

Selective C–H Activation: Ruthenaelectro-Catalysis and Carborane Cage Activation

Dissertation

for the award of the degree

“Doctor rerum naturalium” (Dr.rer.nat.)

of the Georg-August-Universität Göttingen

within the doctoral program of chemistry

of the Georg-August-Universität School of Science (GAUSS)

Submitted by

Long Yang

From Ganzhou (China)



Göttingen, 2021

Thesis Committee

Prof. Dr. Lutz Ackermann, Institute of Organic and Biomolecular Chemistry

Prof. Dr. Shoubhik Das, ORSY Division, Department of Chemistry, Universiteit Antwerpen, Antwerpen, Belgium.

Members of the Examination Board

Reviewer: Prof. Dr. Lutz Ackermann, Institute of Organic and Biomolecular Chemistry, Göttingen

Second Reviewer: Prof. Dr. Shoubhik Das, ORSY Division, Department of Chemistry, Universiteit Antwerpen, Antwerpen, Belgium.

Further members of the Examination Board

Prof. Dr. Dietmar Stalke, Institute of Inorganic Chemistry, Göttingen

Jun.-Prof. Dr. Johannes C. L. Walker, Institute of Organic and Biomolecular Chemistry, Göttingen

Dr. Michael John, Institute of Organic and Biomolecular Chemistry, Göttingen

Dr. Daniel Janßen-Müller, Institute of Organic and Biomolecular Chemistry, Göttingen

Date of the Oral Examination: 30.09.2021

Contents

1. Introduction	1
1.1 Transition Metal-Catalyzed C–H Functionalization.....	1
1.2 General Modes for Metal-Mediated C–H Activation Processes.....	2
1.3 General Strategies for Selective C–H Functionalizations	4
1.4 Ruthenium-Catalyzed Selective C–H Activation.....	5
1.4.1 Ruthenium-Catalyzed <i>ortho</i> -Selective C–H Activation	5
1.4.2 Ruthenium-Catalyzed <i>meta</i> -Selective C–H Activation	12
1.4.3 Ruthenium-Catalyzed <i>para</i> -Selective C–H Activation	14
1.5 Transition Metal-Catalyzed Electrochemical C–H Activation	15
1.5.1 Palladaelectro-Oxidative C–H Activation	15
1.5.2 Rhodaelectro-Oxidative C–H Activation.....	17
1.5.3 Ruthenaelectro-Oxidative C–H Activation.....	19
1.5.4 Iridaelectro-Oxidative C–H Activation	21
1.5.5 Cobaldaelectro-Oxidative C–H Activation	22
1.5.6 Nickellaelectro-Oxidative C–H Activation.....	24
1.5.7 Cupraelectro-Oxidative C–H Activation.....	25
1.5.8 Ferraelectro-Oxidative C–H Activation.....	26
1.5.9 Manganaelectro-Oxidative C–H Activation	27
1.6 Transition Metal Catalyzed B–H Cage Activation of <i>o</i> -Carborane	27
1.6.1 Transition Metal-Catalyzed Cage B(3,6)–H Functionalization	29
1.6.2 Transition Metal-Catalyzed Cage B(4,5,7,11)–H Functionalization	31
1.6.3 Transition Metal-Catalyzed Cage B(8,9,10,12)–H Functionalization	39
1.7 Electrochemical Functionalization of Carboranes	40
2. Objectives	42
3. Results and Discussion	46
3.1 Ruthenium(IV) Intermediates in C–H Annulation by Weak O-Coordination	46
3.1.1 Optimization and Scope.....	46
3.1.2. Proposed Mechanism.....	48
3.2 Twofold C–H/N–H Annulations towards π -Extended Polyaromatics.....	50
3.2.1. Optimization and Scope	50
3.2.2. UV-Vis Absorption and Fluorescence Spectroscopy	52

Contents

3.3 Ruthenaelectro(II/III/I)-Catalyzed Alkyne Annulations	53
3.3.1. Optimization and Scope of Alkenyl Imidazole	53
3.3.2. Optimization and Scope of of benzimidazoles	56
3.3.3 Mechanistic Studies.....	58
3.3.3.1 H/D Exchange and Competition Experiments	58
3.3.3.2 Isolation and Characterization of Ruthenium(II) Intermediate	59
3.3.3.3 Cyclic Voltammetry Studies of Ruthenium(II) Intermediate	60
3.3.3.4 Proposed Mechanism.....	61
3.4 Regioselective B(3,4)-H Arylation of <i>o</i> -Carboranes	63
3.4.1. Optimization and Scope of B(3,4)-H Arylation of <i>o</i> -Carboranes.....	63
3.4.2 Proposed Mechanism.....	66
3.5 Electrochemical B-H Nitrogenation of <i>nido</i> -Carboranes	68
3.5.1 Optimization and Scope	68
3.5.2 Competition Experiments	72
3.5.3 Cyclic Voltammetry and Stability of 156a	73
3.5.4 Spectroscopic Data of BODIPY-Labelled <i>nido</i> -Carborane	74
3.5.5 Proposed Mechanism.....	74
3.6 Cupraelectro-Catalyzed Chalcogenations of <i>o</i> -Carboranes	76
3.6.1 Optimization and Scope	76
3.6.2 Late-stage Functionalization.....	80
3.6.3 Control Experiments and Cyclic Voltammograms	80
3.6.4 Proposed Mechanism.....	82
4. Summary and Outlook.....	83
5. Experimental Section.....	87
5.1 General Remarks	87
5.2 General Procedures	90
5.3 Experimental Procedures and Analytical Data	94
5.3.1 Ruthenium(IV) Intermediates in C-H Annulation	94
5.3.1.1 Characterization Data.....	94
5.3.2 Twofold C-H/N-H Annulations towards π -Extended Polyaromatics	103
5.3.2.1 Characterization Data.....	103
5.3.2.2 Investigation of Rotameric Species.....	108
5.3.3 Ruthenaelectro(II/III/I)-Catalyzed Alkyne Annulations	111
5.3.3.1 Characterization Data.....	111

Contents

5.3.3.2 H/D Exchange Experiment	131
5.3.3.3 Competition Experiments.....	134
5.3.3.4 Synthesis of Ruthenium Complexes	136
5.3.3.5 Ruthenium Complexes Catalyzed C–H/N–H Activation	138
5.3.3.6 Oxidatively Induced Reductive Elimination	138
5.3.3.7 On-Line NMR Monitoring in Flow.....	139
5.3.3.8 GC-Headspace Detection.....	141
5.3.3.9 Cyclic Voltammetry	142
5.3.4 Regioselective B(3,4)–H Arylation of <i>o</i> -Carboranes.....	143
5.3.4.1 Characterization Data.....	143
5.3.5 Electrochemical B–H Nitrogenation of <i>nido</i> -Carboranes	153
5.3.5.1 Characterization Data.....	153
5.3.5.2 Competition Experiments.....	172
5.3.5.3 GC-Headspace Detection.....	173
5.3.5.3 Cyclic Voltammetry	174
5.3.5.3 Stability Test	175
5.3.6 Cupraelectro-Catalyzed Chalcogenations of <i>o</i> -Carboranes	179
5.3.6.1 Characterization Data.....	179
5.3.6.2 Late-stage Diversification	191
5.3.6.3 Mechanistic Studies.....	193
5.3.6.4 Cyclic Voltammetry	193
5.3.6.5 EPR studies.....	195
6. Reference.....	197
7. NMR Spectra.....	207
7.1 Ruthenium(II/IV)-Catalyzed Annulation	207
7.2 Ruthenium(II)-Catalyzed DPP Annulation	226
7.3 Ruthenaelectro(II/III/I)-Catalyzed Annulation.....	235
7.4 Palladium(II)-Catalyzed B(3,4)-Arylation of <i>o</i> -Carboranes	280
7.5 Electrochemical B–H Nitrogenation of <i>nido</i> -Carboranes	310
7.6 Cupraelectro-Oxidative Chalcogenation of <i>o</i> -Carboranes.....	383
Acknowledgement.....	458
Curriculum Vitae.....	460

List of Abbreviations

Ac	acetyl
acac	acetyl acetonate
Ad	Adamantane
Alk	alkyl
AMLA	ambiphilic metal-ligand activation
aq.	aqueous
Ar	aryl
atm	atmospheric pressure
BDMAE	bis(2-dimethylaminoethyl)ether
BHT	butylated hydroxytoluene
BIES	base-assisted internal electrophilic substitution
Bn	benzyl
Boc	<i>tert</i> -butyloxycarbonyl
bpy	2,2'-bipyridyl
BQ	1,4-benzoquinone
Bu	butyl
Bz	benzoyl
calc.	calculated
<i>cat.</i>	catalytic
CCE	constant current electrode
CMD	concerted-metalation-deprotonation
cod	1,5-cyclooctadiene
conv.	conversion
Cp	cyclopentadienyl
Cp*	1,2,3,4,5-pentamethylcyclopenta-1,3-dienyl
Cy	cyclohexyl
δ	chemical shift
d	doublet
DBU	1,8-diazabicyclo[5.4.0]undec-7-ene
DCE	1,2-dichloroethane
DCIB	dichloro- <i>iso</i> -butane
dcype	1,2-bis-(dicyclohexylphosphino)ethane
dd	doublet of doublet
DFT	density functional theory
DG	directing group
DME	dimethoxyethane
DMA	<i>N,N</i> -dimethylacetamide
DMAP	4-dimethylaminopyridine
DMF	<i>N,N</i> -dimethylformamide
DMPU	1,3-dimethyltetrahydropyrimidin-2(1 <i>H</i>)-one

List of Abbreviations

dppbz	1,2-bis(diphenylphosphino)benzene
dt	doublet of triplet
EI	electron ionization
equiv	equivalent
ES	electrophilic substitution
ESI	electrospray ionization
Et	ethyl
Fc	Ferrocene
FG	functional group
g	gram
GC	gas chromatography
GVL	γ -valerolactone
h	hour
Hal	halogen
Het	heteroatom
Hept	heptyl
Hex	hexyl
HFIP	1,1,1,3,3,3-hexafluoro-2-propanol
HPLC	high performance liquid chromatography
HR-MS	high resolution mass spectrometry
Hz	Hertz
<i>i</i>	<i>iso</i>
IPr•HCl	1,3-bis-(2,6-diisopropylphenyl) imidazolium chloride
IR	infrared spectroscopy
IES	internal electrophilic substitution
<i>J</i>	coupling constant
KIE	kinetic isotope effect
L	ligand
<i>m</i>	<i>meta</i>
m	multiplet
M	molar
[M] ⁺	molecular ion peak
Me	methyl
Mes	mesityl
mg	milligram
MHz	megahertz
min	minute
mL	milliliter
mmol	millimole
M.p.	melting point
MQ	6-methylquinoline
Ms	Mesyl
MS	mass spectrometry

List of Abbreviations

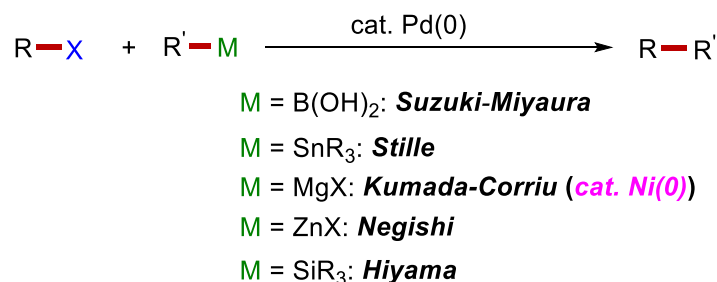
<i>m/z</i>	mass-to-charge ratio
NBA	nitrobenzoic acid
NBE	norbornene
NMO	<i>N</i> -methylmorpholine oxide
NMP	<i>N</i> -methylpyrrolidinone
NMR	nuclear magnetic resonance
n.r.	no reaction
<i>o</i>	<i>ortho</i>
OPV	oil pump vacuum
<i>p</i>	<i>para</i>
PAHs	<i>polycyclic aromatic hydrocarbons</i>
Ph	phenyl
Phen	1,10-phenanthroline
Piv	pivaloyl
ppm	parts per million
Pr	propyl
Py	pyridyl
Pym	pyrimidine
PyO	2-aminopyridine-1-oxide
q	quartet
Q	quinoline
RT	room temperature
s	singlet
sat.	saturated
SCE	saturated calomel electrode
SPS	solvent purification system
<i>t</i>	<i>tert</i>
t	triplet
T	temperature
TBAA	tetrabutylammonium acetate
TBAB	tetrabutylammonium bromide
TBAI	tetrabutylammonium iodide
TBHP	<i>tert</i> -butyl hydroperoxide
TEMPO	2,2,6,6-Tetramethylpiperidine-1-oxyl
Tf	triflate
TFE	2,2,2-trifluoroethanol
THF	tetrahydrofuran
TIPS	triisopropylsilyl
TM	transition metal
TMA	tetramethylammonium
TMEDA	<i>N,N,N',N'</i> -tetramethylethane-1,2-diamine
TMS	trimethylsilyl
Ts	<i>para</i> -toluenesulfonyl

1. Introduction

Synthetic organic chemistry mainly focuses on the cleavage and formation of bonds in a practical and selective fashion, where the formation of carbon-carbon (C–C)^[1] and C–Heteroatom (C–Het)^[2] bonds constitutes one of the most important subjects. During the last century, great progress has been made in organic synthesis, with considerable applications to pharmaceutical industry, materials chemistry, and crop-protection field, among others.^[3] However, the environmental issues associated with organic synthesis are inevitable in terms of chemical waste and toxic reagents. Therefore, significant attention has been paid to the development of sustainable strategies for molecular assembly in terms of both the economic and environmental benefits.^[4] In 1988, Anastas and Warner introduced the twelve principles of green chemistry as guidelines for minimizing the environmental footprint of chemical syntheses.^[5] According to these guidelines, the application of catalysis to organic chemistry is essential to increase the economic benefits and reduce waste formation by avoiding stoichiometric amounts of metal-based catalysts, oxidants or reductants.

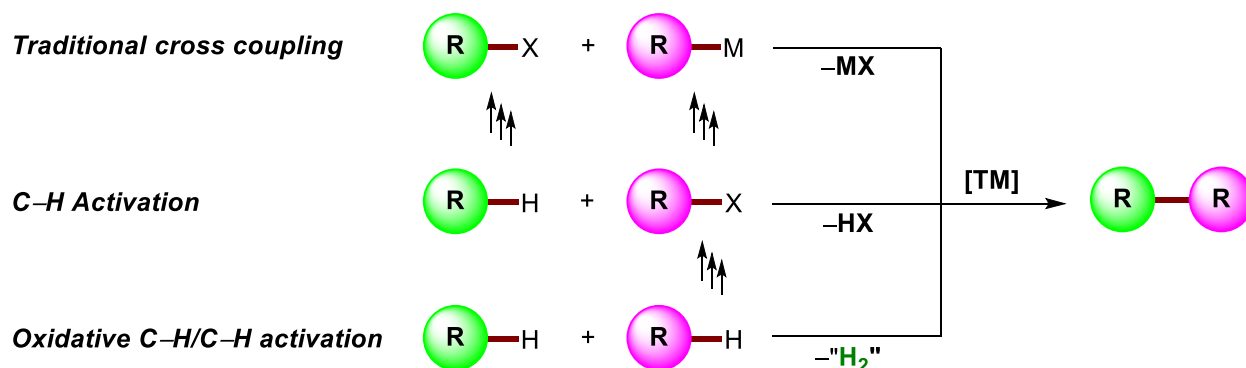
1.1 Transition Metal-Catalyzed C–H Functionalization

Since the early contributions using stoichiometric or catalytic amounts of copper in the coupling reactions by Glaser^[6] and Ullmann^[7] in the late of 19th century, significant progress has been witnessed in transition-metal-catalyzed cross-coupling reactions between a (hetero)aryl halide and an organometallic reagent for the construction of C–C bonds, such as the Suzuki-Miyaura coupling,^[8] the Stille coupling,^[9] the Hiyama coupling,^[10] the Kumada-Corriu coupling,^[11] and the Negishi coupling^[12] reactions ([Scheme 1.1](#)). Additionally, transition-metal-catalyzed cross-coupling reactions, such as the Buchwald-Hartwig amination,^[13] the Ullmann–Goldberg,^[14] and the Chan–Evans–Lam-coupling,^[15] were successfully explored for C–Het bond formations. These important contributions were recognized with the award of the 2010 Nobel Prize in Chemistry to Heck, Negishi and Suzuki “for palladium-catalyzed cross-couplings in organic synthesis”.^[16]



Scheme 1.1. Transition metal-catalyzed cross-coupling reactions.

Although traditional cross-coupling reactions represent one of the most reliable methods to access (hetero)-aryl-(hetero)aryl moieties, this method requires two fully prefunctionalized starting materials, namely organic (pseudo)halides and organometallic reagents *e.g.* Grignard reagents, organostannanes, organozinc and organolithium compounds, which are typically sensitive to air and moisture, and require multistep synthetic procedures,^[17] and generate stoichiometric amounts of salt waste. In contrast, transition metal-catalyzed C–H functionalizations^[18] provide an opportunity to overcome these limitations to some extent.^[19] In particular, cross dehydrogenative couplings (CDC) between two aromatic C–H bonds represent one of the most straightforward and sustainable concepts to forge bi(hetero)aryl structures (C–H/C–H type) with molecular hydrogen as the sole byproduct (**Scheme 1.2.**)^[20]



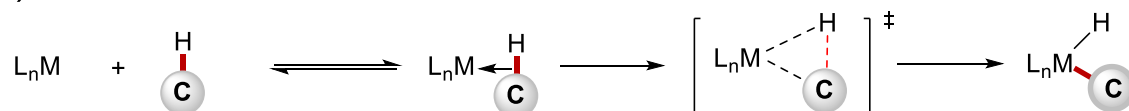
Scheme 1.2. Traditional cross-coupling reactions *versus* C–H activation.

1.2 General Modes for Metal-Mediated C–H Activation Processes

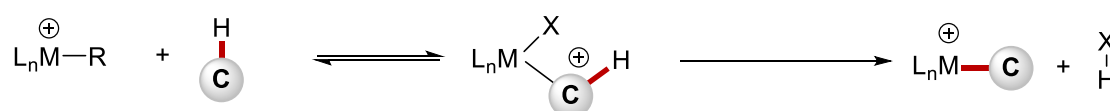
In general terms, the transition-metal-facilitated cleavage of C–H bond is the common key step in C–H functionalization strategies. Computational chemistry has made a particularly strong contribution to the understanding of the range of possible mechanisms for the C–H scission.^[21]

Excluding radical C–H activation or radical cross-coupling reactions,^[22] five different pathways can be classified depending on the electronic properties and the nature of the metal (**Scheme 1.3**). Electron-rich complexes of late transition metals are prone to cleave the inert C–H bonds by oxidative addition, while this mode of action is unfavorable for early transition metals (**Scheme 1.3a**).^[23] Most late transition metals in higher oxidation states often act as a Lewis acid to cleave C–H bond by an electrophilic substitution mode (**Scheme 1.3b**).^[24] The σ -bond metathesis is observed for early transition metals which cannot undergo oxidative addition (**Scheme 1.3c**).^[25] Metals containing an unsaturated M=X bond tend to undergo C–H activation via 1,2-addition (**Scheme 1.3d**).^[26] Furthermore, a base-assisted C–H activation event^[21b, 27] is proposed by the combination of electrophilic attack of the metal with deprotonation by carboxylate or carbonate ligands (**Scheme 1.3e**).

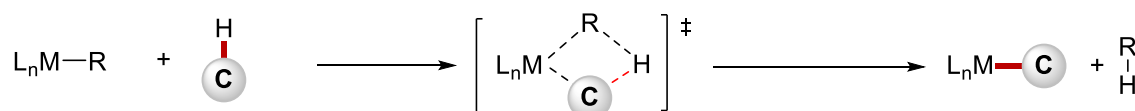
a) Oxidative addition



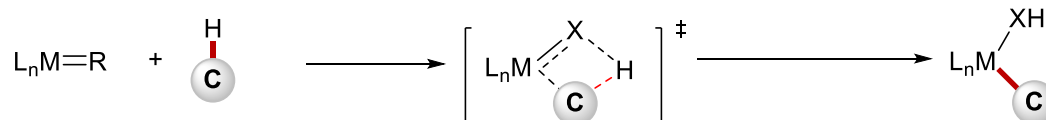
b) Electrophilic substitution



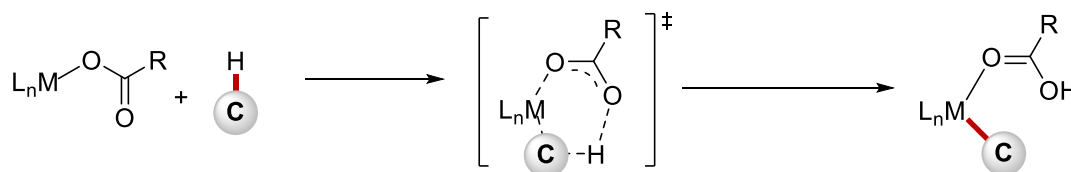
c) σ -Bond metathesis



d) 1,2-Addition



e) Base-assisted metalation



Scheme 1.3. Mechanistic pathways for C–H activation.

Meanwhile, the base-assisted mechanism was further investigated in detail to unveil the important role of an internal base for the C–H cleavage processes, and this base-assisted mechanism could be further categorized by concerted metalation-deprotonation (CMD),^[28] ambiphilic metal-ligand activation (AMLA)^[29] and base-assisted internal electrophilic substitution (BIES).^[30] (Scheme 1.4). Both CMD and AMLA mechanisms involving metalation and deprotonation steps proceed through a six-membered transition state and are favorable for electron-deficient substrates with high kinetic C–H acidity. In sharp contrast the BIES mechanism was preferential observed for electron-rich arenes with acetate or carboxylate ligands and proceeds *via* an electrophilic substitution-type pathway.^[30-31]

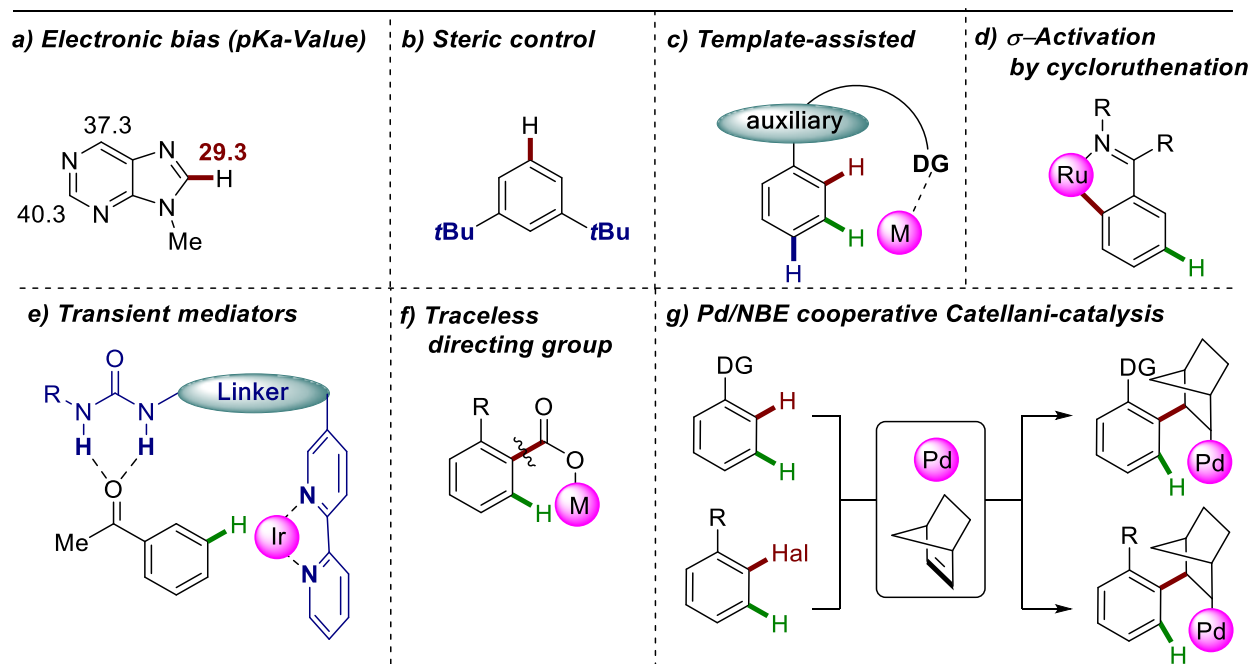


Scheme 1.4. Distinct transition state models for base-assisted C–H metalation.

1.3 General Strategies for Selective C–H Functionalizations

Since C–H bonds are ubiquitous in organic molecules and exhibit similar bond dissociation energies (113.5 kcal/mol for C(sp²)–H bonds in benzene),^[32] the site-selective activation of several C–H bonds in a molecule is a major challenge. To overcome this problem, different approaches have been introduced (Scheme 1.5). One of the methods to differentiate the C–H bonds in heterocycles is by the inherent reactivity in their kinetic acidities and bond dissociation energies (Scheme 1.5a).^[33] Another strategy is the introduction of a bulky substituent on the substrate, resulting in a steric control by preventing access to the adjacent C–H bonds (Scheme 1.5b). Nevertheless, both steric bias and electronic bias have intrinsically limited applications in molecular synthesis owing to the requirement for particular substrates. A more extensively used approach is the installation of Lewis-basic directing groups to precoordinate the transition metal center, thus activating the proximal C–H bond and further facilitating the key C–H activation step selectively (Scheme 1.5c).^[34] In addition, transient directing groups that can be reversibly installed *in situ* and removed in the catalytic C–H cleavage possess have been developed in recent years and have great potential to decrease the number of tedious synthetic steps (Scheme 1.5e).^[35] Moreover, ruthenium-catalyzed σ -activation by strongly influencing the electronic properties of the aromatic ring (Scheme 1.5d),^[36] and exploiting carboxylic acids as

traceless directing groups (Scheme 1.5f)^[37] are the alternative strategies for the remote *meta*-selective C–H activation. In contrast, the palladium/norbornene (NBE) cooperative Catellani-type reaction has emerged as a powerful approach to achieve site-selective C–H activation (Scheme 1.5g).^[38] Here, the *ortho* selective C–H activation occurs in the presence of Pd/NBE to generate a palladium-norbornene species, which can further activate the adjacent C–H bond to finally achieve the remote selective *meta*-C–H bond functionalizations.



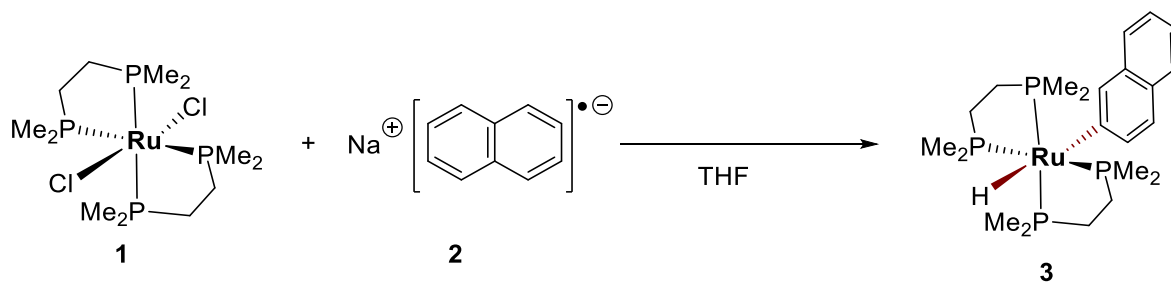
Scheme 1.5. Different strategies for selective C–H functionalizations.

1.4 Ruthenium-Catalyzed Selective C–H Activation

While tremendous contributions have been made in the field of palladium or rhodium complexes-catalyzed C–H bond activation to promote C–C bond formation, the application of cost-effective ruthenium catalysts is now useful and highly desirable for the efficient catalytic conversion of C–H bonds.^[35a]

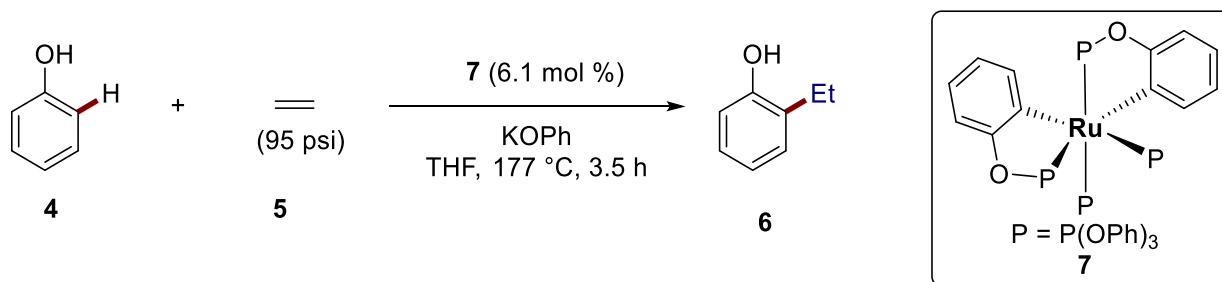
1.4.1 Ruthenium-Catalyzed *ortho*-Selective C–H Activation

As early as 1965, Chatt and Davidson presented the ruthenium-mediated C–H activation, in which the ruthenium(II)-phosphine complex $[\text{RuCl}_2(\text{Me}_2\text{PCH}_2\text{CH}_2\text{PMe}_2)_2]$ **1** was employed to achieve the C–H bond cleavage of sodium arene **2** in THF for the generation of hydride-ruthenium(II) complex **3** (Scheme 1.6).^[39]



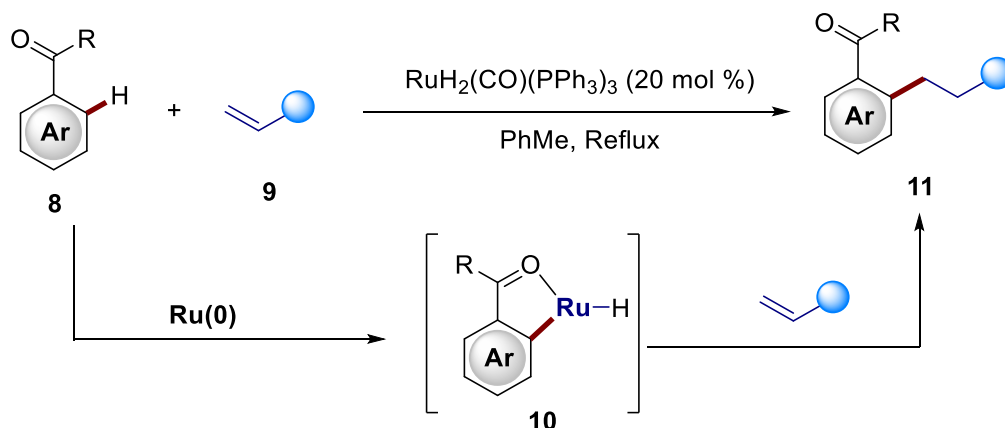
Scheme 1.6. Ruthenium-mediated C–H activation.

In 1986, the first *ortho*-metalated ruthenium complex **7** catalyzed regioselective C–H ethylation was reported by Lewis and Smith, thus inspiring further developments in C–H activation by ruthenium catalysis. A proposed mechanism for the insertion reaction involves phosphite substitution by ethylene, insertion of ethylene for C–C bond formation into the Ru–C bond, and finally reductive elimination to give an ethyl group (**Scheme 1.7**).^[40]



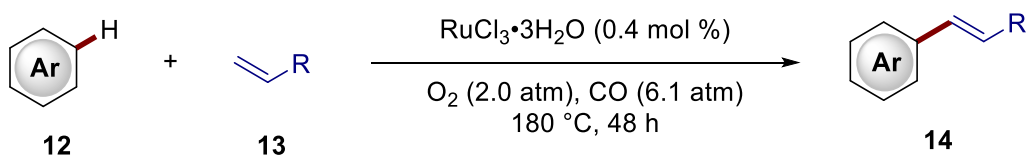
Scheme 1.7. Ruthenium-catalyzed C–H alkylation.

In 1993, a subsequent report in transition-metal-catalyzed C–H bond activation was achieved by the Murai–Chatani–Kakiuchi (**Scheme 1.8**).^[41] This was the first example of chelation-assisted catalytic alkylation of aromatic ketones **8** in the presence of a ruthenium(0) catalyst. This reaction proceeded by an initial insertion of ruthenium(0) into a C–H bond for the generation of active C–Ru–H species, and subsequent reaction of this metal complex with unsaturated substrates to provide the desired product **11**. Importantly, the use of chelation assistance to form the cyclometalated ruthenium-hydride **10** proved crucial for the C–H cleavage.



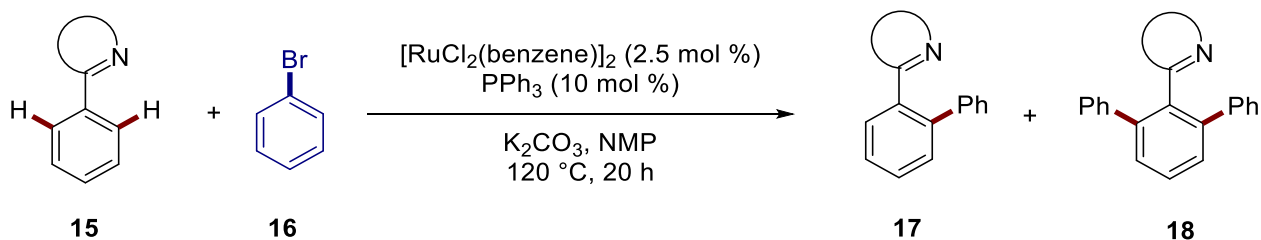
Scheme 1.8. Ruthenium-catalyzed C–H alkylation of aromatic ketones.

In 2001, Milstein and coworkers introduced a novel ruthenium-catalyzed oxidative coupling of olefin **13** with arene **12** to furnish aryl alkene **14**, where either dioxygen or the alkene **13** can play a role of an oxidant, eventually leading to reasonable turnover numbers (Scheme 1.9).^[42]



Scheme 1.9. Ruthenium-catalyzed oxidative coupling

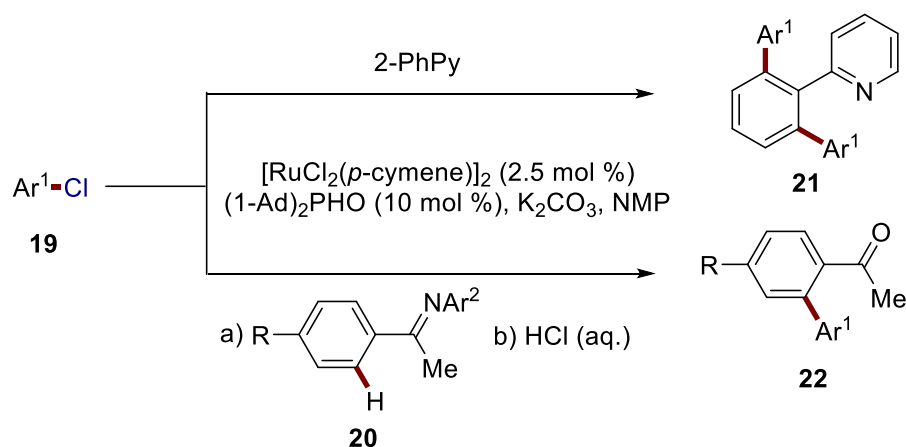
In the same year, the first *ortho*-selective C–H mono- or di-arylations of the aromatic ring in 2-arylpiperidines, 2-aryloxazolines and 2-arylimidazolines **15** with organic halides **16** in the presence of a ruthenium(II)-phosphine complex as the catalyst were reported by Oi and Inoue (Scheme 1.10).^[43] However, this protocol was later shown not to be reproducible. Thus, low-level impurities of γ -butyrolactone were found in the NMP solvent, which could hydrolyze under the basic conditions to generate a carboxylate.^[44]



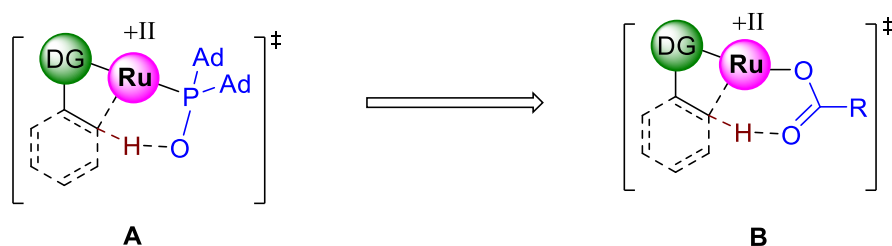
Scheme 1.10. Ruthenium-catalyzed *ortho*-selective C–H arylation.

In 2005, the first generally applicable method for the direct arylation of functionalized arenes using ruthenium(II) catalysts was reported by Ackermann^[45] by the introduction of phosphine oxide $\text{R}_2\text{P}(\text{O})\text{H}$ additives that were shown to activate the ruthenium(II) catalyst more efficiently than tertiary phosphine ligand^[44] (Scheme 1.11). In this case, the air-stable adamantyl-

substituted secondary phosphine oxide (SPO) (1-Ad)₂P(O)H was used as the preligand, leading to the effective arylation with the less reactive, but readily available aryl chlorides **19**. As to this working mode of the SPO-based ruthenium(II) catalyst, a base-assisted metalation was proposed to be the decisive feature *via* transition state **A** (Scheme 1.12). Later, the same group embarked on exploration of other bifunctional ligands, such as carboxylates, for direct arylations that were expected to give rise to transition state **B**.^[46]



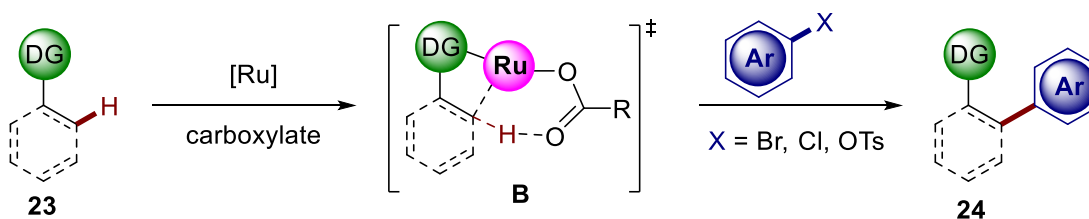
Scheme 1.11. Ruthenium-catalyzed *ortho*-selective C–H arylation using phosphine oxide as preligand.



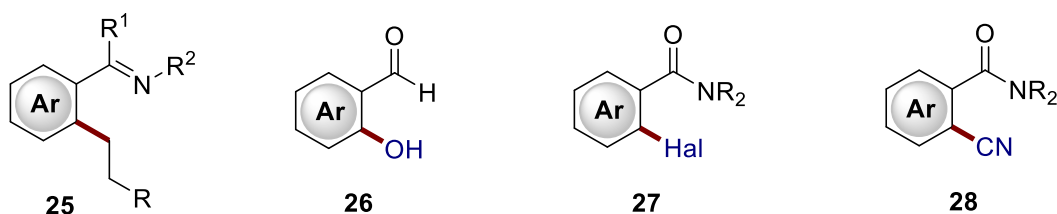
Scheme 1.12. Proposed transition states for base-assisted ruthenations.

In 2008, the Ackermann group demonstrated the first case of carboxylate-assisted ruthenium(II)-catalyzed C–H activation, even in apolar solvent, involving the possible generation of a six-membered ruthenium-carboxylate species (Scheme 1.13a).^[47] Subsequently, this most powerful strategy also enabled site- and chemo-selective C–H alkylations **25**,^[48] C–H oxygenations **26**,^[49] C–H halogenations **27**,^[50] or C–H cyanations **28** (Scheme 1.13b).^[51]

a) Carboxylate-assisted ruthenium(II)-catalyzed C–H arylation

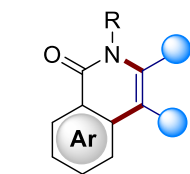
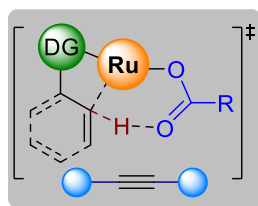


b) Carboxylate-assisted ruthenium(II)-catalyzed C–H alkylation, hydroxylation, halogenation and cyanation

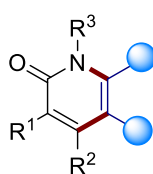


Scheme 1.13. Ruthenium-catalyzed C–H arylation, alkylation, hydroxylation, halogenation and cyanation under carboxylate assistance.

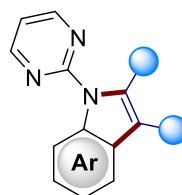
The robust nature of the ruthenium(II)-catalyzed C–H activation was not limited to direct arylation chemistry. Indeed, this general concept of carboxylate-assisted ruthenium-catalyst was found to be broadly applicable for various heterocyclic molecular synthesis in terms of oxidative annulations for C–H/N–H^[52] and C–H/O–H bond^[53] activations in the presence of copper(II) oxidants (Scheme 1.14).^[54]



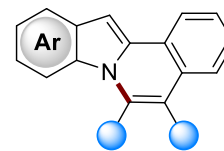
a) Ackermann, 2011



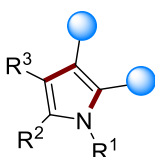
b) Ackermann, 2011



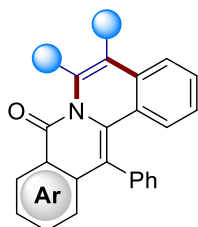
c) Ackermann, 2012



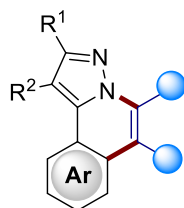
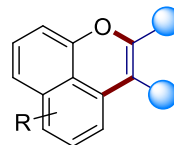
d) Ackermann, 2012



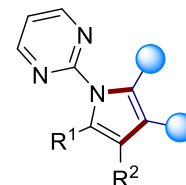
e) Ackermann, 2012



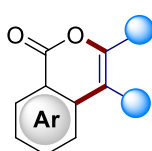
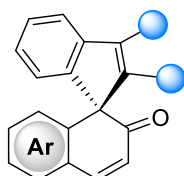
f) Wang, 2012

g) Ackermann, 2012
Jeganmohan, 2012

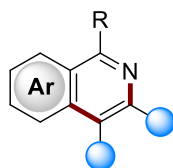
h) Ackermann, 2012



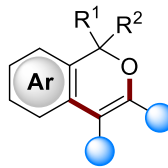
i) Ackermann, 2013

j) Ackermann
2012/2013

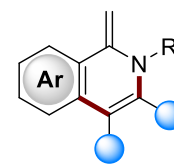
k) Luan, 2013



l) Urriolabeitia, 2013



m) Ackermann, 2014

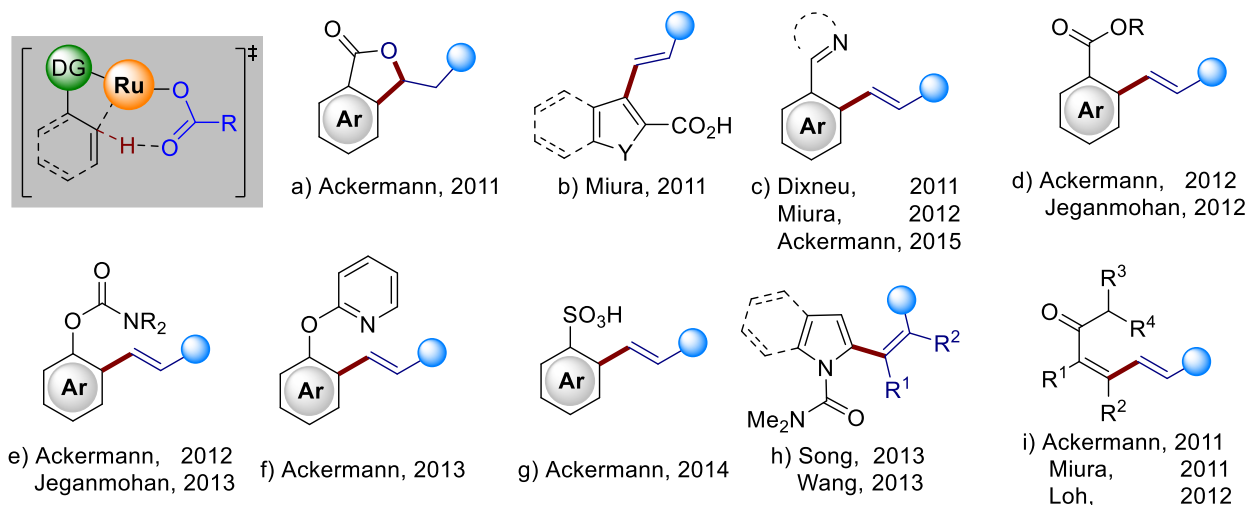


n) Ackermann, 2014

Scheme 1.14. Ruthenium-catalyzed oxidative C–H/X–H annulations with alkynes.

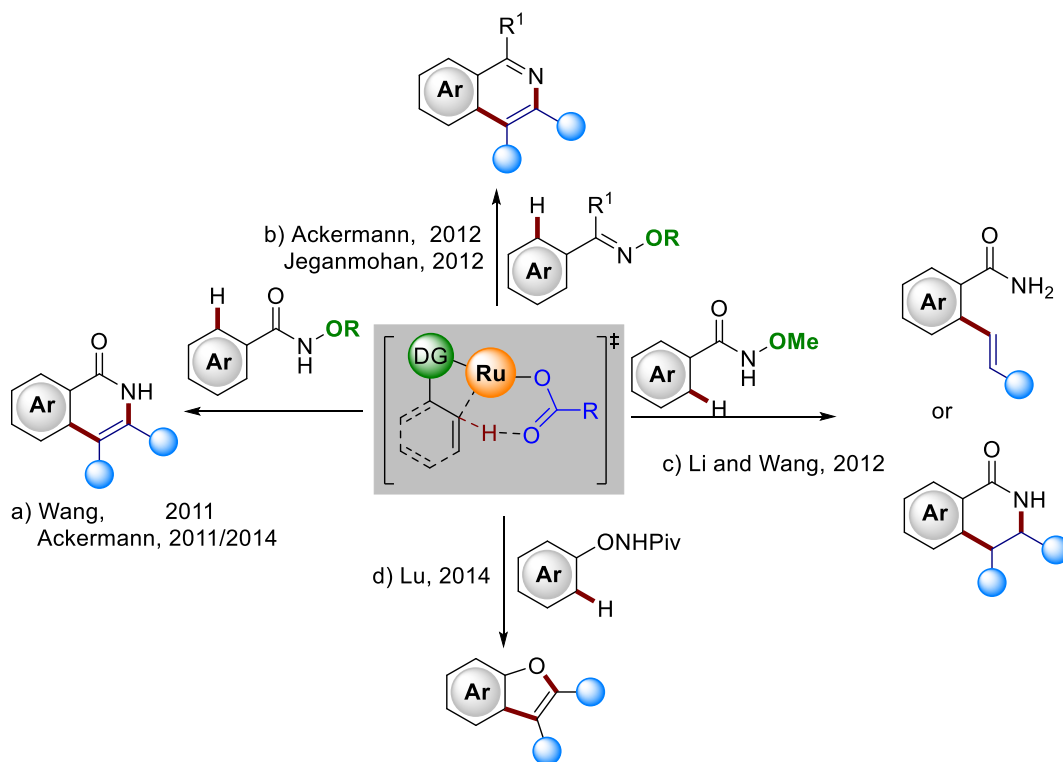
Furthermore, carboxylate assisted ruthenium-catalyzed selective oxidative C(sp²)–H olefinations of heteroarenes were accomplished to generate the desired aryl alkenes (Scheme 1.15). Different directing groups were explored for these transformations by the Ackermann group, among others, such as, carboxylic acids,^[55] oxazoles/triazoles,^[56] ketones/aldehydes,^[57] esters,^[58] carbamates,^[59] 2-pyridyloxys,^[60] sulfonic acids,^[30b] *N*-dimethylcarbamoyls^[61] and amides.^[62]

Introduction



Scheme 1.15. Ruthenium-catalyzed oxidative annulation and olefinations with olefines.

Most of these reactions used copper acetate, which acted not only as the oxidant, but also served as the essential source of acetate for the carboxylate-assisted ruthenation manifold. In order to avoid using the copper salt as an oxidant, an alternative strategy was viable through the use of substrates bearing N–O bonds as “internal oxidants” for the syntheses of isoquinolones, isoquinolines,^[63] olefination or alkyl annulation^[64] and benzofuran derivatives (Scheme 1.16).^[65]

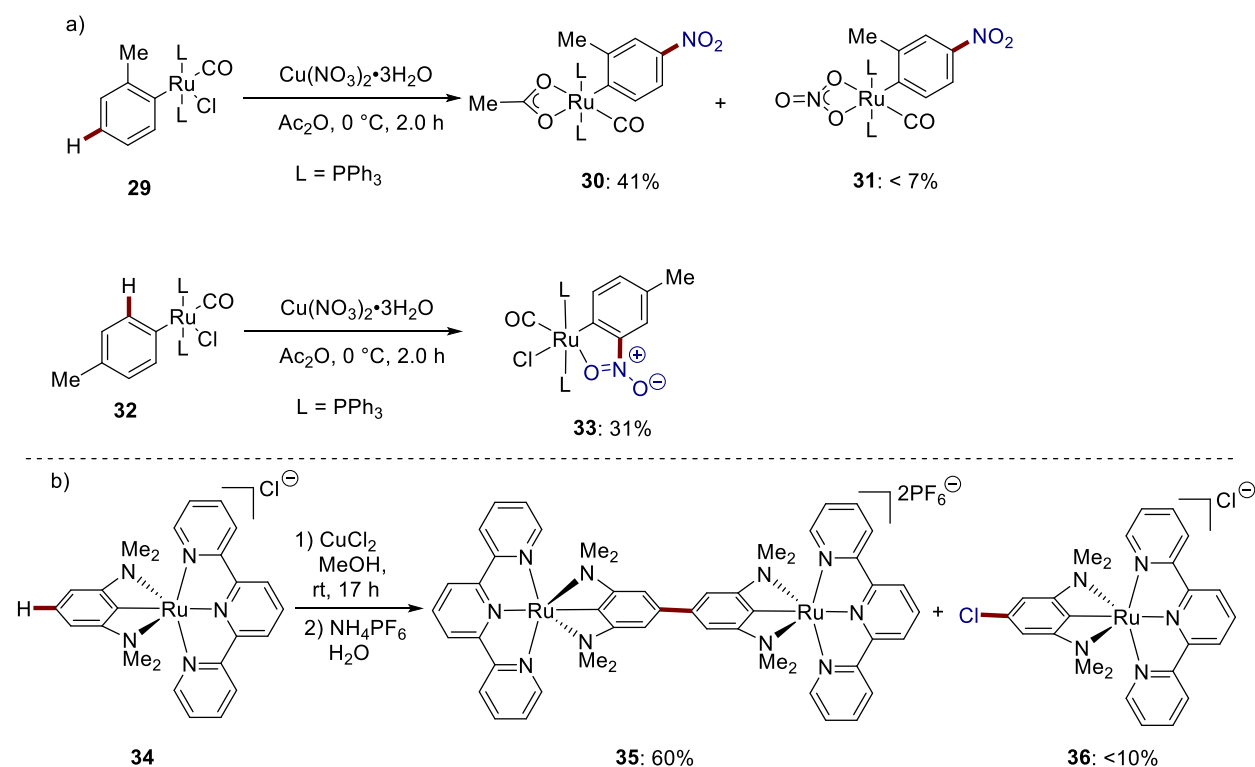


Scheme 1.16. Ruthenium-catalyzed redox-neutral annulation and olefinations with olefines.

1.4.2 Ruthenium-Catalyzed *meta*-Selective C–H Activation

meta-Selective C–H functionalizations can be elegantly achieved *via* σ -activation through cyclometallation.^[36, 66] This strategy usually installs a directing group at the *ortho*-position to produce a significant electronic bias at the arene ring, thus allowing for subsequent functionalizations to take place at the *para* position with respect to the Ru–C bond, leading to an overall *meta*-selective functionalization.

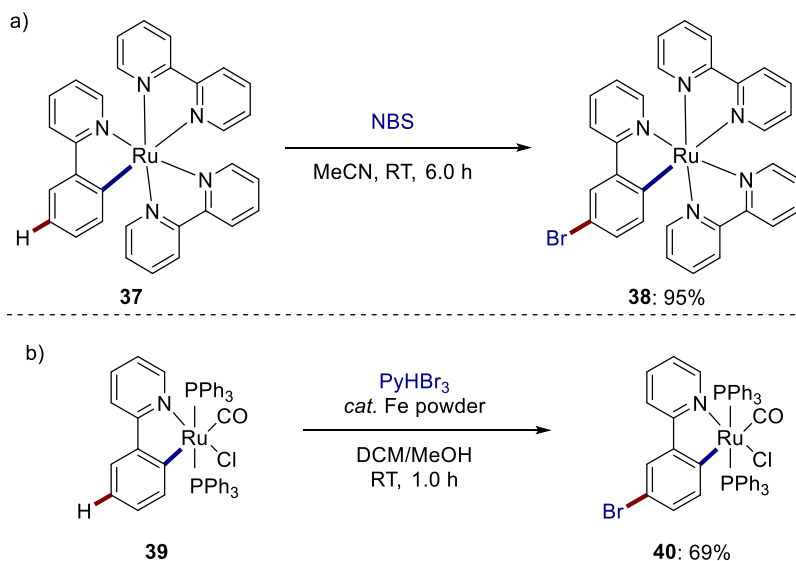
In 1994, Roper reported the *ortho/para*-selective stoichiometric nitration of ruthenium aryl complexes **29** via σ -activation strategy (Scheme 1.17a).^[67] Later, van Koten reported the first chelation-assisted oxidative *para* C–H/C–H functionalization of a ruthenium-arene complex **34**, furnishing the binuclear complex **35** as well as small amounts of chlorinated ruthenium complex **36**. (Scheme 1.17b).^[68] These results presumably clarified that the site-selectivity of C–H activation could be controlled by the formation of C–Ru bond *via* the electronic influence on the arene ring.



Scheme 1.17. C–H activation of cyclometalated ruthenium complexes.

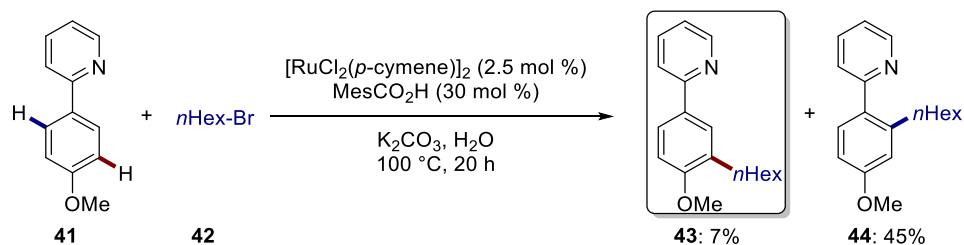
In 1998, the group of Coudret achieved the electrophilic C–H *meta*-bromination of phenylpyridine-ruthenium complex **37** with *N*-bromosuccinimide (NBS) in excellent yield and regioselectivity (Scheme 1.18a).^[69] Afterwards, Roper and Wright disclosed the electrophilic *meta*-selective C–H bromination of phenylpyridine-ruthenium complex **39** with PyHBr₃ as the

halogenating reagent and iron powder as catalyst (Scheme 1.18b).^[70] These observations suggested that the site-selective electrophilic transformation could be controllable by the electronic directing effect of the metal centers.



Scheme 1.18. Remote C–H bromination of cycloruthenium complexes.

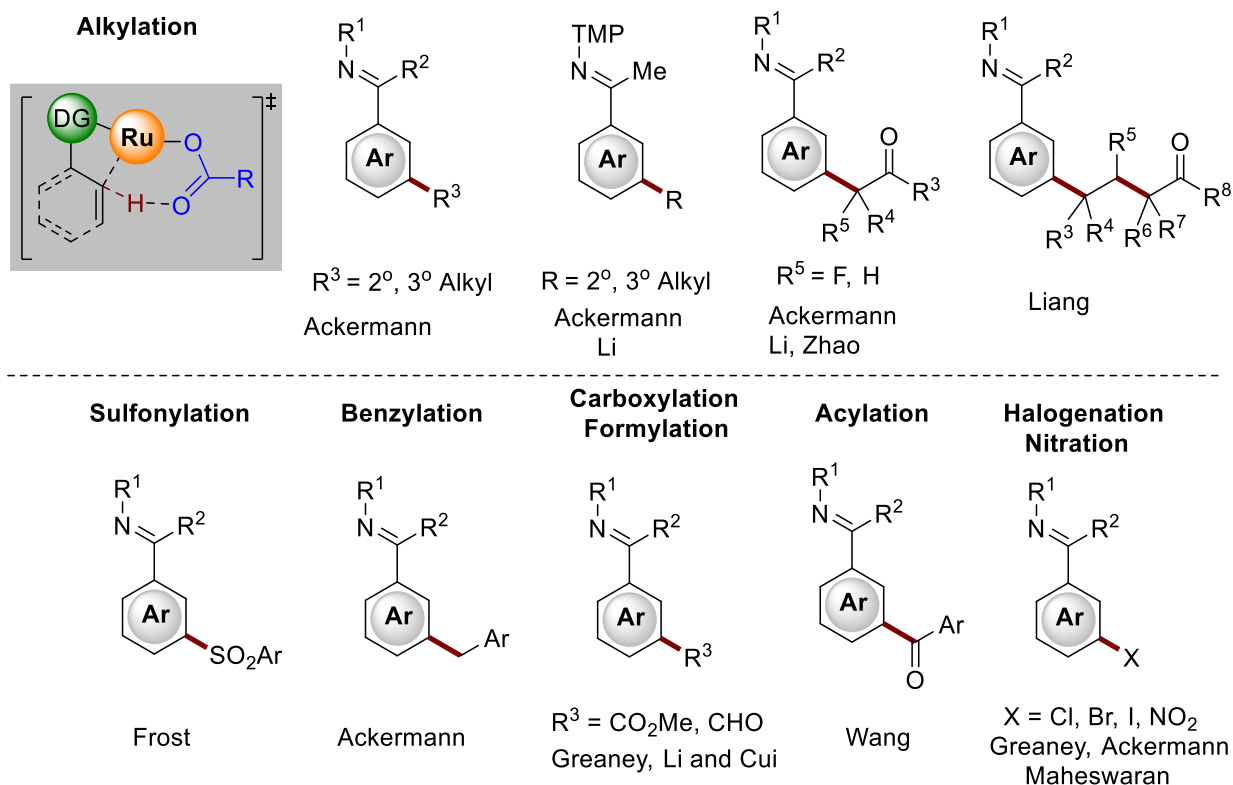
The first observation for the ruthenium-catalyzed *meta*-selective C–H functionalization was reported by the Ackermann group in 2011 (Scheme 1.19).^[71] While chelation assisted ruthenium-catalyzed *ortho*-selective C–H alkylations of the phenylpyridine was the major product, an unprecedented *meta*-alkylated arene **43** was also observed, albeit in rather low yield.



Scheme 1.19. The first ruthenium-catalyzed *meta*-C–H alkylation.

Inspired by this initial result of ruthenium-catalyzed *meta*-selective C–H alkylation, Ackermann^[72] and other groups^[73] independently disclosed this method for remote *meta*-C–H alkylations using secondary and tertiary alkyl bromides through an *ortho*-ruthenation strategy (Scheme 1.20). The catalytic remote alkylations were applicable to pyridines, pyrimidines, azoles and imines as directing groups, leading to the formation of *meta*-alkylated arenes with excellent levels of position-selectivity. Detailed mechanistic studies of this remote functionalization were supportive of a radical mechanism, involving a reversible C–H ruthenation and a subsequent site-selective alkylation, which was rationalized by the strong electronic effect of the Ru–C(sp²) bond.^[72b-d] Recently, a breakthrough in *meta*-C–H alkylations under photoredox conditions, using a

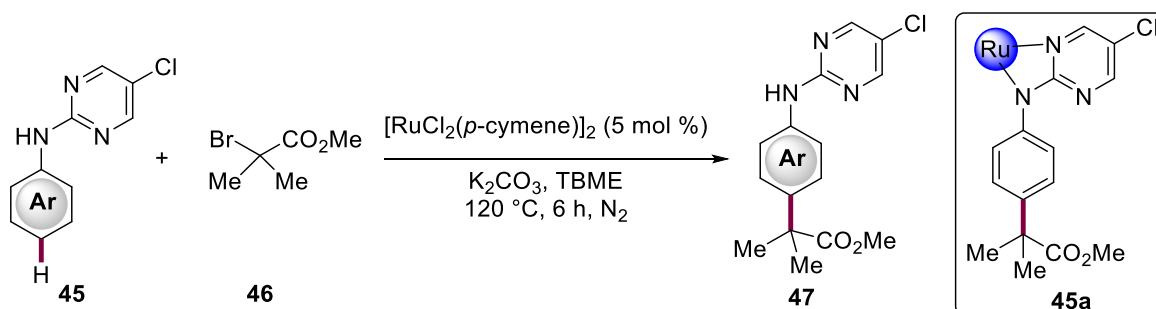
polymer-based hybrid ruthenium catalyst and in a decarboxylative manner were demonstrated by the Ackermann group.^[74] Furthermore, ruthenium-catalyzed carboxylate-assisted *meta*-C–H sulfonylations,^[75] benzylations,^[76] carboxylations,^[77] formylations,^[78] acylations,^[79] halogenations^[80] and nitrations^[81] were developed, respectively, illustrating the key importance of carboxylate-assisted C–H activation with ruthenium(II) complexes in the molecular modifications (Scheme 1.20).^[35a]



Scheme 1.20. Ruthenium-catalyzed selective *meta*-C–H activation in the presence of nitrogen-containing directing groups.

1.4.3 Ruthenium-Catalyzed *para*-Selective C–H Activation

In contrast to the significant progress in *meta*-selective C–H functionalizations, challenging C–H functionalizations at *para* position remain underdeveloped.^[82] In 2017, Frost reported ruthenium-catalyzed *para*-selective C–H alkylations with α -bromo esters **46** (Scheme 1.21).^[83] Mechanistic studies by experiments and DFT calculations suggested a four-membered ruthenacycle **45a** as the key intermediate for the transformations. Afterwards, ruthenium-catalyzed *para*-selective C–H fluoroalkylation of anilides and ketoximes with α -bromo esters **46** were also demonstrated by the Zhao and Ackermann groups.^[84]



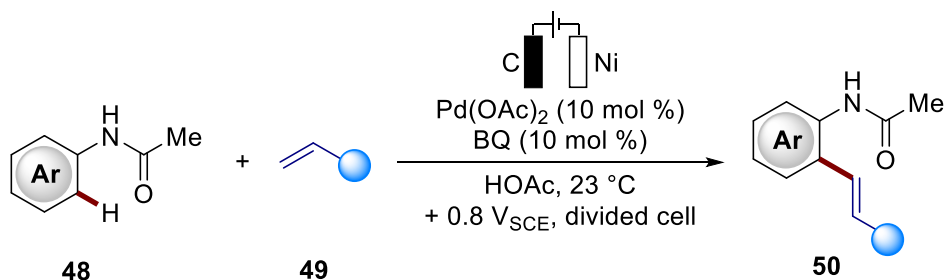
Scheme 1.21. Ruthenium-catalyzed selective *para*-C–H alkylation.

1.5 Transition Metal-Catalyzed Electrochemical C–H Activation

Since early contributions from Volta,^[85] Kolbe,^[86] and Faraday,^[87] electrosynthesis with inexpensive and waste-free electricity as a viable redox equivalent has recently experienced a renaissance,^[88] holding huge potential to accomplish excellent levels of oxidant and resource economy.^[89] In contrast to classical metal-free electrosynthesis, metalla-electrocatalysis sets the stage for transition-metal-catalyzed site-selective C–H activations,^[90] forming C–C or C–Het bonds without stoichiometric chemical oxidants.

1.5.1 Palladaelectro-Oxidative C–H Activation

A pioneering contribution in palladaelectro-oxidative C–H olefinations **50** was reported by the Amatore and Jutand group in 2007 (Scheme 1.22).^[91] This modified Fujiwara-Moritani-type reaction^[92] employed catalytic amounts of benzoquinone as the redox mediator and electricity as a terminal redox equivalent to replace stoichiometric silver(I) and copper(II) salts as oxidants, albeit with a limited scope.



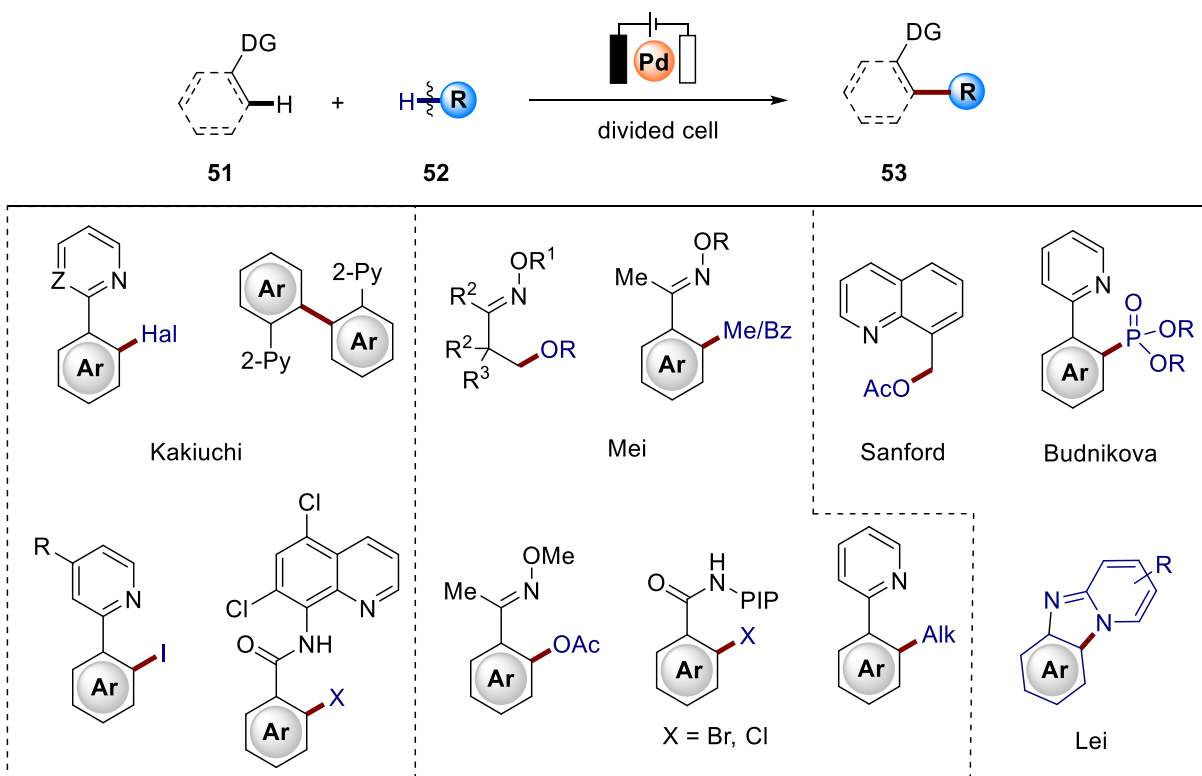
Scheme 1.22. Pallada-electrochemical C–H olefination.

Subsequently, Kakiuchi exploited palladium-catalyzed electrochemical C–H halogenation of 2-phenyl pyridine with hydrogen halides or iodine as the halogenation reagents (Scheme 1.23).^[93] Then, this protocol was further expanded to achieve *ortho*-selective chlorination using bidentate directing groups.^[94] The versatility of pyridine as a chelating group was not only explored for C–H

halogenation of arenes by palladaelectro-catalysis, but also for electrocatalytic homocoupling of arenes *via* intermolecular C–H arylation.^[95]

In 2017, a further contribution was made in electrochemical palladium-catalyzed C(sp³)–H oxygenation by Mei (Scheme 1.23).^[96] This protocol offered a broad scope of synthetically useful oxime derivatives under rather mild reaction conditions.^[97] In subsequent efforts, the efficient palladium-catalyzed oxidative *ortho*-C(sp²)–H methylation and benzylation of oximes were reported by the Mei group using methyltrifluoroborates and benzoyl acetic acids as coupling partners, respectively.^[98] Also, palladium-catalyzed anodic *ortho*-C(sp²)–H acetoxylation,^[99] halogenation^[100] and alkylation^[101] were also achieved by the same group.

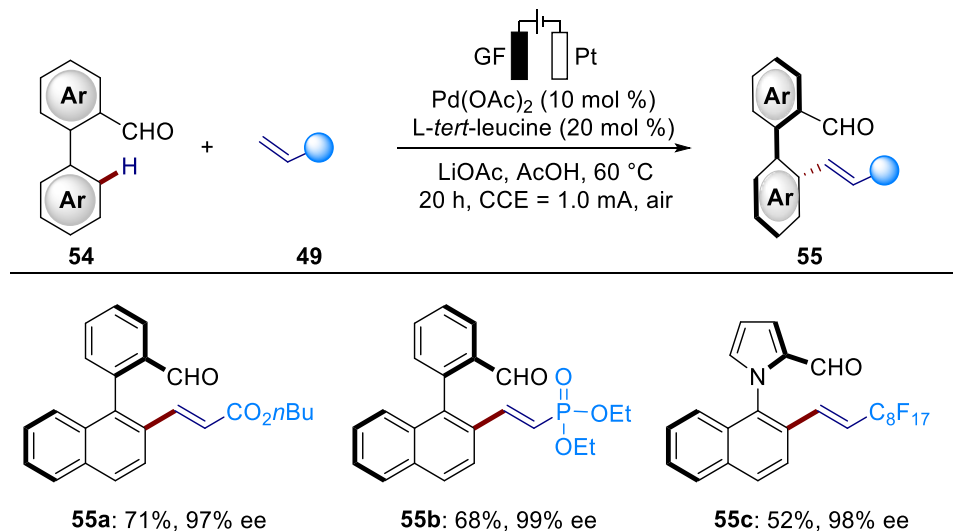
Another example of palladium-catalyzed electrooxidative C(sp³)–H acetoxylation of 8-methylquinoline with tetramethylammonium acetate (TMAOAc, a stronger nucleophile) was introduced by the Sanford group (Scheme 1.23).^[102] In addition, a pyridine-directed palladium-catalyzed electrochemical C(sp²)–H bond phosphonation was also reported by Budnikova.^[103] Moreover, in 2020, the Lei group developed a palladium-catalyzed electro-oxidative intramolecular C–H/N–H annulation reaction without an additive, offering a variety of pyrido[1,2-*a*]benzimidazoles.^[104]



Scheme 1.23. Pallada-electrooxidative C–H activation.

In 2020, the first asymmetric pallada-electrocatalyzed C–H olefination was achieved by the Ackermann group through the synergistic cooperation with a chiral transient directing group for

the construction of various axially chiral biaryls **55a-55c**. Pleasingly the reaction proceeded under undivided cell setup. Further conversion of the thus-obtained products **55** gave expedient access to enantioenriched BINOLs, dicarboxylic acids and helicenes (Scheme 1.24).^[105]



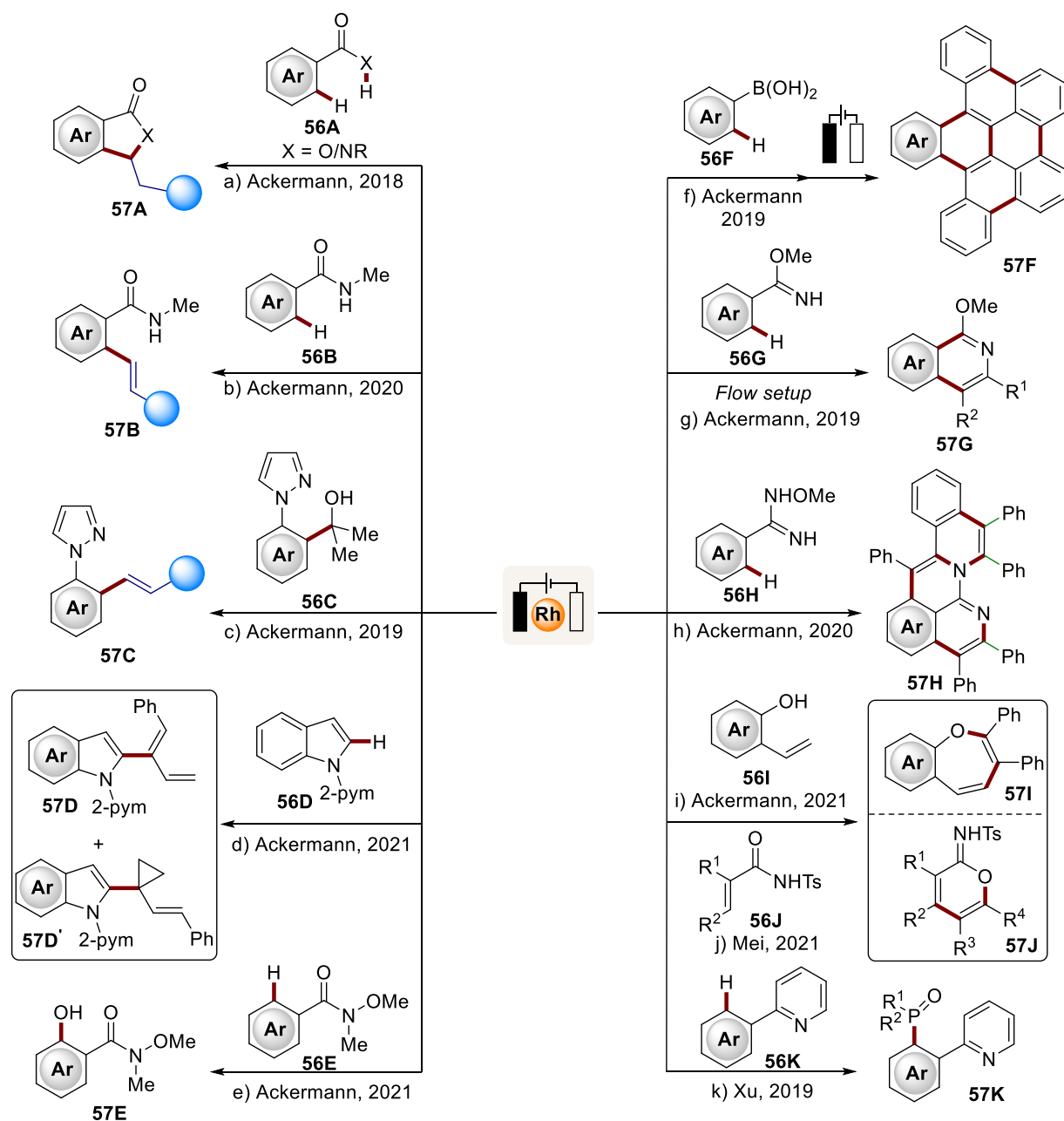
Scheme 1.24. First examples for asymmetric pallada-electrooxidative C–H activation.

1.5.2 Rhodaelectro-Oxidative C–H Activation

Rhodaelectro-oxidative C–H activations have been well documented by Ackermann (Scheme 1.25). In 2018, they reported the first electrochemical cross-dehydrogenative alkene annulation under rhodium catalysis with benzoic acids, amides and indoles **56A** (Scheme 1.25a).^[106] The olefinations of challenging electron-poor benzamides **56B** were established in a fully dehydrogenative fashion using rhodaelectro-catalysis by the same group in 2020, featuring a broad substrate scope (Scheme 1.25b).^[107] In 2019, the first electrochemical C–C activation was accomplished by expedient oxidative rhodium(III) catalysis. This organometallic C–C activation manifold proceeded with ample scope and excellent levels of chemo- and position-selectivities, providing unique access to challenging densely substituted arenes **57C**, which are not viable by any C–H activation methods (Scheme 1.25c).^[108]

Subsequently, the Ackermann group achieved rhodaelectro-catalyzed cascade C–H annulation for the synthesis of novel non-planar polycyclic aromatic hydrocarbons (PAHs) **57F** from simple arylboronic acids **56F** (Scheme 1.25f).^[109] Later, nitrogen-doped polycyclic aromatic hydrocarbons (aza-PAHs) **57H** were obtained *via* a rhodium-catalyzed electrochemical cascade C–H annulations of amidoximes **56H** with alkynes (Scheme 1.25h).^[110] In addition, a flow-rhodaelectro-catalyzed C–H alkyne annulation was firstly established by the same group. Two key rhodacycles were synthesized and detailed mechanistic studies suggest an oxidatively-induced reductive elimination pathway on rhodium(III) in an electrocatalytic regime (Scheme

1.25g).^[111] Recently, an efficient electrooxidative rhodium-catalyzed alkyne annulation *via* C–H/O–H activations was realized using electricity as the sole oxidant, featuring ample substrate scope and high site-selectivities (Scheme 1.25i,j).^[112]



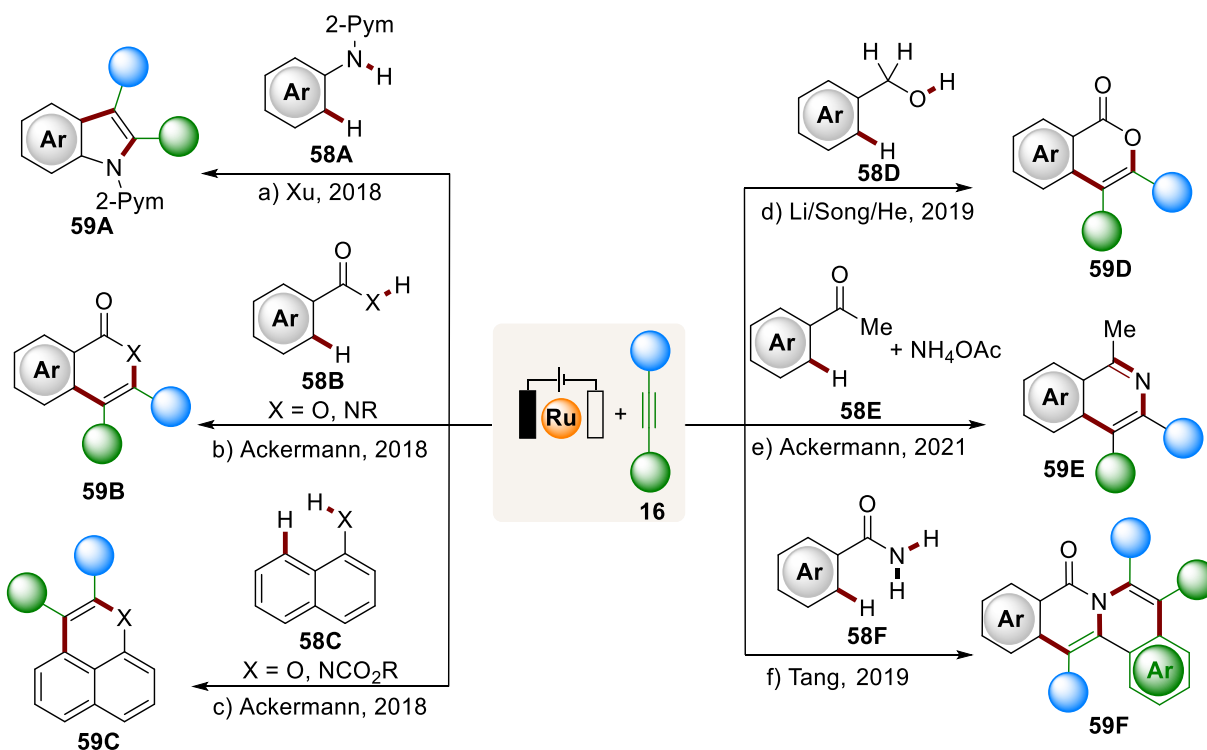
Scheme 1.25. Rhoda-electrooxidative C–H activations.

In 2021, the Ackermann group demonstrated a rhodaelectro-catalyzed C–H activation of indole **56D** with alkydicyclopropanes (ACPs) for the chemo-selective assembly of cyclopropanes or dienes. This unique strategy allowed for the control of selectivity within different mechanistic pathways by either β –H or β –C elimination (Scheme 1.25d).^[113] Moreover, electrocatalyzed arene C–H oxygenation using bimetallic rhodium complex by weakly O-coordinating amides and

ketones **56E** were reported by Ackermann (Scheme 1.25e).^[114] On a different note, a rhodium-catalyzed electrochemical phosphorylation of 2-phenylpyridine **56K** was also reported by Xu and coworkers (Scheme 1.25k).^[115]

1.5.3 Ruthenalectro-Oxidative C–H Activation

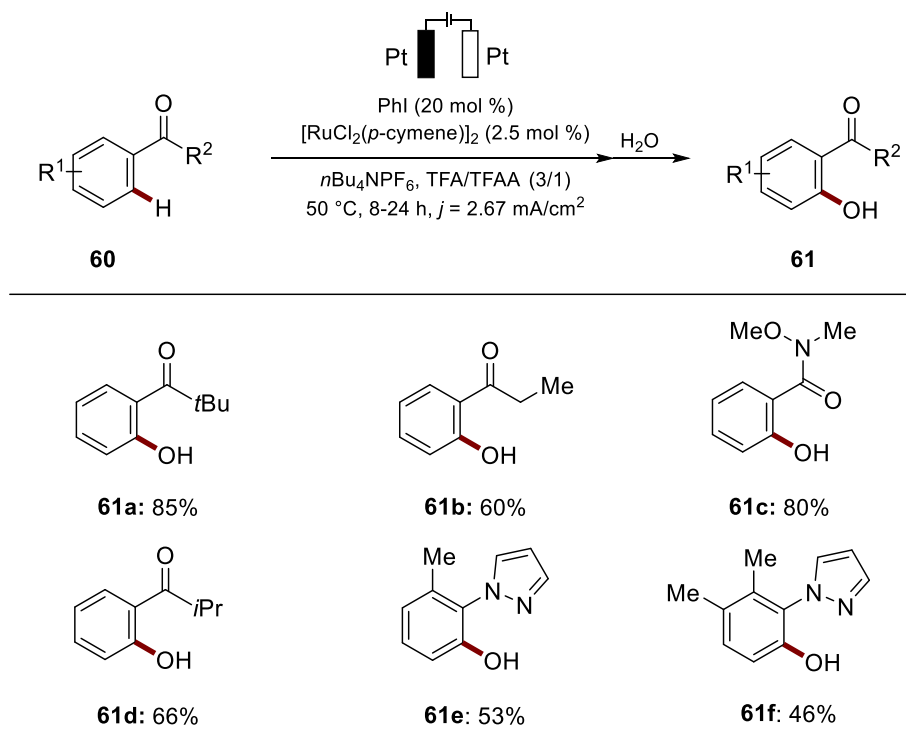
In 2018, Xu and Ackermann^[116] (Scheme 1.26a-b) independently reported ruthenalectrooxidative C–H alkyne annulations with aniline derivatives **58A** and weakly O-coordinating benzoic acid **58B**, leading to the cost-effective preparation of indole derivatives **59A** and isocoumarins **59B**, respectively. Subsequently, naphthol, aromatic carbamates **58C**, benzylic alcohols **58D**, acetophenones **58E** and benzoylamides **58F** proved to be viable substrates for ruthenium-catalyzed dehydrogenative C–H/Het–H alkyne annulations (Scheme 1.26c-f).^[117]



Scheme 1.26. Ruthenalectrooxidative C–H/X–H annulation. (X = N, O).

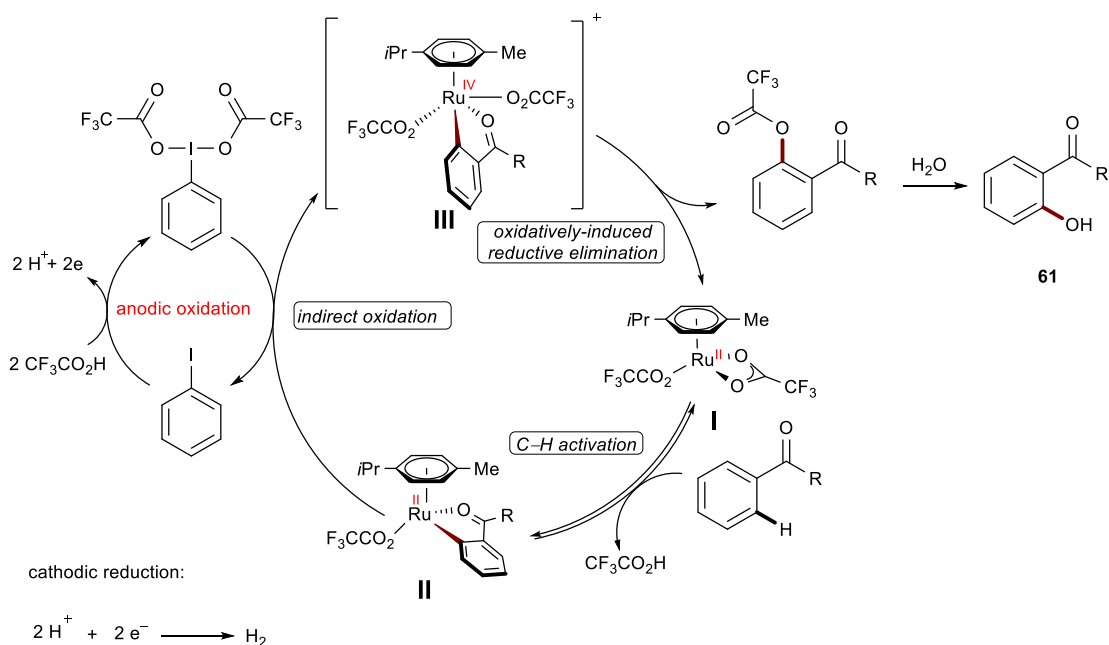
In 2020, Ackermann developed a novel electrochemical co-catalytic system for the C–H oxygenation of synthetically useful amides and ketones **60**, employing dual catalysis with electrogenerated hypervalent iodine(III) and ruthenium(II) complexes. Thus, catalytic amounts of iodoarenes and ruthenium(II) catalyst allowed for versatile C–H oxygenations with ample scope and high functional group tolerance **61a-61f** (Scheme 1.27).^[118]

Introduction



Scheme 1.27. Ruthenaelectro-catalyzed C–H activation of ketones, amides, and pyrazoles.

Based on the detailed mechanistic studies, a plausible catalytic cycle was proposed for the ioda/ruthena-electrocatalyzed C–H oxygenation ([Scheme 1.28](#)). The catalytic cycle is initiated by C–H activation on the amide with the ruthenium(II) catalyst. Then, the anodically generated iodine(III) reagent oxidizes the ruthenium(II) intermediate **II**, delivering ruthenium(IV) intermediate **III**, which then undergoes rapid reductive elimination and subsequent hydrolysis to furnish hydroxylation product **61** and regenerate the active catalyst **I**.



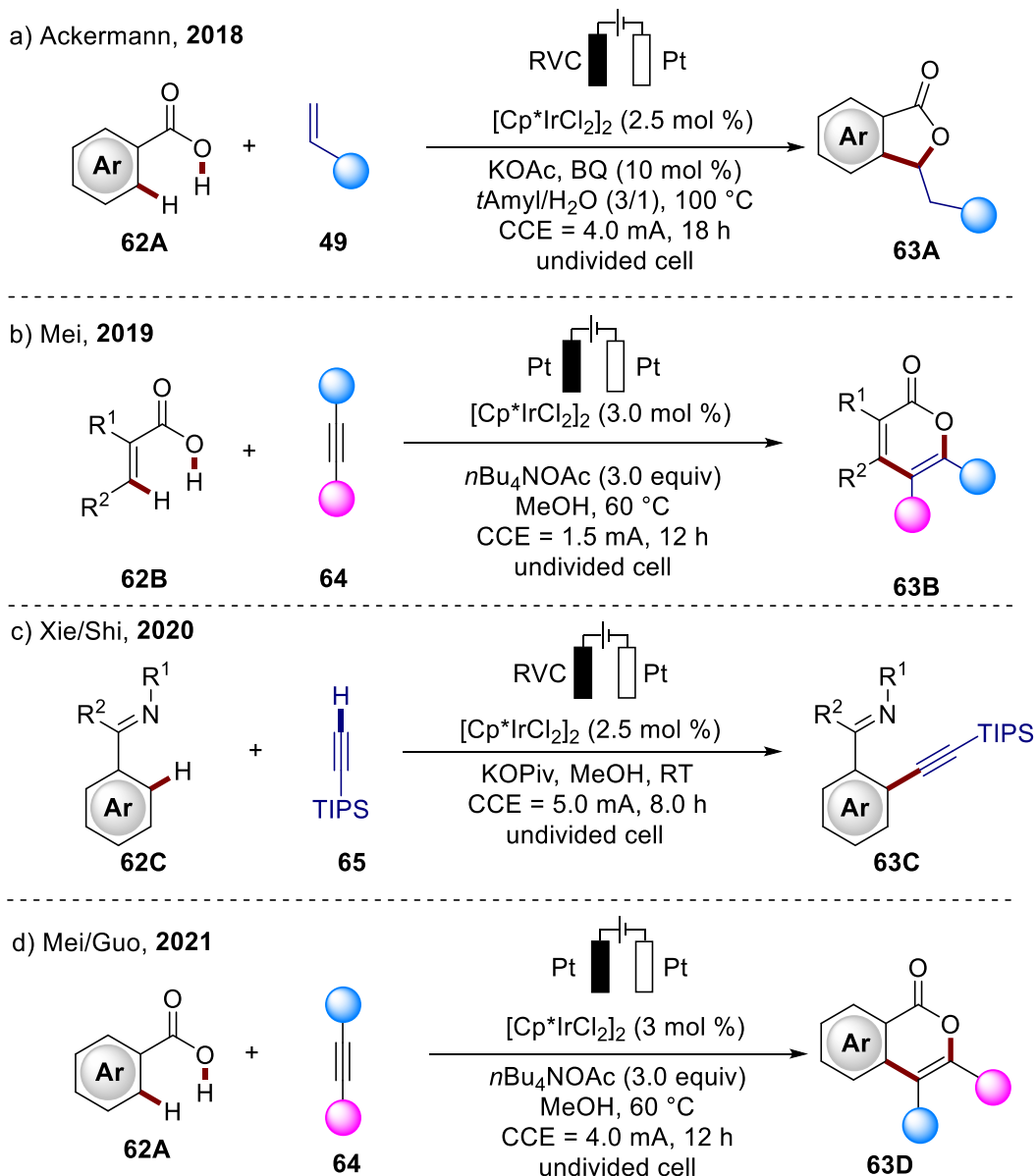
Scheme 1.28. Proposed catalytic cycle for the ruthenaelectro-catalyzed C–H oxygenation.

1.5.4 Iridaelectro-Oxidative C–H Activation

Besides ruthenium and rhodium catalysts, 5d transition metal iridium complexes have also been proven as effective catalysts in C–H functionalizations.^[119] While the oxidative reaction in this research arena was largely dominated by chemical oxidants, Ackermann made a pioneering contribution to the electrooxidative iridium-catalyzed C–H activation with weak O-coordinating benzoic acids **62A** (Scheme 1.29a).^[120] These C–H transformations using *p*-benzoquinone (BQ) as redox mediator presented a high functional-group tolerance, delivering a series of 5-membered heterocycles **63A**. Very recently, the Mei and Guo groups independently reported this type of electrochemical annulation with alkynes by iridium catalysis (Scheme 1.29d).^[121]

In 2019, Mei reported the irida-electrochemical vinylic C–H alkyne annulation of acrylic acids **62B** with alkynes, affording α -pyrones **63B** with good to excellent yields. In this case, preliminary mechanistic studies show that the anodic oxidation was crucial for releasing the product **63B** and regeneration of the active iridium(III) catalyst (Scheme 1.29b).^[122]

In 2020, the Shi and Xie groups developed an electrochemical approach in promoting directed C–H alkylation with terminal alkyne **65** via iridium catalysis. Detailed mechanistic studies in terms of isolation of key iridium(III) intermediates and control experiments suggested an oxidatively-induced reductive elimination, giving the desired aromatic alkynes **63C** in good yields without the addition of external oxidants (Scheme 1.29c).^[123]



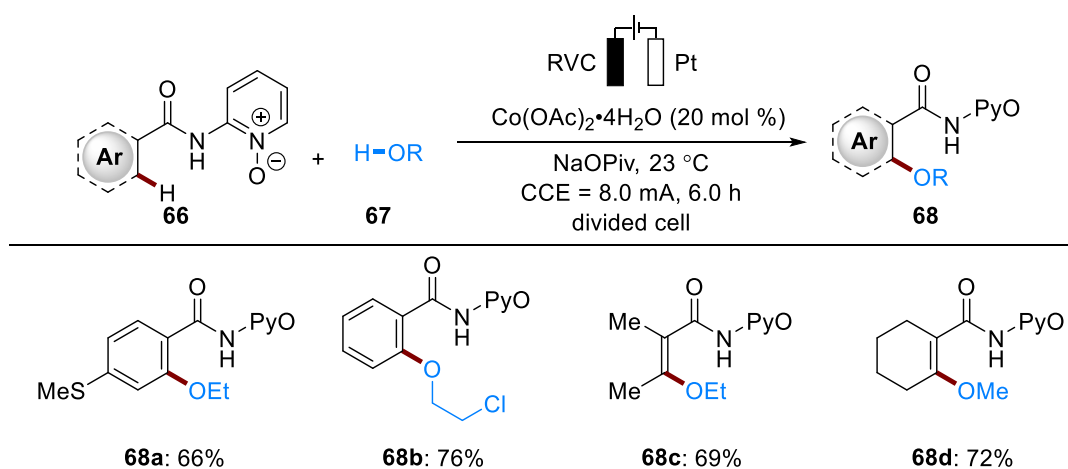
Scheme 1.29. Irida-electrooxidative C–H/O–H annulation.

1.5.5 Cobaltaelectro-Oxidative C–H Activation

The merger of C–H activation and electrochemistry set the stage to establish new reactivities with high levels of resource economy. Despite indisputable advances in electrocatalytic organometallic C–H activations with the precious 4d and 5d transition metals, the development of less toxic, cost-effective and the sustainable nature of Earth-abundant 3d metals in the electrosynthesis is a more environmentally-benign and economically-attractive alternative.

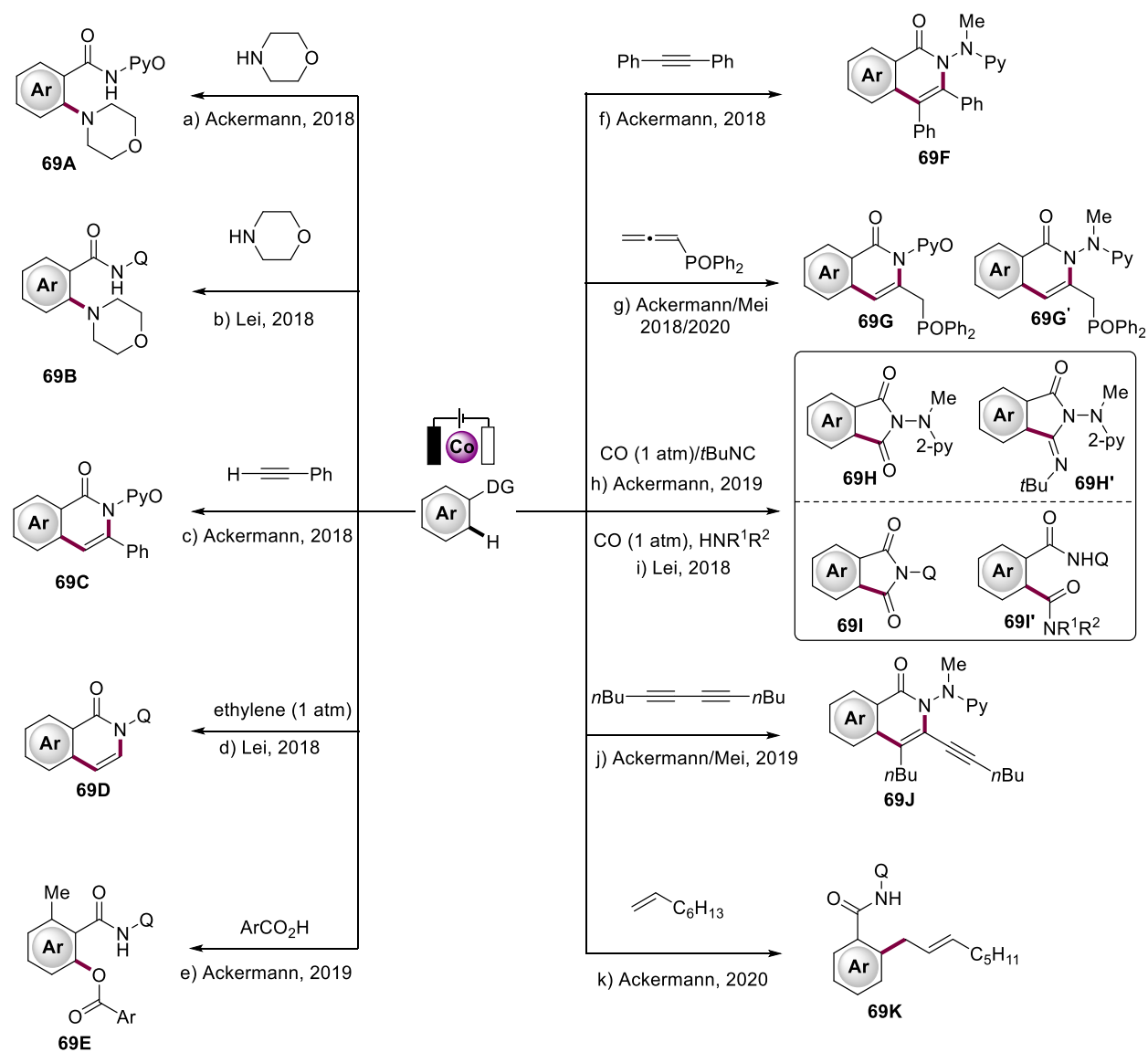
In 2017, the Ackermann group reported the first 3d metallaelectro-catalysis for C–H activation

with cobalt catalysts. This proof of concept study realized the direct C–H oxygenation of aryl and alkenyl amides **66** with inexpensive and Earth-abundant $\text{Co}(\text{OAc})_2 \cdot 4\text{H}_2\text{O}$ as the catalyst (Scheme 1.30).^[124] Based on detailed experimental studies, including the full characterization of key cyclometalated intermediates of cobalt-electrocatalyzed C–H activation, Ackermann proposed a plausible reaction pathway by involving a Co(III/IV/II) manifold.^[125]



Scheme 1.30. Cobalta-electrooxidative aryl and vinylic C–H oxygenation.

The cobalt-electrocatalyzed C–H activation was not limited to C–O bond formations. Thus, Ackermann and Lei established an intermolecular C–H amination protocol under mild reaction conditions with different directing groups (*N,O*- or *N,N*-coordinating auxiliaries) for the C–Het formation (Scheme 1.31a,b).^[126] Thereafter, Ackermann described a cobalt-catalyzed C–O bond formation for the electrochemically promoted C–H acyloxylations (Scheme 1.31e).^[127] Moreover, cobalt-electrocatalysis was extremely effective for the C–H/*N*–H annulation of arene and olefin derivatives with alkynes,^[128] alkenes,^[129] allenes,^[130] carbon monoxide or isocyanides^[131] to generate biorelevant heterocycles (Scheme 1.31c,d,f,j). More recently, the robust and versatile cobalt catalysis also enabled the electrochemical C–H allylation with non-activated alkenes in the biomass-derived solvent γ -valerolactone, generating allylated benzamides with high levels of functional group tolerance and regioselectivity (Scheme 1.31k).^[132]



Scheme 1.31. Cobalt-electrooxidative C–H activation.

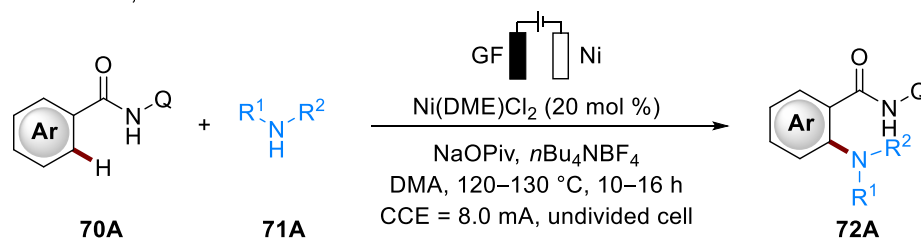
1.5.6 Nickellaelectro-Oxidative C–H Activation

Regarding its Earth-abundance, economical reliability and reactivities, nickel is often considered to be a potential alternative to expensive palladium catalysts. For this reason, a plethora of C–H activations have been achieved by utilizing nickel catalysis.^[133] Despite this indisputable progress, nickella-electrochemical C–H activation remained elusive until recently.

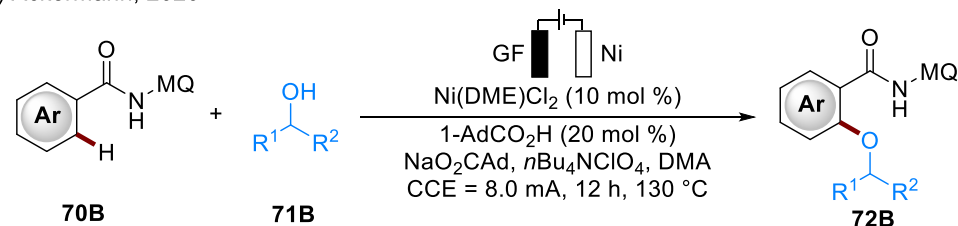
In 2018, the Ackermann group reported the first example of nickella-electrooxidative C–H aminations with ample scope and high levels of chemo- and position-selectivity (Scheme 1.32a).^[134] In contrast to previous metal-catalyzed electrochemical C–H activations, this nickel

electrosynthesis proved particularly potent in the C–H amination **72A** of electron-deficient arenes **70A**. Afterwards, the same group developed nickella-electrocatalyzed alkoxylation^[135] **72B** with challenging secondary alcohols **71B** and phosphorylations **72C** (Scheme 1.32b,c).^[136] Detailed mechanistic studies provided strong support for a nickel(III/IV/II) manifold for these transformations.

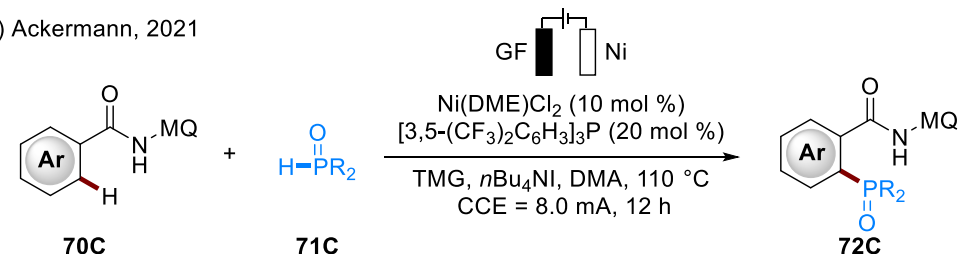
a) Ackermann, 2018



b) Ackermann, 2020



c) Ackermann, 2021



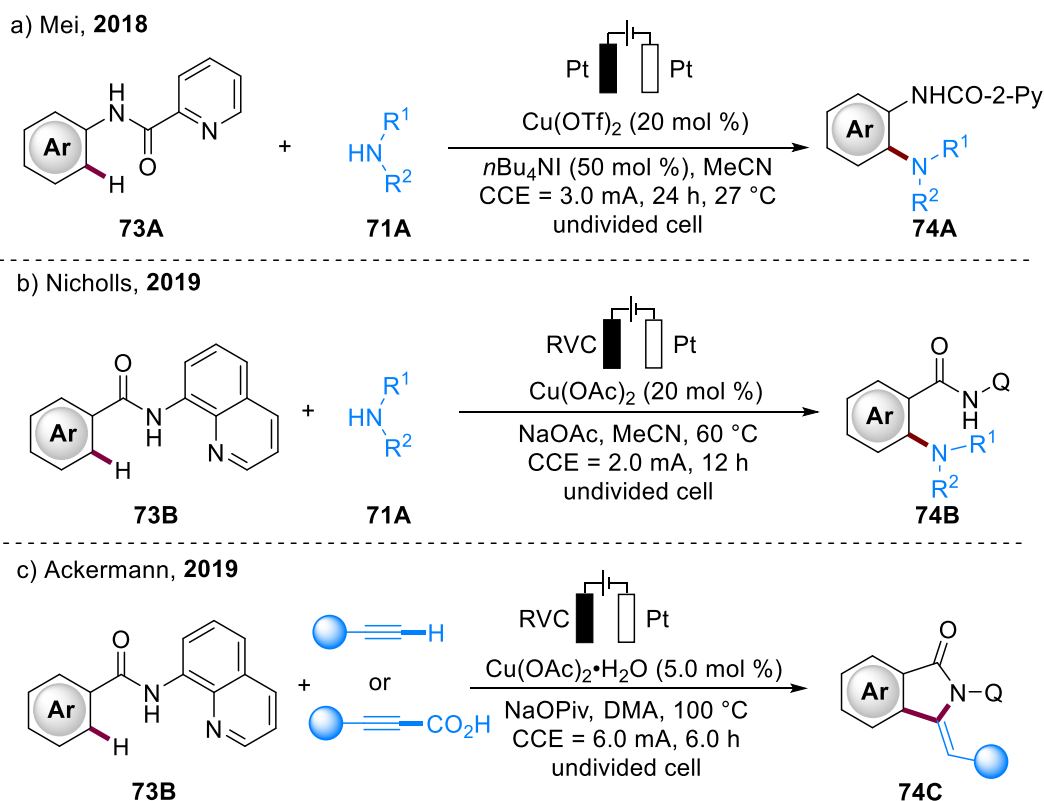
Scheme 1.32. Nickella-electrooxidative C–H aminations.

1.5.7 Cupraelectro-Oxidative C–H Activation

Recently, the Mei group successfully highlighted the efficiency of copper catalysis^[137] in electrochemical C–H functionalizations (Scheme 1.33a).^[138] Here, they employed catalytic amounts of $\text{Cu}(\text{OTf})_2$ and $n\text{-Bu}_4\text{NI}$ as the redox mediator to facilitate the *ortho*-selective C–H amination of aryl amines **73A** bearing the picolinamide (PA) directing group. The detailed experimental studies suggested a single electron transfer (SET) and a high valent copper(III) species to be involved in the reaction mechanism. In a subsequent report, a redox mediator-free condition was applied by Nicholls for the cupraelectro-oxidative C–H amination of benzamides

73B with AQ as a directing group (Scheme 1.33b).^[139] The synthetic utility of this protocol was well explored for various amines containing active pharmaceutical ingredients.

The copper electrocatalysis was not restricted to C–H aminations. Indeed, the Ackermann group revealed a first example of cupraelectro-catalyzed C–H/N–H alkyne annulation with electricity as the terminal oxidant to provide the bioactive five-membered isoindolones **74C** in both a dehydrogenative and decarboxylative manner (Scheme 1.33c).^[140]

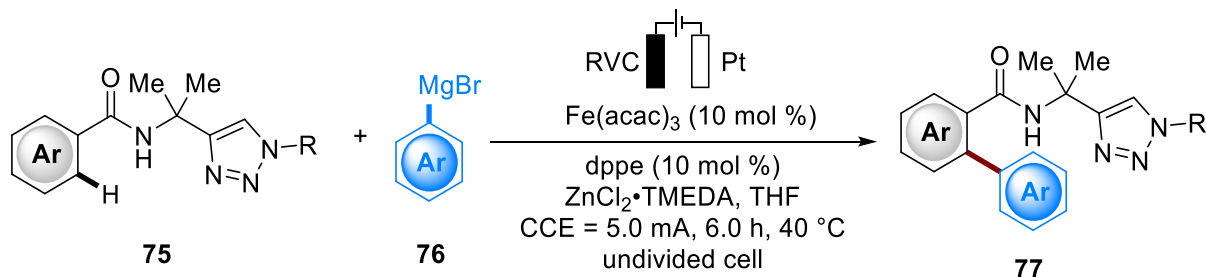


Scheme 1.33. Cupraelectro-oxidative C–H activation.

1.5.8 Ferraelectro-Oxidative C–H Activation

Due to growing interest in chemical utilization of less toxic, natural Earth-abundance and cost-effective metal catalysts, iron catalysis has become a rapidly increasing research area for sustainable molecular syntheses *via* C–H activation.^[141] Despite indisputable advances, the iron-catalyzed oxidative C–H transformations strongly relied on superstoichiometric amounts of cost-intensive 1,2-dichloroisobutane (DCIB) as the sacrificial oxidant, thereby generating stoichiometric amounts of waste. To overcome this major restriction, the Ackermann group

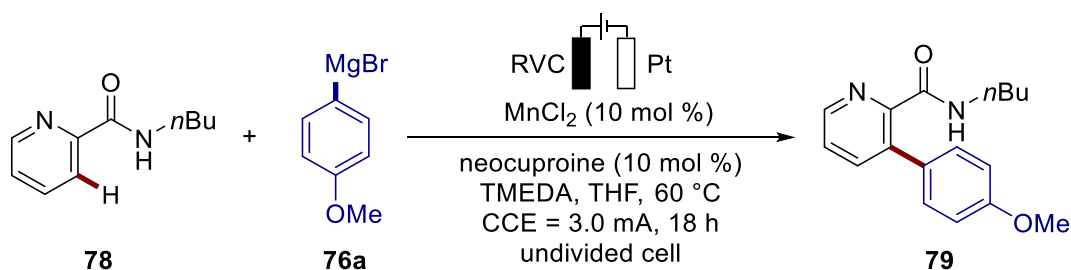
disclosed the unprecedented ferraelectrocatalytic strategy for oxidative C–H arylation with Grignard reagent **76** for the synthesis of biaryls **77** (Scheme 1.34).^[142] Furthermore, detailed mechanistic studies in terms of experiments and DFT calculations suggested an electrooxidative iron(II/III/I) manifold.^[142-143]



Scheme 1.34. Ferra-electrooxidative C–H activation.

1.5.9 Manganoelectro-Oxidative C–H Activation

The sustainable electrochemical organometallic C–H activation was further investigated in the presence of non-toxic and readily accessible manganese catalysts. As a proof of concept, Ackermann showcased the potential of MnCl_2 in combination with electrocatalysis for the transformative C–H arylation of picolinic acids in the assistance of zinc salt (Scheme 1.35).^[142]

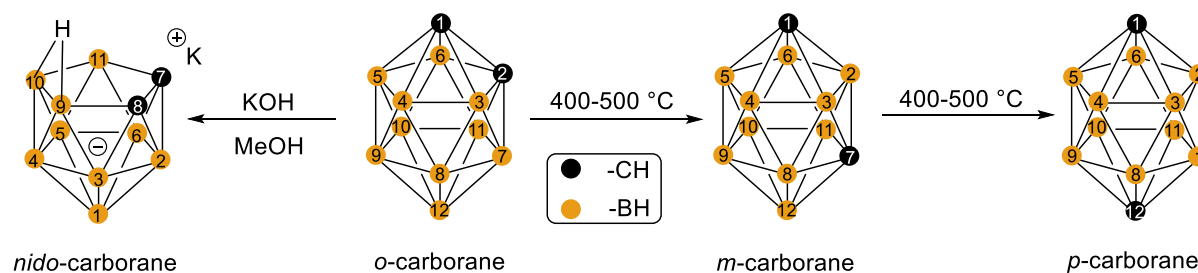


Scheme 1.35. Manganoelectro-oxidative C–H arylation.

1.6 Transition Metal Catalyzed B–H Cage Activation of *o*-Carborane

Carboranes, polyhedral boron-carbon molecular clusters, have one or more of the BH vertices replaced by CH units (Scheme 1.36).^[144] Among them, icosahedral 1,2-dicarba-*closo*-dodecaborane (*o*- $\text{C}_2\text{B}_{10}\text{H}_{12}$), which was first reported in 1963,^[145] has attracted significant attention because of its high symmetry, remarkable stability and subsequent commercial availability. This cluster comprises ten boron atoms and two neighboring carbon atoms, and each atom is hexacoordinated, featuring 26 delocalized electrons over the entire structure of the cluster.^[146] Over the past decades, *o*-carboranes have been extensively studied and have found

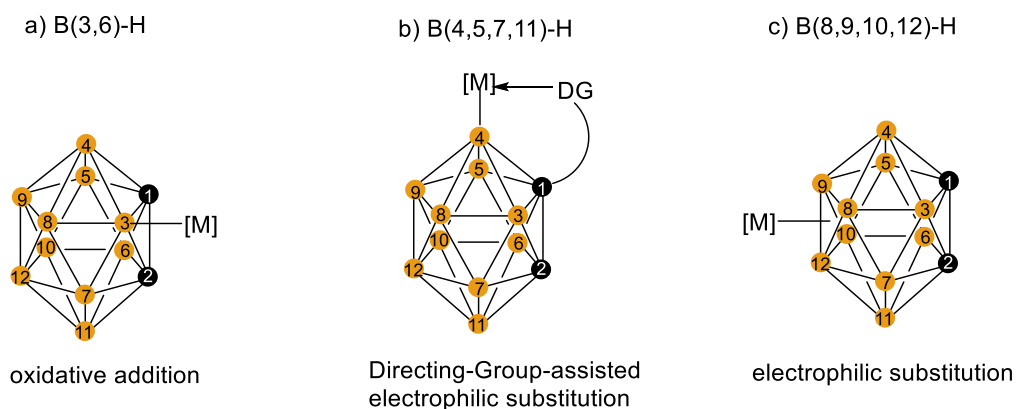
wide applications as useful functional building blocks in supramolecular design or nanomaterials,^[147] in medicine as boron neutron capture therapy (BNCT) agents or pharmacophores,^[148] in organometallic/coordination chemistry^[149] and more. Owing to the strongly electron-withdrawing character of the *o*-carborane unit toward carbon substituents, the C–H bonds are weakly acidic in this cage ($pK_a = 22.0$)^[150] and can be deprotonated with strong bases, such as alkyllithium or Grignard reagents. Thus, a larger number of carbon-substituted *o*-carboranes have been prepared by the reaction of negatively charged carbon atoms with electrophilic reagents (alkylhalides, carbonyl derivatives, and chlorosilanes). In sharp contrast, selective functionalization of chemically very similar ten B–H vertices in *o*-carboranes is very challenging and less explored.^[151]



Scheme 1.36. Molecular *nido*-carborane and geometry of *o*-, *m*-, *p*-dicarba-*closo*-dodecarboranes, IUPAC numbering of the cage atoms and their chemical transformations.

Generally, according to differences in electronegativity and the distance between boron and carbon atoms, the 10 B–H bonds of *o*-carboranes have different electron density, leading to the electrophilic substitution reactions of carborane derivatives with the reaction rate $B(9,12)\text{--}H > B(8,10)\text{--}H > B(4,5,7,11)\text{--}H > B(3,6)\text{--}H$, which also corresponds to the calculated charge distribution on the cage.^[152] As charge differences are very small, achieving high regioselectivity in these substitution reactions is usually problematic.

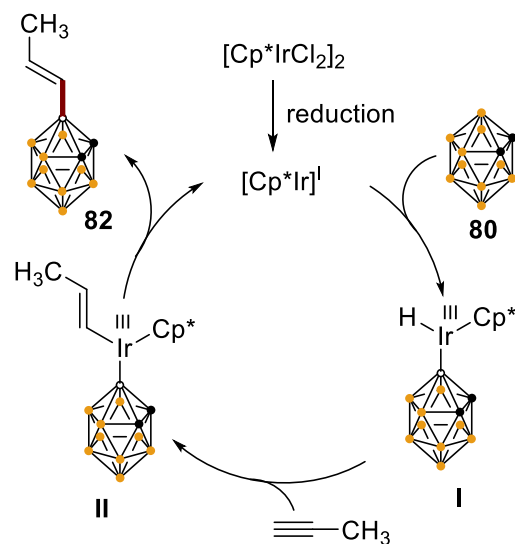
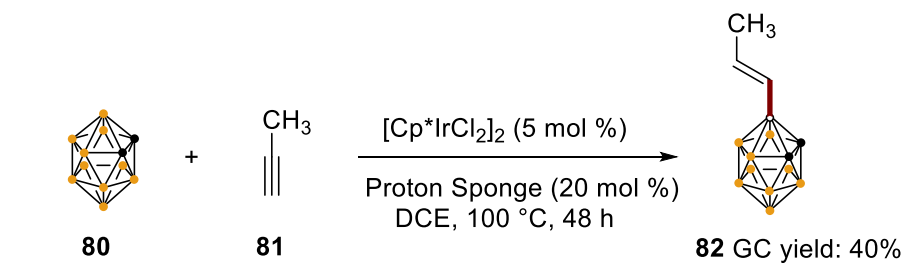
A general strategy for transition metal-catalyzed selective cage B–H functionalization of *o*-carboranes involves three principles:^[153] (1) electron-rich transition metal catalysts preferably functionalize the most electron-deficient B(3,6)–H bonds, which are bonded to both cage carbons; (2) electrophilic transition metal catalysts would be appropriate for the functionalization of electron-rich B(8,9,10,12)–H bonds (not bonded to any cage carbons); and (3) employing directing group with electrophilic transition metal catalysts is essential for B(4,5,7,11)–H functionalization proximal to only one cage carbon (Scheme 1.37).



Scheme 1.37. General strategy for catalytic selective cage B–H functionalization.

1.6.1 Transition Metal-Catalyzed Cage B(3,6)–H Functionalization

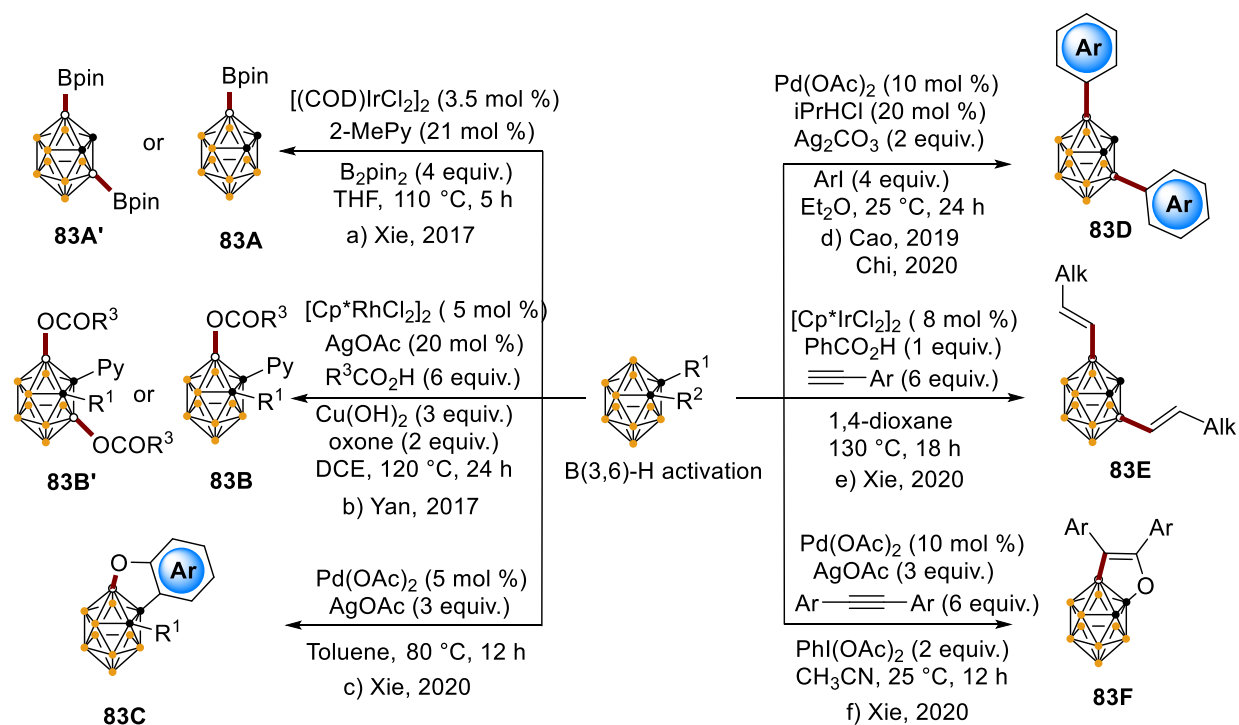
In 1977, a transition metal-catalyzed cage B(3,6)–H deuteration of *o*-carborane **80** with D₂ was described by Hawthorne.^[154] In 1988, Sneddon developed [Cp*IrCl₂]₂/Proton Sponge catalyst system for the selective cage B(3)–H propenylation of *o*-carborane with propyne **81** (Scheme 1.38).^[155] A plausible catalytic cycle is proposed in Scheme 1.38, which commences with a reduction of complex [Cp*IrCl₂]₂ to the active iridium(I) species under the reaction conditions. Subsequently, oxidative addition of the most electron-deficient cage B(3)–H with the iridium(I) species generates the B(3)–Ir intermediate **I**. Thereafter, propyne **81** insertion followed by reductive elimination affords the desired product **82** and regenerates the active iridium(I) catalyst. Although only propyne was examined with low reaction efficacy, this example indicated the feasibility of transition metal-catalyzed selective cage B–H functionalization of *o*-carboranes.



Proton Sponge: 1,8-bis(dimethylamino)naphthalene

Scheme 1.38. Iridium-catalyzed cage B(3)-propenylation of *o*-carborane.

In 2017, the Xie group disclosed an efficient iridium-catalyzed selective cage B(3,6)-diborylation of *o*-carboranes with B_2pin_2 as coupling partner in THF at 110 °C for 5 h, affording B(3,6)-diborylated *o*-carboranes **83A'** in high yields (Scheme 1.39a).^[156] Later, a pyridyl-assisted rhodium-catalyzed selective B(3)-acyloxylation of *o*-carboranes and a palladium-catalyzed intramolecular B–H/O–H dehydrogenative coupling reaction were reported by Yan^[157] and Xie,^[158] respectively (Scheme 1.39b,c). In addition, Pd/NHC (NHC = *N*-heterocyclic carbene) catalyzed cage B(3,6)-arylation of *o*-carboranes was achieved by Cao (Scheme 1.39d).^[159] Concurrently, another phosphine-directed rhodium-catalyzed B(3,6)-diarylation of 1- PAR_2 -*o*-carboranes with aryl bromides was reported by Chi,^[160] offering a series of B(3,6)-diarylated *o*-carboranes **83D** (Scheme 1.39d). Inspired by the Sneddon's work,^[155] Xie recently described iridium-catalyzed cage B(3,6)-alkenylation of *o*-carboranes (Scheme 1.39e).^[161] A plausible mechanism involving a Ir(III/V/III) pathway is proposed for this cage B(3,6)-alkenylation. Thereafter, the same group revealed a palladium-catalyzed B(3)-oxidative annulation of 1-hydroxy-*o*-carborane with internal alkynes, leading to facile synthesis of a class of *o*-carborane-fused oxaboroles **83F** in moderate yields (Scheme 1.39f).^[162]



Scheme 1.39. Cage B(3,6)-H functionalization of *o*-carboranes.

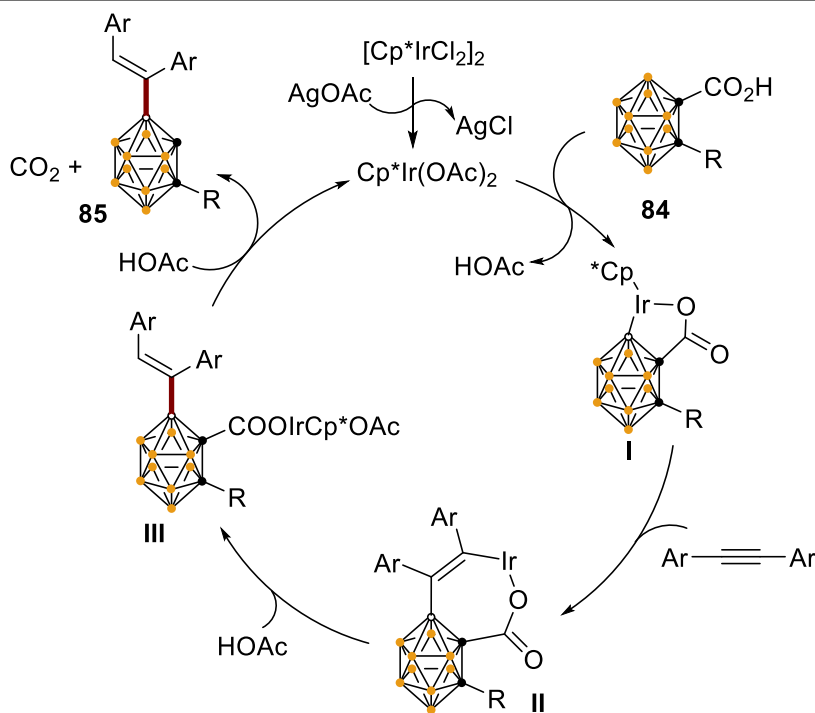
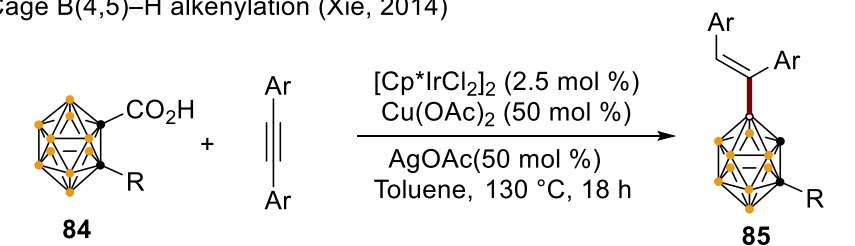
1.6.2 Transition Metal-Catalyzed Cage B(4,5,7,11)-H Functionalization

A general strategy to realize the cage B(4,5,7,11)-H functionalization is introduction of the directing group on one of the cage carbon vertices.

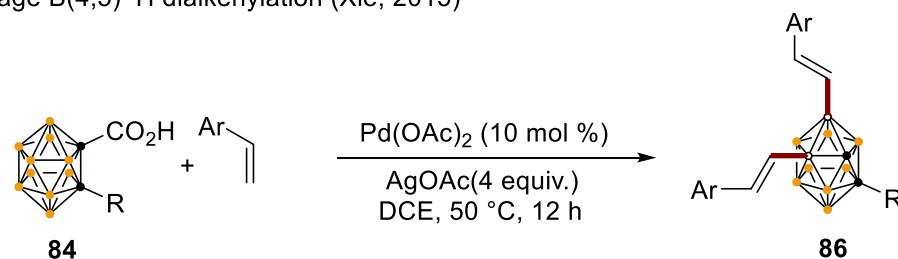
In 2014, Xie disclosed an irridium-catalyzed B(4)-alkenylation of *o*-carboranes by employing a carboxylic acid as the traceless directing group at the cage carbon vertex, generating a range of B(4)-alkenylated *o*-carboranes **85** in high yield with excellent regioselectivity.^[163] A plausible catalytic cycle is proposed involving a cage B(4)-H activation, followed by alkyne insertion, protonation and decarboxylation give the final products **85** (Scheme 1.40a). Later, the same group extended this research to B(4,5)-dialkenylation through palladium catalysis (Scheme 1.40b).^[164] Applying a similar methodology, the Lu group synthesized a series of B(4)- and B(4,5)-substituted *o*-carboranes (**87A** and **87A'**) containing α,β -unsaturated carbonyls in moderate to good yields by employing Pd(TFA) as the catalyst (Scheme 1.40c).^[165]

Introduction

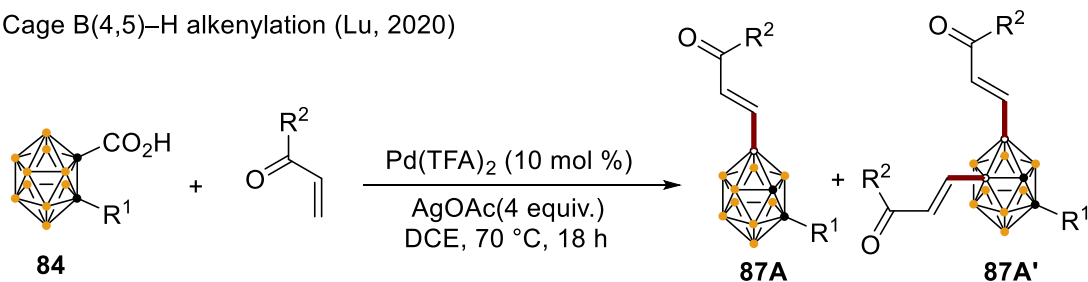
a) Cage B(4,5)-H alkenylation (Xie, 2014)



b) Cage B(4,5)-H dialkenylation (Xie, 2015)



c) Cage B(4,5)-H alkenylation (Lu, 2020)

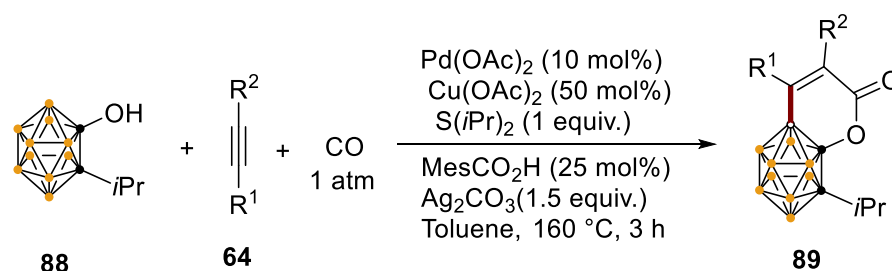


Scheme 1.40. Cage B(4,5)-H alkenylation of α -carboranes.

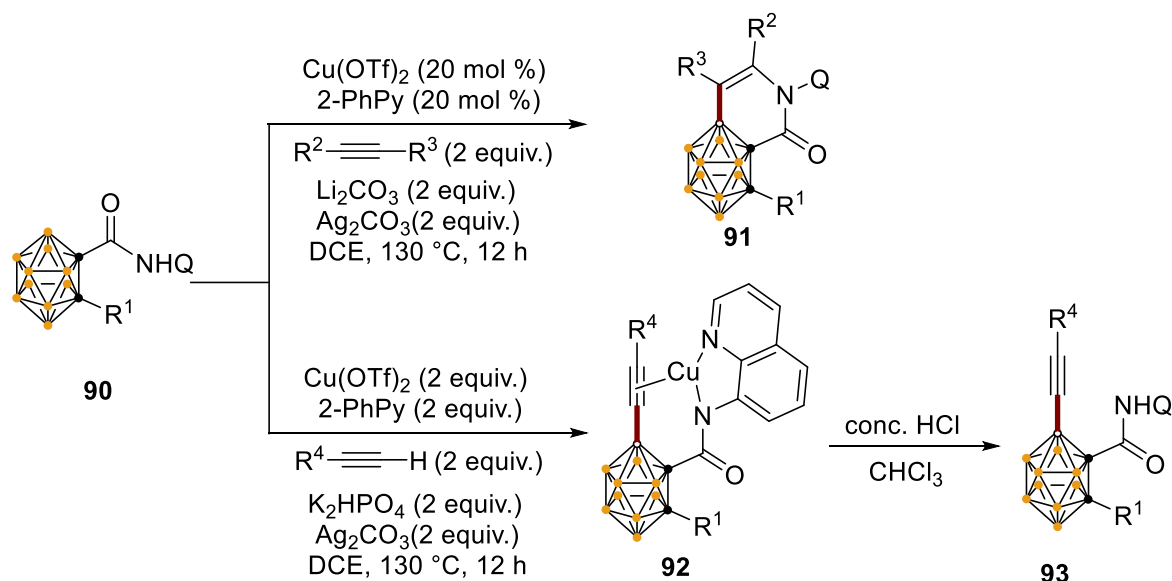
In 2020, the Xie group revealed an efficient palladium-catalyzed three-component carbonylative

annulation of 1-hydroxyl-*o*-carboranes **88** with internal alkynes **64** and CO (Scheme 1.41a).^[166] This protocol provided a new class of C,B-substituted carborano-coumarin derivatives **89** with potential applications to pharmaceuticals in moderate to good yields. Although most selective cage B–H functionalizations of *o*-carboranes were catalyzed by noble transition metal catalysts, Xie established the unprecedented copper-catalyzed regioselective cage B–H alkyne annulation of carboranyl amides **90** with internal alkynes in the presence of a bidentate directing group at the cage carbon position, affording previously inaccessible C,B-substituted *o*-carborane-fused-pyridone derivatives **91** (Scheme 1.41b).^[167] Likewise, terminal alkynes led to dehydrogenative B–H/C–H alkylation. The copper(I) complex **92** was isolated, which underwent protonation with concentrated hydrochloric acid to afford the B(4)-alkynylated compounds **93**.

a) Cage B(4)–H carbonylative annulation (Xie, 2020)



b) Cage B(4)–H alkyne annulation (Xie, 2019)

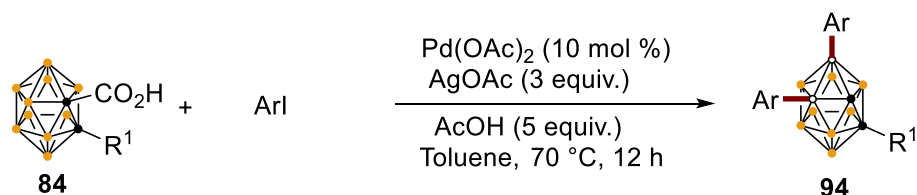


Scheme 1.41. Cage B(4)–H annulation of *o*-carboranes

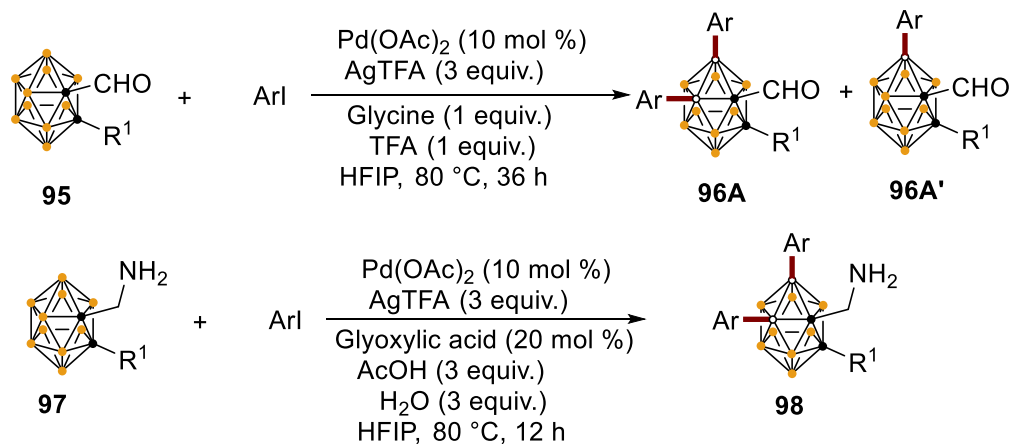
In 2016, palladium-catalyzed cage B(4,5)-diarylation was accomplished by the treatment of carboranyl carboxylic acids **84** with aryl iodides (Scheme 1.42a).^[168] Moreover, using glycine or

glyoxylic acid as a transient directing group for palladium-catalyzed B(4)-arylation or B(4,5)-diarylation of carboranyl aldehydes **95** or methylamines **97** was also reported by Yan (Scheme 1.42b).^[169] Meantime, with the assistance of an acyl amino directing group at the cage B(9) position **99**, palladium-catalyzed regioselective B(4)-arylation of *o*-carboranes with aryl boronic acids was achieved by Cao in 2018 (Scheme 1.42c).^[170] Importantly, a proof-of-principle study of palladium-catalyzed enantioselective intramolecular B–H arylation of *o*-carboranes **101** was first introduced by Xie in the presence of chiral phosphine ligand **L1** (Scheme 1.42d).^[171]

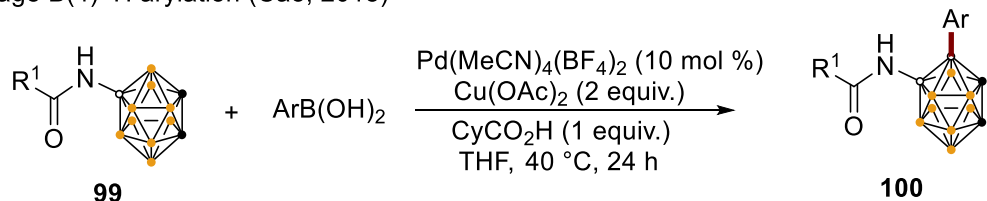
a) Cage B(4,5)–H diarylation (Xie, 2016)



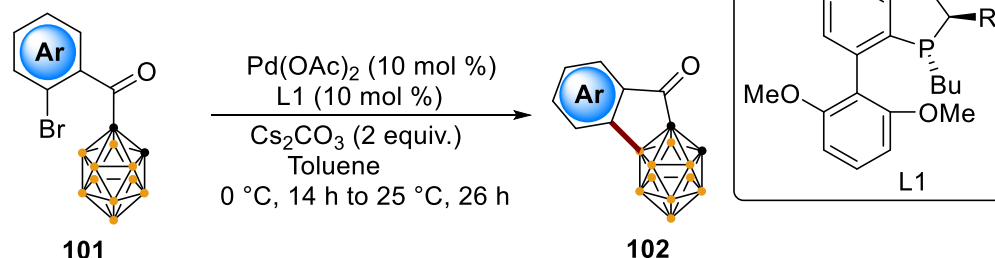
b) Cage B(4,5)–H arylation by transient DG (Yan, 2017/2018)



c) Cage B(4)–H arylation (Cao, 2018)

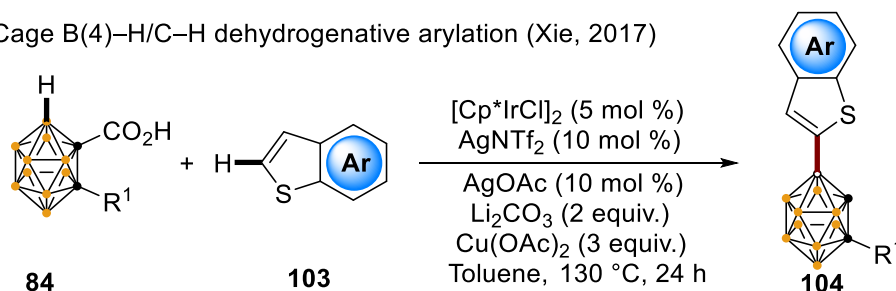


d) Cage B(4)–H enantioselective arylation (Xie, 2018)

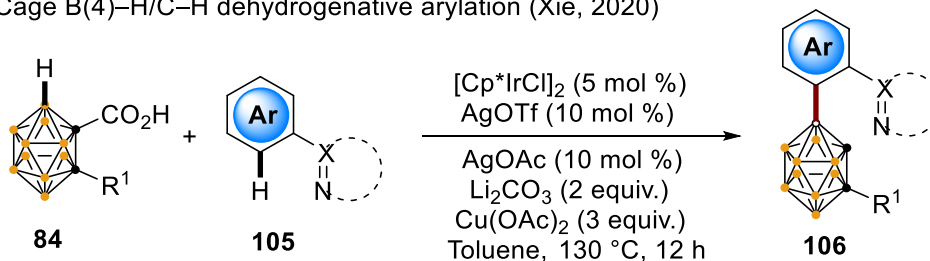
Scheme 1.42. Cage B(4,5)–H arylation of *o*-carboranes

In the aforementioned aryl coupling reactions, aryl iodides were employed. In 2017, another protocol with atom- and step-economical cross-dehydrogenative coupling of carboranyl carboxylic acids **84** with thiophenes was developed in the presence of an iridium catalyst, affording B(4)-thienylated *o*-carboranes **104** in moderate to high yields (Scheme 1.43a).^[172] Afterwards, this dehydrogenative coupling reaction of *o*-carboranes was extended to (hetero)aryls using a double directing groups strategy. In the presence of iridium(III) catalyst, carboranyl carboxylic acids **84** reacted with (hetero)arenes **105** to provide the corresponding B(4)-C(sp²) coupling products **106** in high yields (Scheme 1.43b).^[173]

a) Cage B(4)–H/C–H dehydrogenative arylation (Xie, 2017)



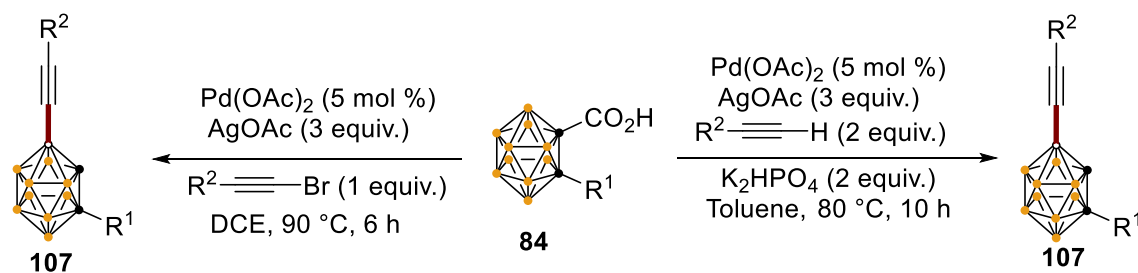
b) Cage B(4)–H/C–H dehydrogenative arylation (Xie, 2020)

Scheme 1.43. Cage B(4)–H/C–H dehydrogenative arylation of *o*-carboranes

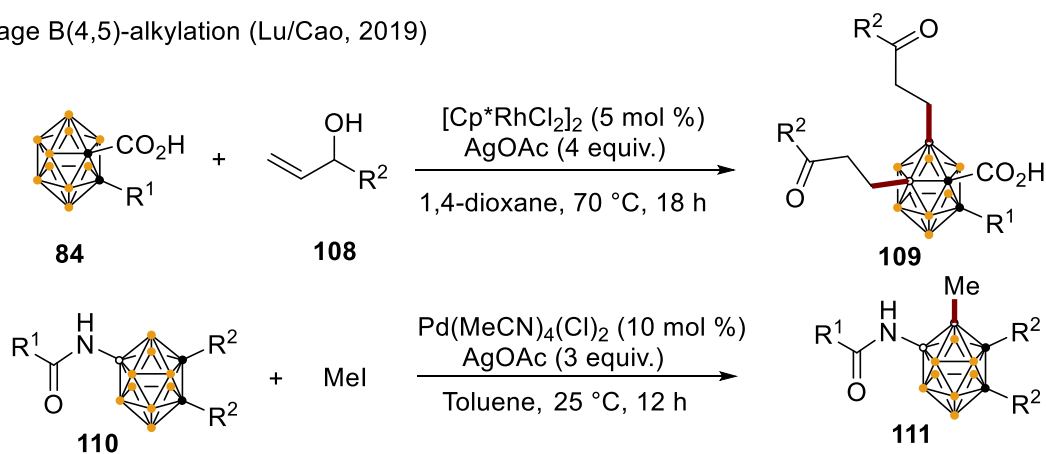
In 2016, two protocols for palladium-catalyzed regioselective cage B(4)-alkynylation of *o*-carboranes were established by treatment of carboranyl carboxylic acids **84** with 1 equivalent of alkynyl bromides or 2 equivalent of terminal alkynes in the presence of palladium catalyst, giving the B(4)-alkynylated *o*-carborane derivatives **107** in moderate to good yields (Scheme 1.44a).^[174]

A carboxylic acid directed rhodium-catalyzed B(4,5)-dialkylation of *o*-carboranes with allylic alcohols was described by Lu (Scheme 1.44b).^[175] This method was well compatible with various aryl- or alkyl-substituted allyl alcohols to provide the corresponding β -aryl or -alkyl ketone products **109** in high efficiency. In contrast, B(9)-acyl amino group directed palladium-catalyzed B(4)-methylation of *o*-carboranes with methyl iodide as coupling partner was also described for B(4)-alkylation of *o*-carboranes **111** (Scheme 1.44b).^[176] Furthermore, a carboranyl carboxylic acid-directed rhodium-catalyzed B(4)-hydroxylation with O₂ gas was disclosed by Xie, leading to a sequence of 4-OH-*o*-carboranes **112** in high yields with excellent regioselectivity (Scheme 1.44c).^[177]

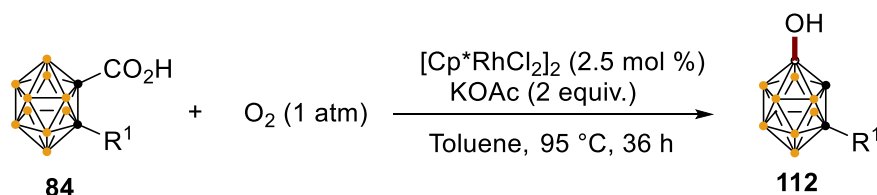
a) Cage B(4)-alkynylation (Xie, 2016)



b) Cage B(4,5)-alkylation (Lu/Cao, 2019)



c) Cage B(4,5)-oxygenation (Xie, 2016)

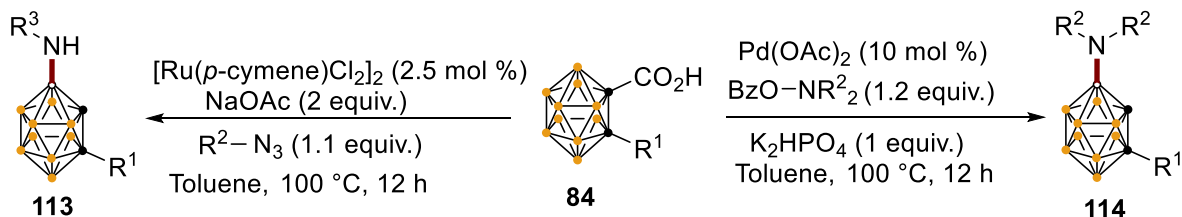


Scheme 1.44. Cage B(4,5)-alkynylation, alkylation, oxygenation of *o*-carboranes

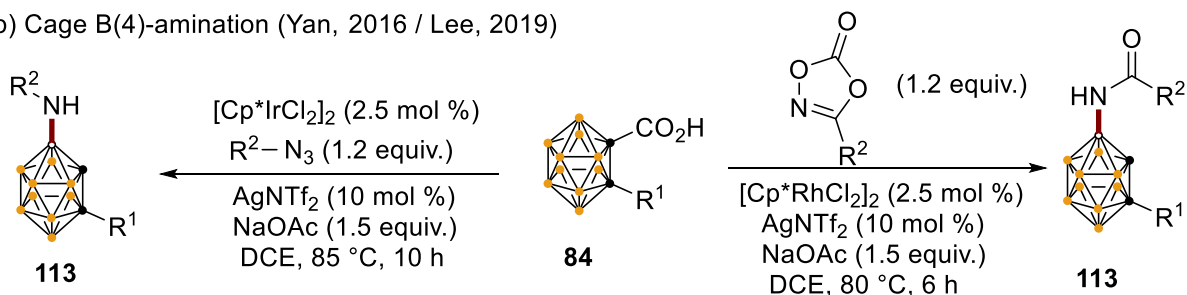
In 2016, palladium- and ruthenium-catalyzed B(4)-amination of carboranyl carboxylic acids **84** with *O*-benzoyl hydroxylamines and sulfonyl azides were realized, respectively, by Xie. This B–N

coupling reaction led to a series of tertiary carboranyl amines **114** and secondary carboranyl amines **113** with high functional group tolerance (Scheme 1.45a).^[178] Later, Yan reported an iridium-catalyzed B(4)-amination of carboranyl carboxylic acids **84** with organic azides and Lee disclosed a similar B(4)-amination by employing dioxazolones as the coupling partner and rhodium as the catalyst (Scheme 1.45b).^[179]

a) Cage B(4)-amination (Xie, 2016)



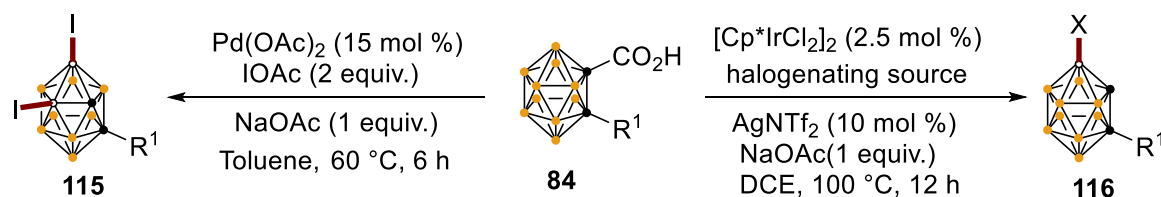
b) Cage B(4)-amination (Yan, 2016 / Lee, 2019)



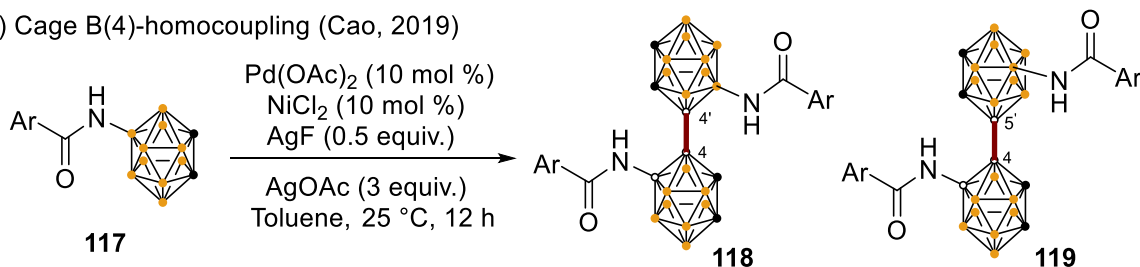
Scheme 1.45. Cage B(4,5)-amination of *o*-carboranes

Recently, Transition metal catalyzed B(4)-halogenation **116**, B(4,5)-diiodination **115**,^[180] B(4)-homocoupling (**118,119**)^[181] and B(4,5)-disulfenylation **121**^[182] of *o*-carboranes were reported by the Xie and Cao group, respectively. These protocols have a wide variety of functional group tolerance, offering a series of functionalized carboranes (Scheme 1.46).

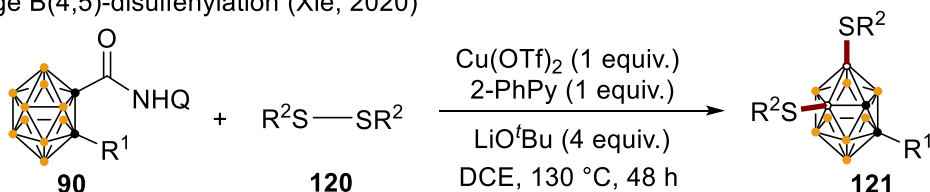
a) Cage B(4,5)-halogenation (Xie, 2017)



b) Cage B(4)-homocoupling (Cao, 2019)



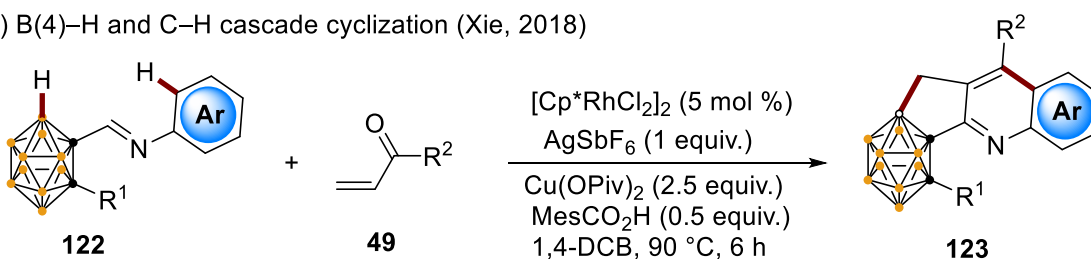
c) Cage B(4,5)-disulfenylation (Xie, 2020)



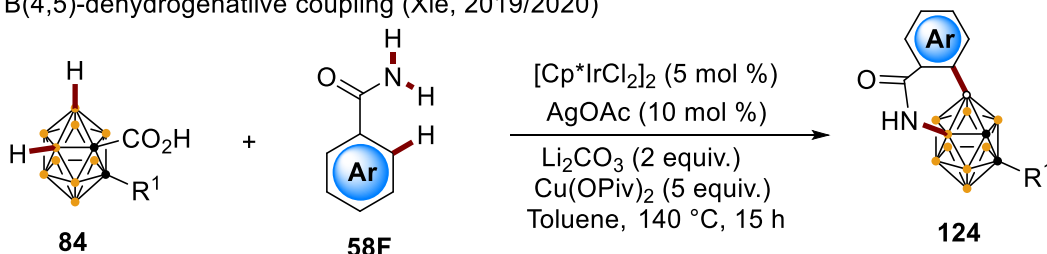
Scheme 1.46. Cage B(4,5)-halogenation, homocoupling and disulfenylation of *o*-carboranes

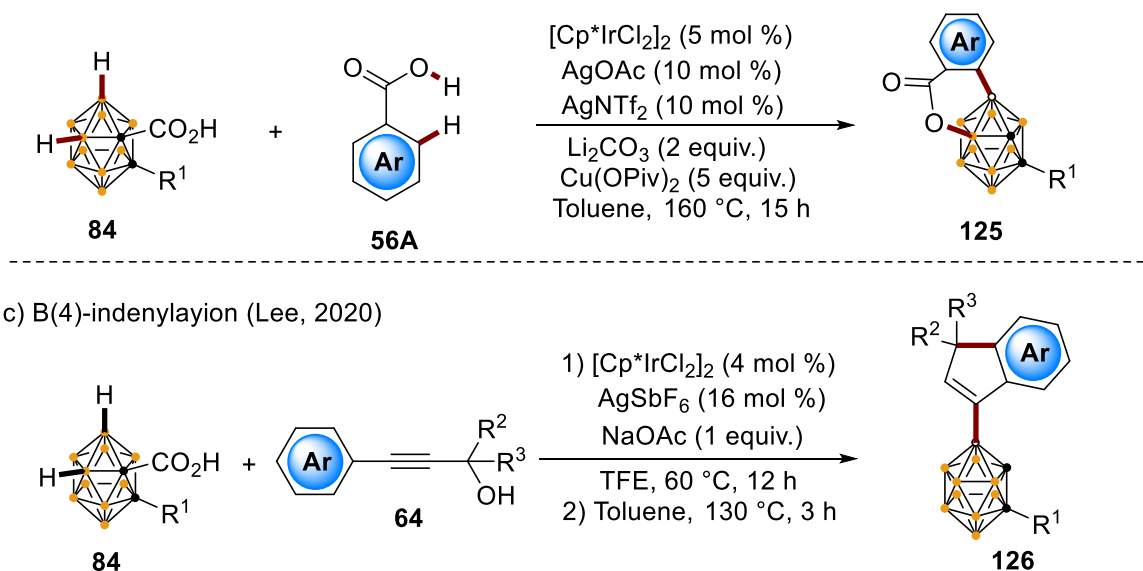
With respect to step-economy and bond-forming efficiency, synthetic methods merging multiple reaction steps into a simple one-pot process have attracted massive research interests. Thereby, a rhodium-catalyzed B(4)-H/C-H cascade cyclization of carboranyl *N*-arylimines **122** with vinyl ketones **49** was developed (Scheme 1.47a).^[183] Very recently, a proof-of-concept investigation of cascade cross-dehydrogenative coupling featuring two B-H, one C-H and one N-H bonds activation was also disclosed. Subsequently, the Xie group extended their studies to include the cascade cross-dehydrogenative coupling of carboranyl carboxylic acids **84** with benzoic acids **56A** (Scheme 1.47b).^[184] More recently, Lee reported an iridium-catalyzed cyclative indenylation of carboranyl carboxylic acids **84** with propargyl alcohols **64**, leading to previously unavailable B(4)-indenylated *o*-carboranes **126** in high yields (Scheme 1.47c).^[185]

a) B(4)-H and C-H cascade cyclization (Xie, 2018)



b) B(4,5)-dehydrogenative coupling (Xie, 2019/2020)



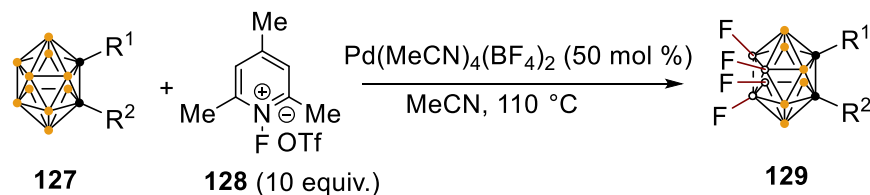


Scheme 1.47. Cage B(4,5)-cascade reaction of *o*-carboranes

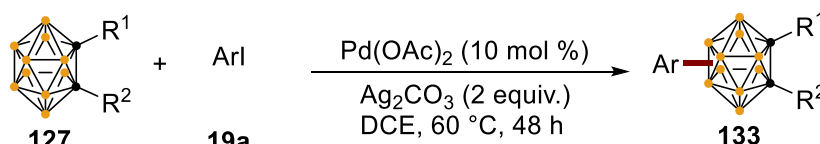
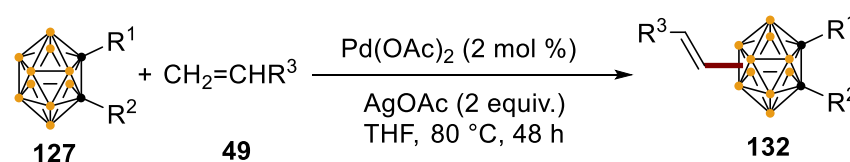
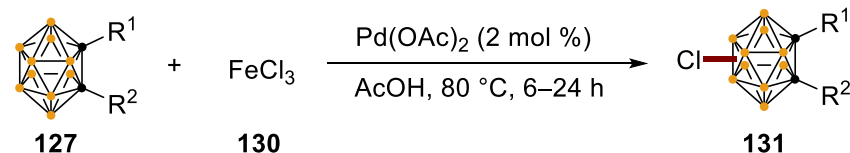
1.6.3 Transition Metal-Catalyzed Cage B(8,9,10,12)–H Functionalization

Owing to the small differences in electron density at the vertices B(8,9,10,12)–H, palladium-catalyzed tetrafluorination **129**^[186] and tetraacetoxylation **137**^[187] of *o*-carboranes were described by Xie and Cao, respectively (Scheme 1.48a,d). Since then, B(8/9)-chlorination **131**,^[188] -alkenylation **132**,^[189] and -arylation **133**^[190] were efficiently achieved with the palladium as the catalyst by the Cao group (Scheme 1.48b). A breakthrough on regioselective B(8)-arylation of *o*-carboranes **134** was disclosed under the assistance of an acyl amino group at B(3) position (Scheme 1.48c).^[191]

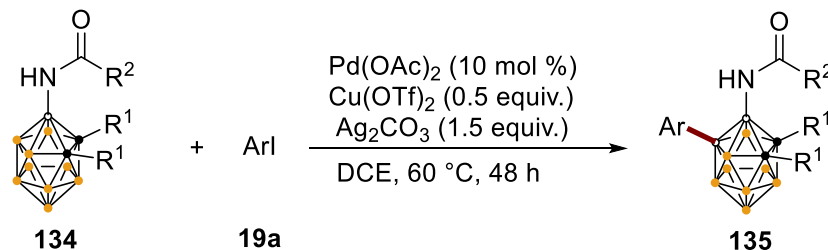
a) Cage B(8,9,10,12)-tetrafluorination (Xie, 2013)



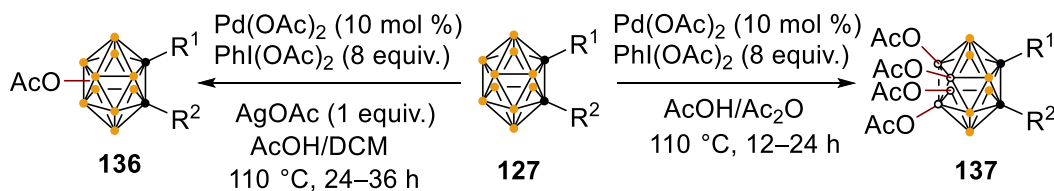
b) Cage B(8/9)-chlorination, alkenylation and arylation (Cao, 2017, 2015, 2015)



c) Cage B(8)-arylation (Xie, 2019)



d) Cage B(8,9,10,12)-tetraacetoxylation (Cao, 2016/2018)

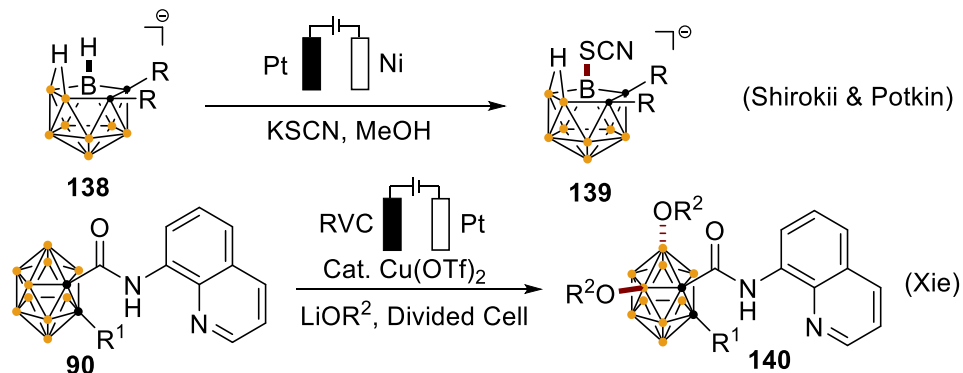


Scheme 1.48. Cage B(8,9,10,12)-halogenation, alkenylation, arylation and tetraacetoxylation of *o*-carboranes

1.7 Electrochemical Functionalization of Carboranes

While significant progress have been realized by the merger of electrocatalysis with organometallic C–H activation,^[192] electrochemical functionalization of carborane continues to be scarce. As early as 2005, Shirokii and Potkin group described the metal-free electrochemical thiocyanation of *nido*-carboranes **138**.^[193] Recently, the Xie group reported a copper-catalyzed

electrochemical B–H oxygenation of *o*-carboranes **90** using a divided cell setup at room temperature. This reaction does not require any additional chemical oxidants and generates H₂ and lithium salt as by-products. The control experiments indicate that a high valent copper(III) species is likely involved in the electrochemical process (Scheme 1.49).^[194]

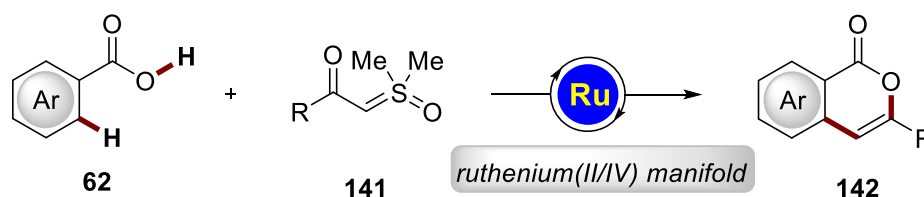


Scheme 1.49. Electrochemical functionalization of carboranes

2. Objectives

During the last decades, transition metal-catalyzed C–H functionalization^[18] has emerged as a powerful tool for the construction of C–C and C–Het bonds due to the excellent levels of atom-^[195] and step-economy.^[196] C–H bonds are ubiquitous in organic compounds, thus, chemo- and position-selective functionalizations of C–H bonds are challenging and extremely important. In contrast to other 4d transition metal catalysts, such as palladium and rhodium, cost-effective ruthenium catalysts^[197] are highly desirable for selective C–H activations.

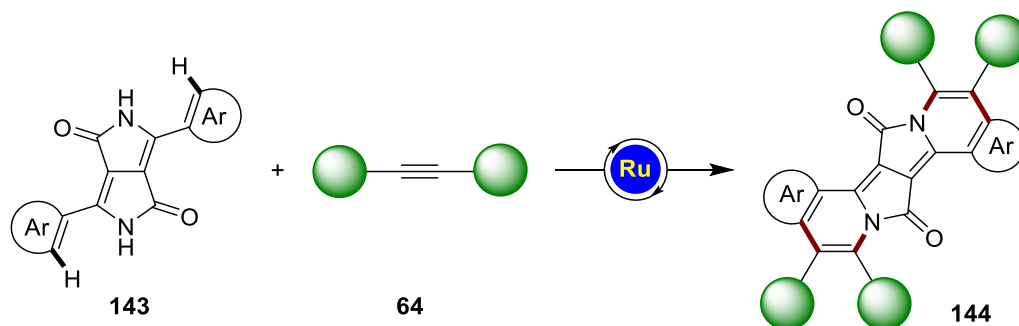
The mechanistic understanding of the fundamental aspects on C–H activation^[198] is vital to the development of synthetically useful C–H functionalization methods.^[21b] In recent years, ruthenium(II)-catalyzed C–H activation^[198c, 199] has emerged as a transformative tool in molecular synthesis, with key applications to drug discovery^[200] and agrochemistry.^[201] In stark contrast to recent findings on rhodium(V)^[202] and iridium(V)-catalyzed^[119c, 203] C–H activation, detailed mechanistic insights into the importance of ruthenium(IV) intermediates in C–H activation processes continues to be limited.^[204] In this context, a ruthenium(II/IV) manifold enabled C–H activation *via* weak O-coordination should be explored (Scheme 2.1).



Scheme 2.1. Ruthenium (II/IV)-catalyzed C–H activation by weak O-coordination

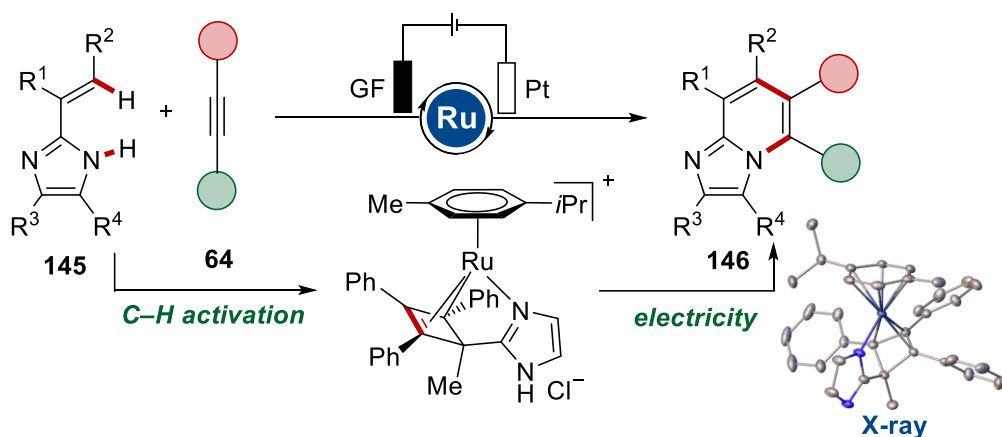
Diketopyrrolopyrroles (DPPs)^[205] **143** – relevant small molecules and conjugated semiconducting polymers – have attracted the attention of researchers from different areas, including optoelectronic materials^[206] and bioimaging probes.^[207] In comparison to the numerous efforts devoted to the modification of the DPP periphery *via* C–H functionalization or direct arylation polymerization (DAP),^[208] their *de novo* assembly leading to π -extended structures continuous to be underdeveloped. Thus, ruthenium-catalyzed twofold C–H/N–H activation for sustainable alkyne annulations towards π -extended polyaromatics should be investigated (Scheme 2.2).

Objectives



Scheme 2.2. Ruthenium (II/IV)-catalyzed double C–H/N–H annulation for diketopyrrolopyroles (DPPs) **144**.

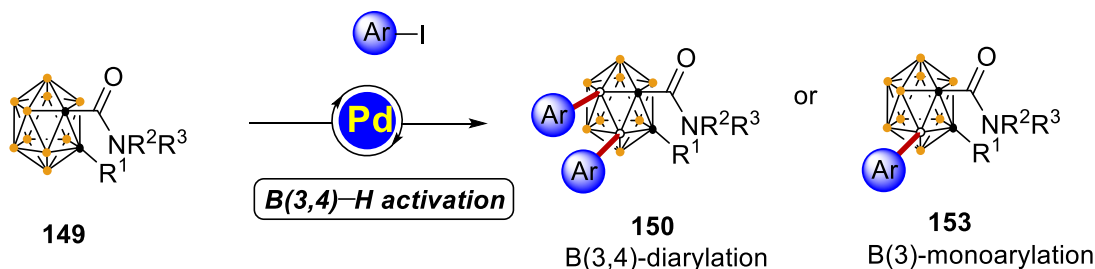
Recently, the elegant merger of metalla-electrocatalyzed oxidative C–H functionalization without expensive and toxic metal oxidants holds the unique power for the resource-economical and environmentally-benign molecular construction.^[90, 209] Despite considerable progress,^[122, 140, 210] the development of new catalytic manifolds is still hampered by a lack of mechanistic understanding. This holds especially true for ruthenaelectrocatalysis, which continues to be underdeveloped.^[116-118] Therefore, another main objective of the thesis is the C–H activation by ruthenaelectro-catalysis ([Scheme 2.3](#)).



Scheme 2.3. Ruthenaelectro(II/III/I)-catalyzed alkyne annulations.

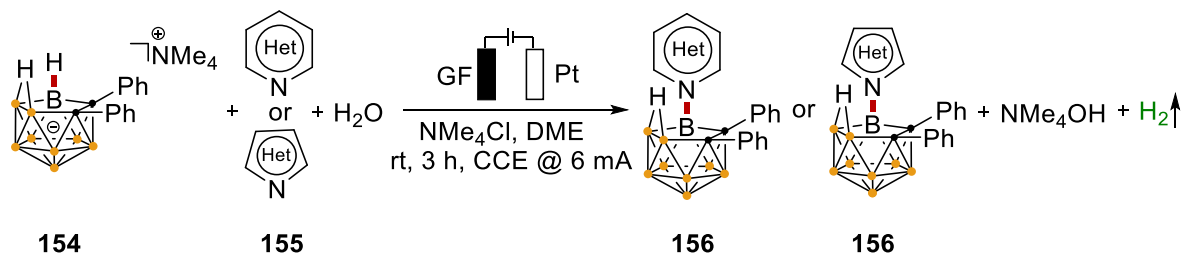
Objectives

In recent years, transition metal-catalyzed cage B–H activation for the regioselective boron functionalization of *o*-carboranes has emerged as a powerful tool for molecular syntheses.^[151] However, the electron density of the 10 B–H bonds in *o*-carboranes are not equal, which results in selectivity issues. Despite indisputable progress, efficient approaches for complementary site-selective functionalizations of *o*-carboranes are hence in high demand. Therefore, we wish to develop an efficient approach for the regioselective B(3,4)–H arylations of *o*-carboranes (Scheme 2.4).



Scheme 2.4. Palladium-catalyzed B(3,4)-arylations.

Moreover, nitrogen-containing carboranes have received increasing attention in recent years, because they possess major potential in drug discovery^[211] as well as molecule catalysis.^[212] In contrast to transition metal-catalyzed regioselective B–H functionalization of *closo*-carborane, B–H functionalization of *nido*-carborane ($7,8\text{-C}_2\text{B}_9\text{H}_{12}^-$) remains in its infancy.^[213] One major challenge is represented by the negatively charged cluster, which inhibits the B–H bond from undergoing nucleophilic substitutions. While significant recent impetus was gained by the merger of electrocatalysis with organometallic C–H activation,^[90, 209] electrochemical regioselective cage B–H functionalization continues to be scarce,^[193-194, 214] Thus, the merger of electrocatalysis with B–H functionalization of *nido*-carborane ($7,8\text{-C}_2\text{B}_9\text{H}_{12}^-$) should be studied (Scheme 2.5).

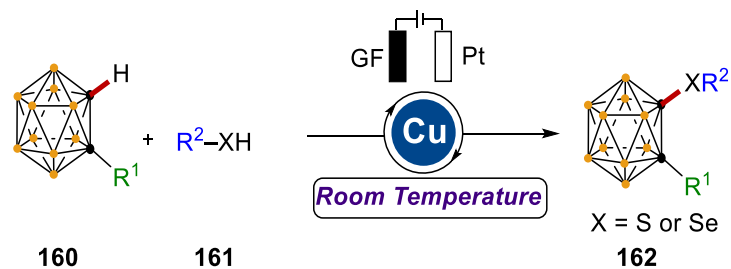


Scheme 2.5. Electrooxidative cage B–H nitrogenation of *nido*-carboranes **154**.

While C–S bonds are important structural motifs in various biologically active molecules and functional materials,^[215] strategies for the assembly of chalcogen-substituted carboranes are relatively rare.^[149a, 182] A major challenge is hence represented by the strong coordination abilities

Objectives

of thiols to most transition metals, which often leads to catalyst deactivation.^[216] Furthermore, oxidative cage B/C–H functionalizations largely call for noble transition metal catalysts^[170, 217] and stoichiometric amounts of expensive chemical oxidants, such as silver(I) salts.^[176, 183, 191] Thus, we explored the copper-catalyzed electrochemical cage C–H chalcogenations of *o*-carboranes in a dehydrogenative manner, assembling a variety of C-sulfenylated and C-selenylated *o*-carboranes (Scheme 2.6).



Scheme 2.6. Cupraelectro-oxidative cage C–H chalcogenation *o*-carboranes **160**.

3. Results and Discussion

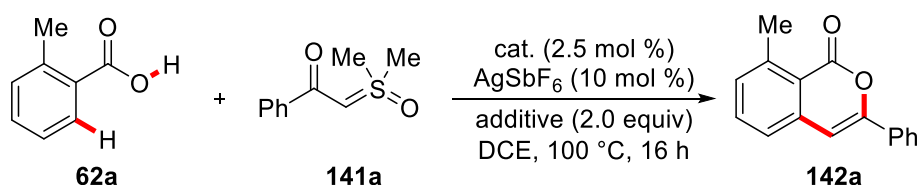
3.1 Ruthenium(IV) Intermediates in C–H Annulation by Weak O-Coordination

The mechanistic understanding of the C–H activation is crucial to develop new type of reactions (vide supra). In this regard, we developed the annulations of sulfoxonium ylides **141** with benzoic acids **62** to provide an expedient access to diversely decorated isocoumarins with ample scope.

3.1.1 Optimization and Scope

Optimization studies on the ruthenium(II)-catalyzed C–H annulation were done by Dr. Yu-Feng Liang as shown in Table 3.1.1.^[218] We commenced our studies by probing the envisioned redox-neutral C–H/O–H functionalization of weakly O-coordinating benzoic acid **62** with sulfoxonium ylide **141** using $[\text{RuCl}_2(p\text{-cymene})]_2$ as the catalyst. A base additive was found essential for the desired C–H annulation, with NEt_3 identified as being optimal (entries 1-5). Interestingly, different ruthenium precursors could be employed, highlighting the importance of carboxylate assistance (entries 6-8). In contrast, frequently used rhodium, iridium and cobalt complexes fell short in delivering the desired product **142** (entries 9-12).

Table 3.1.1. Optimization of reaction conditions.^[a]



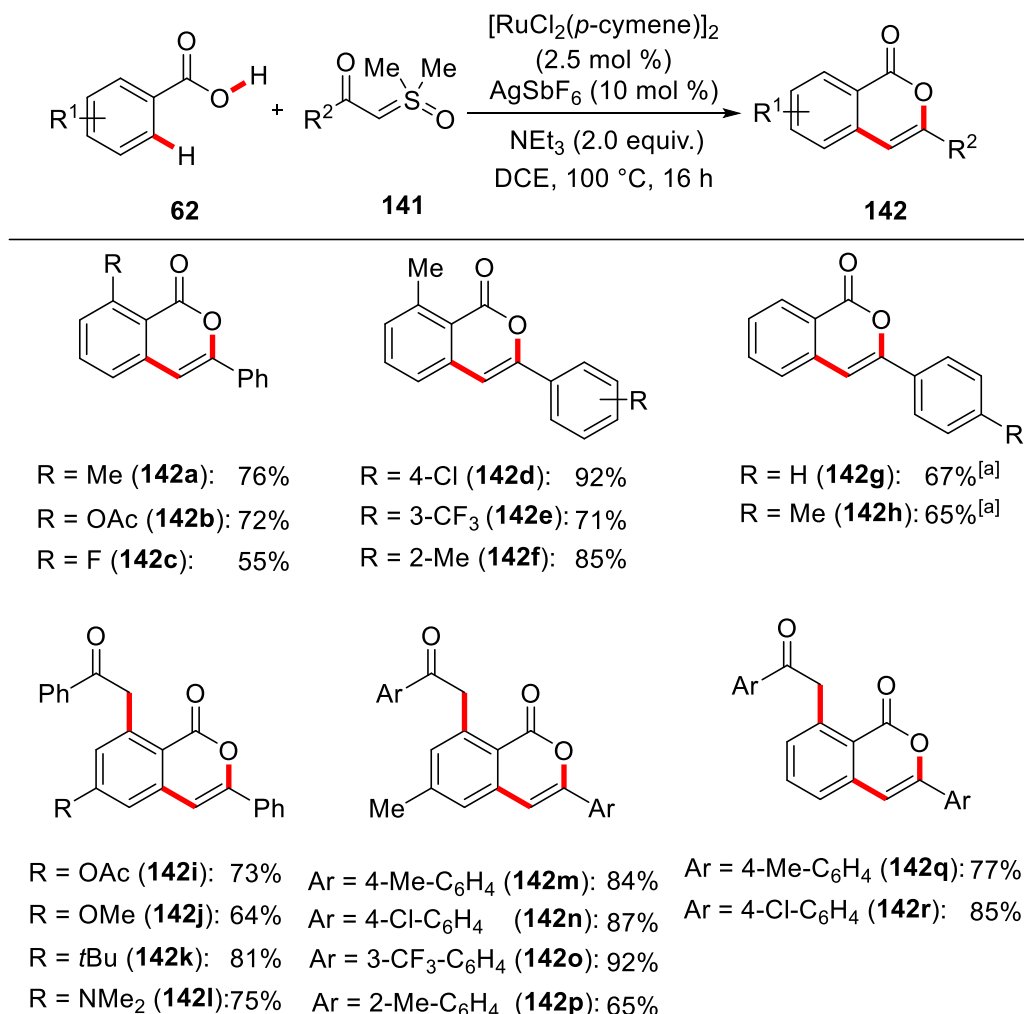
Entry	Cat.	Additive	Yield of 3aa [%] ^[b]
1	$[\text{RuCl}_2(p\text{-cymene})]_2$	—	---
2	$[\text{RuCl}_2(p\text{-cymene})]_2$	NaOAc	30
3	$[\text{RuCl}_2(p\text{-cymene})]_2$	Na_2CO_3	51
4	$[\text{RuCl}_2(p\text{-cymene})]_2$	KO^tBu	23
5	$[\text{RuCl}_2(p\text{-cymene})]_2$	NEt_3	76
6	$[\text{RuCl}_2(p\text{-cymene})]_2$	NEt_3	33 ^[c]
7	$\text{Ru}(\text{OAc})_2(p\text{-cymene})$	NEt_3	65 ^[c,d]

Results and Discussion

8	Ru(O ₂ CMe) ₂ (<i>p</i> -cymene)	NEt ₃	63 ^[c,d]
9	—	NEt ₃	---
10	[Cp*RhCl ₂] ₂	NEt ₃	13
11	[Cp*IrCl ₂] ₂	NEt ₃	<3
12	Cp*Co(CO)I ₂	NEt ₃	---

[a] Reaction conditions: **62a** (0.25 mmol), **141a** (0.38 mmol), cat. (2.5 mol %), AgSbF₆ (10 mol %), additive (0.50 mmol), DCE (2.0 mL), at 100 °C for 16 h. [b] Yields of isolated products. [c] Without AgSbF₆. [d] 5.0 mol % of catalyst.

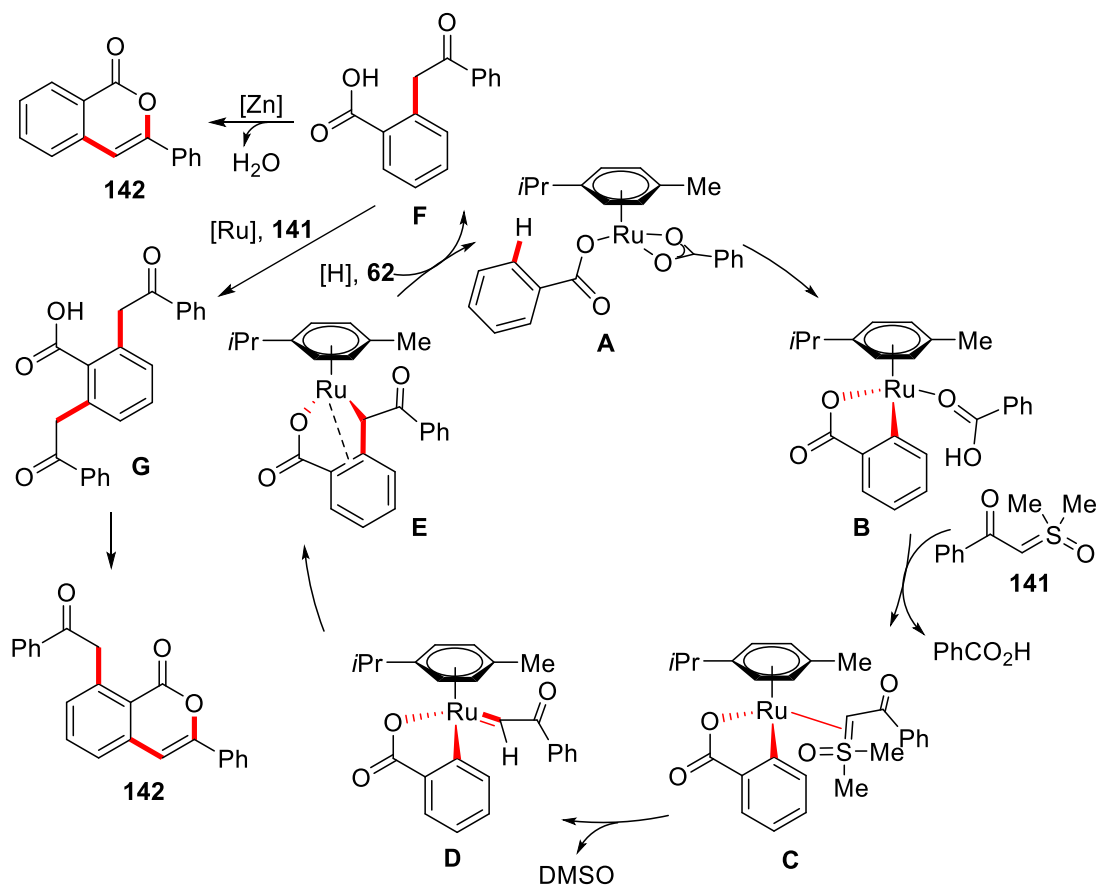
Utilizing the optimized conditions, we next evaluated the versatility of the redox-neutral annulation (Scheme 3.1.1a). Thus, benzoic acids **62** featuring *ortho*-substituents smoothly reacted with sulfoxonium ylides **141**. Moreover, *mono*-C–H functionalization products **142** were selectively obtained, when employing Zn(OAc)₂ as the Lewis-acid additive. Interestingly, the double C–H functionalization products **142i-142r** were selectively generated from *meta*- and *para*-substituted benzoic acids **62** by the judicious choice of the stoichiometry. Thereby, the versatile ruthenium catalysis manifold proved amenable to both electron-rich as well as electron-deficient arenes **62** (Scheme 3.1.1a). Valuable electrophilic functional groups were fully tolerated. Likewise, aryl-substituted sulfoxonium ylides bearing electron-donating or electron-withdrawing groups delivered the desired products (**142m-142r**).



Scheme 3.1.1. Ruthenium-catalyzed C–H/O–H annulation with sulfoxonium ylides **141**. ^[a] Zn(OAc)₂ (50 mol %).

3.1.2. Proposed Mechanism

Based on experimental mechanistic studies, a plausible catalytic cycle was proposed in Scheme 3.1.2. The cyclometalated intermediate **B** is coordinated by the sulfoxonium ylide **141**, leading to ruthenium(II) species **C**. This intermediate **C** is transformed into key ruthenium(IV) species **D** by α -elimination of DMSO. Insertion with the ruthenium(IV) species generates six-membered ruthenacycle **E**. Finally, proto-demetalation affords the acyclic compound, which undergoes a cyclization to get product **142**.



Scheme 3.1.2. Proposed catalytic cycle through a ruthenium(II/IV) manifold.

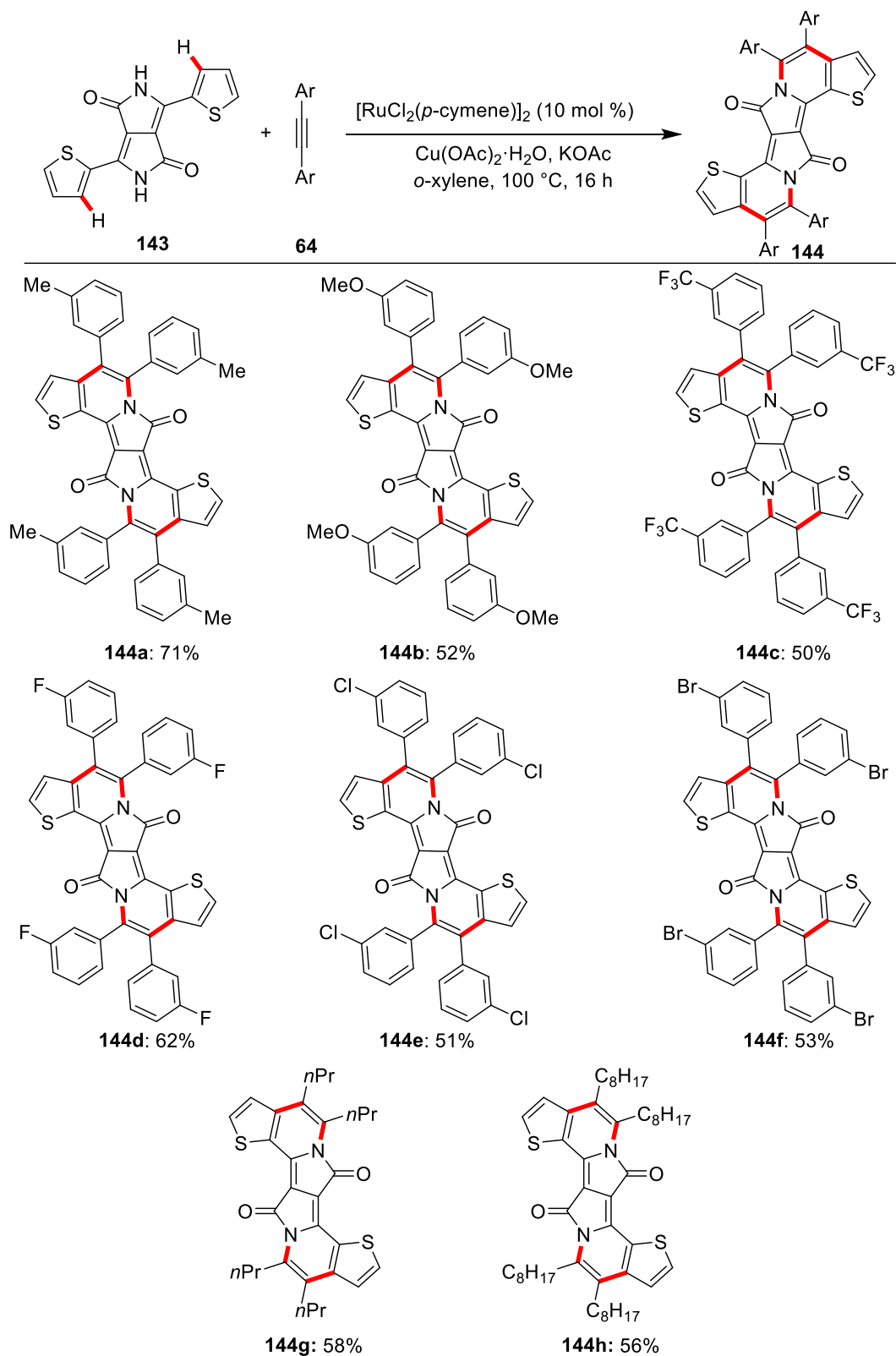
3.2 Twofold C–H/N–H Annulations towards π -Extended Polyaromatics

The widespread applications of substituted diketopyrrolopyrroles (DPPs) call for the development of efficient methods for their modular assembly. Herein, we developed a novel and efficient π -expansion-strategy of DPPs core in a mild and sustainable fashion, employing versatile ruthenium catalysis in the process of a C–H activation of DPPs.^[219]

3.2.1. Optimization and Scope

Optimization studies on the ruthenium(II)-catalyzed C–H allylations were done by Dr. Elżbieta Gońka.^[219] After testing various bases and solvents, the catalytic reaction conditions comprised of $[\text{RuCl}_2(p\text{-cymene})]_2$ (10 mol %), KOAc (1.0 equiv), CuOAc (4.0 equiv) in *o*-xylene at 100 °C for 16 h was identified as optimal. With the optimized catalytic conditions in hand, we tested the versatility of the ruthenium(II)-catalyzed double C–H/N–H annulation of DPP **143** with different diaryl alkynes **64** (Scheme 3.2.1). Thereby, π -extended PAHs were accessed from electron-rich as well as electron-deficient alkynes in an efficient manner, including sensitive tetra-bromo/chloro DPPs **144e-144f**, which should prove instrumental for further modifications and applications of the DPPs **144**. The double ruthenium-catalyzed C–H/N–H annulation was not restricted to aromatic alkynes. Indeed, the reaction also proceeded well with alkyl alkynes, delivering the corresponding products **144g** and **144h** efficiently.

Results and Discussion



Scheme 3.2.1. Ruthenium-catalyzed double C–H/N–H annulation with aryl alkynes.

3.2.2. UV-Vis Absorption and Fluorescence Spectroscopy

The optical properties of the thus-obtained novel compounds **144a–144h** were studied by UV-Vis absorption and fluorescence spectroscopy (Table 3.2.2). The unprecedented DPPs exhibited very intense absorption in the UV and visible region, with absorption maxima between 600 – 640 nm, which results in intense blue to purple color. The absorption maximum in all synthesized derivatives is bathochromically shifted in comparison with the previously synthesized, unsubstituted compounds,^[220] whereas both Stoke shift and absorption coefficient are similar.

Table 3.2.2. Spectroscopic data of π -extended diketopyrrolopyrroles **144a–144h**.

Compound	λ_{max}^{abs}	λ_{max}^{em}	Stokes shift [cm^{-1}]	$\epsilon_{max}[\text{M}^{-1} \text{cm}^{-1}]$
144a	635	645	244	52083
144b	635	646	268	71946
144c	632	641	222	66051
144d	631	640	223	47269
144e	633	644	270	76626
144f	633	643	246	76107
144g	630	639	223	71598
144h	631	642	272	84835

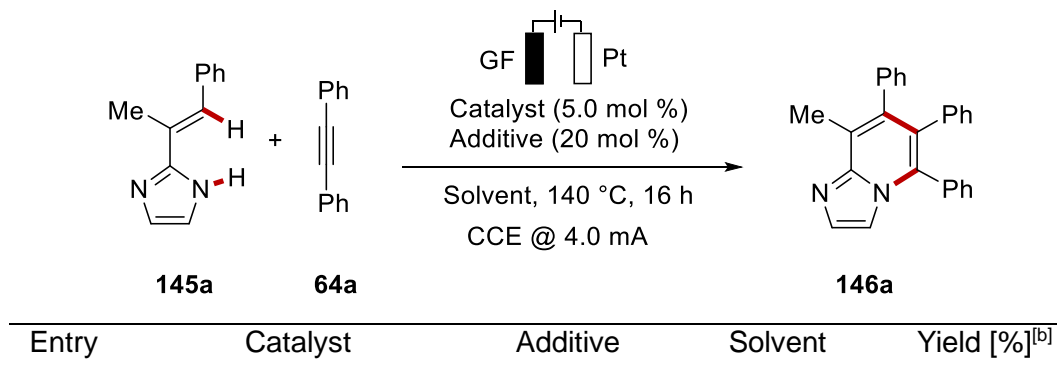
3.3 Ruthenaelectro(II/III/I)-Catalyzed Alkyne Annulations

In this section, a ruthenium-catalyzed electrochemical dehydrogenative annulation reaction of imidazoles with alkynes was developed, allowing for the synthesis of various bridgehead *N*-fused [5,6]-bicyclic heteroarenes through regioselective electrochemical C–H/N–H annulation without chemical oxidants. Novel aza-ruthena-bicyclo-[3.2.0]-heptadienes were fully characterized and identified as the key intermediates for this transformation. Experimental and DFT mechanistic studies were suggestive of an oxidatively-induced reductive elimination pathway within a ruthenium(II/III) regime.^[221]

3.3.1. Optimization and Scope of Alkenyl Imidazole

The study was commenced by probing various reaction conditions for the envisioned ruthenium-catalyzed electrooxidative C–H/N–H annulation of alkenyl imidazole **145** with alkyne **64** in an operationally simple undivided cell setup equipped with a GF (graphite felt) anode and a Pt cathode (Table 3.3.1). After considerable preliminary experimentations, we observed that the desired product **146a** was obtained by catalytic amounts of $[\text{RuCl}_2(\textit{p}\text{-cymene})]_2$, along with KPF_6 as the optimal catalytic additive, and DMF as the best solvent (entries 1-5). The yield was found to be reduced when sodium salts were used, such as NaCl and NaPF_6 (entries 6-7). Gratifyingly, reducing the reaction time to 8 h led to the same yield of product **146a** (entry 8). The reaction with a Pt anode resulted in a sharp drop in yield (entry 10). The addition of the redox mediator of BQ did not improve the performance of the ruthenium catalyst (entries 11-12). Control experiments verified the essential role of the electricity, the additive, and the ruthenium catalyst (entries 13 – 15). A set of otherwise typical transition metal catalysts were also probed but gave none or significantly reduced amounts of product **146a** (entries 16-20).

Table 3.3.1. Optimization of ruthenaelectro-catalyzed annulation.^[a]



Results and Discussion

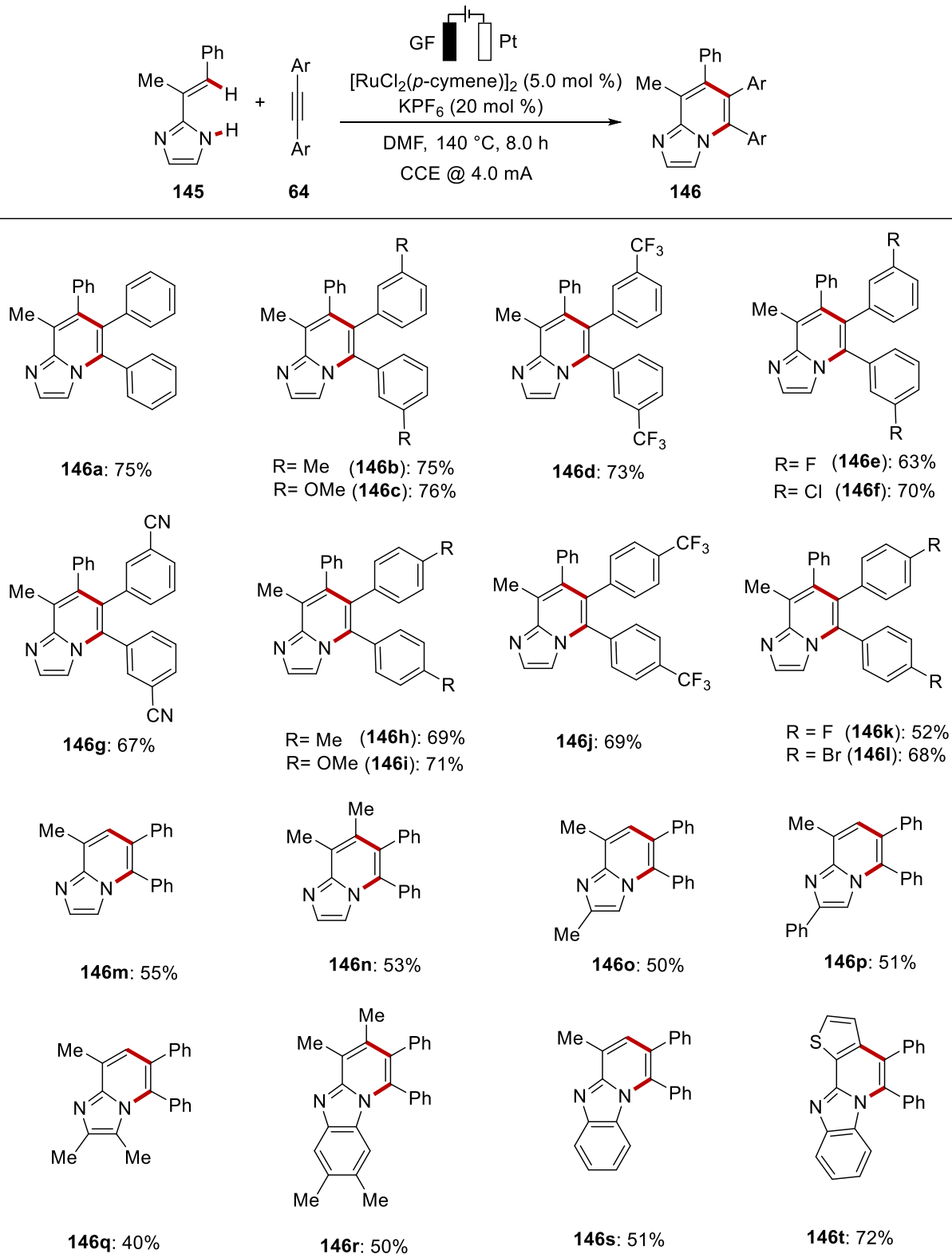
1	[RuCl ₂ (<i>p</i> -cymene)] ₂	KPF ₆	MeOH	10% ^[c]
2	[RuCl ₂ (<i>p</i> -cymene)] ₂	KPF ₆	<i>t</i> -AmOH/H ₂ O	12% ^[d]
3	[RuCl ₂ (<i>p</i> -cymene)] ₂	KPF ₆	DMA	33%
4	[RuCl ₂ (<i>p</i> -cymene)] ₂	KPF ₆	NMP	10%
5	[RuCl ₂ (<i>p</i> -cymene)] ₂	KPF ₆	DMF	75%
6	[RuCl ₂ (<i>p</i> -cymene)] ₂	NaCl	DMF	50%
7	[RuCl ₂ (<i>p</i> -cymene)] ₂	NaPF ₆	DMF	66%
8	[RuCl₂(<i>p</i>-cymene)]₂	KPF₆	DMF	75%^[e]
9	[RuCl ₂ (<i>p</i> -cymene)] ₂	KPF ₆	DMF	56% ^[f]
10	[RuCl ₂ (<i>p</i> -cymene)] ₂	KPF ₆	DMF	46% ^[g]
11	[RuCl ₂ (<i>p</i> -cymene)] ₂	KPF ₆	DMF	33% ^[h]
12	[RuCl ₂ (<i>p</i> -cymene)] ₂	KPF ₆	DMF	28% ^[i]
13	[RuCl ₂ (<i>p</i> -cymene)] ₂	KPF ₆	DMF	10% ^[j]
14	[RuCl ₂ (<i>p</i> -cymene)] ₂	---	DMF	50%
15	---	KPF ₆	DMF	---
16	Ru(<i>p</i> -cymene)(OAc) ₂	KPF ₆	DMF	53%
17	Co(OAc) ₂ ·4H ₂ O	KPF ₆	DMF	---
18	[Cp* ⁺ RhCl ₂] ₂	KPF ₆	DMF	36%
19	[Cp* ⁺ IrCl ₂] ₂	KPF ₆	DMF	10%
20	Pd(OAc) ₂	KPF ₆	DMF	---

[a] Reaction conditions: undivided cell, **145** (0.40 mmol), **64** (0.80 mmol), catalyst (5.0 mol %), additive (20 mol %), solvent (4.0 mL), 140 °C, 16 h, constant current at 4.0 mA, GF anode, Pt-plate cathode. [b] Yields of isolated products. [c] 60 °C. [d] *t*-AmOH/H₂O = 1/1, 100 °C. [e] 8.0 h. [f] 5.0 h. [g] Pt-plate as anode. [h] BQ (10 mol %). [i] BQ (10 mol %), 100 °C. [j] no electricity. DMF = *N,N*-Dimethylformamide, BQ = 1,4-Benzoquinone.

With the optimal reaction conditions in hand, we explored the versatility of the electrochemical annulations with diversely decorated alkynes **64** (Scheme 3.1.1). Electron-rich as well as electron-poor aromatic moieties at the alkynes **64** were amenable to the ruthenaelectrocatalyzed C–H functionalizations. Thereby, a variety of synthetically useful electrophilic functional groups, such as chloro (**146f**), cyano (**146g**) and bromo (**146i**) substituents, were fully tolerated, which should prove invaluable for late-stage manipulations. We next turned our attention to diversified alkenyl imidazoles **145**. Imidazoles bearing a range of substituents at different sites on the alkene or the imidazole were effectively transferable to deliver products **146m–146q**. In addition, benzimidazole substrates with a β-methyl group and without a β-substituent on the alkene were effective for C–H/N–H activation **146r–146s**. Notably, thiophenyl

Results and Discussion

substituted benzimidazole also was a competent substrate, giving the corresponding annulation product **146t** with high efficacy.



Scheme 3.3.1. Scope of the electrochemical C-H/N-H activation with alkynes **64**. (**146c**, **146h**, **146i** and **146l** did by Msc. Ralf Steinbock)

3.3.2. Optimization and Scope of benzimidazoles

Next, we investigated the electrooxidative annulation of benzimidazoles **147** with alkyne **64**, as shown in Table 3.3.2. After considerable optimizations of ruthenium complexes, bases and solvents, a catalytic system containing $[\text{Ru}(p\text{-cymene})\text{Cl}_2]$ (5 mol%), KOAc (2.0 equiv) in a mixture of solvents of *t*-AmOH and H_2O at 100 °C for 4 h was identified as the ideas reaction condition (entry 5). Control experiments highlighted the essential role of the ruthenium catalyst and electricity (entries 6-12).

Table 3.3.2: Optimization of Electrochemical annulation with benzimidazole **147**.^[a]

Reaction scheme: **147a** (x mmol) + **64a** (y mmol) $\xrightarrow[\text{Base, Solvent}]{[\text{RuCl}_2(p\text{-cymene})_2]_2 (5.0 \text{ mol } \%), 1\text{-AdCO}_2\text{H} (20 \text{ mol } \%)}$ **148a**

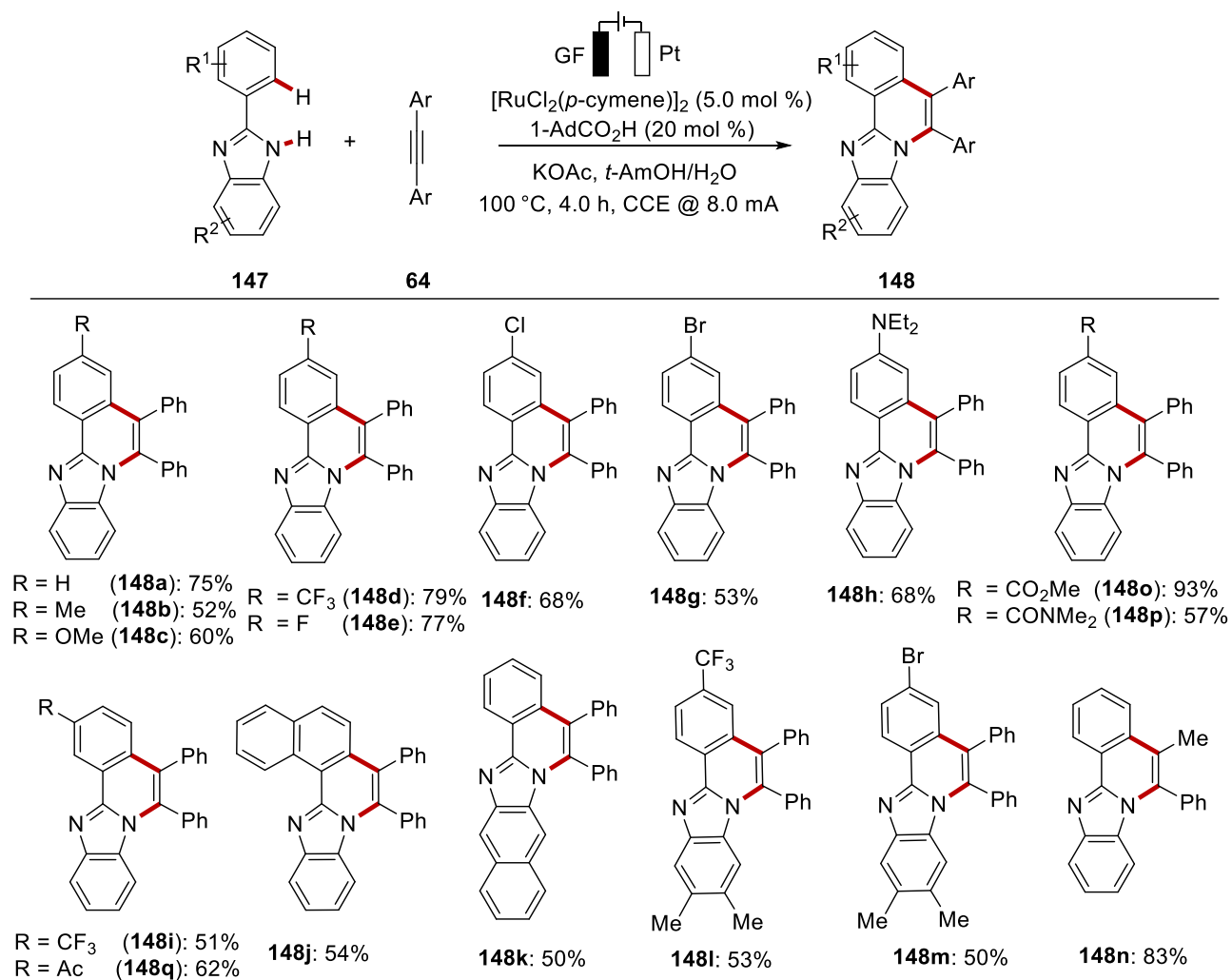
Conditions: 100 °C, 16 h, CCE @ 4.0 mA

Entry	x	y	Base	Solvent	Yield of 148a [%]
1	0.4	0.8	---	<i>t</i> -AmOH/ H_2O (3/1, 4 mL)	48% ^[b]
2	0.4	0.8	K_2CO_3 (1 equiv)	<i>t</i> -AmOH/ H_2O (3/1, 4 mL)	46% ^[c]
3	0.2	0.4	K_2CO_3 (1 equiv)	<i>t</i> -AmOH/ H_2O (1/1, 6 mL)	47% ^[d]
4	0.2	0.4	KOAc (2 equiv)	<i>t</i> -AmOH/ H_2O (1/1, 6 mL)	70% ^[d]
5	0.2	0.4	KOAc (2 equiv)	<i>t</i> -AmOH/ H_2O (1/1, 6 mL)	75% ^[e]
6	0.2	0.4	KOAc (2 equiv)	<i>t</i> -AmOH/ H_2O (1/1, 6 mL)	--- ^[e,f]
7	0.2	0.4	KOAc (2 equiv)	<i>t</i> -AmOH/ H_2O (1/1, 6 mL)	24% ^[e,g]
8	0.2	0.4	KOAc (2 equiv)	<i>t</i> -AmOH/ H_2O (1/1, 6 mL)	40% ^[e,h]
9	0.2	0.4	KOAc (2 equiv)	<i>t</i> -AmOH/ H_2O (1/1, 6 mL)	56% ^[e,i]
10	0.2	0.4	KOAc (2 equiv)	<i>t</i> -AmOH/ H_2O (1/1, 6 mL)	--- ^[e,j]
11	0.2	0.4	KOAc (2 equiv)	<i>t</i> -AmOH/ H_2O (1/1, 6 mL)	--- ^[e,k]
12	0.2	0.4	KOAc (2 equiv)	<i>t</i> -AmOH/ H_2O (1/1, 6 mL)	--- ^[e,l]

Results and Discussion

^[a] Reaction conditions: Undivided cell, **147** (x mmol), **64** (y mmol), $[\text{RuCl}_2(p\text{-cymene})]_2$ (5.0 mol %), 100 °C, 16 h under N_2 , constant current at 4.0 mA, GF anode, Pt-plate cathode, isolated yields. ^[b] KPF_6 (20 mol %) as additive. ^[c] 10 h. ^[d] 8 h. ^[e] 8 mA, 4 h. ^[f] no catalyst. ^[g] no current. ^[h] Pt instead of GF. ^[i] $[\text{Cp}^*\text{RhCl}_2]_2$ (5.0 mol %) as catalyst. ^[j] $\text{Pd}(\text{OAc})_2$ (10 mol %) as catalyst. ^[k] $\text{Co}(\text{OAc})_2 \cdot 4 \text{H}_2\text{O}$ (10 mol %) as catalyst. ^[l] $[\text{Cp}^*\text{IrCl}_2]_2$ (5.0 mol %) as catalyst.

With the best conditions in hand, we next investigated the generality of the metalla-electrocatalysis by the assembly of the benzimidazoquinoline skeleton **148** through annulation of alkynes **64** with 2-arylimidazoles **147** (Scheme 3.3.2). Substitutions at the 2-aryl group and the benzimidazole gave the desired benzimidazoquinolines (**148b-148q**). Likewise, 2-naphthylbenzimidazole and 2-phenylnaphthoimidazole also afforded the corresponding products (**148j,148k**). The unsymmetrical 1-phenyl-1-propyne gave the product **148n** with a high level of regioselectivity. Importantly, chloro, bromo, ester, amide and enolizable ketone substituents were thereby fully tolerated to deliver products **148f-148g**, **148o-148q**.



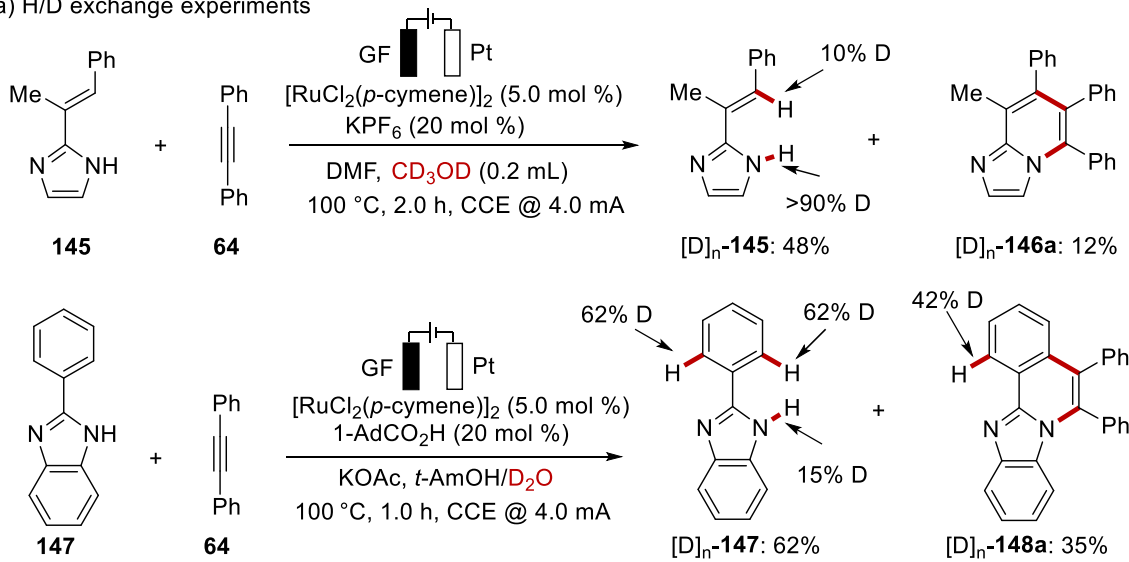
Scheme 3.3.2. Electrochemical C-H/N-H activation with alkynes **64**. (**148d**, **148f**, **148h** and **148n** did by Msc. Ralf Steinbock)

3.3.3 Mechanistic Studies

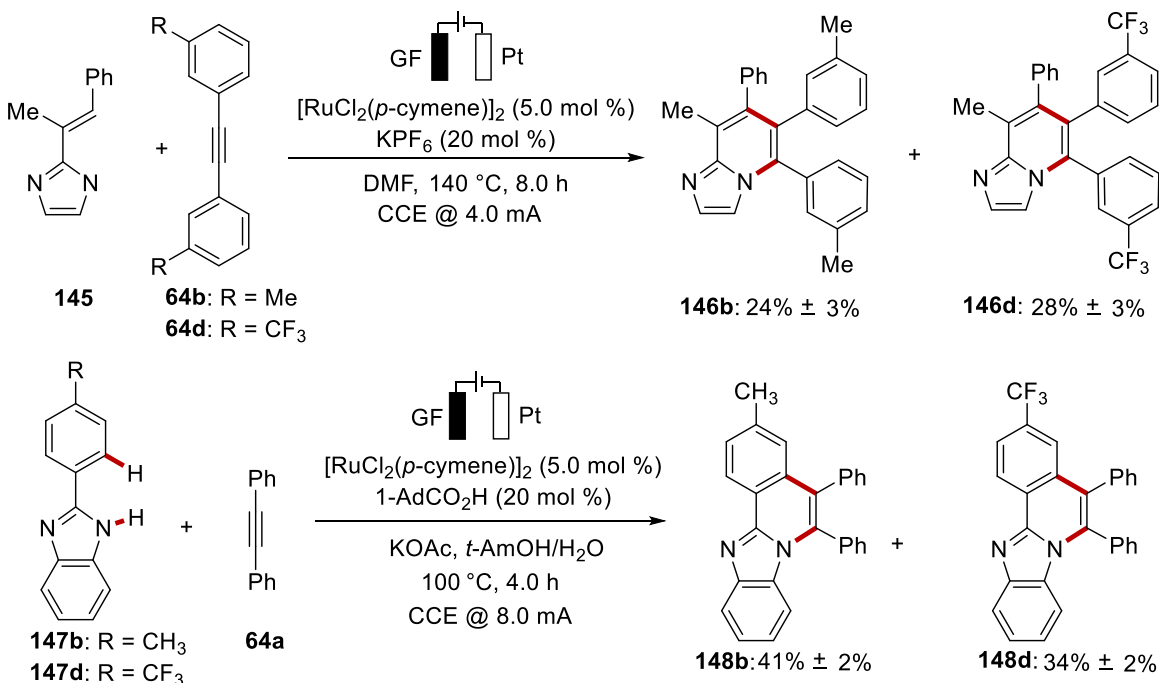
3.3.3.1 H/D Exchange and Competition Experiments

The optimized reaction was conducted in the presence of the cosolvent CD₃OD and D₂O. A H/D scrambling was observed in the reisolated substrate **145a** and the product **146a**, which suggested a reversible C–H cleavage, occurring by an organometallic C–Ru bond formation (Scheme 3.3.3.1a). Intermolecular competition experiments showed a slight preference for electron-poor alkynes **64** and electron-rich arenes **147** (Scheme 3.3.3.1b).

a) H/D exchange experiments



b) competition experiments

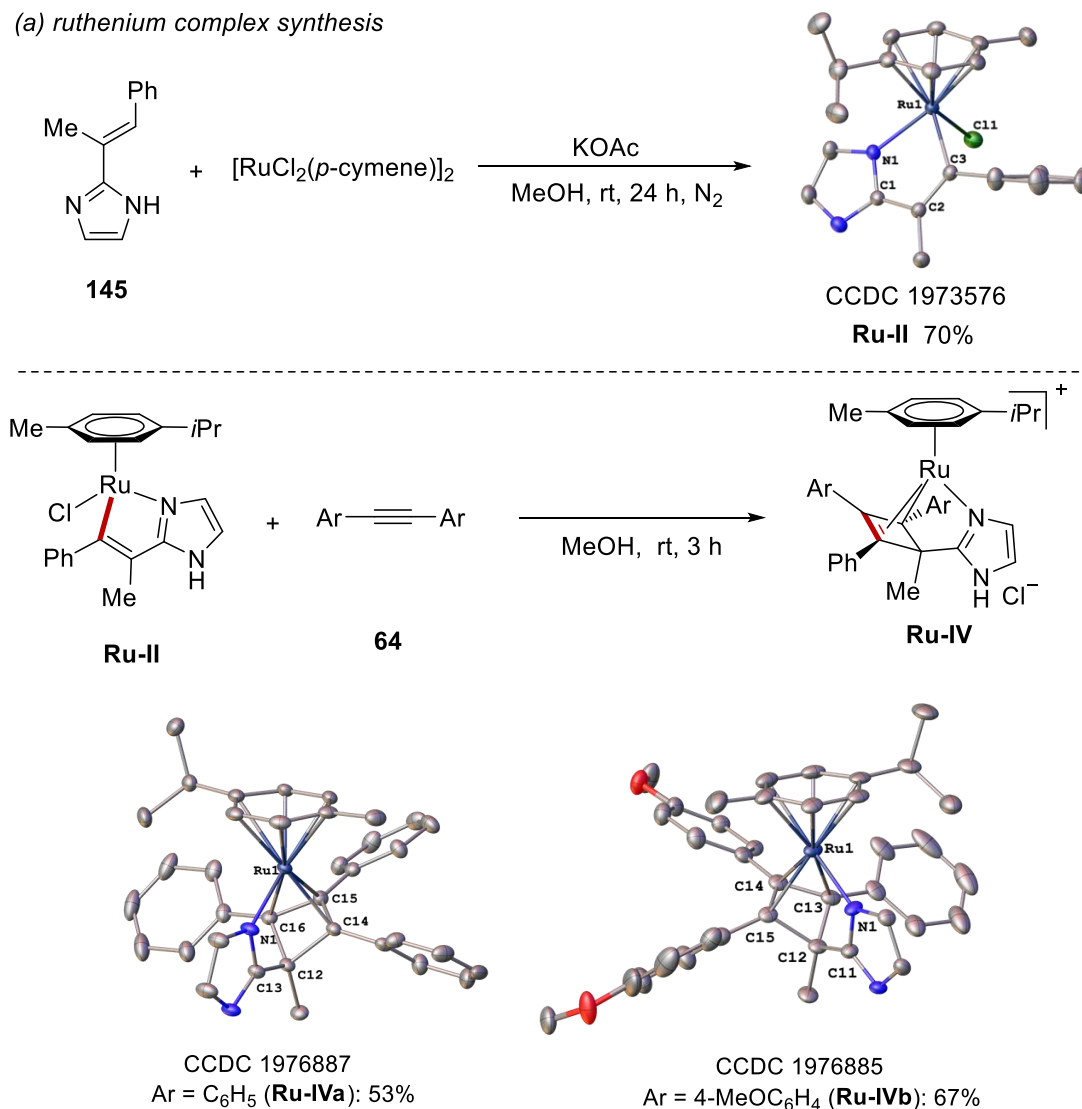


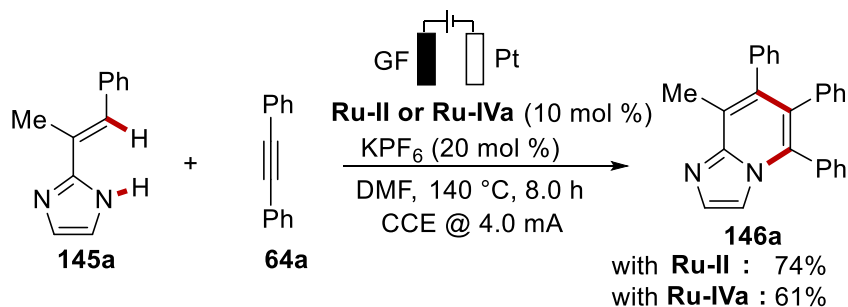
Scheme 3.3.3.1. Mechanistic studies. (Competition experiments did by Msc. Ralf Steinbock)

3.3.3.2 Isolation and Characterization of Ruthenium(II) Intermediate

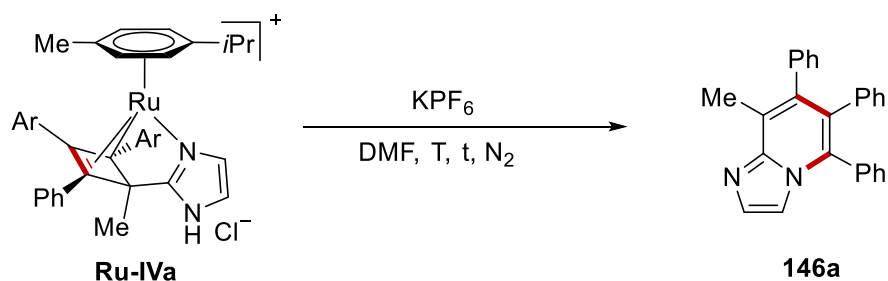
Next, we probed the isolation of intermediates by stoichiometric experimentation. Thus, we first selectively prepared the ruthenacycle **Ru-II** (Scheme 3.3.3.2a). Second, the ruthenacycle **Ru-II** delivered the unprecedented aza-ruthena(II)-bicyclo-[3.2.0]-heptadienes **Ru-IVa** and **Ru-IVb** upon stoichiometric reaction with the alkynes **64**. **Ru-IVa** and **Ru-IVb** were unambiguously characterized by X-ray diffraction analysis. Notably, the metallacycles **Ru-II** and **Ru-IV** proved also to be competent under catalytic reaction conditions (Scheme 3.3.3.2b). It is noteworthy that the aza-ruthena(II)-bicyclo-[3.2.0]-heptadiene **Ru-IVa** was stable, but gave the product **146a** under electrolysis, being suggestive of an oxidation-induced reductive elimination within a ruthenium(II/III) manifold (Scheme 3.3.3.2c).

(a) ruthenium complex synthesis



(b) catalytic reactivity of **Ru-II** and **Ru-IVa**

(c) oxidatively induced reductive elimination

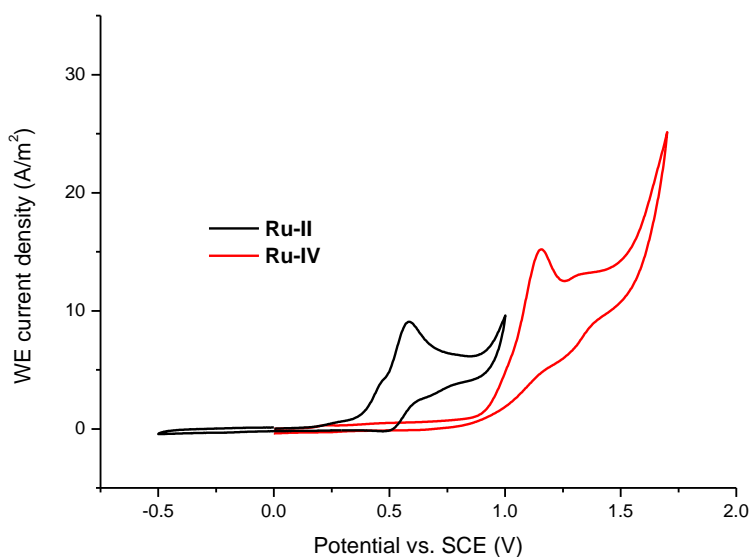


Entry	t/min	T/°C	Current	Ru-IVa	146a
1	10	rt	---	100%	---
2	10	rt	4.0 mA	67%	17%
3	10	80	---	100%	---
4	10	80	4.0 mA	57%	24%
5	60	80	---	77%	---
6	60	80	4.0 mA	---	53%

Scheme 3.3.3.2. Isolation and characterization of ruthenium(II) complexes. (a) ruthenium complex synthesis; (b) catalytic reactivity of ruthenium complex; (c) oxidatively-induced reductive elimination.

3.3.3.3 Cyclic Voltammetry Studies of Ruthenium(II) Intermediate

Furthermore, we probed the electrochemical C–H activation by means of cyclic voltammetric analysis of the well-defined ruthenacycles along with Msc. Alexej Scheremetjew in the Ackermann group ([Scheme 3.3.3.3](#)). Thus, we observed at ambient temperature an irreversible oxidation of the ruthenium(II) complex **Ru-II** at $E_p = 0.60$ V vs. SCE. The aza-ruthena(II)-bicyclo-[3.2.0]-heptadiene **Ru-IVa** featured a considerably higher oxidation wave at $E_p = 1.20$ V vs. SCE, both of which could be rationalized by an oxidation-induced reductive elimination within a ruthenium(II/III) regime.

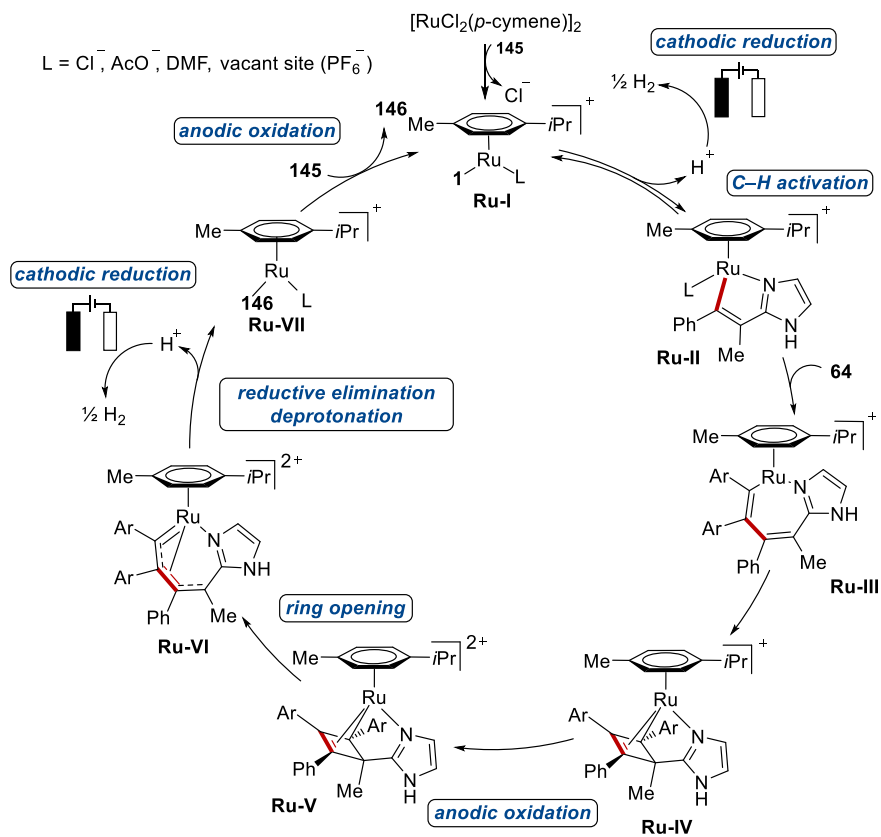


Scheme 3.3.3.3. Cyclic voltammetry in DMF with 100 mM KPF₆ under N₂ at 100 mV/s of **Ru-II** (5 mM) and **Ru-V** (5 mM). CV was performed by Msc. Alexej Scheremetjew.

3.3.3.4 Proposed Mechanism

Finally, based on our mechanistic studies, we proposed a plausible catalytic cycle to commence by a fast organometallic C–H activation ([Scheme 3.3.3.4](#)). Thereby, ruthena(II)cycle **Ru-II** is generated. Thereafter, alkyne **64** coordination and migratory insertion furnish the aza-ruthena-bicyclo-[3.2.0]-heptadiene **Ru-IV**, which undergoes anodic oxidation to deliver the ruthenium(III) complex **Ru-V**. Subsequent pericyclic ring opening yields ruthenium(III) complex **Ru-VI**. Oxidation-induced reductive elimination forms ruthenium(I) complex **Ru-VII**, which is anodically reoxidized to release the product and regenerate ruthenium(II) catalyst.

Results and Discussion



Scheme 3.3.3.4. Proposed mechanism of ruthenium(II/III/I)-catalyzed alkyne annulations.

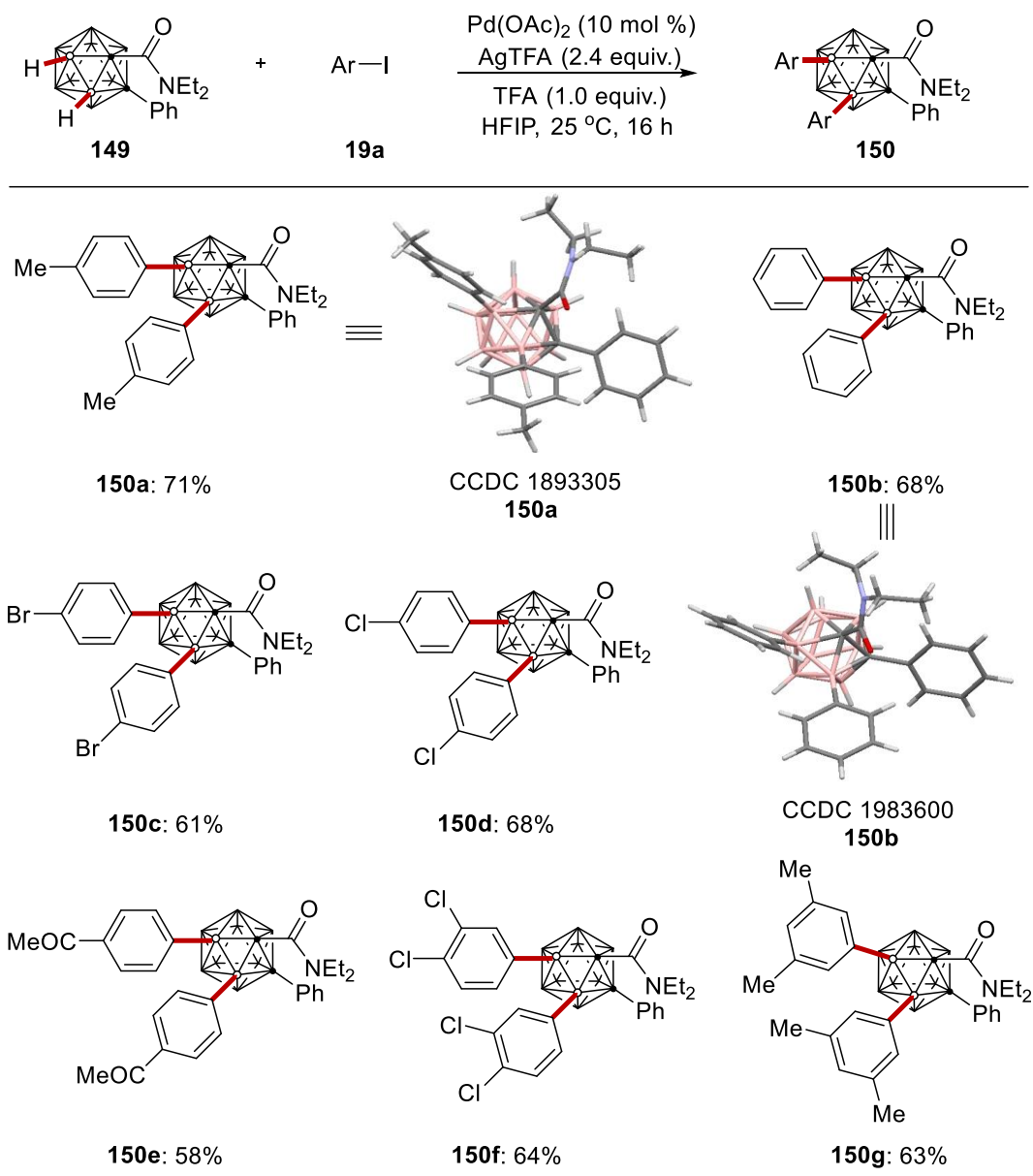
3.4 Regioselective B(3,4)–H Arylation of *o*-Carboranes

Significant progress has been achieved in the regioselective functionalization of *o*-carboranes (vide supra). Despite indisputable advances,^[151] efficient approaches for complementary site-selective functionalizations of *o*-carboranes are hence in high demand. Thus, metal-catalyzed position-selective B(3,4)–H functionalizations of *o*-carboranes has thus far not been reported. In this chapter, a palladium-catalyzed regioselective di- or mono-arylation of *o*-carboranes was achieved by weakly coordinating amides at room temperature.^[222] Thereby, a series of B(3,4)-diarylated and B(3)-monoarylated *o*-carboranes anchored with valuable functional groups were accessed for the first time. This strategy provided an efficient approach for the selective activation of B(3,4)–H bonds for functionalizations of *o*-carboranes.

3.4.1. Optimization and Scope of B(3,4)–H Arylation of *o*-Carboranes

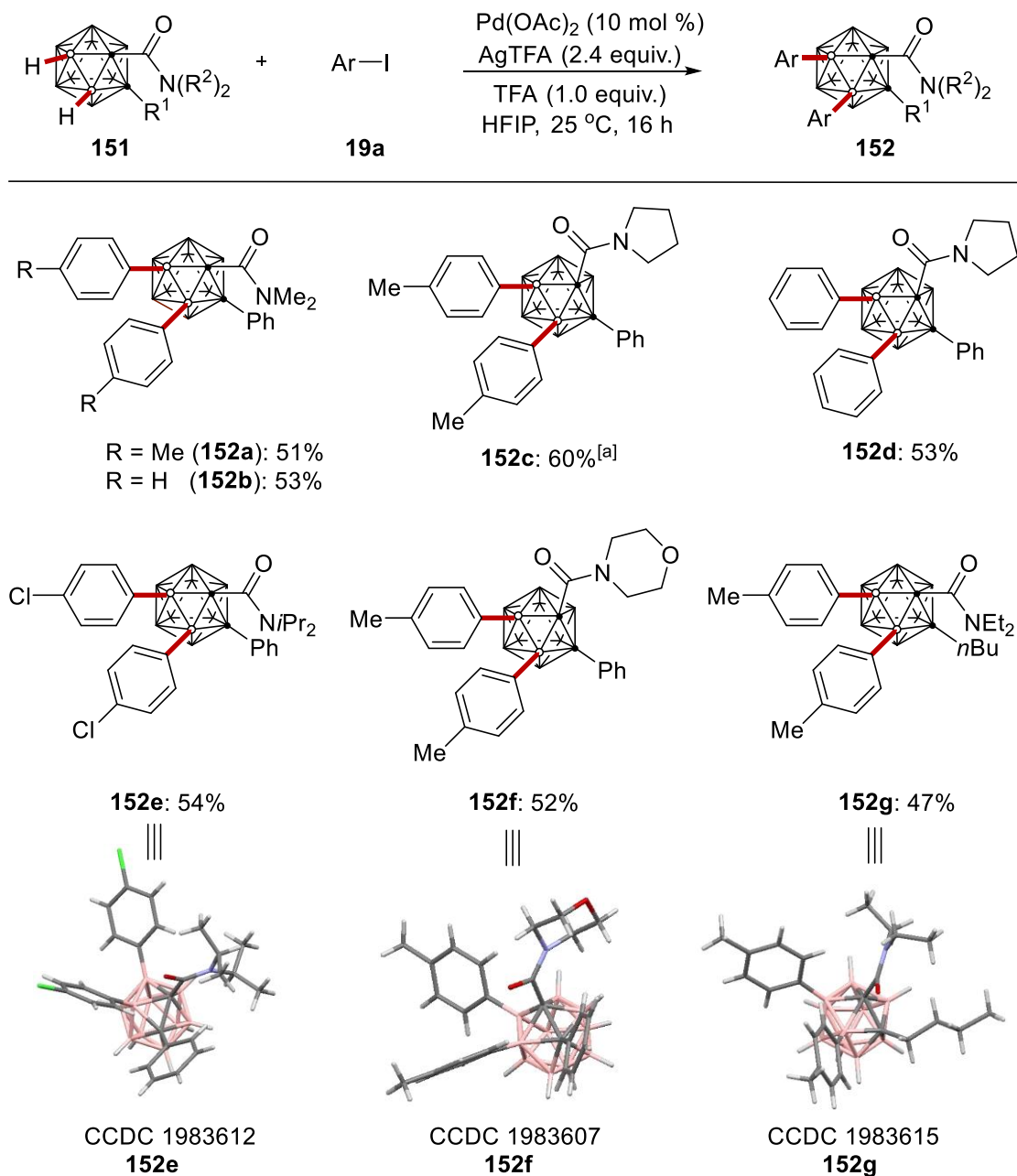
Optimization studies on the palladium-catalyzed B(3,4)–H arylation were initially performed by Dr. Yu-Feng Liang^[222] and after testing various additives and solvents, catalytic reaction conditions comprised of Pd(OAc)₂ (10 mol %), AgTFA (2.0 equiv) and TFA (1.0 equiv.) in HFIP at room temperature for 16 h were identified as optimal for the uncommon B(3,4)-di-arylated product **150**. While replacing AgTFA with Ag₂CO₃ resulted in the formation of B(3)–H mono-arylation product **153** as the major product. With the optimized reaction conditions in hand, Dr. Yu-Feng Liang probed the scope of the B–H di-arylation of *o*-carboranes **149** with different aryl iodides **19a** (Scheme 3.4.1.1). The versatility of the room temperature B(3,4)–H di-arylation was demonstrated by tolerating valuable functional groups, including bromo (**150c**), chloro (**150d**, **150f**), and enolizable ketone (**150e**) substituents.

Results and Discussion



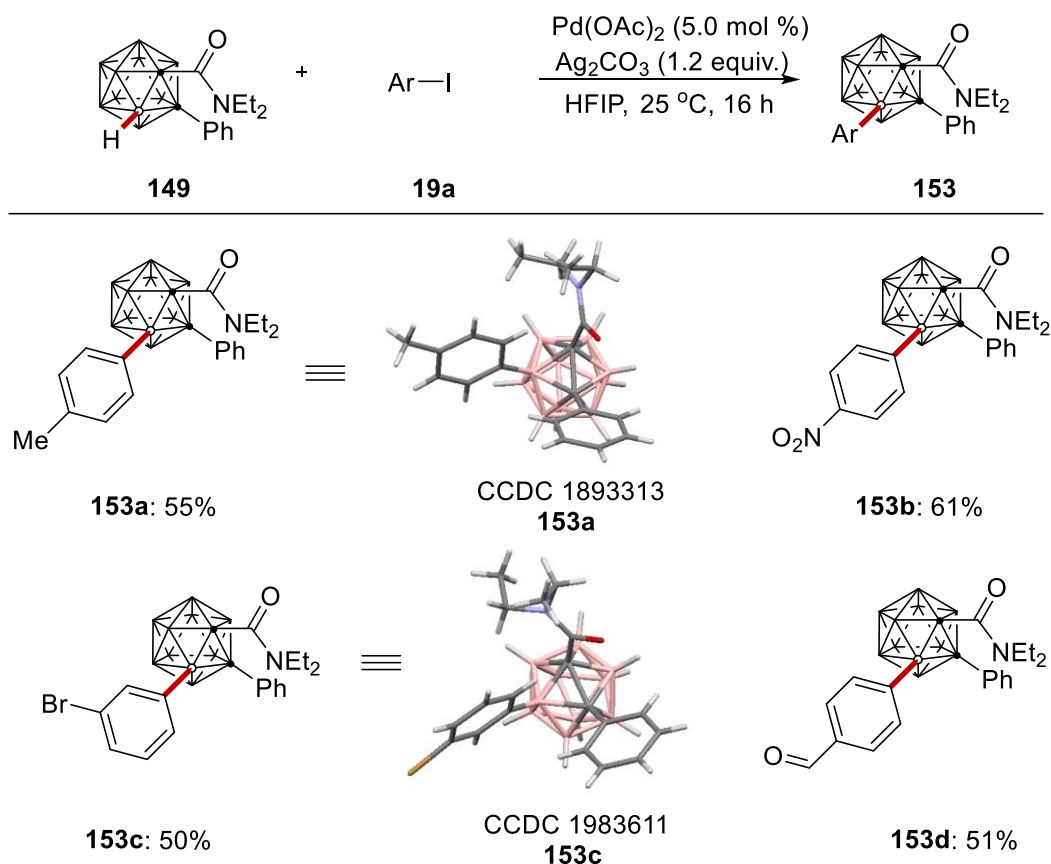
Scheme 3.4.1.1. Palladium-catalyzed B(3,4)-diarylation carried out by Dr. Yu-Feng Liang.

Next, we explored the effect exerted by the *N*-substituent at the amide moiety ([Scheme 3.4.1.2](#)). Tertiary amides **151** proved to be suitable substrates with optimal conditions. The effect of varying the cage carbon substituents R^1 on the reaction was also probed, and both aryl and alkyl substituents gave the B–H arylation products **152a–152g**.



Scheme 3.4.1.2. Palladium-catalyzed B(3,4)-diarylation with different *o*-carboranes. (**152c** did by Becky Bongsuiru Jei)

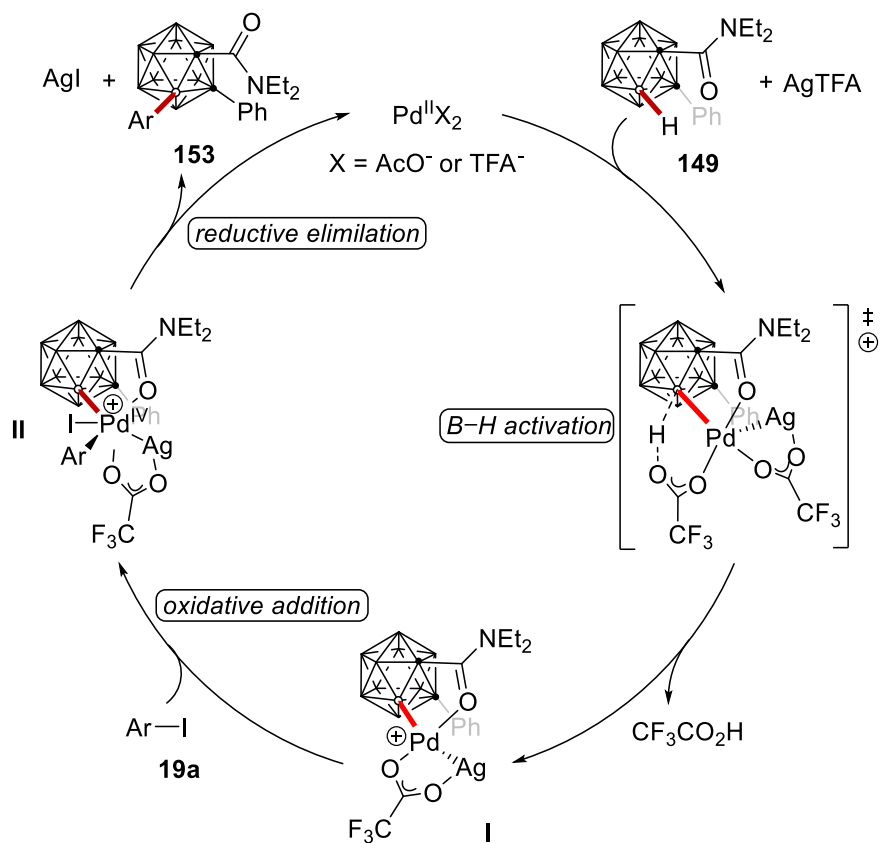
Thereafter, the robustness of the palladium-catalyzed B–H functionalization was subsequently investigated by Dr. Yu-Feng Liang and Becky Bongsuiru Jei for the challenging catalytic B–H monoarylation of *o*-carboranes (**Scheme 3.4.1.3**). The B(3)–H monoarylation proceeded smoothly with valuable functional groups, featuring aldehyde (**153d**) bromo (**153c**) and nitro (**153b**) substituents, which allow for invaluable further late-stage manipulation.



Scheme 3.4.1.3. Palladium-catalyzed B(3)-arylation. (**153a**, **153b** and **153d** did by Dr. Yu-Feng Liang. **153c** did by Becky Bongsuiru Jei)

3.4.2 Proposed Mechanism

A plausible reaction mechanism is proposed to commence by an organometallic B(3)–H activation of **149** by weak assistance of the amide group and AgTFA to form cationic intermediate **I** (Scheme 3.4.2). Oxidative addition with ArI **19a** affords proposed palladium(IV) cationic intermediate **II**, followed by reductive elimination to give the B(3)-mono-arylation product **153**. Subsequent B(4)-arylation occurs assisted by the weakly-coordinating amide to generate the B(3,4)-di-arylation product **150**. Due to the innate reactivity of the B(4)–H bond in **153**, which is inherently higher than that of the B(6)–H bond, the B(3,6)-di-arylation product is not formed.



Scheme 3.4.2. Proposed mechanism for palladium-catalyzed B(3,4)-arylation.

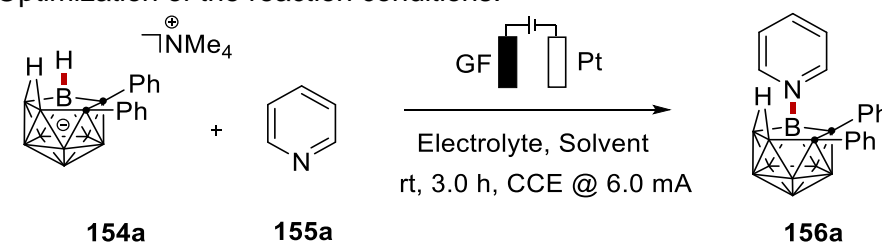
3.5 Electrochemical B–H Nitrogenation of *nido*-Carboranes

While the use of electricity as a redox reagent to facilitate chemical reactions has been recognized as an increasingly viable and environmentally-friendly strategy,^[90, 209] the merger of electrosynthesis with cage B–H functionalization of carboranes continues to be scarce. In this context, we have developed a strategy for unprecedented electrochemical regioselective cage B–H nitrogenation of *nido*-carborane in a dehydrogenative manner, assembling a variety of *N*-heterocycle-, amino acid- and BODIPY-labeled *nido*-carboranes.^[223]

3.5.1 Optimization and Scope

The study was started by probing various reaction conditions for the envisioned electrochemical-catalyzed B–N coupling of *nido*-carborane **154** with pyridine **155** at room temperature in an operationally simple undivided cell setup equipped with a GF (Graphite Felt) anode and a Pt-plate cathode (Table 3.5.1). After considerable preliminary experimentation, we were delighted to observe that the desired B-pyridine *nido*-carborane product **156** was obtained in 60% yield in DME/H₂O as the reaction medium (entries 1-4). Further electrolyte optimization indicated that NMe₄Cl was best (entries 5-7). Increasing the amount of H₂O to 1.0 mL led to a significant decrease in the yield (entries 8-9), while reducing it to 0.2 mL increased the catalytic efficiency to 83% isolated yield of product **156** (entry 10). Control experiments confirmed the essential role of the H₂O, the electricity, the NMe₄Cl additive and the GF as the anode material (entries 11-16).

Table 3.5.1: Optimization of the reaction conditions.^[a]



Entry	Electrolyte	Solvent	Yield [%] ^[b]
1	---	MeOH/H ₂ O	8% ^[c]
2	---	THF/H ₂ O	36% ^[c]
3	---	CH ₃ CN/H ₂ O	40% ^[c]
4	---	DME/H ₂ O	60% ^[c]
5	<i>n</i> BuNPF ₆	DME/H ₂ O	20% ^[c]

Results and Discussion

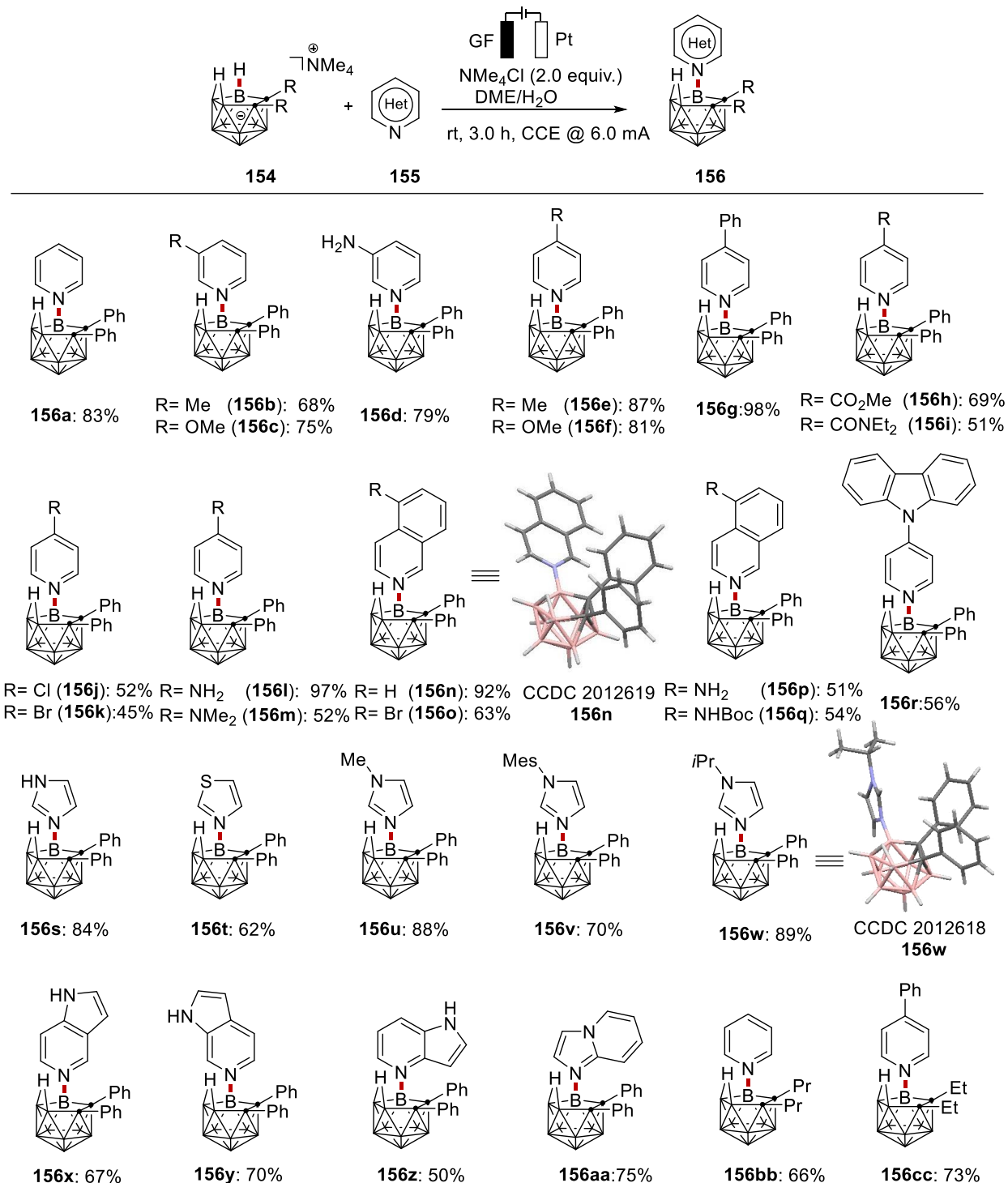
6	<i>n</i> BuNBF ₄	DME/H ₂ O	63% ^[c]
7	NMe ₄ Cl	DME/H ₂ O	65% ^[c]
8	NMe ₄ Cl	DME/H ₂ O	32% ^[d]
9	NMe ₄ Cl	DME/H ₂ O	50% ^[e]
10	NMe₄Cl	DME/H₂O	87% (83%)^[f]
11	NMe ₄ Cl	DME	10%
12	NMe ₄ Cl	DME/H ₂ O	--- ^[g]
13	---	DME/H ₂ O	67%
14	KCl	DME/H ₂ O	75%
15	NaCl	DME/H ₂ O	70%
16	NMe ₄ Cl	DME/H ₂ O	73% ^[h]

[a] Reaction conditions: **154** (0.10 mmol), **155** (0.30 mmol), electrolyte (2 equiv.), DME (4.0 mL), H₂O (0.2 mL), 25 °C, 3 h. [b] Yield was determined by ¹H NMR with CH₂Br₂ as the standard. [c] H₂O (0.5 mL). [d] H₂O (1.0 mL). [e] DME (5.0 mL), H₂O (1.0 mL). [f] Isolated yields in parenthesis. [g] No electricity. [h] Pt-plate as anode. DME = 1,2-Dimethoxyethane, THF = Tetrahydrofuran.

With the optimized reaction conditions in hand, we probed its versatility for the B–N coupling of *nido*-carboranes **154** with different *N*-heterocyclic substrates **155** (Scheme 3.5.1.1). Electron-rich as well as electron-deficient groups on the pyridine **155** were amenable to the electrocatalyzed B–H oxidation coupling, providing the corresponding products in good to excellent yields (**156a-156m**). Thereby, a variety of synthetically useful functional groups, such as ester (**156h**), amide (**156i**), chloro (**156j**) and bromo (**156k**), were fully tolerated, which could prove instrumental for further late-stage manipulations. In addition, various isoquinolines (**155n-155q**) and even the carbazole-substituted pyridine (**155r**), afforded the corresponding electro-oxidative B–N coupling product in good to excellent yields (**156n-156r**). Notably, the free *NH*₂-amino group (**155d**, **155l**) was also tolerated under the mild electro-oxidative conditions, although the amine-substituted and *Boc*-protected amino isoquinoline products (**156p-156q**) were isolated in somewhat lower yields. Interestingly, the Steglich catalyst 4-dimethylaminopyridine (DMAP) was also a competent pyridine derivative in the electrochemical reaction, providing the DMAP decorated *nido*-carborane product (**156m**) with good efficacy.

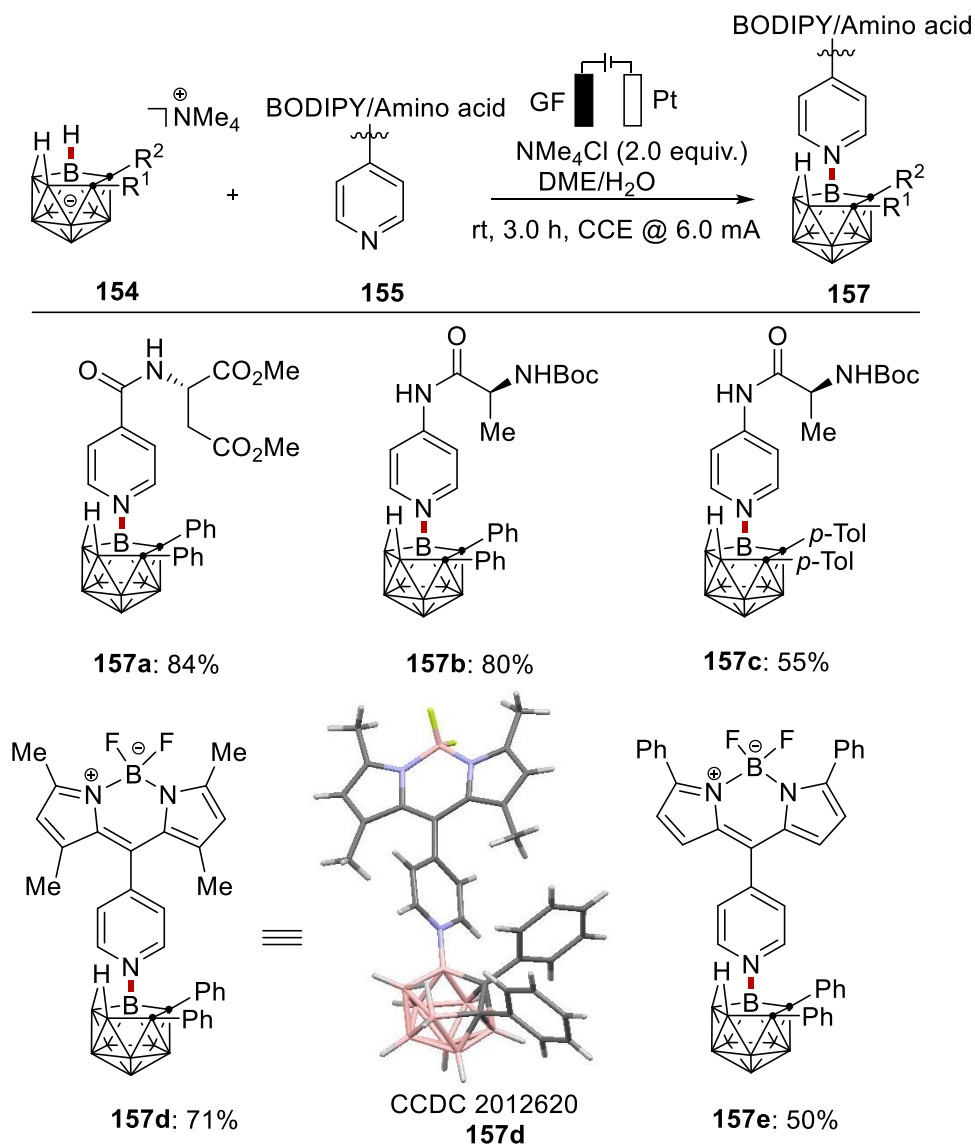
The robustness of the electrooxidative B–N formation at room temperature was next evaluated by other *N*-heterocyclic substrates, such as imidazole with *N* = 11.47 in MeCN according to the Mayr's scale,^[224] *N*-substituted derivatives of imidazoles, thiazole and azaindoles, giving the corresponding B–N products in good to excellent yields (**156s-156aa**). In addition, dialkyl

substituted *nido*-carboranes at the C(cage) site also proceed well under these electrochemical conditions, providing the corresponding B–N coupling products in good yields (**156bb-156cc**). Thus, the oxidant- and catalyst-free electrochemical oxidative B–N coupling provides a new route to a convenient and versatile synthesis of *N*-heterocycle-substituted *nido*-carboranes.



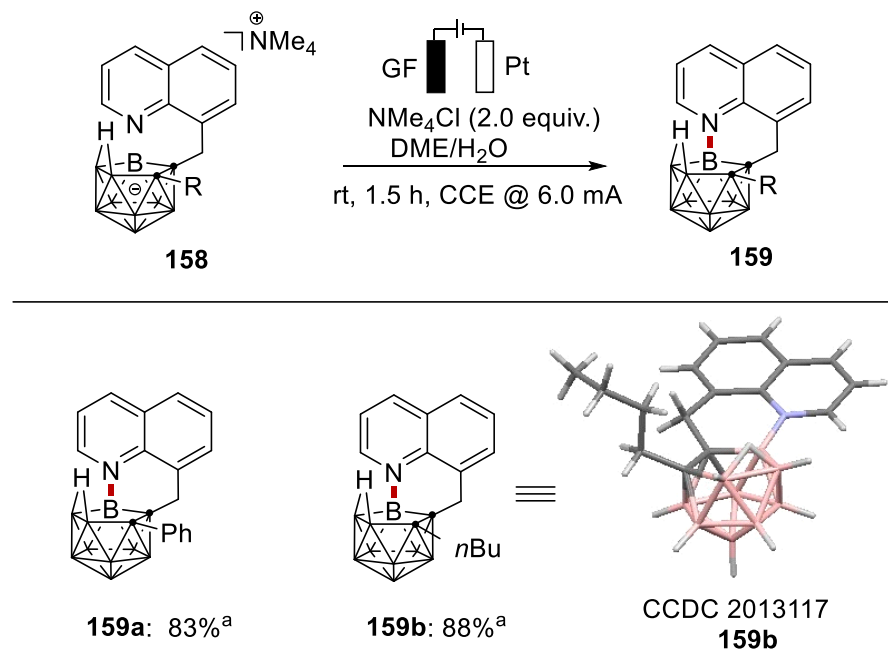
Scheme 3.5.1.1. Electrooxidative B–H nitrogenation of *nido*-carborane with *N*-heterocycles. (**156b-156g**, **156i-156k**, **156q**, **156s**, **156t** and **156x-156aa** did by Becky Bongsuiru Jei)

Encouraged by the unique efficiency of the electrocatalyzed metal-free B–N oxidative coupling with various *N*-heterocyclic substrates, we became intrigued to explore the late-stage amino acid and BODIPY diversification of structurally complex *nido*-carboranes (Scheme 3.5.1.2). Both amino acid- and BODIPY-labeled pyridine proved to be suitable substrates (**157a–157e**).



Scheme 3.5.1.2. Electrooxidative B–H nitrogenation of *nido*-carborane with amino acids and BODIPY pyridines. (**157c** did by Becky Bongsuiru Jei)

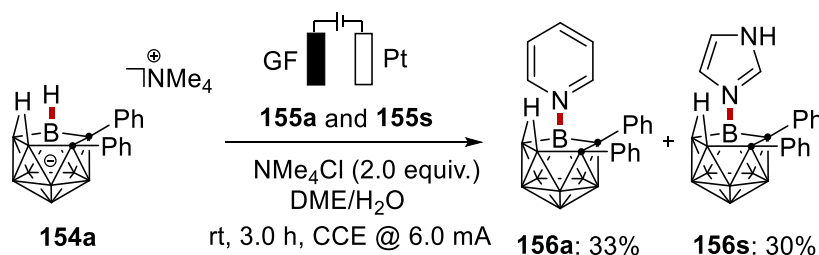
The strategy was not restricted to intermolecular transformations. Actually, the intramolecular B–N couplings of *nido*-carborane **158** was likewise accomplished (Scheme 3.5.1.3), and either aryl or alkyl substituents at the cage-carbon site afforded comparable results (**159a**, **159b**).



Scheme 3.5.1.3. Electrooxidative intramolecular B–N annulation.

3.5.2 Competition Experiments

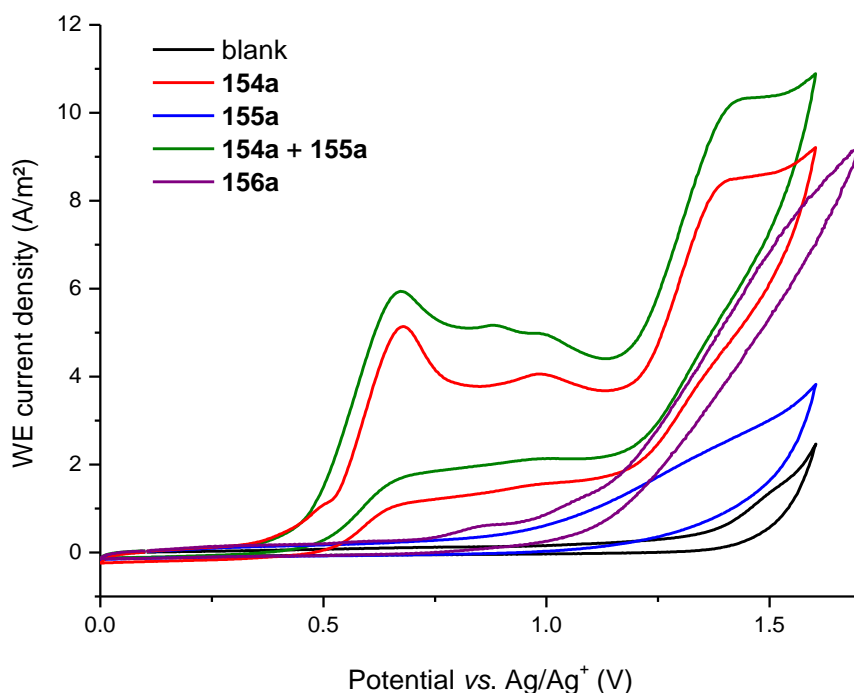
The high efficacy of the electrocatalyzed B–H activation for the synthesis of *N*-heterocyclic *nido*-carboranes motivated us to delineate its mode of action. Thus, an intermolecular competition experiment between pyridine and imidazole revealed a slight preference for pyridine, likely due to the higher nucleophilicity of pyridine when compared to imidazole (pyridine: $N = 11.05$ in H₂O, imidazole: $N = 9.63$ in H₂O)^[224] (Scheme 3.5.2).



Scheme 3.5.2. Competition experiments.

3.5.3 Cyclic Voltammetry and Stability of 156a

Furthermore, we probed the electrochemical B–H activation by means of cyclic voltammetric analysis of the *nido*-carborane along with Msc. Alexej Scheremetjew in the Ackermann group (Scheme 3.5.3). Thus, we observed an irreversible oxidation of the *nido*-carborane at $E_{p/2} = 0.56$ V vs. Ag/Ag⁺ at ambient temperature, which is indicative of a direct oxidation of the *nido*-carborane under electrochemical condition. Furthermore, the calculated half-wave oxidation potential of **154a** using DFT computation by Dr. Rositha Kuniyil at the B97D3/def2-QZVP+CPCM(DME)//B97D3/def2-TZVP level of theory is in good agreement with the one observed in our CV studies (exp: $E_{p/2} = 0.87$ V vs. SCE, calc: $E_{1/2} = 0.86$ V vs. SCE). Then, we also analyzed the thermal and chemical stability of **156a**. We found that compound **156a** (0.4 mL DMSO-*d*₆) was quite stable when being heated to 120 °C for 10 h with only minor decomposition. In addition, the solution of **156a** (0.4 mL CD₃CN) was treated with 0.1 mL H₂O, HCl, or NaOH, respectively. To this end, the ¹¹B NMR experiments demonstrate that **156a** has an excellent stability in a neutral environment, however, it is not stable in strongly acidic or alkaline environments.



Scheme 3.5.3. Cyclic voltammograms at 100 mV/s, *n*Bu₄NPF₆ (0.1M in DME), concentration of substrates 1.0 mM. CV was performed by Msc. Alexej Scheremetjew.

3.5.4 Spectroscopic Data of BODIPY-Labelled *nido*-Carborane

The optical properties of the thus-obtained novel BODIPY-labeled *nido*-carborane **157d** and **157e** were studied in detail by UV-Vis absorption and fluorescence spectroscopy in various solvents (Table 3.5.4). The unprecedented BODIPY-labeled *nido*-carboranes exhibited very intense absorption in the UV and visible region, with an absorption maximum between 507–582 nm and high Stokes shift, resulting in an intense red to purple color. This could be rationalized by the possible donor–acceptor–donor structure of the compounds **157d** and **157e**, as the *nido*-carborane core is an electron acceptor. These spectroscopic data indicated the unique potential applications of the BODIPY-labeled *nido*-carborane compounds in pharmaceuticals, luminescent materials and bioimaging.

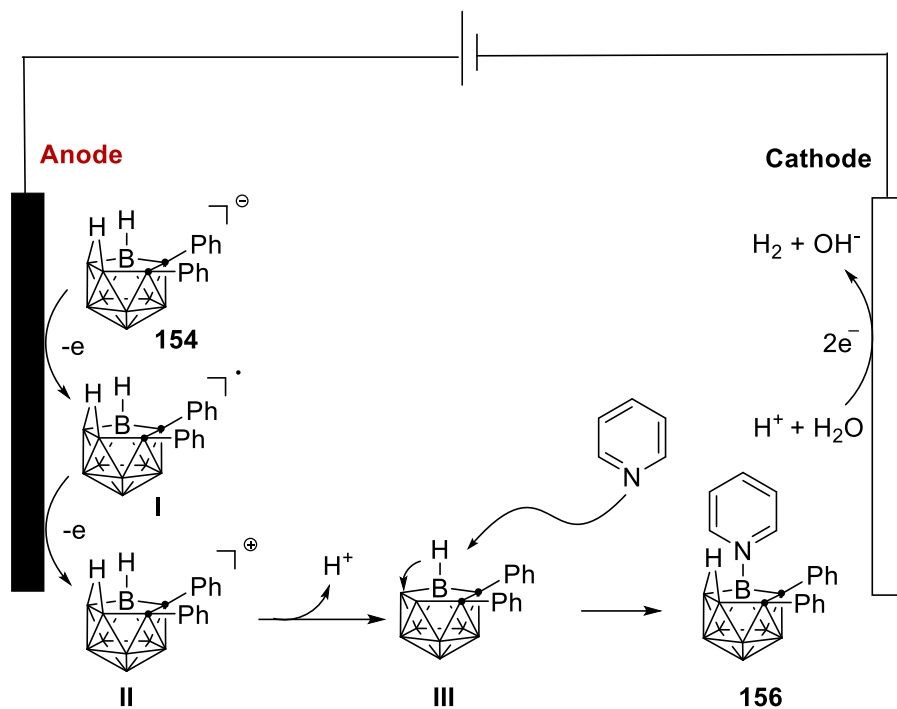
Table 3.5.4. Spectroscopic data of BODIPY-labelled *nido*-carboranes **157d** and **157e**.

Compound	Solvent	$^{Max}\lambda_{abs}$ [nm]	$^{Max}\lambda_{em}$ [nm]	Stokes shift [cm^{-1}]	ϵ_{max} [$M^{-1}cm^{-1}$]
157d	DCM	512	569	1956	68812
	CHCl ₃	513	567	1856	69790
	Actone	507	559	1834	73746
	DMF	509	561	1821	69557
	THF	509	562	1852	72549
157e	DCM	577	634	1558	63459
	CHCl ₃	582	640	1557	60882
	Actone	570	623	1492	65681
	DMF	574	602	810	58557
	THF	575	630	1518	67718

3.5.5 Proposed Mechanism

Based on CV analysis and literature reports,^[225] a plausible reaction mechanism is proposed in Scheme 3.5.5, which commences with an anodic single electron-transfer (SET) process from *nido*-carborane anion to form intermediate **I**, followed by the oxidation to generate intermediate **II**. Subsequently, deprotonation of the bridge proton results in the formation of cage-open carborane intermediate **III**. Finally, the pyridine undergoes nucleophilic attack on the electron

deficient B(9/11)-H site of the intermediate **III** with consecutive transfer of H to the B(10) and B(11) forming a new bridge proton. In addition, molecular H₂ is generated as the by-product through cathodic proton reduction, which was confirmed by head-space GC analysis.



Scheme 3.5.5. Proposed reaction mechanism.

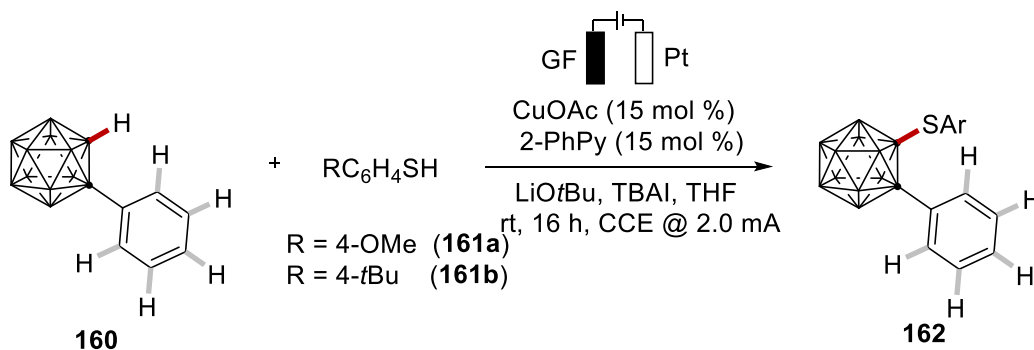
3.6 Cupraelectro-Catalyzed Chalcogenations of *o*-Carboranes

In this section, we will disclose copper-catalyzed electrochemical direct chalcogenations of *o*-carboranes at room temperature. Thereby, a series of cage C-sulfonylated and C-selenylated *o*-carboranes anchored with valuable functional groups were accessed with high levels of position- and chemo-selectivity control. The cupraelectrocatalysis provided efficient approaches to activate otherwise inert cage C–H bonds for the late-stage diversification of *o*-carboranes.

3.6.1 Optimization and Scope

We commenced our studies by probing various reaction conditions for the envisioned copper-catalyzed cage C–H thiolation of *o*-carborane in an operationally simple undivided cell setup equipped with a GF (graphite felt) anode and a Pt cathode (Table 3.6.1). After extensive experimentation, we observed that the thiolation of substrate **160** proceeded efficiently with catalytic amounts of CuOAc and 2-phenylpyridine in the presence of LiOtBu as the base, *n*-Bu₄NI as the electrolyte at room temperature under a constant current of 2 mA (entry 1). The yield was reduced when other copper sources or additives were used (entries 2-5). Surprisingly, *n*-Bu₄NPF₆ as the electrolyte failed to facilitate the carborane modification, indicating that *n*-Bu₄NI operates not only as electrolyte, but also as a redox mediator (entry 6). Altering the stoichiometry of the electrolyte or using KI did not improve the performance (entries 7,8). Product formation was not observed, when the reaction was conducted with DCE as the solvent, while CH₃CN resulted in a drop of the catalytic performance (entries 9,10). Control experiments confirmed the essential role of the electricity and the catalyst (entries 11,12), while a sequential procedure was found to be beneficial (entries 13-15).

Table 3.6.1: Optimization of the reaction conditions.^[a]



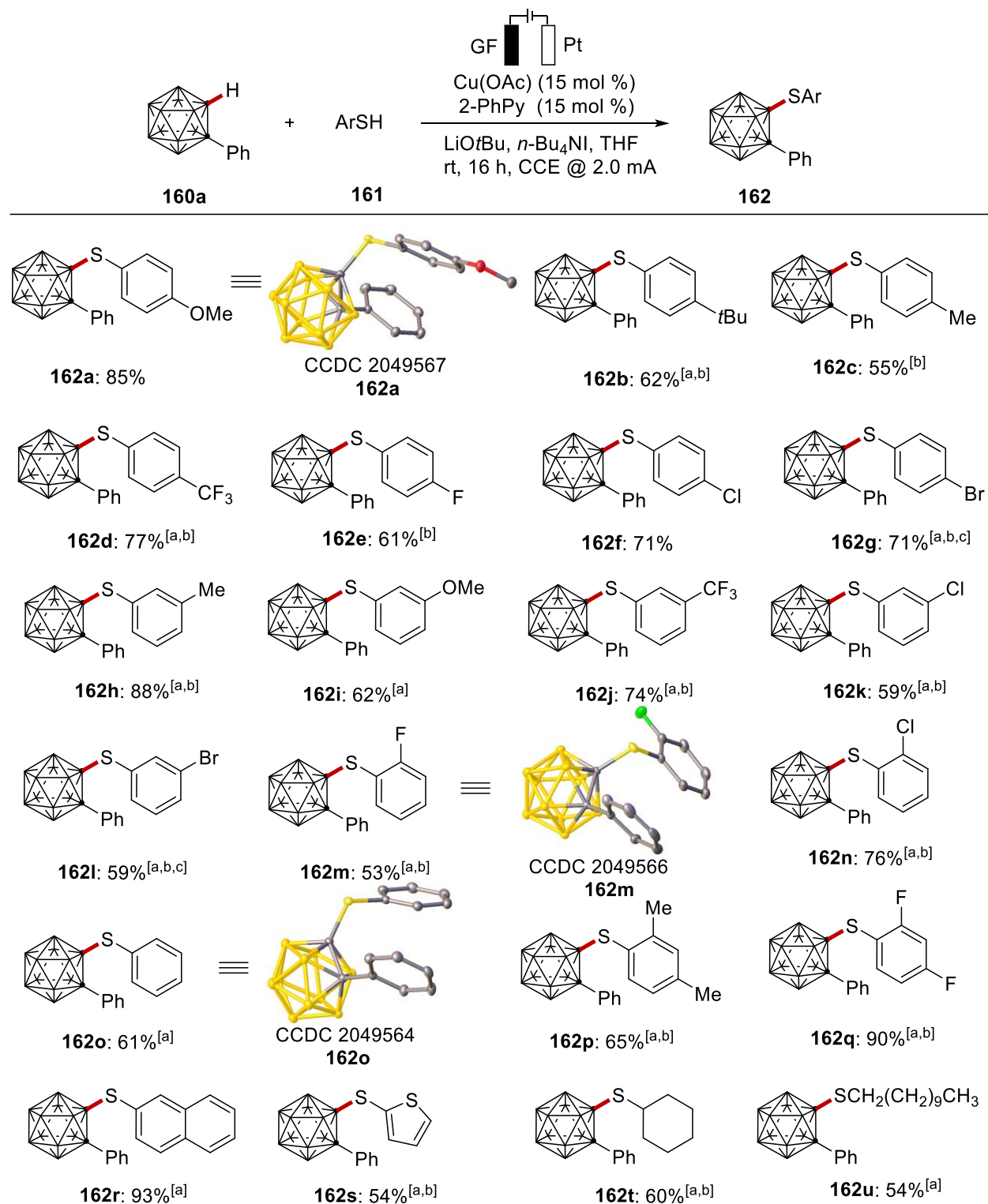
Results and Discussion

Entry	Deviation from standard conditions	Yield [%] ^[b]
1	none	90% (85%) ^[c]
2	Cu(OAc) ₂ instead of CuOAc	51%
3	CuI instead of CuOAc	43%
4	2,6-Lutidine instead of 2-PhPy	71%
5	1,10-Phen instead of 2-PhPy	16%
6	TBAPF ₆ instead of TBAI	---
7	TBAI (3 equiv.)	49%
8	KI (1 equiv) as additive	67%
9	DCE instead of THF	---
10	CH ₃ CN instead of THF	49%
11	No electricity	14% ^[d]
12	No [Cu]	---
13	Procedure B (161b)	66% (62%) ^[e,d]
14	Procedure B: second step without electricity (161b)	--- ^[f]
15	Procedure B (161a)	92% ^[e]

[a] Reaction conditions: Procedure A: **160a** (0.10 mmol), **161a** (0.3 mmol), CuOAc (15 mol %), 2-PhPy (15 mol %), LiOtBu (0.2 mmol), TBAI (2.0 equiv.), solvent (3.0 mL), platinum cathode (10 mm × 15 mm × 0.25 mm), graphite felt (GF) anode (10 mm × 15 mm × 6 mm), 2 mA, under air, rt, 16 h. [b] Yield was determined by ¹H NMR with CH₂Br₂ as the internal standard. [c] Isolated yields in parenthesis. [d] KI (1.0 equiv) as additive. [e] Procedure B: **161a** (0.3 mmol), LiOtBu (0.2 mmol), TBAI (2.0 equiv.), solvent (3.0 mL), 2 mA, rt, 3 h, then adding **160a** (0.10 mmol), 2-PhPy (15 mol %), CuOAc (15 mol %), 2 mA, rt, 16 h. [f] **161b** (0.3 mmol), LiOtBu (0.2 mmol), KI (1.0 equiv.), TBAI (2.0 equiv.), solvent (3.0 mL), 2 mA, rt, 3 h, then adding **160a** (0.10 mmol), 2-PhPy (15 mol %), CuOAc (15 mol %), rt, 16 h.

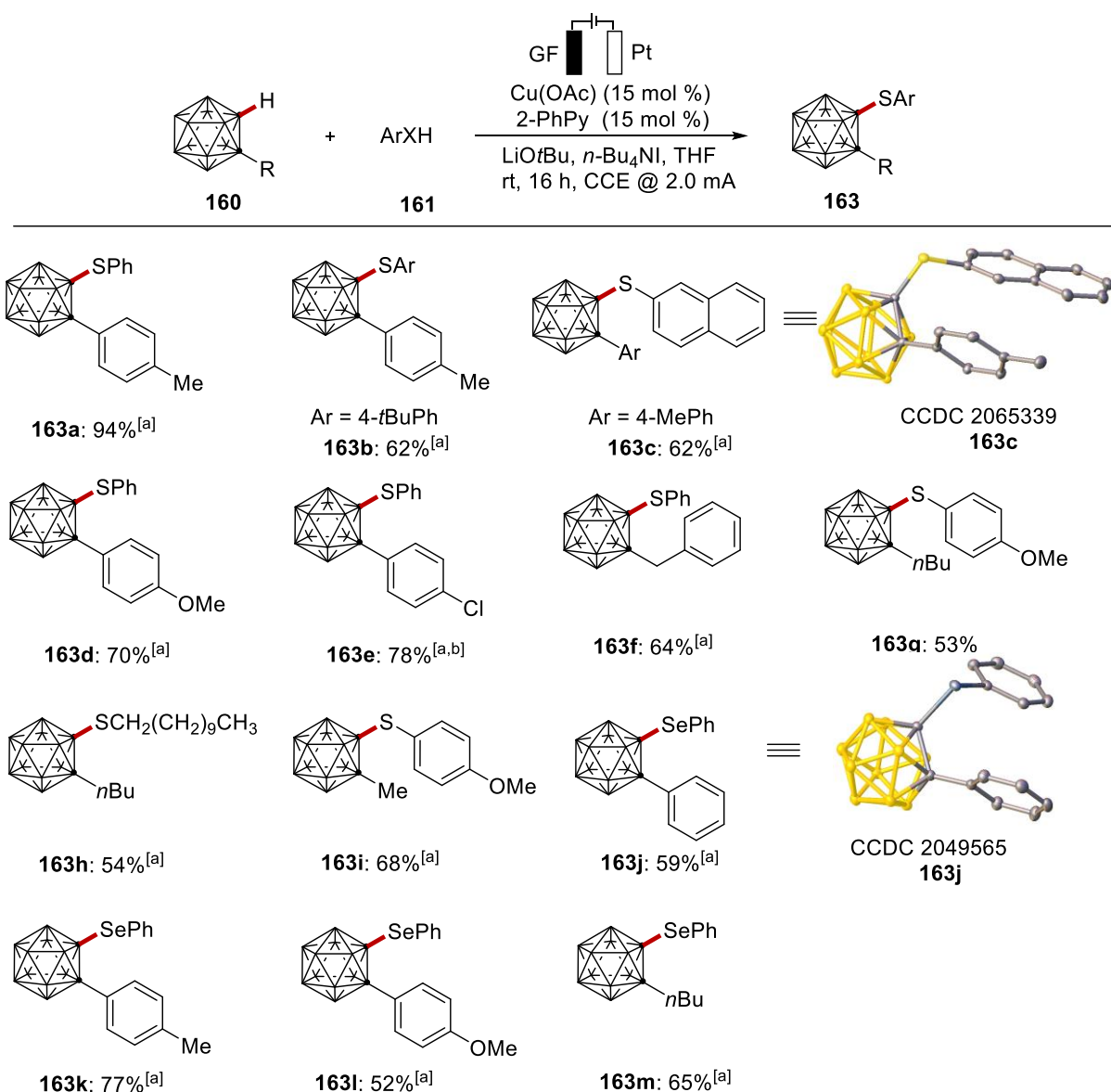
With the optimized reaction conditions in hand, we explored the versatility of the cage C–H thiolation of *o*-carborane **160a** with different thiols **161** (Scheme 3.6.1.1). Electron-rich as well as electron-deficient substituents on the arenes were found to be suitable for the electrocatalyzed C–H activation, providing the corresponding thiolation products **162a-162o** in good to excellent yields. Thereby, a variety of synthetically useful functional groups, such as fluoro (**162e** and **162m**), chloro (**162f**, **162k**, and **162n**) and bromo (**162g** and **162l**), were fully tolerated, which should prove instrumental for further late-stage manipulations. Various disubstituted aromatic and heterocyclic thiols afforded the corresponding cage C–S modified products **162p-162s**. Notably, aliphatic thiols efficiently underwent the electrochemical transformation to provide the corresponding cage alkylthiolated products **162t-162u**.

Results and Discussion



Scheme 3.6.1.1. Electrochemical C–H thiolation of *o*-carborane. ^[a] Procedure B. ^[b] KI (1 equiv.). ^[c] Cul as the catalyst. (162c–162d, 162g–162h, 162j–162l, 162n, 162p–162r, 162t did by Becky Bongsuiru Jei)

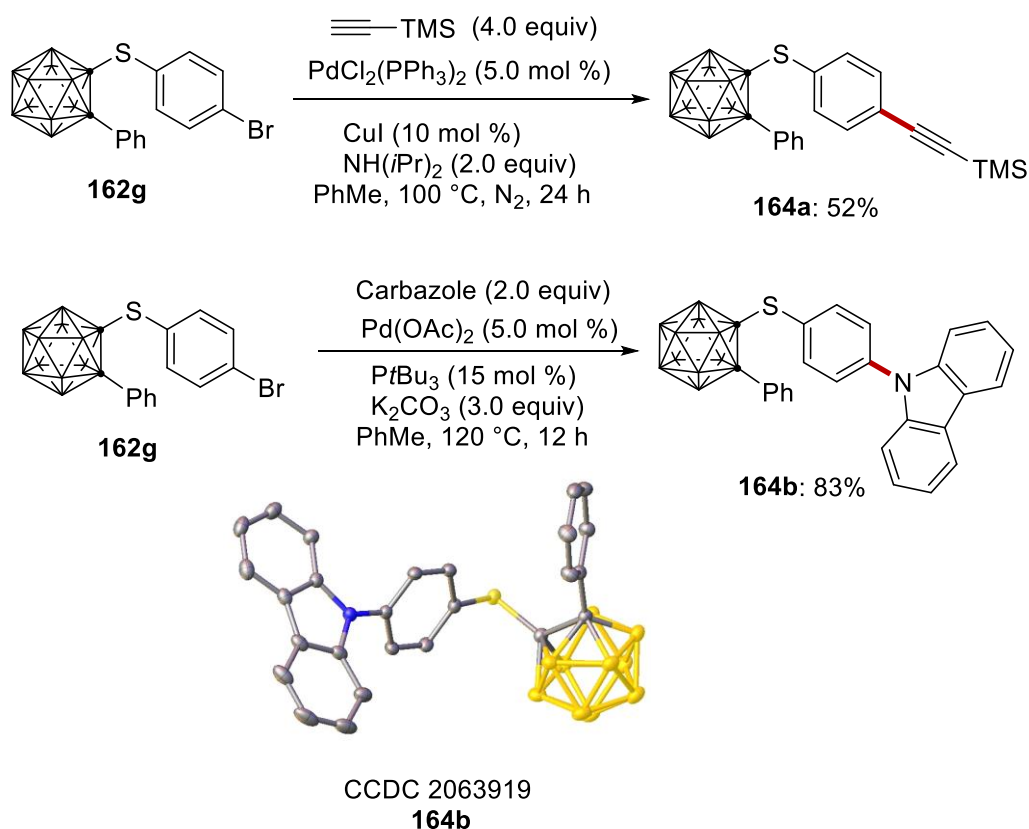
Encouraged by the efficiency of the cupraelectro-oxidative cage C–H thiolation, we became intrigued to explore the chalcogenation of differently-decorated *o*-carboranes **160** (Scheme 3.6.1.2). Electronically diverse *o*-carboranes **160** served as competent coupling partners, giving the corresponding thiolation products (**163a-163e**) with high levels of efficacy in a position-selective manner. The strategy was not restricted to phenyl-substituted *o*-carboranes. Indeed, substrates bearing benzyl and even alkyl groups also performed well to deliver the desired products **163f-163i**. It is noteworthy that the C–H activation approach was also compatible with selenols to give the *o*-carborane **163j**.



Scheme 3.6.1.2. Electrochemical C–H chalcogenation of *o*-carboranes. ^[a] Procedure B. ^[b] KI (1 equiv.). (**163a**, **163c**, **163d** and **163e** did by Becky Bongsuiru Jei)

3.6.2 Late-stage Functionalization

Next, late-stage functionalization of the thus obtained carborane **162g** was studied. Sonogashira-Hagihara coupling of carborane **162g** with trimethylsilylacetylene gave the alkynylated derivative **164a** (Scheme 3.6.2). Buchwald-Hartwig amination of carborane **162g** with carbazole selectivity resulted in the formation of amine **164b**, which offers a new route to cage C-substituted carborane-based host materials for possible applications to phosphorescent organic light-emitting diodes.^[226]



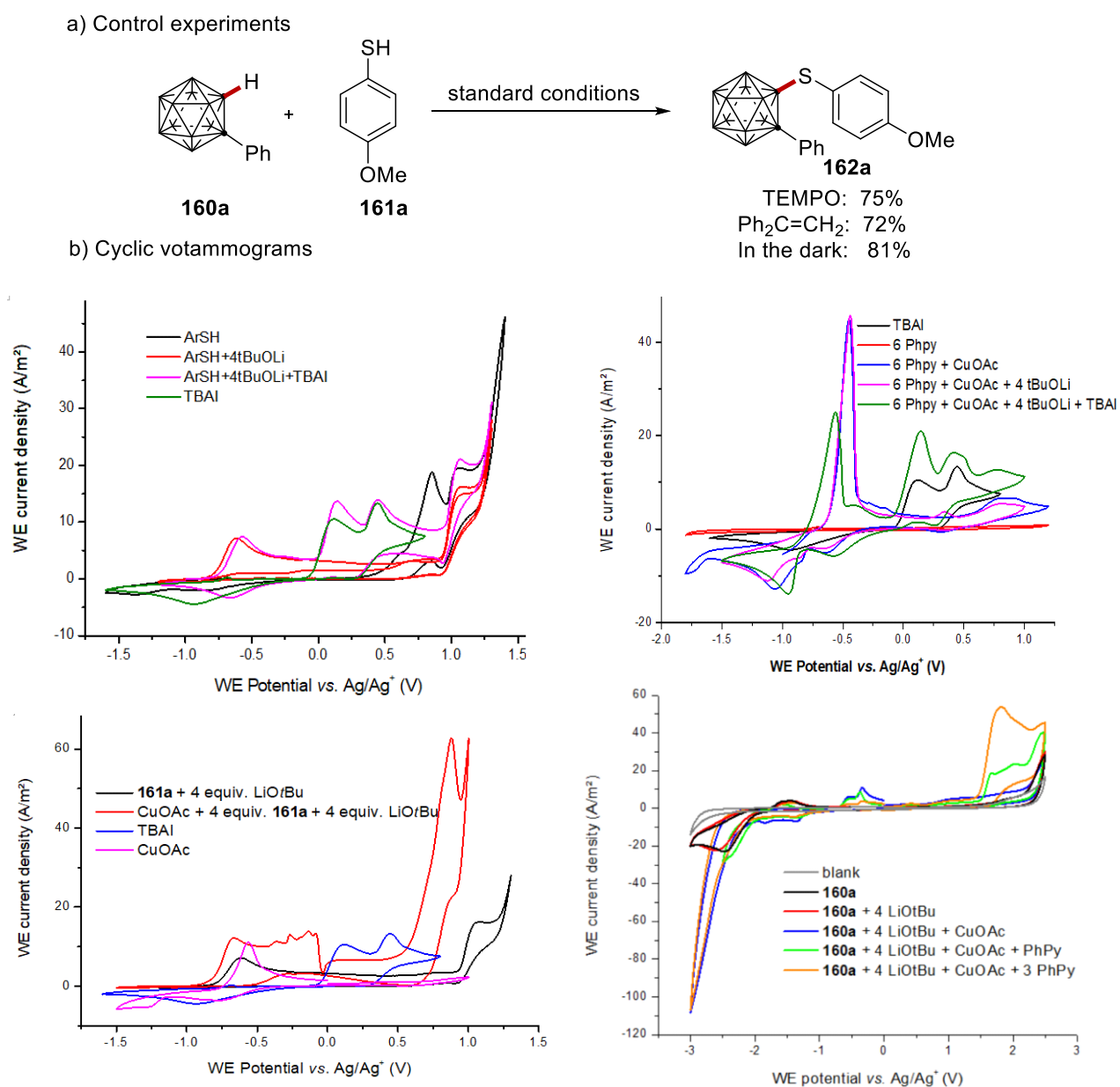
Scheme 3.6.2. Late-stage diversification.

3.6.3 Control Experiments and Cyclic Voltammograms

The high efficacy of the cupraelectro-catalyzed cage C–H chalcogenation motivated us to delineate the mode of action. To this end, control experiments were performed (Scheme 3.6.3a). First, electrocatalysis in the presence of TEMPO or $\text{Ph}_2\text{C}=\text{CH}_2$ gave the desired product **162a**. Second, the cupraelectrocatalysis occurred efficiently in the dark. Third, detailed

Results and Discussion

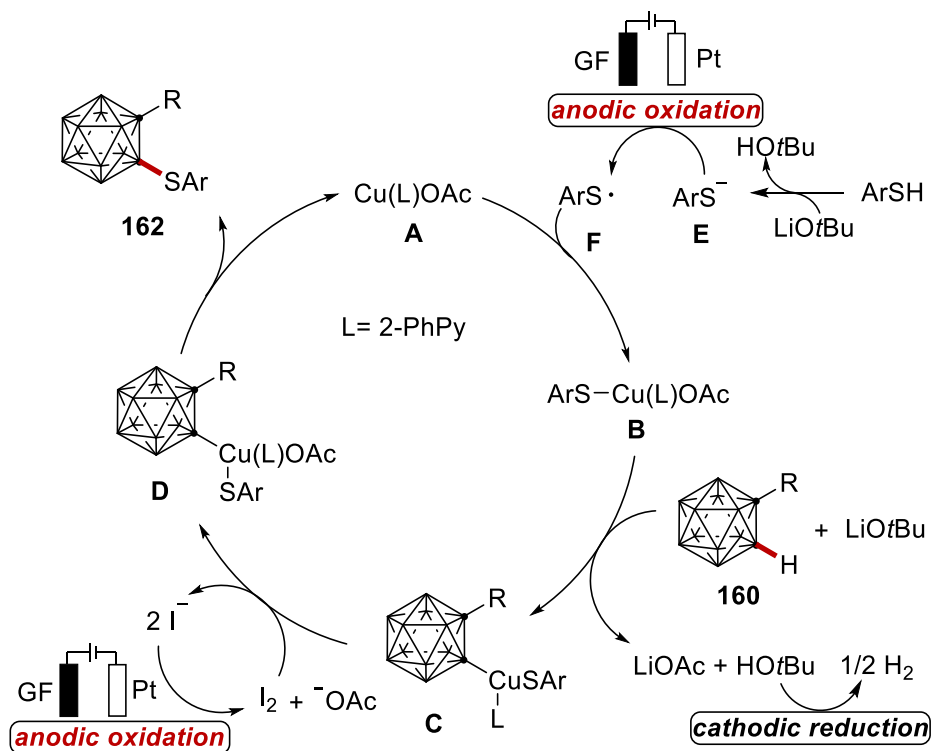
cyclovoltammetric analysis of the thiol and iodide mediator by Msc. Alexej Scheremetjew (Scheme 3.6.3b) showed an irreversible oxidation of the thiol anion at $E_p = -0.62$ V vs. Ag/Ag⁺ and two oxidation events for the iodide at $E_p = 0.12$ V vs. Ag/Ag⁺ and $E_p = 0.44$ V vs. Ag/Ag⁺, which is in agreement with the literature reported iodide oxidation potential^[227] and suggestive of the preferential oxidation of the iodide as redox mediator. Moreover, the use of *n*-Bu₄NI as a redox mediator to achieve copper-catalyzed electrochemical C–H amination of arenes was also documented.^[138]



Scheme 3.6.3. Control experiments and cyclic voltammograms. CV studies did by Msc. Alexej Scheremetjew.

3.6.4 Proposed Mechanism

Based on the findings, a plausible reaction mechanism is proposed in Scheme 3.6.4, which commences with an anodic single electron-transfer (SET) oxidation of the thiol anion **E** to form the sulfur-centered radical **F**. Subsequently, the copper(I) species **A** reacts with the sulfur radical **F** to deliver copper(II) complex **B**, which next reacts with *o*-carborane **160a** in the presence of LiOtBu to generate a copper(II)-*o*-carborane complex **C**. Thereafter, the complex **C** is oxidized by the anodically generated redox mediator I₂ to furnish the copper(III) species **D**, which subsequently undergoes reductive elimination, affording the final product and regenerating the catalytically active complex **A**. Alternatively, the direct oxidation of copper(II) complex **C** by electricity to generate copper(III) species **D** can not be excluded at this stage.



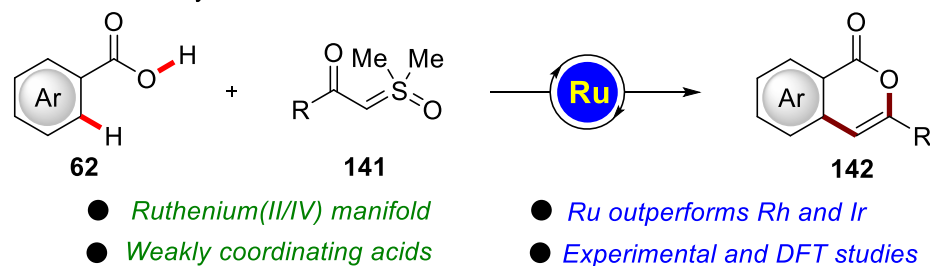
Scheme 3.6.4. Proposed reaction mechanism.

4. Summary and Outlook

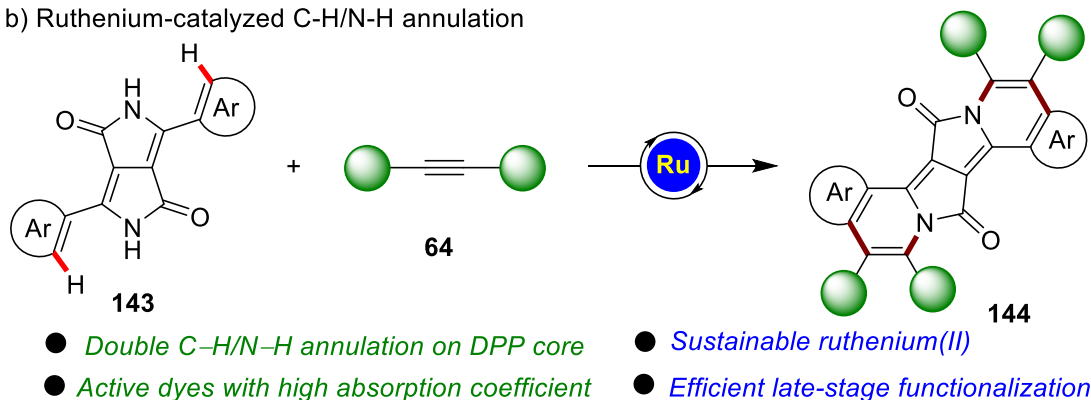
The development of highly step- and atom-economical C–H, and B–H activations by inexpensive and Earth-abundant metals has emerged as an increasingly powerful tool in molecular syntheses. The selective functionalization of otherwise inert C–H bonds remains a big challenge due to the ubiquitous C–H bonds in organic compounds. Despite remarkable advances in the field, most of the reported approaches largely relied on precious metal catalysts, harsh reaction conditions and the necessity of stoichiometric amounts of chemical oxidants, compromising the overall sustainability of the strategy. In this thesis, new methods have been developed for sustainable selective C–H activation and cage B–H/C–H activation of carboranes by cost-effective ruthenium, ruthenaelectro-catalysis and cupraelectro-catalysis.

In the first part, we have unraveled ruthenium(IV) complexes as key intermediates in redox-neutral C–H/O–H activation of benzoic acid with easily-accessible sulfoxonium ylides by weak O-coordination. Based on the experimental and computational studies, a ruthenium(II/IV) catalysis manifold was proposed for the synthesis of various isocomarin derivatives ([Scheme 4.1a](#)). Furthermore, a new strategy towards the synthesis of π -extended DPPs was presented that employed sustainable, inexpensive, and widely applicable ruthenium catalysis. This method allowed for the rapid synthesis of new DPP derivatives, featuring various substituents on the ethylene bridge ([Scheme 4.1b](#)).

a) Ruthenium-catalyzed C–H/O–H annulation



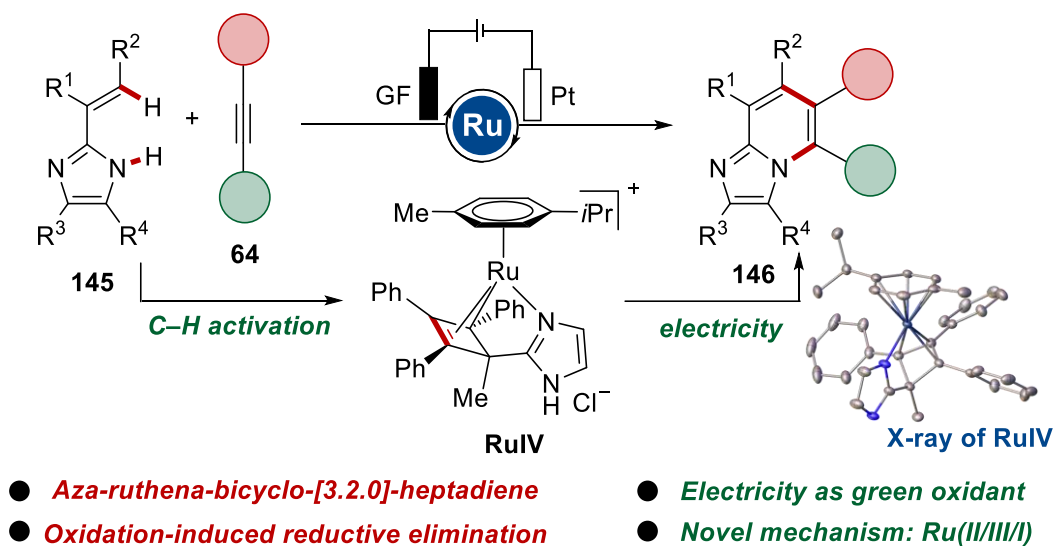
b) Ruthenium-catalyzed C–H/N–H annulation



Scheme 4.1. Ruthenium-catalyzed annulations.

In contrast to the chemical oxidative C–H functionalizations, electrocatalytic C–H activations employ electricity as the redox reagent to replace toxic and expensive chemical oxidants, which has been recognized as an increasingly viable, environmentally-friendly strategy and closely related to the trend of atom- and step-economy.

In the second part, we have reported on the electrocatalytic organometallic C–H/N–H functionalization of imidazoles (Scheme 4.2). Novel aza-ruthena-bicyclo-[3.2.0]-heptadienes were isolated and identified as the key intermediates, setting the stage for alkyne annulations from synthetically meaningful alkenyl and aryl imidazoles with ample scope. The C–H activation employed electricity as the only oxidant and generated molecular hydrogen as the sole byproduct. Mechanistic studies by experiment and DFT provided strong support for an oxidation-induced reductive elimination of aza-ruthena-bicyclo-[3.2.0]-heptadienes by environmentally-benign electricity. These findings should prove instrumental for the mechanistic understanding and design of ruthenium(II)-catalyzed oxidative C–H activations.

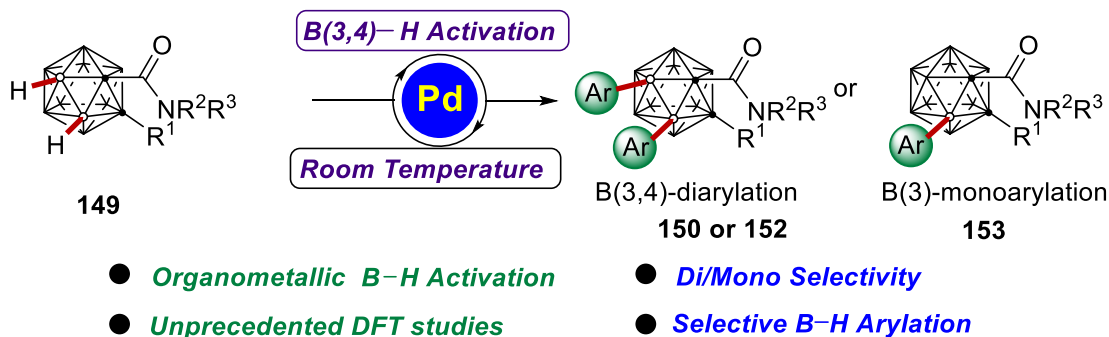


Scheme 4.2. Ruthenaelectro(II/III/I)-catalyzed alkyne annulations.

In the third part, we described the cage B–H/C–H functionalizations of carboranes.

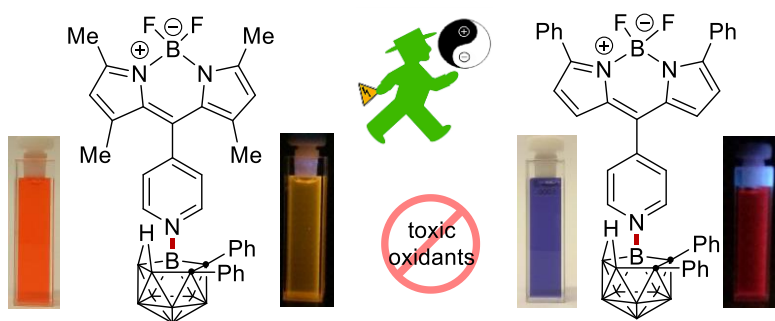
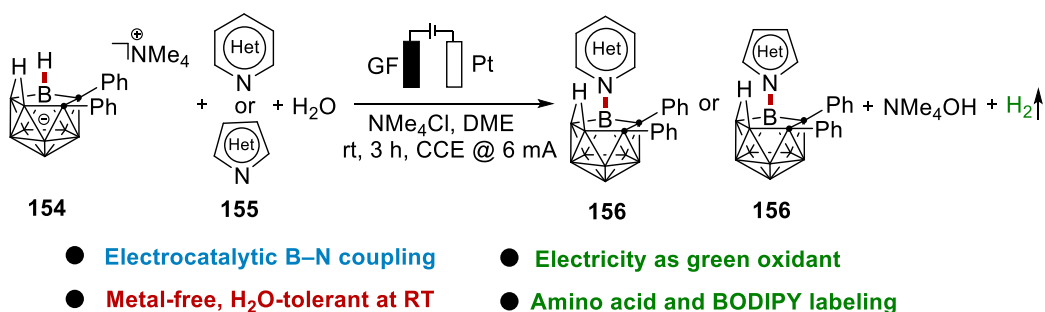
First, a palladium-catalyzed direct arylations at cage B(3,4) positions in *o*-carboranes has been achieved at room temperature with the aid of weakly-coordinating, synthetically useful amides (Scheme 4.3). Thus, palladium-catalyzed B–H activations enabled the assembly of a variety of arylated *o*-carboranes. This method featured high position-selectivity, high tolerance of functional groups, and mild reaction conditions, thereby offering a platform for the design and synthesis of boron-substituted *o*-carboranes. Our findings offered a facile strategy for selective activations of

B(3,4)-H bonds, which will be instrumental for future design of optoelectronics nanomaterials, and boron neutron capture therapy agents.



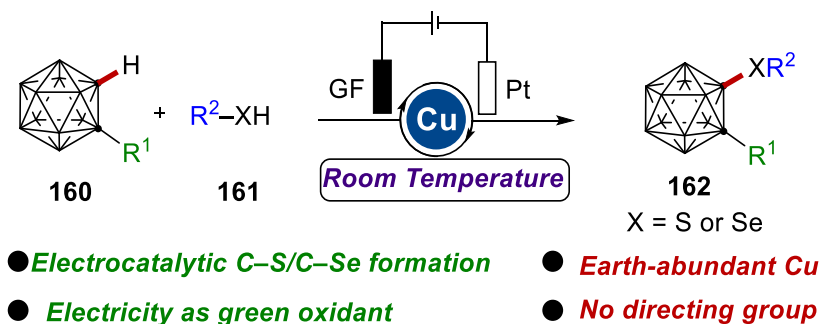
Scheme 4.3. Palladium(II)-catalyzed B(3,4)-H arylation of *o*-carboranes.

Second, metal-free electrocatalyzed direct B-N oxidative couplings of *nido*-carborane with *N*-heterocyclic compound have been achieved at room temperature with molecular hydrogen as the sole by-product (Scheme 4.4). This method featured mild reaction conditions and high tolerance of functional groups leading to various amino acid- and BODIPY-labeled *nido*-carboranes, thereby offering a new platform for the design and synthesis of *N*-substituted *nido*-carborane by environmentally-benign electricity. A plausible mechanism was established by cyclic voltammetry studies and computation. The thus-obtained BODIPY-labeled *nido*-carborane displayed enhanced spectroscopic features.



Scheme 4.4. Electrocatalyzed B-H nitrogenation of *nido*-carboranes.

Last, an efficient and operationally-benign electrocatalytic organometallic cage C–H chalcogenation of *o*-carboranes with thionols and selenols has been achieved at room temperature. This strategy featured mild reaction conditions and high tolerance of functional groups, leading to the facile assembly of a series of *o*-carboranes, thereby offering a new platform for the design of cage C–S/Se substituted *o*-carboranes by environmentally-sound electricity. A plausible mechanism was established by control experiments and detailed cyclic voltammetry studies. Our findings should prove instrumental for the further development of decorated carboranes and boron clusters by molecular electrocatalysis.



Scheme 4.5. Cupraelectro-catalyzed C–H chalcogenation of *o*-carboranes **160**.

5. Experimental Section

5.1 General Remarks

Catalytic reactions under an atmosphere of air were conducted in the sealed tubes or Schlenk tubes. Unless otherwise noted, other reactions were performed under N₂ atmosphere using pre-dried glassware and standard Schlenk techniques.

If not otherwise noted, yields refer to isolated compounds, estimated to be >95% pure as determined by ¹H NMR.

Vacuum

The following pressures were measured on the used vacuum pump and were not corrected: membrane pump vacuum (MPV): 0.5 mbar, oil pump vacuum (OPV): 0.1 mbar.

Melting Points (M.p.)

Melting points were measured using a *Stuart*® Melting Point Apparatus *SMP3* from BARLOWORLD SCIENTIFIC. The reported values are uncorrected.

Chromatography

Analytical thin layer chromatography (TLC) was performed on 0.25 mm silica gel 60F-plates (MACHEREY-NAGEL) with 254 nm fluorescent indicator from MERCK. Plates were visualized under UV-light. Chromatographic purification of products was accomplished by flash column chromatography on MERCK silica gel, grade 60 (0.040–0.063 mm and 0.063–0.200 mm).

Gas Chromatography (GC)

The conversions of the reactions were monitored by applying coupled gas chromatography/mass spectrometry using G1760C GCDplus with mass detector *HP 5971*, *5890 Series II* with mass detector *HP 5972* from HEWLETT-PACKARD and 7890A GC-System with mass detector *5975C (Triplex-Axis-Detector)* from AGILENT TECHNOLOGIES equipped with *HP-5MS* columns (30 m × 0.25 mm × 0.25 m).

Gel Permeation Chromatography (GPC)

GPC purifications were performed on a JAI system (*JAI-LC-9260 II NEXT*) equipped with two sequential columns (*JAIGEL-2HR*, gradient rate: 5.000; *JAIGEL-2.5HR*, gradient rate: 20.000; internal diameter = 20 mm; length = 600 mm; Flush rate = 10.0 mL/min and chloroform (HPLC-quality with 0.6% ethanol as stabilizer) was used as the eluent.

Infrared Spectroscopy

Infrared spectra were recorded with a BRUKER *Alpha-P ATR FT-IR* spectrometer. Liquid samples were measured as a film, solid samples neat. The analysis of the spectra was carried out using the software from BRUKER *OPUS 6*. The absorption was given in wave numbers (cm^{-1}) and the spectra were recorded in the range of 4000–400 cm^{-1} .

Mass Spectrometry

Electron-ionization (EI) mass spectra were recorded on a Jeol AccuTOF instrument at 70 eV. Electrospray-ionization (ESI) mass spectra were obtained on Bruker micrOTOF and maXis instruments. All systems were equipped with time-of-flight (TOF) analyzers. The ratios of mass to charge (m/z) were reported and the intensity relative to the base peak ($I = 100$) is given in parenthesis.

Nuclear Magnetic Resonance Spectroscopy (NMR)

Nuclear magnetic resonance (NMR) spectra were recorded on VARIAN *Inova 500, 600*, VARIAN *Mercury 300, VX 300*, VARIAN *Avance 300*, VARIAN *VNMRS 300* and BRUKER *Avance III 300, 400* and *HD 500* spectrometers. All chemical shifts were given as δ -values in ppm relative to the residual proton peak of the deuterated solvent or its carbon atom, respectively. ^1H and ^{13}C NMR spectra were referenced using the residual proton or solvent carbon peak (see table), respectively. ^{13}C and ^{19}F NMR were measured as proton-decoupled spectra.

	^1H NMR	^{13}C NMR
CDCl_3	7.26	77.16
$[\text{D}]_6\text{-DMSO}$	2.50	39.52

The observed resonance-multiplicities were described by the following abbreviations: s (singlet), d (doublet), t (triplet), q (quartet), hept (heptet), m (multiplet) or analogous representations. The coupling constants J were reported in Hertz (Hz). Analysis of the recorded spectra was carried out with *MestReNova 10* software.

EPR Spectroscopy

EPR spectra were measured on a Bruker ELEXSYS E500 spectrometer, equipped with the digital temperature control system ER 4131VT using nitrogen as coolant. All spectra were measured at room temperature or at temperatures around 150K, and were recorded at about 9.4 GHz microwave frequency, 100 kHz field modulation frequency, and around 10 mW microwave power.

Electrochemistry

Platinum electrodes (10 mm \times 15 mm \times 0.25 mm, 99.9%; obtained from ChemPur® Karlsruhe,

Germany) and graphite felt (GF) electrodes (10 mm × 15 mm × 6 mm, SIGRACELL®GFA 6 EA, obtained from SGL Carbon, Wiesbaden, Germany) were connected using stainless steel adapters. Electrolysis was conducted using an AXIOMET AX-3003P potentiostat in constant current mode. For reactions performed with the standardized electrochemistry kit, *ElectraSyn 2.0* from Ika, the commercialized electrodes and 10 mL undivided cells were used, if not stated otherwise. For reactions in flow an Ismatec REGLO Digital MS-2/12 (ISM 596) peristaltic pump was employed. CV studies were performed using a Metrohm Autolab PGSTAT204 workstation and Nova 2.0 software. Divided cells separated by a P4-glassfrit were obtained from Glasgerätebau Ochs Laborfachhandel e. K. (Bovenden, Germany).

Solvents

All solvents for reactions involving moisture-sensitive reagents were dried, distilled and stored under inert atmosphere (N₂) according to the following standard procedures.

Purified by solvent purification system (SPS-800, M. Braun): CH₂Cl₂, toluene, tetrahydrofuran, dimethylformamide, diethylether, 1,2-dichloroethane, *N*-methyl-2-pyrrolidone (NMP), *N,N*-dimethylacetamide (DMA), dimethylsulfoxide (DMSO) and γ -valerolactone (GVL) was dried over CaH₂ for 8 h, degassed and distilled under reduced pressure. 1,2-dimethoxyethane (DME) was dried over sodium and freshly distilled under N₂. 1,1,1,3,3,3-hexafluoropropan-2-ol (HFIP) was distilled from 3 Å molecular sieves. 2,2,2-trifluoroethanol (TFE) was stirred over CaSO₄ and distilled under reduced pressure. Water was degassed by repeated *Freeze-Pump-Thaw* degassing procedure. 1,4-dioxane and di-*n*-butyl-ether (*n*Bu₂O) were distilled from sodium benzophenone ketyl.

Reagents

Chemicals obtained from commercial sources with purity above 95% were used without further purification. The following compounds were known and were synthesized according to previously described methods.

Sulfoxonium ylides **141**^[228], **143**^[229], **64**^[230], **145**^[231], **147**^[232], **149**^[233], **154**^[225] and **160**^[233].

The following compounds were synthesized and provided by the persons listed below:

Karsten Rauch: [RuCl₂(*p*-cymene)]₂, [Cp*RhCl₂]₂, [Cp*IrCl₂]₂, [Ru(O₂CMe)₂(*p*-cymene)], [Ru(OAc)₂(*p*-cymene).

Cooperation clarification:

In the project of ruthenaelectro-catalytic C–H/N–H annulation, Ralf Steinbock carried out some experiments for the scope (**146c**, **146h**, **146i**, **146l**, **148d**, **148f**, **148h**, **148n**), competition

experiments and GC-Headspace analysis. CV studies were performed by Alexej Scheremetjew. DFT calculations were performed Dr. Rositha Kuniyil. On-line NMR monitoring in flow was performed by Dr. Lars H. Finger. Dr. Antonis M. Messinis helped to get the crystal of ruthenium intermediates.

In the project of metal-free electrocatalytic B–H nitrogenation of *nido*-carboranes, Becky Bongsuiru Jei carried out some experiments for the scope (**156b**, **156c**, **156d**, **156e**, **156f**, **156g**, **156i**, **156j**, **156k**, **156q**, **156s**, **156t**, **156x**, **156y**, **156z**, **156aa**, **157c**). Alexej Scheremetjew carried out GC-Headspace analysis and CV studies. DFT calculations were performed by Dr. Rositha Kuniyil.

In the project of cupraelectro-catalytic C–H chalcogenation of *o*-carboranes, Becky Bongsuiru Jei carried out some experiments for the scope (**162c**, **162d**, **162g**, **162h**, **162j**, **162k**, **162l**, **162n**, **162p**, **162q**, **162r**, **162t**, **163a**, **163c**, **163d**, **163e**). Alexej Scheremetjew carried out CV studies. Binbin Yuan carried out DFT studies. Dr. A. Claudia Stückl carried out EPR measurements and analyzed all EPR data. Dr. Christopher Golz analyzed all the X-ray data in the thesis.

5.2 General Procedures

General Procedure A: Ruthenium(II)-Catalyzed C–H/O–H Annulation of *ortho*-Substituted Benzoic Acids

Benzoic acid **62** (0.25 mmol), sulfoxonium ylide **141** (0.38 mmol), [RuCl₂(*p*-cymene)]₂ (3.8 mg, 2.5 mol %), AgSbF₆ (8.6 mg, 10 mol %), NEt₃ (51 mg, 2.0 equiv), and DCE (2.0 mL) were placed in a 25 mL Schlenk flask under N₂ atmosphere. The mixture was stirred at 100 °C for 16 h. At ambient temperature, the reaction mixture was transferred into a separatory funnel with EtOAc (20 mL) and washed with brine (5.0 mL). The mixture was extracted with EtOAc (3 × 20 mL) and the combined organic layer was dried over Na₂SO₄, concentrated under reduced pressure and purified by column chromatography on silica gel using a mixture of *n*-hexane and EtOAc to afford the desired product **142**.

General Procedure B: Ruthenium(II)-Catalyzed *mono*-C–H Activation of *meta*- and *para*-substituted Benzoic Acids

Benzoic acid **62** (0.75 mmol), sulfoxonium ylide **141** (0.083 mmol), [RuCl₂(*p*-cymene)]₂ (3.8 mg, 2.5 mol %), AgSbF₆ (8.6 mg, 10 mol %), Zn(OAc)₂ (23 mg, 50 mol %), NEt₃ (76 mg, 3.0 equiv), and DCE (2.0 mL) were placed in a 25 mL Schlenk flask under N₂ atmosphere. The mixture was stirred at 100 °C for 2 h. Then, sulfoxonium ylide **141** (0.083 mmol) dissolved in DCE (0.5 mL) was added. And 2 h later, another portion of sulfoxonium ylide **141** (0.083 mmol) dissolved in

DCE (0.5 mL) was added. The resulting mixture was then stirred for 12 h. At ambient temperature, the reaction mixture was transferred into a separatory funnel with EtOAc (20 mL) and washed with brine (5.0 mL). The mixture was extracted with EtOAc (3 × 20 mL) and the combined organic layer was dried over Na₂SO₄, concentrated under reduced pressure and purified by column chromatography on silica gel using a mixture of *n*-hexane and EtOAc to afford the desired product **142**.

General Procedure C: Ruthenium(II)-Catalyzed double C–H Activation of *meta*- and *para*-substituted Benzoic Acids

Benzoic acid **62** (0.25 mmol), sulfoxonium ylide **141** (0.75 mmol), [RuCl₂(*p*-cymene)]₂ (7.7 mg, 5.0 mol %), AgSbF₆ (17.2 mg, 20 mol %), NEt₃ (51 mg, 2.0 equiv), and DCE (2.0 mL) were placed in a 25 mL Schlenk flask under N₂ atmosphere. The mixture was stirred at 100 °C for 16 h. At ambient temperature, the reaction mixture was transferred into a round bottom flask with EtOAc (20 mL) and washed with brine (5.0 mL). The mixture was extracted with EtOAc (3 × 20 mL) and the combined organic layer was dried over Na₂SO₄, concentrated under reduced pressure and purified by column chromatography on silica gel using a mixture of *n*-hexane and EtOAc to afford the desired product **142**.

General Procedure D: Ruthenium(II)-Catalyzed Double C-H/N-H Annulation

To the pre-oven dried 25 mL Schlenk flask diketopyrrolopyrrole **143** (0.25 mmol, 1.0 equiv), alkyne **64** (1.00 mmol, 4.0 equiv), [RuCl₂(*p*-cymene)]₂ (10 mol %), Cu(OAc)₂·H₂O (1.00 mmol, 4.0 equiv), KOAc (0.25 mmol, 1.0 equiv) were added. The Schlenk tube was evaporated and refilled with N₂ and *o*-xylene (2 mL) was added. The reaction was stirred at 100 °C for 16 h under a N₂ atmosphere. At ambient temperature, the reaction mixture was transferred to the separation funnel with the CH₂Cl₂ and washed with the NH₄Cl(aq) solution and dried over Na₂SO₄. The solvent was removed under *vacuo* and the remaining residue was washed with *n*-hexane. The precipitate was separated by the centrifuge, dissolved in CH₂Cl₂ and filtrated through filtration paper giving the desired product.

General Procedure E: Ruthenium(II)-Catalyzed Double Double C-H/N-H Annulation

To the pre-oven dried 25 mL Schlenk flask diketopyrrolopyrrole **143** (0.25 mmol, 1.0 equiv), alkyne **64** (1.00 mmol, 4.0 equiv), [RuCl₂(*p*-cymene)]₂ (10 mol %), Cu(OAc)₂·H₂O (1.00 mmol, 4.0 equiv), KOAc (0.25 mmol, 1.0 equiv) were added. The Schlenk tube was evaporated and refilled with N₂ and *o*-xylene (2 mL) was added. The reaction was stirred at 100 °C for 16 h

under a N₂ atmosphere. At ambient temperature, the reaction mixture was transferred to the separation funnel with CH₂Cl₂ and washed with the NH₄Cl(aq) solution and dried over Na₂SO₄. The solvent was removed under *vacuo* and the remaining residue was purified by column chromatography on silica gel (*n*-hexane:CH₂Cl₂) giving the desired product.

General Procedure F: Electrochemical C–H/N–H Activation with Alkenyl Imidazoles

The electrocatalysis was carried out in an undivided cell under N₂, with a graphite felt (GF) anode (10 mm × 15 mm × 6 mm) and a platinum cathode (10 mm × 15 mm × 0.25 mm). Alkenyl imidazoles **145** (0.4 mmol, 1.0 equiv), alkyne **64** (0.8 mmol, 2.0 equiv), KPF₆ (14.7 mg, 20 mol %) and [RuCl₂(*p*-cymene)]₂ (12.5 mg, 5.0 mol %) were dissolved in DMF (4.0 mL). Electrocatalysis was performed at 140 °C with a constant current of 4.0 mA maintained for 8 h. The GF anode was washed with EtOAc (3×10 mL) in an ultrasonic bath. Evaporation of the solvent and subsequent purification by column chromatography on silica gel afforded the corresponding products **146**.

General Procedure G: Electrochemical C–H/N–H Activation of 2-Phenylbenzimidazoles

The electrocatalysis was carried out in an undivided cell under N₂, with a graphite felt GF anode (10 mm × 15 mm × 6 mm) and a platinum cathode (10 mm × 15 mm × 0.25 mm). 2-Phenylbenzimidazoles **147** (0.2 mmol, 1.0 equiv), alkyne **64** (0.4 mmol, 2.0 equiv), KOAc (0.4 mmol, 2.0 equiv), 1-AdCO₂H (7.2 mg, 20 mol %) and [RuCl₂(*p*-cymene)]₂ (6.2 mg, 5.0 mol %) were dissolved in *t*-AmOH/H₂O (1/1, 6.0 mL). Electrocatalysis was performed at 100 °C with a constant current of 8.0 mA maintained for 4 h. The GF anode was washed with EtOAc (3×10 mL) in an ultrasonic bath. Evaporation of the solvent and subsequent purification by column chromatography on silica gel afforded the corresponding products **148**.

General Procedure H: Palladium-Catalyzed B(3,4)–H Diarylation

o-Carborane **149a** (1-CONEt₂-2-Ph-*o*-C₂B₁₀H₁₀) (0.20 mmol), 4-iodotoluene **19a** (0.48 mmol), Pd(OAc)₂ (10 mol %), AgTFA (0.48 mmol), TFA (0.20 mmol) and HFIP (0.50 mL) were placed in a 25 mL Schlenk tube under N₂ atmosphere. The mixture was stirred at 25 °C for 16 h. Then, the reaction solution was concentrated to dryness in vacuum and purified by column chromatography on silica gel using a mixture of *n*-hexane and EtOAc (20/1 in v/v) and Gel Permeation Chromatography (GPC) to afford the desired product **150a**.

General Procedure I: Palladium-Catalyzed B(3)–H Arylation of *o*-Carboranes

o-Carborane **149a** (1-CONEt₂-2-Ph-*o*-C₂B₁₀H₁₀) (0.20 mmol), 4-iodotoluene **19a** (0.08 mmol),

Pd(OAc)₂ (10 mol %), Ag₂CO₃ (0.24 mmol) and HFIP (0.50 mL) were placed in a 25 mL Schlenk tube under N₂ atmosphere. The mixture was stirred at 25 °C for 4 h. Then, 4-iodotoluene **19a** (0.08 mmol) was added. And 4 h later, another portion of 4-iodotoluene **19a** (0.08 mmol) was added. The resulting mixture was then stirred for 8 h. Then, the reaction solution was concentrated to dryness in vacuum and purified by column chromatography on silica gel using a mixture of *n*-hexane and EtOAc (20/1 in v/v) and Gel Permeation Chromatography (GPC) to afford the desired product **153a**.

General Procedure J: Electrochemical-Catalyzed B–H Nitrogenation of *nido*-Carboranes

The electrocatalysis was carried out in an undivided cell under air, with a graphite felt (GF) anode (10 mm × 15 mm × 6 mm) and a platinum cathode (10 mm × 15 mm × 0.25 mm). *nido*-Carborane **154a** (0.10 mmol, 1.0 equiv), pyridine **155a** (0.30 mmol, 3.0 equiv), and NMe₄Cl (0.20 mmol, 2.0 equiv) were dissolved in DME (4.0 mL) and H₂O (0.2 mL). Electrocatalysis was performed at room temperature with a constant current of 6.0 mA maintained for 3 h. The GF anode was washed with CH₂Cl₂ (3×10 mL). Evaporation of the solvent and subsequent purification by column chromatography on silica gel with CH₂Cl₂/*n*-hexane (1/1) afforded the corresponding products **156a**.

General Procedure K: Cupraelectro-Catalyzed C–H Chalcogenation of *o*-Carboranes

The electrocatalysis was carried out in an undivided cell under air, with a graphite felt (GF) anode (10 mm × 15 mm × 6 mm) and a platinum cathode (10 mm × 15 mm × 0.25 mm). *o*-Carborane **160** (0.10 mmol, 1.0 equiv), thiol **161** (0.30 mmol, 3.0 equiv), CuOAc (15 mol %), 2-PhPy (15 mol %), LiOtBu (0.2 mmol, 2.0 equiv) and TBAI (0.2 mmol, 2.0 equiv) were dissolved in THF (3.0 mL). Electrocatalysis was performed at room temperature with a constant current of 2.0 mA maintained for 16 h. The GF anode was washed with ethyl acetate (3×10 mL). Evaporation of the solvent and subsequent purification by column chromatography on silica gel with *n*-hexane or gel permeation chromatography (GPC) afford the corresponding products **162**.

General Procedure L: Cupraelectro-Catalyzed C–H Chalcogenation of *o*-Carboranes

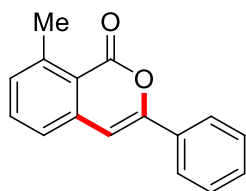
The electrocatalysis was carried out in an undivided cell under air, with a graphite felt (GF) anode (10 mm × 15 mm × 6 mm) and a platinum cathode (10 mm × 15 mm × 0.25 mm). Thiol **161** (0.30 mmol, 3.0 equiv), LiOtBu (0.2 mmol, 2.0 equiv) and TBAI (0.2 mmol, 2.0 equiv) were dissolved in THF (3.0 mL). Electrocatalysis was performed at room temperature with a constant current of 2.0 mA maintained for 3 h. Then, *o*-carborane **160** (0.10 mmol, 1.0 equiv), CuOAc (15 mol %) and 2-PhPy (15 mol %) were added to the reaction mixture and electrocatalysis was

performed at room temperature with a constant current of 2.0 mA maintained for another 16 h. The GF anode was washed with ethyl acetate (3×10 mL). Evaporation of the solvent and subsequent purification by column chromatography on silica gel with *n*-hexane or gel permeation chromatography (GPC) afford the corresponding products **162**.

5.3 Experimental Procedures and Analytical Data

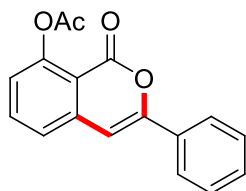
5.3.1 Ruthenium(IV) Intermediates in C–H Annulation

5.3.1.1 Characterization Data



Methyl-3-phenyl-1*H*-isochromen-1-one (**142a**).

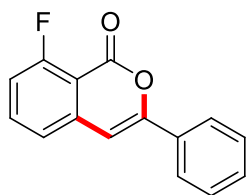
The representative procedure **A** was followed using 2-methylbenzoic acid (**62a**) (34 mg, 0.25 mmol) and 2-[dimethyl(oxo)- λ^6 -sulfaneylidene]-1-phenylethan-1-one (**141a**) (74 mg, 0.38 mmol). Isolation by column chromatography (*n*-hexane/EtOAc: 10/1) yielded **142a** (45 mg, 76%) as a colorless solid. **M.p.** = 133 °C. **¹H NMR** (300 MHz, CDCl₃): δ = 7.94–7.84 (m, 2H), 7.60–7.52 (m, 1H), 7.52–7.41 (m, 3H), 7.35–7.26 (m, 2H), 6.89 (s, 1H), 2.87 (s, 3H). **¹³C NMR** (75 MHz, CDCl₃): δ = 161.7 (C_q), 153.1 (C_q), 143.6 (C_q), 139.0 (C_q), 134.0 (CH), 131.9 (C_q), 131.0 (CH), 129.8 (CH), 128.8 (CH), 125.1 (CH), 124.2 (CH), 119.0 (C_q), 102.3 (CH), 23.2 (CH₃). **IR** (ATR): 3061, 1712, 1592, 1471, 1227, 1074, 796, 691 cm⁻¹. **MS** (ESI) *m/z* (relative intensity): 259 (60) [M+Na]⁺, 237 (100) [M+H]⁺. **HR-MS** (ESI): *m/z* calcd. for C₁₆H₁₂O₂ [M+H]⁺: 237.0910, found: 237.0905.



1-Oxo-3-phenyl-1*H*-isochromen-8-yl acetate (**142b**).

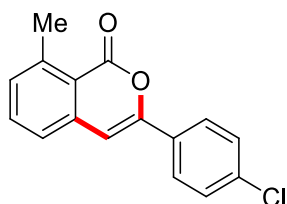
The representative procedure **A** was followed using 2-acetoxybenzoic acid (**62b**) (45 mg, 0.25 mmol) and 2-[dimethyl(oxo)- λ^6 -sulfaneylidene]-1-phenylethan-1-one (**141a**) (74 mg, 0.38 mmol). Isolation by column chromatography (*n*-hexane/EtOAc: 10/1) yielded **142b** (50 mg, 72%) as a

colorless solid. **M.p.** = 137 °C. **¹H NMR** (300 MHz, CDCl₃): δ = 7.90–7.83 (m, 2H), 7.78–7.68 (m, 1H), 7.51–7.44 (m, 3H), 7.39 (d, *J* = 7.9 Hz, 1H), 7.14 (d, *J* = 7.8 Hz, 1H), 6.95 (s, 1H), 2.48 (s, 3H). **¹³C NMR** (75 MHz, CDCl₃): δ = 169.7 (C_q), 158.8 (C_q), 154.2 (C_q), 152.0 (C_q), 140.0 (C_q), 135.6 (CH), 131.6 (C_q), 130.2 (CH), 128.9 (CH), 125.3 (CH), 124.1 (CH), 122.4 (CH), 113.3 (C_q), 101.6 (CH), 21.2 (CH₃). **IR** (ATR): 3068, 1770, 1731, 1609, 1564, 1189, 1079, 689 cm⁻¹. **MS** (ESI) *m/z* (relative intensity): 303 (100) [M+Na]⁺, 281 (20) [M+H]⁺. **HR-MS** (ESI): *m/z* calcd. for C₁₇H₁₂O₄ [M+H]⁺: 281.0806, found: 281.0802. The analytical data correspond with those reported in the literature.^[234]



8-Fluoro-3-phenyl-1*H*-isochromen-1-one (**142c**).

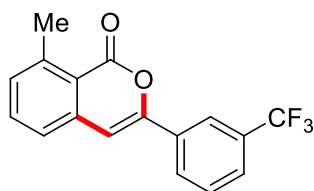
The representative procedure **A** was followed using 2-fluorobenzoic acid (**62c**) (35 mg, 0.25 mmol) and 2-[dimethyl(oxo)-λ⁶-sulfaneylidene]-1-phenylethan-1-one (**141a**) (74 mg, 0.38 mmol). Isolation by column chromatography (*n*-hexane/EtOAc: 10/1) yielded **142c** (33 mg, 55%) as a colorless solid. **M.p.** = 121 °C. **¹H NMR** (300 MHz, CDCl₃): δ = 7.94–7.84 (m, 2H), 7.71–7.67 (m, 1H), 7.53–7.44 (m, 3H), 7.30 (d, *J* = 7.6 Hz, 1H), 7.22–7.11 (m, 1H), 6.94 (s, 1H). **¹³C NMR** (75 MHz, CDCl₃): δ = 163.0 (d, ¹*J* = 265.1 Hz, C_q), 157.8 (C_q), 154.6 (C_q), 140.1 (C_q), 136.3 (d, ³*J* = 10.1 Hz, CH), 131.5 (C_q), 130.3 (CH), 128.9 (CH), 125.4 (CH), 121.8 (d, ⁴*J* = 4.4 Hz, CH), 115.2 (d, ²*J* = 21.2 Hz, CH), 109.3 (C_q), 101.1 (CH). **¹⁹F NMR** (282 MHz, CDCl₃): δ = -107.2. **IR** (ATR): 3105, 1725, 1640, 1475, 1228, 1079, 803, 684 cm⁻¹. **MS** (ESI) *m/z* (relative intensity): 263 (100) [M+Na]⁺, 241 (70) [M+H]⁺. **HR-MS** (ESI): *m/z* calcd. for C₁₅H₉FO₂ [M+H]⁺: 241.0659, found: 241.0655.



3-(4-Chlorophenyl)-8-methyl-1*H*-isochromen-1-one (**142d**).

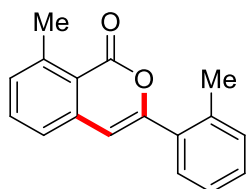
The representative procedure **A** was followed using 2-methylbenzoic acid (**62a**) (34 mg, 0.25 mmol) and 1-(4-chlorophenyl)-2-[dimethyl(oxo)-λ⁶-sulfaneylidene]ethan-1-one (**141b**) (87 mg, 0.38 mmol). Isolation by column chromatography (*n*-hexane/EtOAc: 10/1) yielded **142d** (62 mg,

92%) as a colorless solid. **M.p.** = 156 °C. **¹H NMR** (300 MHz, CDCl₃): δ = 7.78 (d, *J* = 8.7 Hz, 2H), 7.58–7.51 (m, 1H), 7.78 (d, *J* = 8.7 Hz, 2H), 7.33–7.25 (m, 2H), 6.84 (s, 1H), 2.84 (s, 3H). **¹³C NMR** (75 MHz, CDCl₃): δ = 161.3 (C_q), 152.0 (C_q), 143.6 (C_q), 138.8 (C_q), 135.8 (C_q), 134.1 (CH), 131.3 (CH), 130.4 (C_q), 129.0 (CH), 126.3 (CH), 124.3 (CH), 118.9 (C_q), 102.5 (CH), 23.2 (CH₃). **IR** (ATR): 3097, 1714, 1493, 1095, 1074, 1014, 825, 687 cm⁻¹. **MS** (ESI) *m/z* (relative intensity): 293 (60) [M+Na]⁺, 271 (100) [M+H]⁺. **HR-MS** (ESI): *m/z* calcd. for C₁₆H₁₁ClO₂ [M+H]⁺: 271.0520, found: 271.0516.



8-Methyl-3-[3-(trifluoromethyl)phenyl]-1*H*-isochromen-1-one (142e).

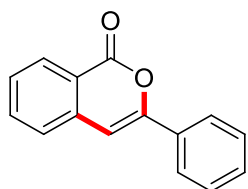
The representative procedure **A** was followed using 2-methylbenzoic acid (**62a**) (34 mg, 0.25 mmol) and 2-[dimethyl(oxo)-λ⁶-sulfaneylidene]-1-[3-(trifluoromethyl)phenyl]ethan-1-one (**141c**) (99 mg, 0.38 mmol). Isolation by column chromatography (*n*-hexane/EtOAc: 10/1) yielded **142e** (54 mg, 71%) as a colorless solid. **M.p.** = 159 °C. **¹H NMR** (300 MHz, CDCl₃): δ = 8.12 (s, 1H), 8.06 (d, *J* = 7.8 Hz, 1H), 7.68 (d, *J* = 7.8 Hz, 1H), 7.64–7.56 (m, 2H), 7.39–7.30 (m, 2H), 6.96 (s, 1H), 2.87 (s, 3H). **¹³C NMR** (75 MHz, CDCl₃): δ = 161.1 (C_q), 151.5 (C_q), 143.8 (C_q), 138.5 (C_q), 134.2 (CH), 132.8 (C_q), 131.6 (CH), 130.9 (q, ²*J* = 32.9 Hz, C_q), 129.4 (CH), 128.2 (CH), 126.3 (q, ³*J* = 3.9 Hz, CH), 124.4 (CH), 123.9 (q, ¹*J* = 270.9 Hz, C_q), 121.9 (q, ³*J* = 3.9 Hz, CH), 119.2 (C_q), 103.4 (CH), 23.2 (CH₃). **¹⁹F NMR** (282 MHz, CDCl₃): δ = -62.7. **IR** (ATR): 2932, 1721, 1333, 1309, 1222, 1166, 1113, 1073 cm⁻¹. **MS** (ESI) *m/z* (relative intensity): 327 (70) [M+Na]⁺, 305 (100) [M+H]⁺. **HR-MS** (ESI): *m/z* calcd. for C₁₇H₁₁F₃O₂ [M+H]⁺: 305.0784, found: 305.0777.



8-Methyl-3-(*o*-tolyl)-1*H*-isochromen-1-one (142f).

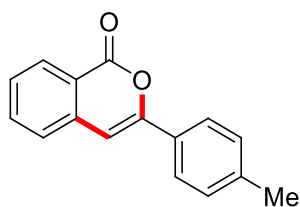
The representative procedure **A** was followed using 2-methylbenzoic acid (**62a**) (34 mg, 0.25 mmol) and 2-[dimethyl(oxo)-λ⁶-sulfaneylidene]-1-(*o*-tolyl)ethan-1-one (**141d**) (79 mg, 0.38 mmol).

Isolation by column chromatography (*n*-hexane/EtOAc: 10/1) yielded **142f** (51 mg, 85%) as a colorless solid. **M.p.** = 141 °C. **¹H NMR** (300 MHz, CDCl₃): δ = 7.63–7.50 (m, 2H), 7.37–7.25 (m, 5H), 6.56 (s, 1H), 2.89 (s, 3H), 2.54 (s, 3H). **¹³C NMR** (75 MHz, CDCl₃): δ = 162.0 (C_q), 155.2 (C_q), 143.5 (C_q), 139.1 (C_q), 136.8 (C_q), 134.0 (CH), 132.8 (C_q), 131.1 (CH), 131.1 (CH), 129.7 (CH), 129.1 (CH), 126.0 (CH), 124.1 (CH), 118.8 (C_q), 106.4 (CH), 23.3 (CH₃), 20.8 (CH₃). **IR** (ATR): 2926, 1710, 1646, 1593, 1573, 1490, 1223, 723 cm⁻¹. **MS** (ESI) *m/z* (relative intensity): 273 (90) [M+Na]⁺, 251 (100) [M+H]⁺. **HR-MS** (ESI): *m/z* calcd. for C₁₇H₁₄O₂ [M+H]⁺: 251.1067, found: 251.1062.



3-Phenyl-1*H*-isochromen-1-one (142g).

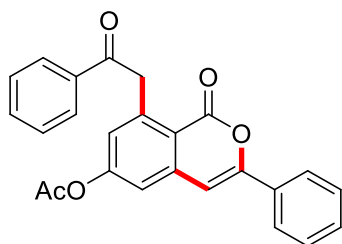
The representative procedure **B** was followed using benzoic acid (**62d**) (92 mg, 0.75 mmol) and 2-[dimethyl(oxo)-λ⁶-sulfaneylidene]-1-phenylethan-1-one (**141a**) (49 mg, 0.25 mmol). Isolation by column chromatography (*n*-hexane/EtOAc: 10/1) yielded **142g** (37 mg, 67%) as a colorless solid. **M.p.** = 90 °C. **¹H NMR** (300 MHz, CDCl₃): δ = 8.31 (d, *J* = 8.0 Hz, 1H), 7.88 (dd, *J* = 7.8, 1.8 Hz, 2H), 7.76–7.67 (m, 1H), 7.53–7.42 (m, 5H), 6.95 (s, 1H). **¹³C NMR** (75 MHz, CDCl₃): δ = 162.3 (C_q), 153.6 (C_q), 137.5 (C_q), 134.9 (CH), 132.0 (C_q), 130.0 (CH), 129.6 (CH), 128.8 (CH), 128.2 (CH), 126.0 (CH), 125.2 (CH), 120.5 (C_q), 101.8 (CH). **IR** (ATR): 3062, 1720, 1636, 1607, 1483, 1234, 1107, 767, 690 cm⁻¹. **MS** (ESI) *m/z* (relative intensity): 245 (50) [M+Na]⁺, 223 (100) [M+H]⁺. **HR-MS** (ESI): *m/z* calcd. for C₁₅H₁₀O₂ [M+H]⁺: 223.0754, found: 223.0758. The analytical data correspond with those reported in the literature.^[235]



3-(*p*-Tolyl)-1*H*-isochromen-1-one (142h).

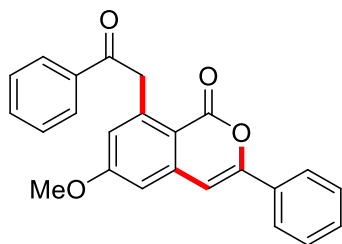
The representative procedure **B** was followed using benzoic acid (**62d**) (92 mg, 0.75 mmol) and 2-[dimethyl(oxo)-λ⁶-sulfaneylidene]-1-(*p*-tolyl)ethan-1-one (**141e**) (53 mg, 0.25 mmol). Isolation by column chromatography (*n*-hexane/EtOAc: 10/1) yielded **142h** (38 mg, 65%) as a colorless solid. **M.p.** = 114 °C. **¹H NMR** (300 MHz, CDCl₃): δ = 8.32 (d, *J* = 8.5 Hz, 1H), 7.79 (d, *J* = 8.2 Hz, 2H), 7.76–7.69 (m, 1H), 7.53–7.46 (m, 2H), 7.31–7.26 (m, 2H), 6.92 (s, 1H), 2.42 (s, 3H). **¹³C**

NMR (75 MHz, CDCl₃): δ = 162.4 (C_q), 153.9 (C_q), 140.3 (C_q), 137.7 (C_q), 134.8 (CH), 129.6 (CH), 129.5 (CH), 129.2 (C_q), 127.9 (CH), 125.9 (CH), 125.2 (CH), 120.4 (C_q), 101.1 (CH), 21.4 (CH₃). **IR** (ATR): 2918, 1731, 1630, 1066, 1008, 816, 752, 688 cm⁻¹. **MS** (ESI) *m/z* (relative intensity): 259 (90) [M+Na]⁺, 237 (100) [M+H]⁺. **HR-MS** (ESI): *m/z* calcd. for C₁₆H₁₂O₂ [M+H]⁺: 237.0910, found: 237.0905. The analytical data correspond with those reported in the literature.^[236]



1-Oxo-8-(2-oxo-2-phenylethyl)-3-phenyl-1*H*-isochromen-6-yl acetate (**142i**).

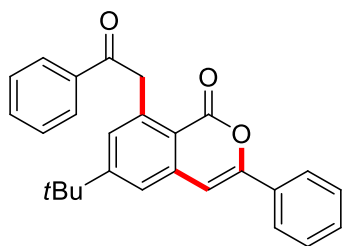
The representative procedure **C** was followed using 4-acetoxybenzoic acid (**62e**) (45 mg, 0.25 mmol) and 2-[dimethyl(oxo)- λ^6 -sulfaneylidene]-1-phenylethan-1-one (**141a**) (147 mg, 0.75 mmol). Isolation by column chromatography (*n*-hexane/EtOAc: 10/1) yielded **142i** (73 mg, 73%) as a colorless solid. **M.p.** = 195 °C. **¹H NMR** (300 MHz, CDCl₃): δ = 8.17–8.08 (m, 2H), 7.88–7.80 (m, 2H), 7.66–7.59 (m, 1H), 7.57–7.50 (m, 2H), 7.48–7.42 (m, 3H), 7.28 (s, 1H), 7.09 (d, *J* = 2.2 Hz, 1H), 6.92 (s, 1H), 4.91 (s, 2H), 2.36 (s, 3H). **¹³C NMR** (75 MHz, CDCl₃): δ = 196.7 (C_q), 168.5 (C_q), 161.1 (C_q), 154.7 (C_q), 154.1 (C_q), 142.0 (C_q), 141.1 (C_q), 137.2 (C_q), 133.1 (CH), 131.5 (C_q), 130.2 (CH), 128.9 (CH), 128.6 (CH), 128.3 (CH), 125.6 (CH), 125.3 (CH), 117.6 (CH), 116.6 (C_q), 102.0 (CH), 45.6 (CH₂), 21.3 (CH₃). **IR** (ATR): 2000, 1643, 1603, 1575, 1061, 1003, 910, 530 cm⁻¹. **MS** (ESI) *m/z* (relative intensity): 421 (95) [M+Na]⁺, 399 (100) [M+H]⁺. **HR-MS** (ESI): *m/z* calcd. for C₂₅H₁₈O₅ [M+H]⁺: 399.1227, found: 399.1218.



6-Methoxy-8-(2-oxo-2-phenylethyl)-3-phenyl-1*H*-isochromen-1-one (**142j**).

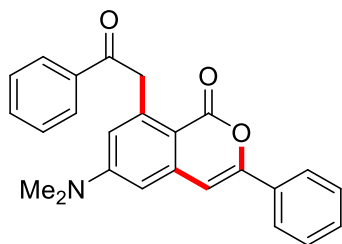
The representative procedure **C** was followed using 4-methoxybenzoic acid (**62f**) (38 mg, 0.25 mmol) and 2-[dimethyl(oxo)- λ^6 -sulfaneylidene]-1-phenylethan-1-one (**141a**) (147 mg, 0.75 mmol). Isolation by column chromatography (*n*-hexane/EtOAc: 10/1) yielded **142j** (59 mg, 64%) as a colorless solid. **M.p.** = 188 °C. **¹H NMR** (300 MHz, CDCl₃): δ = 8.17–8.08 (m, 2H), 7.88–7.79 (m,

2H), 7.64–7.57 (m, 1H), 7.57–7.49 (m, 2H), 7.49–7.40 (m, 3H), 6.94–6.82 (m, 3H), 4.86 (s, 2H), 3.93 (s, 3H). **¹³C NMR** (75 MHz, CDCl₃): δ = 197.1 (C_q), 163.7 (C_q), 161.4 (C_q), 153.8 (C_q), 141.9 (C_q), 141.7 (C_q), 137.4 (C_q), 132.9 (CH), 131.8 (C_q), 129.9 (CH), 128.8 (CH), 128.6 (CH), 128.3 (CH), 125.2 (CH), 120.6 (CH), 112.3 (C_q), 107.5 (CH), 102.4 (CH), 55.6 (CH₃), 45.7 (CH₂). **IR** (ATR): 3059, 1711, 1599, 1468, 1212, 1160, 735, 628 cm⁻¹. **MS** (ESI) *m/z* (relative intensity): 393 (50) [M+Na]⁺, 371 (100) [M+H]⁺. **HR-MS** (ESI): *m/z* calcd. for C₂₄H₁₈O₄ [M+H]⁺: 371.1278, found: 371.1276.



6-(*tert*-Butyl)-8-(2-oxo-2-phenylethyl)-3-phenyl-1*H*-isochromen-1-one (142k).

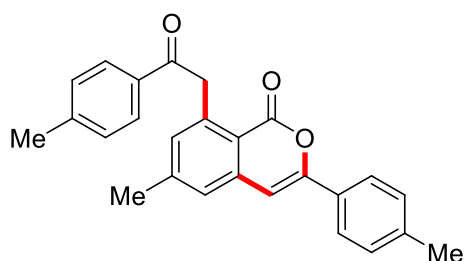
The representative procedure **C** was followed using 4-(*tert*-butyl)benzoic acid (**62g**) (45 mg, 0.25 mmol) and 2-[dimethyl(oxo)-λ⁶-sulfaneylidene]-1-phenylethan-1-one (**141a**) (147 mg, 0.75 mmol). Isolation by column chromatography (*n*-hexane/EtOAc: 10/1) yielded **142k** (80 mg, 81%) as a colorless solid. **M.p.** = 198 °C. **¹H NMR** (300 MHz, CDCl₃): δ = 8.20–8.12 (m, 2H), 7.90–7.83 (m, 2H), 7.65–7.58 (m, 1H), 7.57–7.50 (m, 2H), 7.49–7.40 (m, 4H), 7.36 (d, *J* = 1.9 Hz, 1H), 6.99 (s, 1H), 4.93 (s, 2H), 1.43 (s, 9H). **¹³C NMR** (75 MHz, CDCl₃): δ = 197.3 (C_q), 161.8 (C_q), 158.0 (C_q), 153.2 (C_q), 139.3 (C_q), 139.1 (C_q), 137.5 (C_q), 132.9 (CH), 132.0 (C_q), 130.2 (CH), 129.8 (CH), 128.8 (CH), 128.6 (CH), 128.3 (CH), 125.1 (CH), 122.3 (CH), 116.8 (C_q), 102.9 (CH), 45.9 (CH₂), 35.2 (C_q), 31.0 (CH₃). **IR** (ATR): 2965, 1716, 1688, 1600, 1496, 1212, 756, 688 cm⁻¹. **MS** (ESI) *m/z* (relative intensity): 419 (30) [M+Na]⁺, 397 (100) [M+H]⁺. **HR-MS** (ESI): *m/z* calcd. for C₂₇H₂₄O₃ [M+H]⁺: 397.1798, found: 397.1800.



6-(Dimethylamino)-8-(2-oxo-2-phenylethyl)-3-phenyl-1*H*-isochromen-1-one (142l).

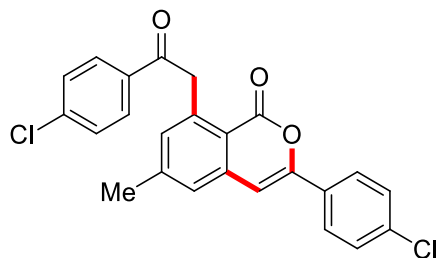
The representative procedure **C** was followed using 4-(dimethylamino)benzoic acid (**62h**) (41 mg, 0.25 mmol) and 2-[dimethyl(oxo)-λ⁶-sulfaneylidene]-1-phenylethan-1-one (**141a**) (147 mg, 0.75

mmol). Isolation by column chromatography (*n*-hexane/EtOAc: 10/1) yielded **142i** (72 mg, 75%) as a colorless solid. **M.p.** = 189 °C. **¹H NMR** (300 MHz, CDCl₃): δ = 8.17–8.12 (m, 2H), 7.83 (dd, *J* = 7.9, 1.7 Hz, 2H), 7.62–7.57 (m, 1H), 7.54–7.48 (m, 2H), 7.46–7.38 (m, 3H), 6.83 (s, 1H), 6.61 (d, *J* = 2.5 Hz, 1H), 6.49 (d, *J* = 2.5 Hz, 1H), 4.83 (s, 2H), 3.08 (s, 6H). **¹³C NMR** (75 MHz, CDCl₃): δ = 197.7 (C_q), 162.0 (C_q), 153.4 (C_q), 153.0 (C_q), 141.0 (C_q), 140.9 (C_q), 137.6 (C_q), 132.7 (CH), 132.3 (C_q), 129.5 (CH), 128.6 (CH), 128.5 (CH), 128.3 (CH), 125.1 (CH), 116.7 (CH), 107.2 (C_q), 105.4 (CH), 102.8 (CH), 46.1 (CH₂), 39.9 (CH₃). **IR** (ATR): 3051, 1694, 1597, 1494, 1448, 1388, 1335, 559 cm⁻¹. **MS** (ESI) *m/z* (relative intensity): 406 (40) [M+Na]⁺, 384 (100) [M+H]⁺. **HR-MS** (ESI): *m/z* calcd. for C₂₅H₂₁NO₃ [M+H]⁺: 384.1594, found: 384.1588.



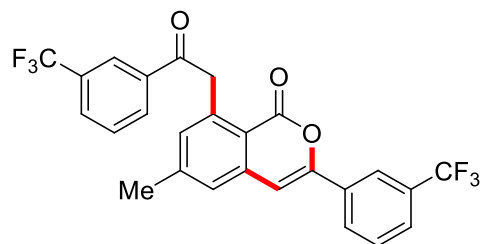
6-Methyl-8-[2-oxo-2-(*p*-tolyl)ethyl]-3-(*p*-tolyl)-1*H*-isochromen-1-one (**142m**).

The representative procedure **C** was followed using 4-methylbenzoic acid (**62i**) (34 mg, 0.25 mmol) and 2-[dimethyl(oxo)-λ⁶-sulfaneylidene]-1-(*p*-tolyl)ethan-1-one (**141f**) (158 mg, 0.75 mmol). Isolation by column chromatography (*n*-hexane/EtOAc: 10/1) yielded **142m** (80 mg, 84%) as a colorless solid. **M.p.** = 201 °C. **¹H NMR** (300 MHz, CDCl₃): δ = 8.04 (d, *J* = 8.2 Hz, 2H), 7.73 (d, *J* = 8.3 Hz, 2H), 7.32 (d, *J* = 8.0 Hz, 2H), 7.28–7.20 (m, 3H), 7.11 (s, 1H), 6.84 (s, 1H), 4.84 (s, 2H), 2.45 (s, 3H), 2.43 (s, 3H), 2.40 (s, 3H). **¹³C NMR** (75 MHz, CDCl₃): δ = 197.0 (C_q), 161.8 (C_q), 153.5 (C_q), 145.1 (C_q), 143.6 (C_q), 140.0 (C_q), 139.7 (C_q), 139.5 (C_q), 135.0 (C_q), 133.4 (CH), 129.5 (CH), 129.3 (CH), 129.2 (C_q), 128.4 (CH), 125.6 (CH), 125.0 (CH), 116.5 (C_q), 101.6 (CH), 45.3 (CH₂), 21.7 (CH₃), 21.6 (CH₃), 21.3 (CH₃). **IR** (ATR): 2919, 1716, 1686, 1567, 1408, 1333, 1272, 765, 690 cm⁻¹. **MS** (ESI) *m/z* (relative intensity): 405 (20) [M+Na]⁺, 383 (100) [M+H]⁺. **HR-MS** (ESI): *m/z* calcd. for C₂₆H₂₂O₃ [M+H]⁺: 383.1642, found: 383.1645.



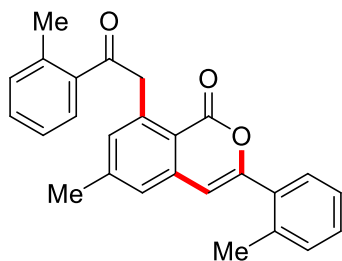
3-(4-Chlorophenyl)-8-[2-(4-chlorophenyl)-2-oxoethyl]-6-methyl-1*H*-isochromen-1-one

(**142n**). The representative procedure **C** was followed using 4-methylbenzoic acid (**62i**) (34 mg, 0.25 mmol) and 1-(4-chlorophenyl)-2-[dimethyl(oxo)- λ^6 -sulfaneylidene]ethan-1-one (**141g**) (173 mg, 0.75 mmol). Isolation by column chromatography (*n*-hexane/EtOAc: 10/1) yielded **142n** (92 mg, 87%) as a colorless solid. **M.p.** = 212 °C. **¹H NMR** (300 MHz, CDCl₃): δ = 8.07 (d, J = 8.7 Hz, 2H), 7.76 (d, J = 8.7 Hz, 2H), 7.50 (d, J = 8.7 Hz, 2H), 7.42 (d, J = 8.7 Hz, 2H), 7.26 (s, 1H), 7.15 (s, 1H), 6.88 (s, 1H), 4.81 (s, 2H), 2.48 (s, 3H). **¹³C NMR** (75 MHz, CDCl₃): δ = 196.2 (C_q), 161.5 (C_q), 152.3 (C_q), 145.5 (C_q), 139.3 (C_q), 139.2 (C_q), 139.1 (C_q), 135.9 (C_q), 135.7 (C_q), 133.9 (CH), 130.3 (C_q), 129.7 (CH), 129.1 (CH), 128.9 (CH), 126.4 (CH), 126.0 (CH), 116.6 (C_q), 102.5 (CH), 45.4 (CH₂), 21.8 (CH₃). **IR** (ATR): 2916, 1717, 1690, 1589, 1568, 1400, 1168, 966 cm⁻¹. **MS** (ESI) m/z (relative intensity): 445 (70) [M+Na]⁺, 423 (100) [M+H]⁺. **HR-MS** (ESI): m/z calcd. for C₂₄H₁₆Cl₂O₃ [M+H]⁺: 423.0549, found: 423.0545.



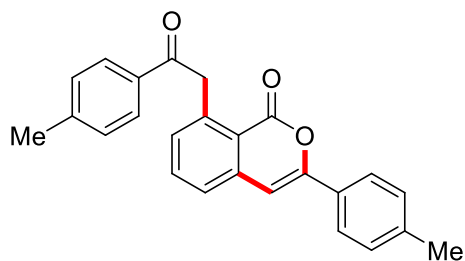
6-Methyl-8-(2-oxo-2-[3-(trifluoromethyl)phenyl]ethyl)-3-[3-(trifluoromethyl)phenyl]-1H-

isochromen-1-one (142o). The representative procedure **C** was followed using 4-methylbenzoic acid (**62i**) (34 mg, 0.25 mmol) and 2-[dimethyl(oxo)- λ^6 -sulfaneylidene]-1-[3-(trifluoromethyl)phenyl]ethan-1-one (**141h**) (198 mg, 0.75 mmol). Isolation by column chromatography (*n*-hexane/EtOAc: 10/1) yielded **142o** (113 mg, 92%) as a colorless solid. **M.p.** = 220 °C. **¹H NMR** (300 MHz, CDCl₃): δ = 8.38 (s, 1H), 8.33 (d, J = 7.8 Hz, 1H), 8.08 (s, 1H), 8.01 (d, J = 7.8 Hz, 1H), 7.88 (d, J = 7.8 Hz, 1H), 7.73–7.65 (m, 2H), 7.63–7.54 (m, 1H), 7.31 (s, 1H), 7.19 (s, 1H), 7.00 (s, 1H), 4.85 (s, 2H), 2.50 (s, 3H). **¹³C NMR** (75 MHz, CDCl₃): δ = 195.9 (C_q), 161.4 (C_q), 151.7 (C_q), 145.8 (C_q), 139.0 (C_q), 138.8 (C_q), 137.8 (C_q), 134.2 (CH), 132.6 (C_q), 131.4 (CH), 130.4 (q, 1J = 268.2 Hz, C_q), 129.7 (q, 3J = 3.6 Hz, CH), 129.4 (CH), 129.3 (CH), 128.1 (CH), 127.4 (q, 1J = 270.1 Hz, C_q), 126.3 (q, 3J = 3.8 Hz, CH), 126.2 (CH), 125.6 (q, 2J = 27.3 Hz, C_q), 125.0 (q, 3J = 3.8 Hz, CH), 124.0 (q, 2J = 26.4 Hz, C_q), 121.9 (q, 3J = 3.8 Hz, CH), 116.7 (C_q), 103.3 (CH), 45.5 (CH₂), 21.7 (CH₃). **¹⁹F NMR** (282 MHz, CDCl₃): δ = -62.7, -62.8. **IR** (ATR): 3082, 1718, 1643, 1611, 1321, 1166, 1125, 695 cm⁻¹. **MS** (ESI) m/z (relative intensity): 513 (70) [M+Na]⁺, 491 (100) [M+H]⁺. **HR-MS** (ESI): m/z calcd. for C₂₆H₁₆F₆O₃ [M+H]⁺: 491.1076, found: 491.1079.



6-Methyl-8-[2-oxo-2-(*o*-tolyl)ethyl]-3-(*o*-tolyl)-1*H*-isochromen-1-one (142p).

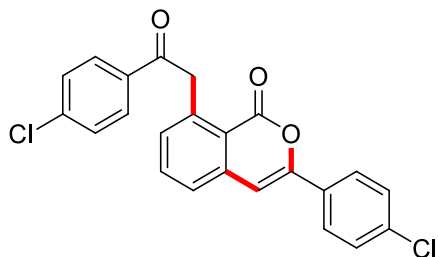
The representative procedure **C** was followed using 4-methylbenzoic acid (**62i**) (34 mg, 0.25 mmol) and 2-[dimethyl(oxo)- λ^6 -sulfaneylidene]-1-(*o*-tolyl)ethan-1-one (**141i**) (158 mg, 0.75 mmol). Isolation by column chromatography (*n*-hexane/EtOAc: 10/1) yielded **142p** (62 mg, 65%) as a colorless solid. **M.p.** = 196 °C. **¹H NMR** (300 MHz, CDCl₃): δ = 8.02 (dd, *J* = 7.6, 1.2 Hz, 1H), 7.57–7.50 (m, 1H), 7.45–7.39 (m, 1H), 7.38–7.25 (m, 6H), 7.18 (s, 1H), 6.58 (s, 1H), 4.82 (s, 2H), 2.55 (s, 3H), 2.52 (s, 3H), 2.51 (s, 3H). **¹³C NMR** (75 MHz, CDCl₃): δ = 201.0 (C_q), 162.0 (C_q), 155.3 (C_q), 145.3 (C_q), 139.5 (C_q), 139.3 (C_q), 138.5 (C_q), 138.1 (C_q), 136.7 (C_q), 133.8 (CH), 132.7 (C_q), 131.9 (CH), 131.2 (CH), 131.1 (CH), 129.7 (CH), 129.1 (CH), 128.7 (CH), 126.0 (CH), 125.7 (CH), 125.6 (CH), 116.5 (C_q), 106.5 (CH), 48.5 (CH₂), 21.8 (CH₃), 21.2 (CH₃), 20.8 (CH₃). **IR** (ATR): 2963, 1716, 1645, 1458, 1326, 1047, 994, 727 cm⁻¹. **MS** (ESI) *m/z* (relative intensity): 405 (60) [M+Na]⁺, 383 (100) [M+H]⁺. **HR-MS** (ESI): *m/z* calcd. for C₂₆H₂₂O₃ [M+H]⁺: 383.1642, found: 383.1646.



6-[2-Oxo-2-(*p*-tolyl)ethyl]-3-(*p*-tolyl)-1*H*-isochromen-1-one (142q).

The representative procedure **C** was followed using benzoic acid (**62d**) (31 mg, 0.25 mmol) and 2-[dimethyl(oxo)- λ^6 -sulfaneylidene]-1-(*p*-tolyl)ethan-1-one (**141f**) (158 mg, 0.75 mmol). Isolation by column chromatography (*n*-hexane/EtOAc: 10/1) yielded **142q** (71 mg, 77%) as a colorless solid. **M.p.** = 205 °C. **¹H NMR** (300 MHz, CDCl₃): δ = 8.04 (d, *J* = 8.2 Hz, 2H), 7.75 (d, *J* = 8.2 Hz, 2H), 7.68–7.64 (m, 1H), 7.45 (d, *J* = 7.9 Hz, 1H), 7.36–7.28 (m, 3H), 7.26 (d, *J* = 8.2 Hz, 2H), 6.93 (s, 1H), 4.90 (s, 2H), 2.46 (s, 3H), 2.41 (s, 3H). **¹³C NMR** (75 MHz, CDCl₃): δ = 196.9 (C_q), 161.8 (C_q), 153.5 (C_q), 143.6 (C_q), 140.2 (C_q), 139.7 (C_q), 139.6 (C_q), 134.9 (C_q), 134.2 (CH), 131.9 (CH), 129.5 (CH), 129.3 (CH), 129.1 (C_q), 128.4 (CH), 125.6 (CH), 125.1 (CH), 119.0 (C_q), 101.6 (CH), 45.5 (CH₂), 21.7 (CH₃), 21.4 (CH₃). **IR** (ATR): 2920, 1719, 1676, 1572, 1337, 1223,

1000, 768 cm^{-1} . **MS** (ESI) m/z (relative intensity): 391 (80) $[\text{M}+\text{Na}]^+$, 369 (100) $[\text{M}+\text{H}]^+$. **HR-MS** (ESI): m/z calcd. for $\text{C}_{25}\text{H}_{20}\text{O}_3$ $[\text{M}+\text{H}]^+$: 369.1485, found: 369.1484.

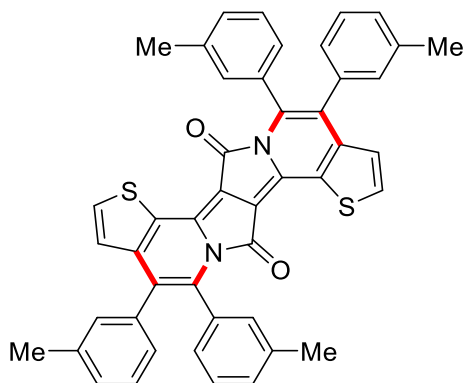


1-(4-Chlorophenyl)-8-(2-(4-chlorophenyl)-2-oxoethyl)-1H-isochromen-1-one (**142r**).

The representative procedure **C** was followed using benzoic acid (**62d**) (31 mg, 0.25 mmol) and 1-(4-chlorophenyl)-2-[dimethyl(oxo)- λ^6 -sulfaneylidene]ethan-1-one (**141g**) (174 mg, 0.75 mmol). Isolation by column chromatography (*n*-hexane/EtOAc: 10/1) yielded **142r** (87 mg, 85%) as a colorless solid. **M.p.** = 218 $^{\circ}\text{C}$. **$^1\text{H NMR}$** (300 MHz, CDCl_3): δ = 8.07 (d, J = 8.9 Hz, 2H), 7.77 (d, J = 8.9 Hz, 2H), 7.72–7.65 (m, 1H), 7.53–7.39 (m, 5H), 7.35–7.31 (m, 1H), 6.95 (s, 1H), 4.86 (s, 2H). **$^{13}\text{C NMR}$** (75 MHz, CDCl_3): δ = 196.0 (C_q), 161.5 (C_q), 152.3 (C_q), 139.4 (C_q), 139.3 (C_q), 139.2 (C_q), 136.0 (C_q), 135.7 (C_q), 134.5 (CH), 132.4 (CH), 130.2 (C_q), 129.7 (CH), 129.1 (CH), 128.9 (CH), 126.4 (CH), 126.0 (CH), 119.0 (C_q), 102.6 (CH), 45.6 (CH_2). **IR** (ATR): 2921, 1730, 1686, 1590, 1492, 1072, 997, 687 cm^{-1} . **MS** (ESI) m/z (relative intensity): 431 (100) $[\text{M}+\text{Na}]^+$, 409 (20) $[\text{M}+\text{H}]^+$. **HR-MS** (ESI): m/z calcd. for $\text{C}_{23}\text{H}_{14}\text{Cl}_2\text{O}_3$ $[\text{M}+\text{H}]^+$: 409.0393, found: 409.0389.

5.3.2 Twofold C–H/N–H Annulations towards π -Extended Polyaromatics

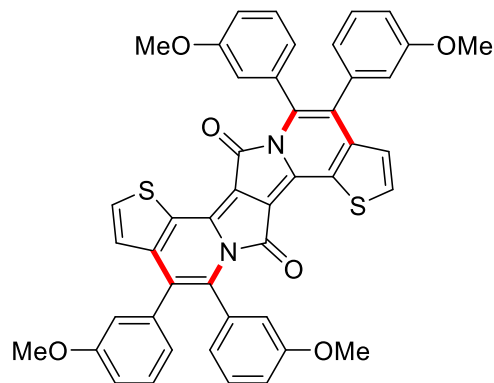
5.3.2.1 Characterization Data



4,5,11,12-tetra-*m*-tolyl-7H,14H-thieno[3',2':7,8]indolizino[2,1-a]thieno[3,2-g]indolizine-7,14-dione (**144a**):

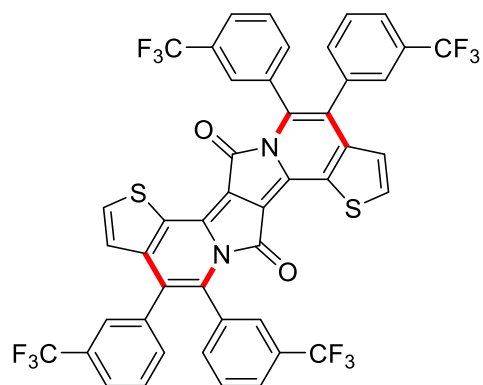
The general procedure **D** was followed using 3,6-di(thiophen-2-yl)-2,5-dihydropyrrolo[3,4-

c]pyrrole-1,4-dione **143a** (0.2 mmol, 60 mg) and 1,2-di-*m*-tolylethyne **64a** (0.8 mmol, 165 mg) yielding **144a** (100 mg, 71%) as the purple crystals. **M. p.** = over the limit of the detection. **¹H NMR** (300 MHz, CDCl₃) δ = 7.60 (d, *J* = 5.2 Hz, 2H), 7.20 – 6.80 (m, 18H), 2.35 – 2.15 (m, 12H). **¹³C NMR** (126 MHz, CDCl₃) δ = 156.5 (C_q), 143.6 (C_q), 138.0 (C_q), 137.4 (C_q), 137.3 (C_q), 136.7 (C_q), 136.4 (C_q), 136.3 (C_q), 135.7 (C_q), 133.1 (CH), 132.5 (C_q), 132.4 (C_q), 131.3 (CH), 131.2 (CH), 131.0 (CH), 130.9 (CH), 128.7 (CH), 128.7 (CH), 128.0 (C_q), 127.8 (CH), 127.7 (CH), 127.6 (CH), 127.6 (CH), 127.5 (CH), 127.4 (CH), 127.3 (CH), 126.8 (CH), 126.7 (CH), 124.8 (CH), 123.8 (C_q), 96.6 (C_q), 21.4 (CH₃), 21.3 (CH₃), 21.3 (CH₃). **IR** (ATR): 3089, 1687, 1628, 1502, 1347, 1095, 1033, 788, 757, 692, 490 cm⁻¹. (The lack of symmetry is caused by the presence of rotameric species at the room temperature). **HR-MS** (ESI) *m/z* calc. for C₄₆H₃₃N₂O₂S₂ [M+H]⁺: 709.1978, found: 709.1985.



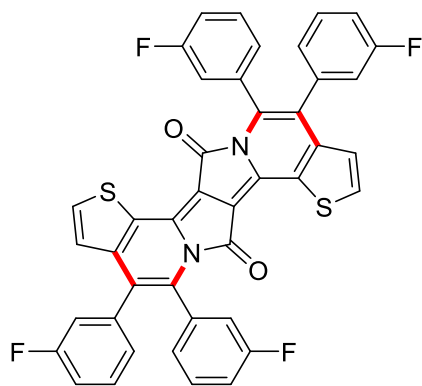
4,5,11,12-tetrakis(3-methoxyphenyl)-7H,14H-thieno[3',2':7,8]indolizino[2,1-a]thieno[3,2-g]indolizine-7,14-dione (144b).

The general procedure **D** was followed using 3,6-di(thiophen-2-yl)-2,5-dihydropyrrolo[3,4-c]pyrrole-1,4-dione **143a** (0.2 mmol, 60 mg) and 1,2-bis(3-methoxyphenyl)ethyne **64b** (0.8 mmol, 191 mg) yielding **144b** (80 mg, 52%) as the purple crystals. **M. p.** = 346 °C. **¹H NMR** (400 MHz, CDCl₃) δ = 7.57 (d, *J* = 5.2 Hz, 2H), 7.22-7.07 (m, 4H), 6.98-6.93 (m, 1H), 6.89-6.83 (m, 3H), 6.83-6.60 (m, 9H), 6.51 (s, 1H), 3.70-3.59 (m, 12H). **¹³C NMR** (101 MHz, CDCl₃) δ = 159.1 (C_q), 159.1 (C_q), 158.5 (C_q), 158.4 (C_q), 156.3 (C_q), 143.3 (C_q), 137.5 (C_q), 137.0 (C_q), 137.0 (C_q), 136.7 (C_q), 133.7 (CH), 133.3 (CH), 129.0 (CH), 128.9 (CH), 128.2 (CH), 128.2 (CH), 128.0 (CH), 124.8 (CH), 123.5 (C_q), 123.1 (CH), 123.0 (CH), 122.9 (CH), 115.9 (CH), 115.9 (CH), 115.8 (CH), 115.7 (CH), 115.7 (CH), 114.0 (CH), 113.9 (CH), 113.5 (CH), 113.4 (CH), 113.2 (CH), 113.2 (CH), 96.6 (C_q), 55.2 (CH₃), 55.1 (CH₃), 55.1 (CH₃), 55.1 (CH₃). (The lack of symmetry is caused by the presence of rotameric species at the room temperature). **IR** (ATR): 3090, 1685, 1632, 1575, 1475, 1284, 778, 756, 488 cm⁻¹. **HR-MS** (ESI) *m/z* calc. for C₄₆H₃₃N₂O₆S₂⁺ [M+H]⁺: 773.1775, found: 773.1766.



4,5,11,12-tetrakis(3-(trifluoromethyl)phenyl)-7H,14H-thieno[3',2':7,8]indolizino[2,1-a]thieno[3,2-g]indolizine-7,14-dione (144c).

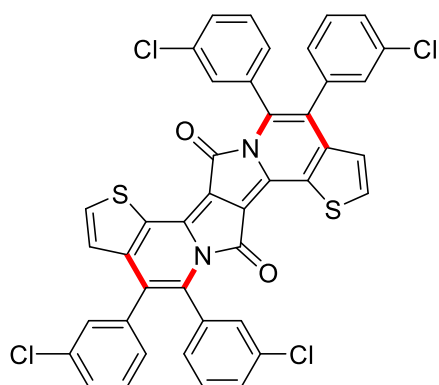
The general procedure **D** was followed using 3,6-di(thiophen-2-yl)-2,5-dihydropyrrolo[3,4-c]pyrrole-1,4-dione **143a** (0.2 mmol, 60 mg) and 1,2-bis(3-methoxyphenyl)ethyne **64c** (0.8 mmol, 251 mg), yielding **144c** (92 mg, 50%) as the purple crystals. **M. p.** = over the limit of the detection. **¹H NMR** (400 MHz, CDCl₃) δ = 7.75 – 7.68 (m, 1H), 7.65 – 7.33 (m, 7H), 7.26 – 7.15 (m, 1H), 6.91 – 6.80 (m, 1H). **¹³C NMR** (126 MHz, CDCl₃) δ = 156.2 (C_q), 142.7 (C_q), 142.6 (C_q), 136.7 (C_q), 136.5 (C_q), 135.9 (C_q), 135.9 (C_q), 134.3 (CH), 134.3 (CH), 133.8 (CH), 133.5 (CH), 133.4 (CH), 133.4 (CH), 133.4 (CH), 133.3 (CH), 133.3 (CH), 133.3 (CH), 132.8 (C_q), 132.7 (C_q), 128.8 (CH), 128.7 (C_q), 127.7 (CH), 127.5 (CH), 127.3 (CH), 127.0 (CH), 125.1 (CH), 125.0 (CH), 124.8 (C_q), 124.8 (C_q), 124.8 (C_q), 124.8 (C_q), 124.7 (C_q), 124.4 (C_q), 124.4 (CH), 124.4 (CH), 124.3 (CH), 122.9 (C_q), 122.8 (C_q), 122.7 (C_q), 122.6 (C_q), 122.6 (C_q), 122.5 (C_q), 96.8 (C_q). **¹⁹F NMR** (471 MHz, CDCl₃): δ = -62.79, -62.93, -62.97, -63.08. (The lack of symmetry is caused by the presence of rotameric species at the room temperature). **IR** (ATR): 2927, 2851, 1706, 1632, 1326, 1164, 1070, 803, 699, 664 cm⁻¹. **HR-MS** (ESI) m/z calc. for C₄₆H₂₁F₁₂N₂O₂S₂⁺ [M+H]⁺: 925.0847, found: 925.0839.



4,5,11,12-tetrakis(3-fluorophenyl)-7H,14H-thieno[3',2':7,8]indolizino[2,1-a]thieno[3,2-

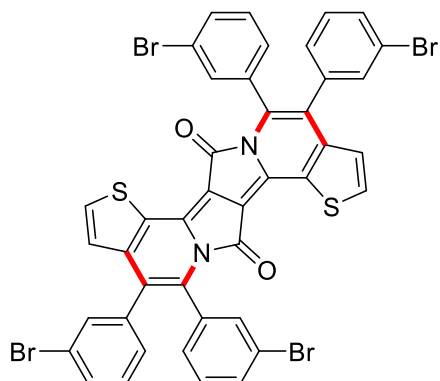
g]indolizine-7,14-dione (144d).

The general procedure **D** was followed using 3,6-di(thiophen-2-yl)-2,5-dihydropyrrolo[3,4-c]pyrrole-1,4-dione **143a** (0.2 mmol, 60 mg) and 1,2-bis(3-methoxyphenyl)ethyne **64d** (0.8 mmol, 171 mg). yielding **144d** (90 mg, 62%) as the purple crystals. **M. p.** = over the limit of the detection. **¹H NMR** (500 MHz, CDCl₃) δ = 7.62 (d, J = 5.2 Hz, 2H), 7.24–7.14 (m, 4H), 7.06 (d, J = 7.6 Hz, 2H), 7.03–6.74 (m, 12H). **¹³C NMR** (126 MHz, CDCl₃) δ = 162.4 (d, $^1J_{C-F}$ = 247 Hz, C_q), 161.8 (d, $^1J_{C-F}$ = 247 Hz, C_q), 156.2 (C_q), 142.9 (C_q), 137.3 (d, $^4J_{C-F}$ = 7.9 Hz, C_q), 136.6 (C_q), 136.4 (C_q), 134.1 (d, $^3J_{C-F}$ = 8.5 Hz, C_q), 133.9 (CH), 129.8 (d, $^3J_{C-F}$ = 9 Hz, CH), 129.7 (d, $^3J_{C-F}$ = 9 Hz, CH), 129.0 (d, $^3J_{C-F}$ = 8.5 Hz, CH), 128.8 (d, $^4J_{C-F}$ = 8.3 Hz, CH), 128.4 (C_q), 126.2 (d, $^2J_{C-F}$ = 19.5 Hz, CH), 124.5 (CH), 122.6 (C_q), 117.4 (d, $^2J_{C-F}$ = 20 Hz, CH), 115.4 (d, $^2J_{C-F}$ = 21 Hz, CH), 114.6 (d, $^2J_{C-F}$ = 21 Hz, CH), 96.7 (C_q). **¹⁹F NMR** (471 MHz, CDCl₃): δ = -112.58, -112.85, -113.30, -113.56. (The lack of symmetry is caused by the presence of rotameric species at the room temperature). **IR** (ATR): 1702, 1610, 1582, 1479, 1431, 1146, 758, 695, 489 cm⁻¹. **HR-MS** (ESI) m/z calc. for C₄₂H₂₁F₄N₂O₂S₂⁺ [M+H]⁺: 725.0975, found: 725.0961.

**4,5,11,12-tetrakis(3-chlorophenyl)-7H,14H-thieno[3',2':7,8]indolizino[2,1-a]thieno[3,2-g]indolizine-7,14-dione (144e).**

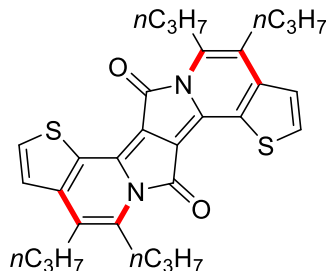
The general procedure **D** was followed using 3,6-bis(5-octylthiophen-2-yl)-2,5-dihydropyrrolo[3,4-c]pyrrole-1,4-dione **143a** (0.2 mmol, 60 mg) and 1,2-bis(3-chlorophenyl)ethyne **64e** (0.8 mmol, 198 mg). yielding **144e** (81 mg, 51%) as the purple crystals **M. p.** = over the limit of the detection. **¹H NMR** (400 MHz, CDCl₃) δ = 7.68 (d, J = 5.1 Hz, 2H), 7.28 – 7.15 (m, 13H), 7.11 (s, 1H), 7.02 (s, 1H), 6.96 (d, J = 7.7 Hz, 1H), 6.91 – 6.83 (m, 2H). **¹³C NMR** (101 MHz, CDCl₃) 156.2 (C_q), 142.9 (C_q), 137.0 (C_q), 136.7 (C_q), 136.4 (C_q), 134.2 (C_q), 134.1 (C_q), 134.0 (CH), 133.9 (C_q), 133.5 (C_q), 133.3 (C_q), 130.5 (CH), 130.4 (CH), 130.2 (CH), 129.6 (CH), 129.5 (CH), 128.8 (CH), 128.7 (CH), 128.6 (CH), 128.5 (CH), 127.9 (CH), 124.5 (CH), 122.6 (C_q), 96.7 (C_q). (The lack of symmetry is caused by the presence of rotameric species at the room temperature). **IR** (ATR): 1698, 1635, 1565, 1472, 1095, 1029, 789, 751,

707,486 cm^{-1} . **HR-MS** (ESI) m/z calc. for $\text{C}_{42}\text{H}_{21}\text{Cl}_4\text{N}_2\text{O}_2\text{S}_2^+$ $[\text{M}+\text{H}]^+$: 788.9793, found: 788.9787.



4,5,11,12-tetrakis(3-bromophenyl)-7H,14H-thieno[3',2':7,8]indolizino[2,1-a]thieno[3,2-g]indolizine-7,14-dione (144f)

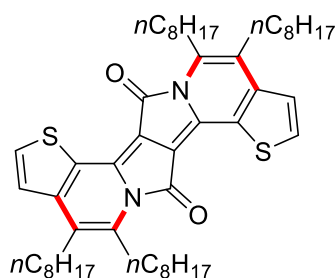
The general procedure **D** was followed using 3,6-bis(5-octylthiophen-2-yl)-2,5-dihydropyrrolo[3,4-c]pyrrole-1,4-dione **143a** (0.2 mmol, 60 mg) and 1,2-bis(3-bromophenyl)ethyne **64f** (0.8 mmol, 269 mg). yielding **144f** (103 mg, 53%) as the purple crystals. **M. p.** = over the limit of the detection. $^1\text{H NMR}$ (300 MHz, CDCl_3) δ = 7.68 (d, J = 5.2 Hz, 2H), 7.47 – 7.37 (m, 6H), 7.34 (s, 1H), 7.27 – 7.05 (m, 8H), 6.99 (d, J = 7.9 Hz, 1H), 6.87 (d, J = 5.4 Hz, 2H). $^{13}\text{C NMR}$ (126 MHz, CDCl_3) δ = 156.2 (C_q), 142.8 (C_q), 137.2 (C_q), 137.1 (C_q), 136.6 (C_q), 136.3 (C_q), 134.0 (CH), 133.5 (CH), 133.3 (CH), 133.0 (CH), 132.9 (CH), 131.4 (CH), 130.8 (CH), 129.8 (CH), 129.7 (CH), 129.2 (CH), 129.1 (CH), 128.9 (CH), 128.7 (CH), 128.5 (C_q), 124.5, 122.6 (C_q), 122.2 (C_q), 122.1 (C_q), 121.5 (C_q), 121.4 (C_q), 96.7 (C_q). (The lack of symmetry is caused by the presence of rotameric species at the room temperature). **IR** (ATR): 1697, 1635, 1559, 1470, 1347, 1094, 787, 746, 682, 482 cm^{-1} . **HR-MS** (ESI) m/z calc. for $\text{C}_{42}\text{H}_{21}\text{Br}_4\text{N}_2\text{O}_2\text{S}_2^+$ $[\text{M}+\text{H}]^+$: 964.7772, found: 964.7712.



4,5,11,12-tetra-*n*-propyl-7H,14H-thieno[3',2':7,8]indolizino[2,1-a]thieno[3,2-g]indolizine-7,14-dione (144g).

The general procedure **D** was followed using 3,6-di(thiophen-2-yl)-2,5-dihydropyrrolo[3,4-c]pyrrole-1,4-dione **143a** (0.2 mmol, 60 mg) and oct-4-yne **64g** (0.8 mmol, 88 mg). yielding **144g**

(60 mg, 58%) as the purple crystals. **M. p.** = 333 °C. **¹H NMR** (300 MHz, CDCl₃) δ = 7.74 (d, *J* = 5.3 Hz, 2H), 7.27 (d, 2H), 3.48-3.39 (m, 4H), 2.80-2.71 (m, 4H), 1.86-1.76 (m, 4H), 1.72-1.62 (m, 4H), 1.14 (t, *J* = 6.6 Hz, 6H), 1.09 (t, *J* = 6.6 Hz, 6H). **¹³C NMR** (126 MHz, CDCl₃) δ = 157.5 (C_q), 143.5 (C_q), 141.1 (C_q), 137.2 (C_q), 133.1 (CH), 127.4 (C_q), 122.8 (CH), 120.2 (C_q), 96.1 (C_q), 30.9 (CH₂), 30.6 (CH₂), 28.2 (CH₂), 24.1 (CH₂), 23.7 (CH₂), 14.4 (CH₃), 14.3 (CH₃). **IR** (ATR): 3074, 2963, 2951, 2928, 2867, 1683, 1640, 1546, 1028, 768, 698, 467 cm⁻¹. **HR-MS** (ESI) *m/z* calc. for C₃₀H₃₃N₂O₂S₂ [M+H]⁺: 517.1978, found: 517.1974.



4,5,11,12-tetrakis(3-*n*-octylphenyl)-7H,14H-thieno[3',2':7,8]indolizino[2,1-a]thieno[3,2-g]indolizine-7,14-dione (144h).

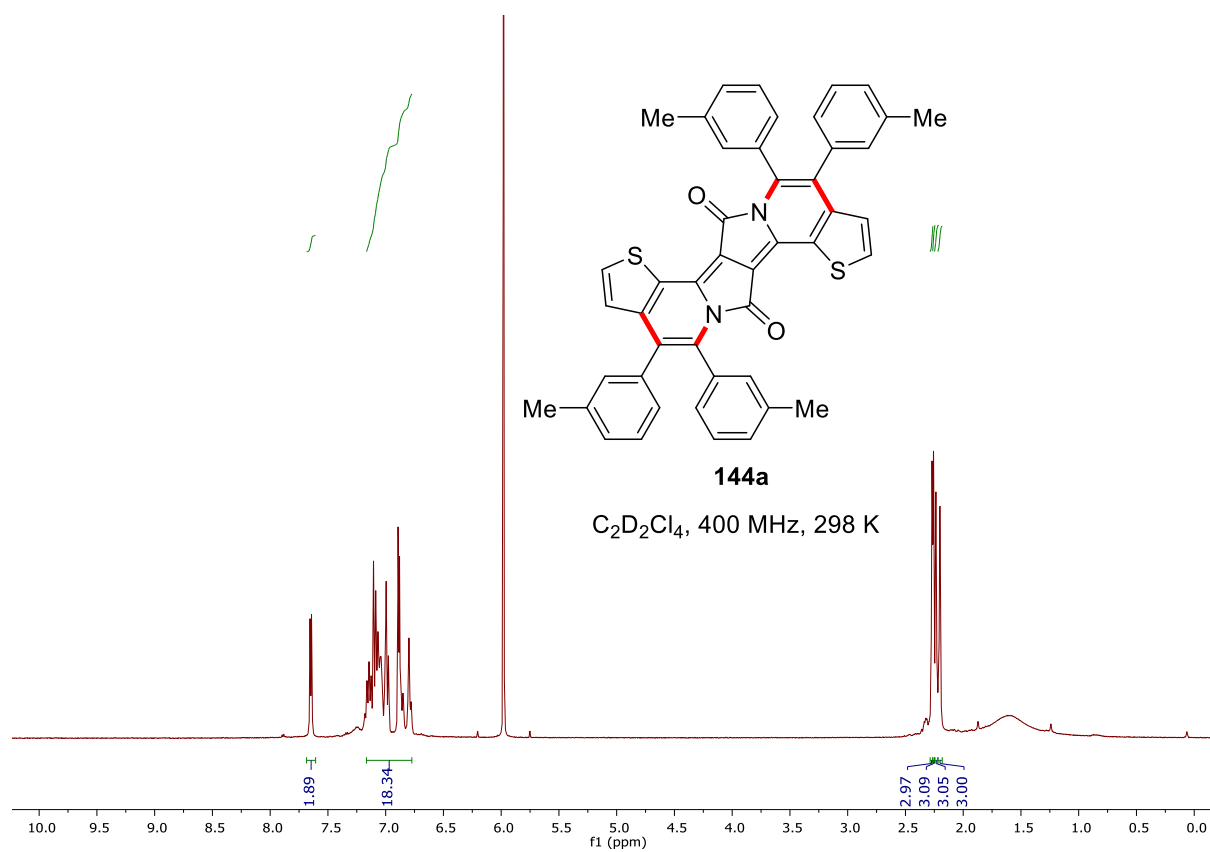
The general procedure **D** was followed using 3,6-di(thiophen-2-yl)-2,5-dihydropyrrolo[3,4-c]pyrrole-1,4-dione **143a** (0.2 mmol, 60 mg) and octadec-9-yne **64h** (0.8 mmol, 200 mg). yielding **144h** (89 mg, 56%) as the purple crystals. **M. p.** = 287 °C. **¹H NMR** (400 MHz, CDCl₃) δ = 7.73 (d, *J* = 5.2 Hz, 2H), 7.27 (d, *J* = 5.5 Hz, 2H), 3.44 (t, *J* = 8.0 Hz, 4H), 2.75 (t, *J* = 8.1 Hz, 4H), 1.81 – 1.71 (m, 4H), 1.68 – 1.59 (m, 4H), 1.53 – 1.28 (m, 40H), 0.95 – 0.88 (m, 12H). **¹³C NMR** (101 MHz, CDCl₃) δ = 157.5 (C_q), 143.6 (C_q), 141.3 (C_q), 137.1 (C_q), 133.1 (CH), 127.4 (C_q), 122.7 (CH), 120.3 (C_q), 96.1 (C_q), 31.9 (CH₂), 31.9 (CH₂), 30.8 (CH₂), 30.5 (CH₂), 29.9 (CH₂), 29.8 (CH₂), 29.5 (CH₂), 29.4 (CH₂), 29.3 (CH₂), 28.6 (CH₂), 26.3 (CH₂), 22.7 (CH₂), 22.7 (CH₂), 14.1 (CH₃), 14.1 (CH₃). **IR** (ATR): 2954, 2918, 2848, 1676, 1538, 1505, 1349, 1017, 772, 700 cm⁻¹. **HR-MS** (ESI) *m/z* calc. for C₅₀H₇₃N₂O₂S₂ [M+H]⁺: 797.5108, found: 797.5091.

5.3.2.2 Investigation of Rotameric Species

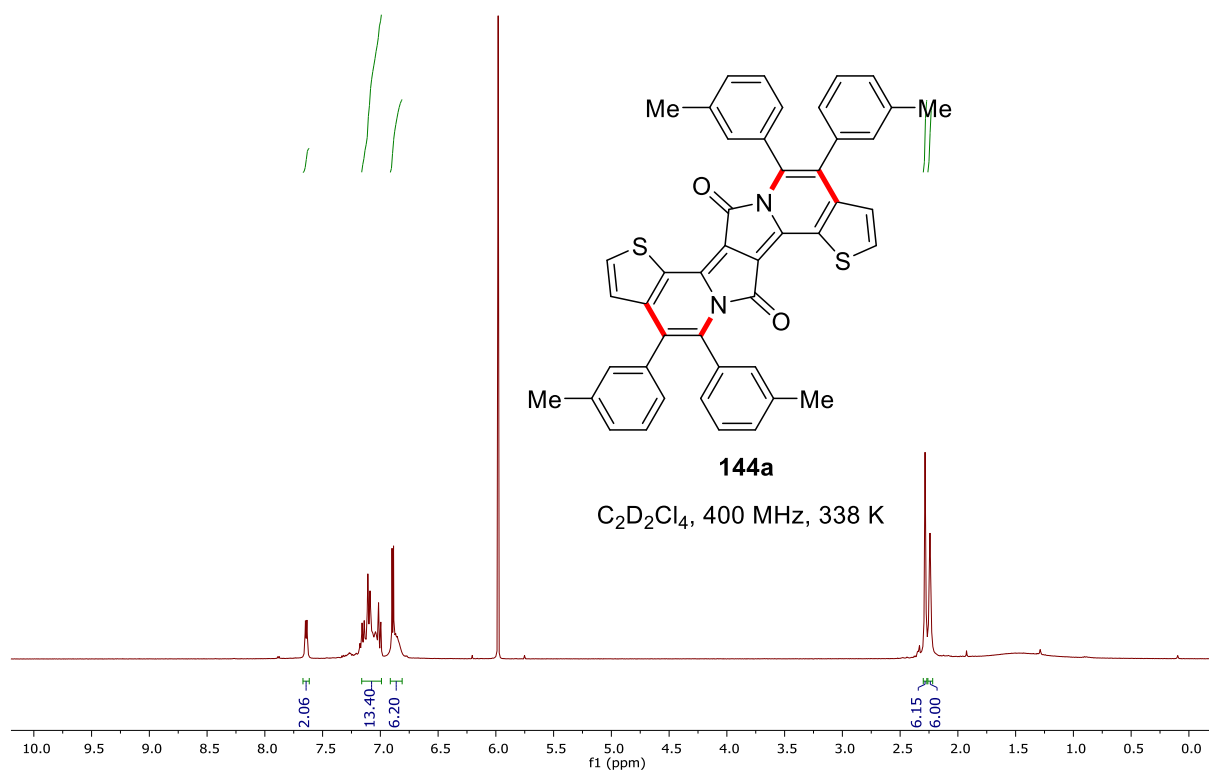
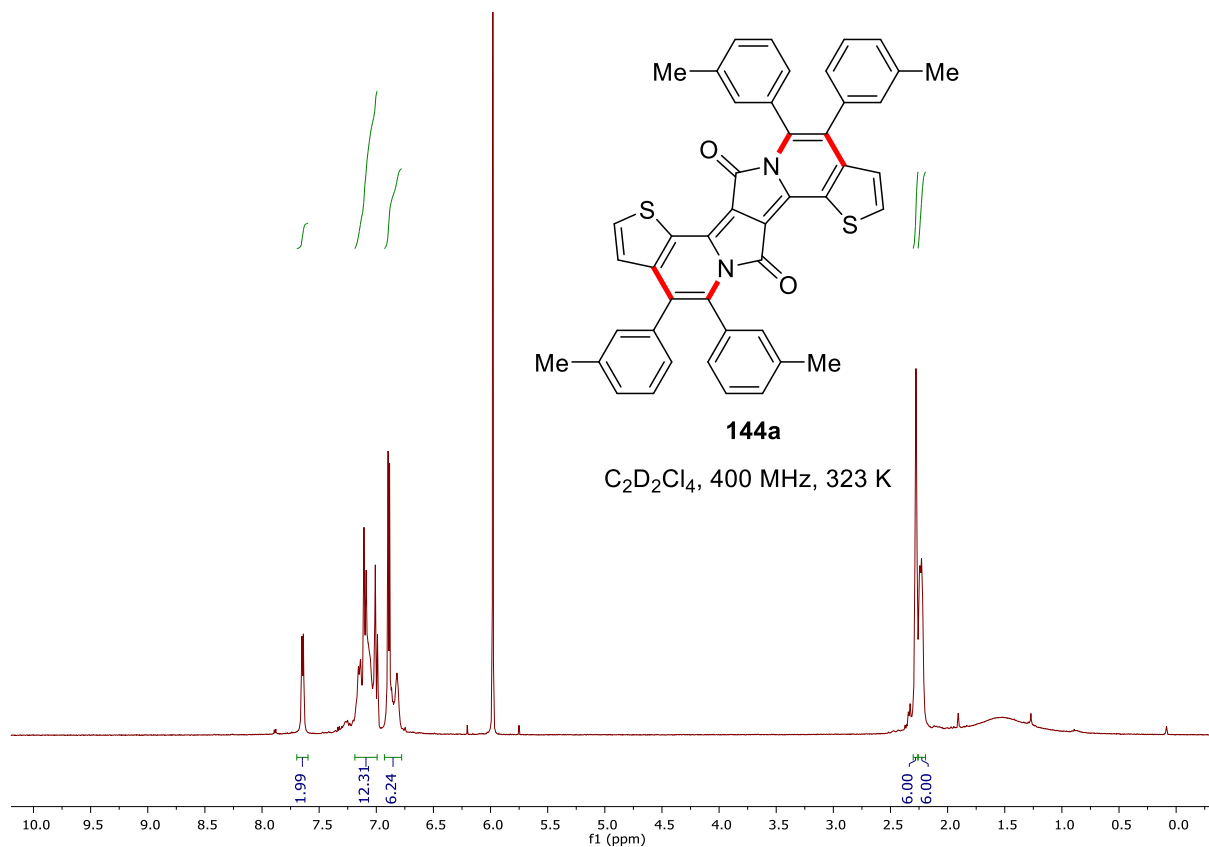
Due to the lack of the symmetry on the ¹H NMR spectra for compounds **144a-144f**, we have investigated the possibility of the presence of the rotameric species at the room temperature. In order to do that, we have measured ¹H NMR spectra for compound **144a** in different temperatures using 1,1,2,2-tetrachloroethane-d₂ as a solvent. In comparison to the ¹H NMR spectrum measured at 298 K, where four signals for all methyl groups can be easily distinguished, at higher temperatures (323 K and 338 K) only two signals are visible. Our

Experimental Section

observation clearly shows that the lack of symmetry, observed on spectra at room temperature of *meta*-substituted derivatives, is caused by the presence of rotameric species.

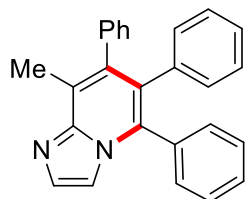


Experimental Section



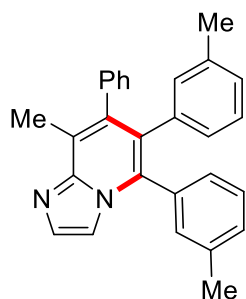
5.3.3 Ruthenaelectro(II/III/I)-Catalyzed Alkyne Annulations

5.3.3.1 Characterization Data



8-Methyl-5,6,7-triphenylimidazo[1,2-a]pyridine (146a)

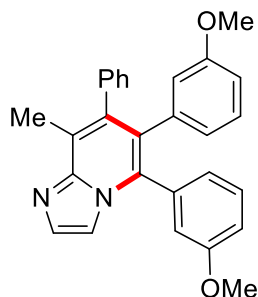
The general procedure **F** was followed using **145a** (74 mg, 0.4 mmol) and **64a** (142 mg, 0.8 mmol) at 140 °C for 8 h. Purification by column chromatography on silica gel (*n*-hexane/EtOAc = 5:1) yielded **146a** (108 mg, 75%) as a white solid. **M.p.**: 242 °C. **¹H NMR** (300 MHz, CDCl₃): δ = 7.64 (d, *J* = 1.2 Hz, 1H), 7.34 – 7.27 (m, 6H), 7.23 – 7.13 (m, 3H), 7.07 – 7.02 (m, 2H), 6.95 – 6.88 (m, 3H), 6.86 – 6.79 (m, 2H), 2.53 (s, 3H). **¹³C NMR** (101 MHz, CDCl₃): δ = 145.8 (C_q), 138.6 (C_q), 137.8 (C_q), 137.3 (C_q), 133.9 (C_q), 133.3 (C_q), 133.1 (CH), 131.5 (CH), 130.2 (CH), 130.2 (CH), 128.7 (CH), 127.6 (overlapped, CH), 127.0 (CH), 126.7 (C_q), 126.6 (CH), 126.1 (CH), 123.8 (C_q), 112.2 (CH), 15.2 (CH₃). **IR (ATR)**: 2922, 1495, 1474, 1443, 1285, 1141, 752, 700, 515 cm⁻¹. **MS (ESI)** *m/z* (relative intensity): 361 (100) [M+H]⁺. **HR-MS (ESI)** *m/z* calc. for C₂₆H₂₁N₂ [M+H]⁺: 361.1699, found: 361.1706. The analytical data corresponds with those reported in the literature. [231]



9-Methyl-7-phenyl-5,6-di-*m*-tolylimidazo[1,2-a]pyridine (146b)

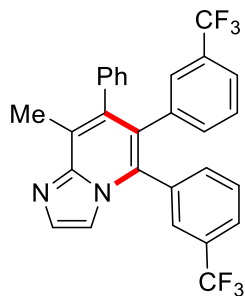
The general procedure **F** was followed using **145a** (74 mg, 0.4 mmol) and **64b** (165 mg, 0.8 mmol) at 140 °C for 8 h. Purification by column chromatography on silica gel (*n*-hexane/EtOAc = 5:1) yielded **146b** (117 mg, 75%) as a white solid. **M.p.**: 183 °C. **¹H NMR** (400 MHz, CDCl₃): δ = 7.63 (s, 1H), 7.29 (s, 1H), 7.22 – 6.96 (m, 9H), 6.79 (t, *J* = 7.6 Hz, 1H), 6.71 (d, *J* = 7.6 Hz, 1H), 6.62 (d, *J* = 8.5 Hz, 2H), 2.52 (t, *J* = 1.4 Hz, 3H), 2.29 (s, 3H), 2.03 (s, 3H). **¹³C NMR** (101 MHz, CDCl₃): δ = 145.7 (C_q), 138.8 (C_q), 138.2 (C_q), 138.0 (C_q), 137.1 (C_q), 136.3 (C_q), 133.9 (C_q), 133.4 (C_q), 132.9 (CH), 132.4 (CH), 130.7 (CH), 130.2 (CH), 129.3 (CH), 128.6 (CH), 128.4 (CH),

127.5 (CH), 127.2 (CH), 126.7 (CH), 126.7 (CH), 126.5 (CH), 123.5 (C_q, overlapped), 112.3 (CH), 21.3 (CH₃), 21.1 (CH₃), 15.2 (CH₃). **IR (ATR):** 2920, 1583, 1475, 1287, 1141, 775, 701, 530 cm⁻¹. **MS (ESI)** m/z (relative intensity): 389 (100) [M+H]⁺. **HR-MS (ESI)** m/z calc. for C₂₈H₂₅N₂ [M+H]⁺: 389.2012, found: 389.2014.



5,6-Bis(3-methoxyphenyl)-8-methyl-7-phenylimidazo[1,2-a]pyridine (146c)

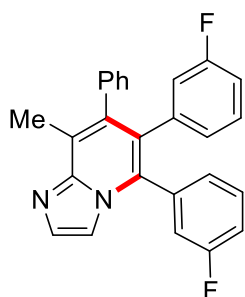
The general procedure **F** was followed using **145a** (74 mg, 0.4 mmol) and **64c** (190 mg, 0.8 mmol) at 140 °C for 8 h. Purification by column chromatography on silica gel (*n*-hexane/EtOAc = 5:1) yielded **146c** (127 mg, 76%) as a white solid. **M.p.:** 262 °C. **¹H NMR** (300 MHz, CDCl₃): δ = 7.61 (d, *J* = 1.3 Hz, 1H), 7.35 – 7.32 (m, 1H), 7.25 – 7.12 (m, 4H), 7.10 – 6.96 (m, 2H), 6.91 (d, *J* = 7.6 Hz, 1H), 6.85 – 6.76 (m, 3H), 6.51 – 6.29 (m, 3H), 3.66 (s, 3H), 3.48 (s, 3H), 2.50 (s, 3H). **¹³C NMR** (101 MHz, CDCl₃): δ = 159.8 (C_q), 158.5 (C_q), 145.8 (C_q), 138.7 (C_q), 138.7 (C_q), 137.8 (C_q), 135.2 (C_q), 133.2 (C_q), 133.2 (CH), 130.2 (CH), 129.8 (CH), 128.1 (CH), 127.7 (CH), 126.8 (CH), 126.5 (C_q), 124.3 (CH), 124.0 (C_q), 122.5 (CH), 117.0 (CH), 115.6 (CH), 114.8 (CH), 112.5 (CH), 112.4 (CH), 55.3 (CH₃), 55.2 (CH₃), 15.3 (CH₃). **IR (ATR):** 1599, 1474, 1473, 1430, 1316, 1287, 1244, 1045, 762 cm⁻¹. **MS (ESI)** m/z (relative intensity): 421 (100) [M+H]⁺, 185 (10). **HR-MS (ESI)** m/z calc. For C₂₈H₂₅N₂O₂ [M+H]⁺: 421.1916 found: 421.1911.



8-Methyl-7-phenyl-5,6-bis[3-(trifluoromethyl)phenyl]imidazo[1,2-a]pyridine (146d)

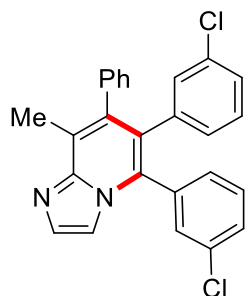
The general procedure **F** was followed using **145a** (74 mg, 0.4 mmol) and **64d** (251 mg, 0.8 mmol) at 140 °C for 8 h. Purification by column chromatography on silica gel (*n*-hexane/EtOAc = 5:1) yielded **146d** (145 mg, 73%) as a white solid. **M.p.:** 183 °C. **¹H NMR** (400 MHz, CDCl₃): δ =

7.70 (s, 1H), 7.60 (t, $J = 4.7$ Hz, 1H), 7.57 – 7.46 (m, 3H), 7.27 – 7.11 (m, 5H), 7.11 – 6.90 (m, 5H), 2.55 (s, 3H). **^{13}C NMR** (101 MHz, CDCl_3): $\delta = 145.8$ (C_q), 137.8 (overlapped, C_q), 137.2 (C_q), 134.5 (CH), 134.2 (C_q), 133.8 (CH), 133.3 (CH), 131.8 (C_q), 131.5 (q, $^2J_{\text{C-F}} = 18$ Hz, C_q), 131.2 (q, $^2J_{\text{C-F}} = 18$ Hz, C_q), 130.0 (CH), 129.5 (CH), 128.4 (q, $^3J_{\text{C-F}} = 3$ Hz, CH), 127.9 (CH), 127.8 (CH), 127.3 (q, $^3J_{\text{C-F}} = 3$ Hz, CH), 127.1 (CH), 126.0 (C_q), 125.8 (q, $^3J_{\text{C-F}} = 3$ Hz, CH), 125.2 (C_q), 123.6 (q, $^1J_{\text{C-F}} = 272$ Hz, C_q), 123.5 (q, $^1J_{\text{C-F}} = 272$ Hz, C_q), 123.2 (q, $^3J_{\text{C-F}} = 5$ Hz, CH), 112.0 (CH), 15.2 (CH₃). **^{19}F NMR** (376 MHz, CDCl_3): $\delta = -63.3$ (s), -63.4 (s). **IR (ATR)**: 1343, 1314, 1297, 1163, 1117, 1076, 780, 705, 668 cm^{-1} . **MS (ESI)** m/z (relative intensity): 497 (100) $[\text{M}+\text{H}]^+$, 519 (10) $[\text{M}+\text{Na}]^+$. **HR-MS (ESI)** m/z calc. for $\text{C}_{28}\text{H}_{19}\text{N}_2\text{F}_6$ $[\text{M}+\text{H}]^+$: 497.1447, found: 497.1449.



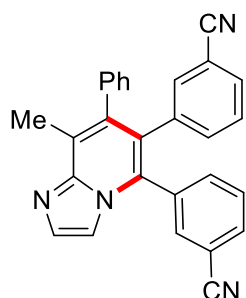
5,6-Bis(3-fluorophenyl)-8-methyl-7-phenylimidazo[1,2-a]pyridine (146e)

The general procedure **F** was followed using **145a** (74 mg, 0.4 mmol) and **64e** (171 mg, 0.8 mmol) at 140 °C for 8 h. Purification by column chromatography on silica gel (*n*-hexane/EtOAc = 5:1) yielded **146e** (100 mg, 63%) as a white solid. **M.p.**: 182 °C. **^1H NMR** (300 MHz, CDCl_3): $\delta = 7.67$ (s, 1H), 7.44 – 7.28 (m, 2H), 7.26 – 7.15 (m, 3H), 7.11 – 6.98 (m, 5H), 6.90 (t, $J = 7.2$ Hz, 1H), 6.70 – 6.59 (m, 2H), 6.55 (dd, $J = 9.5, 2.4$ Hz, 1H), 2.52 (s, 3H). **^{13}C NMR** (101 MHz, CDCl_3): $\delta = 162.7$ (d, $^1J_{\text{C-F}} = 248$ Hz, C_q), 161.7 (d, $^1J_{\text{C-F}} = 246$ Hz, C_q), 145.7 (C_q), 139.2 (d, $^3J_{\text{C-F}} = 8$ Hz, C_q), 138.0 (C_q), 137.3 (C_q), 135.5 (d, $^3J_{\text{C-F}} = 8$ Hz, C_q), 133.5 (CH), 131.8 (C_q), 130.6 (d, $^3J_{\text{C-F}} = 7$ Hz, CH), 130.0 (CH), 128.7 (d, $^3J_{\text{C-F}} = 7$ Hz, CH), 127.8 (CH), 127.2 (d, $^4J_{\text{C-F}} = 3$ Hz, CH), 127.0 (CH), 125.9 (d, $^4J_{\text{C-F}} = 3$ Hz, CH), 125.7 (C_q), 124.7 (C_q), 118.2 (d, $^2J_{\text{C-F}} = 21$ Hz, CH), 117.1 (d, $^2J_{\text{C-F}} = 22$ Hz, CH), 116.1 (d, $^2J_{\text{C-F}} = 22$ Hz, CH), 113.4 (d, $^2J_{\text{C-F}} = 21$ Hz, CH), 112.1 (CH), 15.2 (CH₃). **^{19}F NMR** (376 MHz, CDCl_3): $\delta = -111.7$ (s), -114.3 (s). **IR (ATR)**: 3029, 1611, 1579, 1472, 1430, 1227, 931, 765, 695 cm^{-1} . **MS (ESI)** m/z (relative intensity): 397 (100) $[\text{M}+\text{H}]^+$, 419 (10) $[\text{M}+\text{Na}]^+$. **HR-MS (ESI)** m/z calc. for $\text{C}_{26}\text{H}_{19}\text{N}_2\text{F}_2$ $[\text{M}+\text{H}]^+$: 397.1511, found: 397.1512.



5,6-Bis(3-chlorophenyl)-8-methyl-7-phenylimidazo[1,2-a]pyridine (146f)

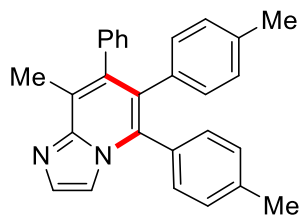
The general procedure **F** was followed using **145a** (74 mg, 0.4 mmol) and **64f** (198 mg, 0.8 mmol) at 140 °C for 8 h. Purification by column chromatography on silica gel (*n*-hexane/EtOAc = 5:1) yielded **146f** (120 mg, 70%) as a white solid. **M.p.**: 198 °C. **¹H NMR** (400 MHz, CDCl₃): δ = 7.67 (s, 1H), 7.39 – 7.28 (m, 4H), 7.26 – 7.12 (m, 4H), 7.08 – 6.98 (m, 2H), 6.96 – 6.81 (m, 3H), 6.73 (t, *J* = 6.8 Hz, 1H), 2.52 (s, 3H). **¹³C NMR** (101 MHz, CDCl₃): δ = 145.7 (C_q), 138.8 (C_q), 138.0 (C_q), 137.4 (C_q), 135.2 (C_q), 134.7 (C_q), 133.5 (CH), 133.0 (C_q), 131.8 (C_q), 131.4 (CH), 130.3 (CH), 130.1 (CH), 130.0 (CH), 129.6 (CH), 129.3 (CH), 128.5 (CH), 128.4 (CH), 127.9 (CH), 127.0 (CH), 126.7 (CH), 125.7 (C_q), 124.8 (C_q), 112.1 (CH), 15.2 (CH₃). **IR (ATR)**: 3046, 1592, 1564, 1463, 1289, 1145, 770, 697, 533 cm⁻¹. **MS (ESI)** *m/z* (relative intensity): 429 (100) [M+H]⁺. **HR-MS (ESI)** *m/z* calc. for C₂₆H₁₉N₂³⁵Cl₂ [M+H]⁺: 429.0920, found: 429.0921.



3,3'-(8-Methyl-7-phenylimidazo[1,2-a]pyridine-5,6-diyl)dibenzonitrile (146g)

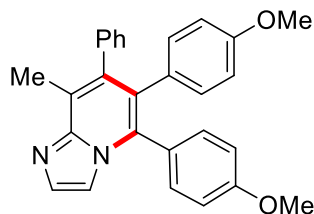
The general procedure **F** was followed using **145a** (74 mg, 0.4 mmol) and **64g** (183 mg, 0.8 mmol) at 140 °C for 8 h. Purification by column chromatography on silica gel (*n*-hexane/EtOAc = 5:1) yielded **146g** (110 mg, 67%) as a white solid. **M.p.**: 240 °C. **¹H NMR** (400 MHz, CDCl₃): δ = 7.70 (s, 1H), 7.70 – 7.65 (m, 1H), 7.63 – 7.49 (m, 3H), 7.31 – 7.24 (m, 2H), 7.23 – 7.17 (m, 3H), 7.14 – 7.05 (m, 3H), 7.05 – 6.92 (m, 2H), 2.53 (s, 3H). **¹³C NMR** (101 MHz, CDCl₃): δ = 145.8 (C_q), 138.3 (C_q), 137.5 (C_q), 137.0 (C_q), 135.6 (CH), 134.8 (CH), 134.6 (C_q), 134.4 (CH), 134.2 (CH), 133.6 (CH), 132.8 (CH), 130.9 (C_q), 130.4 (CH), 130.1 (CH), 130.0 (CH), 128.3 (CH), 128.1 (CH), 127.4 (CH), 126.0 (C_q), 125.4 (C_q), 118.0 (C_q), 117.4 (C_q), 113.9 (C_q), 111.9 (C_q), 111.8 (CH), 15.1 (CH₃). **IR (ATR)**: 3029, 2230, 1473, 1291, 1143, 811, 781, 695 cm⁻¹. **MS (ESI)**

m/z (relative intensity): 411 (100) [M+H]⁺, 433 (10) [M+Na]⁺. **HR-MS (ESI)** m/z calc. for C₂₈H₁₉N₄ [M+H]⁺: 411.1604, found: 411.1604.



8-Methyl-7-phenyl-5,6-di-*p*-tolylimidazo[1,2-*a*]pyridine (146h)

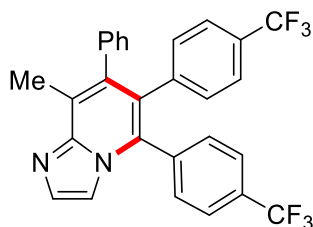
The general procedure **F** was followed using **145a** (74 mg, 0.4 mmol) and **64h** (165 mg, 0.8 mmol) at 140 °C for 8 h. Purification by column chromatography on silica gel (*n*-hexane/EtOAc = 5:1) yielded **146h** (107 mg, 69%) as a white solid. **M.p.**: 259 °C. **¹H NMR** (300 MHz, CDCl₃): δ = 7.63 (d, *J* = 1.1 Hz, 1H), 7.31 – 7.29 (m, 1H), 7.24 – 7.11 (m, 7H), 7.05 – 7.00 (m, 2H), 6.75 – 6.66 (m, 4H), 2.52 (s, 3H), 2.35 (s, 3H), 2.13 (s, 3H). **¹³C NMR** (101 MHz, CDCl₃): δ = 145.9 (C_q), 130.0 (C_q), 138.5 (C_q), 138.3 (C_q), 135.4 (C_q), 134.3 (C_q), 133.4 (C_q), 132.8 (CH), 131.3 (CH), 131.1 (C_q), 130.3 (CH), 130.1 (CH), 129.5 (CH), 127.9 (CH), 127.7 (CH), 127.1 (C_q), 126.6 (CH), 123.6 (C_q), 112.4 (CH), 21.5 (CH₃), 21.2 (CH₃), 15.3 (CH₃). **IR (ATR)**: 1600, 1513, 1483, 1442, 1287, 1144, 817, 731, 702 cm⁻¹. **MS (ESI)** m/z (relative intensity): 389 (100) [M+H]⁺. **HR-MS (ESI)** m/z calc. for C₂₈H₂₅N₂ [M+H]⁺: 389.2018, found: 389.2012.



5,6-Bis(4-methoxyphenyl)-8-methyl-7-phenylimidazo[1,2-*a*]pyridine (146i)

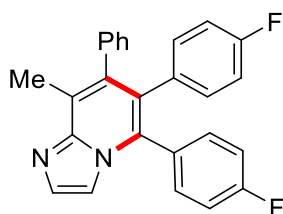
The general procedure **F** was followed using **145a** (74 mg, 0.4 mmol) and **64i** (165 mg, 0.8 mmol) at 140 °C for 8 h. Purification by column chromatography on silica gel (*n*-hexane/EtOAc = 5:1) yielded **146i** (119 mg, 71%) as a white solid. **M.p.**: 197 °C. **¹H NMR** (400 MHz, CDCl₃): δ = 7.62 (d, *J* = 1.3 Hz, 1H), 7.31 (d, *J* = 1.3 Hz, 1H), 7.23 – 7.13 (m, 5H), 7.05 – 7.00 (m, 2H), 6.85 (d, *J* = 8.7 Hz, 2H), 6.71 (d, *J* = 8.7 Hz, 2H), 6.47 (d, *J* = 8.7 Hz, 2H), 3.80 (s, 3H), 3.64 (s, 3H), 2.50 (s, 3H). **¹³C NMR** (101 MHz, CDCl₃): δ = 159.4 (C_q), 157.5 (C_q), 145.8 (C_q), 138.9 (C_q), 138.2 (C_q), 133.3 (C_q), 132.9 (CH), 132.5 (CH), 131.4 (CH), 130.2 (CH), 129.8 (C_q), 127.6 (CH), 126.5 (CH), 126.4 (overlapped, C_q), 123.5 (C_q), 114.1 (CH), 112.5 (CH), 112.1 (CH), 55.2 (CH₃), 54.9 (CH₃), 15.2 (CH₃). **IR (ATR)**: 3022, 2959, 2835, 1605, 1511, 1478, 1288, 1240, 701 cm⁻¹.

MS (ESI) m/z (relative intensity): 421 (100) $[M+H]^+$, 185 (10). **HR-MS (ESI)** m/z calc. for $C_{28}H_{25}N_2O_2$ $[M+H]^+$: 421.1911, found: 421.1912.



8-Methyl-7-phenyl-5,6-bis[4-(trifluoromethyl)phenyl]imidazo[1,2-a]pyridine (146j)

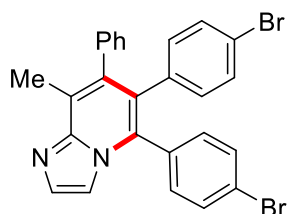
The general procedure **F** was followed using **145a** (74 mg, 0.4 mmol) and **64j** (251 mg, 0.8 mmol) at 140 °C for 8 h. Purification by column chromatography on silica gel (*n*-hexane/EtOAc = 5:1) yielded **146j** (137 mg, 69%) as a white solid. **M.p.**: 266 °C. **¹H NMR** (300 MHz, $CDCl_3$): δ = 7.68 (d, J = 1.1 Hz, 1H), 7.63 (d, J = 8.0 Hz, 2H), 7.42 (d, J = 8.0 Hz, 2H), 7.25 – 7.17 (m, 6H), 7.04 – 6.98 (m, 2H), 6.95 (d, J = 8.0 Hz, 2H), 2.54 (s, 3H). **¹³C NMR** (101 MHz, $CDCl_3$): δ = 145.8 (C_q), 140.8 (C_q), 137.7 (C_q), 137.2 (C_q), 137.1 (C_q), 133.7 (CH), 131.7 (C_q), 131.7 (CH), 131.2 (q, $^2J_{C-F}$ = 33 Hz, C_q), 130.7 (CH), 130.0 (CH), 128.6 (q, $^2J_{C-F}$ = 33 Hz, C_q), 127.9 (CH), 127.1 (CH), 126.0 (q, $^3J_{C-F}$ = 4 Hz, CH), 125.8 (C_q), 125.2 (C_q), 124.2 (q, $^3J_{C-F}$ = 4 Hz, CH), 123.8 (q, $^1J_{C-F}$ = 273 Hz, C_q), 123.5 (q, $^1J_{C-F}$ = 273 Hz, C_q), 112.0 (CH), 15.2 (CH₃). **¹⁹F NMR** (282 MHz, $CDCl_3$): δ = –62.7 (s), –62.9 (s). **IR (ATR)**: 1615, 1323, 1157, 1109, 1065, 1019, 850, 704 cm^{-1} . **MS (ESI)** m/z (relative intensity): 497 (100) $[M+H]^+$, 519 (10) $[M+Na]^+$. **HR-MS (ESI)** m/z calc. for $C_{28}H_{19}N_2F_6$ $[M+H]^+$: 497.1447, found: 497.1449.



5,6-Bis(4-fluorophenyl)-8-methyl-7-phenylimidazo[1,2-a]pyridine (146k)

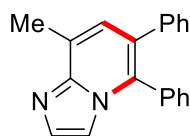
The general procedure **A** was followed using **145a** (74 mg, 0.4 mmol) and **64k** (171 mg, 0.8 mmol) at 140 °C for 8 h. Purification by column chromatography on silica gel (*n*-hexane/EtOAc = 5:1) yielded **146k** (82 mg, 52%) as a white solid. **M.p.**: 249 °C. **¹H NMR** (400 MHz, $CDCl_3$): δ = 7.66 (d, J = 1.2 Hz, 1H), 7.29 – 7.26 (m, 2H), 7.25 – 7.14 (m, 4H), 7.07 – 6.99 (m, 4H), 6.79 – 6.74 (m, 2H), 6.68 – 6.60 (m, 2H), 2.52 (s, 3H). **¹³C NMR** (101 MHz, $CDCl_3$): δ = 162.5 (d, $^1J_{C-F}$ = 250 Hz, C_q), 161.1 (d, $^1J_{C-F}$ = 250 Hz, C_q), 145.7 (C_q), 138.3 (C_q), 137.8 (C_q), 133.2 (CH), 133.1 (d, $^4J_{C-F}$ = 3 Hz, C_q), 132.9 (d, $^3J_{C-F}$ = 8 Hz, CH), 132.4 (C_q), 132.0 (d, $^3J_{C-F}$ = 8 Hz, CH), 130.1

(CH), 129.7 (d, $^4J_{C-F} = 4$ Hz, C_q), 127.8 (CH), 126.8 (CH), 126.1 (C_q), 124.3 (C_q), 116.1 (d, $^2J_{C-F} = 22$ Hz, CH), 114.2 (d, $^2J_{C-F} = 22$ Hz, CH), 112.0 (CH), 15.2 (CH₃). **¹⁹F NMR** (377 MHz, CDCl₃): $\delta = -111.3$ (s), -115.6 (s). **IR (ATR)**: 3025, 1601, 1508, 1481, 1288, 1216, 1143, 782, 700 cm⁻¹. **MS (ESI)** m/z (relative intensity): 397 (100) [M+H]⁺, 419 (10) [M+Na]⁺. **HR-MS (ESI)** m/z calc. for C₂₆H₁₉N₂F₂ [M+H]⁺: 397.1511, found: 397.1511.



5,6-Bis(4-bromophenyl)-8-methyl-7-phenylimidazo[1,2-a]pyridine (146l)

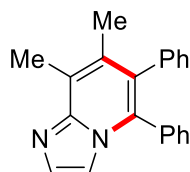
The general procedure **F** was followed using **145a** (74 mg, 0.4 mmol) and **64I** (269 mg, 0.8 mmol) at 140 °C for 8 h. Purification by column chromatography on silica gel (*n*-hexane/EtOAc = 5:1) yielded **146l** (141 mg, 68%) as a white solid. **M.p.**: 276 °C. **¹H NMR** (300 MHz, CDCl₃): $\delta = 7.65$ (d, $J = 1.2$ Hz, 1H), 7.50 (d, $J = 8.4$ Hz, 2H), 7.27 – 7.17 (m, 4H), 7.17 – 7.12 (m, 2H), 7.11 – 7.05 (m, 2H), 7.03 – 6.97 (m, 2H), 6.68 (d, $J = 8.4$ Hz, 2H), 2.50 (s, 3H). **¹³C NMR** (75 MHz, CDCl₃): $\delta = 145.7$ (C_q), 138.1 (C_q), 137.4 (C_q), 136.1 (C_q), 133.4 (CH), 132.9 (CH), 132.5 (C_q), 132.3 (CH), 132.0 (C_q), 131.7 (CH), 130.5 (CH), 130.1 (CH), 127.9 (CH), 127.0 (CH), 125.7 (C_q), 124.6 (C_q), 123.3 (C_q), 120.7 (C_q), 112.0 (CH), 15.2 (CH₃). **IR (ATR)**: 2149, 1977, 1948, 1474, 1070, 1011, 822, 732, 700 cm⁻¹. **MS (ESI)** m/z (relative intensity): 516 (100) [M+H]⁺, 441 (10). **HR-MS (ESI)** m/z calc. for C₂₆H₁₉N₂⁷⁹Br₂ [M+H]⁺: 516.9910, found: 516.9913.



8-Methyl-5,6-diphenylimidazo[1,2-a]pyridine (146m)

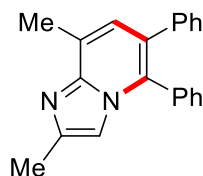
The general procedure **F** was followed using **145b** (43 mg, 0.4 mmol) and **64a** (143 mg, 0.8 mmol) at 140 °C for 8 h. Purification by column chromatography on silica gel (*n*-hexane/EtOAc = 5:1) yielded **146m** (63 mg, 55%) as a white solid. **M.p.**: 135 °C. **¹H NMR** (300 MHz, CDCl₃): $\delta = 7.59$ (d, $J = 1.3$ Hz, 1H), 7.41 – 7.36 (m, 3H), 7.35 (d, $J = 1.3$ Hz, 1H), 7.34 – 7.29 (m, 2H), 7.23 – 7.17 (m, 4H), 7.17 – 7.12 (m, 2H), 2.72 (s, 3H). **¹³C NMR** (75 MHz, CDCl₃): $\delta = 145.7$ (C_q), 138.6 (C_q), 133.6 (C_q), 133.0 (C_q), 132.9 (CH), 130.3 (CH), 129.9 (CH), 129.0 (CH), 128.9 (CH), 128.0 (CH), 126.9 (CH), 126.8 (CH), 126.1 (C_q), 125.6 (C_q), 112.2 (CH), 17.0 (CH₃). **IR (ATR)**: 2918, 1477, 1442, 1307, 1265, 1146, 763, 696 cm⁻¹. **MS (ESI)** m/z (relative intensity): 285 (100)

[M+H]⁺. **HR-MS (ESI)** m/z calc. for C₂₀H₁₇N₂ [M+H]⁺: 285.1386, found: 285.1388. The analytical data corresponds with those reported in the literature.^[231]



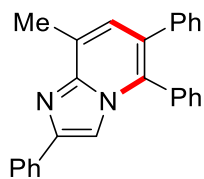
7,8-Dimethyl-5,6-diphenylimidazo[1,2-a]pyridine (146n)

The general procedure **F** was followed using **145c** (49 mg, 0.4 mmol) and **64a** (143 mg, 0.8 mmol) at 140 °C for 8 h. Purification by column chromatography on silica gel (*n*-hexane/EtOAc = 5:1) yielded **146n** (63 mg, 53%) as a white solid. **M.p.**: 196 °C. **¹H NMR** (300 MHz, CDCl₃): δ = 7.57 – 7.49 (m, 1H), 7.33 – 7.27 (m, 3H), 7.25 – 7.16 (m, 5H), 7.15 – 7.12 (m, 1H), 7.10 – 7.02 (m, 2H), 2.70 (s, 3H), 2.10 (s, 3H). **¹³C NMR** (75 MHz, CDCl₃): δ = 146.1 (C_q), 137.9 (C_q), 133.9 (C_q), 133.1 (C_q), 132.4 (CH), 131.6 (C_q), 130.7 (CH), 130.0 (CH), 128.6 (CH), 128.5 (CH), 127.8 (CH), 127.6 (C_q), 126.8 (CH), 123.2 (C_q), 111.7 (CH), 17.1 (CH₃), 13.9 (CH₃). **IR (ATR)**: 1979, 1474, 1442, 1306, 869, 755, 695 cm⁻¹. **MS (ESI)** m/z (relative intensity): 299 (100) [M+H]⁺. **HR-MS (ESI)** m/z calc. for C₂₁H₁₉N₂ [M+H]⁺: 299.1543, found: 299.1544.

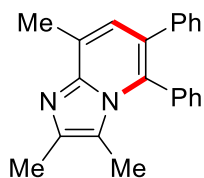


2,8-Dimethyl-5,6-diphenylimidazo[1,2-a]pyridine (146o)

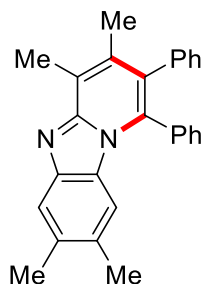
The general procedure **F** was followed using **145d** (49 mg, 0.4 mmol) and **64a** (143 mg, 0.8 mmol) at 140 °C for 8 h. Purification by column chromatography on silica gel (*n*-hexane/EtOAc = 5:1) yielded **146o** (60 mg, 50%) as a white solid. **M.p.**: 189 °C. **¹H NMR** (400 MHz, CDCl₃): δ = 7.42 – 7.36 (m, 3H), 7.32 – 7.28 (m, 2H), 7.23 – 7.17 (m, 3H), 7.16 – 7.12 (m, 3H), 7.10 (s, 1H), 2.70 (s, 3H), 2.45 (s, 3H). **¹³C NMR** (101 MHz, CDCl₃): δ = 145.3 (C_q), 142.6 (C_q), 138.8 (C_q), 133.8 (C_q), 132.5 (C_q), 130.3 (CH), 129.9 (CH), 128.9 (CH), 128.9 (CH), 127.9 (CH), 126.7 (CH), 126.6 (CH), 125.1 (C_q), 125.0 (C_q), 109.4 (CH), 17.1 (CH₃), 14.5 (CH₃). **IR (ATR)**: 2017, 1989, 1476, 1437, 1320, 1180, 768, 699 cm⁻¹. **MS (ESI)** m/z (relative intensity): 299 (100) [M+H]⁺. **HR-MS (ESI)** m/z calc. for C₂₁H₁₉N₂ [M+H]⁺: 299.1543, found: 299.1543.

**8-Methyl-2,5,6-triphenylimidazo[1,2-a]pyridine (146p)**

The general procedure **F** was followed using **145e** (74 mg, 0.4 mmol) and **64a** (143 mg, 0.8 mmol) at 140 °C for 8 h. Purification by column chromatography on silica gel (*n*-hexane/EtOAc = 5:1) yielded **146p** (74 mg, 51%) as a white solid. **M.p.**: 205 °C. **¹H NMR** (300 MHz, CDCl₃): δ = 7.98 – 7.90 (m, 2H), 7.63 (s, 1H), 7.45 – 7.41 (m, 4H), 7.41 – 7.28 (m, 4H), 7.24 – 7.13 (m, 6H), 2.79 (s, 3H). **¹³C NMR** (75 MHz, CDCl₃): δ = 146.0 (C_q), 145.3 (C_q), 138.7 (C_q), 134.2 (C_q), 133.7 (C_q), 132.8 (C_q), 130.4 (CH), 129.9 (CH), 129.0 (overlapped, CH), 128.6 (CH), 128.0 (CH), 127.7 (CH), 127.2 (CH), 126.8 (CH), 126.2 (CH), 126.1 (C_q), 125.6 (C_q), 108.0 (CH), 17.1 (CH₃). **IR (ATR)**: 1979, 1950, 1475, 724, 695, 583, 509 cm⁻¹. **MS (ESI)** m/z (relative intensity): 361 (100) [M+H]⁺. **HR-MS (ESI)** m/z calc. for C₂₆H₂₁N₂ [M+H]⁺: 361.1699, found: 361.1699.

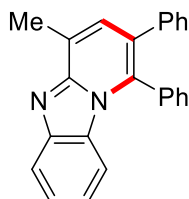
**2,3,8-Trimethyl-5,6-diphenylimidazo[1,2-a]pyridine (146q)**

The general procedure **F** was followed using **145f** (55 mg, 0.4 mmol) and **64a** (143 mg, 0.8 mmol) at 140 °C for 8 h. Purification by column chromatography on silica gel (*n*-hexane/EtOAc = 5:1) yielded **146q** (50 mg, 40%) as a white solid. **M.p.**: 185 °C. **¹H NMR** (400 MHz, CDCl₃): δ = 7.38 – 7.24 (m, 5H), 7.19 – 7.13 (m, 3H), 7.11 – 7.06 (m, 2H), 6.99 (s, 1H), 2.68 (s, 3H), 2.40 (s, 3H), 1.66 (s, 3H). **¹³C NMR** (101 MHz, CDCl₃): δ = 144.6 (C_q), 140.5 (C_q), 139.3 (C_q), 133.7 (C_q), 133.5 (C_q), 131.9 (CH), 130.0 (CH), 128.5 (CH), 127.6 (CH), 127.3 (CH), 126.4 (CH), 126.3 (C_q), 125.4 (CH), 125.1 (C_q), 118.6 (C_q), 17.2 (CH₃), 13.7 (CH₃), 12.0 (CH₃). **IR (ATR)**: 2148, 2085, 1978, 1438, 1251, 710, 697, 642 cm⁻¹. **MS (ESI)** m/z (relative intensity): 313 (100) [M+H]⁺. **HR-MS (ESI)** m/z calc. for C₂₂H₂₁N₂ [M+H]⁺: 313.1699, found: 313.1704.



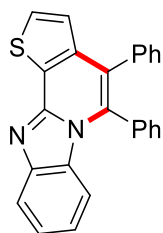
3,4,7,8-Tetramethyl-1,2-diphenylbenzo[4,5]imidazo[1,2-a]pyridine (146r)

The general procedure **F** was followed using **145g** (80 mg, 0.4 mmol) and **64a** (143 mg, 0.8 mmol) at 140 °C for 8 h. Purification by column chromatography on silica gel (*n*-hexane/EtOAc = 5:1) yielded **146r** (75 mg, 50%) as a white solid. **M.p.**: 256 °C. **¹H NMR** (300 MHz, CDCl₃): δ = 7.70 (s, 1H), 7.42 – 7.33 (m, 3H), 7.27 – 7.16 (m, 5H), 7.13 – 7.08 (m, 2H), 5.75 (s, 1H), 2.78 (s, 3H), 2.36 (s, 3H), 2.13 (s, 3H), 2.06 (s, 3H). **¹³C NMR** (101 MHz, CDCl₃): δ = 149.3 (C_q), 143.8 (C_q), 137.6 (C_q), 135.6 (C_q), 135.5 (C_q), 134.2 (C_q), 133.8 (overlapped, C_q), 130.9 (CH), 130.4 (CH), 128.8 (CH), 128.8 (C_q), 128.6 (CH), 127.8 (CH), 126.8 (CH), 126.2 (C_q), 122.7 (C_q), 119.1 (CH), 114.6 (CH), 20.7 (CH₃), 20.5 (CH₃), 17.7 (CH₃), 14.4 (CH₃). **IR (ATR)**: 2152, 2086, 2045, 1464, 856, 726, 697 cm⁻¹. **MS (ESI)** *m/z* (relative intensity): 377 (100) [M+H]⁺. **HR-MS (ESI)** *m/z* calc. for C₂₇H₂₅N₂ [M+H]⁺: 377.2012, found: 377.2014.



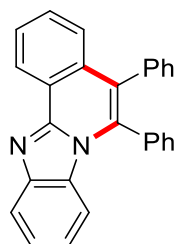
4-Methyl-1,2-diphenylbenzo[4,5]imidazo[1,2-a]pyridine (146s)

The general procedure **F** was followed using **145h** (63 mg, 0.4 mmol) and **64a** (143 mg, 0.8 mmol) at 140 °C for 8 h. Purification by column chromatography on silica gel (*n*-hexane/EtOAc = 5:1) yielded **146s** (68 mg, 51%) as a white solid. **M.p.**: 232 °C. **¹H NMR** (300 MHz, CDCl₃): δ = 7.98 (d, *J* = 8.0 Hz, 1H), 7.53 – 7.34 (m, 7H), 7.26 – 7.15 (m, 5H), 6.91 (t, *J* = 7.8 Hz, 1H), 6.20 (d, *J* = 8.5 Hz, 1H), 2.82 (s, 3H). **¹³C NMR** (75 MHz, CDCl₃): δ = 149.3 (C_q), 145.0 (C_q), 138.2 (C_q), 135.9 (C_q), 133.3 (C_q), 131.1 (CH), 130.7 (CH), 130.4 (C_q), 130.0 (CH), 129.5 (CH), 129.0 (CH), 127.9 (CH), 126.7 (CH), 126.1 (C_q), 124.8 (CH), 124.5 (C_q), 120.3 (CH), 119.7 (CH), 114.9 (CH), 17.6 (CH₃). **IR (ATR)**: 2149, 2096, 1476, 1448, 1382, 1361, 730, 699 cm⁻¹. **MS (ESI)** *m/z* (relative intensity): 335 (100) [M+H]⁺, 357 (10) [M+Na]⁺. **HR-MS (ESI)** *m/z* calc. for C₂₄H₁₉N₂ [M+H]⁺: 335.1543, found: 335.1541.



4,5-Diphenylbenzo[4,5]imidazo[1,2-a]thieno[2,3-c]pyridine (146t)

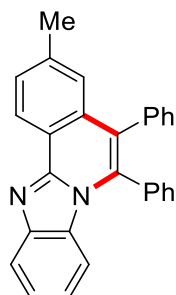
The general procedure **F** was followed using **145i** (80 mg, 0.4 mmol) and **64a** (143 mg, 0.8 mmol) at 140 °C for 8 h. Purification by column chromatography on silica gel (*n*-hexane/EtOAc = 5:1) yielded **146t** (108 mg, 72%) as a white solid. **M.p.**: 255 °C. **¹H NMR** (300 MHz, CDCl₃): δ = 7.97 (dt, *J* = 8.2, 1.0 Hz, 1H), 7.63 (d, *J* = 5.2 Hz, 1H), 7.50 – 7.34 (m, 6H), 7.31 – 7.23 (m, 5H), 7.07 (d, *J* = 5.2 Hz, 1H), 6.93 (ddd, *J* = 8.5, 7.1, 1.2 Hz, 1H), 6.10 (dt, *J* = 8.5, 0.9 Hz, 1H). **¹³C NMR** (75 MHz, CDCl₃): δ = 145.2 (C_q), 144.9 (C_q), 140.3 (C_q), 136.1 (C_q), 135.0 (C_q), 133.2 (C_q), 130.8 (CH), 130.8 (CH), 130.7 (C_q), 129.4 (CH), 129.2 (CH), 128.9 (CH), 128.0 (CH), 127.3 (CH), 125.7 (C_q), 125.3 (CH), 124.5 (CH), 121.5 (C_q), 120.7 (CH), 119.4 (CH), 114.4 (CH). **IR (ATR)**: 2010, 1979, 1950, 1629, 1483, 1410, 733, 695 cm⁻¹. **MS (ESI)** *m/z* (relative intensity): 377 (100) [M+H]⁺, 399 (10) [M+Na]⁺. **HR-MS (ESI)** *m/z* calc. for C₂₅H₁₇N₂S [M+H]⁺: 377.1107, found: 377.1109. The analytical data correspond with those reported in the literature.^[237]



5,6-Diphenylbenzo[4,5]imidazo[2,1-a]isoquinoline (148a)

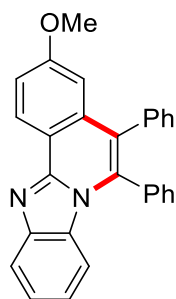
The general procedure **G** was followed using **147a** (39 mg, 0.2 mmol) and **64a** (72 mg, 0.4 mmol) at 100 °C for 4 h. Purification by column chromatography on silica gel (*n*-hexane/EtOAc = 5:1) yielded **148a** (56 mg, 75%) as a white solid. **M.p.**: 275 °C. **¹H NMR** (300 MHz, CDCl₃): δ = 9.02 (d, *J* = 8.3 Hz, 1H), 8.02 (d, *J* = 8.1 Hz, 1H), 7.71 (t, *J* = 7.5 Hz, 1H), 7.59 (t, *J* = 7.7 Hz, 1H), 7.47 – 7.34 (m, 7H), 7.33 – 7.23 (m, 5H), 6.96 (t, *J* = 7.8 Hz, 1H), 6.04 (d, *J* = 8.5 Hz, 1H). **¹³C NMR** (101 MHz, CDCl₃): δ = 147.8 (C_q), 144.3 (C_q), 135.7 (C_q), 135.1 (C_q), 133.7 (C_q), 132.7 (C_q), 131.5 (CH), 131.2 (C_q), 130.6 (CH), 129.9 (CH), 129.2 (CH), 128.7 (CH), 128.0 (CH), 127.8 (CH), 127.3 (CH), 126.4 (CH), 125.1 (CH), 124.1 (CH), 123.5 (C_q), 122.9 (C_q), 121.2 (CH), 119.6 (CH), 114.1 (CH). **IR (ATR)**: 2142, 2021, 1522, 1487, 1443, 1330, 744, 700 cm⁻¹. **MS (ESI)** *m/z* (relative intensity): 371 (100) [M+H]⁺. **HR-MS (ESI)** *m/z* calc. for C₂₇H₁₉N₂ [M+H]⁺: 371.1543,

found: 371.1547. The analytical data correspond with those reported in the literature.^[238]



3-Methyl-5,6-diphenylbenzo[4,5]imidazo[2,1-a]isoquinoline (148b)

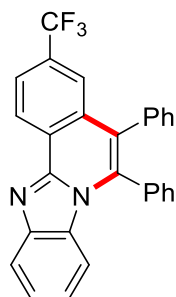
The general procedure **G** was followed using **147b** (42 mg, 0.2 mmol) and **64a** (72 mg, 0.4 mmol) at 100 °C for 4 h. Purification by column chromatography on silica gel (*n*-hexane/EtOAc = 5:1) yielded **148b** (40 mg, 52%) as a white solid. **M.p.**: 264 °C. **¹H NMR** (300 MHz, CDCl₃): δ = 8.90 (d, *J* = 8.2 Hz, 1H), 7.99 (d, *J* = 8.5 Hz, 1H), 7.55 (dd, *J* = 8.2, 1.6 Hz, 1H), 7.45 – 7.33 (m, 6H), 7.33 – 7.28 (m, 3H), 7.26 – 7.21 (m, 2H), 7.13 (s, 1H), 6.93 (td, *J* = 8.4, 1.1 Hz, 1H), 6.01 (dd, *J* = 8.5, 0.9 Hz, 1H), 2.45 (s, 3H). **¹³C NMR** (75 MHz, CDCl₃): δ = 148.0 (C_q), 144.3 (C_q), 140.3 (C_q), 135.8 (C_q), 135.1 (C_q), 133.8 (C_q), 132.8 (C_q), 131.5 (CH), 131.2 (C_q), 130.7 (CH), 129.3 (CH), 129.1 (CH), 128.7 (CH), 128.0 (CH), 127.2 (CH), 126.1 (CH), 125.0 (CH), 124.0 (CH), 123.4 (C_q), 121.0 (CH), 120.7 (C_q), 119.4 (CH), 114.1 (CH), 22.0 (CH₃). **IR (ATR)**: 2046, 1625, 1524, 1486, 1444, 1326, 1257, 819, 779 cm⁻¹. **MS (ESI)** *m/z* (relative intensity): 385 (100) [M+H]⁺. **HR-MS (ESI)** *m/z* calc. for C₂₈H₂₁N₂ [M+H]⁺: 385.1699, found: 385.1699. The analytical data correspond with those reported in the literature.^[237]



3-Methoxy-5,6-diphenylbenzo[4,5]imidazo[2,1-a]isoquinoline (148c)

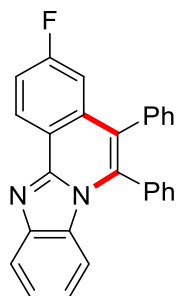
The general procedure **G** was followed using **147c** (45 mg, 0.2 mmol) and **64a** (72 mg, 0.4 mmol) at 100 °C for 4 h. Purification by column chromatography on silica gel (*n*-hexane/EtOAc = 5:1) yielded **148c** (48 mg, 60%) as a white solid. **M.p.**: 235 °C. **¹H NMR** (400 MHz, CDCl₃): δ = 8.93 (d, *J* = 8.8 Hz, 1H), 7.97 (d, *J* = 8.1 Hz, 1H), 7.45 – 7.34 (m, 6H), 7.34 – 7.26 (m, 4H), 7.25 – 7.22 (m, 2H), 6.92 (t, *J* = 7.7 Hz, 1H), 6.76 (d, *J* = 2.5 Hz, 1H), 6.00 (d, *J* = 8.5 Hz, 1H), 3.77 (s,

3H). **¹³C NMR** (101 MHz, CDCl₃): δ = 161.0 (C_q), 148.0 (C_q), 144.4 (C_q), 135.7 (C_q), 135.6 (C_q), 134.6 (C_q), 133.8 (C_q), 131.4 (CH), 131.2 (C_q), 130.6 (CH), 129.2 (CH), 128.7 (CH), 128.1 (CH), 127.3 (CH), 127.0 (CH), 124.0 (CH), 123.2 (C_q), 120.8 (CH), 119.2 (CH), 116.8 (C_q), 116.4 (CH), 114.0 (CH), 108.8 (CH), 55.3 (CH₃). **IR (ATR)**: 2138, 1609, 1464, 1444, 1221, 725, 696, 567 cm⁻¹. **MS (ESI)** m/z (relative intensity): 401 (100) [M+H]⁺. **HR-MS (ESI)** m/z calc. for C₂₈H₂₁N₂O [M+H]⁺: 401.1648, found: 401.1649. The analytical data correspond with those reported in the literature.^[238]



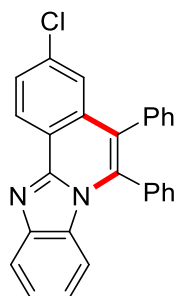
5,6-Diphenyl-3-(trifluoromethyl)benzo[4,5]imidazo[2,1-a]isoquinoline (148d)

The general procedure **G** was followed using **147d** (52 mg, 0.2 mmol) and **64a** (72 mg, 0.4 mmol) at 100 °C for 4 h. Purification by column chromatography on silica gel (*n*-hexane/EtOAc = 5:1) yielded **148d** (69 mg, 79%) as a white solid. **M.p.**: 240 °C. **¹H NMR** (300 MHz, CDCl₃): δ = 9.13 (d, *J* = 8.4 Hz, 1H), 8.04 (dt, *J* = 8.2, 1.0 Hz, 1H), 7.92 (ddd, *J* = 8.4, 1.8, 0.6 Hz, 1H), 7.63 (dt, *J* = 1.7, 0.8 Hz, 1H), 7.50 – 7.40 (m, 4H), 7.39 – 7.30 (m, 5H), 7.26 – 7.20 (m, 2H), 7.01 (ddd, *J* = 8.5, 7.2, 1.2 Hz, 1H), 6.05 (dt, *J* = 8.5, 0.9 Hz, 1H). **¹³C NMR** (101 MHz, CDCl₃): δ = 146.8 (C_q), 144.4 (C_q), 136.7 (C_q), 134.8 (C_q), 133.4 (C_q), 132.6 (C_q), 131.6 (q, ²*J*_{C-F} = 32 Hz, C_q), 131.5 (CH), 131.3 (C_q), 130.6 (CH), 129.7 (CH), 129.0 (CH), 128.5 (CH), 127.9 (CH), 126.1 (CH), 125.4 (C_q), 124.7 (CH), 124.1 (q, ¹*J*_{C-F} = 273 Hz, C_q), 124.0 (q, ³*J*_{C-F} = 3 Hz, CH), 123.6 (q, ³*J*_{C-F} = 4 Hz, CH), 123.3 (C_q), 122.1 (CH), 120.1 (CH), 114.5 (CH). **¹⁹F NMR** (377 MHz, CDCl₃): δ = -62.5 (s). **IR (ATR)**: 1450, 1432, 1416, 1321, 1167, 1122, 1065, 1017, 850, 744 cm⁻¹. **MS (ESI)** m/z (relative intensity): 439 (100) [M+H]⁺. **HR-MS (ESI)** m/z calc. for C₂₈H₁₈F₃N₂ [M+H]⁺: 439.1422 found: 439.1417. The analytical data correspond with those reported in the literature.^[238]



3-Fluoro-5,6-diphenylbenzo[4,5]imidazo[2,1-a]isoquinoline (148e)

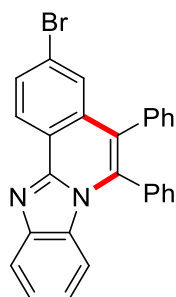
The general procedure **G** was followed using **147e** (42 mg, 0.2 mmol) and **64a** (72 mg, 0.4 mmol) at 100 °C for 4 h. Purification by column chromatography on silica gel (*n*-hexane/EtOAc = 5:1) yielded **148e** (60 mg, 77%) as a white solid. **M.p.**: 251 °C. **¹H NMR** (300 MHz, CDCl₃): δ = 9.00 (dd, *J* = 8.9, 5.7 Hz, 1H), 7.99 (dt, *J* = 8.2, 0.9 Hz, 1H), 7.50 – 7.28 (m, 10H), 7.26 – 7.19 (m, 2H), 7.01 (dd, *J* = 10.4, 2.5 Hz, 1H), 6.95 (t, *J* = 8.4 Hz, 1H), 6.02 (dt, *J* = 8.5, 0.9 Hz, 1H). **¹³C NMR** (75 MHz, CDCl₃): δ = 163.7 (d, ¹*J*_{C-F} = 248 Hz, C_q), 147.3 (C_q), 144.3 (C_q), 136.3 (C_q), 135.1 (C_q), 134.8 (d, ³*J*_{C-F} = 9.1 Hz, C_q), 133.4 (C_q), 131.4 (CH), 131.1 (C_q), 130.5 (CH), 129.4 (CH), 128.8 (CH), 128.2 (CH), 127.7 (d, ³*J*_{C-F} = 9.3 Hz, CH), 127.6 (CH), 124.3 (CH), 122.9 (d, ⁴*J*_{C-F} = 3.4 Hz, C_q), 121.3 (CH), 119.5 (CH), 119.5 (C_q), 116.4 (d, ²*J*_{C-F} = 24 Hz, CH), 114.1 (CH), 111.7 (d, ²*J*_{C-F} = 23 Hz, CH). **¹⁹F NMR** (282 MHz, CDCl₃): δ = -108.3 (s). **IR (ATR)**: 2140, 2014, 1467, 1444, 1324, 1267, 1201, 730 cm⁻¹. **MS (ESI)** *m/z* (relative intensity): 389 (100) [M+H]⁺. **HR-MS (ESI)** *m/z* calc. for C₂₇H₁₈N₂F [M+H]⁺: 389.1449, found: 389.1447. The characterization data correspond with those reported in the literature.^[237]



3-Chloro-5,6-diphenylbenzo[4,5]imidazo[2,1-a]isoquinoline (148f)

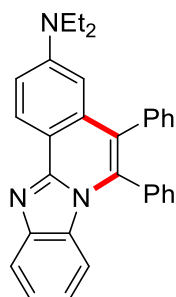
The general procedure **G** was followed using **147f** (46 mg, 0.2 mmol) and **64a** (72 mg, 0.4 mmol) at 100 °C for 4 h. Purification by column chromatography on silica gel (*n*-hexane/EtOAc = 5:1) yielded **148f** (55 mg, 68%) as a white solid. **M.p.**: 295 °C. **¹H NMR** (400 MHz, CDCl₃): δ = 8.94 (d, *J* = 8.6 Hz, 1H), 8.00 (d, *J* = 8.2 Hz, 1H), 7.67 (d, *J* = 8.6 Hz, 1H), 7.49 – 7.38 (m, 4H), 7.38 – 7.29 (m, 6H), 7.26 – 7.18 (m, 2H), 6.97 (t, *J* = 7.8 Hz, 1H), 6.02 (d, *J* = 8.5 Hz, 1H). **¹³C NMR** (101 MHz, CDCl₃): δ = 147.1 (C_q), 144.3 (C_q), 136.4 (C_q), 136.2 (C_q), 134.9 (C_q), 133.9 (C_q),

133.4 (C_q), 131.4 (CH), 131.1 (C_q), 130.4 (CH), 129.4 (CH), 128.8 (CH), 128.3 (CH), 128.2 (CH), 127.6 (CH), 126.7 (CH), 125.7 (CH), 124.4 (CH), 122.6 (C_q), 121.5 (CH), 121.3 (C_q), 119.6 (CH), 114.2 (CH). **IR (ATR):** 2141, 2046, 2022, 1920, 1444, 733, 710 cm⁻¹. **MS (ESI)** m/z (relative intensity): 405 (100) [M+H]⁺, 371 (10). **HR-MS (ESI)** m/z calc. for C₂₇H₁₈N₂³⁵Cl [M+H]⁺: 405.1153, found: 405.1156. The analytical data correspond with those reported in the literature.^[237]



3-Bromo-5,6-diphenylbenzo[4,5]imidazo[2,1-a]isoquinoline (148g)

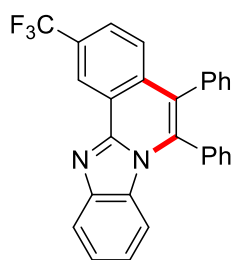
The general procedure **G** was followed using **147g** (55 mg, 0.2 mmol) and **64a** (72 mg, 0.4 mmol) at 100 °C for 4 h. Purification by column chromatography on silica gel (*n*-hexane/EtOAc = 5:1) yielded **148g** (48 mg, 53%) as a white solid. **M.p.:** 297 °C. **¹H NMR** (400 MHz, CDCl₃): δ = 8.87 (d, *J* = 8.5 Hz, 1H), 7.99 (dd, *J* = 8.2, 1.0 Hz, 1H), 7.81 (d, *J* = 8.7 Hz, 1H), 7.49 (s, 1H), 7.46 – 7.38 (m, 4H), 7.37 – 7.29 (m, 5H), 7.24 – 7.19 (m, 2H), 6.97 (t, *J* = 8.4 Hz, 1H), 6.02 (dd, *J* = 8.6, 0.9 Hz, 1H). **¹³C NMR** (101 MHz, CDCl₃): δ = 147.2 (C_q), 144.3 (C_q), 136.4 (C_q), 134.9 (C_q), 134.1 (C_q), 133.4 (C_q), 131.4 (CH), 131.1 (C_q), 131.0 (CH), 130.5 (CH), 129.4 (CH), 128.8 (CH), 128.8 (CH), 128.2 (CH), 127.6 (CH), 126.7 (CH), 124.6 (C_q), 124.4 (CH), 122.5 (C_q), 121.6 (C_q), 121.6 (CH), 119.7 (CH), 114.2 (CH). **IR (ATR):** 3049, 1599, 1486, 1443, 1417, 1324, 732, 702 cm⁻¹. **MS (ESI)** m/z (relative intensity): 449 (100) [M+H]⁺, 631 (30). **HR-MS (ESI)** m/z calc. for C₂₇H₁₈N₂⁷⁹Br [M+H]⁺: 449.0648, found: 449.0647. The analytical data correspond with those reported in the literature.^[237]



N,N-Diethyl-5,6-diphenylbenzo[4,5]imidazo[2,1-a]isoquinolin-3-amine (148h)

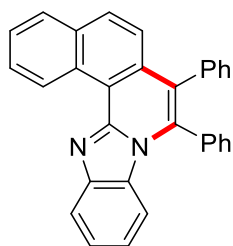
The general procedure **G** was followed using **147h** (53 mg, 0.2 mmol) and **64a** (72 mg, 0.4 mmol)

at 100 °C for 4 h. Purification by column chromatography on silica gel (*n*-hexane/EtOAc = 5:1) yielded **148h** (60 mg, 68%) as a white solid. **M.p.**: 260 °C. **¹H NMR** (400 MHz, CDCl₃): δ = 8.78 (d, *J* = 9.0 Hz, 1H), 7.91 (d, *J* = 8.1 Hz, 1H), 7.43 – 7.34 (m, 5H), 7.33 – 7.28 (m, 3H), 7.26 – 7.22 (m, 3H), 7.10 (dd, *J* = 9.1, 2.6 Hz, 1H), 6.86 (t, *J* = 7.3 Hz, 1H), 6.35 (d, *J* = 2.6 Hz, 1H), 5.95 (d, *J* = 8.4 Hz, 1H), 3.32 (q, *J* = 7.1 Hz, 4H), 1.10 (t, *J* = 7.0 Hz, 6H). **¹³C NMR** (101 MHz, CDCl₃): δ = 148.8 (C_q), 148.8 (C_q), 144.7 (C_q), 136.3 (C_q), 135.0 (C_q), 134.8 (C_q), 134.2 (C_q), 131.5 (CH), 131.3 (C_q), 130.7 (CH), 129.0 (CH), 128.6 (CH), 127.8 (CH), 127.0 (CH), 126.6 (CH), 123.6 (CH), 123.4 (C_q), 120.0 (CH), 118.7 (CH), 113.7 (CH), 113.4 (CH), 111.9 (C_q), 106.2 (CH), 44.6 (CH₂), 12.4 (CH₃). **IR (ATR)**: 3051, 2972, 1626, 1604, 1484, 1442, 1253, 1073, 700 cm⁻¹. **MS (ESI)** *m/z* (relative intensity): 442 (100) [M+H]⁺. **HR-MS (ESI)** *m/z* calc. for C₃₁H₂₈N₃ [M+H]⁺: 442.2278, found: 442.2279. The analytical data correspond with those reported in the literature.^[237]



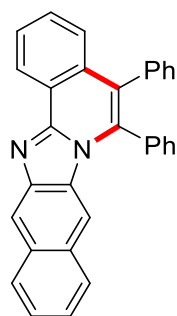
5,6-Diphenyl-2-(trifluoromethyl)benzo[4,5]imidazo[2,1-a]isoquinoline (**148i**)

The general procedure **G** was followed using **147i** (52 mg, 0.2 mmol) and **64a** (72 mg, 0.4 mmol) at 100 °C for 4 h. Purification by column chromatography on silica gel (*n*-hexane/EtOAc = 5:1) yielded **148i** (45 mg, 51%) as a white solid. **M.p.**: 285 °C. **¹H NMR** (400 MHz, CDCl₃): δ = 9.32 (d, *J* = 2.0 Hz, 1H), 8.03 (d, *J* = 8.2 Hz, 1H), 7.77 (dd, *J* = 8.6, 1.8 Hz, 1H), 7.50 – 7.37 (m, 7H), 7.36 – 7.29 (m, 3H), 7.26 – 7.22 (m, 2H), 6.99 (ddd, *J* = 8.4, 7.2, 1.3 Hz, 1H), 6.05 (d, *J* = 8.5 Hz, 1H). **¹³C NMR** (101 MHz, CDCl₃): δ = 146.9 (C_q), 144.2 (C_q), 137.2 (C_q), 135.0 (C_q), 134.8 (C_q), 133.2 (C_q), 131.4 (CH), 131.1 (C_q), 130.4 (CH), 129.6 (q, ²*J*_{C-F} = 33 Hz, C_q), 129.5 (CH), 128.9 (CH), 128.3 (CH), 127.6 (CH), 127.2 (CH), 125.8 (q, ³*J*_{C-F} = 3.4 Hz, CH), 124.6 (CH), 124.0 (q, ¹*J*_{C-F} = 272 Hz, C_q), 122.8 (C_q), 122.8 (C_q), 122.6 (q, ³*J*_{C-F} = 4.1 Hz, CH), 121.9 (CH), 119.8 (CH), 114.3 (CH). **¹⁹F NMR** (377 MHz, CDCl₃): δ = -62.16 (s). **IR (ATR)**: 2270, 2149, 1977, 1948, 1474, 1070, 1011, 732, 700 cm⁻¹. **MS (ESI)** *m/z* (relative intensity): 439 (100) [M+H]⁺. **HR-MS (ESI)** *m/z* calc. for C₂₈H₁₈N₂F₃ [M+H]⁺: 439.1417, found: 439.1417. The analytical data correspond with those reported in the literature.^[237]



7,8-Diphenylbenzo[h]benzo[4,5]imidazo[2,1-a]isoquinoline (148j)

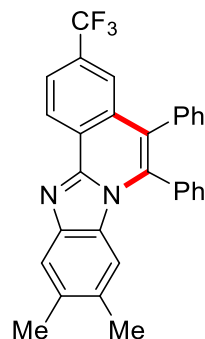
The general procedure **G** was followed using **147j** (49 mg, 0.2 mmol) and **64a** (72 mg, 0.4 mmol) at 100 °C for 4 h. Purification by column chromatography on silica gel (*n*-hexane/EtOAc = 5:1) yielded **148j** (45 mg, 54%) as a white solid. **M.p.**: 236 °C. **¹H NMR** (400 MHz, CDCl₃): δ = 11.17 (d, *J* = 8.5 Hz, 1H), 8.16 (t, *J* = 8.1 Hz, 1H), 8.06 – 7.94 (m, 3H), 7.76 (t, *J* = 7.6 Hz, 1H), 7.51 – 7.38 (m, 7H), 7.37 – 7.29 (m, 5H), 6.99 (t, *J* = 7.8 Hz, 1H), 6.12 (d, *J* = 8.4 Hz, 1H). **¹³C NMR** (101 MHz, CDCl₃): δ = 147.9 (C_q), 144.7 (C_q), 136.4 (C_q), 136.1 (C_q), 134.0 (C_q), 132.6 (overlapped, C_q), 132.4 (C_q), 131.7 (CH), 130.8 (CH), 130.6 (overlapped, CH), 130.2 (C_q), 129.9 (C_q), 129.2 (CH), 128.8 (CH), 128.3 (CH), 128.2 (CH), 128.1 (CH), 127.3 (CH), 126.8 (CH), 124.3 (CH), 124.0 (CH), 121.1 (CH), 119.9 (CH), 118.1 (C_q), 114.4 (CH). **IR (ATR)**: 2905, 1745, 1590, 1481, 1447, 1377, 1175, 825, 730 cm⁻¹. **MS (ESI)** *m/z* (relative intensity): 421 (100) [M+H]⁺. **HR-MS (ESI)** *m/z* calc. for C₃₁H₂₁N₂ [M+H]⁺: 421.1699, found: 421.1699. The analytical data correspond with those reported in the literature.^[237]



5,6-Diphenylnaphtho[2',3':4,5]imidazo[2,1-a]isoquinoline (148k)

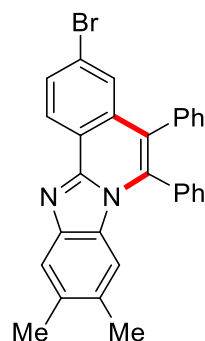
The general procedure **G** was followed using **147k** (49 mg, 0.2 mmol) and **64a** (72 mg, 0.4 mmol) at 100 °C for 4 h. Purification by column chromatography on silica gel (*n*-hexane/EtOAc = 5:1) yielded **148k** (42 mg, 50%) as a white solid. **M.p.**: 287 °C. **¹H NMR** (300 MHz, CDCl₃): δ = 9.18 (d, *J* = 7.9 Hz, 1H), 8.49 (s, 1H), 8.03 (d, *J* = 8.4 Hz, 1H), 7.77 (t, *J* = 7.5 Hz, 1H), 7.68 (t, *J* = 7.7 Hz, 1H), 7.59 – 7.38 (m, 8H), 7.37 – 7.26 (m, 6H), 6.40 (s, 1H). **¹³C NMR** (75 MHz, CDCl₃): δ = 135.5 (C_q), 135.2 (overlapped, C_q), 133.8 (C_q), 133.4 (C_q), 131.5 (CH), 131.4 (CH), 131.3 (C_q), 131.2 (overlapped, C_q), 130.7 (CH), 129.5 (CH), 129.0 (overlapped, C_q), 128.9 (CH), 128.4 (CH), 128.2 (CH), 128.2 (CH), 127.8 (CH), 127.5 (CH), 126.5 (CH), 126.1 (CH), 124.8 (CH), 124.0 (CH), 121.6 (C_q), 115.0 (CH), 111.8 (CH). **IR (ATR)**: 2196, 1528, 1487, 1439, 1254, 859, 769,

729, 696 cm^{-1} . **MS (ESI)** m/z (relative intensity): 421 (100) $[\text{M}+\text{H}]^+$, 381 (10). **HR-MS (ESI)** m/z calc. for $\text{C}_{31}\text{H}_{21}\text{N}_2$ $[\text{M}+\text{H}]^+$: 421.1699, found: 421.1700.



9,10-Dimethyl-5,6-diphenyl-3-(trifluoromethyl)benzo[4,5]imidazo[2,1-a]isoquinoline (148I)

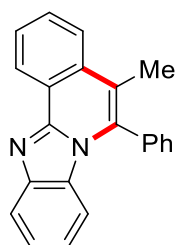
The general procedure **G** was followed using **147I** (58 mg, 0.2 mmol) and **64a** (72 mg, 0.4 mmol) at 100 °C for 4 h. Purification by column chromatography on silica gel (*n*-hexane/EtOAc = 5:1) yielded **148I** (49 mg, 53%) as a white solid. **M.p.**: 309 °C. **^1H NMR** (400 MHz, CDCl_3): δ = 9.06 (d, J = 8.4 Hz, 1H), 7.88 (dd, J = 8.5, 1.8 Hz, 1H), 7.76 (s, 1H), 7.63 – 7.61 (m, 1H), 7.50 – 7.42 (m, 3H), 7.40 – 7.30 (m, 5H), 7.27 – 7.23 (m, 2H), 5.73 (s, 1H), 2.38 (s, 3H), 2.09 (s, 3H). **^{13}C NMR** (101 MHz, CDCl_3): δ = 145.9 (C_q), 142.9 (C_q), 136.5 (C_q), 134.8 (C_q), 133.8 (C_q), 133.5 (C_q), 132.1 (C_q), 131.4 (CH), 131.1 (C_q), 130.9 (q, $^2J_{\text{C-F}}$ = 32 Hz, C_q), 130.5 (CH), 129.5 (C_q), 129.2 (CH), 128.7 (CH), 128.2 (CH), 127.6 (CH), 125.6 (CH), 125.2 (C_q), 124.0 (q, $^1J_{\text{C-F}}$ = 272 Hz, C_q), 123.5 (q, $^3J_{\text{C-F}}$ = 3 Hz, CH), 123.3 (q, $^3J_{\text{C-F}}$ = 4 Hz, CH), 122.5 (C_q), 119.6 (CH), 114.3 (CH), 20.7 (CH_3), 20.4 (CH_3). **^{19}F NMR** (377 MHz, CDCl_3): δ = –62.3 (s). **IR (ATR)**: 2920, 1487, 1458, 1357, 1313, 1151, 1125, 698 cm^{-1} . **MS (ESI)** m/z (relative intensity): 467 (100) $[\text{M}+\text{H}]^+$. **HR-MS (ESI)** m/z calc. for $\text{C}_{30}\text{H}_{22}\text{N}_2\text{F}_3$ $[\text{M}+\text{H}]^+$: 467.1730, found: 467.1732.



3-Bromo-9,10-dimethyl-5,6-diphenylbenzo[4,5]imidazo[2,1-a]isoquinoline (148m)

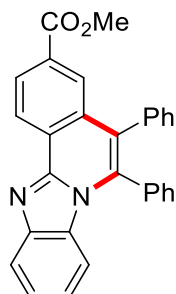
The general procedure **G** was followed using **147m** (60 mg, 0.2 mmol) and **64a** (72 mg, 0.4 mmol) at 100 °C for 4 h. Purification by column chromatography on silica gel (*n*-hexane/EtOAc =

5:1) yielded **148m** (48 mg, 50%) as a white solid. **M.p.**: 307 °C. **¹H NMR** (400 MHz, CDCl₃): δ = 8.80 (d, *J* = 8.6 Hz, 1H), 7.76 (dd, *J* = 8.6, 1.9 Hz, 1H), 7.73 (s, 1H), 7.48 – 7.39 (m, 4H), 7.36 – 7.28 (m, 5H), 7.25 – 7.21 (m, 2H), 5.69 (s, 1H), 2.37 (s, 3H), 2.08 (s, 3H). **¹³C NMR** (101 MHz, CDCl₃): δ = 146.5 (C_q), 142.9 (C_q), 136.3 (C_q), 135.1 (C_q), 133.9 (C_q), 133.6 (C_q), 133.6 (C_q), 131.5 (CH), 130.8 (CH), 130.6 (C_q), 130.5 (CH), 129.5 (C_q), 129.2 (CH), 128.7 (CH), 128.7 (CH), 128.2 (CH), 127.5 (CH), 126.5 (CH), 124.1 (C_q), 121.9 (C_q), 121.7 (C_q), 119.4 (CH), 114.3 (CH), 20.8 (CH₃), 20.4 (CH₃). **IR (ATR)**: 1598, 1522, 1444, 1416, 1072, 872, 703, 661 cm⁻¹. **MS (ESI)** *m/z* (relative intensity): 477 (100) [M+H]⁺, 659 (20). **HR-MS (ESI)** *m/z* calc. for C₂₉H₂₂N₂⁷⁹Br [M+H]⁺: 477.0961, found: 477.0957.



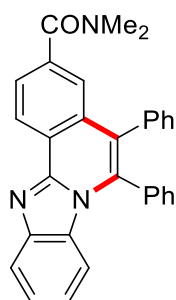
5-Methyl-6-phenylbenzo[4,5]imidazo[2,1-a]isoquinoline (**148n**)

The general procedure **G** was followed using **147a** (39 mg, 0.2 mmol) and **64m** (46 mg, 0.4 mmol) at 100 °C for 4 h. Purification by column chromatography on silica gel (*n*-hexane/EtOAc = 5:1) yielded **148n** (51 mg, 83%) as a white solid. **M.p.**: 238 °C. **¹H NMR** (300 MHz, CDCl₃): δ = 8.99 (dd, *J* = 7.6, 1.4 Hz, 1H), 8.00 – 7.93 (m, 2H), 7.82 – 7.72 (m, 2H), 7.73 – 7.65 (m, 3H), 7.54 – 7.49 (m, 2H), 7.39 – 7.34 (m, 1H), 6.93 (ddd, *J* = 8.4, 7.2, 1.2 Hz, 1H), 5.96 (d, *J* = 8.5 Hz, 1H), 2.34 (s, 3H). **¹³C NMR** (101 MHz, CDCl₃): δ = 147.7 (C_q), 144.1 (C_q), 134.7 (C_q), 134.4 (C_q), 132.5 (C_q), 131.3 (C_q), 130.4 (CH), 130.2 (CH), 129.9 (CH), 129.7 (CH), 127.8 (CH), 125.5 (CH), 124.2 (CH), 124.0 (CH), 123.3 (C_q), 121.2 (CH), 119.6 (CH), 115.6 (C_q), 114.0 (CH), 14.6 (CH₃). **IR (ATR)**: 1524, 1448, 1376, 1253, 907, 906, 730, 701, 650 cm⁻¹. **MS (ESI)** *m/z* (relative intensity): 309 (100) [M+H]⁺. **HR-MS (ESI)** *m/z* calc. for C₂₂H₁₇N₂ [M+H]⁺: 309.1392 found: 309.1386. The analytical data correspond with those reported in the literature.^[238]

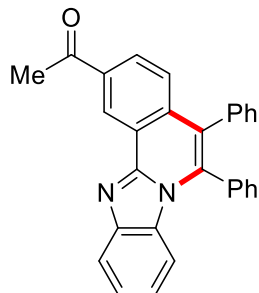


Methyl 5,6-diphenylbenzo[4,5]imidazo[2,1-a]isoquinoline-3-carboxylate (148o)

The general procedure **G** was followed using **147n** (51 mg, 0.2 mmol) and **64a** (72 mg, 0.4 mmol) at 100 °C for 4 h. Purification by column chromatography on silica gel (*n*-hexane/EtOAc = 5:1) yielded **148o** (80 mg, 93%) as a white solid. **M.p.**: 265 °C. **¹H NMR** (400 MHz, CDCl₃): δ = 9.07 (d, *J* = 8.4 Hz, 1H), 8.33 (dd, *J* = 8.4, 1.6 Hz, 1H), 8.09 (s, 1H), 8.03 (d, *J* = 8.4 Hz, 1H), 7.49 – 7.40 (m, 4H), 7.40 – 7.26 (m, 6H), 7.26 – 7.24 (m, 1H), 7.00 (t, *J* = 8.4 Hz, 1H), 6.05 (d, *J* = 8.5 Hz, 1H), 3.92 (s, 3H). **¹³C NMR** (101 MHz, CDCl₃): δ = 166.7 (C_q), 146.9 (C_q), 144.4 (C_q), 136.0 (C_q), 134.9 (C_q), 133.5 (C_q), 132.3 (C_q), 131.5 (CH), 131.2 (C_q), 131.1 (C_q), 130.6 (CH), 129.4 (CH), 128.8 (CH), 128.2 (overlapped, CH), 127.9 (CH), 127.6 (CH), 126.0 (C_q), 125.3 (CH), 124.5 (CH), 123.6 (C_q), 121.9 (CH), 119.9 (CH), 114.3 (CH), 52.4 (CH₃). **IR (ATR)**: 2920, 1722, 1446, 1266, 738, 709, 500, 467, 449 cm⁻¹. **MS (ESI)** *m/z* (relative intensity): 429 (100) [M+H]⁺. **HR-MS (ESI)** *m/z* calc. for C₂₉H₂₁N₂O₂ [M+H]⁺: 429.1598 found: 429.1602.

***N,N*-Dimethyl-5,6-diphenylbenzo[4,5]imidazo[2,1-a]isoquinoline-3-carboxamide (148p)**

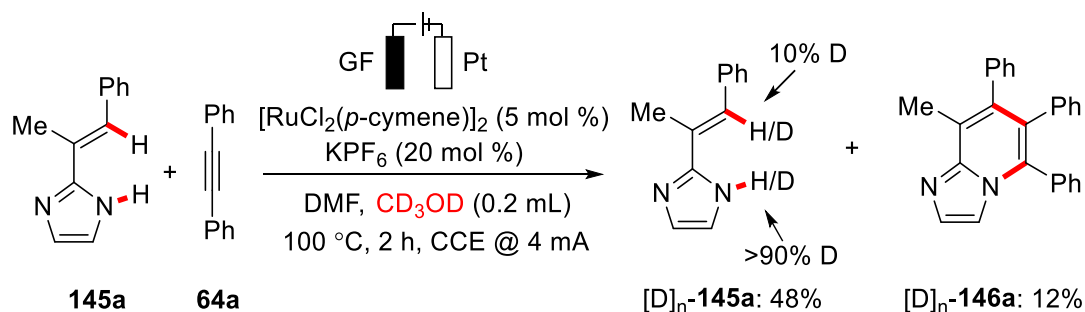
The general procedure **G** was followed using **64o** (53 mg, 0.2 mmol) and **64a** (72 mg, 0.4 mmol) at 100 °C for 4 h. Purification by column chromatography on silica gel (*n*-hexane/EtOAc = 1:1) yielded **148p** (50 mg, 57%) as a white solid. **M.p.**: 310 °C. **¹H NMR** (400 MHz, CDCl₃): δ = 9.04 (d, *J* = 8.2 Hz, 1H), 8.02 (d, *J* = 8.2 Hz, 1H), 7.74 (dd, *J* = 8.2, 1.6 Hz, 1H), 7.47 – 7.34 (m, 7H), 7.33 – 7.22 (m, 5H), 6.98 (t, *J* = 7.9 Hz, 1H), 6.04 (d, *J* = 8.5 Hz, 1H), 3.11 (s, 3H), 2.95 (s, 3H). **¹³C NMR** (101 MHz, CDCl₃): δ = 170.8 (C_q), 147.2 (C_q), 144.3 (C_q), 137.6 (C_q), 136.0 (C_q), 135.1 (C_q), 133.5 (C_q), 132.5 (C_q), 131.5 (CH), 131.2 (C_q), 130.5 (CH), 129.4 (CH), 128.8 (CH), 128.2 (CH), 127.5 (CH), 126.2 (CH), 125.3 (CH), 125.1 (CH), 124.4 (CH), 123.5 (C_q), 123.3 (C_q), 121.6 (CH), 119.8 (CH), 114.2 (CH), 39.5 (CH₃), 35.3 (CH₃). **IR (ATR)**: 1624, 1485, 1442, 1391, 1071, 839, 744, 722 cm⁻¹. **MS (ESI)** *m/z* (relative intensity): 442 (100) [M+H]⁺. **HR-MS (ESI)** *m/z* calc. for C₃₀H₂₄N₃O [M+H]⁺: 442.1914 found: 442.1915.



1-[5,6-Diphenylbenzo[4,5]imidazo[2,1-a]isoquinolin-2-yl]ethan-1-one (**148q**)

The general procedure **G** was followed using **147p** (47 mg, 0.2 mmol) and **64a** (72 mg, 0.4 mmol) at 100 °C for 4 h. Purification by column chromatography on silica gel (*n*-hexane/EtOAc = 5:1) yielded **148q** (51 mg, 62%) as a white solid. **M.p.**: 275 °C. **¹H NMR** (400 MHz, CDCl₃): δ = 9.55 (d, *J* = 1.9 Hz, 1H), 8.19 (dd, *J* = 8.6, 1.9 Hz, 1H), 8.04 (d, *J* = 8.2 Hz, 1H), 7.51 – 7.40 (m, 5H), 7.40 – 7.35 (m, 2H), 7.35 – 7.28 (m, 3H), 7.25 – 7.20 (m, 2H), 6.99 (t, *J* = 8.5 Hz, 1H), 6.05 (d, *J* = 8.5 Hz, 1H), 2.87 (s, 3H). **¹³C NMR** (101 MHz, CDCl₃): δ = 197.5 (C_q), 147.4 (C_q), 144.2 (C_q), 137.4 (C_q), 135.8 (C_q), 135.8 (C_q), 135.1 (C_q), 133.3 (C_q), 131.4 (CH), 131.1 (C_q), 130.3 (CH), 129.5 (CH), 128.9 (CH), 128.3 (CH), 128.2 (CH), 127.6 (CH), 126.9 (CH), 126.2 (CH), 124.6 (CH), 123.2 (C_q), 122.6 (C_q), 121.7 (CH), 119.7 (CH), 114.3 (CH), 27.0 (CH₃). **IR (ATR)**: 1683, 1608, 1421, 1257, 916, 825, 700 cm⁻¹. **MS (ESI)** *m/z* (relative intensity): 413 (100) [M+H]⁺. **HR-MS (ESI)** *m/z* calc. for C₂₉H₂₁N₂O [M+H]⁺: 413.1648 found: 413.1651.

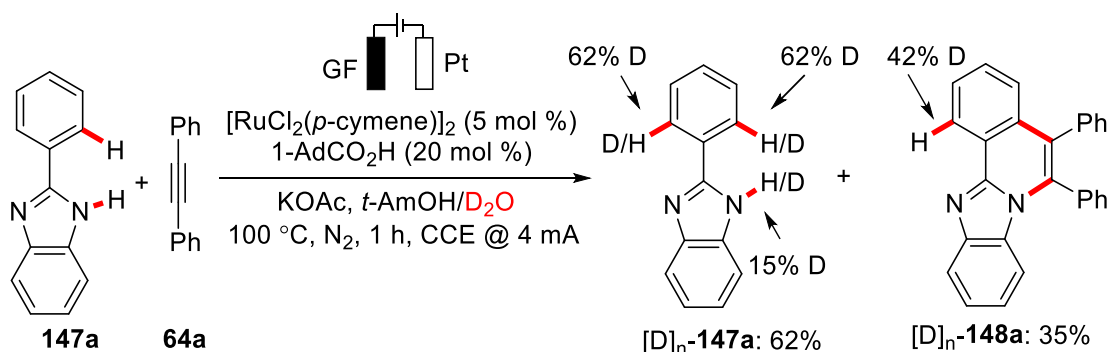
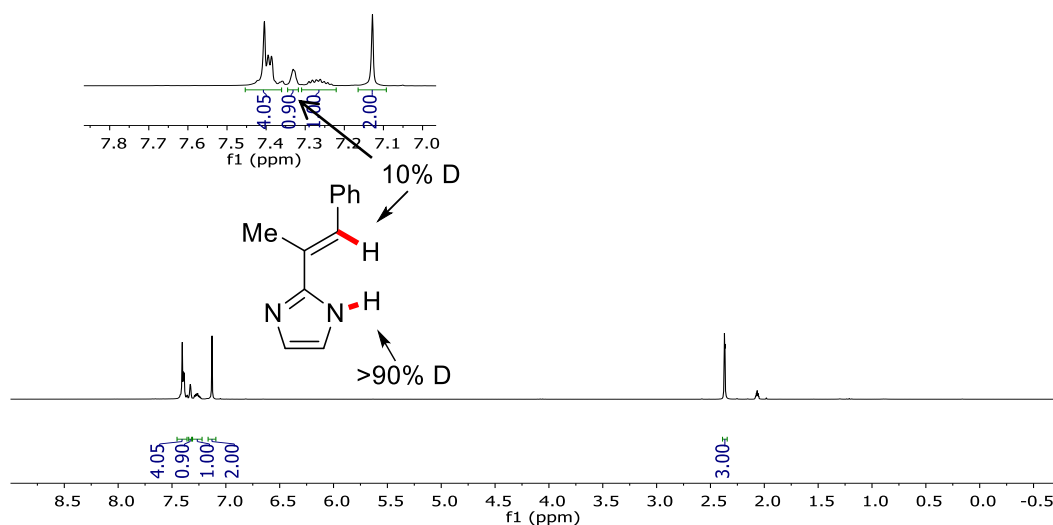
5.3.3.2 H/D Exchange Experiment



In an undivided cell equipped with a GF anode (10 mm × 15 mm × 6 mm) and a platinum cathode (10 mm × 15 mm × 0.25 mm), **145a** (74 mg, 0.4 mmol), alkyne **64a** (142.4 mg, 0.8 mmol), KPF₆ (15 mg, 20.0 mol %) and [RuCl₂(*p*-cymene)]₂ (12.5 mg, 5.0 mol %) were dissolved in DMF (4 mL) and CD₃OD (0.2 mL) under N₂. Electrocatalysis was performed at 100 °C with a constant current of 4.0 mA maintained for 2 h. After the reaction, the GF anode was washed with EtOAc (3×10 mL) in an ultrasonic bath. The combined organic phases were added to the reaction mixture. Evaporation of the solvent and subsequent column chromatography (*n*-hexane/EtOAc = 10:1 → 5:1) yielded [D]_n-**145a** (35 mg, 48%) as a white solid and [D]_n-**146a** (17

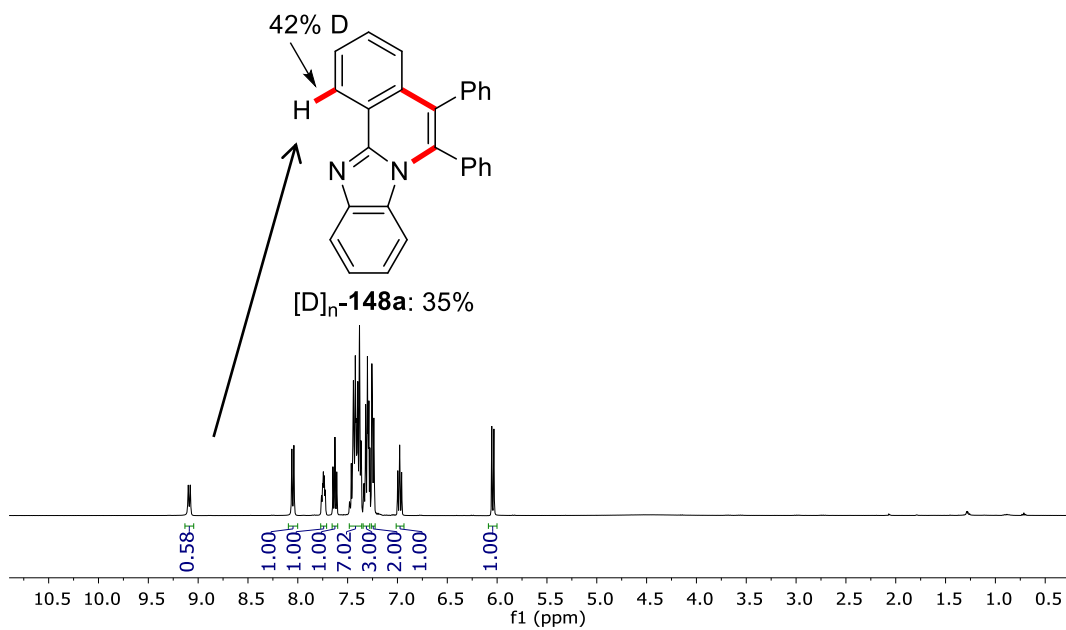
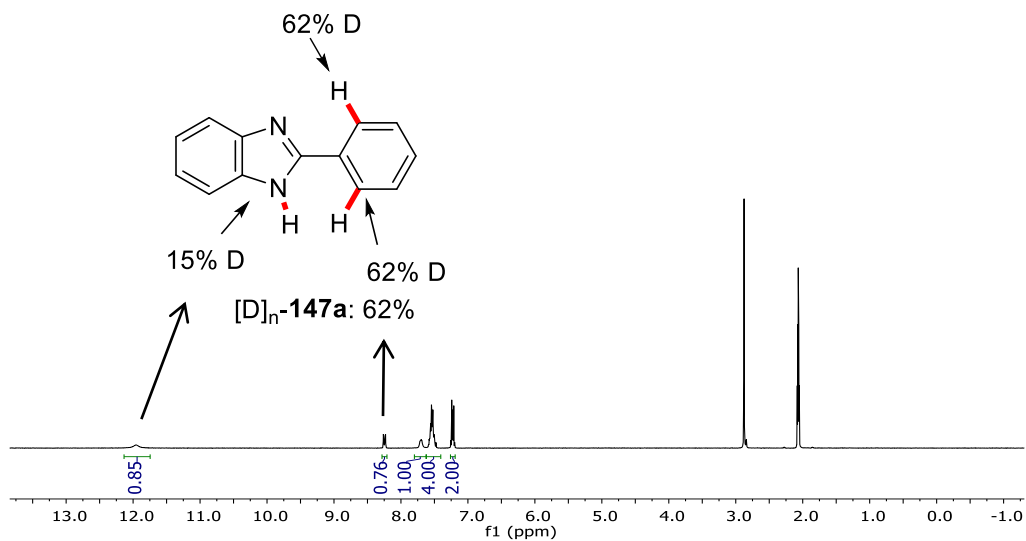
Experimental Section

mg, 12%) as a white solid. The D-incorporation was estimated by ^1H NMR spectroscopy.

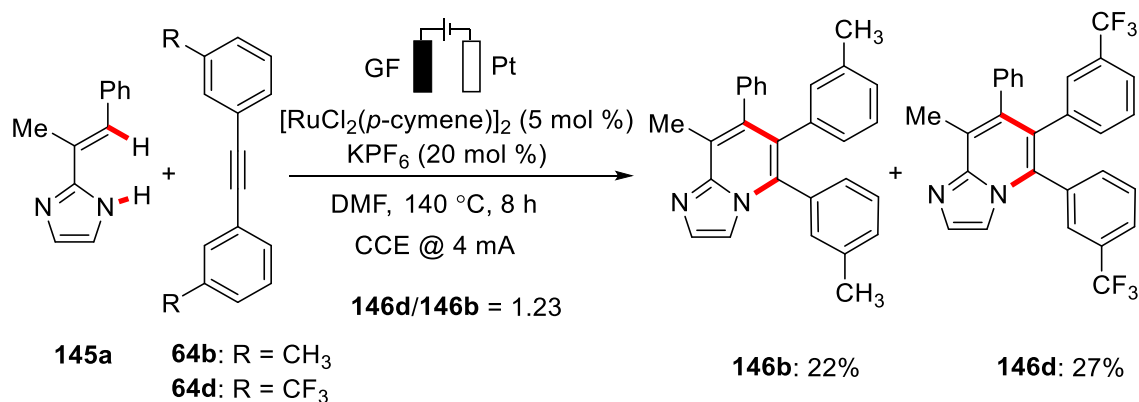


In an undivided cell equipped with a GF anode (10 mm × 15 mm × 6 mm) and a platinum cathode (10 mm × 15 mm × 0.25 mm), **147a** (39 mg, 0.2 mmol), alkyne **64a** (71 mg, 0.4 mmol), 1-AdCO₂H (7.2 mg, 20.0 mol %) and [RuCl₂(*p*-cymene)]₂ (6.2 mg, 5.0 mol %) were dissolved in *t*-AmOH (3 mL) and D₂O (3 mL) under N₂. Electrocatalysis was performed at 100 °C with a constant current of 4.0 mA maintained for 1 h. The GF anode was washed with ethyl acetate (3×10 mL) in an ultrasonic bath. Evaporation of the solvent and subsequent column chromatography (*n*-hexane/EtOAc = 10:1 → 5:1) yielded [D]_n-**147a** (24 mg, 62%) as a white solid and [D]_n-**148a** (26 mg, 35%) as a white solid. The D-incorporation was estimated by ^1H NMR spectroscopy.

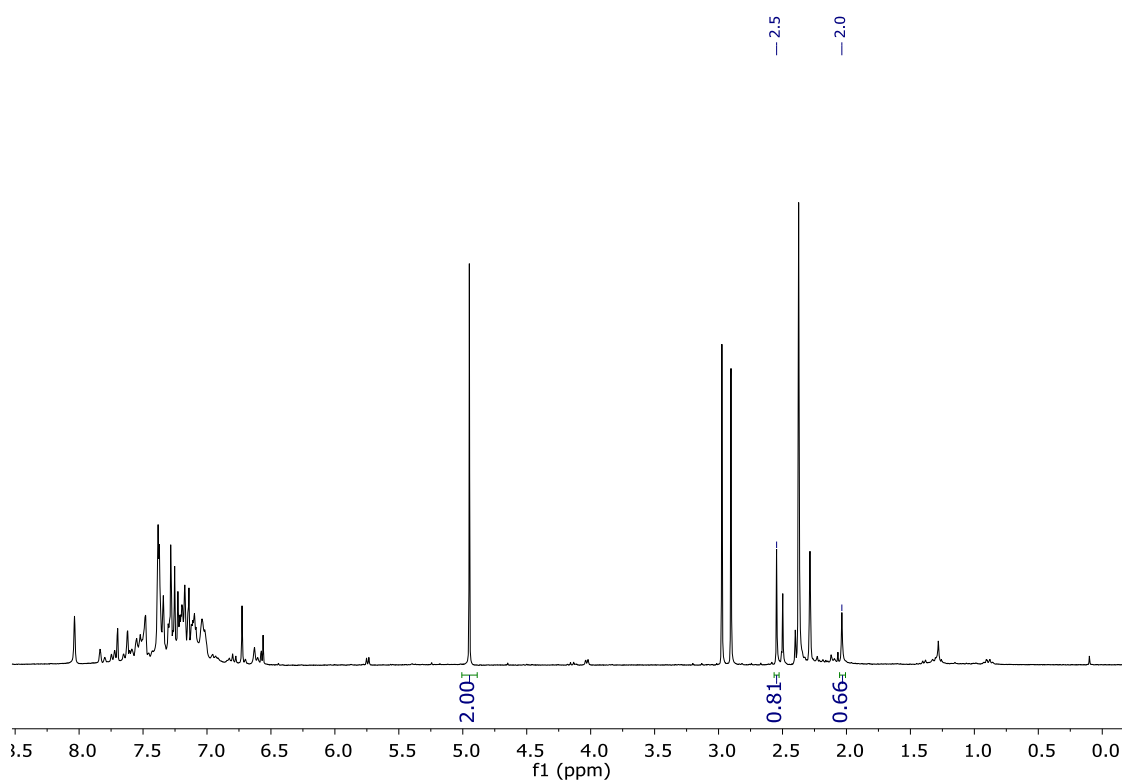
Experimental Section



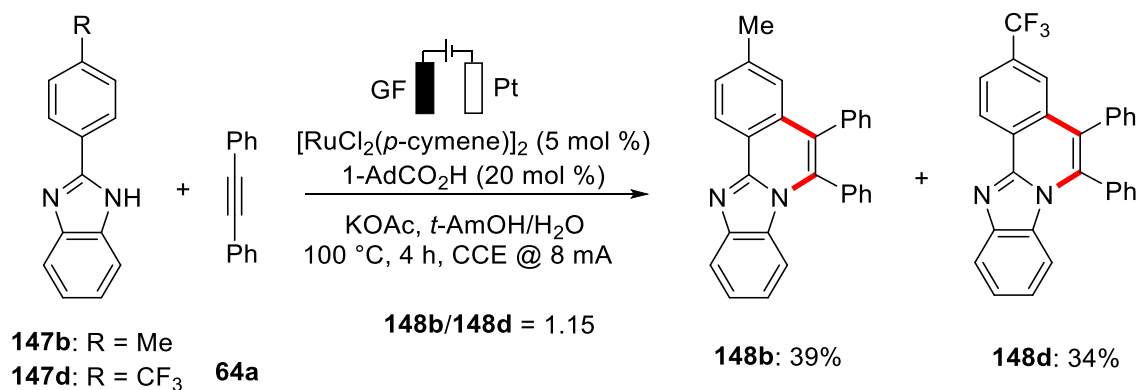
5.3.3.3 Competition Experiments



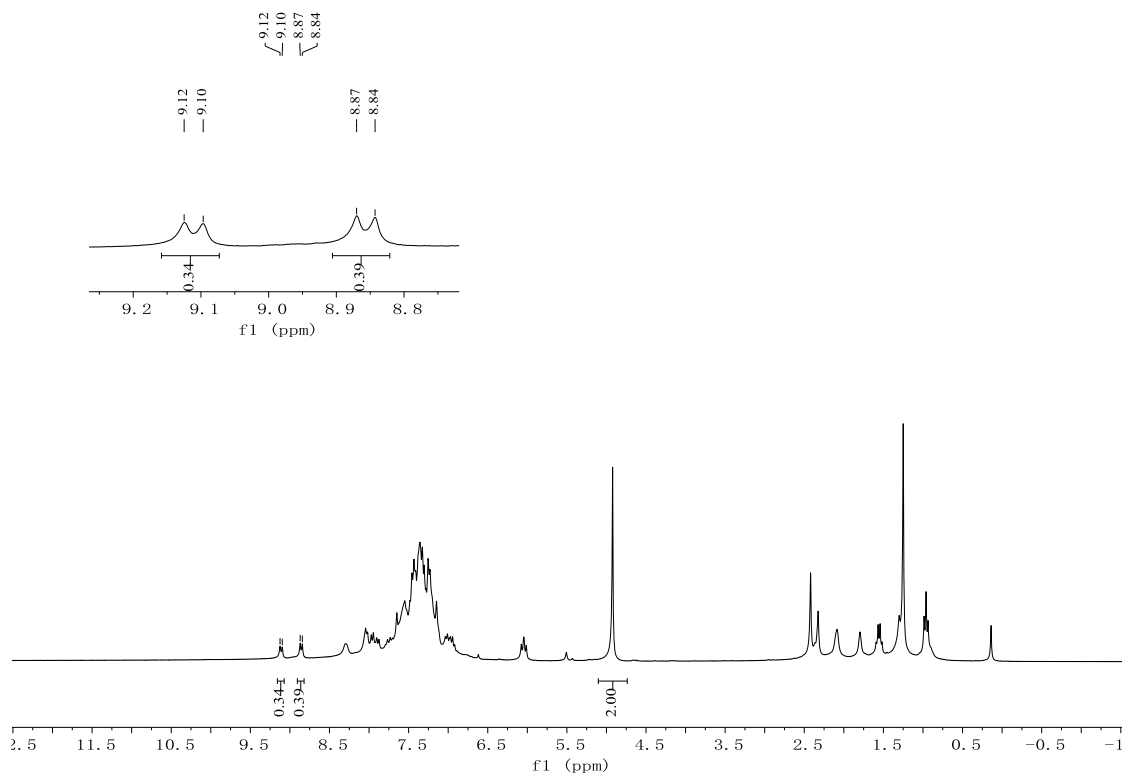
The general procedure **F** was followed using **145a** (74 mg, 0.40 mmol), alkyne **64b** (82 mg, 0.40 mmol) and **64d** (125 mg, 0.40 mmol). Then, the crude reaction mixture was filtered through a short pad of Celite. The conversion to **146b** (22%) and **146d** (27%) were determined by crude ¹H NMR spectroscopy with CH₂Br₂ as the internal standard. Then, repeated this reaction another two times got **146b** (27%), **146d** (31%) and **146b** (22%), **146d** (26%), respectively.



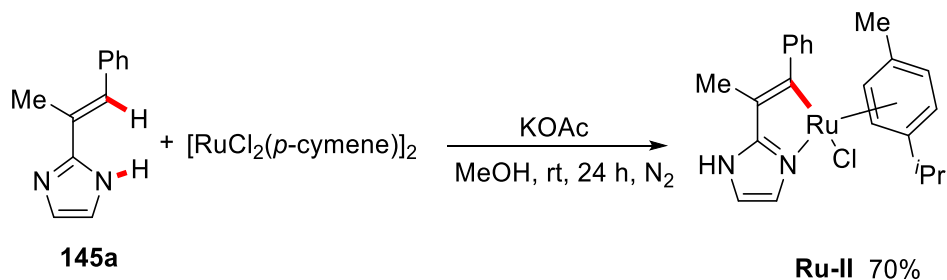
Experimental Section



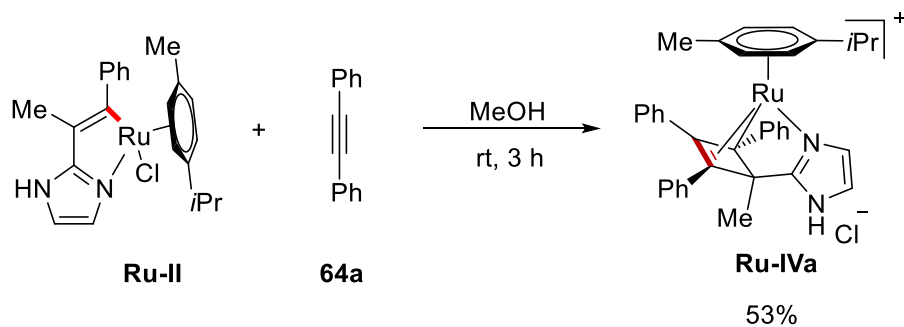
The general procedure **G** was followed using **147b** (42 mg, 0.20 mmol), **147d** (52 mg, 0.20 mmol) and alkyne **64a** (36 mg, 0.20 mmol). Then, the crude reaction mixture was filtered through a short pad of Celite. The conversions to **148b** and **148d** were determined by crude ¹H NMR spectroscopy with CH₂Br₂ as the internal standard. Then, repeated this reaction another two times got **148b** (42%), **148d** (33%) and **148b** (42%), **148d** (35%), respectively.



5.3.3.4 Synthesis of Ruthenium Complexes



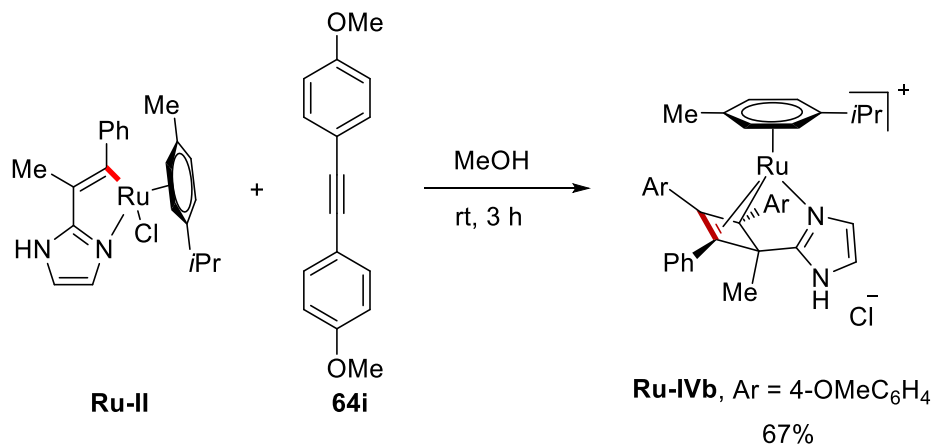
A 15 mL Schlenk tube was charged with **145a** (18.4 mg, 0.10 mmol), $[\text{RuCl}_2(p\text{-cymene})]_2$ (31.2 mg, 0.05 mmol), KOAc (20 mg, 0.20 mmol), and MeOH (2.0 mL). The mixture was stirred at ambient temperature for 24 h, and then MeOH was removed *in vacuo*. After column chromatography on silica gel ($\text{CH}_2\text{Cl}_2/\text{MeOH} = 50 : 1$) and crystallization (CH_2Cl_2 and *n*-pentane), **Ru-II** was isolated as a red solid (32 mg, 70%). **$^1\text{H NMR}$** (400 MHz, CDCl_3): $\delta = 10.24$ (s, 1H), 7.37 – 7.29 (m, 4H), 7.17 (t, $J = 6.6$ Hz, 1H), 7.06 (s, 1H), 6.44 (s, 1H), 5.29 – 5.24 (m, 2H), 4.87 (d, $J = 5.5$ Hz, 1H), 4.29 (d, $J = 5.5$ Hz, 1H), 2.20 (p, $J = 6.9$ Hz, 1H), 1.93 (s, 3H), 1.55 (s, 3H), 0.96 (d, $J = 7.0$ Hz, 3H), 0.79 (d, $J = 6.9$ Hz, 3H). **$^{13}\text{C NMR}$** (101 MHz, CDCl_3): $\delta = 187.0$ (C_q), 157.4 (C_q), 153.2 (C_q), 128.1 (CH), 127.4 (CH), 125.7 (CH), 124.3 (CH), 121.2 (C_q), 115.5 (CH), 96.7 (C_q), 95.9 (C_q), 89.0 (CH), 87.6 (CH), 84.3 (CH), 83.0 (CH), 30.8 (CH), 23.2 (CH_3), 20.9 (CH_3), 18.6 (CH_3), 13.3 (CH_3). **IR (ATR)**: 3078, 3050, 1626, 1600, 1484, 1442, 1253, 760, 704 cm^{-1} . **MS (ESI)** m/z (relative intensity): 419 (100) $[\text{M}-\text{Cl}]^+$. **HR-MS (ESI)** m/z calcd for $\text{C}_{22}\text{H}_{25}\text{N}_2\text{Ru}$ $[\text{M}-\text{Cl}]^+$: 419.1062, found: 419.1064.



A 15 mL Schlenk tube was charged with **Ru-II** (13.6 mg, 0.03 mmol), **64a** (5.9 mg, 0.033 mmol) and MeOH (2.0 mL). The mixture was stirred at ambient temperature for 3 h, and then MeOH was removed *in vacuo*. After column chromatography on silica gel ($\text{CH}_2\text{Cl}_2/\text{MeOH} = 50 : 1$), **Ru-IVa** was isolated as a yellow solid (10 mg, 53%), which could be crystallized in MeOH and Et_2O . **$^1\text{H NMR}$** (400 MHz, CDCl_3): $\delta = 14.31$ (s, 1H), 7.69 – 7.61 (m, 2H), 7.50 – 7.40 (m, 3H), 7.32 – 7.26 (m, 6H), 7.10 – 7.02 (m, 6H), 5.14 (d, $J = 5.7$ Hz, 2H), 4.90 (d, $J = 6.2$ Hz, 2H), 2.38 – 2.28

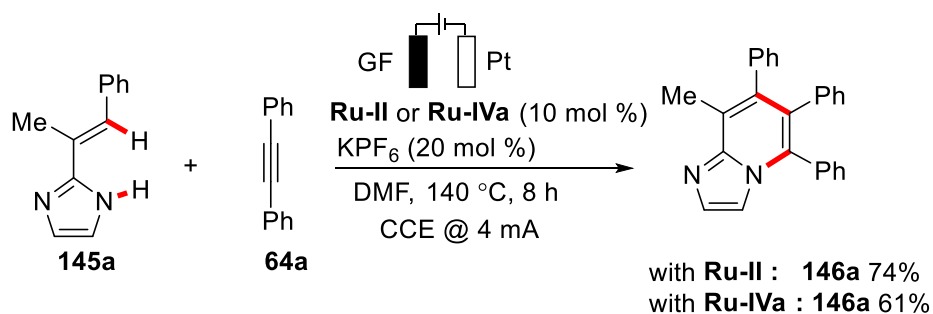
Experimental Section

(m, 1H), 1.92 (s, 3H), 1.64 (s, 3H), 0.86 (d, $J = 6.9$ Hz, 6H). **^{13}C NMR** (101 MHz, CDCl_3): $\delta = 157.1$ (C_q), 134.5 (overlapped, C_q), 134.1 (C_q), 129.3 (CH), 128.9 (overlapped, CH), 128.6 (overlapped, CH), 127.6 (overlapped, CH), 127.0 (overlapped, CH), 126.6 (CH), 118.4 (CH), 117.1 (C_q), 108.6 (C_q), 106.7 (C_q), 96.1 (overlapped, C_q), 87.8 (overlapped, CH), 86.4 (overlapped, CH), 61.8 (C_q), 30.3 (CH), 22.4 (overlapped, CH_3), 20.8 (CH_3), 17.7 (CH_3). **IR (ATR)**: 2958, 2148, 1706, 1494, 1293, 1208, 726, 693 cm^{-1} . **MS (ESI)** m/z (relative intensity): 597 (100) $[\text{M}-\text{Cl}]^+$. **HR-MS (ESI)** m/z calcd for $\text{C}_{36}\text{H}_{35}\text{N}_2\text{Ru}$ $[\text{M}-\text{Cl}]^+$: 597.1848, found: 597.1842.



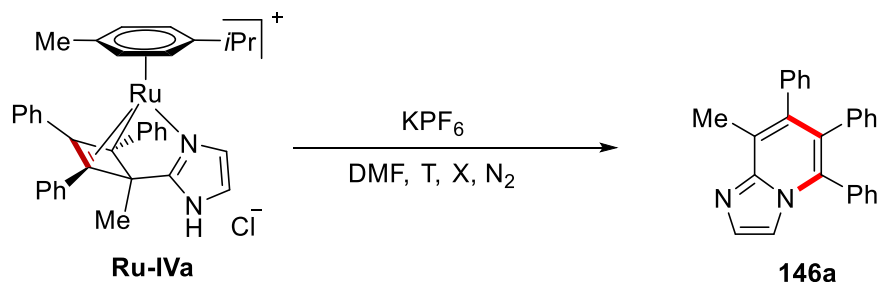
A 15 mL Schlenk tube was charged with **Ru-II** (13.6 mg, 0.03 mmol), **64i** (7.9 mg, 0.033 mmol) and MeOH (2 mL). The mixture was stirred at ambient temperature for 3 h, and then MeOH was removed *in vacuo*. After column chromatography on silica gel ($\text{CH}_2\text{Cl}_2/\text{MeOH} = 50 : 1$), **Ru-IVb** was isolated as yellow solid (14 mg, 67%), which could be crystallized in MeOH and diethyl ether. **^1H NMR** (400 MHz, CDCl_3): $\delta = 14.38$ (s, 1H), 7.60 (d, $J = 8.5$ Hz, 2H), 7.29 (d, $J = 0.9$ Hz, 3H), 7.13 – 7.06 (m, 3H), 7.05 – 6.99 (m, 3H), 6.97 (d, $J = 8.6$ Hz, 2H), 6.82 (d, $J = 8.4$ Hz, 2H), 5.06 (dd, $J = 18.7, 5.9$ Hz, 2H), 4.81 (d, $J = 39.5$ Hz, 2H), 3.90 (s, 3H), 3.82 (s, 3H), 2.42 – 2.32 (m, 1H), 1.94 (s, 3H), 1.62 (s, 3H), 0.91 (d, $J = 6.8$ Hz, 3H), 0.86 (d, $J = 6.8$ Hz, 3H). **^{13}C NMR** (101 MHz, CDCl_3): $\delta = 160.0$ (C_q), 159.0 (C_q), 157.2 (C_q), 134.9 (C_q), 130.0 (CH), 128.9 (CH), 128.6 (CH), 127.4 (CH), 126.9 (CH), 126.6 (C_q), 126.3 (CH), 126.0 (C_q), 118.4 (CH), 116.6 (C_q), 114.4 (CH), 113.9 (CH), 108.2 (C_q), 107.3 (C_q), 96.4 (C_q), 95.5 (C_q), 87.3 (CH), 87.1 (CH), 86.1 (CH), 85.7 (CH), 61.7 (C_q), 55.4 (CH_3), 55.4 (CH_3), 30.3 (CH), 22.7 (CH_3), 22.3 (CH_3), 20.9 (CH_3), 17.9 (CH_3). **IR (ATR)**: 2959, 1604, 1499, 1439, 1288, 1245, 1173, 1022, 832 cm^{-1} . **MS (ESI)** m/z (relative intensity): 657 (100) $[\text{M}-\text{Cl}]^+$. **HR-MS (ESI)** m/z calcd for $\text{C}_{38}\text{H}_{39}\text{N}_2\text{RuO}_2$ $[\text{M}-\text{Cl}]^+$: 657.2060, found: 657.2062.

5.3.3.5 Ruthenium Complexes Catalyzed C–H/N–H Activation



In an undivided cell with GF anode (10 mm × 10 mm × 6 mm) and a platinum cathode (20 mm × 10 mm × 0.25 mm), alkenyl imidazole **145a** (0.4 mmol, 1.0 equiv), alkyne **64a** (0.8 mmol, 2.0 equiv), KPF₆ (14.7 mg, 20 mol %) and **Ru-II** (18 mg, 10.0 mol %) were dissolved in DMF (4.0 mL) under N₂. Electrocatalysis was performed at 140 °C with a constant current of 4.0 mA maintained for 8 h. The GF anode was washed with EtOAc (3×10 mL) in an ultrasonic bath. The combined organic phases were added to the reaction mixture. Evaporation of the solvent and subsequent column chromatography on silica gel afforded the corresponding product **146a** (74% based on **145a**). The analogous procedure with **Ru-IVa** (25 mg, 10.0 mol %) yielded **146a** (61% based on **145a**).

5.3.3.6 Oxidatively Induced Reductive Elimination

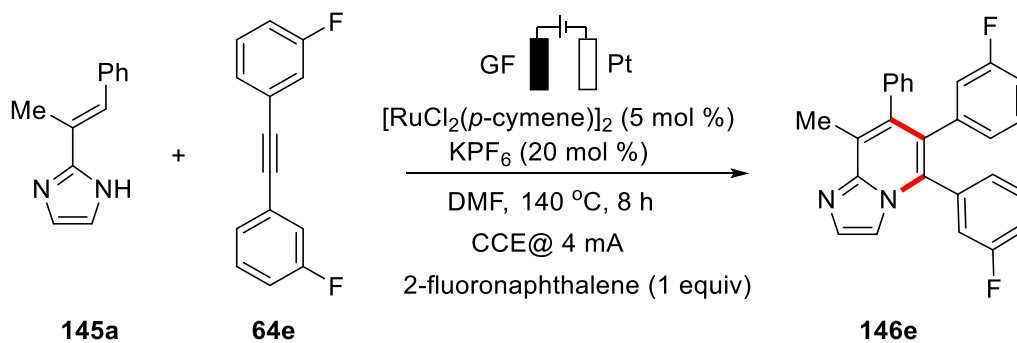


Entry	X/min	T/°C	Current	Ru-IVa	146a
1	10	rt	---	100%	---
2	10	rt	4 mA	67%	17%
3	10	80	---	100%	---
4	10	80	4 mA	57%	24%
5	60	80	---	77%	---
6	60	80	4 mA	---	53%
7	10	140	---	43%	14%
8	10	140	4 mA	20%	70%

A 15 mL Schlenk tube was charged with **Ru-IVa** (9.5 mg, 0.015 mmol) and KPF_6 (14.7 mg, 0.08 mmol). The tube was evacuated and filled with N_2 three times. Then, DMF (4 mL) was added and the mixture was electrolyzed at a constant current of 4 mA for 10 min or 60 min at ambient temperature or 80 °C or 140 °C (GF anode, (10 mm × 15 mm × 6 mm) and a platinum cathode (10 mm × 15 mm × 0.25 mm)). The solvent was removed *in vacuo* and trimethoxybenzene (5.05 mg, 0.03 mmol) was added as standard. Then, the residue was dissolved in CDCl_3 (0.8 mL) and subjected to ^1H NMR spectroscopy.

5.3.3.7 On-Line NMR Monitoring in Flow

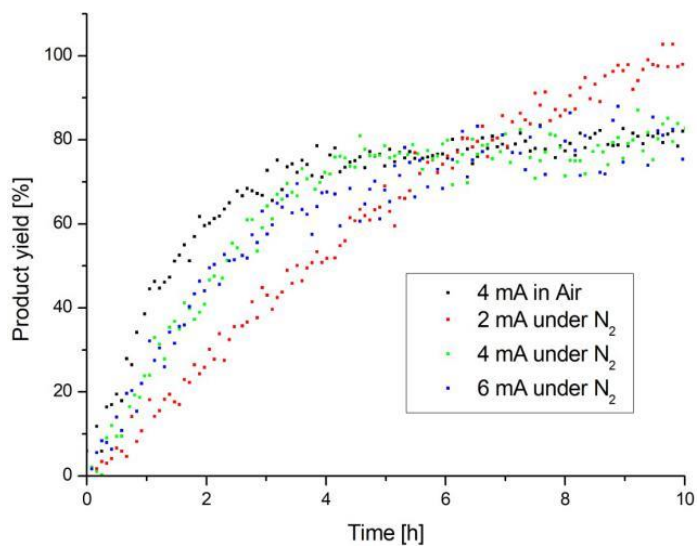
On-line monitoring in flow was performed by Dr. Lars H. Finger. The ^{19}F NMR spectroscopy experiments in flow were performed on a Magritek Spinsolve 60^{ULTRA} (from Magritek GmbH, Germany) with the reaction monitoring kit supplied by the manufacturer. For pumping the solution to the spectrometer, an Ismatec REGLO Digital MS-2/12 (ISM 596) peristaltic pump was employed. The flow rate was 0.4 mL/min.



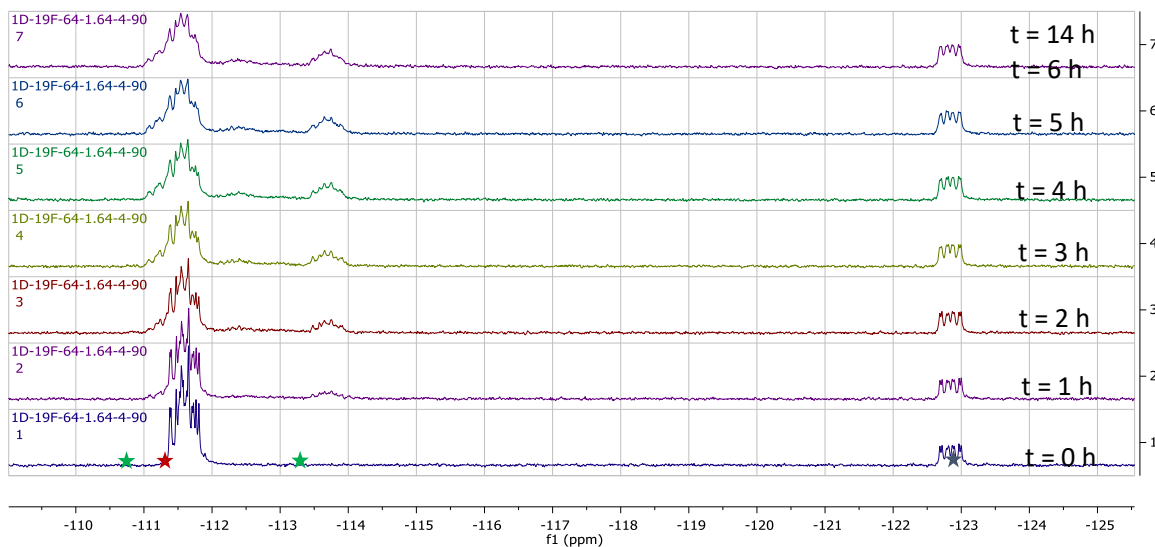
CCE	NMR Yield
4 mA air	67%
4 mA N_2	67%
2 mA N_2	65%
6 mA N_2	55%

A 15 mL Schlenk tube was charged with **145a** (110.4 mg, 0.60 mmol, 1.0 equiv), **64e** (256.8 mg, 1.2 mmol, 2.0 equiv), KPF_6 (22.1 mg, 0.12 mmol), 2-fluoronaphthalene (65.8 μL , 0.6 mmol), $[\text{RuCl}_2(p\text{-cymene})]_2$ (18.7 mg, 5.0 mol %) and DMF (6 mL). The solution was pumped to the NMR spectrometer by a peristaltic pump with a flow speed of 0.4 mL/min. The electrocatalysis was performed at 140 °C with a constant current of 4.0 mA maintained for 8 h. After evaporation of the solvent, the reaction yield of **146e** was determined by ^1H NMR with CH_2Br_2 as internal

standard.

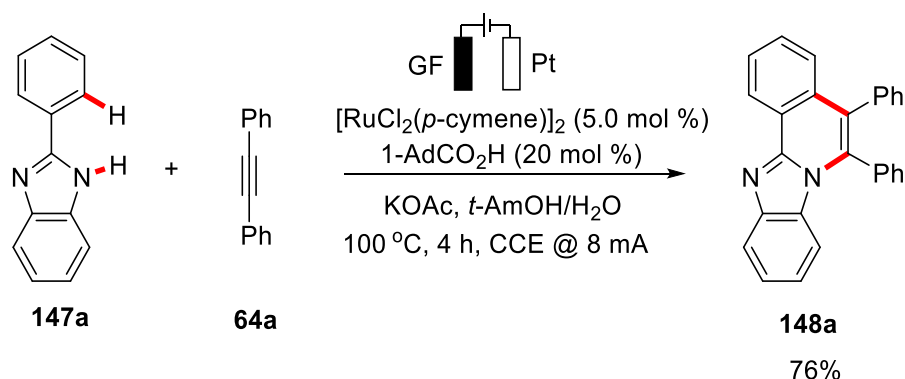


Scheme 5.3.3.7a Reaction profile determined by ^{19}F NMR spectroscopic monitoring in flow.

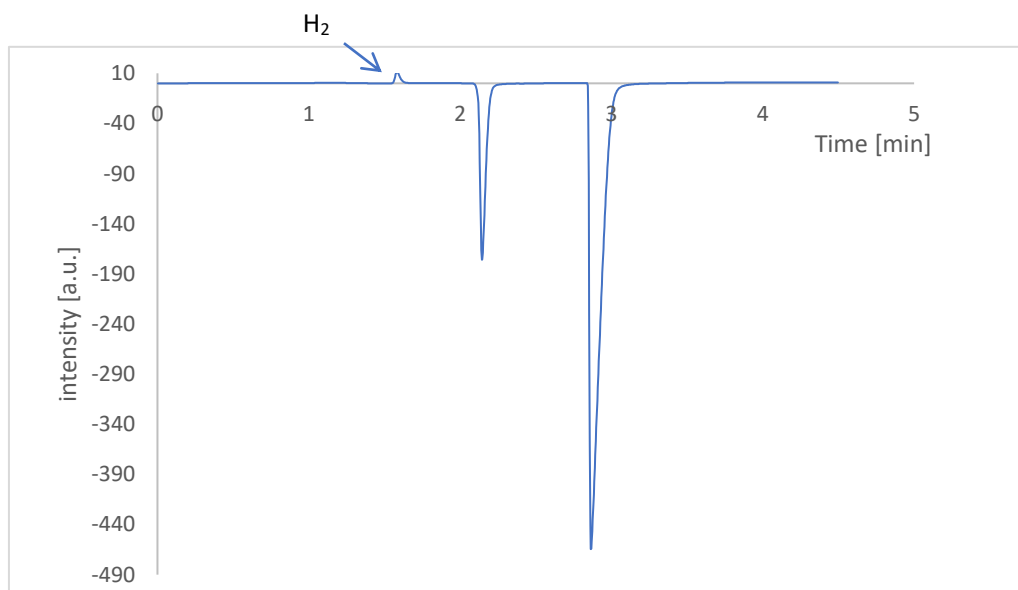


Scheme 5.3.3.7b ^{19}F NMR spectra recorded in flow from the reaction mixture at 4 mA in air at selected times (★: Product **146e**, ★: Starting material **64e**, ★: Internal standard (2-fluoronaphthalene)).

5.3.3.8 GC-Headspace Detection

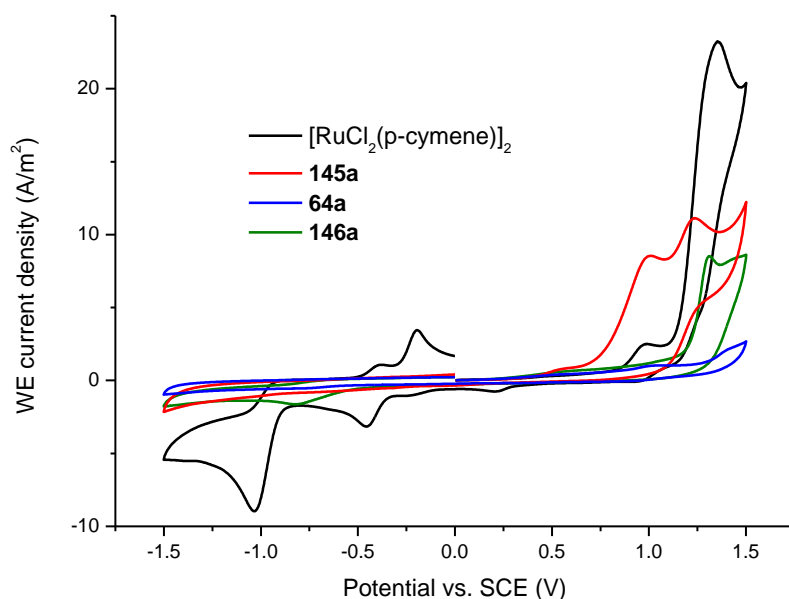


In an undivided cell equipped with a GF anode (10 mm × 15 mm × 6 mm) and a platinum cathode (10 mm × 15 mm × 0.25 mm), **147a** (39 mg, 0.2 mmol), alkyne **64a** (71 mg, 0.4 mmol), KOAc (39 mg, 0.4 mmol), 1-AdCO₂H (7.2 mg, 20.0 mol %) and $[\text{RuCl}_2(p\text{-cymene})]_2$ (6.2 mg, 5.0 mol %) were dissolved in *t*-AmOH (3 mL) and H₂O (3 mL) under N₂. Electrocatalysis was performed at 100 °C with a constant current of 8.0 mA maintained for 4 h. After the reaction, 1.0 mL of the headspace volume was removed for GC analysis. The graphite felt anode was washed with EtOAc (3 × 20 mL) in an ultrasonic bath. The yield of **148a** (76%) was determined by ¹H NMR spectroscopy.

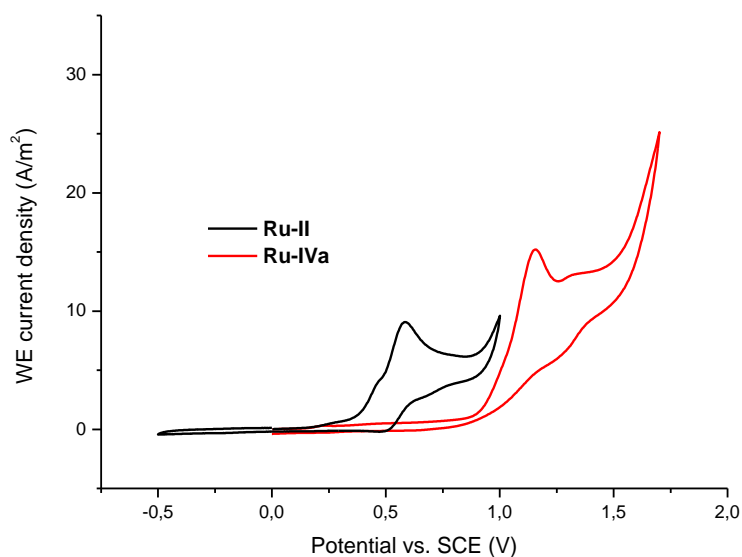


5.3.3.9 Cyclic Voltammetry

CV measurements were conducted with a Metrohm Autolab PGSTAT204 potentiostat and Nova 2.1 software. For all experiments, a glassy carbon working electrode (disk, diameter: 3mm), a platinum wire counter electrode and a saturated calomel reference electrode (SCE) were employed. The voltammograms were recorded at room temperature in DMF at a substrate concentration of 5 mmol/L and with 0.1 mol/L KPF_6 as supporting electrolyte. All solutions were saturated with N_2 prior to the measurement and an overpressure of N_2 was maintained throughout the experiment. The scan rate is 100 mV/s. Deviations from the general experimental setup were indicated in the respective figures and descriptions.



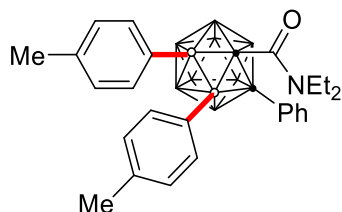
Cyclic voltammograms of $[\text{RuCl}_2(\text{p-cymene})]_2$ (2.5 mM; black line), **145a** (red line), **64a** (blue line), **146a** (green line) at rt. CV performed by Alexej Scheremetjew.



Cyclic voltammograms of **Ru-II** (black line), **Ru-IVa** (red line) in DMF under N₂ at rt, 100 mM KPF₆ at 100 mV/s.

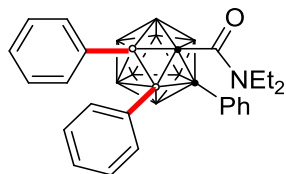
5.3.4 Regioselective B(3,4)-H Arylation of *o*-Carboranes

5.3.4.1 Characterization Data

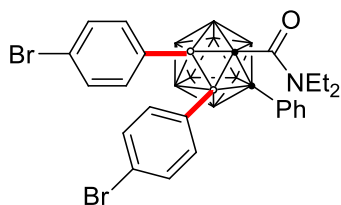


150a. The representative procedure **H** was followed using *o*-carborane **149a** (1-CONEt₂-2-Ph-*o*-C₂B₁₀H₁₀) (64 mg, 0.20 mmol) and 4-iodotoluene **19a** (105 mg, 0.48 mmol). Isolation by column chromatography (*n*-hexane/EtOAc: 20/1) yielded **150a** (71 mg, 71%) as a colorless solid. **M.p.** = 171–172 °C. **¹H NMR** (500 MHz, CDCl₃): δ = 7.45 (d, *J* = 8.5 Hz, 2H), 7.39–7.32 (m, 3H), 7.22 (dd, *J* = 8.5, 7.3 Hz, 2H), 7.17 (d, *J* = 8.0 Hz, 2H), 6.94–6.90 (m, 4H), 3.49–3.44 (m, 2H), 3.26–3.22 (m, 2H), 2.28 (s, 3H), 2.24 (s, 3H), 1.00 (t, *J* = 7.0 Hz, 6H). **¹³C NMR** (125 MHz, CDCl₃): δ = 156.6 (C_q), 138.1 (C_q), 137.7 (C_q), 136.5 (CH), 133.9 (CH), 133.3 (C_q), 130.0 (CH), 129.3 (CH), 128.1 (CH), 127.6 (CH), 127.5 (CH), 85.5 (C_q), 79.3 (C_q), 43.7 (CH₂), 21.2 (CH₃), 21.1 (CH₃), 12.9 (CH₃). **¹¹B NMR** (160 MHz, CDCl₃): δ = 0.65 (2B), -1.38 (1B), -3.61 (1B), -6.20 (1B), -10.54 (5B). **IR** (ATR): 2978, 2566, 1653, 1608, 1415, 1264, 1191, 772 cm⁻¹. **MS** (ESI) *m/z* (relative intensity): 522 (100) [M+Na]⁺, 500 (40) [M+H]⁺. **HR-MS** (ESI): *m/z* calcd. for

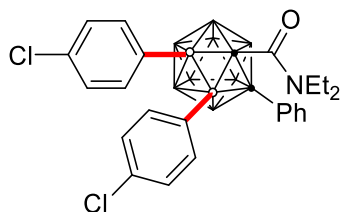
$C_{27}H_{38}^{10}B_2^{11}B_8NO$ $[M+H]^+$: 500.3964, found: 500.3951.



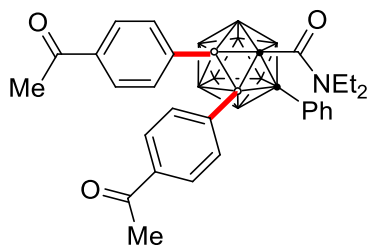
150b. The representative procedure **H** was followed using *o*-carborane **149a** (1- $CONEt_2$ -2-Ph-*o*- $C_2B_{10}H_{10}$) (64 mg, 0.20 mmol) and iodobenzene **19b** (98 mg, 0.48 mmol). Isolation by column chromatography (*n*-hexane/EtOAc: 20/1) yielded **150b** (64 mg, 68%) as a colorless solid. **M.p.** = 197–198 °C. **1H NMR** (400 MHz, $CDCl_3$): δ = 7.53–7.42 (m, 4H), 7.37–7.32 (m, 1H), 7.29–7.15 (m, 6H), 7.14–7.04 (m, 4H), 3.50–3.41 (m, 2H), 3.26–3.20 (m, 2H), 0.99 (t, J = 7.0 Hz, 6H). **^{13}C NMR** (100 MHz, $CDCl_3$): δ = 156.6 (C_q), 136.6 (CH), 134.0 (CH), 133.2 (C_q), 130.1 (CH), 129.4 (CH), 128.4 (CH), 128.0 (CH), 127.6 (CH), 127.2 (CH), 126.6 (CH), 86.0 (C_q), 79.7 (C_q), 43.8 (CH_2), 12.9 (CH_3). **^{11}B NMR** (128 MHz, $CDCl_3$): δ = 0.34 (2B), -1.31 (1B), -3.28 (1B), -5.82 (1B), -10.20 (5B). **IR** (ATR): 2973, 2567, 1647, 1430, 1266, 1208, 696 cm^{-1} . **MS** (ESI) m/z (relative intensity): 494 (100) $[M+Na]^+$, 472 (40) $[M+H]^+$. **HR-MS** (ESI): m/z calcd. for $C_{25}H_{34}^{10}B_2^{11}B_8NO$ $[M+H]^+$: 472.3650, found: 472.3631.



150c. The representative procedure **H** was followed using *o*-carborane **149a** (1- $CONEt_2$ -2-Ph-*o*- $C_2B_{10}H_{10}$) (64 mg, 0.20 mmol) and 1-bromo-4-iodobenzene **19c** (136 mg, 0.48 mmol). Isolation by column chromatography (*n*-hexane/EtOAc: 20/1) yielded **150c** (76 mg, 61%) as a colorless solid. **M.p.** = 205–206 °C. **1H NMR** (300 MHz, $CDCl_3$): δ = 7.50–7.39 (m, 3H), 7.32–7.27 (m, 5H), 7.25–7.22 (m, 3H), 7.21–7.14 (m, 2H), 3.60–3.42 (m, 4H), 1.05 (t, J = 6.9 Hz, 6H). **^{13}C NMR** (75 MHz, $CDCl_3$): δ = 156.2 (C_q), 138.0 (CH), 135.6 (CH), 132.0 (C_q), 130.5 (CH), 129.8 (CH), 129.7 (CH), 129.6 (CH), 127.9 (CH), 123.6 (C_q), 123.2 (C_q), 84.6 (C_q), 78.5 (C_q), 44.0 (CH_2), 13.1 (CH_3). **^{11}B NMR** (96 MHz, $CDCl_3$): δ = 0.22 (3B), -3.11 (1B), -6.02 (1B), -9.94 (5B). **IR** (ATR): 2573, 1647, 1578, 1487, 1381, 1205, 1010, 693 cm^{-1} . **MS** (ESI) m/z (relative intensity): 652 (100) $[M+Na]^+$, 630 (10) $[M+H]^+$. **HR-MS** (ESI): m/z calcd. for $C_{25}H_{31}^{11}B_{10}^{79}Br_2NONa$ $[M+Na]^+$: 652.1657, found: 652.1642.

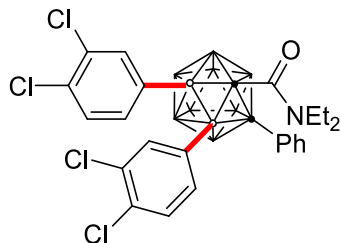


150d. The representative procedure **H** was followed using *o*-carborane **149a** (1-CONEt₂-2-Ph-*o*-C₂B₁₀H₁₀) (64 mg, 0.20 mmol) and 1-chloro-4-iodobenzene **19d** (115 mg, 0.48 mmol). Isolation by column chromatography (*n*-hexane/EtOAc: 20/1) yielded **150d** (73 mg, 68%) as a colorless solid. **M.p.** = 185–186 °C. **¹H NMR** (300 MHz, CDCl₃): δ = 7.48–7.40 (m, 3H), 7.35–7.22 (m, 6H), 7.17–7.08 (m, 4H), 3.54–3.40 (m, 4H), 1.06 (t, *J* = 7.0 Hz, 6H). **¹³C NMR** (75 MHz, CDCl₃): δ = 156.2 (C_q), 137.8 (CH), 135.3 (CH), 135.0 (C_q), 134.7 (C_q), 132.1 (C_q), 129.9 (CH), 129.6 (CH), 128.0 (CH), 127.5 (CH), 126.9 (CH), 84.9 (C_q), 78.9 (C_q), 44.2 (CH₂), 12.9 (CH₃). **¹¹B NMR** (96 MHz, CDCl₃): δ = 0.49 (3B), -3.10 (1B), -6.38 (1B), -10.40 (5B). **IR** (ATR): 2571, 1648, 1584, 1489, 1268, 1205, 1092, 730 cm⁻¹. **MS** (ESI) *m/z* (relative intensity): 564 (100) [M+Na]⁺, 542 (10) [M+H]⁺. **HR-MS** (ESI): *m/z* calcd. for C₂₅H₃₁¹¹B₁₀³⁵Cl₂NONa [M+Na]⁺: 564.2649, found: 564.2640.

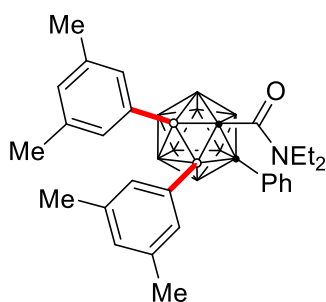


150e. The representative procedure **H** was followed using *o*-carborane **149a** (1-CONEt₂-2-Ph-*o*-C₂B₁₀H₁₀) (64 mg, 0.20 mmol) and 1-(4-iodophenyl)ethanone **19e** (118 mg, 0.48 mmol). Isolation by column chromatography (*n*-hexane/EtOAc: 20/1) yielded **150e** (64 mg, 58%) as a colorless solid. **M.p.** = 244–245 °C. **¹H NMR** (300 MHz, CDCl₃): δ = 7.74 (d, *J* = 8.3 Hz, 2H), 7.66 (d, *J* = 8.3 Hz, 2H), 7.51–7.39 (m, 7H), 7.34–7.27 (m, 2H), 3.60–3.45 (m, 4H), 2.56 (s, 3H), 2.55 (s, 3H), 1.09 (t, *J* = 6.9 Hz, 6H). **¹³C NMR** (75 MHz, CDCl₃): δ = 198.3 (C_q), 198.1 (C_q), 156.0 (C_q), 136.6 (C_q), 136.5 (CH), 136.4 (C_q), 134.2 (CH), 131.8 (C_q), 130.1 (CH), 129.7 (CH), 128.0 (CH), 127.0 (CH), 126.0 (CH), 84.9 (C_q), 78.5 (C_q), 43.9 (CH₂), 26.7 (CH₃), 26.5 (CH₃), 13.0 (CH₃). **¹¹B NMR** (96 MHz, CDCl₃): δ = 0.58 (3B), -2.61 (1B), -5.98 (1B), -9.67 (5B). **IR** (ATR): 2572, 1679, 1642, 1357, 1266, 1200, 730, 590 cm⁻¹. **MS** (ESI) *m/z* (relative intensity): 578 (100) [M+Na]⁺, 556 (10)

$[M+H]^+$. **HR-MS** (ESI): m/z calcd. for $C_{29}H_{37}^{10}B_2^{11}B_8NO_3Na$ $[M+Na]^+$: 578.3683, found: 578.3676.

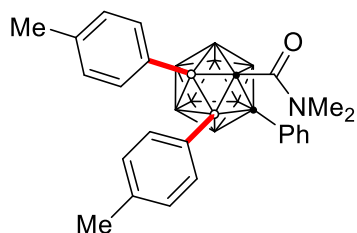


150f. The representative procedure **H** was followed using *o*-carborane **149a** (1-CONEt₂-2-Ph-*o*-C₂B₁₀H₁₀) (64 mg, 0.20 mmol) and 1,2-dichloro-4-iodobenzene **19f** (131 mg, 0.48 mmol). Isolation by column chromatography (*n*-hexane/EtOAc: 20/1) yielded **150f** (78 mg, 64%) as a colorless solid. **M.p.** = 208–209 °C. **¹H NMR** (300 MHz, CDCl₃): δ = 7.48–7.40 (m, 4H), 7.36–7.26 (m, 4H), 7.22–7.11 (m, 3H), 3.60–3.45 (m, 4H), 1.13 (t, J = 6.9 Hz, 6H). **¹³C NMR** (75 MHz, CDCl₃): δ = 155.8 (C_q), 138.1 (CH), 135.6 (CH), 135.4 (CH), 133.2 (CH), 133.0 (C_q), 132.9 (C_q), 132.0 (C_q), 131.5 (C_q), 130.9 (C_q), 130.2 (CH), 129.7 (CH), 129.5 (CH), 128.7 (CH), 128.2 (CH), 85.0 (C_q), 78.2 (C_q), 44.2 (CH₂), 13.0 (CH₃). **¹¹B NMR** (96 MHz, CDCl₃): δ = 0.76 (3B), -3.10 (1B), -6.49 (1B), -10.24 (5B). **IR** (ATR): 2578, 1646, 1473, 1424, 1203, 1028, 695 cm⁻¹. **MS** (ESI) m/z (relative intensity): 632 (100) $[M+Na]^+$, 610 (10) $[M+H]^+$. **HR-MS** (ESI): m/z calcd. for $C_{25}H_{29}^{11}B_{10}^{35}Cl_4NONa$ $[M+Na]^+$: 632.1879, found: 632.1867.

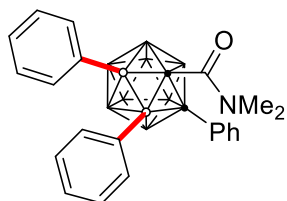


150g. The representative procedure **H** was followed using *o*-carborane **149a** (1-CONEt₂-2-Ph-*o*-C₂B₁₀H₁₀) (64 mg, 0.20 mmol) and 1-iodo-3,5-dimethylbenzene **19g** (112 mg, 0.48 mmol). Isolation by column chromatography (*n*-hexane/EtOAc: 20/1) yielded **150g** (66 mg, 63%) as a colorless solid. **M.p.** = 203–205 °C. **¹H NMR** (300 MHz, CDCl₃): δ = 7.52 (d, J = 7.4 Hz, 2H), 7.40–7.32 (m, 1H), 7.29–7.18 (m, 4H), 7.00–6.90 (m, 3H), 6.87 (s, 1H), 3.62 (q, J = 7.0 Hz, 2H), 3.09 (q, J = 7.0 Hz, 2H), 2.19 (s, 6H), 2.16 (s, 6H), 1.08 (t, J = 7.0 Hz, 6H). **¹³C NMR** (75 MHz,

CDCl₃): δ = 156.8 (C_q), 136.2 (C_q), 135.6 (C_q), 134.3 (CH), 134.3 (C_q), 131.8 (CH), 130.4 (CH), 130.2 (CH), 129.7 (CH), 129.3 (CH), 127.5 (CH), 87.6 (C_q), 80.3 (C_q), 43.5 (CH₂), 21.4 (CH₃), 21.2 (CH₃), 12.7 (CH₃). **¹¹B NMR** (96 MHz, CDCl₃): δ = 0.69 (2B), -1.17 (1B), -3.10 (1B), -5.90 (1B), -10.05 (5B). **IR** (ATR): 2916, 2557, 1646, 1420, 1264, 1183, 855, 689 cm⁻¹. **MS** (ESI) *m/z* (relative intensity): 550 (100) [M+Na]⁺, 528 (10) [M+H]⁺. **HR-MS** (ESI): *m/z* calcd. for C₂₉H₄₁¹⁰B₂¹¹B₈NONa [M+Na]⁺: 550.4097, found: 550.4096.

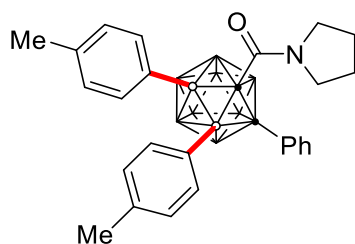


152a. The representative procedure **H** was followed using *o*-carborane **151a** (1-CONMe₂-2-Ph-*o*-C₂B₁₀H₁₀) (58 mg, 0.20 mmol) and 4-iodotoluene **19a** (105 mg, 0.48 mmol). Isolation by column chromatography (*n*-hexane/EtOAc: 20/1) yielded **152a** (48 mg, 51%) as a colorless solid. **M.p.** = 158–159 °C. **¹H NMR** (400 MHz, CDCl₃): δ = 7.45 (d, *J* = 7.4 Hz, 2H), 7.40–7.36 (m, 1H), 7.34–7.23 (m, 4H), 7.20 (d, *J* = 7.9 Hz, 2H), 6.99–6.90 (m, 4H), 3.04 (s, 6H), 2.31 (s, 3H), 2.29 (s, 3H). **¹³C NMR** (100 MHz, CDCl₃): δ = 157.7 (C_q), 138.3 (C_q), 137.9 (C_q), 136.3 (CH), 133.9 (CH), 133.1 (C_q), 130.0 (CH), 129.5 (CH), 128.4 (CH), 127.8 (CH), 127.6 (CH), 85.9 (C_q), 78.6 (C_q), 40.8 (CH₃), 21.3 (CH₃), 21.2 (CH₃). **¹¹B NMR** (128 MHz, CDCl₃): δ = 0.7 (2B), -1.3 (1B), -3.2 (1B), -6.4 (1B), -10.6 (5B). **IR** (ATR): 2921, 2570, 1644, 1393, 1195, 743, 693 cm⁻¹. **MS** (ESI) *m/z* (relative intensity): 473 (100) [M+H]⁺. **HR-MS** (ESI): *m/z* calcd. for C₂₅H₃₄¹⁰B₁¹¹B₉NO [M+H]⁺: 473.3607, found: 473.3606.

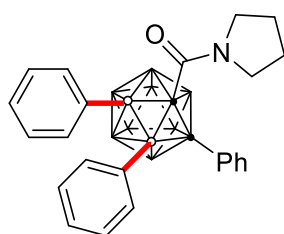


152b. The representative procedure **H** was followed using *o*-carborane **151a** (1-CONMe₂-2-Ph-*o*-C₂B₁₀H₁₀) (58 mg, 0.20 mmol) and iodobenzene **19b** (98 mg, 0.48 mmol). Isolation by column chromatography (*n*-hexane/EtOAc: 20/1) yielded **152b** (47 mg, 53%) as a colorless solid. **M.p.** =

99–100 °C. **¹H NMR** (400 MHz, CDCl₃): δ = 7.47–7.41 (m, 4H), 7.40–7.35 (m, 1H), 7.32–7.29 (m, 2H), 7.28–7.20 (m, 4H), 7.18–7.10 (m, 4H), 3.03 (s, 6H). **¹³C NMR** (100 MHz, CDCl₃): δ = 157.7 (C_q), 136.4 (CH), 133.9 (CH), 133.0 (C_q), 130.0 (CH), 129.6 (CH), 128.6 (CH), 128.2 (CH), 127.9 (CH), 127.5 (CH), 126.8 (CH), 86.4 (C_q), 79.0 (C_q), 40.8 (CH₃). **¹¹B NMR** (128 MHz, CDCl₃): δ = 0.57 (2B), -1.13 (1B), -3.10 (1B), -6.27 (1B), -10.23 (5B). **IR** (ATR): 3053, 2581, 1654, 1493, 1373, 1167, 744 cm⁻¹. **MS** (ESI) *m/z* (relative intensity): 444 (100) [M+H]⁺, 466 (10) [M+Na]⁺. **HR-MS** (ESI): *m/z* calcd. for C₂₃H₃₀¹⁰B₂¹¹B₈NO [M+H]⁺: 444.3336, found: 444.3328.

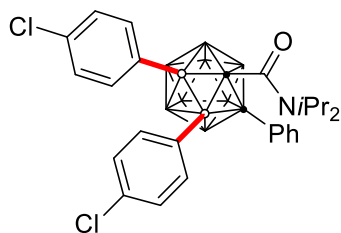


152c. The representative procedure **H** was followed using *o*-carborane **151b** (1-CON(CH₂)₄-2-Ph-*o*-C₂B₁₀H₁₀) (63 mg, 0.20 mmol) and 4-iodotoluene **19a** (105 mg, 0.48 mmol). Isolation by column chromatography (*n*-hexane/EtOAc: 20/1) yielded **152c** (59 mg, 60%) as a pink solid. **M.p.** = 228–230 °C. **¹H NMR** (400 MHz, CDCl₃): δ = 7.44–7.38 (m, 2H), 7.36–7.28 (m, 3H), 7.22–7.16 (m, 2H), 7.16–7.10 (m, 2H), 6.96–6.87 (m, 4H), 3.65–3.28 (m, 4H), 2.25 (s, 3H), 2.23 (s, 3H), 1.80–1.63 (m, 4H). **¹³C NMR** (100 MHz, CDCl₃): δ = 155.7 (C_q), 138.1 (C_q), 137.7 (C_q), 136.6 (CH), 133.6 (CH), 132.9 (C_q), 129.9 (CH), 129.4 (CH), 128.3 (CH), 127.7 (CH), 127.5 (CH), 85.0 (C_q), 78.7 (C_q), 50.5 (overlapped, CH₂), 21.2 (CH₃), 21.2 (CH₃). **¹¹B NMR** (128 MHz, CDCl₃): δ = 0.57 (2B), -1.61 (1B), -3.32 (1B), -6.45 (1B), -10.78 (5B). **IR** (ATR): 2975, 2878, 2570, 1639, 1446, 1225, 865, 753, 690 cm⁻¹. **MS** (ESI) *m/z* (relative intensity): 498 (20) [M+H]⁺, 520 (100) [M+Na]⁺. **HR-MS** (ESI) *m/z* calcd for C₂₇H₃₅¹⁰B₂¹¹B₈NONa [M+Na]⁺ 520.3627, found 520.3623.

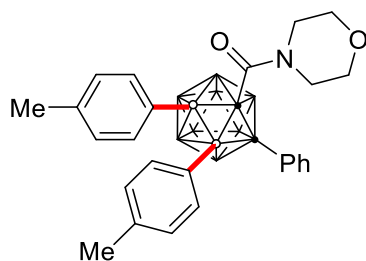


152d. The representative procedure **H** was followed using *o*-carborane **151b** (1-CON(CH₂)₄-2-Ph-*o*-C₂B₁₀H₁₀) (63 mg, 0.20 mmol) and iodobenzene **19b** (98 mg, 0.48 mmol). Isolation by

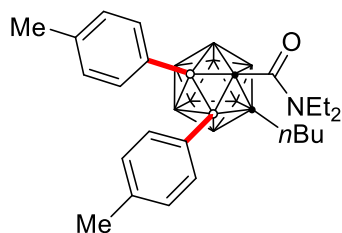
column chromatography (*n*-hexane/EtOAc: 20/1) yielded **152d** (50 mg, 53%) as a colorless solid. **M.p.** = 176–177 °C. **¹H NMR** (500 MHz, CDCl₃): δ = 7.51–7.44 (m, 2H), 7.43–7.38 (m, 2H), 7.35–7.30 (m, 1H), 7.25–7.24 (m, 1H), 7.24–7.16 (m, 5H), 7.13–7.04 (m, 4H), 3.63–3.41 (m, 4H), 1.83–1.61 (m, 4H). **¹³C NMR** (125 MHz, CDCl₃): δ = 155.7 (C_q), 136.7 (CH), 133.6 (CH), 132.8 (C_q), 129.9 (CH), 129.5 (CH), 128.4 (CH), 128.1 (CH), 127.7 (CH), 127.4 (CH), 126.6 (CH), 85.5 (C_q), 79.1 (C_q), 50.5 (overlapped, CH₂). **¹¹B NMR** (96 MHz, CDCl₃): δ = 0.48 (2B), -1.36 (1B), -3.15 (1B), -6.18 (1B), -10.26 (5B). **IR** (ATR): 2921, 2570, 1643, 1389, 1195, 861, 743, 692 cm⁻¹. **MS** (ESI) *m/z* (relative intensity): 471 (100) [M+H]⁺, 493 (10) [M+Na]⁺. **HR-MS** (ESI): *m/z* calcd. for C₂₅H₃₂¹⁰B₁¹¹B₉NO [M+H]⁺: 471.3450, found: 471.3448.



152e. The representative procedure **H** was followed using *o*-carborane **151c** (1-CONⁱPr₂-2-Ph-*o*-C₂B₁₀H₁₀) (70 mg, 0.20 mmol) and 1-chloro-4-iodobenzene **19d** (114 mg, 0.48 mmol). Isolation by column chromatography (*n*-hexane/EtOAc: 20/1) yielded **152e** (61 mg, 54%) as a colorless solid. **M.p.** = 232–233 °C. **¹H NMR** (400 MHz, CDCl₃): δ = 7.52 (d, *J* = 7.4 Hz, 2H), 7.45–7.41 (m, 1H), 7.35 (d, *J* = 8.4 Hz, 2H), 7.32–7.27 (m, 2H), 7.19 (d, *J* = 8.6 Hz, 2H), 7.14 (d, *J* = 8.4 Hz, 2H), 7.07 (d, *J* = 8.4 Hz, 2H), 5.24–5.18 (m, 1H), 3.44–3.39 (m, 1H), 1.29 (d, *J* = 6.7 Hz, 6H), 1.04 (d, *J* = 6.7 Hz, 6H). **¹³C NMR** (100 MHz, CDCl₃): δ = 154.5 (C_q), 137.9 (CH), 136.1 (CH), 134.7 (C_q), 134.5 (C_q), 132.0 (C_q), 129.9 (CH), 129.5 (CH), 128.0 (CH), 127.5 (CH), 126.5 (CH), 83.9 (C_q), 79.1 (C_q), 50.3 (CH), 49.4 (CH), 20.5 (CH₃), 20.3 (CH₃), 19.7 (CH₃), 19.6 (CH₃). **¹¹B NMR** (128 MHz, CDCl₃): δ = 1.47 (1B), -1.05 (2B), -3.30 (1B), -6.75 (1B), -10.90 (5B). **IR** (ATR): 2968, 2620, 2585, 1657, 1586, 1491, 1369, 1296, 691 cm⁻¹. **MS** (ESI) *m/z* (relative intensity): 569 (100) [M+H]⁺, 591 (10) [M+Na]⁺. **HR-MS** (ESI): *m/z* calcd. for C₂₇H₃₆¹⁰B₁¹¹B₉³⁵Cl₂NO [M+H]⁺: 569.3141, found: 569.3142.

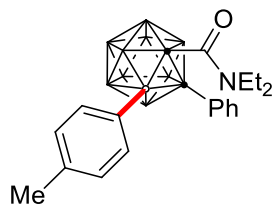


152f. The representative procedure **H** was followed using *o*-carborane **151d** (1-CON(CH₂)₄O-2-Ph-*o*-C₂B₁₀H₁₀) (67 mg, 0.20 mmol) and 4-iodotoluene **19a** (105 mg, 0.48 mmol). Isolation by column chromatography (*n*-hexane/EtOAc: 20/1) yielded **152f** (54 mg, 52%) as a colorless solid. **M.p.** = 258–259 °C. **¹H NMR** (400 MHz, CDCl₃): δ = 7.49–7.41 (m, 2H), 7.40–7.32 (m, 3H), 7.28–7.21 (m, 2H), 7.21–7.14 (m, 2H), 7.01 (d, *J* = 7.9 Hz, 2H), 6.96 (d, *J* = 7.8 Hz, 2H), 3.73–3.58 (m, 4H), 3.48–3.32 (m, 4H), 2.34 (s, 3H), 2.28 (s, 3H). **¹³C NMR** (100 MHz, CDCl₃): δ = 157.6 (C_q), 138.7 (C_q), 138.2 (C_q), 136.2 (CH), 134.2 (CH), 133.4 (C_q), 130.1 (CH), 129.6 (CH), 128.5 (CH), 128.0 (CH), 127.8 (CH), 86.7 (C_q), 78.6 (C_q), 66.5 (CH₂), 47.9 (CH₂), 21.3 (CH₃), 21.2 (CH₃). **¹¹B NMR** (128 MHz, CDCl₃): δ = 0.67 (2B), -0.88 (1B), -3.11 (1B), -6.12 (1B), -10.53 (5B). **IR** (ATR): 2843, 2549, 1660, 1447, 1411, 1264, 1225, 771 cm⁻¹. **MS** (ESI) *m/z* (relative intensity): 514 (70) [M+H]⁺, 536 (100) [M+Na]⁺. **HR-MS** (ESI): *m/z* calcd. for C₂₇H₃₅¹⁰B₂¹¹B₈NO₂Na [M+Na]⁺: 536.3576, found: 536.3557.

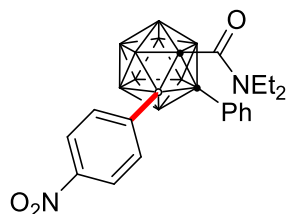


152g. The representative procedure **H** was followed using *o*-carborane **151e** (1-CONEt₂-2-*n*Bu-*o*-C₂B₁₀H₁₀) (60 mg, 0.20 mmol) and 4-iodotoluene **19a** (105 mg, 0.48 mmol). Isolation by column chromatography (*n*-hexane/EtOAc: 20/1) yielded **152g** (45 mg, 47%) as a colorless solid. **M.p.** = 88–89 °C. **¹H NMR** (400 MHz, CDCl₃): δ = 7.39 (d, *J* = 7.9 Hz, 2H), 7.17 (d, *J* = 7.8 Hz, 2H), 7.12 (d, *J* = 7.9 Hz, 2H), 6.99 (d, *J* = 7.8 Hz, 2H), 4.15–3.66 (m, 2H), 3.66–3.46 (m, 2H), 2.56–2.46 (m, 1H), 2.38 (s, 3H), 2.30 (s, 3H), 2.29–2.18 (m, 1H), 1.66–1.56 (m, 1H), 1.54–1.42 (m, 1H), 1.35–1.19 (m, 8H), 0.91 (t, *J* = 7.3 Hz, 3H). **¹³C NMR** (100 MHz, CDCl₃): δ = 156.3 (C_q), 137.9 (C_q), 137.8 (C_q), 134.8 (CH), 133.3 (CH), 128.6 (CH), 127.7 (CH), 83.6 (C_q), 73.6 (C_q), 44.2 (CH₂), 34.5 (CH₂), 32.0 (CH₂), 22.4 (CH₂), 21.4 (CH₃), 21.3 (CH₃), 13.8 (CH₃), 13.1 (CH₃). **¹¹B NMR** (128 MHz, CDCl₃): δ = 2.34 (2B), -1.13 (2B), -2.77 (1B), -7.74 (1B), -10.36 (2B), -12.42 (1B), -13.91 (1B). **IR** (ATR): 2951, 2867, 2568, 1647, 1419, 1265, 809 cm⁻¹. **MS** (ESI) *m/z*

(relative intensity): 480 (100) $[M+H]^+$, 502 (20) $[M+Na]^+$. **HR-MS** (ESI): m/z calcd. for $C_{25}H_{42}^{10}B_2^{11}B_8NO$ $[M+H]^+$: 480.4276, found: 480.4272.

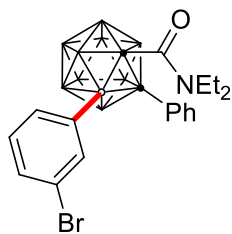


153a. The representative procedure I was followed using *o*-carborane **149a** (1- $CONEt_2$ -2-Ph-*o*- $C_2B_{10}H_{10}$) (64 mg, 0.20 mmol) and 4-iodotoluene **19a** (53 mg, 0.24 mmol). Isolation by column chromatography (*n*-hexane/EtOAc: 20/1) yielded **153a** (45 mg, 55%) as a colorless solid. **M.p.** = 180–181 °C. **1H NMR** (400 MHz, $CDCl_3$): δ = 7.45–7.39 (m, 4H), 7.28–7.22 (m, 1H), 7.16–7.05 (m, 4H), 3.55–3.35 (m, 4H), 2.34 (s, 3H), 1.00 (t, J = 7.1 Hz, 6H). **^{13}C NMR** (100 MHz, $CDCl_3$): δ = 158.3 (C_q), 139.1 (C_q), 134.6 (CH), 134.0 (C_q), 131.9 (CH), 129.2 (CH), 128.5 (CH), 127.0 (CH), 89.5 (C_q), 82.4 (C_q), 43.6 (CH_2), 21.3 (CH_3), 12.2 (CH_3). **^{11}B NMR** (128 MHz, $CDCl_3$): δ = -1.0 (1B), -2.26 (1B), -3.69 (1B), -7.91 (3B), -10.32 (4B). **IR** (ATR): 2635, 2563, 1648, 1476, 1418, 1269, 1208, 1080, 689 cm^{-1} . **MS** (ESI) m/z (relative intensity): 432 (100) $[M+Na]^+$, 410 (10) $[M+H]^+$. **HR-MS** (ESI): m/z calcd. for $C_{20}H_{31}^{10}B_2^{11}B_8NONa$ $[M+Na]^+$: 432.3311, found: 432.3304.

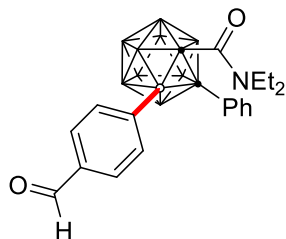


153b. The representative procedure I was followed using *o*-carborane **149a** (1- $CONEt_2$ -2-Ph-*o*- $C_2B_{10}H_{10}$) (64 mg, 0.20 mmol) and 1-iodo-4-nitrobenzene **19h** (60 mg, 0.24 mmol). Isolation by column chromatography (*n*-hexane/EtOAc: 20/1) yielded **153b** (54 mg, 61%) as a colorless solid. **M.p.** = 147–148 °C. **1H NMR** (300 MHz, $CDCl_3$): δ = 8.14 (d, J = 8.7 Hz, 2H), 7.78 (d, J = 8.7 Hz, 2H), 7.41–7.30 (m, 3H), 7.22–7.16 (m, 2H), 3.43–3.32 (m, 4H), 1.03 (t, J = 7.0 Hz, 6H). **^{13}C NMR** (75 MHz, $CDCl_3$): δ = 158.0 (C_q), 148.3 (C_q), 135.5 (CH), 133.5 (C_q), 131.4 (CH), 129.8 (CH), 127.6 (CH), 122.3 (CH), 90.8 (C_q), 83.0 (C_q), 43.7 (CH_2), 14.0 (CH_3). **^{11}B NMR** (96 MHz, $CDCl_3$): δ = -0.10 (2B), -3.09 (2B), -7.61 (3B), -8.98 (2B), -10.71 (1B). **IR** (ATR): 2980, 2561, 1647, 1513, 1346, 1265, 1208, 843, 687 cm^{-1} . **MS** (ESI) m/z (relative intensity): 463 (100) $[M+Na]^+$, 441 (10) $[M+H]^+$.

$[M+H]^+$. **HR-MS** (ESI): m/z calcd. for $C_{19}H_{28}^{10}B_2^{11}B_8N_2O_3Na$ $[M+Na]^+$: 463.3005, found: 463.2995.



153c. The representative procedure **I** was followed using *o*-carborane **149a** (1-CONEt₂-2-Ph-*o*-C₂B₁₀H₁₀) (64 mg, 0.20 mmol) and 1-iodo-3-bromobenzene **19i** (60 mg, 0.24 mmol). Isolation by column chromatography (*n*-hexane/EtOAc: 20/1) yielded **153c** (47.3 mg, 50%) as a colorless solid. **M.p.** = 168–169 °C. **¹H NMR** (400 MHz, CDCl₃): δ = 7.66–7.61 (m, 1H), 7.52–7.45 (m, 2H), 7.40–7.35 (m, 2H), 7.31–7.23 (m, 1H), 7.17–7.09 (m, 3H), 3.36–3.10 (m, 4H), 1.01 (t, J = 7.2 Hz, 6H). **¹³C NMR** (100 MHz, CDCl₃): δ = 158.0 (C_q), 137.1 (CH), 133.8 (C_q), 133.2 (CH), 132.3 (CH), 131.8 (CH), 129.5 (CH), 129.4 (CH), 127.3 (CH), 122.5 (C_q), 90.5 (C_q), 82.8 (C_q), 44.1 (CH₂), 43.7 (CH₂), 14.0 (CH₃), 12.2 (CH₃). **¹¹B NMR** (128 MHz, CDCl₃): δ = -0.49 (2B), -3.35 (2B), -7.81 (3B), -9.66 (3B). **IR** (ATR): 2976, 2575, 1645, 1420, 1266, 1156, 770, 689 cm⁻¹. **MS** (ESI) m/z (relative intensity): 497 (100) $[M+Na]^+$, 475 (20) $[M+H]^+$. **HR-MS** (ESI) m/z calcd for $C_{19}H_{28}^{10}B_1^{11}B_9^{79}BrNONa$ $[M+Na]^+$: 497.2220, found 497.2229.

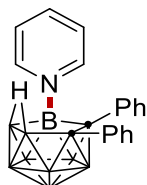


153d. The representative procedure **I** was followed using *o*-carborane **149a** (1-CONEt₂-2-Ph-*o*-C₂B₁₀H₁₀) (64 mg, 0.20 mmol) and 4-iodobenzaldehyde **19j** (56 mg, 0.24 mmol). Isolation by column chromatography (*n*-hexane/EtOAc: 20/1) yielded **153d** (43 mg, 51%) as a colorless solid. **M.p.** = 211–212 °C. **¹H NMR** (300 MHz, CDCl₃): δ = 10.07 (s, 1H), 7.88–7.70 (m, 4H), 7.44–7.37 (m, 2H), 7.35–7.29 (m, 1H), 7.20–7.11 (m, 2H), 3.43–3.30 (m, 4H), 1.03 (t, J = 7.0 Hz, 6H). **¹³C NMR** (75 MHz, CDCl₃): δ = 192.3 (CH), 158.0 (C_q), 136.3 (C_q), 135.3 (CH), 133.7 (C_q), 131.8 (CH), 129.7 (CH), 128.5 (CH), 127.2 (CH), 90.8 (C_q), 83.0 (C_q), 43.7 (CH₂), 13.2 (CH₃). **¹¹B NMR** (96 MHz, CDCl₃): δ = -0.28 (2B), -3.35 (2B), -7.51 (3B), -9.39 (2B), -11.02 (1B). **IR** (ATR): 2980,

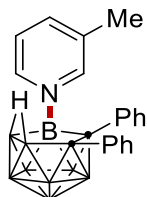
2560, 1719, 1650, 1627, 1420, 1266, 1181, 761, 688 cm^{-1} . **MS** (ESI) m/z (relative intensity): 424 (100) $[\text{M}+\text{H}]^+$. **HR-MS** (ESI): m/z calcd. for $\text{C}_{20}\text{H}_{30}^{10}\text{B}_2^{11}\text{B}_8\text{NO}_2$ $[\text{M}+\text{H}]^+$: 424.3284, found: 424.3266.

5.3.5 Electrochemical B–H Nitrogenation of *nido*-Carboranes

5.3.5.1 Characterization Data

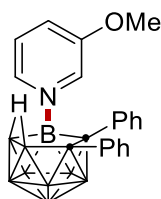


156a. The representative procedure **J** was followed using *nido*-carborane **154a** (36.0 mg, 0.10 mmol) and pyridine **155a** (24.0 mg, 0.30 mmol). Isolation by column chromatography (*n*-hexane/ CH_2Cl_2 : 1/1) yielded **156a** (30.0 mg, 83%) as a colorless solid. **M.p.** = 280 – 282 °C. **^1H NMR** (300 MHz, CD_2Cl_2): δ = 8.75 (d, J = 5.2 Hz, 2H), 8.07 (tt, J = 7.7, 1.5 Hz, 1H), 7.56 – 7.48 (m, 2H), 7.35 – 7.28 (m, 2H), 7.08 – 6.96 (m, 3H), 6.94 – 6.82 (m, 5H), -1.97 (s, 1H). **^{13}C NMR** (101 MHz, CD_2Cl_2): δ = 147.7 (CH), 142.4 (CH), 138.7 (C_q), 136.2 (C_q), 132.1 (CH), 131.1 (CH), 127.5 (CH), 127.1 (CH), 126.6 (CH), 126.3 (CH), 125.8 (CH). **^{11}B NMR** (96 MHz, CD_2Cl_2): δ = 4.92 (1B), -3.89 (1B), -11.50 (1B), -15.73 (2B), -20.65 (1B), -26.08 (1B), -30.97 (1B), -35.87 (1B). **IR** (ATR): 2558, 2536, 2510, 1486, 1456, 1445, 1171, 764, 698 cm^{-1} . **MS** (ESI) m/z (relative intensity): 387 (100) $[\text{M}+\text{Na}]^+$, 365 (20) $[\text{M}+\text{H}]^+$. **HR-MS** (ESI): m/z calcd. for $\text{C}_{19}\text{H}_{24}^{10}\text{B}_1^{11}\text{B}_8\text{N}$ $[\text{M}+\text{Na}]^+$: 387.2688, found: 387.2680. The analytical data corresponds with those reported in the literature.^[225]

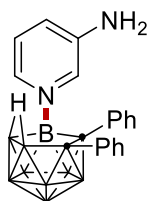


156b. The representative procedure **J** was followed using *nido*-carborane **154a** (36.0 mg, 0.10 mmol) and 3-methylpyridine **155b** (27.9 mg, 0.30 mmol). Isolation by column chromatography (*n*-hexane/ CH_2Cl_2 : 1/1) yielded **156b** (26.0 mg, 68%) as a white solid. **M.p.** = 280 – 283 °C. **^1H NMR** (500 MHz, CDCl_3): δ = 8.54 (d, J = 6.1 Hz, 1H), 8.45 (s, 1H), 7.76 (d, J = 7.7 Hz, 1H), 7.32 (dd, J = 7.9, 5.9 Hz, 1H), 7.28 – 7.24 (m, 2H), 7.00 – 6.87 (m, 3H), 6.86 – 6.77 (m, 5H),

2.27 (s, 3H), -2.08 (s, 1H). $^{13}\text{C NMR}$ (126 MHz, CDCl_3): δ = 147.5 (CH), 144.9 (CH), 142.4 (CH), 138.5 (C_q), 136.4 (C_q), 136.4 (C_q), 132.1 (CH), 131.1 (CH), 127.4 (CH), 127.1 (CH), 126.6 (CH), 126.2 (CH), 124.9 (CH), 18.5 (CH_3). $^{11}\text{B NMR}$ (128 MHz, CDCl_3): δ = 4.46 (1B), -4.56 (1B), -11.28 (1B), -15.95 (2B), -21.01 (1B), -26.04 (1B), -30.94 (1B), -35.69 (1B). **IR** (ATR): 3059, 1487, 1443, 1201, 1155, 1056, 907, 734, 696 cm^{-1} . **MS** (ESI) m/z (relative intensity): 401 (90) $[\text{M}+\text{Na}]^+$, 379 (20) $[\text{M}+\text{H}]^+$. **HR-MS** (ESI): m/z calcd. for $\text{C}_{20}\text{H}_{26}^{10}\text{B}_1^{11}\text{B}_8\text{N}$ $[\text{M}+\text{Na}]^+$: 401.2845, found: 401.2850. The analytical data corresponds with those reported in the literature.^[225]

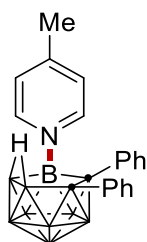


156c. The representative procedure **J** was followed using *nido*-carborane **154a** (36.0 mg, 0.10 mmol) and 3-methoxypyridine **155c** (32.0 mg, 0.30 mmol). Isolation by column chromatography (*n*-hexane/ CH_2Cl_2 : 1/1) yielded **156c** (30.0 mg, 75%) as a yellow solid. **M.p.** = 220 – 223 °C. $^1\text{H NMR}$ (500 MHz, CD_2Cl_2): δ = 8.47 (d, J = 5.8 Hz, 1H), 8.13 (d, J = 2.7 Hz, 1H), 7.51 (ddd, J = 8.7, 2.7, 1.1 Hz, 1H), 7.40 (dd, J = 8.7, 5.8 Hz, 1H), 7.28 – 7.25 (m, 2H), 6.99 – 6.93 (m, 3H), 6.91 – 6.83 (m, 5H), 3.65 (s, 3H), -2.01 (s, 1H). $^{13}\text{C NMR}$ (126 MHz, CD_2Cl_2): δ = 157.1 (C_q), 140.8 (CH), 139.0 (C_q), 136.7 (C_q), 134.7 (CH), 132.4 (CH), 131.5 (CH), 128.2 (CH), 127.8 (CH), 127.4 (CH), 127.0 (CH), 126.6 (CH), 126.3 (CH), 56.8 (CH_3). $^{11}\text{B NMR}$ (128 MHz, CD_2Cl_2): δ = 4.82 (1B), -4.05 (1B), -11.74 (1B), -15.83 (2B), -20.58 (1B), -26.13 (1B), -31.13 (1B), -35.90 (1B). **IR** (ATR): 2526, 1572, 1487, 1443, 1298, 1259, 1056, 881, 693 cm^{-1} . **MS** (ESI) m/z (relative intensity): 417 (100) $[\text{M}+\text{Na}]^+$, 395 (20) $[\text{M}+\text{H}]^+$. **HR-MS** (ESI): m/z calcd. for $\text{C}_{20}\text{H}_{26}^{10}\text{B}_1^{11}\text{B}_8\text{NO}$ $[\text{M}+\text{Na}]^+$: 417.2794, found: 417.2796. The analytical data corresponds with those reported in the literature.^[225]

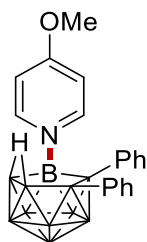


156d. The representative procedure **J** was followed using *nido*-carborane **154a** (36.0 mg, 0.10 mmol) and pyridin-3-amine **155d** (28.2 mg, 0.30 mmol). Isolation by column chromatography (*n*-hexane/ CH_2Cl_2 : 1/1) yielded **156d** (30.0 mg, 79%) as a yellow solid. **M.p.** = 250 – 253 °C. $^1\text{H NMR}$ (500 MHz, CD_2Cl_2): δ = 8.07 (d, J = 2.4 Hz, 1H), 8.04 (d, J = 5.1 Hz, 1H), 7.29 – 7.24

(m, 2H), 7.20 – 7.14 (m, 2H), 6.99 – 6.92 (m, 3H), 6.88 – 6.82 (m, 5H), 4.13 (s, 2H), -2.00 (s, 1H). ^{13}C NMR (126 MHz, CD_2Cl_2): δ = 145.0 (C_q), 139.1 (C_q), 137.8 (CH), 136.8 (C_q), 134.2 (CH), 132.4 (CH), 131.3 (CH), 127.5 (CH), 127.3 (overlapped, CH), 126.8 (CH), 126.5 (CH), 126.0 (CH). ^{11}B NMR (128 MHz, CD_2Cl_2): δ = 4.99 (1B), -4.38 (1B), -12.03 (1B), -15.78 (2B), -21.02 (1B), -26.20 (1B), -31.14 (1B), -36.05 (1B). IR (ATR): 3480, 3388, 2539, 1623, 1583, 1442, 1164, 697 cm^{-1} . MS (ESI) m/z (relative intensity): 402 (100) $[\text{M}+\text{Na}]^+$, 380 (50) $[\text{M}+\text{H}]^+$. HR-MS (ESI): m/z calcd. for $\text{C}_{19}\text{H}_{25}^{10}\text{B}_1^{11}\text{B}_8\text{N}_2$ $[\text{M}+\text{Na}]^+$: 402.2797, found: 402.2796. The analytical data corresponds with those reported in the literature.^[225]

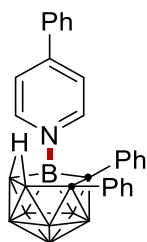


156e. The representative procedure **J** was followed using *nido*-carborane **154a** (36.0 mg, 0.10 mmol) and 4-methylpyridine **155e** (27.9 mg, 0.30 mmol). Isolation by column chromatography (*n*-hexane/ CH_2Cl_2 : 1/1) yielded **156e** (33.0 mg, 87%) as a white solid. **M.p.** = 247 – 250 °C. ^1H NMR (500 MHz, CDCl_3): δ = 8.52 (d, J = 6.6 Hz, 2H), 7.26 – 7.24 (m, 1H), 7.24 – 7.23 (m, 1H), 7.21 (d, J = 7.5 Hz, 2H), 6.95 – 6.88 (m, 3H), 6.85 – 6.77 (m, 5H), 2.45 (s, 3H), -2.06 (s, 1H). ^{13}C NMR (126 MHz, CDCl_3): δ = 155.4 (C_q), 146.9 (CH), 138.5 (C_q), 136.5 (C_q), 132.1 (CH), 131.1 (CH), 127.1 (CH), 127.1 (CH), 126.6 (CH), 126.2 (overlapped, CH), 21.7 (CH_3). ^{11}B NMR (128 MHz, CDCl_3): δ = 4.43 (1B), -3.98 (1B), -11.46 (1B), -15.82 (2B), -20.70 (1B), -26.00 (1B), -30.91 (1B), -35.77 (1B). IR (ATR): 3058, 2540, 2159, 1495, 1444, 761, 697 cm^{-1} . MS (ESI) m/z (relative intensity): 401 (100) $[\text{M}+\text{Na}]^+$, 479 (20) $[\text{M}+\text{H}]^+$. HR-MS (ESI): m/z calcd. for $\text{C}_{20}\text{H}_{26}^{10}\text{B}_1^{11}\text{B}_8\text{N}$ $[\text{M}+\text{Na}]^+$: 401.2845, found: 401.2842. The analytical data corresponds with those reported in the literature.^[225]

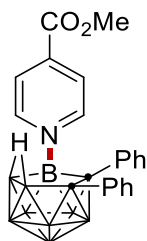


156f. The representative procedure **J** was followed using *nido*-carborane **154a** (36.0 mg, 0.10

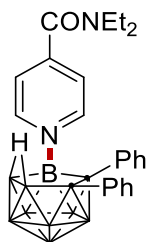
mmol) and 4-methoxypyridine **155f** (32.7 mg, 0.30 mmol). Isolation by column chromatography (*n*-hexane/CH₂Cl₂: 1/1) yielded **156f** (32.0 mg, 81%) as a white solid. **M.p.** = 314 – 317 °C. **¹H NMR** (500 MHz, CD₂Cl₂): δ = 8.49 (d, *J* = 7.5 Hz, 2H), 7.27 (d, *J* = 6.6 Hz, 2H), 7.00 – 6.93 (m, 3H), 6.89 – 6.82 (m, 7H), 3.92 (s, 3H), -2.02 (s, 1H). **¹³C NMR** (126 MHz, CD₂Cl₂): δ = 169.8 (C_q), 149.5 (CH), 139.1 (C_q), 136.8 (C_q), 132.4 (CH), 131.4 (CH), 127.6 (CH), 127.3 (CH), 126.8 (CH), 126.5 (CH), 111.5 (CH), 57.3 (CH₃). **¹¹B NMR** (128 MHz, CD₂Cl₂): δ = 4.80 (1B), -3.95 (1B), -11.52(1B), -15.65 (2B), -20.30 (1B), -25.96 (1B), -30.82 (1B), -35.66 (1B). **IR** (ATR): 2570, 2525, 1631, 1516, 1319, 1162, 1005, 847 cm⁻¹ **MS** (ESI) *m/z* (relative intensity): 417 (100) [M+Na]⁺, 395 (20) [M+H]⁺. **HR-MS** (ESI): *m/z* calcd. for C₂₀H₂₆¹⁰B₁¹¹B₈NO [M+Na]⁺: 417.2794, found: 417.2794. The analytical data corresponds with those reported in the literature.^[225]



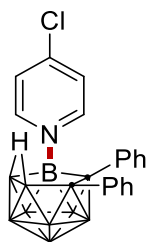
156g. The representative procedure **J** was followed using *nido*-carborane **154a** (36.0 mg, 0.10 mmol) and 4-phenylpyridine **155g** (46.5 mg, 0.30 mmol). Isolation by column chromatography (*n*-hexane/CH₂Cl₂: 1/1) yielded **156g** (43.2 mg, 98%) as a yellow solid. **M.p.** = 242 – 245 °C. **¹H NMR** (500 MHz, CD₂Cl₂): δ = 8.67 (d, *J* = 7.0 Hz, 2H), 7.68 – 7.65 (m, 4H), 7.58 – 7.53 (m, 3H), 7.31 – 7.27 (m, 2H), 7.01 – 6.95 (m, 3H), 6.93 – 6.89 (m, 2H), 6.87 – 6.83 (m, 3H), -1.91 (s, 1H). **¹³C NMR** (126 MHz, CD₂Cl₂): δ = 154.4 (C_q), 147.8 (CH), 139.1 (C_q), 136.6 (C_q), 134.6 (C_q), 132.4 (CH), 131.9 (CH), 131.5 (CH), 129.9 (CH), 127.8 (CH), 127.7 (CH), 127.4 (CH), 126.9 (CH), 126.6 (CH), 123.1 (CH). **¹¹B NMR** (128 MHz, CDCl₃): δ = 6.28 (1B), -0.08 (1B), -7.92 (1B), -10.65 (2B), -16.32 (1B), -20.79 (1B), -26.45 (1B), -31.72 (1B). **IR** (ATR): 2532, 1626, 1486, 1431, 1219, 1172, 1013, 763, 698 cm⁻¹. **MS** (ESI) *m/z* (relative intensity): 463 (100) [M+Na]⁺, 441 (50) [M+H]⁺. **HR-MS** (ESI): *m/z* calcd. for C₂₅H₂₈¹⁰B₁¹¹B₈N [M+Na]⁺: 463.3005, found: 463.2997. The analytical data corresponds with those reported in the literature.^[225]



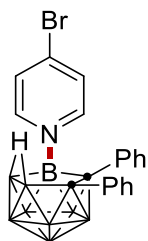
156h. The representative procedure **J** was followed using *nido*-carborane **154a** (36.0 mg, 0.10 mmol) and methyl isonicotinate **155h** (41.0 mg, 0.30 mmol). Isolation by column chromatography (*n*-hexane/CH₂Cl₂: 1/1) yielded **156h** (29.0 mg, 69%) as a colorless solid. **M.p.** = 242 – 246 °C. **¹H NMR** (300 MHz, CD₂Cl₂): δ = 8.84 (d, *J* = 6.9 Hz, 2H), 8.00 (d, *J* = 7.0 Hz, 2H), 7.34 – 7.28 (m, 2H), 7.06 – 6.97 (m, 3H), 6.94 – 6.87 (m, 5H), 4.00 (s, 3H), -1.89 (s, 1H). **¹³C NMR** (101 MHz, CD₂Cl₂): δ = 162.5 (C_q), 148.4 (CH), 142.2(C_q), 138.6(C_q), 135.9(C_q), 132.1 (CH), 131.2 (CH), 127.7 (CH), 127.1 (CH), 126.9 (CH), 126.4 (CH), 125.2 (CH), 53.7 (CH₃). **¹¹B NMR** (128 MHz, CD₂Cl₂): δ = 4.45 (1B), -3.67 (1B), -11.05 (1B), -15.83 (2B), -20.08 (1B), -26.03 (1B), -30.77 (1B), -35.42 (1B). **IR** (ATR): 2529, 1743, 1440, 1427, 1289, 1112, 767, 690 cm⁻¹. **MS** (ESI) *m/z* (relative intensity): 445 (100) [M+Na]⁺, 423 (20) [M+H]⁺. **HR-MS** (ESI): *m/z* calcd. for C₂₁H₂₆¹⁰B₁¹¹B₈NO₂ [M+H]⁺: 423.2925, found: 423.2897. The analytical data corresponds with those reported in the literature.^[225]



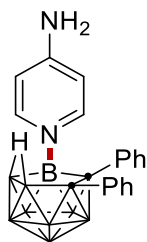
156i. The representative procedure **J** was followed using *nido*-carborane **154a** (36.0 mg, 0.10 mmol) and *N,N*-diethylisonicotinamide **155i** (53.4 mg, 0.30 mmol). Isolation by column chromatography (CH₂Cl₂) yielded **156i** (24.0 mg, 51%) as a yellow solid. **M.p.** = 251 – 254 °C. **¹H NMR** (400 MHz, CD₂Cl₂): δ = 8.72 (d, *J* = 6.8 Hz, 2H), 7.41 – 7.34 (m, 2H), 7.31 – 7.23 (m, 2H), 7.00 – 6.91 (m, 3H), 6.89 – 6.80 (m, 5H), 3.47 (q, *J* = 7.1 Hz, 2H), 2.99 (q, *J* = 7.1 Hz, 2H), 1.19 (t, *J* = 7.2 Hz, 3H), 1.02 (t, *J* = 7.1 Hz, 3H), -2.00 (s, 1H). **¹³C NMR** (101 MHz, CD₂Cl₂): δ = 165.4 (C_q), 150.9 (C_q), 148.4 (CH), 138.9 (C_q), 136.4 (C_q), 132.4 (CH), 131.5(CH), 127.9 (CH), 127.4 (CH), 127.1 (CH), 126.7 (CH), 123.3 (CH), 43.4 (CH₂), 39.9 (CH₂), 14.2 (CH₃), 12.7 (CH₃). **¹¹B NMR** (128 MHz, CD₂Cl₂): δ = 4.59 (1B), -3.84 (1B), -11.22 (1B), -15.78 (2B), -20.43 (1B), -26.04 (1B), -30.87 (1B), -35.68 (1B). **IR** (ATR): 2530, 2223, 2177, 2035, 1991, 1628, 1053, 696 cm⁻¹. **MS** (ESI) *m/z* (relative intensity): 486 (50) [M+Na]⁺, 464 (100) [M+H]⁺. **HR-MS** (ESI): *m/z* calcd. for C₂₄H₃₃¹⁰B₁¹¹B₈N₂O [M+Na]⁺: 486.3375, found: 486.3392.



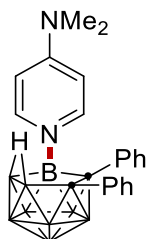
156j. The representative procedure **J** was followed using *nido*-carborane **154a** (36.0 mg, 0.10 mmol) and 4-chloropyridine hydrochloride **155j** (45.0 mg, 0.30 mmol). Isolation by column chromatography (*n*-hexane/CH₂Cl₂: 3/1) yielded **156j** (20.0 mg, 53%) as a yellow solid. **M.p.** = 232 – 234 °C. **¹H NMR** (300 MHz, CDCl₃): δ = 8.62 (d, *J* = 7.0 Hz, 2H), 7.44 (d, *J* = 7.1 Hz, 2H), 7.31 – 7.29 (m, 1H), 7.28 – 7.26 (m, 1H), 7.02 – 6.94 (m, 3H), 6.91 – 6.85 (m, 5H), -2.09 (s, 1H). **¹³C NMR** (101 MHz, CDCl₃): δ = 151.3 (C_q), 148.1 (CH), 138.4 (C_q), 136.1 (C_q), 132.04 (CH), 131.2 (CH), 127.7 (CH), 127.2 (CH), 126.9 (CH), 126.4 (CH), 126.1 (CH). **¹¹B NMR** (128 MHz, CDCl₃): δ = 4.15 (1B), -3.56 (1B), -10.88 (1B), -15.95 (2B), -20.21 (1B), -25.97 (1B), -30.85 (1B), -35.56 (1B). **IR** (ATR): 3112, 2538, 1615, 1487, 1433, 1115, 1055, 696 cm⁻¹. **MS** (ESI) *m/z* (relative intensity): 421 (100) [M+Na]⁺, 399 (20) [M+H]⁺. **HR-MS** (ESI): *m/z* calcd. for C₁₉H₂₃¹⁰B₁¹¹B₈³⁵ClN [M+Na]⁺: 421.2303, found: 421.2298. The analytical data corresponds with those reported in the literature.^[225]



156k. The representative procedure **J** was followed using *nido*-carborane **154a** (36.0 mg, 0.10 mmol) and 4-bromopyridine hydrochloride **155k** (58.2 mg, 0.30 mmol). Isolation by column chromatography (*n*-hexane/CH₂Cl₂: 3/1) yielded **156k** (21.0 mg, 45%) as a yellow solid. **M.p.** = 233 – 236 °C. **¹H NMR** (500 MHz, CD₂Cl₂): δ = 8.46 (d, *J* = 7.0 Hz, 2H), 7.65 – 7.61 (m, 2H), 7.28 – 7.24 (m, 2H), 7.02 – 6.92 (m, 4H), 6.88 – 6.86 (m, 4H), -2.05 (s, 1H). **¹³C NMR** (126 MHz, CD₂Cl₂): δ = 147.9 (CH), 141.1 (C_q), 138.9 (C_q), 136.2 (C_q), 132.4 (CH), 131.5 (CH), 129.7 (CH), 128.0 (CH), 127.4 (CH), 127.2 (CH), 126.7 (CH). **¹¹B NMR** (128 MHz, CD₂Cl₂): δ = 4.35 (1B), -3.85 (1B), -11.36 (1B), -15.88 (2B), -20.30 (1B), -26.02 (1B), -30.90 (1B), -35.68 (1B). **IR** (ATR): 2923, 2852, 2149, 2030, 1974, 1723, 1459, 697 cm⁻¹. **MS** (ESI) *m/z* (relative intensity): 465 (100) [M+Na]⁺. **HR-MS** (ESI) *m/z* calcd for C₁₉H₂₃¹⁰B₁¹¹B₈⁷⁹BrN [M+Na]⁺ 465.1808, found 465.1807. The analytical data corresponds with those reported in the literature.^[225]

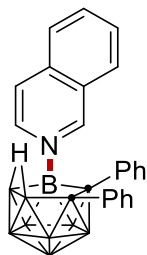


156l. The representative procedure **J** was followed using *nido*-carborane **154a** (36.0 mg, 0.10 mmol) and pyridin-4-amine **155l** (28.0 mg, 0.30 mmol). Isolation by column chromatography (*n*-hexane/CH₂Cl₂: 1/1) yielded **156l** (37.0 mg, 97%) as a colorless solid. **M.p.** = 293 – 296 °C. **¹H NMR** (400 MHz, Acetone-*d*₆): δ = 8.32 – 8.23 (m, 2H), 7.35 – 7.26 (m, 2H), 7.10 (s, 2H), 7.02 – 6.88 (m, 5H), 6.85 – 6.75 (m, 3H), 6.72 – 6.64 (m, 2H), -1.84 (s, 1H). **¹³C NMR** (101 MHz, Acetone-*d*₆): δ = 158.0 (C_q), 147.7 (CH), 139.4 (C_q), 137.4 (C_q), 132.2 (CH), 131.2 (CH), 126.8 (CH), 126.0 (CH), 125.9 (CH), 108.7 (CH), 108.6 (CH). **¹¹B NMR** (96 MHz, Acetone-*d*₆): δ = 5.24 (1B), -5.39 (1B), -13.34 (1B), -15.81 (2B), -22.06 (1B), -26.12 (1B), -31.54 (1B), -36.82 (1B). **IR** (ATR): 3475, 3375, 2538, 1644, 1527, 1182, 831, 694 cm⁻¹. **MS** (ESI) *m/z* (relative intensity): 402 (100) [M+Na]⁺, 380 (30) [M+H]⁺. **HR-MS** (ESI): *m/z* calcd. for C₁₉H₂₅¹⁰B₁¹¹B₈N [M+Na]⁺: 402.2797, found: 402.2792. The analytical data corresponds with those reported in the literature.^[225]

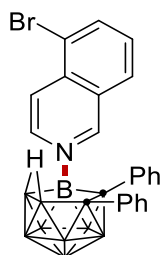


156m. The representative procedure **J** was followed using *nido*-carborane **154a** (36.0 mg, 0.10 mmol) and *N,N*-dimethylpyridin-4-amine **155m** (37.0 mg, 0.30 mmol). Isolation by column chromatography (*n*-hexane/CH₂Cl₂: 1/1) yielded **156m** (21.0 mg, 52%) as a colorless solid. **M.p.** = 336 – 338 °C. **¹H NMR** (300 MHz, DMSO-*d*₆): δ = 8.29 (d, *J* = 7.1 Hz, 2H), 7.30 (d, *J* = 6.4 Hz, 2H), 7.02 – 6.90 (m, 5H), 6.83 – 6.75 (m, 3H), 6.70 (d, *J* = 7.4 Hz, 2H), 3.05 (s, 6H), -1.56 (s, 1H). **¹³C NMR** (101 MHz, DMSO-*d*₆): δ = 155.7 (C_q), 147.0 (CH), 139.4 (C_q), 137.3 (C_q), 132.5 (CH), 131.4 (CH), 127.3 (CH), 127.2 (CH), 126.6 (CH), 126.5 (CH), 106.9 (CH), 39.8 (CH₃). **¹¹B NMR** (128 MHz, DMSO-*d*₆): δ = 5.14 (1B), -6.22 (1B), -15.59 (3B), -21.95 (1B), -26.05 (1B), -31.52 (1B), -37.12 (1B). **IR** (ATR): 2554, 2528, 2502, 1643, 1565, 1441, 1166, 820, 696 cm⁻¹. **MS** (ESI) *m/z* (relative intensity): 430 (100) [M+Na]⁺, 408 (30) [M+H]⁺. **HR-MS** (ESI): *m/z* calcd.

for $C_{21}H_{29}^{10}B_1^{11}B_8N_2$ $[M+Na]^+$: 430.3111, found: 430.3110.

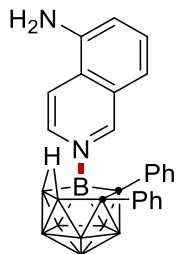


156n. The representative procedure **J** was followed using *nido*-carborane **154a** (36.0 mg, 0.10 mmol) and isoquinoline **155n** (39.0 mg, 0.30 mmol). Isolation by column chromatography (*n*-hexane/ CH_2Cl_2 : 1/1) yielded **156n** (38.0 mg, 92%) as a yellow solid. **M.p.** = 280 – 282 °C. **1H NMR** (300 MHz, CD_2Cl_2): δ = 9.35 (s, 1H), 8.56 (dd, J = 6.8, 1.0 Hz, 1H), 8.03 – 7.96 (m, 3H), 7.87 – 7.81 (m, 2H), 7.37 – 7.32 (m, 2H), 7.06 – 6.99 (m, 3H), 6.97 – 6.93 (m, 2H), 6.85 – 6.78 (m, 3H), -1.85 (s, 1H). **^{13}C NMR** (101 MHz, CD_2Cl_2): δ = 151.9 (CH), 139.1 (C_q), 139.0 (CH), 136.9 (C_q), 136.7 (C_q), 135.9 (CH), 132.5 (CH), 131.5 (CH), 130.7 (CH), 129.8 (CH), 127.7 (CH), 127.6 (C_q), 127.4 (CH), 126.9 (CH), 126.9 (CH), 126.6 (CH), 123.6 (CH). **^{11}B NMR** (128 MHz, CD_2Cl_2): δ = 4.98 (1B), -4.07 (1B), -11.80 (1B), -15.78 (2B), -20.56 (1B), -26.09 (1B), -31.06 (1B), -35.86 (1B). **IR** (ATR): 3376, 2544, 1644, 1598, 1494, 1443, 1179, 697 cm^{-1} . **MS** (ESI) m/z (relative intensity): 437 (100) $[M+Na]^+$, 415 (30) $[M+H]^+$. **HR-MS** (ESI): m/z calcd. for $C_{23}H_{26}^{10}B_1^{11}B_8N$ $[M+Na]^+$: 437.2847, found: 437.2849.

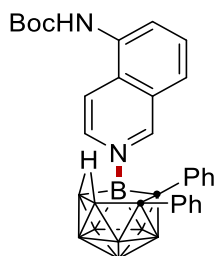


156o. The representative procedure **J** was followed using *nido*-carborane **154a** (36.0 mg, 0.10 mmol) and 5-bromoisoquinoline **155o** (62.0 mg, 0.30 mmol). Isolation by column chromatography (*n*-hexane/ CH_2Cl_2 : 1/1) yielded **156o** (31.0 mg, 63%) as a yellow solid. **M.p.** = 280 – 283 °C. **1H NMR** (400 MHz, CD_2Cl_2): δ = 9.30 – 9.23 (m, 1H), 8.70 – 8.59 (m, 1H), 8.32 – 8.21 (m, 1H), 8.18 – 8.11 (m, 1H), 7.95 – 7.88 (m, 1H), 7.74 – 7.63 (m, 1H), 7.37 – 7.28 (m, 2H), 7.04 – 6.97 (m, 3H), 6.96 – 6.91 (m, 2H), 6.87 – 6.79 (m, 3H), -1.84 (s, 1H). **^{13}C NMR** (101 MHz, CD_2Cl_2): δ = 151.5 (CH), 139.9 (CH), 139.0 (CH), 138.7 (C_q), 136.2 (C_q), 135.8 (C_q), 132.1 (CH), 131.3 (CH), 131.0 (CH), 129.3 (CH), 128.4 (C_q), 127.6 (CH), 127.1 (CH), 126.8 (CH), 126.3 (CH), 122.7 (CH), 121.5 (C_q). **^{11}B NMR** (96 MHz, CD_2Cl_2): δ = 4.90 (1B), -3.78 (1B), -11.27 (1B), -

15.75 (2B), -20.22 (1B), -26.03 (1B), -31.02 (1B), -35.73 (1B). **IR** (ATR): 2923, 2543, 1637, 1595, 1490, 1443, 1215, 748, 698 cm^{-1} . **MS** (ESI) m/z (relative intensity): 516 (100) $[\text{M}+\text{Na}]^+$, 494 (30) $[\text{M}+\text{H}]^+$. **HR-MS** (ESI): m/z calcd. for $\text{C}_{23}\text{H}_{25}^{11}\text{B}_9^{79}\text{BrN}$ $[\text{M}+\text{Na}]^+$: 516.1952, found: 516.1946.

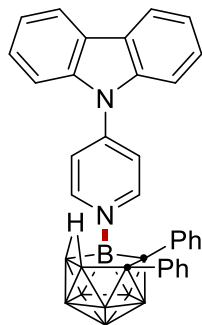


156p. The representative procedure **J** was followed using *nido*-carborane **154a** (36.0 mg, 0.10 mmol) and isoquinolin-5-amine **155p** (43.0 mg, 0.30 mmol). Isolation by column chromatography (*n*-hexane/ CH_2Cl_2 : 1/1) yielded **156p** (22.0 mg, 51%) as a yellow solid. **M.p.** = 291 – 293 $^\circ\text{C}$. **^1H NMR** (400 MHz, CD_2Cl_2): δ = 9.24 (s, 1H), 8.48 – 8.40 (m, 1H), 7.74 – 7.68 (m, 1H), 7.64 – 7.57 (m, 1H), 7.40 – 7.31 (m, 3H), 7.23 – 7.18 (m, 1H), 7.04 – 6.93 (m, 5H), 6.86 – 6.77 (m, 3H), 4.45 (s, 2H), -1.84 (s, 1H). **^{13}C NMR** (101 MHz, CD_2Cl_2): δ = 151.9 (CH), 142.1 (C_q), 138.8 (C_q), 137.0 (CH), 136.4 (C_q), 132.2 (CH), 131.2 (CH), 131.2 (CH), 128.2 (C_q), 127.4 (CH), 127.1 (CH), 126.6 (CH), 126.3 (CH), 125.7 (C_q), 119.3 (CH), 117.7 (CH), 117.4 (CH). **^{11}B NMR** (96 MHz, CD_2Cl_2): δ = 5.02 (1B), -4.05 (1B), -11.73 (1B), -15.70 (2B), -20.59 (1B), -26.07 (1B), -31.04 (1B), -35.90 (1B). **IR** (ATR): 2529, 1627, 1596, 1494, 1399, 1385, 744, 693 cm^{-1} . **MS** (ESI) m/z (relative intensity): 452 (100) $[\text{M}+\text{Na}]^+$, 430 (20) $[\text{M}+\text{H}]^+$. **HR-MS** (ESI): m/z calcd. for $\text{C}_{23}\text{H}_{27}^{10}\text{B}_1^{11}\text{B}_8\text{N}_2$ $[\text{M}+\text{Na}]^+$: 452.2956, found: 452.2954.

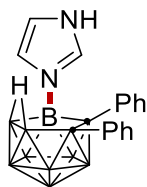


156q. The representative procedure **J** was followed using *nido*-carborane **154a** (36.0 mg, 0.10 mmol) and *tert*-butyl isoquinolin-5-ylcarbamate **155q** (53.4 mg, 0.30 mmol). Isolation by column chromatography (CH_2Cl_2) yielded **156q** (25.1 mg, 54%) as a yellow solid. **M.p.** = 198 – 201 $^\circ\text{C}$. **^1H NMR** (400 MHz, CD_2Cl_2): δ = 9.27 (s, 1H), 8.49 (d, J = 8.0 Hz, 1H), 8.32 (d, J = 7.7 Hz, 1H), 7.81 – 7.73 (m, 2H), 7.71 – 7.66 (m, 1H), 7.32 – 7.27 (m, 2H), 7.01 – 6.94 (m, 3H), 6.93 – 6.86 (m, 3H), 6.82 – 6.76 (m, 3H), 1.52 (s, 9H), -1.88 (s, 1H). **^{13}C NMR** (101 MHz, CD_2Cl_2): δ = 152.9 (C_q), 152.1 (CH), 139.1 (C_q), 138.5 (CH), 136.6 (C_q), 133.8 (C_q), 132.5 (CH), 131.6 (CH), 131.0

(CH), 130.0 (C_q), 128.2 (C_q), 127.8 (CH), 127.4 (overlapped, CH), 127.0 (CH), 126.6 (CH), 125.6 (CH), 117.7 (CH), 82.2 (C_q), 28.2 (CH₃). **¹¹B NMR** (128 MHz, CD₂Cl₂): δ = 4.81 (1B), -3.96 (1B), -11.51 (1B), -15.65 (2B), -20.31 (1B), -25.95 (1B), -30.82 (1B), -35.66 (1B). **IR** (ATR): 2540, 1682, 1521, 1491, 1444, 1252, 1151, 696 cm⁻¹. **MS** (ESI) *m/z* (relative intensity): 530 (50) [M+H]⁺, 552 (100) [M+Na]⁺. **HR-MS** (ESI): *m/z* calcd. for C₂₈H₃₅¹⁰B₁¹¹B₈N₂O₂ [M+Na]⁺: 552.3483, found: 552.3478.

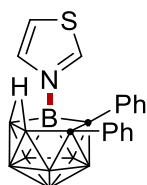


156r. The representative procedure **J** was followed using *nido*-carborane **154a** (36.0 mg, 0.10 mmol) and 9-(pyridin-4-yl)-9*H*-carbazole **155r** (73.0 mg, 0.30 mmol). Isolation by column chromatography (*n*-hexane/CH₂Cl₂: 1/1) yielded **156r** (30.0 mg, 56%) as a yellow solid. **M.p.** = 320 – 321 °C. **¹H NMR** (300 MHz, DMSO-*d*₆): δ = 9.09 (d, *J* = 7.0 Hz, 2H), 8.28 (d, *J* = 7.4 Hz, 2H), 8.12 (d, *J* = 7.1 Hz, 2H), 7.66 – 7.59 (m, 2H), 7.52 (t, *J* = 7.1 Hz, 2H), 7.46 – 7.40 (m, 2H), 7.37 (d, *J* = 6.7 Hz, 2H), 7.09 – 6.94 (m, 5H), 6.90 – 6.81 (m, 3H), -1.42 (s, 1H). **¹³C NMR** (101 MHz, DMSO-*d*₆): δ = 150.7 (CH), 150.0 (C_q), 139.1 (C_q), 138.3 (C_q), 136.6 (C_q), 132.5 (CH), 131.5 (CH), 127.7 (CH), 127.5 (CH), 127.4 (CH), 126.9 (CH), 126.7 (CH), 125.1 (C_q), 123.4 (CH), 121.5 (CH), 121.4 (CH), 111.1 (CH). **¹¹B NMR** (161 MHz, DMSO-*d*₆): δ = 19.79 (1B), 5.14 (1B), -5.31 (1B), -15.72 (2B), -21.29 (1B), -26.27 (1B), -31.13 (1B), -36.92 (1B). **IR** (ATR): 2216, 2176, 2149, 1961, 1510, 1443, 749 cm⁻¹. **MS** (ESI) *m/z* (relative intensity): 552 (100) [M+Na]⁺, 530 (20) [M+H]⁺. **HR-MS** (ESI): *m/z* calcd. for C₃₁H₃₁¹⁰B₁¹¹B₈N₂ [M+Na]⁺: 552.3274, found: 552.3265.

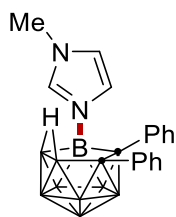


156s. The representative procedure **J** was followed using *nido*-carborane **154a** (36.0 mg, 0.10 mmol) and imidazole **155s** (20.4 mg, 0.30 mmol). Isolation by column chromatography (CH₂Cl₂) yielded **156s** (30.0 mg, 84%) as a white solid. **M.p.** = 283 – 285 °C. **¹H NMR** (500 MHz, Acetone-

d_6): $\delta = 8.47$ (t, $J = 1.4$ Hz, 1H), 7.33 (t, $J = 1.6$ Hz, 1H), 7.32 – 7.24 (m, 3H), 7.04 – 6.98 (m, 2H), 6.97 – 6.91 (m, 2H), 6.92 – 6.85 (m, 1H), 6.86 – 6.77 (m, 3H), 2.87 (s, 1H), -1.81 (s, 1H). ^{13}C NMR (126 MHz, Acetone- d_6): $\delta = 140.4$ (C_q), 138.4 (C_q), 133.0 (CH), 132.1 (CH), 127.7 (CH), 127.6 (overlapped, CH), 127.3 (CH), 126.9 (CH), 126.7 (CH), 119.3 (CH). ^{11}B NMR (128 MHz, Acetone d_6): $\delta = 6.28$ (1B), -0.05 (1B), -7.84 (1B), -10.55 (2B), -16.20 (1B), -20.71 (1B), -26.25 (1B), -31.58 (1B). IR (ATR): 3350, 3151, 2535, 1693, 1494, 1444, 1245, 1058 cm^{-1} MS (ESI) m/z (relative intensity): 376 (100) $[\text{M}+\text{Na}]^+$, 354 (20) $[\text{M}+\text{H}]^+$. HR-MS (ESI): m/z calcd. for $\text{C}_{17}\text{H}_{23}^{10}\text{B}_1^{11}\text{B}_8\text{N}_2$ $[\text{M}+\text{Na}]^+$: 376.2639, found: 376.2637. The analytical data corresponds with those reported in the literature.^[225]

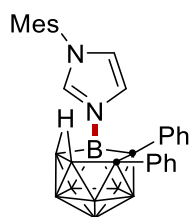


156t. The representative procedure **J** was followed using *nido*-carborane **154a** (36.0 mg, 0.10 mmol) and thiazole **155t** (25.5 mg, 0.30 mmol). Isolation by column chromatography (*n*-hexane/ CH_2Cl_2 : 1/1) yielded **156t** (23.0 mg, 62%) as a white solid. **M.p.** = 278 – 280 °C. ^1H NMR (500 MHz, Acetone- d_6): $\delta = 9.62$ (dd, $J = 2.4, 1.2$ Hz, 1H), 8.19 (dd, $J = 3.6, 1.2$ Hz, 1H), 8.01 (dd, $J = 3.6, 2.3$ Hz, 1H), 7.33 – 7.28 (m, 2H), 7.04 – 6.99 (m, 2H), 6.96 – 6.87 (m, 3H), 6.85 – 6.80 (m, 3H), -1.75 (s, 1H). ^{13}C NMR (126 MHz, Acetone- d_6): $\delta = 160.8$ (CH), 142.5 (C_q), 139.9 (C_q), 137.7 (CH), 132.9 (CH), 131.9 (CH), 127.9 (CH), 127.7 (CH), 127.3 (CH), 126.9 (CH), 124.5 (CH). ^{11}B NMR (128 MHz, Acetone- d_6): $\delta = 2.16$ (1B), -4.51 (1B), -11.95 (1B), -15.68 (2B), -20.65 (1B), -25.91 (1B), -30.68 (1B), -36.28 (1B). IR (ATR): 3110, 2922, 2852, 1975, 1492, 1442, 1248, 688 cm^{-1} . MS (ESI) m/z (relative intensity): 393 (100) $[\text{M}+\text{Na}]^+$, 371 (30) $[\text{M}+\text{H}]^+$. HR-MS (ESI): m/z calcd. for $\text{C}_{17}\text{H}_{22}^{10}\text{B}_1^{11}\text{B}_8\text{NS}$ $[\text{M}+\text{Na}]^+$: 393.2252, found: 393.2252. The analytical data corresponds with those reported in the literature.^[225]

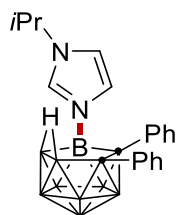


156u. The representative procedure **J** was followed using *nido*-carborane **154a** (36.0 mg, 0.10 mmol) and 1-methyl-1*H*-imidazole **155u** (25.0 mg, 0.30 mmol). Isolation by column chromatography (*n*-hexane/ CH_2Cl_2 : 1/1) yielded **156u** (32.0 mg, 88%) as a colorless solid. **M.p.**

= 270 – 272 °C. **¹H NMR** (400 MHz, CD₂Cl₂): δ = 7.74 (s, 1H), 7.34 – 7.28 (m, 2H), 7.04 – 6.90 (m, 9H), 6.85 (t, *J* = 1.8 Hz, 1H), 3.67 (s, 3H), -1.98 (s, 1H). **¹³C NMR** (101 MHz, CD₂Cl₂): δ = 139.1 (C_q), 137.3 (C_q), 137.2 (CH), 132.2 (CH), 131.2 (CH), 127.2 (CH), 127.1 (CH), 127.0 (CH), 126.4 (CH), 126.1 (CH), 121.6 (CH), 35.5 (CH₃). **¹¹B NMR** (96 MHz, CD₂Cl₂): δ = 0.89 (1B), -4.66 (1B), -12.39 (1B), -15.64 (2B), -20.80 (1B), -25.99 (1B), -31.34 (1B), -36.47 (1B). **IR** (ATR): 3143, 2547, 2506, 1541, 1442, 1172, 829, 750, 689 cm⁻¹. **MS** (ESI) *m/z* (relative intensity): 390 (100) [M+Na]⁺, 368 (20) [M+H]⁺. **HR-MS** (ESI): *m/z* calcd. for C₁₈H₂₅¹⁰B₁¹¹B₈N₂ [M+Na]⁺: 390.2796, found: 390.2795. The analytical data corresponds with those reported in the literature.^[225]

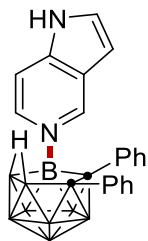


156v. The representative procedure **J** was followed using *nido*-carborane **154a** (36.0 mg, 0.10 mmol) and 1-mesityl-1*H*-imidazole **155v** (56.0 mg, 0.30 mmol). Isolation by column chromatography (*n*-hexane/CH₂Cl₂: 1/1) yielded **156v** (33.0 mg, 70%) as a colorless solid. **M.p.** = 237 – 239 °C. **¹H NMR** (300 MHz, CD₂Cl₂): δ = 7.72 (t, *J* = 1.5 Hz, 1H), 7.47 (t, *J* = 1.6 Hz, 1H), 7.36 – 7.30 (m, 2H), 7.04 – 6.95 (m, 7H), 6.93 – 6.87 (m, 4H), 2.35 (s, 3H), 1.94 (s, 3H), 1.60 (s, 3H), -2.01 (s, 1H). **¹³C NMR** (101 MHz, CD₂Cl₂): δ = 141.3 (C_q), 139.3 (C_q), 137.7 (C_q), 137.4 (CH), 134.8 (C_q), 134.7 (C_q), 132.5 (CH), 131.4 (CH), 131.0 (C_q), 129.7 (CH), 128.3 (CH), 127.6 (CH), 127.3 (CH), 126.7 (CH), 126.4 (CH), 122.5 (CH), 21.1 (CH₃), 17.2 (CH₃), 17.0 (CH₃). **¹¹B NMR** (128 MHz, CD₂Cl₂): δ = 0.52 (1B), -4.70 (1B), -12.44 (1B), -15.97 (2B), -21.20 (1B), -26.06 (1B), -31.28 (1B), -36.54 (1B). **IR** (ATR): 3475, 3375, 2534, 1644, 1527, 1181, 832, 695 cm⁻¹. **MS** (ESI) *m/z* (relative intensity): 494 (100) [M+Na]⁺, 472 (30) [M+H]⁺. **HR-MS** (ESI): *m/z* calcd. for C₂₆H₃₃¹⁰B₁¹¹B₈N₂ [M+Na]⁺: 494.3427, found: 494.3417.

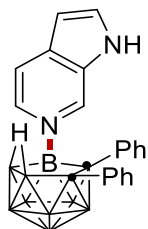


156w. The representative procedure **J** was followed using *nido*-carborane **154a** (36.0 mg, 0.10 mmol) and 1-isopropyl-1*H*-imidazole **155w** (33.0 mg, 0.30 mmol). Isolation by column

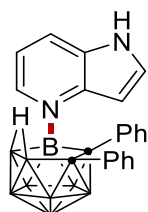
chromatography (*n*-hexane/CH₂Cl₂: 1/1) yielded **156w** (35.0 mg, 89%) as a colorless solid. **M.p.** = 213 – 216 °C. **¹H NMR** (300 MHz, CD₂Cl₂): δ = 7.50 (t, *J* = 1.6 Hz, 1H), 7.34 – 7.30 (m, 2H), 7.21 (t, *J* = 1.7 Hz, 1H), 7.05 – 6.97 (m, 3H), 6.96 – 6.91 (m, 6H), 4.24 (hept, *J* = 6.7 Hz, 1H), 1.35 (d, *J* = 2.5 Hz, 3H), 1.33 (d, *J* = 2.5 Hz, 3H), -2.07 (s, 1H). **¹³C NMR** (101 MHz, CD₂Cl₂): δ = 139.4 (C_q), 137.8 (C_q), 134.8 (CH), 132.4 (CH), 131.5 (CH), 127.6 (CH), 127.5 (CH), 127.3 (CH), 126.7 (CH), 126.4 (CH), 118.7 (CH), 52.4 (CH), 23.1 (CH₃), 22.9 (CH₃). **¹¹B NMR** (128 MHz, CD₂Cl₂): δ = 0.72 (1B), -5.08 (1B), -12.70 (1B), -15.94 (2B), -21.04 (1B), -26.22 (1B), -31.68 (1B), -36.64 (1B). **IR** (ATR): 3142, 2557, 2519, 1537, 1442, 1177, 838, 759, 657 cm⁻¹. **MS** (ESI) *m/z* (relative intensity): 418 (100) [M+Na]⁺, 396 (30) [M+H]⁺. **HR-MS** (ESI): *m/z* calcd. for C₂₀H₂₉¹⁰B₁¹¹B₈N₂ [M+Na]⁺: 418.3111, found: 418.3114.



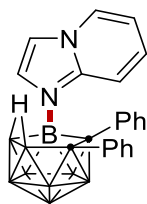
156x. The representative procedure **J** was followed using *nido*-carborane **154a** (36.0 mg, 0.10 mmol) and 1*H*-pyrrolo[3,2-*c*]pyridine **155x** (35.4 mg, 0.30 mmol). Isolation by column chromatography (CH₂Cl₂) yielded **156x** (27.0 mg, 67%) as a white solid. **M.p.** = 280 – 283 °C. **¹H NMR** (500 MHz, Acetone-*d*₆): δ = 11.51 (s, 1H), 9.40 (s, 1H), 8.57 (d, *J* = 7.8 Hz, 1H), 7.75 (dd, *J* = 3.4, 1.9 Hz, 1H), 7.66 (d, *J* = 6.8 Hz, 1H), 7.35 – 7.30 (m, 2H), 7.04 – 6.99 (m, 2H), 6.97 – 6.85 (m, 4H), 6.75 – 6.60 (m, 3H), -1.65 (s, 1H). **¹³C NMR** (126 MHz, Acetone-*d*₆): δ = 144.2 (CH), 141.7 (C_q), 140.2 (C_q), 139.9 (CH), 138.0 (C_q), 133.0 (CH), 132.0 (CH), 131.9 (CH), 127.7 (CH), 127.5 (CH), 126.8 (CH), 126.8 (CH), 125.6 (C_q), 108.8 (CH), 104.6 (CH). **¹¹B NMR** (128 MHz, Acetone-*d*₆): δ = 6.10 (1B), -4.91 (1B), -12.91 (1B), -15.57 (2B), -21.64 (1B), -26.01 (1B), -30.95 (1B), -36.54 (1B). **IR** (ATR): 3386, 2923, 2536, 1631, 1493, 1357, 1225, 697 cm⁻¹. **MS** (ESI) *m/z* (relative intensity): 426 (100) [M+Na]⁺, 404 (30) [M+H]⁺. **HR-MS** (ESI): *m/z* calcd. for C₂₁H₂₅¹⁰B₁¹¹B₈N₂ [M+Na]⁺: 426.2798, found: 426.2794.



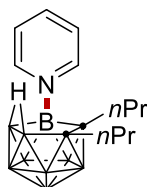
156y. The representative procedure **J** was followed using *nido*-carborane **154a** (36.0 mg, 0.10 mmol) and 1*H*-pyrrolo[2,3-*c*]pyridine **155y** (35.4 mg, 0.30 mmol). Isolation by column chromatography (CH₂Cl₂) yielded **156y** (28.2 mg, 70%) as a white solid. **M.p.** = 171 – 175 °C. **¹H NMR** (500 MHz, Acetone-*d*₆): δ = 11.55 (s, 1H), 9.23 (s, 1H), 8.53 (d, *J* = 6.6 Hz, 1H), 8.07 (d, *J* = 2.9 Hz, 1H), 7.80 (d, *J* = 6.6 Hz, 1H), 7.31 (d, *J* = 7.2 Hz, 2H), 6.99 (d, *J* = 6.8 Hz, 2H), 6.93 (t, *J* = 7.4 Hz, 2H), 6.92 – 6.85 (m, 1H), 6.79 (d, *J* = 2.9 Hz, 1H), 6.73 – 6.63 (m, 3H), -1.64 (s, 1H). **¹³C NMR** (126 MHz, Acetone-*d*₆): δ = 140.1 (C_q), 138.3 (CH), 137.9 (C_q), 137.9 (CH), 136.4 (C_q), 134.8 (CH), 133.0 (CH), 132.6 (C_q), 131.9 (CH), 127.7 (CH), 127.6 (CH), 126.9 (CH), 126.8 (CH), 116.7 (CH), 103.6 (CH). **¹¹B NMR** (128 MHz, Acetone-*d*₆): δ = 6.24 (1B), -4.58 (1B), -12.66 (1B), -15.43 (2B), -21.41 (1B), -25.92 (1B), -30.88 (1B), -36.41 (1B). **IR** (ATR): 2539, 1710, 1639, 1494, 1321, 1140, 836, 693 cm⁻¹. **MS** (ESI) *m/z* (relative intensity): 426 (100) [M+Na]⁺, 404 (50) [M+H]⁺. **HR-MS** (ESI): *m/z* calcd. for C₂₁H₂₅¹⁰B₁¹¹B₈N₂ [M+Na]⁺: 426.2798, found: 426.2798. The analytical data corresponds with those reported in the literature.^[225]



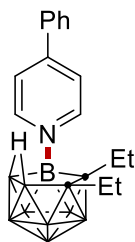
156z. The representative procedure **J** was followed using *nido*-carborane **154a** (36.0 mg, 0.10 mmol) and 1*H*-pyrrolo[3,2-*b*]pyridine **155z** (35.4 mg, 0.30 mmol). Isolation by column chromatography (CH₂Cl₂) yielded **156z** (20.1 mg, 50%) as a white solid. **M.p.** = 283 – 285 °C. **¹H NMR** (500 MHz, Acetone-*d*₆): δ = 11.57 (s, 1H), 8.69 (d, *J* = 6.0 Hz, 1H), 8.30 (d, *J* = 8.1 Hz, 1H), 8.22 (d, *J* = 3.3 Hz, 1H), 7.76 (d, *J* = 3.3 Hz, 1H), 7.38 – 7.29 (m, 3H), 7.02 – 6.85 (m, 5H), 6.62 – 6.50 (m, 3H), -1.67 (s, 1H). **¹³C NMR** (126 MHz, Acetone-*d*₆): δ = 144.0 (C_q), 142.6 (CH), 140.0 (C_q), 137.9 (C_q), 135.3 (CH), 133.1 (CH), 132.7 (CH), 131.6 (C_q), 127.8 (CH), 126.9 (CH), 126.9 (CH), 126.7 (CH), 126.6 (CH), 116.9 (CH), 101.9 (CH). **¹¹B NMR** (128 MHz, Acetone-*d*₆): δ = 4.40 (1B), -4.77 (1B), -12.03 (1B), -15.09 (1B), -15.66 (1B), -22.01 (1B), -25.70 (1B), -29.83 (1B), -36.66 (1B). **IR** (ATR): 3386, 2540, 2199, 2021, 14958, 1425, 1367, 763, 698. cm⁻¹. **MS** (ESI) *m/z* (relative intensity): 426 (100) [M+Na]⁺, 404 (30) [M+H]⁺. **HR-MS** (ESI): *m/z* calcd. for C₂₁H₂₅¹⁰B₁¹¹B₈N₂ [M+Na]⁺: 426.2798, found: 426.2801.



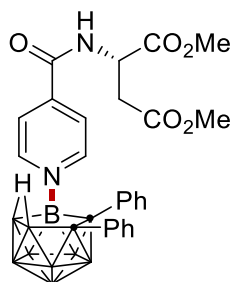
156aa. The representative procedure **J** was followed using *nido*-carborane **154a** (36.0 mg, 0.10 mmol) and *H*-imidazo[1,2-*a*]pyridine **155aa** (35.4 mg, 0.30 mmol). Isolation by column chromatography (CH₂Cl₂) yielded **156aa** (30.0 mg, 75%) as a white solid. **M.p.** = 265 – 268 °C. **¹H NMR** (500 MHz, CD₂Cl₂): δ = 8.76 (d, *J* = 9.3 Hz, 1H), 8.16 (dt, *J* = 6.7, 1.2 Hz, 1H), 7.82 (ddd, *J* = 9.3, 7.0, 1.3 Hz, 1H), 7.53 (d, *J* = 2.1 Hz, 1H), 7.39 (d, *J* = 1.3 Hz, 1H), 7.34 – 7.28 (m, 2H), 7.25 (td, *J* = 6.9, 1.1 Hz, 1H), 7.01 – 6.92 (m, 3H), 6.83 – 6.76 (m, 2H), 6.70 – 6.61 (m, 3H), -1.87 (s, 1H). **¹³C NMR** (126 MHz, CD₂Cl₂): δ = 143.8 (C_q), 139.4 (C_q), 137.8 (C_q), 132.4 (CH), 132.1 (CH), 130.9 (CH), 130.5 (CH), 127.9 (CH), 127.3 (CH), 127.0 (CH), 126.4 (CH), 126.2 (CH), 116.9 (CH), 115.0 (CH), 113.1 (CH). **¹¹B NMR** (128 MHz, CD₂Cl₂): δ = 0.00 (1B), -4.98 (1B), -11.82 (1B), -15.41 (1B), -16.03 (1B), -21.34 (1B), -25.59 (1B), -30.16 (1B), -36.53 (1B). **IR** (ATR): 3144, 2532, 1707, 1642, 1444, 1202, 752, 697 cm⁻¹. **MS** (ESI) *m/z* (relative intensity): 426 (100) [M+Na]⁺, 404 (50) [M+H]⁺. **HR-MS** (ESI): *m/z* calcd. for C₂₁H₂₅¹⁰B₁¹¹B₈N₂ [M+H]⁺: 426.2798, found: 426.2801.



156bb. The representative procedure **J** was followed using *nido*-carborane **154b** (29.1 mg, 0.10 mmol) and pyridine **155a** (24.0 mg, 0.30 mmol). Isolation by column chromatography (*n*-hexane/CH₂Cl₂: 1/1) yielded **156bb** (19.5 mg, 66%) as a yellow solid. **M.p.** = 199 – 200 °C. **¹H NMR** (300 MHz, CD₂Cl₂): δ = 9.09 (d, *J* = 4.9 Hz, 2H), 8.33 (tt, *J* = 7.8, 1.5 Hz, 1H), 7.85 (dd, *J* = 7.7, 6.6 Hz, 2H), 2.04 – 1.85 (m, 6H), 1.01 – 0.86 (m, 5H), 0.61 (t, *J* = 7.3 Hz, 3H), -2.76 (s, 1H). **¹³C NMR** (75 MHz, CD₂Cl₂): δ = 148.9 (CH), 143.1 (CH), 126.5 (CH), 36.7 (CH₂), 33.4 (CH₂), 24.1 (CH₂), 22.9 (CH₂), 14.3 (CH₃), 14.1 (CH₃). **¹¹B NMR** (96 MHz, CD₂Cl₂): δ = 4.42 (1B), -5.99 (1B), -12.19 (1B), -13.83 (1B), -17.06 (1B), -20.53 (1B), -27.25 (1B), -30.97 (1B), -37.54 (1B). **IR** (ATR): 2558, 2527, 2231, 2032, 1960, 1629, 572, 480 cm⁻¹. **MS** (ESI) *m/z* (relative intensity): 319 (100) [M+Na]⁺, 297 (50) [M+H]⁺. **HR-MS** (ESI): *m/z* calcd. for C₁₃H₂₈¹⁰B₁¹¹B₈N [M+Na]⁺: 319.2997, found: 319.2993.

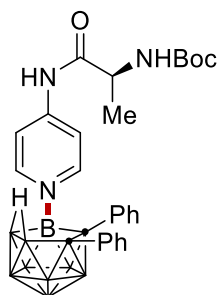


156cc. The representative procedure **J** was followed using *nido*-carborane **154c** (26.3 mg, 0.10 mmol) and 4-phenylpyridine **155g** (46.5 mg, 0.30 mmol). Isolation by column chromatography (*n*-hexane/CH₂Cl₂: 1/1) yielded **156cc** (25.0 mg, 73%) as a yellow solid. **M.p.** = 84 – 85 °C. **¹H NMR** (300 MHz, CD₂Cl₂): δ = 9.06 (d, *J* = 5.6 Hz, 2H), 8.02 (d, *J* = 5.6 Hz, 2H), 7.90 – 7.80 (m, 2H), 7.71 – 7.62 (m, 3H), 2.19 – 1.98 (m, 2H), 1.92 – 1.80 (m, 2H), 1.15 (t, *J* = 7.5 Hz, 3H), 0.65 (t, *J* = 7.5 Hz, 3H), -2.72 (s, 1H). **¹³C NMR** (75 MHz, CD₂Cl₂): δ = 155.0 (C_q), 148.8 (CH), 134.4 (C_q), 131.8 (CH), 129.8 (CH), 127.6 (CH), 123.6 (CH), 27.1 (CH₂), 23.7 (CH₂), 14.9 (CH₃), 13.9 (CH₃). **¹¹B NMR** (96 MHz, CD₂Cl₂): δ = 4.3 (1B), -6.1 (1B), -12.5 (1B), -14.0 (1B), -17.2 (1B), -20.7 (1B), -27.3 (1B), -31.1 (1B), -37.6 (1B). **IR** (ATR): 2527, 2032, 1994, 1961, 1629, 766, 692, 446 cm⁻¹. **MS** (ESI) *m/z* (relative intensity): 367 (100) [M+Na]⁺, 345 (50) [M+H]⁺. **HR-MS** (ESI): *m/z* calcd. for C₁₇H₂₈¹⁰B₁¹¹B₈N [M+Na]⁺: 367.0000, found: 367.2993.

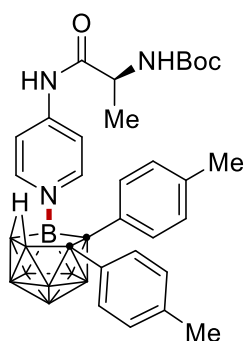


157a. The representative procedure **J** was followed using *nido*-carborane **154a** (36.0 mg, 0.10 mmol) and dimethyl isonicotinoyl-*L*-aspartate **155bb** (80.0 mg, 0.30 mmol). Isolation by column chromatography (MeOH/CH₂Cl₂: 1/100) yielded **157a** (46.0 mg, 84%) as a yellow solid. **M.p.** = 183 – 187 °C. **¹H NMR** (400 MHz, CD₂Cl₂): δ = 8.83 (d, *J* = 6.7 Hz, 2H), 7.82 (d, *J* = 7.0 Hz, 2H), 7.49 – 7.42 (m, 1H), 7.32 (d, *J* = 6.5 Hz, 2H), 7.04 – 6.98 (m, 3H), 6.96 – 6.89 (m, 5H), 5.03 – 4.96 (m, 1H), 3.80 (s, 3H), 3.72 (s, 3H), 3.20 – 3.11 (m, 1H), 3.02 – 2.94 (m, 1H), -1.89 (s, 1H). **¹³C NMR** (101 MHz, CD₂Cl₂): δ = 171.4 (C_q), 170.2 (C_q), 161.8 (C_q), 148.3 (CH), 145.7 (C_q), 138.6 (C_q), 135.8 (C_q), 132.1 (CH), 131.2 (CH), 127.8 (CH), 127.1 (CH), 127.0 (CH), 126.4 (CH), 123.5 (CH), 53.1 (CH₃), 52.2 (CH₃), 49.3 (CH), 35.4 (CH₂). **¹¹B NMR** (96 MHz, CD₂Cl₂): δ = 4.58 (1B), -3.63 (1B), -11.19 (1B), -15.79 (2B), -20.13 (1B), -26.06 (1B), -30.87 (1B), -35.56 (1B). **IR** (ATR): 3335, 2954, 2541, 1738, 1708, 1676, 1434, 1220, 697 cm⁻¹. **MS** (ESI) *m/z* (relative

intensity): 574 (100) $[M+Na]^+$, 552 (20) $[M+H]^+$. **HR-MS** (ESI): m/z calcd. for $C_{26}H_{33}^{10}B_1^{11}B_8N_2O_5$ $[M+Na]^+$: 574.3174, found: 574.3165.



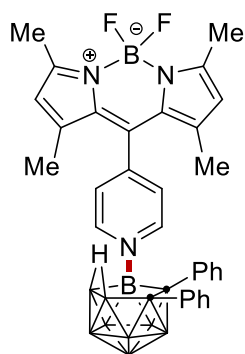
157b. The representative procedure **J** was followed using *nido*-carborane **154a** (36.0 mg, 0.10 mmol) and *tert*-butyl (*S*)-(1-oxo-1-(pyridin-4-ylamino)propan-2-yl)carbamate **155cc** (80.0 mg, 0.30 mmol). Isolation by column chromatography (MeOH/CH₂Cl₂: 1/100) yielded **157b** (44.0 mg, 80%) as a colorless solid. **M.p.** = 230 – 233 °C. **¹H NMR** (400 MHz, CDCl₃): δ = 10.00 (s, 1H), 8.47 (d, J = 3.3 Hz, 2H), 7.51 (t, J = 6.5 Hz, 2H), 7.33 – 7.28 (m, 2H), 7.00 – 6.93 (m, 3H), 6.89 – 6.80 (m, 5H), 4.98 – 4.84 (m, 1H), 4.33 – 4.20 (m, 1H), 1.48 (s, 9H), 1.42 (d, J = 7.2 Hz, 3H), -2.02 (s, 1H). **¹³C NMR** (101 MHz, CDCl₃): δ = 171.8 (C_q), 157.2 (C_q), 149.5 (C_q), 148.3 (CH), 138.6 (C_q), 136.5 (C_q), 132.1 (CH), 131.1 (CH), 127.4 (CH), 127.1 (CH), 126.6 (CH), 126.2 (CH), 113.9 (CH), 82.2 (C_q), 51.1 (CH), 28.2 (CH₃), 15.7 (CH₃). **¹¹B NMR** (96 MHz, CDCl₃): δ = 5.18 (1B), -3.87 (1B), -10.82 (1B), -15.36 (2B), -20.60 (1B), -26.03 (1B), -30.80 (1B), -35.93 (1B). **IR** (ATR): 3475, 3375, 2535, 1681, 1644, 1494, 1443, 1162, 695 cm⁻¹. **MS** (ESI) m/z (relative intensity): 573 (100) $[M+Na]^+$, 551 (50) $[M+H]^+$. **HR-MS** (ESI): m/z calcd. for $C_{27}H_{38}^{10}B_1^{11}B_8N_3O_3$ $[M+Na]^+$: 573.3698, found: 573.3708.



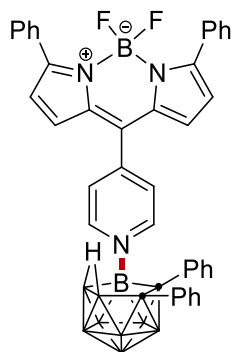
157c. The representative procedure **J** was followed using the toluene derivative of the *nido*-carborane **154d** (38.8 mg, 0.10 mmol) and *tert*-butyl (*S*)-(1-oxo-1-(pyridin-4-ylamino)propan-2-yl)carbamate **155dd** (80.0 mg, 0.30 mmol). Isolation by column chromatography (CH₂Cl₂) yielded **157c** (32.0 mg, 55%) as a white solid. **M.p.** = 220 – 222 °C. **¹H NMR** (300 MHz, CD₂Cl₂):

Experimental Section

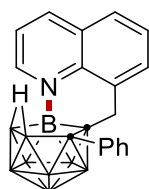
δ = 9.91 (s, 1H), 8.48 (d, J = 7.3 Hz, 2H), 7.57 (d, J = 9.7 Hz, 2H), 7.19 (d, J = 8.1 Hz, 2H), 6.90 – 6.76 (m, 4H), 6.71 (d, J = 7.8 Hz, 2H), 5.01 (d, J = 6.5 Hz, 1H), 4.29 (q, J = 7.0 Hz, 1H), 2.18 (s, 3H), 2.10 (s, 3H), 1.48 (s, 9H), 1.42 (d, J = 7.1 Hz, 3H), -1.98 (s, 1H). **^{13}C NMR** (101 MHz, CD_2Cl_2): δ = 171.9 (C_q), 149.7 (C_q), 148.3 (CH), 136.2 (C_q), 136.2 (C_q), 136.2 (C_q), 135.8 (C_q), 133.5 (C_q), 132.0 (CH), 131.0 (CH), 128.1 (CH), 127.8 (CH), 113.8 (CH), 81.8 (C_q), 29.7 (CH), 27.9 (CH_3), 20.6 (CH_3), 20.6 (CH_3), 20.5 (CH_3). **^{11}B NMR** (128 MHz, CD_2Cl_2): δ = 6.10 (1B), -4.91 (1B), -12.91 (1B), -15.57 (2B), -21.64 (1B), -26.01 (1B), -30.95 (1B), -36.54 (1B). **IR** (ATR): 3210, 2539, 1633, 1517, 1312, 1171, 845, 697 cm^{-1} . **MS** (ESI) m/z (relative intensity): 596 (100) $[\text{M}+\text{NH}_4]^+$. **HR-MS** (ESI): m/z calcd. for $\text{C}_{29}\text{H}_{42}^{10}\text{B}_1^{11}\text{B}_8\text{N}_3\text{O}_3$ $[\text{M}+\text{NH}_4]^+$: 596.4458, found: 596.4449.



157d. The representative procedure **J** was followed using *nido*-carborane **154a** (36.0 mg, 0.10 mmol) and 5,5-difluoro-1,3,7,9-tetramethyl-10-(pyridin-4-yl)-5*H*-4 λ^4 ,5 λ^4 -dipyrrolo[1,2-*c*:2', 1'-*f*][1,3,2]diazaborinine **155ee** (98.0 mg, 0.30 mmol). Isolation by column chromatography (MeOH/ CH_2Cl_2 : 1/100) yielded **157d** (43.0 mg, 71%) as a red solid. **M.p.** = 318 – 319 °C. **^1H NMR** (300 MHz, CD_2Cl_2): δ = 8.94 (d, J = 6.8 Hz, 2H), 7.59 (d, J = 6.8 Hz, 2H), 7.37 – 7.30 (m, 2H), 7.07 – 6.87 (m, 8H), 6.09 (s, 2H), 2.55 (s, 6H), 1.25 (s, 6H), -1.96 (s, 1H). **^{13}C NMR** (101 MHz, CD_2Cl_2): δ = 158.0 (C_q), 150.7 (C_q), 148.5 (CH), 142.1 (C_q), 138.5 (C_q), 136.0 (C_q), 133.5 (C_q), 132.1 (CH), 131.0 (CH), 129.4 (C_q), 127.7 (CH), 127.2 (CH), 126.9 (CH), 126.4 (overlapped, CH), 122.5 (CH), 15.1 (CH_3), 15.1 (CH_3), 14.5 (CH_3), 14.5 (CH_3). **^{11}B NMR** (128 MHz, CD_2Cl_2): δ = 4.61 (1B), 0.53 (t, J = 31.9 Hz, BF_2), -3.67 (1B), -10.68 (1B), -15.76 (2B), -20.49 (1B), -26.01 (1B), -30.72 (1B), -35.65 (1B). **^{19}F NMR** (377 MHz, CD_2Cl_2): δ = -146.29 (dd, J = 64.0, 32.5 Hz). **IR** (ATR): 3478, 3376, 2541, 1644, 1518, 1443, 1197, 1161, 695 cm^{-1} . **MS** (ESI) m/z (relative intensity): 633 (100) $[\text{M}+\text{Na}]^+$. **HR-MS** (ESI): m/z calcd. for $\text{C}_{32}\text{H}_{37}^{10}\text{B}_1^{11}\text{B}_9\text{F}_2\text{N}_3$ $[\text{M}+\text{Na}]^+$: 633.3821, found: 633.3823.

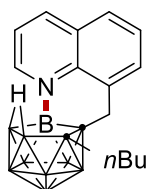


157e. The representative procedure **J** was followed using *nido*-carborane **154a** (36.0 mg, 0.10 mmol) and 5,5-difluoro-3,7-diphenyl-10-(pyridin-4-yl)-5*H*-4 λ^4 ,5 λ^4 -dipyrrolo[1,2-*c*:2',1'-*f*][1,3,2]diazaborinine **155ff** (126.0 mg, 0.30 mmol). Isolation by column chromatography (MeOH/CH₂Cl₂: 1/100) yielded **157e** (35.0 mg, 50%) as a purple solid. **M.p.** = 310 – 312 °C. **¹H NMR** (300 MHz, CD₂Cl₂): δ = 8.91 (d, *J* = 6.8 Hz, 2H), 7.92 – 7.85 (m, 4H), 7.70 (d, *J* = 6.9 Hz, 2H), 7.55 – 7.47 (m, 6H), 7.40 – 7.33 (m, 2H), 7.09 – 6.95 (m, 8H), 6.78 (d, *J* = 4.3 Hz, 2H), 6.62 (d, *J* = 4.4 Hz, 2H), -1.90 (s, 1H). **¹³C NMR** (101 MHz, CD₂Cl₂): δ = 161.2 (C_q), 148.5 (C_q), 147.8 (CH), 138.6 (C_q), 136.2 (C_q), 135.4 (C_q), 134.9 (C_q), 132.1 (CH), 131.8 (C_q), 131.2 (CH), 130.3 (CH), 129.7 (CH), 129.5 (CH), 129.5 (CH), 129.4 (CH), 128.3 (CH), 127.7 (CH), 127.2 (CH), 127.0 (CH), 126.9 (CH), 126.4 (CH), 122.6 (CH). **¹¹B NMR** (128 MHz, CD₂Cl₂): δ = 4.61 (1B), 1.24 (t, *J* = 31.3 Hz, BF₂), -3.79 (1B), -10.90 (1B), -16.09 (2B), -20.64 (1B), -26.21 (1B), -31.07 (1B), -35.67 (1B). **¹⁹F NMR** (377 MHz, CD₂Cl₂): δ = -132.08 (dd, *J* = 63.1, 31.2 Hz). **IR** (ATR): 2220, 2160, 2148, 1990, 1569, 1289, 1136, 1073, 699 cm⁻¹. **MS** (ESI) *m/z* (relative intensity): 729 (100) [M+Na]⁺. **HR-MS** (ESI): *m/z* calcd. for C₄₀H₃₇¹⁰B₁¹¹B₉F₂N₃ [M+Na]⁺: 729.3822, found: 729.3833.



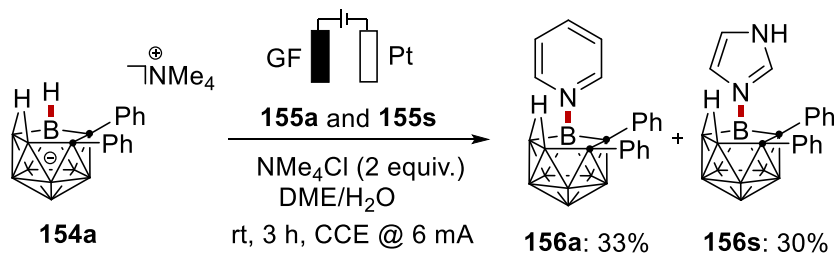
159a. The representative procedure **J** was followed using *nido*-carborane **158a** (43.0 mg, 0.10 mmol). Isolation by column chromatography (MeOH/CH₂Cl₂: 1/100) yielded **159a** (29.0 mg, 83%) as a yellow solid. **M.p.** = 292 – 294 °C. **¹H NMR** (300 MHz, CD₂Cl₂): δ = 9.30 (d, *J* = 5.4 Hz, 1H), 8.63 (dd, *J* = 8.4, 1.6 Hz, 1H), 7.94 (d, *J* = 8.1 Hz, 1H), 7.79 – 7.67 (m, 2H), 7.60 – 7.55 (m, 1H), 7.54 – 7.48 (m, 2H), 7.38 – 7.26 (m, 3H), 3.46 (d, *J* = 18.8 Hz, 1H), 3.10 (d, *J* = 18.8 Hz, 1H), -1.86 (s, 1H). **¹³C NMR** (101 MHz, CD₂Cl₂): δ = 145.5 (CH), 143.3 (CH), 138.9 (C_q), 137.6 (C_q), 134.5 (CH), 132.7 (C_q), 131.9 (CH), 129.6 (C_q), 128.9 (CH), 128.0 (CH), 127.6 (CH), 127.1 (CH),

120.9 (CH), 33.9 (CH₂). **¹¹B NMR** (96 MHz, CD₂Cl₂): δ = 1.14 (1B), -4.04 (1B), -13.02 (3B), -19.21 (1B), -27.64 (1B), -29.35 (1B), -34.55 (1B). **IR** (ATR): 2571, 2543, 2521, 1518, 1373, 829, 766, 695 cm⁻¹. **MS** (ESI) *m/z* (relative intensity): 373 (100) [M+Na]⁺, 351 (20) [M+H]⁺. **HR-MS** (ESI): *m/z* calcd. for C₁₈H₂₂¹⁰B₁¹¹B₈N [M+Na]⁺: 373.2531, found: 373.2524. The analytical data corresponds with those reported in the literature.^[225]

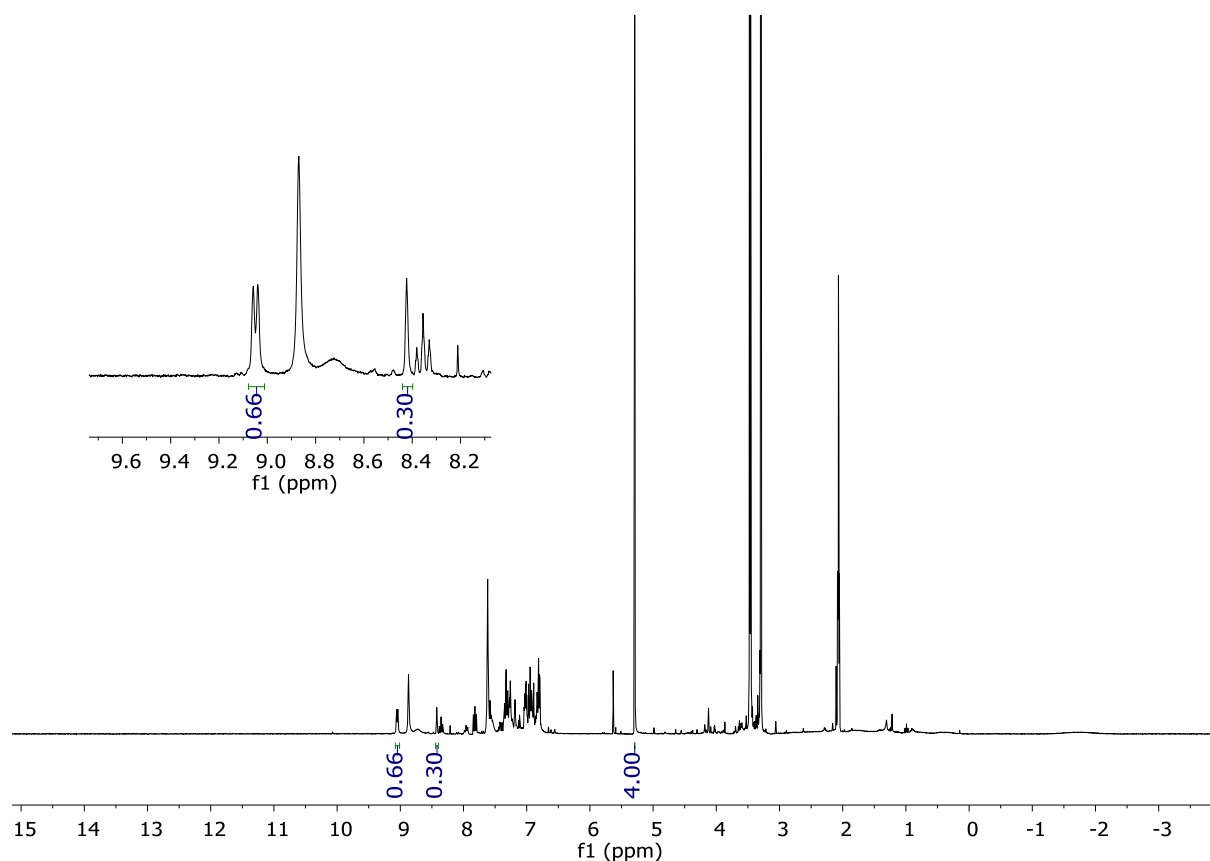


159b. The representative procedure **J** was followed using *nido*-carborane **158b** (41.0 mg, 0.10 mmol). Isolation by column chromatography (MeOH/CH₂Cl₂: 1/100) yielded **159b** (29.0 mg, 88%) as a yellow solid. **M.p.** = 235 – 237 °C. **¹H NMR** (300 MHz, CD₂Cl₂): δ = 9.26 (d, *J* = 4.8 Hz, 1H), 8.61 (dd, *J* = 8.4, 1.6 Hz, 1H), 8.01 – 7.93 (m, 1H), 7.83 – 7.69 (m, 3H), 3.88 (d, *J* = 18.4 Hz, 1H), 3.64 (d, *J* = 18.4 Hz, 1H), 2.09 – 1.86 (m, 2H), 1.73 – 1.47 (m, 2H), 1.43 – 1.29 (m, 2H), 0.95 (t, *J* = 7.3 Hz, 3H), -2.44 (s, 1H). **¹³C NMR** (101 MHz, CD₂Cl₂): δ = 145.3 (CH), 143.0 (CH), 137.7 (C_q), 134.5 (CH), 132.7 (C_q), 129.6 (C_q), 128.9 (CH), 127.6 (CH), 120.9 (CH), 34.1 (CH₂), 33.1 (CH₂), 33.0 (CH₂), 23.1 (CH₂), 13.8 (CH₃). **¹¹B NMR** (96 MHz, CD₂Cl₂): δ = 0.54 (1B), -5.34 (1B), -12.19 (1B), -15.65 (2B), -18.83 (1B), -27.89 (1B), -29.97 (1B), -35.37 (1B). **IR** (ATR): 2931, 2850, 2581, 2522, 1518, 1374, 1005, 826, 767 cm⁻¹. **MS** (ESI) *m/z* (relative intensity): 353 (100) [M+Na]⁺, 331 (20) [M+H]⁺. **HR-MS** (ESI): *m/z* calcd. for C₁₆H₂₆¹⁰B₁¹¹B₈N [M+Na]⁺: 353.2843, found: 353.2834.

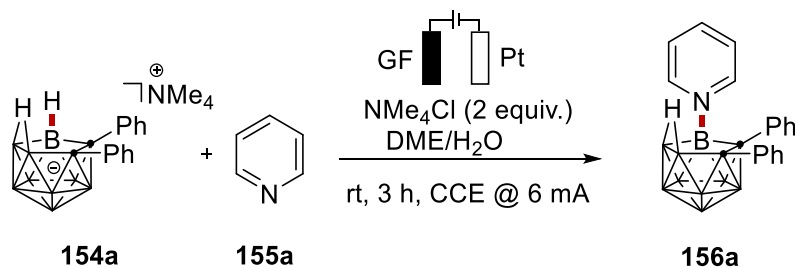
5.3.5.2 Competition Experiments



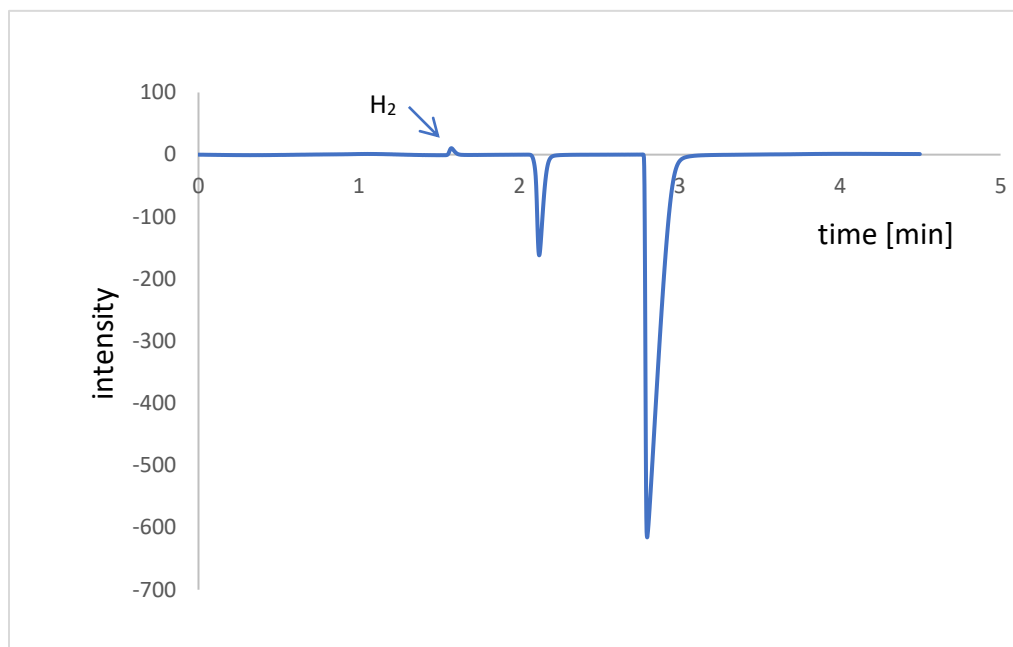
The general procedure **J** was followed using *nido*-carborane **154a** (36 mg, 0.10 mmol), pyridine **155a** (12 mg, 0.15 mmol) and imidazole **155s** (10 mg, 0.15 mmol). The conversions to **156a** and **156s** were determined by crude ¹H NMR spectroscopy with CH₂Br₂ as the internal standard.



5.3.5.3 GC-Headspace Detection



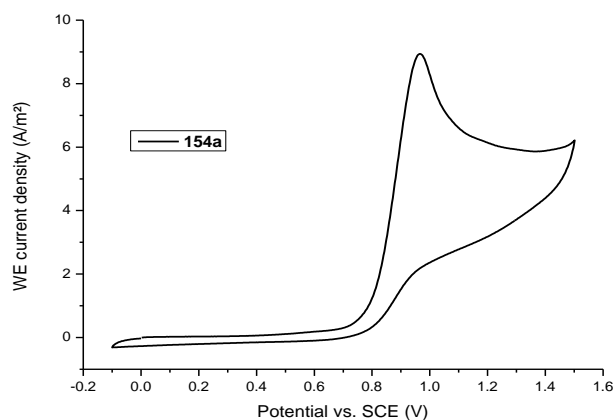
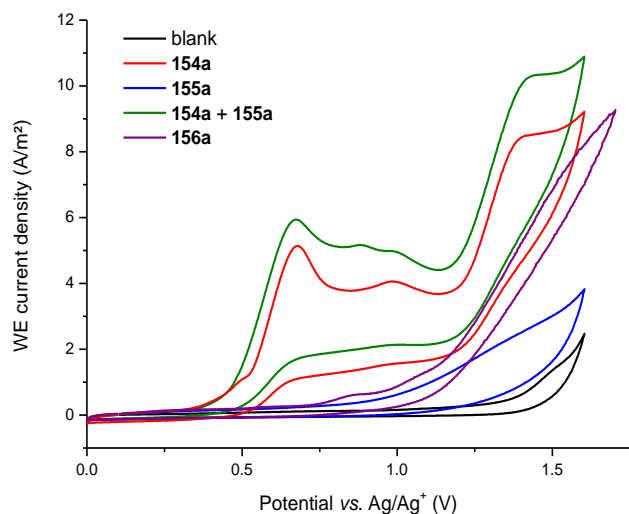
In an undivided cell equipped with a GF anode (10 mm × 15 mm × 6 mm) and a platinum cathode (10 mm × 15 mm × 0.25 mm), *nido*-Carborane **154a** (0.1 mmol, 1.0 equiv), pyridine **155a** (0.3 mmol, 3.0 equiv), and NMe₄Cl (0.2 mmol, 2.0 equiv) were dissolved in DME (4.0 mL) and H₂O (0.2 mL). Electrocatalysis was performed at room temperature under a constant current of 6.0 mA maintained for 3 h. After the reaction, 1.0 mL of the headspace volume was removed for GC analysis. The graphite felt anode was washed with CH₂Cl₂ (3 × 10 mL) in an ultrasonic bath. The yield of **156a** (86%) was determined by ¹H NMR spectroscopy.



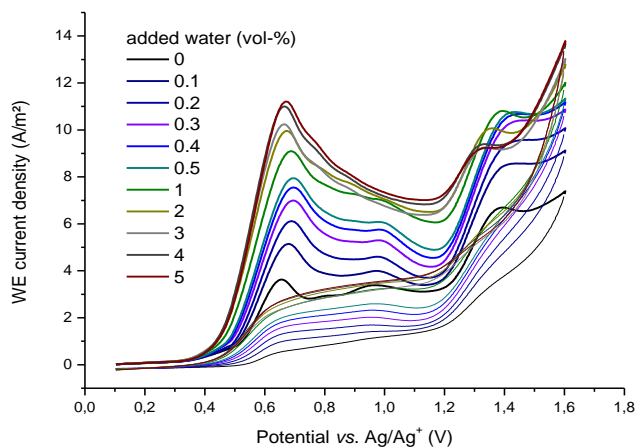
5.3.5.3 Cyclic Voltammetry

CV measurements were conducted with a Metrohm Autolab PGSTAT204 potentiostat and Nova 2.1 software. A glassy carbon working electrode (disk, diameter: 3mm), a coiled platinum wire counter electrode and a non-aqueous Ag/Ag⁺ reference electrode (ALS Japan) were employed. The voltammograms were recorded at room temperature in dry 1,2-dimethoxyethane (DME) at a substrate concentration of 1 mmol/L and with 100 mmol/L *n*-Bu₄NPF₆ as supporting electrolyte. All solutions were degassed with DME-saturated N₂ prior to measurement and an overpressure of protective gas was maintained throughout the experiment. The scan rate is 100 mV/s. Deviations from the general experimental conditions are indicated in the respective figures and descriptions. The measured half-peak potential for the irreversible oxidation process of the *nido*-carborane standard substrate is: +0.87 V vs. SCE in DME/H₂O 19:1, +0.55 V vs. Ag/Ag⁺ in DME/H₂O 19:1, + 0.57 V vs. Ag/Ag⁺ in DME.

1) Reagents



2) Effect of H₂O



5.3.5.3 Stability Test

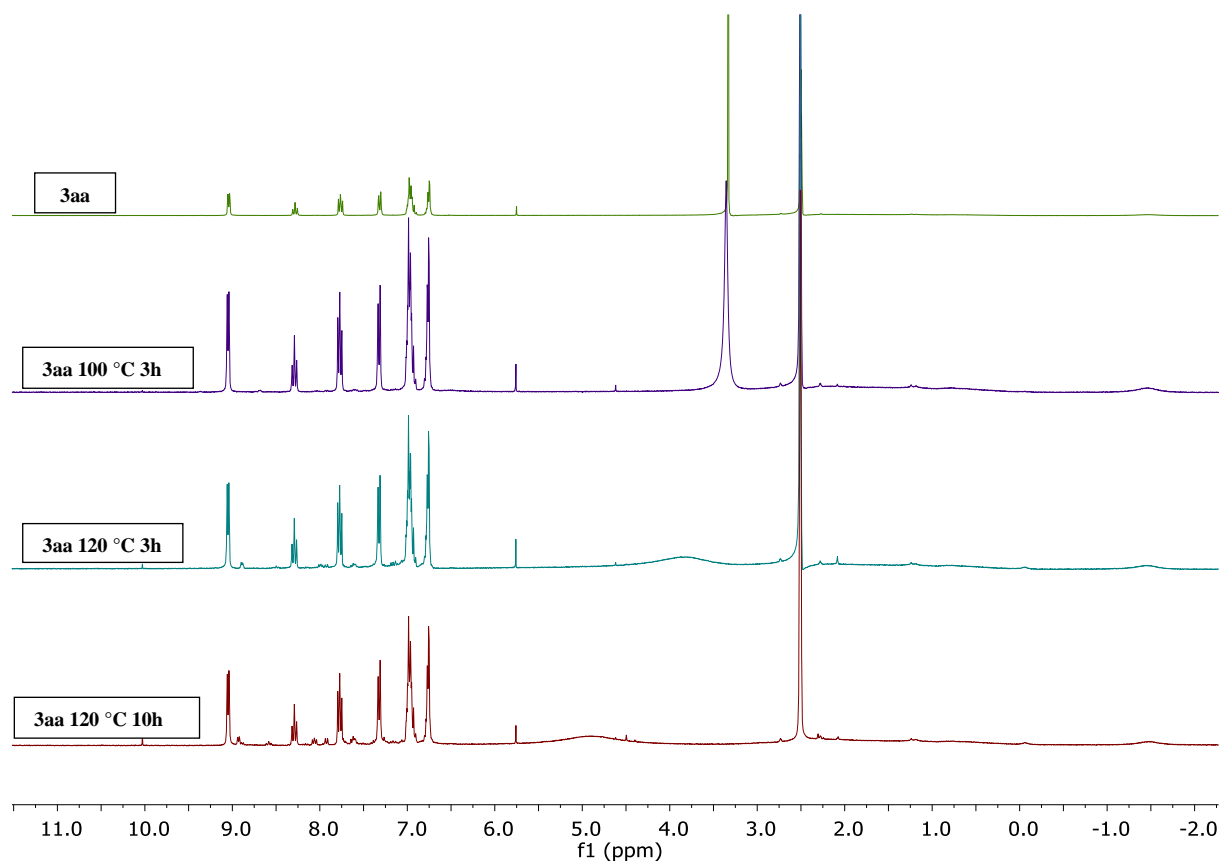
Thermal stability test: compound **156a** was dissolved in an NMR tube (0.4 mL DMSO-d₆), then heated to 100 °C for 3 h, 120 °C for 3 h, and 120 °C for 10 h, respectively. The ¹H NMR and ¹¹B

Experimental Section

NMR tracking experiments show that **156a** was quite stable at 100 °C and 120 °C .

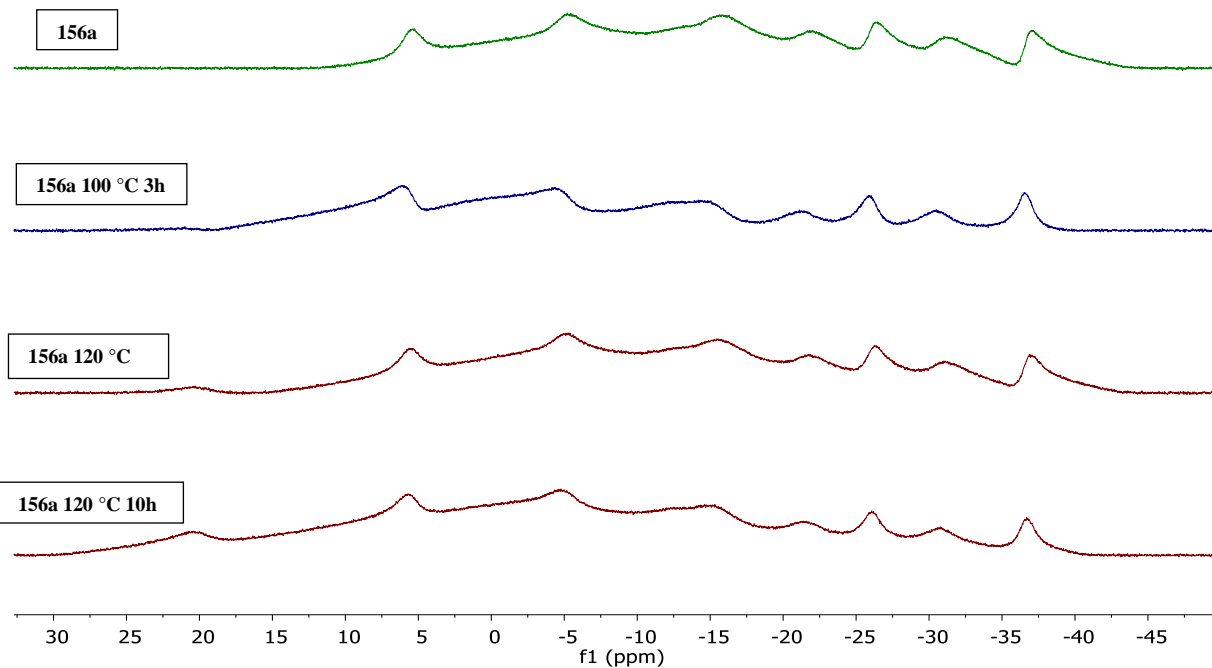
Chemical stability test: compound **156a** was dissolved in an NMR tube (0.4 mL CD₃CN), then 0.1 mL H₂O, HCl (1M) or NaOH (1M) was added into the NMR tube, respectively. The ¹¹B NMR tracking experiments show that **156a** was stable in a neutral environment. However, **156a** starts to decompose in a strong acidic or alkaline environment.

Note: although **156a** was not stable in a strong acidic or alkaline environments, but during our experiments, we found these B - N coupling compounds are very stable in the solid state or even in liquid solution at room temperature for a long time.

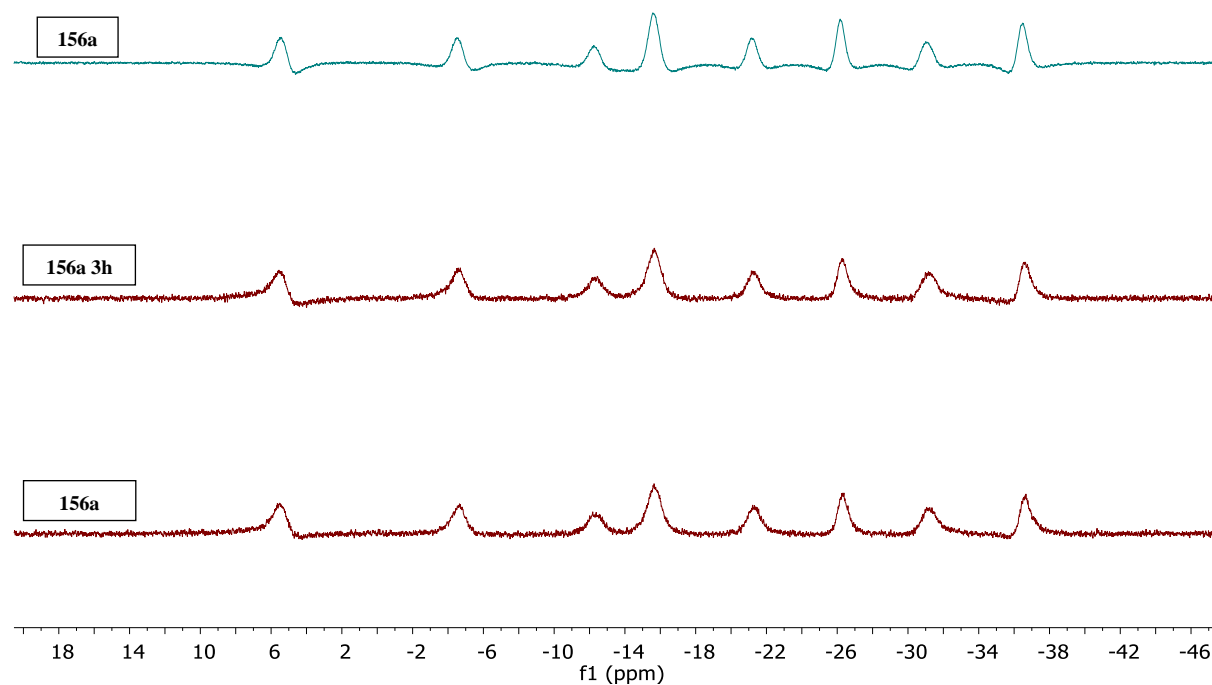


¹H NMR spectra of compound **156a** in DMSO-d₆ at different temperature for stability test.

Experimental Section

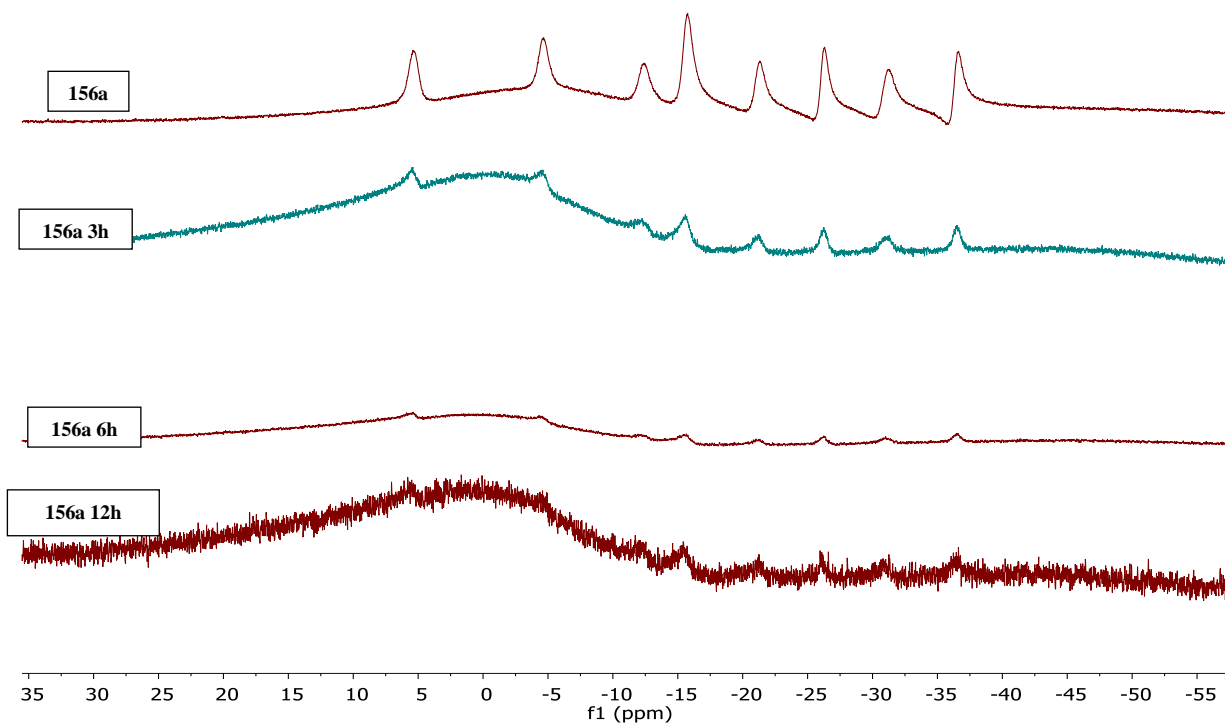


^{11}B NMR spectra of compound **156a** in DMSO-d_6 at different temperature for thermal stability test.

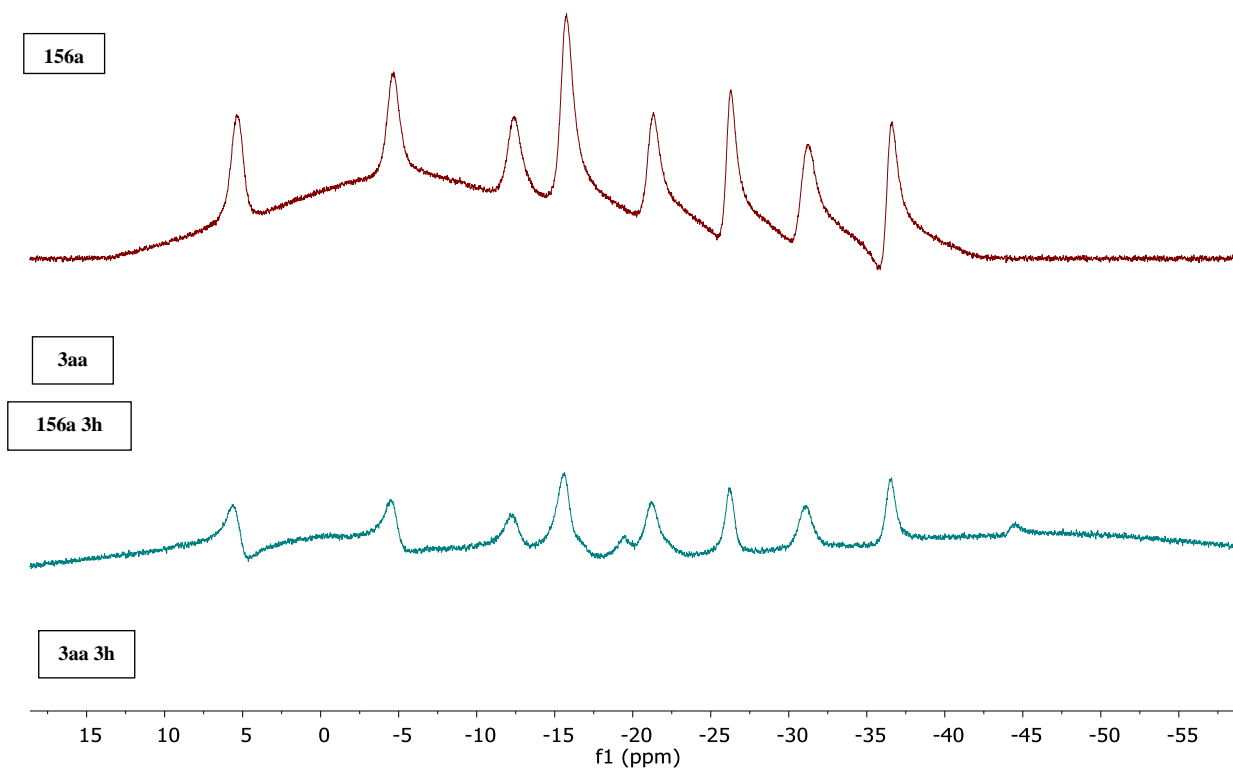


^{11}B NMR spectra of compound **156a** in CD_3CN in $0.1\text{ mL H}_2\text{O}$ for chemical stability test.

Experimental Section



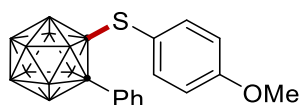
^{11}B NMR spectra of compound **156a** in CD_3CN in 0.1 mL HCl (1M) for chemical stability test.



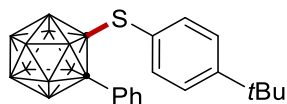
^{11}B NMR spectra of compound **156a** in CD_3CN in 0.1 mL NaOH (1M) for chemical stability test.

5.3.6 Cupraelectro-Catalyzed Chalcogenations of *o*-Carboranes

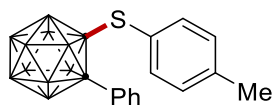
5.3.6.1 Characterization Data



162a. The representative procedure **K** was followed using *o*-carborane **160a** (22.0 mg, 0.10 mmol) and 4-methoxybenzenethiol **161a** (36.9 μ L, 0.30 mmol). Isolation by column chromatography (*n*-hexane) yielded **162a** (30.5 mg, 85%) as a colorless solid. **M.p.** = 141 – 143 $^{\circ}$ C. **1 H NMR** (400 MHz, CDCl_3): δ = 7.66 (d, J = 8.0 Hz, 2H), 7.57 (t, J = 7.4 Hz, 1H), 7.48 (t, J = 7.6 Hz, 2H), 6.86 (d, J = 8.7 Hz, 2H), 6.77 (d, J = 8.8 Hz, 2H), 3.83 (s, 3H). **13 C NMR** (101 MHz, CDCl_3): δ = 161.8 (C_q), 138.5 (CH), 132.2 (CH), 131.0 (C_q), 130.8 (CH), 128.5 (CH), 120.8 (C_q), 114.5 (CH), 87.9 (Cage C), 86.9 (Cage C), 55.4 (CH_3). **11 B NMR** (96 MHz, CDCl_3): δ = -2.78 (2B), -9.14 (3B), -10.46 (3B), -11.59 (2B). **IR** (ATR): 2924, 2853, 2601, 2574, 2561, 1588, 1253, 1170, 1027 cm^{-1} . **MS** (EI) m/z : 358 [M] $^+$. **HR-MS** (EI): m/z calcd. for $\text{C}_{15}\text{H}_{22}^{10}\text{B}_2^{11}\text{B}_8\text{OS}$ [M] $^+$: 358.2397, found: 358.2386.

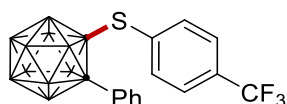


162b. The representative procedure **L** with KI (16.6 mg, 0.10 mmol) was followed using *o*-carborane **160a** (22.0 mg, 0.10 mmol) and 4-(*tert*-butyl)benzenethiol **161b** (49.9 μ L, 0.30 mmol). Isolation by column chromatography (*n*-hexane) yielded **162b** (24.0 mg, 62%) as a colorless solid. **M.p.** = 177 – 179 $^{\circ}$ C. **1 H NMR** (400 MHz, CDCl_3): δ = 7.69 – 7.64 (m, 2H), 7.62 – 7.53 (m, 1H), 7.51 – 7.46 (m, 2H), 7.30 – 7.26 (m, 2H), 6.92 – 6.85 (m, 2H), 1.33 (s, 9H). **13 C NMR** (101 MHz, CDCl_3): δ = 154.7 (C_q), 136.5 (CH), 132.2 (CH), 131.0 (C_q), 130.8 (CH), 128.5 (CH), 126.4 (C_q), 126.1 (CH), 88.1 (Cage C), 86.6 (Cage C), 34.9 (C_q), 31.1 (CH_3). **11 B NMR** (96 MHz, CDCl_3): δ = -3.00 (2B), -9.24 (3B), -10.43 (2B), -11.65 (3B). **IR** (ATR): 2966, 2924, 2866, 2577, 2564, 1446, 1073, 687 cm^{-1} . **MS** (EI) m/z : 384 [M] $^+$. **HR-MS** (EI): m/z calcd. for $\text{C}_{18}\text{H}_{28}^{10}\text{B}_2^{11}\text{B}_8\text{S}$ [M] $^+$: 384.2919, found: 384.2904.

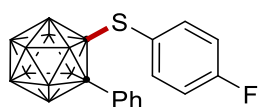


162c. The representative procedure **K** with KI (16.6 mg, 0.10 mmol) was followed using *o*-carborane **160a** (22.0 mg, 0.10 mmol) and 4-methylbenzenethiol **161c** (37.2 mg, 0.30 mmol). Isolation by column chromatography (*n*-hexane) yielded **162c** (18.9 mg, 55%) as a colorless

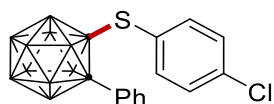
solid. **M.p.** = 146 – 148 °C. **¹H NMR** (400 MHz, CDCl₃): δ = 7.65 – 7.58 (m, 1H), 7.55 – 7.49 (m, 2H), 7.47 – 7.39 (m, 2H), 7.03 (d, *J* = 7.8 Hz, 2H), 6.79 (d, *J* = 8.2 Hz, 2H), 2.32 (s, 3H). **¹³C NMR** (101 MHz, CDCl₃): δ = 141.6 (C_q), 136.7 (CH), 132.2 (CH), 130.9 (C_q), 130.8 (CH), 129.8 (CH), 128.5 (C_q), 126.5 (CH), 88.0 (Cage C), 86.5 (Cage C), 21.37 (CH₃). **¹¹B NMR** (128 MHz, CDCl₃): δ = -2.59 (1B), -3.22 (1B), -8.51 (2B), -9.22 (2B), -10.42 (2B), -11.56 (2B). **IR** (ATR): 2954, 2598, 2568, 1973, 1492, 1446, 1179, 1073, 885 cm⁻¹. **MS** (EI) *m/z*: 342 [M]⁺. **HR-MS** (EI): *m/z* calcd. for C₁₅H₂₂¹⁰B₂¹¹B₈S [M]⁺: 342.2448, found: 342.2435.



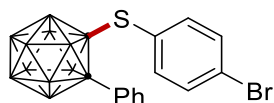
162d. The representative procedure **L** with KI (16.6 mg, 0.10 mmol) was followed using *o*-carborane **160a** (22.0 mg, 0.10 mmol) and 4-(trifluoromethyl)benzenethiol **161d** (41.1 μL, 0.30 mmol). Isolation by column chromatography (*n*-hexane) yielded **162d** (30.6 mg, 77%) as a colorless solid. **M.p.** = 84 – 86 °C. **¹H NMR** (400 MHz, CDCl₃): δ = 7.62 – 7.58 (m, 2H), 7.57 – 7.52 (m, 1H), 7.51 – 7.47 (m, 2H), 7.47 – 7.42 (m, 2H), 7.05 – 7.00 (m, 2H). **¹³C NMR** (101 MHz, CDCl₃): δ = 137.0 (CH), 133.8 (C_q), 133.0 (q, ²*J*_{C-F} = 33 Hz, C_q), 132.1 (CH), 131.0 (CH), 130.7 (C_q), 128.6 (CH), 125.9 (q, ³*J*_{C-F} = 3.7 Hz, CH), 123.4 (q, ¹*J*_{C-F} = 273 Hz, C_q), 88.0 (Cage C), 84.7 (Cage C). **¹¹B NMR** (128 MHz, CDCl₃): δ = -2.47 (2B), -9.09 (4B), -10.22 (2B), -11.48 (2B). **¹⁹F NMR** (376 MHz, CDCl₃): δ = -63.07. **IR** (ATR): 2925, 2572, 1495, 1447, 1322, 1172, 1135, 1062, 842 cm⁻¹. **MS** (EI) *m/z*: 396 [M]⁺. **HR-MS** (EI): *m/z* calcd. for C₁₅H₁₉¹⁰B₂¹¹B₈F₃S [M]⁺: 396.2165, found: 396.2158.



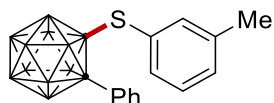
162e. The representative procedure **K** with KI (16.6 mg, 0.10 mmol) was followed using *o*-carborane **160a** (22.0 mg, 0.10 mmol) and 4-fluorobenzenethiol **161e** (32.0 μL, 0.30 mmol). Isolation by column chromatography (*n*-hexane) yielded **162e** (21.0 mg, 61%) as a colorless solid. **M.p.** = 103 – 105 °C. **¹H NMR** (400 MHz, CDCl₃): δ = 7.69 – 7.61 (m, 2H), 7.61 – 7.54 (m, 1H), 7.51 – 7.44 (m, 2H), 7.01 – 6.87 (m, 4H). **¹³C NMR** (101 MHz, CDCl₃): δ = 164.4 (d, ¹*J*_{C-F} = 254 Hz, C_q), 139.0 (d, ³*J*_{C-F} = 8.9 Hz, CH), 132.1 (CH), 130.9 (CH), 130.8 (C_q), 128.6 (CH), 125.3 (d, ⁴*J*_{C-F} = 3.6 Hz, C_q), 116.4 (d, ²*J*_{C-F} = 22 Hz, CH), 87.8 (Cage C), 85.8 (Cage C). **¹¹B NMR** (96 MHz, CDCl₃): δ = -2.67 (2B), -8.91 (4B), -10.32 (2B), -11.54 (2B). **¹⁹F NMR** (282 MHz, CDCl₃): δ = -107.68. **IR** (ATR): 2609, 2572, 2561, 1585, 1486, 1233, 1155, 835, 687 cm⁻¹. **MS** (EI) *m/z*: 346 [M]⁺. **HR-MS** (EI): *m/z* calcd. for C₁₄H₁₉¹⁰B₂¹¹B₈FS [M]⁺: 346.2197, found: 346.2185.



162f. The representative procedure **K** was followed using *o*-carborane **160a** (22.0 mg, 0.10 mmol) and 4-chlorobenzenethiol **161f** (43.0 mg, 0.30 mmol). Isolation by column chromatography (*n*-hexane) yielded **162f** (26.0 mg, 71%) as a colorless solid. **M.p.** = 108 – 110 °C. **¹H NMR** (400 MHz, CDCl₃): δ = 7.68 – 7.62 (m, 2H), 7.61 – 7.54 (m, 1H), 7.52 – 7.44 (m, 2H), 7.28 – 7.22 (m, 2H), 6.90 – 6.81 (m, 2H). **¹³C NMR** (101 MHz, CDCl₃): δ = 138.0 (CH), 137.9 (C_q), 132.1 (CH), 131.0 (CH), 130.8 (C_q), 129.4 (CH), 128.6 (CH), 128.1 (C_q), 87.9 (Cage C), 85.4 (Cage C). **¹¹B NMR** (96 MHz, CDCl₃): δ = -2.60 (2B), -8.90 (4B), -10.31 (2B), -11.54 (2B). **IR** (ATR): 2610, 2567, 1572, 1473, 1445, 1092, 1073, 746 cm⁻¹. **MS** (EI) *m/z*: 362 [M]⁺. **HR-MS** (EI): *m/z* calcd. for C₁₄H₁₉¹⁰B₂¹¹B₈³⁵ClS [M]⁺: 362.1904, found: 362.1893.

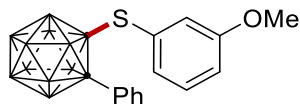


162g. The representative procedure **L** with KI (16.6 mg, 0.10 mmol) and CuI (2.9 mg, 15 mol %) was followed using *o*-carborane **160a** (22.0 mg, 0.10 mmol) and 4-bromobenzenethiol **161g** (56.1 mg, 0.30 mmol). Isolation by column chromatography (*n*-hexane) yielded **162g** (29.0 mg, 71 %) as a colorless solid. **M.p.** = 126 – 128 °C. **¹H NMR** (400 MHz, CDCl₃): δ = 7.62 – 7.58 (m, 2H), 7.56 – 7.50 (m, 1H), 7.46 – 7.41 (m, 2H), 7.39 – 7.34 (m, 2H), 6.78 – 6.70 (m, 2H). **¹³C NMR** (101 MHz, CDCl₃): δ = 138.1 (CH), 132.4 (CH), 132.1 (CH), 130.9 (CH), 130.7 (C_q), 128.6 (C_q), 128.5 (CH), 126.3 (C_q), 87.9 (Cage C), 85.2 (Cage C). **¹¹B NMR** (128 MHz, CDCl₃): δ = -2.46 (2B), -9.13 (4B), -10.31 (2B), -11.52 (2B). **IR** (ATR): 2622, 2596, 1564, 1471, 1446, 1386, 1070, 1010, 810 cm⁻¹. **MS** (EI) *m/z*: 408 [M]⁺. **HR-MS** (EI): *m/z* calcd. for C₁₄H₁₉¹¹B₁₀⁷⁹Br [M]⁺: 408.1363, found: 408.1358.

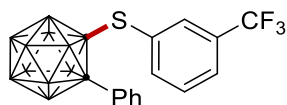


162h. The representative procedure **L** with KI (16.6 mg, 0.10 mmol) was followed using *o*-carborane **160a** (22.0 mg, 0.10 mmol) and 3-methylbenzenethiol **161h** (35.6 μL, 0.30 mmol). Isolation by column chromatography (*n*-hexane) yielded **162h** (30.3 mg, 88%) as a colorless solid. **M.p.** = 58 – 60 °C. **¹H NMR** (400 MHz, CDCl₃): δ = 7.63 – 7.59 (m, 2H), 7.56 – 7.51 (m, 1H), 7.46 – 7.41 (m, 2H), 7.20 – 7.16 (m, 1H), 7.13 (t, *J* = 7.6 Hz, 1H), 6.79 (d, *J* = 7.5 Hz, 1H),

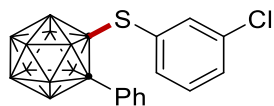
6.55 (s, 1H), 2.22 (s, 3H). ^{13}C NMR (101 MHz, CDCl_3): δ = 138.9 (C_q), 137.3 (CH), 133.6 (CH), 132.2 (CH), 131.8 (CH), 130.8 (C_q), 130.7 (CH), 129.4 (C_q), 128.8 (CH), 128.4 (CH), 87.8 (Cage C), 86.2 (Cage C), 21.1 (CH_3). ^{11}B NMR (128 MHz, CDCl_3): δ = -2.43 (1B), -3.16 (1B), -8.42 (1B), -9.16 (2B), -10.45 (3B), -11.42 (2B). IR (ATR): 2922, 2564, 1591, 1494, 1474, 1446, 1377, 885, 780 cm^{-1} . MS (EI) m/z : 342 $[\text{M}]^+$. HR-MS (EI): m/z calcd. for $\text{C}_{15}\text{H}_{22}^{10}\text{B}_2^{11}\text{B}_8\text{S}$ $[\text{M}]^+$: 342.2448, found: 342.2434.



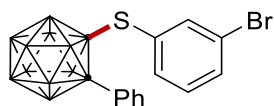
162i. The representative procedure **L** was followed using *o*-carborane **160a** (22.0 mg, 0.10 mmol) and 3-methoxybenzenethiol **161i** (37.2 μL , 0.30 mmol). Isolation by column chromatography (*n*-hexane) yielded **162i** (22.2 mg, 62%) as a colorless oil. ^1H NMR (400 MHz, CDCl_3): δ = 7.66 (d, J = 8.0 Hz, 2H), 7.59 – 7.54 (m, 1H), 7.51 – 7.44 (m, 2H), 7.18 (t, J = 8.0 Hz, 1H), 6.97 (dd, J = 8.4, 2.5 Hz, 1H), 6.56 (d, J = 7.6 Hz, 1H), 6.50 (s, 1H), 3.75 (s, 3H). ^{13}C NMR (101 MHz, CDCl_3): δ = 159.5 (C_q), 132.2 (CH), 131.0 (C_q), 130.8 (CH), 130.6 (C_q), 129.8 (CH), 129.0 (CH), 128.5 (CH), 121.5 (CH), 117.4 (CH), 88.1 (Cage C), 86.1 (Cage C), 55.4 (CH_3). ^{11}B NMR (96 MHz, CDCl_3): δ = -2.69 (2B), -9.12 (4B), -10.34 (2B), -11.44 (2B). IR (ATR): 2961, 2934, 2597, 2564, 1589, 1479, 1249, 1231, 1040, 688 cm^{-1} . MS (EI) m/z : 358 $[\text{M}]^+$. HR-MS (EI): m/z calcd. for $\text{C}_{15}\text{H}_{22}^{10}\text{B}_2^{11}\text{B}_8\text{OS}$ $[\text{M}]^+$: 358.2397, found: 358.2385.



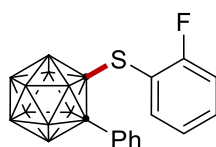
162j. The representative procedure **L** with KI (16.6 mg, 0.10 mmol) was followed using *o*-carborane **160a** (22.0 mg, 0.10 mmol) and 3-(trifluoromethyl)benzenethiol **161j** (40.8 μL , 0.30 mmol). Isolation by column chromatography (*n*-hexane) yielded **162j** (29.5 mg, 74%) as a colorless oil. ^1H NMR (400 MHz, CDCl_3): δ = 7.65 (d, J = 7.8 Hz, 1H), 7.61 – 7.52 (m, 3H), 7.47 – 7.40 (m, 3H), 7.34 – 7.30 (m, 1H), 6.93 – 6.87 (m, 1H). ^{13}C NMR (101 MHz, CDCl_3): δ = 139.9 (CH), 133.5 (q, $^3J_{\text{C-F}}$ = 3.8 Hz, CH), 132.0 (CH), 131.5 (q, $^2J_{\text{C-F}}$ = 33 Hz, C_q), 131.1 (CH), 130.8 (C_q), 130.5 (C_q), 129 (CH), 128.7 (CH), 127.9 (q, $^3J_{\text{C-F}}$ = 3.7 Hz, CH), 123.2 (q, $^1J_{\text{C-F}}$ = 273 Hz, C_q), 88.0 (Cage C), 84.9 (Cage C). ^{11}B NMR (128 MHz, CDCl_3): δ = -2.31 (2B), -9.02 (4B), -10.25 (2B), -11.46 (2B). ^{19}F NMR (376 MHz, CDCl_3): δ = -62.78. IR (ATR): 2755, 1580, 1420, 1320, 1272, 1165, 1122, 1071, 792 cm^{-1} . MS (EI) m/z : 396 $[\text{M}]^+$. HR-MS (EI): m/z calcd. for $\text{C}_{15}\text{H}_{19}^{10}\text{B}_2^{11}\text{B}_8\text{F}_3\text{S}$ $[\text{M}]^+$: 396.2165, found: 396.2154.



162k. The representative procedure **L** with KI (16.6 mg, 0.10 mmol) was followed using *o*-carborane **160a** (22.0 mg, 0.10 mmol) and 3-chlorobenzenethiol **161k** (34.5 μ L, 0.30 mmol). Isolation by column chromatography (*n*-hexane) yielded **162k** (21.4 mg, 59%) as a colorless solid. **M.p.** = 60 – 62 °C. **¹H NMR** (400 MHz, CDCl₃): δ = 7.63 – 7.52 (m, 3H), 7.49 – 7.42 (m, 2H), 7.37 (ddd, *J* = 8.1, 2.1, 1.0 Hz, 1H), 7.23 – 7.17 (m, 1H), 6.95 (ddd, *J* = 7.8, 1.7, 1.1 Hz, 1H), 6.62 (ddd, *J* = 2.1, 1.7, 0.4 Hz, 1H). **¹³C NMR** (101 MHz, CDCl₃): δ = 136.4 (CH), 134.7 (CH), 134.4 (C_q), 132.1 (CH), 131.3 (CH), 131.1 (C_q), 131.0 (CH), 130.6 (C_q), 130.1 (CH), 128.6 (CH), 87.8 (Cage C), 85.1 (Cage C). **¹¹B NMR** (128 MHz, CDCl₃): δ = -2.37 (1B), -2.90 (1B), -9.11 (4B), -10.37 (2B), -11.46 (2B). **IR** (ATR): 2922, 2565, 1573, 1459, 1398, 1116, 1071, 864, 771 cm⁻¹. **MS** (EI) *m/z*: 362 [M]⁺. **HR-MS** (EI): *m/z* calcd. for C₁₄H₁₉¹⁰B₂¹¹B₈S³⁵Cl [M]⁺: 362.1904, found: 362.1893.

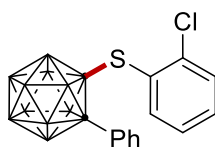


162l. The representative procedure **L** with KI (16.6 mg, 0.10 mmol) and CuI (2.9 mg, 15 mol %) was followed using *o*-carborane **160a** (22.0 mg, 0.10 mmol) and 3-bromobenzenethiol **161l** (31.0 μ L, 0.30 mmol). Isolation by column chromatography (*n*-hexane) yielded **162l** (24.1 mg, 59%) as a colorless oil. **¹H NMR** (400 MHz, CDCl₃): δ = 7.62 – 7.57 (m, 2H), 7.57 – 7.50 (m, 2H), 7.49 – 7.42 (m, 2H), 7.15 (t, *J* = 7.9 Hz, 1H), 7.02 (ddd, *J* = 7.8, 1.7, 1.1 Hz, 1H), 6.75 (t, *J* = 1.8 Hz, 1H). **¹³C NMR** (101 MHz, CDCl₃): δ = 139.2 (CH), 135.1 (CH), 134.2 (CH), 132.1 (CH), 131.4 (C_q), 131.0 (CH), 130.5 (C_q), 130.4 (CH), 128.7 (CH), 122.4 (C_q), 87.8 (Cage C), 85.1 (Cage C). **¹¹B NMR** (128 MHz, CDCl₃): δ = -2.35 (2B), -9.11 (4B), -10.37 (2B), -11.44 (2B). **IR** (ATR): 2918, 2589, 1559, 1455, 1394, 1066, 866, 770, 672 cm⁻¹. **MS** (EI) *m/z*: 408 [M]⁺. **HR-MS** (EI): *m/z* calcd. for C₁₄H₁₉¹¹B₁₀S⁷⁹Br [M]⁺: 408.1363, found: 408.1360.

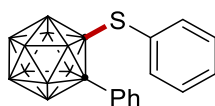


162m. The representative procedure **L** with KI (16.6 mg, 0.10 mmol) was followed using *o*-carborane **160a** (22.0 mg, 0.10 mmol) and 2-fluorobenzenethiol **161m** (32.0 μ L, 0.30 mmol). Isolation by column chromatography (*n*-hexane) yielded **162m** (18.5 mg, 53%) as a colorless solid. **M.p.** = 116 – 118 °C. **¹H NMR** (400 MHz, CDCl₃): δ = 7.73 – 7.66 (m, 2H), 7.61 – 7.54 (m,

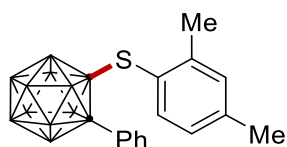
1H), 7.53 – 7.44 (m, 3H), 7.17 – 7.03 (m, 2H), 6.94 – 6.84 (m, 1H). ^{13}C NMR (101 MHz, CDCl_3): δ = 163.3 (d, $^1J_{\text{C-F}}$ = 253 Hz, C_q), 139.4 (CH), 134.1 (d, $^3J_{\text{C-F}}$ = 8.4 Hz, CH), 132.1 (CH), 130.9 (C_q), 130.9 (CH), 128.5 (CH), 124.5 (d, $^3J_{\text{C-F}}$ = 4.0 Hz, CH), 117.0 (d, $^2J_{\text{C-F}}$ = 18.2 Hz, C_q), 116.5 (d, $^2J_{\text{C-F}}$ = 23.1 Hz, CH), 88.7 (Cage C), 85.2 (Cage C). ^{11}B NMR (96 MHz, CDCl_3): δ = -2.87 (2B), -8.30 (2B), -9.21 (1B), -9.90 (3B), -11.53 (2B). ^{19}F NMR (282 MHz, CDCl_3): δ = -102.48. IR (ATR): 2598, 2557, 1470, 1261, 1223, 1067, 755, 689 cm^{-1} . MS (EI) m/z : 346 $[\text{M}]^+$. HR-MS (EI): m/z calcd. for $\text{C}_{14}\text{H}_{19}^{10}\text{B}_2^{11}\text{B}_8\text{FS}$ $[\text{M}]^+$: 346.2197, found: 346.2183.



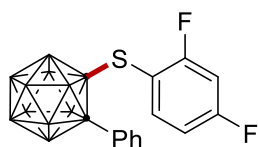
162n. The representative procedure **L** with KI (16.6 mg, 0.10 mmol) was followed using *o*-carborane **160a** (22.0 mg, 0.10 mmol) and 2-chlorobenzenethiol **161n** (33.6 μL , 0.30 mmol). Isolation by column chromatography (*n*-hexane) yielded **162n** (27.5 mg, 76%) as a colorless solid. **M.p.** = 146 – 148 $^\circ\text{C}$. ^1H NMR (400 MHz, CDCl_3): δ = 7.72 – 7.64 (m, 2H), 7.56 – 7.47 (m, 1H), 7.49 – 7.40 (m, 3H), 7.40 – 7.31 (m, 1H), 7.21 – 7.12 (m, 1H), 7.02 (d, J = 7.8 Hz, 1H). ^{13}C NMR (101 MHz, CDCl_3): δ = 141.1 (C_q), 140.0 (CH), 132.7 (CH), 132.1 (CH), 131.1 (C_q), 130.9 (CH), 130.6 (CH), 128.9 (C_q), 128.6 (CH), 127.1 (CH), 89.5 (Cage C), 85.7 (Cage C). ^{11}B NMR (128 MHz, CDCl_3): δ = -2.90 (2B), -8.40 (2B), -9.57 (4B), -11.70 (2B). IR (ATR): 2500, 1945, 1447, 1321, 1259, 1166, 1134, 1070, 749 cm^{-1} . MS (EI) m/z : 362 $[\text{M}]^+$. HR-MS (EI): m/z calcd. for $\text{C}_{14}\text{H}_{19}^{10}\text{B}_2^{11}\text{B}_8\text{S}^{35}\text{Cl}$ $[\text{M}]^+$: 362.1904, found: 362.1893.



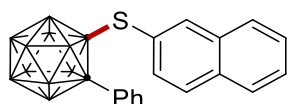
162o. The representative procedure **L** was followed using *o*-carborane **160a** (22.0 mg, 0.10 mmol) and benzenethiol **161o** (31.0 μL , 0.30 mmol). Isolation by column chromatography (*n*-hexane) yielded **162o** (20.0 mg, 61%) as a colorless solid. **M.p.** = 112 – 114 $^\circ\text{C}$. ^1H NMR (300 MHz, CDCl_3): δ = 7.66 (d, J = 7.6 Hz, 2H), 7.61 – 7.54 (m, 1H), 7.51 – 7.40 (m, 3H), 7.32 – 7.25 (m, 2H), 6.96 (d, J = 7.7 Hz, 2H). ^{13}C NMR (75 MHz, CDCl_3): δ = 136.8 (CH), 132.2 (CH), 131.1 (CH), 130.9 (C_q), 130.9 (CH), 129.8 (C_q), 129.1 (CH), 128.5 (CH), 88.1 (Cage C), 86.1 (Cage C). ^{11}B NMR (96 MHz, CDCl_3): δ = -2.78 (2B), -9.14 (3B), -10.35 (3B), -11.50 (2B). IR (ATR): 2612, 2589, 2560, 1585, 1486, 1232, 1077, 686 cm^{-1} . MS (EI) m/z : 328 $[\text{M}]^+$. HR-MS (EI): m/z calcd. for $\text{C}_{14}\text{H}_{20}^{10}\text{B}_2^{11}\text{B}_8\text{S}$ $[\text{M}]^+$: 328.2291, found: 328.2279.



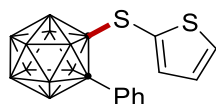
162p. The representative procedure **L** with KI (16.6 mg, 0.10 mmol) was followed using *o*-carborane **160a** (22.0 mg, 0.10 mmol) and 2,4-dimethylbenzenethiol **161p** (40.3 μ L, 0.30 mmol). Isolation by column chromatography (*n*-hexane) yielded **162p** (23.1 mg, 65%) as a colorless solid. **M.p.** = 97 – 99 °C. **¹H NMR** (400 MHz, CDCl₃): δ = 7.71 – 7.64 (m, 2H), 7.55 – 7.47 (m, 1H), 7.49 – 7.40 (m, 2H), 7.05 – 6.99 (m, 1H), 6.91 – 6.84 (m, 1H), 6.75 (d, J = 7.9 Hz, 1H), 2.29 (s, 3H), 2.21 (s, 3H). **¹³C NMR** (101 MHz, CDCl₃): δ = 143.9 (C_q), 141.9 (C_q), 138.6 (CH), 132.1 (CH), 131.7 (CH), 131.3 (C_q), 130.7 (CH), 128.6 (CH), 127.3 (CH), 126.1 (C_q), 89.5 (Cage C), 87.4 (Cage C), 21.3 (CH₃), 20.7 (CH₃). **¹¹B NMR** (128 MHz, CDCl₃): δ = -3.05 (2B), -8.58 (2B), -9.80 (4B), -11.72 (2B). **IR** (ATR): 2919, 2851, 2586, 2569, 1600, 1446, 1232, 1074, 886 cm⁻¹. **MS** (EI) m/z : 356 [M]⁺. **HR-MS** (EI): m/z calcd. for C₁₆H₂₄¹⁰B₂¹¹B₈S [M]⁺: 356.2605, found: 356.2593.



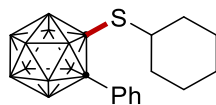
162q. The representative procedure **L** with KI (16.6 mg, 0.10 mmol) was followed using *o*-carborane **160a** (22.0 mg, 0.10 mmol) and 2,4-difluorobenzenethiol **161q** (33.1 μ L, 0.30 mmol). Isolation by column chromatography (*n*-hexane) yielded **162q** (32.8 mg, 65%) as a colorless solid. **M.p.** = 109 – 111 °C. **¹H NMR** (400 MHz, CDCl₃): δ = 7.69 – 7.60 (m, 2H), 7.56 – 7.48 (m, 1H), 7.48 – 7.39 (m, 2H), 6.88 – 6.71 (m, 3H). **¹³C NMR** (101 MHz, CDCl₃): δ = 165.4 (dd, ¹ J_{C-F} = 257 Hz, ³ J_{C-F} = 10.8 Hz, C_q), 163.9 (dd, ¹ J_{C-F} = 256 Hz, ³ J_{C-F} = 13.4 Hz, C_q), 140.6 (dd, ³ J_{C-F} = 10.2, 10.2 Hz, CH), 132.1 (CH), 131.0 (CH), 130.9 (C_q), 128.6 (CH), 112.9 (dd, ² J_{C-F} = 18.5 Hz, ⁴ J_{C-F} = 3.9 Hz, C_q), 112.2 (dd, ² J_{C-F} = 22.0 Hz, ⁴ J_{C-F} = 3.9 Hz, CH), 105.1 (dd, ² J_{C-F} = 25.8, 25.9 Hz, CH), 88.5 (Cage C), 84.9 (Cage C). **¹¹B NMR** (128 MHz, CDCl₃): δ = -2.20 (1B), -3.38 (1B), -7.71 (2B), -9.26 (2B), -10.50 (2B), -12.38 (2B). **¹⁹F NMR** (282 MHz, CDCl₃): δ = -97.08 (d, J = 11.5 Hz), -101.85 (d, J = 11.5 Hz). **IR** (ATR): 3059, 1487, 1443, 1201, 1155, 1056, 907, 734 cm⁻¹. **MS** (EI) m/z : 364 [M]⁺. **HR-MS** (EI): m/z calcd. for C₁₄H₁₈¹⁰B₂¹¹B₈SF₂ [M]⁺: 364.2102, found: 364.2098.



162r. The representative procedure **L** was followed using *o*-carborane **160a** (22.0 mg, 0.10 mmol) and naphthalene-2-thiol **161r** (43.2 mg, 0.30 mmol). Isolation by column chromatography (*n*-hexane) yielded **162r** (35.2 mg, 93%) as a colorless solid. **M.p.** = 129 – 131 °C. **¹H NMR** (400 MHz, CDCl₃): δ = 7.83 – 7.79 (m, 1H), 7.71 (d, *J* = 8.7 Hz, 1H), 7.64 – 7.44 (m, 8H), 7.18 – 7.15 (m, 1H), 7.08 (dd, *J* = 8.5, 1.8 Hz, 1H). **¹³C NMR** (101 MHz, CDCl₃): δ = 137.6 (CH), 133.9 (C_q), 132.8 (C_q), 132.3 (CH), 132.1 (CH), 130.9 (C_q), 130.8 (CH), 128.8 (CH), 128.5 (CH), 128.3 (CH), 128.0 (CH), 127.7 (CH), 126.8 (CH), 126.8 (C_q) 87.8 (Cage C), 85.9 (Cage C). **¹¹B NMR** (128 MHz, CDCl₃): δ = -2.37 (1B), -3.12 (1B), -8.44 (2B), -9.14 (2B), -10.49 (3B), -11.39 (1B). **IR** (ATR): 3057, 2594, 1581, 1494, 1446, 1072, 901, 859, 808, 743 cm⁻¹. **MS** (EI) *m/z*: 378 [M]⁺. **HR-MS** (EI): *m/z* calcd. for C₁₈H₂₂¹⁰B₂¹¹B₈S [M]⁺: 378.2449, found: 378.2436.

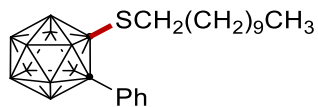


162s. The representative procedure **L** with KI (16.6 mg, 0.10 mmol) was followed using *o*-carborane **160a** (22.0 mg, 0.10 mmol) and benzenethiol **161s** (27.8 μL, 0.30 mmol). Isolation by column chromatography (*n*-hexane) yielded **162s** (18.0 mg, 54%) as a colorless solid. **M.p.** = 83 – 85 °C. **¹H NMR** (300 MHz, CDCl₃): δ = 7.68 (d, *J* = 7.6 Hz, 2H), 7.59 – 7.45 (m, 4H), 6.97 (dd, *J* = 5.3, 3.6 Hz, 1H), 6.64 (d, *J* = 3.9 Hz, 1H). **¹³C NMR** (75 MHz, CDCl₃): δ = 139.3 (CH), 134.1 (CH), 132.1 (CH), 130.9 (CH), 130.6 (C_q), 128.6 (CH), 127.7 (CH), 127.6 (C_q), 87.4 (Cage C), 85.6 (Cage C). **¹¹B NMR** (96 MHz, CDCl₃): δ = -2.70 (2B), -9.16 (3B), -10.37 (3B), -11.72 (2B). **IR** (ATR): 2922, 2852, 2605, 2589, 2559, 1399, 1218, 852, 710 cm⁻¹. **MS** (EI) *m/z*: 334 [M]⁺. **HR-MS** (EI): *m/z* calcd. for C₁₂H₁₈¹⁰B₂¹¹B₈S₂ [M]⁺: 334.1854, found: 334.1845.

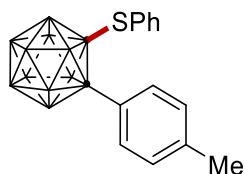


162t. The representative procedure **L** with KI (16.6 mg, 0.10 mmol) was followed using *o*-carborane **160a** (22.0 mg, 0.10 mmol) and cyclohexanethiol **161t** (35.5 μL, 0.30 mmol). Isolation by column chromatography (*n*-hexane) yielded **162t** (20.0 mg, 60%) as a colorless oil. **¹H NMR** (400 MHz, CDCl₃): δ = 7.65 – 7.58 (m, 2H), 7.47 – 7.41 (m, 1H), 7.41 – 7.33 (m, 2H), 2.76 – 2.68 (m, 1H), 1.69 – 1.60 (m, 2H), 1.51 – 1.40 (m, 2H), 1.33 – 0.98 (m, 6H). **¹³C NMR** (101 MHz, CDCl₃): δ = 131.8 (CH), 131.0 (C_q), 130.6 (CH), 128.3 (CH), 88.6 (Cage C), 87.0 (Cage C), 50.5 (CH), 33.9 (CH₂), 25.7 (CH₂), 25.0 (CH₂). **¹¹B NMR** (128 MHz, CDCl₃): δ = -2.81 (2B), -8.18 (2B), -9.37 (2B), -10.21 (2B), -11.07 (2B). **IR** (ATR): 2932, 2852, 2557, 1494, 1447, 1321, 1261, 1075, 884 cm⁻¹. **MS** (EI) *m/z*: 334 [M]⁺. **HR-MS** (EI): *m/z* calcd. for C₁₄H₂₆¹⁰B₂¹¹B₈S [M]⁺: 334.2760,

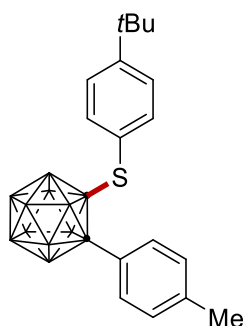
found: 334.2748.



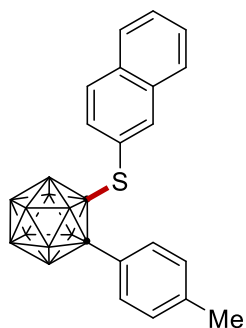
162u. The representative procedure B was followed using *o*-carborane **160a** (22.0 mg, 0.10 mmol) and 1-undecanethiol **161u** (67.9 μ L, 0.30 mmol). Isolation by column chromatography (*n*-hexane) yielded **162u** (22.0 mg, 54%) as a colorless oil. **¹H NMR** (300 MHz, CDCl₃): δ = 7.65 (d, J = 7.6 Hz, 2H), 7.52 – 7.46 (m, 1H), 7.45 – 7.37 (m, 2H), 2.65 (t, J = 7.2 Hz, 2H), 1.37 – 1.12 (m, 18H), 0.95 – 0.88 (m, 3H). **¹³C NMR** (75 MHz, CDCl₃): δ = 131.6 (CH), 131.1 (C_q), 130.7 (CH), 128.5 (CH), 88.7 (Cage C), 86.7 (Cage C), 36.9 (CH₂), 31.9 (CH₂), 29.6 (CH₂), 29.5 (CH₂), 29.3 (2CH₂), 28.8 (CH₂), 28.3 (CH₂), 28.0 (CH₂), 22.7 (CH₂), 14.1 (CH₃). **¹¹B NMR** (96 MHz, CDCl₃): δ = -2.96 (2B), -8.35 (2B), -10.02 (5B), -11.34 (1B). **IR** (ATR): 2957, 2923, 2853, 2593, 1447, 1276, 766, 750 cm⁻¹. **MS** (EI) m/z : 406 [M]⁺. **HR-MS** (EI): m/z calcd. for C₁₉H₃₈¹⁰B₂¹¹B₈S [M]⁺: 406.3702, found: 406.3694.



163a. The representative procedure L was followed using *o*-carborane **160b** (23.4 mg, 0.10 mmol) and benzenethiol **161o** (30.8 μ L, 0.30 mmol). Isolation by column chromatography (*n*-hexane) yielded **163a** (32.2 mg, 94%) as a colorless solid. **M.p.** = 114 – 116 °C. **¹H NMR** (400 MHz, CDCl₃): δ = 7.51 – 7.46 (m, 2H), 7.42 – 7.37 (m, 1H), 7.28 – 7.21 (m, 4H), 7.01 – 6.96 (m, 2H), 2.43 (s, 3H). **¹³C NMR** (101 MHz, CDCl₃): δ = 141.3 (C_q), 137.0 (CH), 132.1 (CH), 131.1 (CH), 129.9 (C_q), 129.2 (CH), 129.1 (CH), 128.2 (C_q), 88.6 (Cage C), 86.3 (Cage C), 21.2 (CH₃). **¹¹B NMR** (128 MHz, CDCl₃): δ = -2.90 (2B), -9.10 (3B), -10.40 (3B), -11.55 (2B). **IR** (ATR): 2922, 2564, 1612, 1509, 1471, 1439, 1260, 1193, 888 cm⁻¹. **MS** (EI) m/z : 342 [M]⁺. **HR-MS** (EI): m/z calcd. for C₁₅H₂₂¹⁰B₂¹¹B₈S [M]⁺: 342.2448, found: 342.2436.

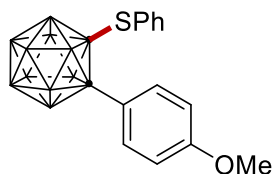


163b. The representative procedure **L** was followed using *o*-carborane **160b** (23.0 mg, 0.10 mmol) and 4-(*tert*-butyl)benzenethiol **161b** (49.9 μ L, 0.30 mmol). Isolation by column chromatography (*n*-hexane) yielded **163b** (24.7 mg, 62%) as a colorless solid. **M.p.** = 106 – 108 $^{\circ}$ C. **$^1\text{H NMR}$** (400 MHz, CDCl_3): δ = 7.51 (d, J = 8.4 Hz, 2H), 7.27 (d, J = 6.0 Hz, 2H), 7.25 (d, J = 6.0 Hz, 2H), 6.93 (d, J = 8.4 Hz, 2H), 2.45 (s, 3H), 1.30 (s, 9H). **$^{13}\text{C NMR}$** (101 MHz, CDCl_3): δ = 154.6 (C_q), 141.2 (C_q), 136.6 (CH), 132.1 (CH), 129.2 (CH), 128.3 (C_q), 126.5 (C_q), 126.1 (CH), 88.6 (Cage C), 86.7 (Cage C), 34.9 (C_q), 31.1 (CH_3), 21.2 (CH_3). **$^{11}\text{B NMR}$** (96 MHz, CDCl_3): δ = -3.14 (2B), -9.15 (3B), -10.52 (3B), -11.76 (2B). **IR** (ATR): 2962, 2924, 2852, 2594, 2572, 1460, 1259, 765 cm^{-1} . **MS** (EI) m/z : 398 [M] $^+$. **HR-MS** (EI): m/z calcd. for $\text{C}_{19}\text{H}_{30}^{10}\text{B}_2^{11}\text{B}_8\text{S}$ [M] $^+$: 398.3076, found: 398.3064.

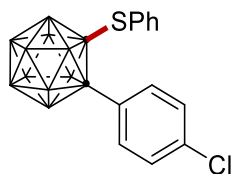


163c. The representative procedure **L** was followed using *o*-carborane **160b** (23.4 mg, 0.10 mmol) and naphthalene-2-thiol **161r** (43.2 mg, 0.30 mmol). Isolation by column chromatography (*n*-hexane) yielded **163c** (39.2 mg, 62%) as a colorless solid. **M.p.** = 165 – 166 $^{\circ}$ C. **$^1\text{H NMR}$** (400 MHz, CDCl_3): δ = 7.84 – 7.79 (m, 1H), 7.72 (dd, J = 8.5, 0.6 Hz, 1H), 7.62 – 7.58 (m, 1H), 7.57 – 7.53 (m, 1H), 7.53 – 7.47 (m, 3H), 7.27 – 7.24 (m, 2H), 7.22 (dd, J = 1.8, 0.9 Hz, 1H), 7.12 (dd, J = 8.5, 1.8 Hz, 1H), 2.49 (s, 3H). **$^{13}\text{C NMR}$** (101 MHz, CDCl_3): δ = 141.3 (C_q), 137.6 (CH), 133.9 (C_q), 132.9 (C_q), 132.2 (CH), 132.2 (CH), 129.2 (CH), 128.8 (CH), 128.2 (CH), 128.2 (C_q), 128.0 (CH), 127.7 (CH), 126.9 (C_q), 126.8 (CH), 88.1 (Cage C), 86.0 (Cage C), 21.3 (CH_3). **$^{11}\text{B NMR}$** (128 MHz, CDCl_3): δ = -2.63 (2B), -9.08 (4B), -10.53 (2B), -11.48 (2B). **IR** (ATR): 2591, 1276, 1259, 816, 766, 748 cm^{-1} . **MS** (EI) m/z : 392 [M] $^+$. **HR-MS** (EI): m/z calcd. for $\text{C}_{19}\text{H}_{24}^{10}\text{B}_2^{11}\text{B}_8\text{S}$ [M] $^+$:

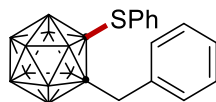
392.2606, found: 392.2600.



163d. The representative procedure **L** was followed using *o*-carborane **160c** (25.1 mg, 0.10 mmol) and benzenethiol **161o** (30.8 μ L, 0.30 mmol). Isolation by column chromatography (*n*-hexane) yielded **163d** (25.1 mg, 70%) as a colorless oil. **¹H NMR** (400 MHz, CDCl₃): δ = 7.51 (d, J = 9.0 Hz, 2H), 7.42 – 7.37 (m, 1H), 7.28 – 7.22 (m, 2H), 6.99 (dd, J = 8.3, 1.3 Hz, 2H), 6.92 (d, J = 9.0 Hz, 2H), 3.88 (s, 3H). **¹³C NMR** (101 MHz, CDCl₃): δ = 161.6 (C_q), 136.9 (CH), 133.7 (CH), 131.1 (CH), 129.9 (C_q), 129.1 (CH), 123.3 (C_q), 113.7 (CH), 88.9 (Cage C), 86.7 (Cage C), 55.5 (CH₃). **¹¹B NMR** (128 MHz, CDCl₃): δ = -3.01 (2B), -9.06 (4B), -10.52 (2B), -11.55 (2B). **IR** (ATR): 2588, 1971, 1607, 1511, 1302, 1261, 1184, 835, 748 cm⁻¹. **MS** (EI) m/z : 358 [M]⁺. **HR-MS** (EI): m/z calcd. for C₁₅H₂₂¹⁰B₂¹¹B₈SO [M]⁺: 358.2395, found: 358.2391.

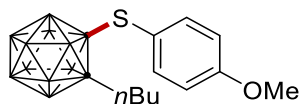


163e. The representative procedure **L** with KI (16.6 mg, 0.10 mmol) was followed using *o*-carborane **160d** (25.4 mg, 0.10 mmol) and benzenethiol **161o** (30.8 μ L, 0.30 mmol). Isolation by column chromatography (*n*-hexane) yielded **163e** (28.2 mg, 78%) as a colorless oil. **¹H NMR** (400 MHz, CDCl₃): δ = 7.55 (d, J = 8.6 Hz, 2H), 7.49 – 7.40 (m, 3H), 7.29 (t, J = 7.8 Hz, 2H), 7.00 (d, J = 7.6 Hz, 2H). **¹³C NMR** (101 MHz, CDCl₃): δ = 137.5 (C_q), 136.8 (CH), 133.4 (CH), 131.3 (CH), 129.7 (C_q), 129.6 (C_q), 129.2 (CH), 128.7 (CH), 87.1 (Cage C), 86.2 (Cage C). **¹¹B NMR** (128 MHz, CDCl₃): δ = -2.39 (1B), -3.00 (1B), -8.40 (2B), -9.20 (1B), -10.19 (3B), -11.56 (2B). **IR** (ATR): 2924, 2593, 1593, 1492, 1401, 1100, 1070, 1016, 887 cm⁻¹. **MS** (EI) m/z : 362 [M]⁺. **HR-MS** (EI): m/z calcd. for C₁₄H₁₉¹⁰B₂¹¹B₈S³⁵Cl [M]⁺: 362.1904, found: 362.1894.

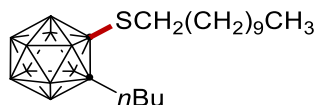


163f. The representative procedure **L** was followed using *o*-carborane **160e** (23.4 mg, 0.10 mmol) and benzenethiol **161o** (31.0 μ L, 0.30 mmol). Isolation by column chromatography (*n*-hexane) yielded **163f** (22.0 mg, 64%) as a colorless solid. **M.p.** = 119 – 121 °C. **¹H NMR** (300

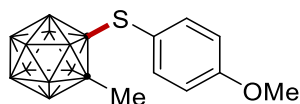
MHz, CDCl₃): δ = 7.70 – 7.66 (m, 2H), 7.60 – 7.55 (m, 1H), 7.53 – 7.46 (m, 2H), 7.43 – 7.33 (m, 3H), 7.29 – 7.25 (m, 2H), 3.80 (s, 2H). **¹³C NMR** (75 MHz, CDCl₃): δ = 137.2 (CH), 135.6 (C_q), 131.5 (CH), 130.4 (CH), 130.0 (C_q), 129.6 (CH), 128.6 (CH), 128.0 (CH), 84.3 (Cage C), 84.2 (Cage C), 40.9 (CH₂). **¹¹B NMR** (96 MHz, CDCl₃): δ = -3.85 (2B), -9.37 (4B), -10.84 (4B). **IR** (ATR): 2923, 2852, 2577, 2560, 1493, 1470, 1439, 1419, 745 cm⁻¹. **MS** (EI) *m/z*: 342 [M]⁺. **HR-MS** (EI): *m/z* calcd. for C₁₅H₂₂¹⁰B₂¹¹B₈S [M]⁺: 342.2448, found: 342.2432.



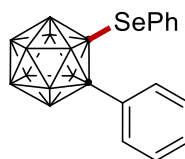
163g. The representative procedure **K** was followed using *o*-carborane **160f** (20.0 mg, 0.10 mmol) and 4-methoxybenzenethiol **161a** (36.9 μ L, 0.30 mmol). Isolation by column chromatography (*n*-hexane) yielded **163g** (18.0 mg, 53%) as a colorless oil. **¹H NMR** (400 MHz, CDCl₃): δ = 7.48 (d, *J* = 8.8 Hz, 2H), 6.94 (d, *J* = 8.7 Hz, 2H), 3.88 (s, 3H), 2.52 – 2.47 (m, 2H), 1.59 – 1.53 (m, 2H), 1.49 – 1.41 (m, 2H), 1.01 (t, *J* = 7.2 Hz, 3H). **¹³C NMR** (101 MHz, CDCl₃): δ = 162.0 (C_q), 138.8 (CH), 120.9 (C_q), 114.9 (CH), 84.7 (Cage C), 84.6 (Cage C), 55.5 (CH₃), 35.0 (CH₂), 31.8 (CH₂), 22.5 (CH₂), 13.8 (CH₃). **¹¹B NMR** (96 MHz, CDCl₃): δ = -4.27 (2B), -9.91 (4B), -10.94 (4B). **IR** (ATR): 2959, 2930, 2564, 1591, 1493, 1254, 1172, 830 cm⁻¹. **MS** (EI) *m/z*: 338 [M]⁺. **HR-MS** (EI): *m/z* calcd. for C₁₃H₂₆¹⁰B₂¹¹B₈OS [M]⁺: 338.2709, found: 338.2703.



163h. The representative procedure **L** was followed using *o*-carborane **160f** (20.0 mg, 0.10 mmol) and 1-undecanethiol **161u** (67.9 μ L, 0.30 mmol). Isolation by column chromatography (*n*-hexane) yielded **163h** (20.7 mg, 54%) as a colorless oil. **¹H NMR** (300 MHz, CDCl₃): δ = 2.86 (t, *J* = 7.2 Hz, 2H), 2.35 – 2.26 (m, 2H), 1.67 – 1.59 (m, 2H), 1.57 – 1.47 (m, 2H), 1.45 – 1.21 (m, 18H), 1.01 – 0.85 (m, 6H). **¹³C NMR** (75 MHz, CDCl₃): δ = 85.0 (Cage C), 83.9 (Cage C), 37.2 (CH₂), 34.6 (CH₂), 31.9 (CH₂), 31.8 (CH₂), 29.6 (CH₂), 29.5 (CH₂), 29.4 (CH₂), 29.3 (CH₂), 29.0 (CH₂), 28.7 (CH₂), 28.2 (CH₂), 22.7 (CH₂), 22.4 (CH₂), 14.1 (CH₃), 13.7 (CH₃). **¹¹B NMR** (96 MHz, CDCl₃): δ = -4.29 (2B), -9.85 (4B), -10.95 (4B). **IR** (ATR): 2958, 2924, 2853, 2606, 2569, 1466, 1259, 748 cm⁻¹. **MS** (EI) *m/z*: 386 [M]⁺. **HR-MS** (EI): *m/z* calcd. for C₁₇H₄₂¹⁰B₂¹¹B₈S [M]⁺: 386.4014, found: 386.4008.

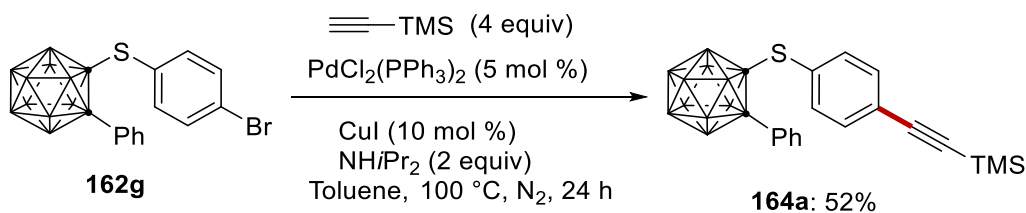


163i. The representative procedure **L** was followed using *o*-carborane **160g** (15.8 mg, 0.10 mmol) and 4-methoxybenzenethiol **161a** (36.9 μ L, 0.30 mmol). Isolation by column chromatography (*n*-hexane) yielded **163i** (20.0 mg, 68%) as a colorless solid. **M.p.** = 81 – 83 °C. **¹H NMR** (300 MHz, CDCl₃): δ = 7.49 (d, *J* = 8.9 Hz, 2H), 6.94 (d, *J* = 9.0 Hz, 2H), 3.87 (s, 3H), 2.24 (s, 3H). **¹³C NMR** (75 MHz, CDCl₃): δ = 162.0 (C_q), 138.9 (CH), 121.0 (C_q), 114.9 (CH), 82.7 (Cage C), 79.3 (Cage C), 55.5 (CH₃), 23.6 (CH₃). **¹¹B NMR** (96 MHz, CDCl₃): δ = -3.86 (1B), -4.97 (1B), -8.82 (2B), -9.90 (6B). **IR** (ATR): 2838, 2600, 2571, 2557, 1590, 1493, 1254, 828 cm⁻¹. **MS** (EI) *m/z*: 296 [M]⁺. **HR-MS** (EI): *m/z* calcd. for C₁₀H₂₀¹⁰B₂¹¹B₈OS [M]⁺: 296.2238, found: 296.2230.



163j. The representative procedure **L** was followed using *o*-carborane **160a** (22.0 mg, 0.10 mmol) and benzeneselenol **161v** (31.9 μ L, 0.30 mmol). Isolation by column chromatography (*n*-hexane) yielded **163j** (22.0 mg, 59%) as a colorless solid. **M.p.** = 112 – 114 °C. **¹H NMR** (300 MHz, CDCl₃): δ = 7.63 – 7.52 (m, 3H), 7.45 (t, *J* = 7.5 Hz, 3H), 7.29 (t, *J* = 7.6 Hz, 2H), 7.16 (d, *J* = 7.3 Hz, 2H). **¹³C NMR** (75 MHz, CDCl₃): δ = 137.6 (CH), 132.0 (CH), 131.7 (C_q), 130.8 (CH), 130.7 (CH), 129.2 (CH), 128.5 (CH), 127.1 (C_q), 86.3 (Cage C), 72.7 (Cage C). **¹¹B NMR** (96 MHz, CDCl₃): δ = -2.44 (2B), -8.29 (1B), -9.00 (1B), -9.78 (3B), -11.45 (3B). **IR** (ATR): 2630, 2609, 2572, 2561, 1585, 1486, 1233, 754 cm⁻¹. **MS** (EI) *m/z*: 376 [M]⁺. **HR-MS** (EI): *m/z* calcd. for C₁₄H₂₀¹⁰B₂¹¹B₈Se [M]⁺: 376.1729, found: 376.1726.

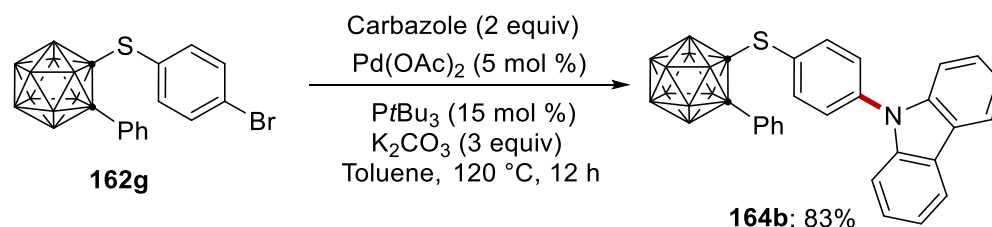
5.3.6.2 Late-stage Diversification



Compound **162g** (40.7 mg, 0.10 mmol), trimethylsilylacetylene (56.5 μ L, 0.40 mmol), PdCl₂(PPh₃)₂ (3.5 mg, 0.005 mmol), CuI (1.9 mg, 0.01 mmol) and NH*t*Pr₂ (28.2 μ L, 0.20 mmol) were combined together in toluene (2.5 mL). The resulting mixture was heated at 100 °C for 24 h

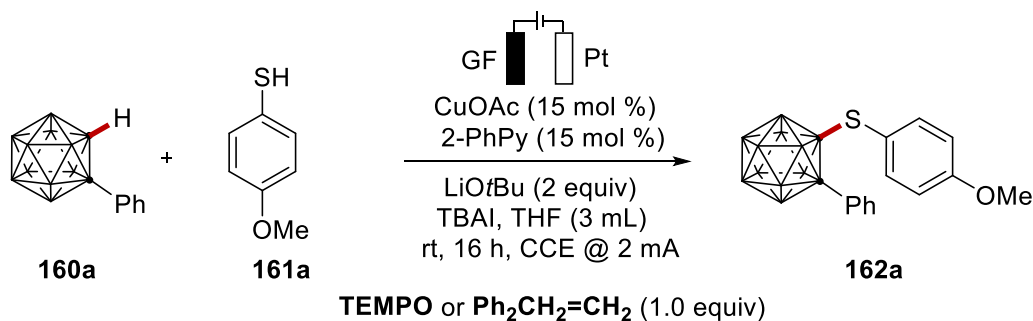
Experimental Section

under N₂. Then, the reaction was quenched with water (10 mL) and extracted with diethyl ether (10 mL x 3). The organic layers were combined and concentrated to dryness in vacuo. The residue was subjected to flash column chromatography on silica gel using n-hexane as eluent to give the product **164a** as a colorless oil (52%). **¹H NMR** (300 MHz, CDCl₃): δ = 7.66 – 7.60 (m, 2H), 7.60 – 7.53 (m, 1H), 7.47 (t, *J* = 7.6 Hz, 2H), 7.34 (d, *J* = 8.0 Hz, 2H), 6.86 (d, *J* = 8.0 Hz, 2H), 0.28 (s, 9H). **¹³C NMR** (101 MHz, CDCl₃): δ = 136.6 (CH), 132.5 (CH), 132.3 (CH), 131.0 (CH), 130.9 (C_q), 129.9 (C_q), 128.7 (CH), 126.3 (C_q), 103.6 (C_q), 98.0 (C_q), 88.1 (Cage C), 85.8 (Cage C), 0.0 (CH₃). **¹¹B NMR** (96 MHz, CDCl₃): δ = -2.65 (2B), -8.99 (3B), -10.46 (5B). **IR** (ATR): 2958, 2923, 2594, 2575, 2158, 1480, 1250, 862, 841 cm⁻¹. **MS** (EI) *m/z*: 424 [M]⁺. **HR-MS** (EI): *m/z* calcd. for C₁₉H₂₈¹⁰B₂¹¹B₈SSi [M]⁺: 424.2690, found: 424.2678.

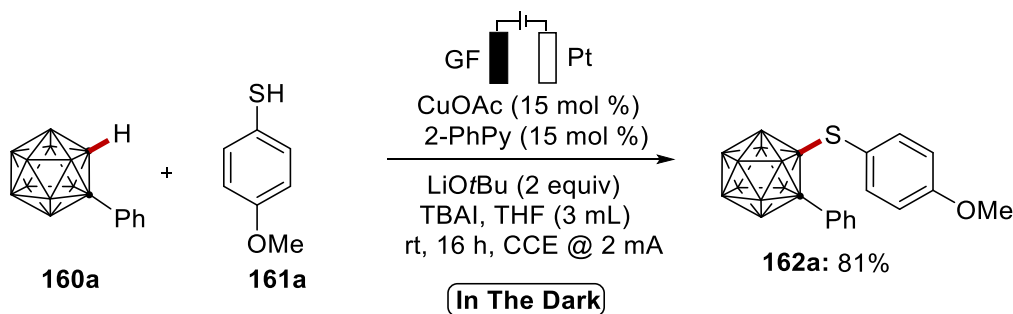


Compound **162g** (40.7 mg, 0.10 mmol), carbazole (33.4 mg, 0.20 mmol), Pd(OAc)₂ (1.1 mg, 0.005 mmol), PtBu₃ (3.0 mg, 0.015 mmol), and K₂CO₃ (41.4 mg, 0.30 mmol) were combined together in toluene (2.5 mL). The resulting mixture was heated at 120 °C for 12 h. Then, the reaction was quenched with water (10 mL) and extracted with diethyl ether (10 mL x 3). The organic layers were combined and concentrated to dryness in vacuo. The residue was subjected to flash column chromatography on silica gel using n-hexane and ethyl acetate (20/1) as eluent to give the product **164b** as a colorless solid (83%). M.p. = 214 – 216 °C. **¹H NMR** (300 MHz, CDCl₃): δ = 8.14 (d, *J* = 7.8 Hz, 2H), 7.70 (d, *J* = 7.7 Hz, 2H), 7.58 – 7.53 (m, 1H), 7.49 (d, *J* = 8.5 Hz, 4H), 7.45 – 7.39 (m, 4H), 7.32 (ddd, *J* = 8.0, 6.1, 2.1 Hz, 2H), 7.14 (d, *J* = 8.4 Hz, 2H). **¹³C NMR** (101 MHz, CDCl₃): δ = 140.5 (C_q), 140.1 (C_q), 138.4 (CH), 132.2 (CH), 131.0 (CH), 130.9 (C_q), 128.6 (CH), 128.0 (C_q), 127.0 (CH), 126.2 (CH), 123.8 (C_q), 120.7 (CH), 120.5 (CH), 109.6 (CH), 87.9 (Cage C), 85.7 (Cage C). **¹¹B NMR** (96 MHz, CDCl₃): δ = -2.51 (2B), -9.09 (4B), -10.13 (4B). **IR** (ATR): 2921, 2851, 2595, 2565, 2555, 1586, 1446, 1223, 720 cm⁻¹. **MS** (EI) *m/z*: 493 [M]⁺. **HR-MS** (EI): *m/z* calcd. for C₂₆H₂₇¹⁰B₂¹¹B₈NS [M]⁺: 493.2875, found: 493.2861.

5.3.6.3 Mechanistic Studies



The general procedure **K** was followed using *o*-carborane **160a** (0.10 mmol, 1.0 equiv), 4-methoxybenzenethiol **161a** (36.9 μL , 0.30 mmol) and TEMPO or $\text{Ph}_2\text{CH}_2=\text{CH}_2$ (0.1 mmol, 1.0 equiv). Electrocatalysis was performed at room temperature with a constant current of 2.0 mA maintained for 16 h. The GF anode was washed with ethyl acetate (3 \times 10 mL). Evaporation of the solvent and subsequent purification by column chromatography on silica gel with *n*-hexane afforded the corresponding product **162a** (TEMPO: 75%, $\text{Ph}_2\text{CH}_2=\text{CH}_2$: 72%).



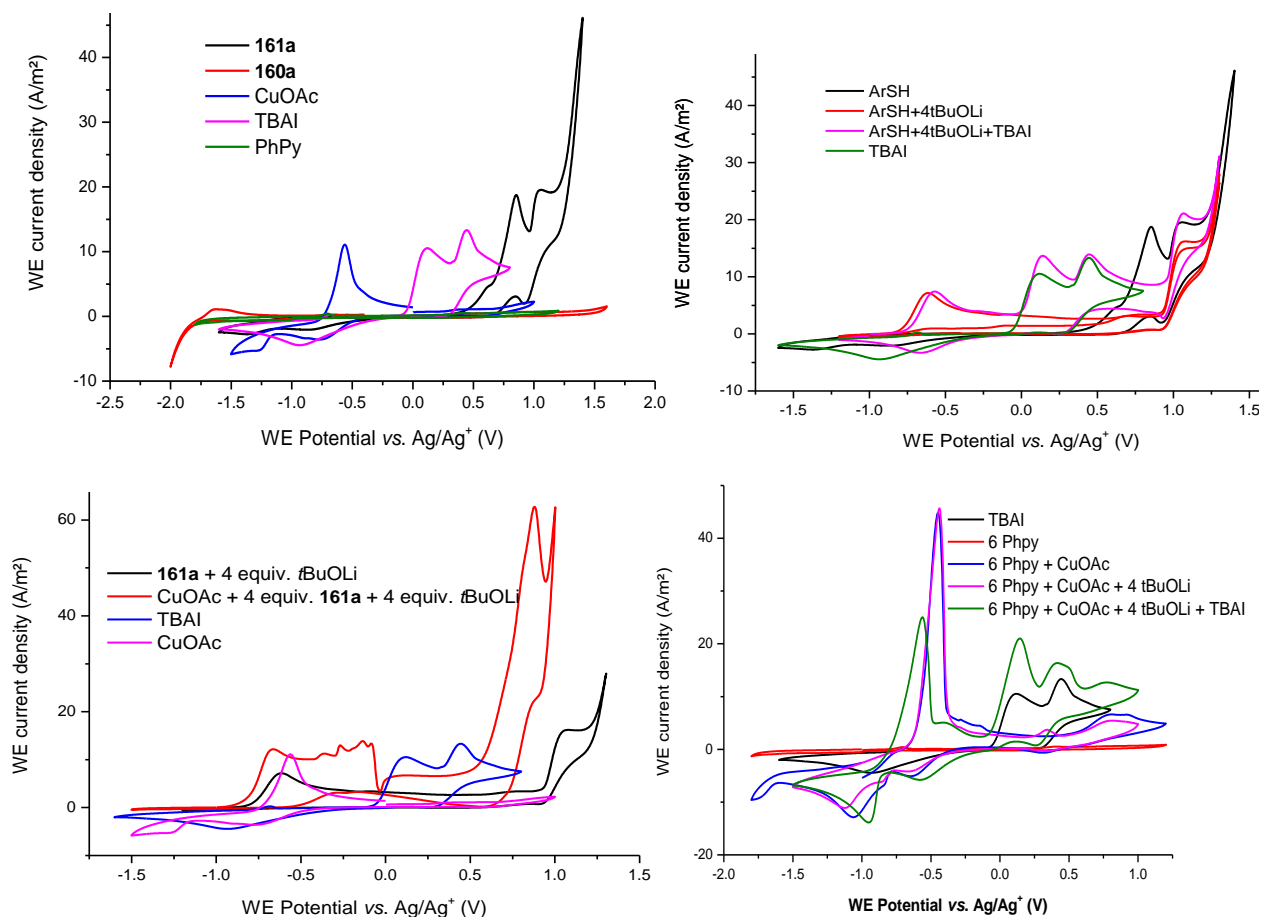
The general procedure **K** was followed using *o*-carborane **160a** (0.10 mmol, 1.0 equiv), 4-methoxybenzenethiol **161a** (36.9 μL , 0.30 mmol). Electrocatalysis was performed in the dark at room temperature with a constant current of 2.0 mA maintained for 16 h. The GF anode was washed with ethyl acetate (3 \times 10 mL). Evaporation of the solvent and subsequent purification by column chromatography on silica gel with *n*-hexane afforded the corresponding product **162a** (81%).

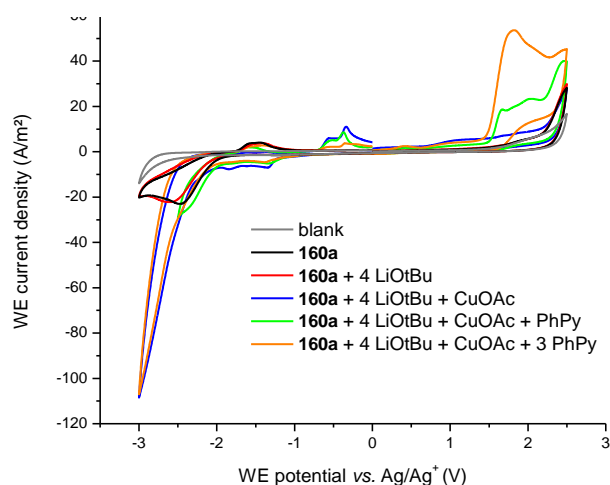
5.3.6.4 Cyclic Voltammetry

CV measurements were conducted by Alexej Scheremetjew with a Metrohm Autolab PGSTAT204 potentiostat and Nova 2.1 software. A glassy carbon working electrode (disk, diameter: 3mm), a coiled platinum wire counter electrode and a non-aqueous Ag/Ag^+ reference electrode (ALS Japan, 10 mmol/L AgNO_3 and 100 mmol/L *n*- Bu_4NPF_6 in acetonitrile) were

Experimental Section

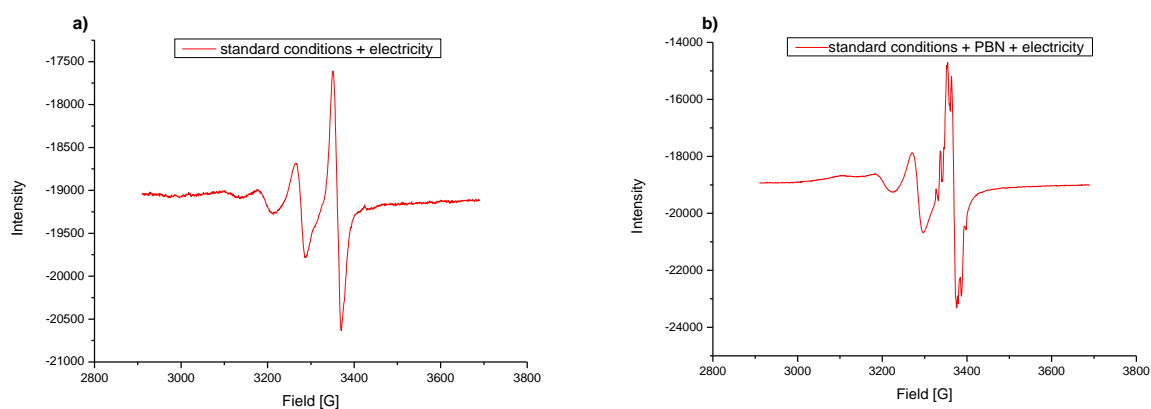
employed. The voltammograms were recorded at room temperature in dry acetonitrile at a substrate concentration of 5 mmol/L and with 100 mmol/L $n\text{-Bu}_4\text{NPF}_6$ as supporting electrolyte. Prior to each measurement, the working electrode was thoroughly polished with 0.05 μm alumina polishing powder and rinsed with water and methanol. All measured solutions were saturated with nitrogen gas and an overpressure of protective gas was maintained throughout the experiment. The nitrogen gas was previously saturated with solvent vapour by passing it through a gas washing bottle with acetonitrile. The scan rate is 100 mV/s. Deviations from the general experimental conditions are indicated in the respective figures.





5.3.6.5 EPR studies

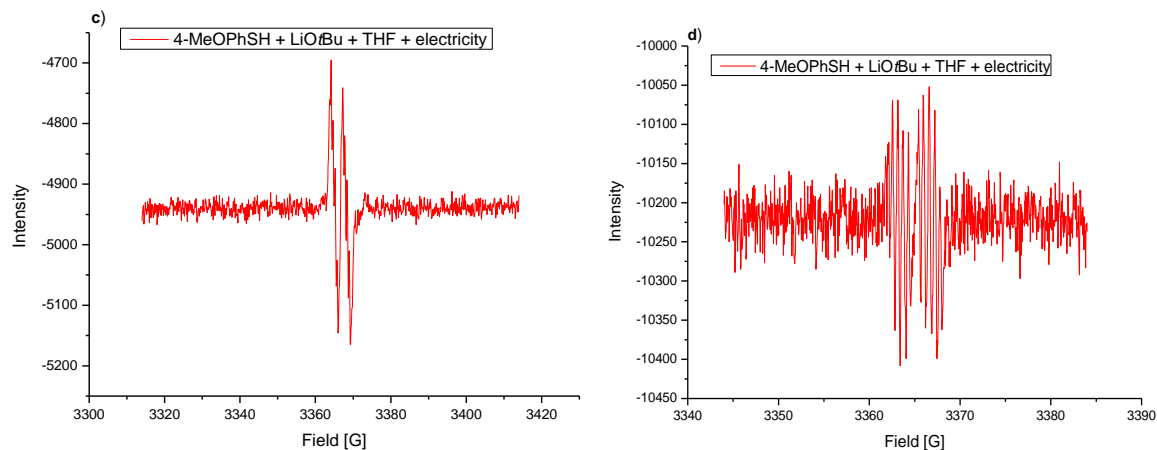
(EPR spectroscopy analysis did by Dr. A. Claudia Stcökl). The electrocatalysis was carried out in an undivided cell under air, with a graphite felt (GF) anode (10 mm × 15 mm × 6 mm) and a platinum cathode (10 mm × 15 mm × 0.25 mm). *o*-Carborane **160a** (0.10 mmol, 1.0 equiv), 4-methoxybenzenethiol **161a** (0.30 mmol, 3.0 equiv), CuOAc (15 mol %), 2-PhPy (15 mol %), LiOtBu (0.2 mmol, 2.0 equiv) and TBAI (0.2 mmol, 2.0 equiv) were dissolved in THF (3.0 mL). Electrocatalysis was performed at room temperature with a constant current of 2.0 mA maintained for 2 h. Then PBN (*N*-tert-butyl- α -Phenylnitrone) (5 equiv.) (if noted) was added into the reaction system. After stirring 2 minutes, the mixture was immediately transferred into the EPR tube for EPR measurement.



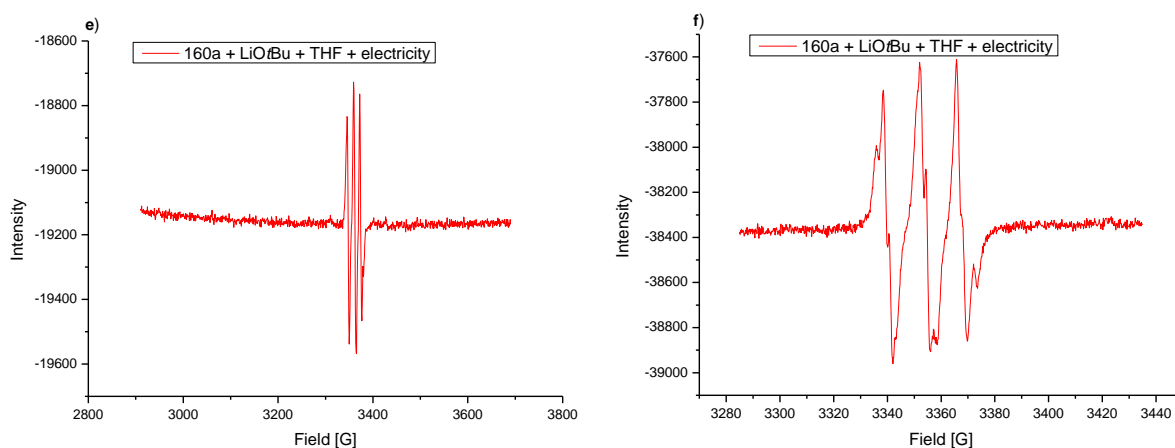
The electrocatalysis was carried out in an undivided cell under air, with a graphite felt (GF) anode (10 mm × 15 mm × 6 mm) and a platinum cathode (10 mm × 15 mm × 0.25 mm). 4-methoxybenzenethiol **161a** (0.30 mmol) and LiOtBu (0.2 mmol) were dissolved in THF (3.0 mL). Electrocatalysis was performed at room temperature with a constant current of 2.0 mA maintained for 2 h. Then PBN (*N*-tert-butyl- α -Phenylnitrone) (5 equiv.) was added into the reaction system. After stirring 2 minutes, the mixture was immediately transferred into the EPR

Experimental Section

tube for EPR measurement. This EPR result showed a small radical signal, which is not stable for longer time even after trapping with PBN and might be attributed to one of the possible thiols containing radical species.^[239]



The electrocatalysis was carried out in an undivided cell under air, with a graphite felt (GF) anode (10 mm × 15 mm × 6 mm) and a platinum cathode (10 mm × 15 mm × 0.25 mm). *o*-carborane **160a** (0.10 mmol) and LiOtBu (0.2 mmol) were dissolved in THF (3.0 mL). Electrocatalysis was performed at room temperature with a constant current of 2.0 mA maintained for 2 h. Then PBN (*N*-tert-butyl- α -Phenylnitron) (5 equiv.) was added into the reaction system. After stirring 2 minutes, the mixture was immediately transferred into the EPR tube for EPR measurement.



6. Reference

- [1] a) J. Xie, H. Jin, A. S. K. Hashmi, *Chem. Soc. Rev.* **2017**, *46*, 5193–5203; b) C. C. Johansson Seechurn, M. O. Kitching, T. J. Colacot, V. Snieckus, *Angew. Chem. Int. Ed.* **2012**, *51*, 5062–5085.
- [2] a) Q. Wang, Y. Su, L. Li, H. Huang, *Chem. Soc. Rev.* **2016**, *45*, 1257–1272; b) C. Shen, P. Zhang, Q. Sun, S. Bai, T. S. Hor, X. Liu, *Chem. Soc. Rev.* **2015**, *44*, 291–314.
- [3] a) J. Börgel, T. Ritter, *Chem* **2020**, *6*, 1877–1887; b) W. Wang, M. M. Lorion, J. Shah, A. R. Kapdi, L. Ackermann, *Angew. Chem. Int. Ed.* **2018**, *57*, 14700–14717; c) D. J. Schipper, K. Fagnou, *Chem. Mater.* **2011**, *23*, 1594–1600.
- [4] S. A. Matlin, G. Mehta, H. Hopf, A. Krief, *Nat. Chem.* **2016**, *8*, 393–398.
- [5] a) P. T. Anastas, J. C. Warner, *Green Chemistry: Theory and Practice*, Oxford Universal Press, Oxford, **1998**; b) P. T. Anastas, T. C. Williamson, *Green Chemistry: Designing Chemistry for the Environment*, ACS Publications, Washington, D.C., **1996**.
- [6] C. Glaser, *Ber. Dtsch. Chem. Ges.* **1869**, *2*, 422–424.
- [7] a) P. E. Fanta, *Synthesis* **1974**, *1974*, 9–21; b) F. Ullmann, J. Bielecki, *Ber. Dtsch. Chem. Ges.* **1901**, *34*, 2174–2185.
- [8] a) N. Miyaura, A. Suzuki, *Chem. Rev.* **1995**, *95*, 2457–2483; b) N. Miyaura, K. Yamada, A. Suzuki, *Tetrahedron Lett.* **1979**, *20*, 3437–3440.
- [9] a) J. K. Stille, *Angew. Chem. Int. Ed.* **1986**, *25*, 508–524; b) D. Milstein, J. K. Stille, *J. Am. Chem. Soc.* **1978**, *100*, 3636–3638; c) M. Kosugi, Y. Shimizu, T. Migita, *Chem. Lett.* **1977**, *6*, 1423–1424.
- [10] a) T. Hiyama, in *Metal-Catalyzed Cross-Coupling Reactions* (Eds.: A. de Meijere, F. Diederich), Wiley-VCH, Weinheim, **1998**; b) M. Fujita, T. Hiyama, *J. Org. Chem.* **1988**, *53*, 5415–5421; c) T. Hiyama, M. Obayashi, I. Mori, H. Nozaki, *J. Org. Chem.* **1983**, *48*, 912–914.
- [11] K. Tamao, Y. Kiso, K. Sumitani, M. Kumada, *J. Am. Chem. Soc.* **1972**, *94*, 9268–9269.
- [12] a) E.-I. Negishi, *Acc. Chem. Res.* **1982**, *15*, 340–348; b) E.-I. Negishi, A. O. King, N. Okukado, *J. Org. Chem.* **1977**, *42*, 1821–1823; c) S. Baba, E.-I. Negishi, *J. Am. Chem. Soc.* **1976**, *98*, 6729–6731.
- [13] a) J. F. Hartwig, *Nature* **2008**, *455*, 314–322; b) A. R. Muci, S. L. Buchwald, *Top. Curr. Chem.* **2002**, *219*, 131–209; c) J. F. Hartwig, *Angew. Chem. Int. Ed.* **1998**, *37*, 2046–2067.
- [14] a) H. Lin, D. Sun, *Org. Prep. Proced. Int.* **2013**, *45*, 341–394; b) F. Monnier, M. Taillefer, *Angew. Chem. Int. Ed.* **2009**, *48*, 6954–6971.
- [15] J. X. Qiao, P. Y. S. Lam, *Synthesis* **2011**, 829–856.
- [16] The nobel prize in chemistry 2010 - press release: https://www.nobelprize.org/nobel_prizes/chemistry/laureates/2010/press.html (accessed on 07.02.2021).
- [17] L. Ackermann, *Modern Arylation Methods*, Wiley-VCH: Weinheim, **2009**.
- [18] a) T. Rogge, N. Kaplaneris, N. Chatani, J. Kim, S. Chang, B. Punji, L. L. Schafer, D. G. Musaev, J. Wencel-Delord, C. A. Roberts, R. Sarpong, Z. E. Wilson, M. A. Brimble, M. J. Johansson, L. Ackermann, *Nat. Rev. Methods Primers* **2021**, *1*, 43; b) L. Guillemard, N. Kaplaneris, L. Ackermann, M. J. Johansson, *Nat. Rev. Chem.* **2021**, *5*, 522–545; c) S. Rej, Y. Ano, N. Chatani, *Chem. Rev.* **2020**, *120*, 1788–1887; d) F. Colobert, J. Wencel-Delord, *C–H Activation for Asymmetric Synthesis*, Wiley-VCH, Weinheim, **2019**; e) L. Ackermann, T. B. Gunnoe, L. G. Habgood, *Catalytic Hydroarylation of Carbon-Carbon Multiple Bonds*, Wiley-VCH, Weinheim, **2017**; f) P. H. Dixneuf, H. Doucet, *C–H Bond Activation and Catalytic Functionalization II*, Springer International Publishing, Switzerland, **2016**; g) P. H. Dixneuf, H. Doucet, *C–H Bond Activation and Catalytic Functionalization I*, Springer International Publishing, Switzerland, **2016**; h) J. J. Li, *C–H Bond Activation in Organic Synthesis*, CRC Press, Taylor & Francis Group, LLC, **2015**; i) X. Ribas, *C–H and C–X Bond Functionalization: Transition Metal Mediation*, Royal Society of Chemistry, Thomas Graham House, Cambridge, **2013**; j) J.-Q. Yu, Z. Shi, *C–H Activation*, Springer-Verlag Berlin,

Reference

- Heidelberg, **2010**.
- [19] a) R. C. Samanta, T. H. Meyer, I. Siewert, L. Ackermann, *Chem. Sci.* **2020**, *11*, 8657–8670; b) P. Gandeepan, L. H. Finger, T. H. Meyer, L. Ackermann, *Chem. Soc. Rev.* **2020**, *49*, 4254–4272; c) L. Ackermann, S.-L. You, M. Oestreich, S. Meng, D. MacFarlane, Y. Yin, *Trends Chem.* **2020**, *2*, 275–277; d) T. H. Meyer, L. H. Finger, P. Gandeepan, L. Ackermann, *Trends Chem.* **2019**, *1*, 63–76.
- [20] a) S. A. Girard, T. Knauber, C.-J. Li, *Angew. Chem. Int. Ed.* **2014**, *53*, 74–100; b) C. S. Yeung, V. M. Dong, *Chem. Rev.* **2011**, *111*, 1215–1292; c) C. J. Scheuermann, *Chem. Asian J.* **2010**, *5*, 436–451; d) C.-J. Li, Z. Li, *Pure Appl. Chem.* **2006**, *78*, 935–945.
- [21] a) D. L. Davies, S. A. Macgregor, C. L. McMullin, *Chem. Rev.* **2017**, *117*, 8649–8709; b) L. Ackermann, *Chem. Rev.* **2011**, *111*, 1315–1345; c) D. Balcells, E. Clot, O. Eisenstein, *Chem. Rev.* **2010**, *110*, 749–823.
- [22] H. Yi, G. Zhang, H. Wang, Z. Huang, J. Wang, A. K. Singh, A. Lei, *Chem. Rev.* **2017**, *117*, 9016–9085.
- [23] a) J. R. Webb, S. A. Burgess, T. R. Cundari, T. B. Gunnoe, *Dalton Trans.* **2013**, *42*, 16646–16665; b) T. G. P. Harper, P. J. Desrosiers, T. C. Flood, *Organometallics* **1990**, *9*, 2523–2528.
- [24] J. Kua, X. Xu, R. A. Periana, W. A. Goddard, *Organometallics* **2002**, *21*, 511–525.
- [25] Z. Lin, *Coord. Chem. Rev.* **2007**, *251*, 2280–2291.
- [26] a) T. R. Cundari, T. R. Klinckman, P. T. Wolczanski, *J. Am. Chem. Soc.* **2002**, *124*, 1481–1487; b) J. L. Bennett, P. T. Wolczanski, *J. Am. Chem. Soc.* **1997**, *119*, 10696–10719; c) C. C. Cummins, S. M. Baxter, P. T. Wolczanski, *J. Am. Chem. Soc.* **1988**, *110*, 8731–8733; d) P. J. Walsh, F. J. Hollander, R. G. Bergman, *J. Am. Chem. Soc.* **1988**, *110*, 8729–8731.
- [27] J. M. Duff, B. L. Shaw, *J. Chem. Soc., Dalton Trans.* **1972**, 2219–2225.
- [28] S. I. Gorelsky, D. Lapointe, K. Fagnou, *J. Am. Chem. Soc.* **2008**, *130*, 10848–10849.
- [29] a) Y. Boutadla, D. L. Davies, S. A. Macgregor, A. I. Poblador-Bahamonde, *Dalton Trans.* **2009**, 5887–5893; b) D. L. Davies, S. M. A. Donald, S. A. Macgregor, *J. Am. Chem. Soc.* **2005**, *127*, 13754–13755.
- [30] a) D. Zell, M. Bursch, V. Müller, S. Grimme, L. Ackermann, *Angew. Chem. Int. Ed.* **2017**, *56*, 10378–10382; b) W. Ma, R. Mei, G. Tenti, L. Ackermann, *Chem. Eur. J.* **2014**, *20*, 15248–15251.
- [31] T. Rogge, J. C. A. Oliveira, R. Kuniyil, L. Hu, L. Ackermann, *ACS Catal.* **2020**, *10*, 10551–10558.
- [32] J. M. Brown, S. Murai, H. Alper, A. Furstner, P. Dixneuf, R. Gossage, S. Murai, V. Grushin, L. Hegedus, M. Hidai, *Activation of Unreactive Bonds and Organic Synthesis*, Springer-Verlag Berlin, Heidelberg, **1999**.
- [33] a) K. Shen, Y. Fu, J.-N. Li, L. Liu, Q.-X. Guo, *Tetrahedron* **2007**, *63*, 1568–1576; b) L. Ackermann, in *Directed Metallation* (Ed.: N. Chatani), Springer Berlin Heidelberg, Berlin, Heidelberg, **2007**, pp. 35–60.
- [34] a) G. Cera, L. Ackermann, *Top. Curr. Chem.* **2016**, *374*, 191–224; b) L. Ackermann, J. Li, *Nat. Chem.* **2015**, *7*, 686–687; c) L. Ackermann, R. Vicente, *Top. Curr. Chem.* **2010**, *292*, 211–229; d) L. Ackermann, R. Vicente, A. R. Kapdi, *Angew. Chem. Int. Ed.* **2009**, *48*, 9792–9826.
- [35] a) L. Ackermann, K. Korvorapun, R. C. Samanta, T. Rogge, *Synthesis* **2021**, *53*, 2911–2946; b) P. Gandeepan, L. Ackermann, *Chem* **2018**, *4*, 199–222; c) J. Li, S. De Sarkar, L. Ackermann, *Top. Organomet. Chem.* **2016**, *55*, 217–257.
- [36] J. A. Leitch, C. G. Frost, *Chem. Soc. Rev.* **2017**, *46*, 7145–7153.
- [37] a) M. Font, J. M. Quibell, G. J. P. Perry, I. Larrosa, *Chem. Commun.* **2017**, *53*, 5584–5597; b) N. Y. P. Kumar, A. Bechtoldt, K. Raghuvanshi, L. Ackermann, *Angew. Chem. Int. Ed.* **2016**, *55*, 6929–6932.
- [38] a) J. Wang, G. Dong, *Chem. Rev.* **2019**, *119*, 7478–7528; b) M. Catellani, F. Frignani, A. Rangoni, *Angew. Chem. Int. Ed.* **1997**, *36*, 119–122.
- [39] J. Chatt, J. M. Davidson, *J. Chem. Soc.* **1965**, 843–855.
- [40] L. N. Lewis, J. F. Smith, *J. Am. Chem. Soc.* **1986**, *108*, 2728–2735.
- [41] S. Murai, F. Kakiuchi, S. Sekine, Y. Tanaka, A. Kamatani, M. Sonoda, N. Chatani, *Nature* **1993**, *366*, 529–531.

Reference

- [42] H. Weissman, X. Song, D. Milstein, *J. Am. Chem. Soc.* **2001**, *123*, 337–338.
- [43] a) S. Oi, E. Aizawa, Y. Ogino, Y. Inoue, *J. Org. Chem.* **2005**, *70*, 3113–3119; b) S. Oi, S. Fukita, N. Hirata, N. Watanuki, S. Miyano, Y. Inoue, *Org. Lett.* **2001**, *3*, 2579–2581.
- [44] S. G. Ouellet, A. Roy, C. Molinaro, R. Angelaud, J.-F. Marcoux, P. D. O’Shea, I. W. Davies, *J. Org. Chem.* **2011**, *76*, 1436–1439.
- [45] L. Ackermann, *Org. Lett.* **2005**, *7*, 3123–3125.
- [46] a) L. Ackermann, *Org. Process Res. Dev.* **2015**, *19*, 260–269; b) L. Ackermann, *Acc. Chem. Res.* **2014**, *47*, 281–295.
- [47] L. Ackermann, R. Vicente, A. Althammer, *Org. Lett.* **2008**, *10*, 2299–2302.
- [48] a) M. Schinkel, I. Marek, L. Ackermann, *Angew. Chem. Int. Ed.* **2013**, *52*, 3977–3980; b) L. Ackermann, *Chem. Commun.* **2010**, *46*, 4866–4877; c) L. Ackermann, P. Novák, R. Vicente, N. Hofmann, *Angew. Chem. Int. Ed.* **2009**, *48*, 6045–6048.
- [49] a) X. Yang, Y. Sun, Z. Chen, Y. Rao, *Adv. Syn. Catal.* **2014**, *356*, 1625–1630; b) F. Yang, K. Rauch, K. Kettelhoit, L. Ackermann, *Angew. Chem. Int. Ed.* **2014**, *53*, 11285–11288; c) V. S. Thirunavukkarasu, S. I. Kozhushkov, L. Ackermann, *Chem. Commun.* **2014**, *50*, 29–39.
- [50] L. Wang, L. Ackermann, *Chem. Commun.* **2014**, *50*, 1083–1085.
- [51] W. Liu, L. Ackermann, *Chem. Commun.* **2014**, *50*, 1878–1881.
- [52] a) L. Wang, L. Ackermann, *Org. Lett.* **2013**, *15*, 176–179; b) W. Ma, K. Graczyk, L. Ackermann, *Org. Lett.* **2012**, *14*, 6318–6321; c) B. Li, H. Feng, N. Wang, J. Ma, H. Song, S. Xu, B. Wang, *Chem. Eur. J.* **2012**, *18*, 12873–12879; d) L. Ackermann, L. Wang, A. V. Lygin, *Chem. Sci.* **2012**, *3*, 177–180; e) L. Ackermann, A. V. Lygin, *Org. Lett.* **2012**, *14*, 764–767; f) L. Ackermann, A. V. Lygin, N. Hofmann, *Org. Lett.* **2011**, *13*, 3278–3281; g) L. Ackermann, A. V. Lygin, N. Hofmann, *Angew. Chem. Int. Ed.* **2011**, *50*, 6379–6382.
- [53] a) M. Deponti, S. I. Kozhushkov, D. S. Yufit, L. Ackermann, *Org. Biomol. Chem.* **2013**, *11*, 142–148; b) V. S. Thirunavukkarasu, M. Donati, L. Ackermann, *Org. Lett.* **2012**, *14*, 3416–3419; c) R. K. Chinnagolla, M. Jeganmohan, *Chem. Commun.* **2012**, *48*, 2030–2032; d) L. Ackermann, J. Pospech, K. Graczyk, K. Rauch, *Org. Lett.* **2012**, *14*, 930–933.
- [54] L. Ackermann, *Acc. Chem. Res.* **2014**, *47*, 281–295.
- [55] T. Ueyama, S. Mochida, T. Fukutani, K. Hirano, T. Satoh, M. Miura, *Org. Lett.* **2011**, *13*, 706–708.
- [56] a) C. Tirlor, L. Ackermann, *Tetrahedron* **2015**, *71*, 4543–4551; b) B. Li, K. Devaraj, C. Darcel, P. H. Dixneuf, *Green Chem.* **2012**, *14*, 2706–2709; c) H. Yuto, U. Takumi, F. Tatsuya, H. Koji, S. Tetsuya, M. Masahiro, *Chem. Lett.* **2011**, *40*, 1165–1166; d) P. B. Arockiam, C. Fischmeister, C. Bruneau, P. H. Dixneuf, *Green Chem.* **2011**, *13*, 3075–3078.
- [57] a) K. Padala, M. Jeganmohan, *Org. Lett.* **2012**, *14*, 1134–1137; b) K. Padala, M. Jeganmohan, *Org. Lett.* **2011**, *13*, 6144–6147.
- [58] a) K. Padala, S. Pimparkar, P. Madasamy, M. Jeganmohan, *Chem. Commun.* **2012**, *48*, 7140–7142; b) K. Graczyk, W. Ma, L. Ackermann, *Org. Lett.* **2012**, *14*, 4110–4113.
- [59] a) M. C. Reddy, M. Jeganmohan, *Eur. J. Org. Chem.* **2013**, 1150–1157; b) J. Li, C. Kornhaas, L. Ackermann, *Chem. Commun.* **2012**, *48*, 11343–11345.
- [60] W. Ma, L. Ackermann, *Chem. Eur. J.* **2013**, *19*, 13925–13928.
- [61] a) L.-Q. Zhang, S. Yang, X. Huang, J. You, F. Song, *Chem. Commun.* **2013**, *49*, 8830–8832; b) B. Li, J. Ma, W. Xie, H. Song, S. Xu, B. Wang, *J. Org. Chem.* **2013**, *78*, 9345–9353.
- [62] a) J. Zhang, T.-P. Loh, *Chem. Commun.* **2012**, *48*, 11232–11234; b) Y. Hashimoto, T. Ortloff, K. Hirano, T. Satoh, C. Bolm, M. Miura, *Chem. Lett.* **2012**, *41*, 151–153; c) L. Ackermann, L. Wang, R. Wolfram, A. V. Lygin, *Org. Lett.* **2012**, *14*, 728–731.
- [63] a) F. Yang, L. Ackermann, *J. Org. Chem.* **2014**, *79*, 12070–12082; b) C. Kornhaas, J. Li, L. Ackermann, *J. Org. Chem.* **2012**, *77*, 9190–9198; c) R. K. Chinnagolla, S. Pimparkar, M. Jeganmohan, *Org. Lett.* **2012**, *14*, 3032–3035; d) B. Li, H. Feng, S. Xu, B. Wang, *Chem. Eur. J.* **2011**, *17*, 12573–12577; e) L. Ackermann, S. Fenner, *Org. Lett.* **2011**, *13*, 6548–6551.

Reference

- [64] B. Li, J. Ma, N. Wang, H. Feng, S. Xu, B. Wang, *Org. Lett.* **2012**, *14*, 736–739.
- [65] Z. Zhou, G. Liu, Y. Shen, X. Lu, *Org. Chem. Front.* **2014**, *1*, 1161–1165.
- [66] J. Li, S. De Sarkar, L. Ackermann, *Top. Organomet. Chem.* **2016**, *55*, 217–257.
- [67] G. R. Clark, C. E. L. Headford, W. R. Roper, L. J. Wright, V. P. D. Yap, *Inorg. Chim. Acta* **1994**, *220*, 261–272.
- [68] J.-P. Sutter, D. M. Grove, M. Beley, J.-P. Collin, N. Veldman, A. L. Spek, J.-P. Sauvage, G. van Koten, *Angew. Chem. Int. Ed.* **1994**, *33*, 1282–1285.
- [69] C. Coudret, S. Fraysse, *Chem. Commun.* **1998**, 663–664.
- [70] A. M. Clark, C. E. F. Rickard, W. R. Roper, L. J. Wright, *Organometallics* **1999**, *18*, 2813–2820.
- [71] L. Ackermann, N. Hofmann, R. Vicente, *Org. Lett.* **2011**, *13*, 1875–1877.
- [72] a) K. Korvorapun, N. Kaplaneris, T. Rogge, S. Warratz, A. C. Stückl, L. Ackermann, *ACS Catal.* **2018**, *8*, 886–892; b) Z. Ruan, S. K. Zhang, C. Zhu, P. N. Ruth, D. Stalke, L. Ackermann, *Angew. Chem. Int. Ed.* **2017**, *56*, 2045–2049; c) J. Li, K. Korvorapun, S. De Sarkar, T. Rogge, D. J. Burns, S. Warratz, L. Ackermann, *Nat. Commun.* **2017**, *8*, 1–8; d) J. Li, S. Warratz, D. Zell, S. De Sarkar, E. E. Ishikawa, L. Ackermann, *J. Am. Chem. Soc.* **2015**, *137*, 13894–13901; e) N. Hofmann, L. Ackermann, *J. Am. Chem. Soc.* **2013**, *135*, 5877–5884.
- [73] a) X.-G. Wang, Y. Li, H.-C. Liu, B.-S. Zhang, X.-Y. Gou, Q. Wang, J.-W. Ma, Y.-M. Liang, *J. Am. Chem. Soc.* **2019**, *141*, 13914–13922; b) A. J. Paterson, C. J. Heron, C. L. McMullin, M. F. Mahon, N. J. Press, C. G. Frost, *Org. Biomol. Chem.* **2017**, *15*, 5993–6000; c) G. Li, P. Gao, X. Lv, C. Qu, Q. Yan, Y. Wang, S. Yang, J. Wang, *Org. Lett.* **2017**, *19*, 2682–2685; d) Z. Y. Li, L. Li, Q. L. Li, K. Jing, H. Xu, G. W. Wang, *Chem. Eur. J.* **2017**, *23*, 3285–3290; e) A. J. Paterson, S. St John-Campbell, M. F. Mahon, N. J. Press, C. G. Frost, *Chem. Commun.* **2015**, *51*, 12807–12810.
- [74] a) I. Choi, V. Müller, Y. Wang, K. Xue, R. Kuniyil, L. B. Andreas, V. Karius, J. G. Alauzun, L. Ackermann, *Chem. Eur. J.* **2020**, *26*, 15290–15297; b) K. Korvorapun, M. Moselage, J. Struwe, T. Rogge, A. M. Messinis, L. Ackermann, *Angew. Chem. Int. Ed.* **2020**, *59*, 18795–18803; c) P. Gandeepan, J. Koeller, K. Korvorapun, J. Mohr, L. Ackermann, *Angew. Chem. Int. Ed.* **2019**, *58*, 9820–9825; d) M. Moselage, J. Li, F. Kramm, L. Ackermann, *Angew. Chem. Int. Ed.* **2017**, *56*, 5341–5344.
- [75] O. Saidi, J. Marafie, A. E. W. Ledger, P. M. Liu, M. F. Mahon, G. Kociok-Köhn, M. K. Whittlesey, C. G. Frost, *J. Am. Chem. Soc.* **2011**, *133*, 19298–19301.
- [76] K. Korvorapun, R. Kuniyil, L. Ackermann, *ACS Catal.* **2019**, *10*, 435–440.
- [77] H. L. Barlow, C. J. Teskey, M. F. Greaney, *Org. Lett.* **2017**, *19*, 6662–6665.
- [78] C. Jia, N. Wu, X. Cai, G. Li, L. Zhong, L. Zou, X. Cui, *J. Org. Chem.* **2020**, *85*, 4536–4542.
- [79] K. Jing, Z.-Y. Li, G.-W. Wang, *ACS Catal.* **2018**, *8*, 11875–11881.
- [80] a) G. M. Reddy, N. S. Rao, H. Maheswaran, *Org. Chem. Front.* **2018**, *5*, 1118–1123; b) S. Warratz, D. J. Burns, C. Zhu, K. Korvorapun, T. Rogge, J. Scholz, C. Jooss, D. Gelman, L. Ackermann, *Angew. Chem. Int. Ed.* **2017**, *56*, 1557–1560; c) C. J. Teskey, A. Y. W. Lui, M. F. Greaney, *Angew. Chem. Int. Ed.* **2015**, *54*, 11677–11680; d) Q. Yu, L. a. Hu, Y. Wang, S. Zheng, J. Huang, *Angew. Chem. Int. Ed.* **2015**, *54*, 15284–15288.
- [81] Z. Fan, J. Ni, A. Zhang, *J. Am. Chem. Soc.* **2016**, *138*, 8470–8475.
- [82] W. Liu, L. Ackermann, *Org. Lett.* **2013**, *15*, 3484–3486.
- [83] J. A. Leitch, C. L. McMullin, A. J. Paterson, M. F. Mahon, Y. Bhonoah, C. G. Frost, *Angew. Chem. Int. Ed.* **2017**, *56*, 15131–15135.
- [84] a) C. Yuan, L. Zhu, C. Chen, X. Chen, Y. Yang, Y. Lan, Y. Zhao, *Nat. Commun.* **2018**, *9*, 1189; b) C. Yuan, L. Zhu, R. Zeng, Y. Lan, Y. Zhao, *Angew. Chem. Int. Ed.* **2018**, *57*, 1277–1281.
- [85] A. Volta, *Philos. Trans. R. Soc. London* **1800**, *90*, 403–431.
- [86] a) H. Kolbe, *Liebigs Ann. Chem.* **1849**, *69*, 257–294; b) H. Kolbe, *Liebigs Ann. Chem.* **1848**, *64*, 339–341.
- [87] M. Faraday, *Philos. Trans. R. Soc. London* **1825**, 440–466.

Reference

- [88] a) L. Zeng, H. Li, J. Hu, D. Zhang, J. Hu, P. Peng, S. Wang, R. Shi, J. Peng, C.-W. Pao, J.-L. Chen, J.-F. Lee, H. Zhang, Y.-H. Chen, A. Lei, *Nat. Catal.* **2020**, *3*, 438–445; b) J. C. Siu, N. Fu, S. Lin, *Acc. Chem. Res.* **2020**, *53*, 547–560; c) P. Xiong, H.-C. Xu, *Acc. Chem. Res.* **2019**, *52*, 3339–3350; d) A. Wiebe, T. Gieshoff, S. Möhle, E. Rodrigo, M. Zirbes, S. R. Waldvogel, *Angew. Chem. Int. Ed.* **2018**, *57*, 5594–5619; e) Y. Jiang, K. Xu, C. Zeng, *Chem. Rev.* **2018**, *118*, 4485–4540; f) M. Yan, Y. Kawamata, P. S. Baran, *Chem. Rev.* **2017**, *117*, 13230–13319; g) R. Feng, J. A. Smith, K. D. Moeller, *Acc. Chem. Res.* **2017**, *50*, 2346–2352; h) E. J. Horn, B. R. Rosen, P. S. Baran, *ACS Cent. Sci.* **2016**, *2*, 302–308; i) R. Francke, R. D. Little, *Chem. Soc. Rev.* **2014**, *43*, 2492–2521; j) J.-i. Yoshida, K. Kataoka, R. Horcajada, A. Nagaki, *Chem. Rev.* **2008**, *108*, 2265–2299; k) A. Jutand, *Chem. Rev.* **2008**, *108*, 2300–2347; l) E. Duñach, D. Franco, S. Olivero, *Eur. J. Org. Chem.* **2003**, 1605–1622.
- [89] T. H. Meyer, L. H. Finger, P. Gandeepan, L. Ackermann, *Trends Chem.* **2019**, *1*, 63–76.
- [90] a) L. Ackermann, *Acc. Chem. Res.* **2020**, *53*, 84–104; b) Y. Qiu, J. Struwe, L. Ackermann, *Synlett* **2019**, *30*, 1164–1173; c) Q.-L. Yang, P. Fang, T.-S. Mei, *Chin. J. Chem.* **2018**, *36*, 338–352; d) S. Tang, Y. Liu, A. Lei, *Chem* **2018**, *4*, 27–45; e) C. Ma, P. Fang, T.-S. Mei, *ACS Catal.* **2018**, *8*, 7179–7189; f) N. Sauermann, T. H. Meyer, Y. Qiu, L. Ackermann, *ACS Catal.* **2018**, *8*, 7086–7103; g) N. Sauermann, T. H. Meyer, L. Ackermann, *Chem. Eur. J.* **2018**, *24*, 16209–16217.
- [91] C. Amatore, C. Cammoun, A. Jutand, *Adv. Synth. Catal.* **2007**, *349*, 292–296.
- [92] a) Y. Fujiwara, I. Moritani, S. Danno, R. Asano, S. Teranishi, *J. Am. Chem. Soc.* **1969**, *91*, 7166–7169; b) Y. Fujiwara, I. Moritani, M. Matsuda, S. Teranishi, *Tetrahedron Lett.* **1968**, *9*, 633–636; c) I. Moritani, Y. Fujiwara, *Tetrahedron Lett.* **1967**, *8*, 1119–1122.
- [93] a) H. Aiso, T. Kochi, H. Mutsutani, T. Tanabe, S. Nishiyama, F. Kakiuchi, *J. Org. Chem.* **2012**, *77*, 7718–7724; b) F. Kakiuchi, T. Kochi, H. Mutsutani, N. Kobayashi, S. Urano, M. Sato, S. Nishiyama, T. Tanabe, *J. Am. Chem. Soc.* **2009**, *131*, 11310–11311.
- [94] M. Konishi, K. Tsuchida, K. Sano, T. Kochi, F. Kakiuchi, *J. Org. Chem.* **2017**, *82*, 8716–8724.
- [95] F. Saito, H. Aiso, T. Kochi, F. Kakiuchi, *Organometallics* **2014**, *33*, 6704–6707.
- [96] K.-J. Jiao, Y.-K. Xing, Q.-L. Yang, H. Qiu, T.-S. Mei, *Acc. Chem. Res.* **2020**, *53*, 300–310.
- [97] Q.-L. Yang, Y.-Q. Li, C. Ma, P. Fang, X.-J. Zhang, T.-S. Mei, *J. Am. Chem. Soc.* **2017**, *139*, 3293–3298.
- [98] C. Ma, C.-Q. Zhao, Y.-Q. Li, L.-P. Zhang, X.-T. Xu, K. Zhang, T.-S. Mei, *Chem. Commun.* **2017**, *53*, 12189–12192.
- [99] Y.-Q. Li, Q.-L. Yang, P. Fang, T.-S. Mei, D. Zhang, *Org. Lett.* **2017**, *19*, 2905–2908.
- [100] a) X.-Y. W. Q.-L. Yang, X.-J. Weng, X. Yang, X.-T. Xu, X., P. F. Tong, X.-Y. Wu, T.-S. Mei, *Acta Chim. Sinica* **2019**, *77*, 866–873; b) Q.-L. Yang, X.-Y. Wang, T.-L. Wang, X. Yang, D. Liu, X. Tong, X.-Y. Wu, T.-S. Mei, *Org. Lett.* **2019**, *21*, 2645–2649.
- [101] Q.-L. Yang, C.-Z. Li, L.-W. Zhang, Y.-Y. Li, X. Tong, X.-Y. Wu, T.-S. Mei, *Organometallics* **2019**, *38*, 1208–1212.
- [102] A. Shrestha, M. Lee, A. L. Dunn, M. S. Sanford, *Org. Lett.* **2018**, *20*, 204–207.
- [103] T. V. Grayaznova, Y. B. Dudkina, D. R. Islamov, O. N. Kataeva, O. G. Sinyashin, D. A. Vicic, Y. H. Budnikova, *J. Organomet. Chem.* **2015**, *785*, 68–71.
- [104] Z. Duan, L. Zhang, W. Zhang, L. Lu, L. Zeng, R. Shi, A. Lei, *ACS Catal.* **2020**, *10*, 3828–3831.
- [105] U. Dhawa, C. Tian, T. Wdowik, J. C. A. Oliveira, J. Hao, L. Ackermann, *Angew. Chem. Int. Ed.* **2020**, *59*, 13451–13457.
- [106] Y. Qiu, W.-J. Kong, J. Struwe, N. Sauermann, T. Rogge, A. Scheremetjew, L. Ackermann, *Angew. Chem. Int. Ed.* **2018**, *57*, 5828–5832.
- [107] Y. Zhang, J. Struwe, L. Ackermann, *Angew. Chem. Int. Ed.* **2020**, *59*, 15076–15080.
- [108] Y. Qiu, A. Scheremetjew, L. Ackermann, *J. Am. Chem. Soc.* **2019**, *141*, 2731–2738.
- [109] W.-J. Kong, L. H. Finger, J. C. A. Oliveira, L. Ackermann, *Angew. Chem. Int. Ed.* **2019**, *58*, 6342–6346.
- [110] W.-J. Kong, Z. Shen, L. H. Finger, L. Ackermann, *Angew. Chem. Int. Ed.* **2020**, *59*, 5551–5556.
- [111] W.-J. Kong, L. H. Finger, A. M. Messinis, R. Kuniyil, J. C. A. Oliveira, L. Ackermann, *J. Am. Chem. Soc.*

Reference

- 2019**, *141*, 17198–17206.
- [112] a) Y. Wang, J. C. A. Oliveira, Z. Lin, L. Ackermann, *Angew. Chem. Int. Ed.* **2021**, *60*, 6419–6424; b) Y.-K. Xing, X.-R. Chen, Q.-L. Yang, S.-Q. Zhang, H.-M. Guo, X. Hong, T.-S. Mei, *Nat. Commun.* **2021**, *12*, 930.
- [113] Z. Shen, I. Maksso, R. Kuniyil, T. Rogge, L. Ackermann, *Chem. Commun.* **2021**, *57*, 3668–3671.
- [114] X. Tan, L. Massignan, X. Hou, J. Frey, J. C. A. Oliveira, M. N. Hussain, L. Ackermann, *Angew. Chem. Int. Ed.* **2021**, *60*, 13264–13270.
- [115] Z.-J. Wu, F. Su, W. Lin, J. Song, T.-B. Wen, H.-J. Zhang, H.-C. Xu, *Angew. Chem. Int. Ed.* **2019**, *58*, 16770–16774.
- [116] a) F. Xu, Y.-J. Li, C. Huang, H.-C. Xu, *ACS Catal.* **2018**, *8*, 3820–3824; b) Y. Qiu, C. Tian, L. Massignan, T. Rogge, L. Ackermann, *Angew. Chem. Int. Ed.* **2018**, *57*, 5818–5822.
- [117] a) X. Tan, X. Hou, T. Rogge, L. Ackermann, *Angew. Chem. Int. Ed.* **2021**, *60*, 4619–4624; b) L. Yang, R. Steinbock, A. Scheremetjew, R. Kuniyil, L. H. Finger, A. M. Messinis, L. Ackermann, *Angew. Chem. Int. Ed.* **2020**, *59*, 11130–11135; c) M.-J. Luo, M. Hu, R.-J. Song, D.-L. He, J.-H. Li, *Chem. Commun.* **2019**, *55*, 1124–1127; d) M.-J. Luo, T.-T. Zhang, F.-J. Cai, J.-H. Li, D.-L. He, *Chem. Commun.* **2019**, *55*, 7251–7254; e) Z.-Q. Wang, C. Hou, Y.-F. Zhong, Y.-X. Lu, Z.-Y. Mo, Y.-M. Pan, H.-T. Tang, *Org. Lett.* **2019**, *21*, 9841–9845; f) R. Mei, J. Koeller, L. Ackermann, *Chem. Commun.* **2018**, *54*, 12879–12882.
- [118] L. Massignan, X. Tan, T. H. Meyer, R. Kuniyil, A. M. Messinis, L. Ackermann, *Angew. Chem. Int. Ed.* **2020**, *59*, 3184–3189.
- [119] a) K. Shin, Y. Park, M.-H. Baik, S. Chang, *Nat. Chem.* **2018**, *10*, 218–224; b) G. Tan, Q. You, J. Lan, J. You, *Angew. Chem. Int. Ed.* **2018**, *57*, 6309–6313; c) S. Y. Hong, Y. Park, Y. Hwang, Y. B. Kim, M.-H. Baik, S. Chang, *Science* **2018**, *359*, 1016–1021; d) B. A. Arndtsen, R. G. Bergman, *Science* **1995**, *270*, 1970.
- [120] Y. Qiu, M. Stangier, T. H. Meyer, J. C. A. Oliveira, L. Ackermann, *Angew. Chem. Int. Ed.* **2018**, *57*, 14179–14183.
- [121] Q.-L. Yang, H.-W. Jia, Y. Liu, Y.-K. Xing, R.-C. Ma, M.-M. Wang, G.-R. Qu, T.-S. Mei, H.-M. Guo, *Org. Lett.* **2021**, *23*, 1209–1215.
- [122] Q.-L. Yang, Y.-K. Xing, X.-Y. Wang, H.-X. Ma, X.-J. Weng, X. Yang, H.-M. Guo, T.-S. Mei, *J. Am. Chem. Soc.* **2019**, *141*, 18970–18976.
- [123] X. Ye, C. Wang, S. Zhang, J. Wei, C. Shan, L. Wojtas, Y. Xie, X. Shi, *ACS Catal.* **2020**, *10*, 11693–11699.
- [124] N. Sauermann, T. H. Meyer, C. Tian, L. Ackermann, *J. Am. Chem. Soc.* **2017**, *139*, 18452–18455.
- [125] T. H. Meyer, J. C. A. Oliveira, D. Ghorai, L. Ackermann, *Angew. Chem. Int. Ed.* **2020**, *59*, 10955–10960.
- [126] a) N. Sauermann, R. Mei, L. Ackermann, *Angew. Chem. Int. Ed.* **2018**, *57*, 5090–5094; b) X. Gao, P. Wang, L. Zeng, S. Tang, A. Lei, *J. Am. Chem. Soc.* **2018**, *140*, 4195–4199.
- [127] C. Tian, U. Dhawa, J. Struwe, L. Ackermann, *Chin. J. Chem.* **2019**, *37*, 552–556.
- [128] a) R. Mei, W. Ma, Y. Zhang, X. Guo, L. Ackermann, *Org. Lett.* **2019**, *21*, 6534–6538; b) C. Tian, L. Massignan, T. H. Meyer, L. Ackermann, *Angew. Chem. Int. Ed.* **2018**, *57*, 2383–2387; c) R. Mei, N. Sauermann, J. C. A. Oliveira, L. Ackermann, *J. Am. Chem. Soc.* **2018**, *140*, 7913–7921.
- [129] S. Tang, D. Wang, Y. Liu, L. Zeng, A. Lei, *Nat. Commun.* **2018**, *9*, 798.
- [130] a) R. Mei, X. Fang, L. He, J. Sun, L. Zou, W. Ma, L. Ackermann, *Chem. Commun.* **2020**, *56*, 1393–1396; b) T. H. Meyer, J. C. A. Oliveira, S. C. Sau, N. W. J. Ang, L. Ackermann, *ACS Catal.* **2018**, *8*, 9140–9147.
- [131] a) S. C. Sau, R. Mei, J. Struwe, L. Ackermann, *ChemSusChem* **2019**, *12*, 3023–3027; b) L. Zeng, H. Li, S. Tang, X. Gao, Y. Deng, G. Zhang, C.-W. Pao, J.-L. Chen, J.-F. Lee, A. Lei, *ACS Catal.* **2018**, *8*, 5448–5453.
- [132] U. Dhawa, C. Tian, W. Li, L. Ackermann, *ACS Catal.* **2020**, *10*, 6457–6462.

Reference

- [133] P. Gandeepan, T. Müller, D. Zell, G. Cera, S. Warratz, L. Ackermann, *Chem. Rev.* **2019**, *119*, 2192–2452.
- [134] S.-K. Zhang, R. C. Samanta, N. Sauermann, L. Ackermann, *Chem. Eur. J.* **2018**, *24*, 19166–19170.
- [135] S.-K. Zhang, J. Struwe, L. Hu, L. Ackermann, *Angew. Chem. Int. Ed.* **2020**, *59*, 3178–3183.
- [136] S.-K. Zhang, A. Del Vecchio, R. Kuniyil, A. M. Messinis, Z. Lin, L. Ackermann, *Chem* **2021**, *7*, 1379–1392.
- [137] a) A. E. Wendlandt, A. M. Suess, S. S. Stahl, *Angew. Chem. Int. Ed.* **2011**, *50*, 11062–11087; b) O. Daugulis, H.-Q. Do, D. Shabashov, *Acc. Chem. Res.* **2009**, *42*, 1074–1086; c) L. Ackermann, H. K. Potukuchi, D. Landsberg, R. Vicente, *Org. Lett.* **2008**, *10*, 3081–3084.
- [138] Q.-L. Yang, X.-Y. Wang, J.-Y. Lu, L.-P. Zhang, P. Fang, T.-S. Mei, *J. Am. Chem. Soc.* **2018**, *140*, 11487–11494.
- [139] S. Kathiravan, S. Suriyanarayanan, I. A. Nicholls, *Org. Lett.* **2019**, *21*, 1968–1972.
- [140] C. Tian, U. Dhawa, A. Scheremetjew, L. Ackermann, *ACS Catal.* **2019**, *9*, 7690–7696.
- [141] a) R. Shang, L. Ilies, E. Nakamura, *Chem. Rev.* **2017**, *117*, 9086–9139; b) G. Cera, L. Ackermann, *Top. Curr. Chem.* **2016**, *374*, 191–224.
- [142] C. Zhu, M. Stangier, J. C. A. Oliveira, L. Massignan, L. Ackermann, *Chem. Eur. J.* **2019**, *25*, 16382–16389.
- [143] T. E. Boddie, S. H. Carpenter, T. M. Baker, J. C. DeMuth, G. Cera, W. W. Brennessel, L. Ackermann, M. L. Neidig, *J. Am. Chem. Soc.* **2019**, *141*, 12338–12345.
- [144] a) R. N. Grimes, *Dalton Trans.* **2015**, *44*, 5939–5956; b) C. Douvris, J. Michl, *Chem. Rev.* **2013**, *113*, PR179–PR233.
- [145] a) T. Heying, J. Ager Jr, S. Clark, D. Mangold, H. Goldstein, M. Hillman, R. Polak, J. Szymanski, *Inorg. Chem.* **1963**, *2*, 1089–1092; b) M. M. Fein, J. Bobinski, N. Mayes, N. Schwartz, M. S. Cohen, *Inorg. Chem.* **1963**, *2*, 1111–1115.
- [146] a) J. Poater, M. Solà, C. Viñas, F. Teixidor, *Chem. Eur. J.* **2016**, *22*, 7437–7443; b) J. Poater, M. Solà, C. Viñas, F. Teixidor, *Angew. Chem. Int. Ed.* **2014**, *53*, 12191–12195.
- [147] a) A. Saha, E. Oleshkevich, C. Vinas, F. Teixidor, *Adv. Mater.* **2017**, *29*, 1704238; b) E. A. Qian, A. I. Wixtrom, J. C. Axtell, A. Saebi, D. Jung, P. Rehak, Y. Han, E. H. Mouilly, D. Mosallaei, S. Chow, M. S. Messina, J. Y. Wang, A. T. Royappa, A. L. Rheingold, H. D. Maynard, P. Kral, A. M. Spokoyny, *Nat. Chem.* **2017**, *9*, 333–340; c) C. J. Villagómez, T. Sasaki, J. M. Tour, L. Grill, *J. Am. Chem. Soc.* **2010**, *132*, 16848–16854; d) M. Koshino, T. Tanaka, N. Solin, K. Suenaga, H. Isobe, E. Nakamura, *Science* **2007**, *316*, 853–853.
- [148] a) F. Issa, M. Kassiou, L. M. Rendina, *Chem. Rev.* **2011**, *111*, 5701–5722; b) M. Scholz, E. Hey-Hawkins, *Chem. Rev.* **2011**, *111*, 7035–7062.
- [149] a) X. Zhang, H. Yan, *Coord. Chem. Rev.* **2019**, *378*, 466–482; b) W.-B. Yu, P.-F. Cui, W.-X. Gao, G.-X. Jin, *Coord. Chem. Rev.* **2017**, *350*, 300–319; c) Z.-J. Yao, G.-X. Jin, *Coord. Chem. Rev.* **2013**, *257*, 2522–2535.
- [150] a) V. Bregadze, Z. Xie, *Eur. J. Inorg. Chem.* **2017**, *2017*, 4344; b) R. N. Grimes, *Carboranes*, Academic Press, **2016**; c) Z. Xie, G.-X. Jin, *Dalton Trans.* **2014**, *43*, 4924–4924.
- [151] a) Y. K. Au, Z. Xie, *Bull. Chem. Soc. Jpn.* **2021**, *94*, 879–899; b) Y. Quan, Z. Xie, *Chem. Soc. Rev.* **2019**, *48*, 3660–3673.
- [152] F. Teixidor, G. Barberà, A. Vaca, R. Kivekäs, R. Sillanpää, J. Oliva, C. Viñas, *J. Am. Chem. Soc.* **2005**, *127*, 10158–10159.
- [153] Y. Quan, Z. Qiu, Z. Xie, *Chem. Eur. J.* **2018**, *24*, 2795–2805.
- [154] E. L. Hoel, M. Talebinasab-Savari, M. Hawthorne, *J. Am. Chem. Soc.* **1977**, *99*, 4356–4367.
- [155] M. G. Mirabelli, L. G. Sneddon, *J. Am. Chem. Soc.* **1988**, *110*, 449–453.
- [156] R. Cheng, Z. Qiu, Z. Xie, *Nat. Commun.* **2017**, *8*, 14827.
- [157] C. X. Li, H. Y. Zhang, T. Y. Wong, H. J. Cao, H. Yan, C. S. Lu, *Org. Lett.* **2017**, *19*, 5178–5181.
- [158] C.-X. Cui, J. Zhang, Z. Qiu, Z. Xie, *Dalton Trans.* **2020**, *49*, 1380–1383.

Reference

- [159] T.-T. Xu, K. Cao, C.-Y. Zhang, J. Wu, L.-F. Ding, J. Yang, *Org. Lett.* **2019**, *21*, 9276–9279.
- [160] Z. Y. Zhang, X. Zhang, J. Yuan, C. D. Yue, S. Meng, J. Chen, G. A. Yu, C. M. Che, *Chem. Eur. J.* **2020**, *26*, 5037–5050.
- [161] R. Cheng, Z. Qiu, Z. Xie, *Chem. Eur. J.* **2020**, *26*, 7212–7218.
- [162] R. Cheng, Z. Qiu, Z. Xie, *Chin. J. Chem.* **2020**, *38*, 1575–1578.
- [163] Y. Quan, Z. Xie, *J. Am. Chem. Soc.* **2014**, *136*, 15513–15516.
- [164] H. Lyu, Y. Quan, Z. Xie, *Angew. Chem. Int. Ed.* **2015**, *54*, 10623–10626.
- [165] C. Zhang, Q. Wang, S. Tian, J. Zhang, J. Li, L. Zhou, J. Lu, *Org. Bio. Chem.* **2020**, *18*, 4723–4727.
- [166] Y. K. Au, Y. Quan, Z. Xie, *Chem. Asian J.* **2020**, *15*, 2170–2173.
- [167] Y. Chen, Y. K. Au, Y. Quan, Z. Xie, *Sci. China Chem.* **2018**, *62*, 74–79.
- [168] Y. Quan, Z. Xie, *Angew. Chem. Int. Ed.* **2016**, *55*, 1295–1298.
- [169] a) X. Zhang, H. Yan, *Chem. Sci.* **2018**, *9*, 3964–3969; b) X. Zhang, H. Zheng, J. Li, F. Xu, J. Zhao, H. Yan, *J. Am. Chem. Soc.* **2017**, *139*, 14511–14517.
- [170] T. T. Xu, K. Cao, C. Y. Zhang, J. Wu, L. Jiang, J. Yang, *Chem. Commun.* **2018**, *54*, 13603–13606.
- [171] R. Cheng, B. Li, J. Wu, J. Zhang, Z. Qiu, W. Tang, S.-L. You, Y. Tang, Z. Xie, *J. Am. Chem. Soc.* **2018**, *140*, 4508–4511.
- [172] Y. Quan, H. Lyu, Z. Xie, *Chem. Commun.* **2017**, *53*, 4818–4821.
- [173] Y. Chen, Y. Quan, Z. Xie, *Chem. Commun.* **2020**, *56*, 7001–7004.
- [174] Y. Quan, C. Tang, Z. Xie, *Chem. Sci.* **2016**, *7*, 5838–5845.
- [175] Q. Wang, S. Tian, C. Zhang, J. Li, Z. Wang, Y. Du, L. Zhou, J. Lu, *Org. Lett.* **2019**, *21*, 8018–8021.
- [176] K. Cao, C.-Y. Zhang, T.-T. Xu, J. Wu, L.-F. Ding, L. Jiang, J. Yang, *J. Organomet. Chem.* **2019**, *902*, 120956.
- [177] H. Lyu, Y. Quan, Z. Xie, *Angew. Chem. Int. Ed.* **2016**, *55*, 11840–11844.
- [178] H. Lyu, Y. Quan, Z. Xie, *J. Am. Chem. Soc.* **2016**, *138*, 12727–12730.
- [179] a) Y. Baek, S. Kim, J.-Y. Son, K. Lee, D. Kim, P. H. Lee, *ACS Catal.* **2019**, 10418–10425; b) H. Li, F. Bai, H. Yan, C. Lu, V. I. Bregadze, *Eur. J. Org. Chem.* **2017**, 2017, 1343–1352.
- [180] H. Lyu, Y. Quan, Z. Xie, *Chem. Eur. J.* **2017**, *23*, 14866–14871.
- [181] a) J. Wu, K. Cao, C. Y. Zhang, T. T. Xu, X. Y. Wen, B. Li, J. Yang, *Inorg. Chem.* **2020**, *59*, 17340–17346; b) J. Wu, K. Cao, C.-Y. Zhang, T.-T. Xu, L.-F. Ding, B. Li, J. Yang, *Org. Lett.* **2019**, *21*, 5986–5989.
- [182] Y. Chen, Y. Quan, Z. Xie, *Chem. Commun.* **2020**, *56*, 12997–13000.
- [183] H. Lyu, Y. Quan, Z. Xie, *Chem. Sci.* **2018**, *9*, 6390–6394.
- [184] a) Y. K. Au, H. Lyu, Y. Quan, Z. Xie, *Chin. J. Chem.* **2020**, *38*, 383–388; b) Y. K. Au, H. Lyu, Y. Quan, Z. Xie, *J. Am. Chem. Soc.* **2019**, *141*, 12855–12862.
- [185] Y. Baek, K. Cheong, G. H. Ko, G. U. Han, S. H. Han, D. Kim, K. Lee, P. H. Lee, *J. Am. Chem. Soc.* **2020**, *142*, 9890–9895.
- [186] Z. Qiu, Y. Quan, Z. Xie, *J. Am. Chem. Soc.* **2013**, *135*, 12192–12195.
- [187] a) T.-T. Xu, K. Cao, J. Wu, C.-Y. Zhang, J. Yang, *Inorg. Chem.* **2018**, *57*, 2925–2932; b) K. Cao, T.-T. Xu, J. Wu, L. Jiang, J. Yang, *Chem. Commun.* **2016**, *52*, 11446–11449.
- [188] T. T. Xu, C. Y. Zhang, K. Cao, J. Wu, L. Jiang, J. Li, B. Li, J. Yang, *ChemistrySelect* **2017**, *2*, 3396–3399.
- [189] J. Wu, K. Cao, T.-T. Xu, X.-J. Zhang, L. Jiang, J. Yang, Y. Huang, *RSC Adv.* **2015**, *5*, 91683–91685.
- [190] K. Cao, Y. Huang, J. Yang, J. Wu, *Chem. Commun.* **2015**, *51*, 7257–7260.
- [191] H. Lyu, J. Zhang, J. Yang, Y. Quan, Z. Xie, *J. Am. Chem. Soc.* **2019**, *141*, 4219–4224.
- [192] P. Gandeepan, L. H. Finger, T. H. Meyer, L. Ackermann, *Chem. Soc. Rev.* **2020**, *49*, 4254–4272.
- [193] a) D. A. Rudakov, V. I. Potkin, I. V. Lantsova, *Russ. J. Electrochem.* **2009**, *45*, 813–817; b) D. Rudakov, V. Shirokii, V. Potkin, N. Maier, V. Bragin, P. Petrovskii, I. Sivaev, V. Bregadze, A. Kisin, *Russ. Chem. Bull.* **2005**, *54*, 1599–1602.
- [194] Y. K. Au, H. Lyu, Y. Quan, Z. Xie, *J. Am. Chem. Soc.* **2020**, *142*, 6940–6945.
- [195] a) B. M. Trost, *Angew. Chem. Int. Ed.* **1995**, *34*, 259–281; b) B. Trost, *Science* **1991**, *254*, 1471–1477.

Reference

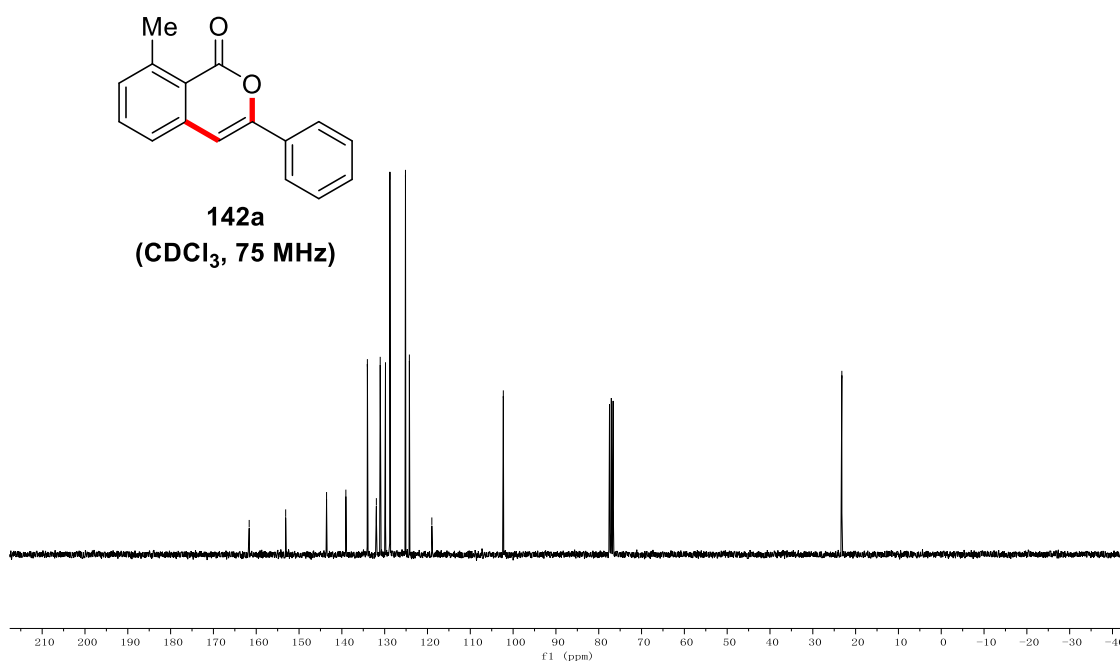
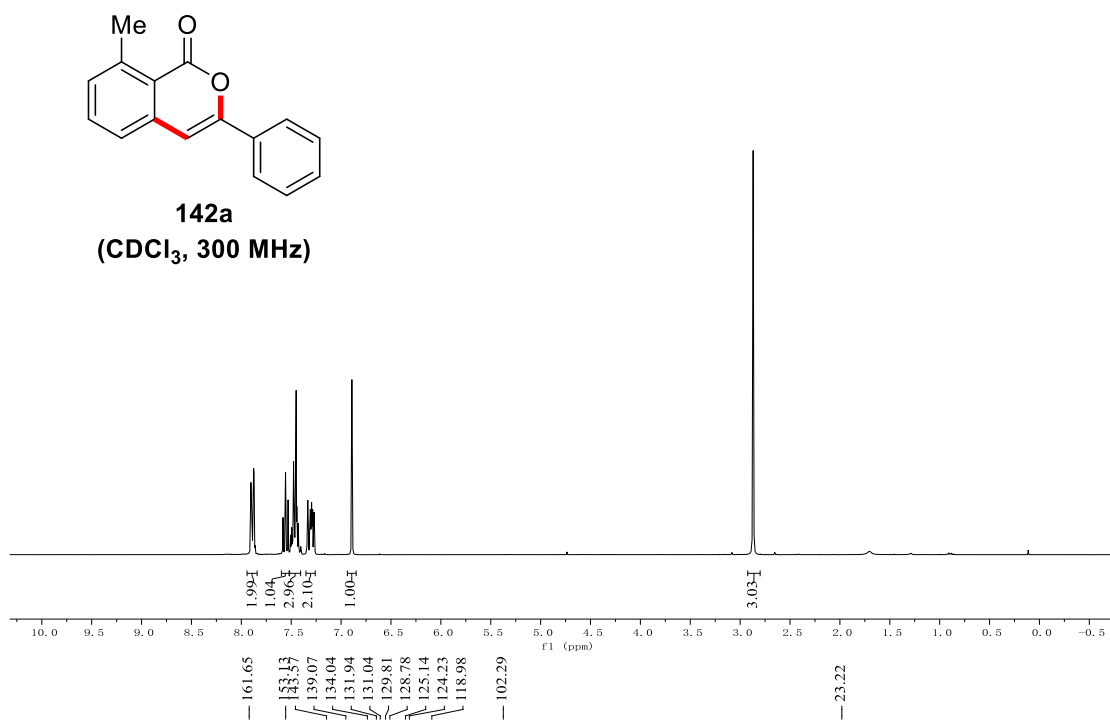
- [196] a) P. A. Wender, B. L. Miller, *Nature* **2009**, *460*, 197–201; b) P. A. Wender, M. P. Croatt, B. Witulski, *Tetrahedron* **2006**, *62*, 7505–7511.
- [197] a) S. I. Kozhushkov, L. Ackermann, *Chem. Sci.* **2013**, *4*, 886–896; b) P. B. Arockiam, C. Bruneau, P. H. Dixneuf, *Chem. Rev.* **2012**, *112*, 5879–5918; c) L. Ackermann, R. Vicente, in *C–H Activation* (Eds.: J.-Q. Yu, Z. Shi), Springer Berlin Heidelberg, Berlin, Heidelberg, **2010**, pp. 211–229; d)
- [198] a) J. C. Chu, T. Rovis, *Angew. Chem. Int. Ed.* **2018**, *57*, 62–101; b) P. Gandeepan, L. Ackermann, *Chem* **2018**, *4*, 199–222; c) G. Rouquet, N. Chatani, *Angew. Chem. Int. Ed.* **2013**, *52*, 11726–11743; d) L. Ackermann, R. Vicente, A. R. Kapdi, *Angew. Chem. Int. Ed.* **2009**, *48*, 9792–9826.
- [199] P. B. Arockiam, C. Bruneau, P. H. Dixneuf, *Chem. Rev.* **2012**, *112*, 5879–5918.
- [200] a) M. Seki, *Org. Process Res. Dev.* **2016**, *20*, 867–877; b) L. Ackermann, *Org. Process Res. Dev.* **2015**, *19*, 260–269.
- [201] J. Hubrich, T. Himmler, L. Rodefeld, L. Ackermann, *ACS Catal.* **2015**, *5*, 4089–4093.
- [202] S. Vasquez-Céspedes, X. Wang, F. Glorius, *ACS Catal.* **2018**, *8*, 242–257.
- [203] Y. Park, J. Heo, M.-H. Baik, S. Chang, *J. Am. Chem. Soc.* **2016**, *138*, 14020–14029.
- [204] a) M. Simonetti, D. M. Cannas, X. Just-Baringo, I. J. Vitorica-Yrezabal, I. Larrosa, *Nat. Chem.* **2018**, *10*, 724–731; b) L. Ackermann, R. Born, P. Álvarez-Bercedo, *Angew. Chem. Int. Ed.* **2007**, *46*, 6364–6367; c) L. Ackermann, A. Althammer, R. Born, *Synlett* **2007**, 2833–2836; d) L. Ackermann, A. Althammer, R. Born, *Angew. Chem. Int. Ed.* **2006**, *45*, 2619–2622.
- [205] D. G. Farnum, G. Mehta, G. G. I. Moore, F. P. Siegal, *Tetrahedron Lett.* **1974**, *15*, 2549–2552.
- [206] a) C. Zhao, Y. Guo, Y. Zhang, N. Yan, S. You, W. Li, *J. Mater. Chem. A* **2019**, *7*, 10174–10199; b) Y. Patil, R. Misra, *Chem. Asian J.* **2018**, *13*, 220–229; c) W. Li, K. H. Hendriks, M. M. Wienk, R. A. J. Janssen, *Acc. Chem. Res.* **2016**, *49*, 78–85; d) M. J. Robb, S.-Y. Ku, F. G. Brunetti, C. J. Hawker, *J. Polym. Sci., Part A: Polym. Chem.* **2013**, *51*, 1263–1271; e) Y. Wu, W. Zhu, *Chem. Soc. Rev.* **2013**, *42*, 2039–2058; f) Y. Li, P. Sonar, L. Murphy, W. Hong, *Energy Environ. Sci.* **2013**, *6*, 1684–1710; g) B. Tieke, A. R. Rabindranath, K. Zhang, Y. Zhu, *Beilstein J. Org. Chem.* **2010**, *6*, 830–845.
- [207] M. Kaur, D. H. Choi, *Chem. Soc. Rev.* **2015**, *44*, 58–77.
- [208] a) Z. Ni, H. Wang, H. Dong, Y. Dang, Q. Zhao, X. Zhang, W. Hu, *Nat. Chem.* **2019**, *11*, 271–277; b) D. Feng, G. Barton, C. N. Scott, *Org. Lett.* **2019**, *21*, 1973–1978; c) S.-Y. Liu, D.-G. Wang, A.-G. Zhong, H.-R. Wen, *Org. Chem. Front.* **2018**, *5*, 653–661; d) W. Masayuki, O. Fumiyuki, *Asian J. Org. Chem.* **2018**, *7*, 1206–1216; e) S. Yu, F. Liu, J. Yu, S. Zhang, C. Cabanetos, Y. Gao, W. Huang, *J. Mater. Chem. C* **2017**, *5*, 29–40.
- [209] K.-J. Jiao, Y.-K. Xing, Q.-L. Yang, H. Qiu, T.-S. Mei, *Acc. Chem. Res.* **2020**, *53*, 300–310.
- [210] a) Z.-J. Wu, F. Su, W. Lin, J. Song, T.-B. Wen, H.-J. Zhang, H.-C. Xu, *Angew. Chem. Int. Ed.* **2019**, *58*, 16770–16774; b) W.-J. Kong, L. H. Finger, J. C. A. Oliveira, L. Ackermann, *Angew. Chem. Int. Ed.* **2019**, *58*, 6342–6346.
- [211] a) T. O. Olusanya, G. Calabrese, D. G. Fatouros, J. Tsibouklis, J. R. Smith, *Biophys. Chem.* **2019**, *247*, 25–33; b) I. V. Korolkov, A. L. Kozlovskiy, Y. G. Gorin, A. V. Kazantsev, D. I. Shlimas, M. V. Zdorovets, N. K. Ualieva, V. S. Rusakov, *J. Nanopart. Res.* **2018**, *20*, 1–11.
- [212] a) H. Shen, Z. Xie, *J. Am. Chem. Soc.* **2010**, *132*, 11473–11480; b) Z. Xie, *Coord. Chem. Rev.* **2006**, *250*, 259–272; c) N. S. Hosmane, J. A. Maguire, *Eur. J. Inorg. Chem.* **2003**, *2003*, 3989–3999.
- [213] a) A. Shmal'ko, S. Anufriev, A. Anisimov, M. Y. Stogniy, I. Sivaev, V. Bregadze, *Russ. Chem. Bull.* **2019**, *68*, 1239–1247; b) M. Y. Stogniy, S. A. Erokhina, K. Y. Suponitsky, A. A. Anisimov, I. B. Sivaev, V. I. Bregadze, *New J. Chem.* **2018**, *42*, 17958–17967; c) S. A. Anufriev, I. B. Sivaev, K. Y. Suponitsky, I. A. Godovikov, V. I. Bregadze, *Eur. J. Inorg. Chem.* **2017**, *2017*, 4436–4443.
- [214] M. Chen, D. Zhao, J. Xu, C. Li, C. Lu, H. Yan, *Angew. Chem. Int. Ed.* **2021**, *60*, 7838–7844.
- [215] a) A. Gangjee, Y. Zeng, T. Talreja, J. J. McGuire, R. L. Kisliuk, S. F. Queener, *J. Med. Chem.* **2007**, *50*, 3046–3053; b) Z.-Y. Sun, E. Botros, A.-D. Su, Y. Kim, E. Wang, N. Z. Baturay, C.-H. Kwon, *J. Med. Chem.* **2000**, *43*, 4160–4168.
- [216] a) V. Hirschbeck, P. H. Gehrtz, I. Fleischer, *Chem. Eur. J.* **2018**, *24*, 7092–7107; b) I. P. Beletskaya, V.

Reference

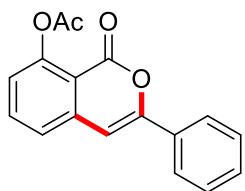
- P. Ananikov, *Chem. Rev.* **2011**, *111*, 1596–1636; c) M. Mellah, A. Voituriez, E. Schulz, *Chem. Rev.* **2007**, *107*, 5133–5209.
- [217] F. Lin, J.-L. Yu, Y. Shen, S.-Q. Zhang, B. Spingler, J. Liu, X. Hong, S. Duttwyler, *J. Am. Chem. Soc.* **2018**, *140*, 13798–13807.
- [218] Y. F. Liang, L. Yang, T. Rogge, L. Ackermann, *Chem. Eur. J.* **2018**, *24*, 16548–16552.
- [219] E. Gońka, L. Yang, R. Steinbock, F. Pesciaioli, R. Kuniyil, L. Ackermann, *Chem. Eur. J.* **2019**, *25*, 16246–16250.
- [220] M. Grzybowski, E. Glodkowska-Mrowka, T. Stoklosa, D. T. Gryko, *Org. Lett.* **2012**, *14*, 2670–2673.
- [221] L. Yang, R. Steinbock, A. Scheremetjew, R. Kuniyil, L. H. Finger, A. M. Messinis, L. Ackermann, *Angew. Chem. Int. Ed.* **2020**, *59*, 11130–11135.
- [222] Y.-F. Liang, L. Yang, B. B. Jei, R. Kuniyil, L. Ackermann, *Chem. Sci.* **2020**, *11*, 10764–10769.
- [223] L. Yang, B. Bongsuiru Jei, A. Scheremetjew, R. Kuniyil, L. Ackermann, *Angew. Chem. Int. Ed.* **2021**, *60*, 1482–1487.
- [224] a) H. Mayr, A. R. Ofial, *Acc. Chem. Res.* **2016**, *49*, 952–965; b) M. Baidya, F. Brotzel, H. Mayr, *Org. Bio. Chem.* **2010**, *8*, 1929–1935; c) F. Brotzel, B. Kempf, T. Singer, H. Zipse, H. Mayr, *Chem. Eur. J.* **2007**, *13*, 336–345.
- [225] Z. Yang, W. Zhao, W. Liu, X. Wei, M. Chen, X. Zhang, X. Zhang, Y. Liang, C. Lu, H. Yan, *Angew. Chem. Int. Ed.* **2019**, *58*, 11886–11892.
- [226] a) K.-R. Wee, W.-S. Han, D. W. Cho, S. Kwon, C. Pac, S. O. Kang, *Angew. Chem. Int. Ed.* **2012**, *51*, 2677–2680; b) K.-R. Wee, Y.-J. Cho, S. Jeong, S. Kwon, J.-D. Lee, I.-H. Suh, S. O. Kang, *J. Am. Chem. Soc.* **2012**, *134*, 17982–17990.
- [227] F. Wang, S. S. Stahl, *Angew. Chem. Int. Ed.* **2019**, *58*, 6385–6390.
- [228] Y. Xu, X. Yang, X. Zhou, L. Kong, X. Li, *Org. Lett.* **2017**, *19*, 4307–4310.
- [229] M. Grzybowski, E. Glodkowska-Mrowka, T. Stoklosa, D. T. Gryko, *Org. Lett.* **2012**, *14*, 2670–2673.
- [230] M. J. Mio, L. C. Kopel, J. B. Braun, T. L. Gadzikwa, K. L. Hull, R. G. Brisbois, C. J. Markworth, P. A. Grieco, *Org. Lett.* **2002**, *4*, 3199–3202.
- [231] K. S. Halskov, H. S. Roth, J. A. Ellman, *Angew. Chem. Int. Ed.* **2017**, *56*, 9183–9187.
- [232] J. M. Villar, J. Suárez, J. s. A. Varela, C. Saá, *Org. Lett.* **2017**, *19*, 1702–1705.
- [233] A. Toppino, A. R. Genady, M. E. El-Zaria, J. Reeve, F. Mostofian, J. Kent, J. F. Valliant, *Inorg. Chem.* **2013**, *52*, 8743–8749.
- [234] K. Nozawa, M. Yamada, Y. Tsuda, K. Kawai, S. Nakajima, *Chem. Pharm. Bull.* **1981**, *29*, 2491–2495.
- [235] M. Uchiyama, H. Ozawa, K. Takuma, Y. Matsumoto, M. Yonehara, K. Hiroya, T. Sakamoto, *Org. Lett.* **2006**, *8*, 5517–5520.
- [236] S. A. Shahzad, C. Venin, T. Wirth, *Eur. J. Org. Chem.* **2010**, 3465–3472.
- [237] P. K. Dutta, S. Sen, *Chem. Eur. J.* **2018**, *2018*, 5512–5519.
- [238] A. Obata, A. Sasagawa, K. Yamazaki, Y. Ano, N. Chatani, *Chem. Sci.* **2019**, *10*, 3242–3248.
- [239] O. Ito, M. Matsuda, *Bull. Chem. Soc. Jpn.* **1984**, *57*, 1745–1749.

7. NMR Spectra

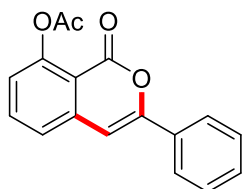
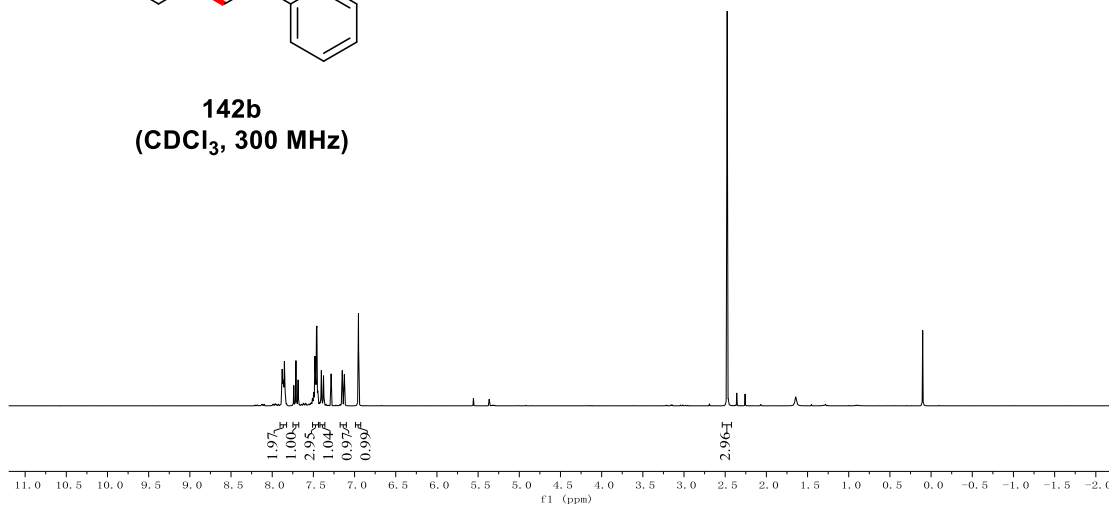
7.1 Ruthenium(II/IV)-Catalyzed Annulation



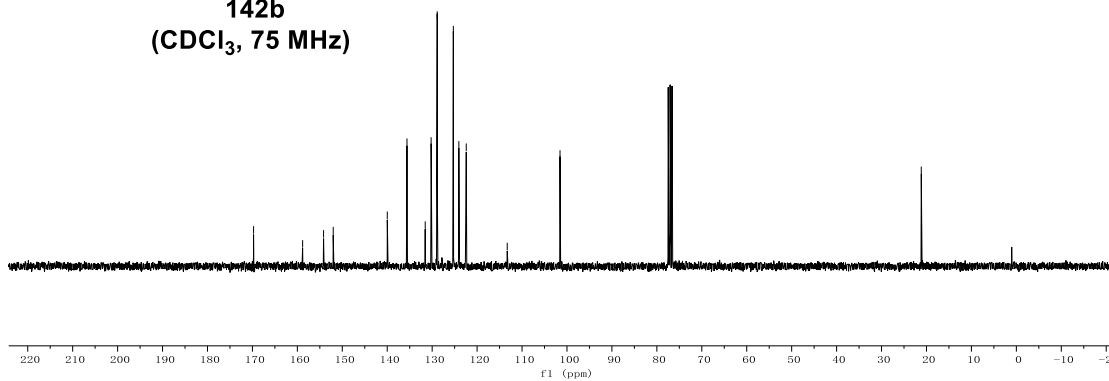
NMR Spectra



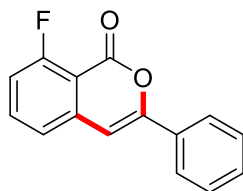
142b
(CDCl₃, 300 MHz)



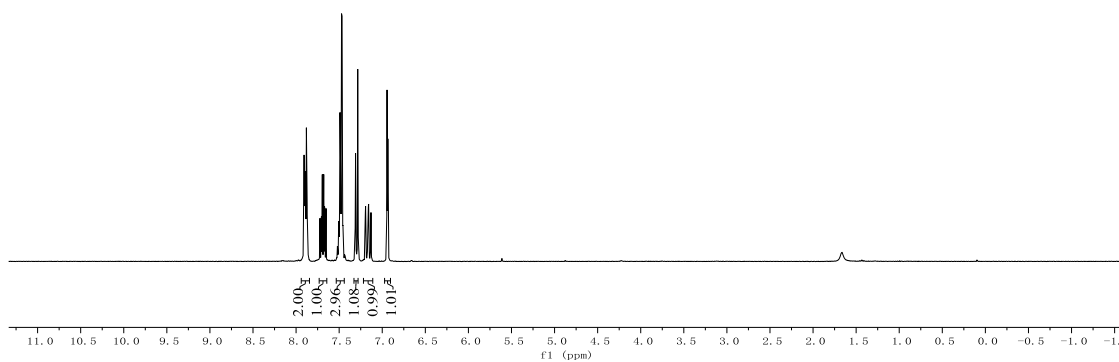
142b
(CDCl₃, 75 MHz)



NMR Spectra



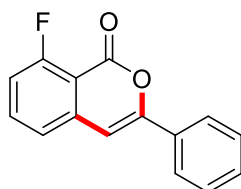
142c
(CDCl₃, 300 MHz)



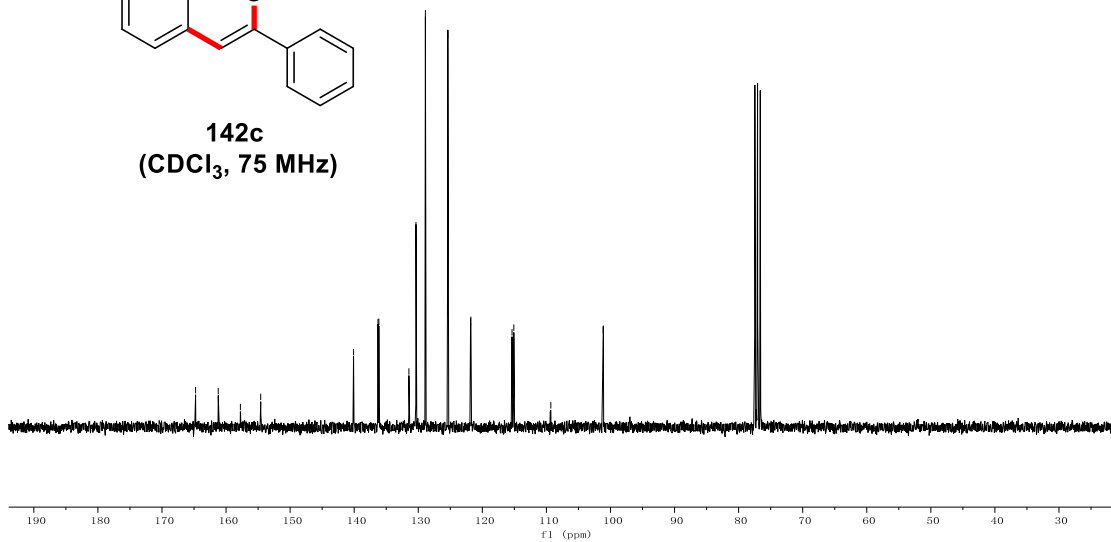
164.75
161.22
157.76
154.59

140.10
136.28
136.15
131.46
130.36
128.89
125.39
121.84
121.78
115.37
115.08

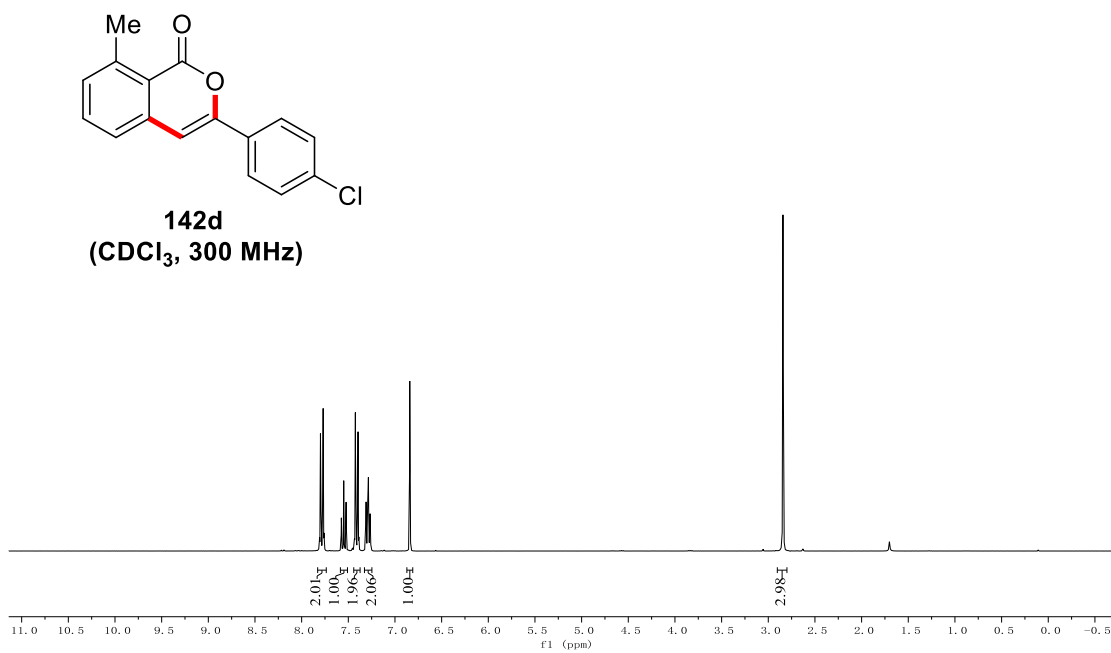
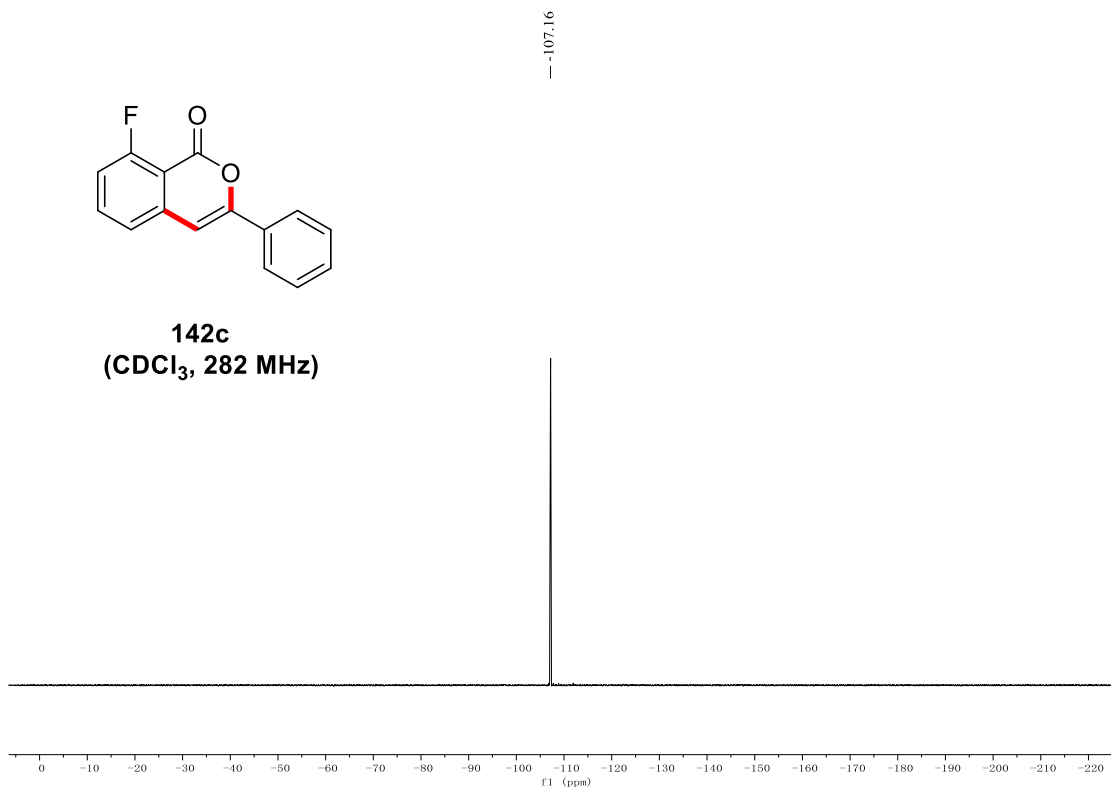
109.31
101.16
101.11



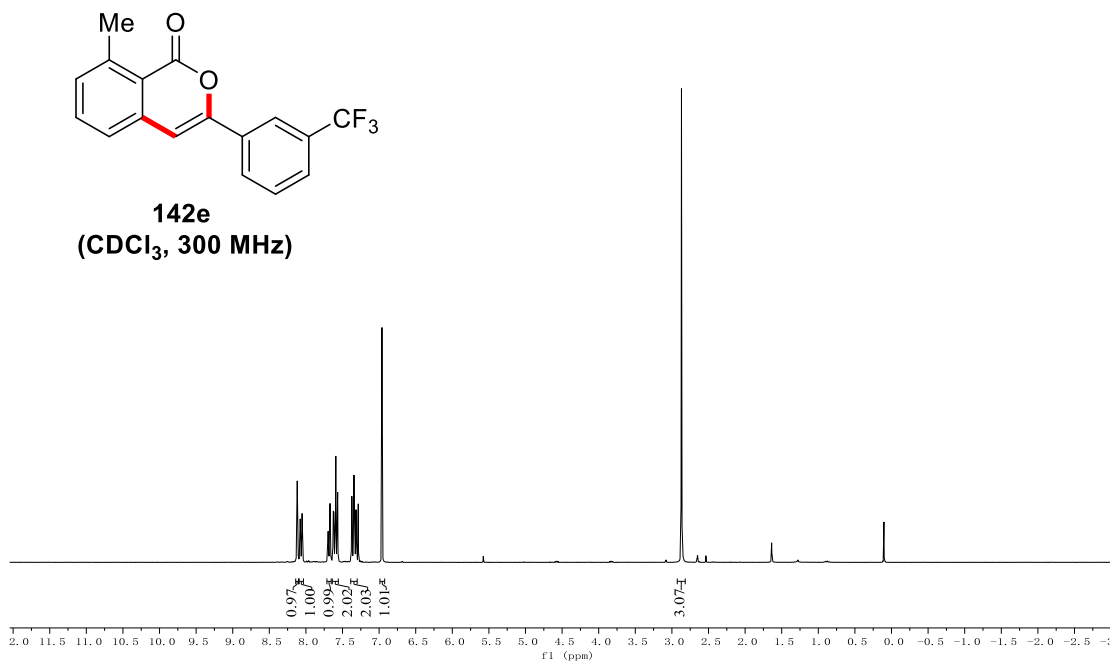
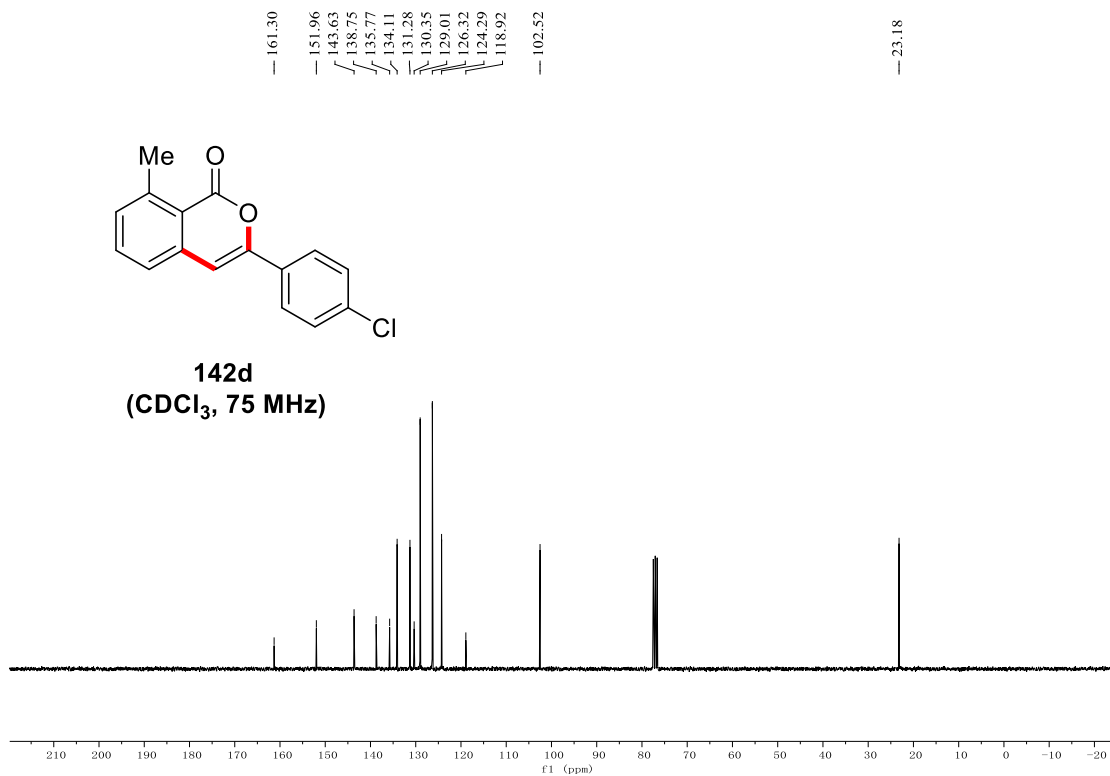
142c
(CDCl₃, 75 MHz)



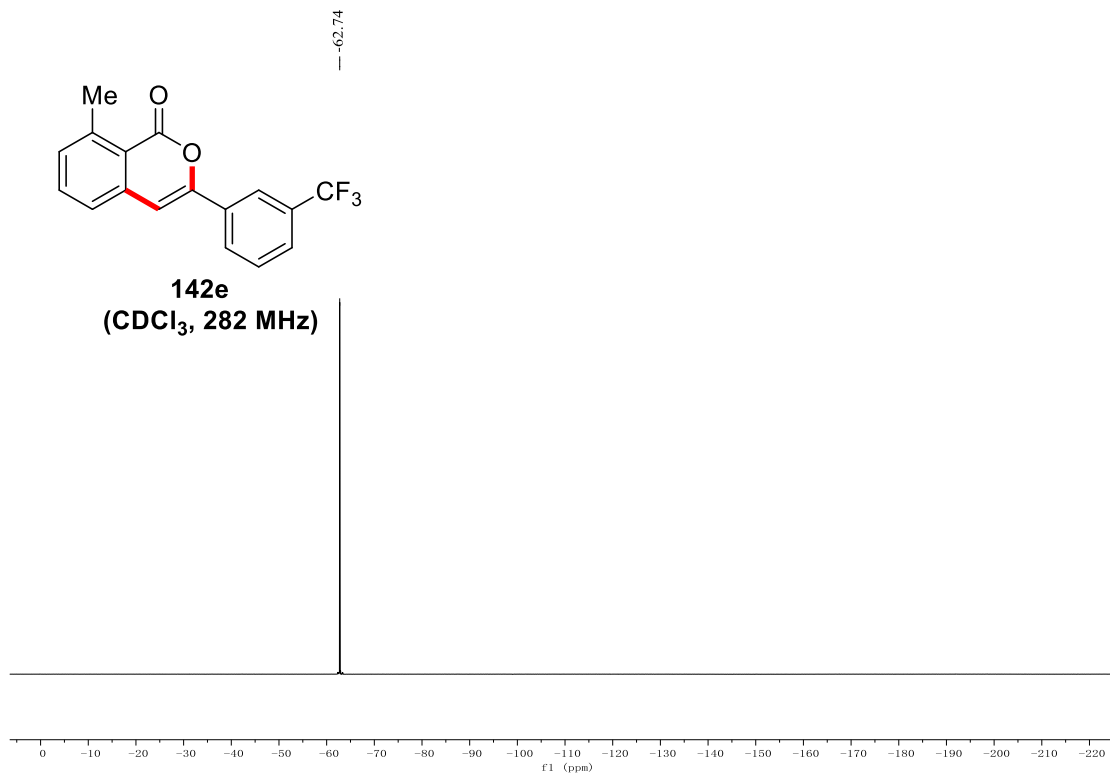
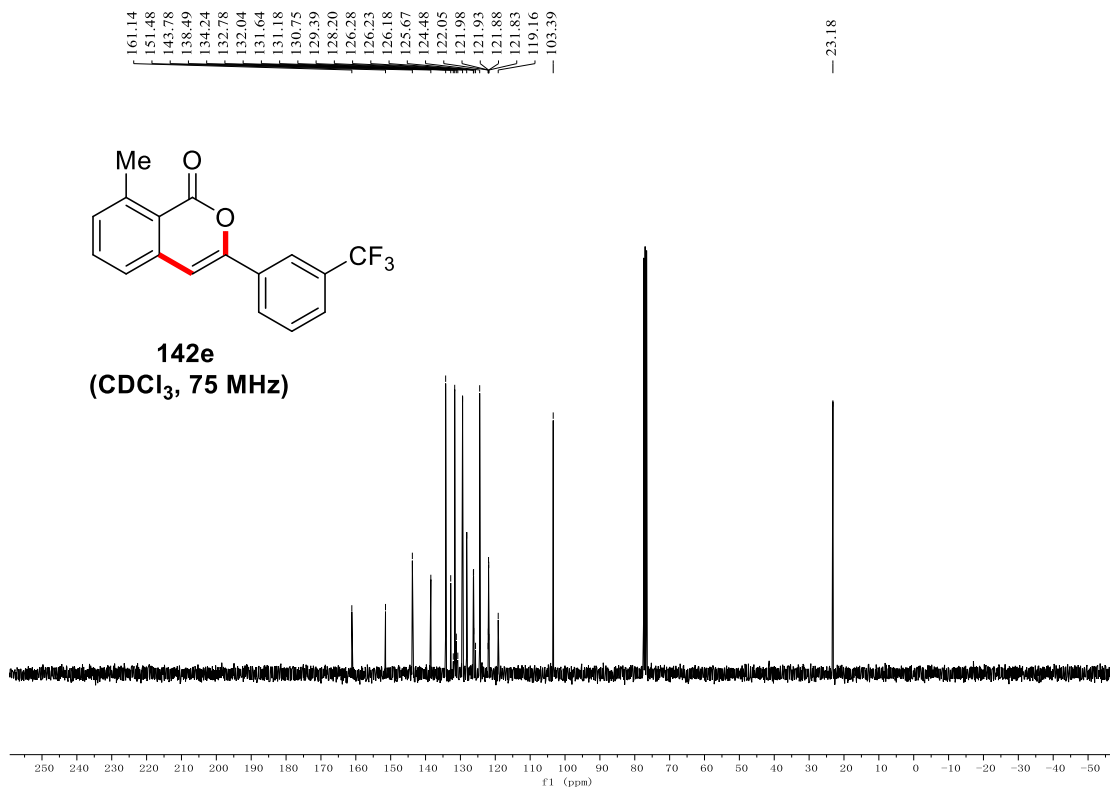
NMR Spectra



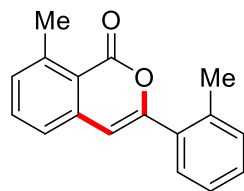
NMR Spectra



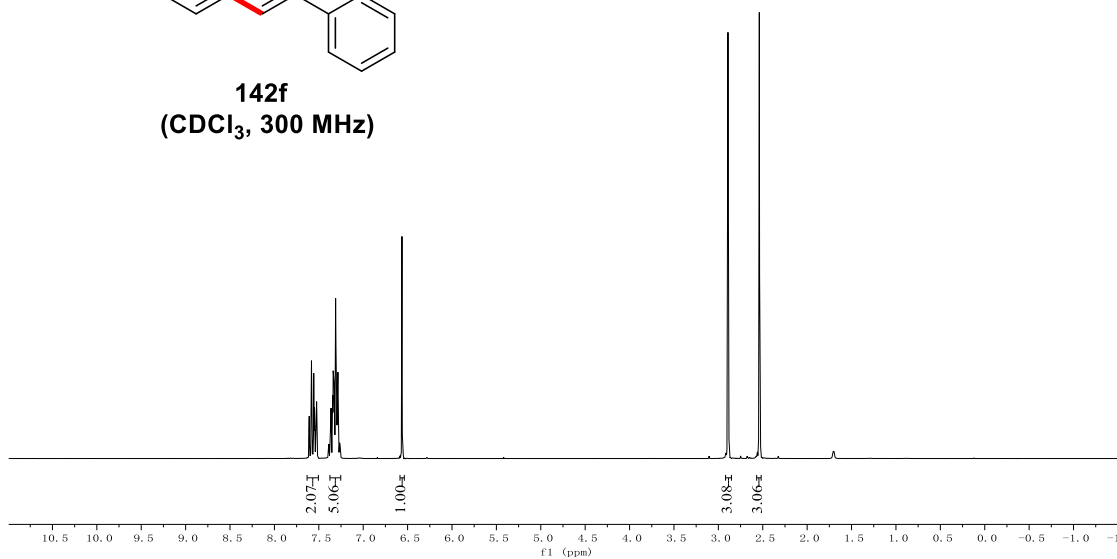
NMR Spectra



NMR Spectra

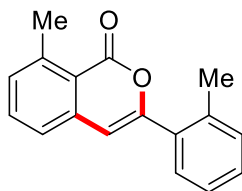


142f
(CDCl₃, 300 MHz)

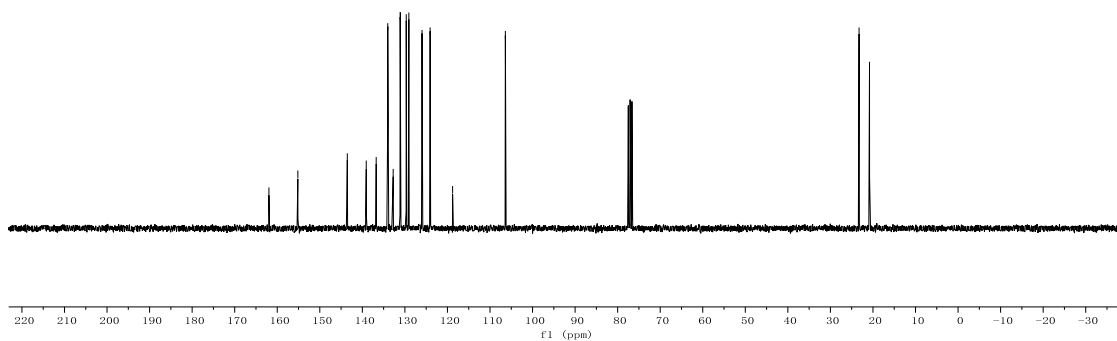


161.96
155.16
143.54
139.08
136.75
134.03
132.75
131.11
131.05
129.68
129.07
125.97
124.07
118.79
106.39

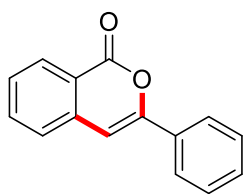
23.27
20.81



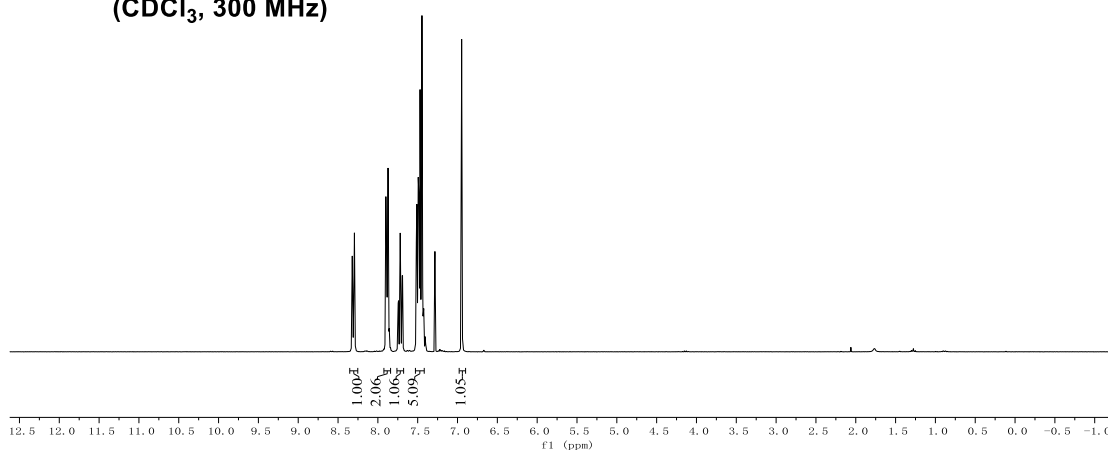
142f
(CDCl₃, 75 MHz)



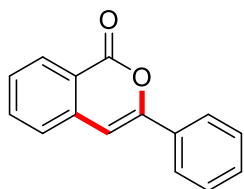
NMR Spectra



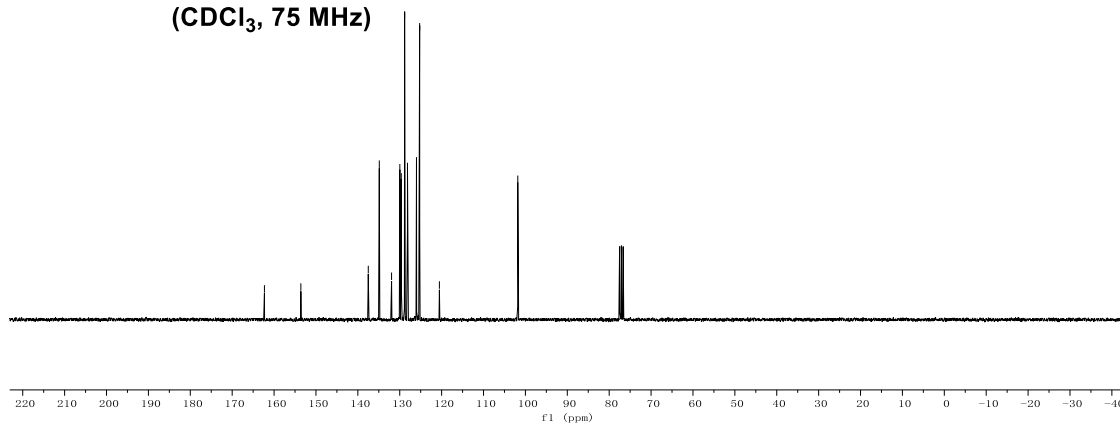
142g
(CDCl₃, 300 MHz)



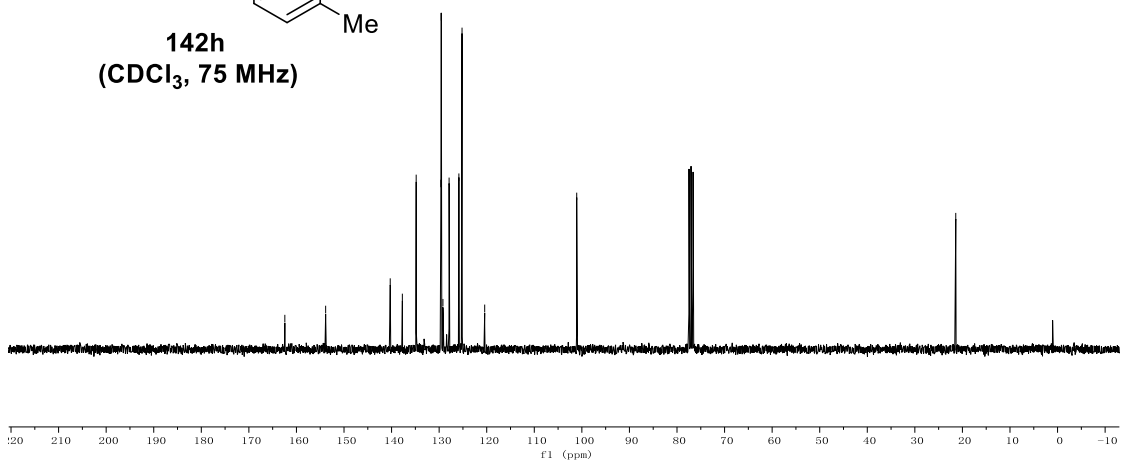
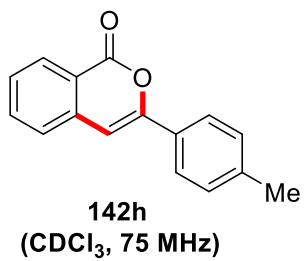
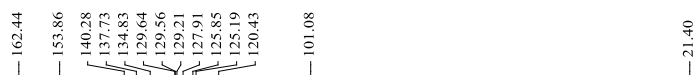
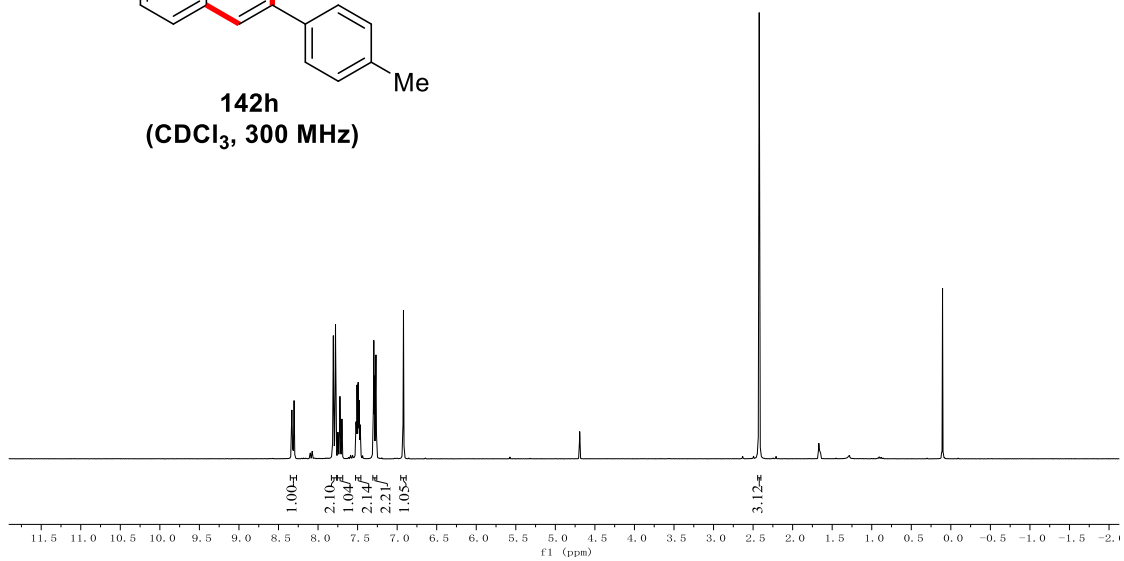
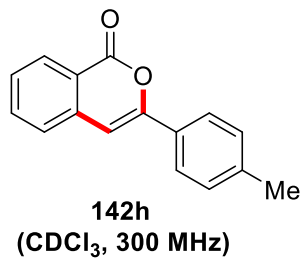
162.50
153.60
137.51
134.88
131.95
129.98
129.63
128.83
128.15
126.00
125.24
120.53
101.82



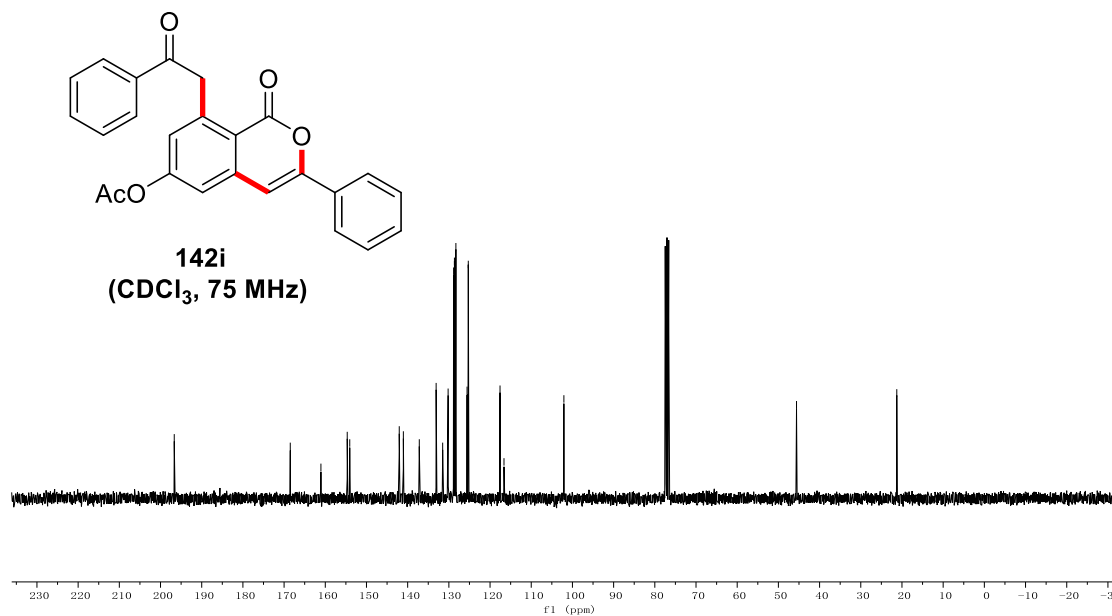
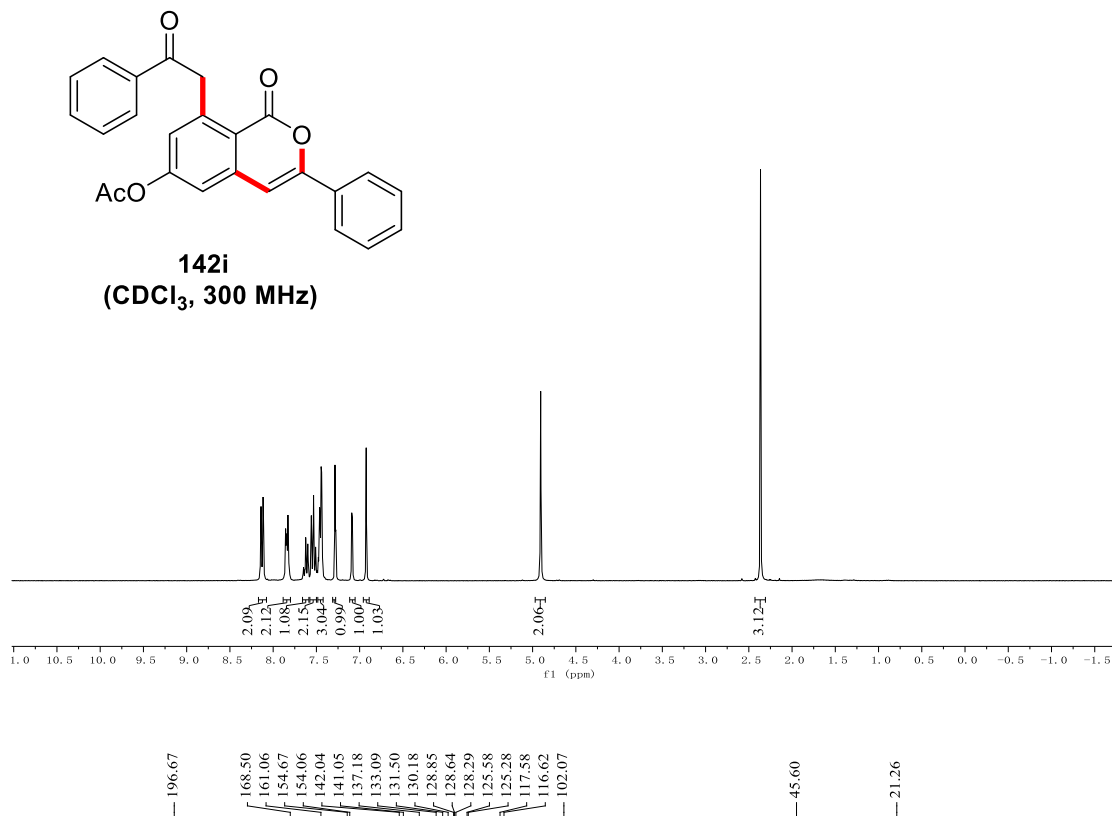
142g
(CDCl₃, 75 MHz)



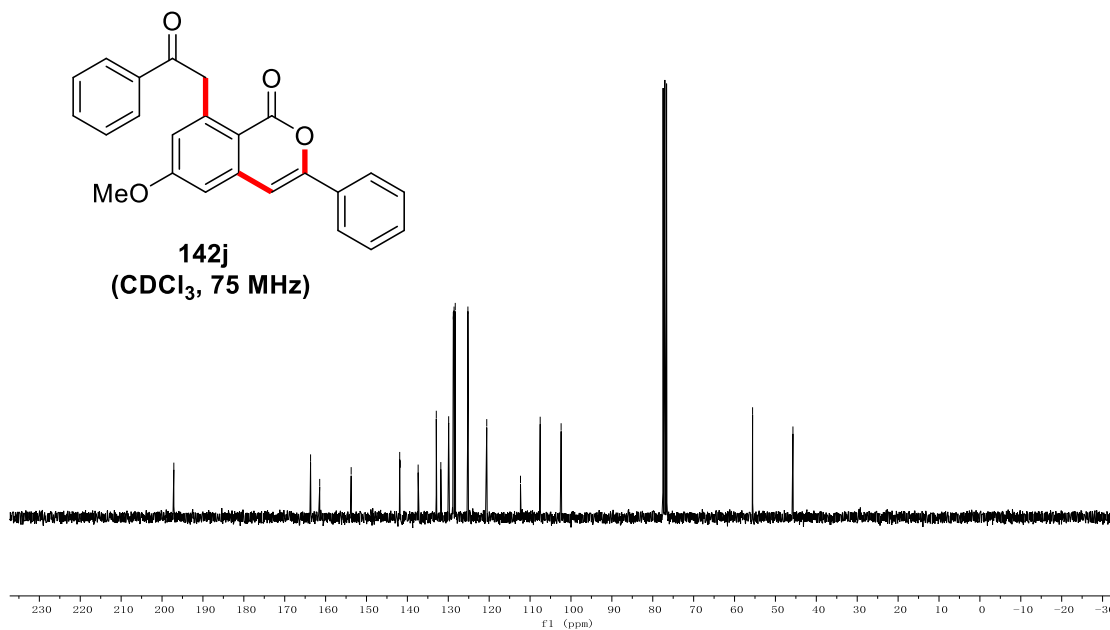
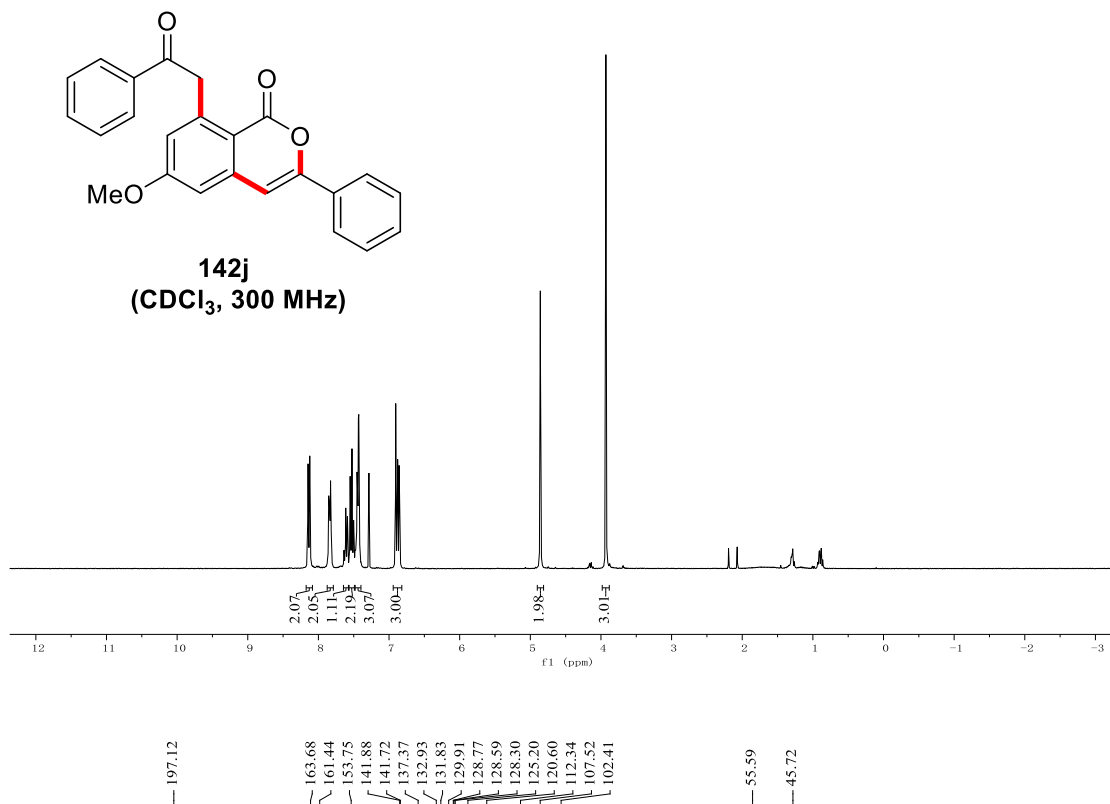
NMR Spectra



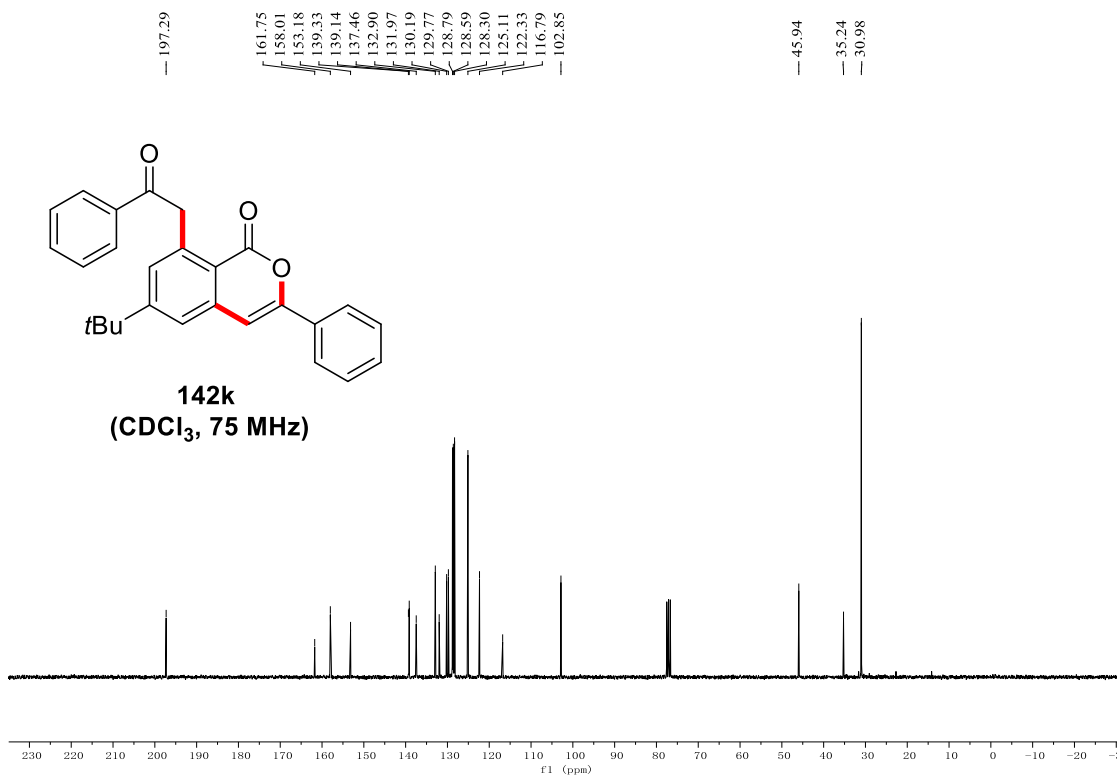
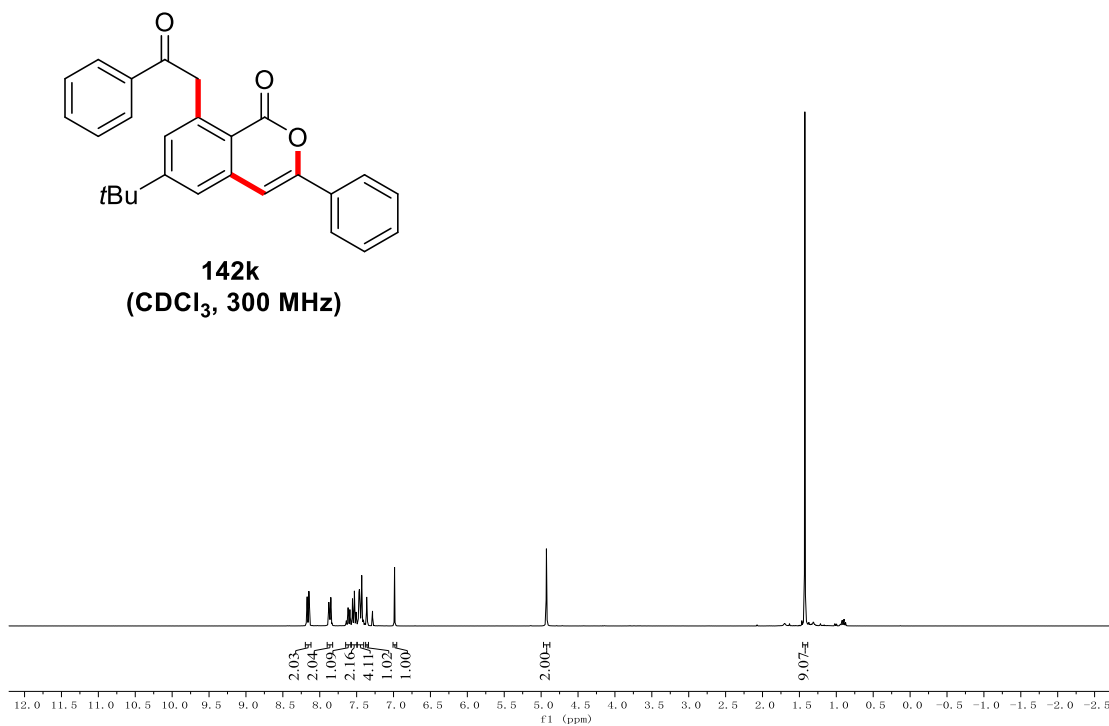
NMR Spectra



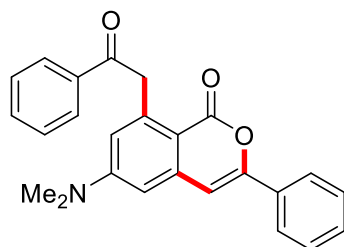
NMR Spectra



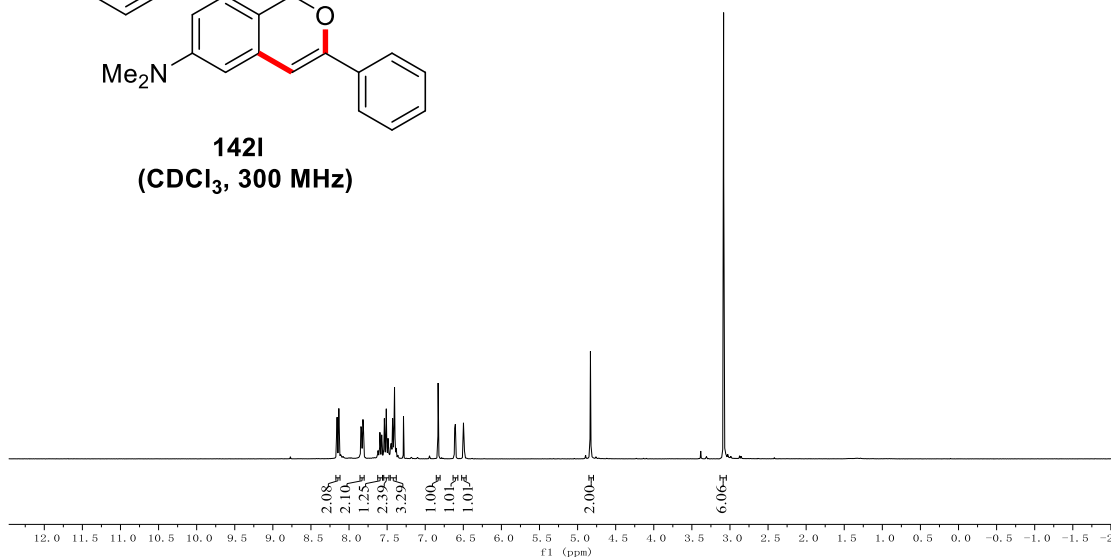
NMR Spectra



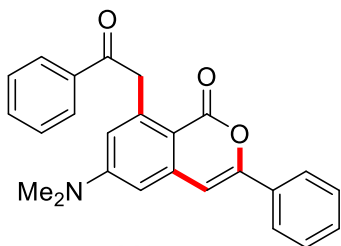
NMR Spectra



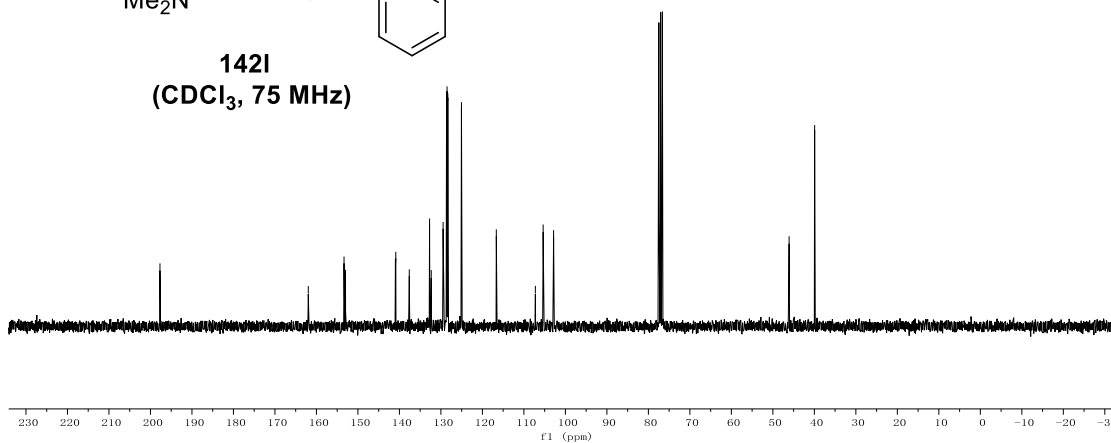
142I
(CDCl₃, 300 MHz)



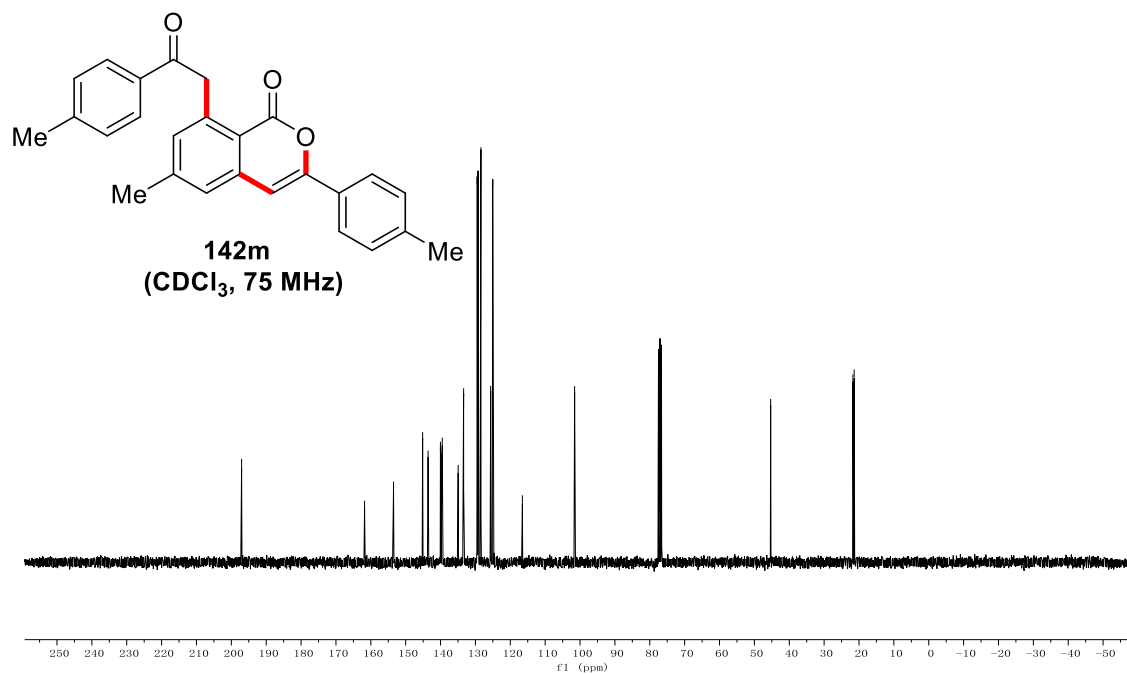
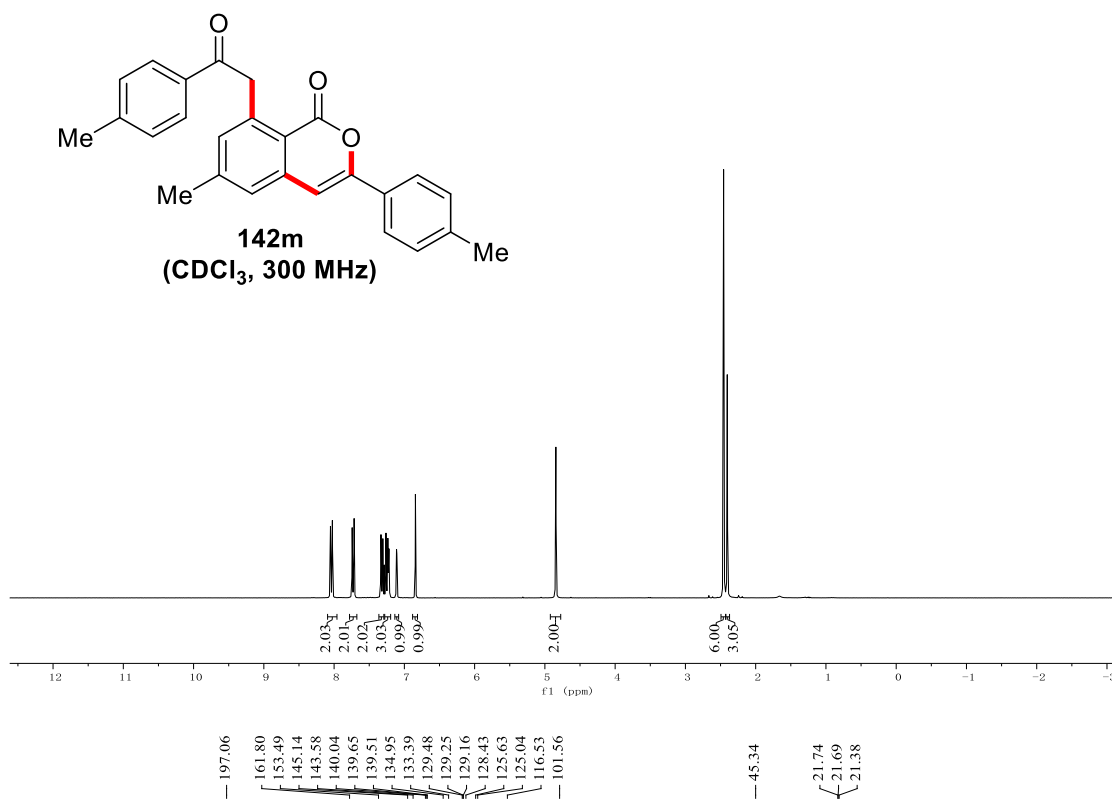
197.71
161.96
153.35
152.99
140.97
140.87
137.62
132.73
132.33
129.47
128.64
128.52
128.34
125.05
116.65
107.23
105.36
102.84
46.09
39.93



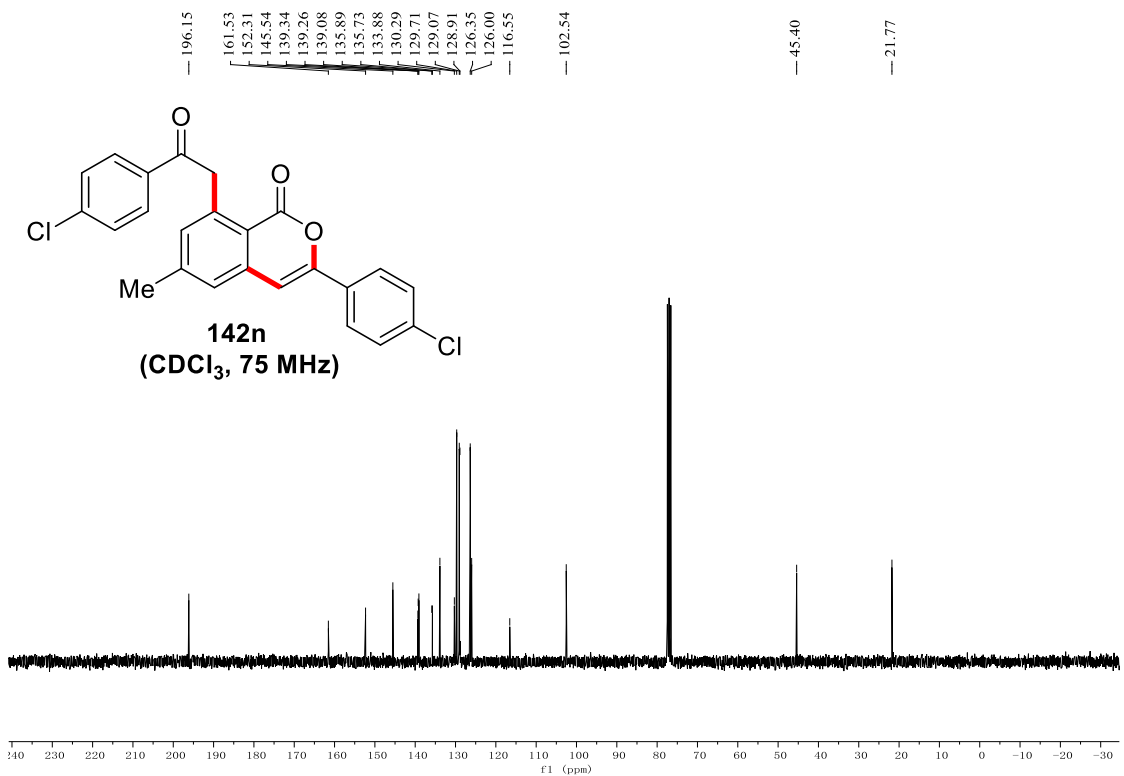
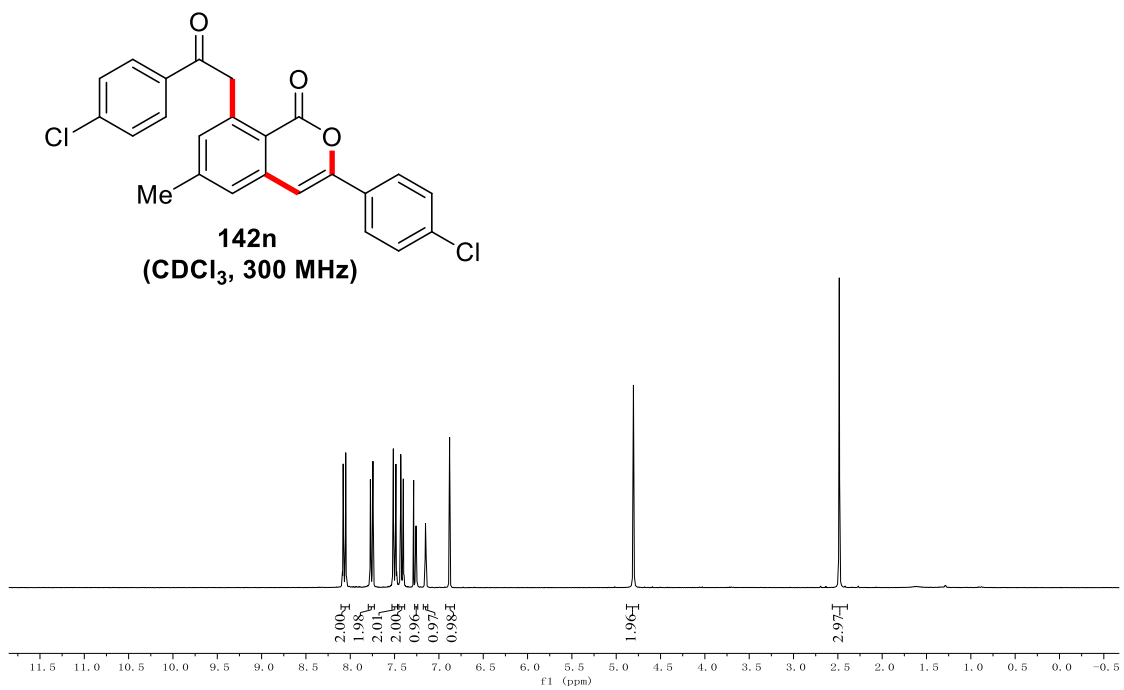
142I
(CDCl₃, 75 MHz)



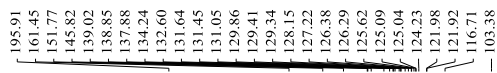
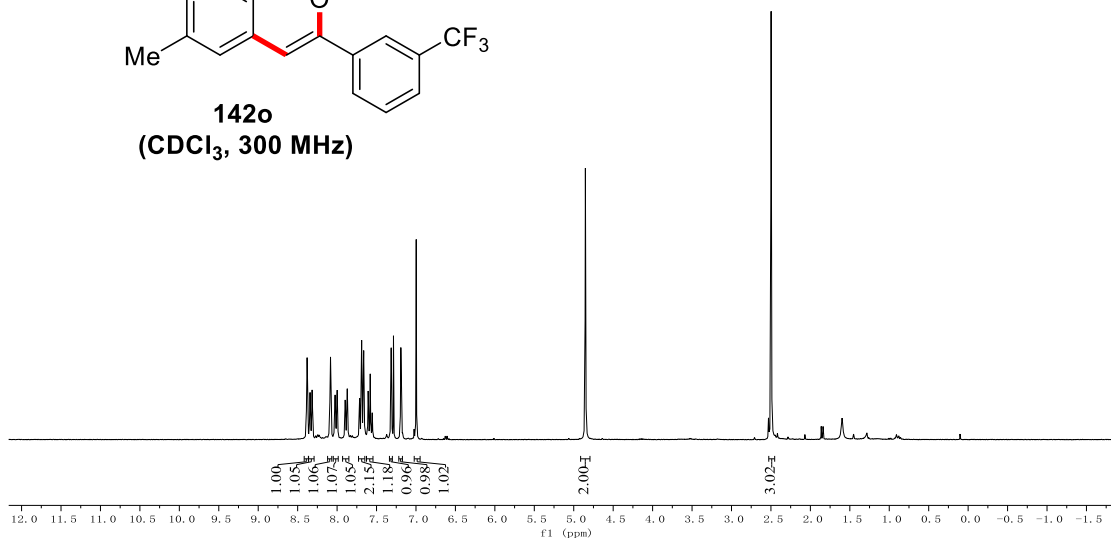
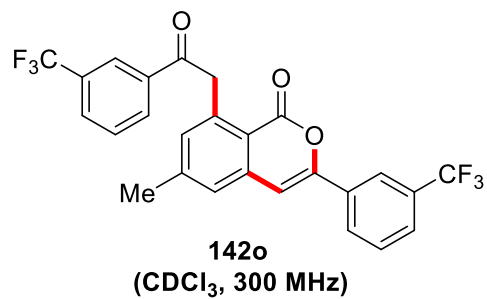
NMR Spectra



NMR Spectra

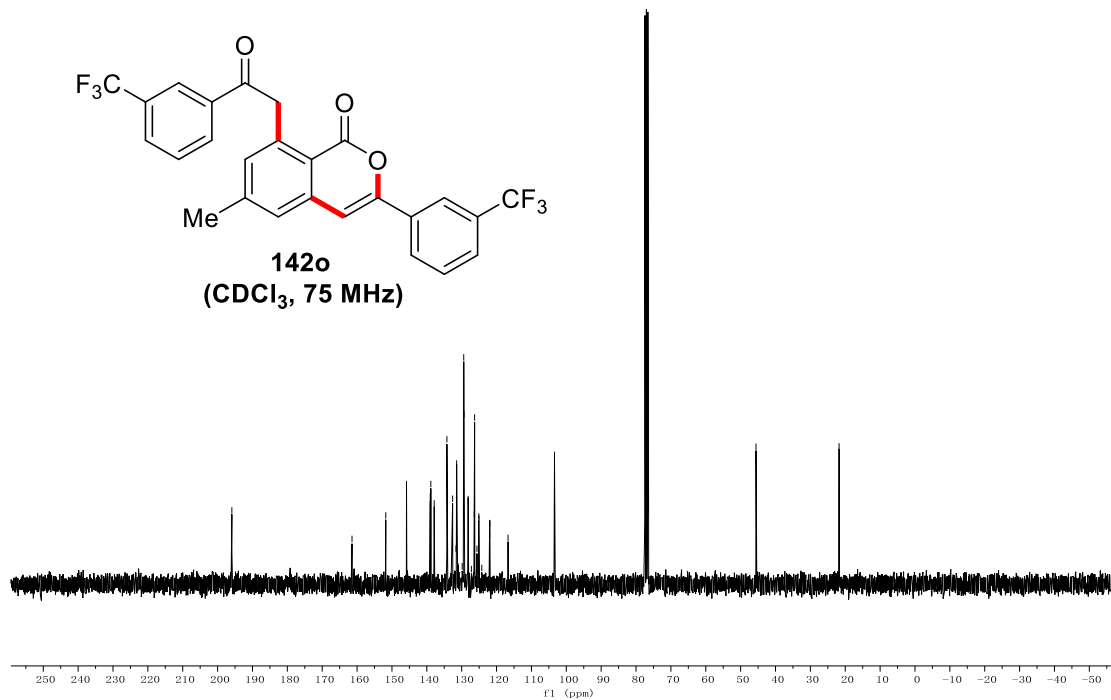
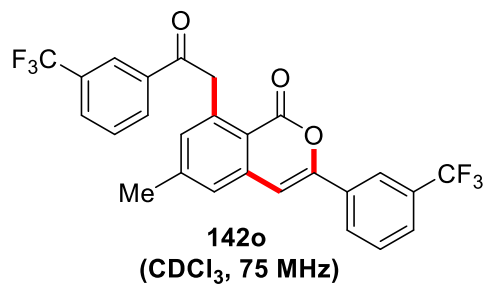


NMR Spectra

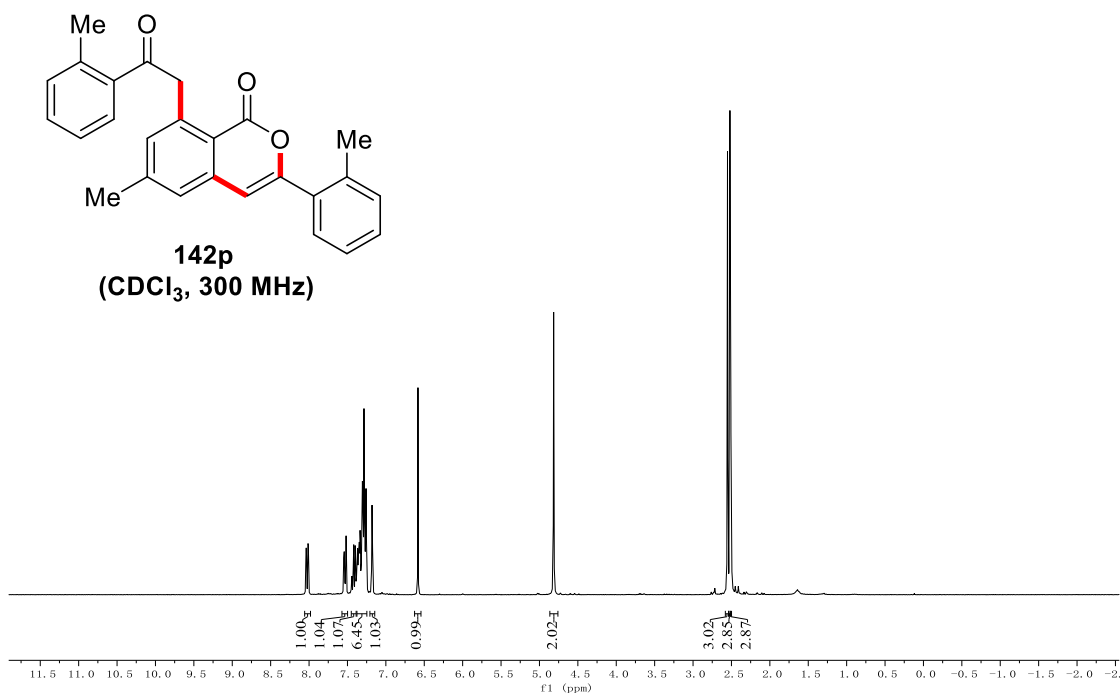
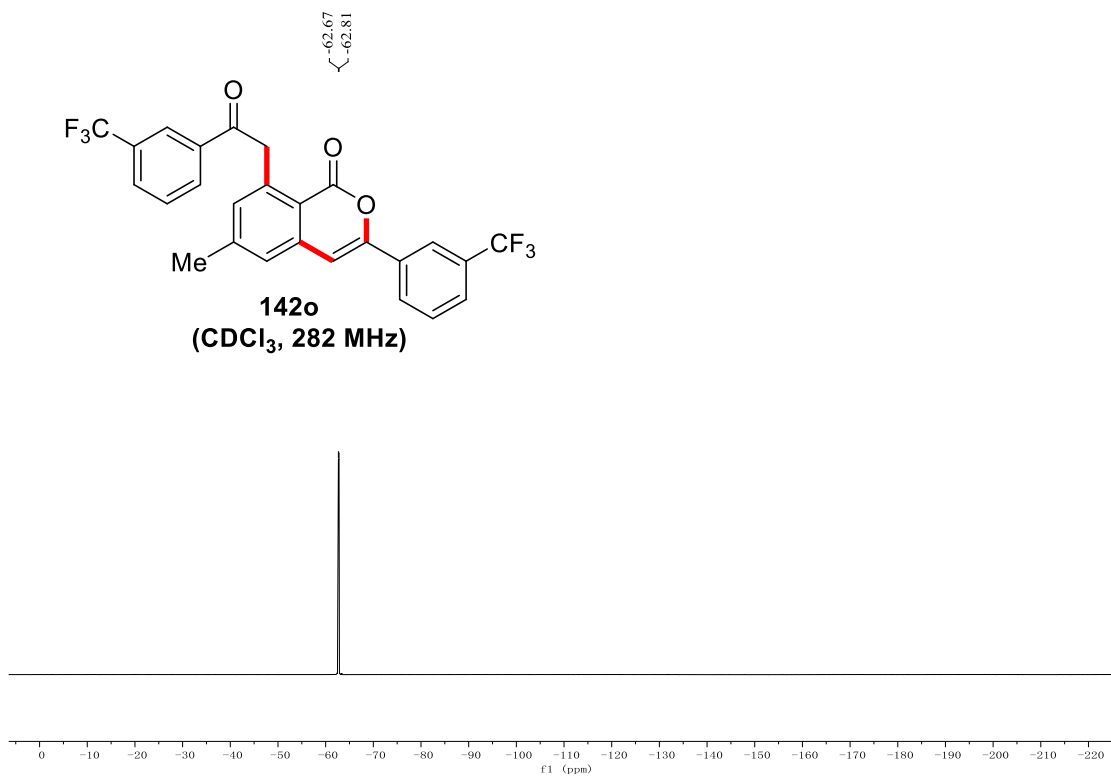


— 45.59

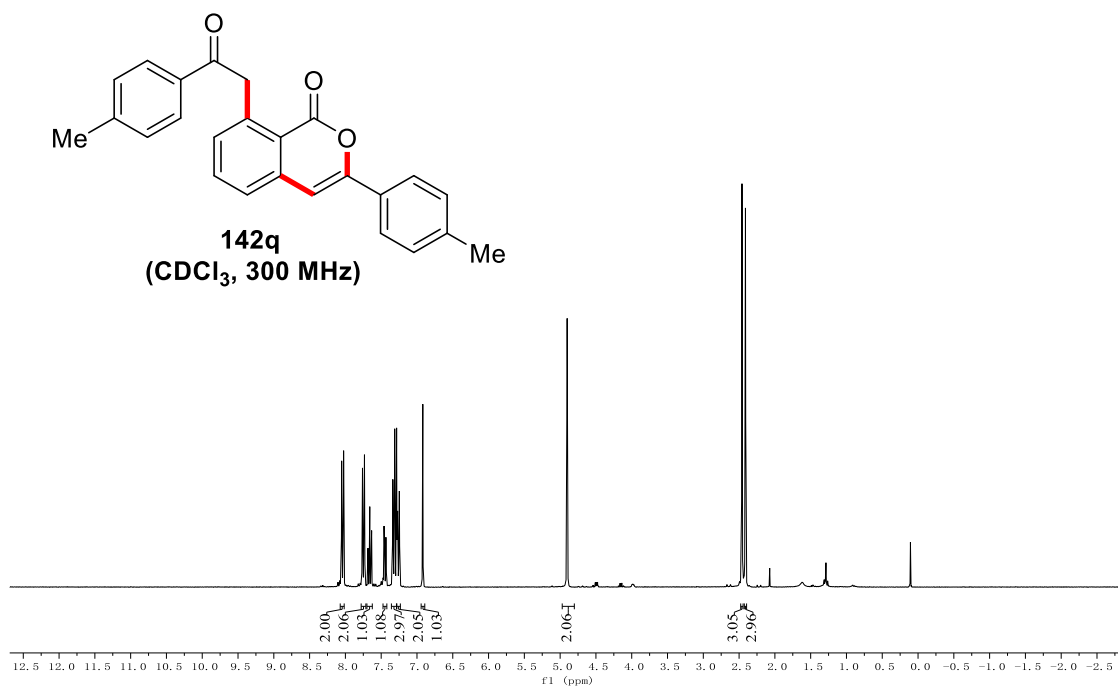
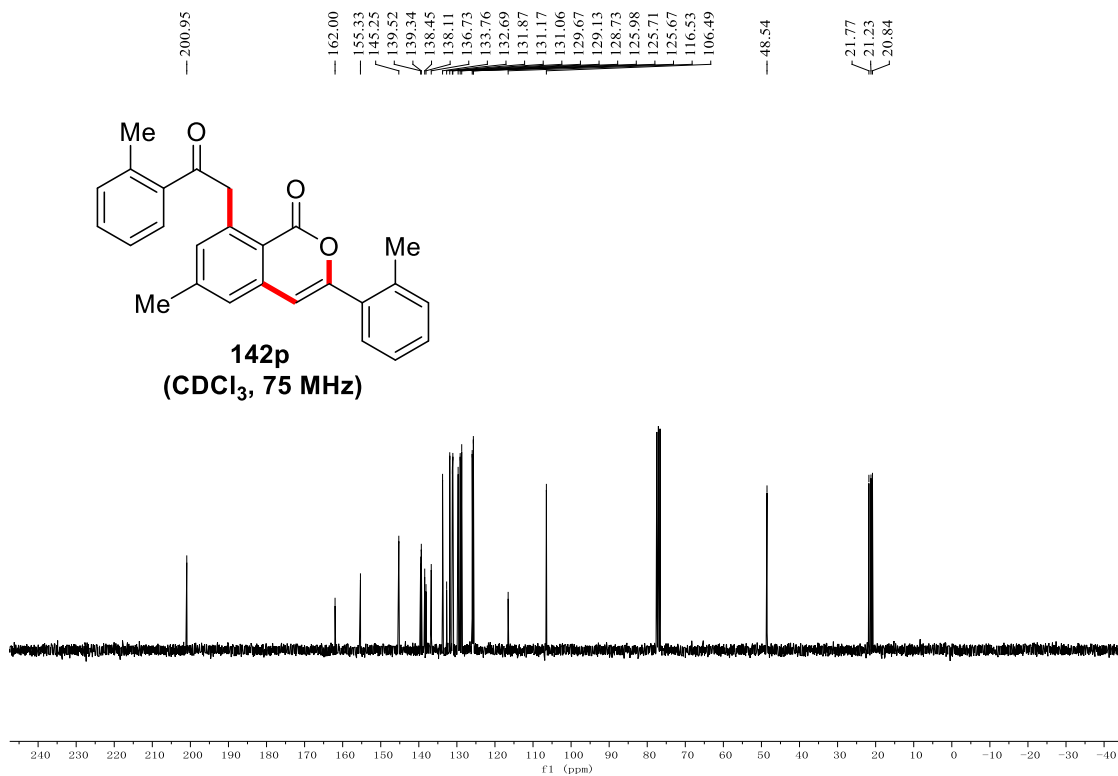
— 21.77



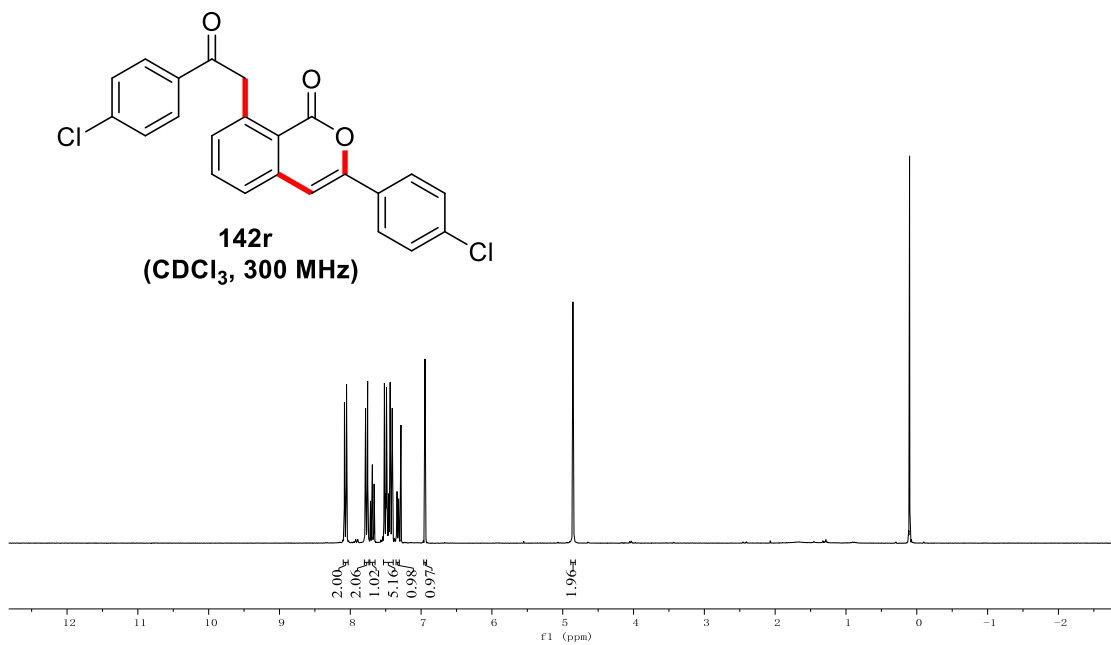
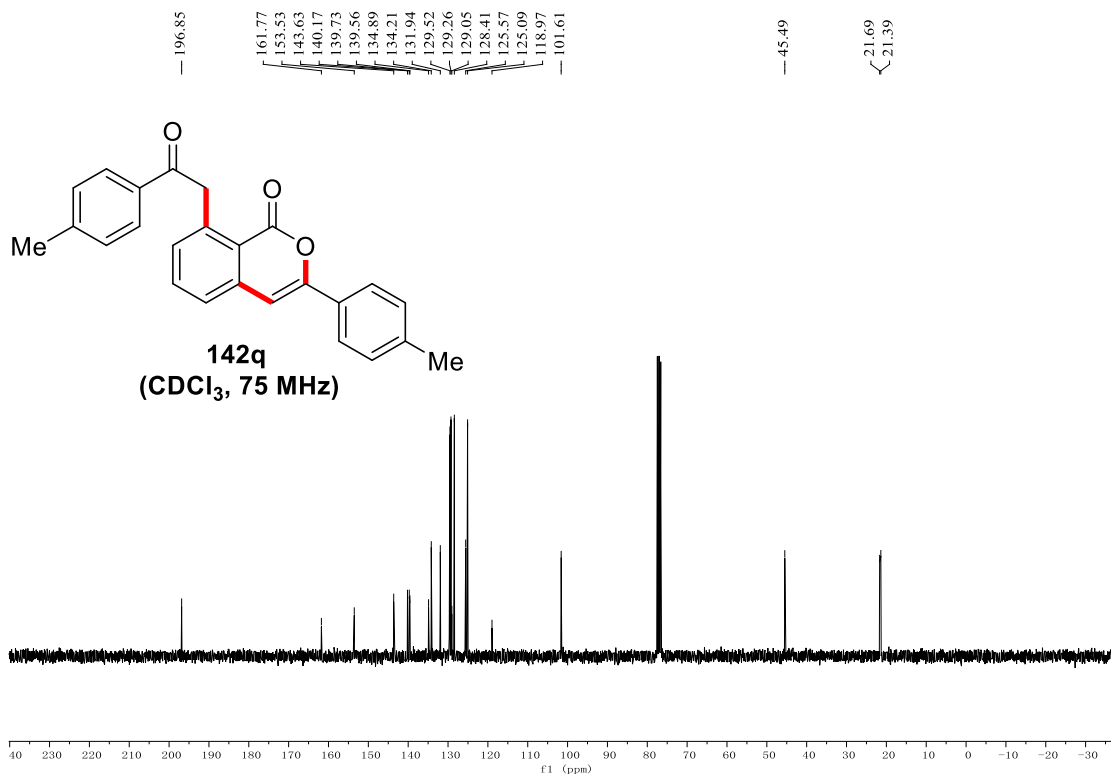
NMR Spectra



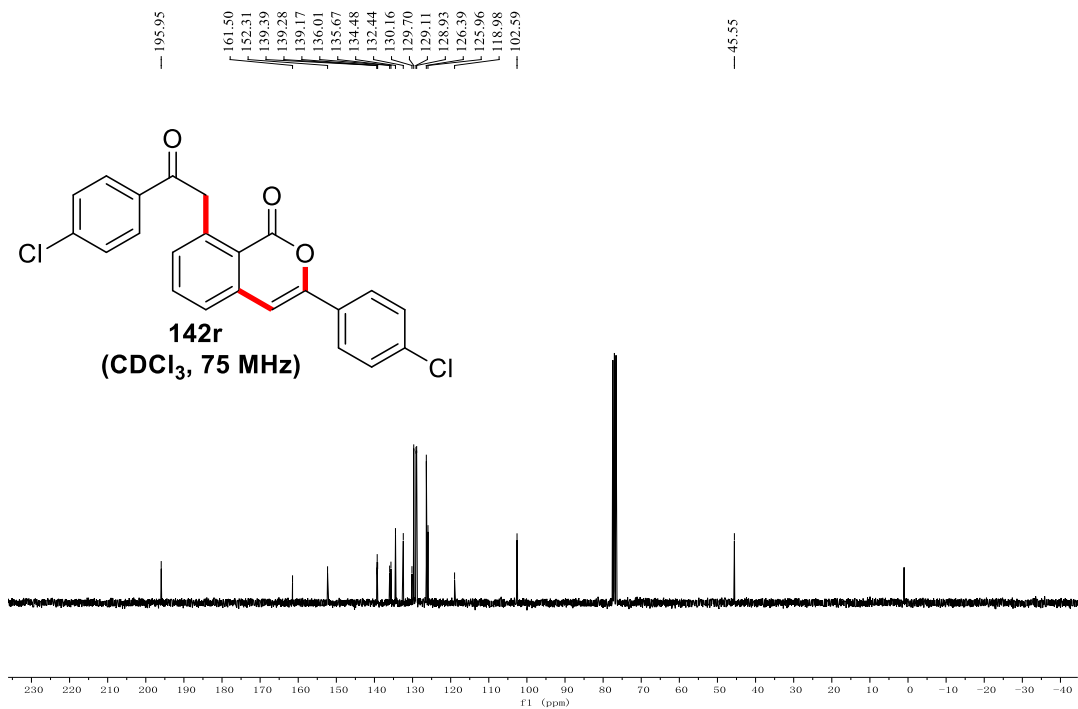
NMR Spectra



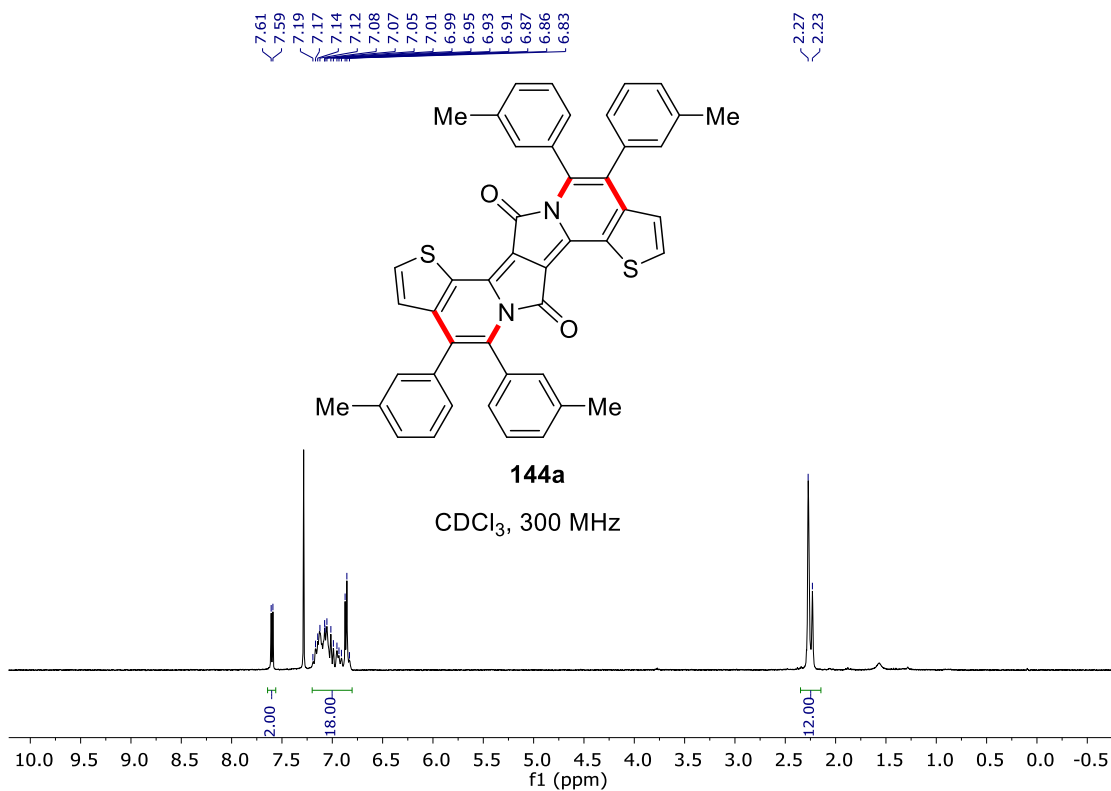
NMR Spectra



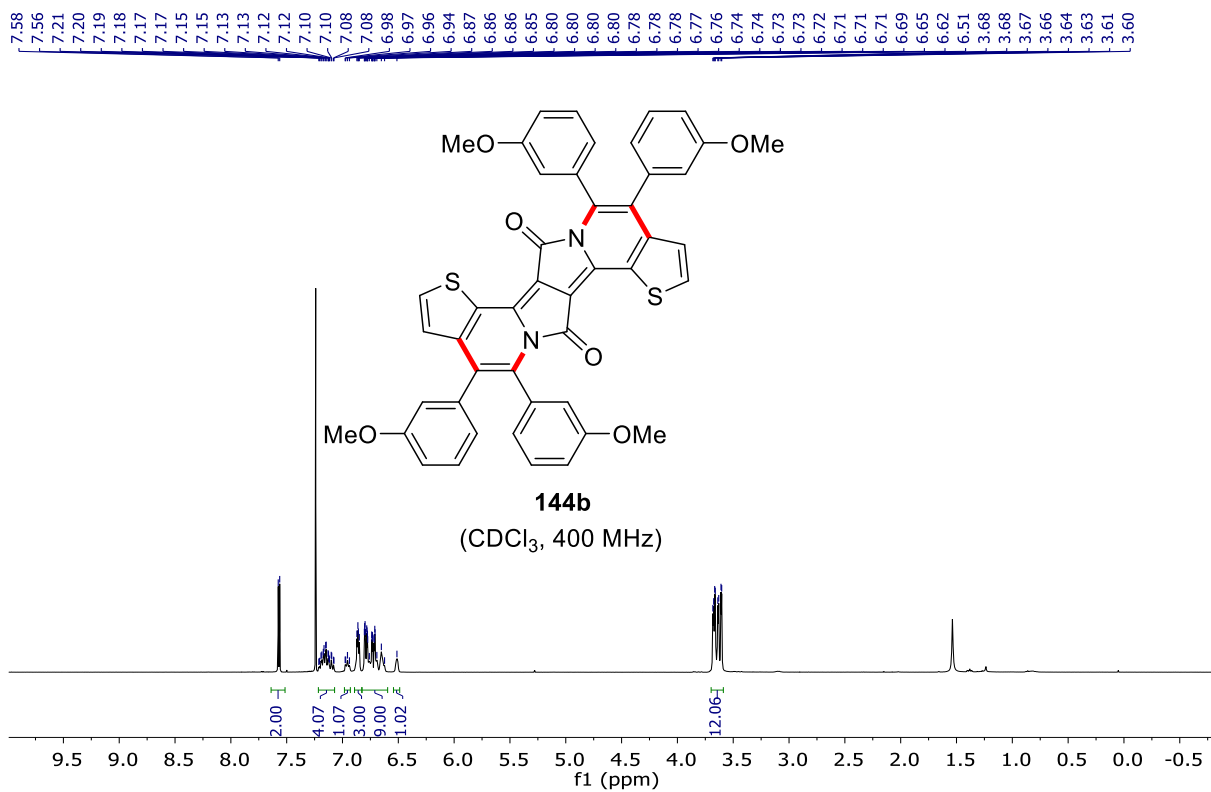
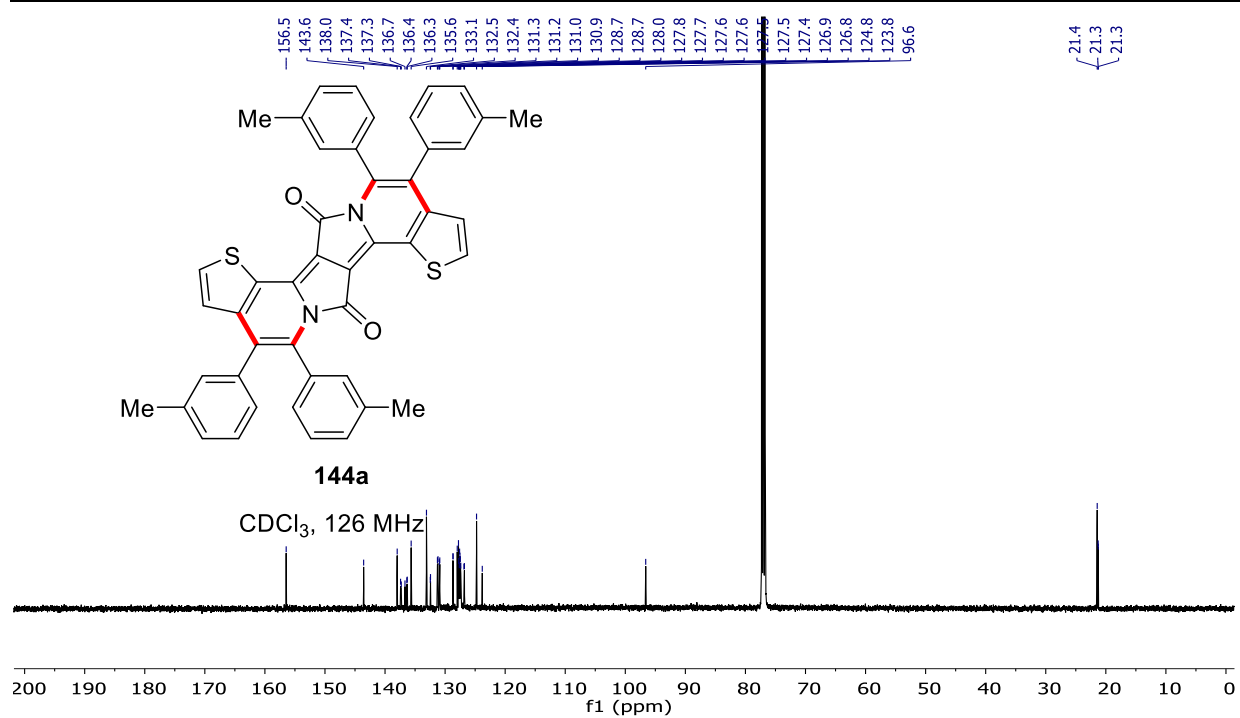
NMR Spectra



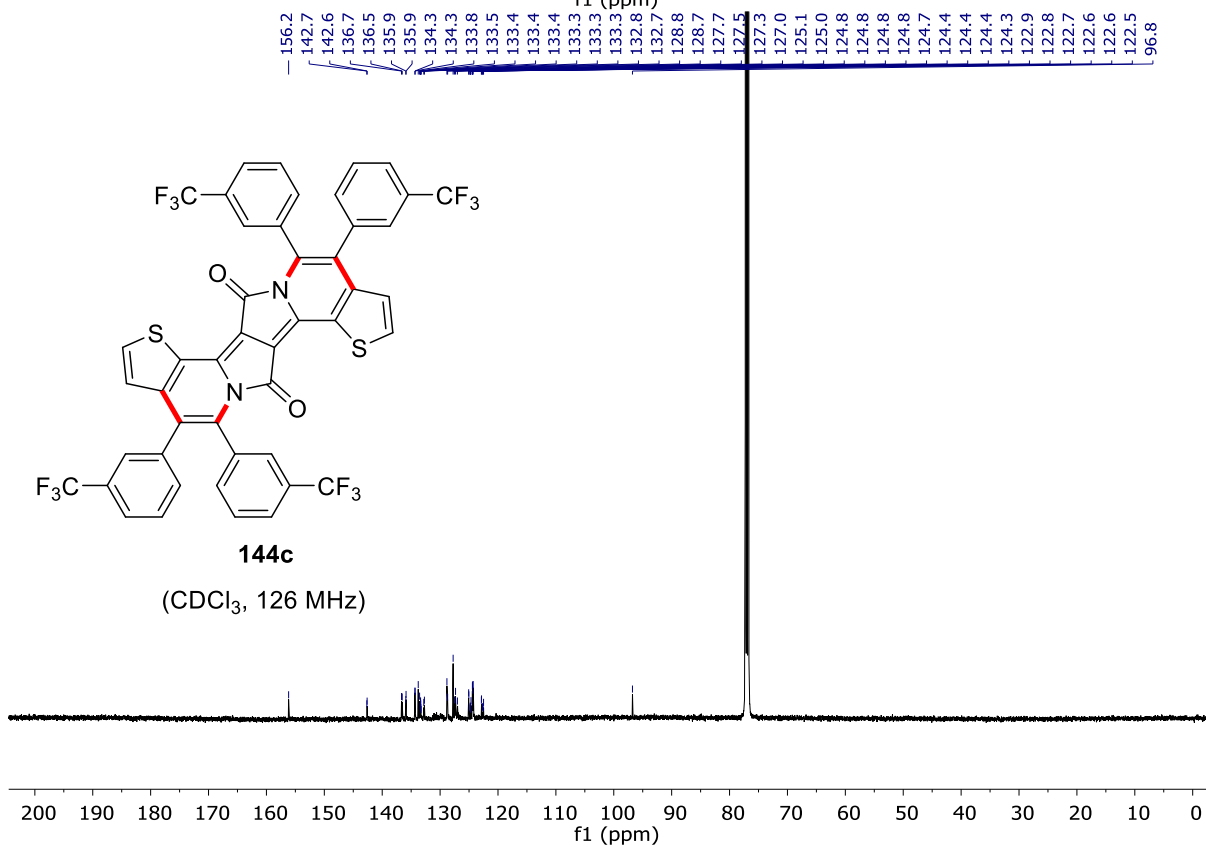
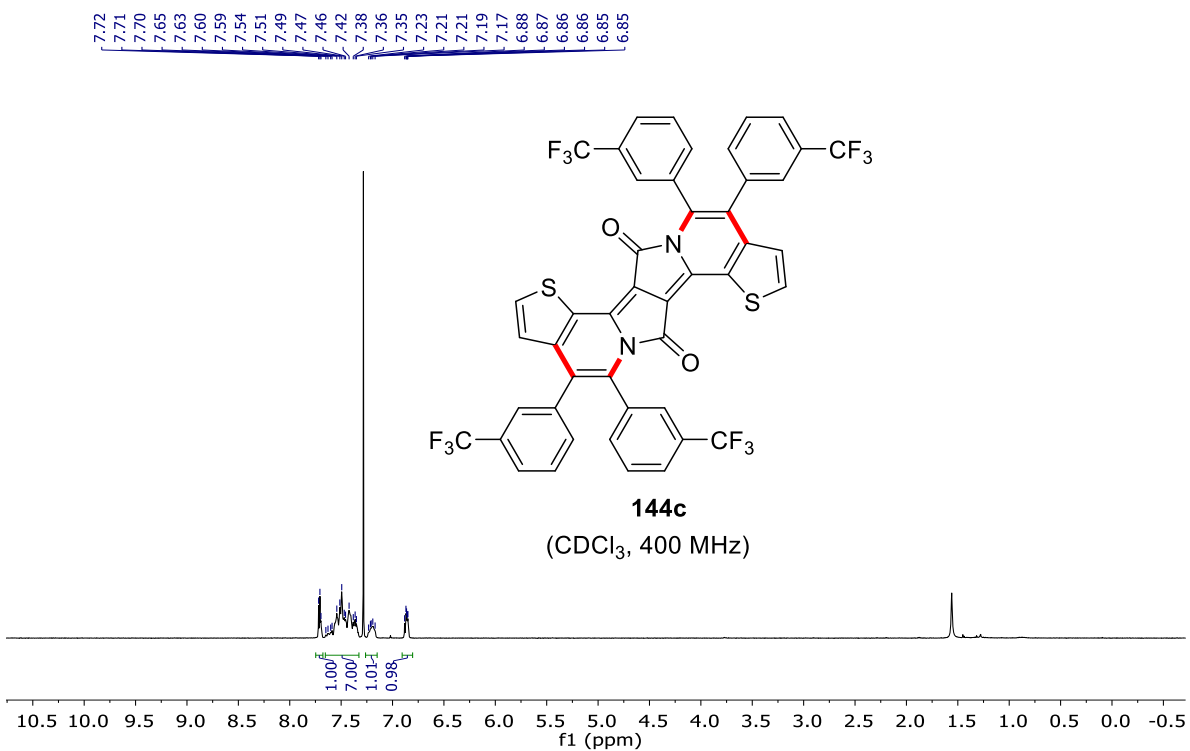
7.2 Ruthenium(II)-Catalyzed DPP Annulation



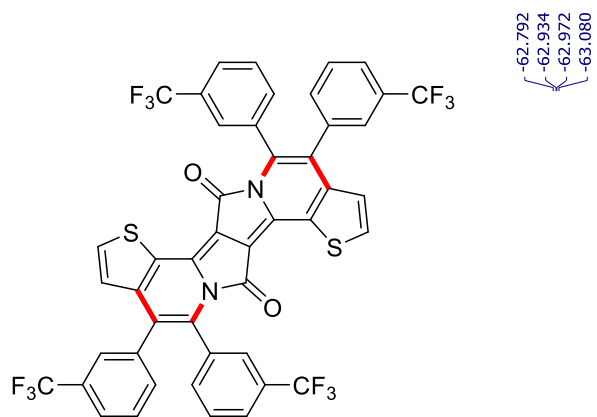
NMR Spectra



NMR Spectra

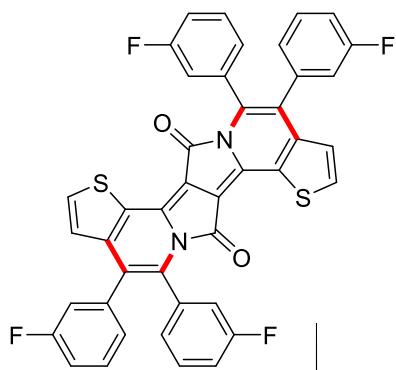
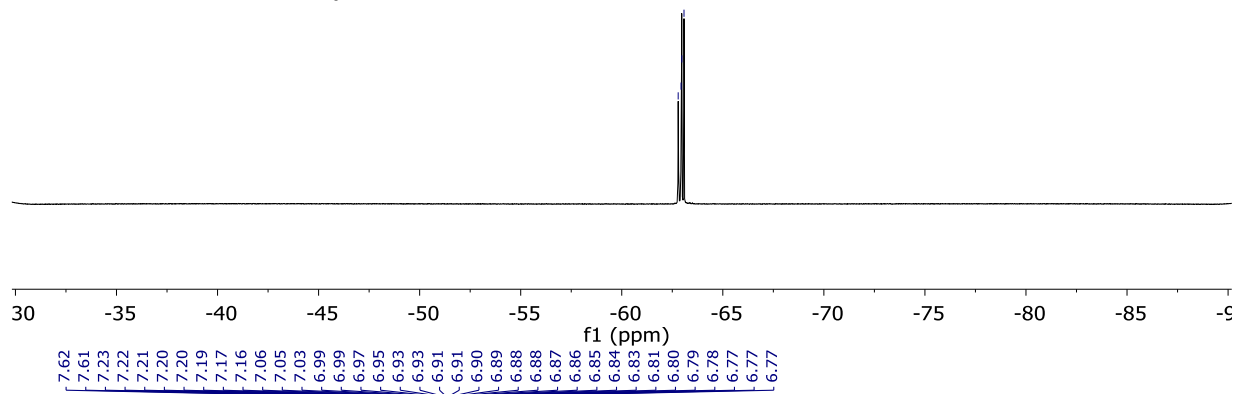


NMR Spectra



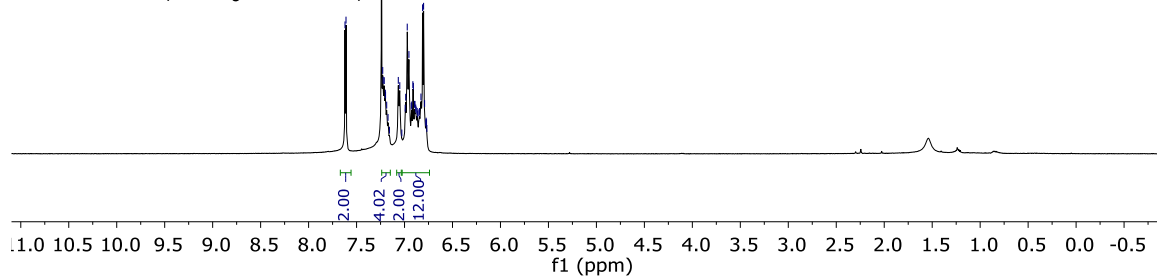
144c

(CDCl_3 , 477 MHz)

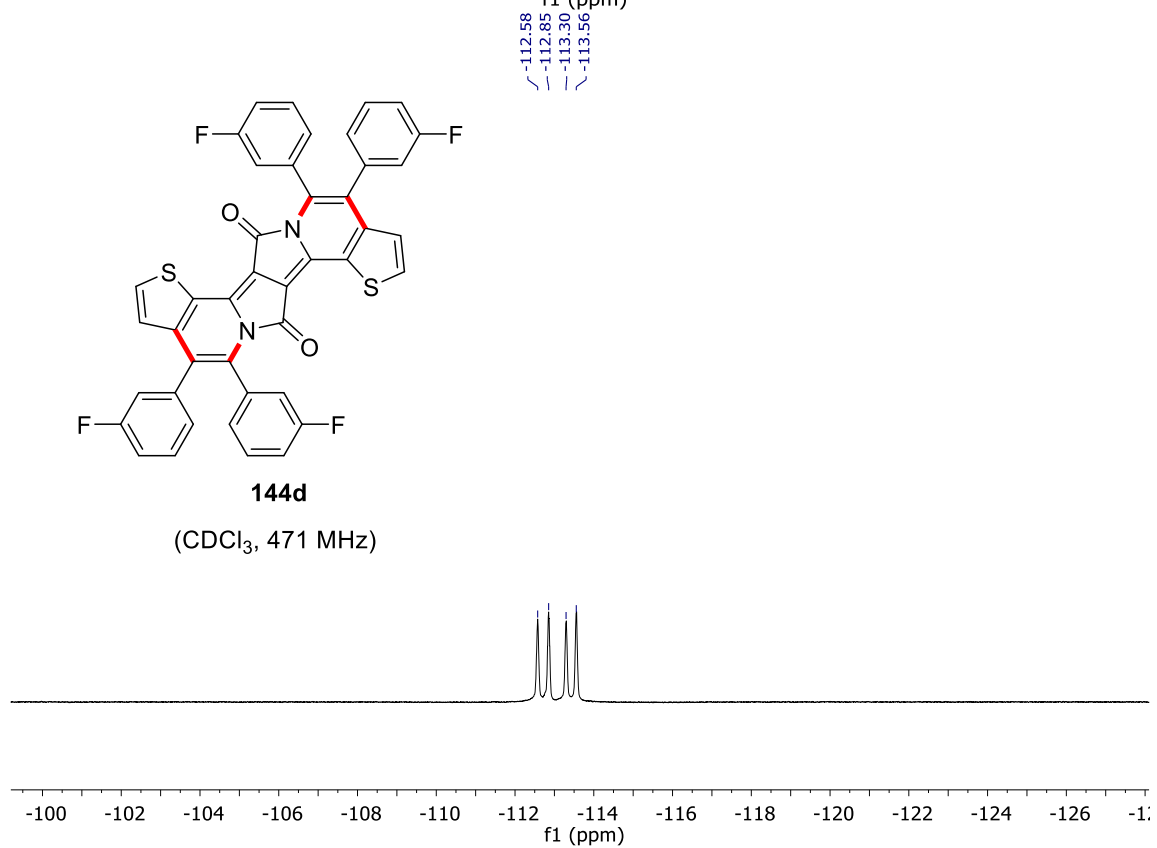
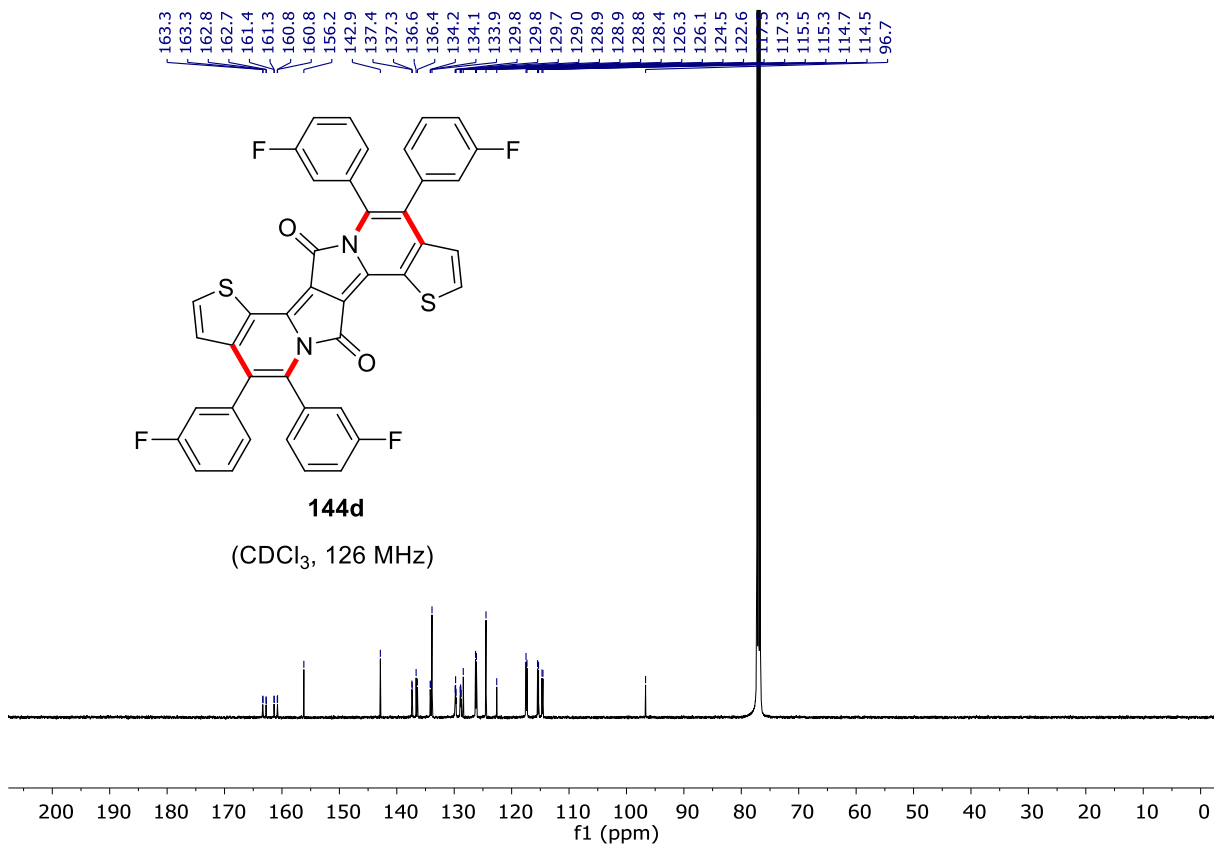


144d

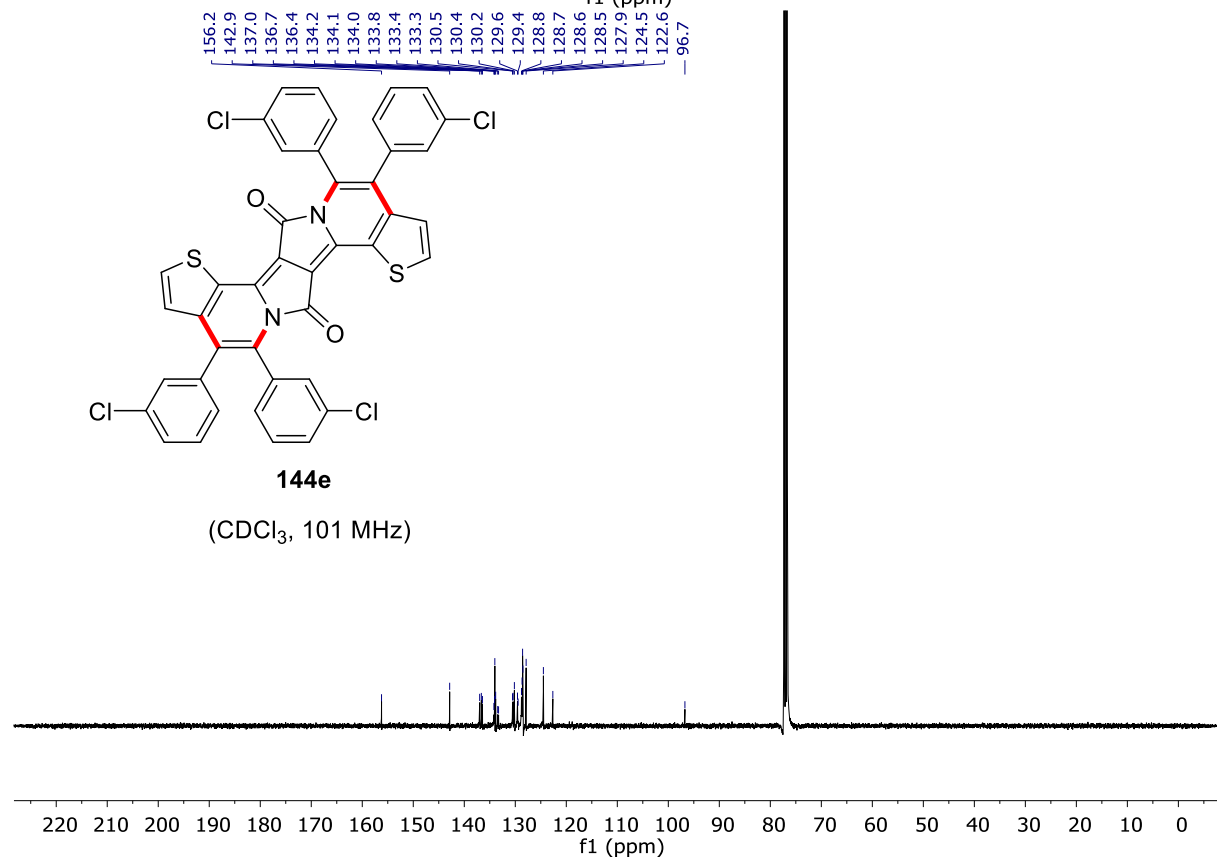
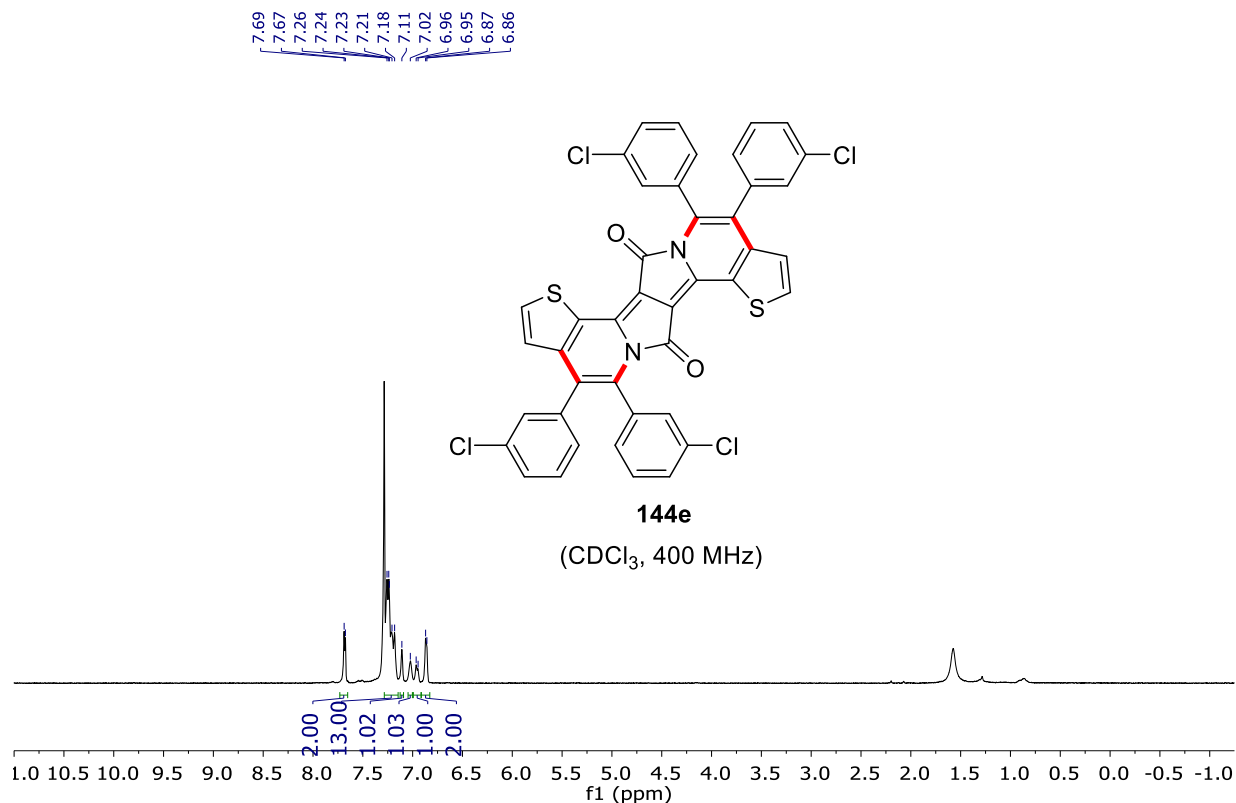
(CDCl_3 , 500 MHz)



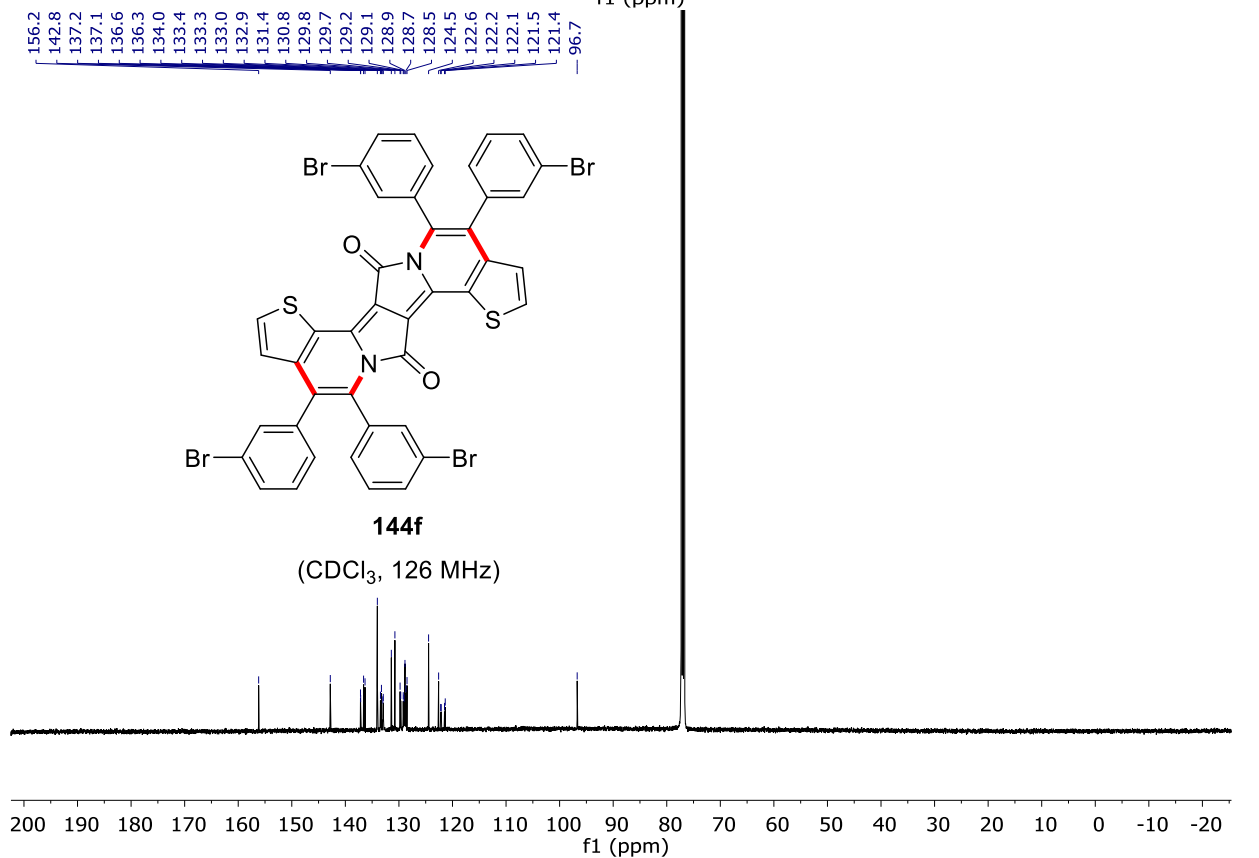
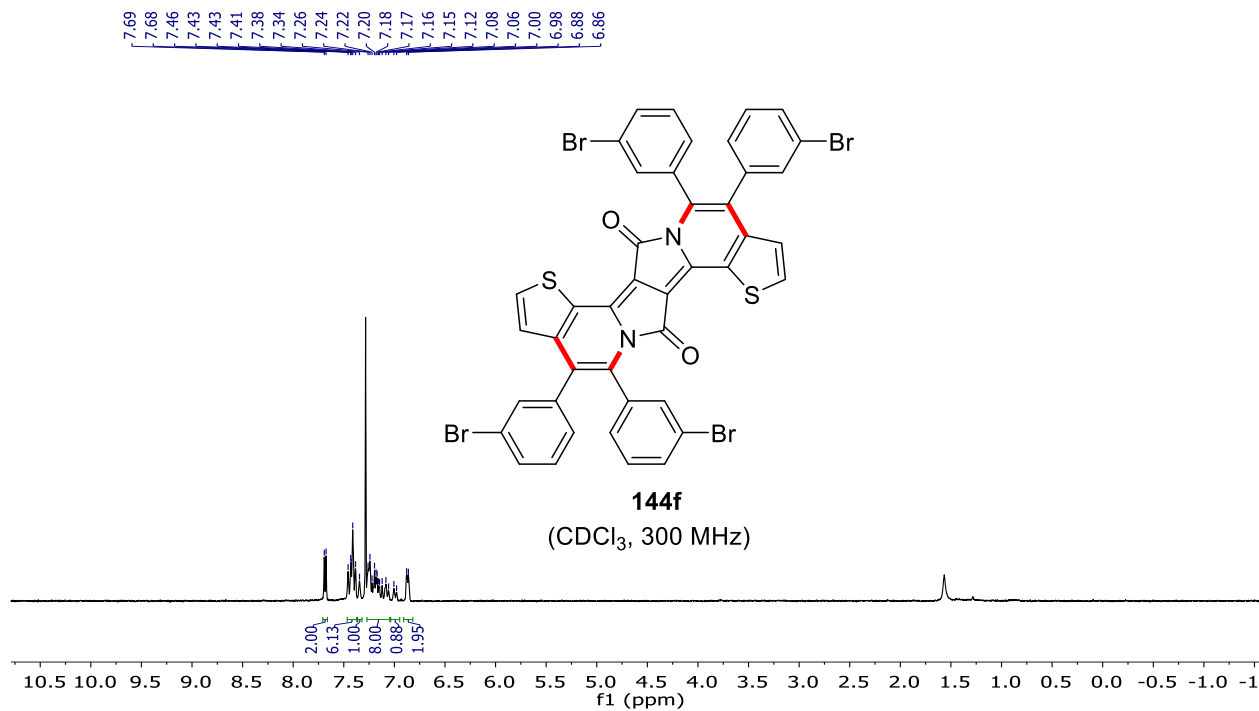
NMR Spectra



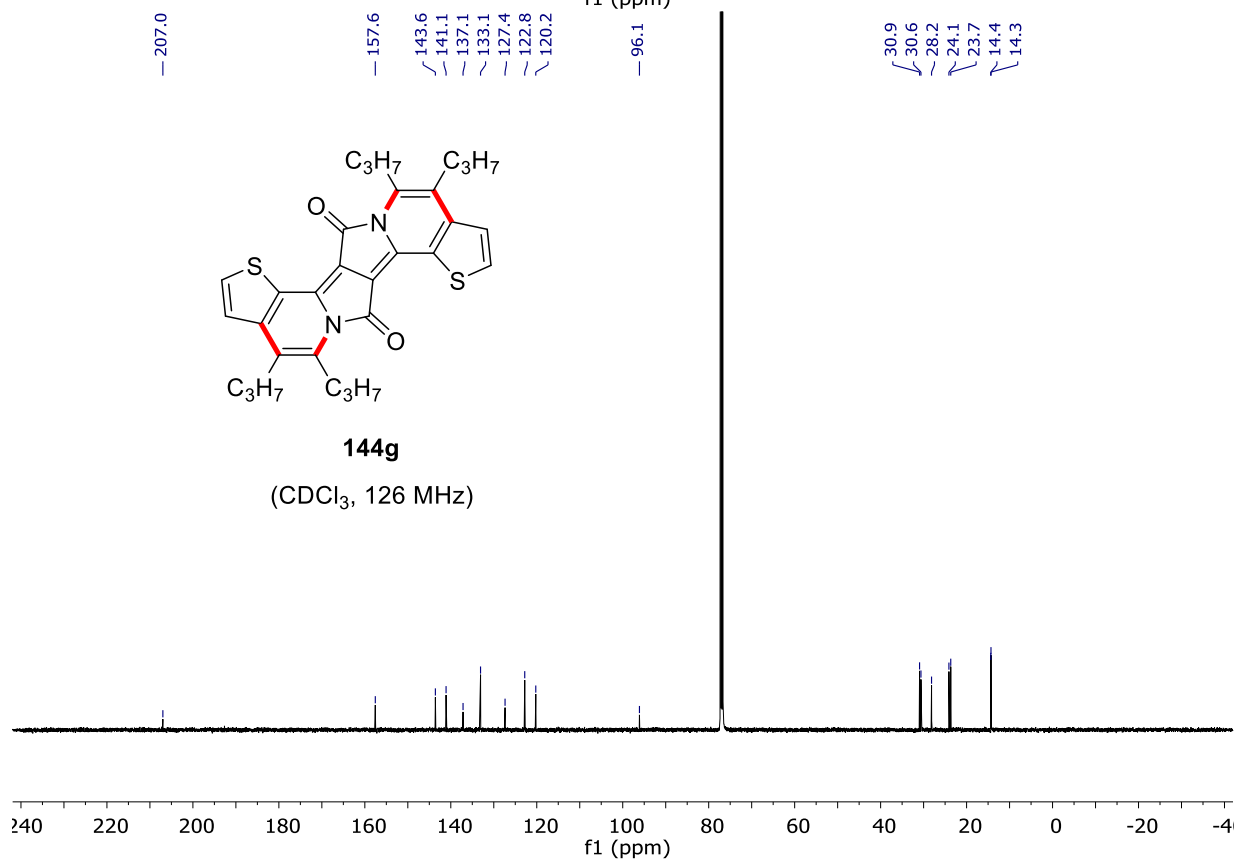
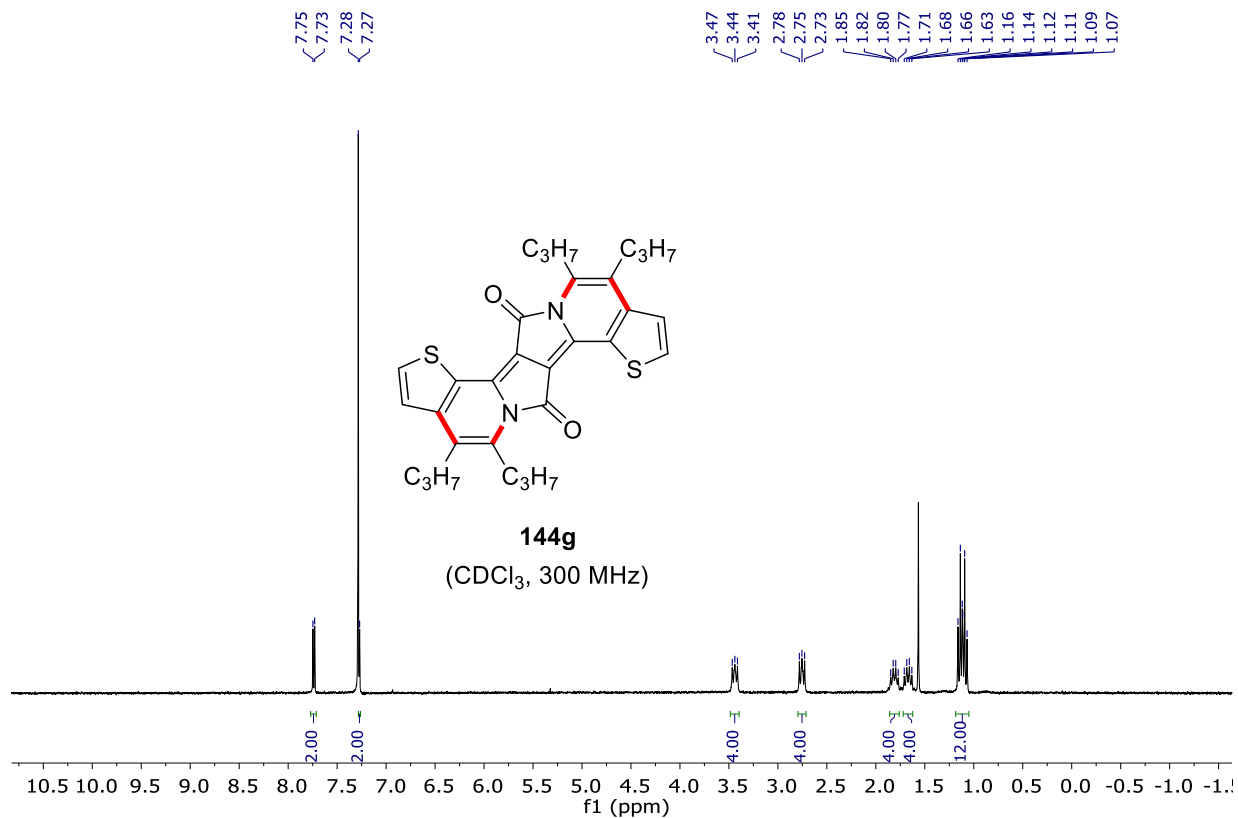
NMR Spectra



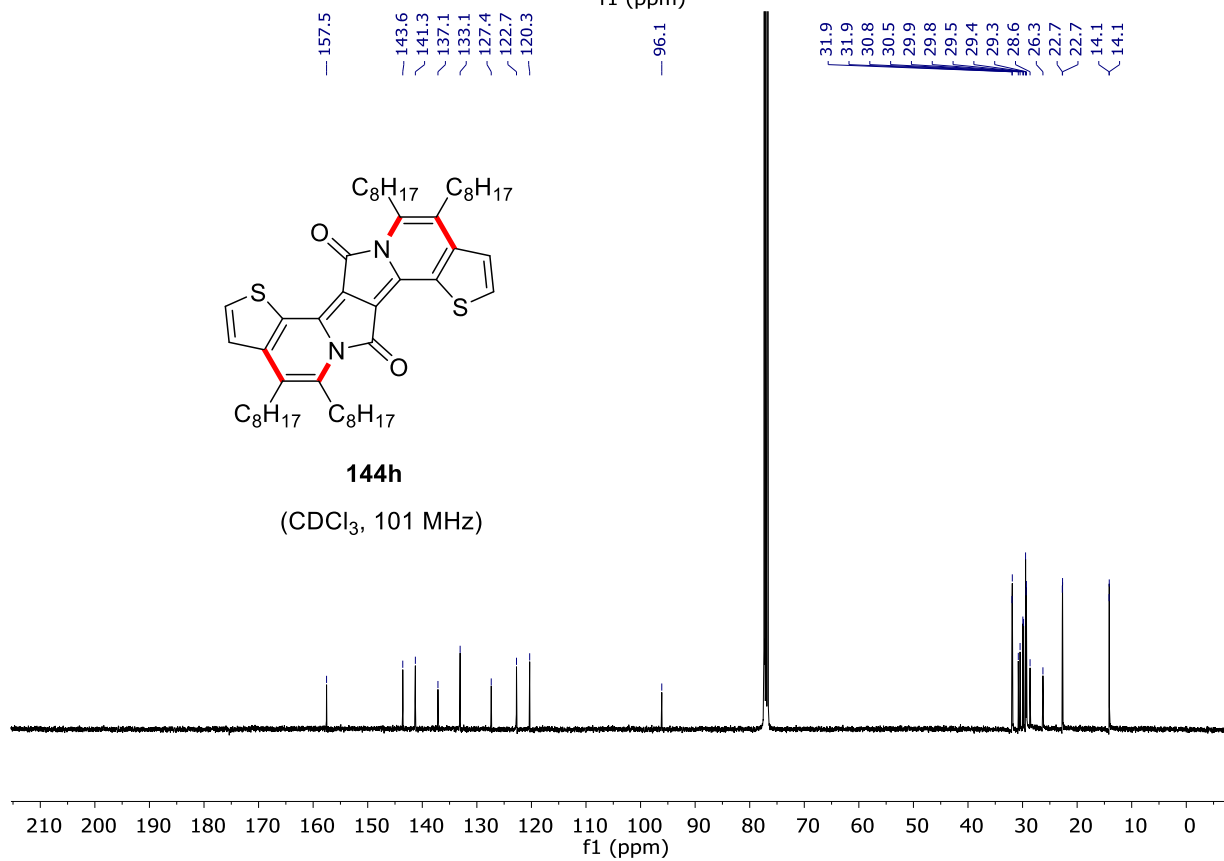
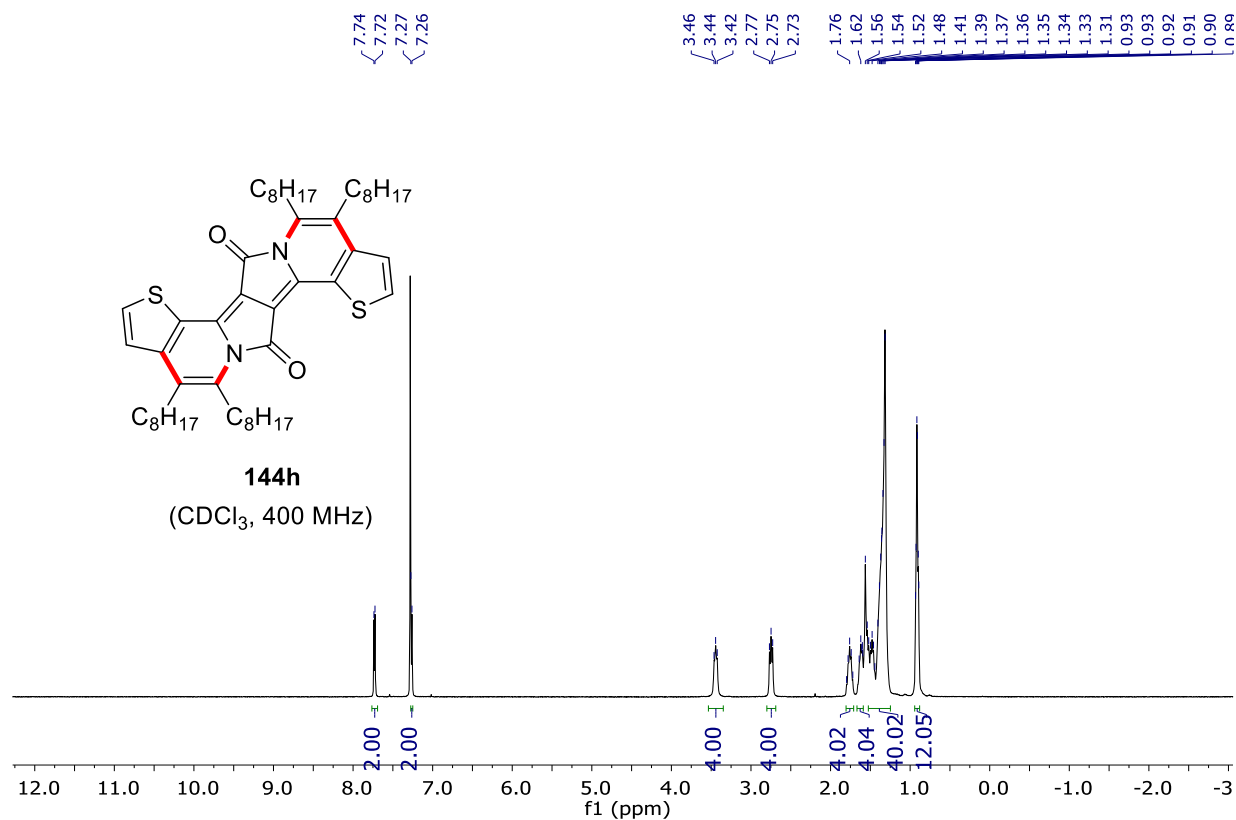
NMR Spectra



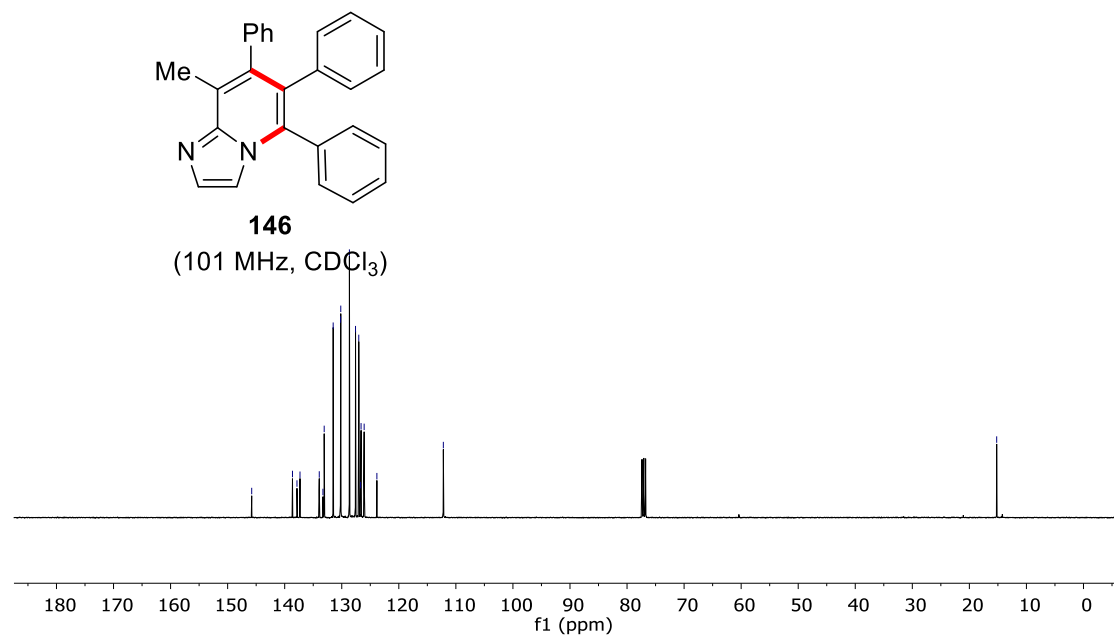
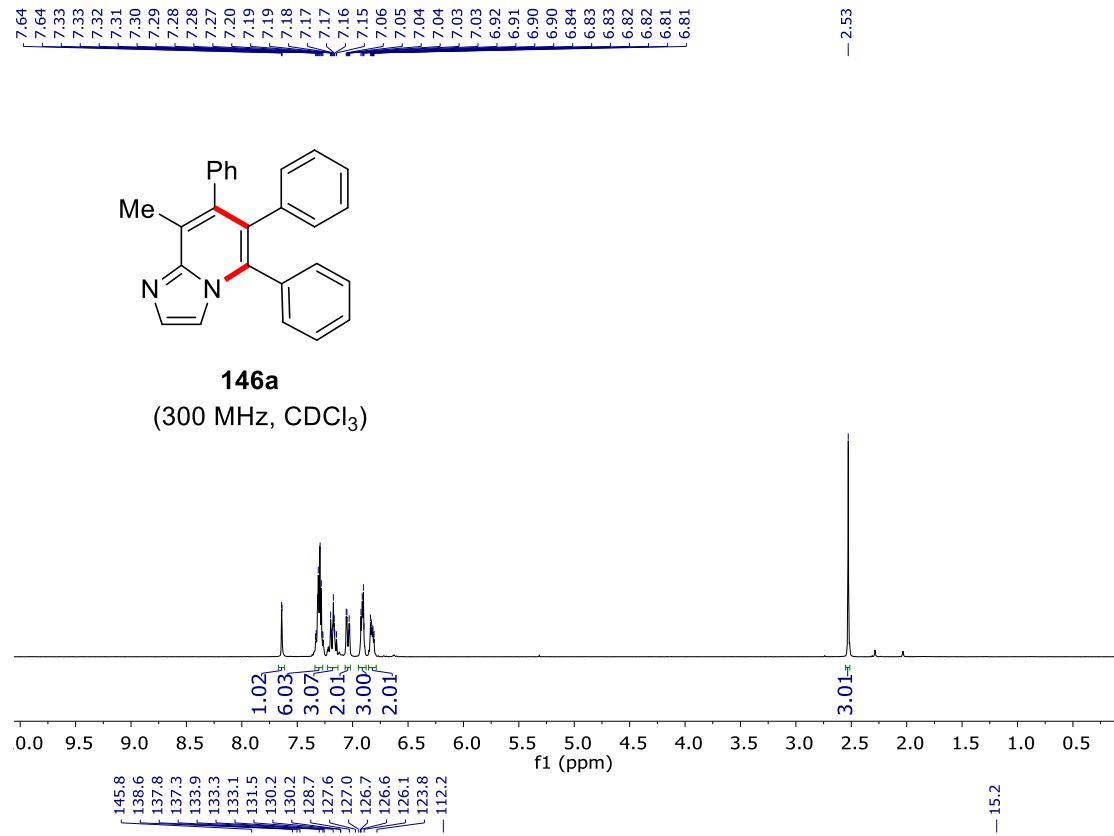
NMR Spectra



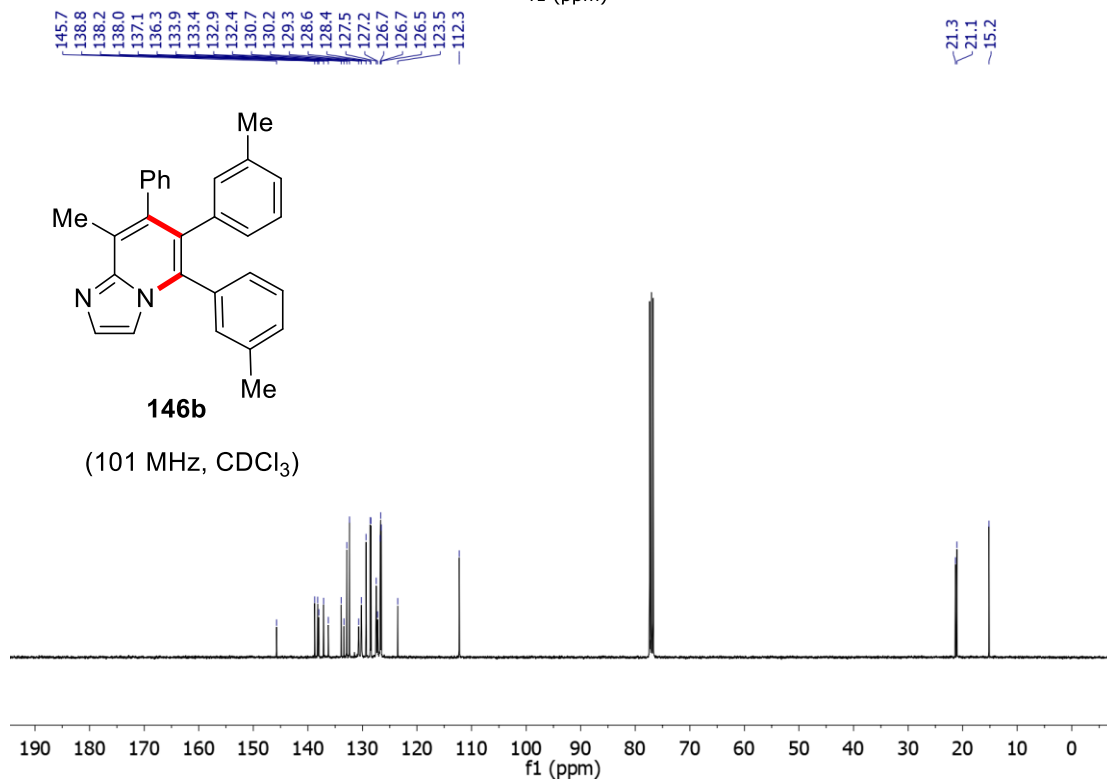
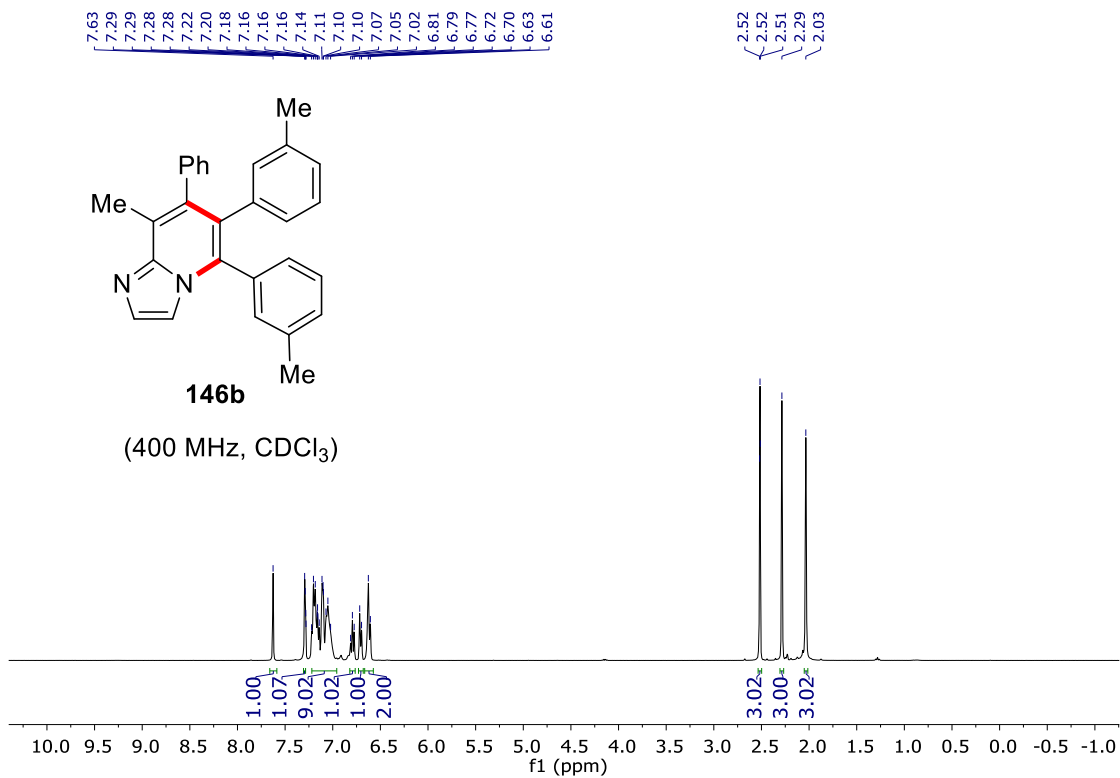
NMR Spectra



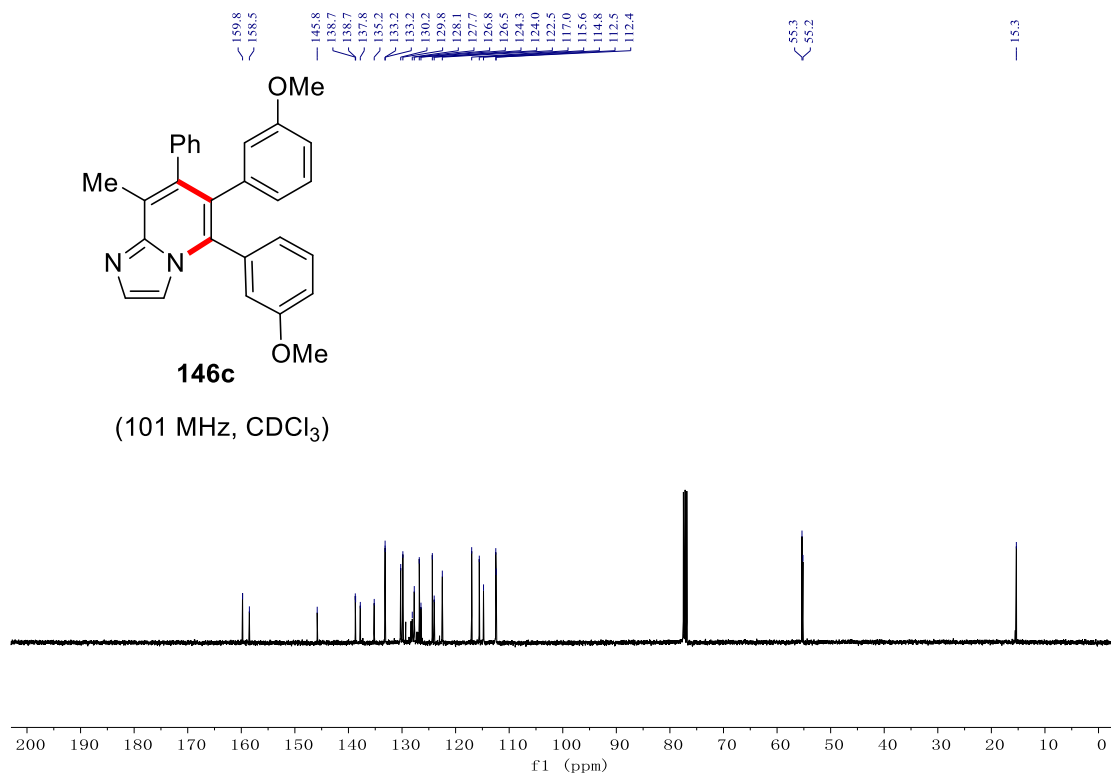
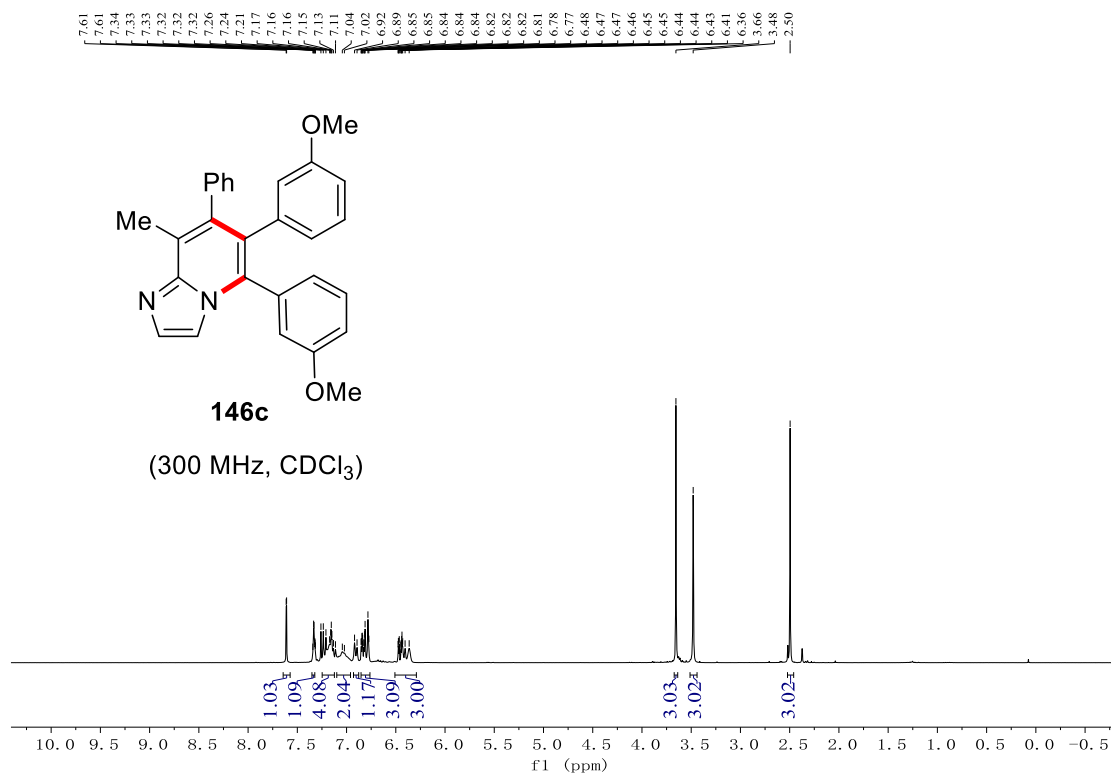
7.3 Ruthenaelectro(II/III/I)-Catalyzed Annulation



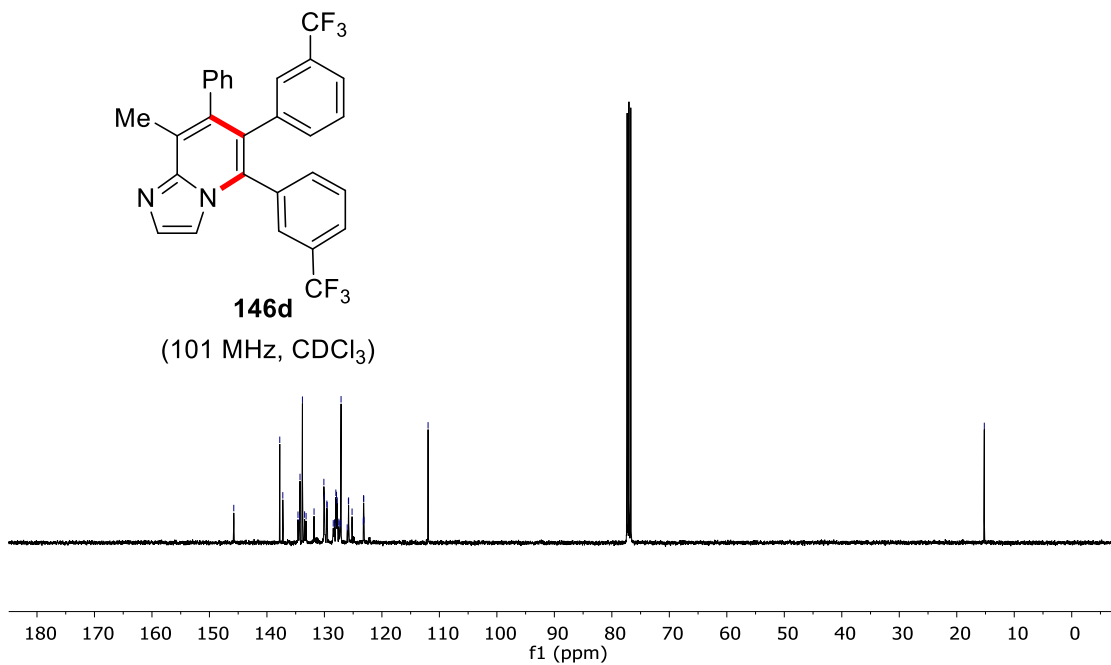
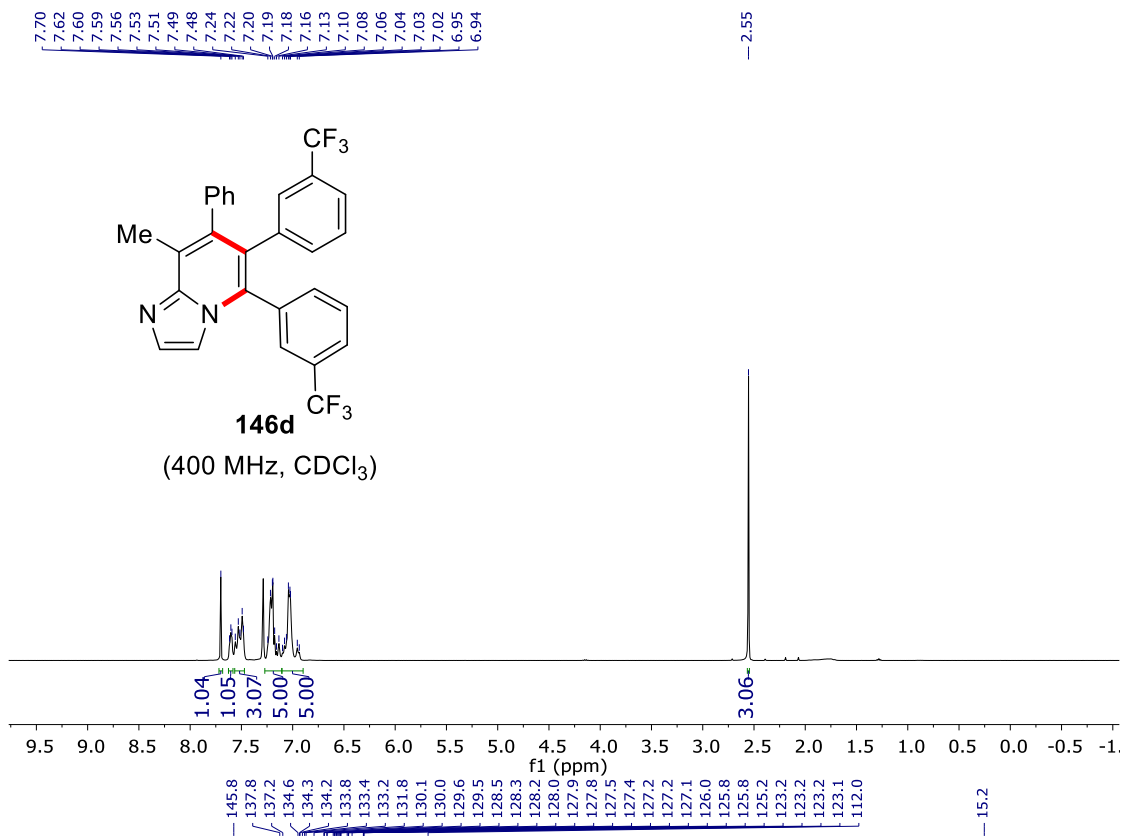
NMR Spectra



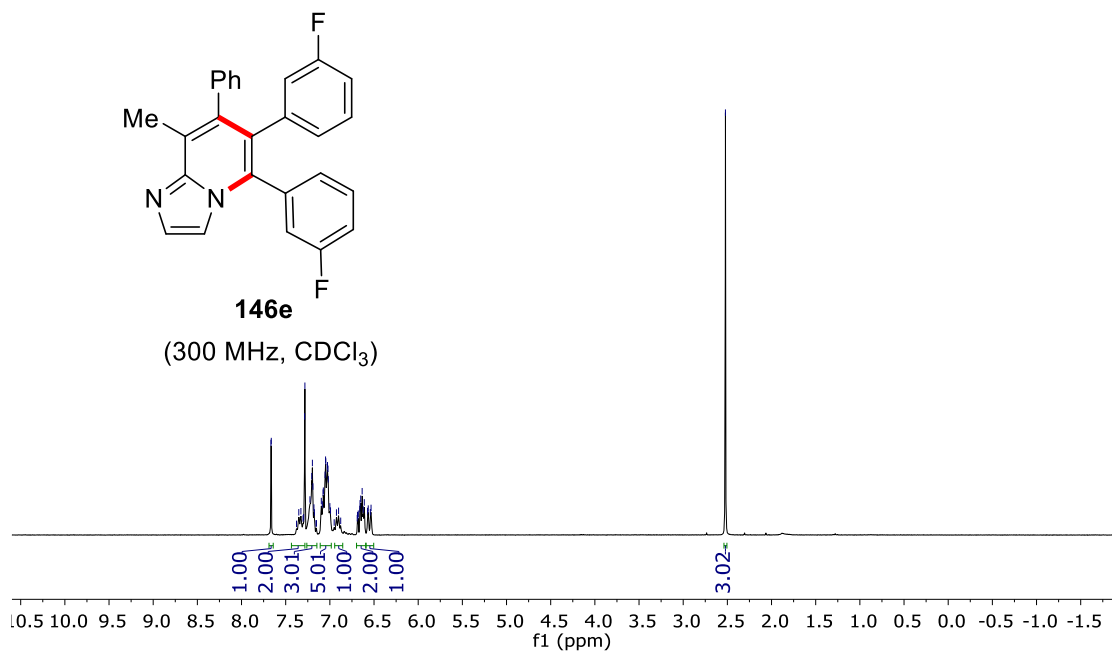
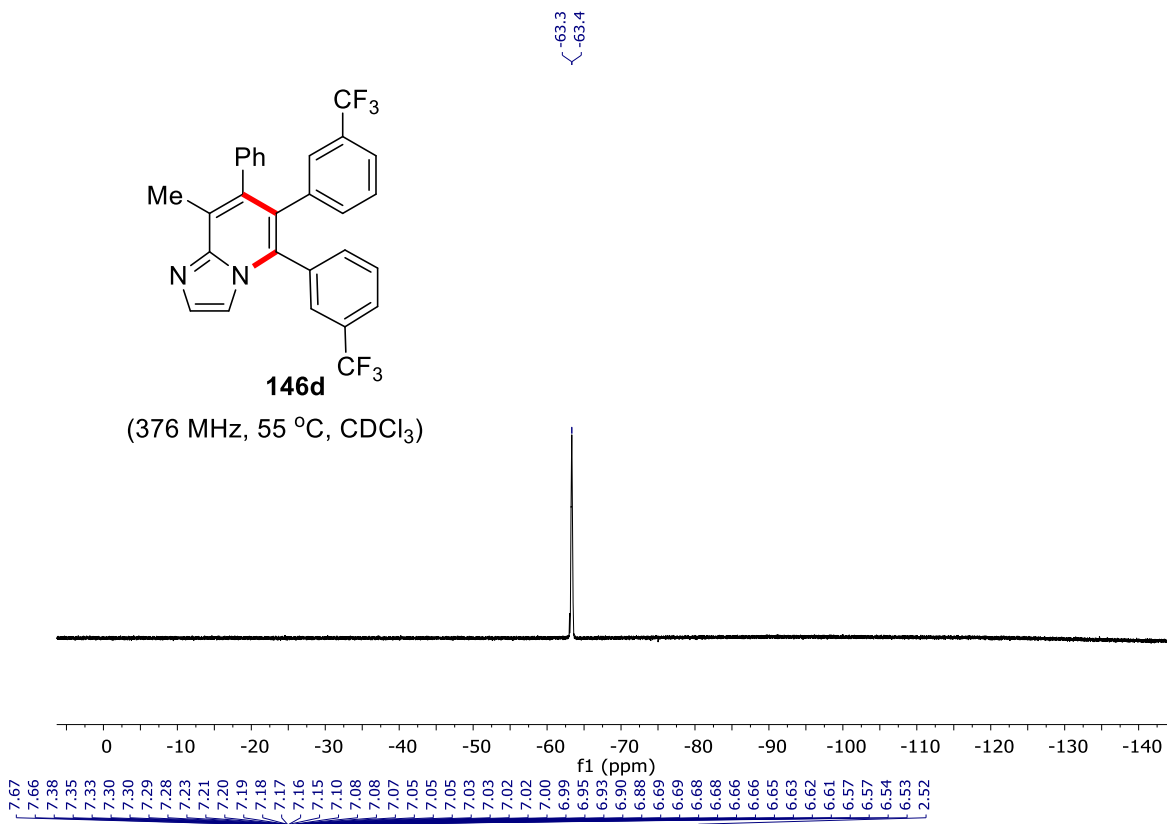
NMR Spectra



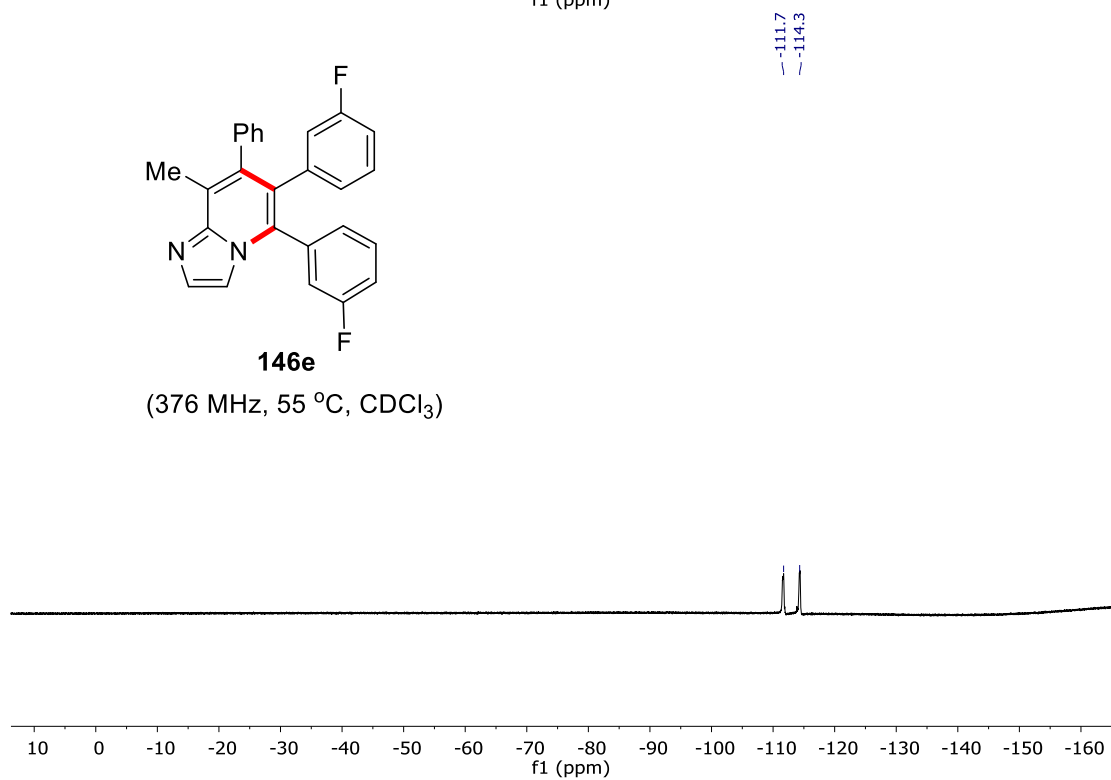
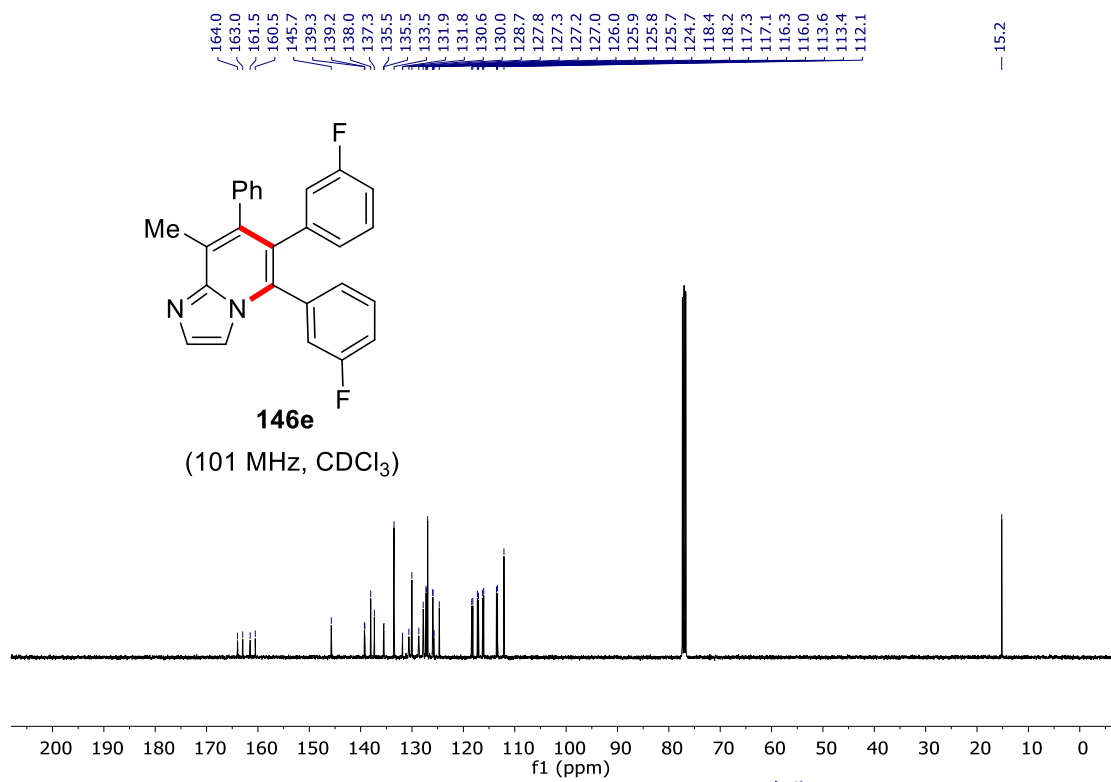
NMR Spectra



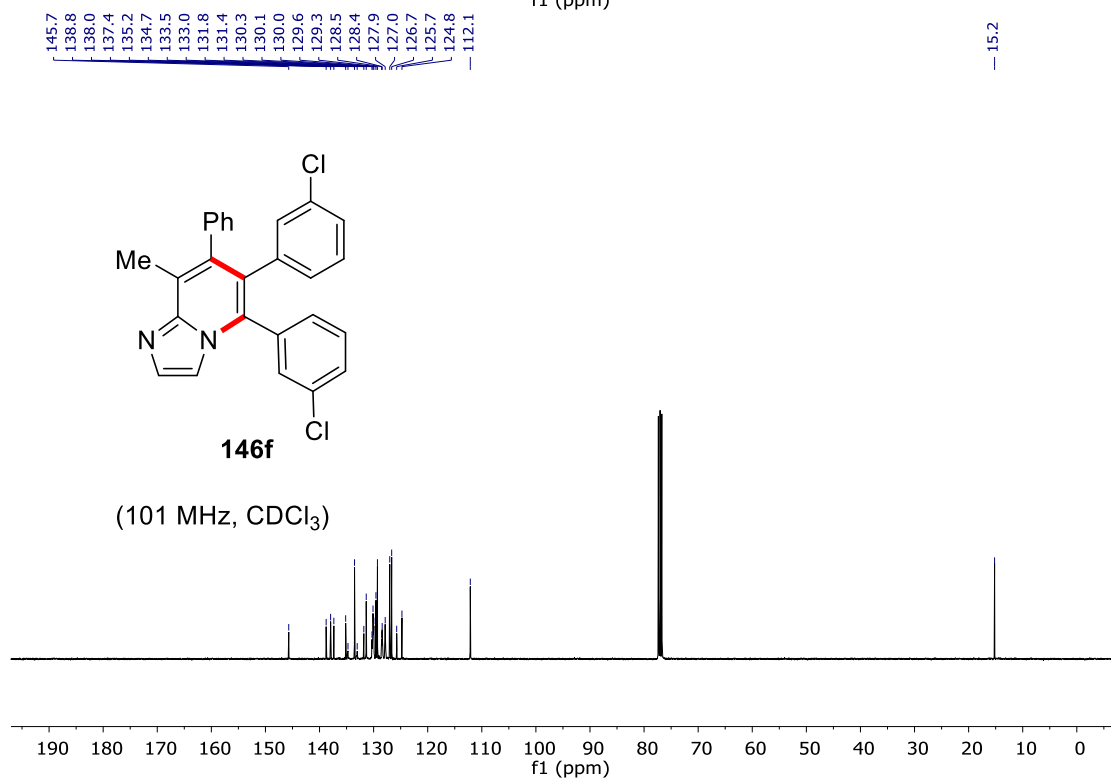
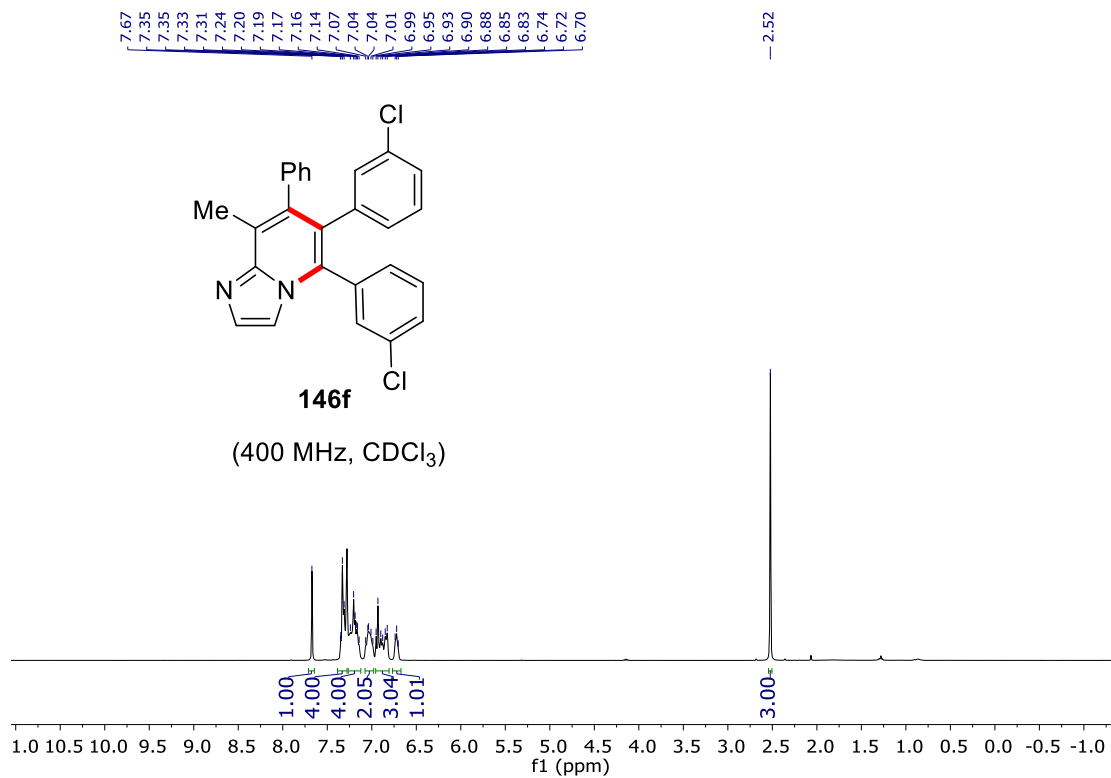
NMR Spectra



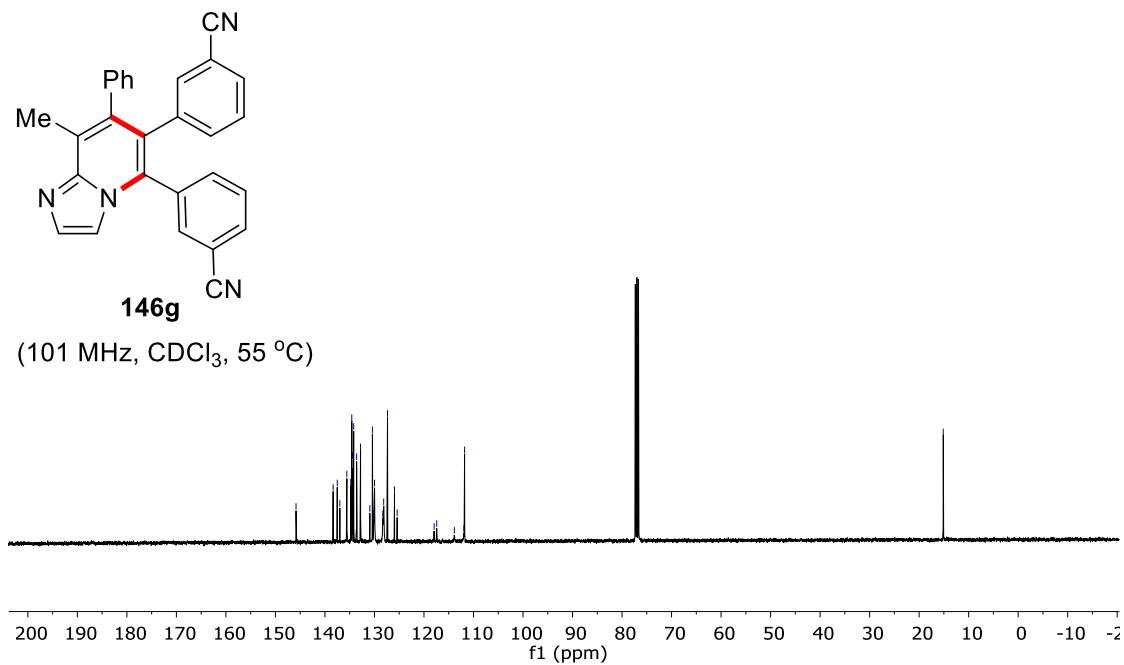
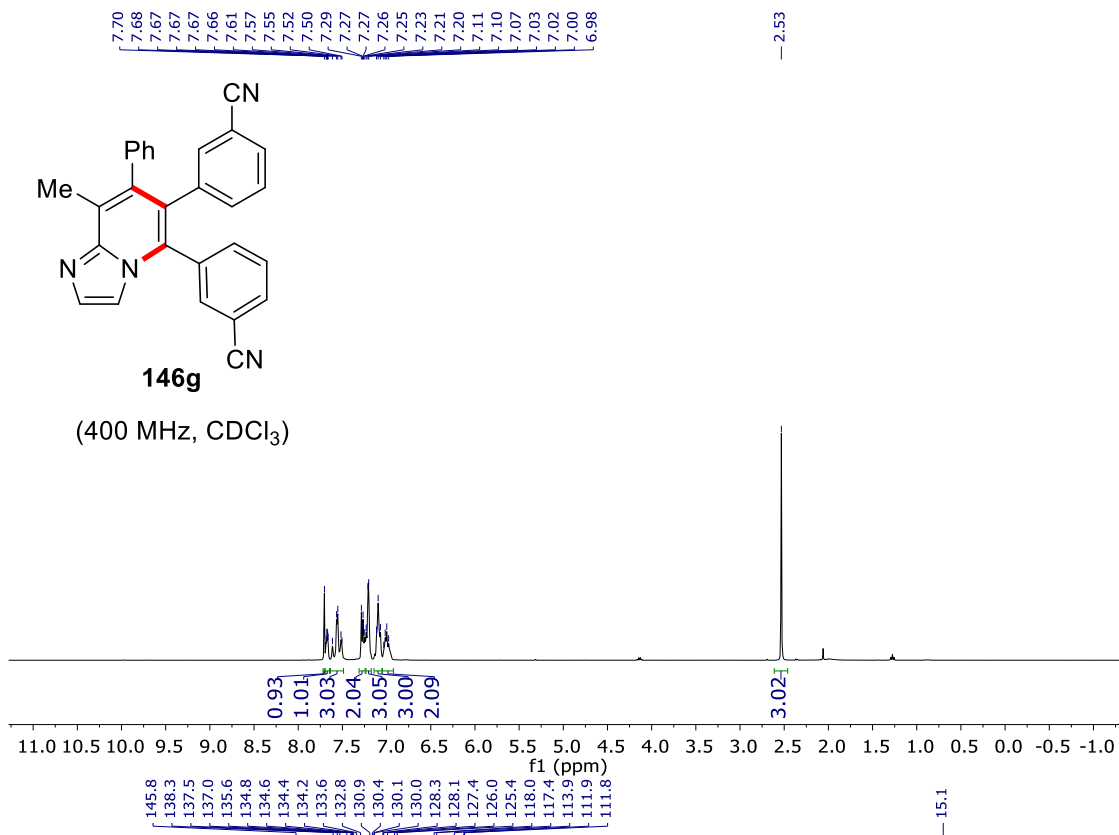
NMR Spectra



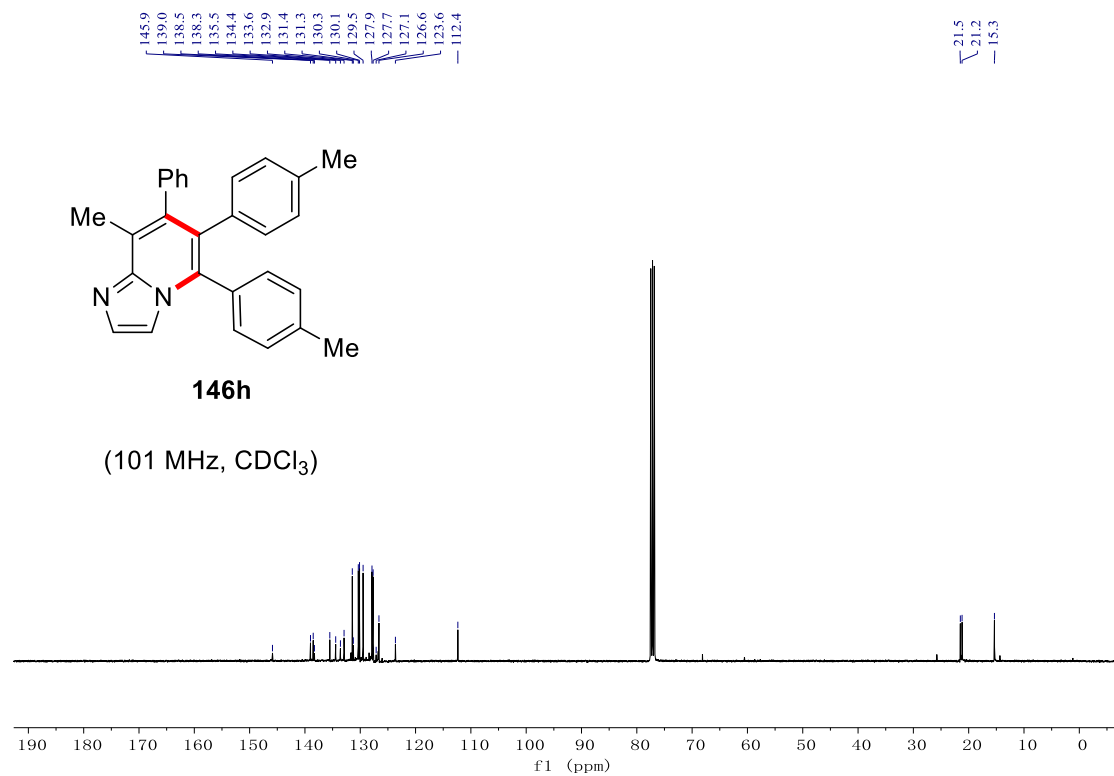
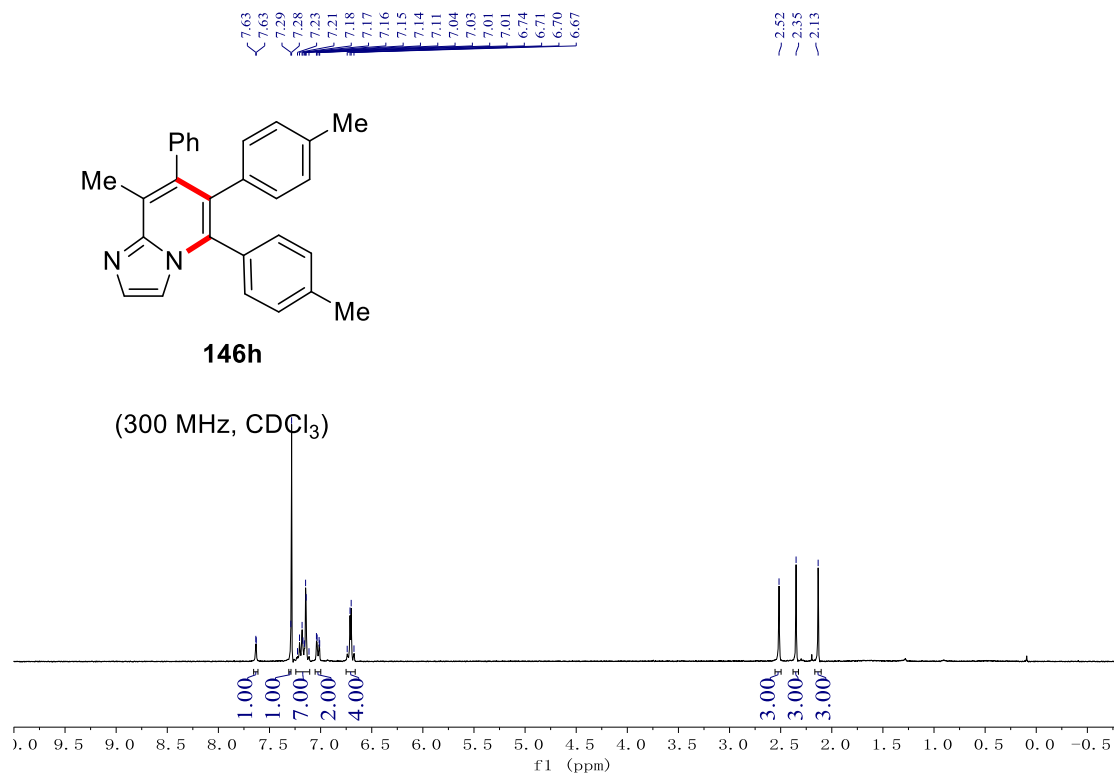
NMR Spectra



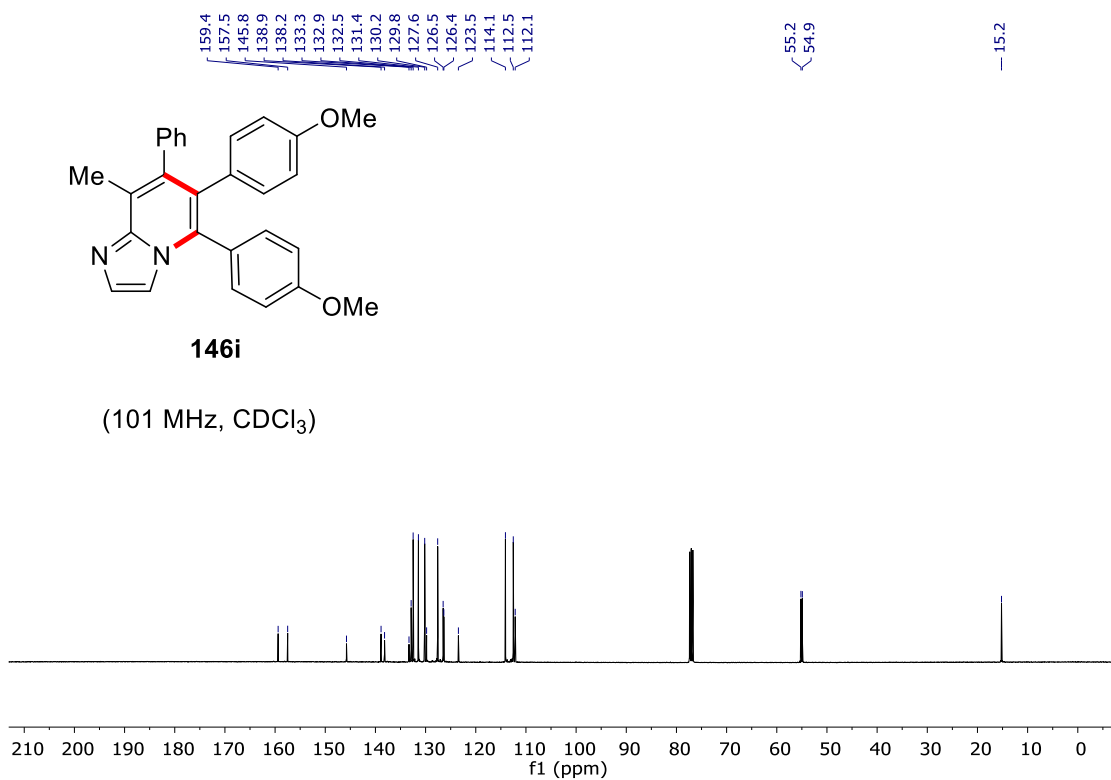
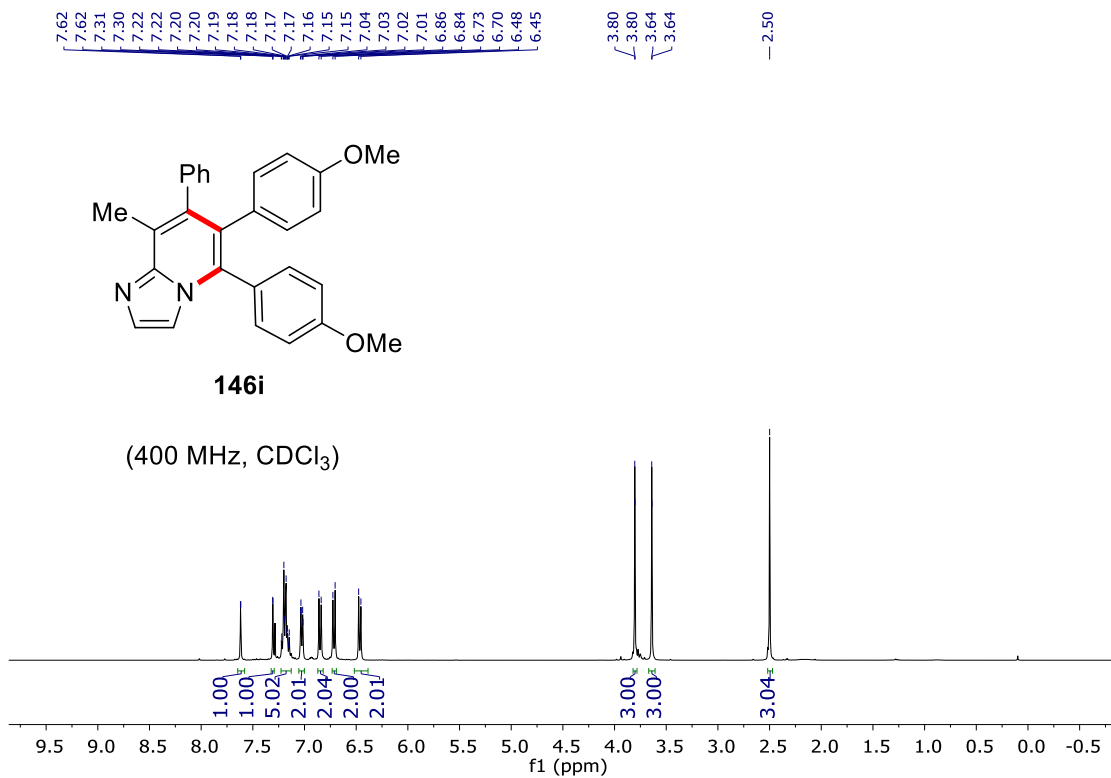
NMR Spectra



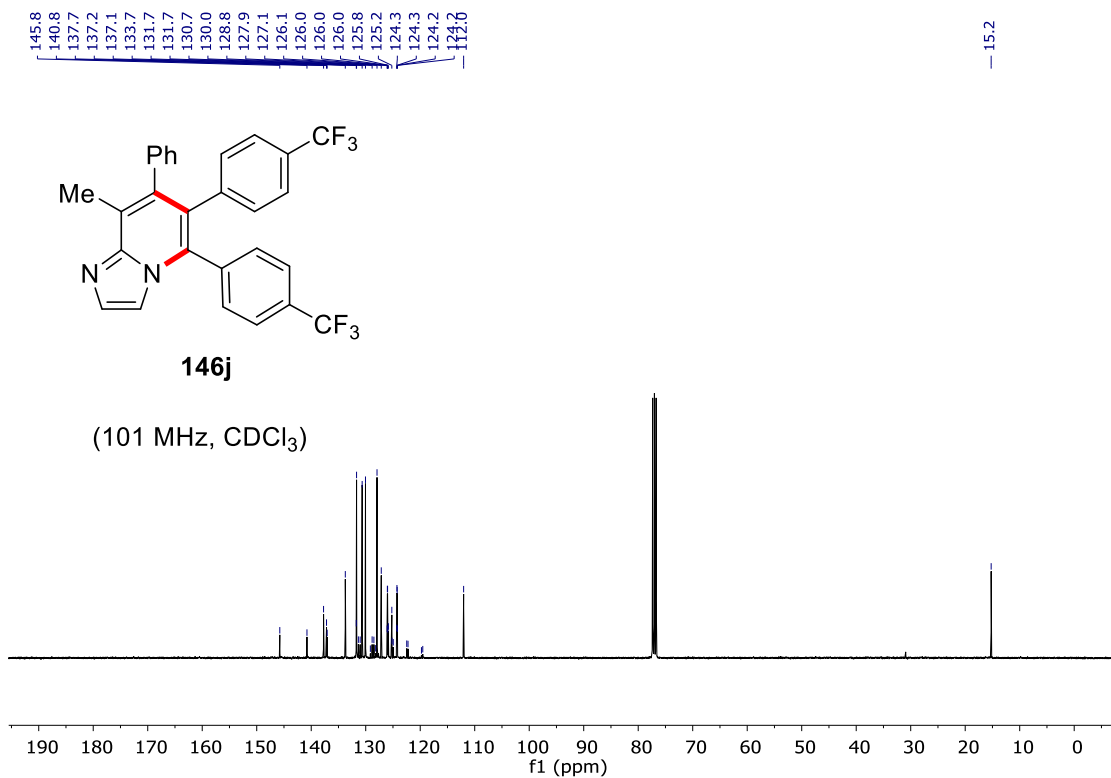
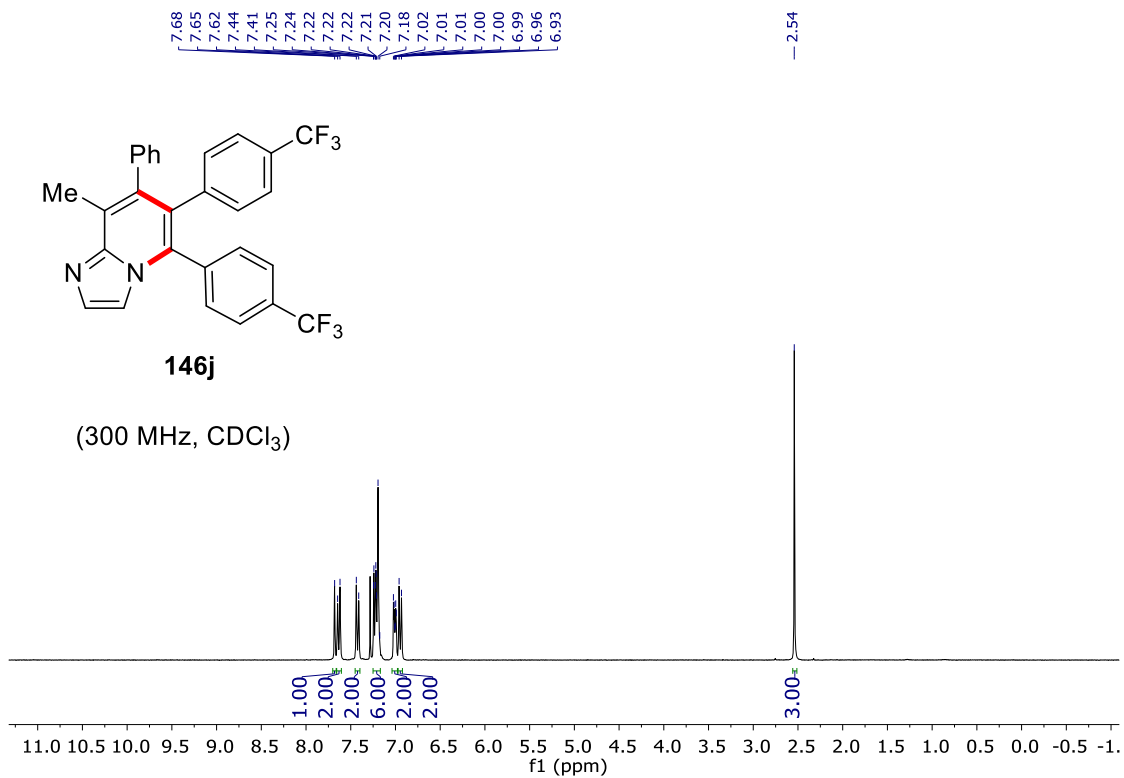
NMR Spectra



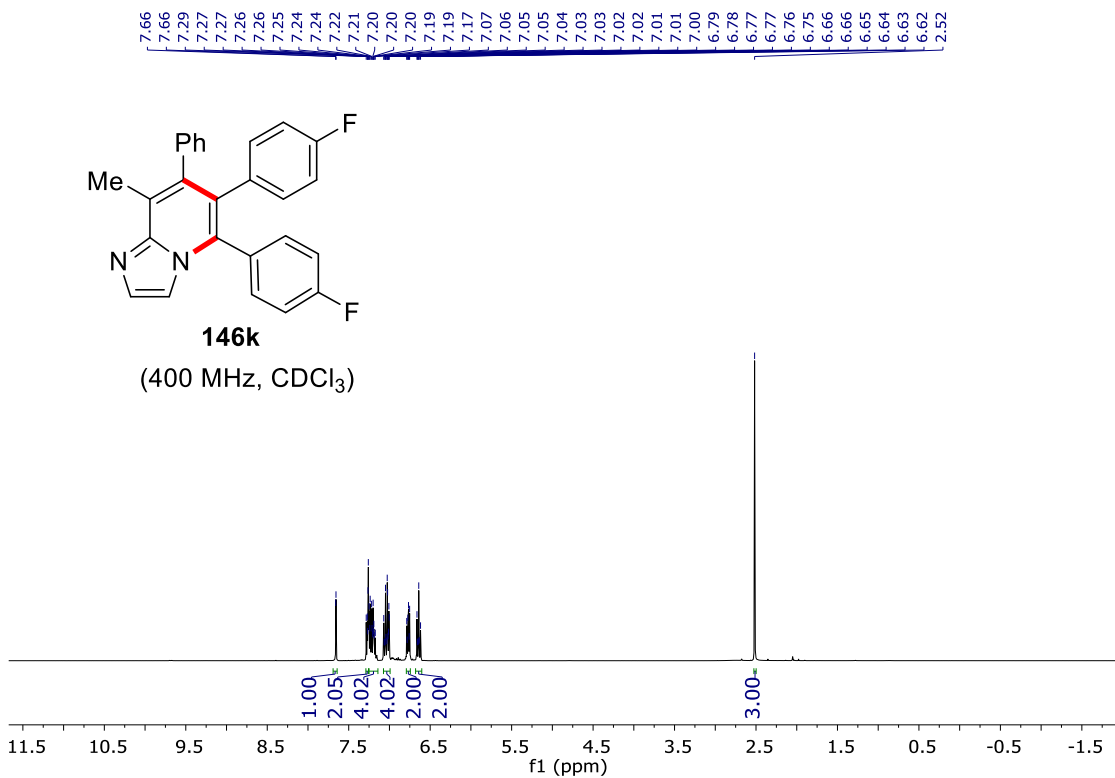
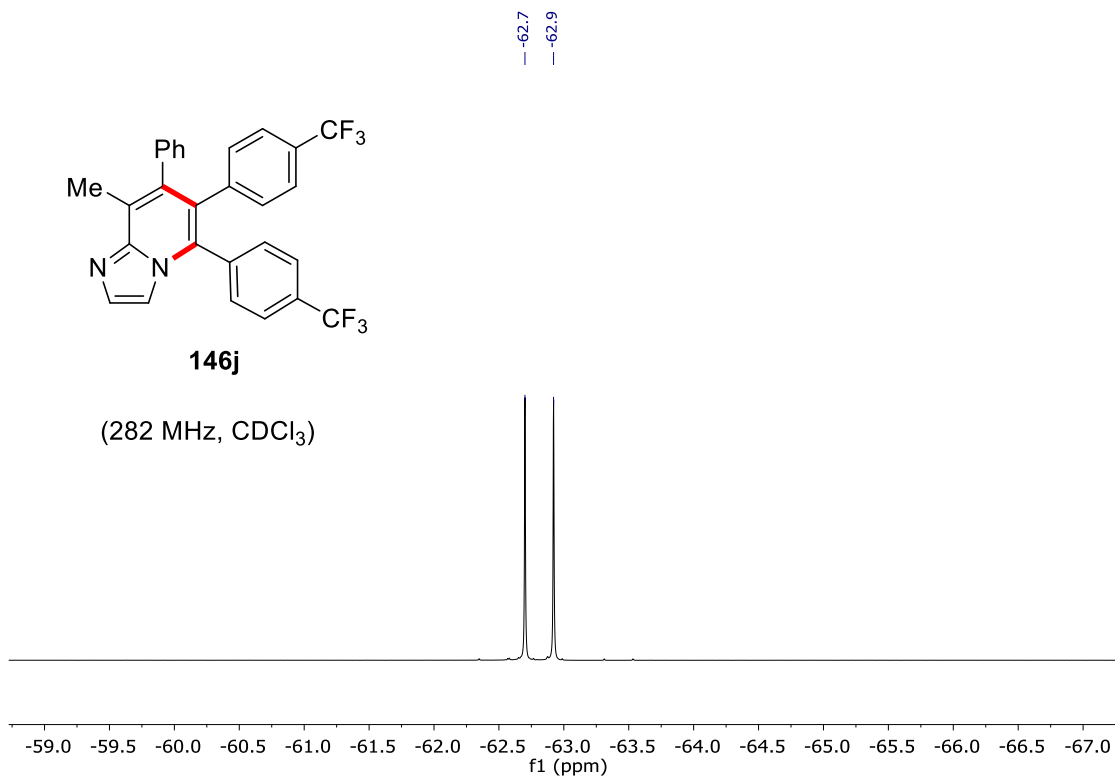
NMR Spectra



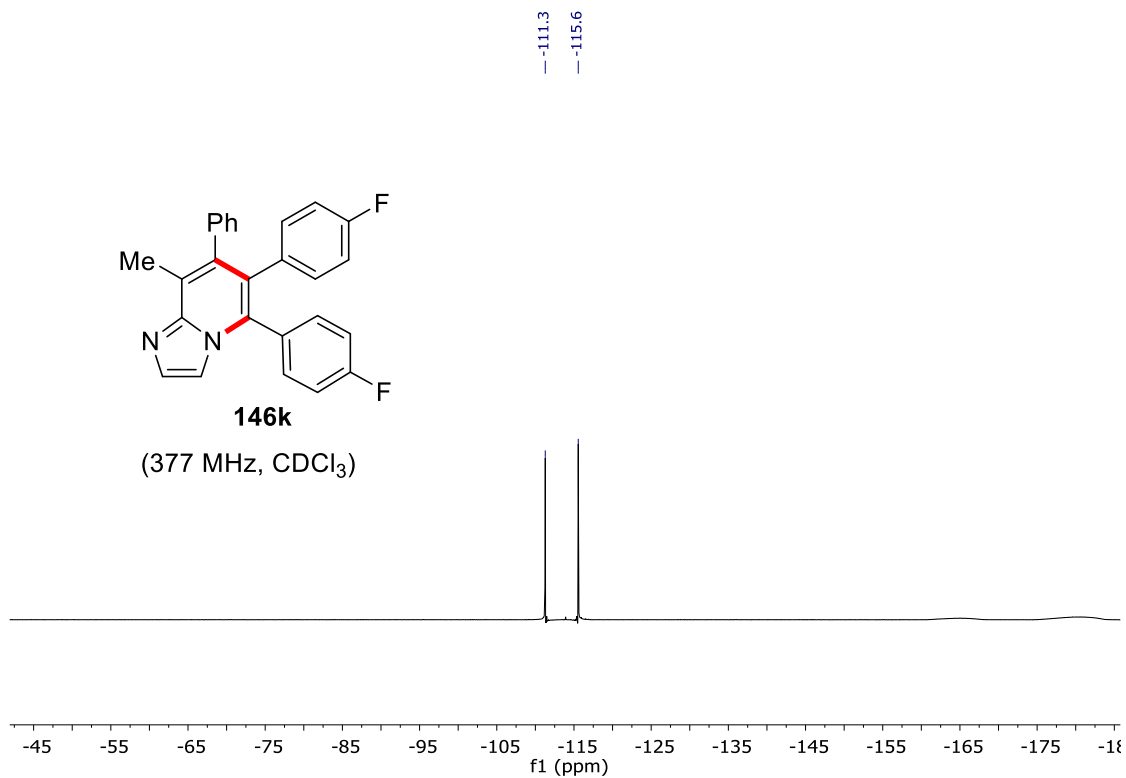
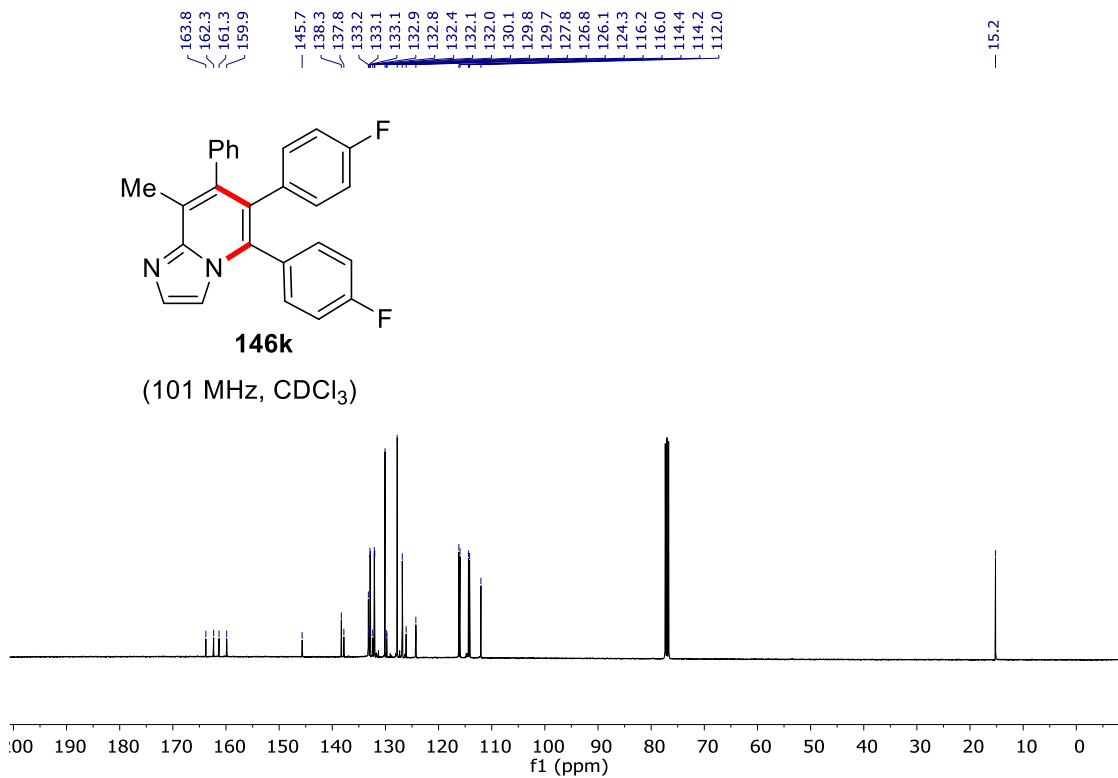
NMR Spectra



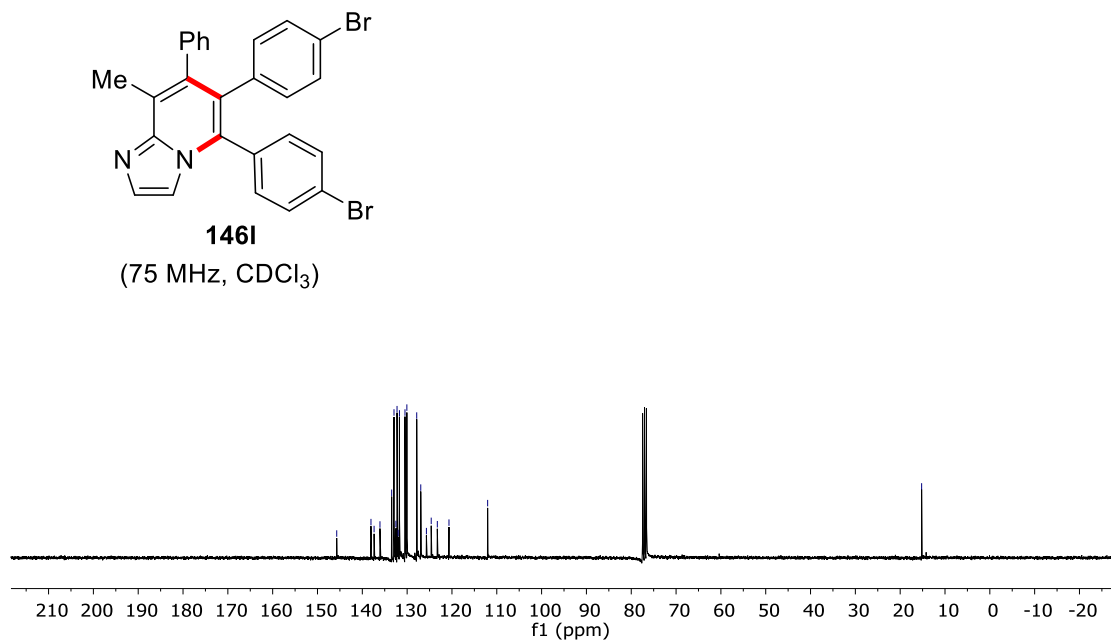
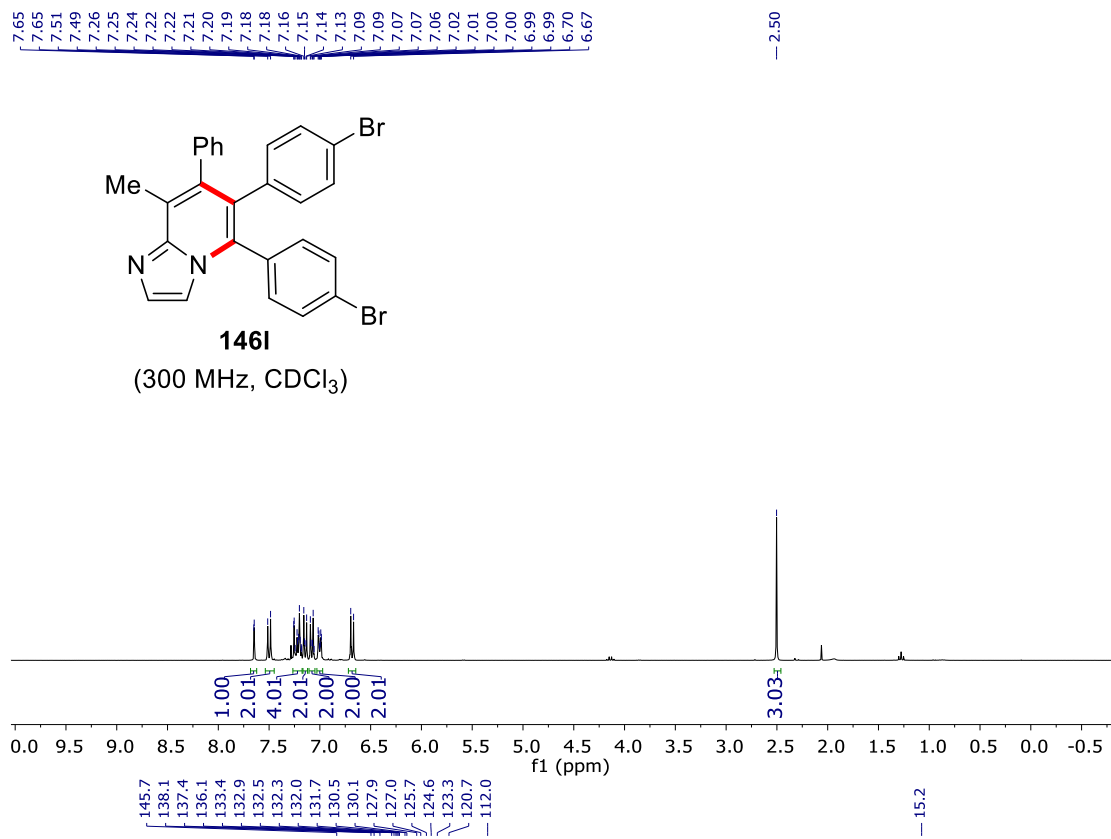
NMR Spectra



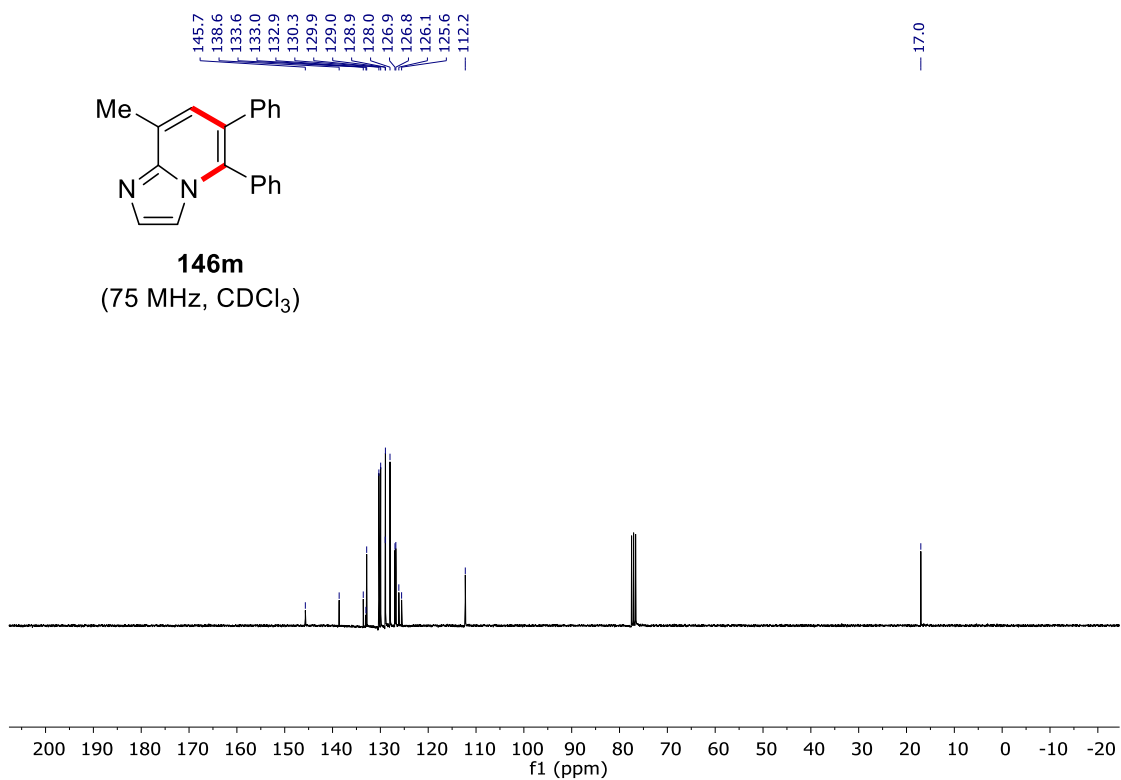
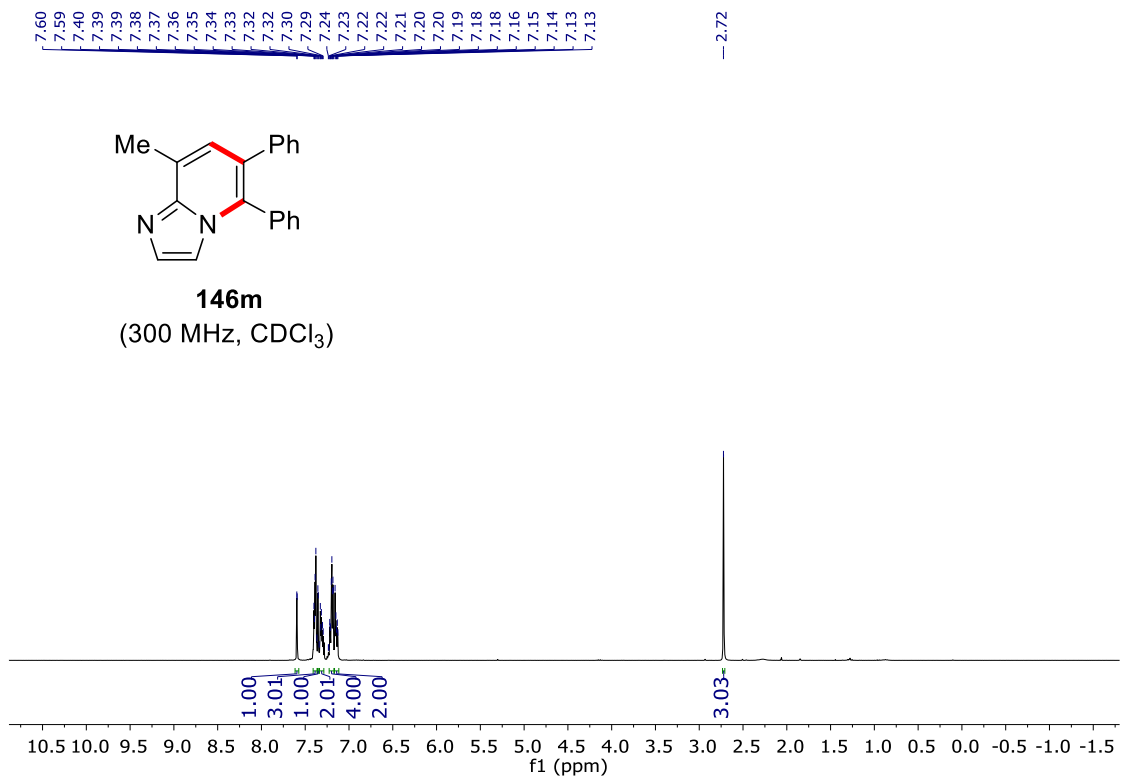
NMR Spectra



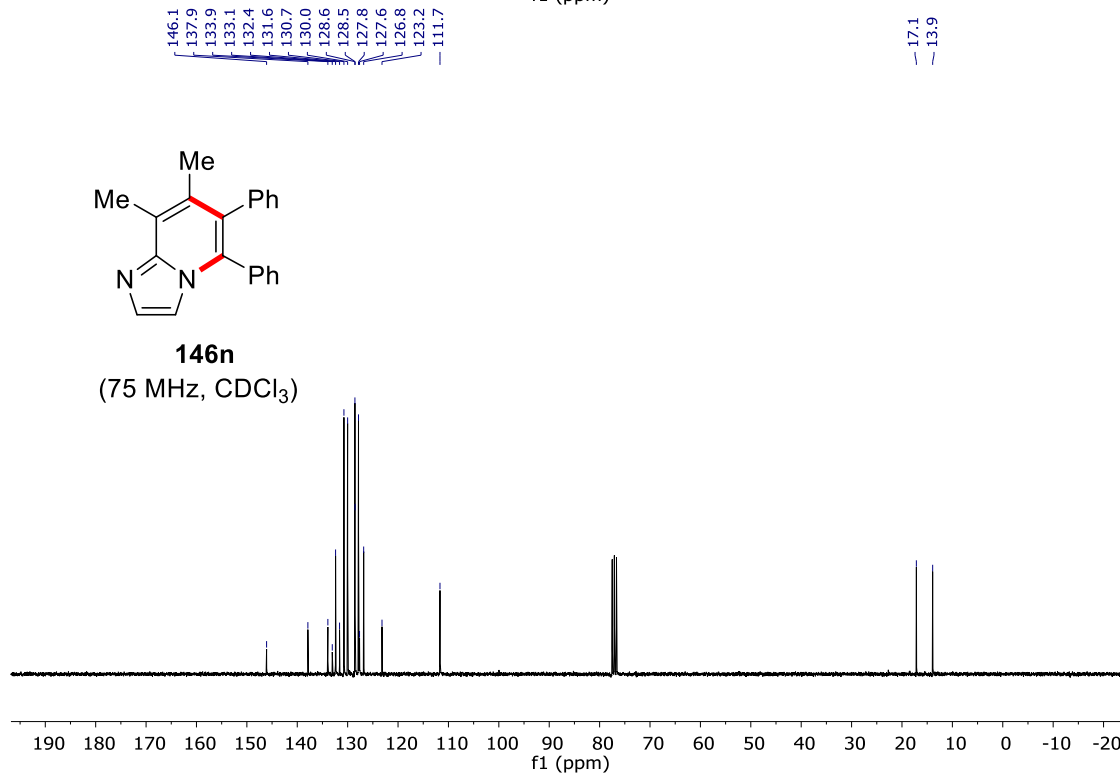
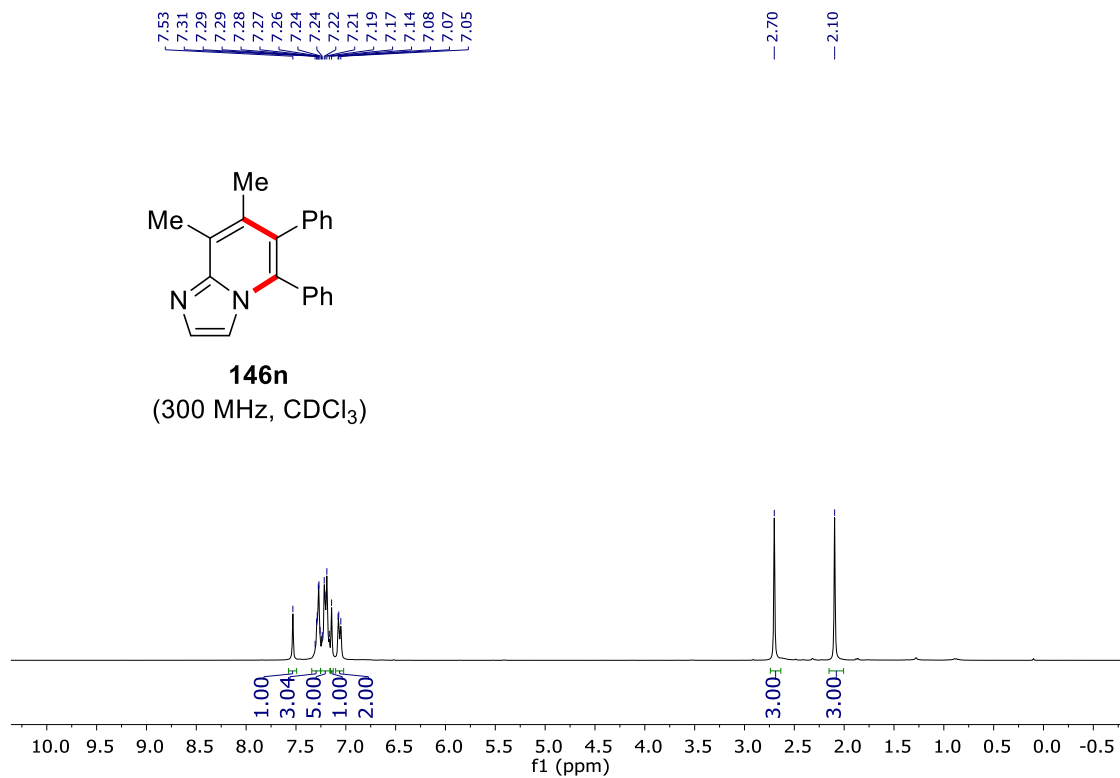
NMR Spectra



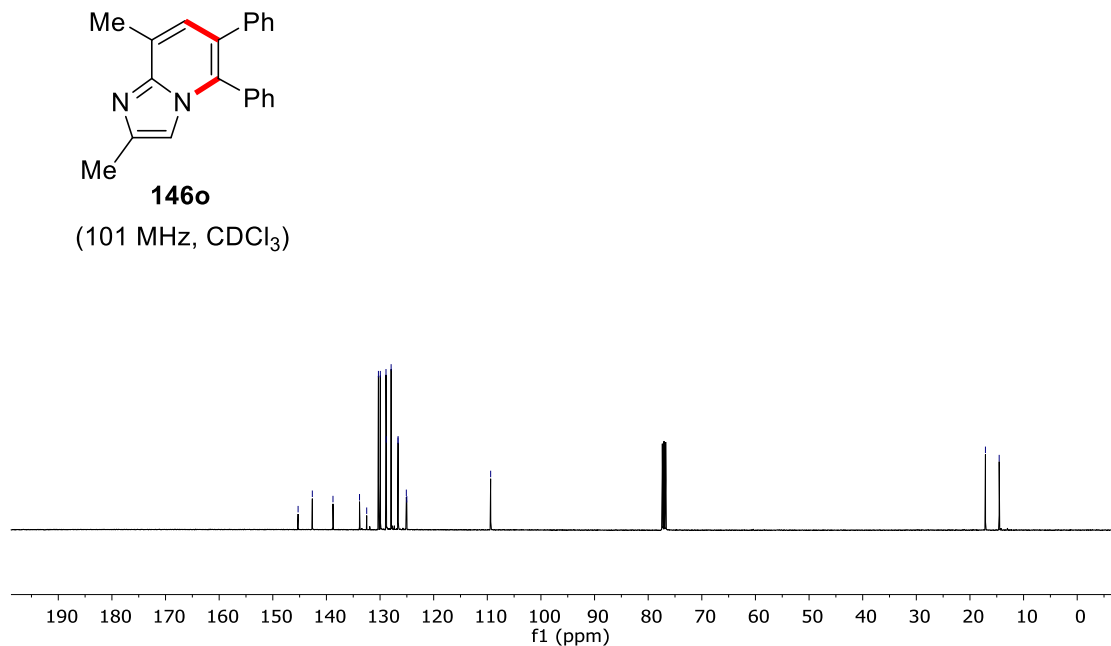
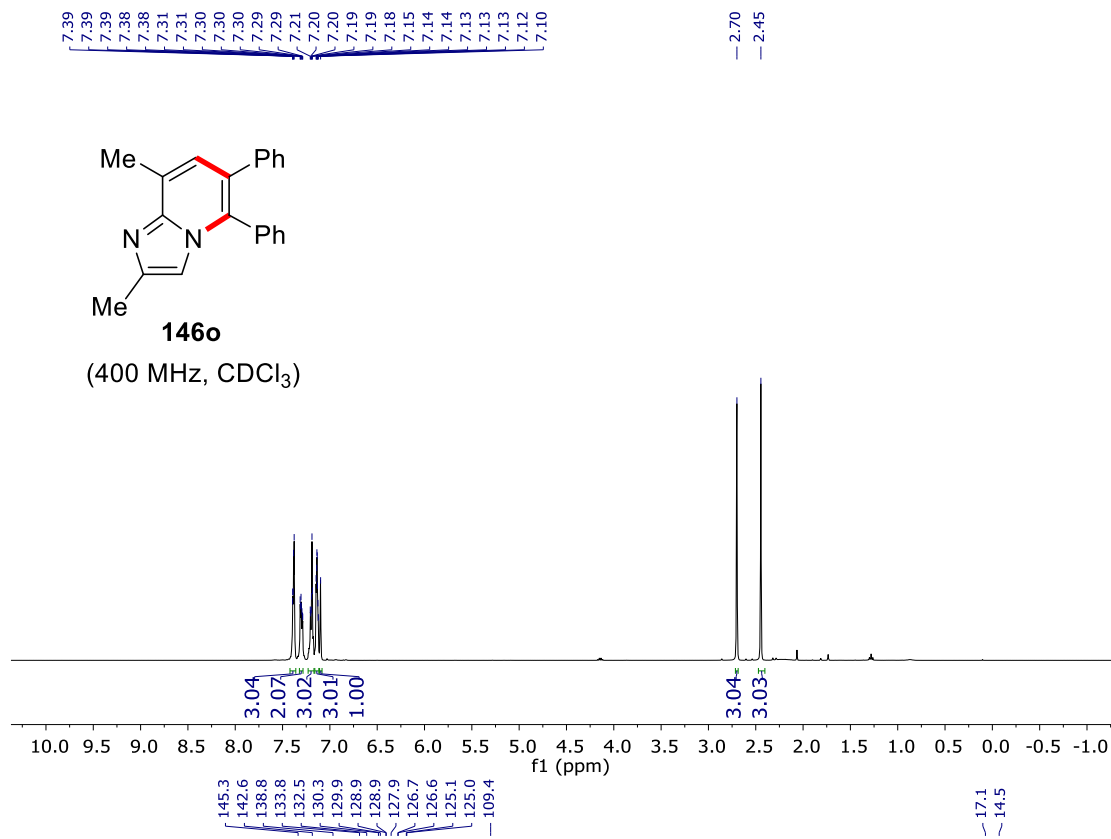
NMR Spectra



NMR Spectra



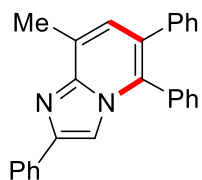
NMR Spectra



NMR Spectra

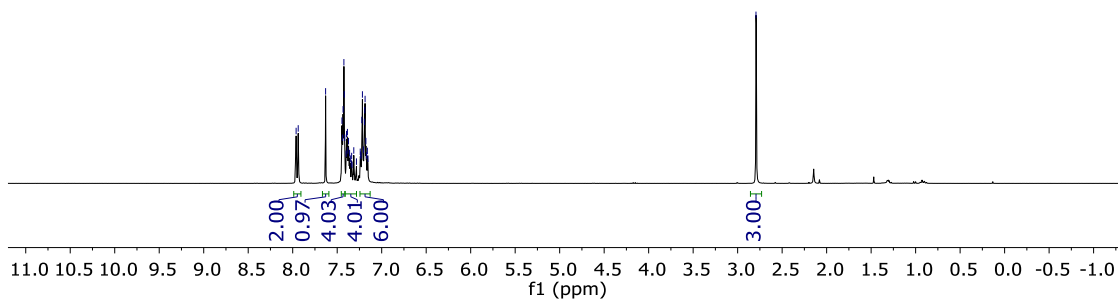
7.96
7.94
7.63
7.45
7.44
7.43
7.42
7.42
7.40
7.40
7.38
7.38
7.37
7.36
7.35
7.34
7.34
7.33
7.31
7.28
7.24
7.23
7.22
7.22
7.21
7.19
7.19
7.18
7.17
7.16
7.15

-2.79



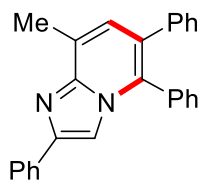
146p

(300 MHz, CDCl₃)



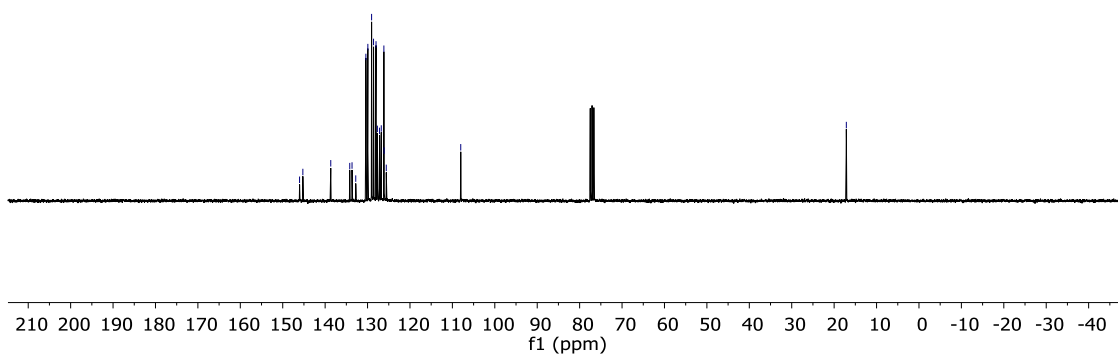
146.0
145.3
138.7
134.2
133.7
132.8
130.4
129.9
129.0
128.6
128.0
127.7
127.2
126.8
126.2
126.1
125.6
108.0

-17.1

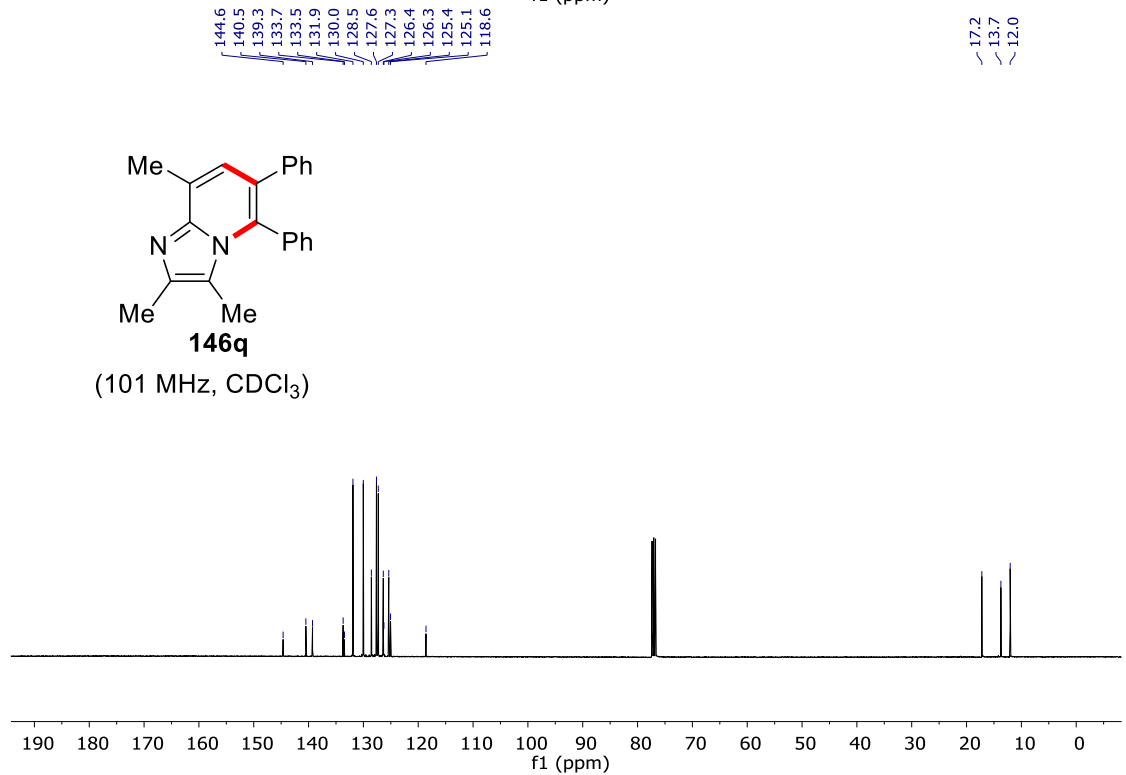
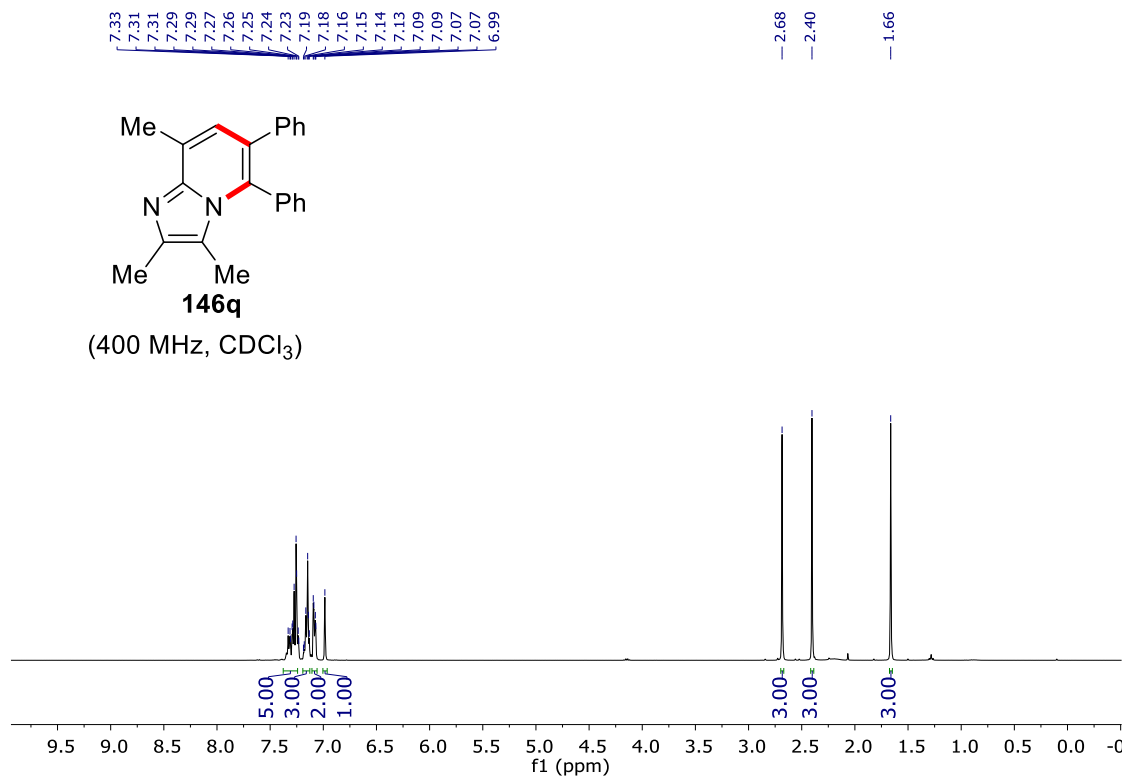


146p

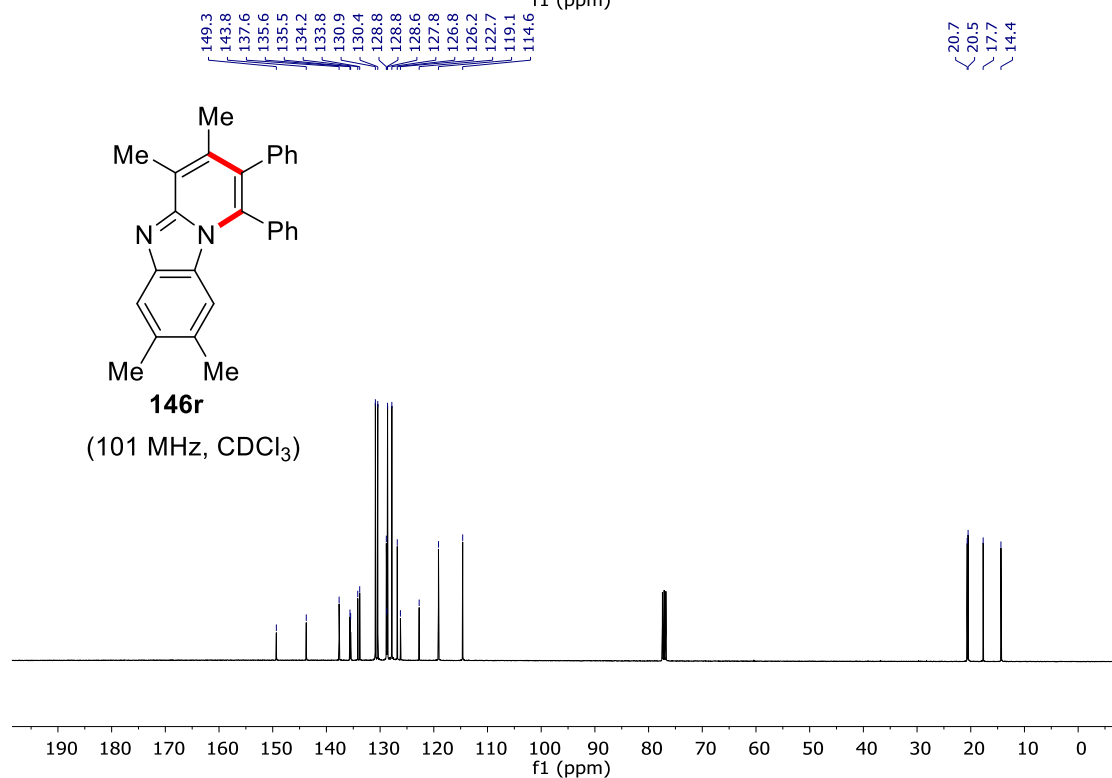
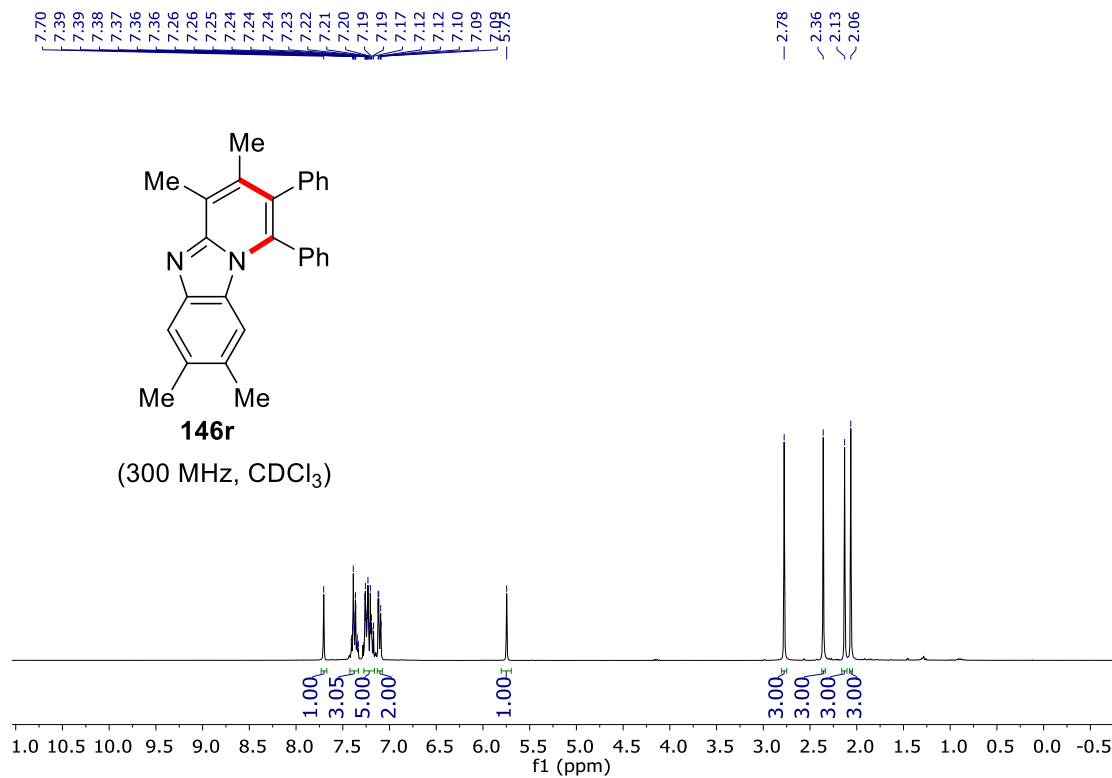
(75 MHz, CDCl₃)



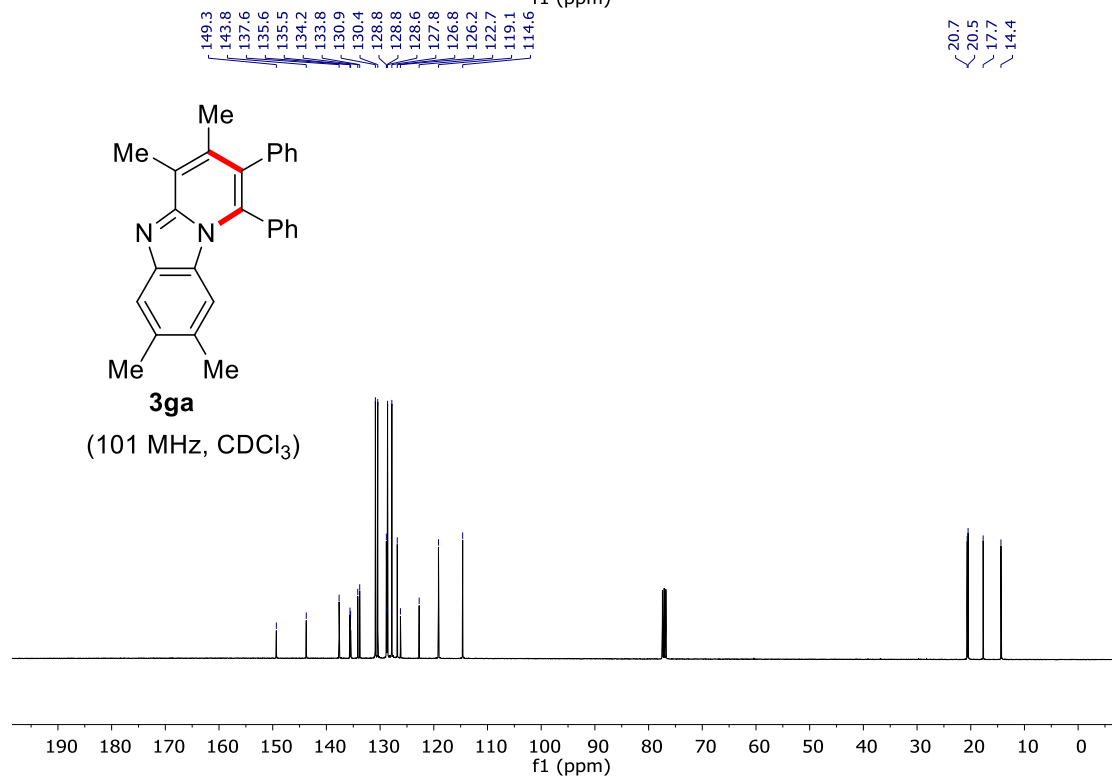
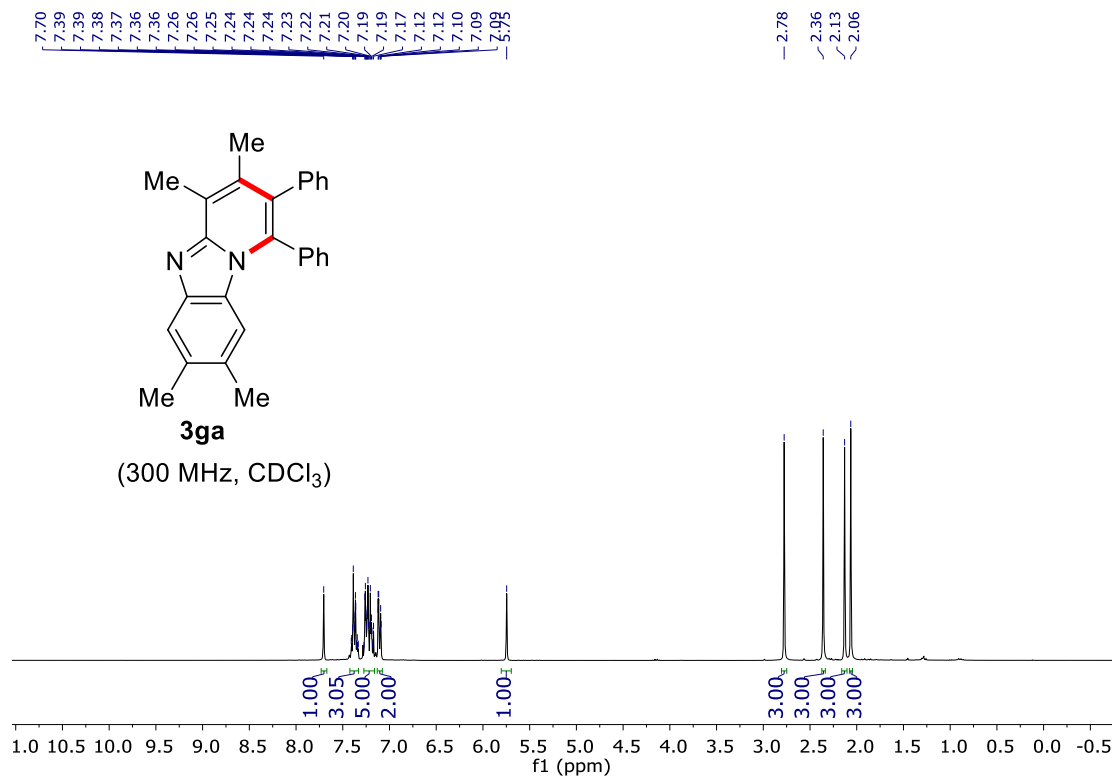
NMR Spectra



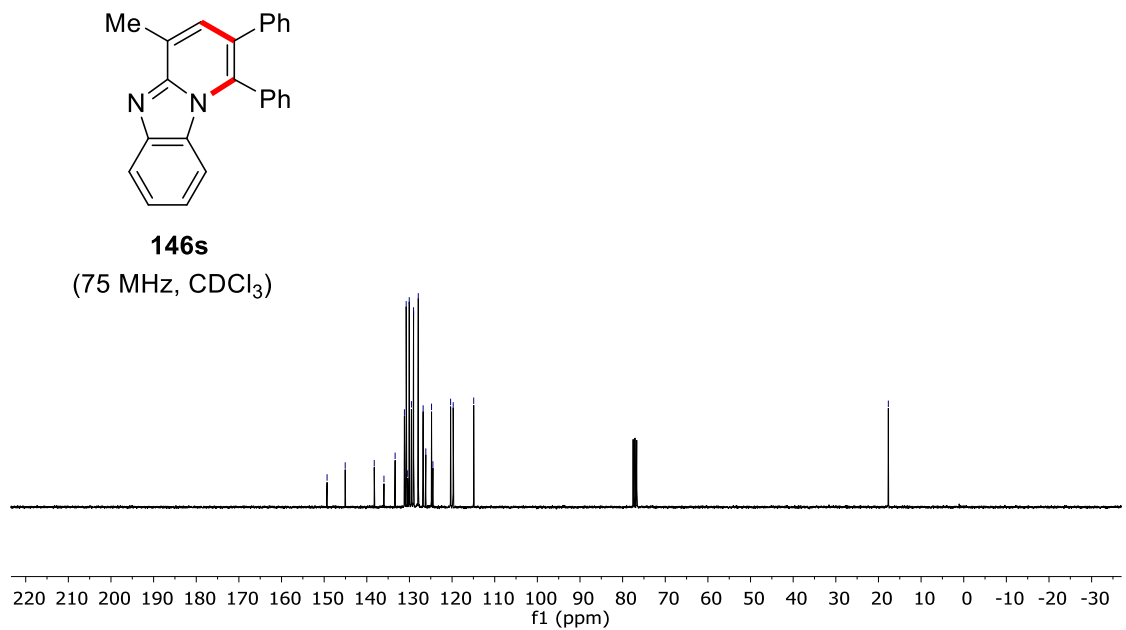
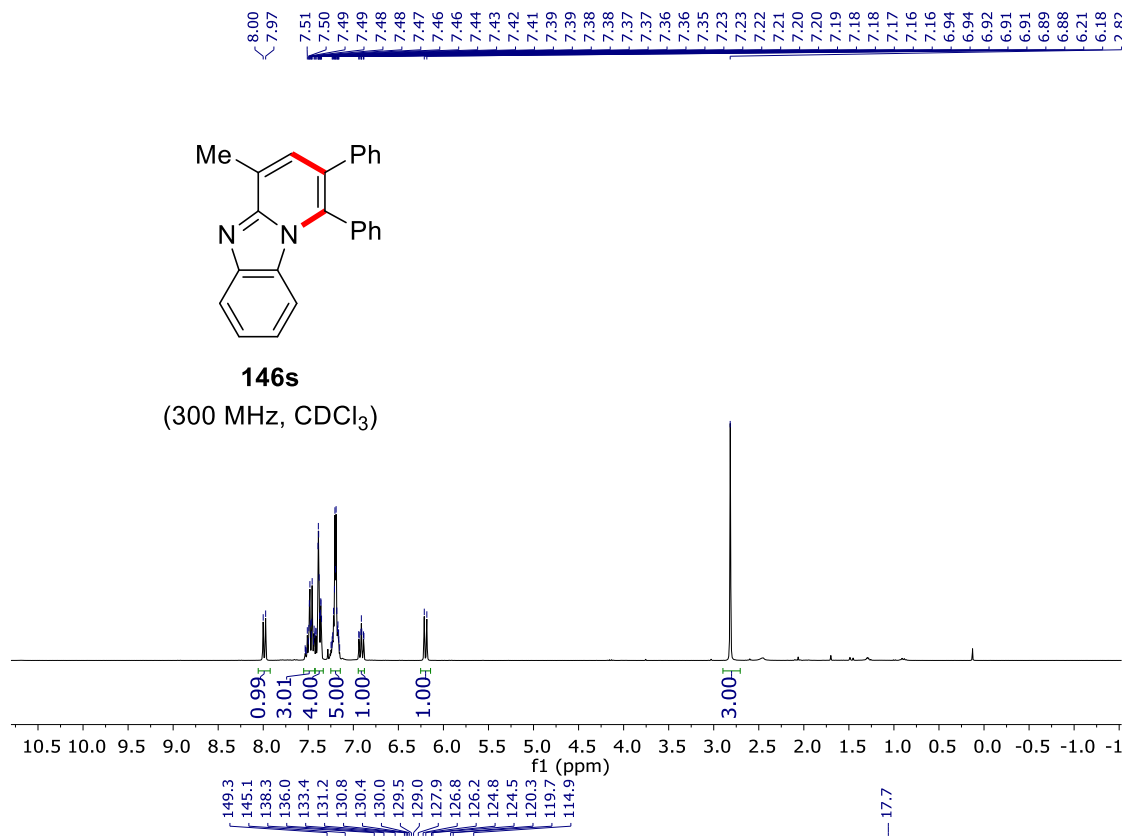
NMR Spectra



NMR Spectra

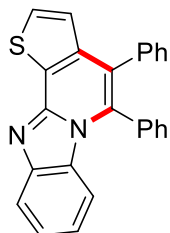


NMR Spectra



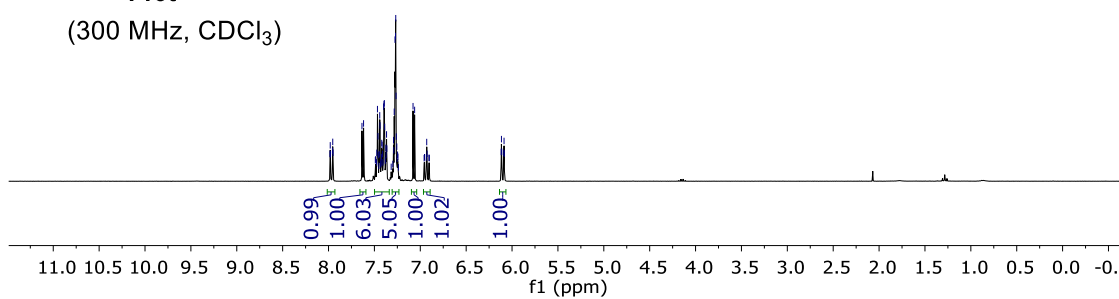
NMR Spectra

7.98
7.98
7.96
7.95
7.64
7.62
7.49
7.49
7.47
7.46
7.46
7.45
7.44
7.44
7.42
7.42
7.41
7.41
7.40
7.40
7.39
7.38
7.38
7.37
7.37
7.36
7.29
7.29
7.28
7.28
7.27
7.27
7.26
7.26
7.26
7.25
7.25
7.24
7.24
7.06
6.96
6.95
6.93
6.93
6.91
6.90
6.12
6.11
6.09
6.09
6.08

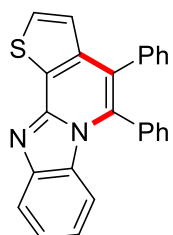


146t

(300 MHz, CDCl₃)

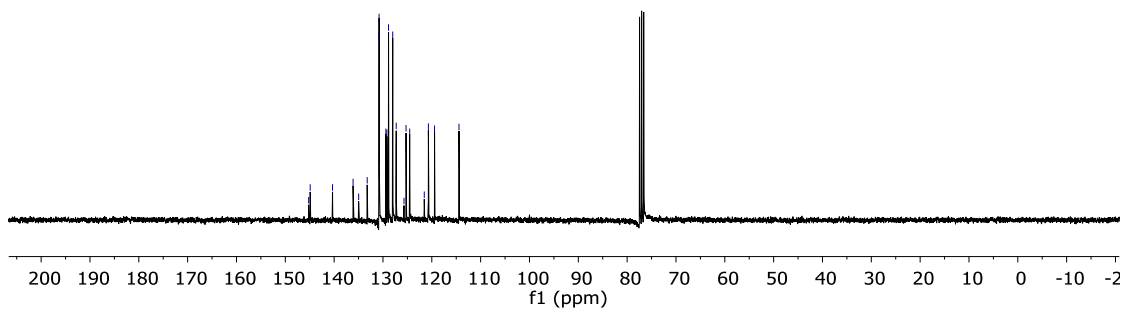


145.2
144.9
140.3
136.1
135.0
133.2
130.8
130.8
130.7
129.4
129.2
128.9
128.0
127.3
125.7
125.3
124.5
121.5
120.7
119.4
114.4

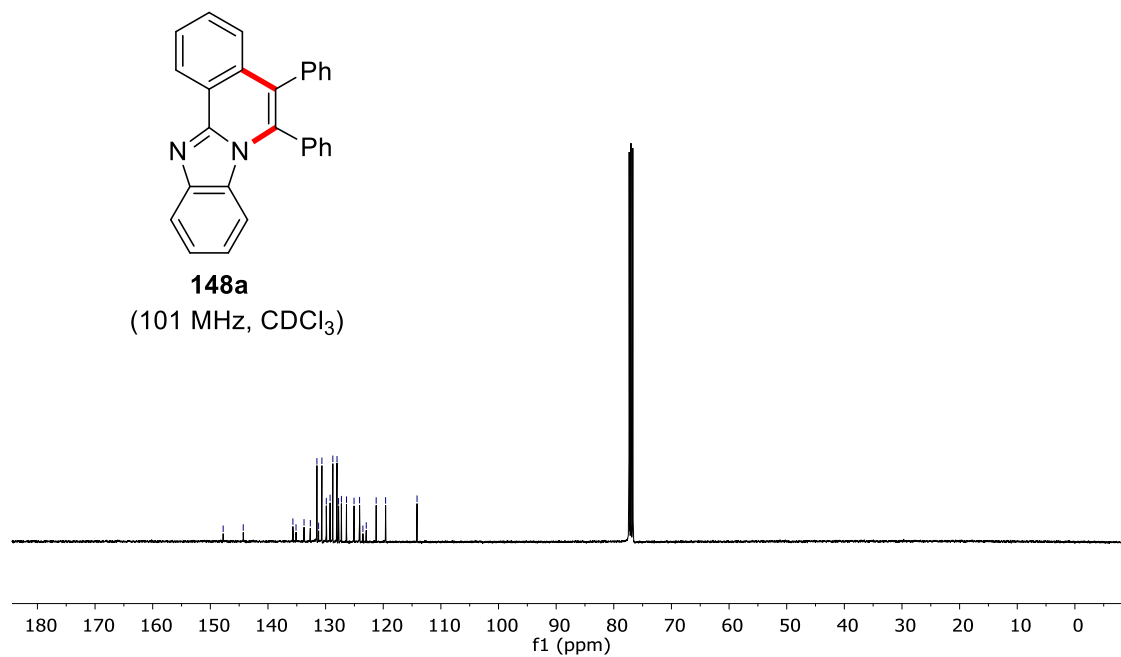
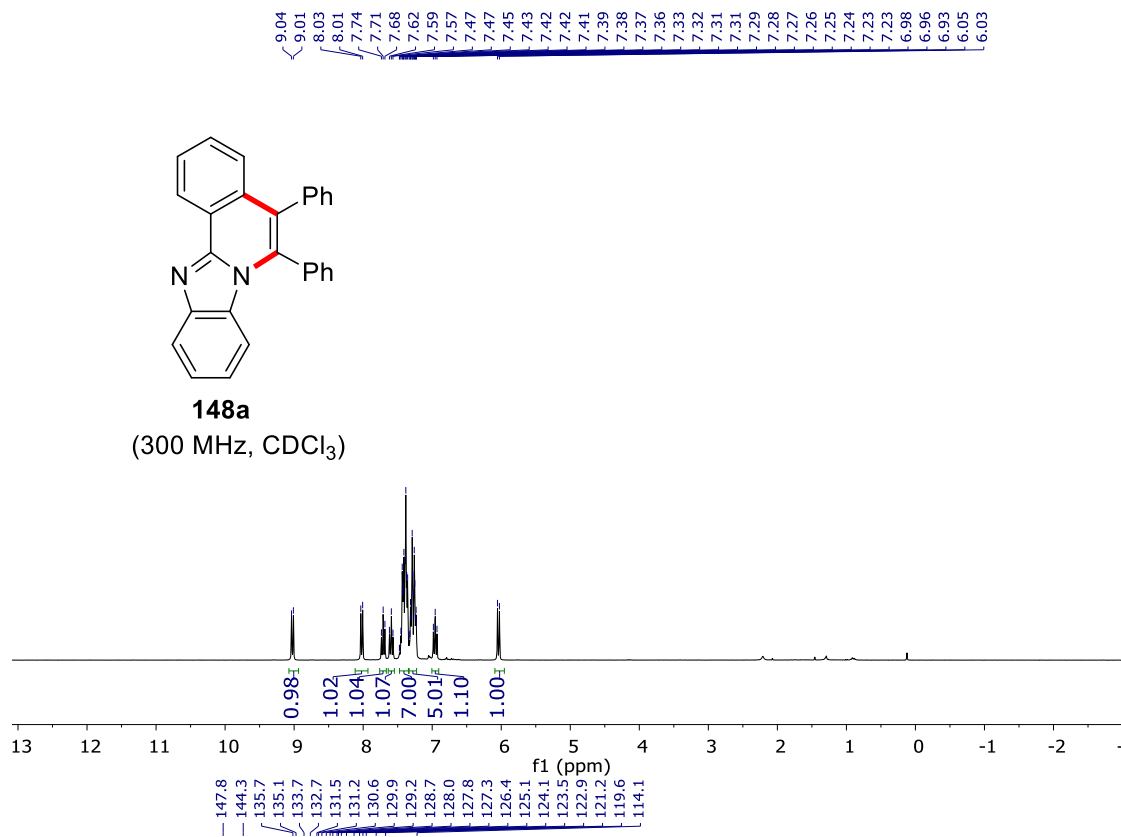


146t

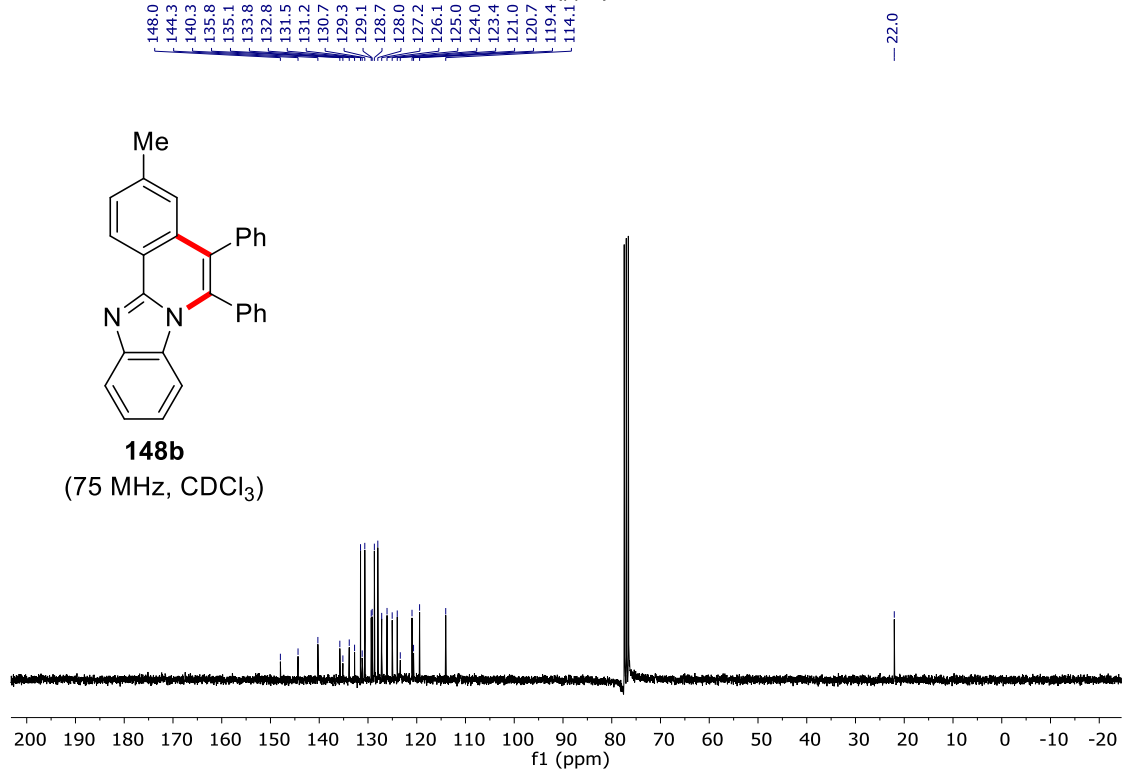
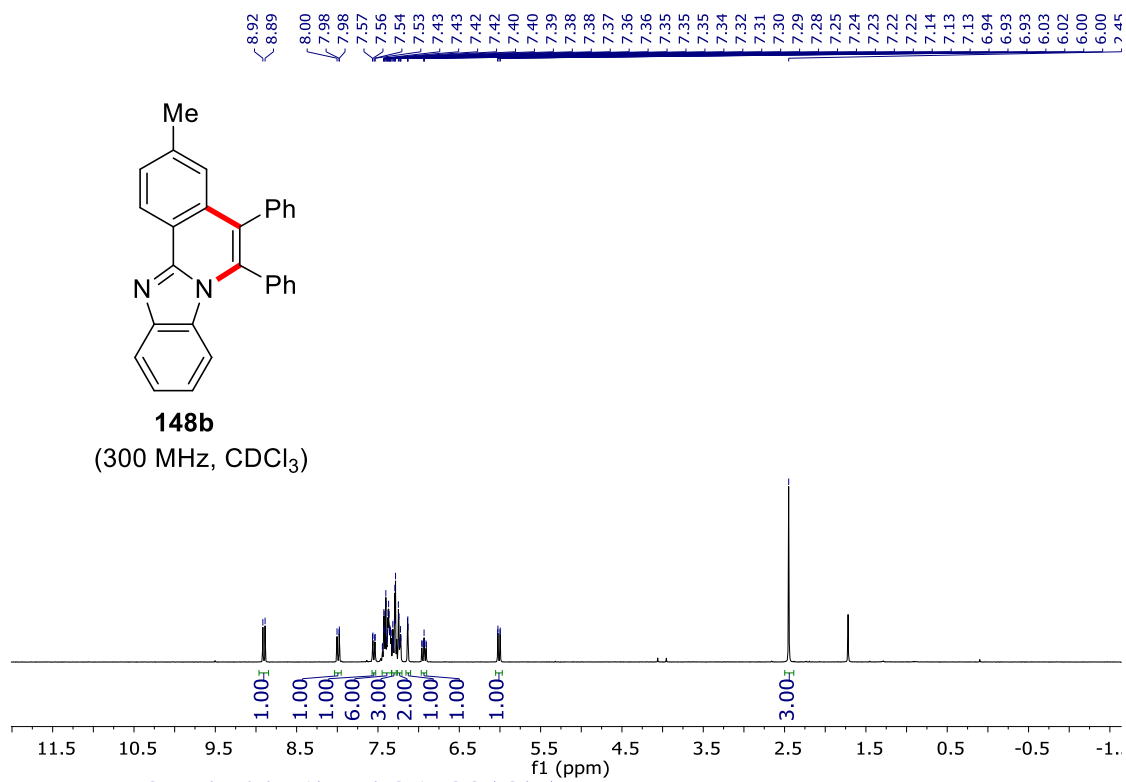
(75 MHz, CDCl₃)



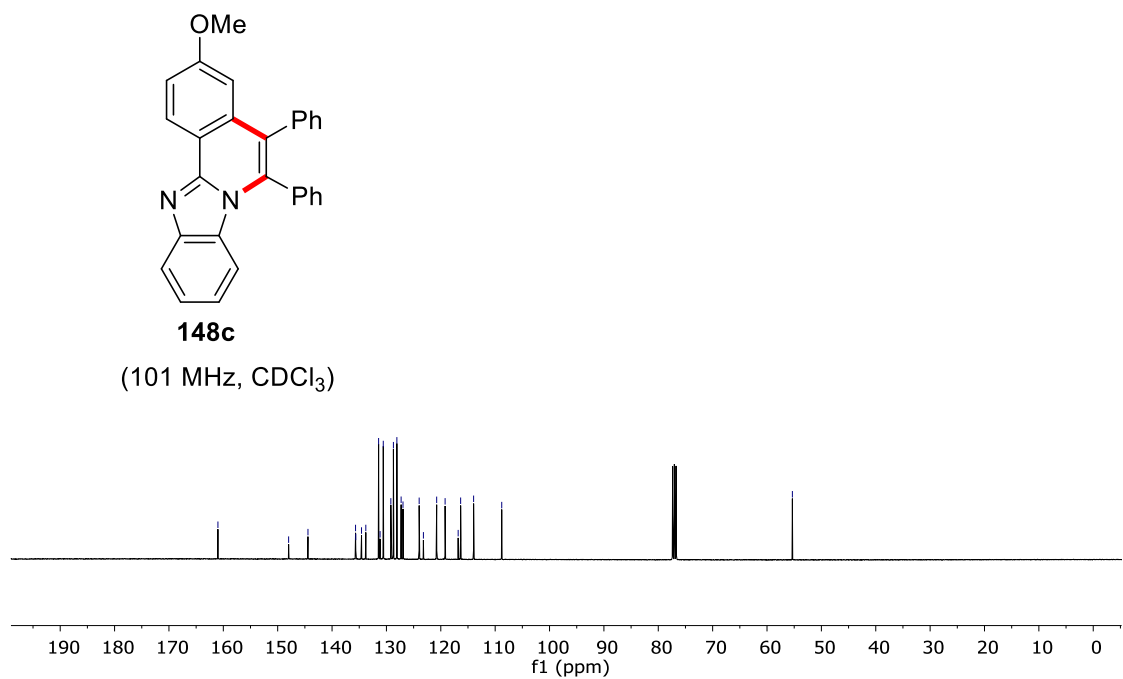
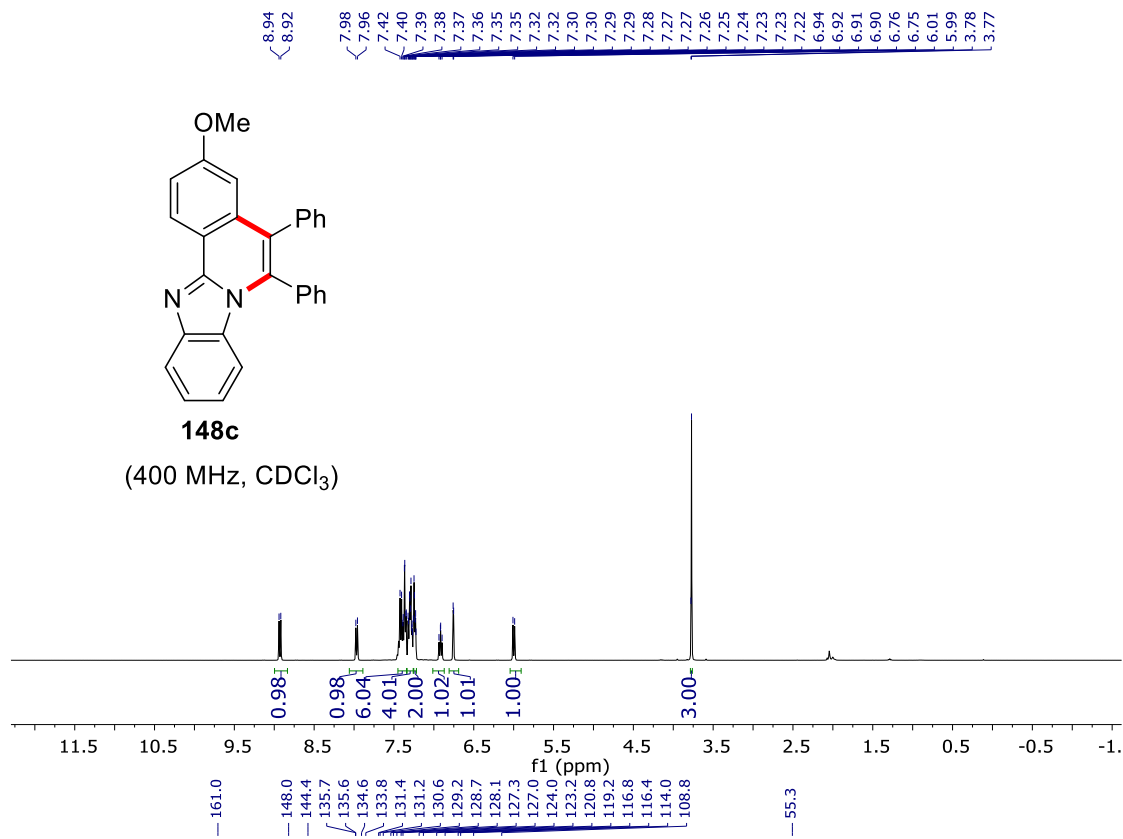
NMR Spectra



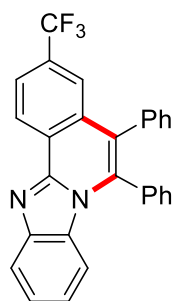
NMR Spectra



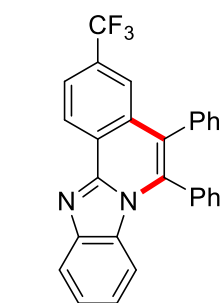
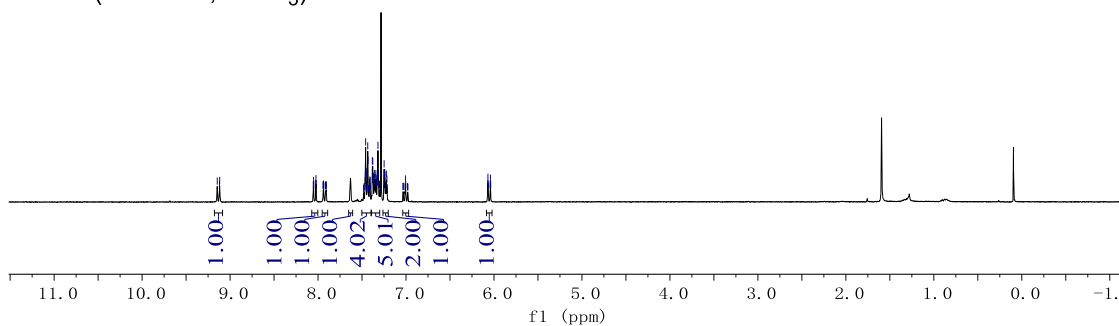
NMR Spectra



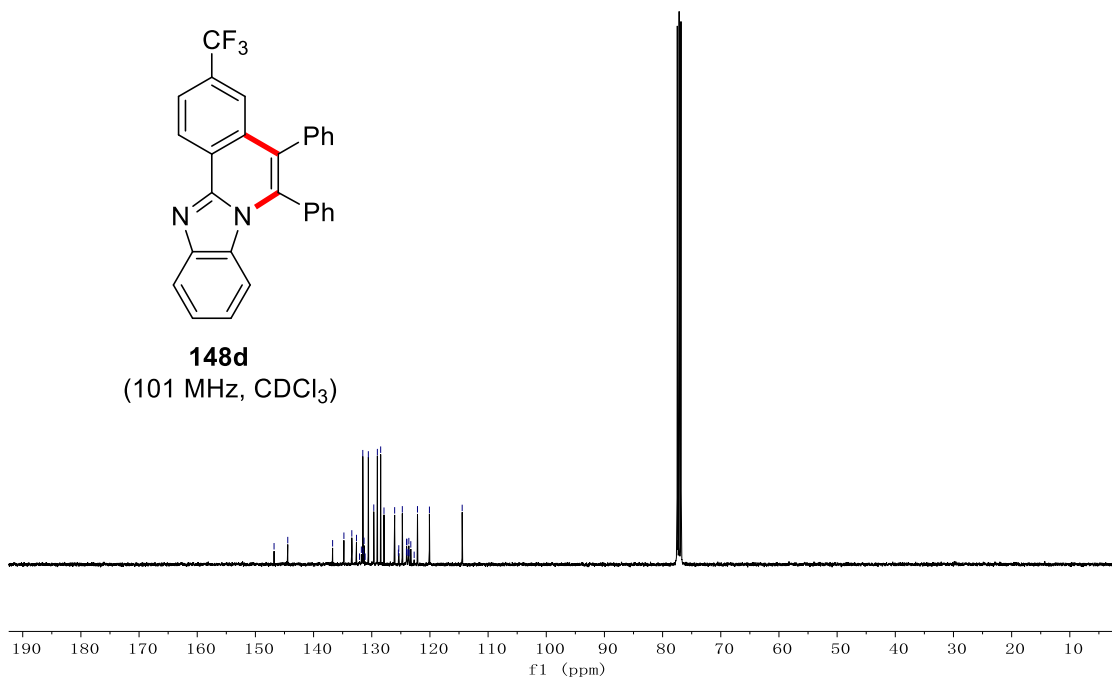
NMR Spectra



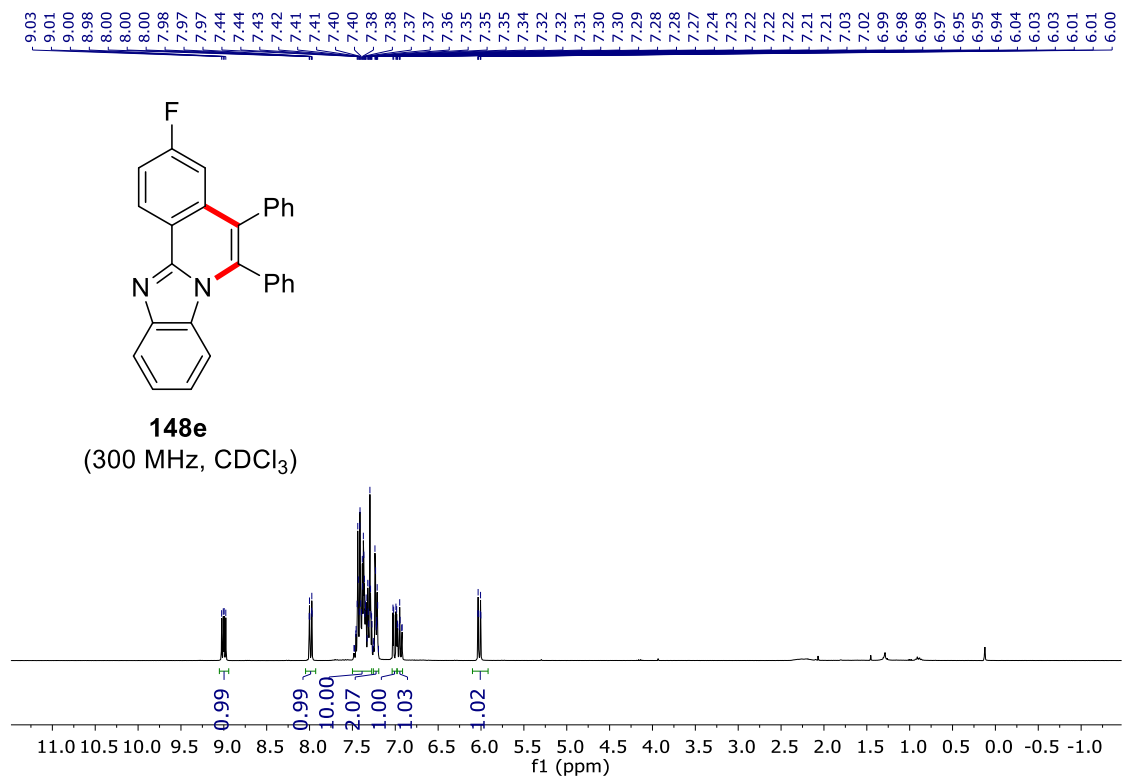
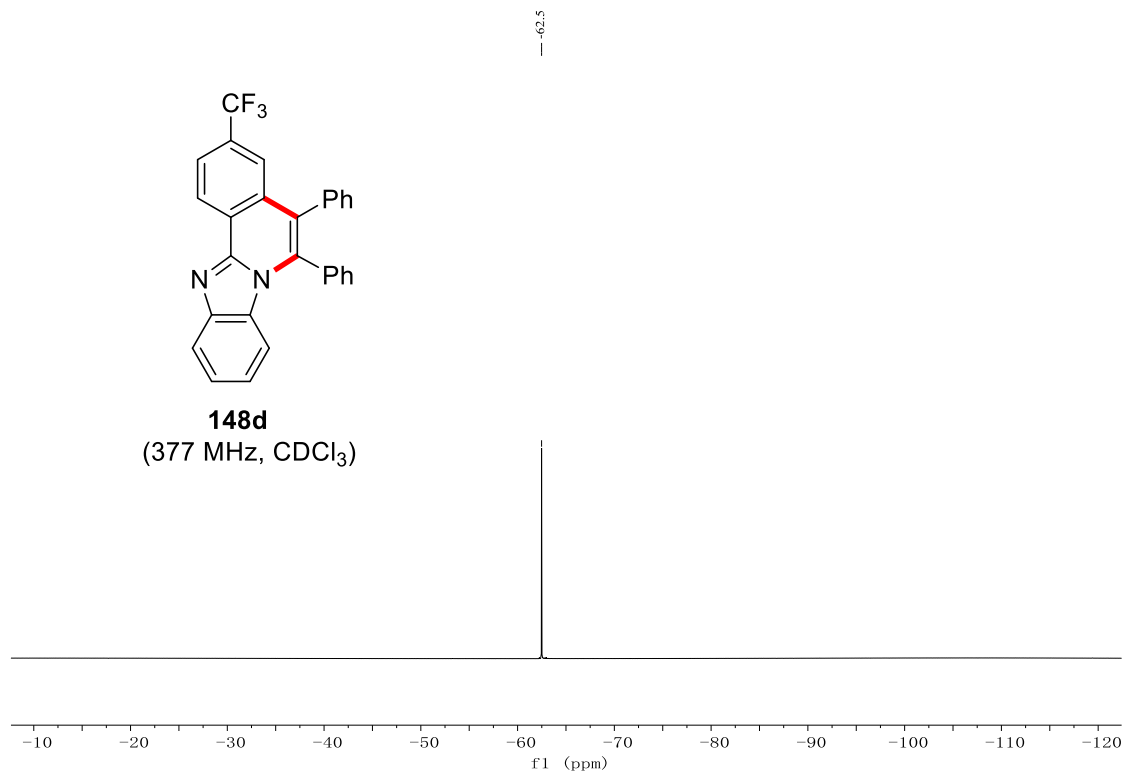
148d
(400 MHz, CDCl₃)



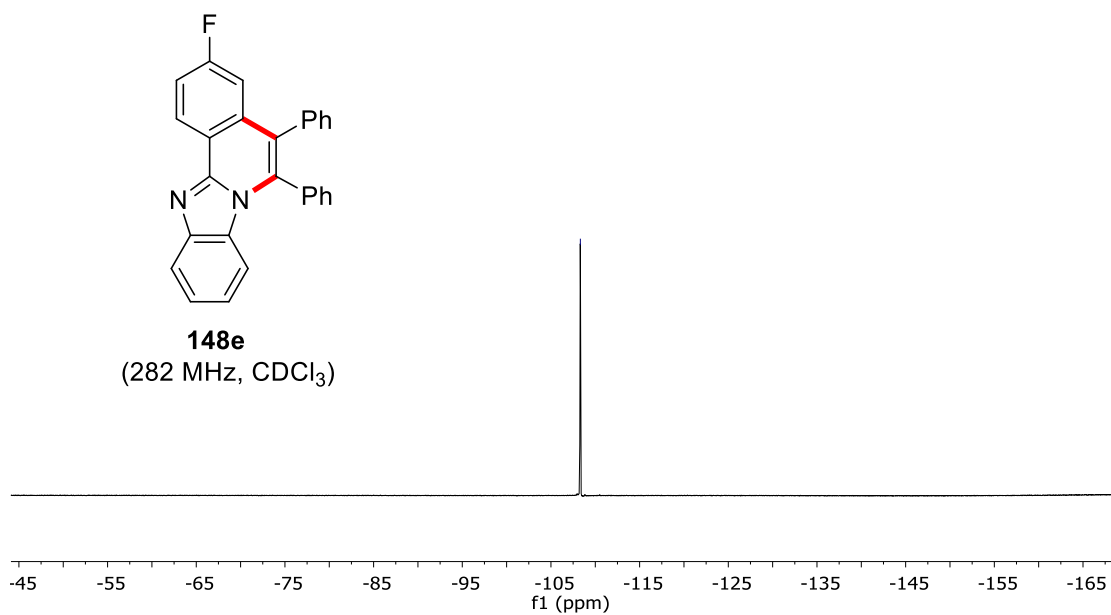
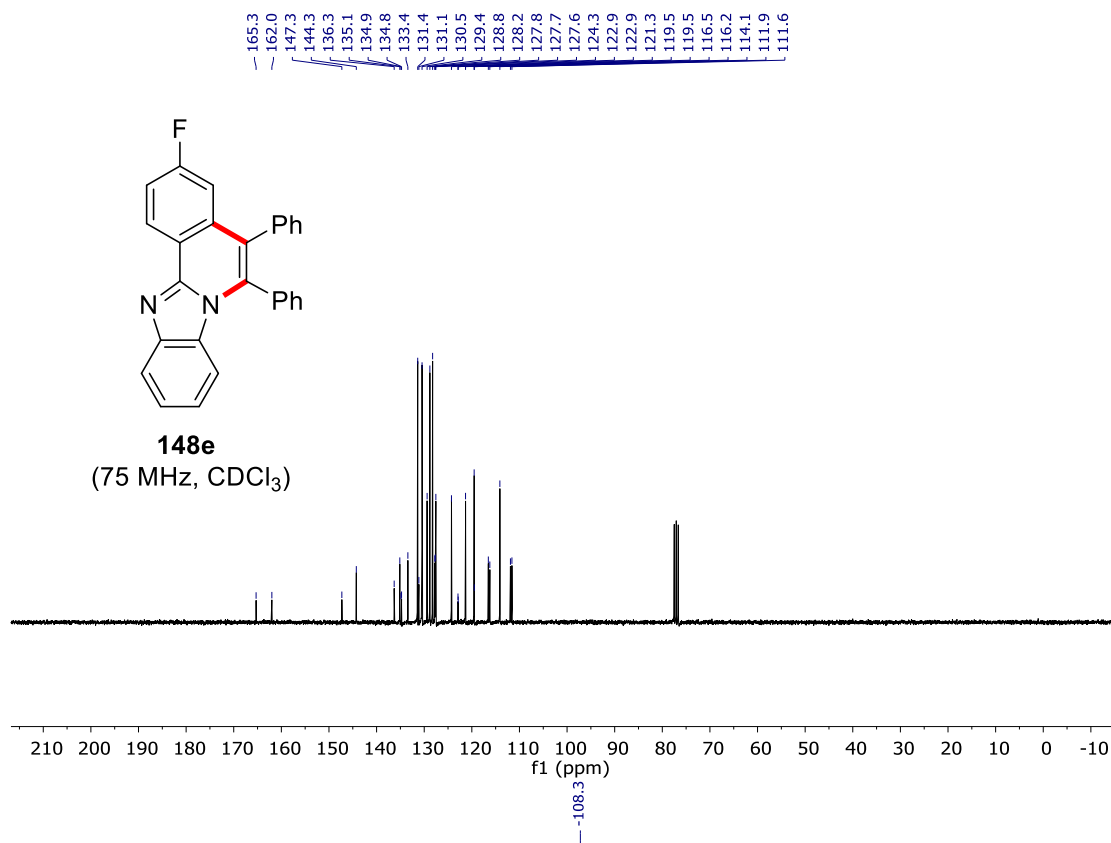
148d
(101 MHz, CDCl₃)



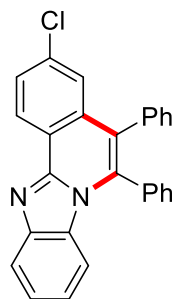
NMR Spectra



NMR Spectra

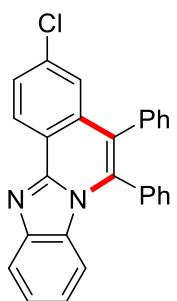
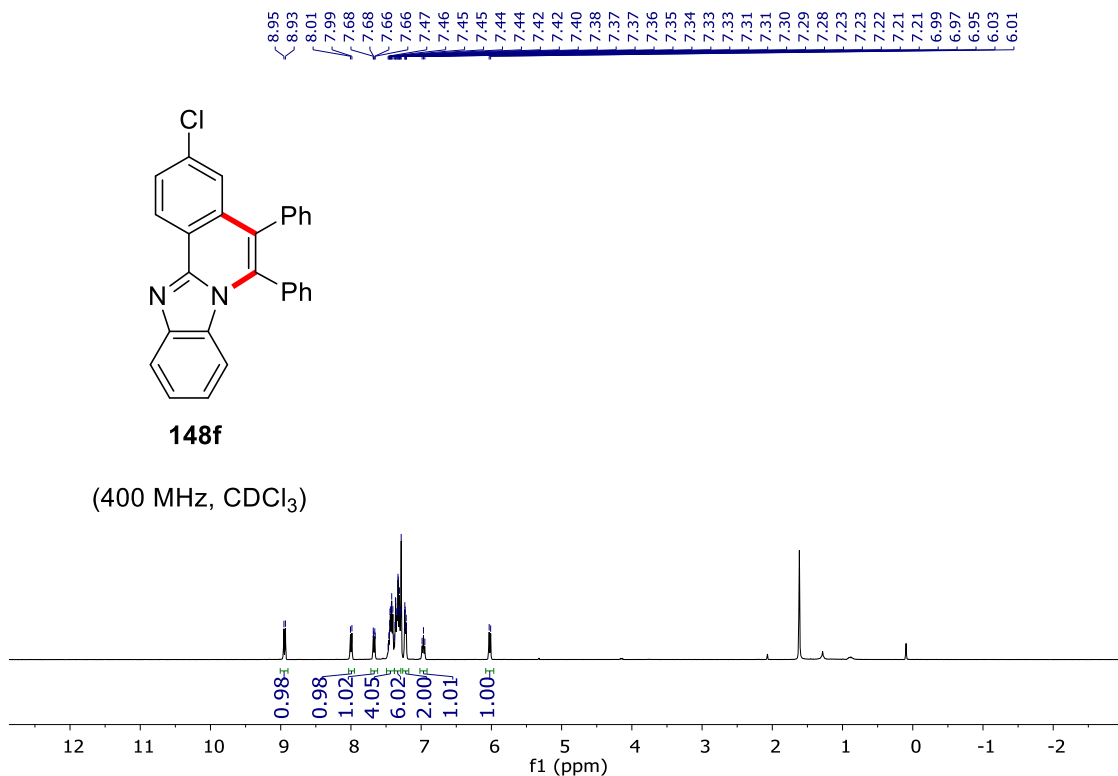


NMR Spectra



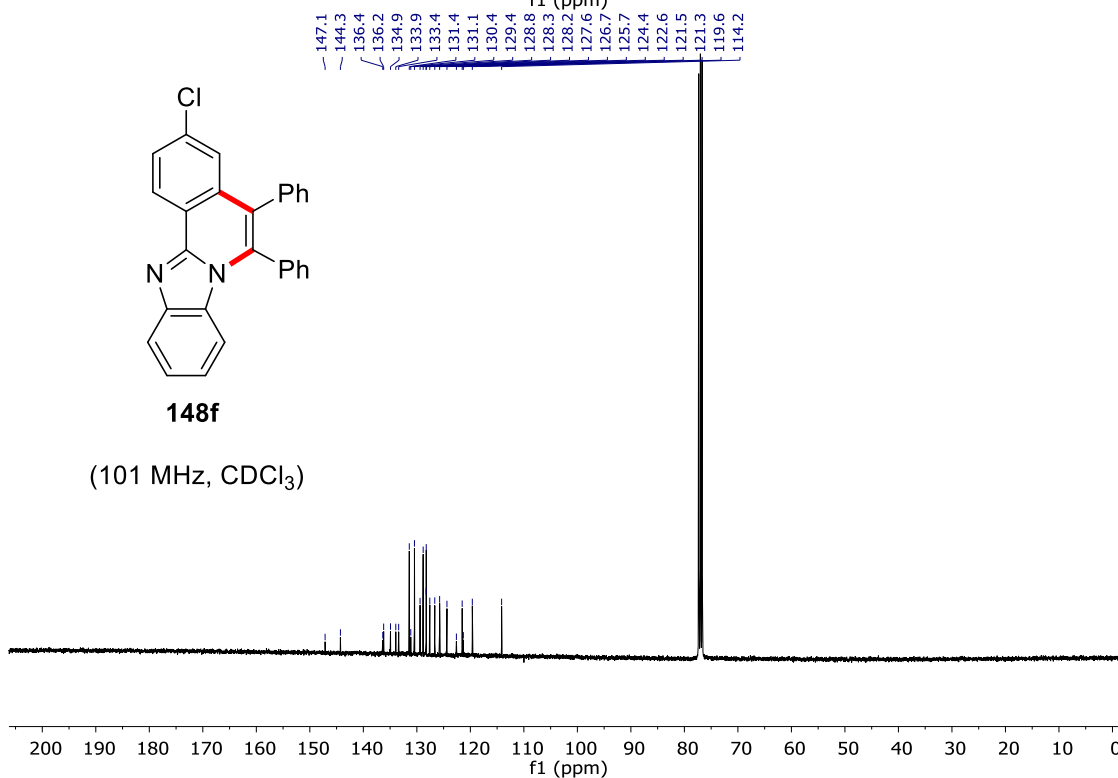
148f

(400 MHz, CDCl₃)



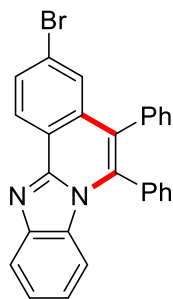
148f

(101 MHz, CDCl₃)



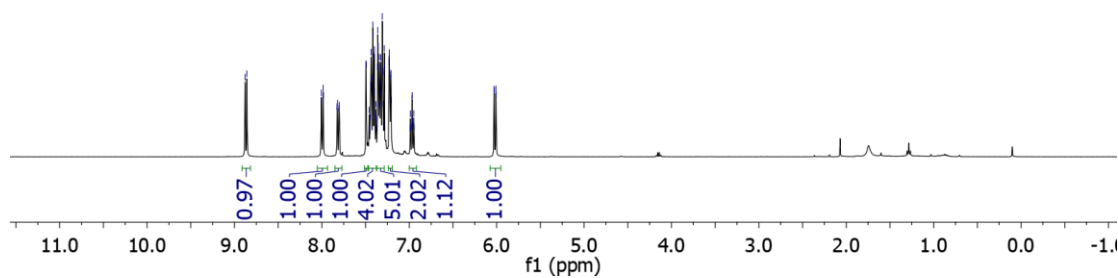
NMR Spectra

8.88
8.86
8.01
8.00
7.99
7.98
7.83
7.82
7.80
7.50
7.49
7.46
7.45
7.44
7.44
7.42
7.42
7.42
7.40
7.40
7.39
7.38
7.38
7.36
7.36
7.36
7.35
7.35
7.34
7.34
7.34
7.33
7.32
7.31
7.30
7.29
7.29
7.28
7.28
7.23
7.23
7.21
7.21
7.21
6.99
6.97
6.97
6.97
6.96
6.95
6.95
6.03
6.01
6.01

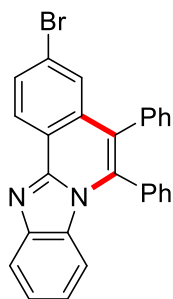


148g

(400 MHz, CDCl₃)

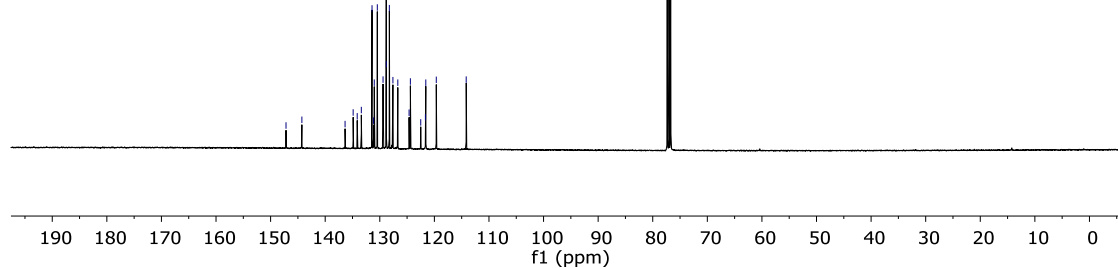


147.2
144.3
144.3
136.4
134.9
134.1
133.4
133.4
131.4
131.1
131.0
130.5
129.4
128.8
128.8
128.2
127.6
126.7
124.6
124.4
124.4
122.5
121.6
121.6
119.7
114.2

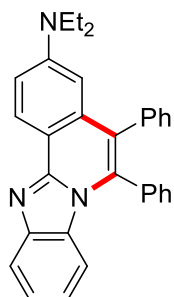


148g

(101 MHz, CDCl₃)

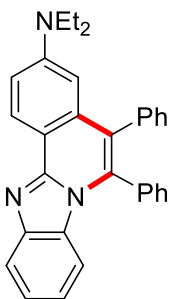
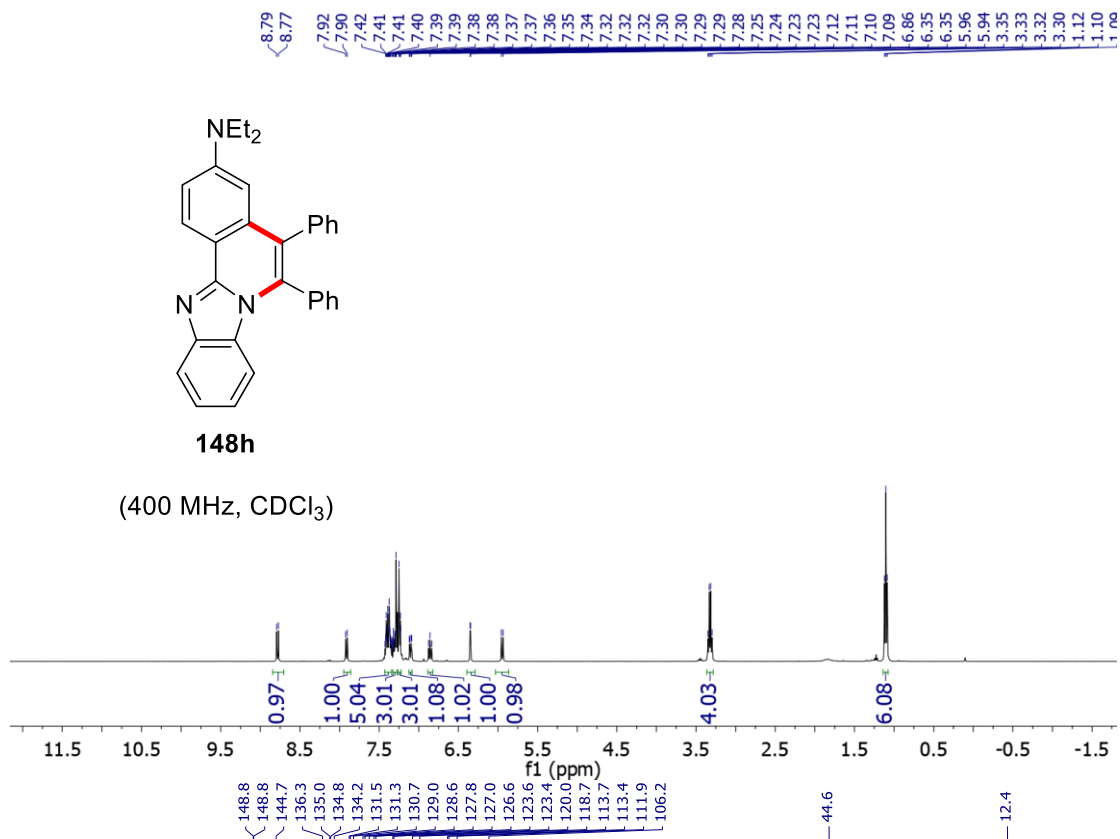


NMR Spectra



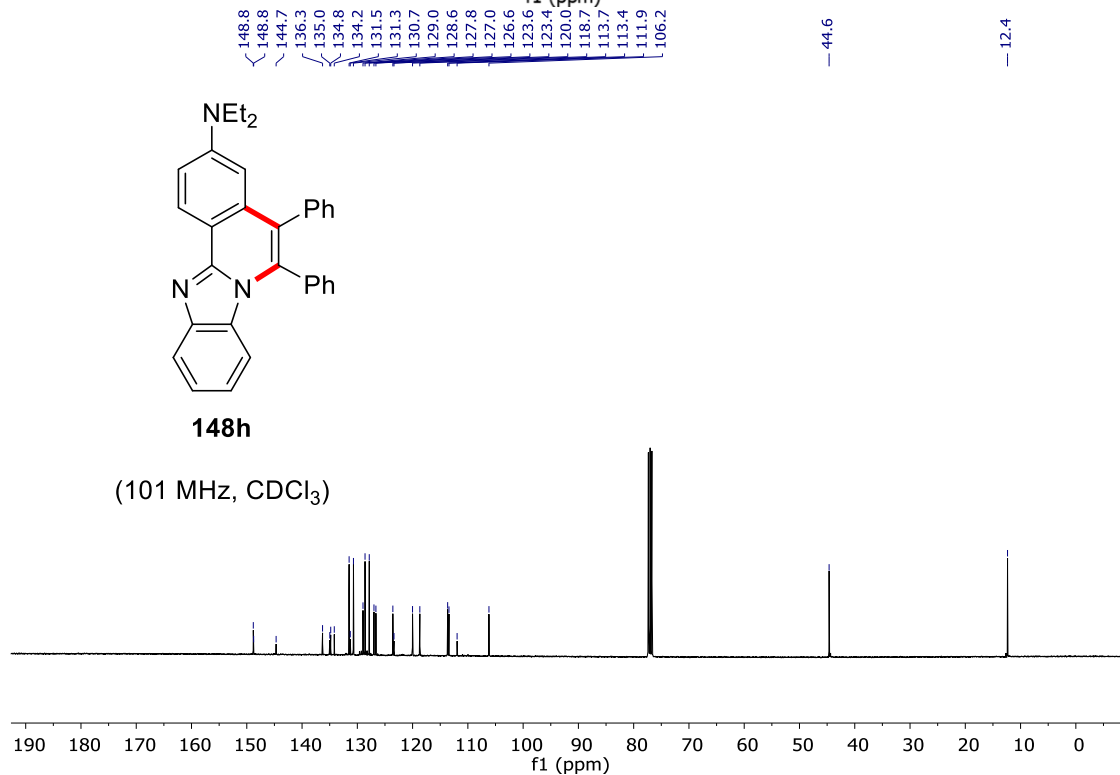
148h

(400 MHz, CDCl_3)

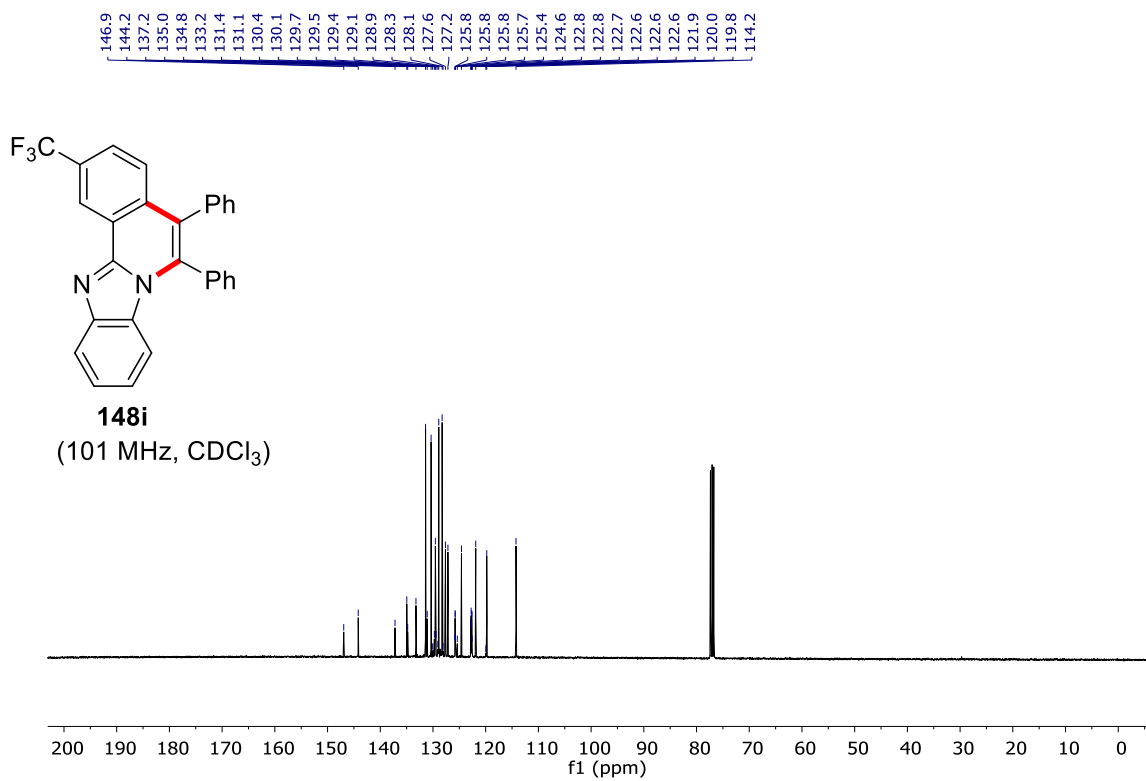
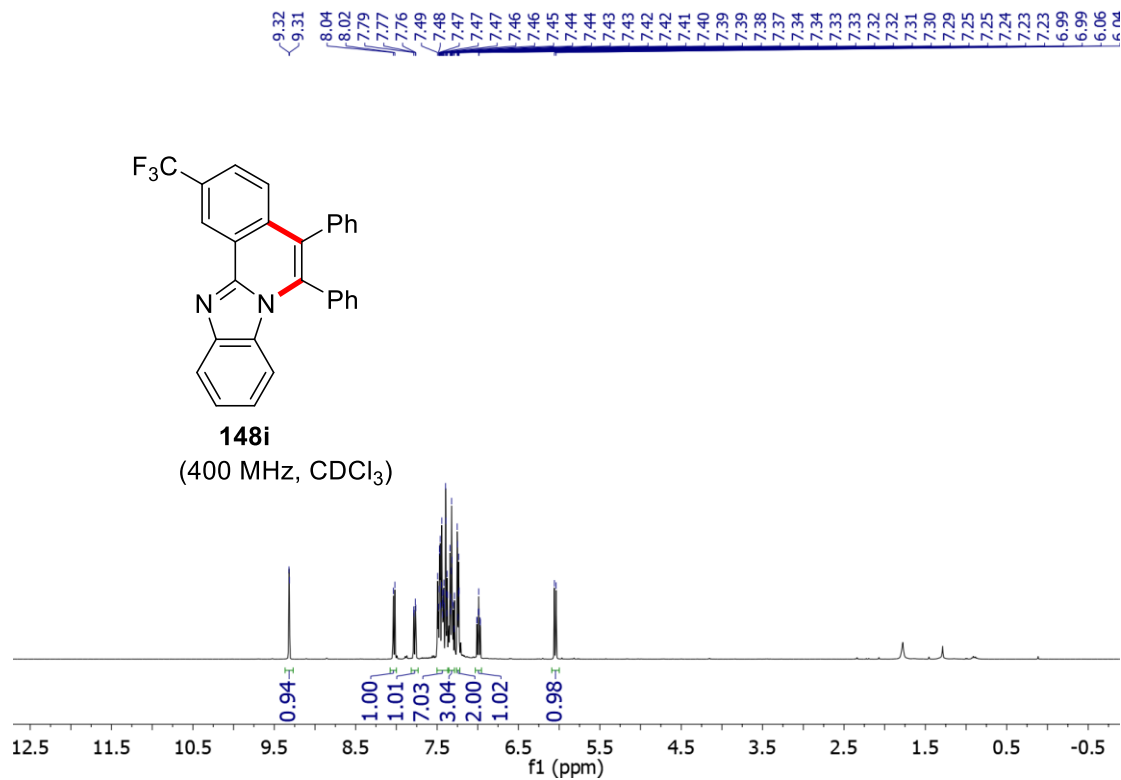


148h

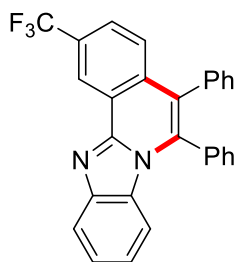
(101 MHz, CDCl_3)



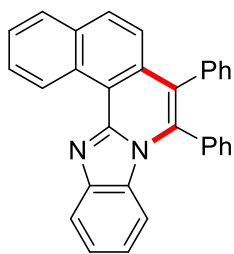
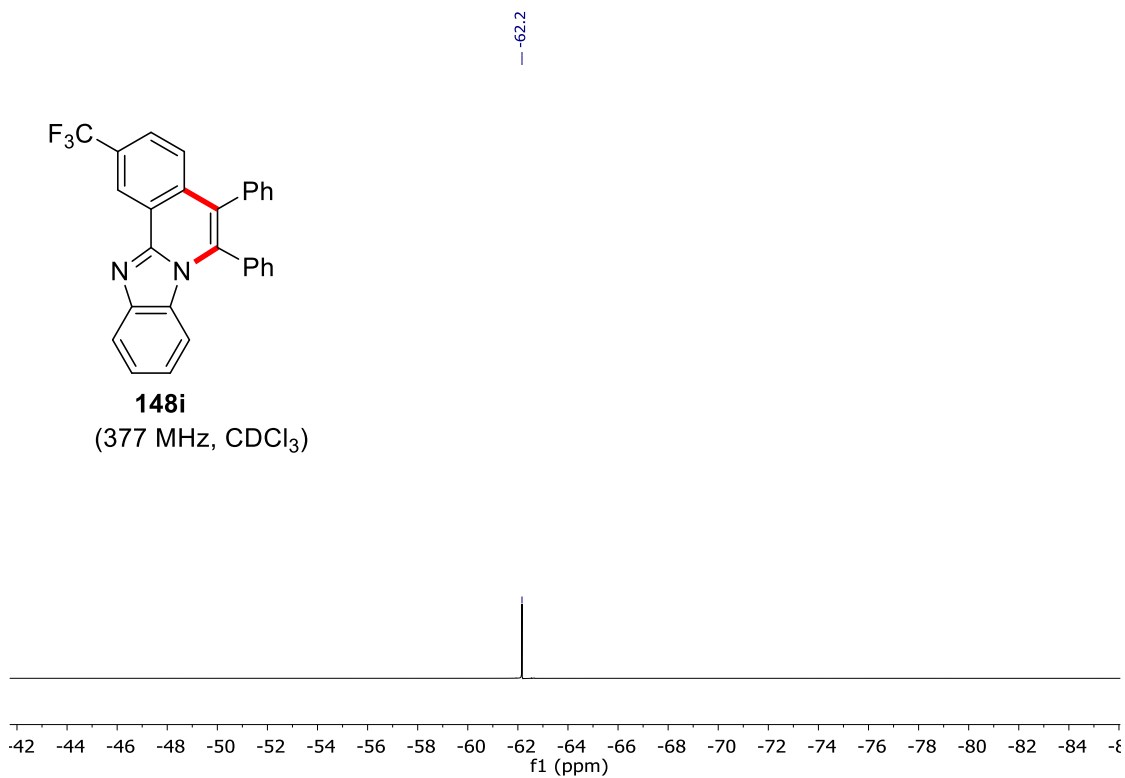
NMR Spectra



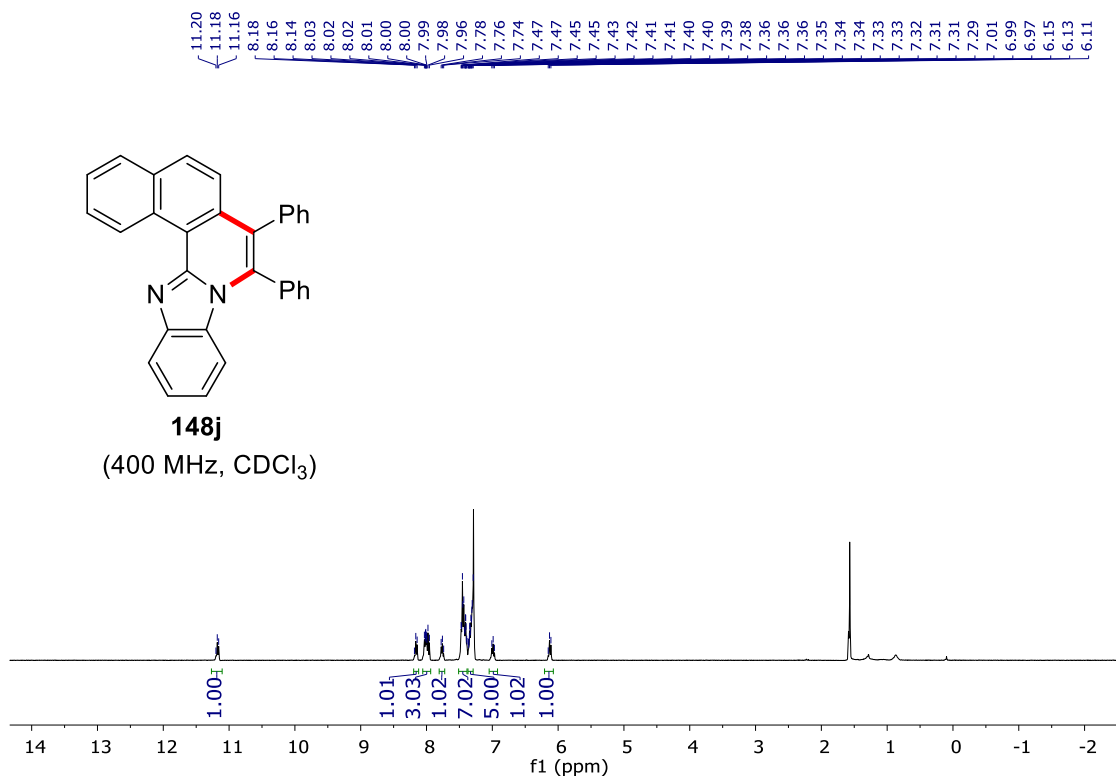
NMR Spectra



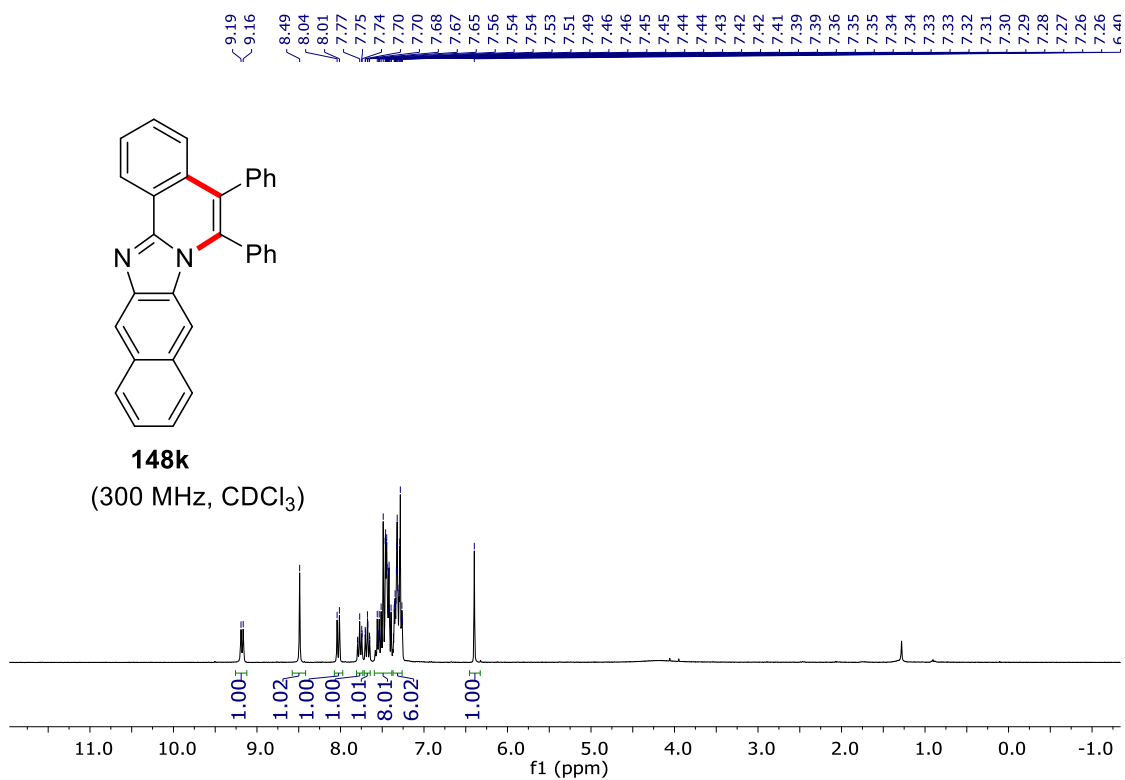
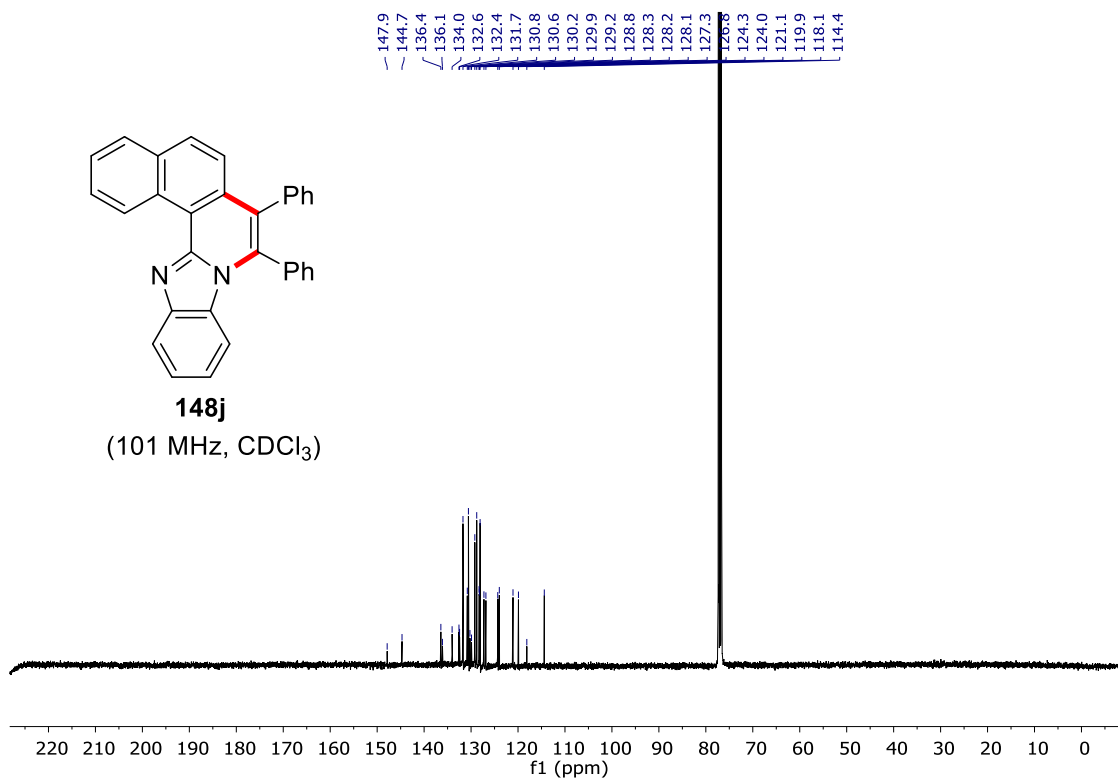
148i
(377 MHz, CDCl₃)



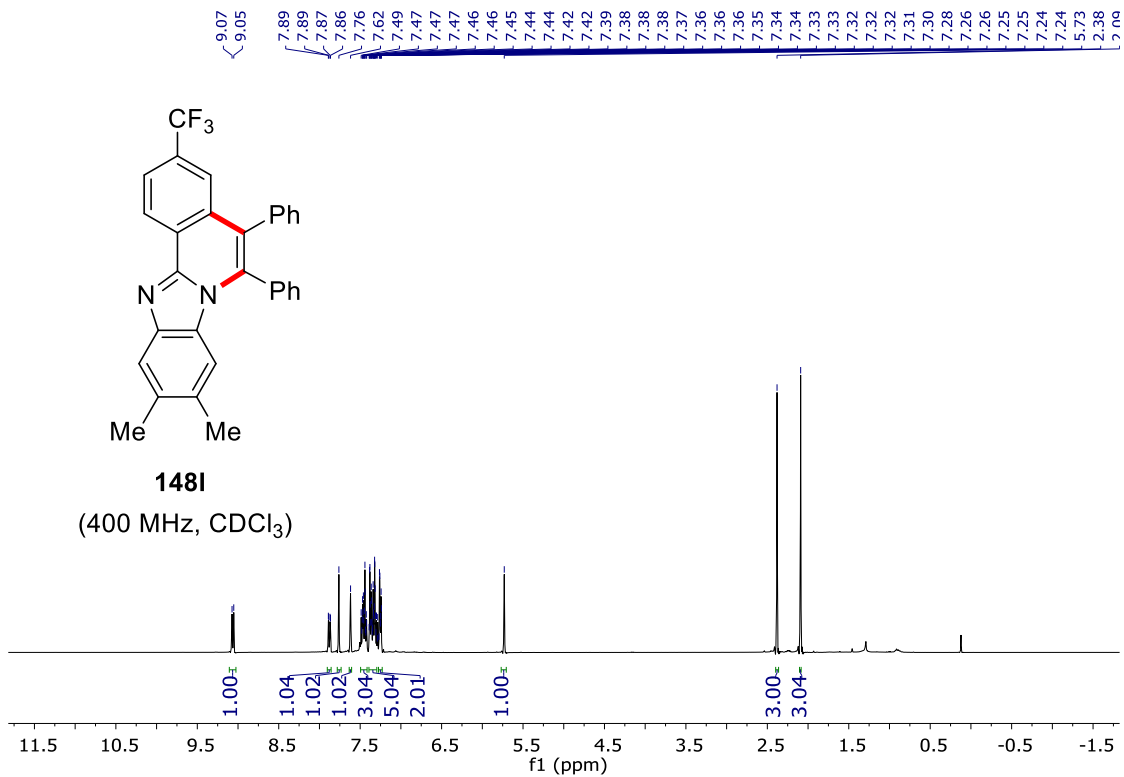
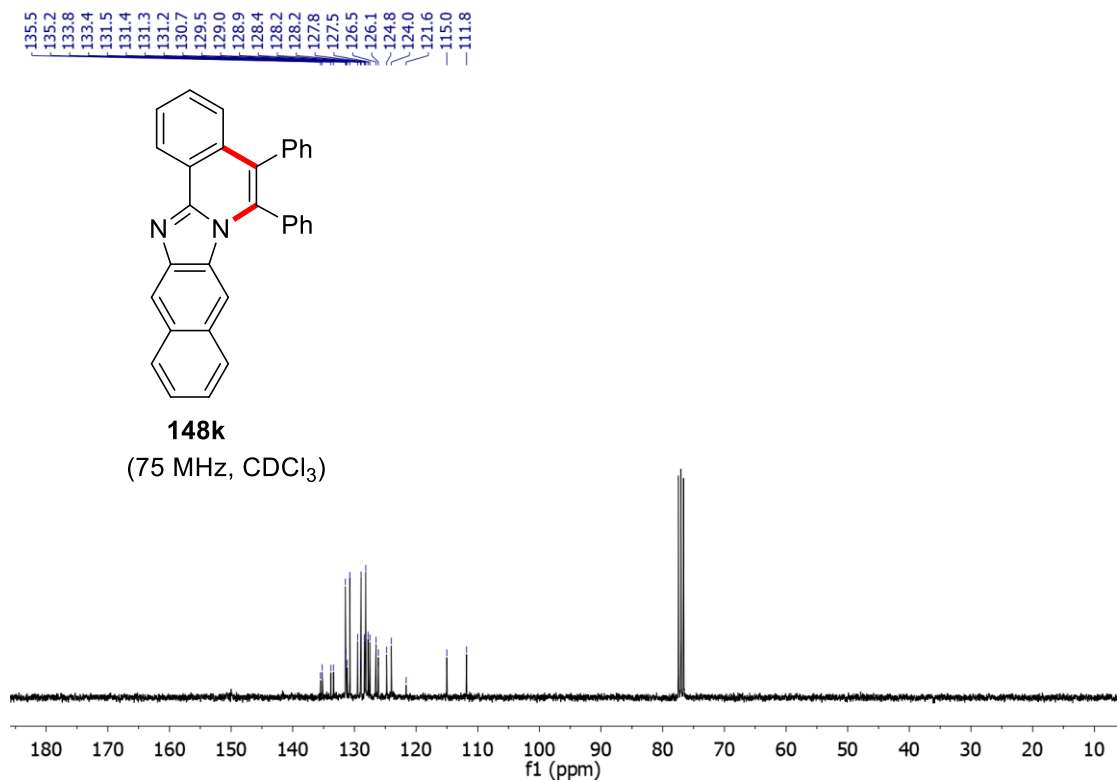
148j
(400 MHz, CDCl₃)



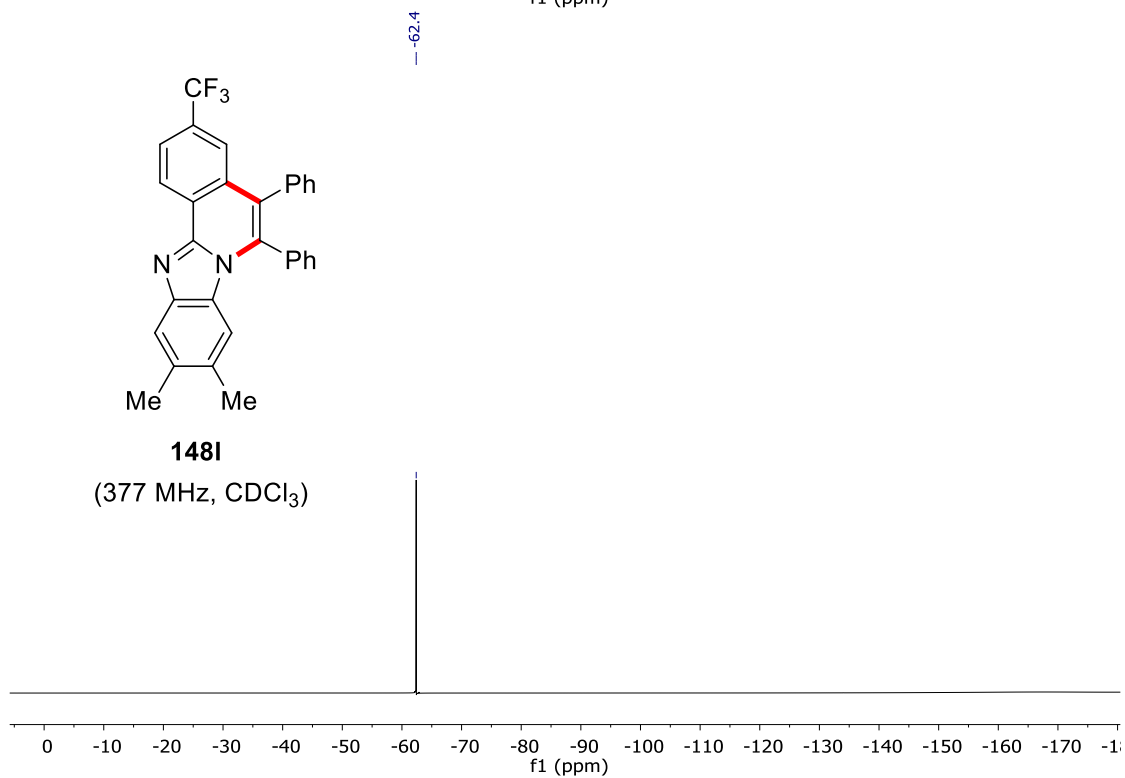
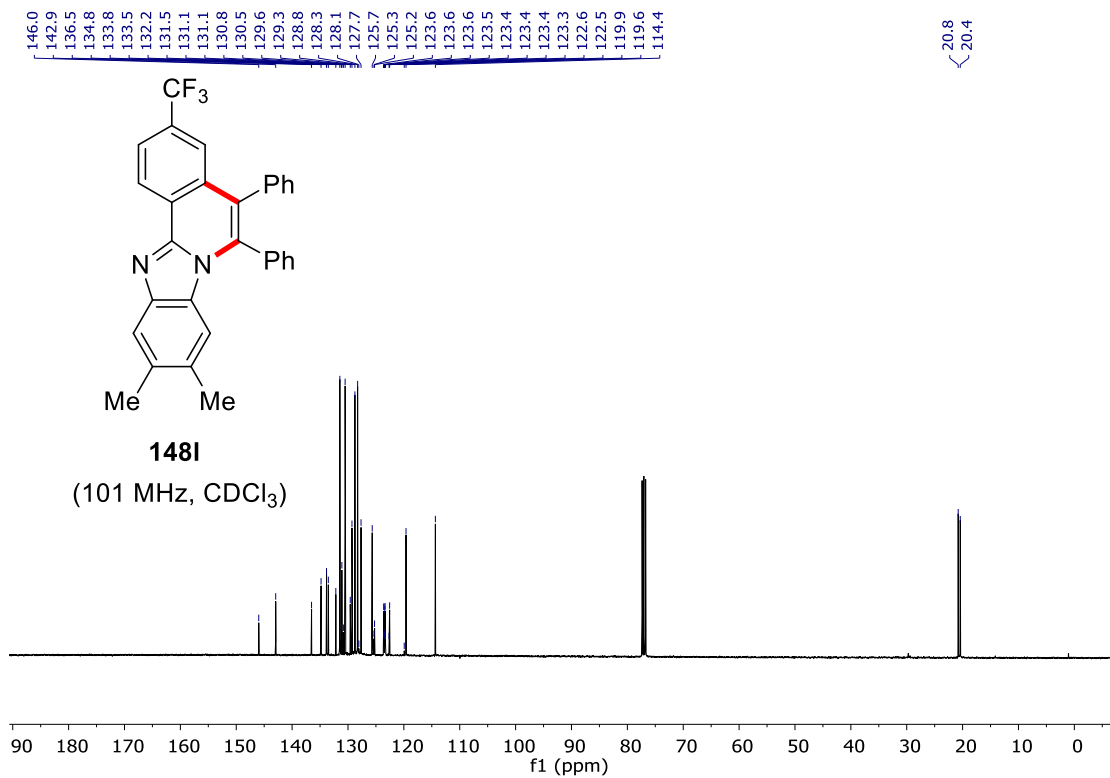
NMR Spectra



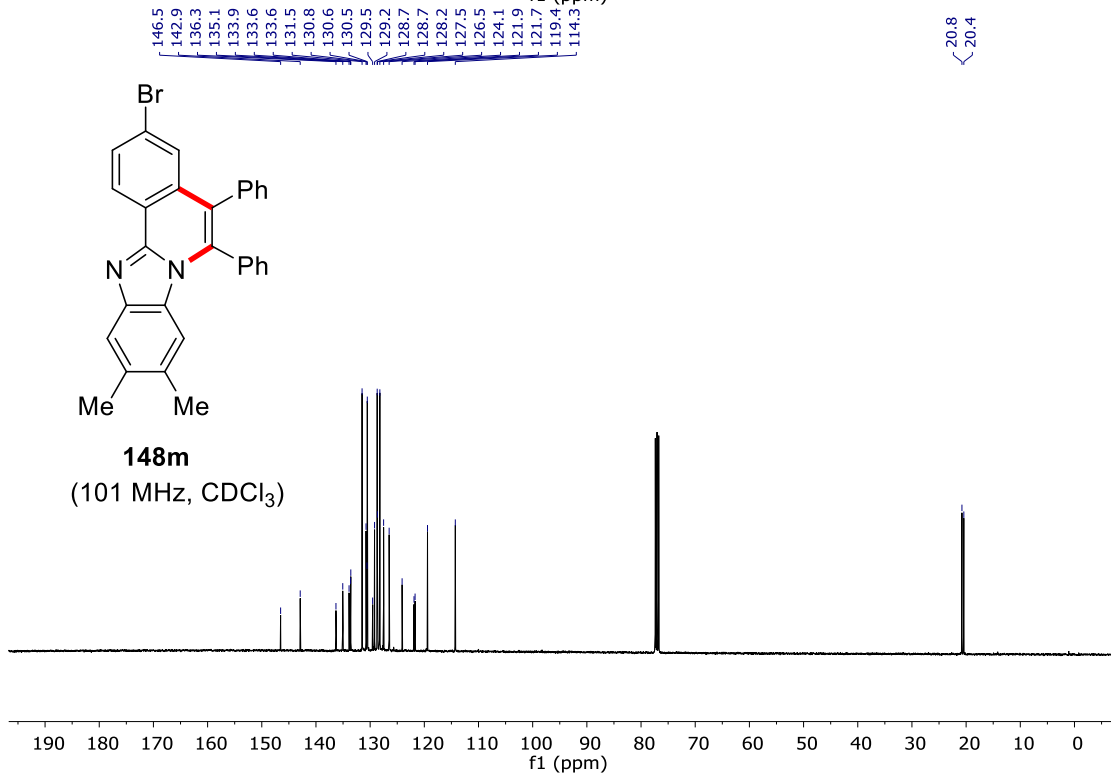
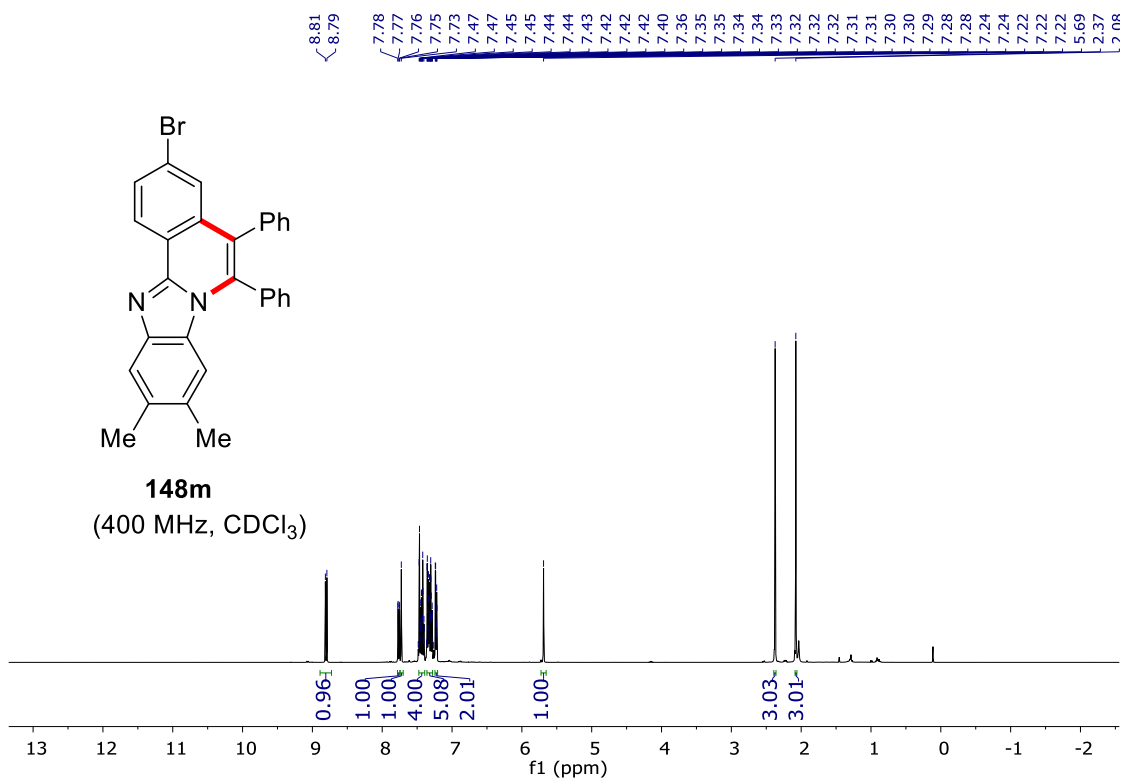
NMR Spectra



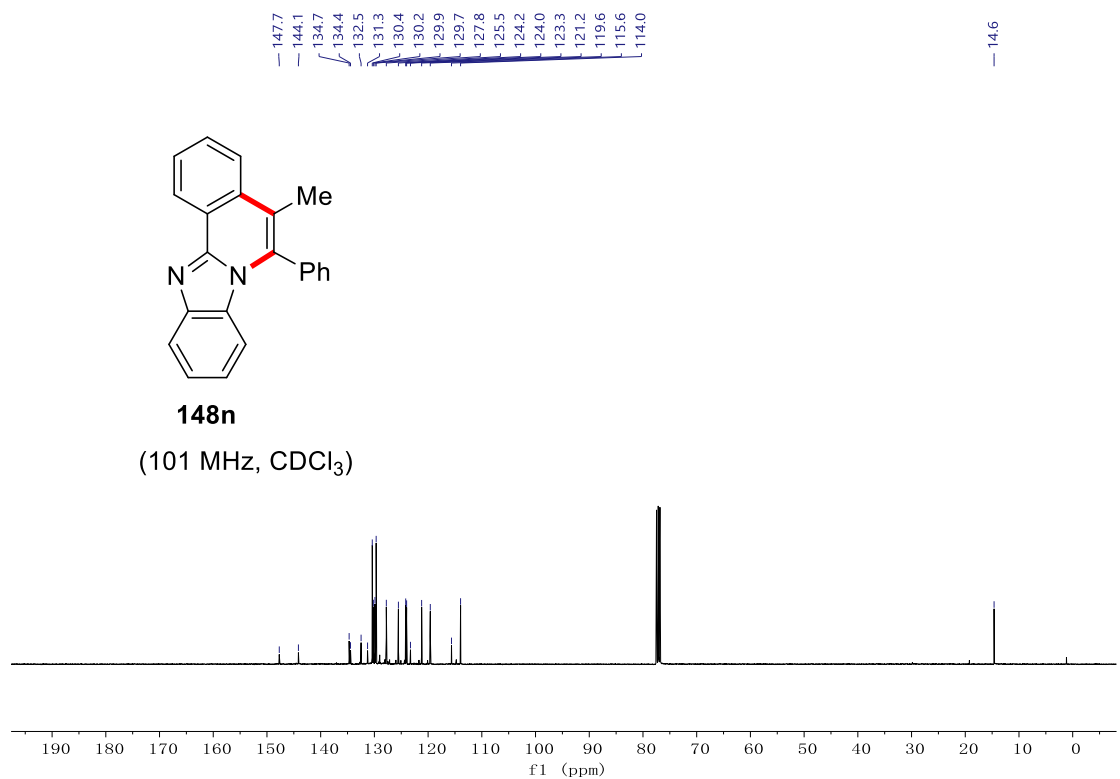
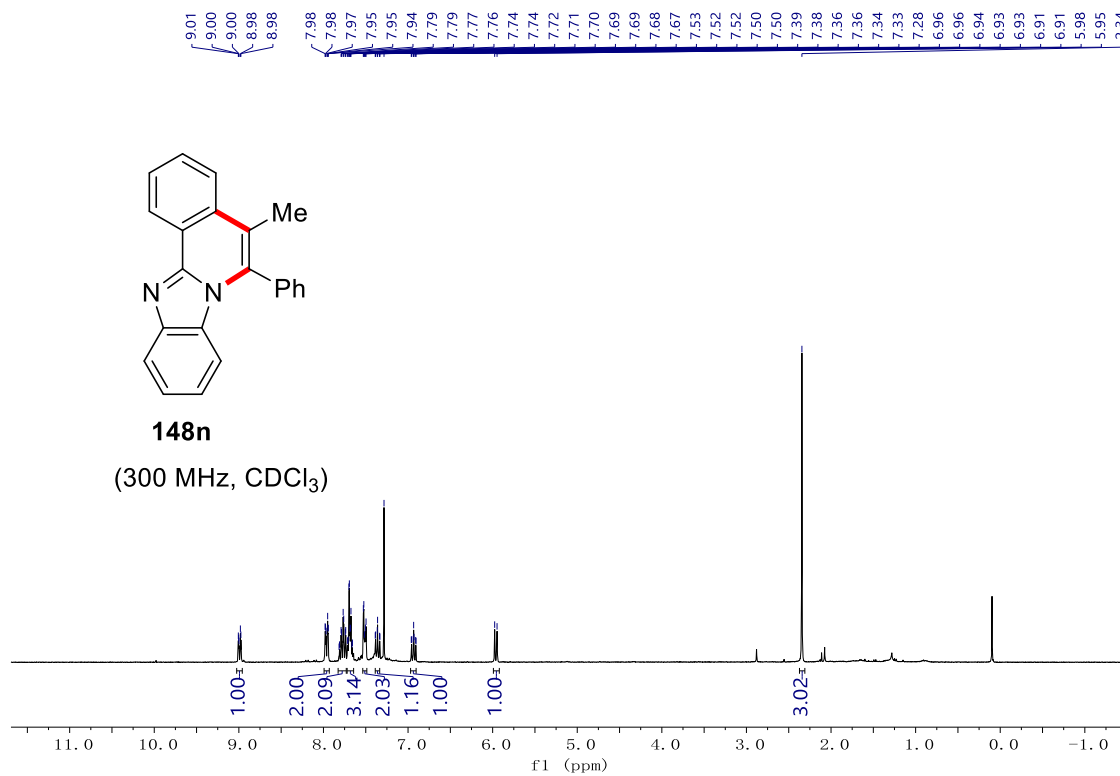
NMR Spectra



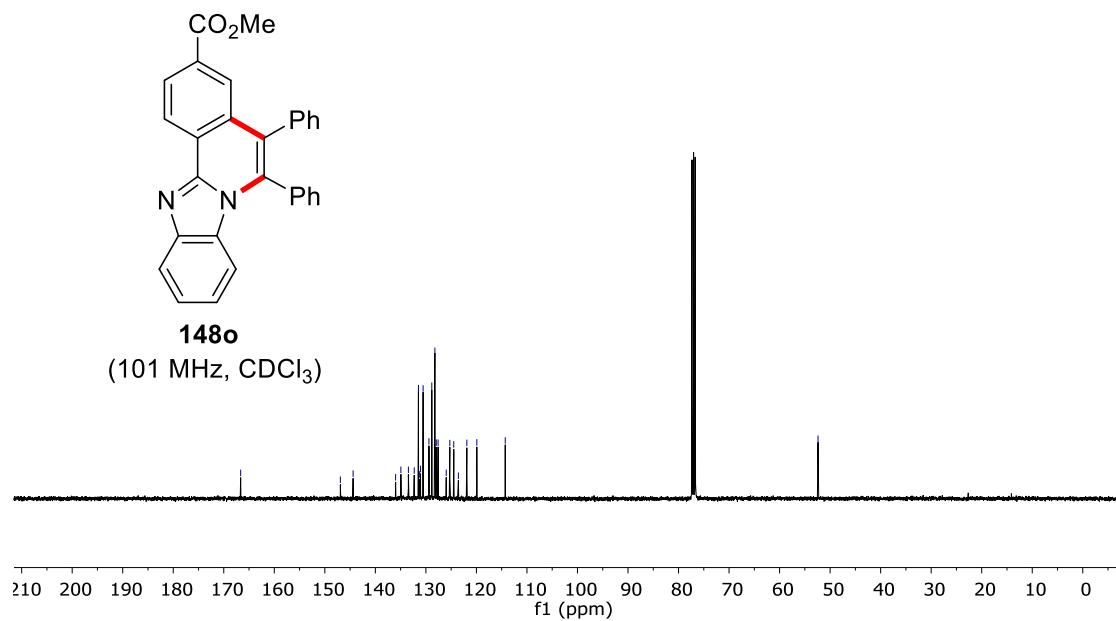
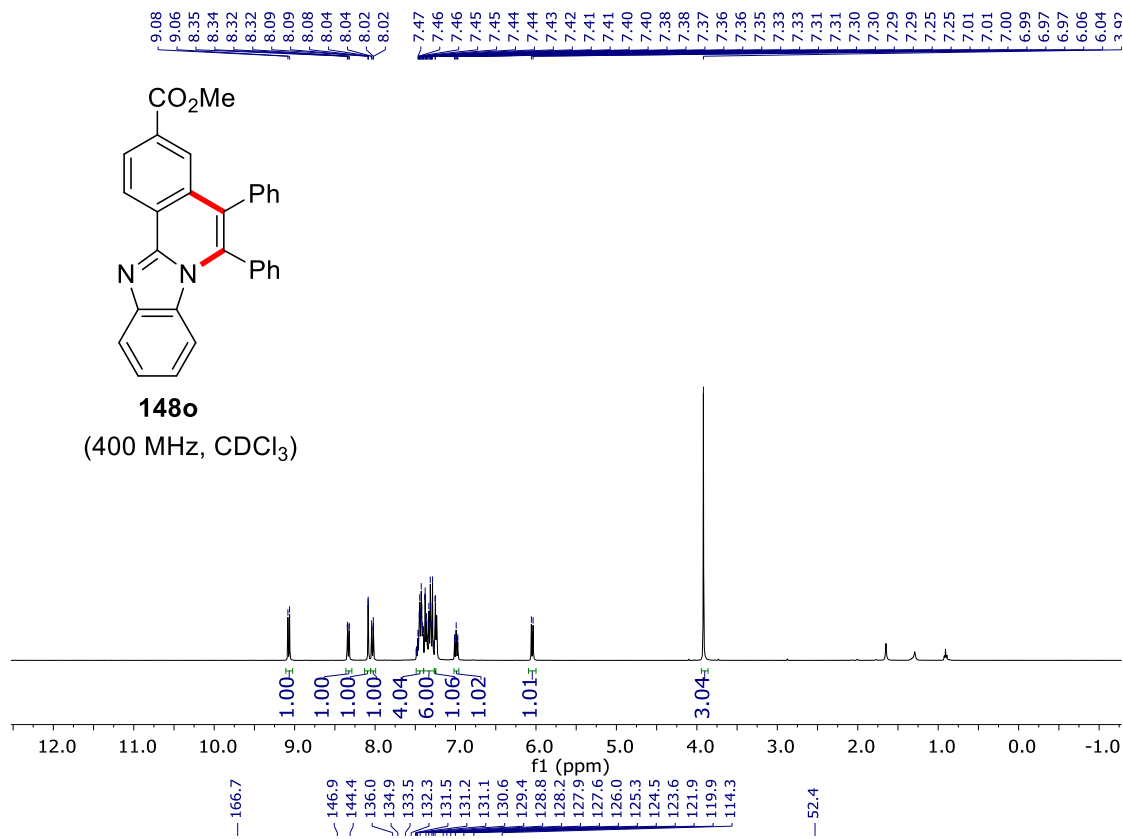
NMR Spectra



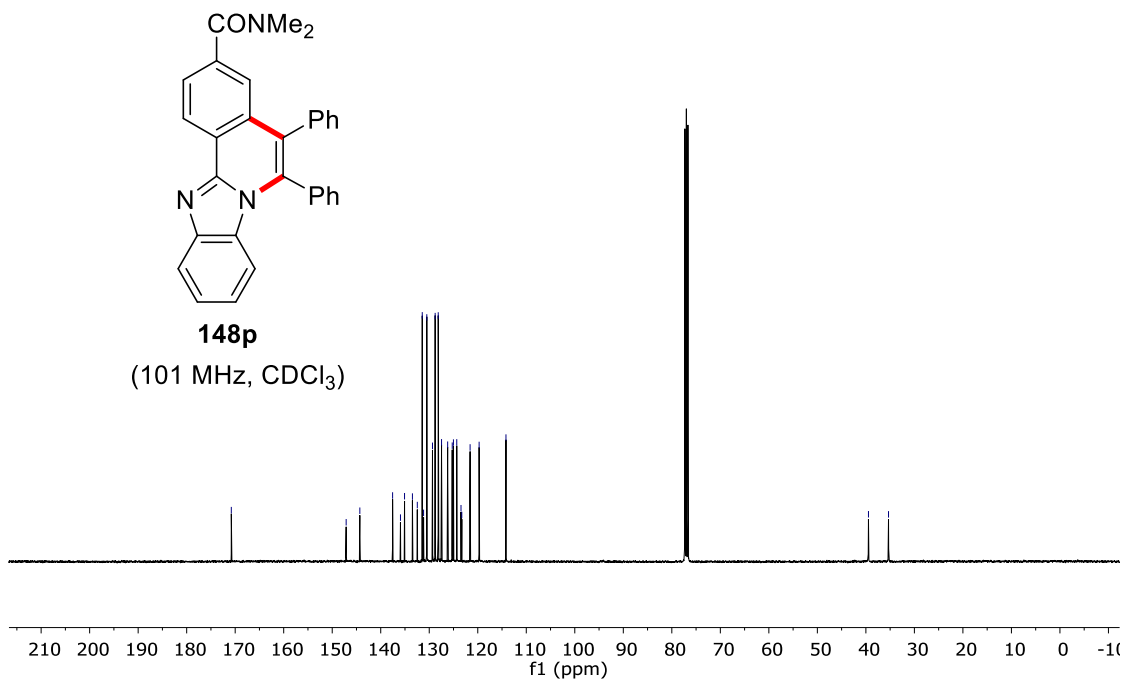
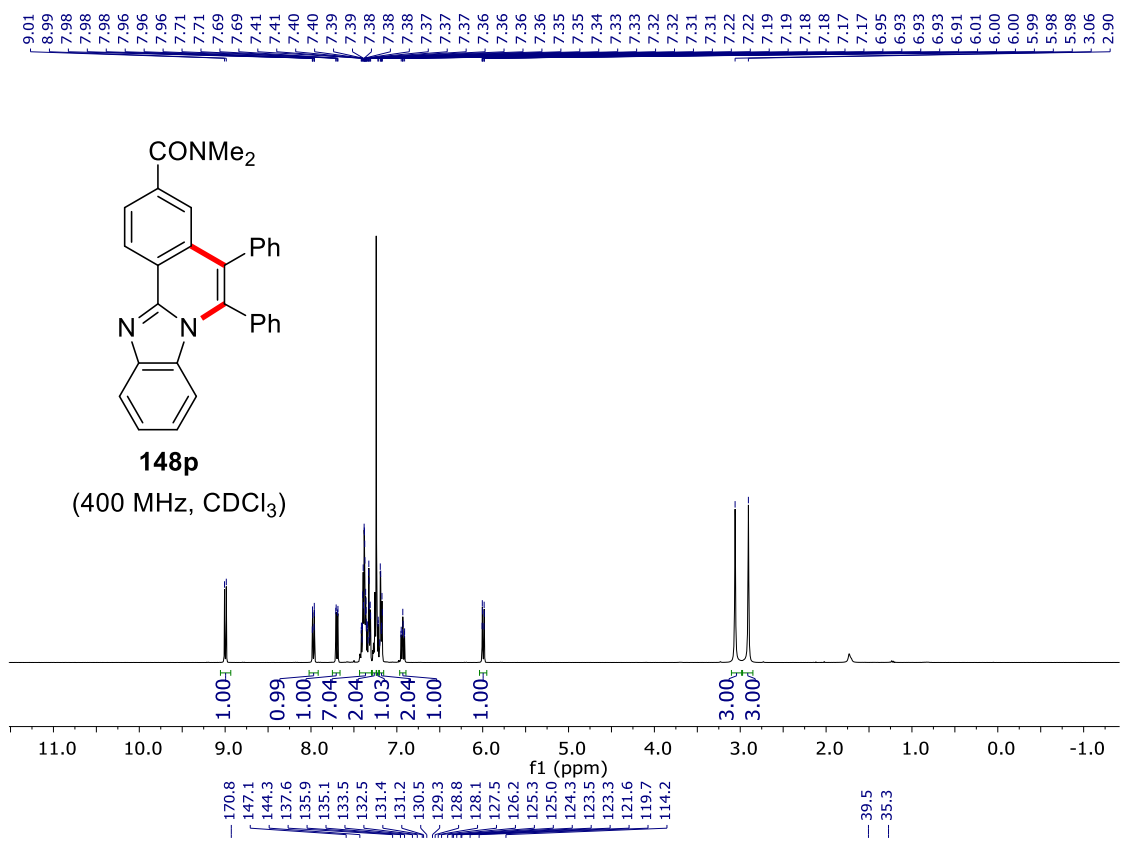
NMR Spectra



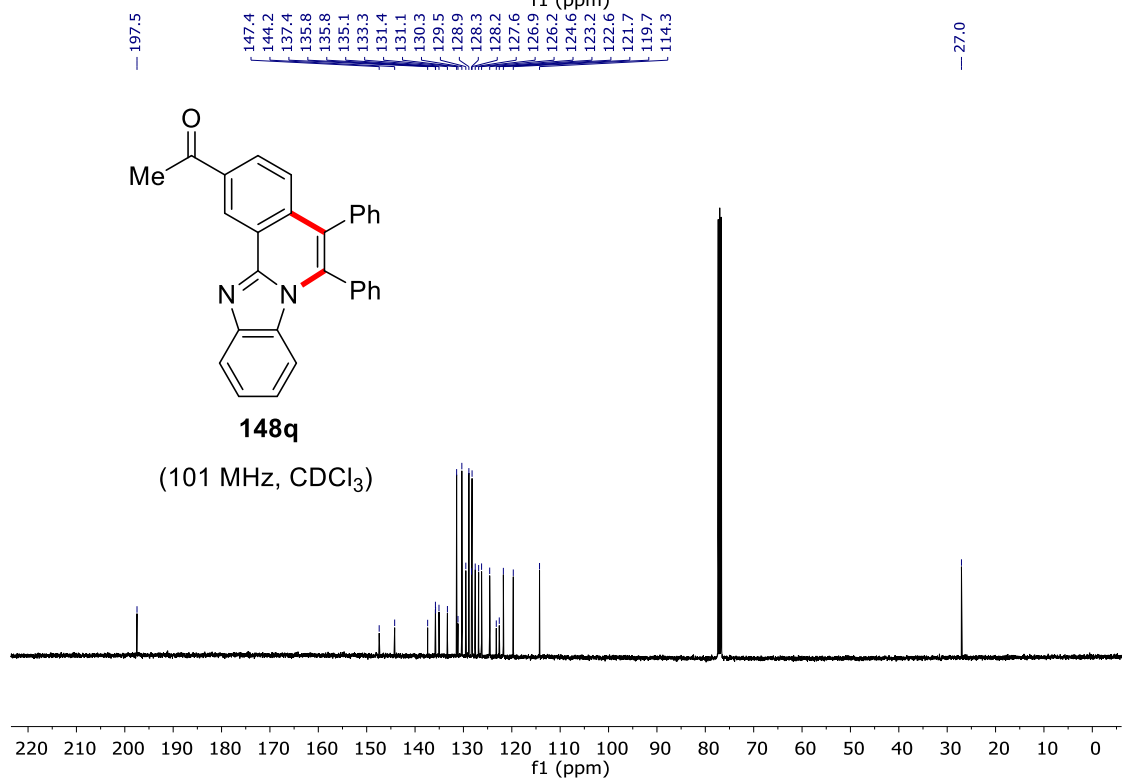
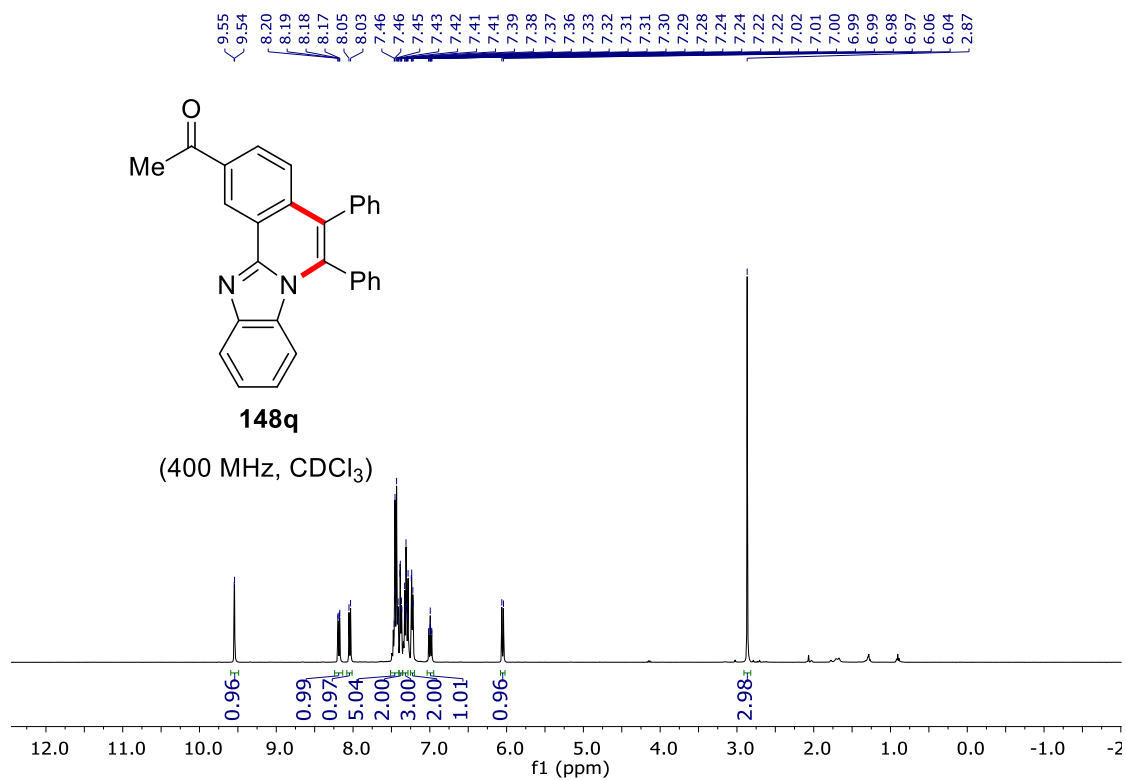
NMR Spectra



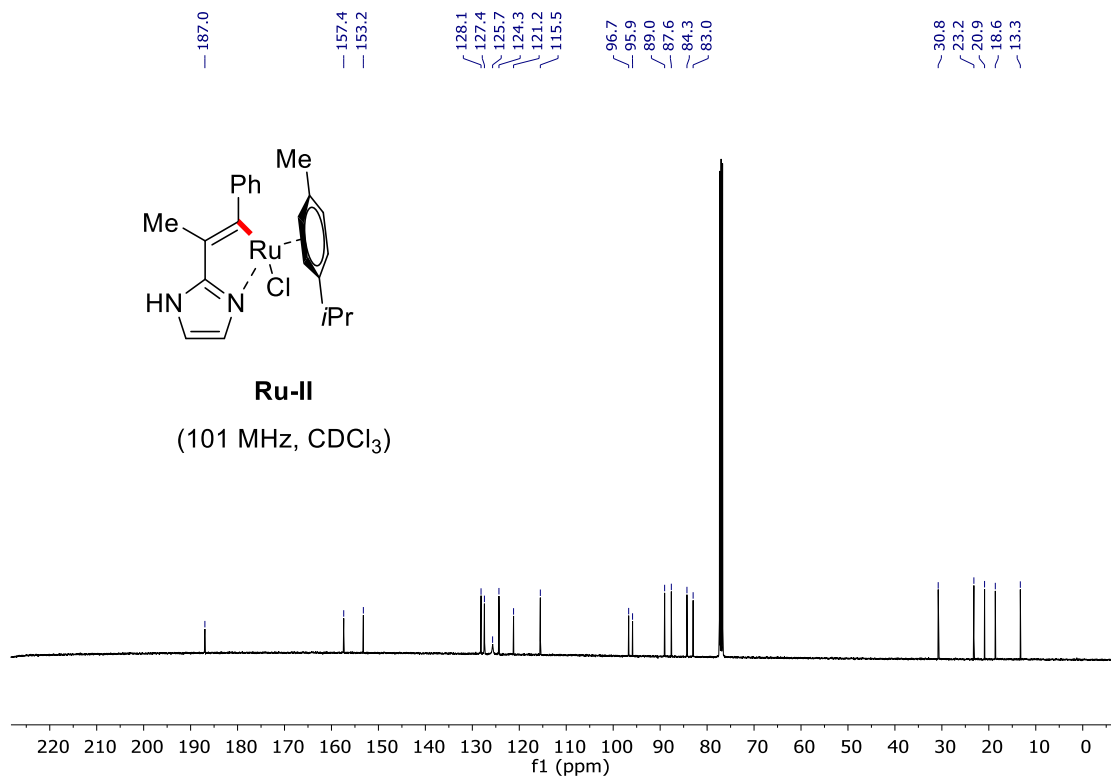
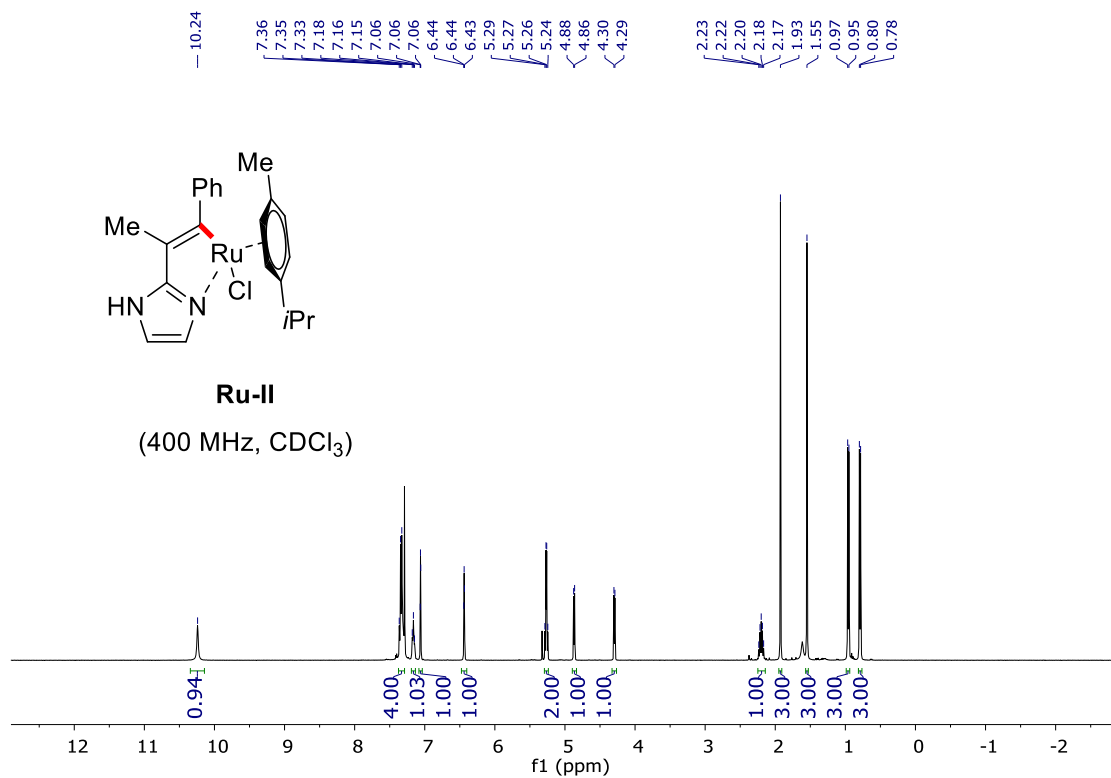
NMR Spectra



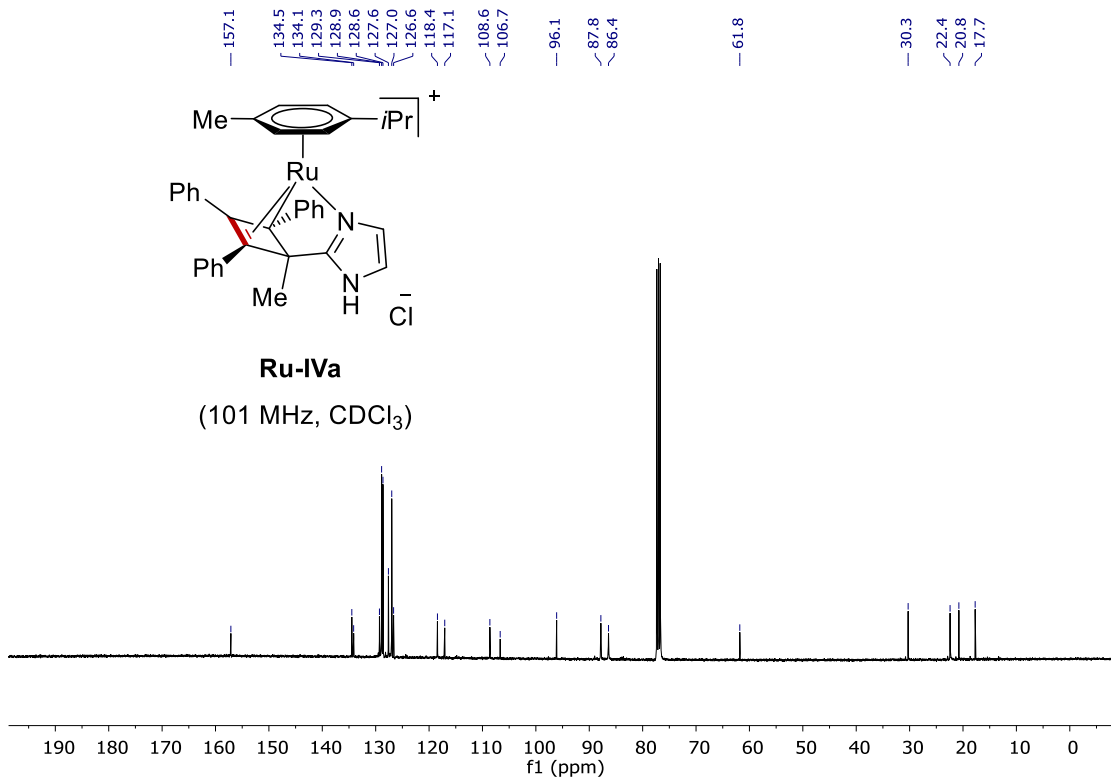
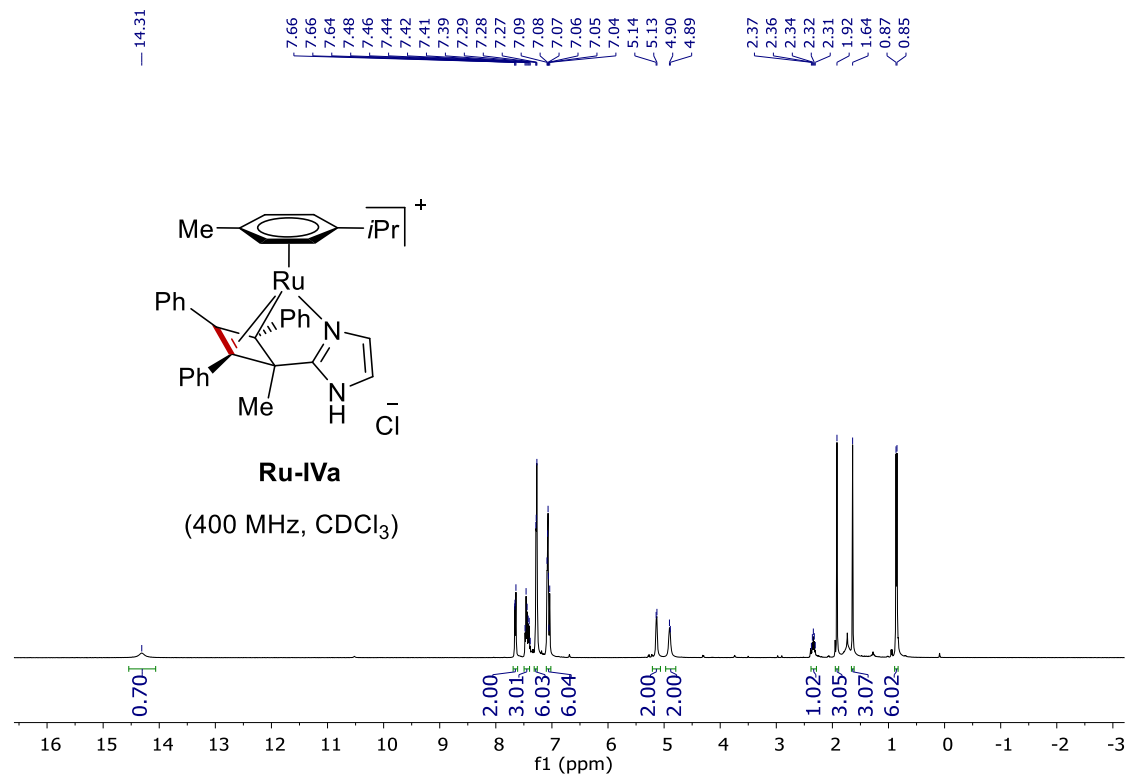
NMR Spectra



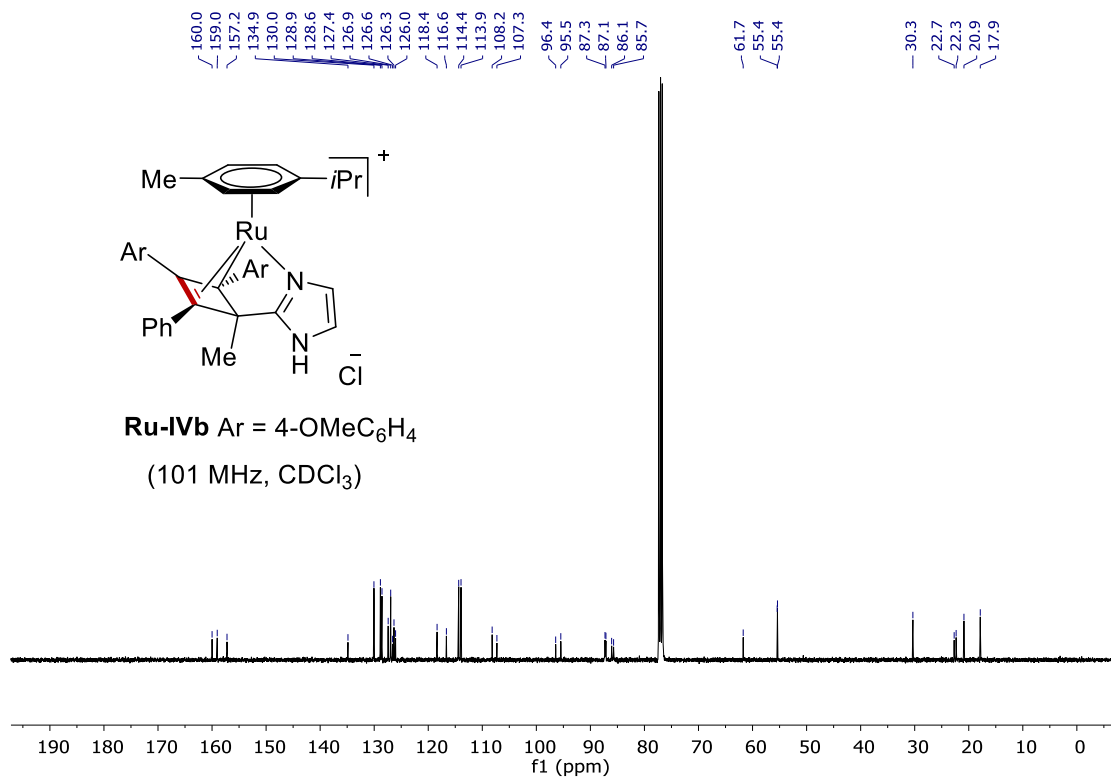
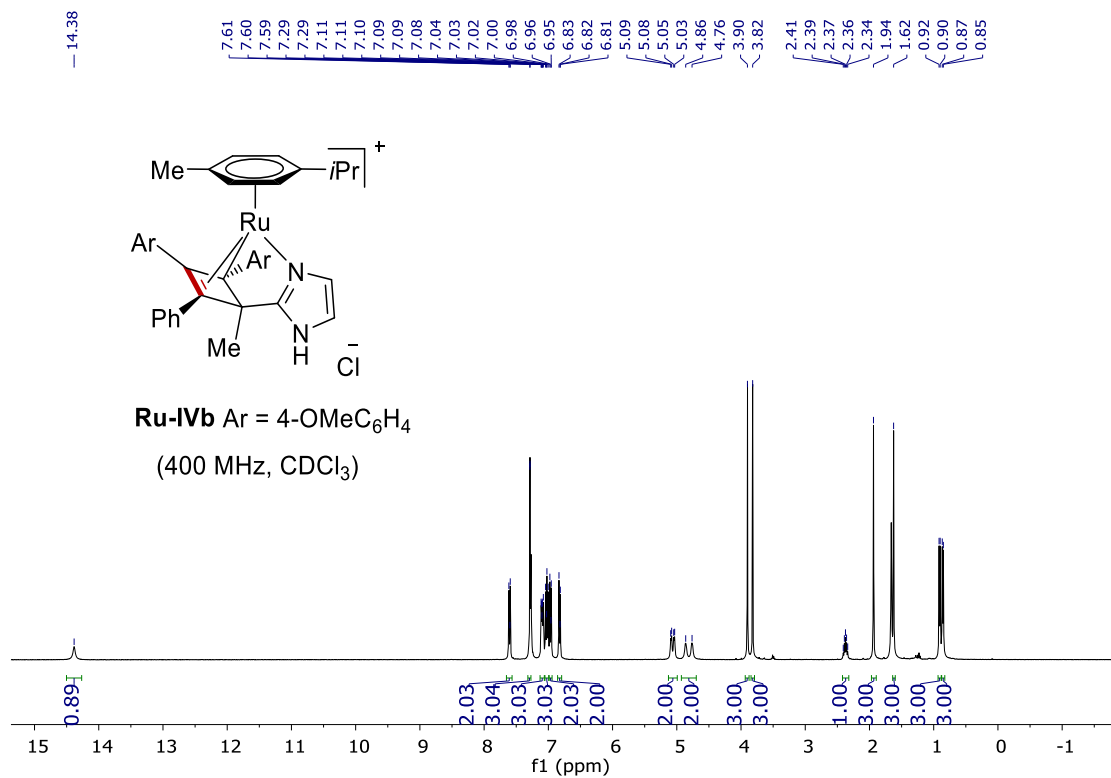
NMR Spectra

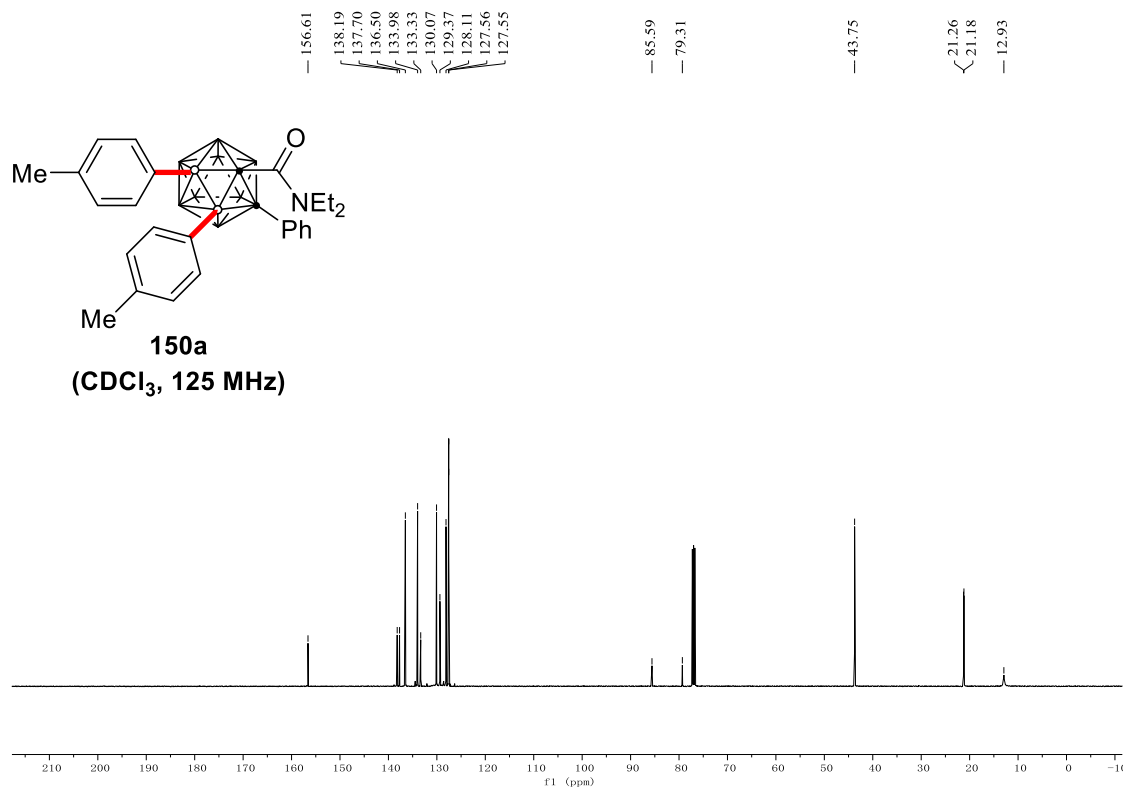
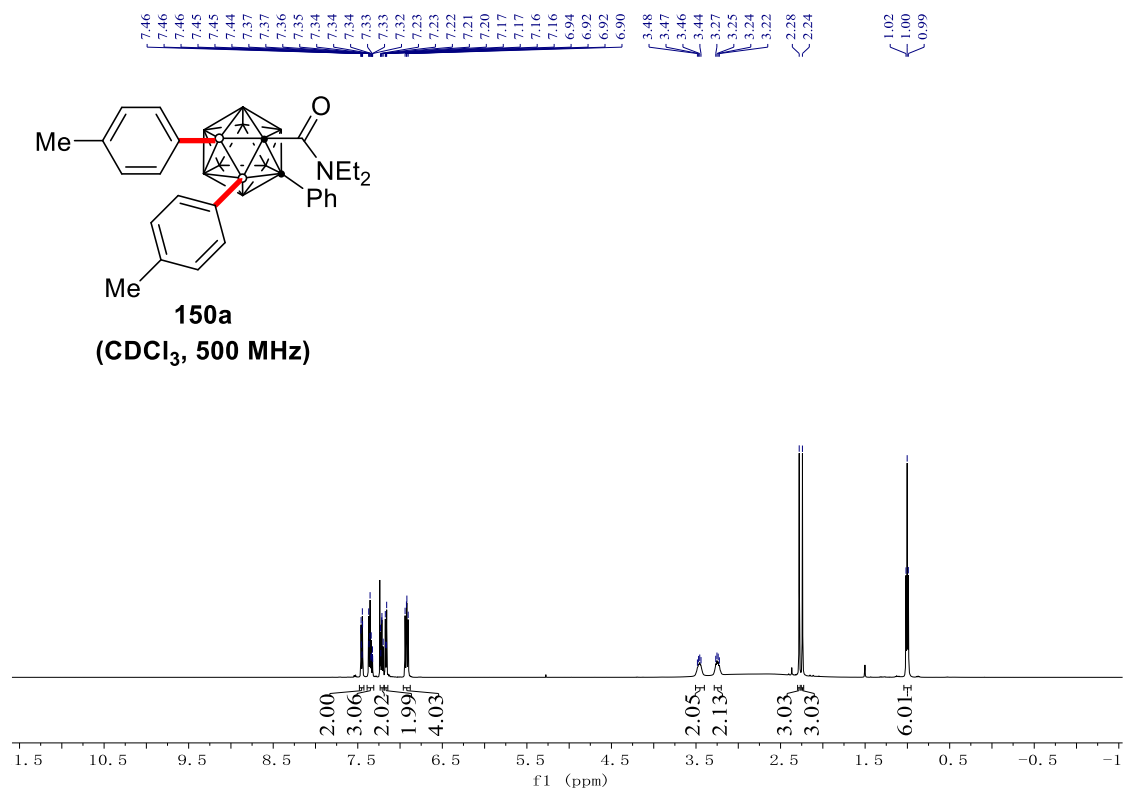


NMR Spectra

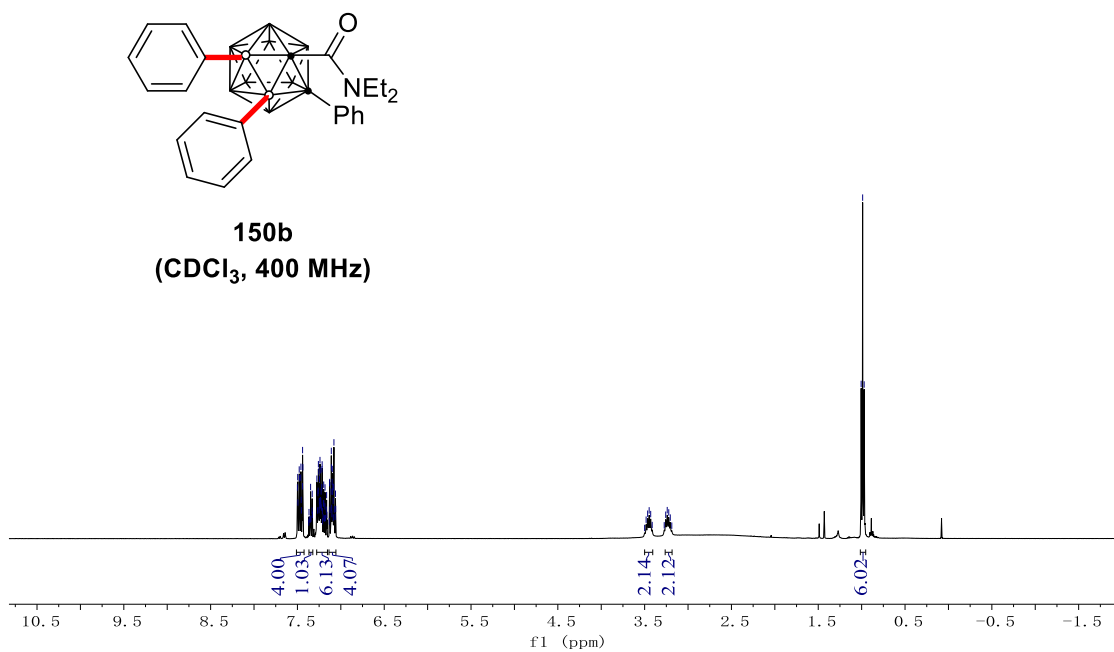
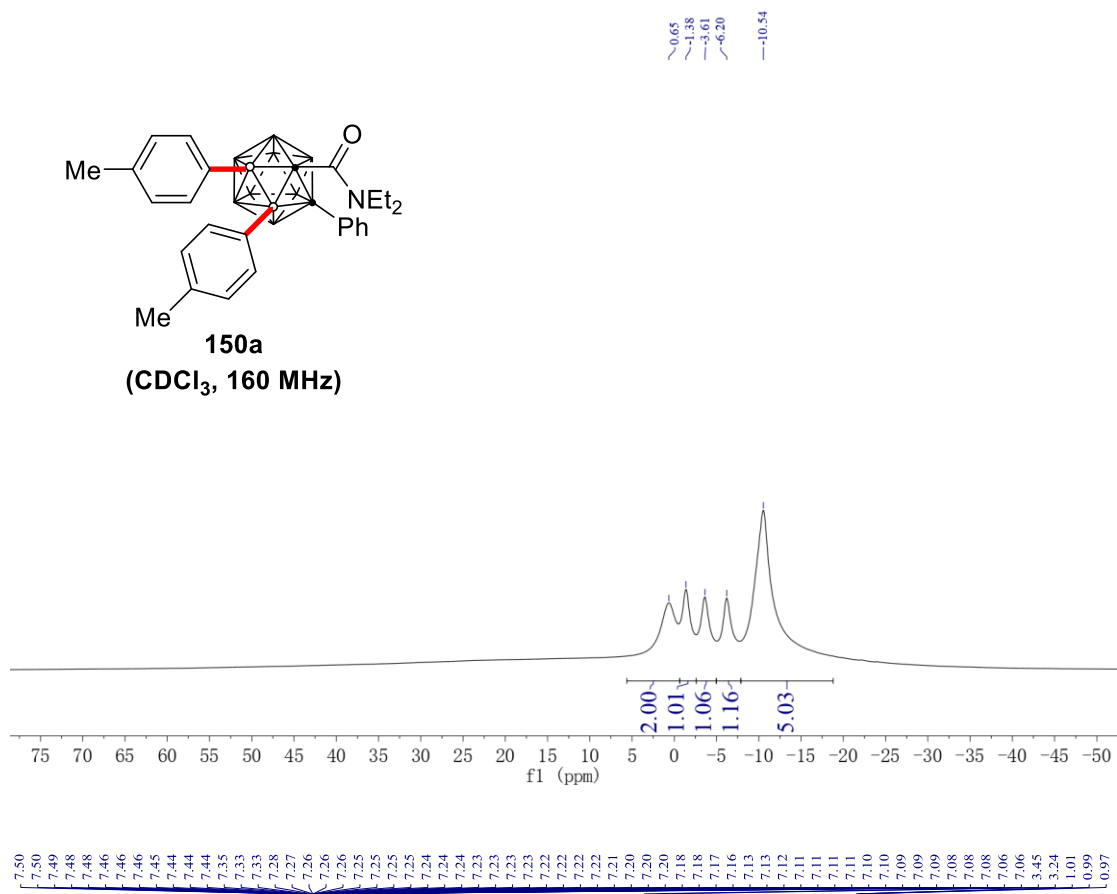


NMR Spectra

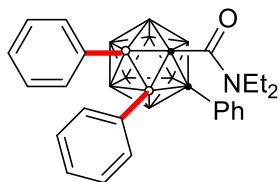


7.4 Palladium(II)-Catalyzed B(3,4)-Arylation of *o*-Carboranes

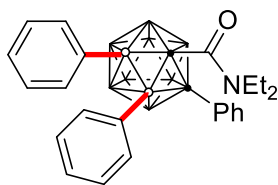
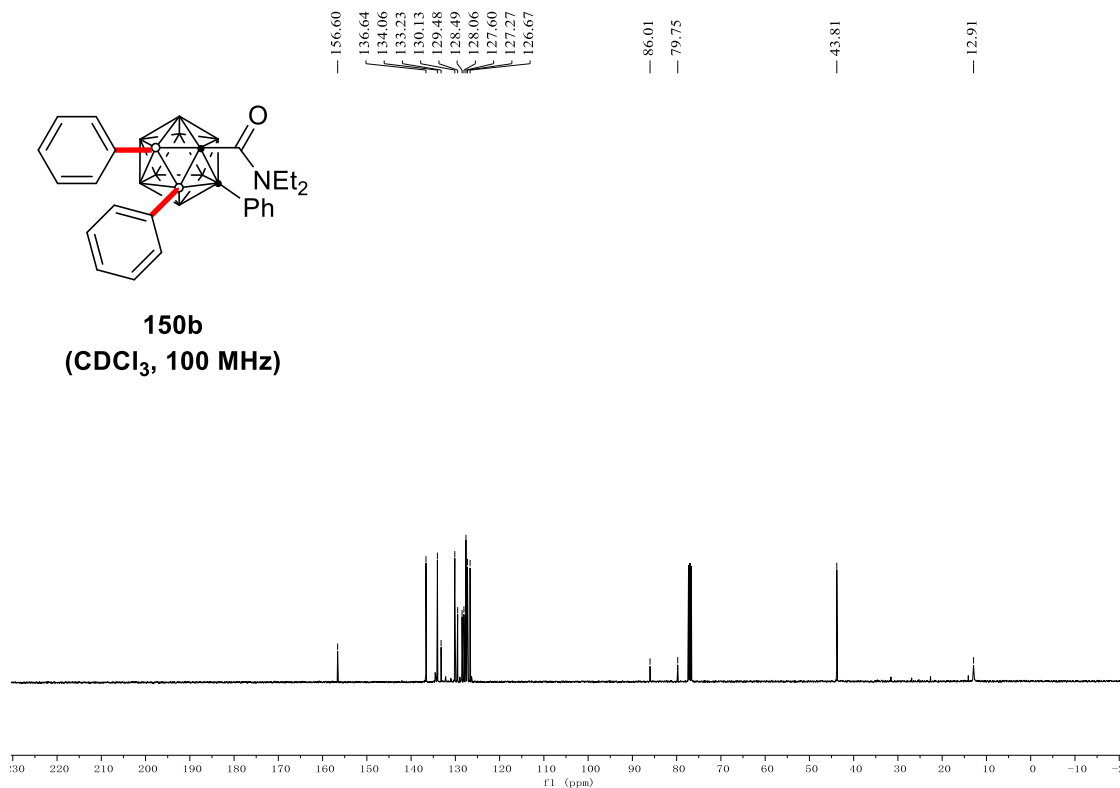
NMR Spectra



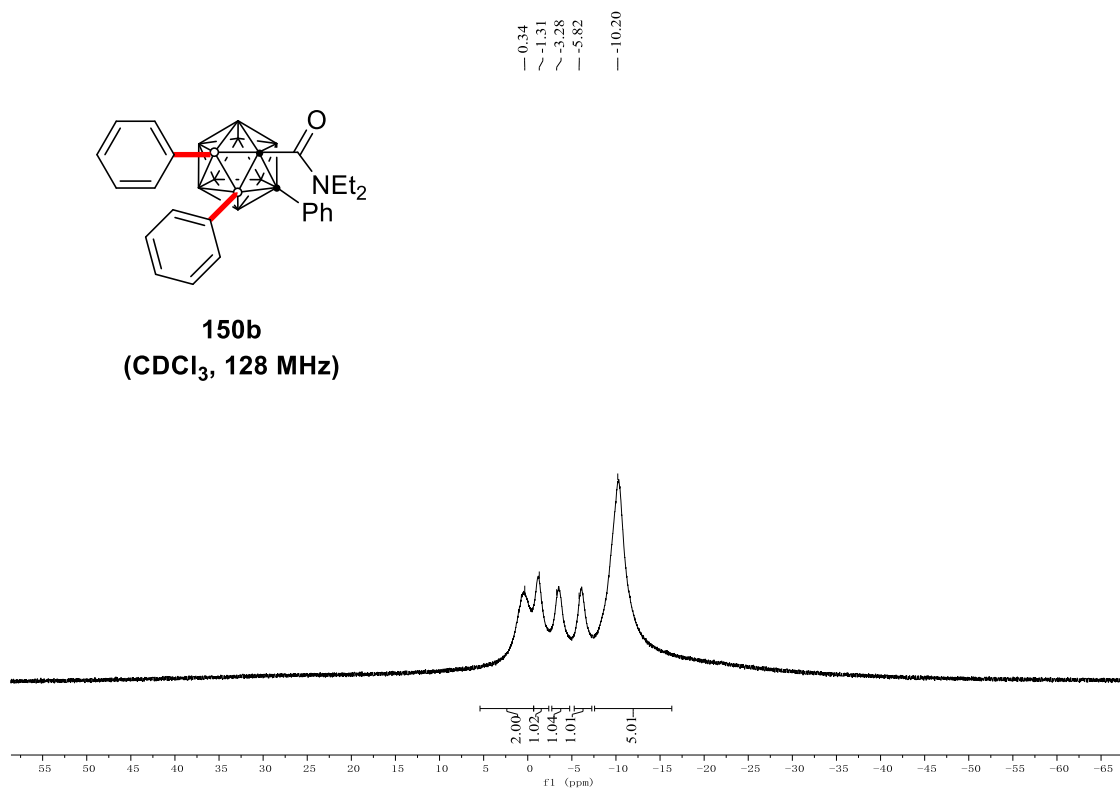
NMR Spectra



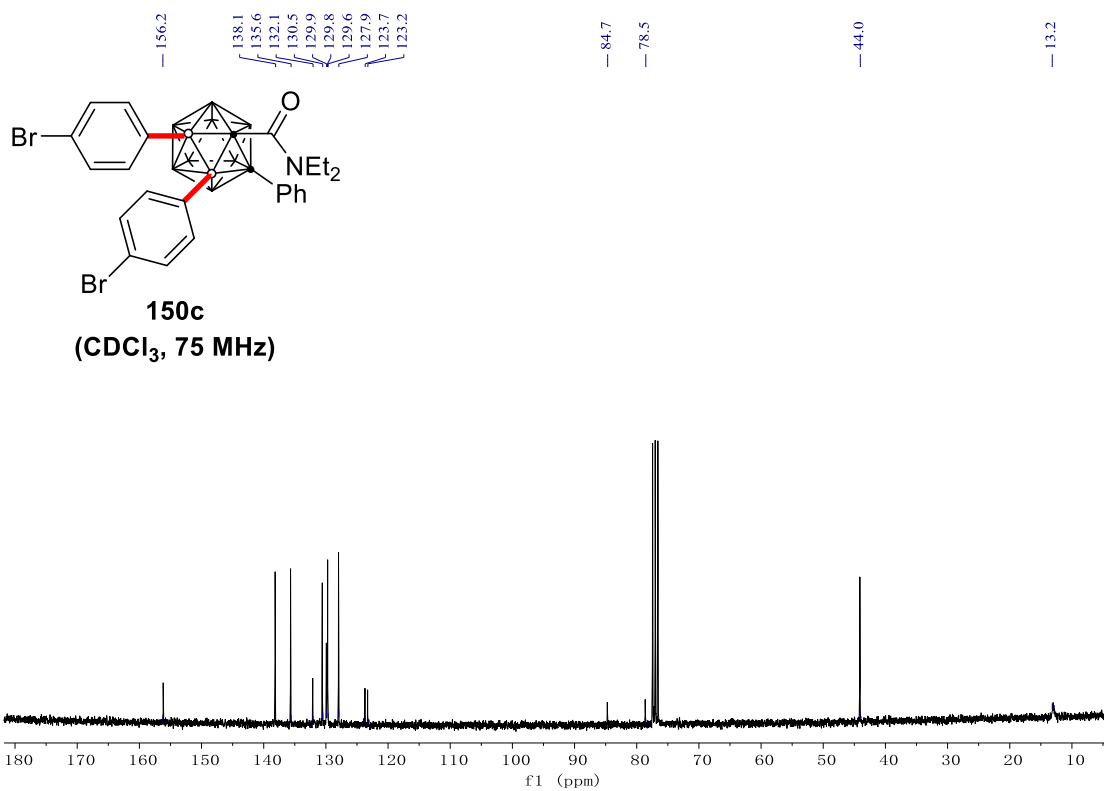
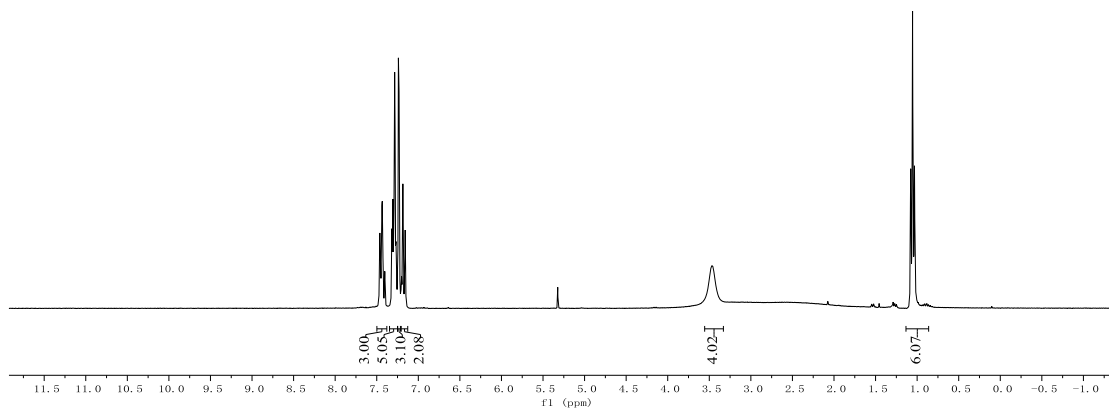
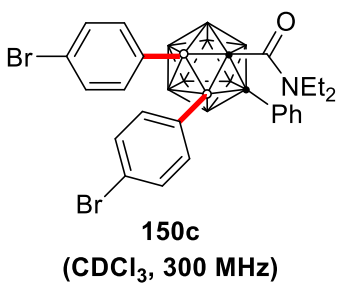
150b
(CDCl₃, 100 MHz)



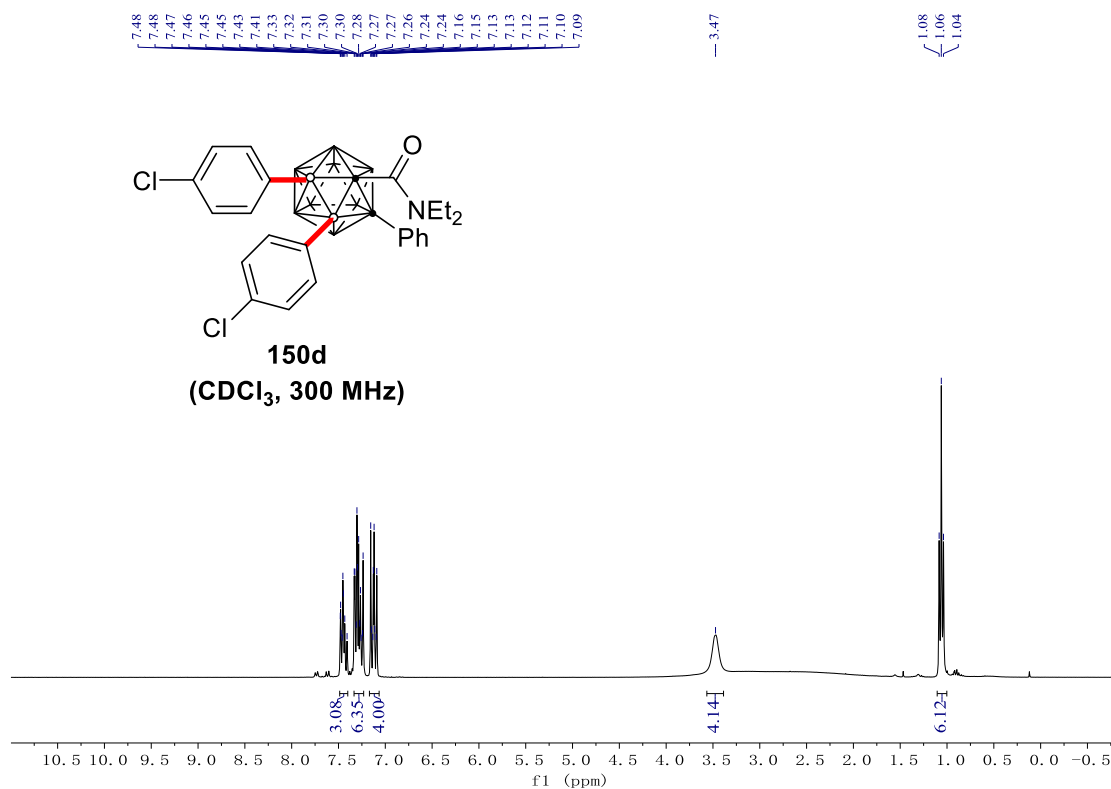
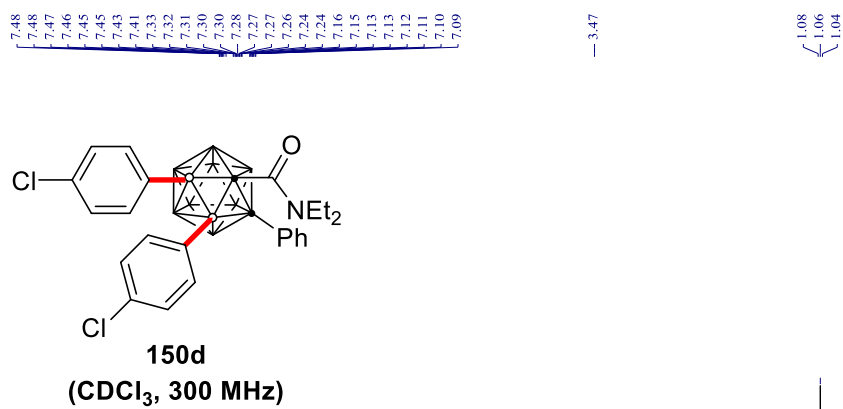
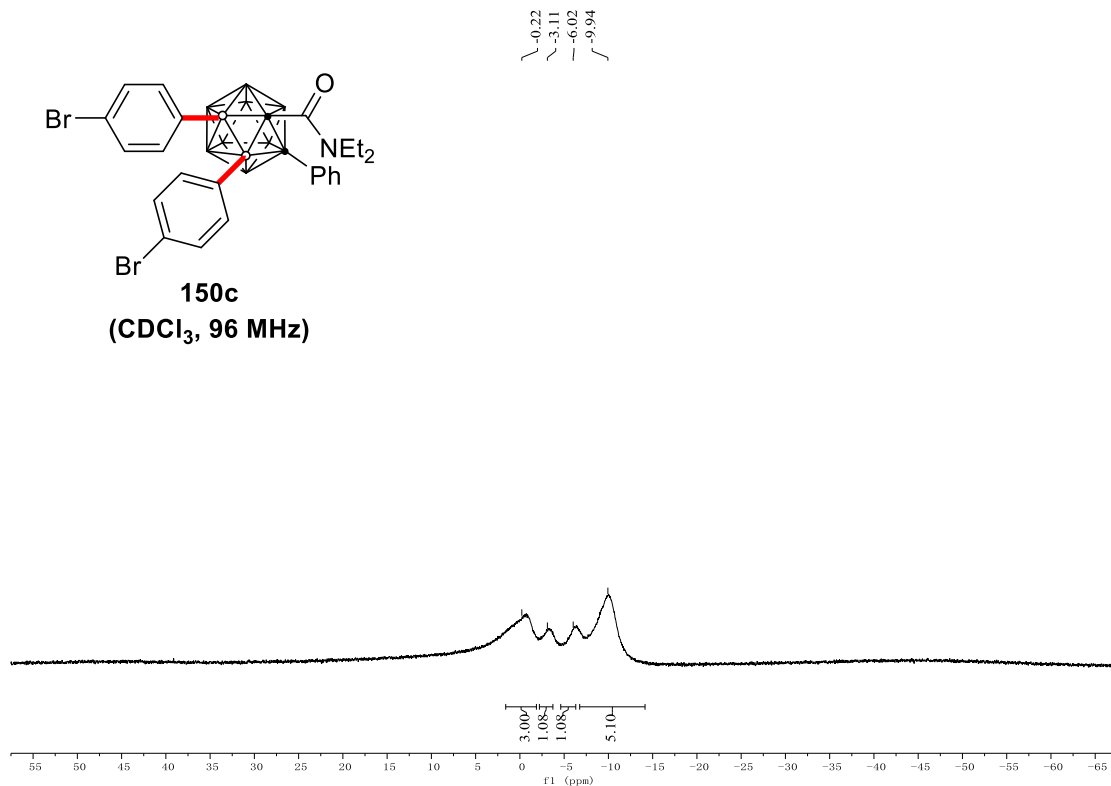
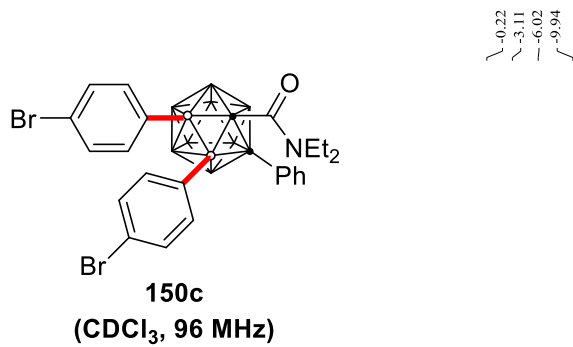
150b
(CDCl₃, 128 MHz)



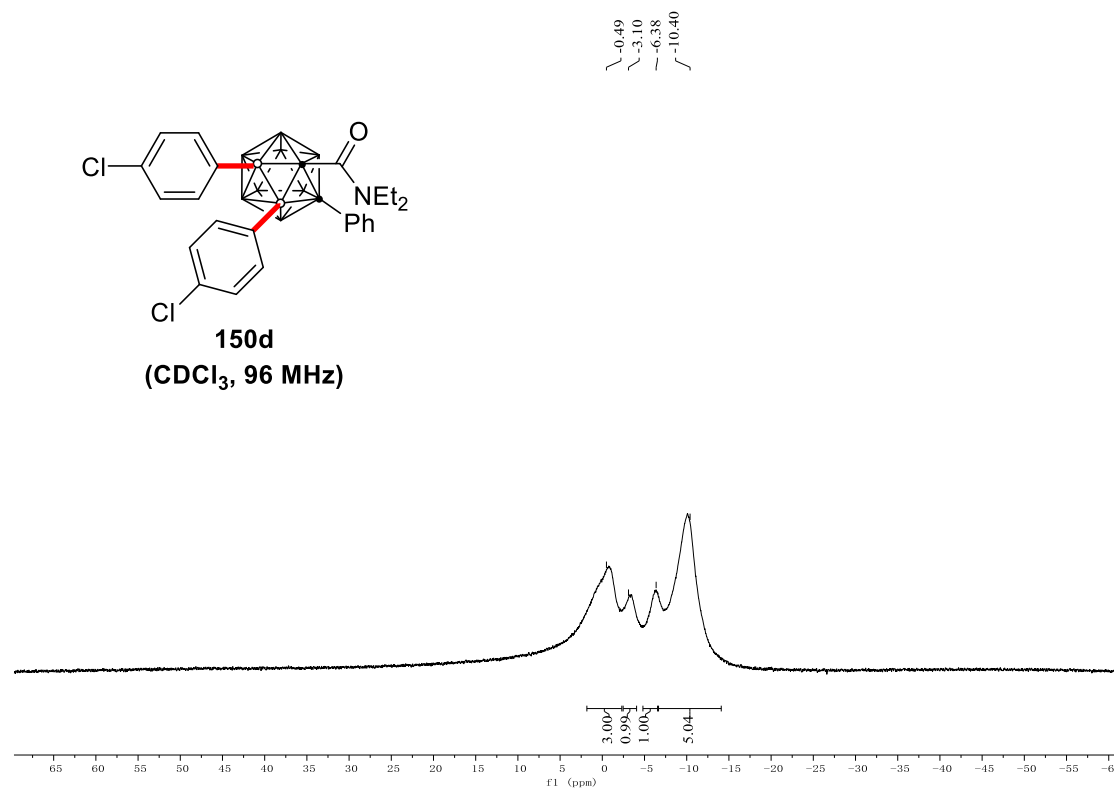
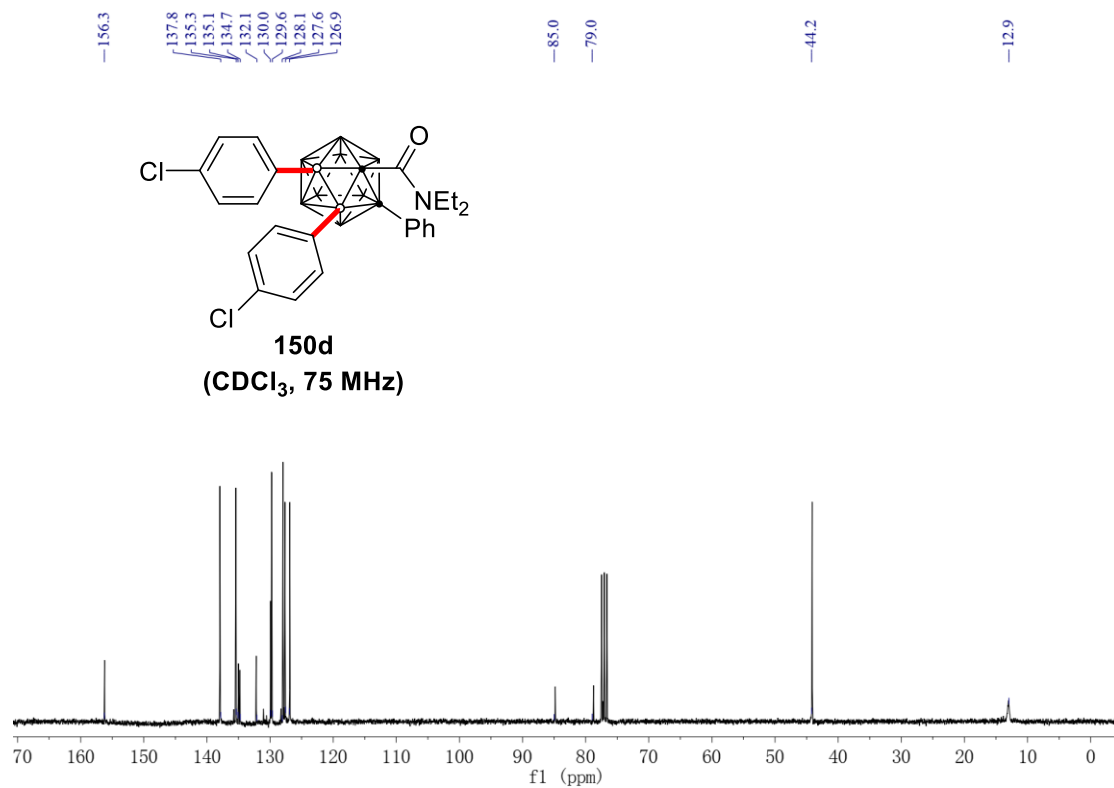
NMR Spectra



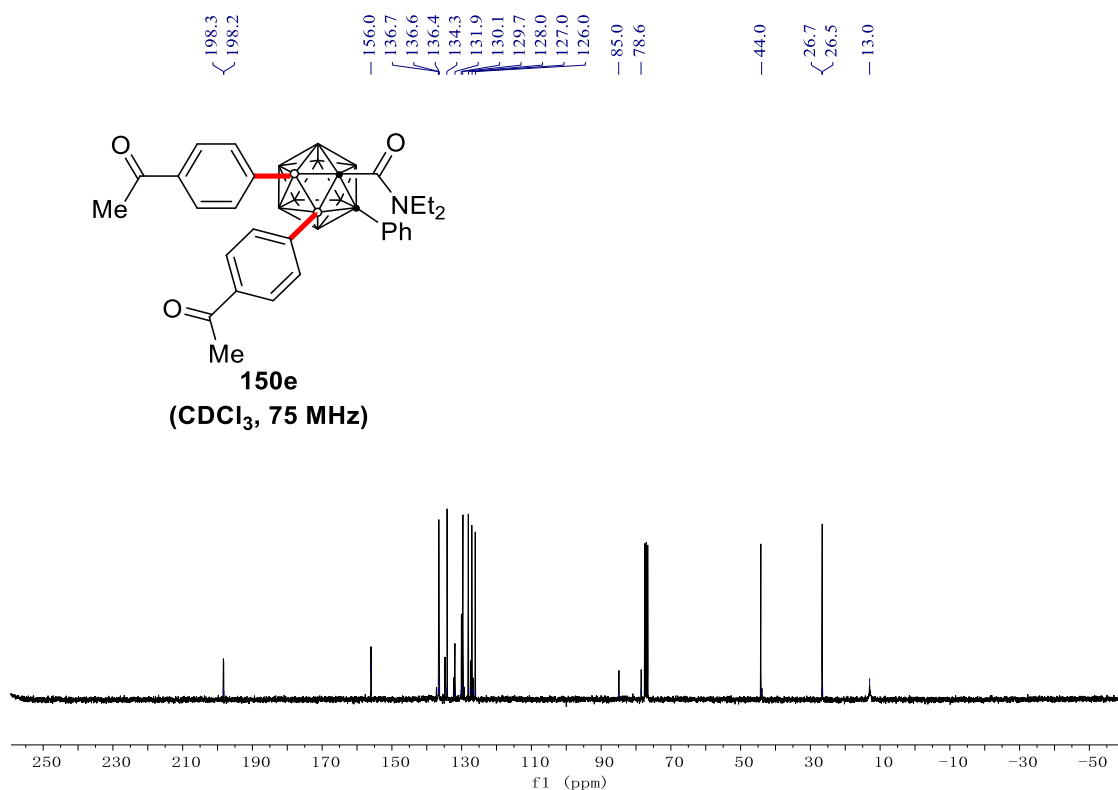
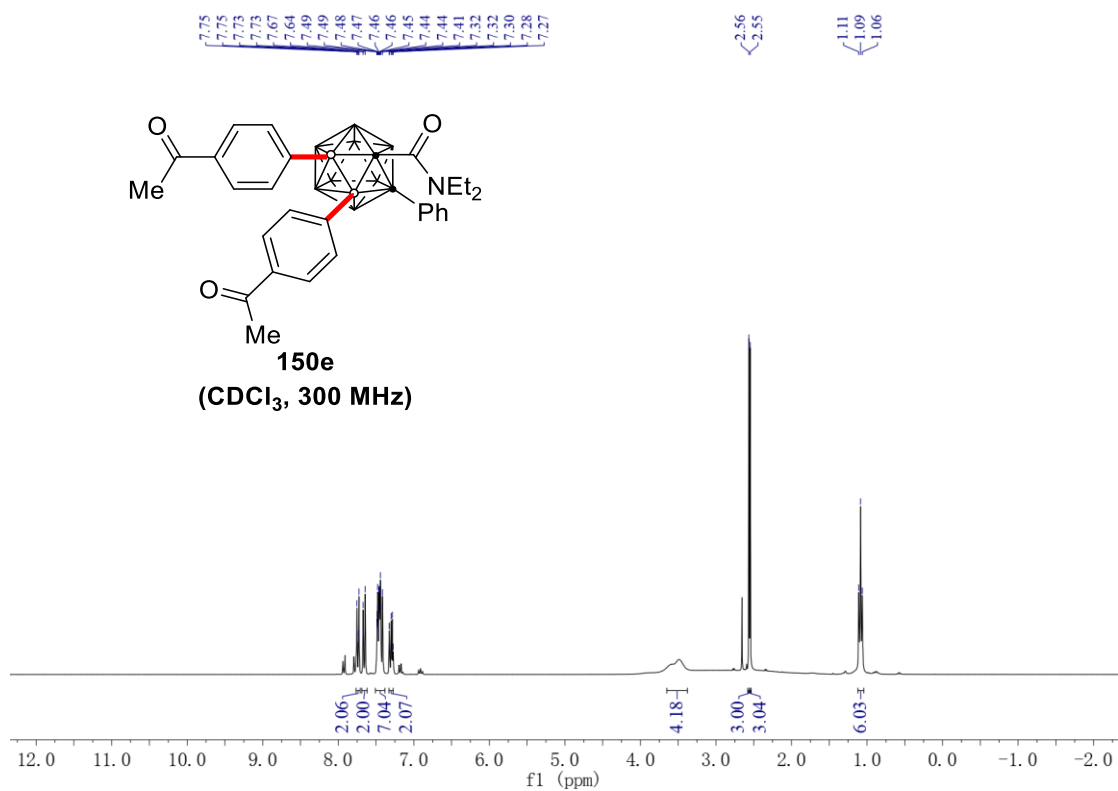
NMR Spectra



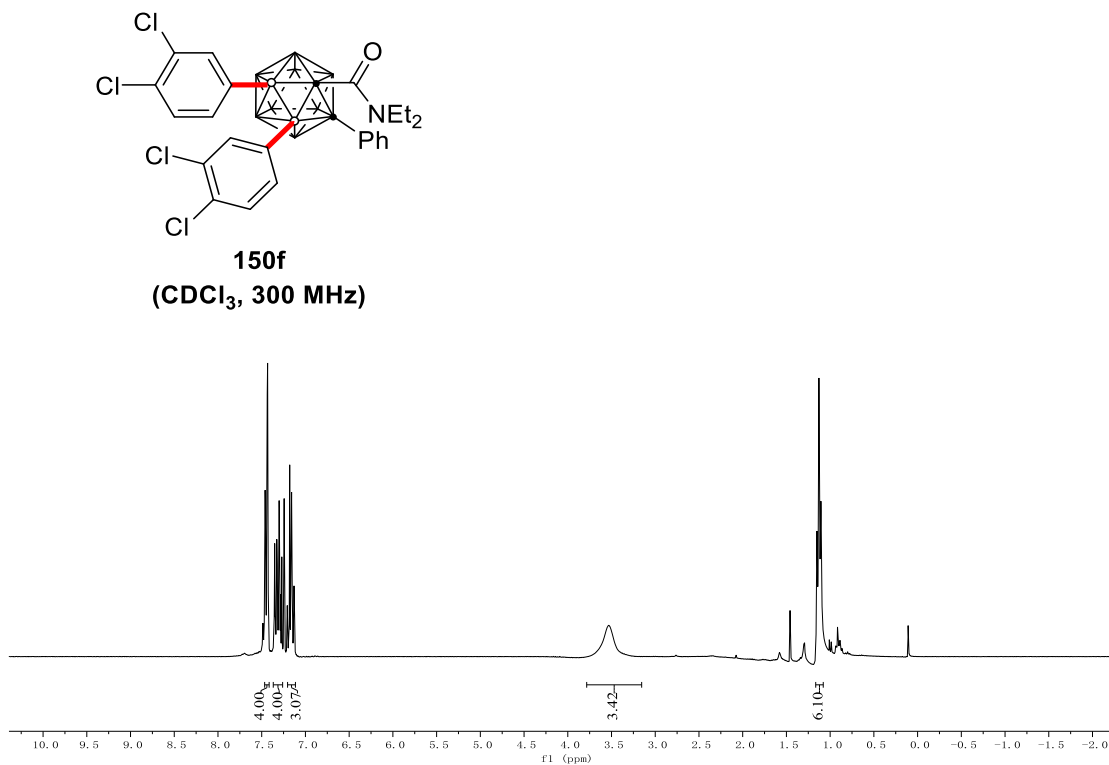
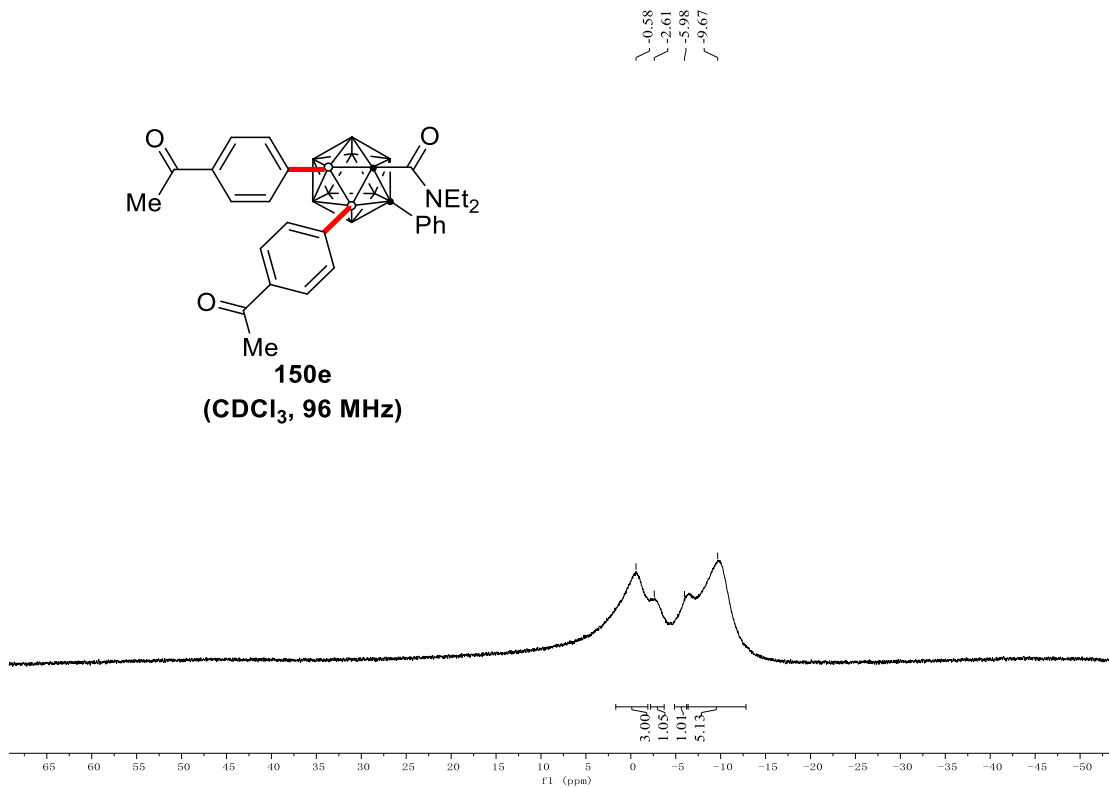
NMR Spectra



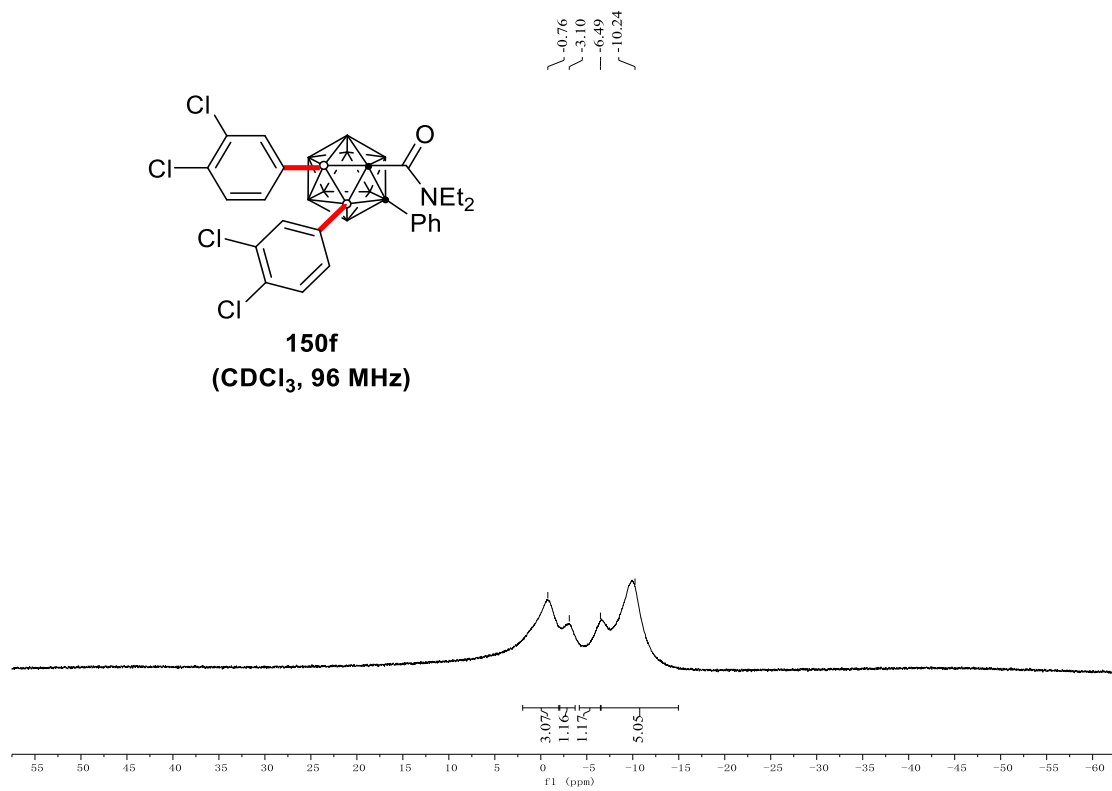
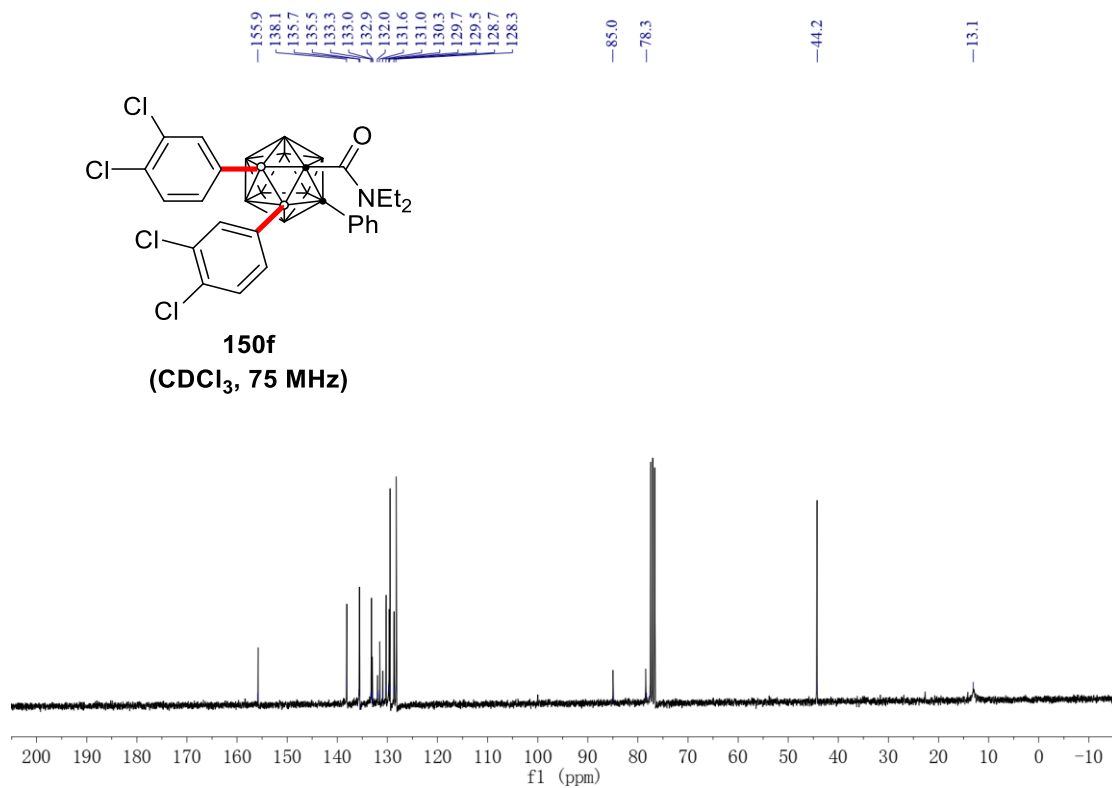
NMR Spectra



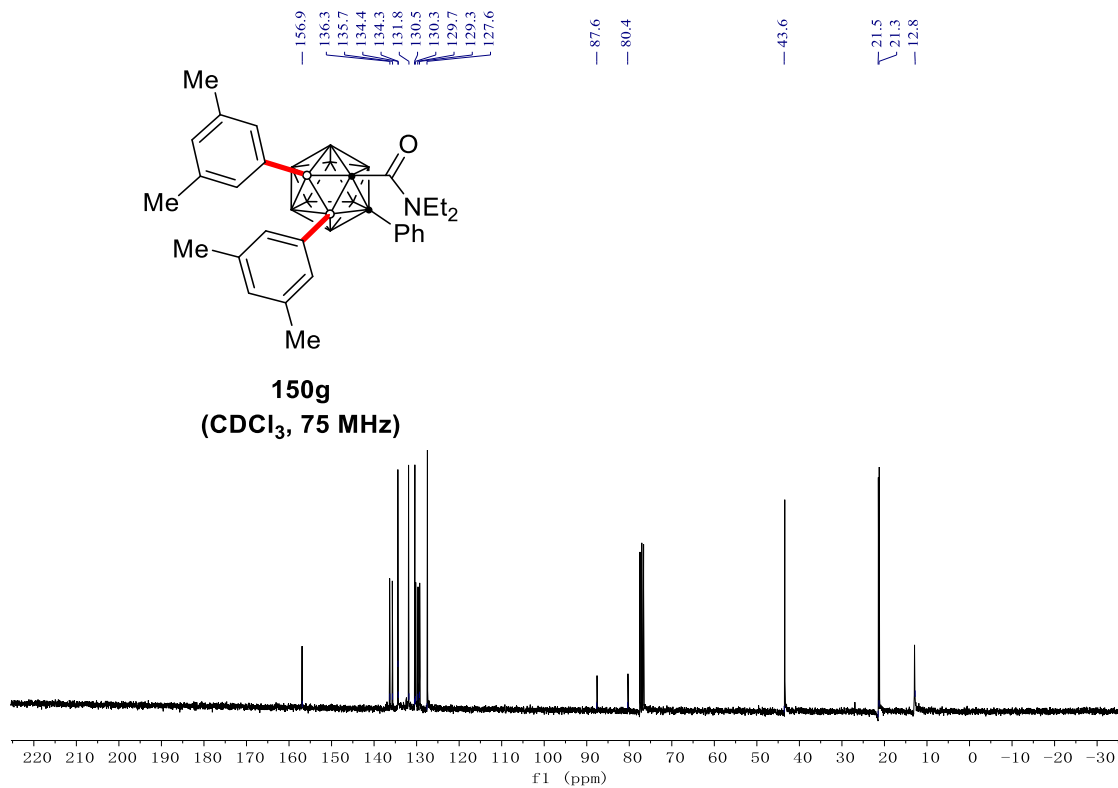
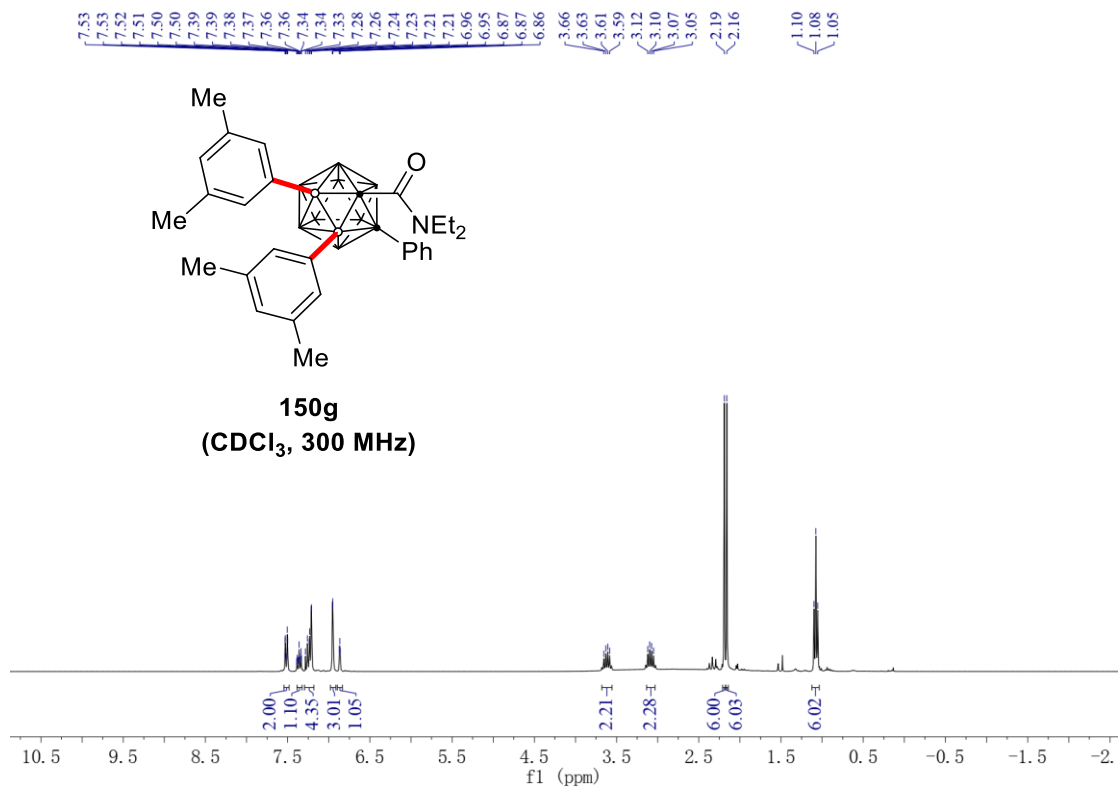
NMR Spectra



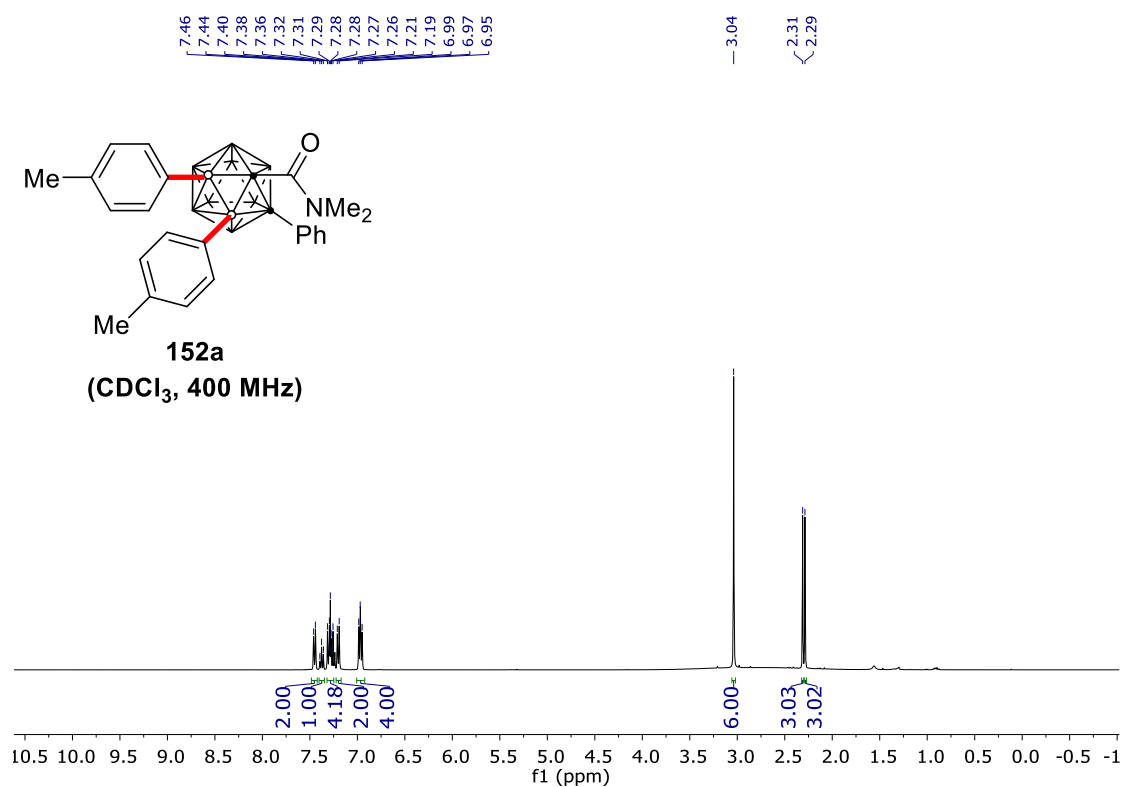
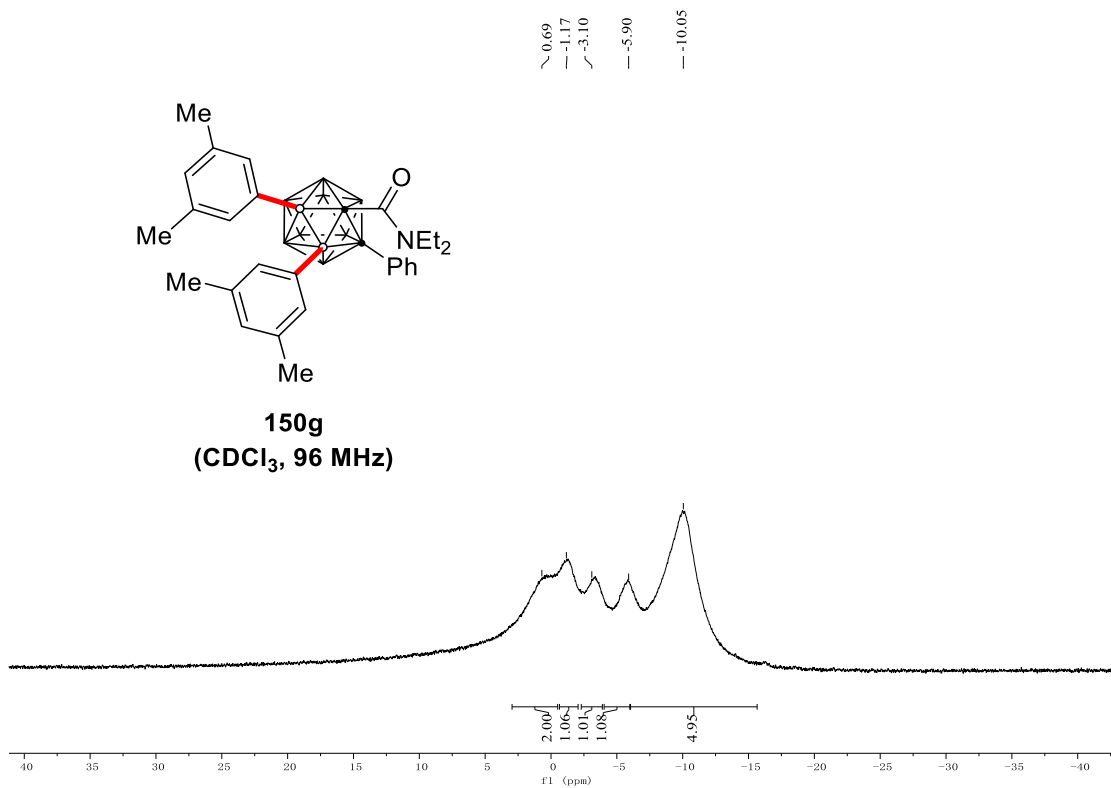
NMR Spectra



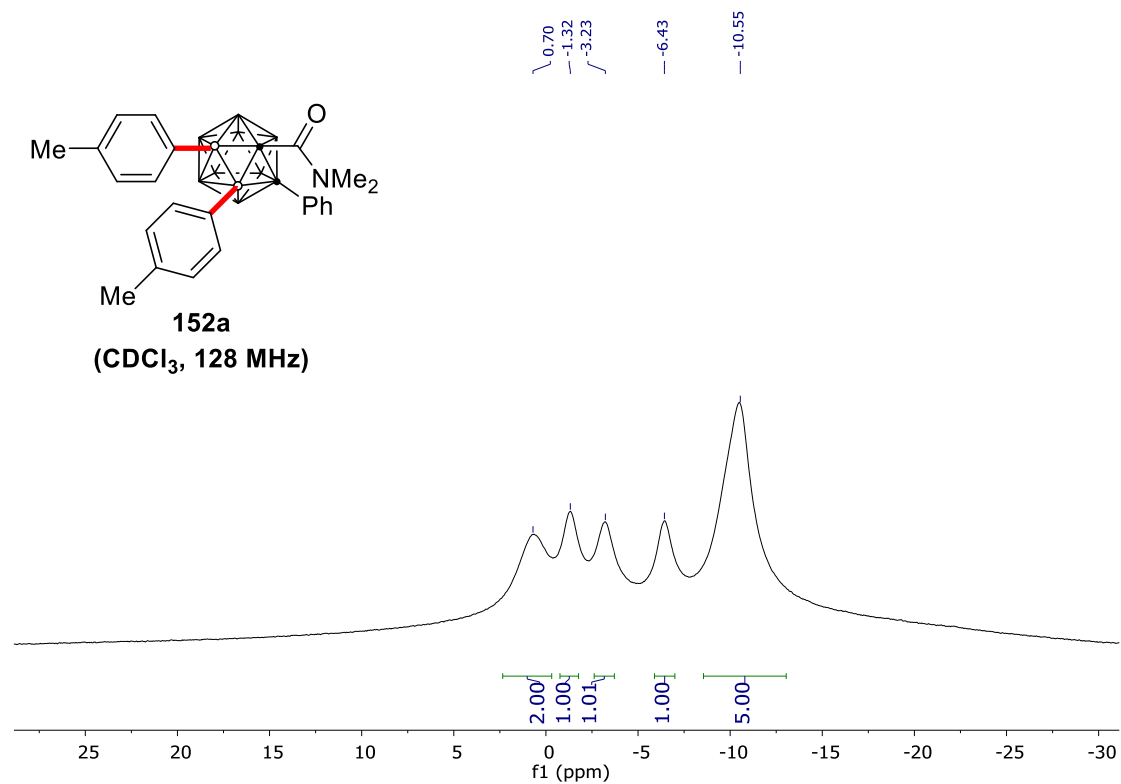
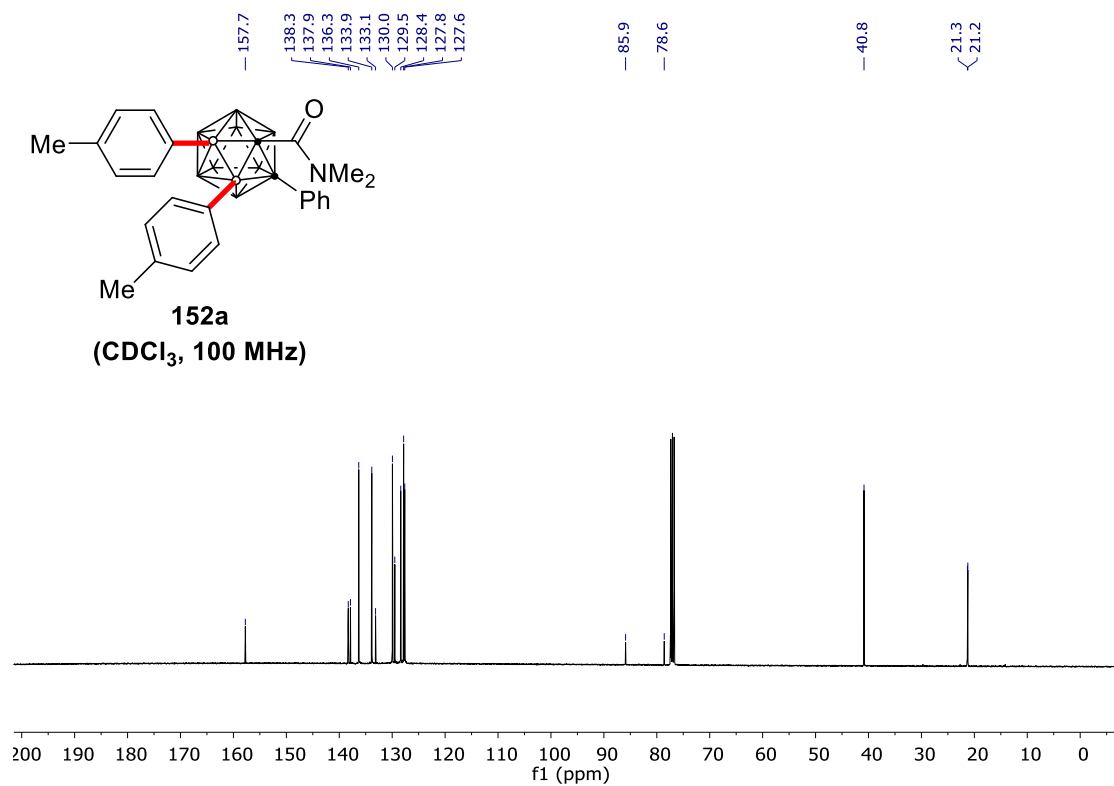
NMR Spectra



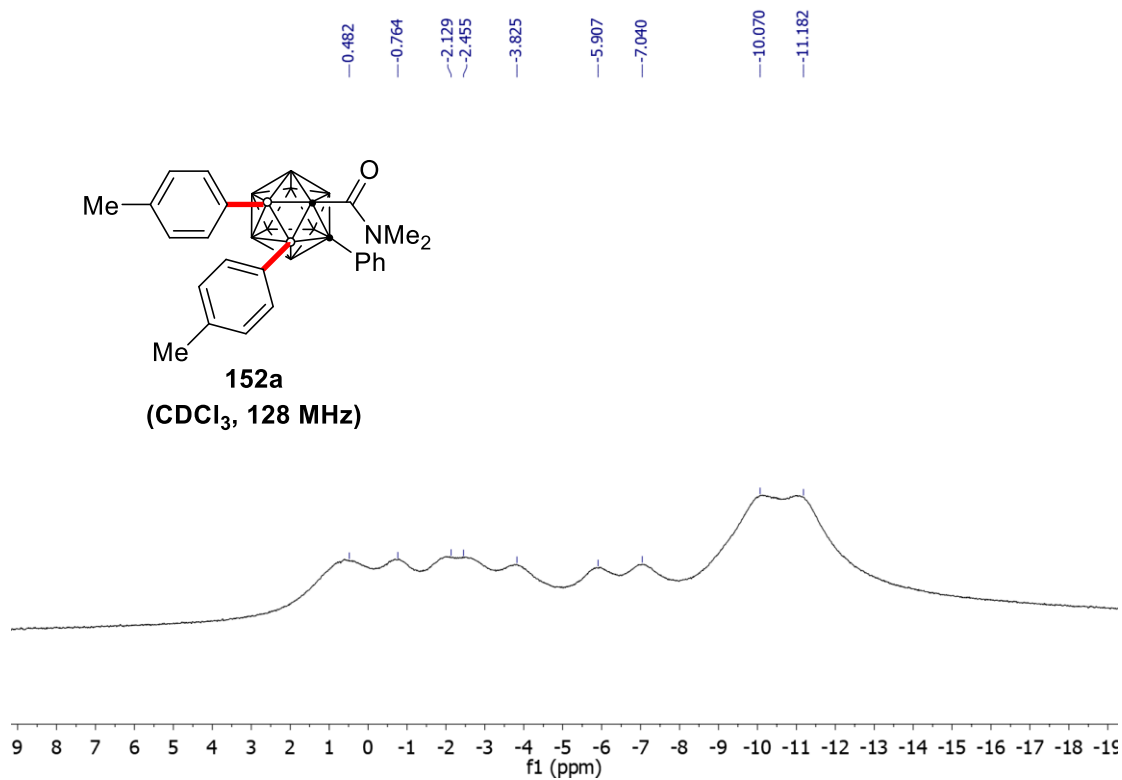
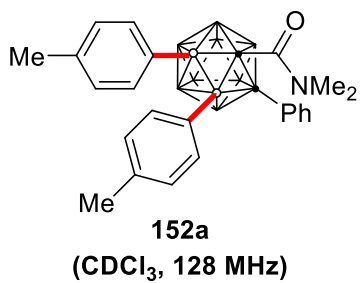
NMR Spectra



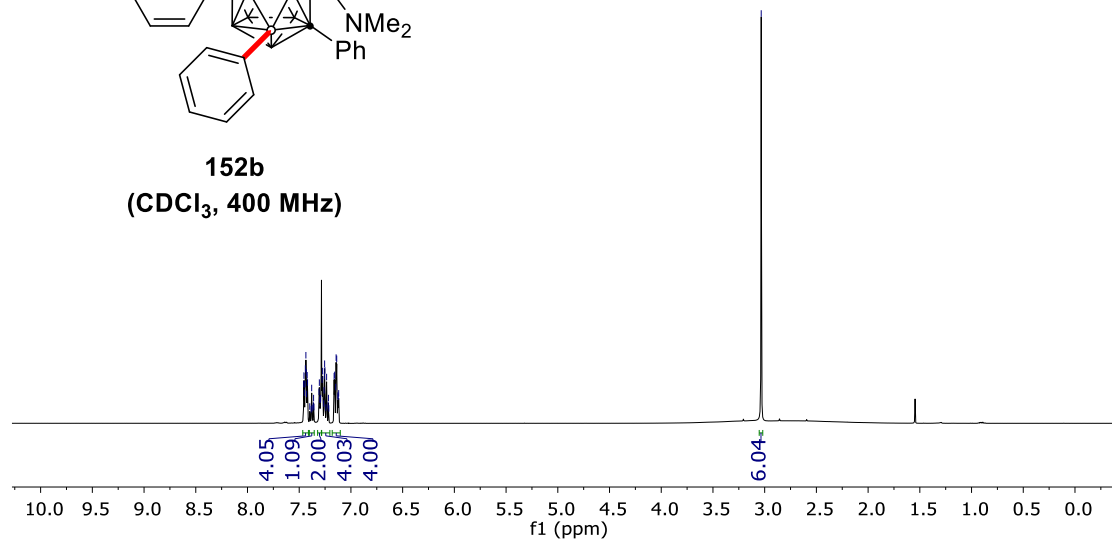
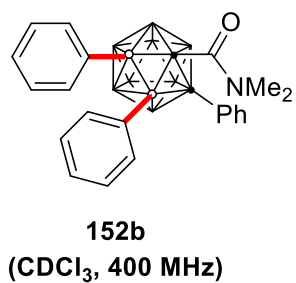
NMR Spectra



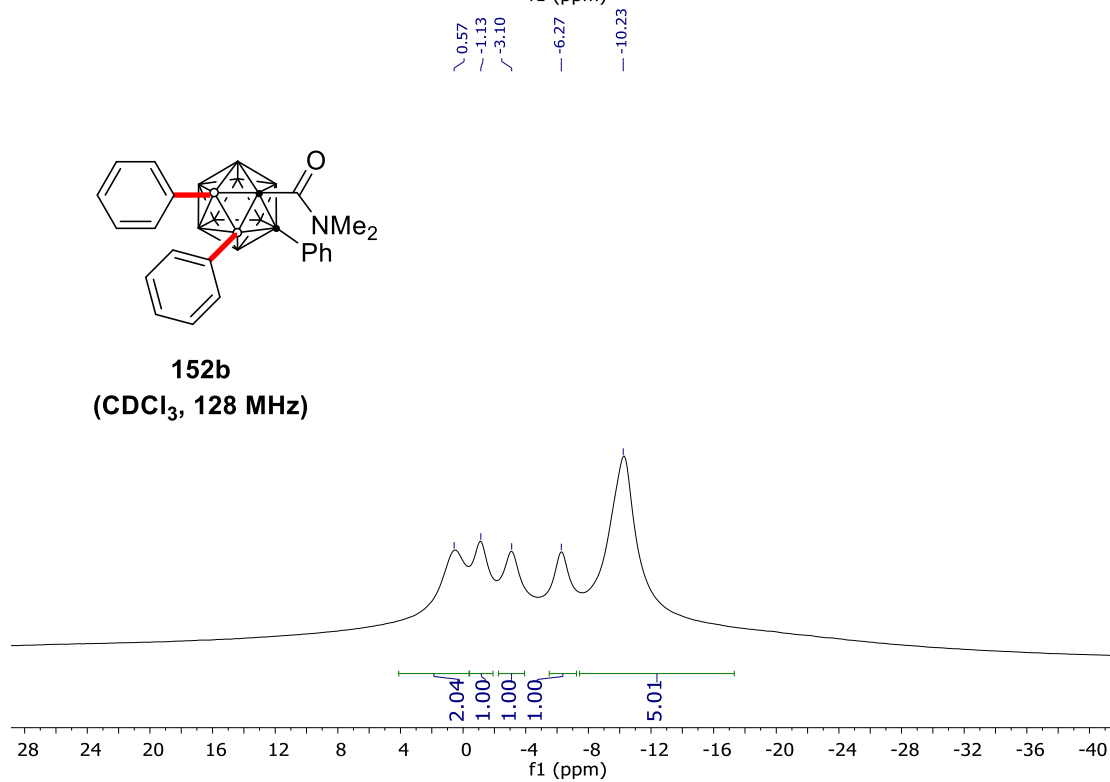
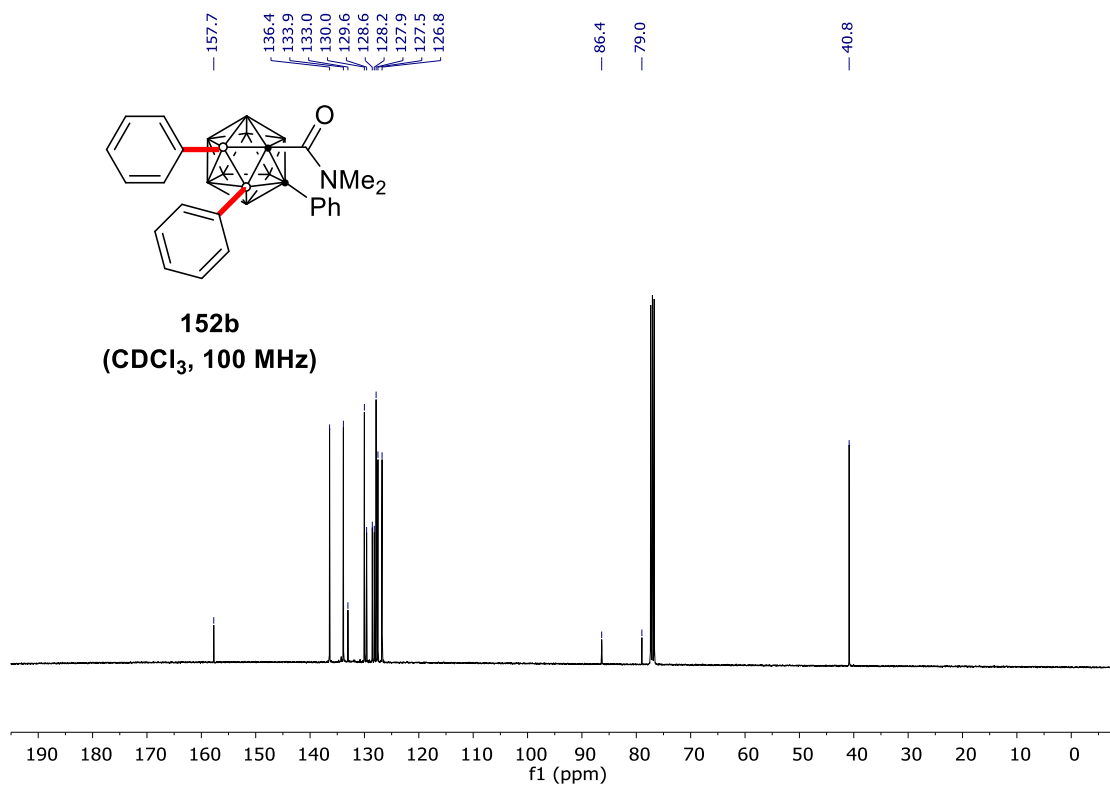
NMR Spectra



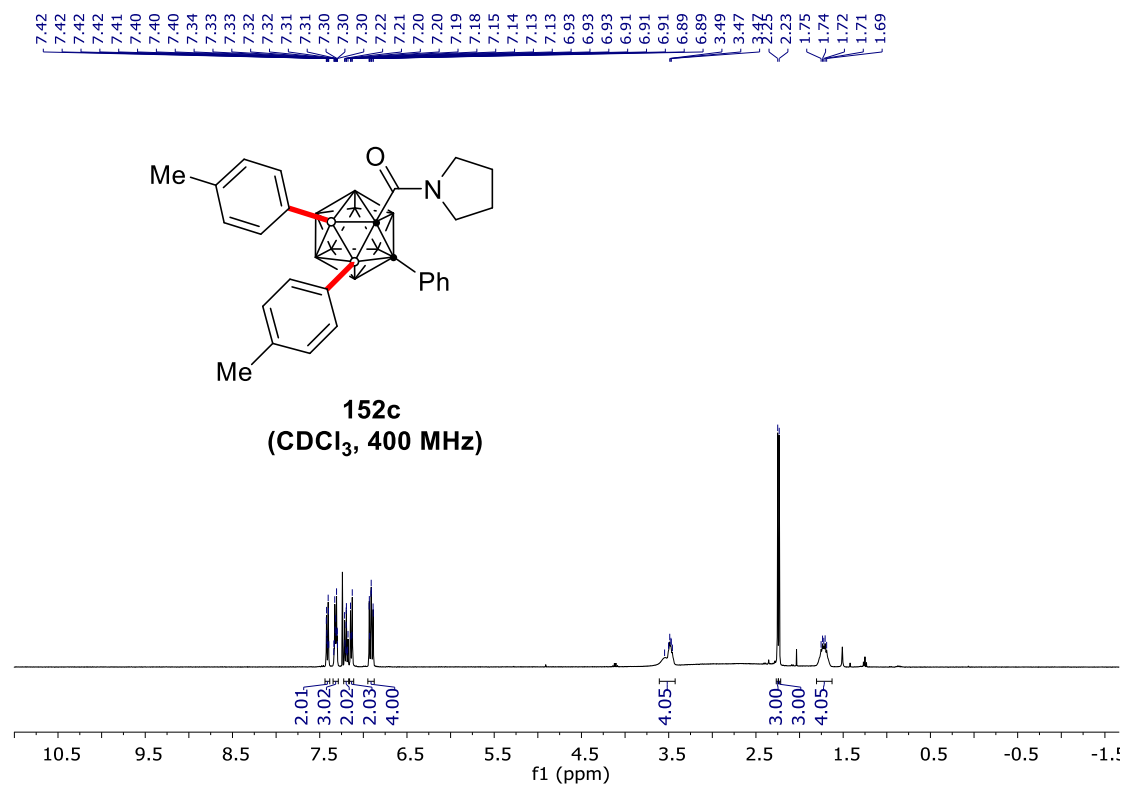
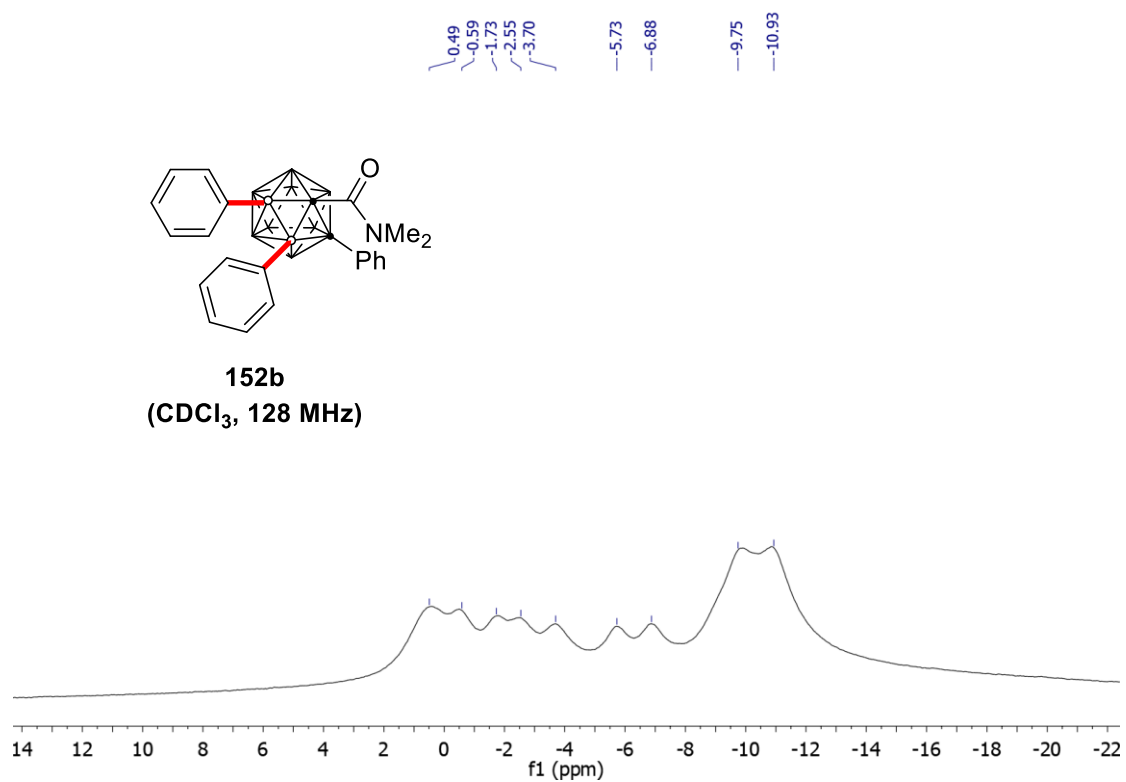
7.46, 7.45, 7.45, 7.44, 7.44, 7.44, 7.43, 7.43, 7.42, 7.42, 7.40, 7.38, 7.38, 7.38, 7.36, 7.36, 7.36, 7.31, 7.31, 7.30, 7.30, 7.29, 7.28, 7.27, 7.26, 7.26, 7.26, 7.25, 7.25, 7.24, 7.24, 7.22, 7.22, 7.21, 7.16, 7.16, 7.15, 7.14, 7.14, 7.13, 7.12, 7.12, 3.03



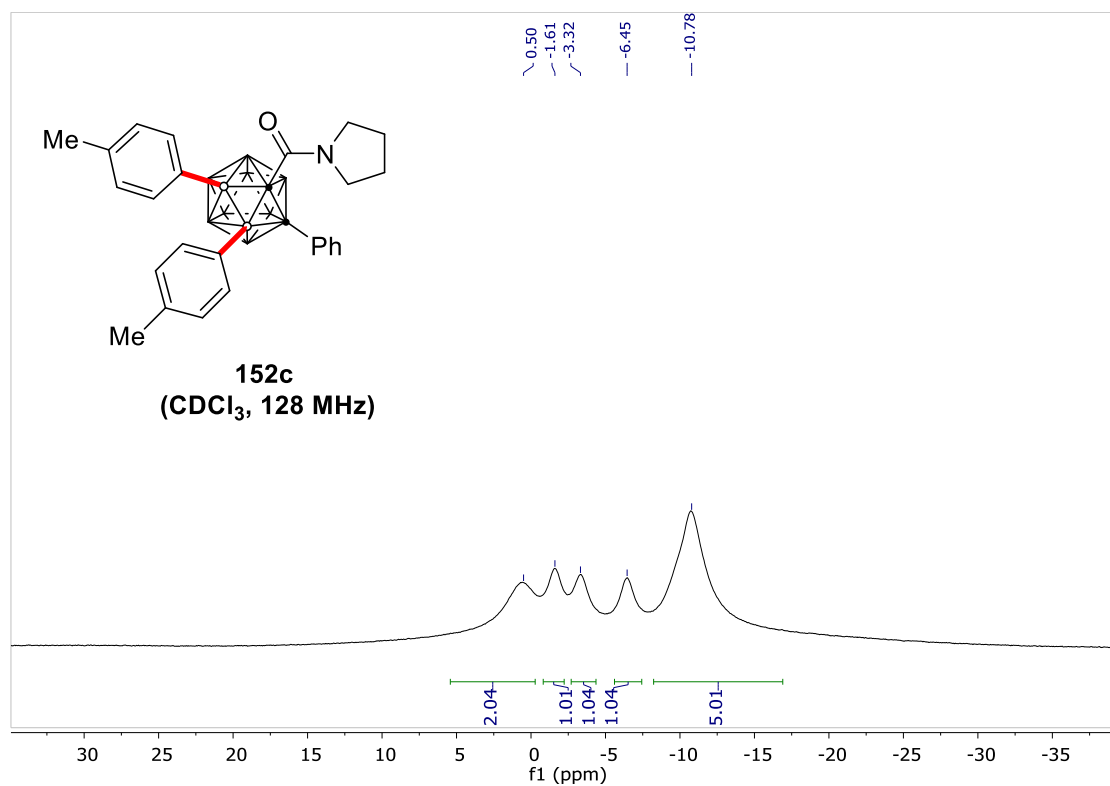
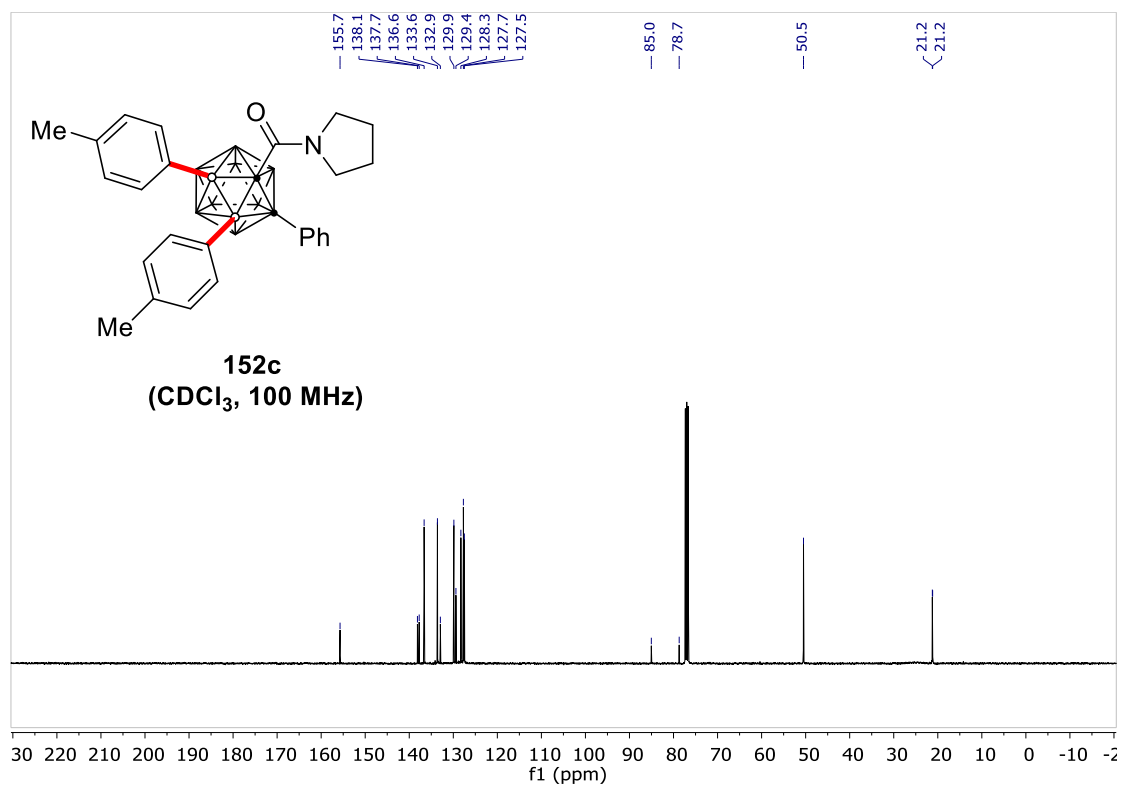
NMR Spectra



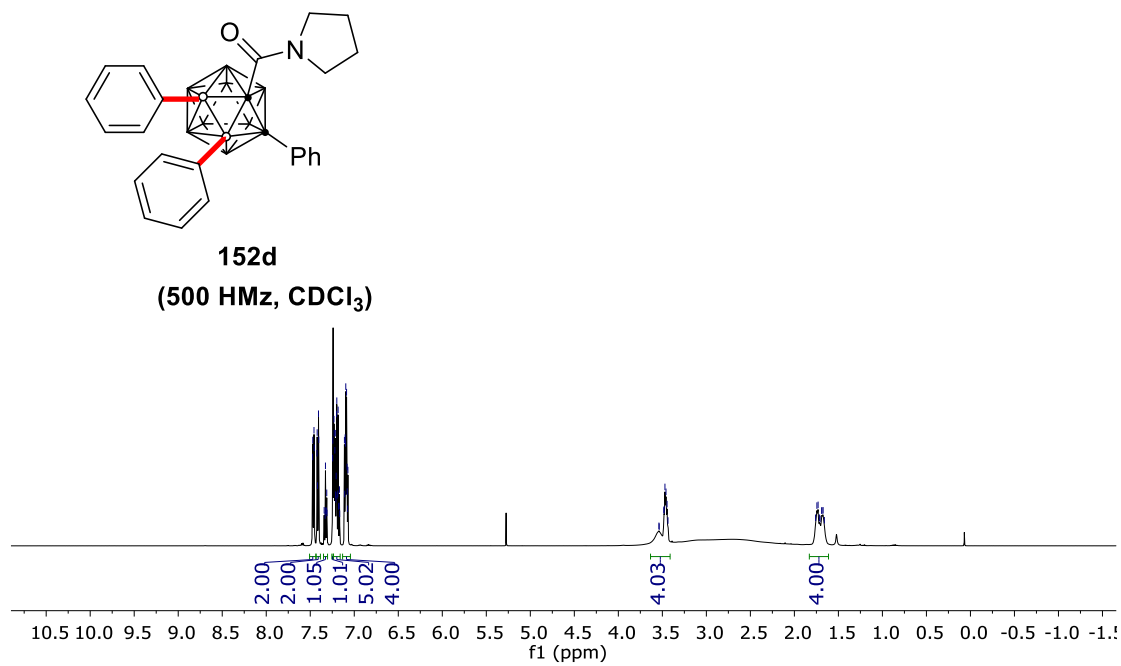
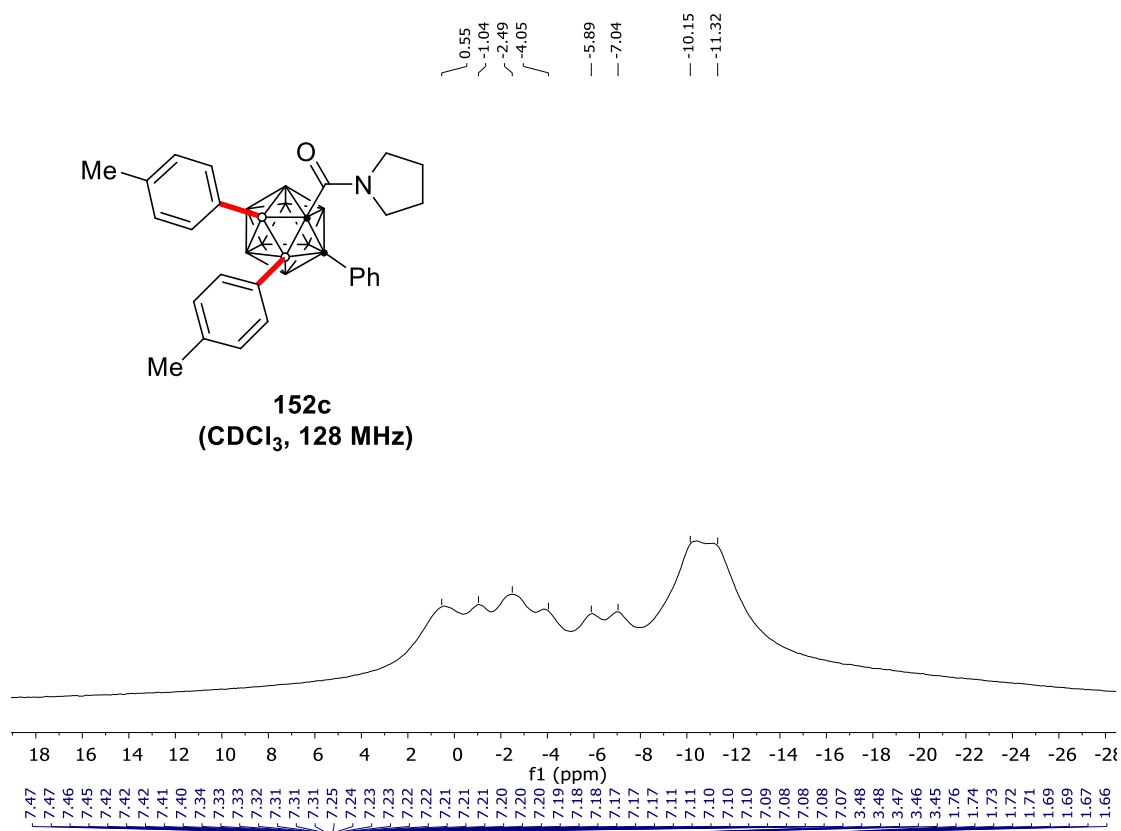
NMR Spectra



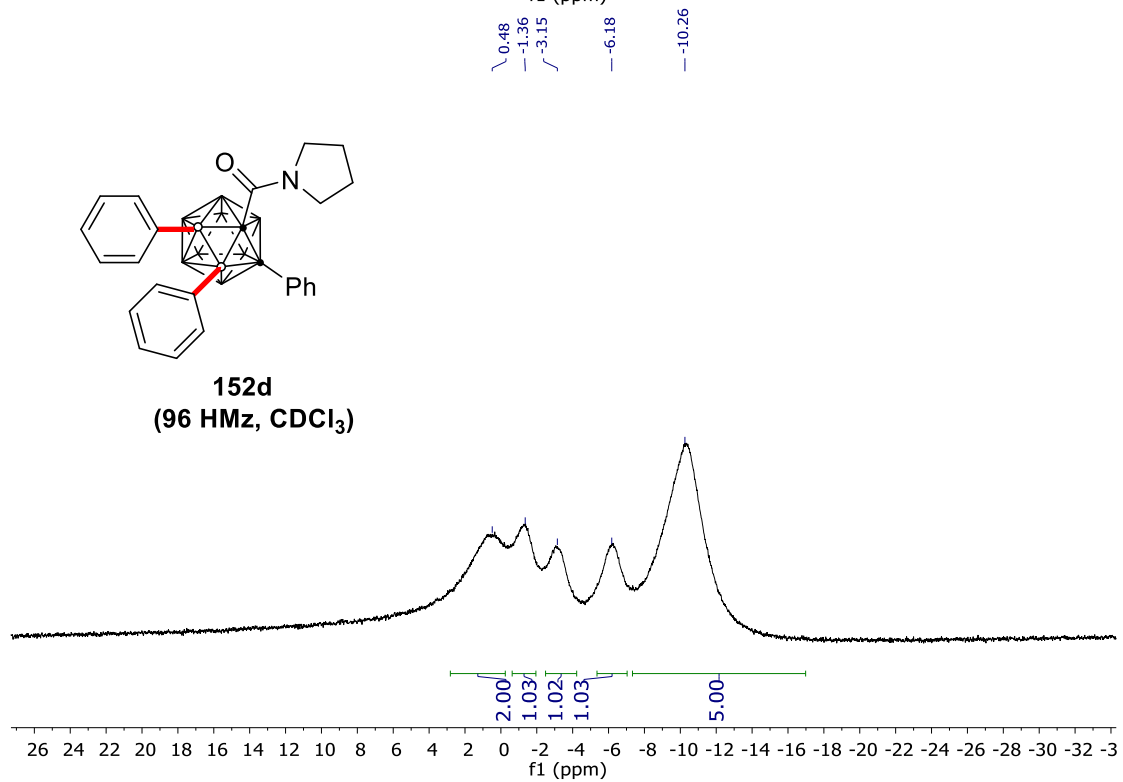
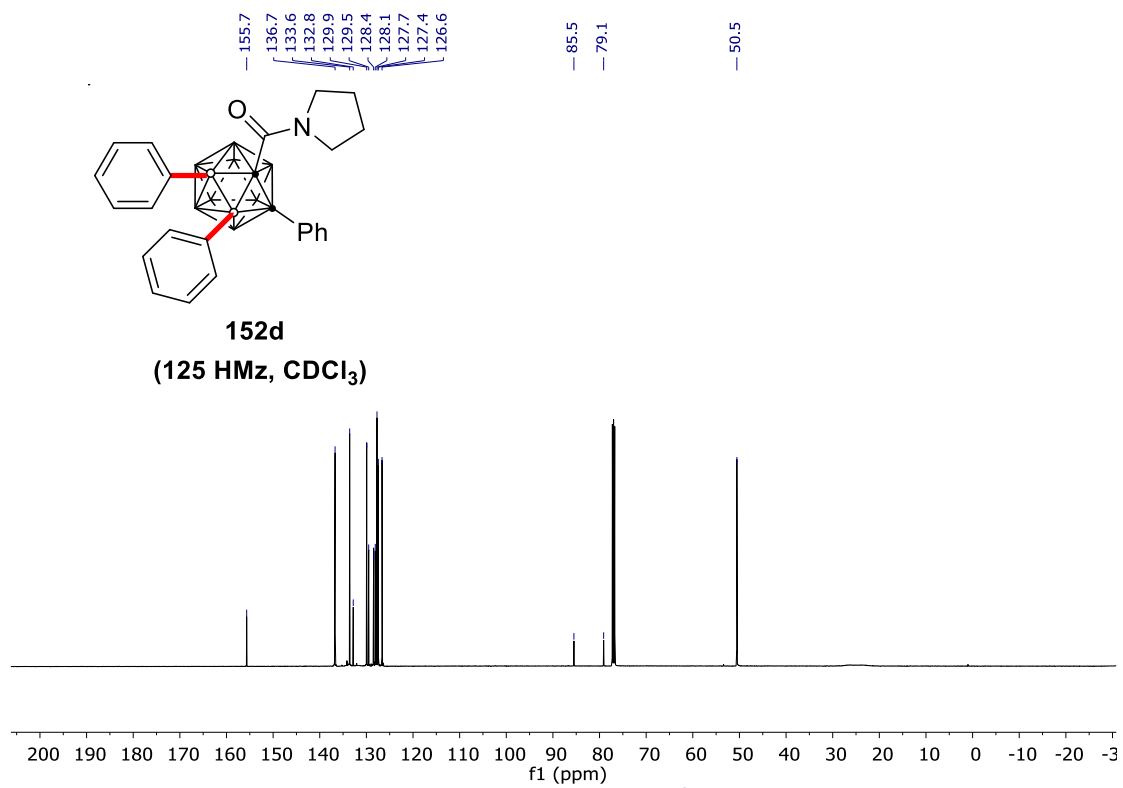
NMR Spectra



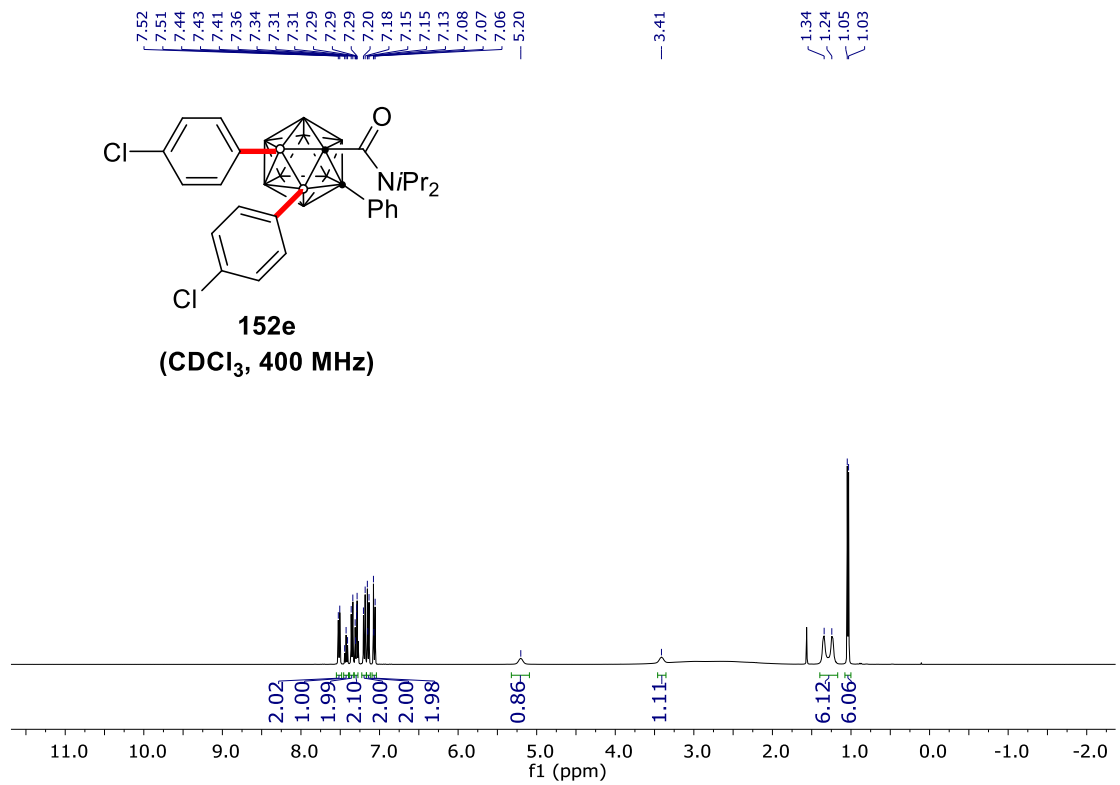
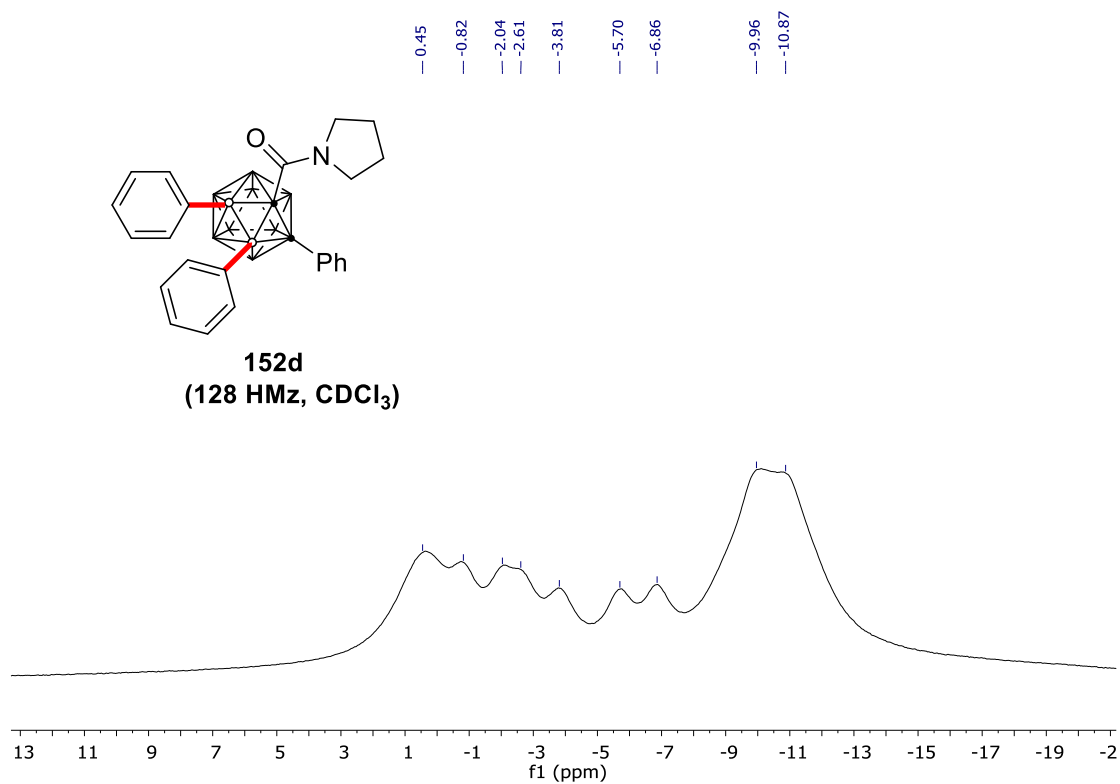
NMR Spectra



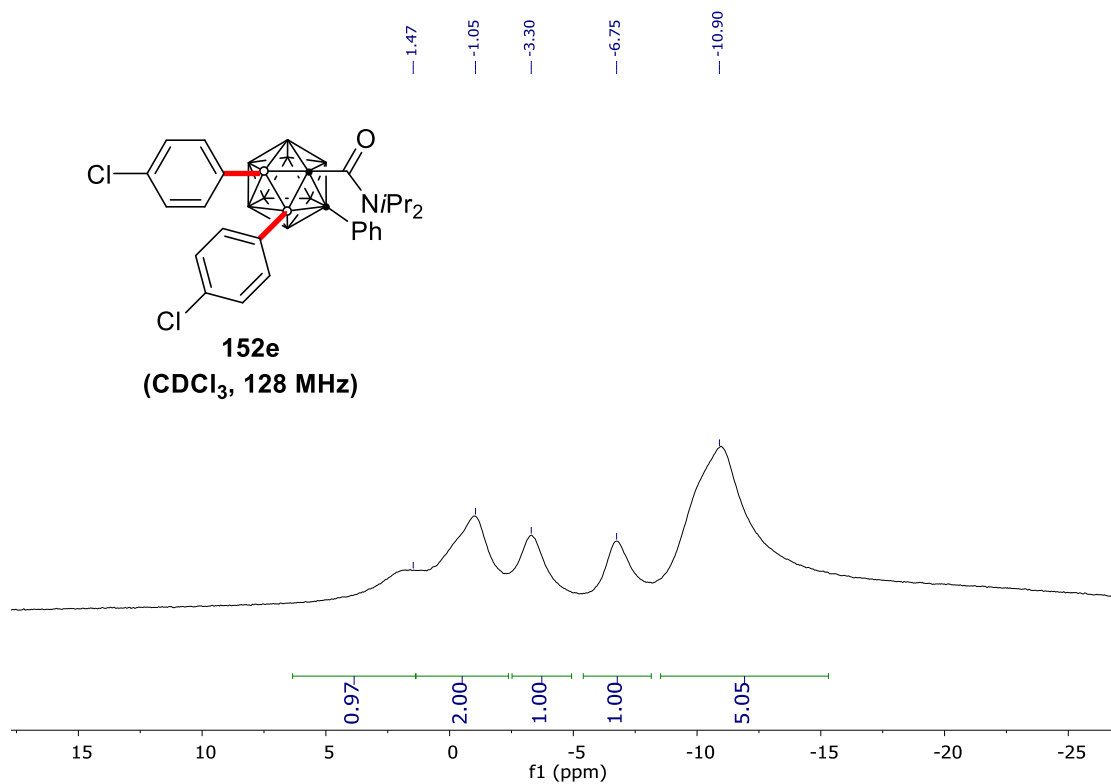
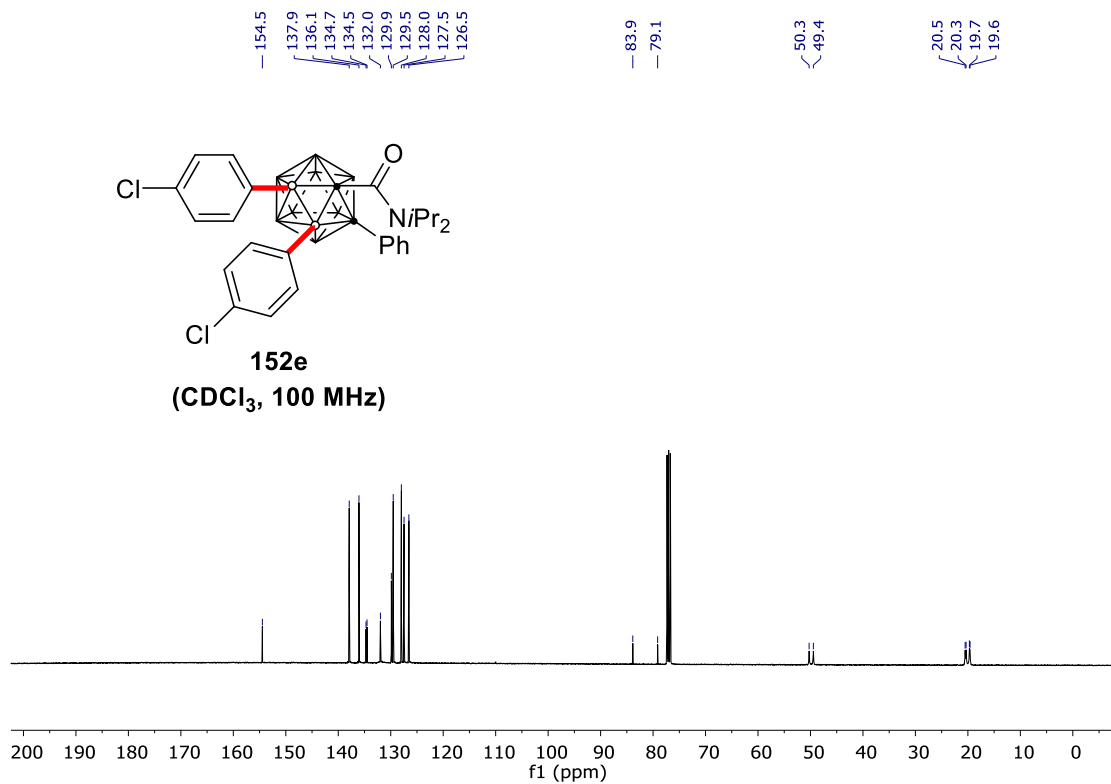
NMR Spectra



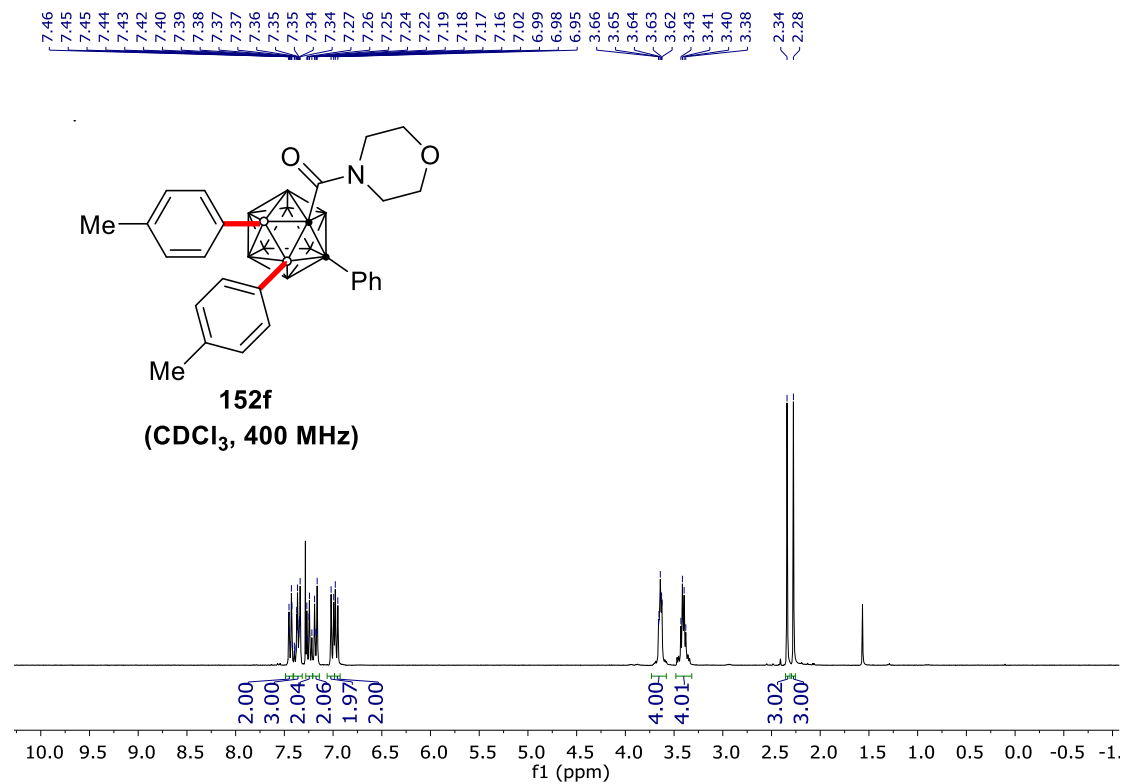
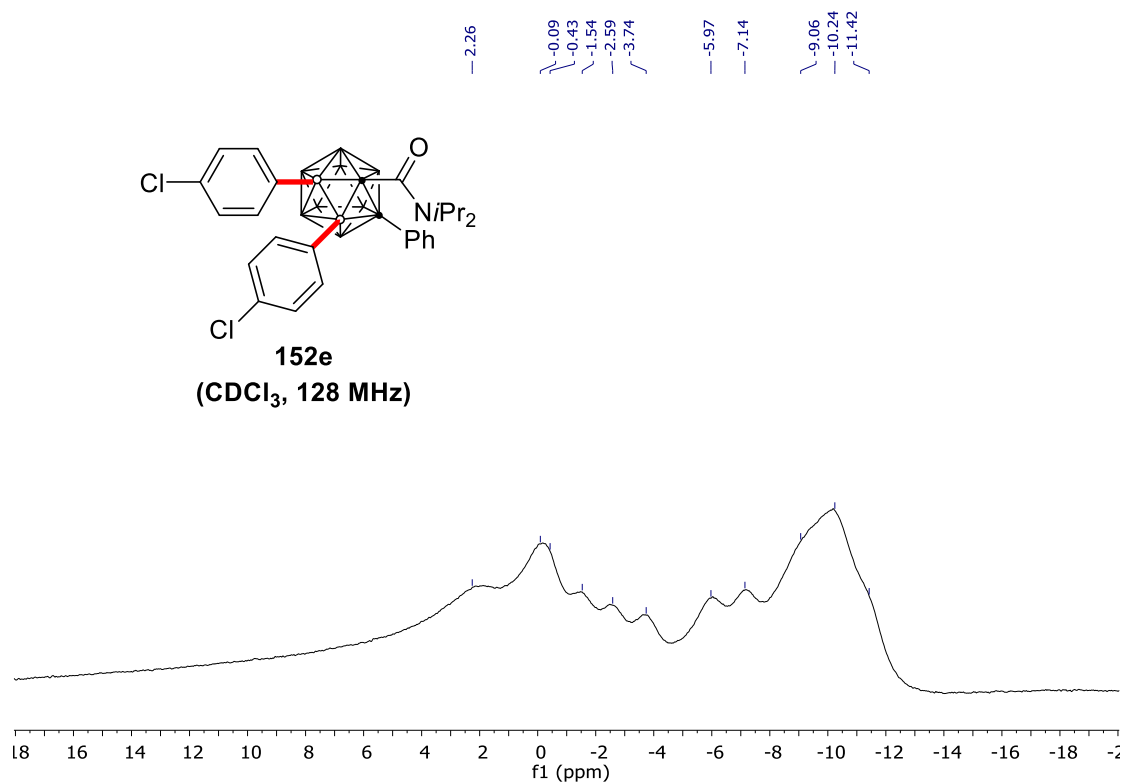
NMR Spectra



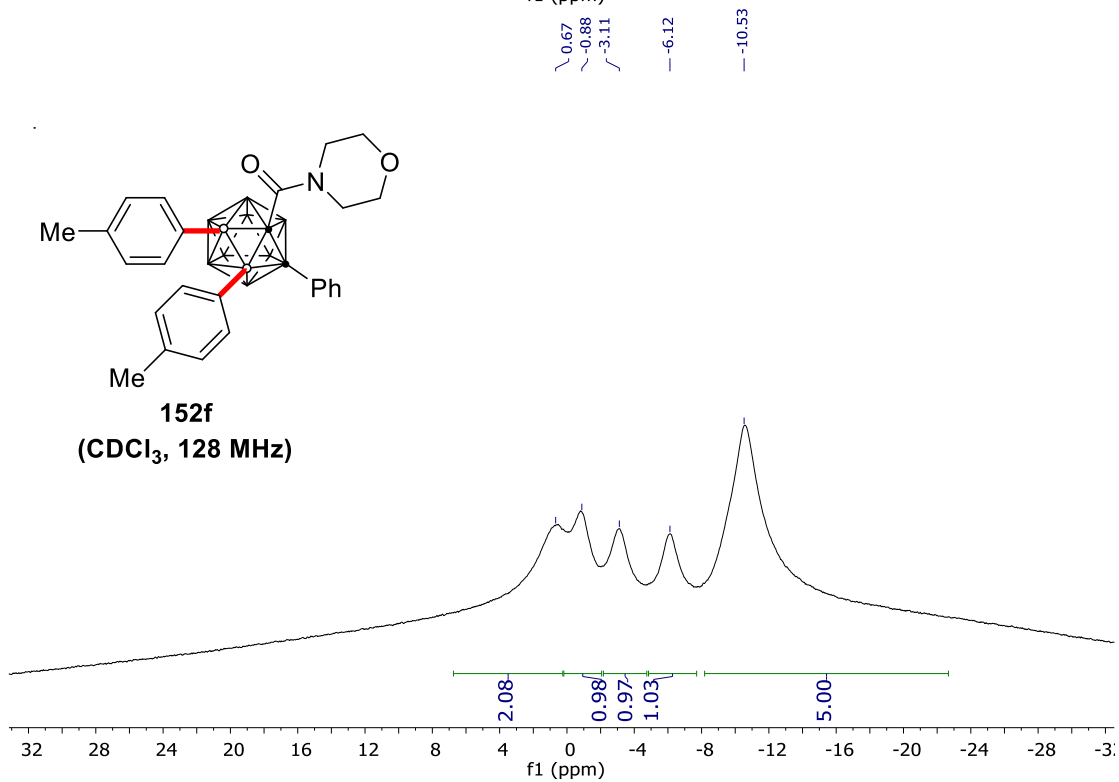
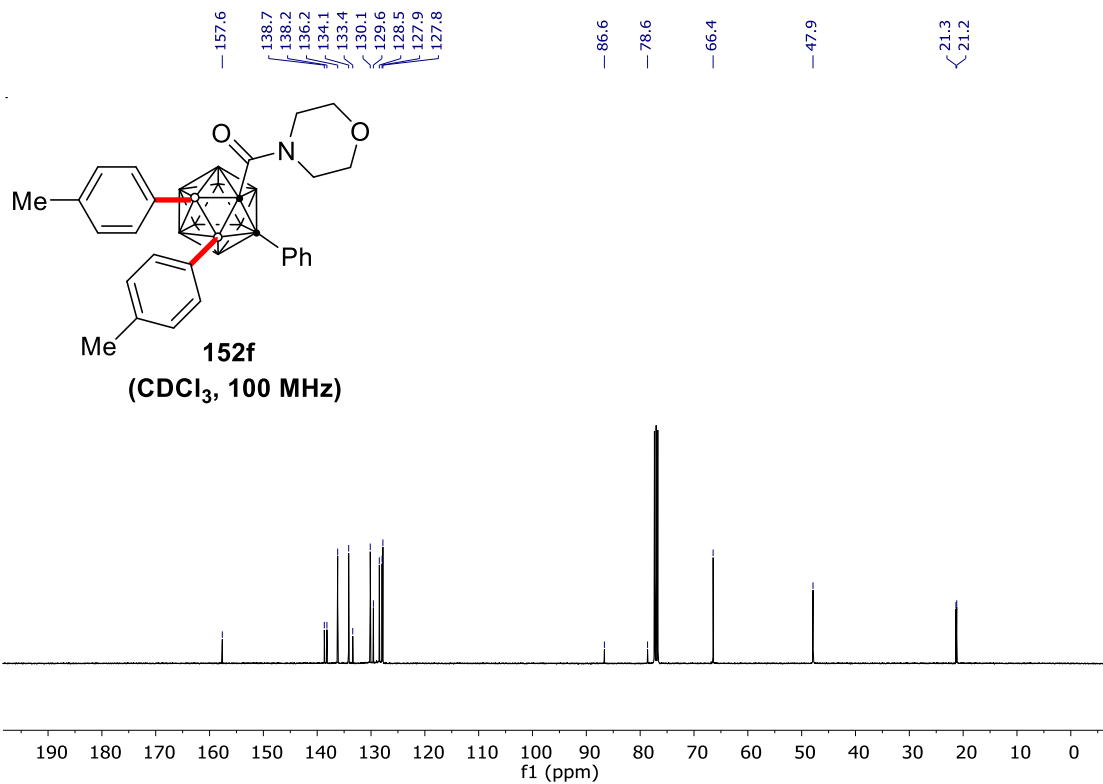
NMR Spectra



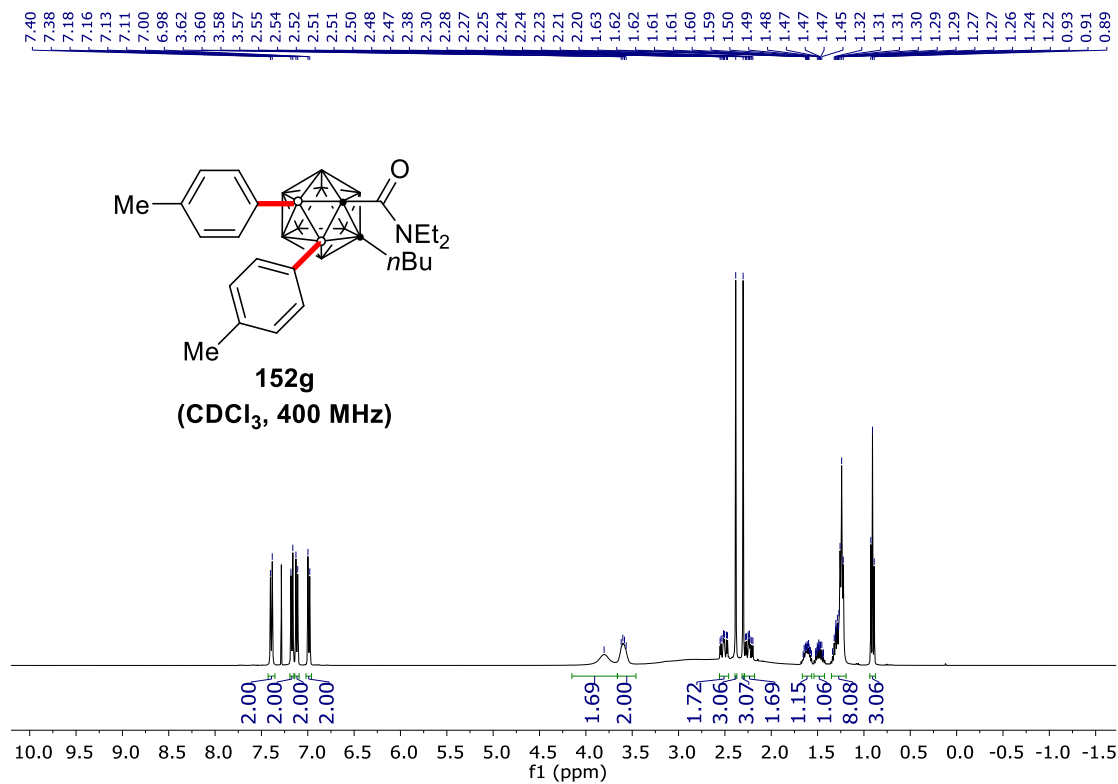
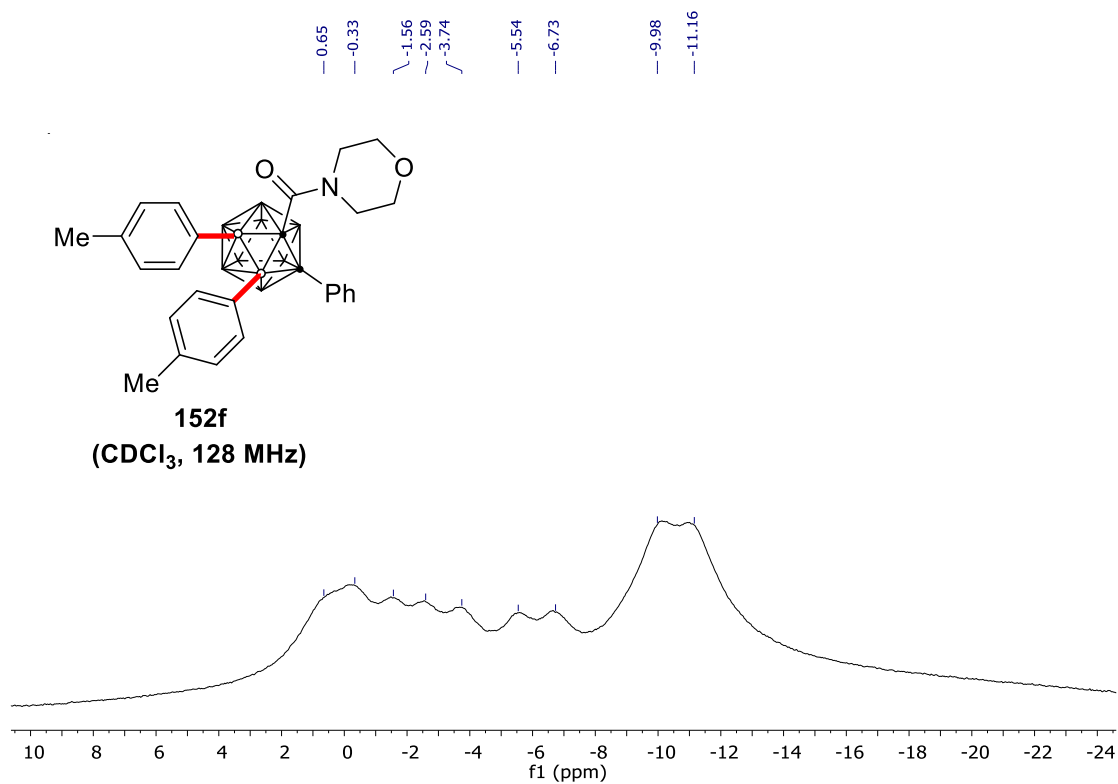
NMR Spectra



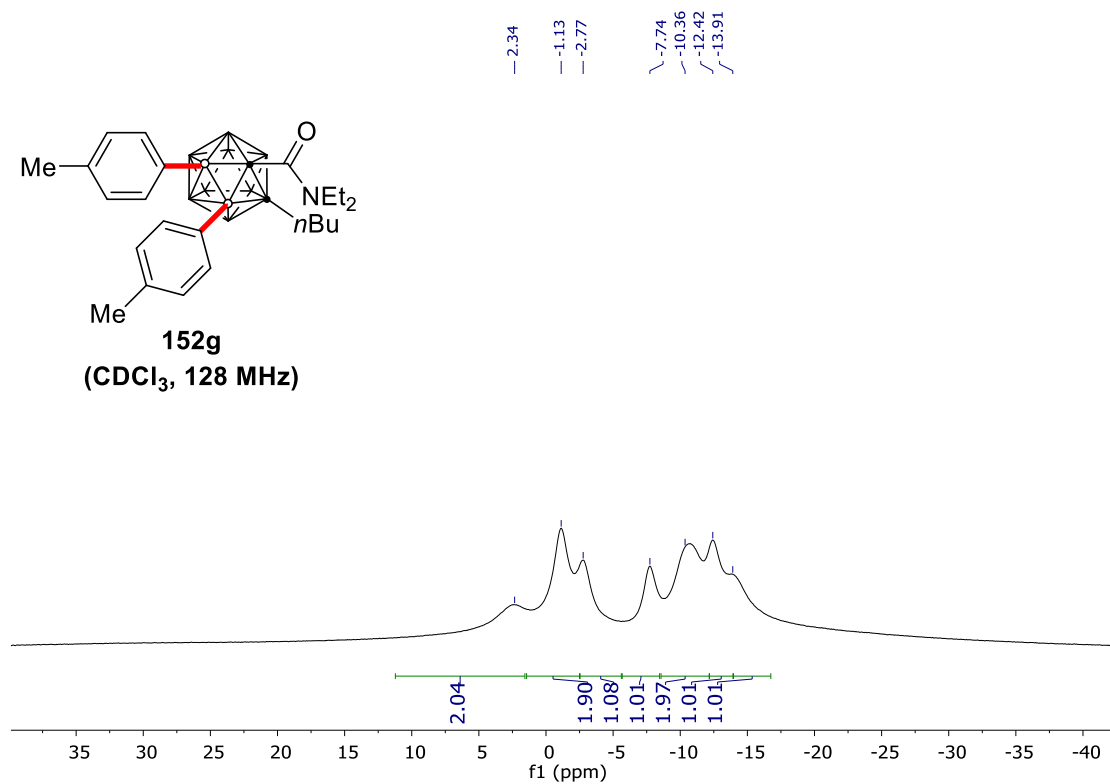
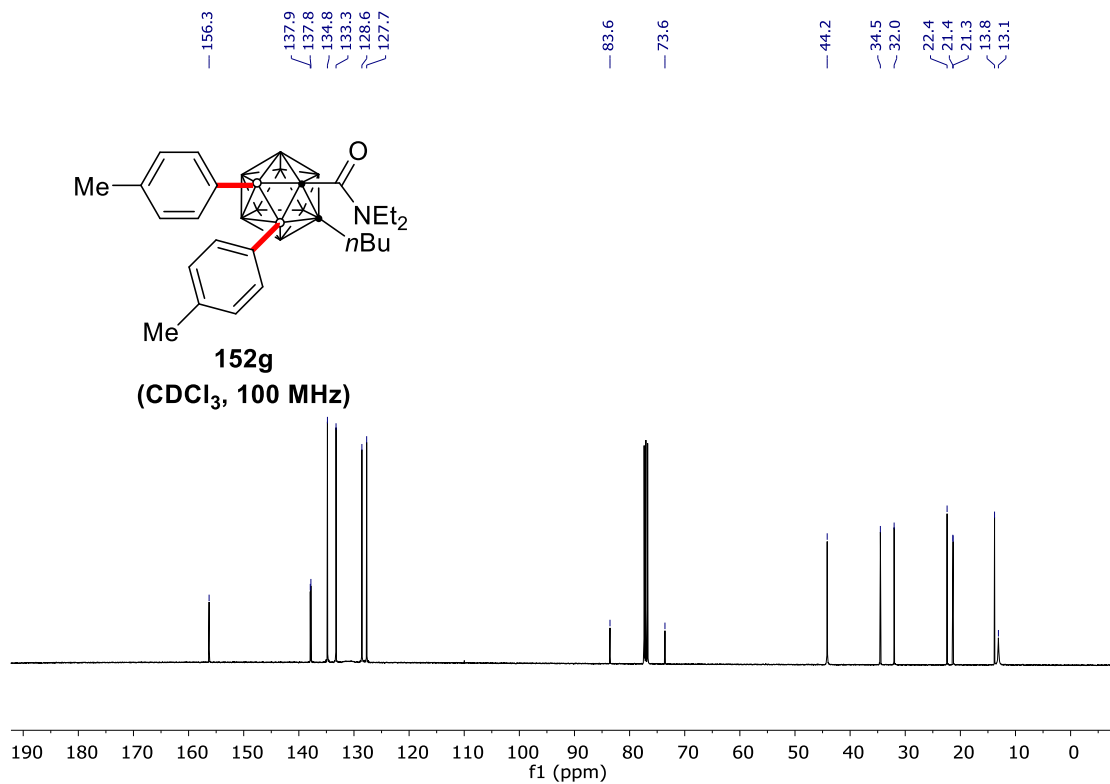
NMR Spectra



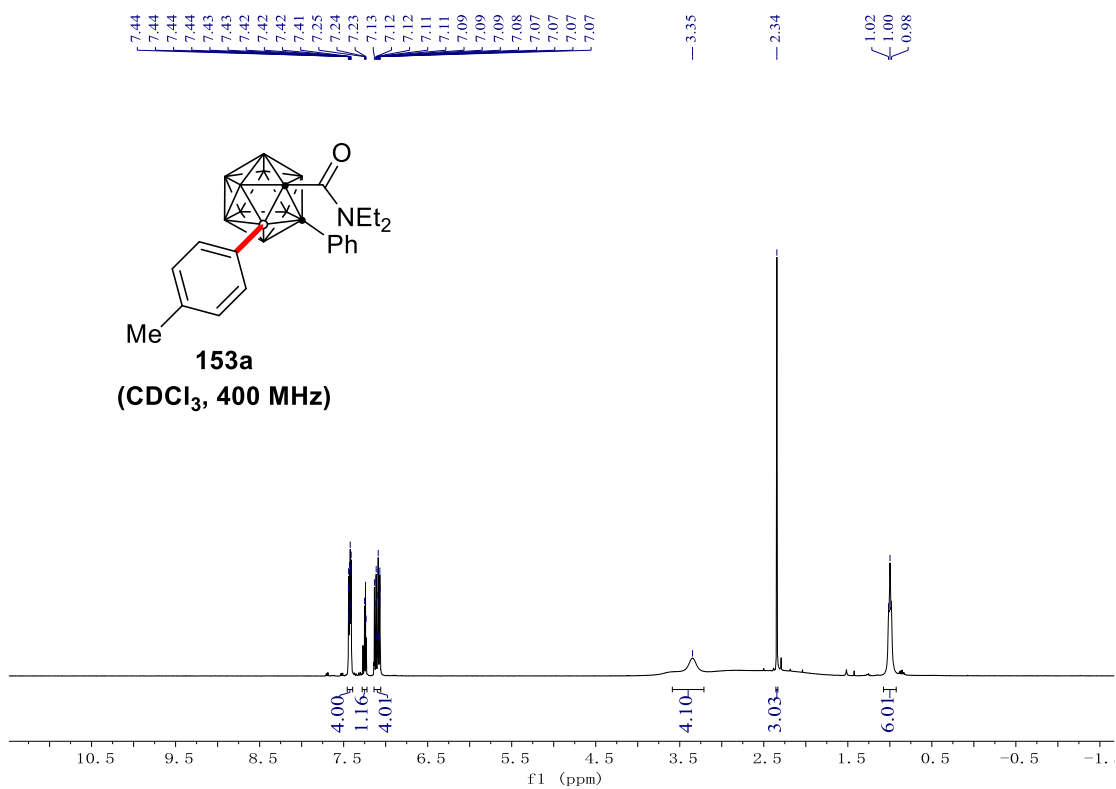
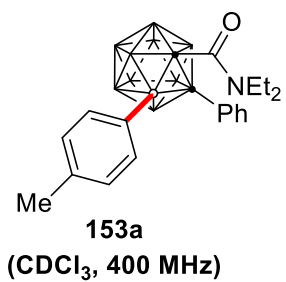
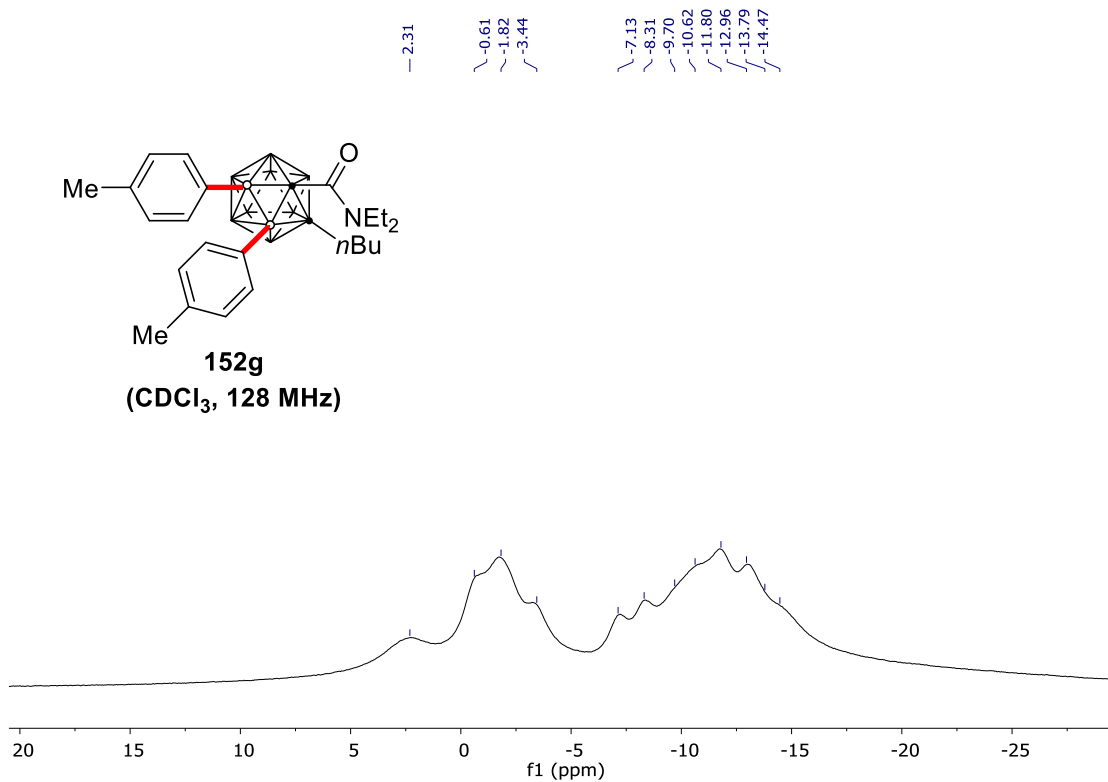
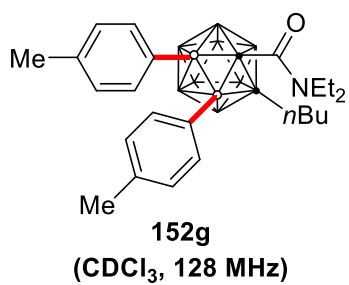
NMR Spectra



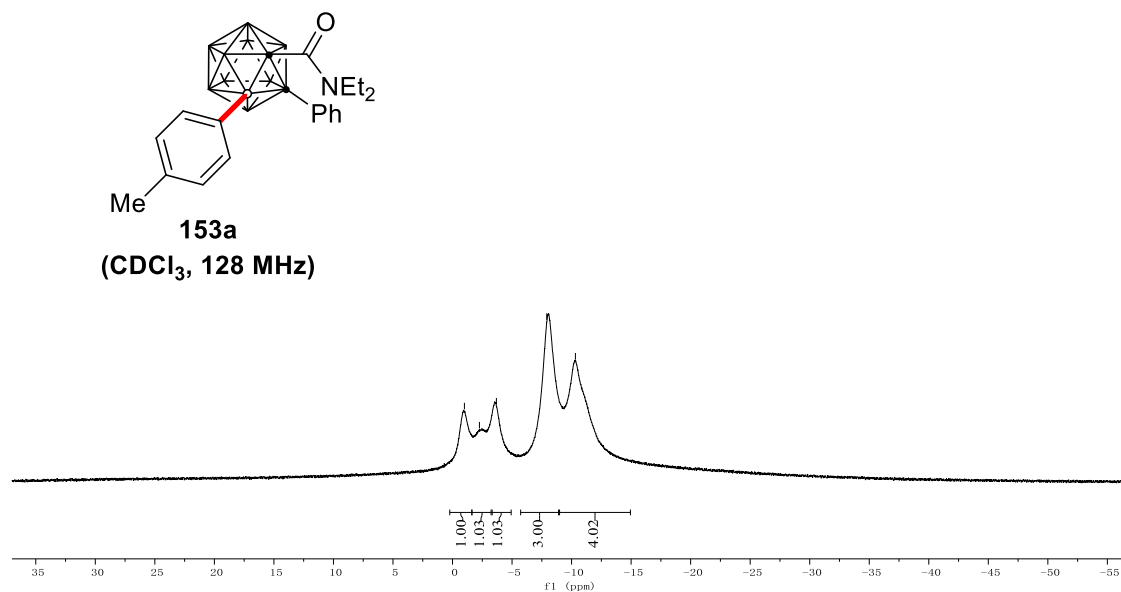
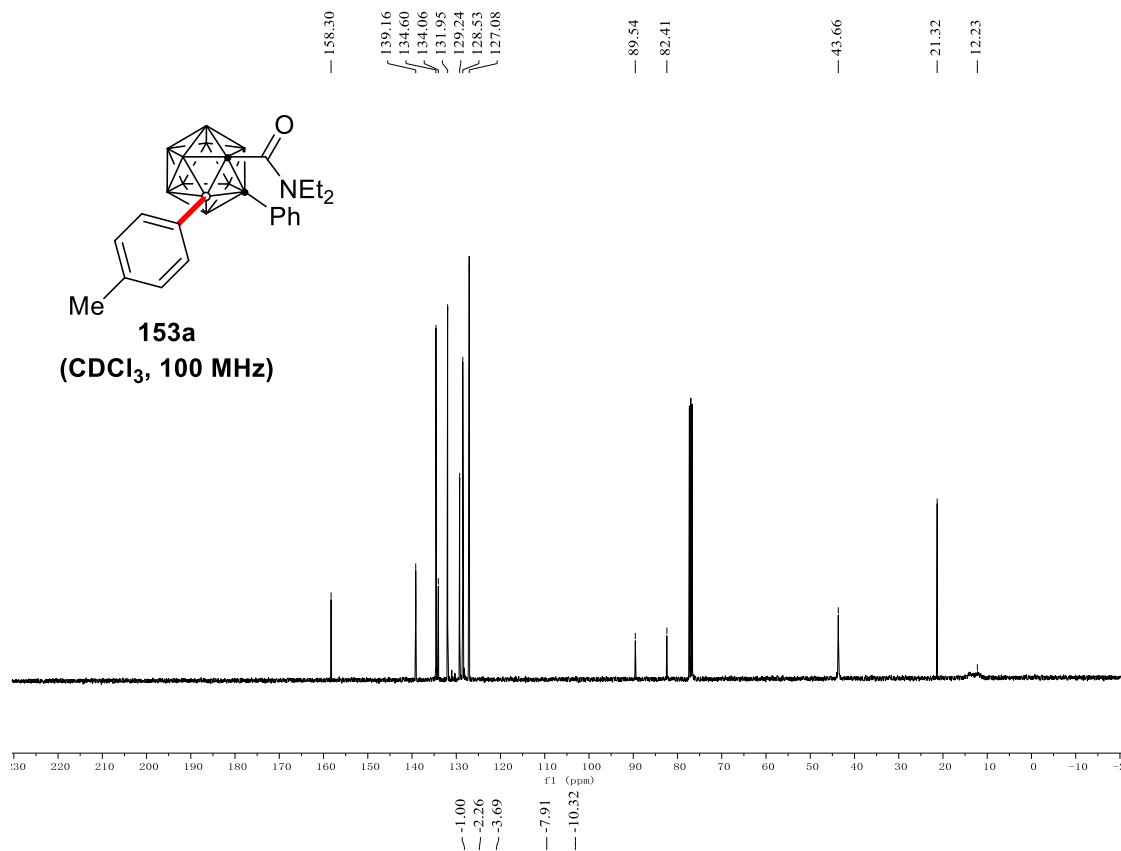
NMR Spectra



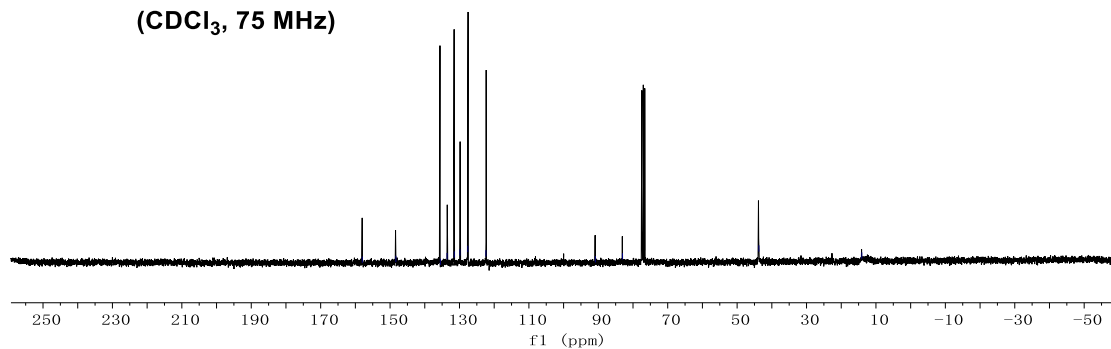
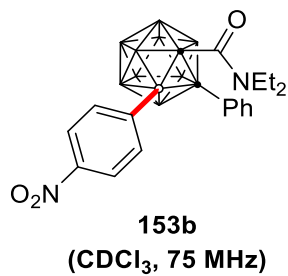
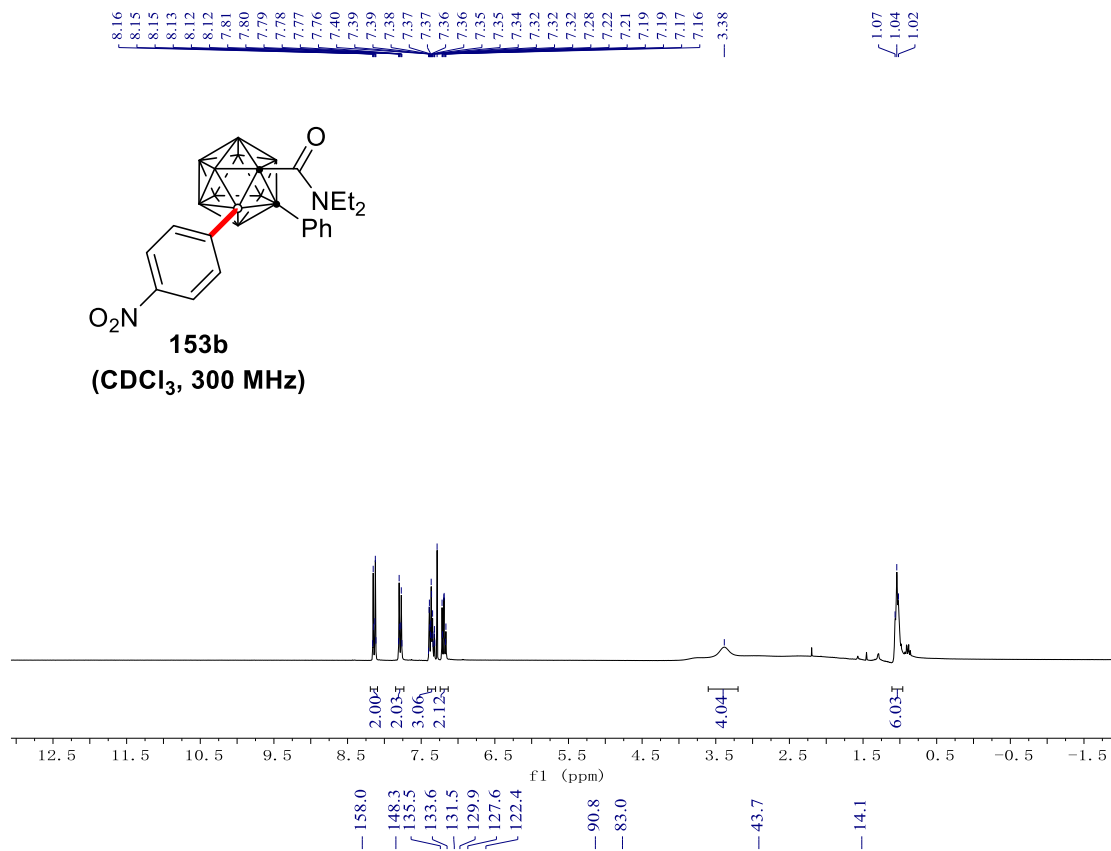
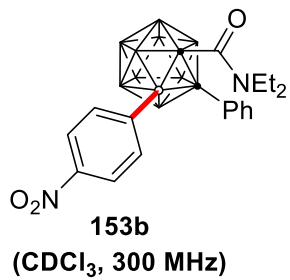
NMR Spectra



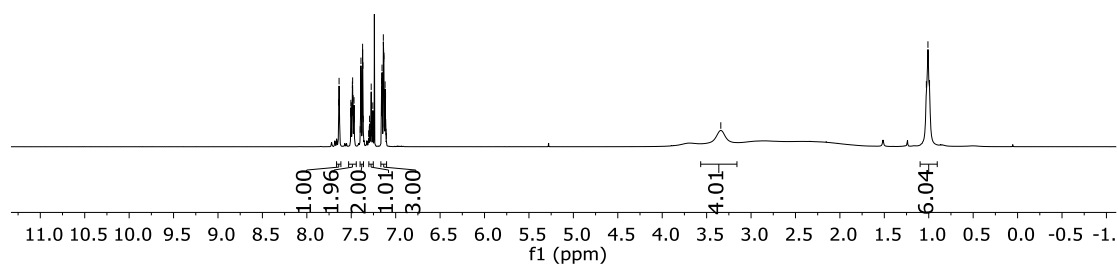
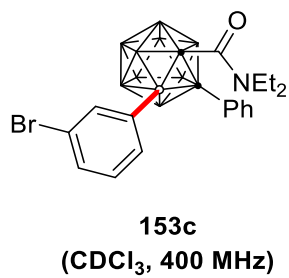
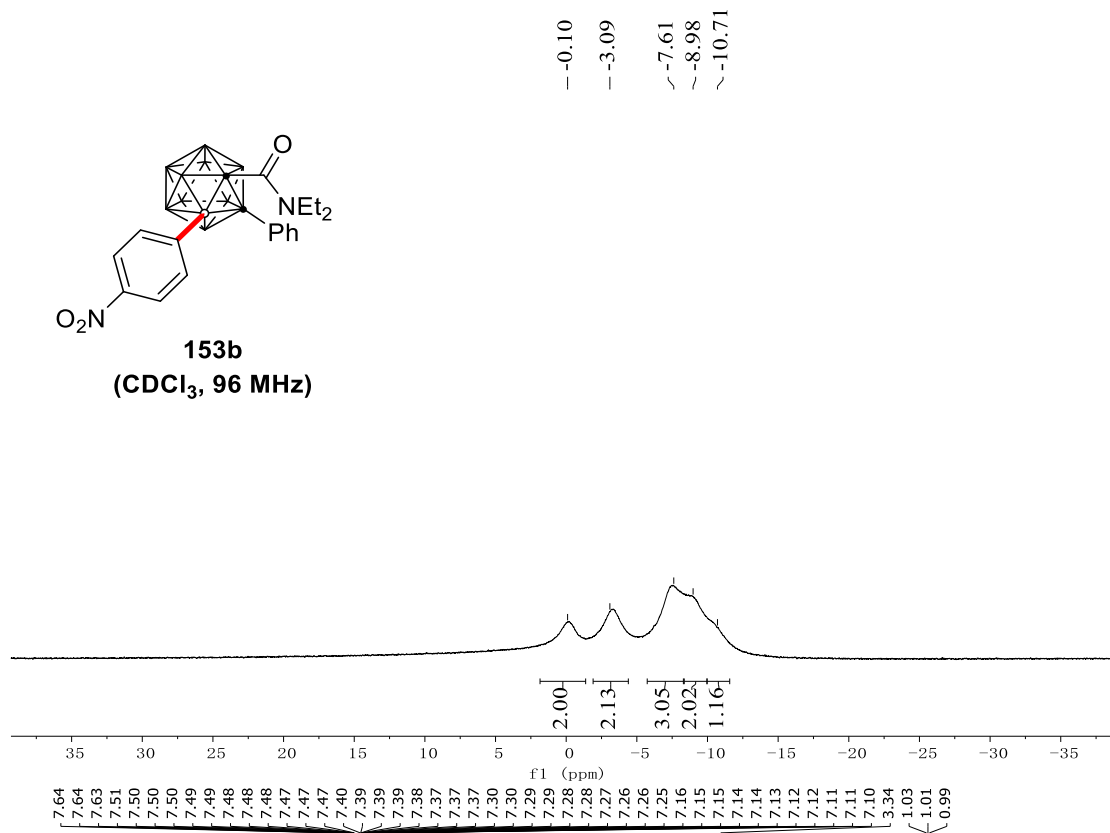
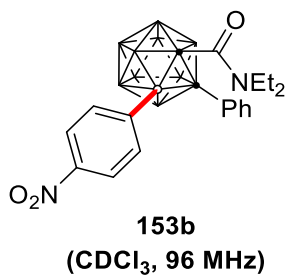
NMR Spectra



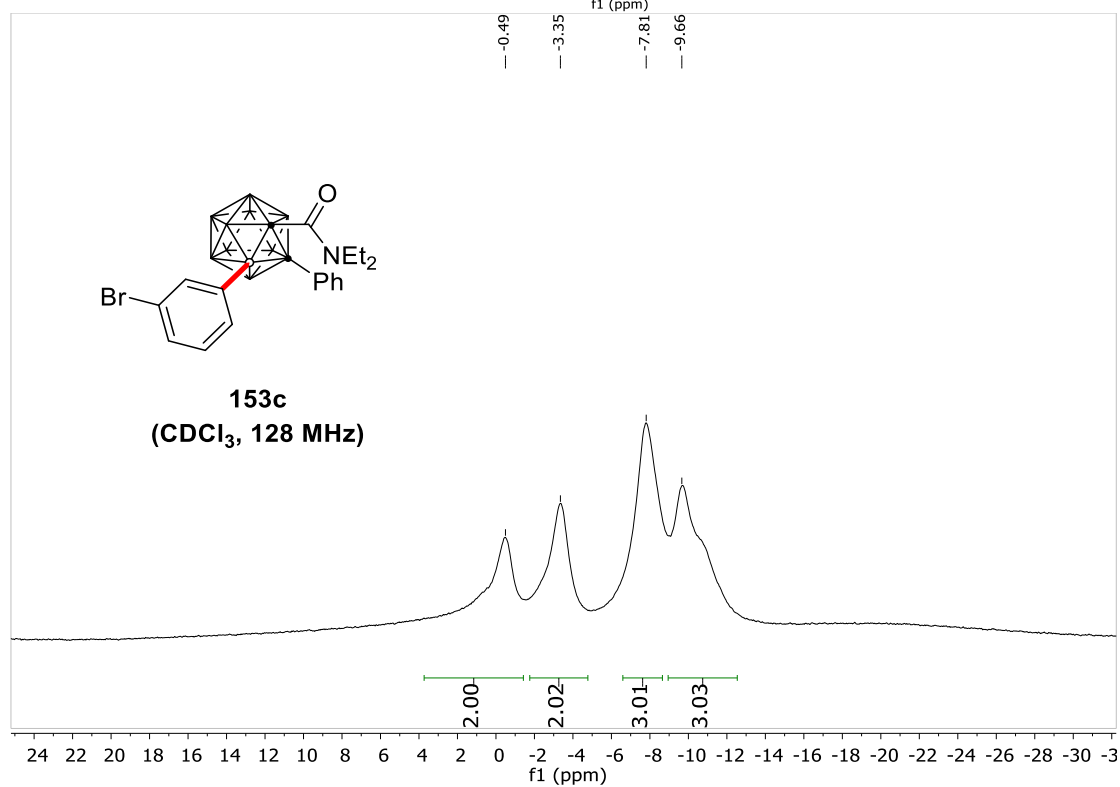
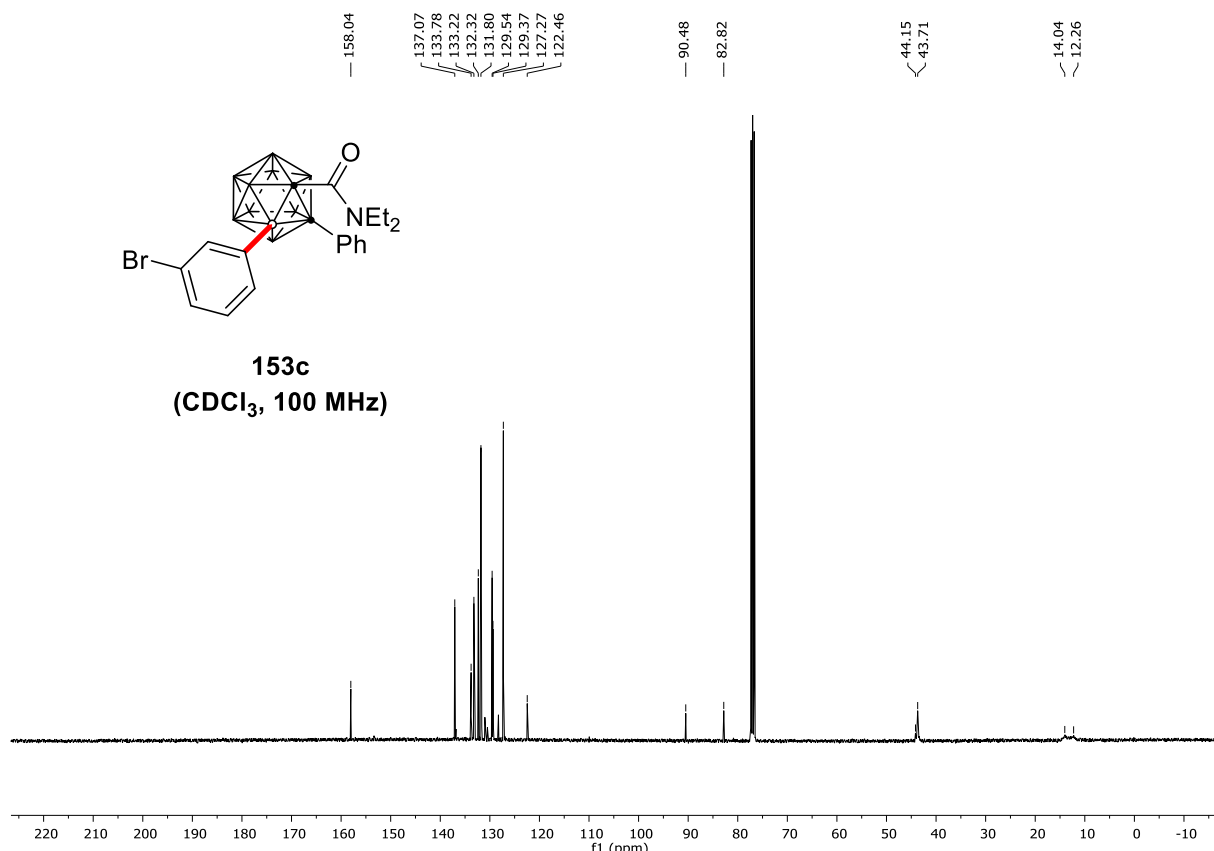
NMR Spectra



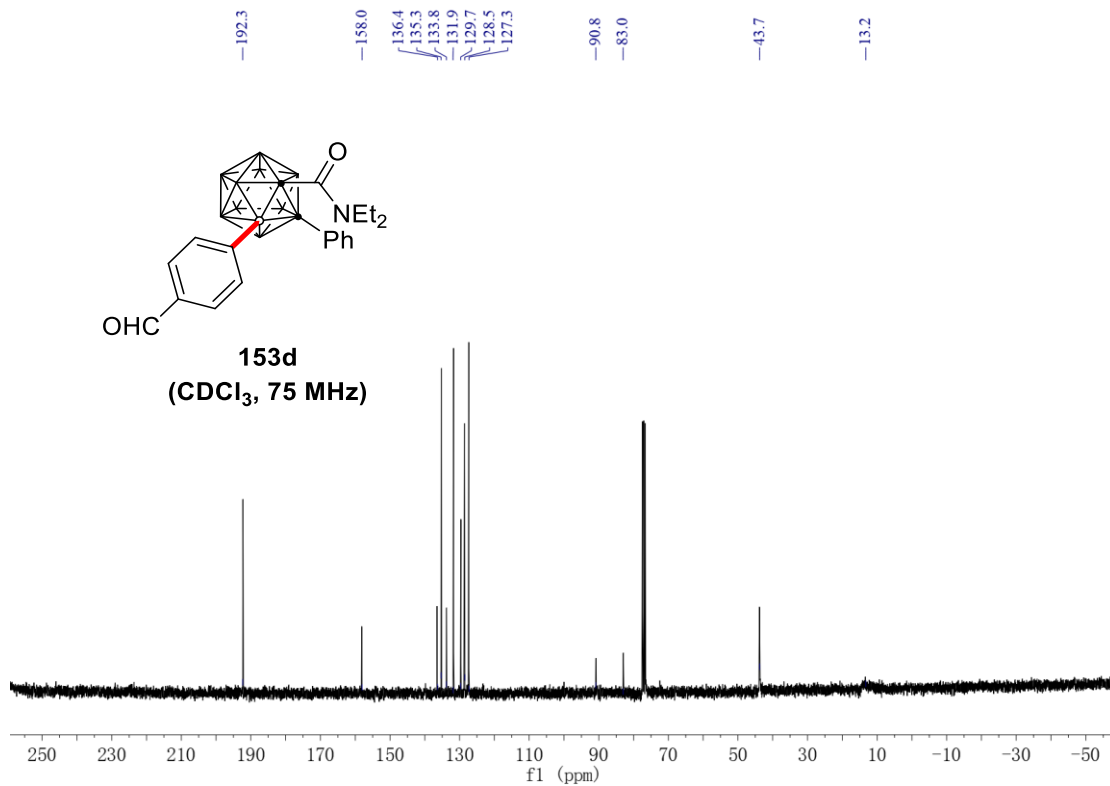
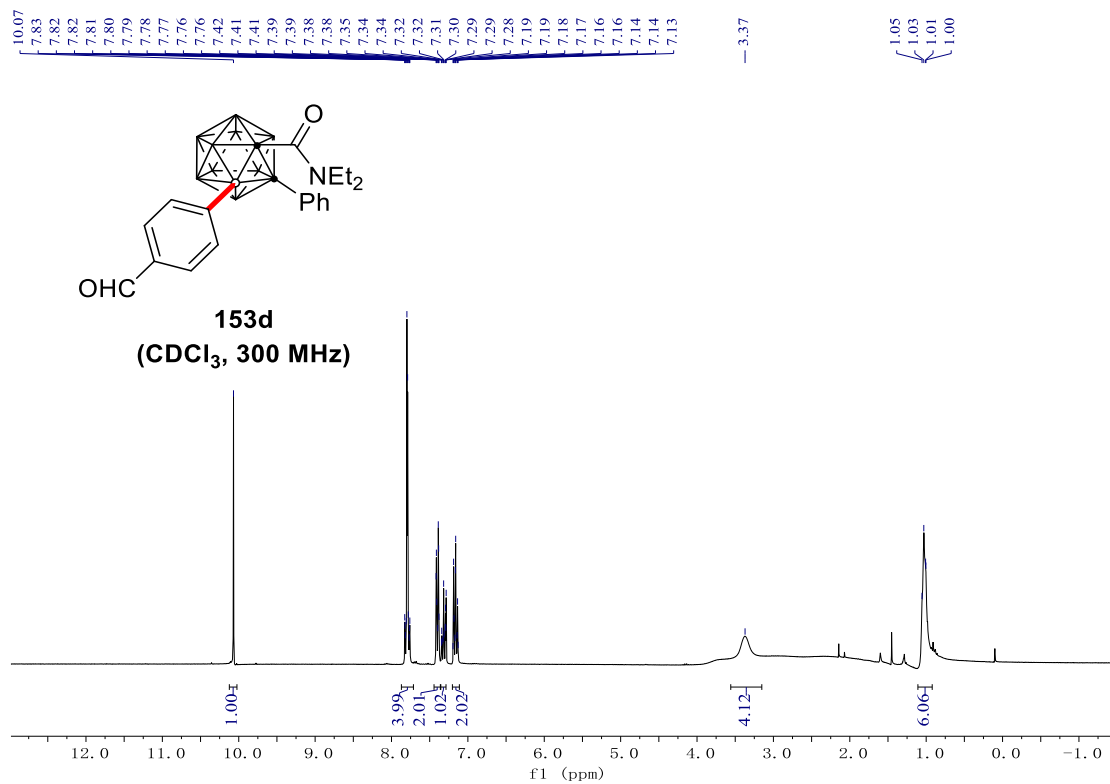
NMR Spectra



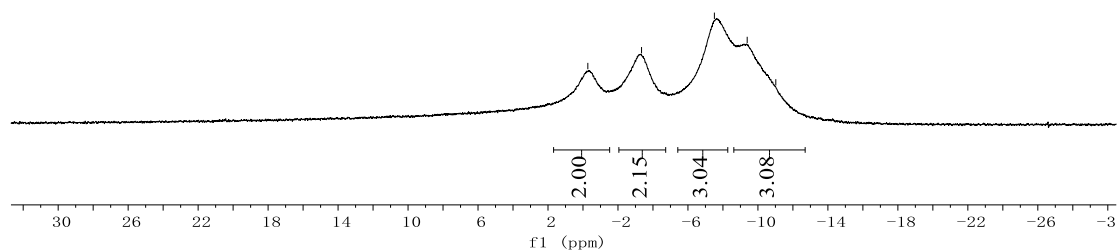
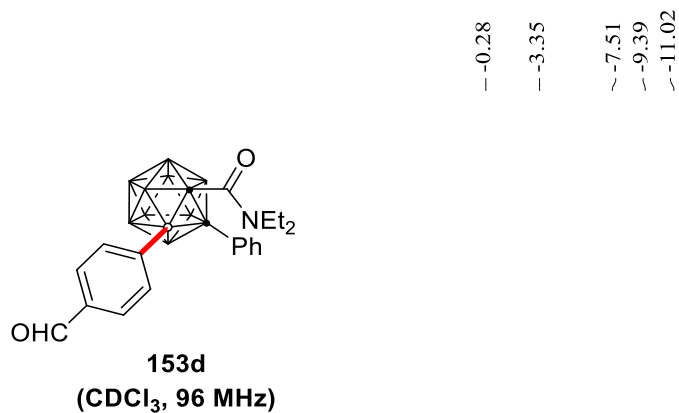
NMR Spectra



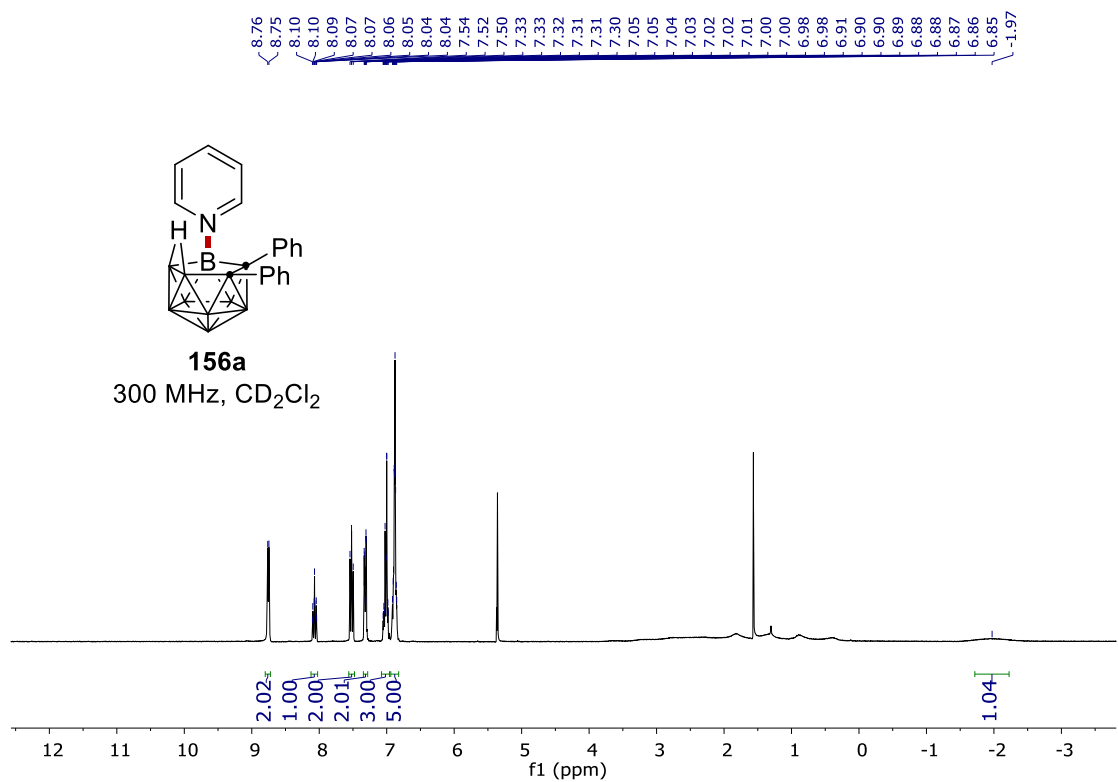
NMR Spectra



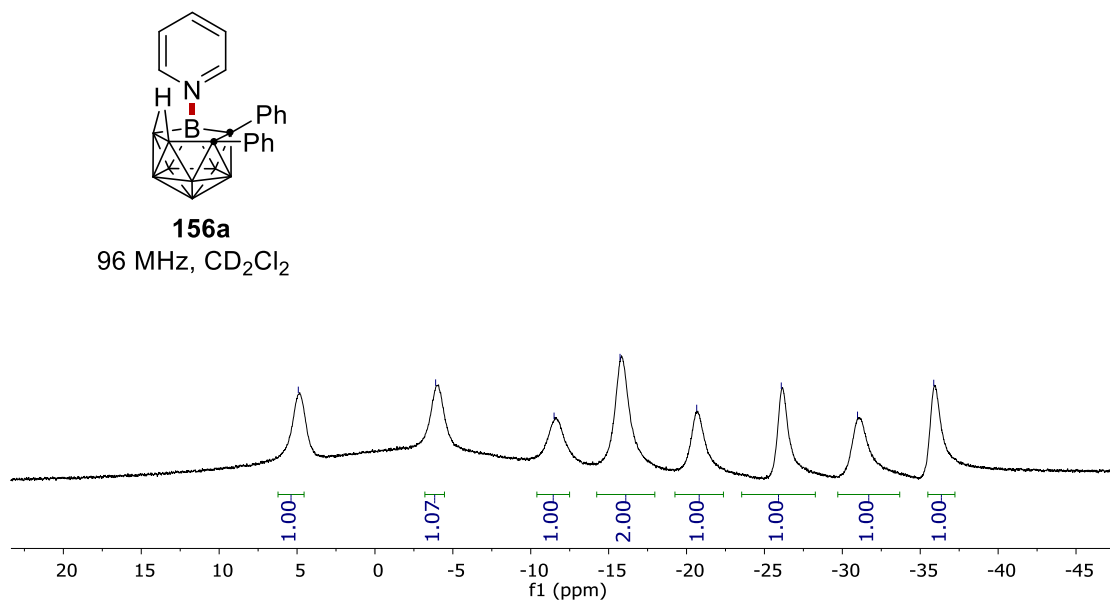
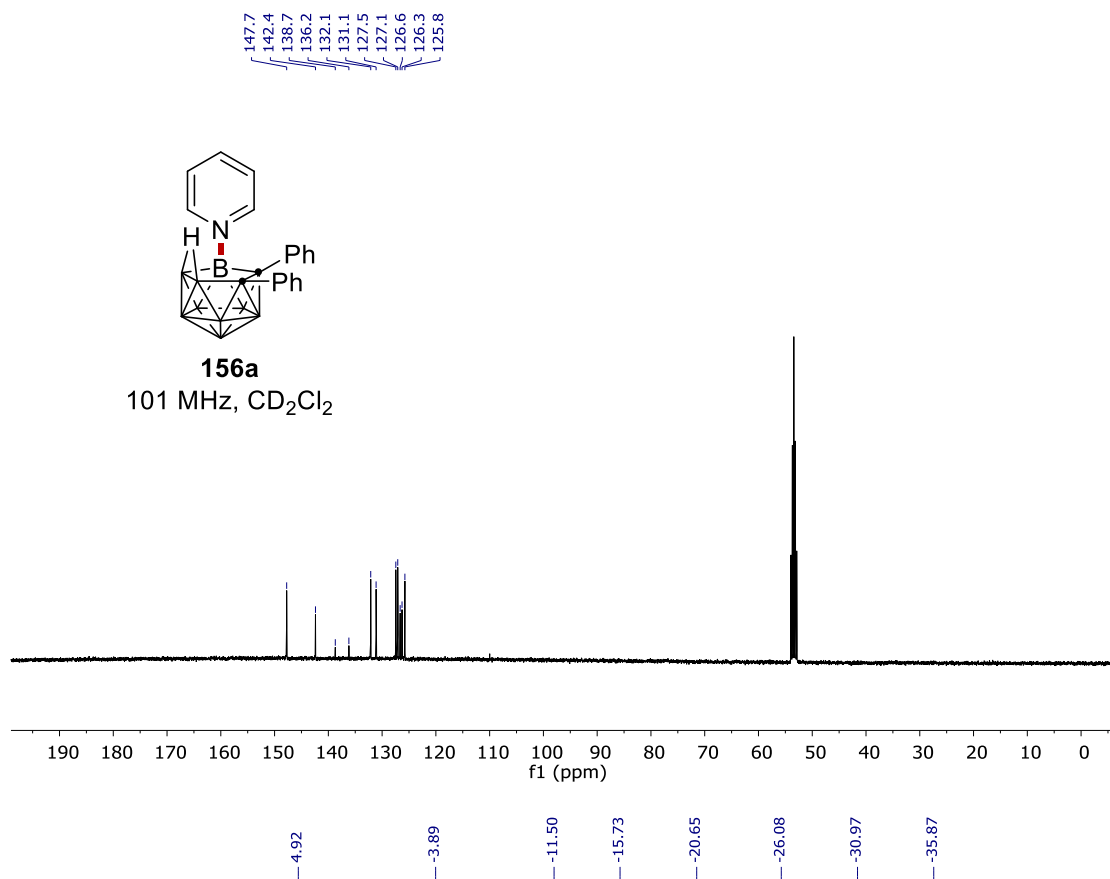
NMR Spectra



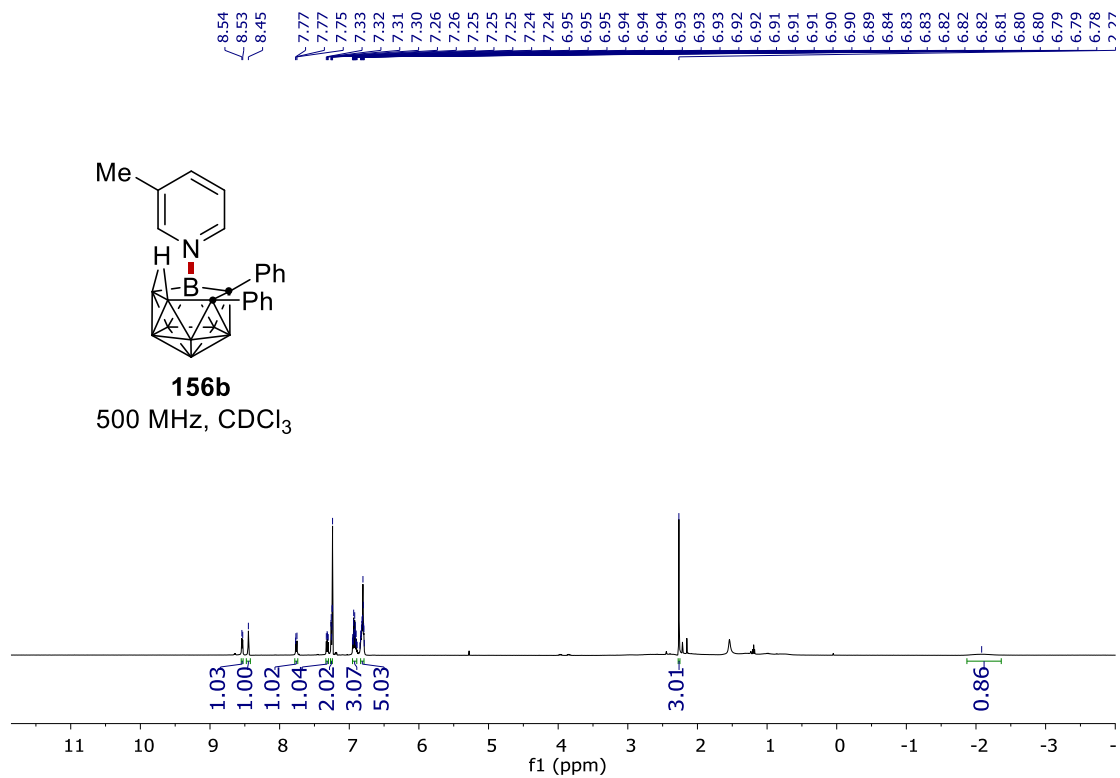
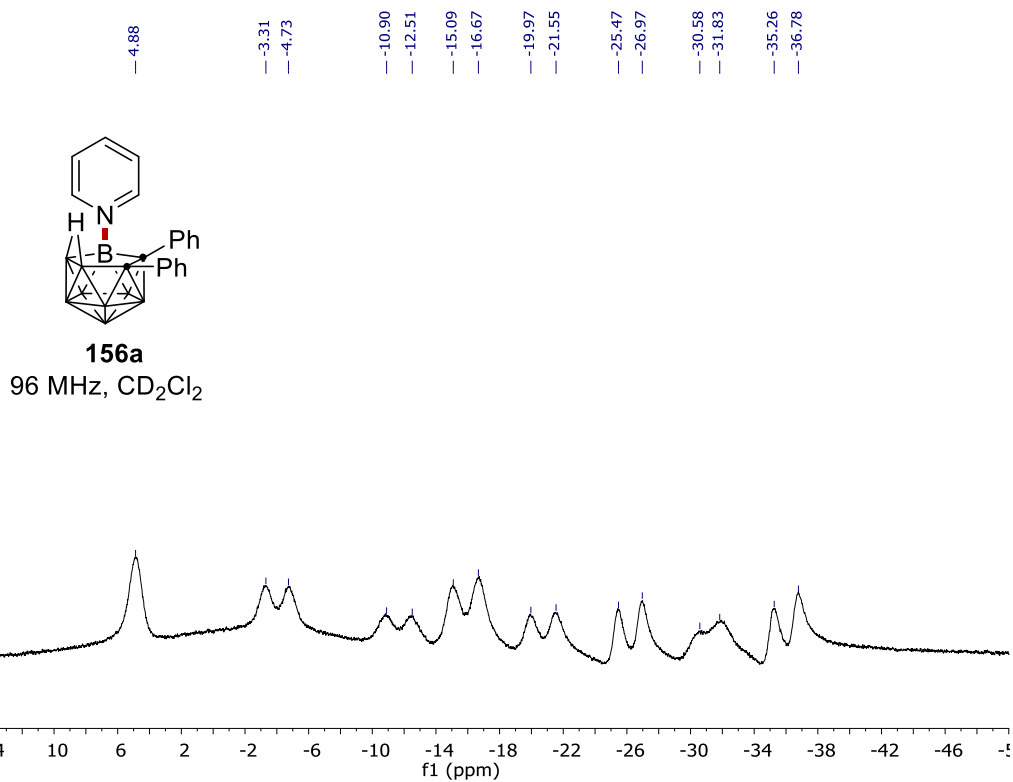
7.5 Electrochemical B–H Nitrogenation of *nido*-Carboranes



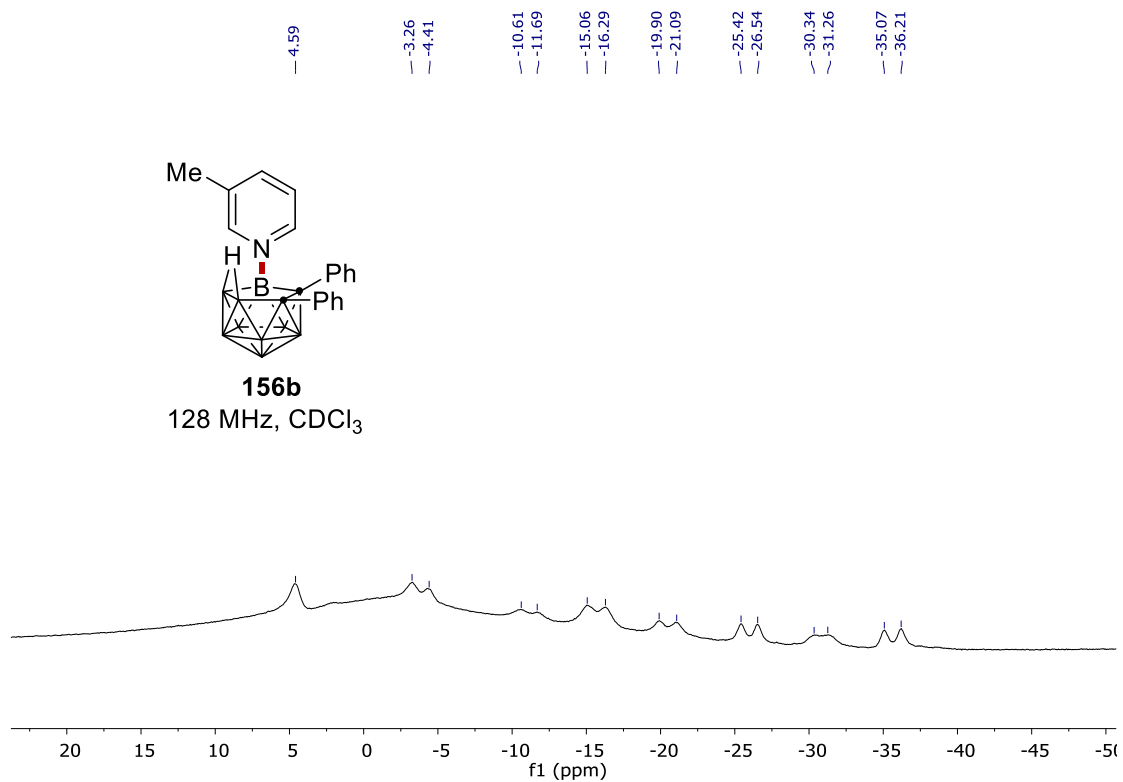
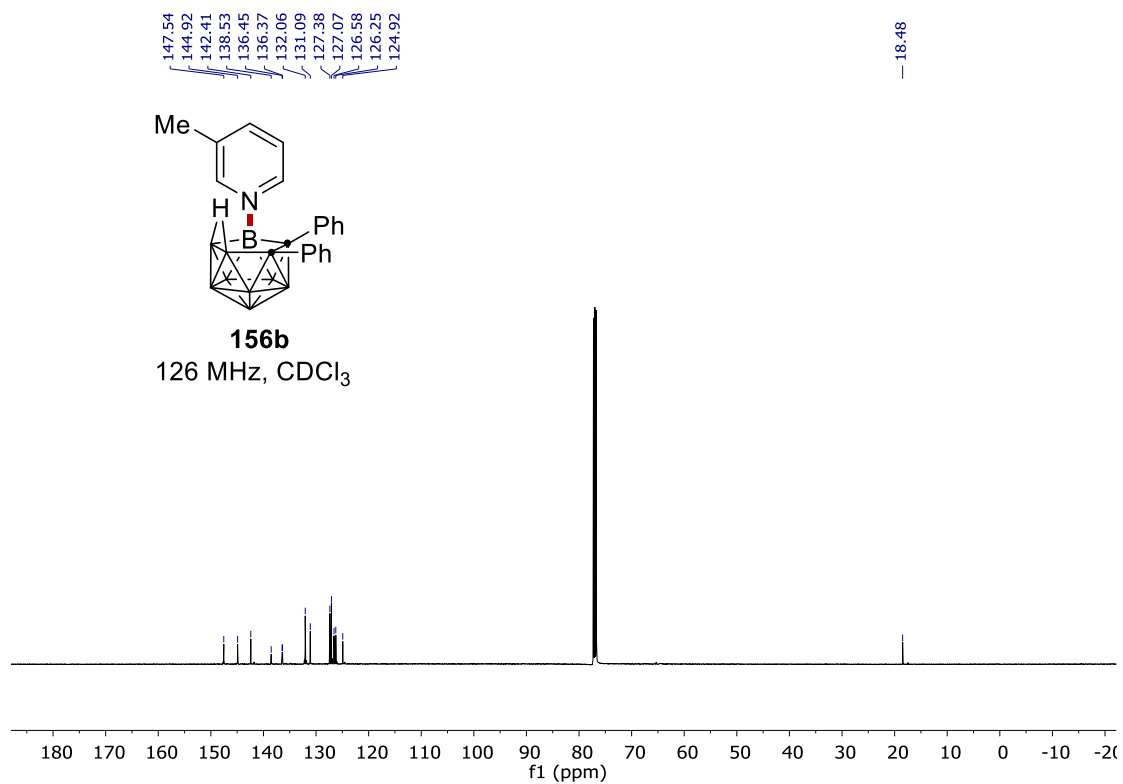
NMR Spectra



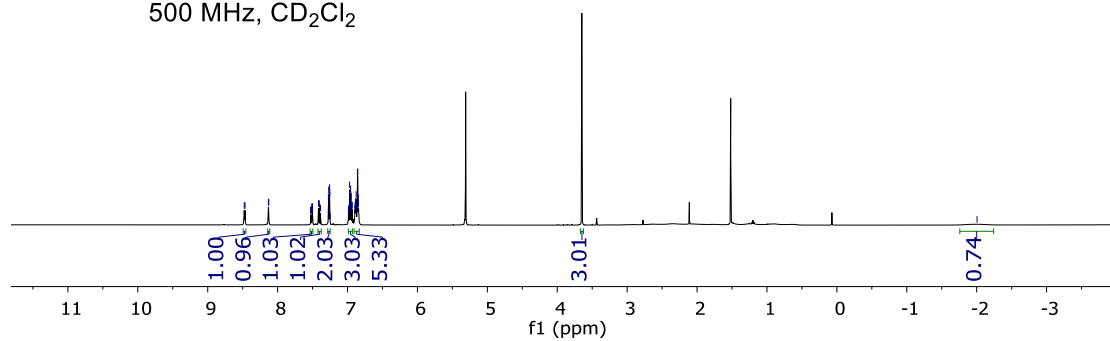
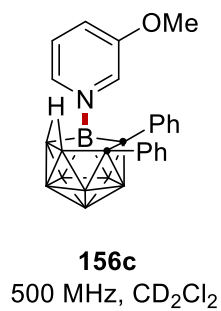
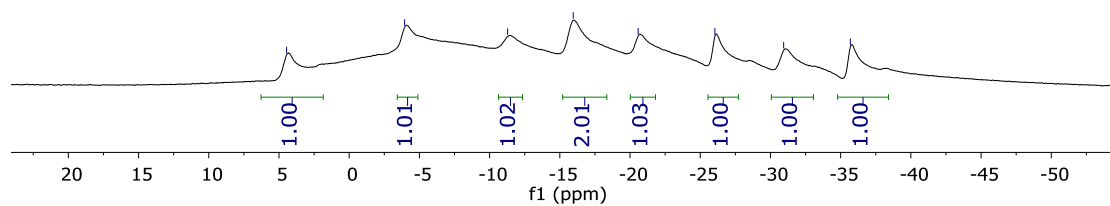
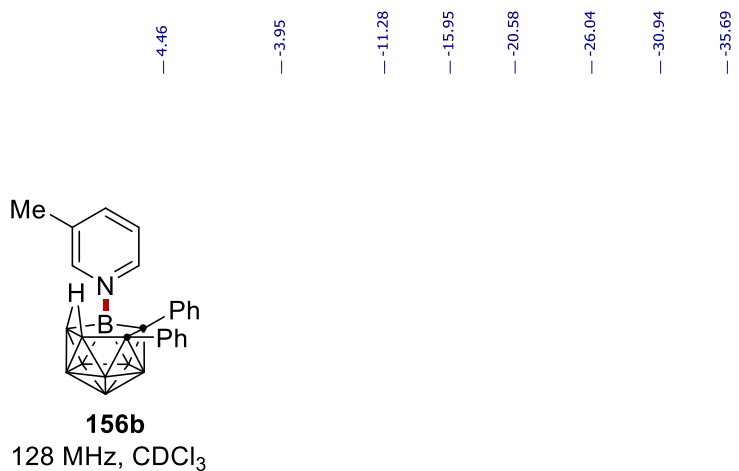
NMR Spectra



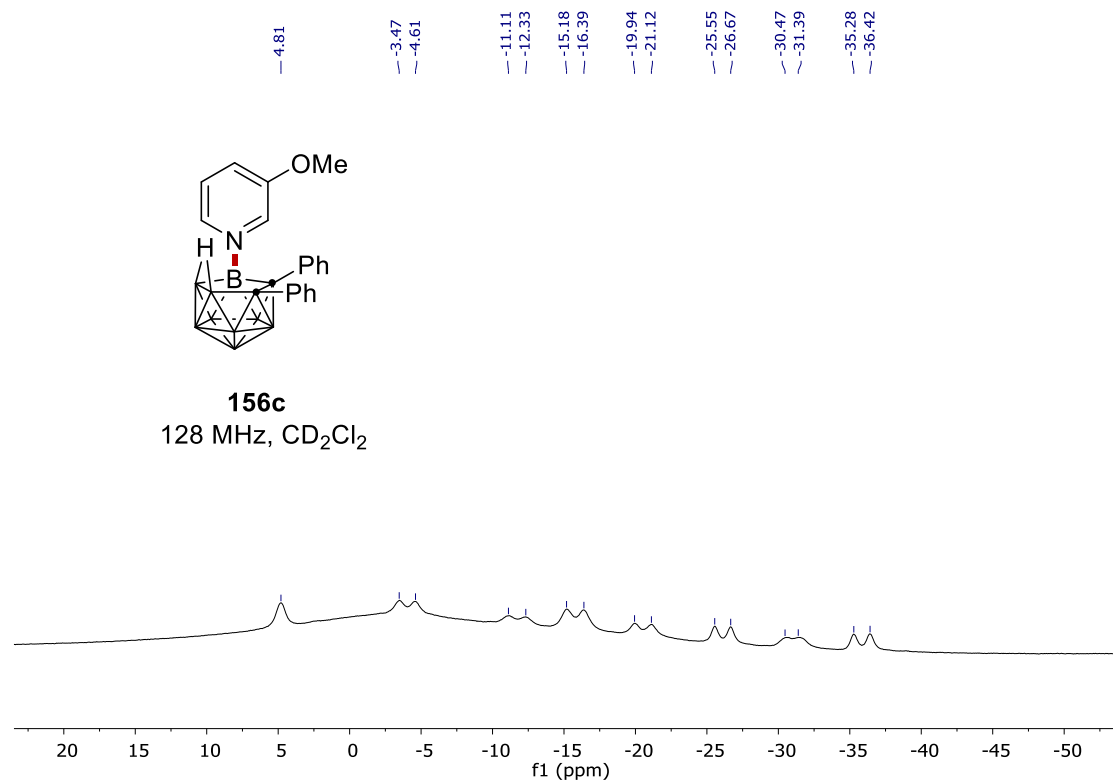
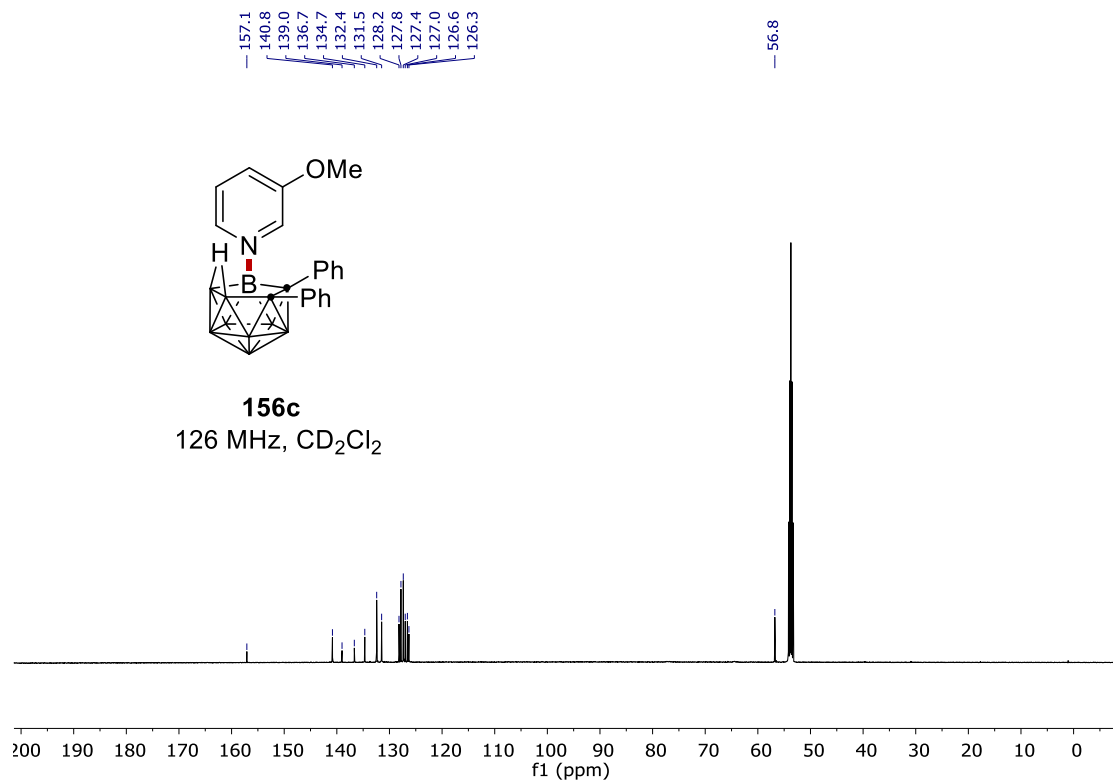
NMR Spectra



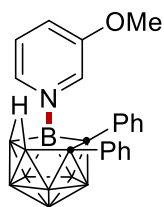
NMR Spectra



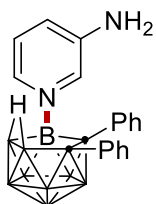
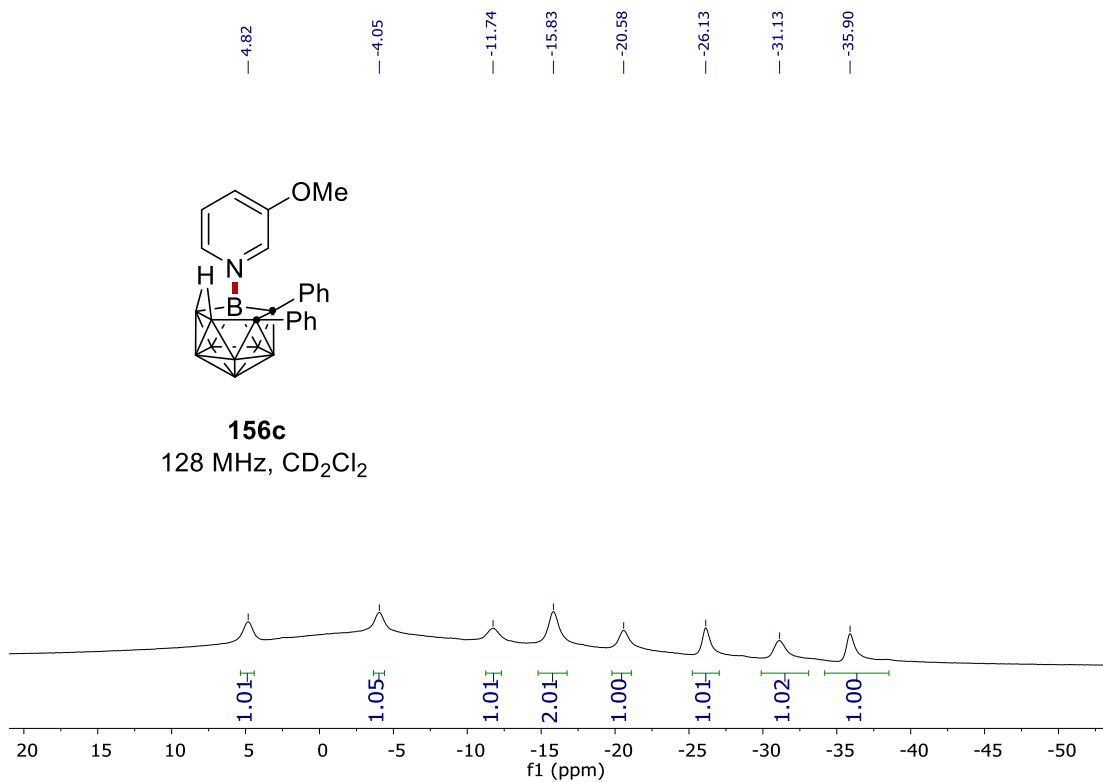
NMR Spectra



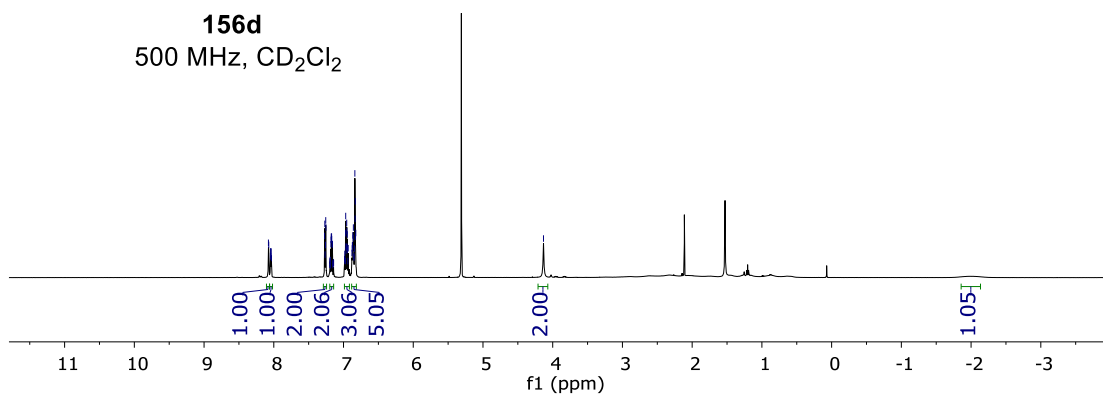
NMR Spectra



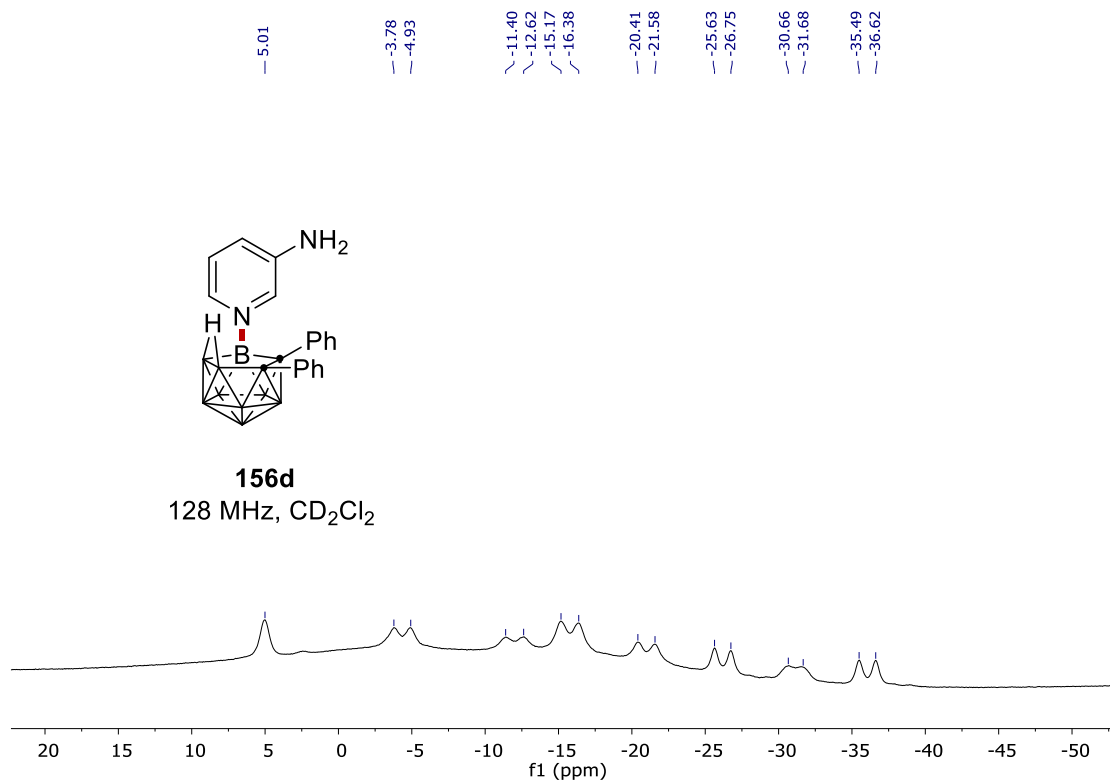
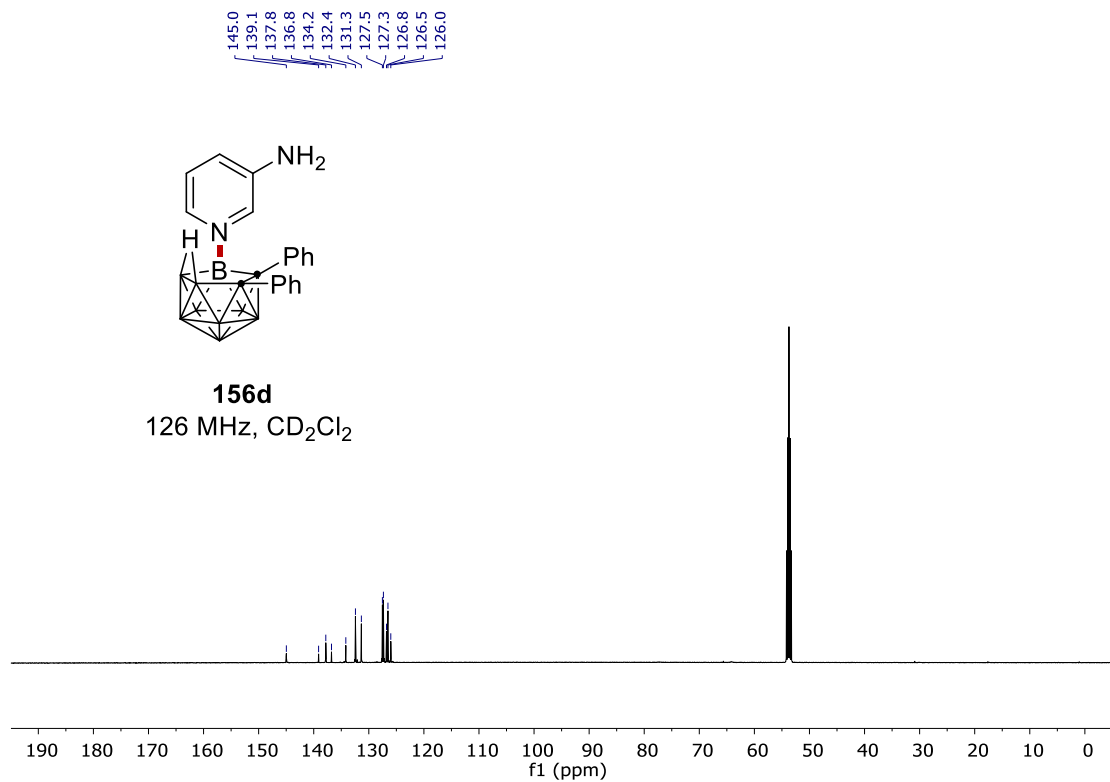
156c
128 MHz, CD₂Cl₂



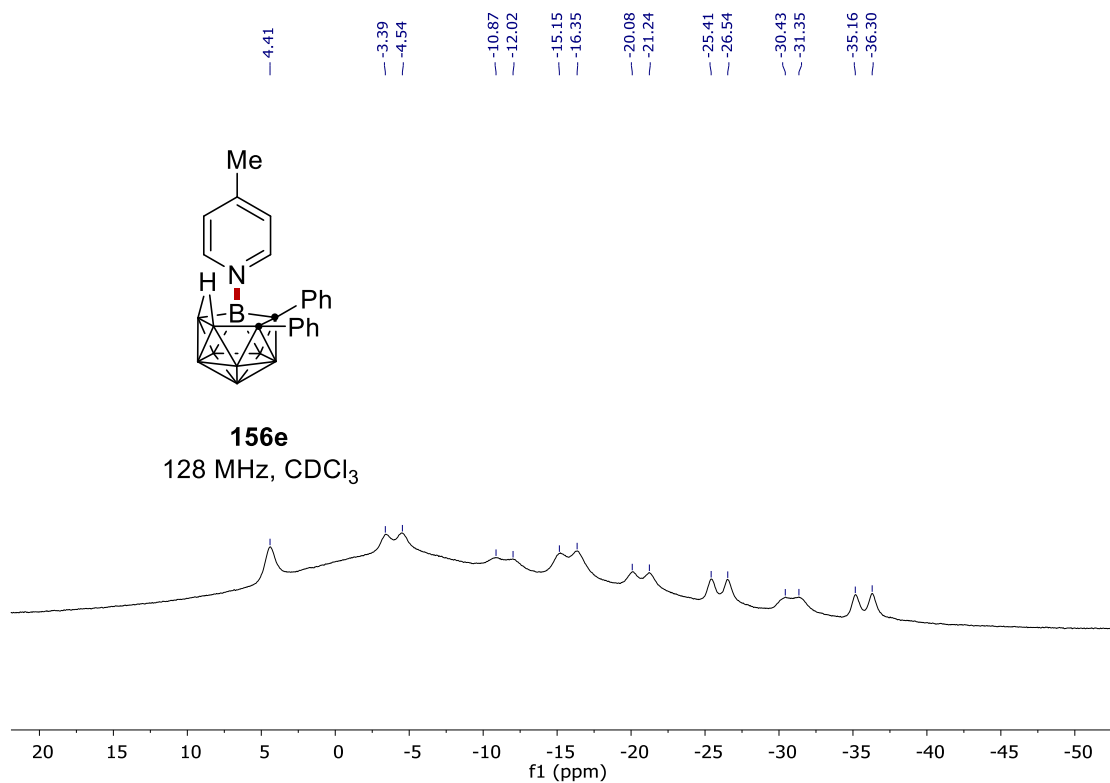
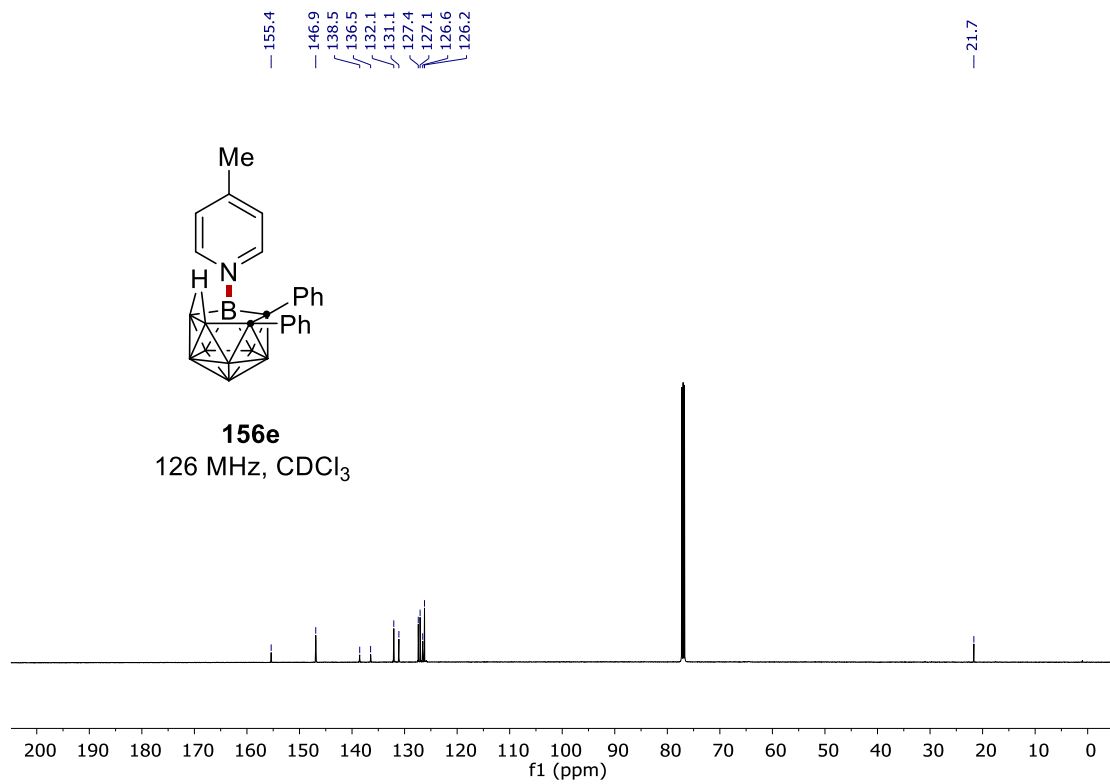
156d
500 MHz, CD₂Cl₂



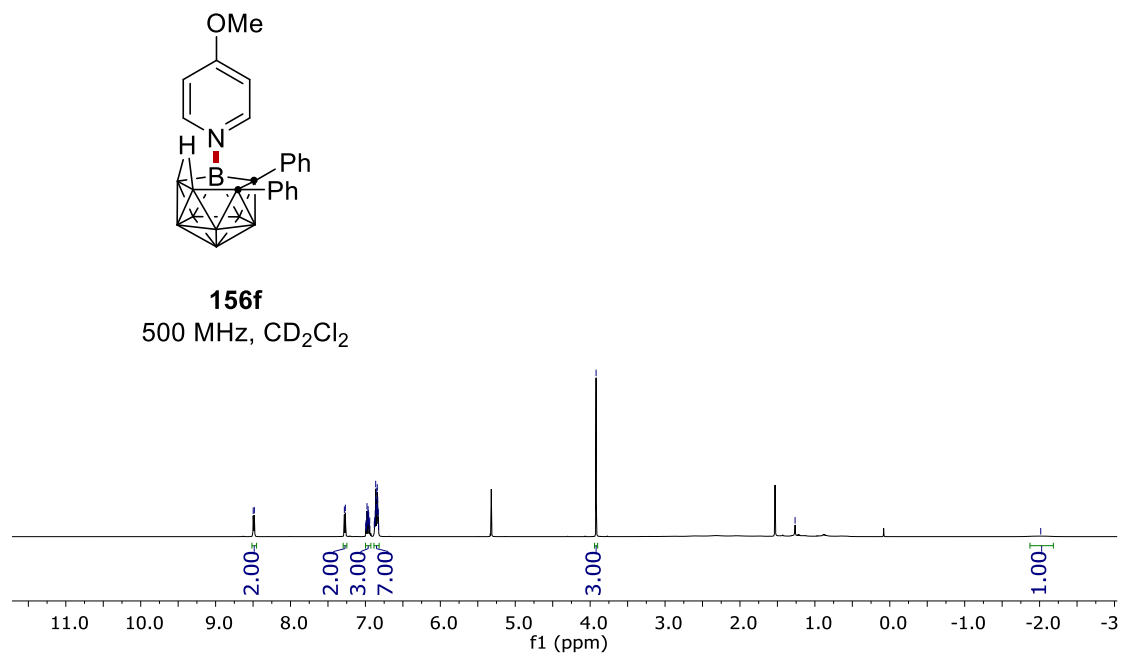
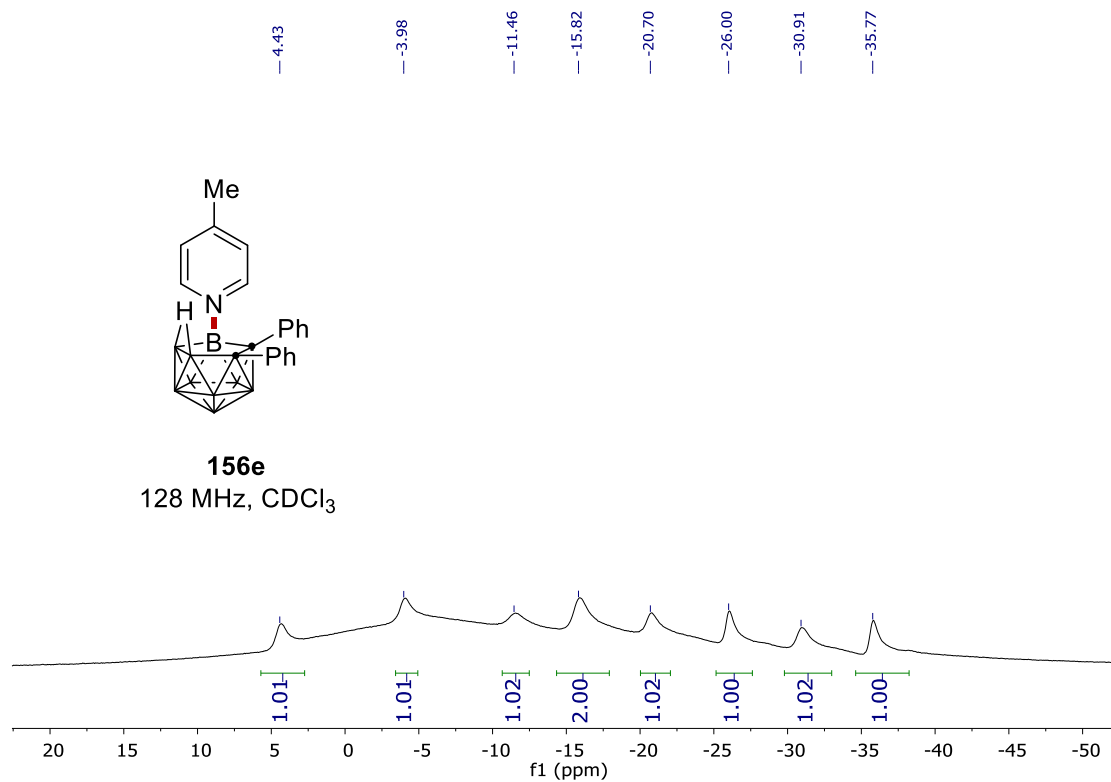
NMR Spectra



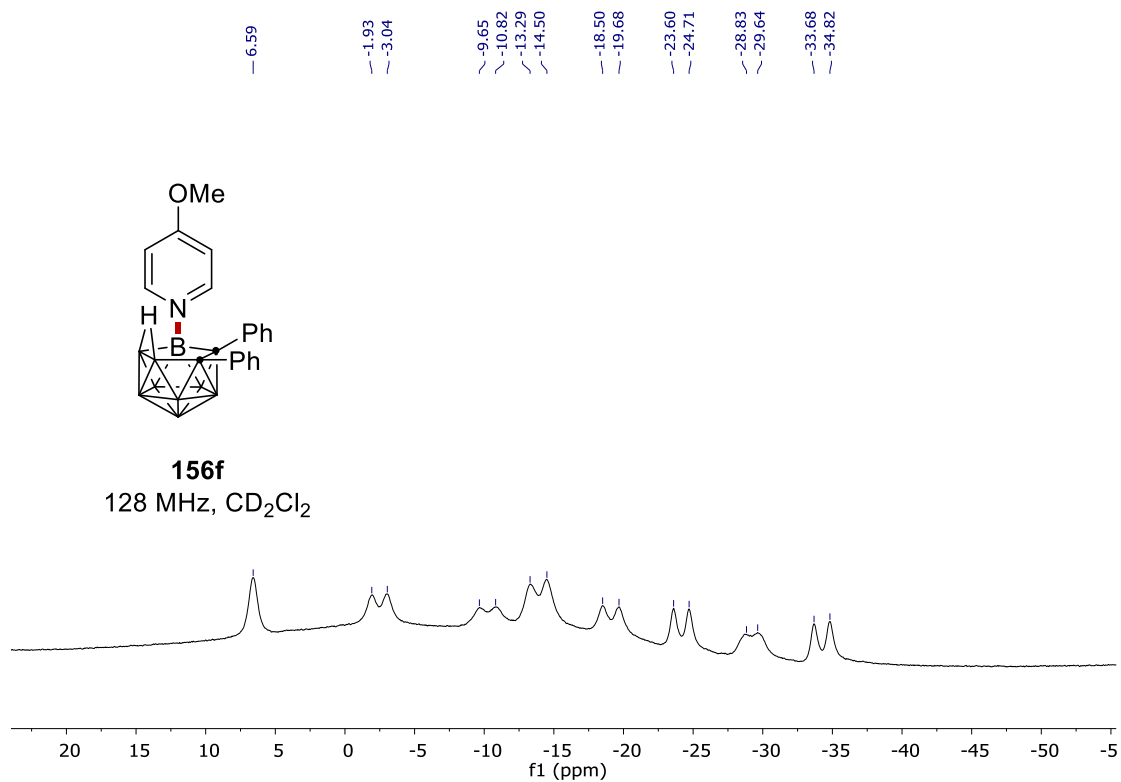
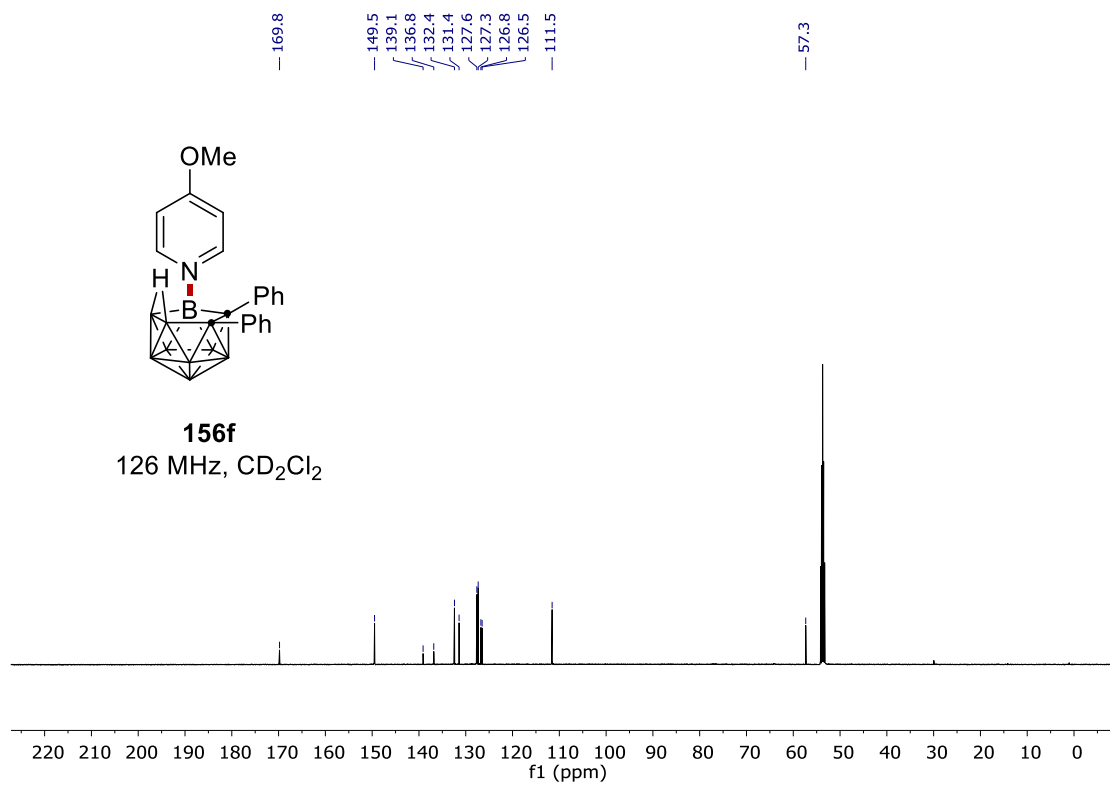
NMR Spectra



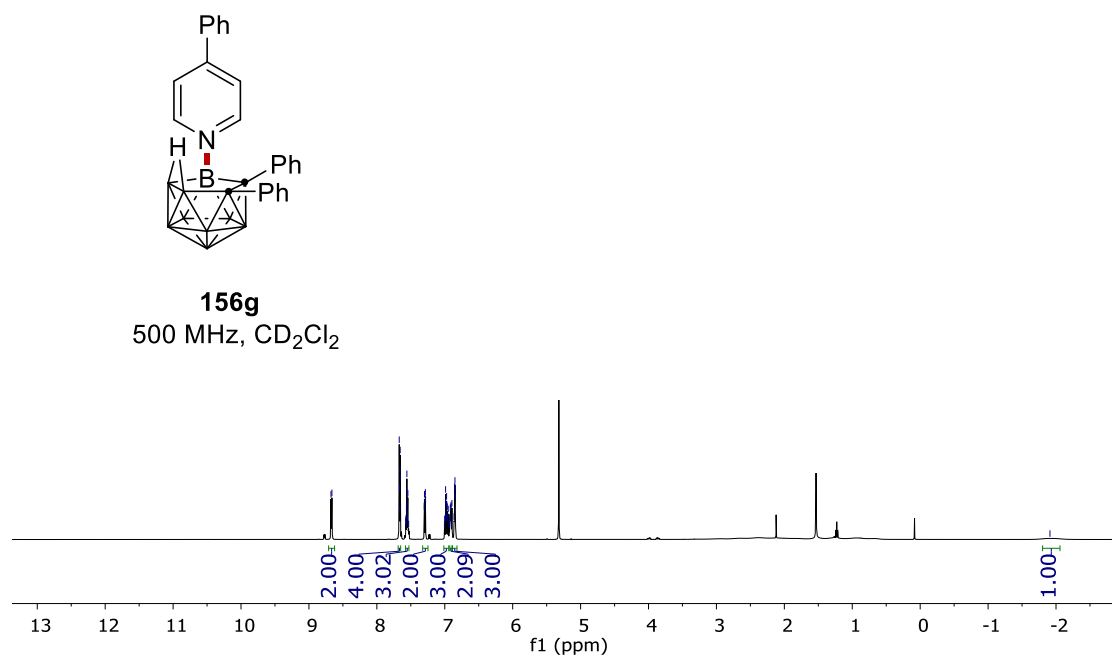
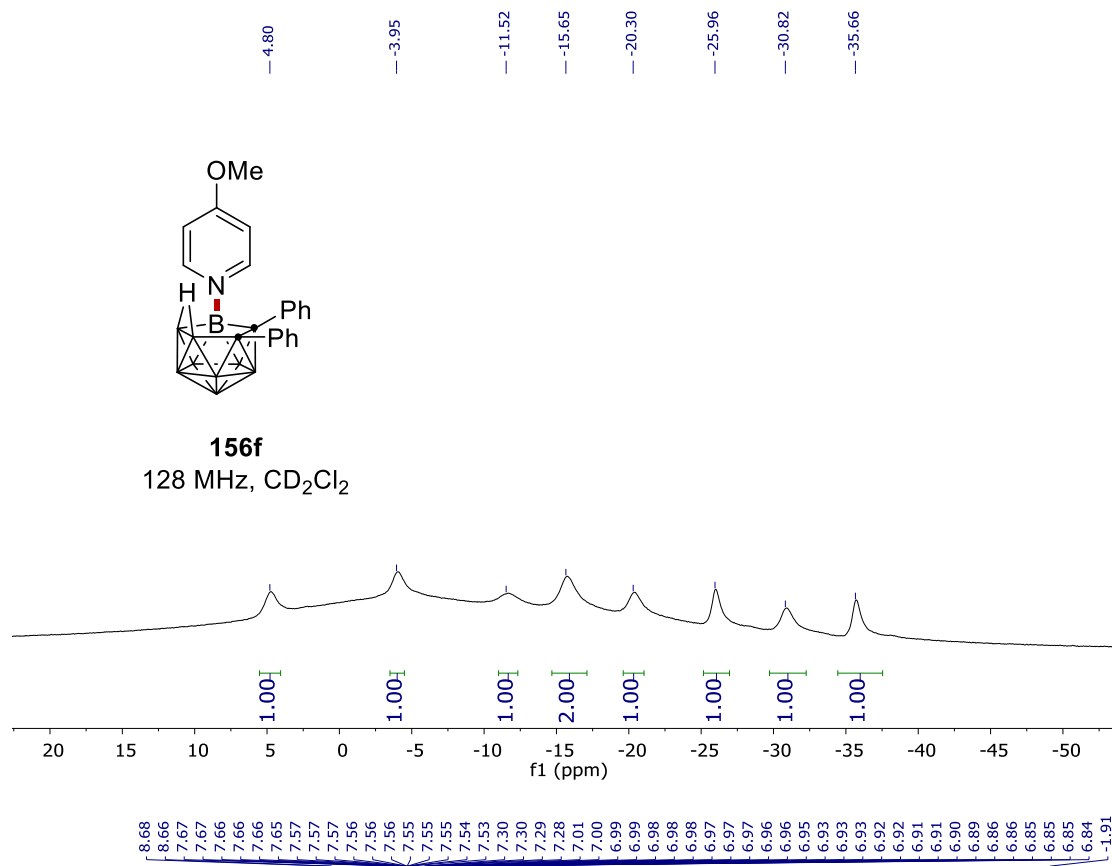
NMR Spectra



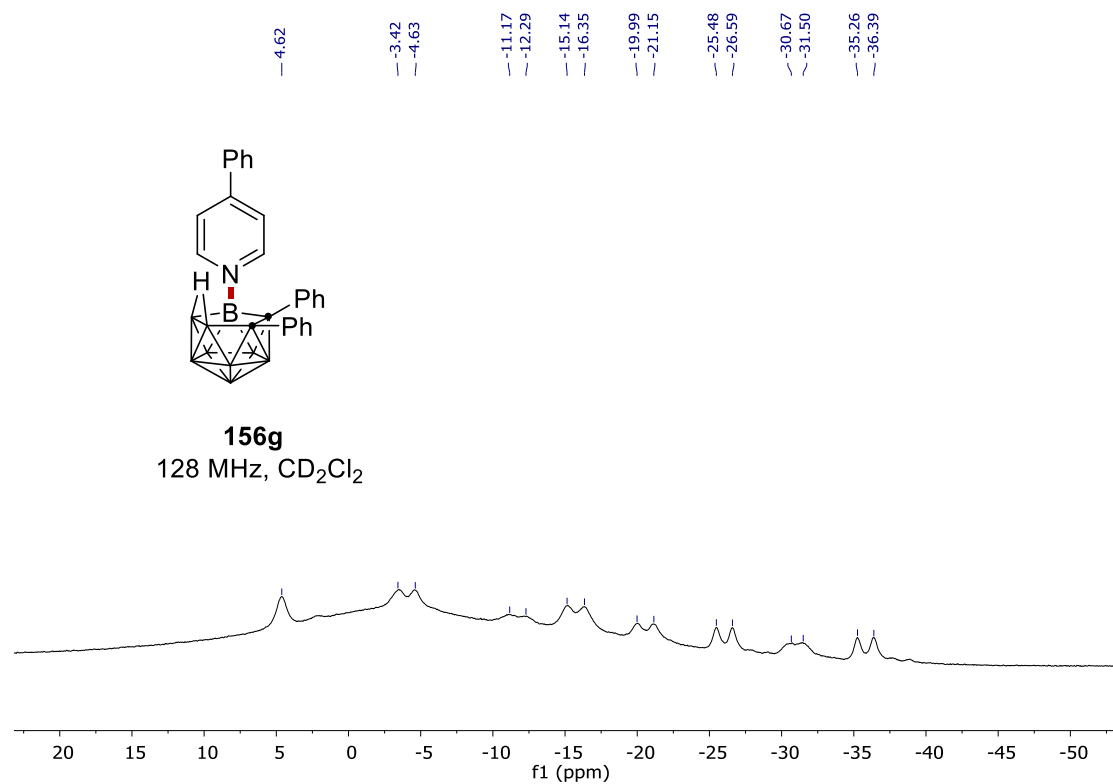
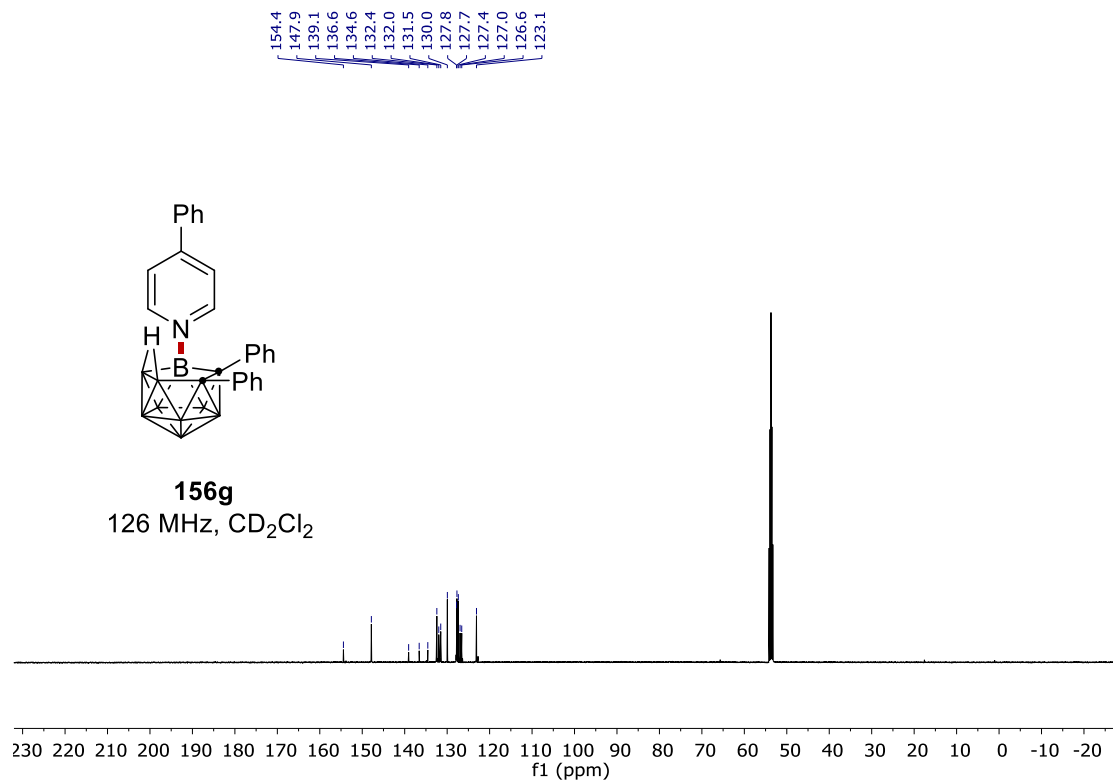
NMR Spectra



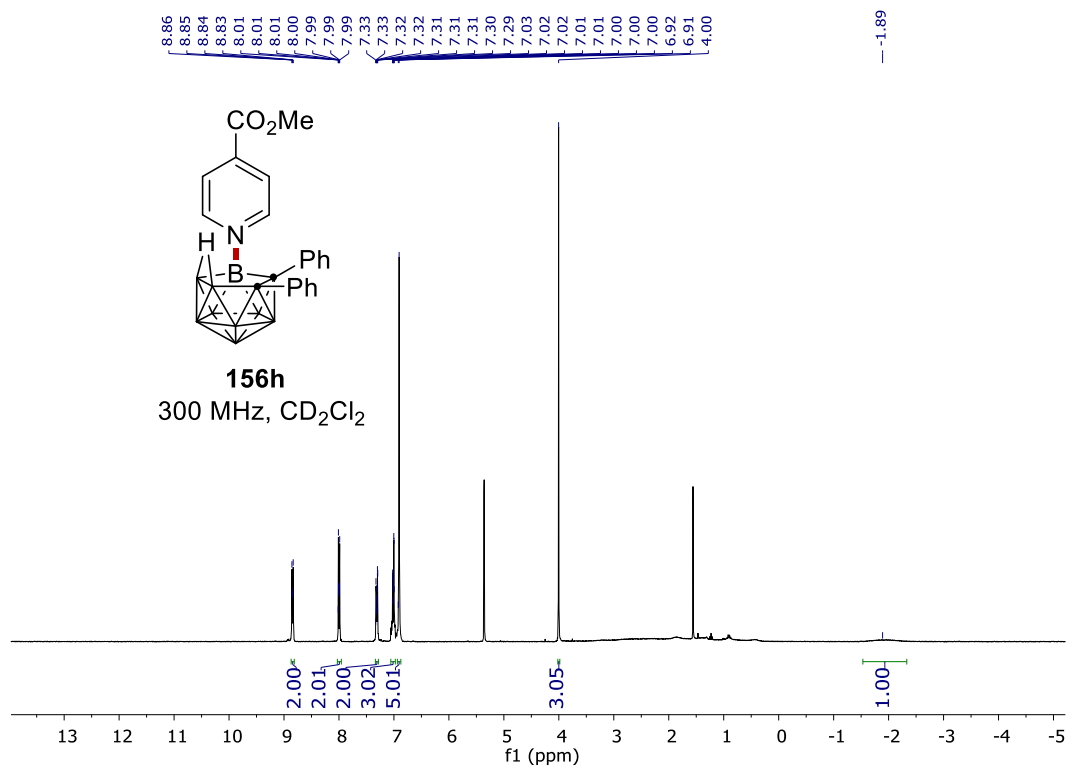
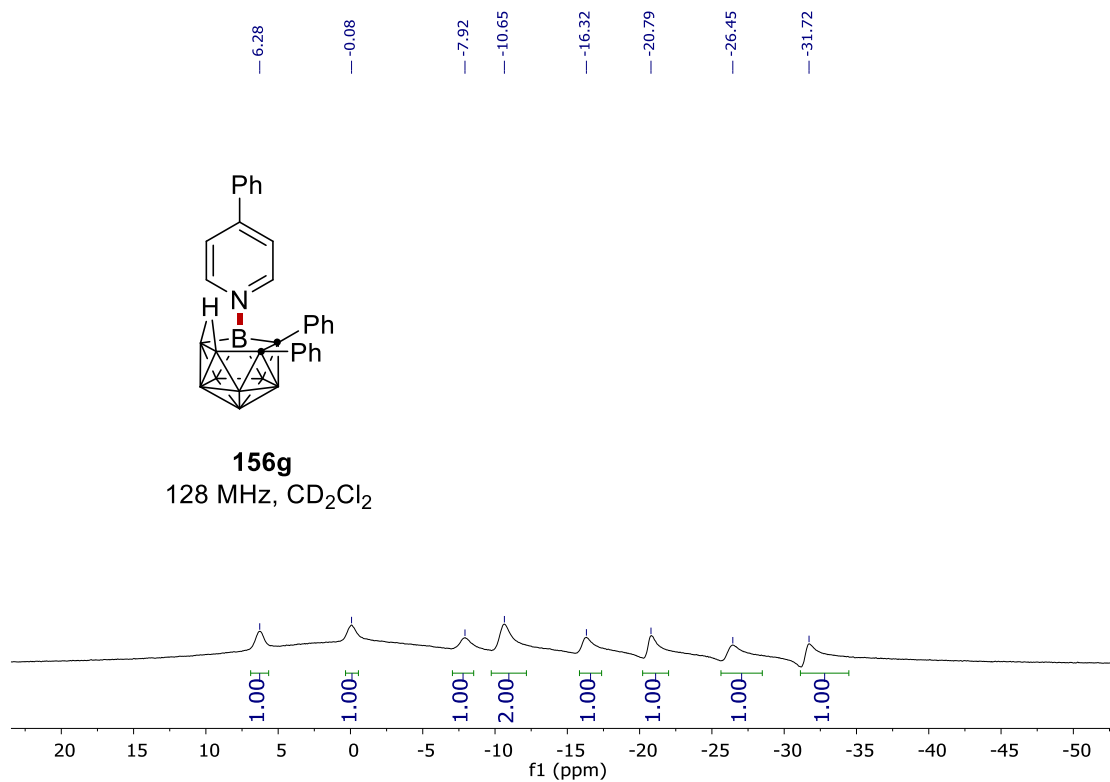
NMR Spectra



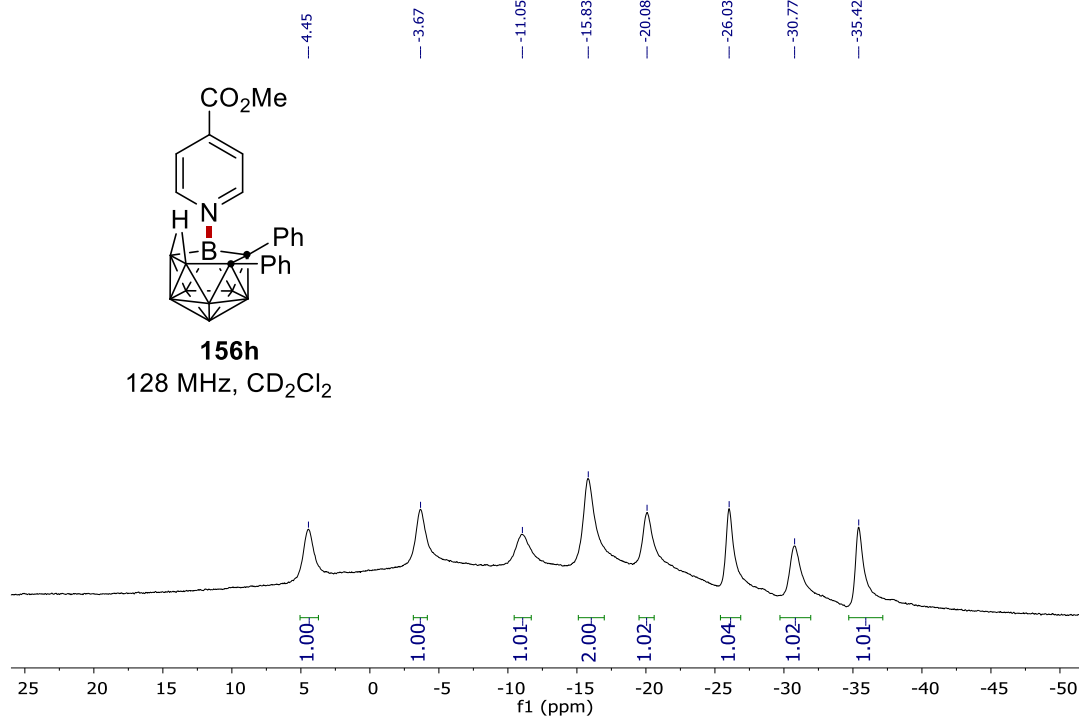
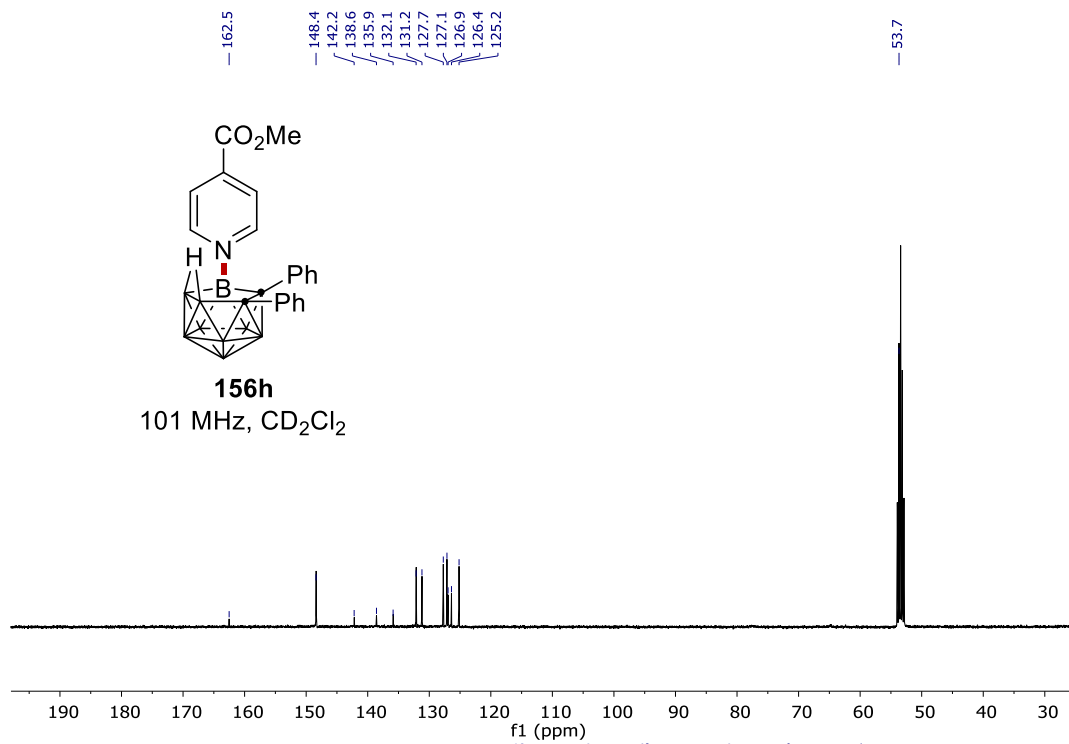
NMR Spectra



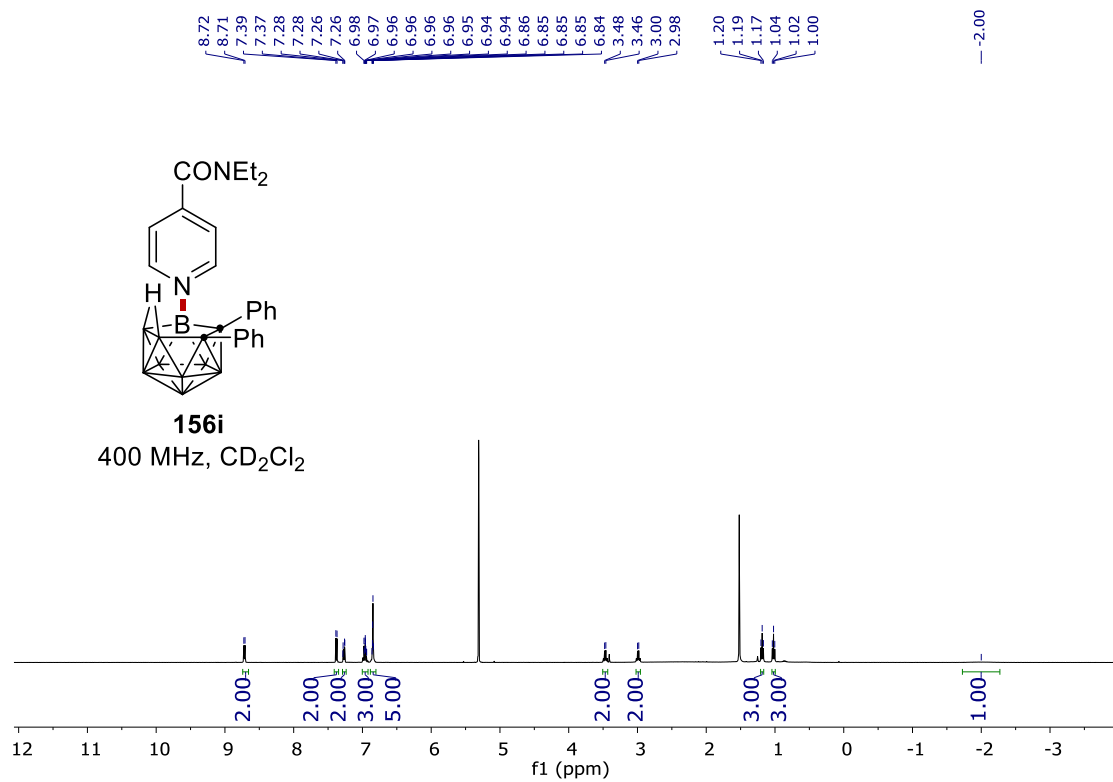
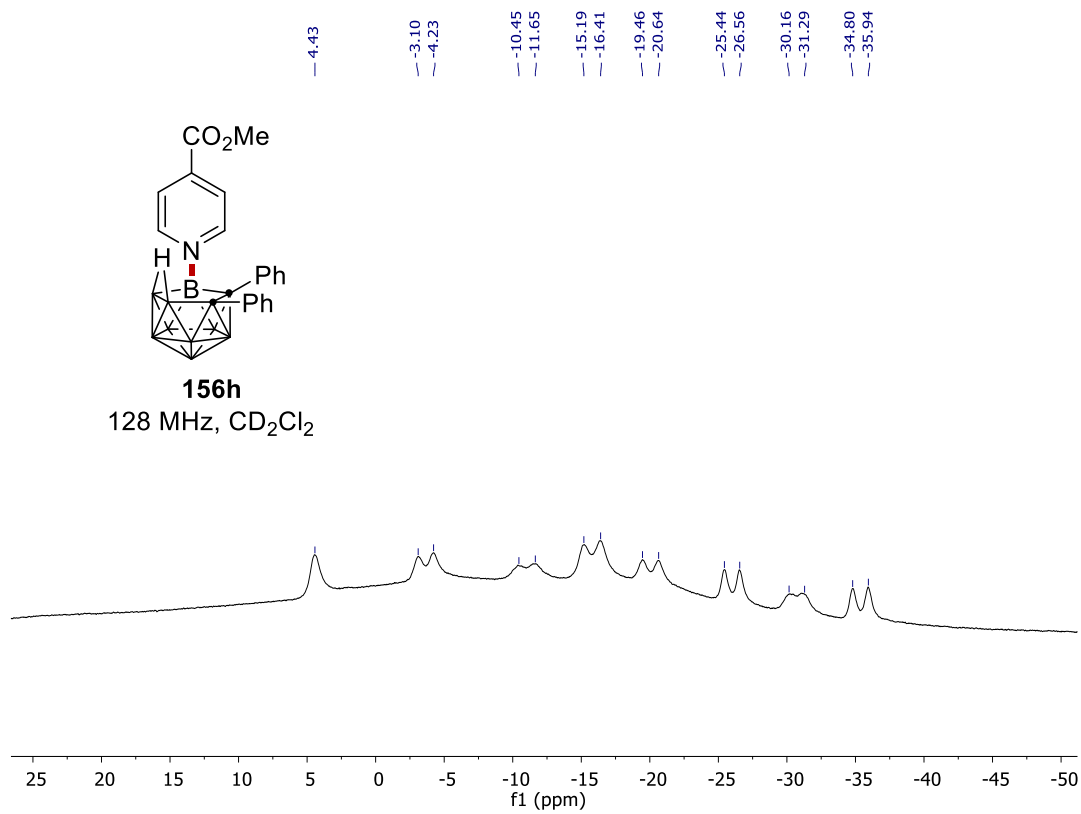
NMR Spectra



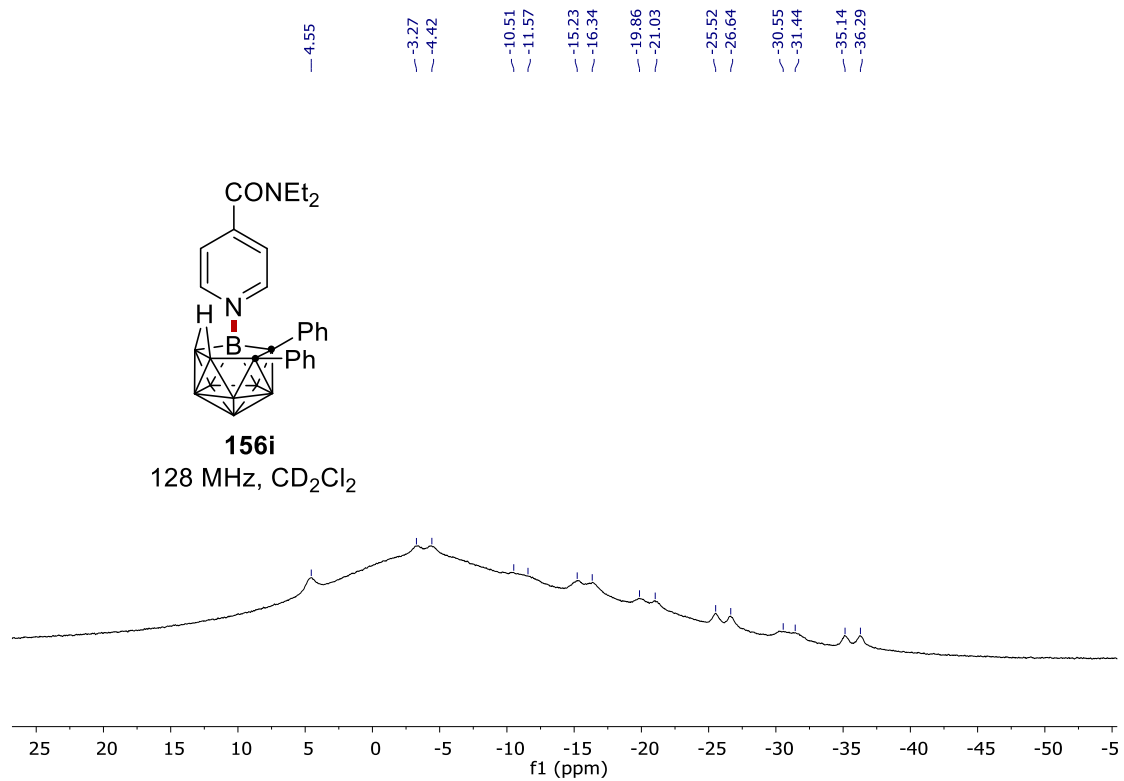
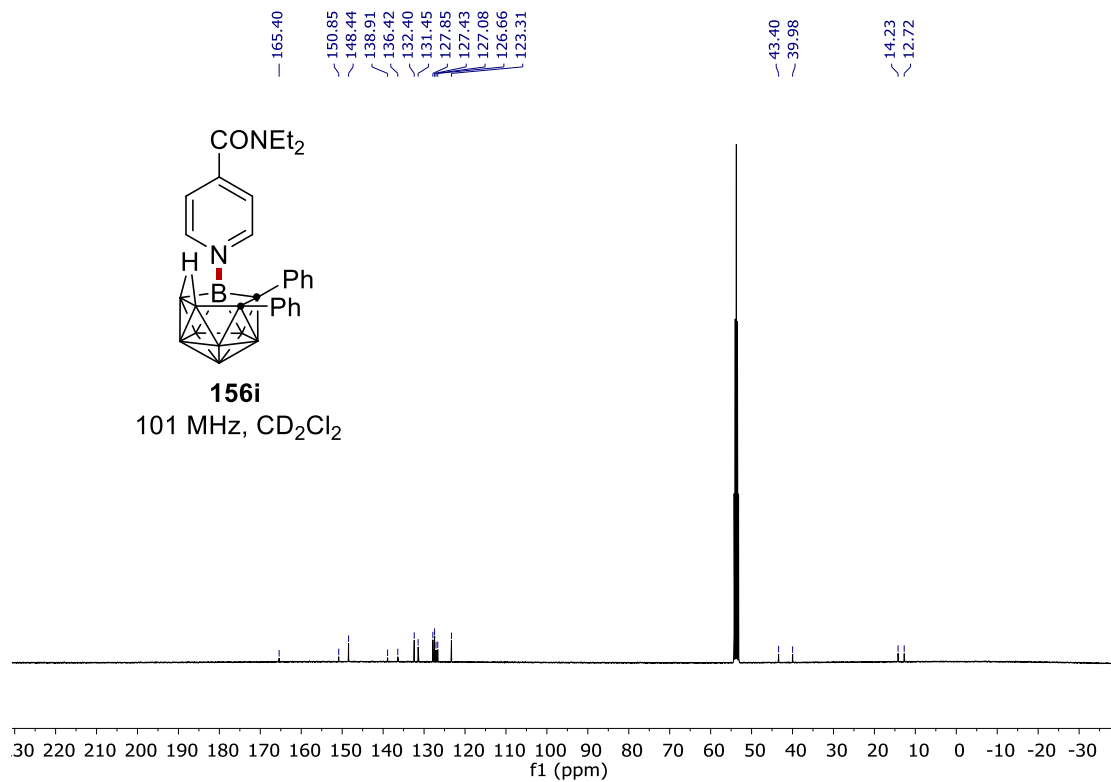
NMR Spectra



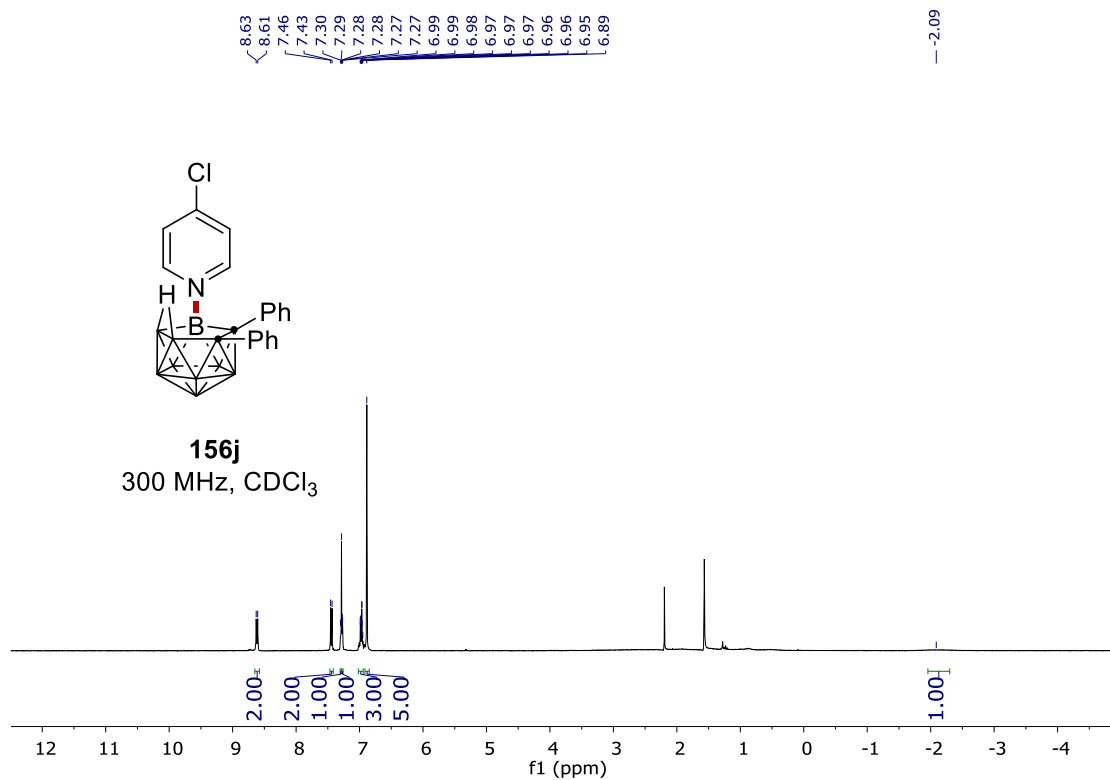
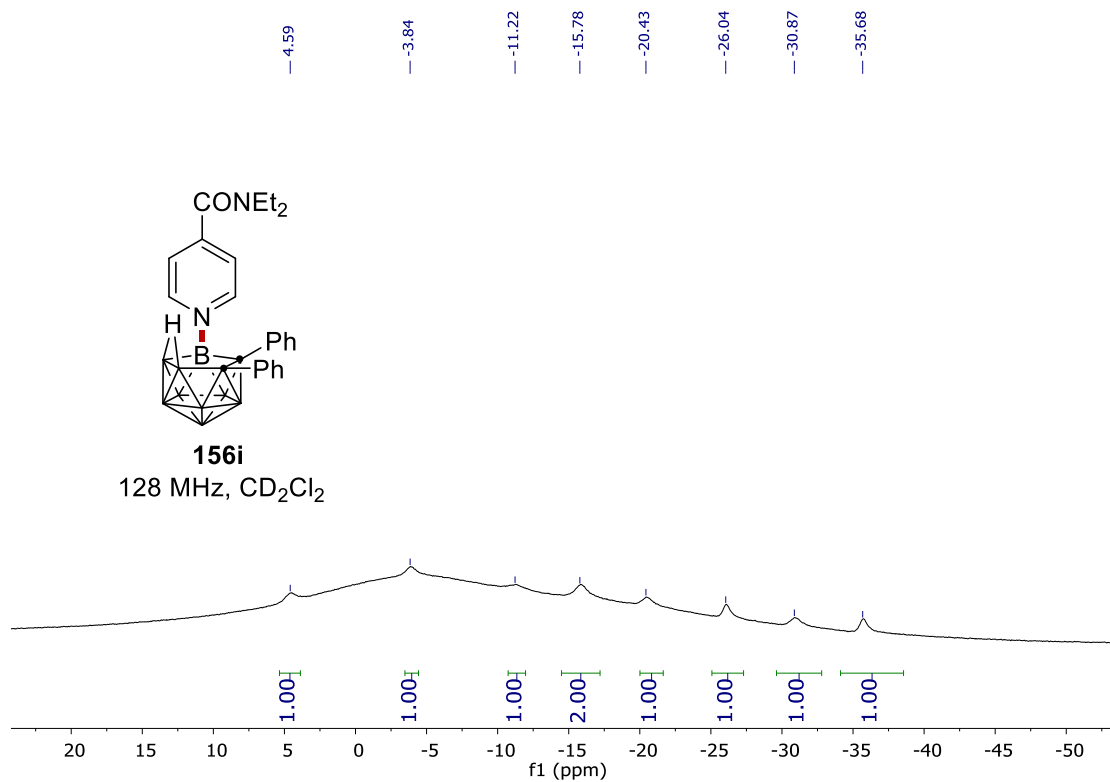
NMR Spectra



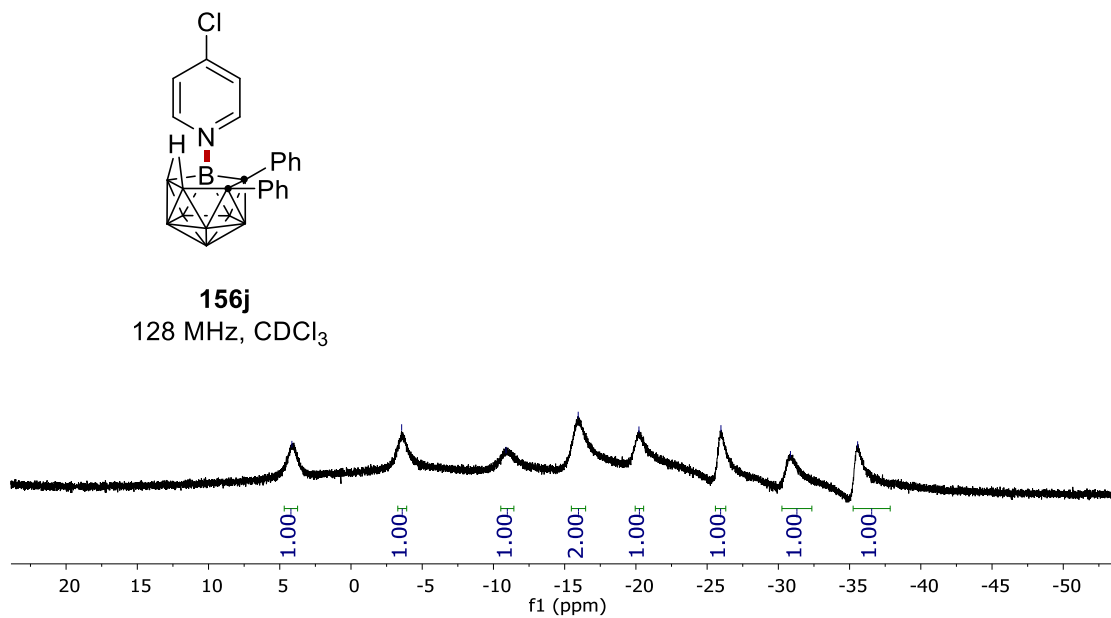
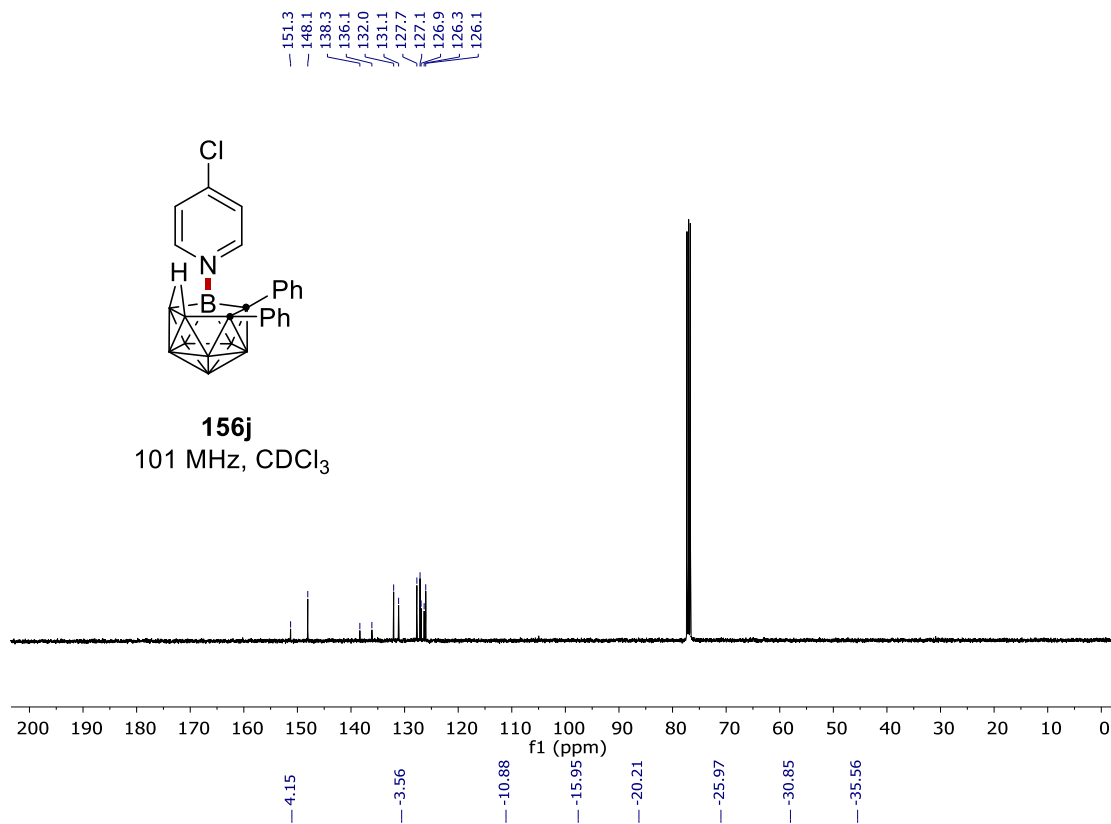
NMR Spectra



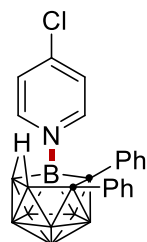
NMR Spectra



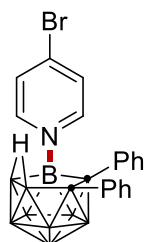
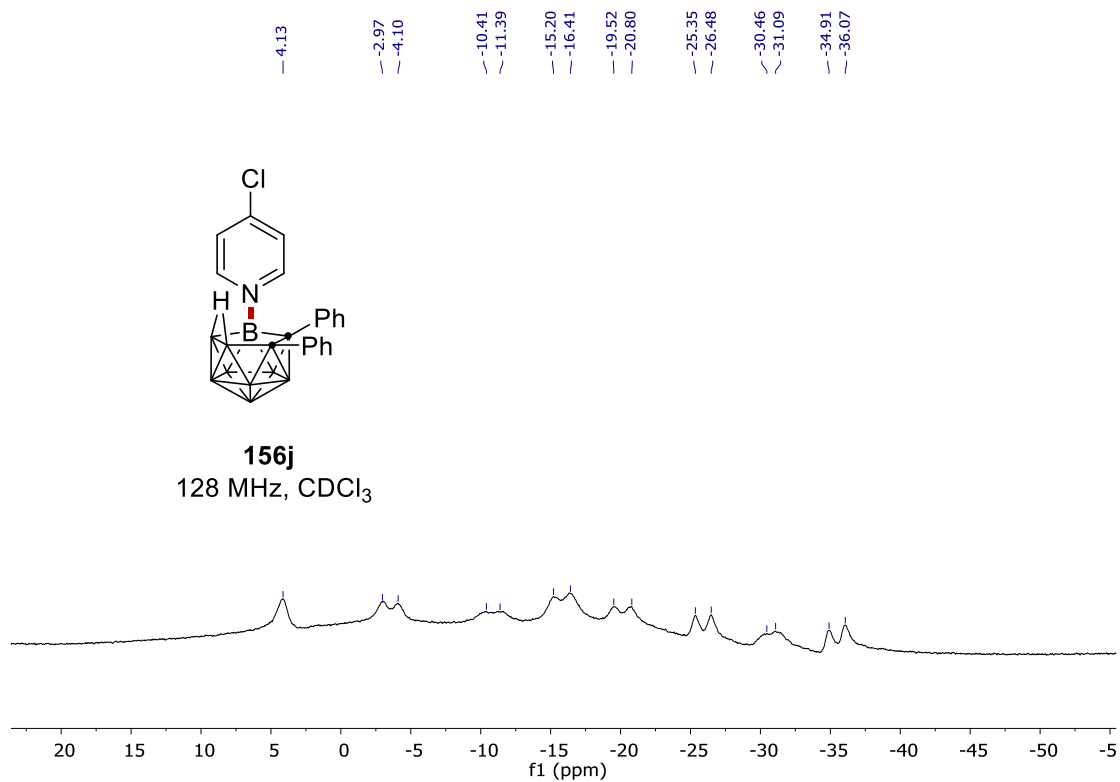
NMR Spectra



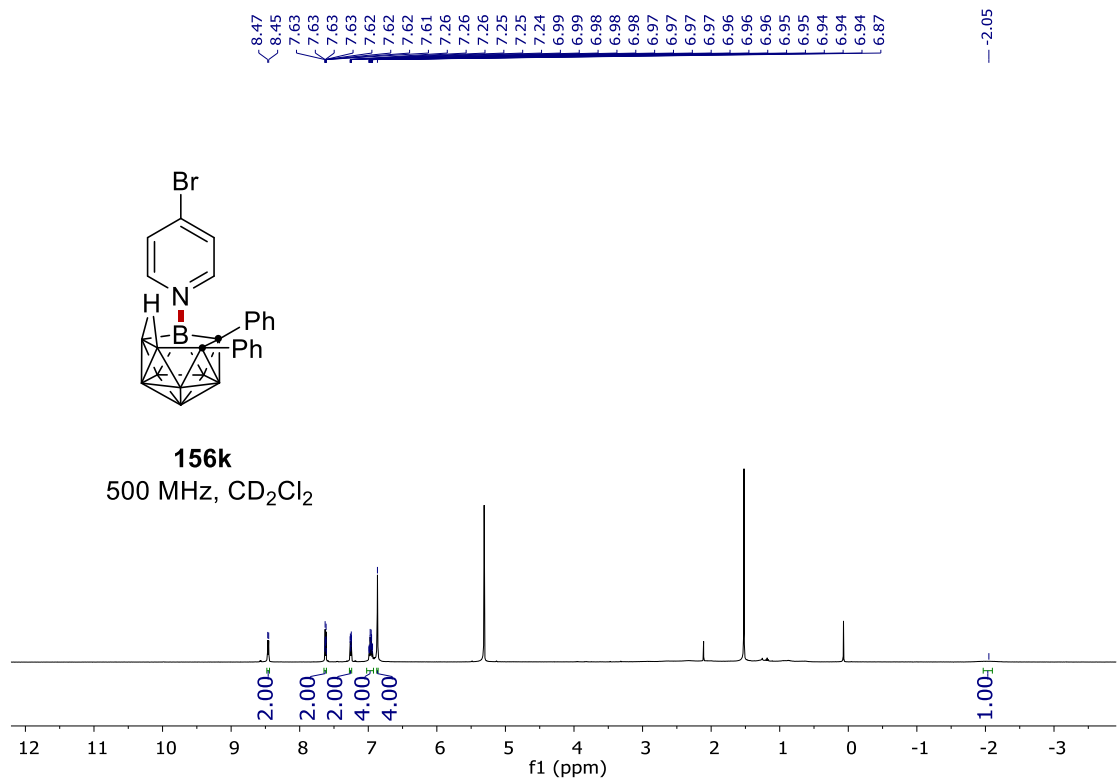
NMR Spectra



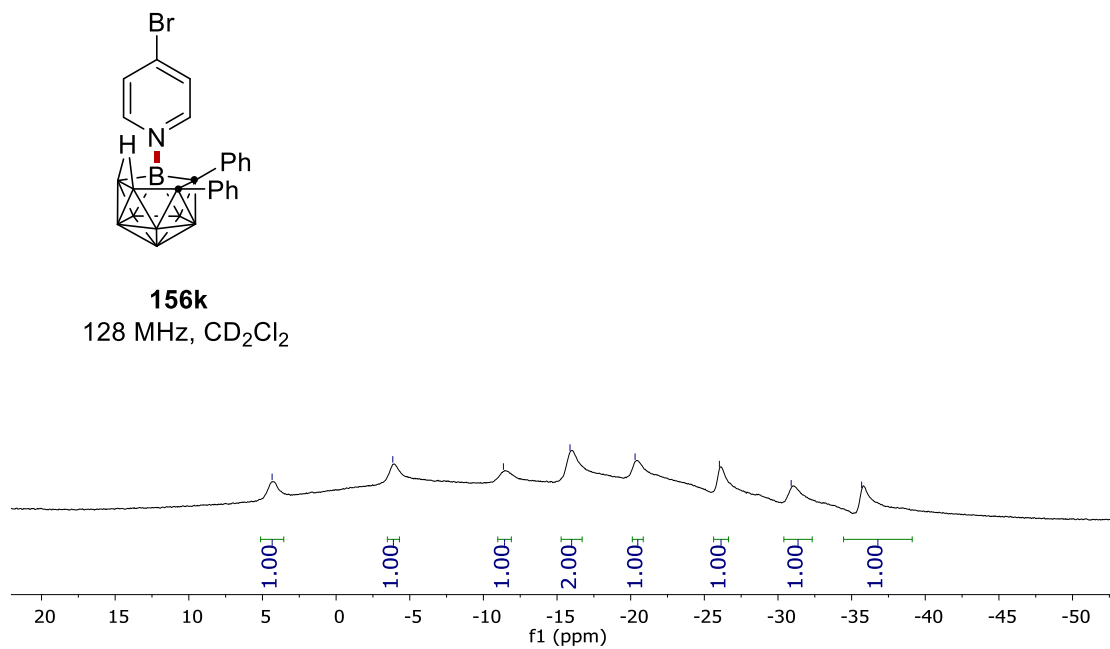
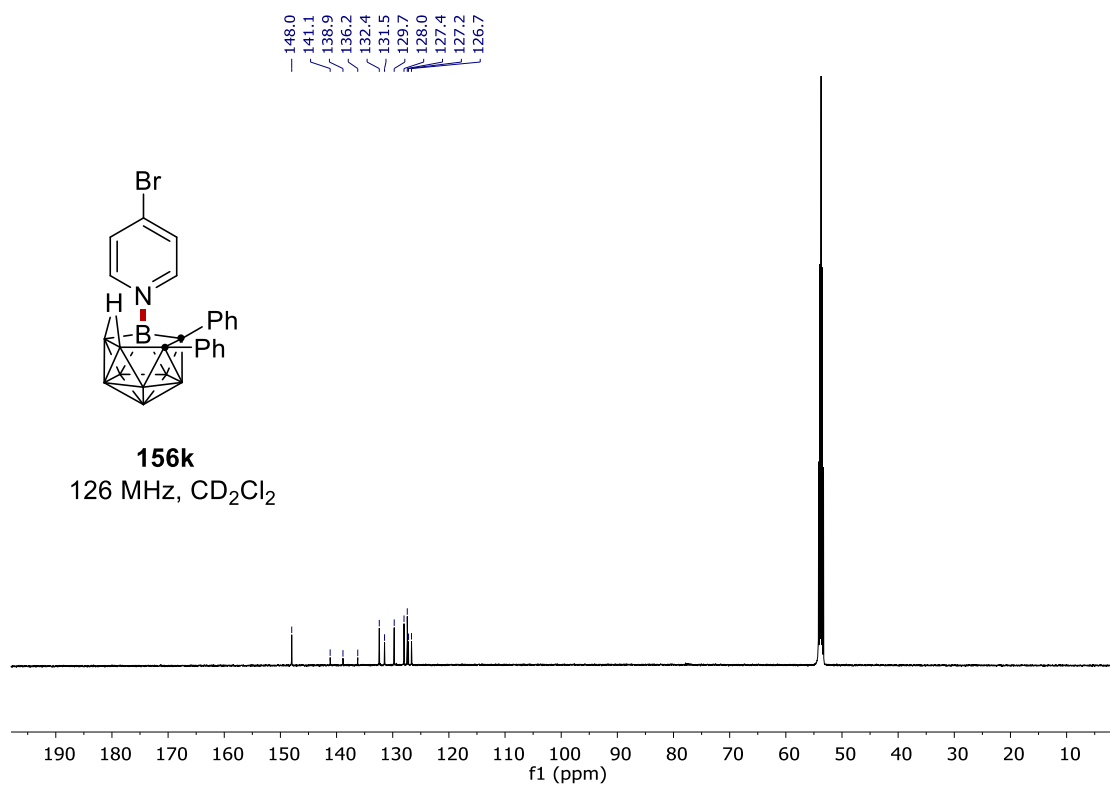
156j
128 MHz, CDCl₃



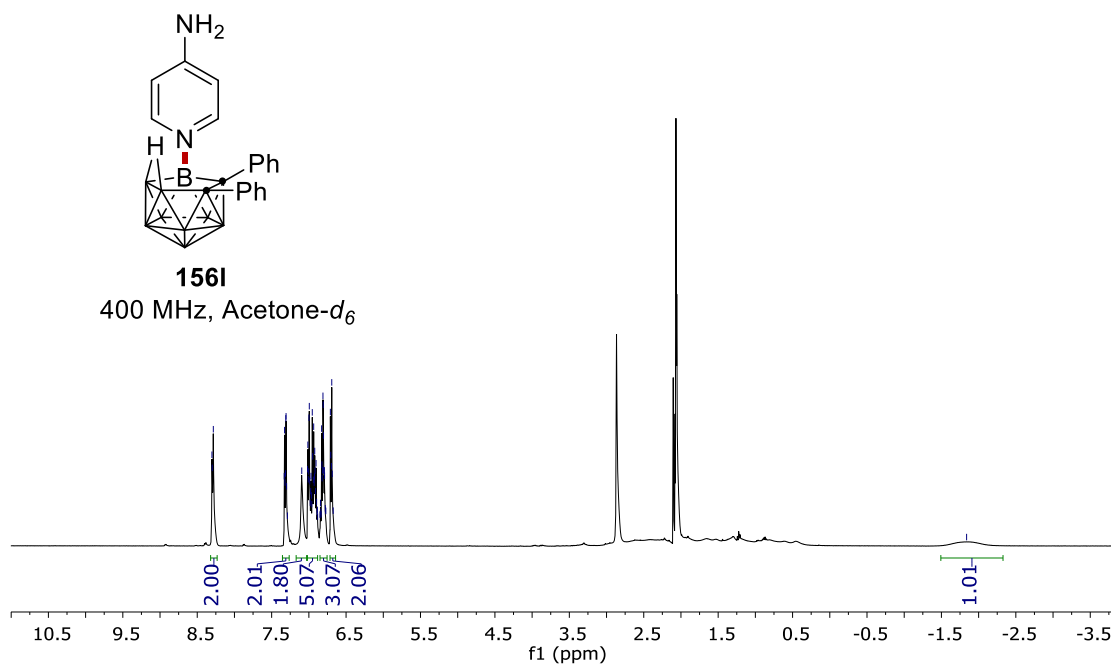
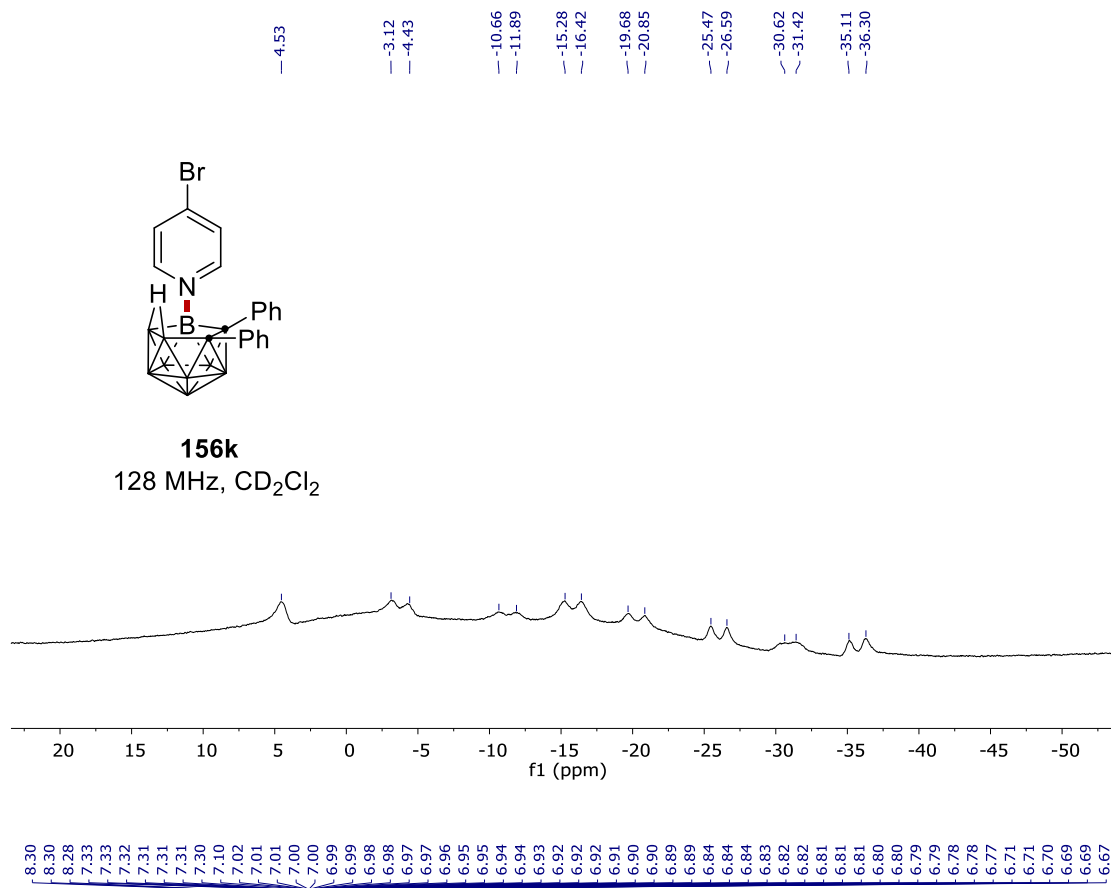
156k
500 MHz, CD₂Cl₂



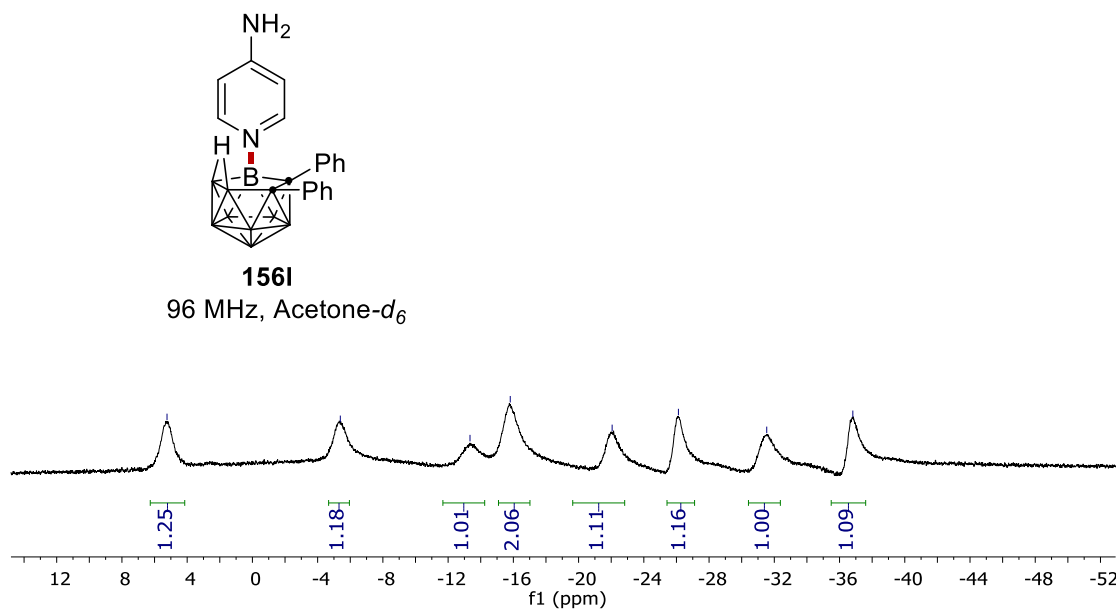
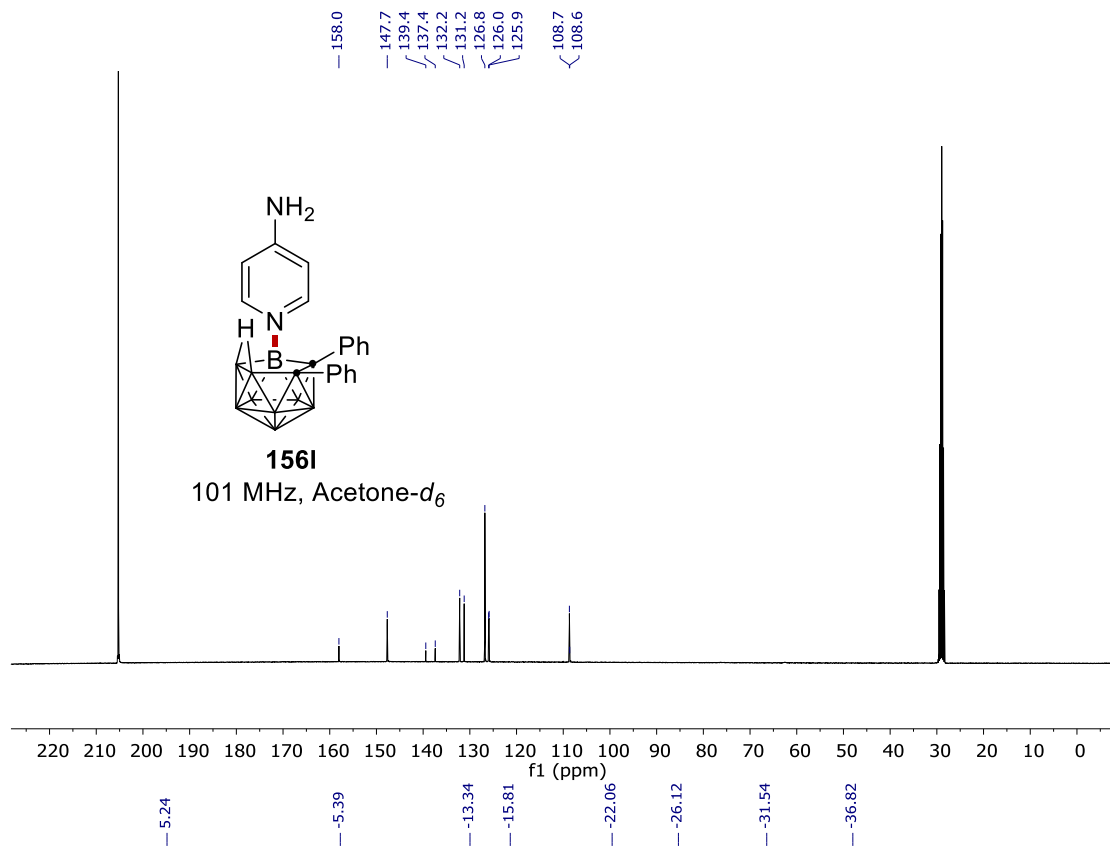
NMR Spectra



NMR Spectra

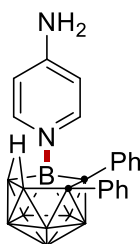


NMR Spectra



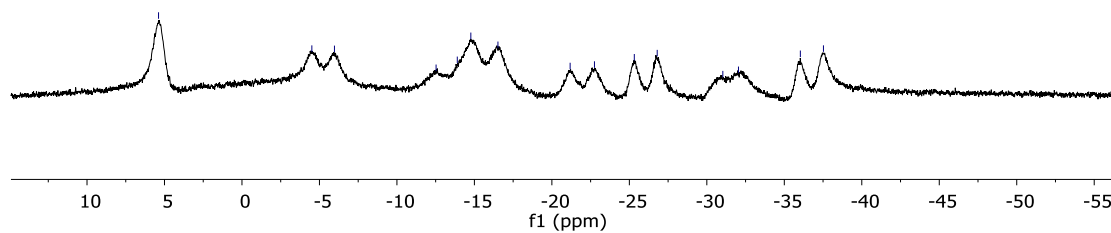
NMR Spectra

-5.38
 -4.51
 -5.97
 -12.53
 -13.90
 -14.77
 -16.52
 -21.18
 -22.75
 -25.32
 -26.80
 -31.03
 -32.04
 -36.04
 -37.53

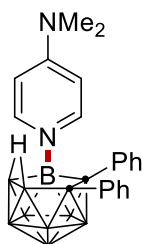


156I

96 MHz, Acetone- d_6

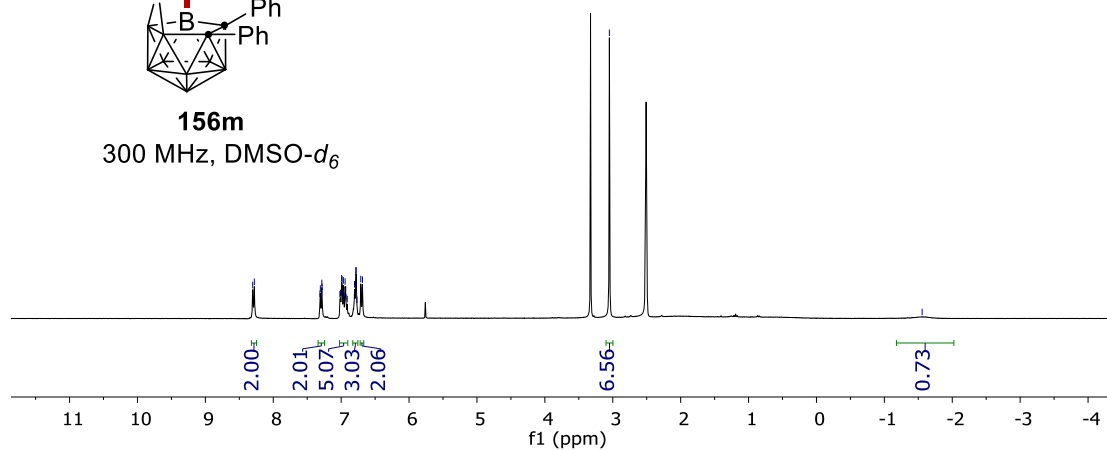


8.30
 8.28
 7.31
 7.29
 7.29
 7.28
 7.02
 7.01
 6.99
 6.99
 6.97
 6.96
 6.94
 6.93
 6.93
 6.91
 6.80
 6.78
 6.78
 6.77
 6.71
 6.69
 6.69
 3.05
 -1.56

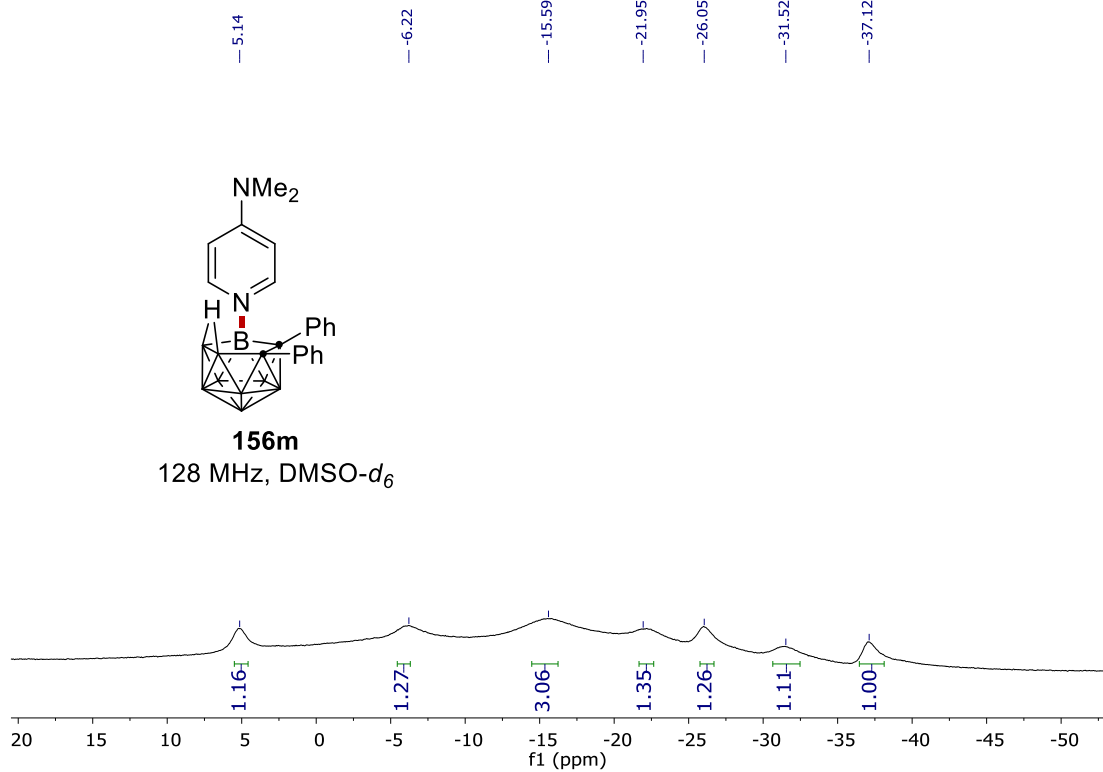
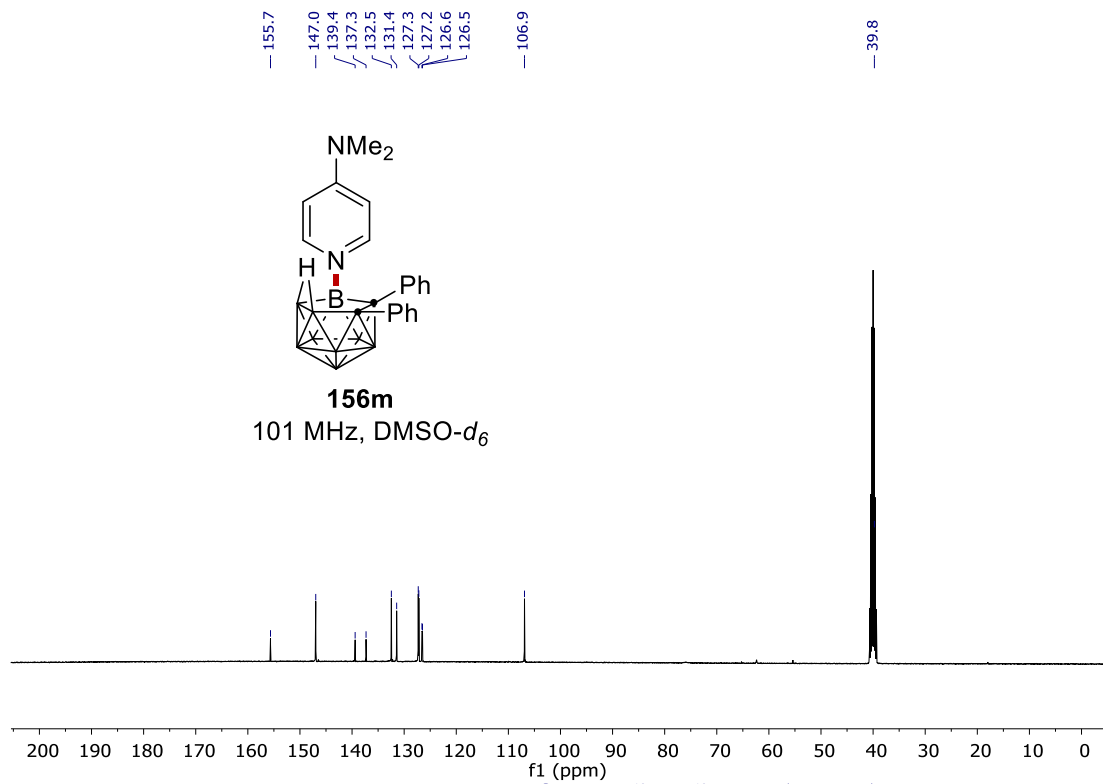


156m

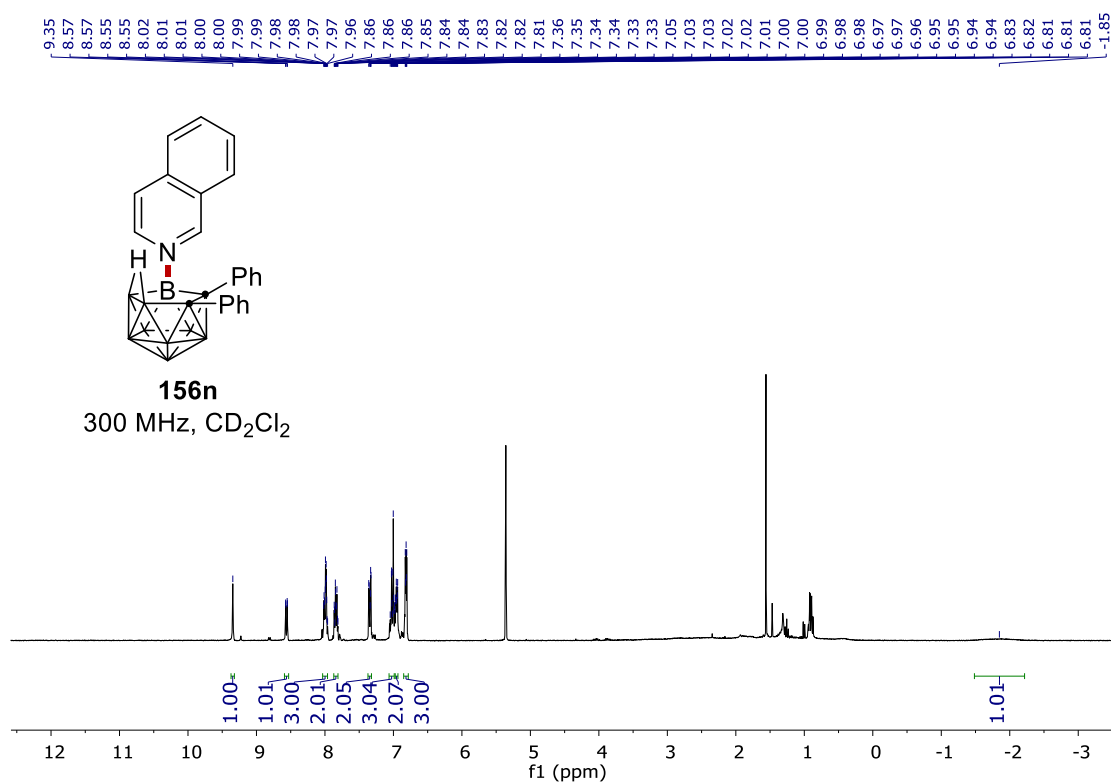
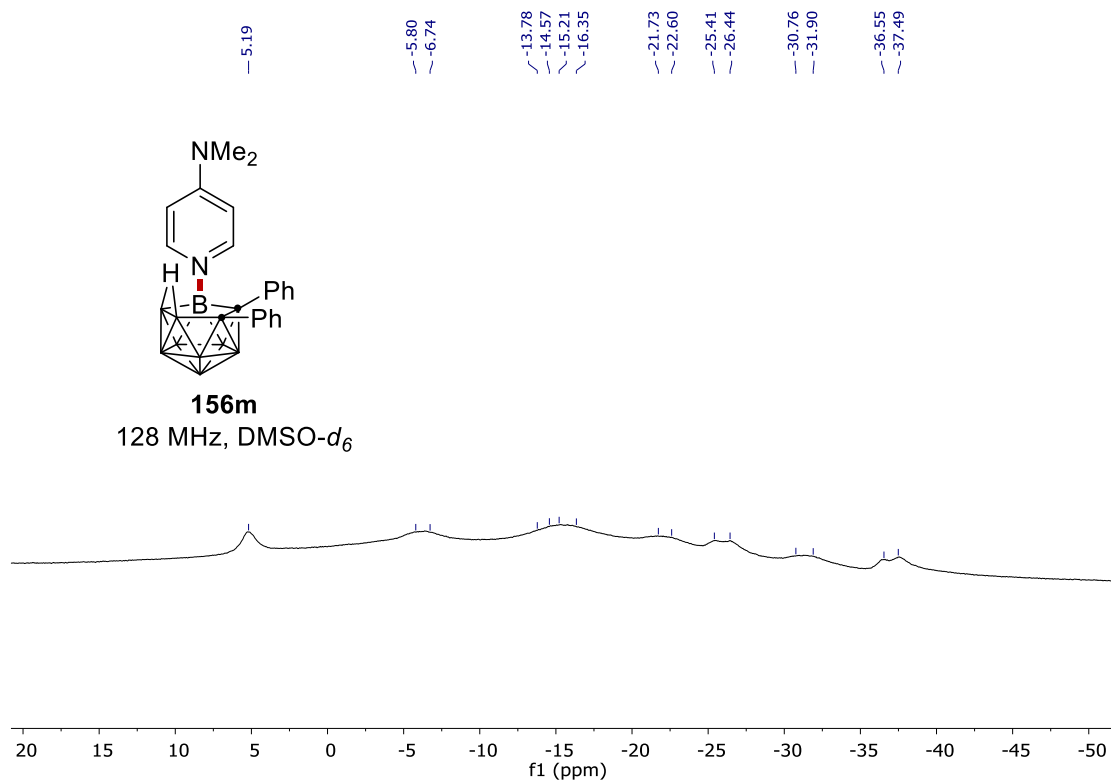
300 MHz, DMSO- d_6



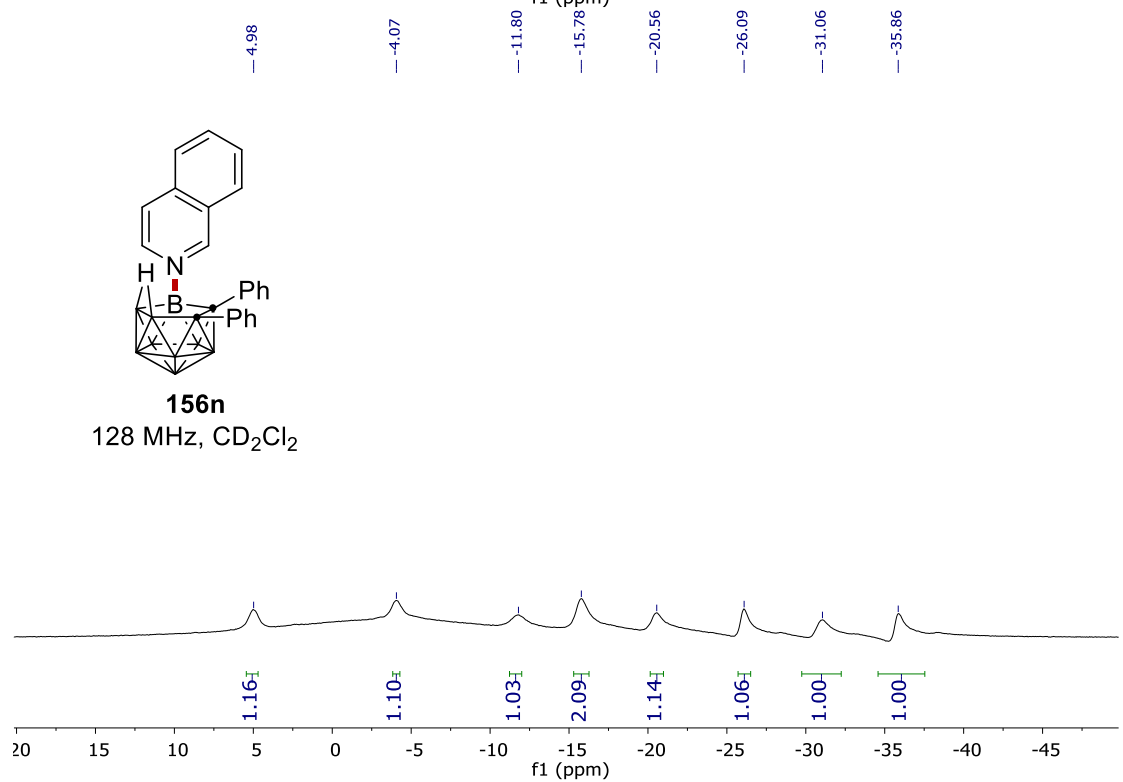
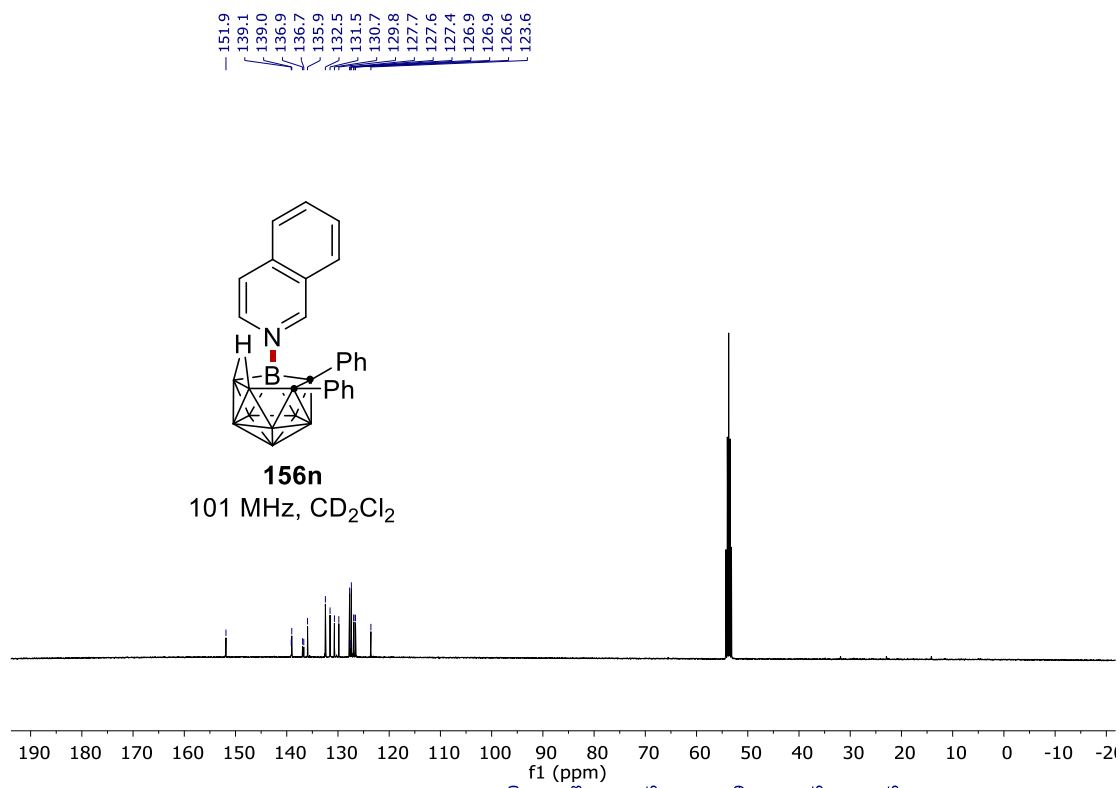
NMR Spectra



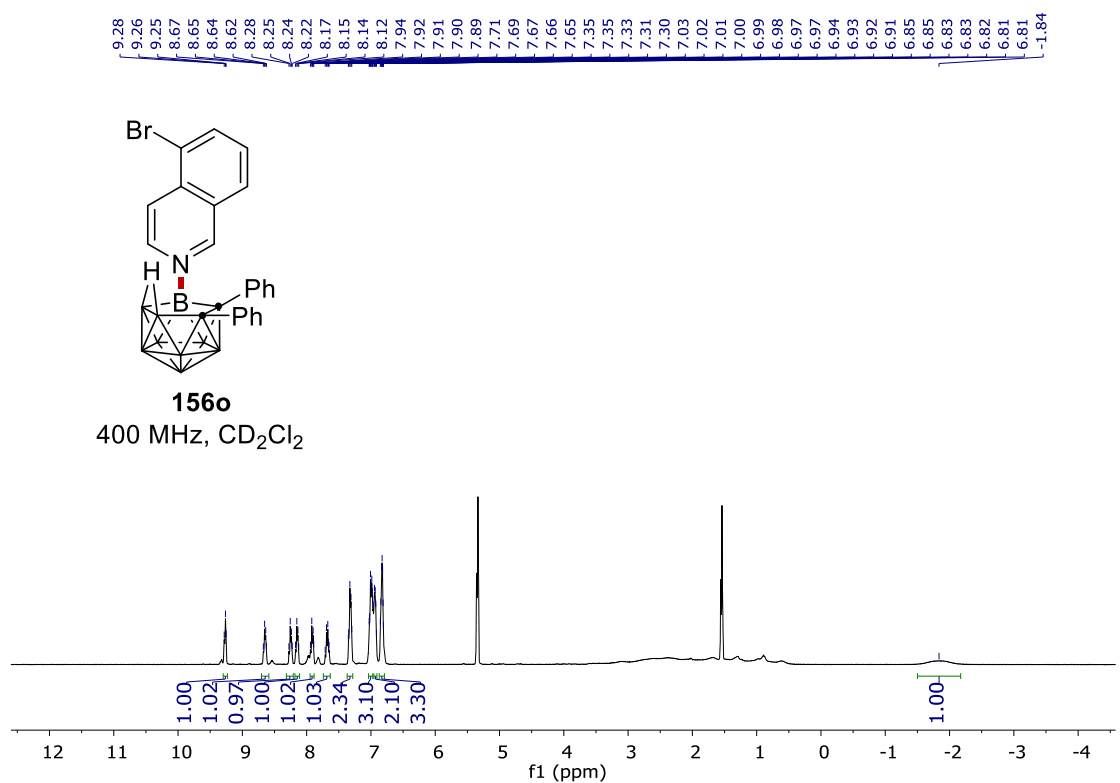
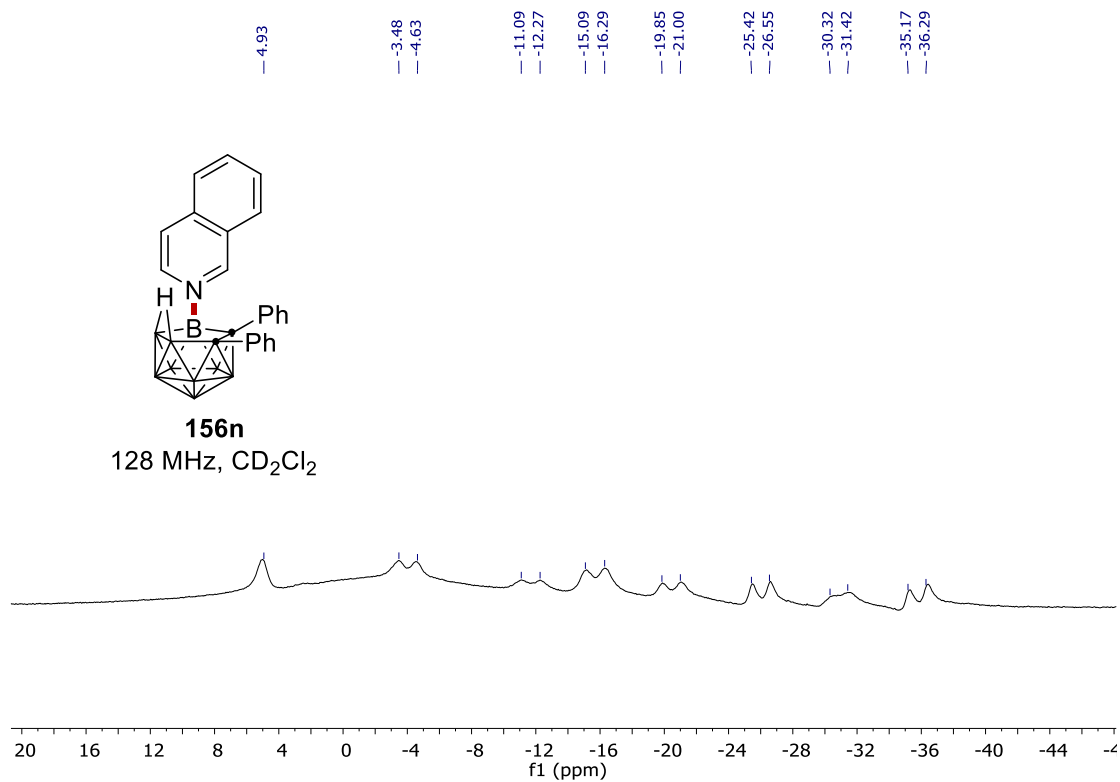
NMR Spectra



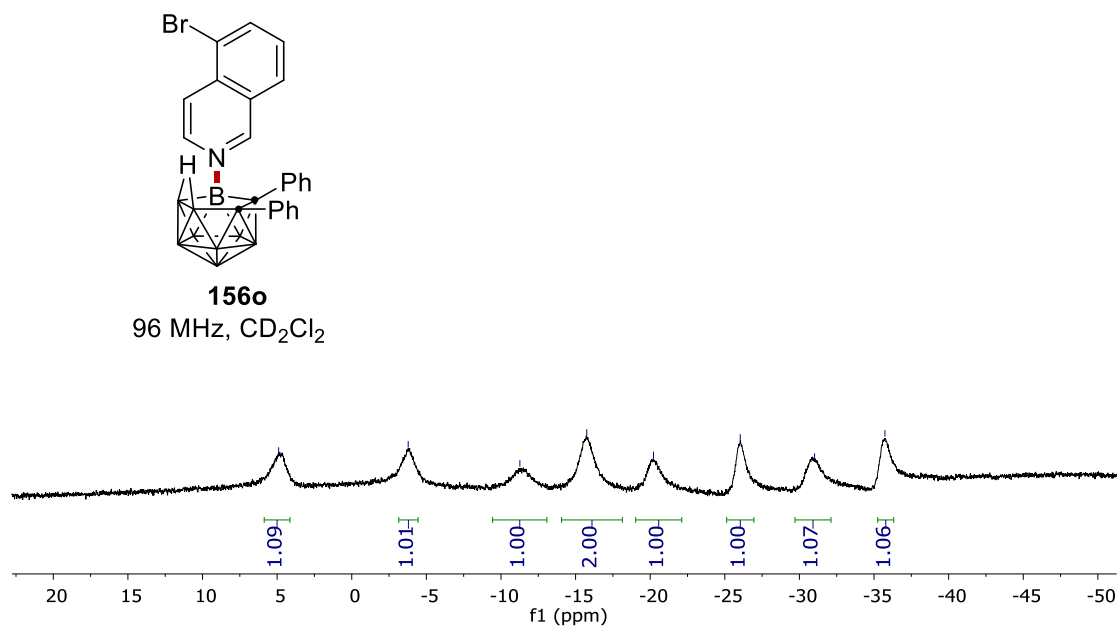
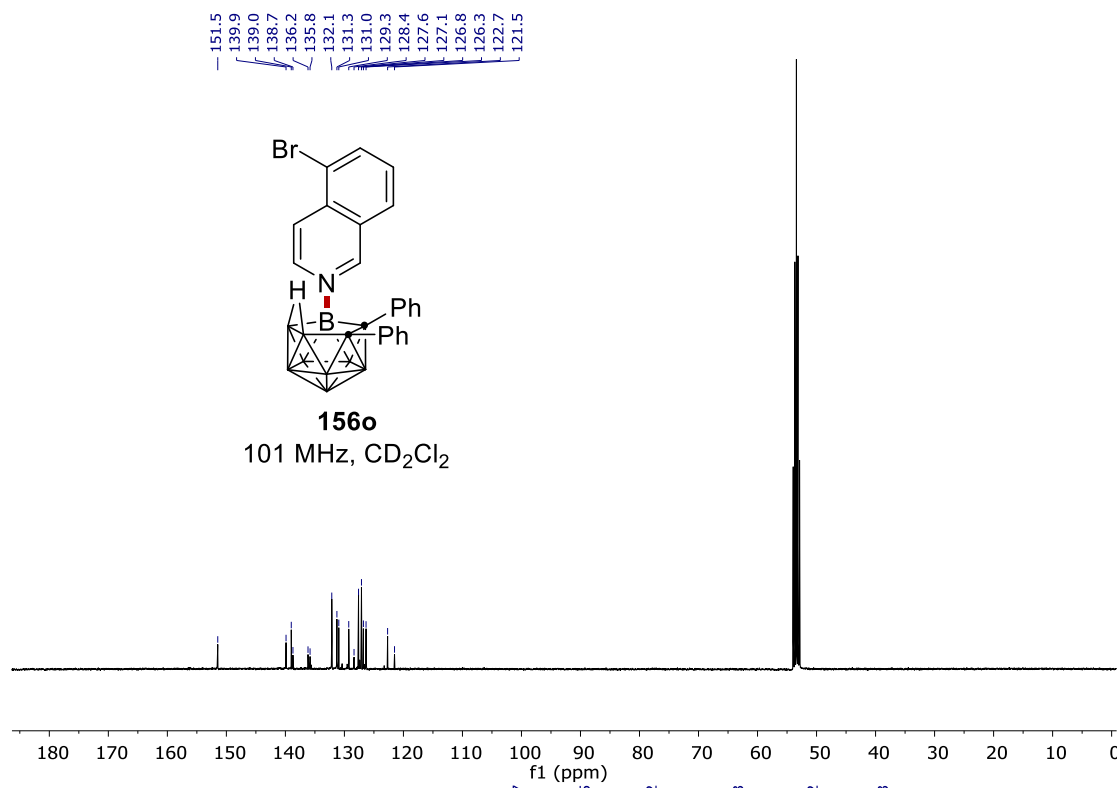
NMR Spectra



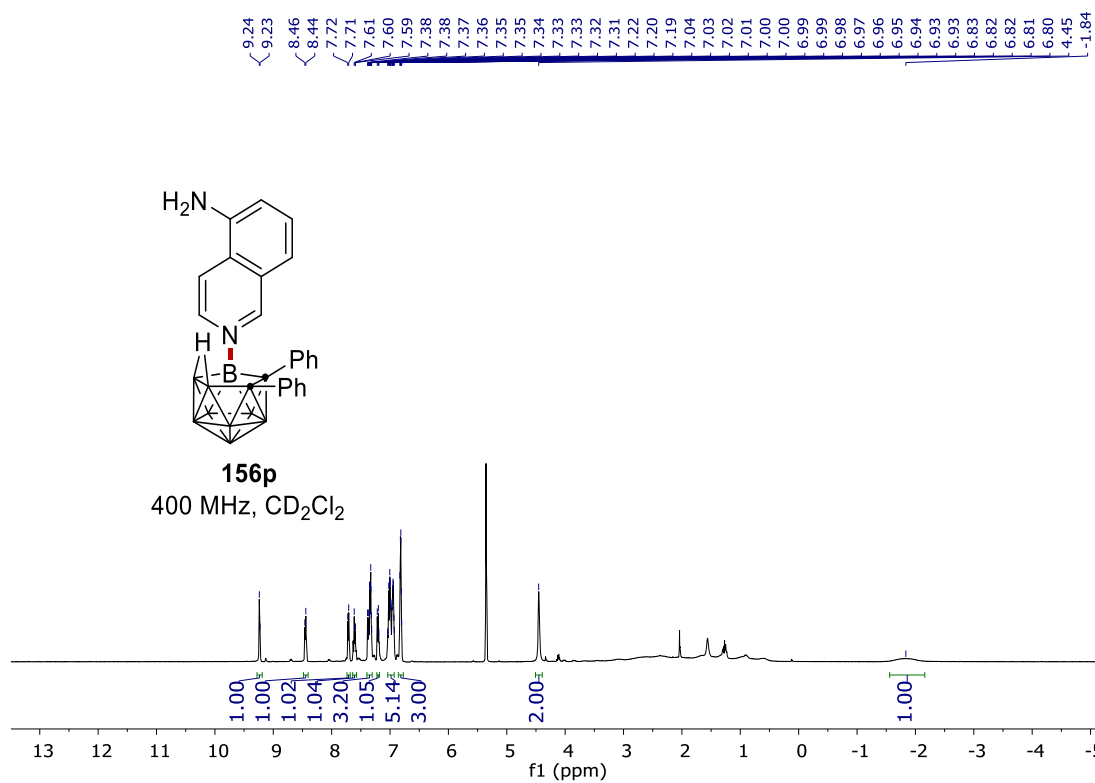
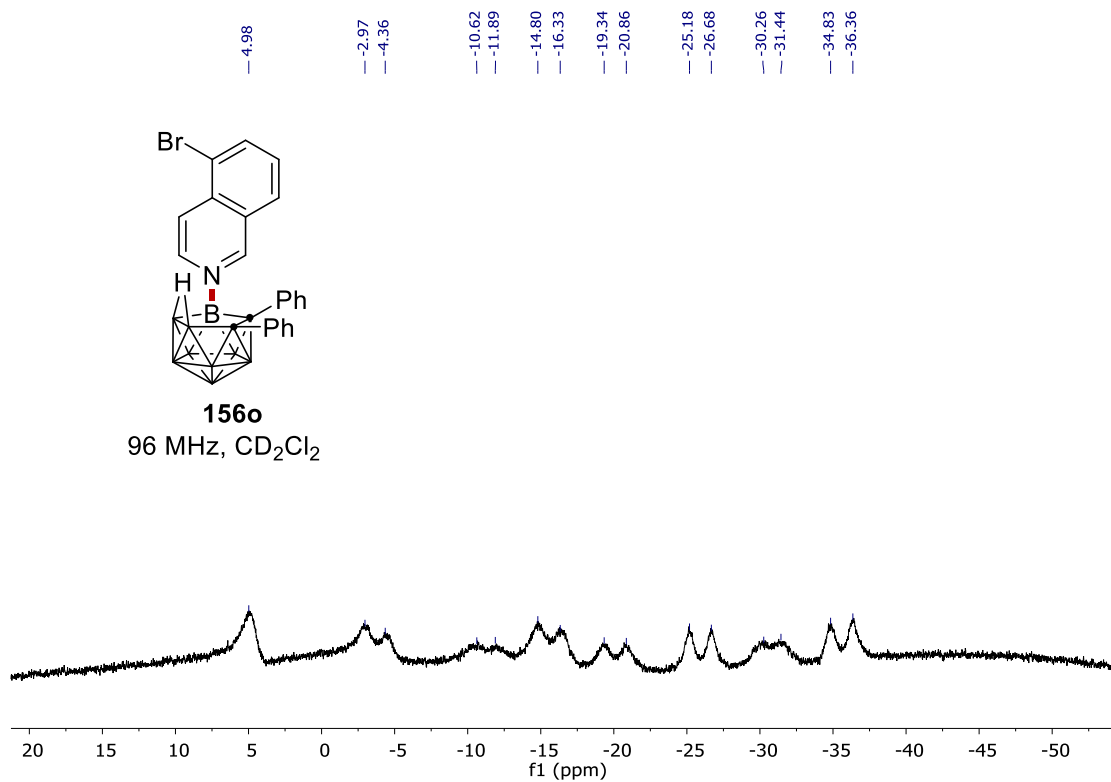
NMR Spectra



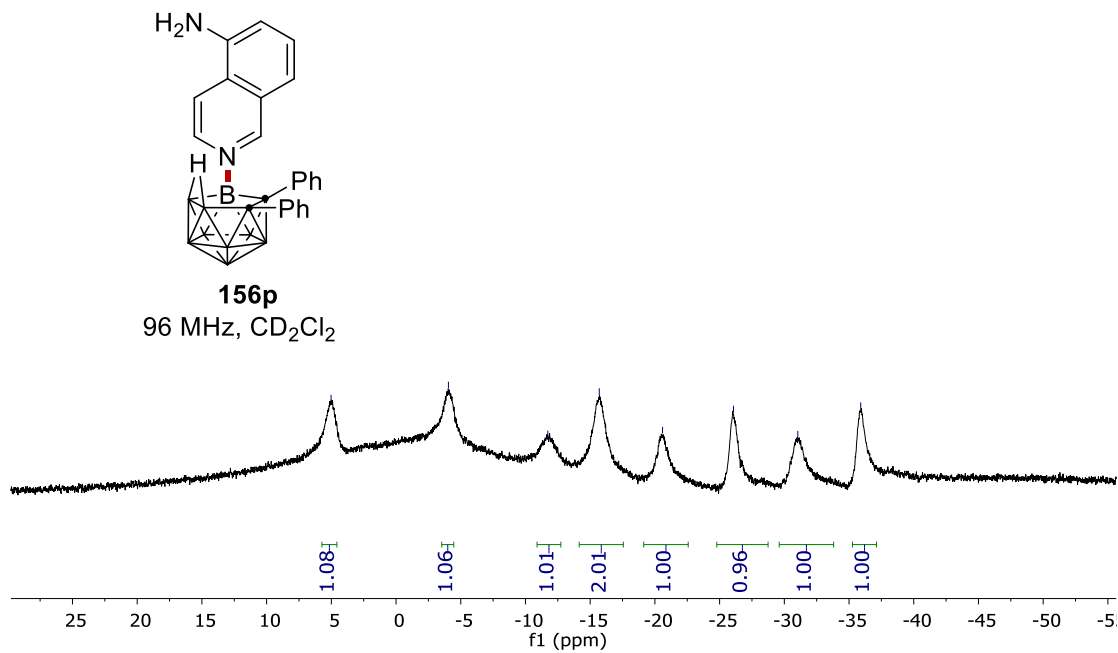
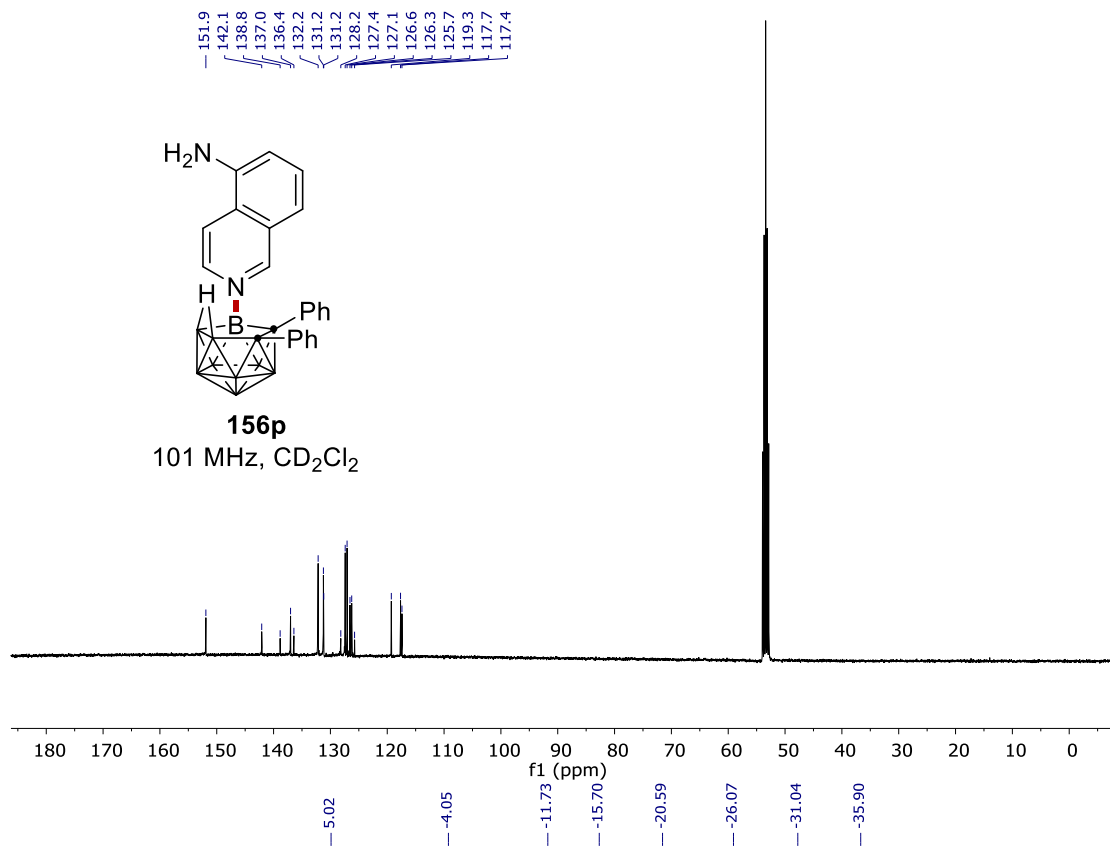
NMR Spectra



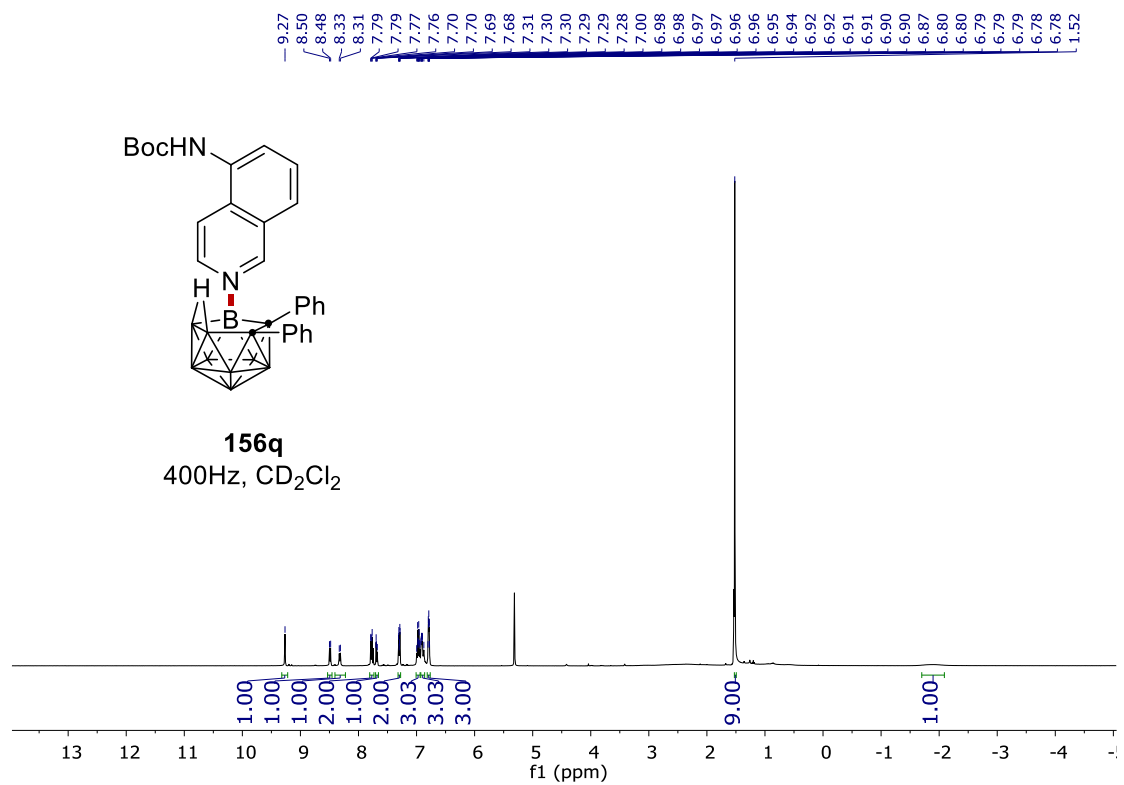
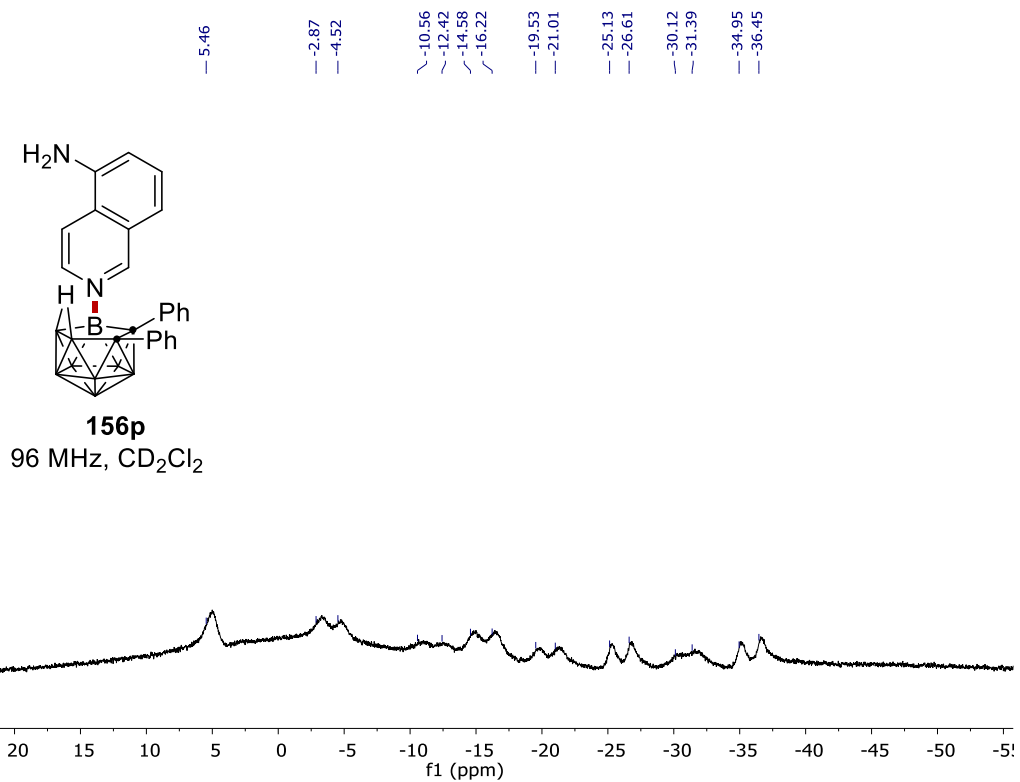
NMR Spectra



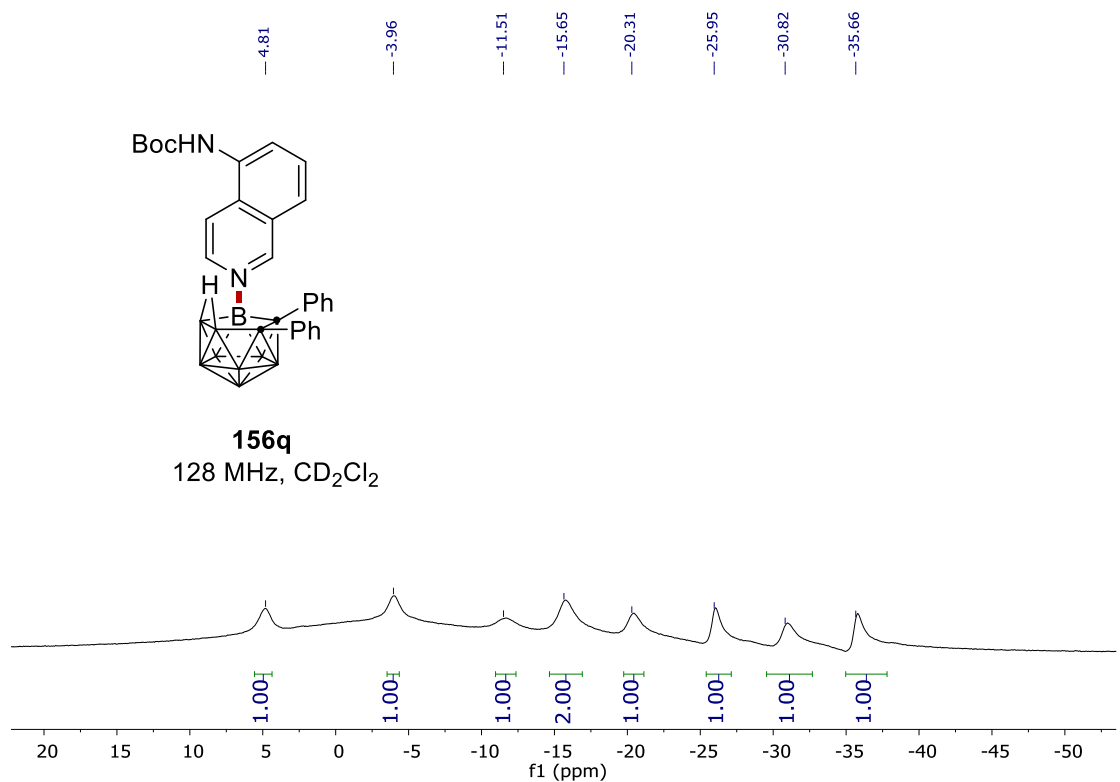
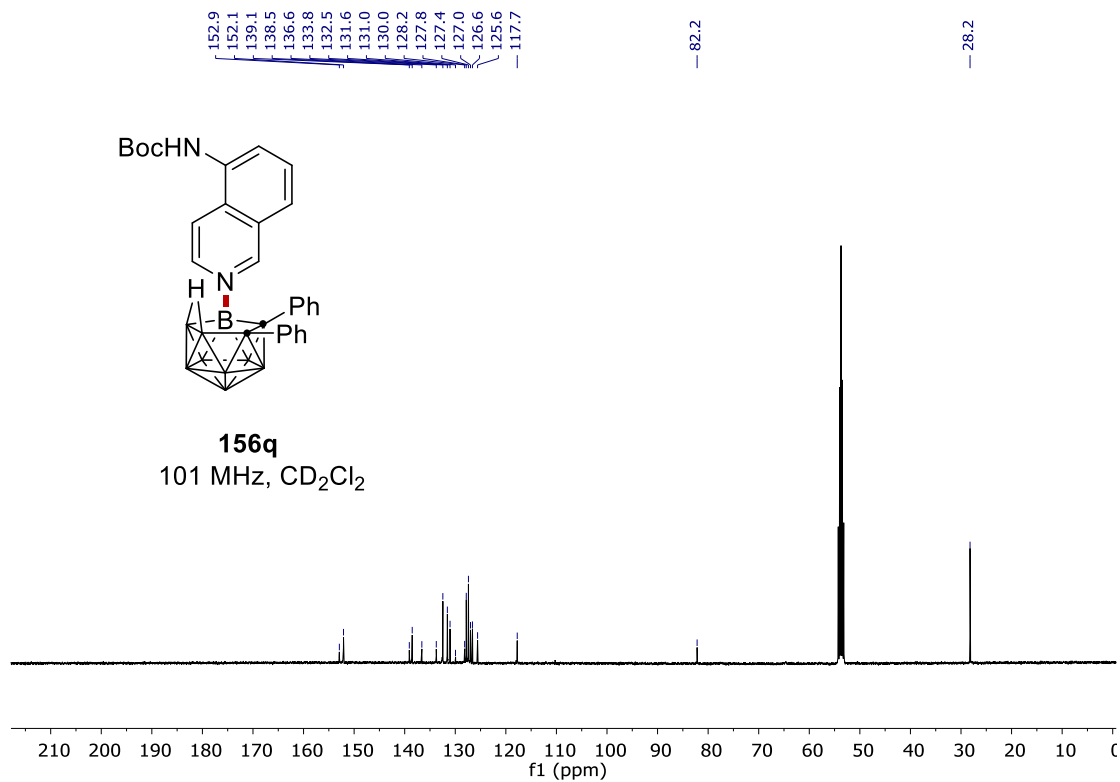
NMR Spectra



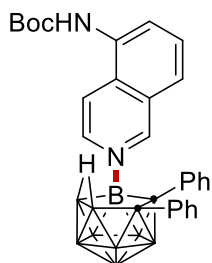
NMR Spectra



NMR Spectra

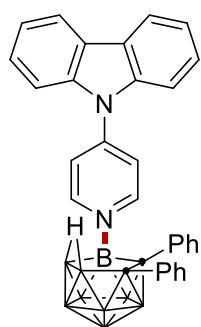
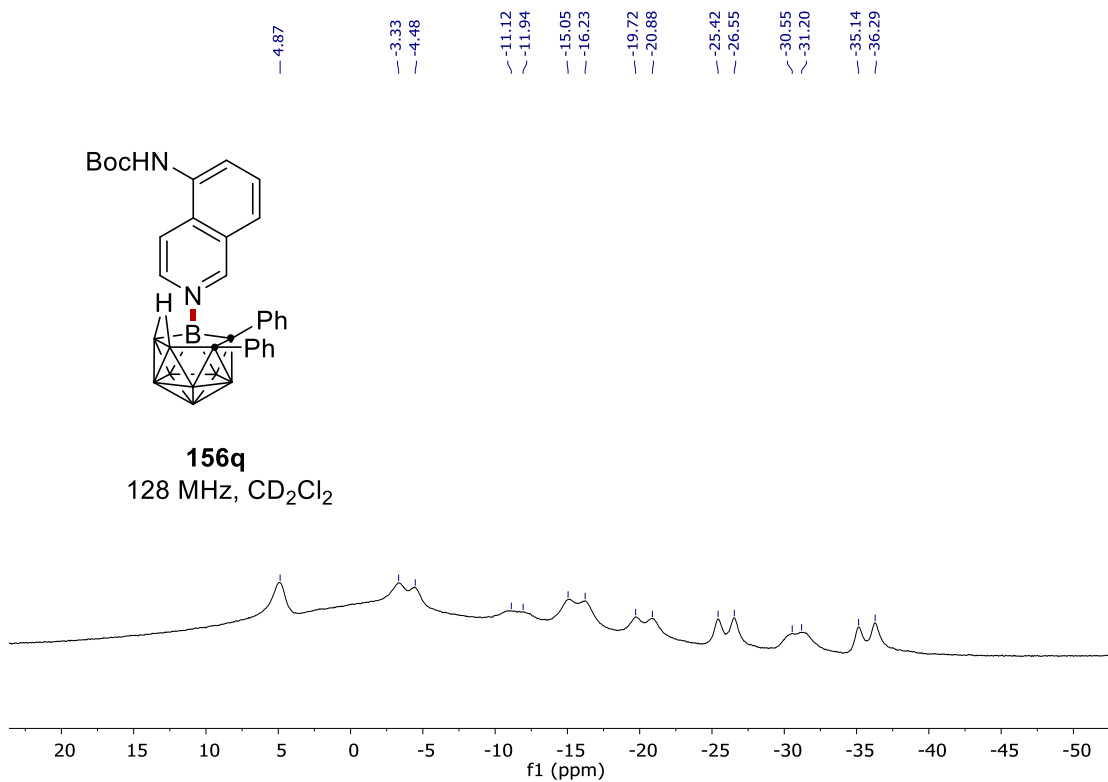


NMR Spectra



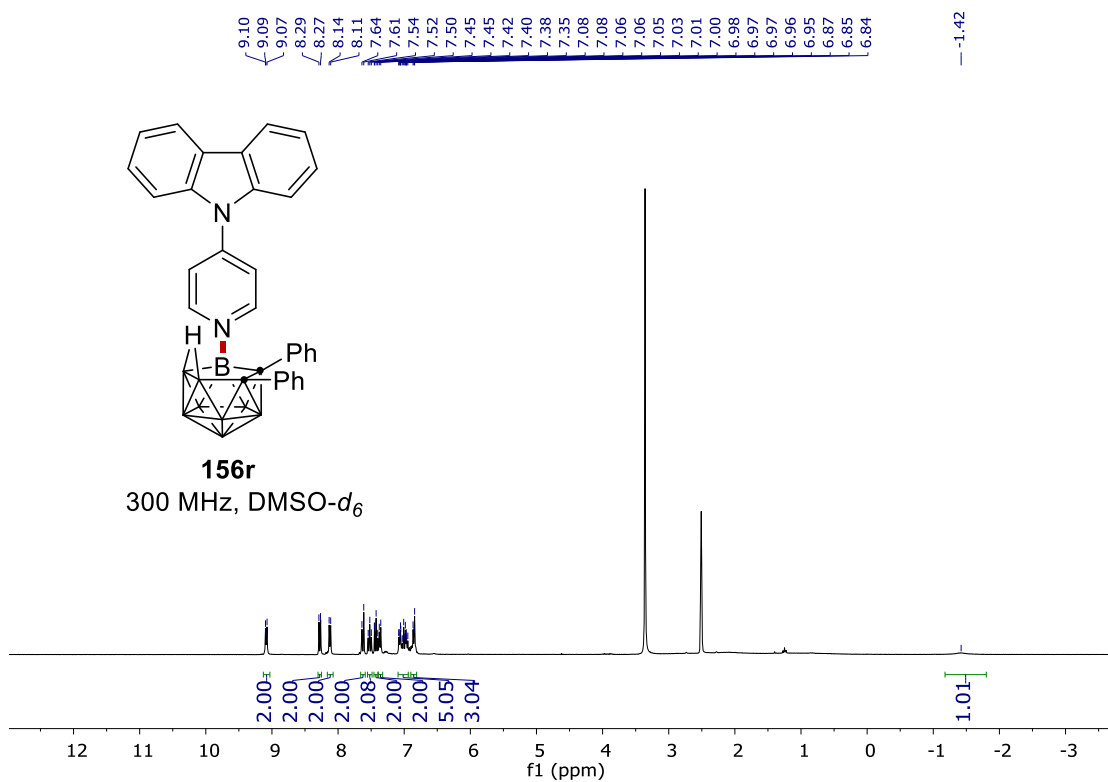
156q

128 MHz, CD₂Cl₂

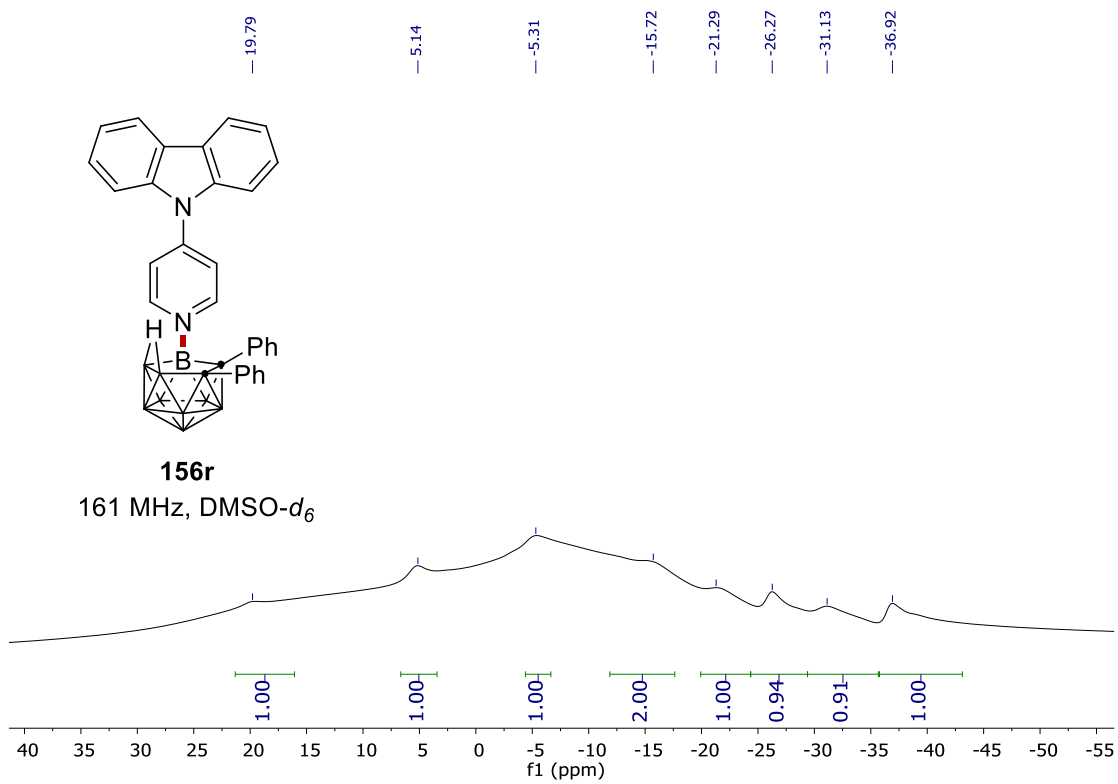
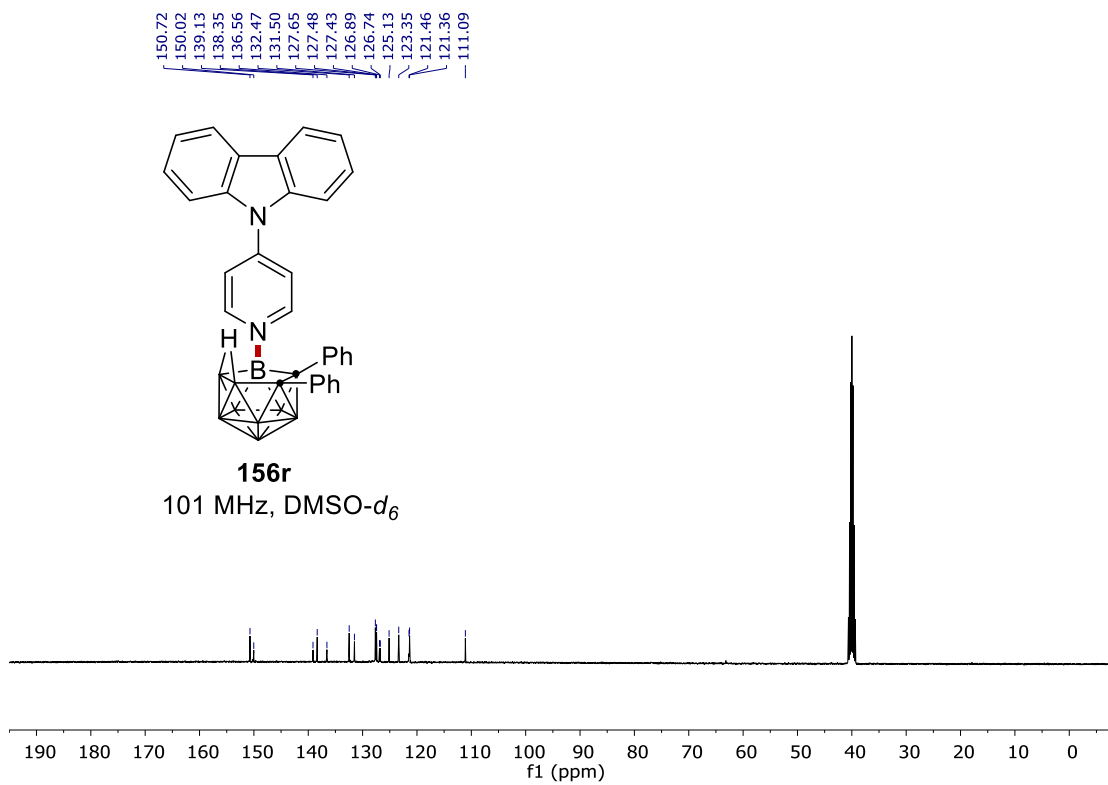


156r

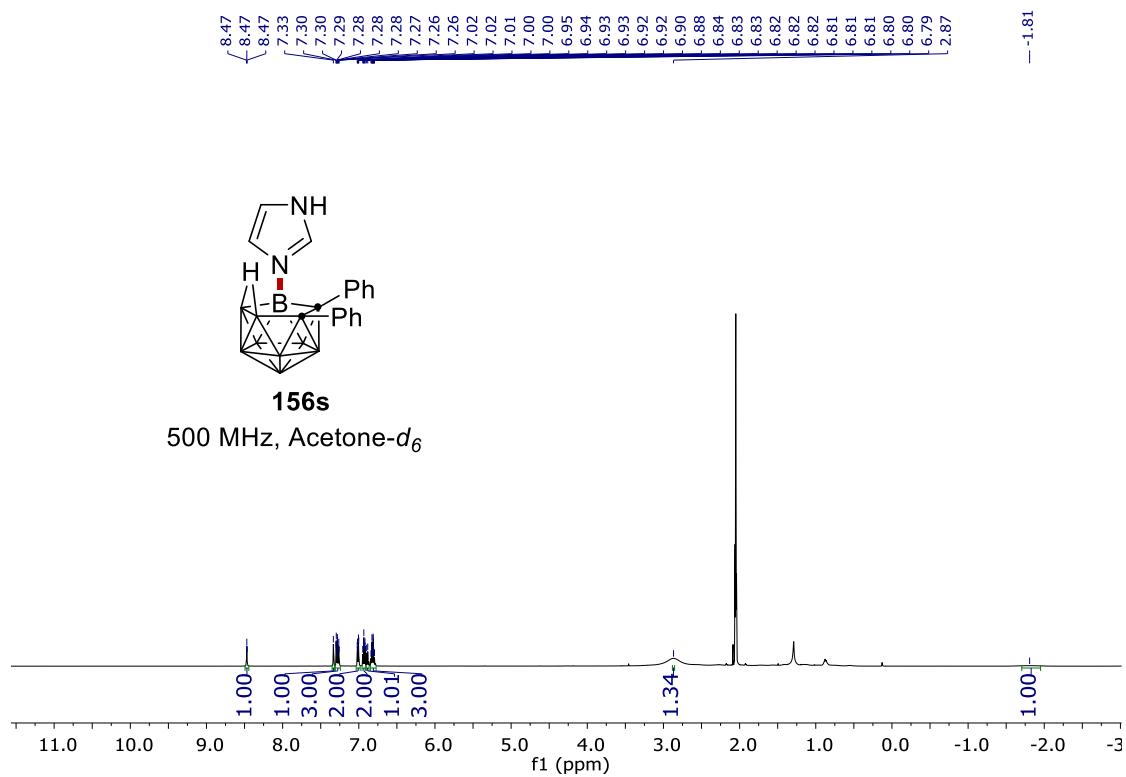
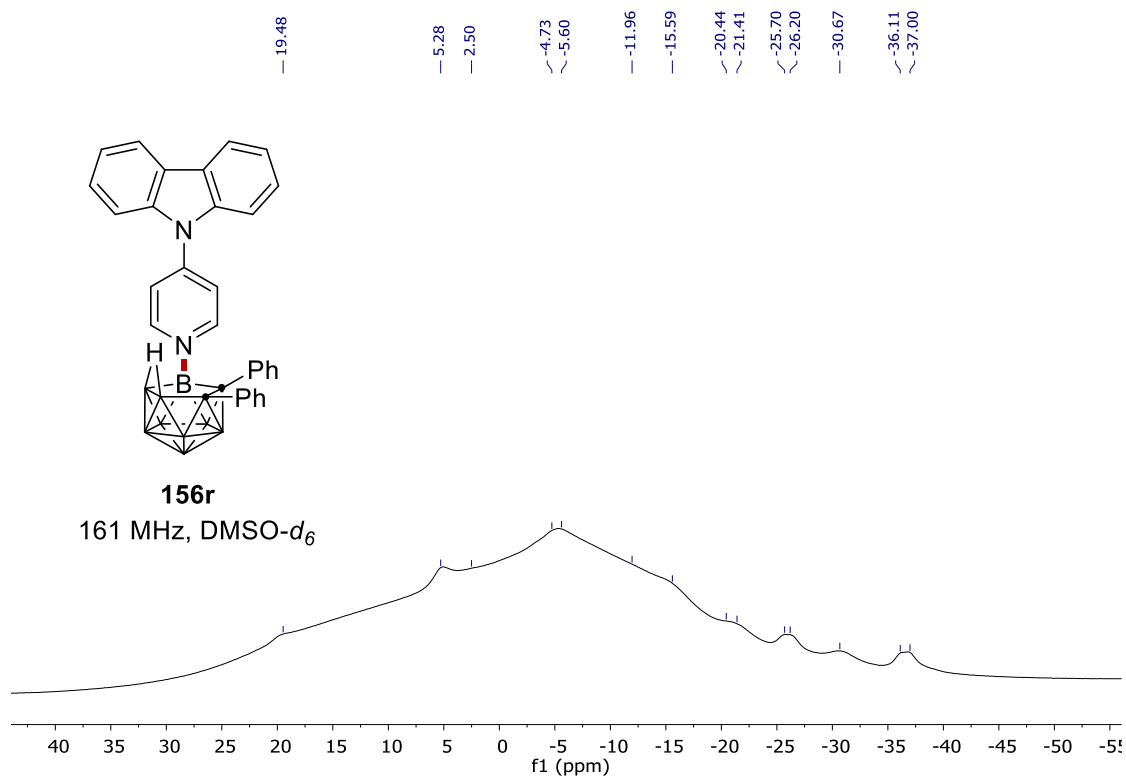
300 MHz, DMSO-*d*₆



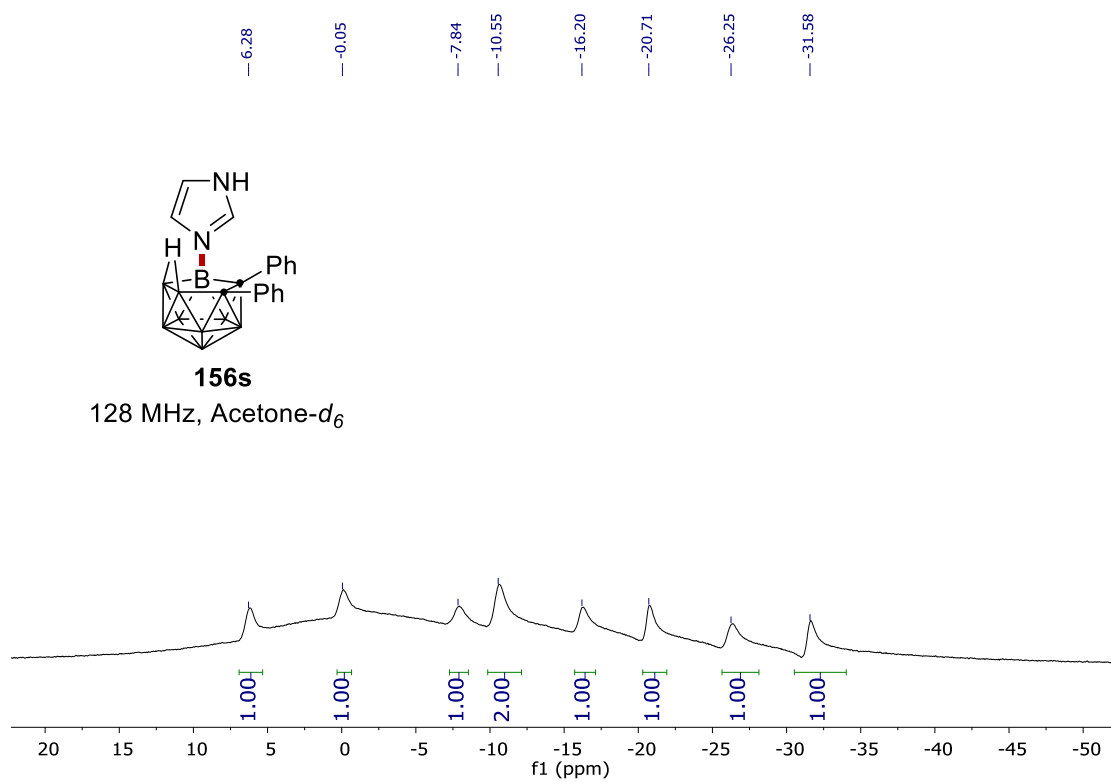
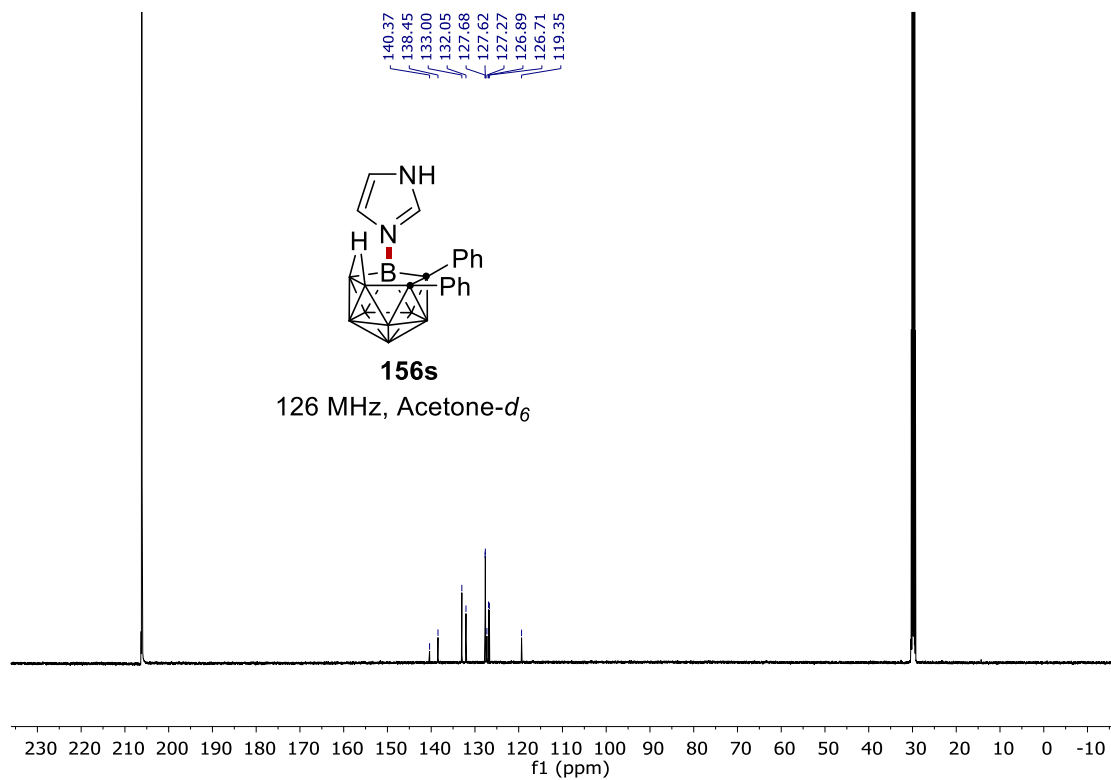
NMR Spectra



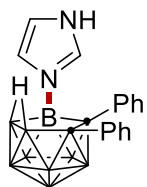
NMR Spectra



NMR Spectra

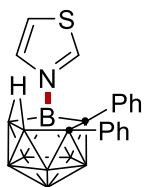
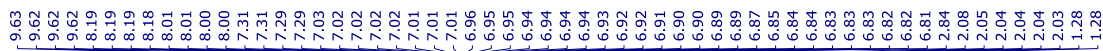
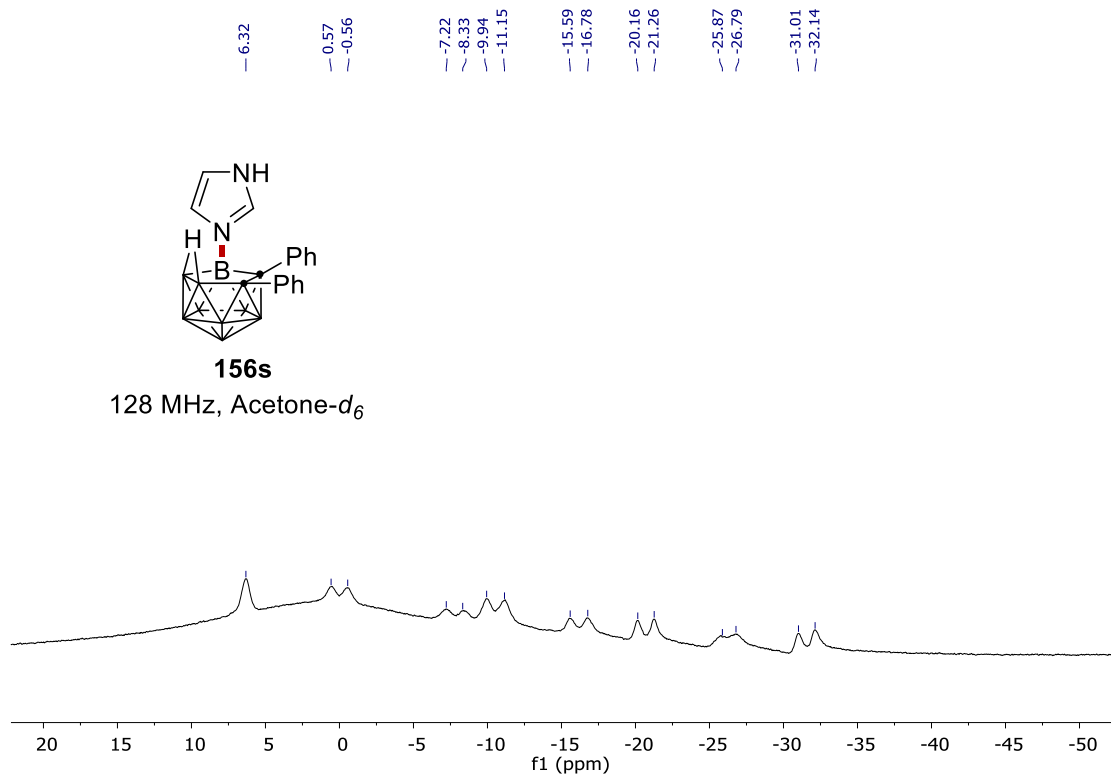


NMR Spectra



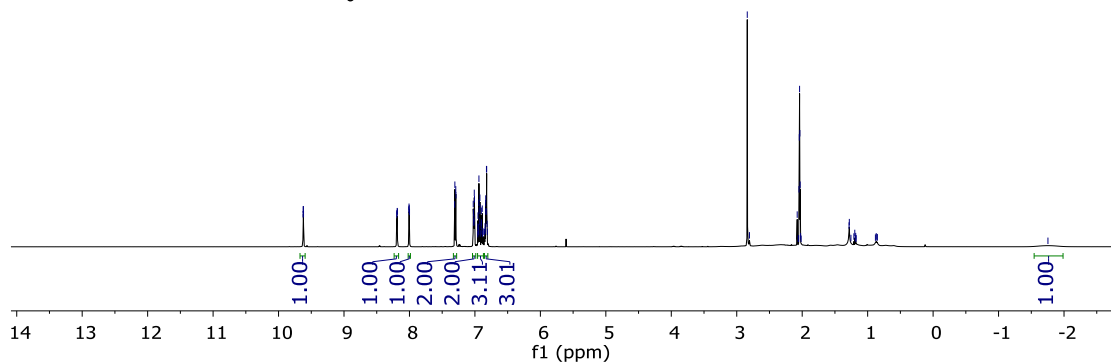
156s

128 MHz, Acetone- d_6

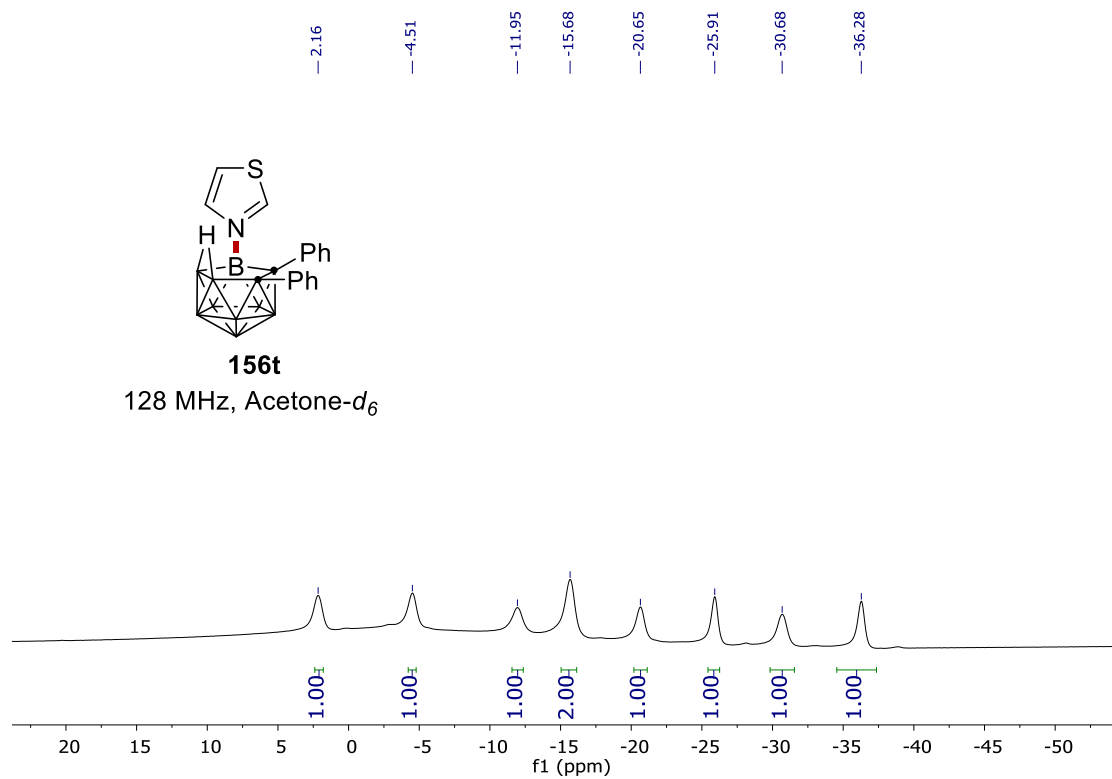
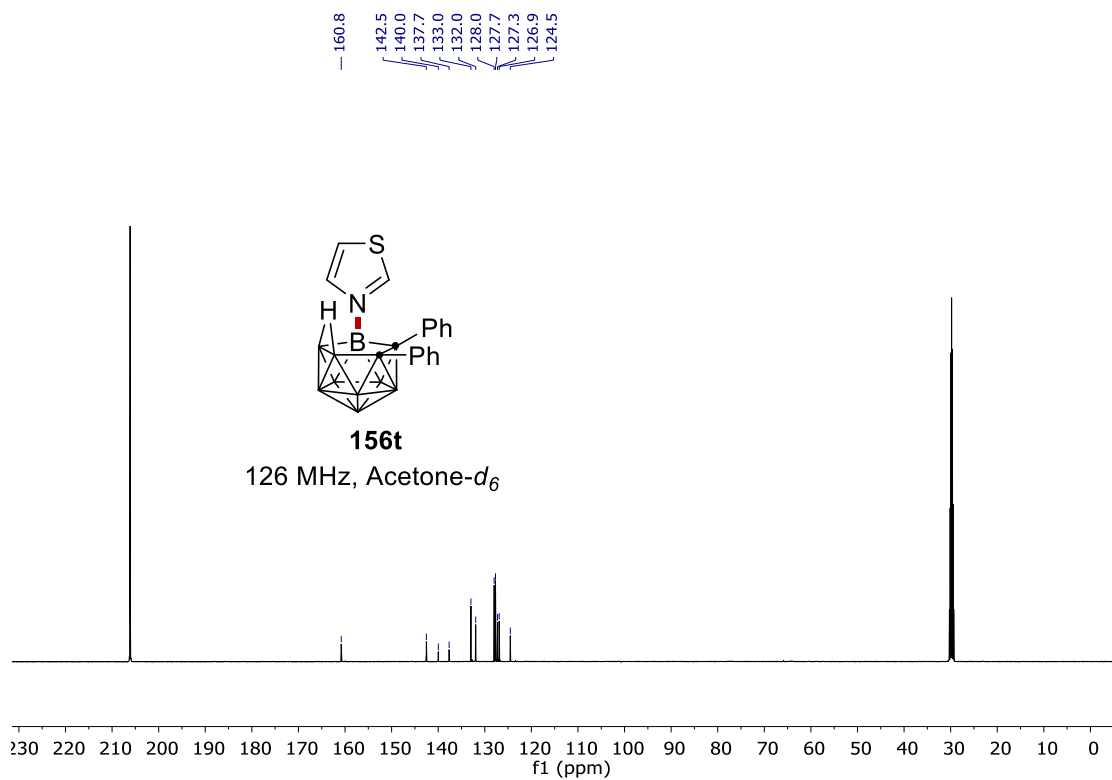


156t

500 MHz, Acetone- d_6

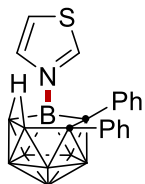


NMR Spectra



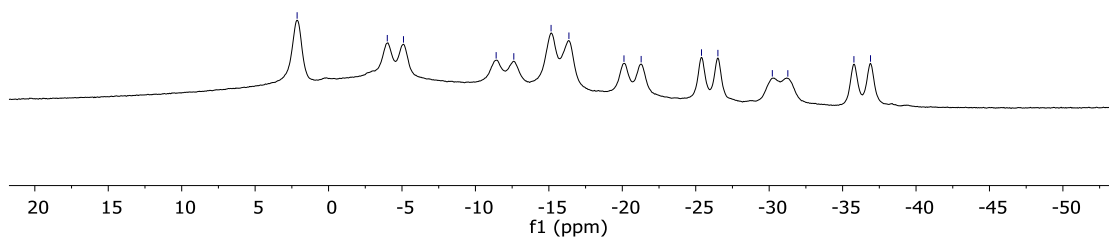
NMR Spectra

-2.14
 -4.00
 -5.10
 -11.41
 -12.61
 -15.15
 -16.37
 -20.11
 -21.28
 -25.39
 -26.51
 -30.22
 -31.27
 -35.77
 -36.90

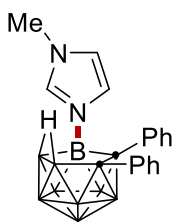


156t

128 MHz, Acetone- d_6

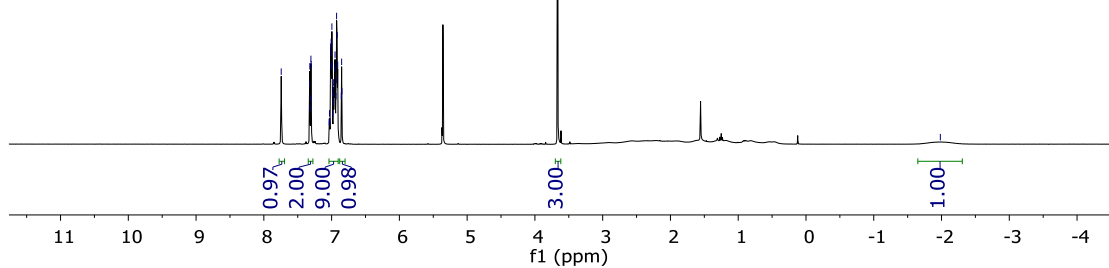


7.74
 7.33
 7.32
 7.32
 7.31
 7.31
 7.30
 7.03
 7.01
 7.01
 7.00
 7.00
 6.99
 6.99
 6.97
 6.96
 6.95
 6.95
 6.94
 6.93
 6.92
 6.91
 6.86
 6.85
 6.85
 -1.98

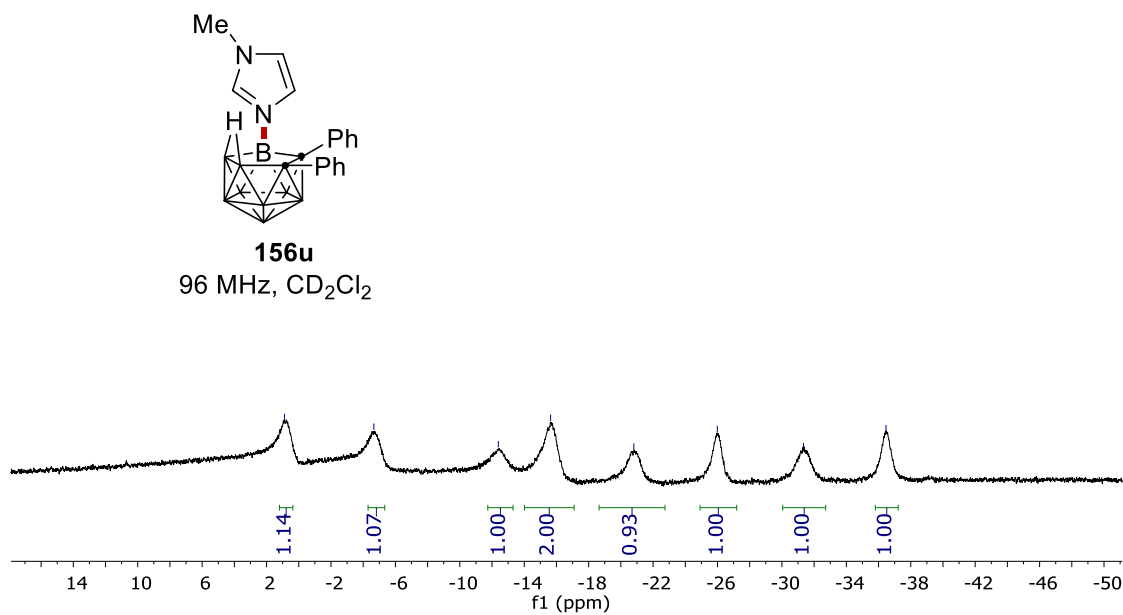
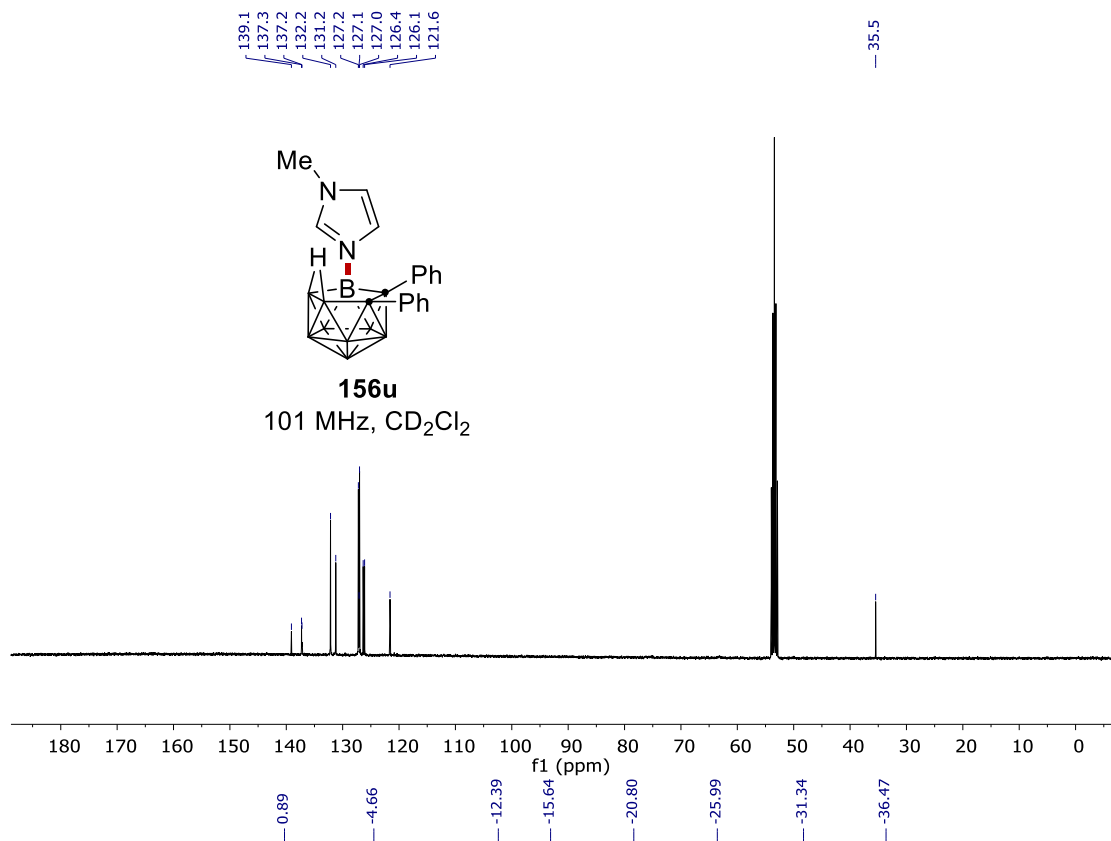


156u

400 MHz, CD_2Cl_2

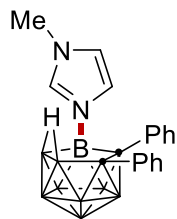


NMR Spectra

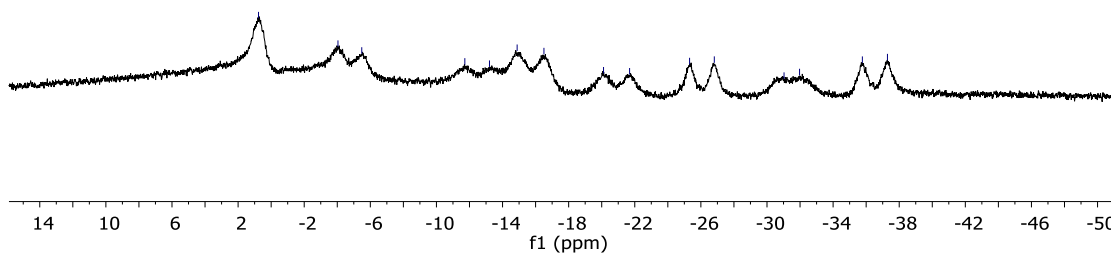


NMR Spectra

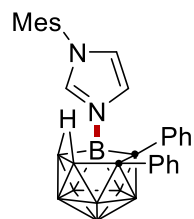
-0.77
 -4.04
 -5.48
 -11.72
 -13.21
 -14.88
 -16.50
 -20.11
 -21.69
 -25.32
 -26.81
 -31.03
 -31.97
 -35.77
 -37.29



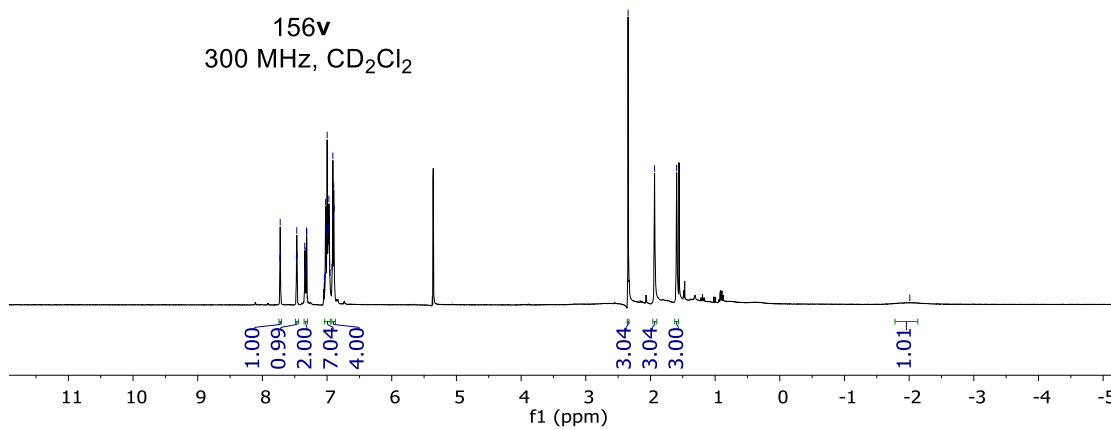
156u
96 MHz, CD₂Cl₂



7.73
 7.72
 7.72
 7.47
 7.46
 7.35
 7.34
 7.34
 7.33
 7.33
 7.32
 7.32
 7.31
 7.04
 7.04
 7.03
 7.02
 7.02
 7.02
 7.01
 7.01
 7.00
 6.99
 6.99
 6.98
 6.98
 6.97
 6.97
 6.96
 6.95
 6.92
 6.92
 6.91
 6.91
 6.90
 6.89
 2.35
 1.94
 1.60
 -2.01

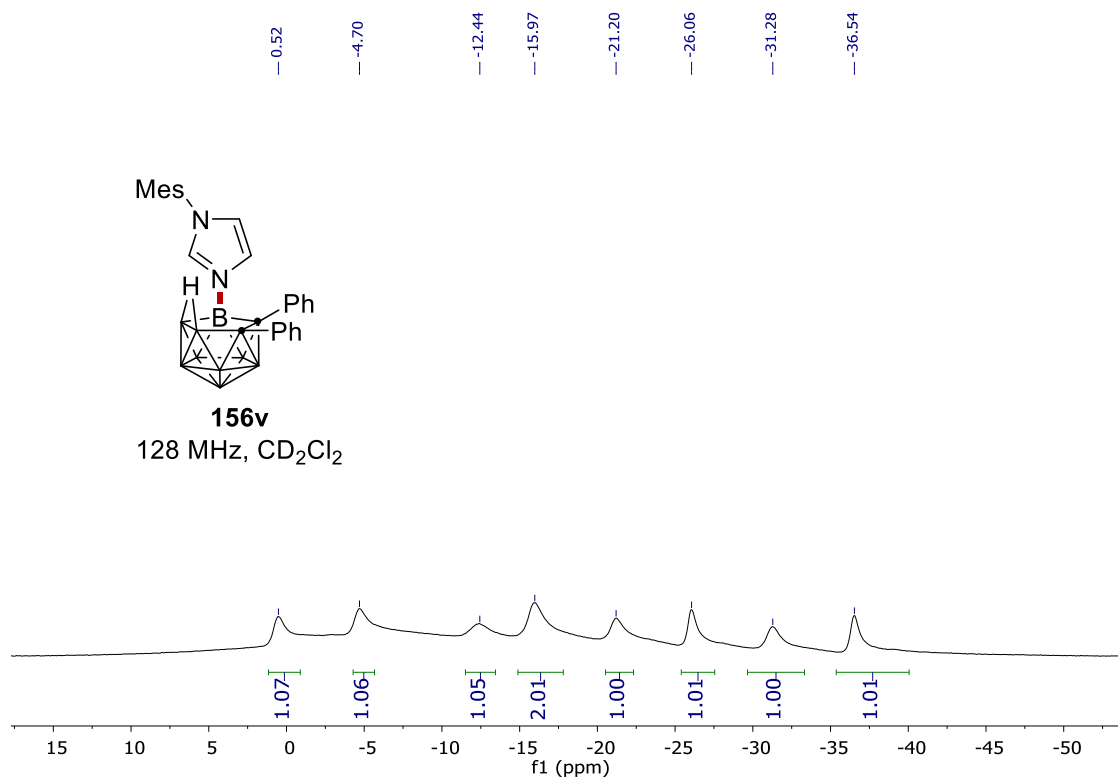
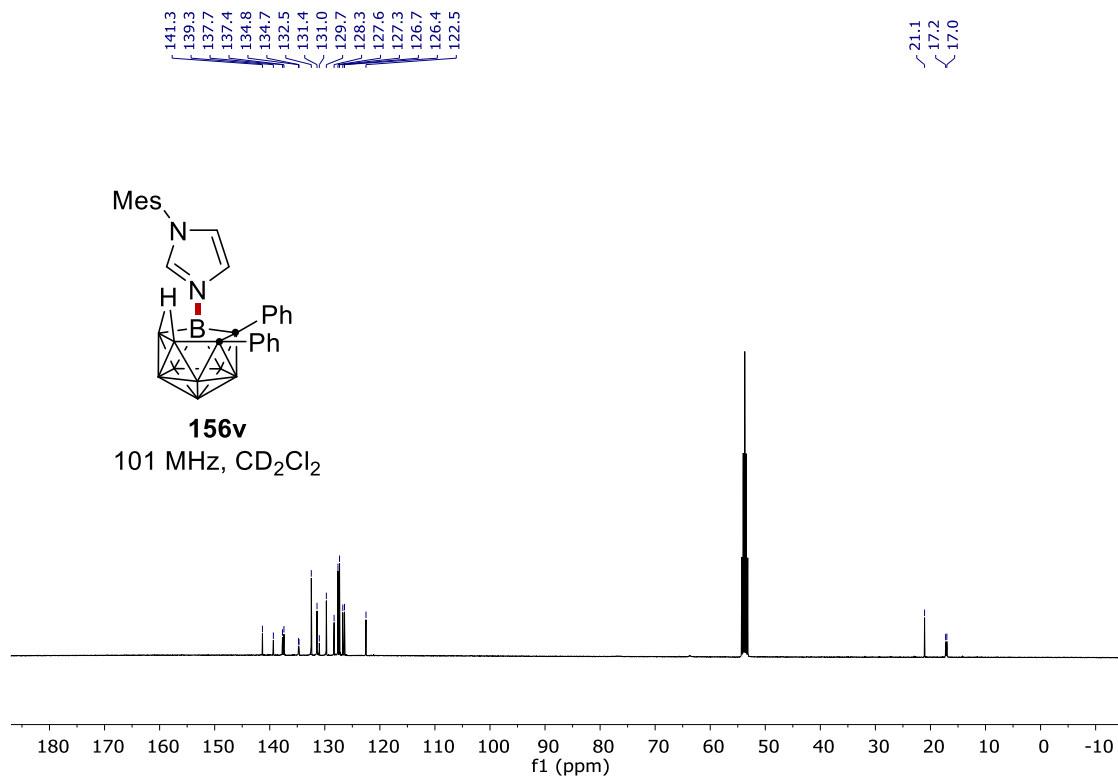


156v
300 MHz, CD₂Cl₂

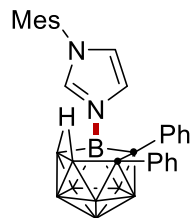


1.00
 0.99
 2.00
 7.04
 4.00
 3.04
 3.04
 3.00
 1.01

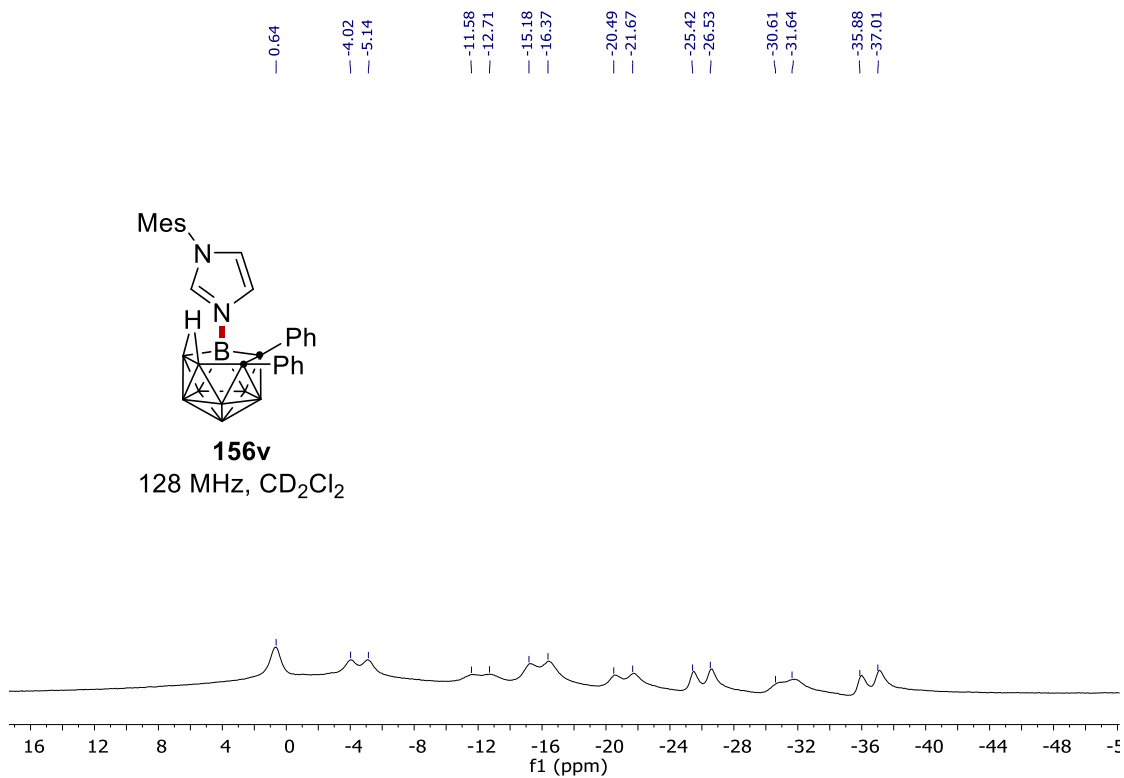
NMR Spectra



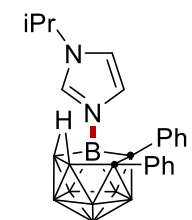
NMR Spectra



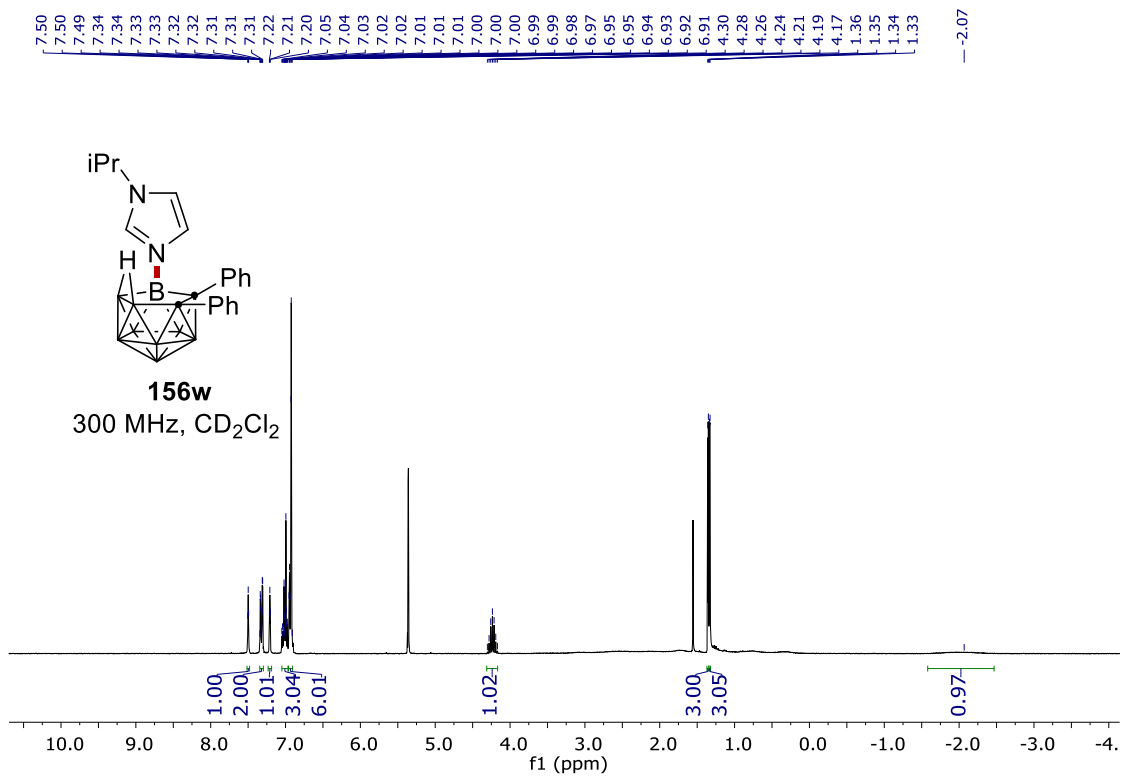
156v
128 MHz, CD₂Cl₂



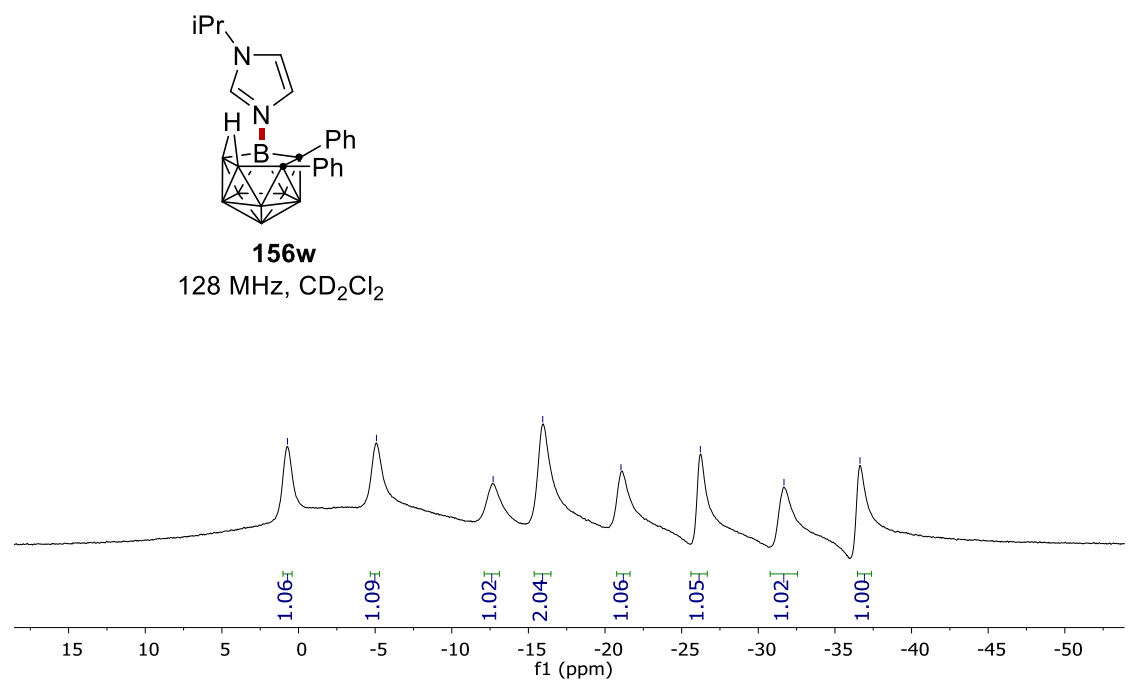
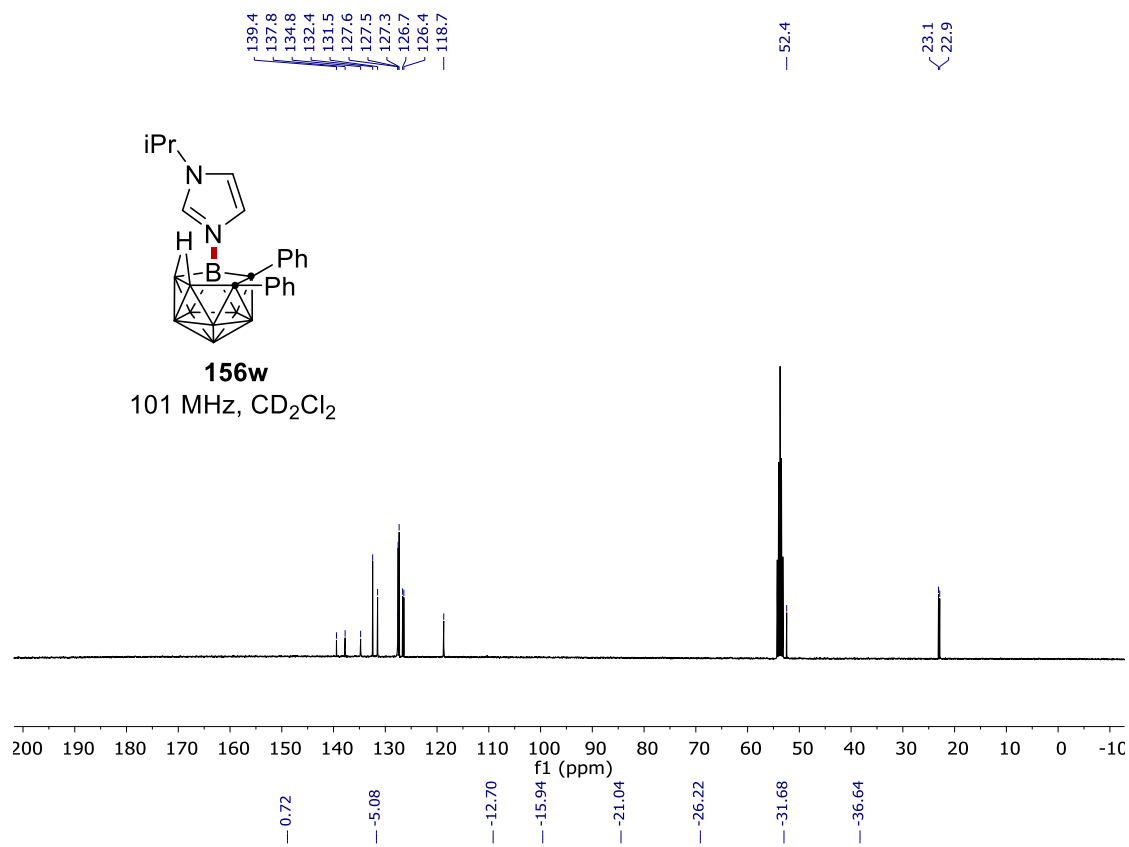
7.50, 7.50, 7.49, 7.34, 7.34, 7.33, 7.33, 7.32, 7.32, 7.31, 7.31, 7.22, 7.21, 7.20, 7.05, 7.04, 7.03, 7.02, 7.01, 7.01, 7.00, 7.00, 7.00, 6.99, 6.99, 6.98, 6.97, 6.95, 6.94, 6.93, 6.92, 6.91, 4.30, 4.28, 4.26, 4.24, 4.21, 4.19, 4.17, 1.36, 1.35, 1.34, 1.33, -2.07



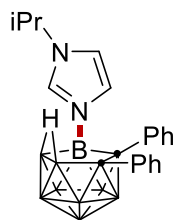
156w
300 MHz, CD₂Cl₂



NMR Spectra

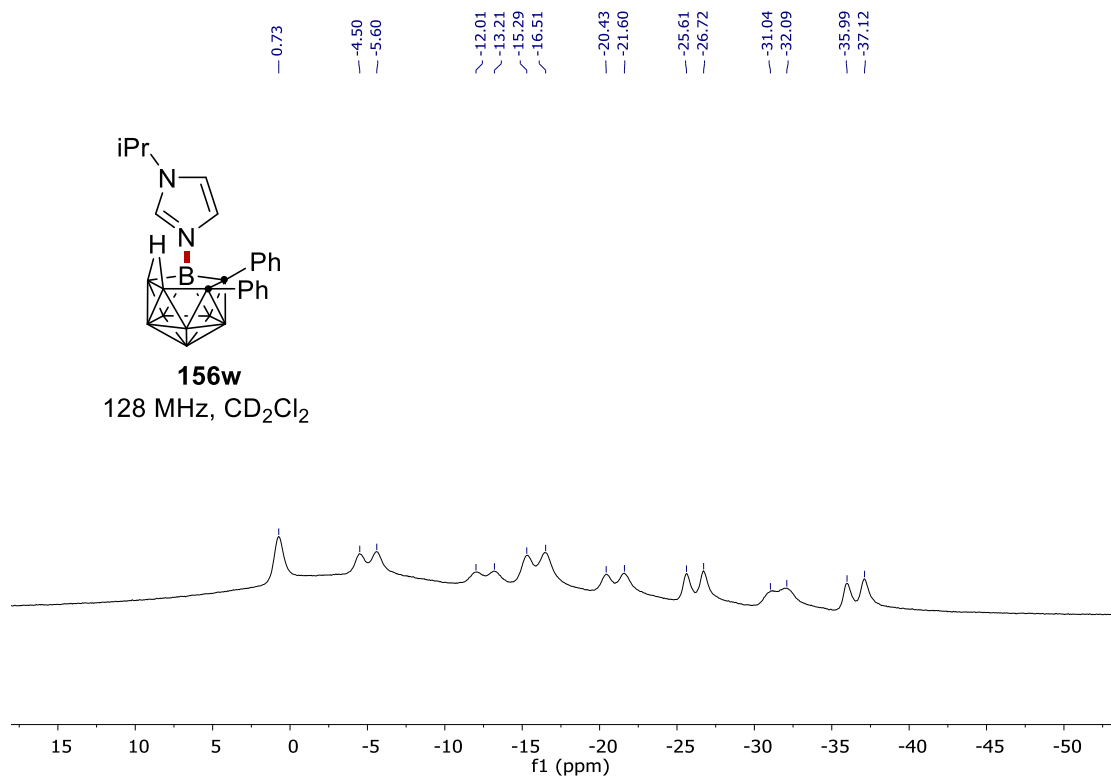


NMR Spectra

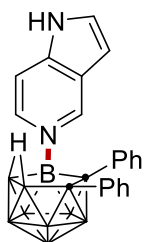


156w

128 MHz, CD₂Cl₂

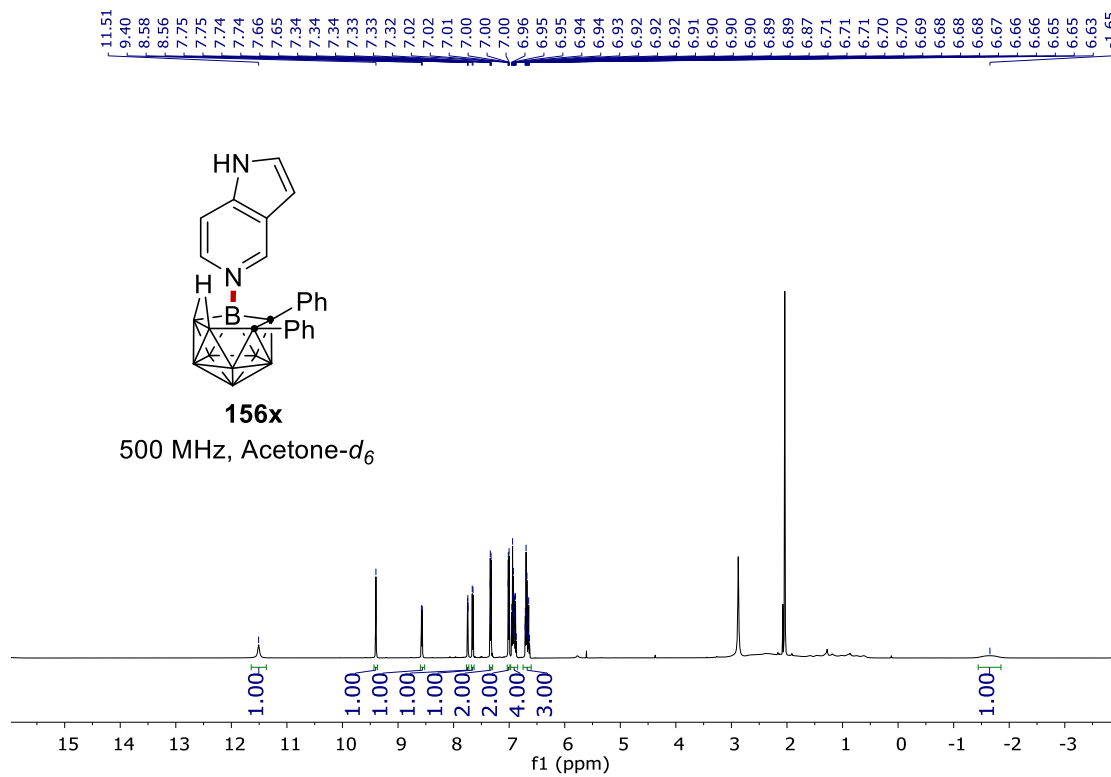


11.51, 9.40, 8.58, 8.56, 7.75, 7.75, 7.74, 7.74, 7.66, 7.65, 7.34, 7.34, 7.34, 7.33, 7.33, 7.32, 7.02, 7.02, 7.01, 7.00, 7.00, 6.96, 6.95, 6.95, 6.94, 6.94, 6.93, 6.92, 6.92, 6.91, 6.90, 6.90, 6.90, 6.89, 6.89, 6.87, 6.87, 6.71, 6.71, 6.70, 6.70, 6.69, 6.68, 6.68, 6.68, 6.67, 6.66, 6.66, 6.65, 6.65, 6.63, 6.63, -1.65

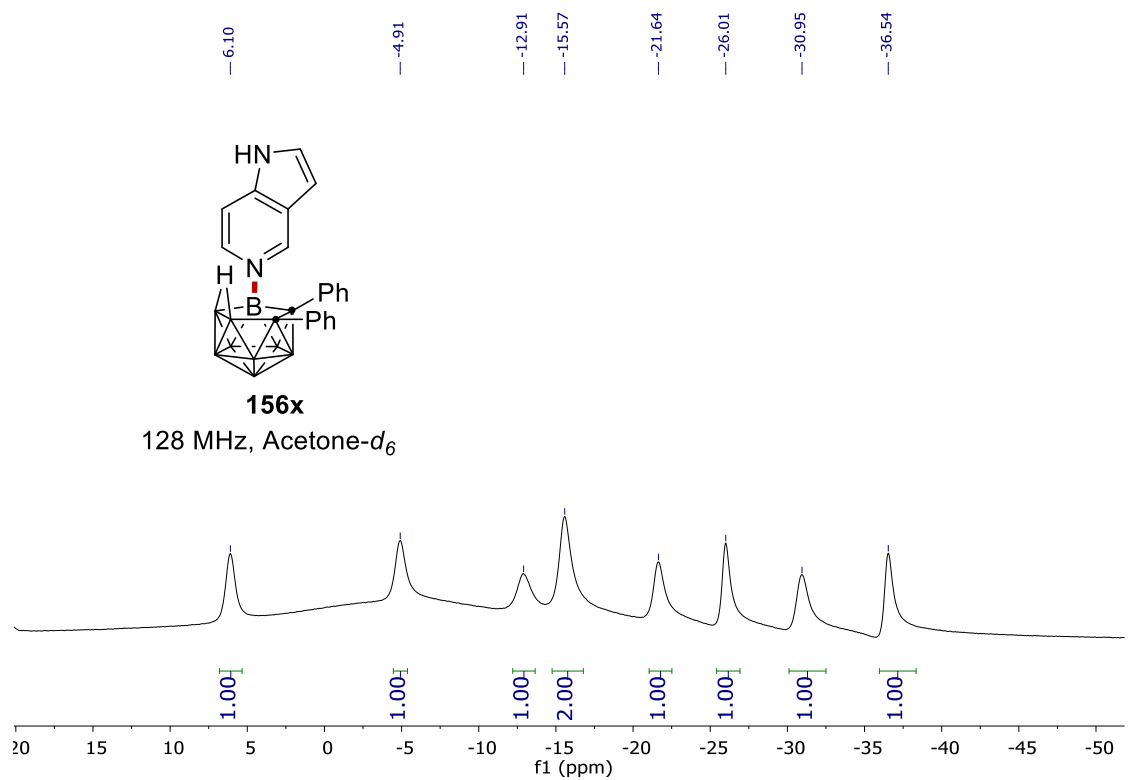
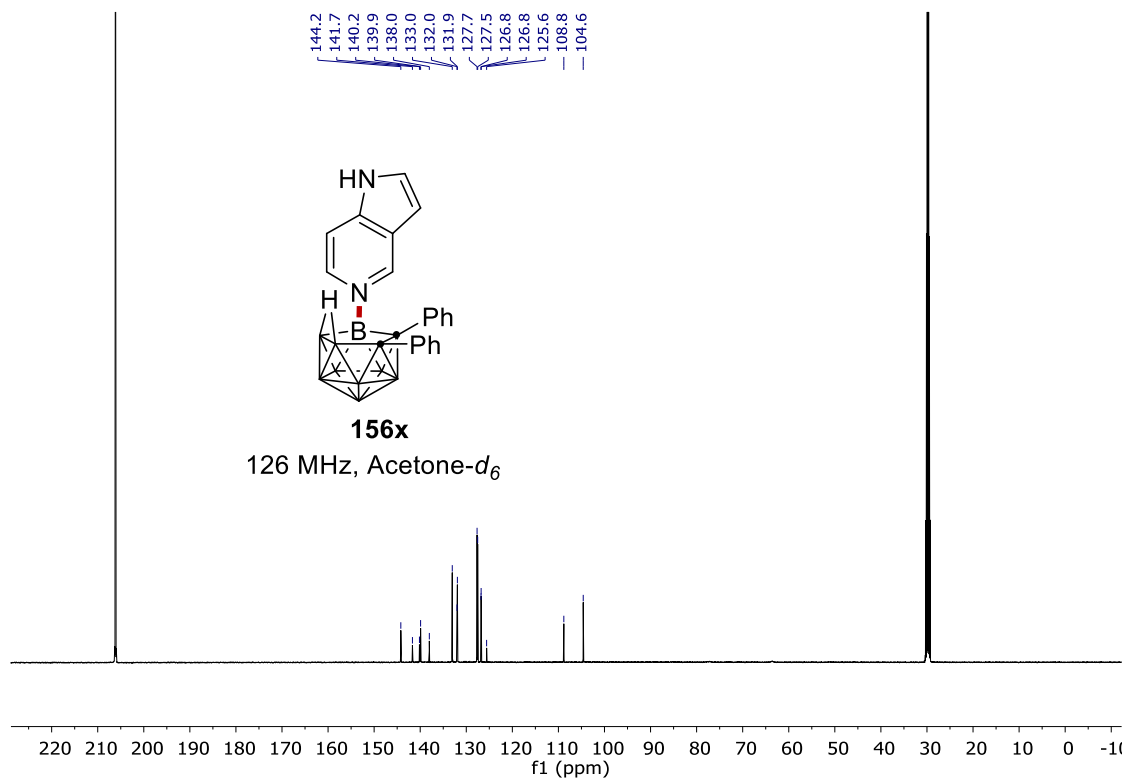


156x

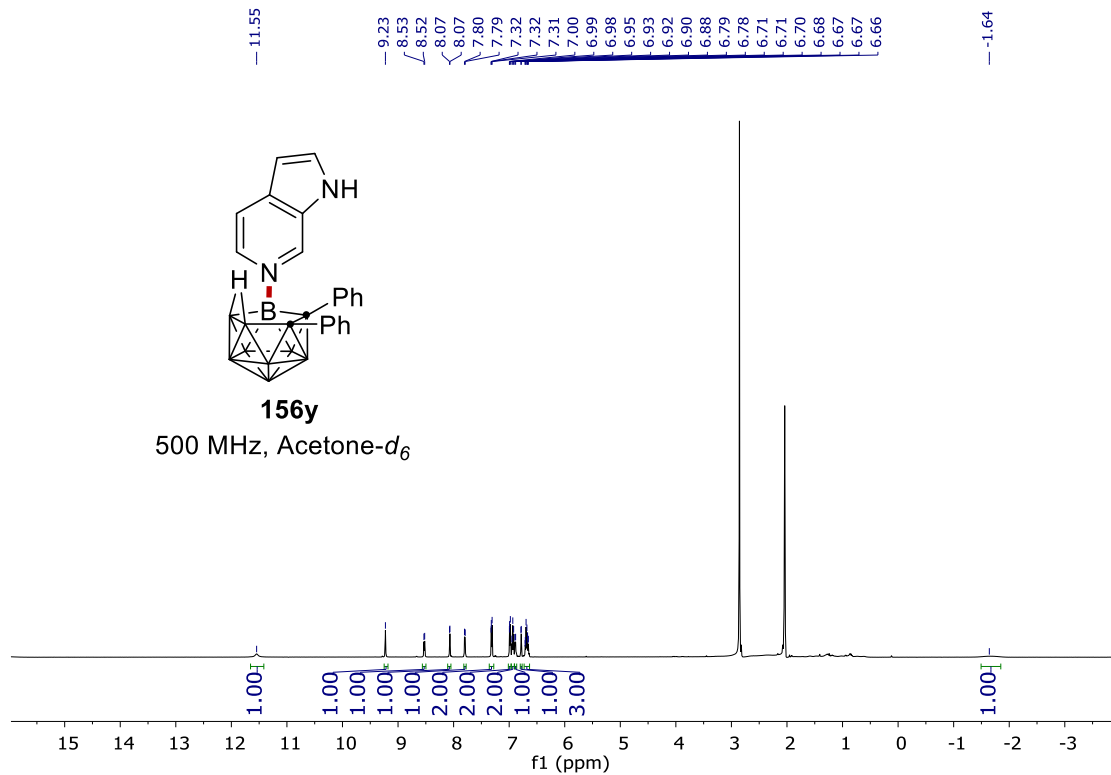
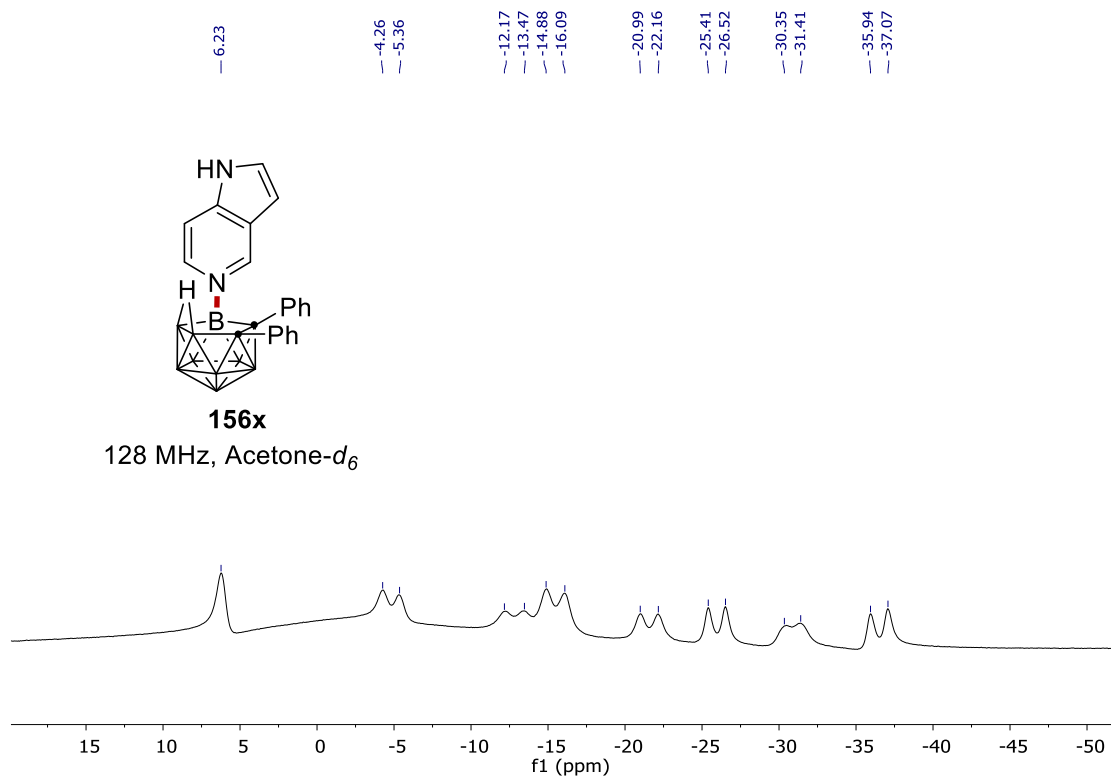
500 MHz, Acetone-*d*₆



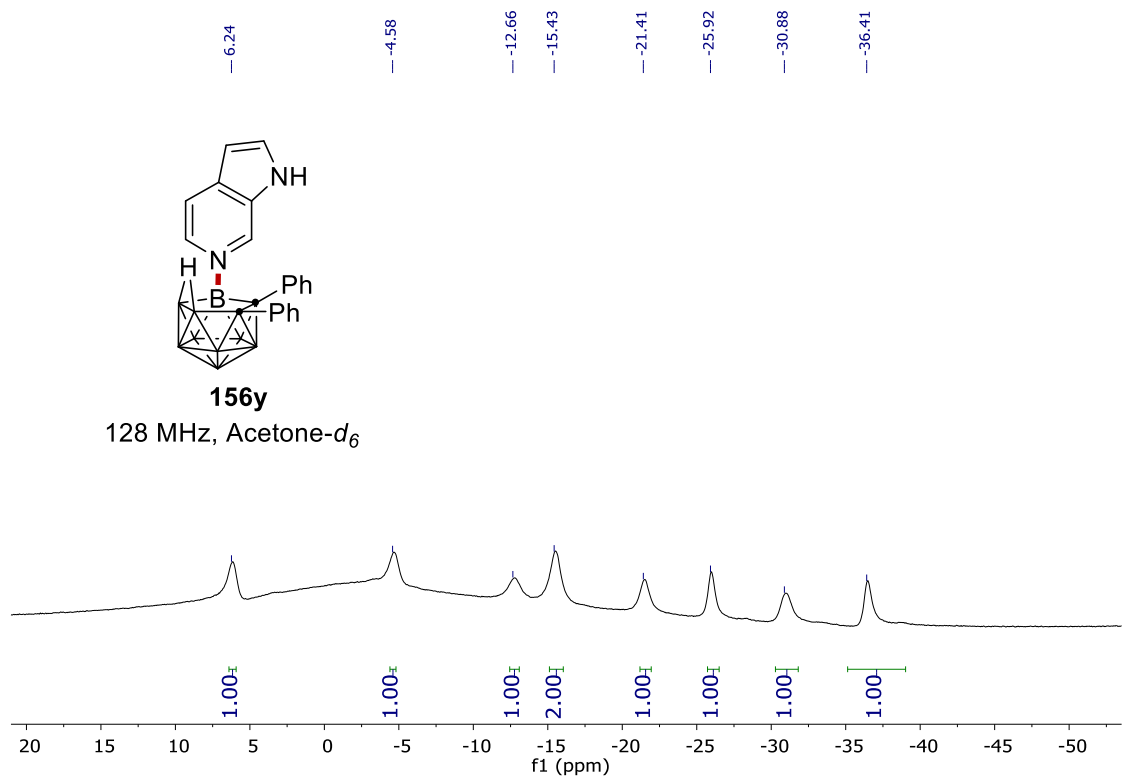
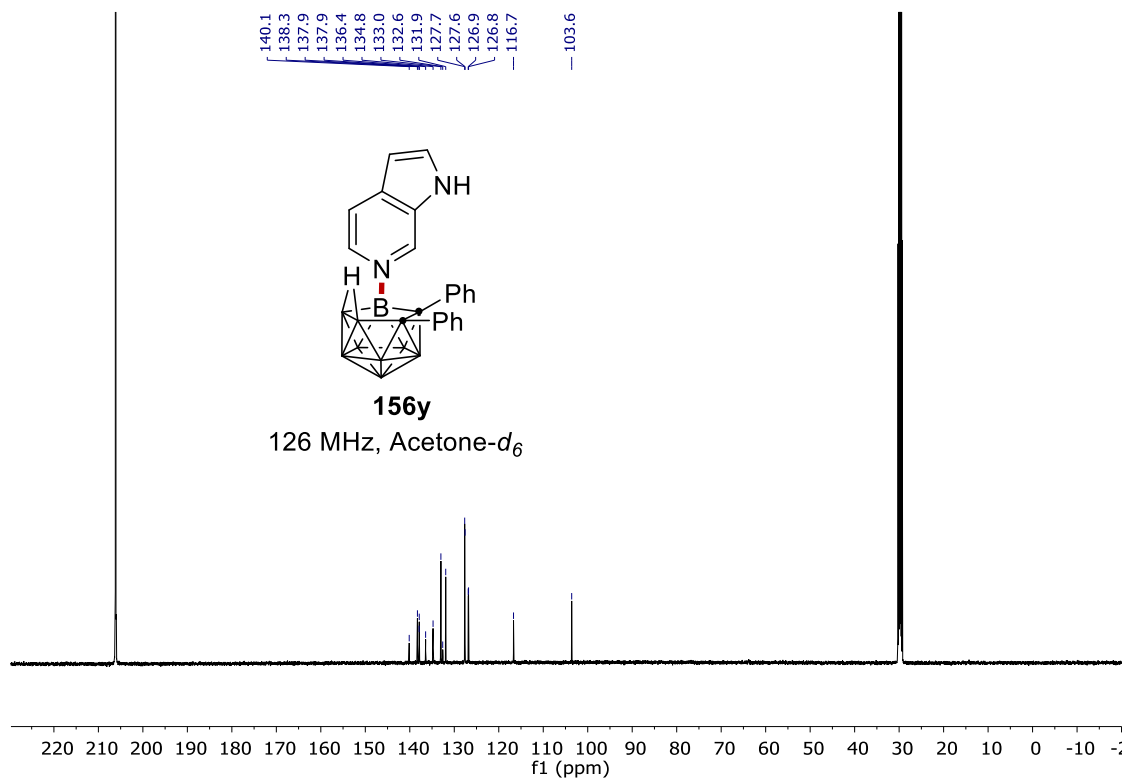
NMR Spectra



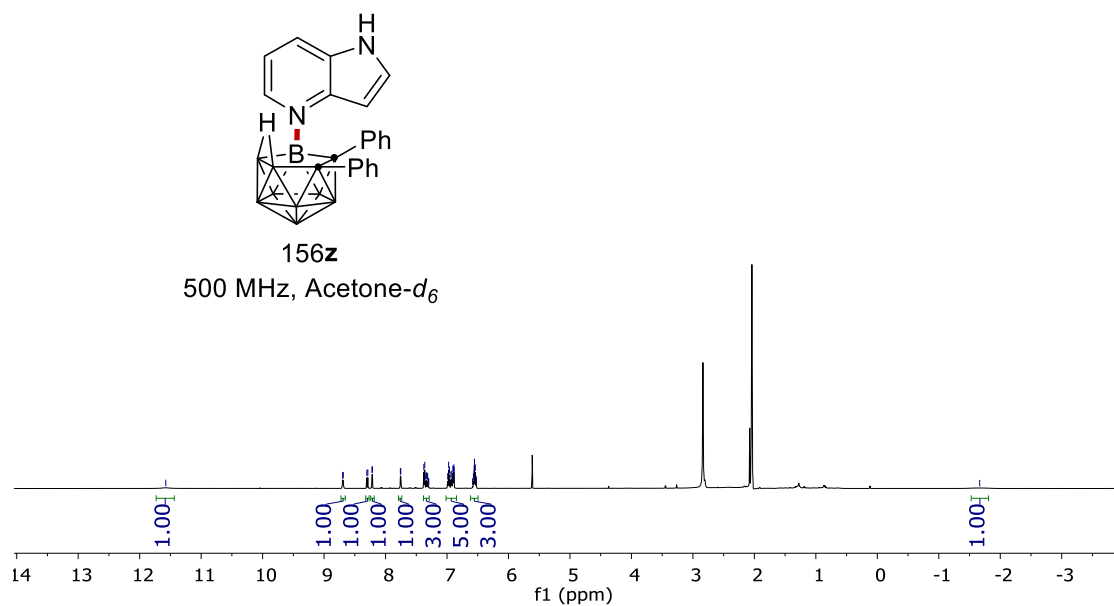
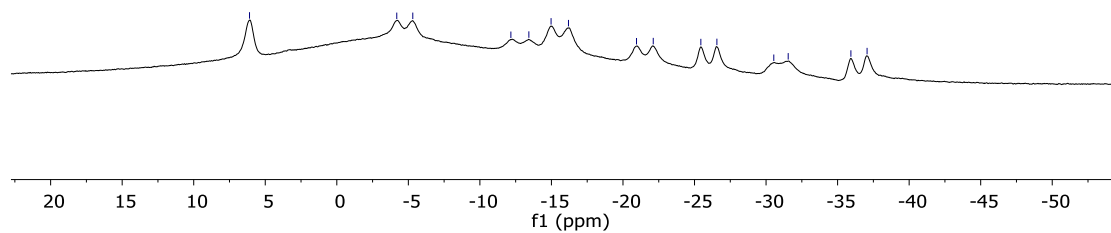
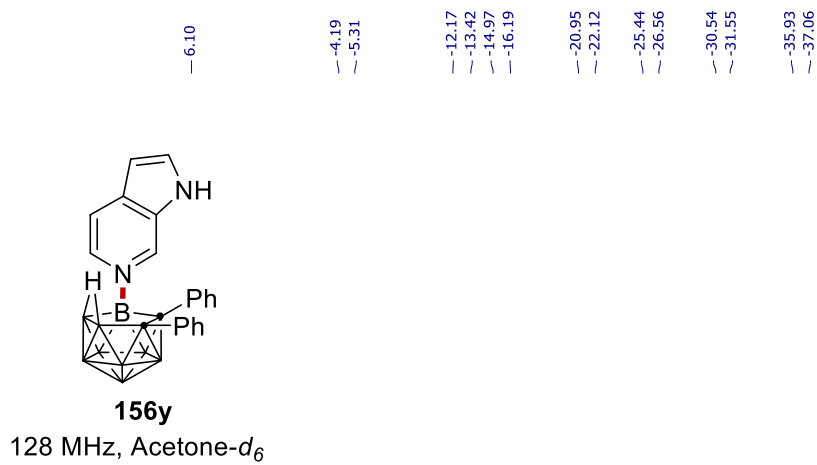
NMR Spectra



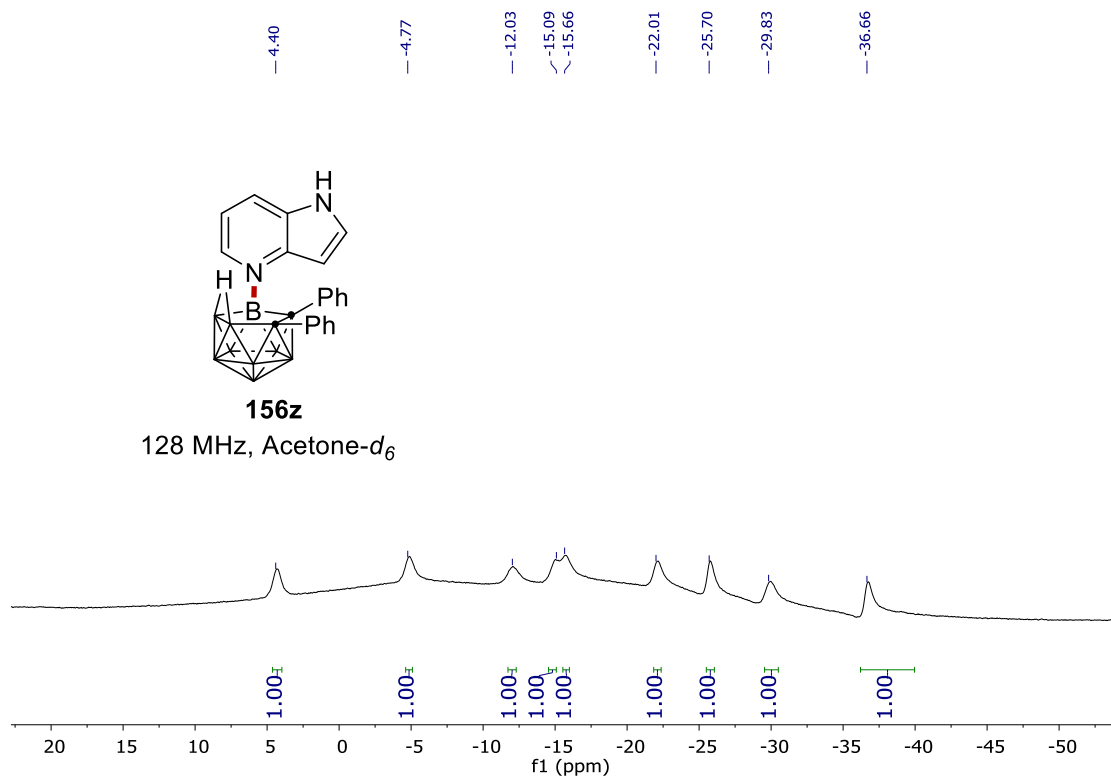
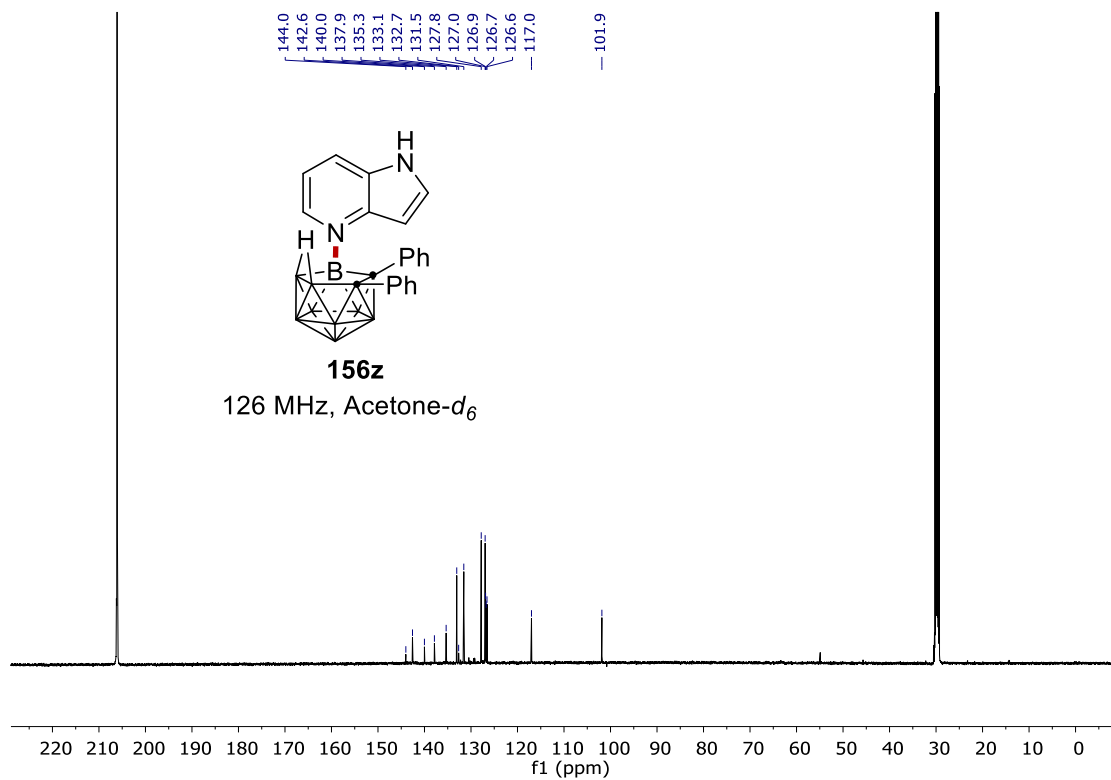
NMR Spectra



NMR Spectra

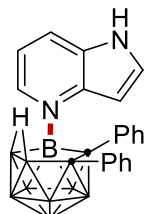


NMR Spectra



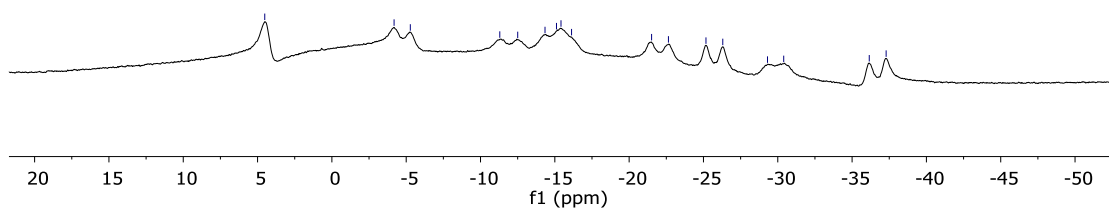
NMR Spectra

-4.52
 -4.18
 -5.28
 -11.30
 -12.50
 -14.34
 -15.11
 -15.41
 -16.12
 -21.51
 -22.64
 -25.17
 -26.30
 -29.31
 -30.40
 -36.15
 -37.29

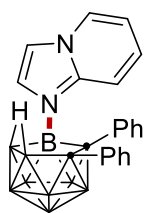


156z

128 MHz, Acetone- d_6

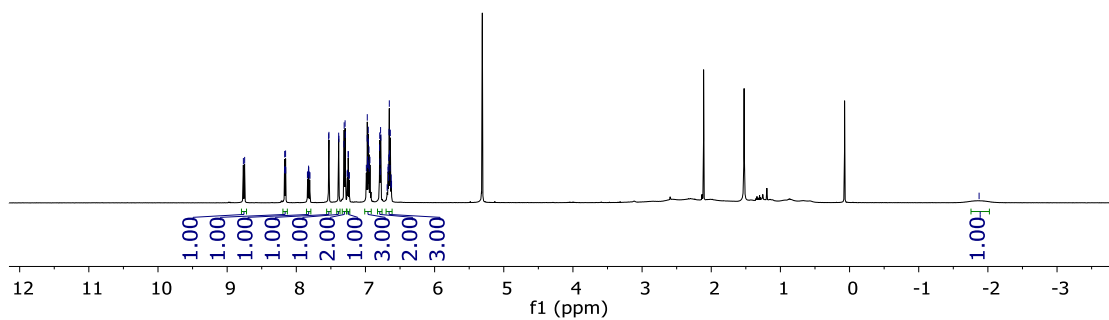


8.77
 8.75
 8.17
 8.17
 8.17
 8.16
 8.15
 8.15
 7.84
 7.84
 7.82
 7.82
 7.82
 7.81
 7.81
 7.80
 7.53
 7.53
 7.39
 7.38
 7.38
 7.31
 7.31
 7.29
 7.29
 7.26
 7.26
 7.25
 7.25
 7.24
 7.24
 7.23
 7.23
 6.99
 6.98
 6.97
 6.97
 6.97
 6.96
 6.96
 6.96
 6.96
 6.95
 6.95
 6.95
 6.94
 6.94
 6.80
 6.80
 6.79
 6.79
 6.79
 6.78
 6.78
 6.78
 6.67
 6.67
 6.67
 6.66
 6.66
 6.66
 6.66
 6.65
 6.65
 6.65
 6.64
 6.64

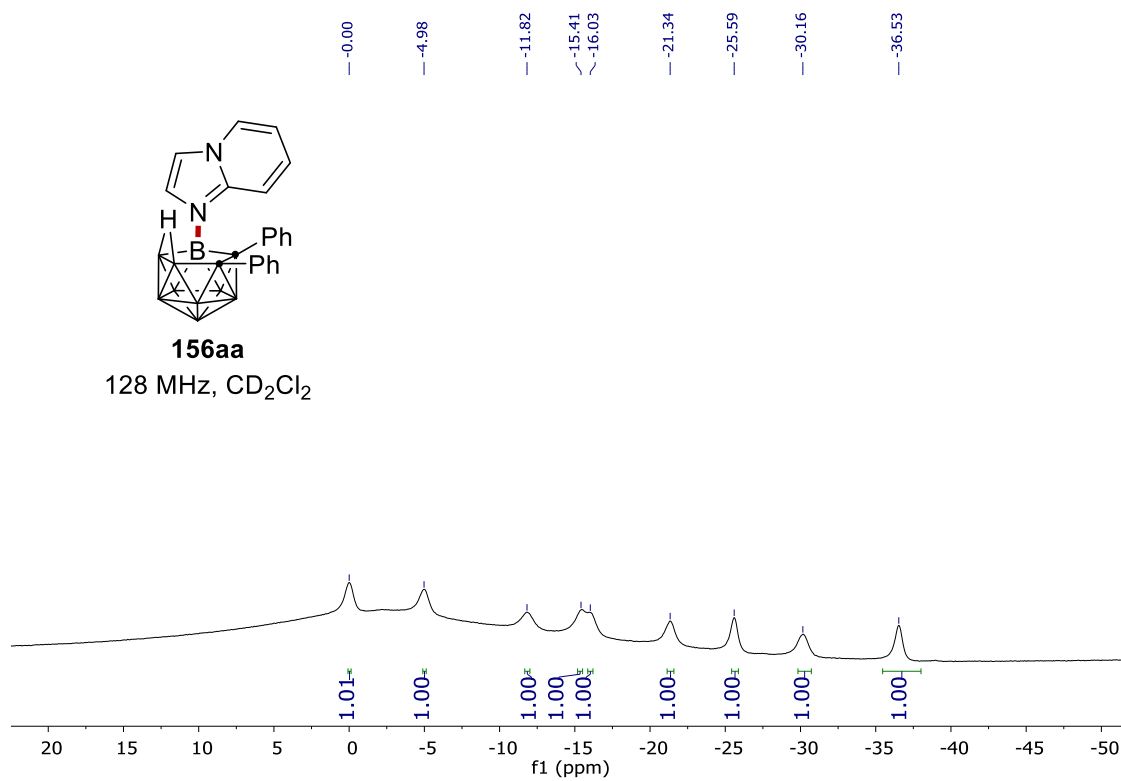
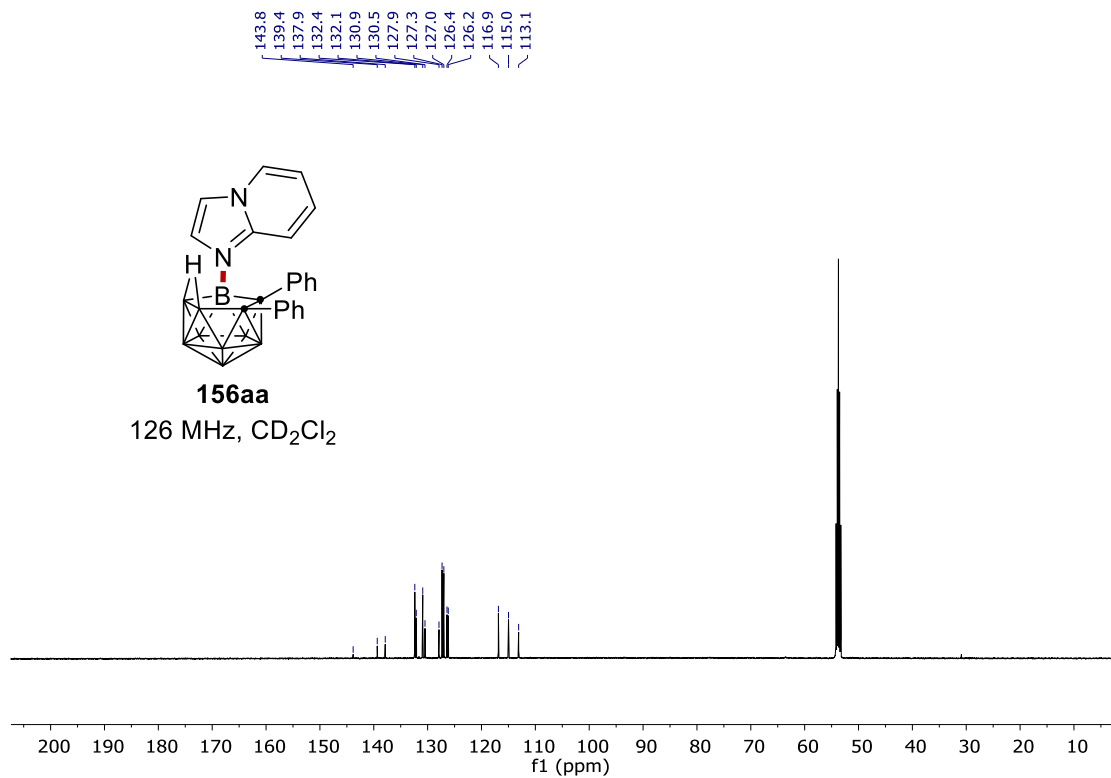


156aa

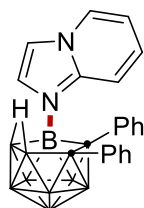
500 MHz, CD_2Cl_2



NMR Spectra

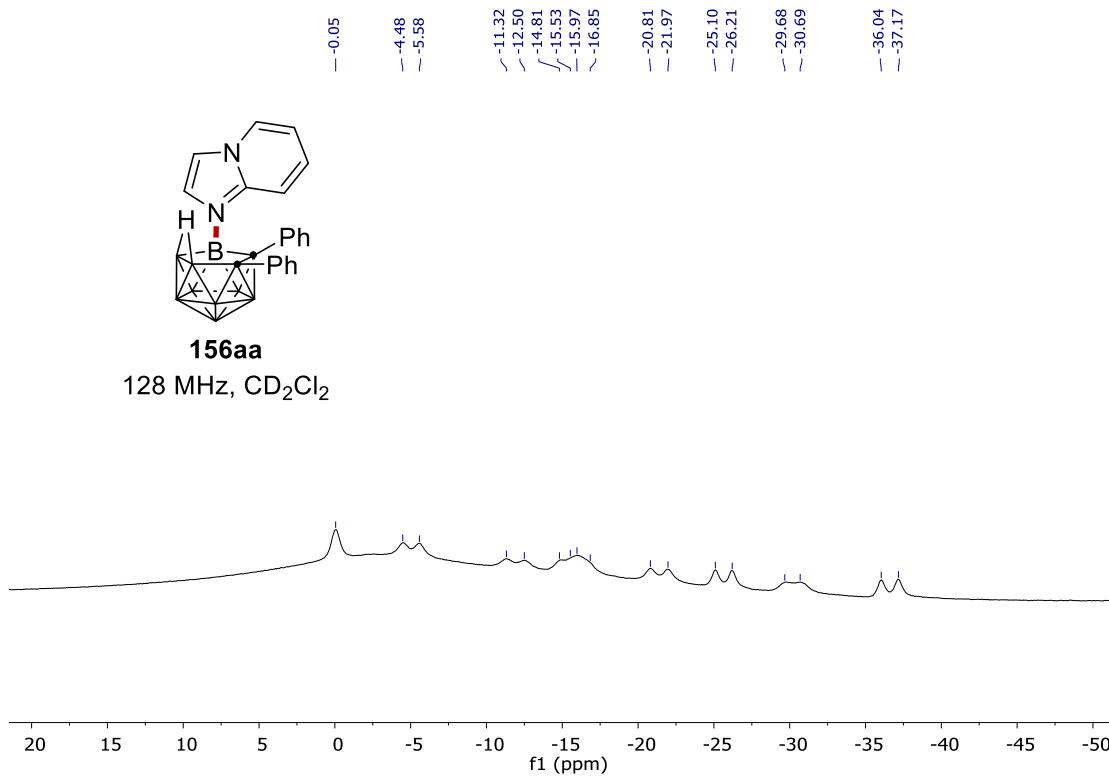


NMR Spectra

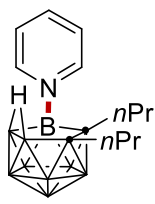


156aa

128 MHz, CD₂Cl₂

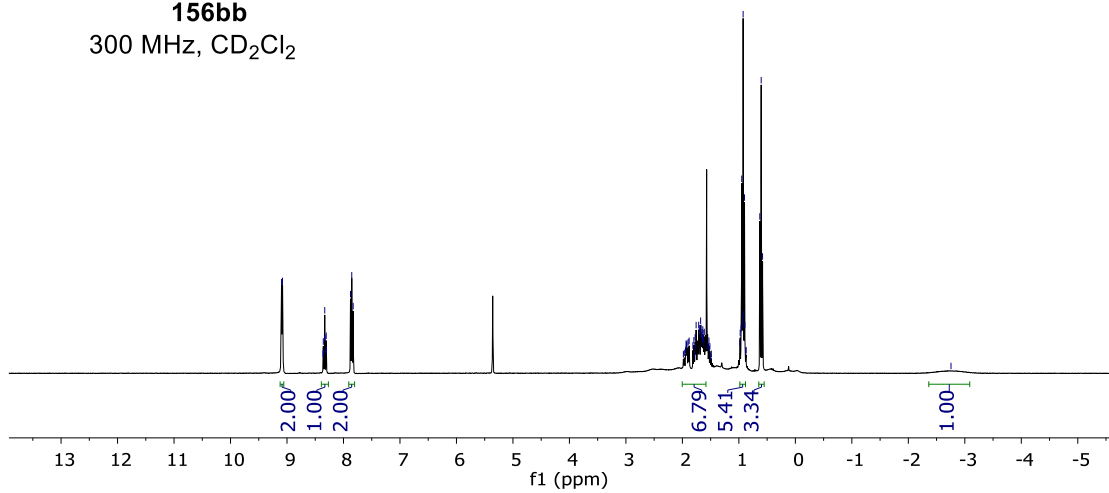


9.10, 9.08, 8.36, 8.36, 8.36, 8.35, 8.34, 8.33, 8.33, 8.31, 8.31, 8.30, 8.30, 7.88, 7.85, 7.83, 1.97, 1.94, 1.94, 1.93, 1.92, 1.90, 1.88, 1.81, 1.81, 1.80, 1.77, 1.77, 1.76, 1.71, 1.70, 1.69, 1.68, 1.67, 1.66, 1.65, 1.65, 1.64, 1.64, 1.63, 1.63, 1.62, 1.61, 1.55, 1.54, 1.53, 1.51, 0.98, 0.98, 0.96, 0.95, 0.94, 0.93, 0.92, 0.92, 0.90, 0.89, 0.88, 0.87, 0.63, 0.61, 0.58

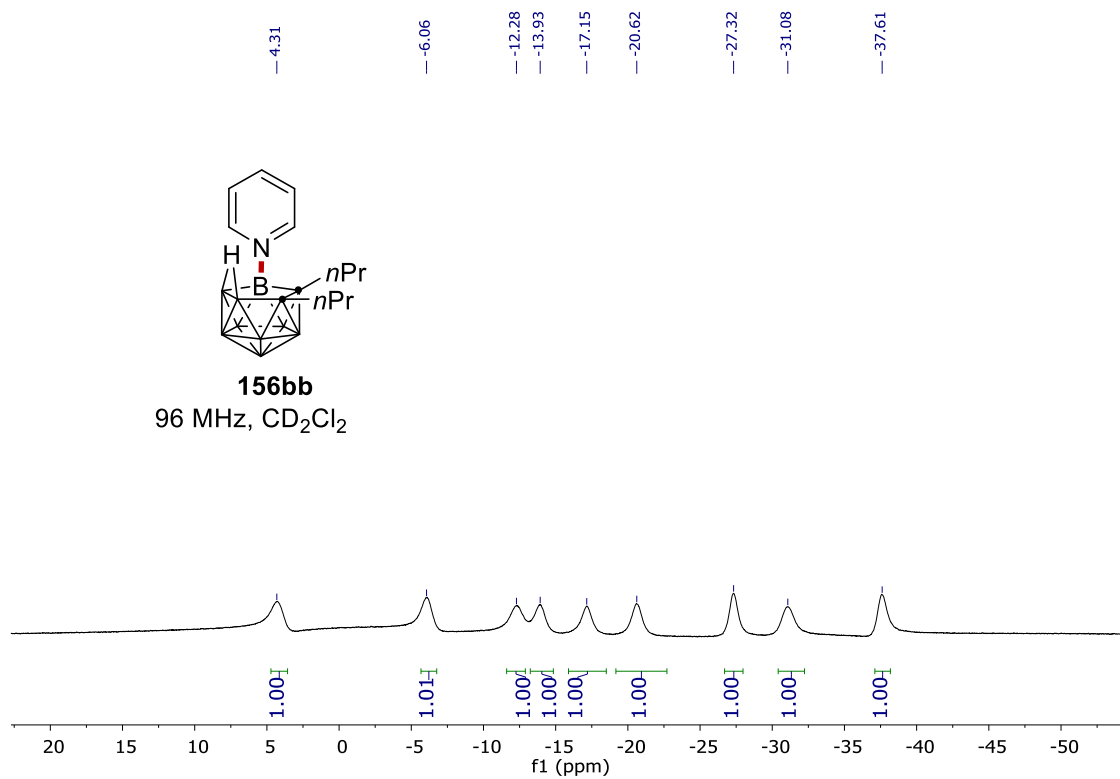
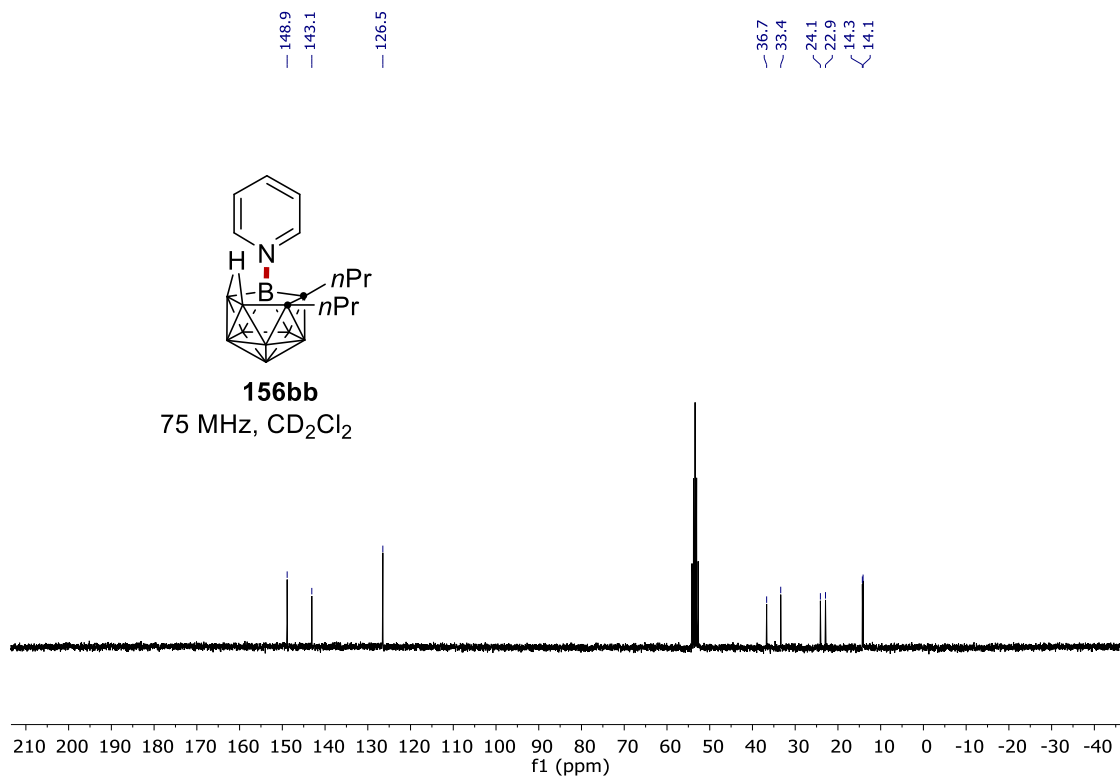


156bb

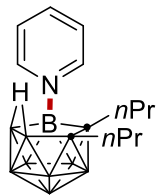
300 MHz, CD₂Cl₂



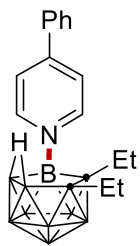
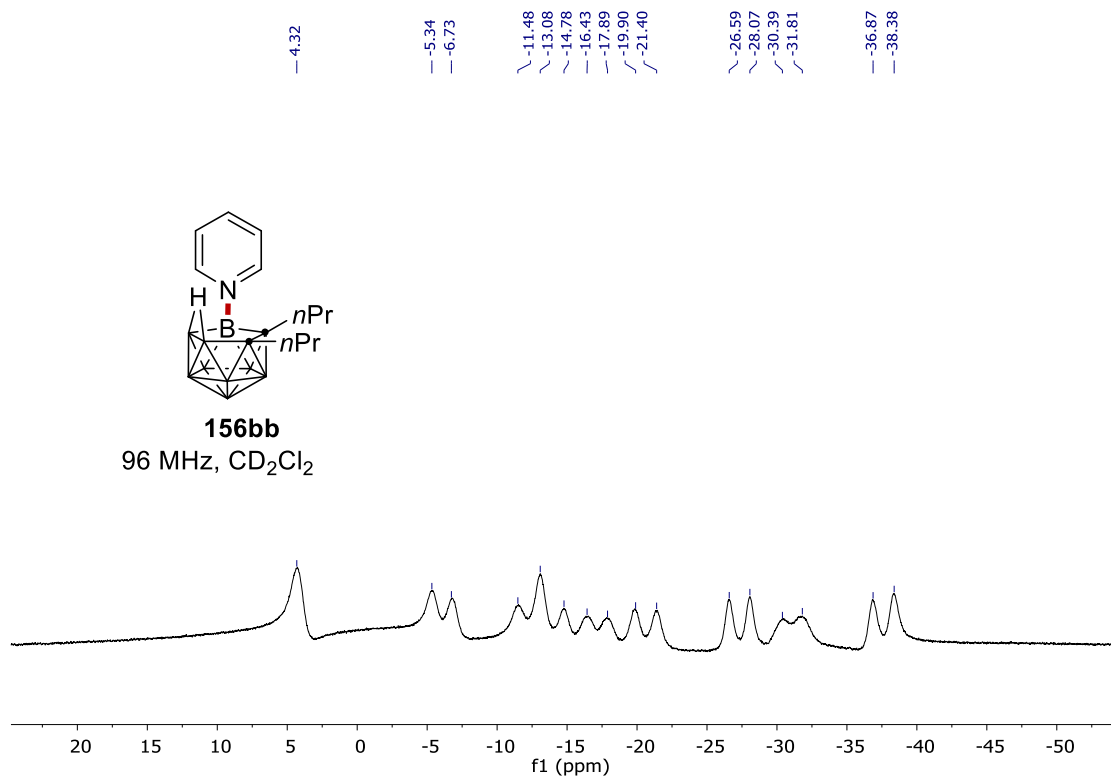
NMR Spectra



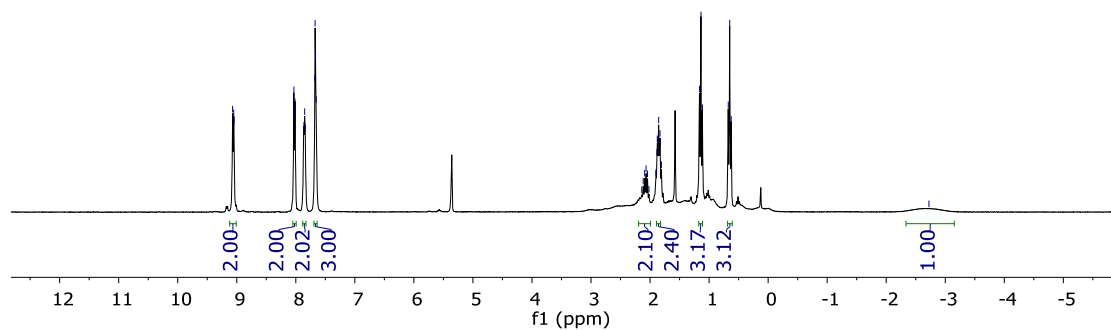
NMR Spectra



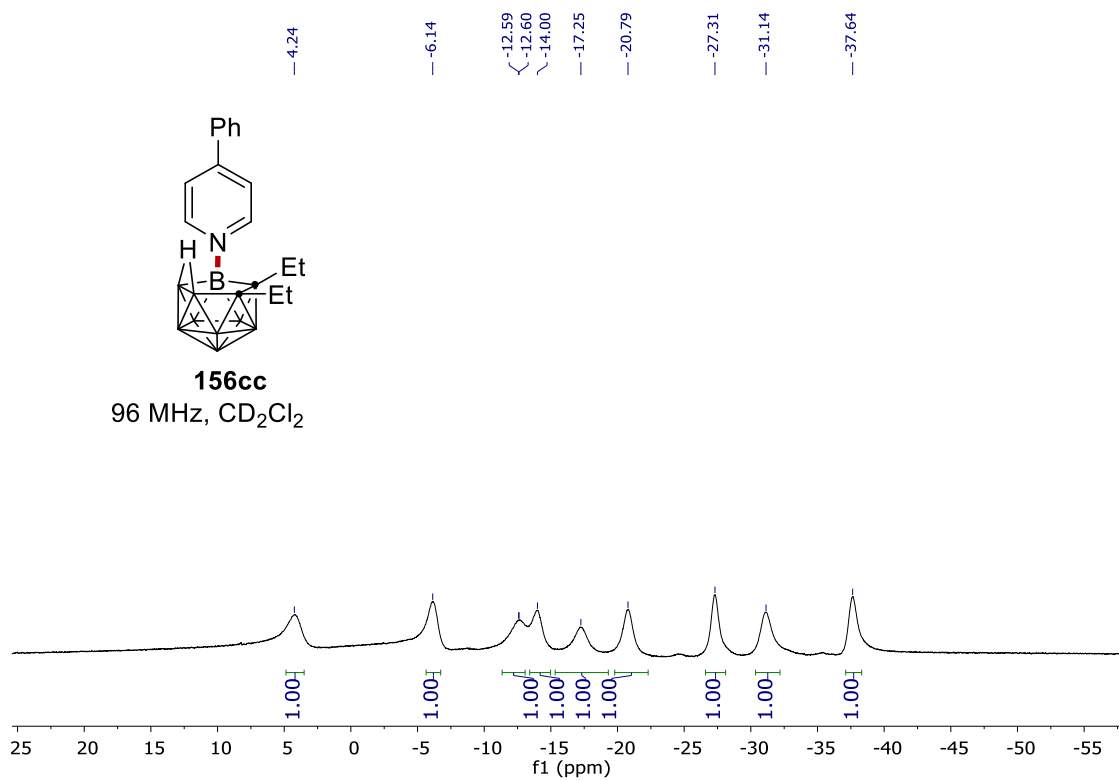
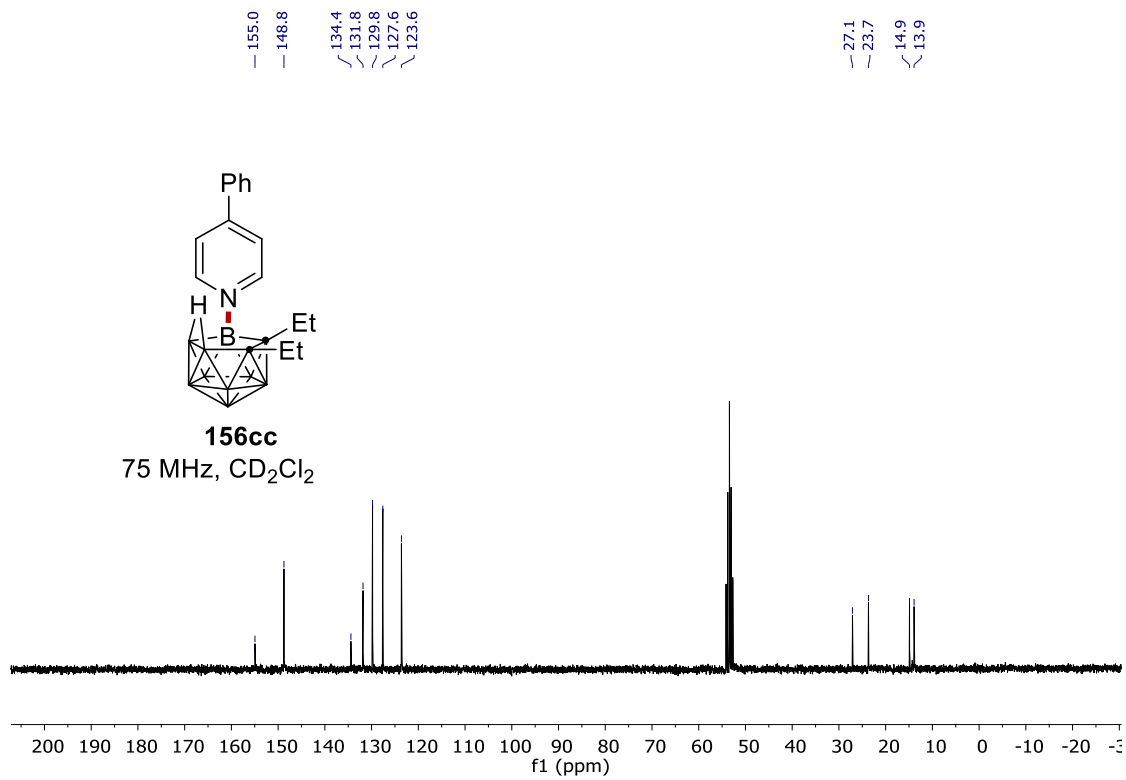
156bb
96 MHz, CD₂Cl₂



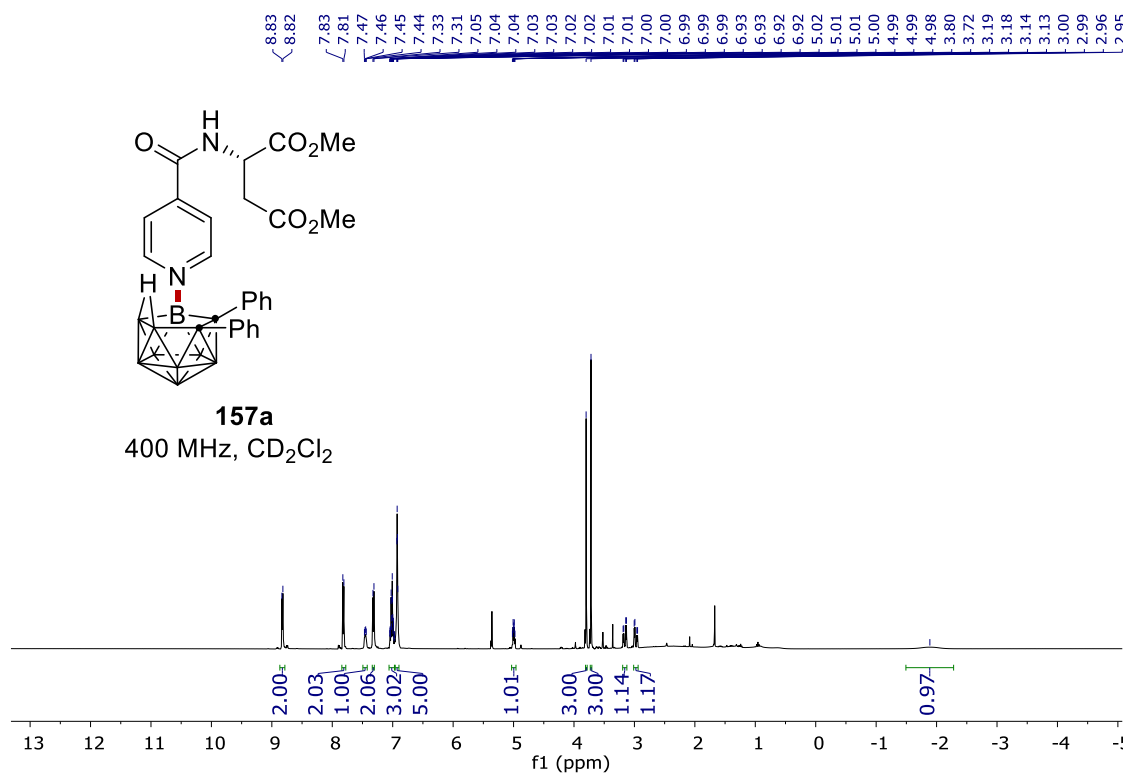
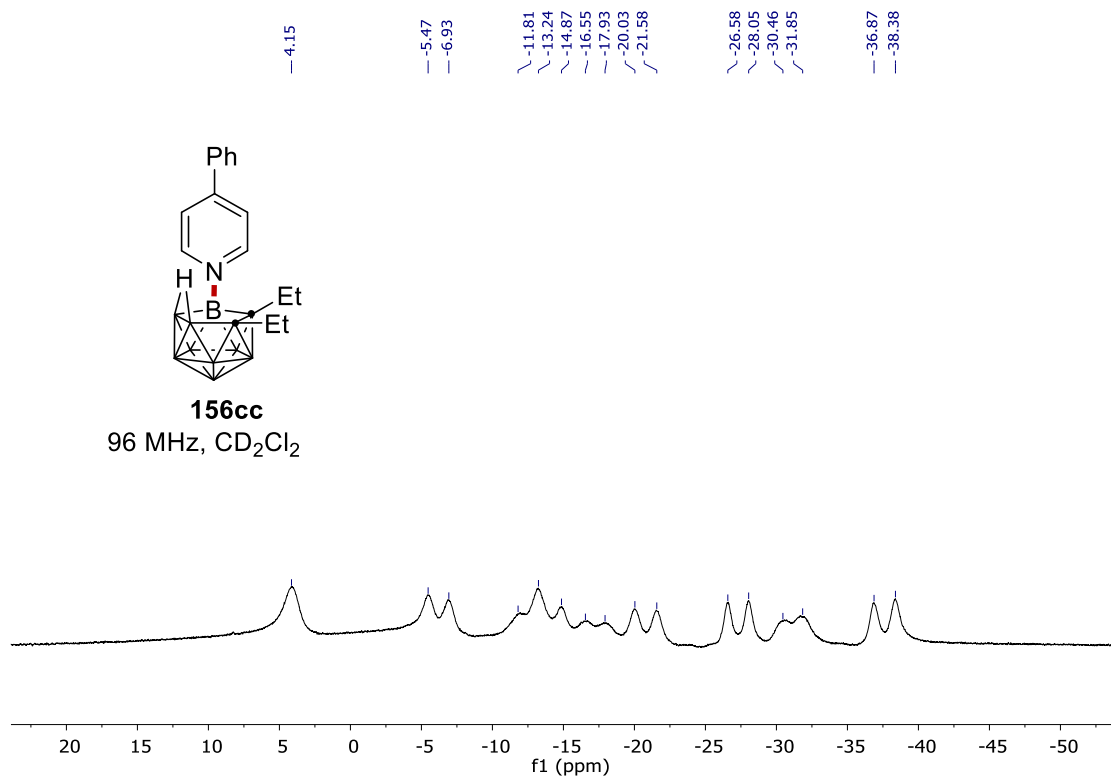
156cc
300 MHz, CD₂Cl₂



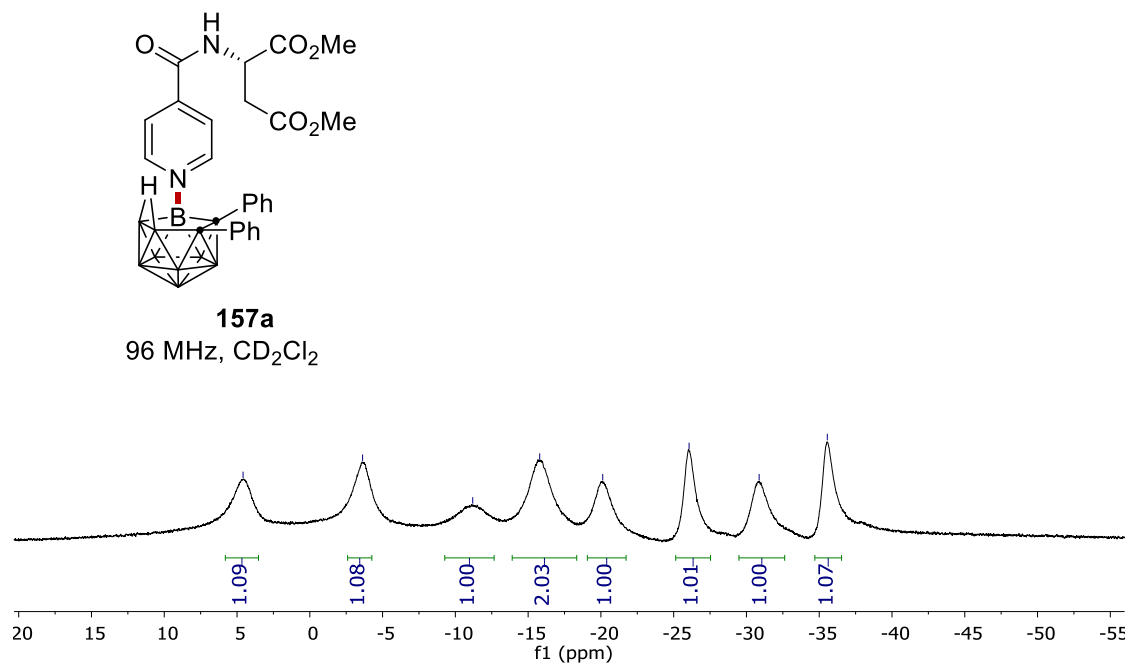
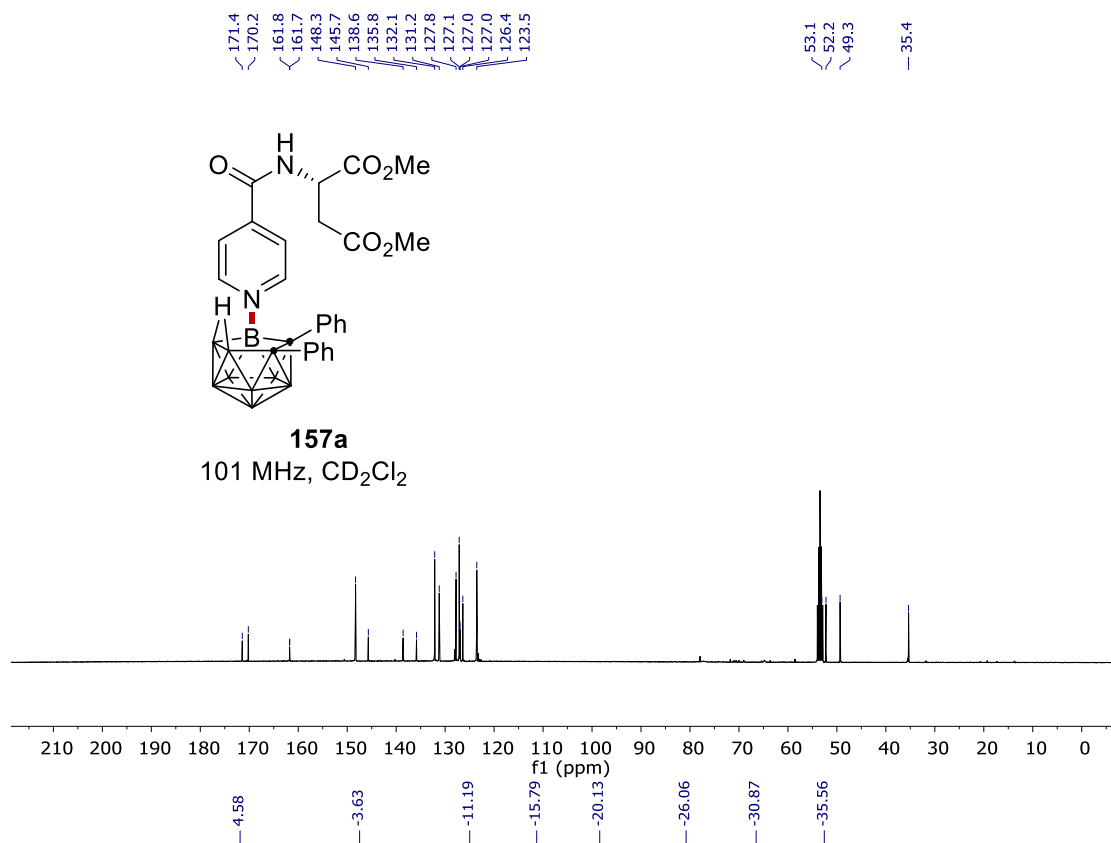
NMR Spectra



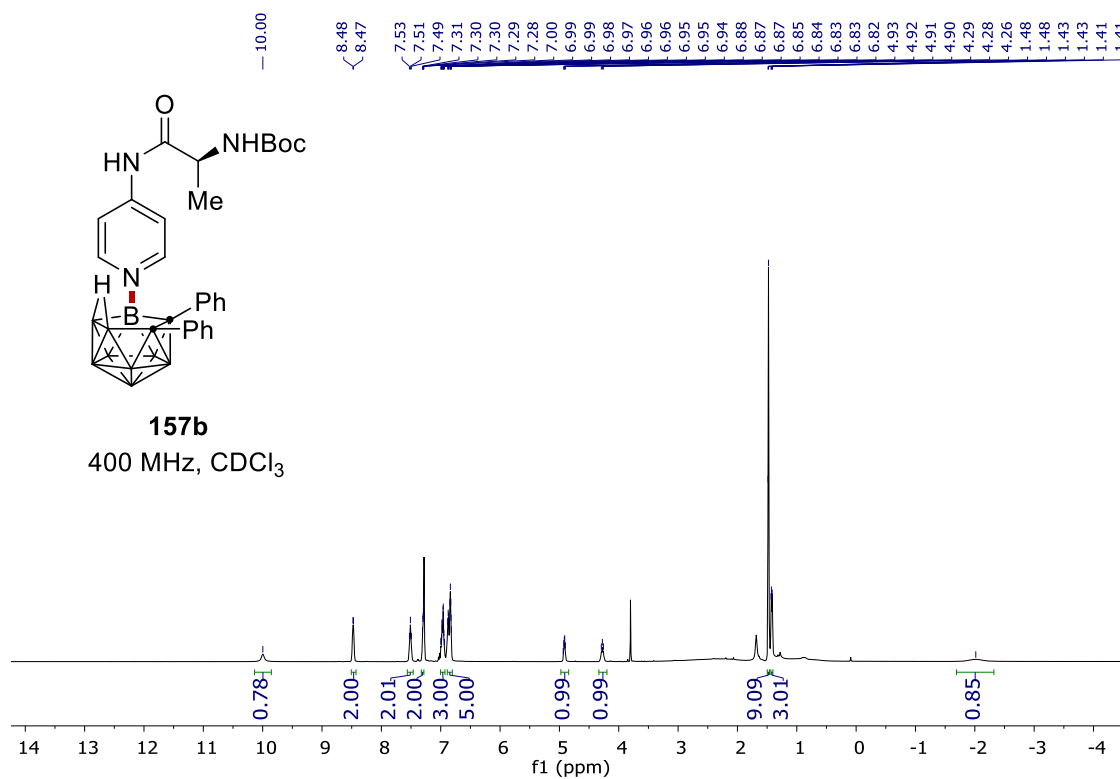
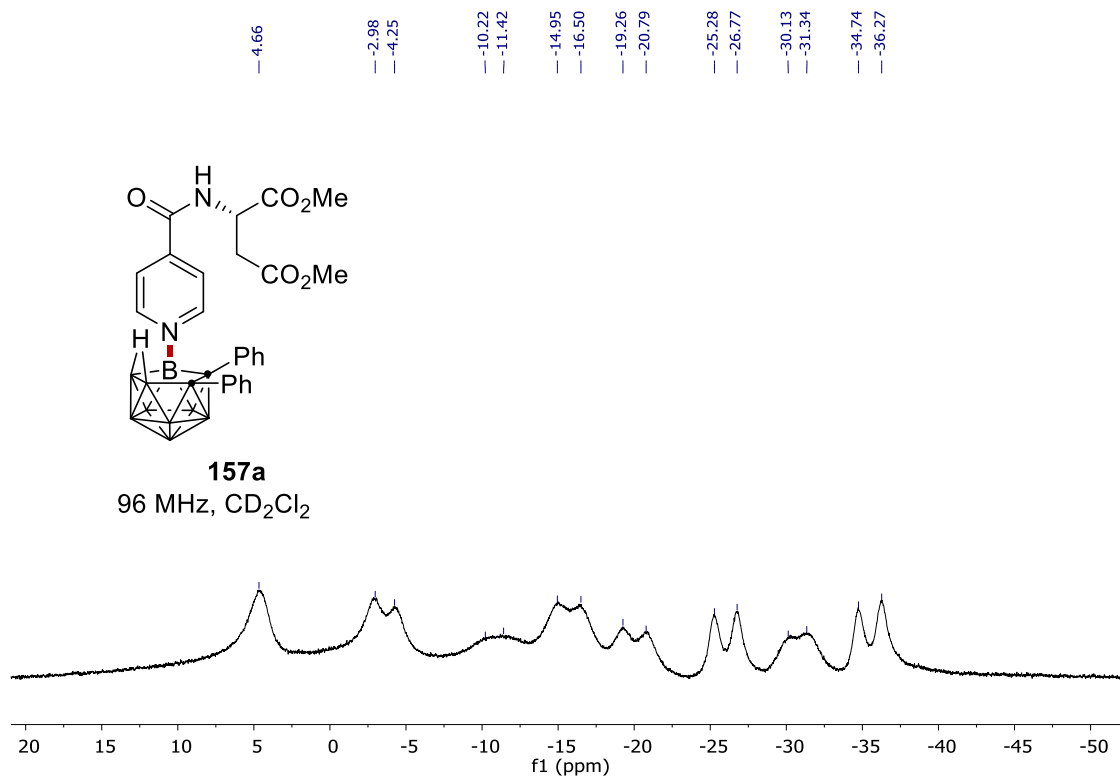
NMR Spectra



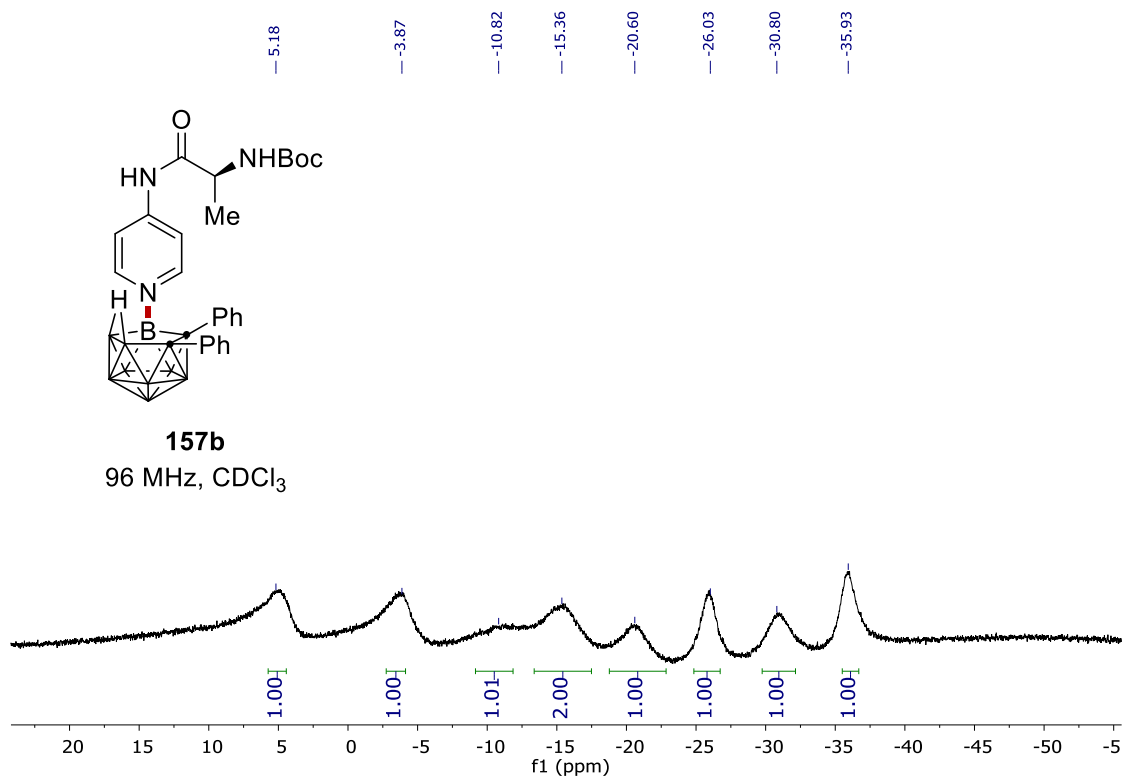
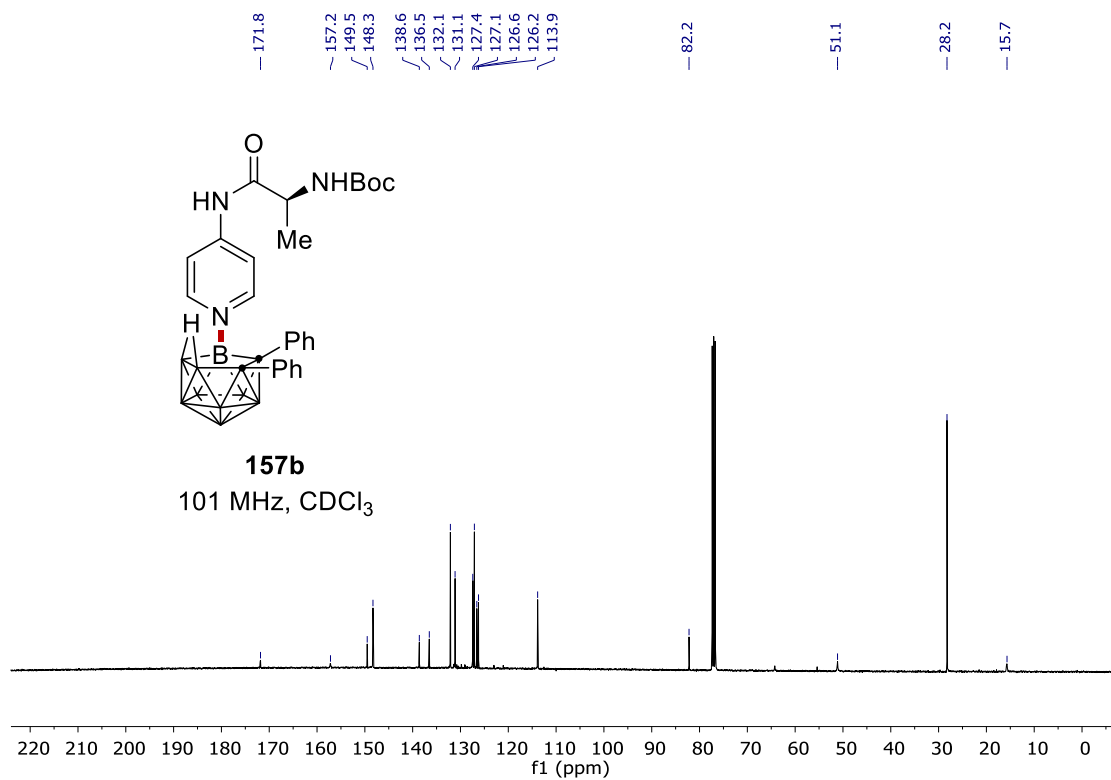
NMR Spectra



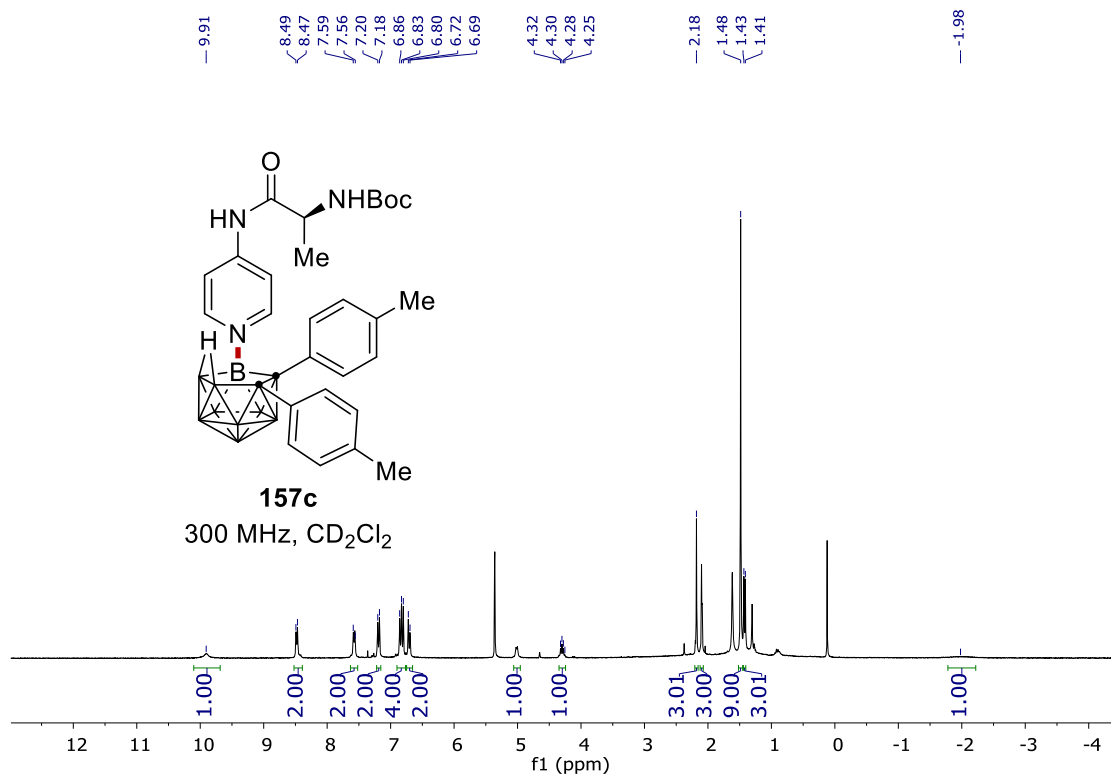
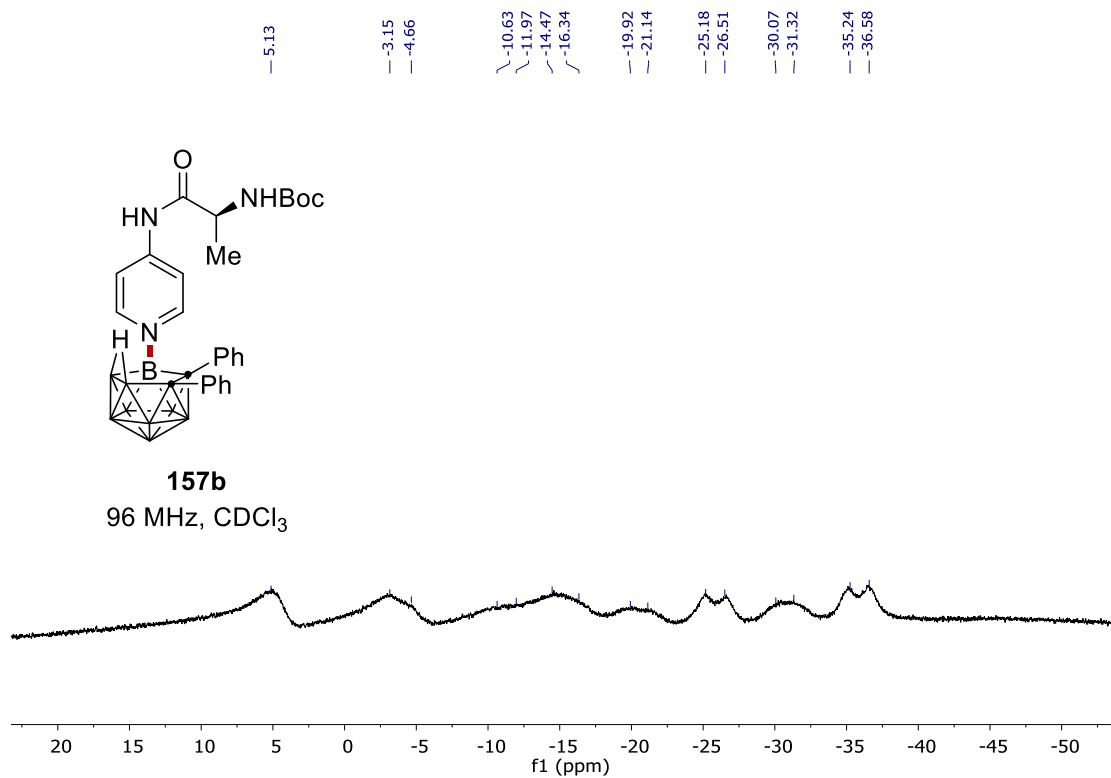
NMR Spectra



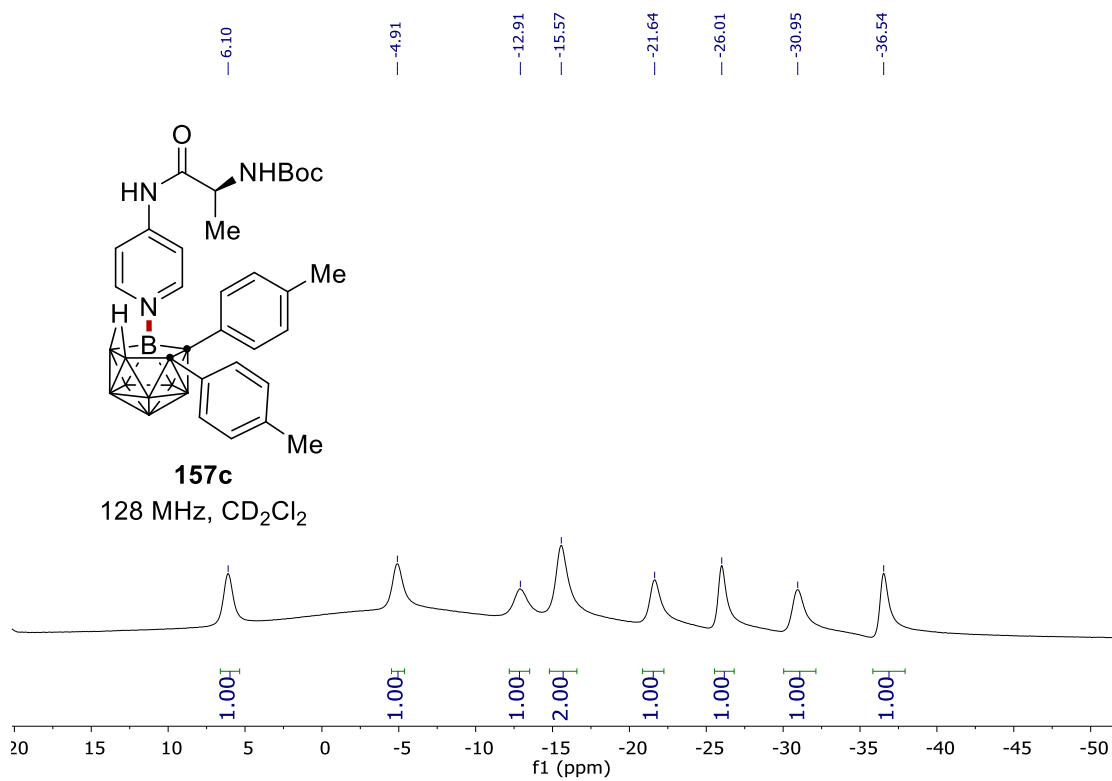
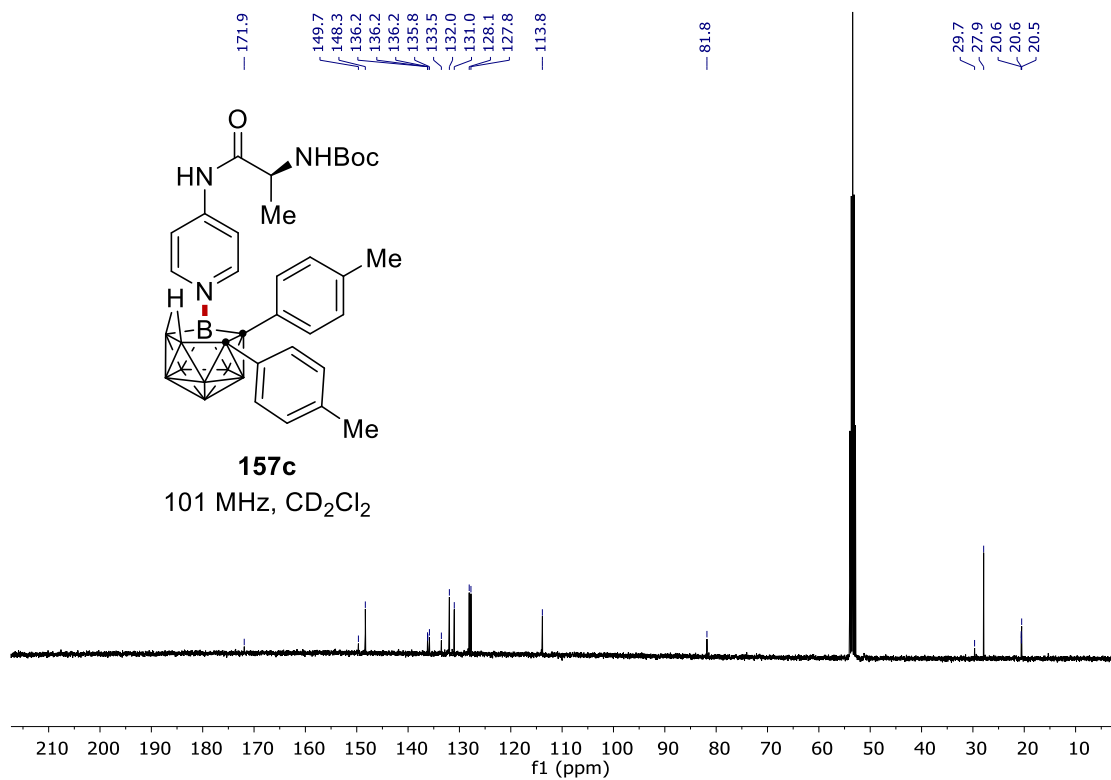
NMR Spectra



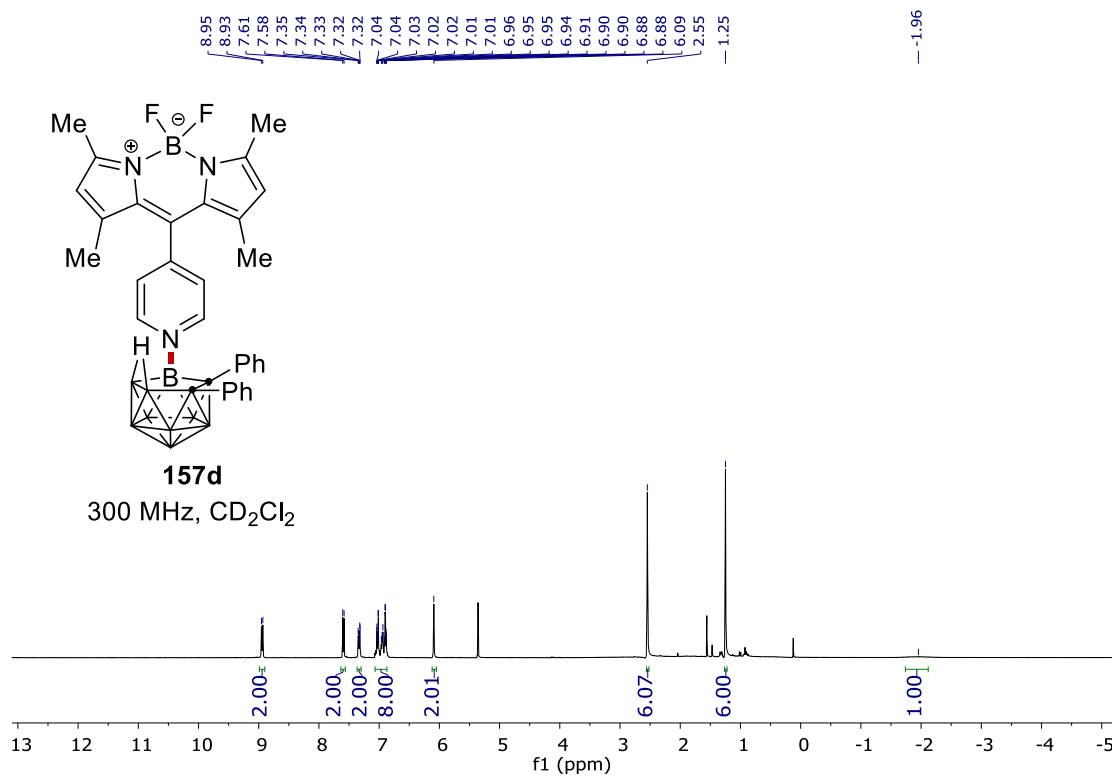
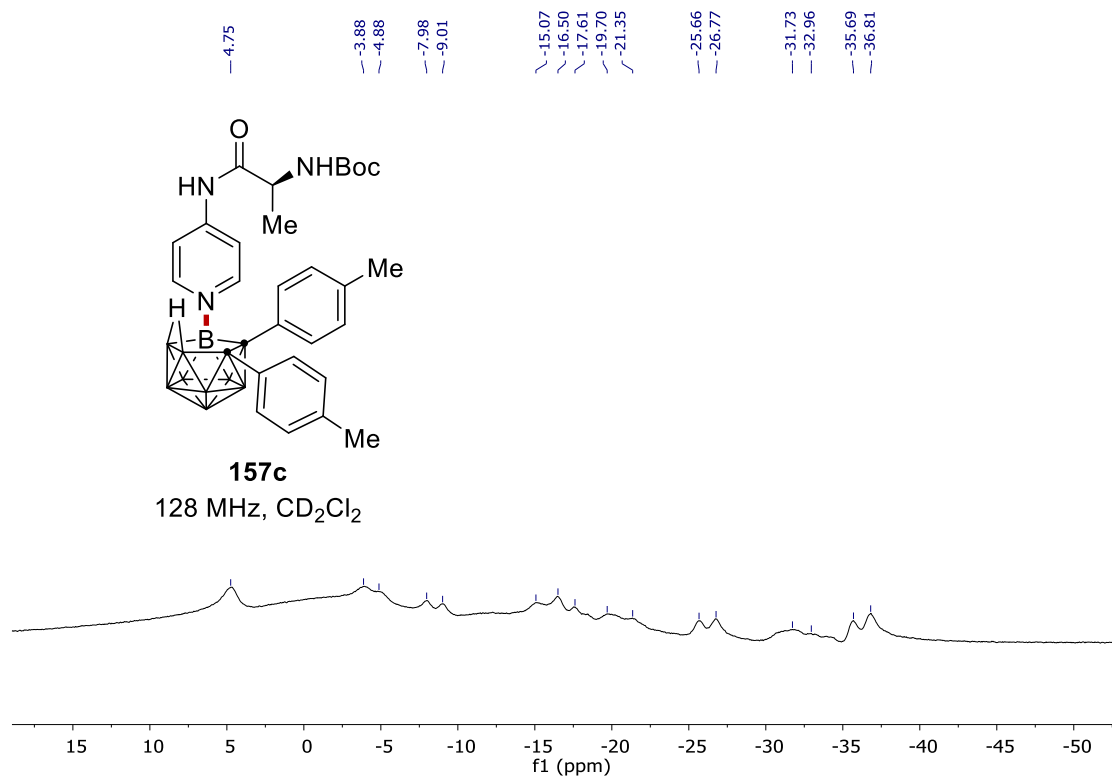
NMR Spectra



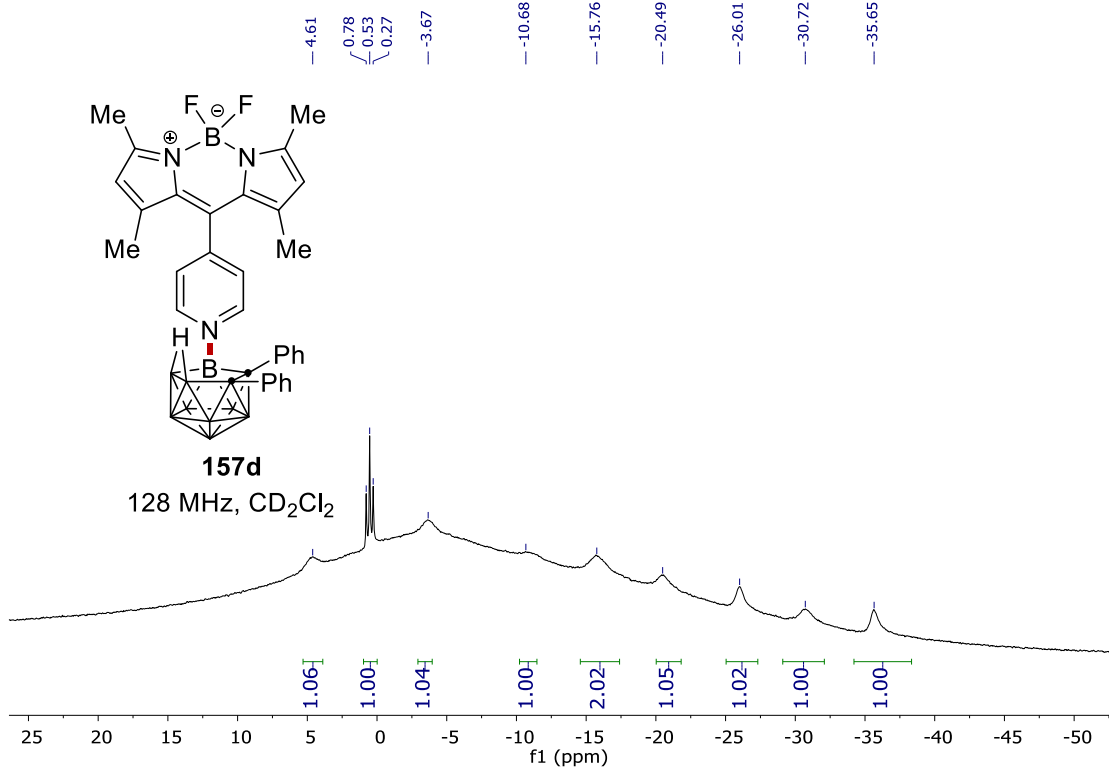
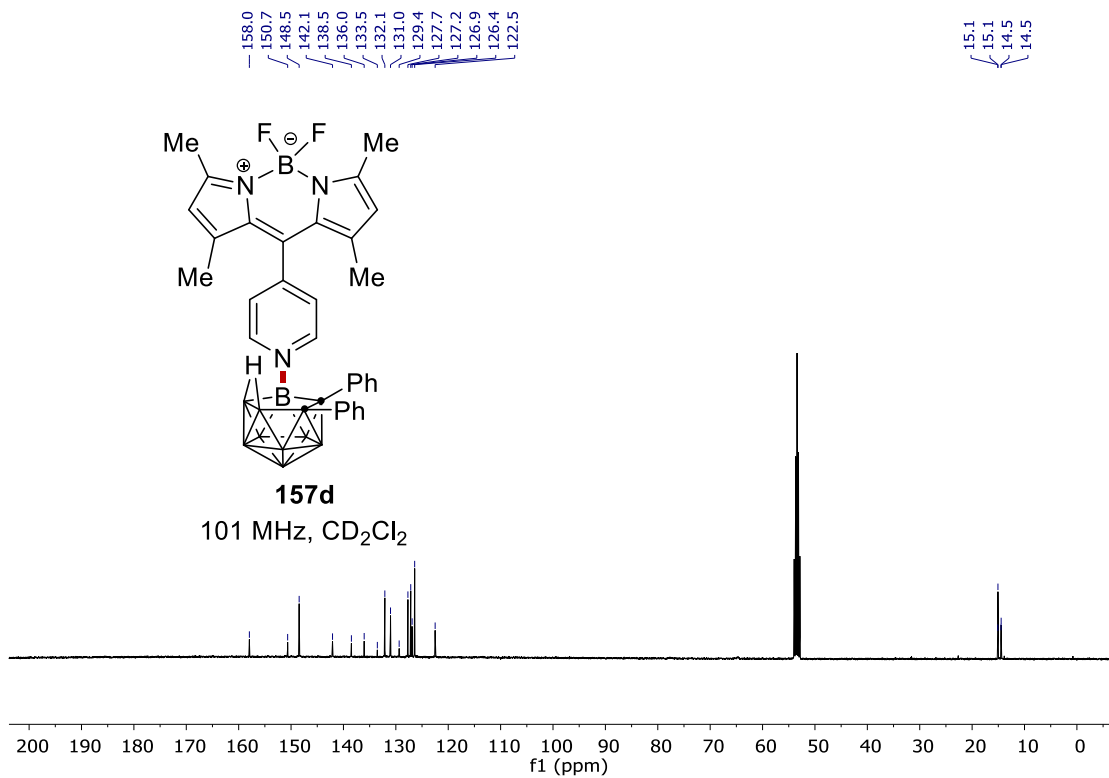
NMR Spectra



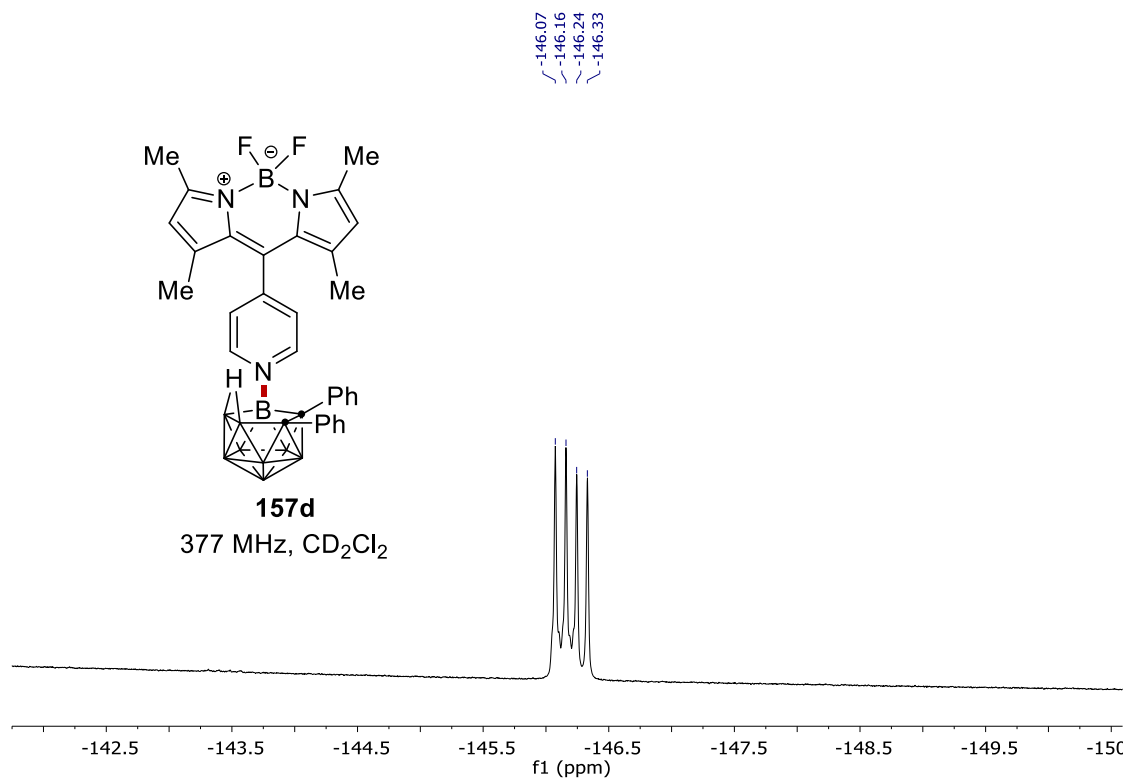
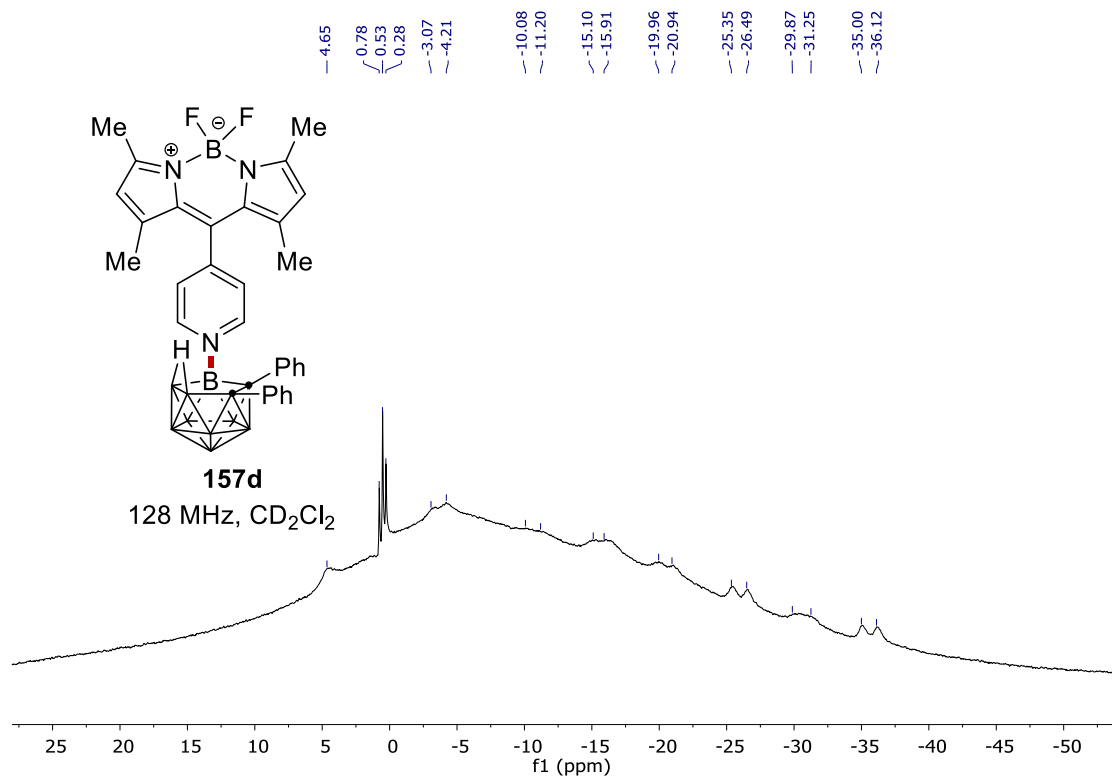
NMR Spectra



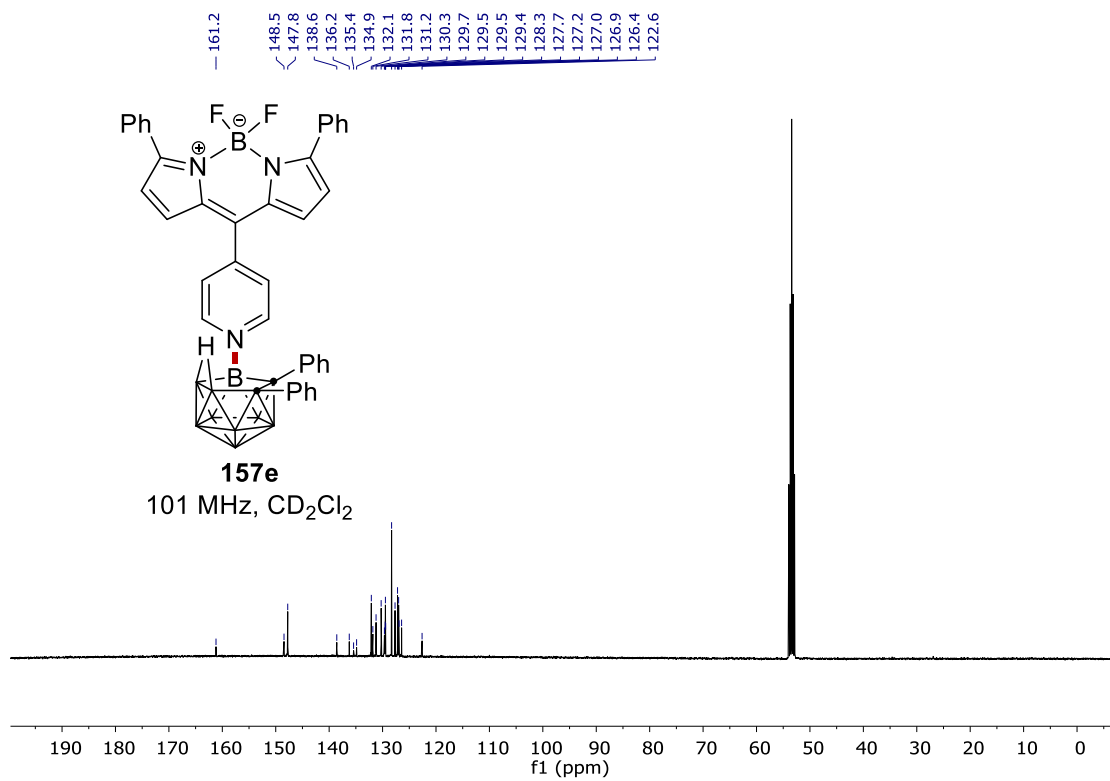
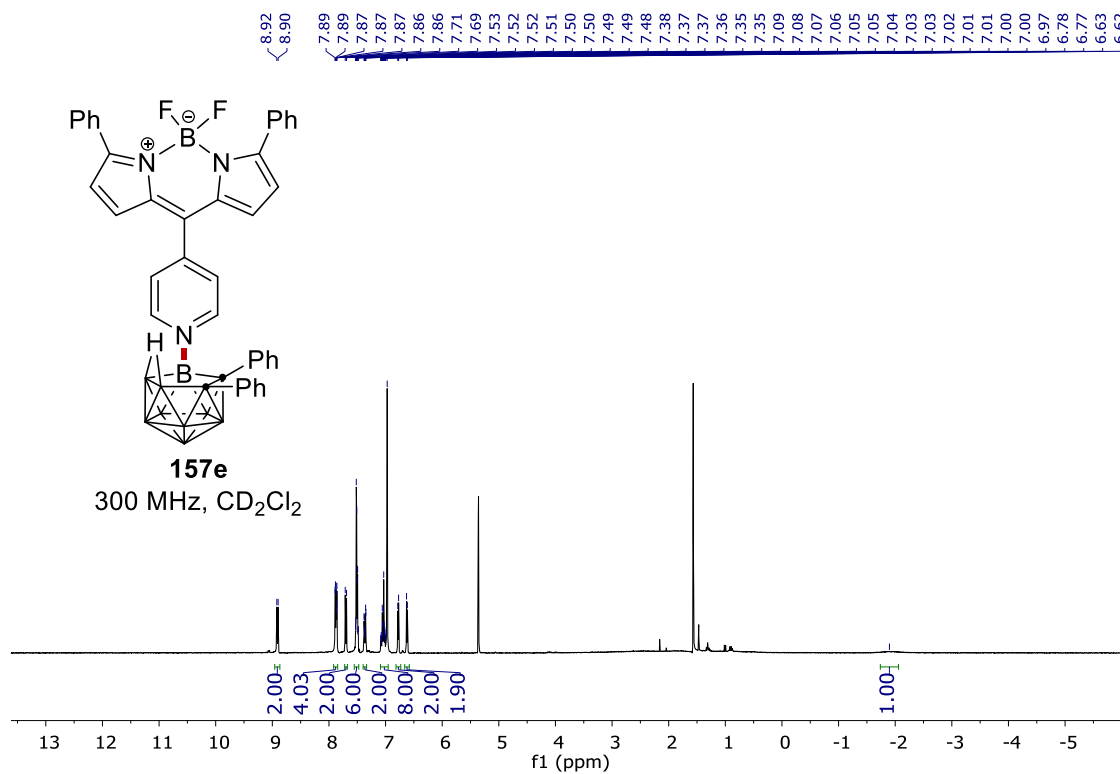
NMR Spectra



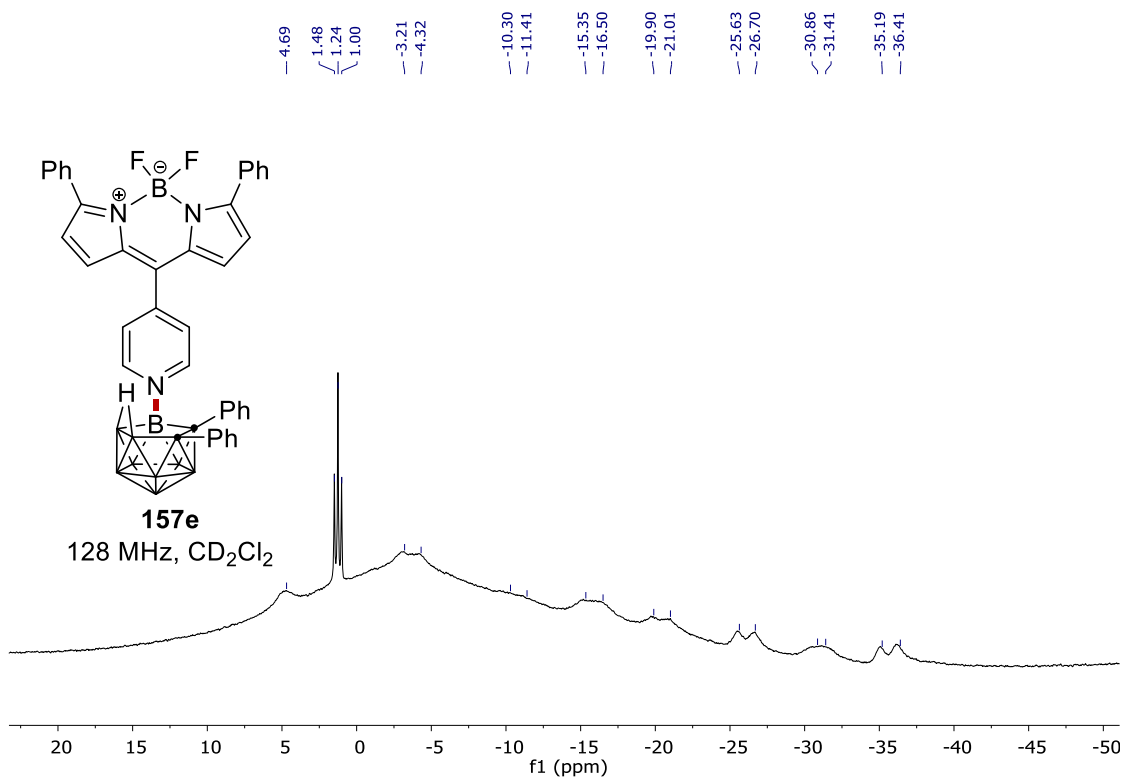
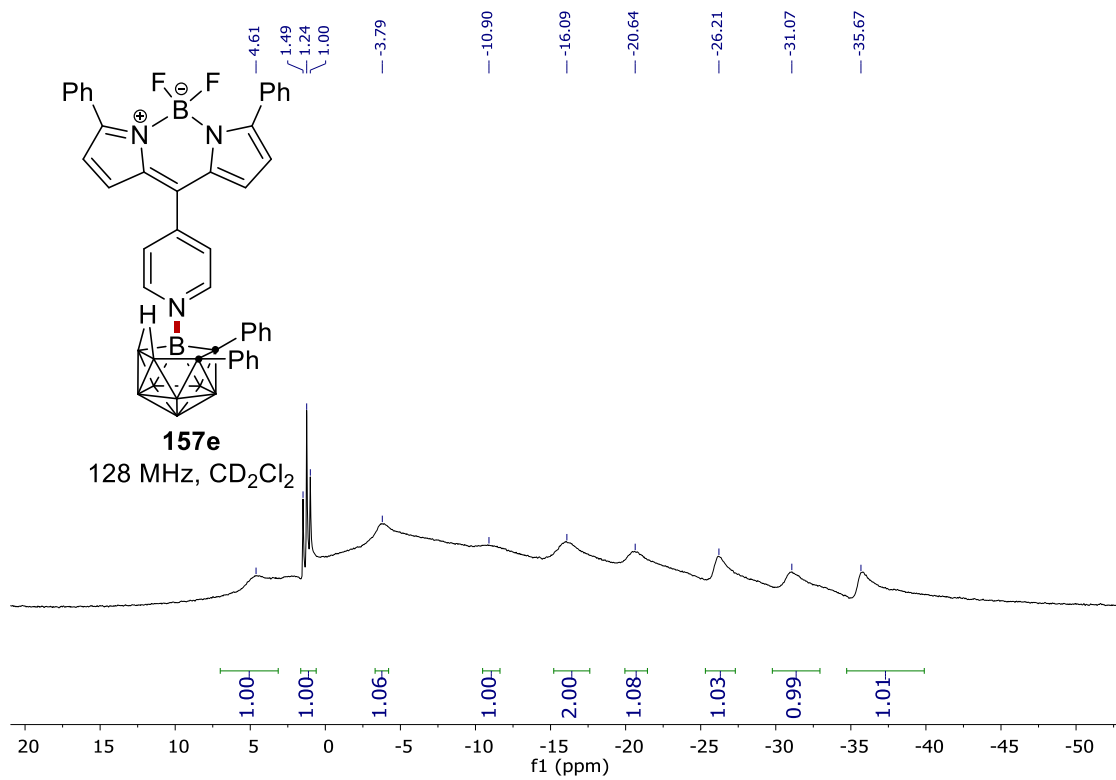
NMR Spectra



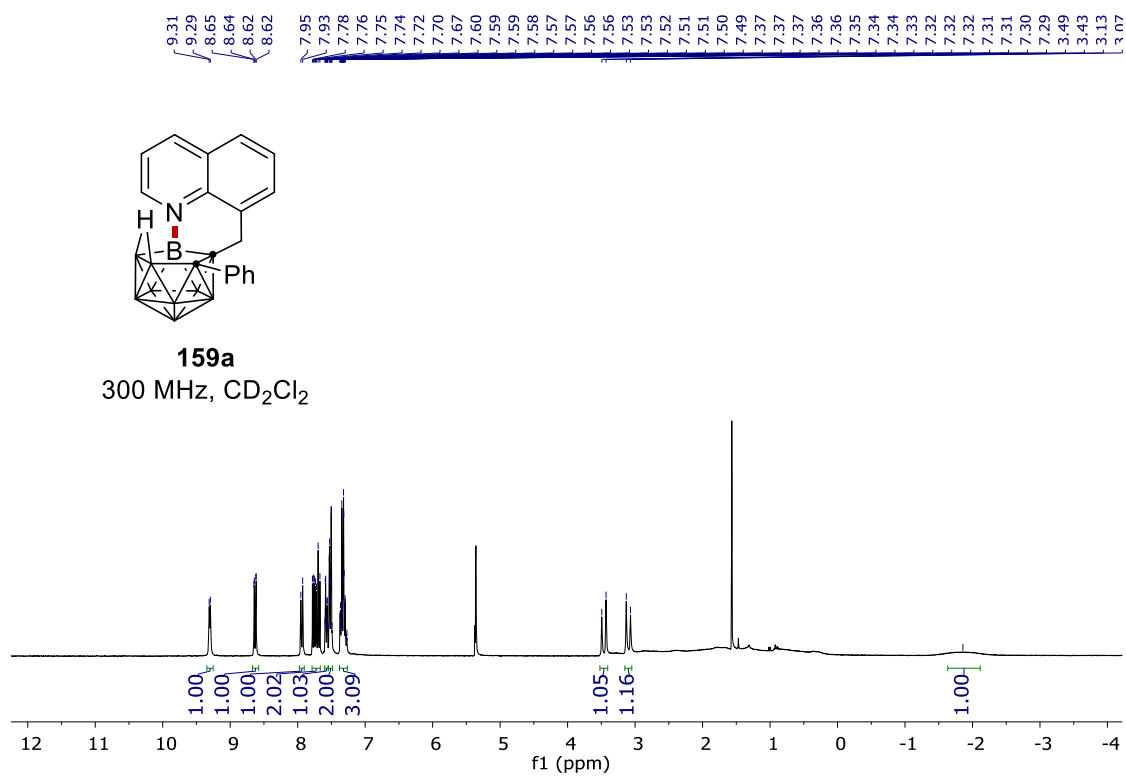
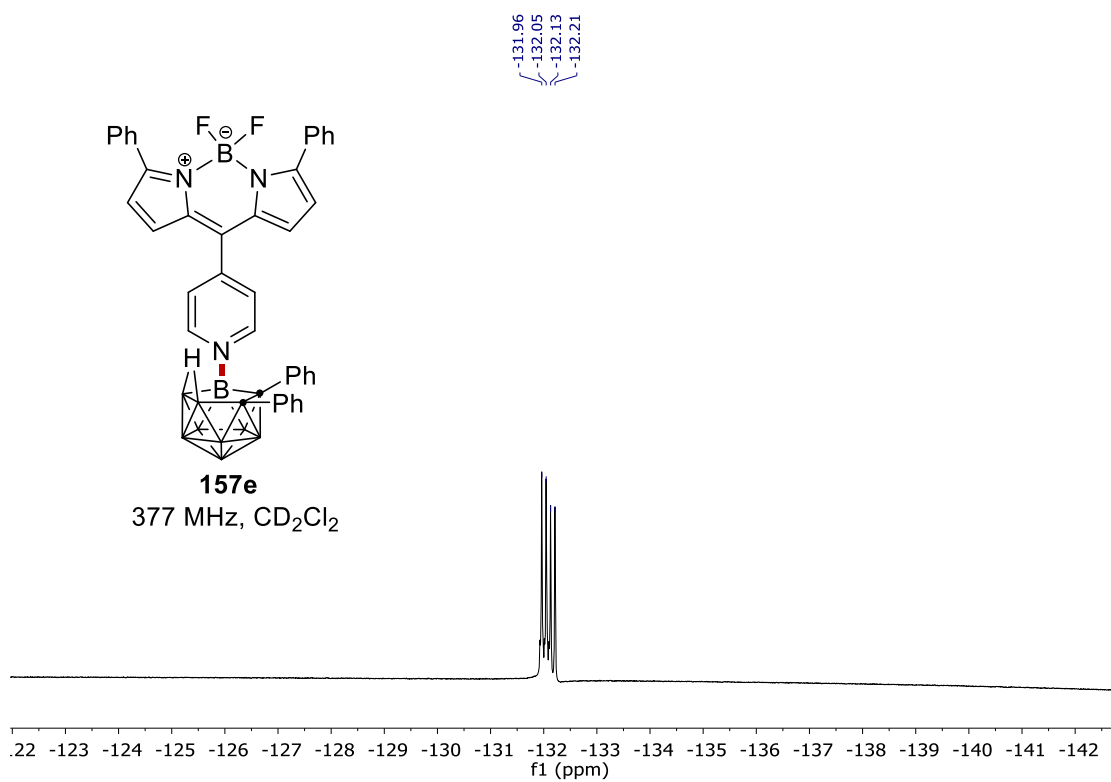
NMR Spectra



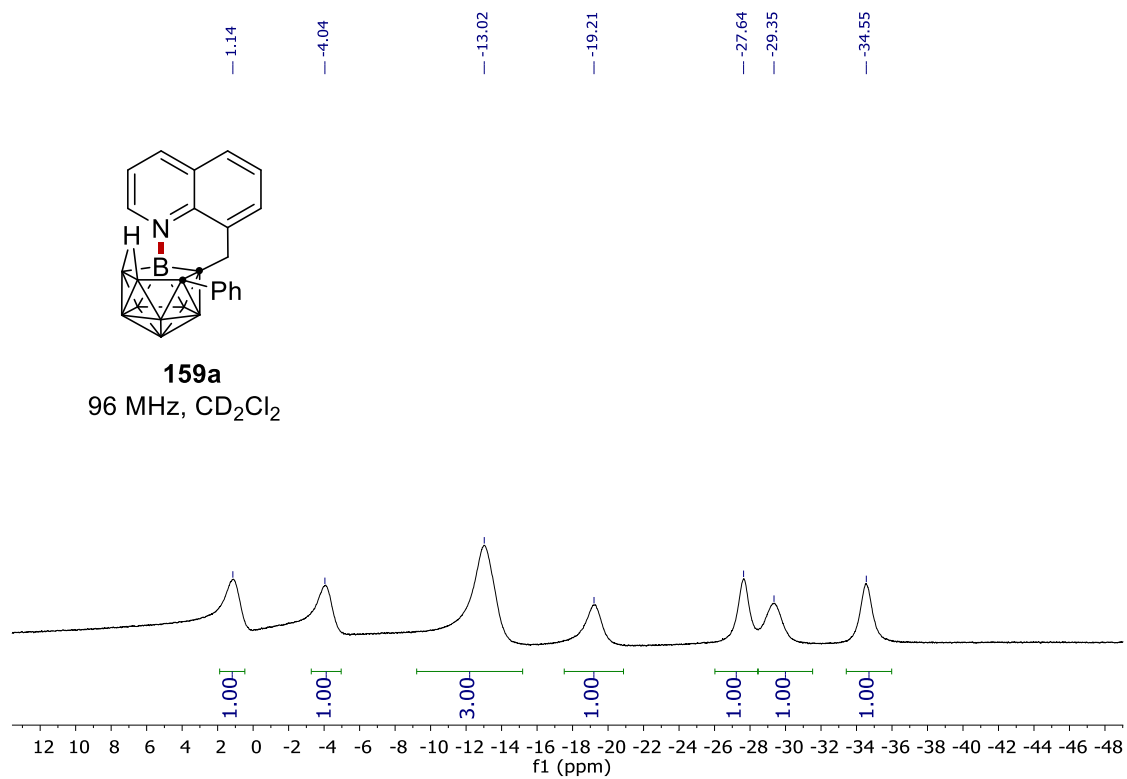
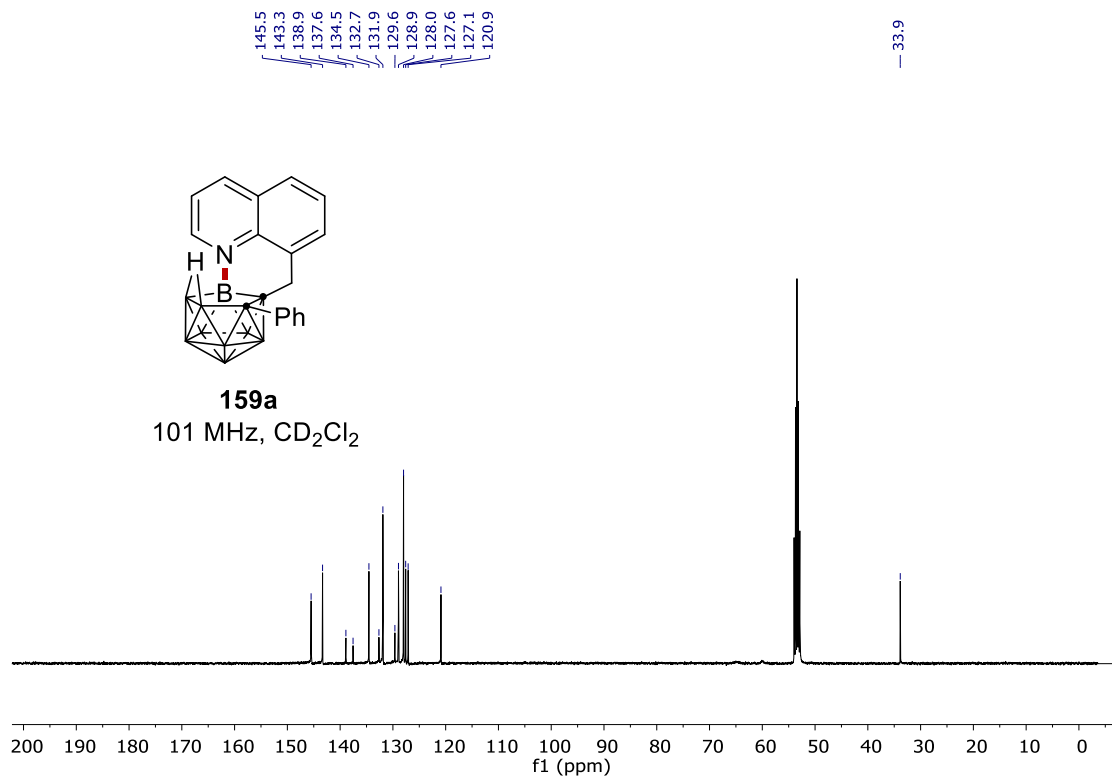
NMR Spectra



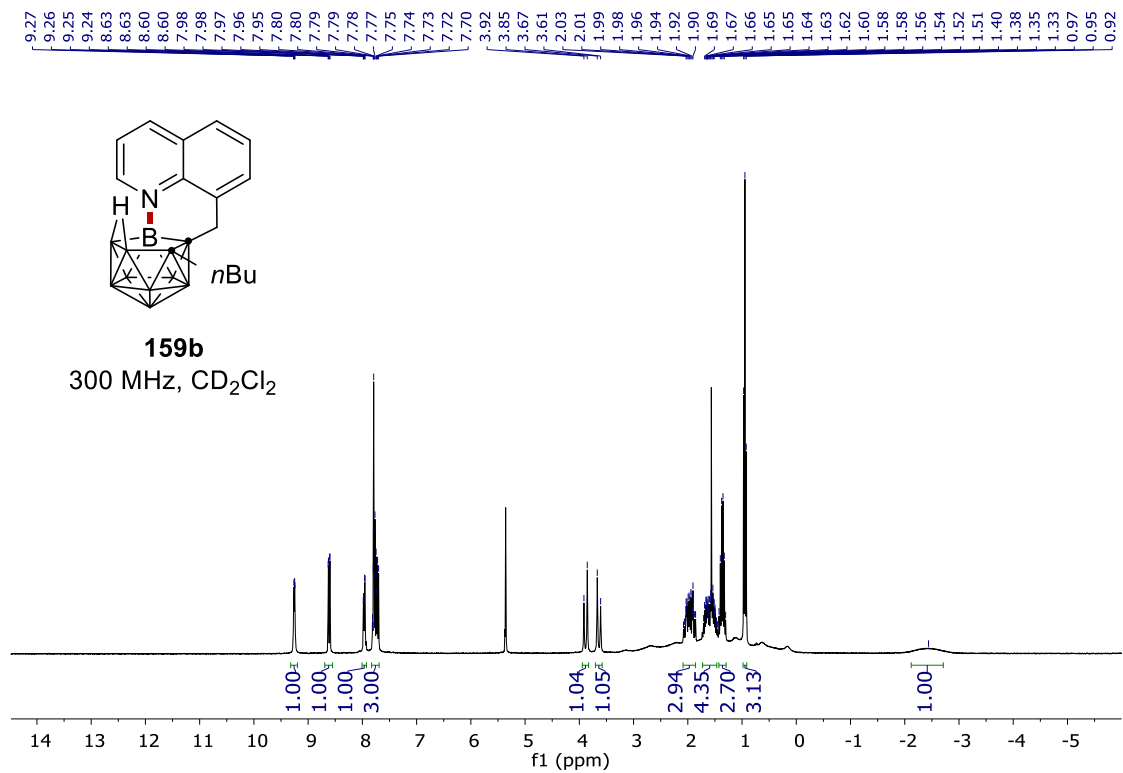
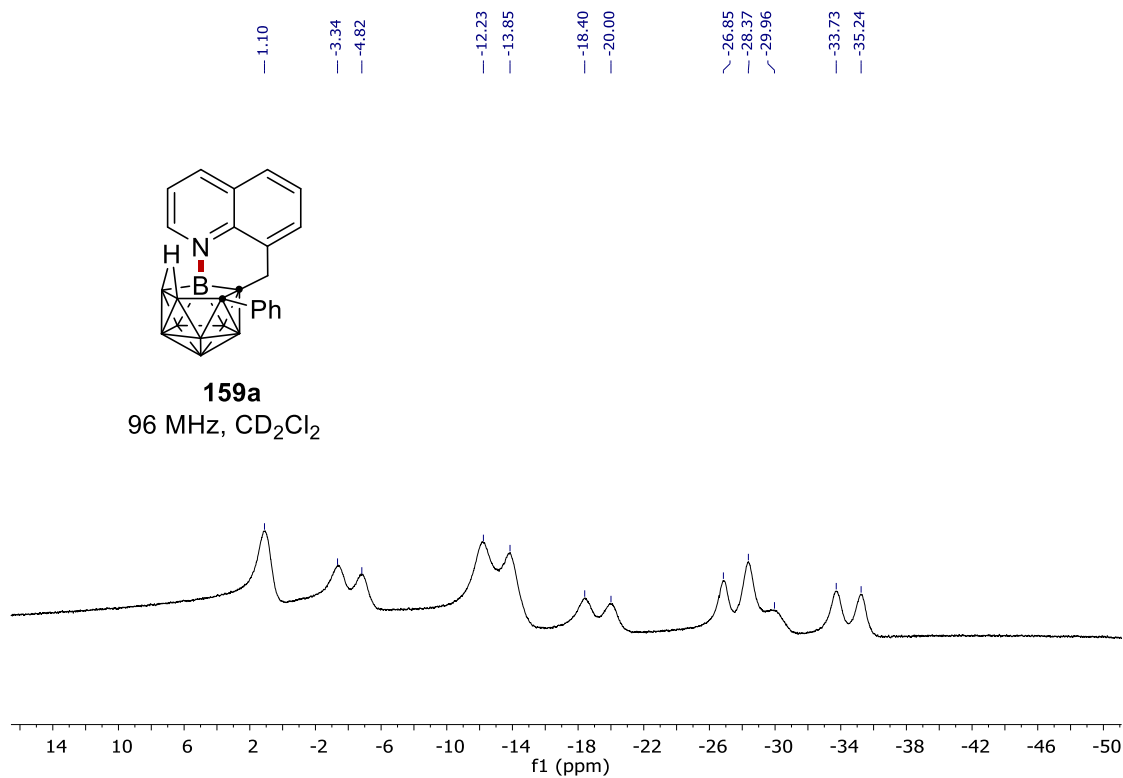
NMR Spectra



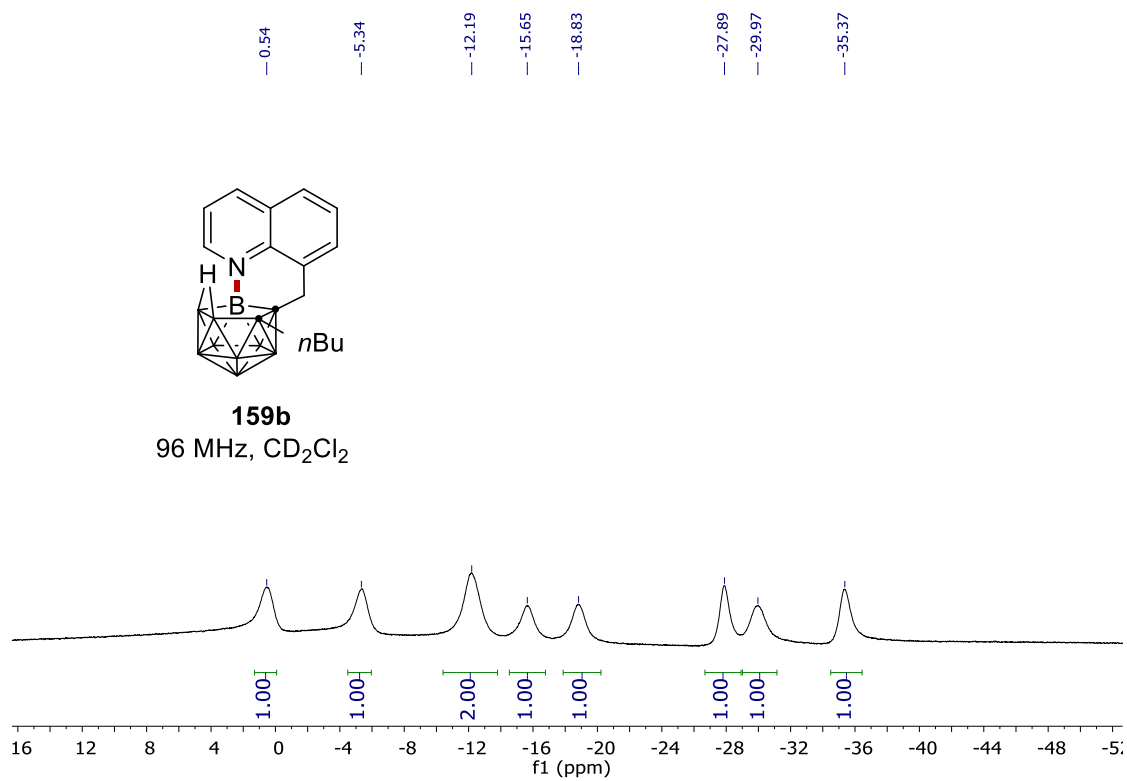
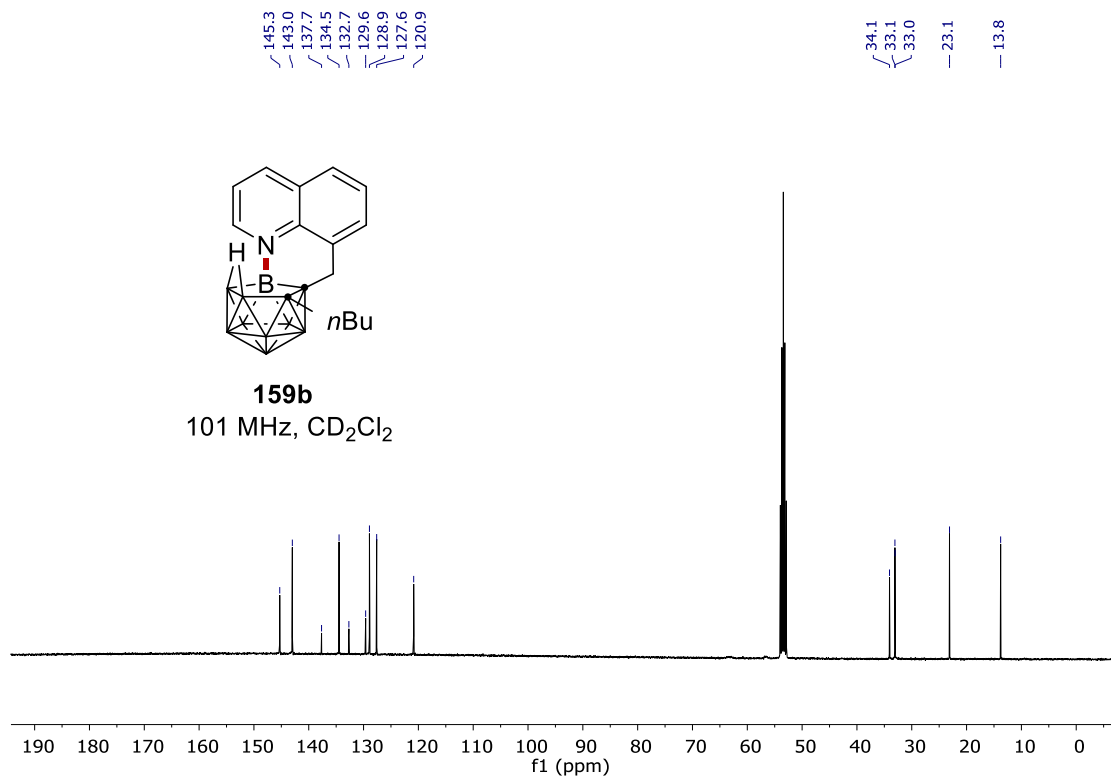
NMR Spectra



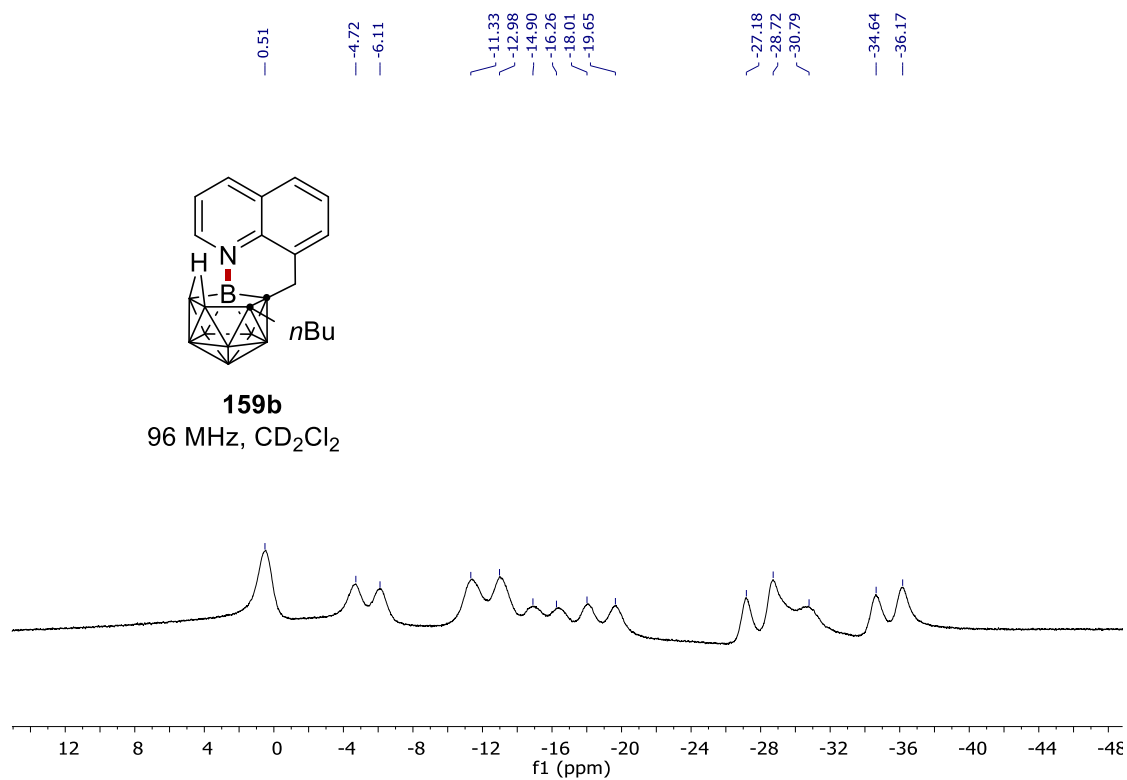
NMR Spectra



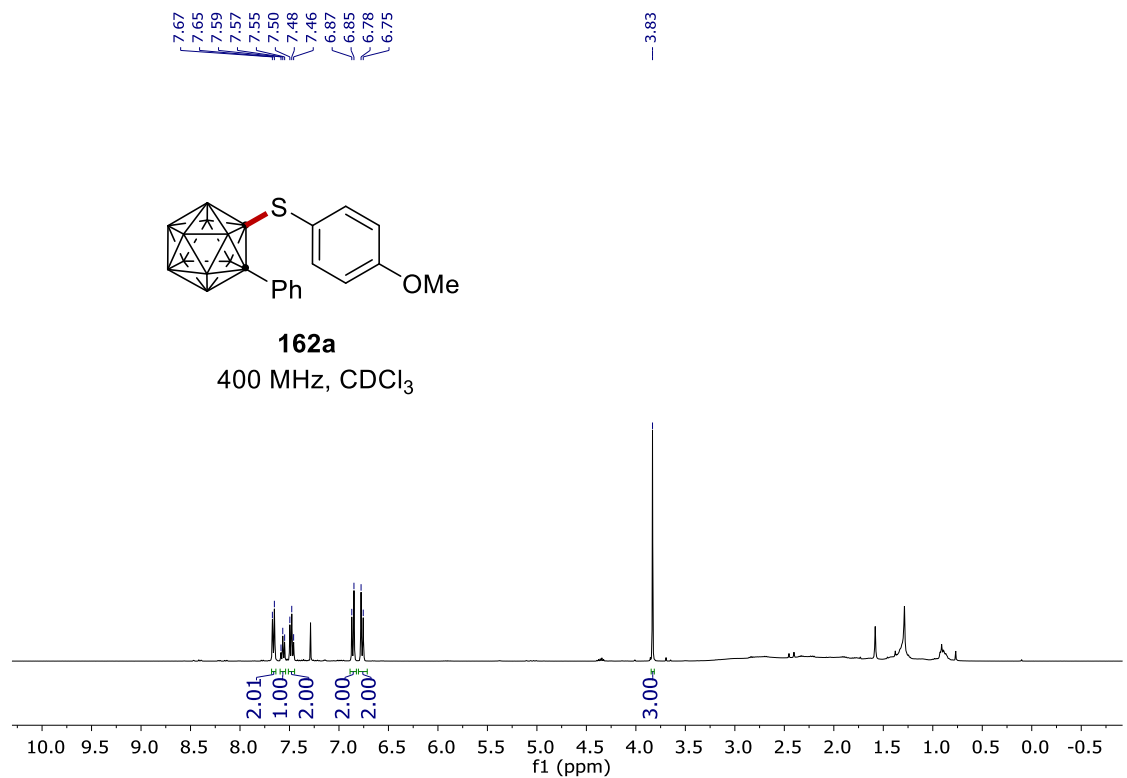
NMR Spectra



NMR Spectra



7.6 Cupraelectro-Oxidative Chalcogenation of o-Carboranes

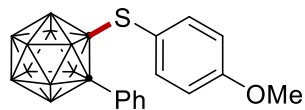


NMR Spectra

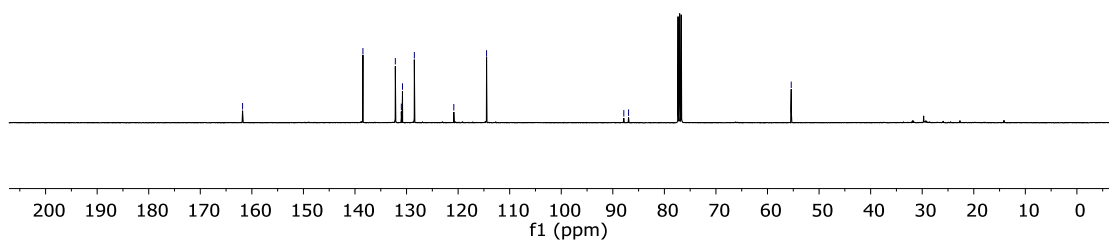
161.8
138.5
132.2
131.0
130.8
128.5
120.8
114.5

87.9
86.9

55.4

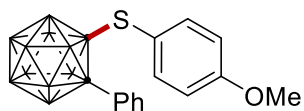


162a
101 MHz, CDCl₃

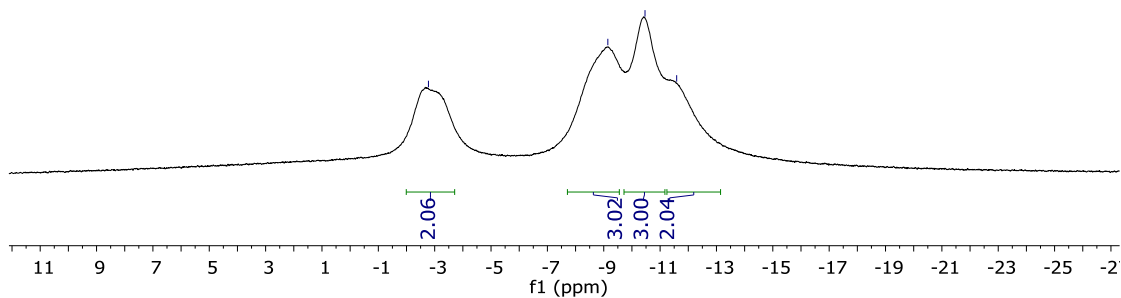


-2.78

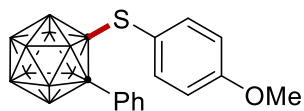
-9.14
-10.46
-11.59



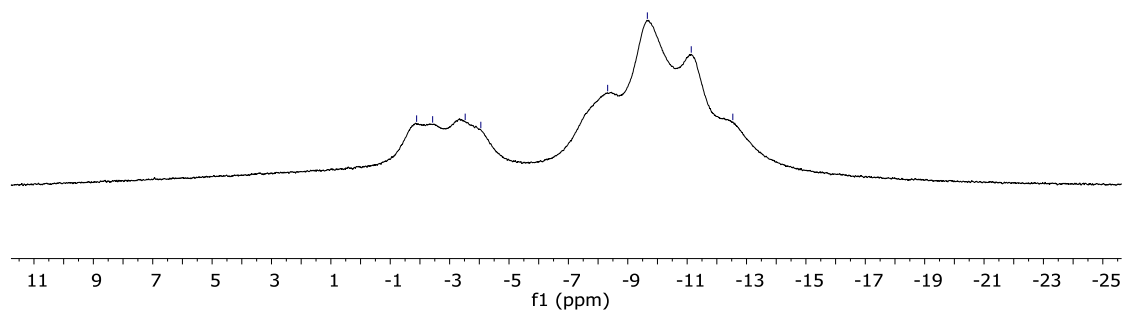
162a
96 MHz, CDCl₃



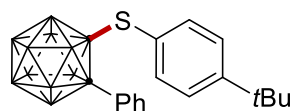
NMR Spectra



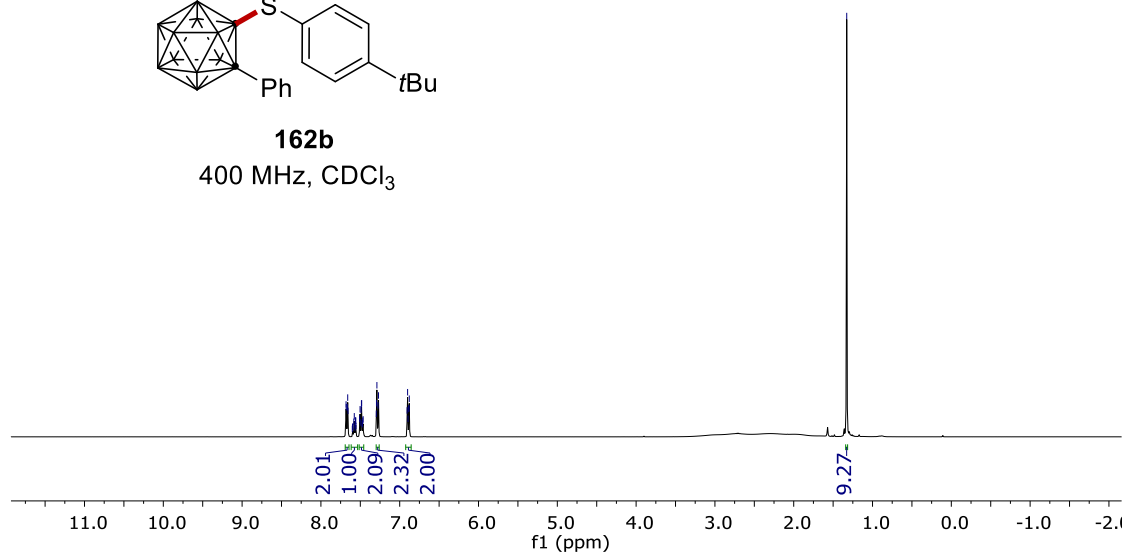
162a
96 MHz, CDCl₃



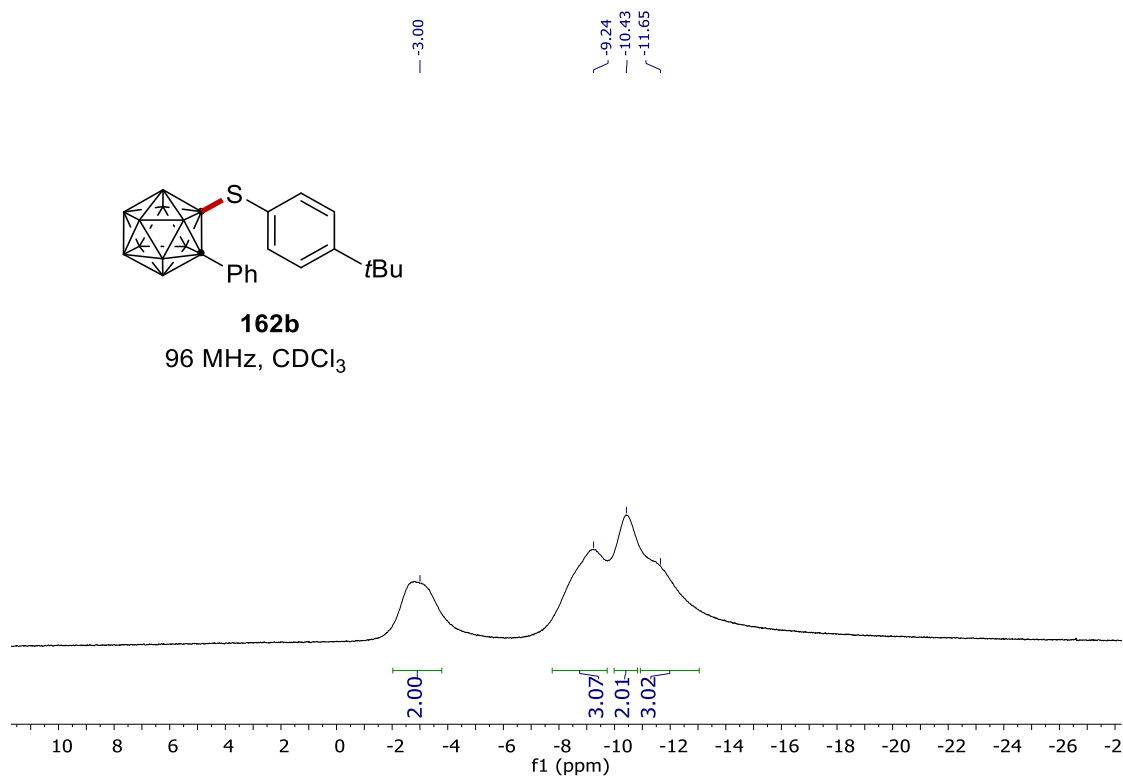
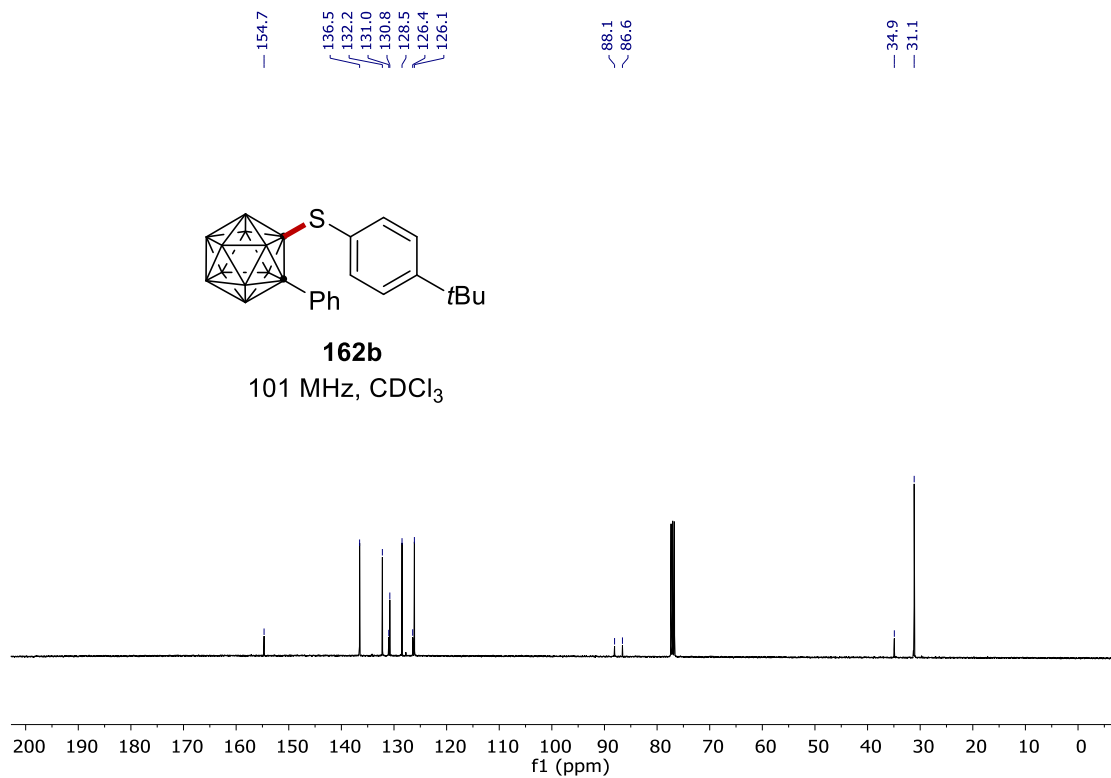
7.68
7.66
7.66
7.66
7.60
7.60
7.59
7.58
7.58
7.57
7.56
7.56
7.56
7.55
7.55
7.51
7.50
7.49
7.49
7.48
7.48
7.48
7.47
7.47
7.46
7.30
7.29
7.29
7.28
7.27
6.91
6.90
6.89
6.89
6.88
6.88
-1.33



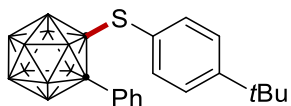
162b
400 MHz, CDCl₃



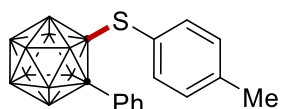
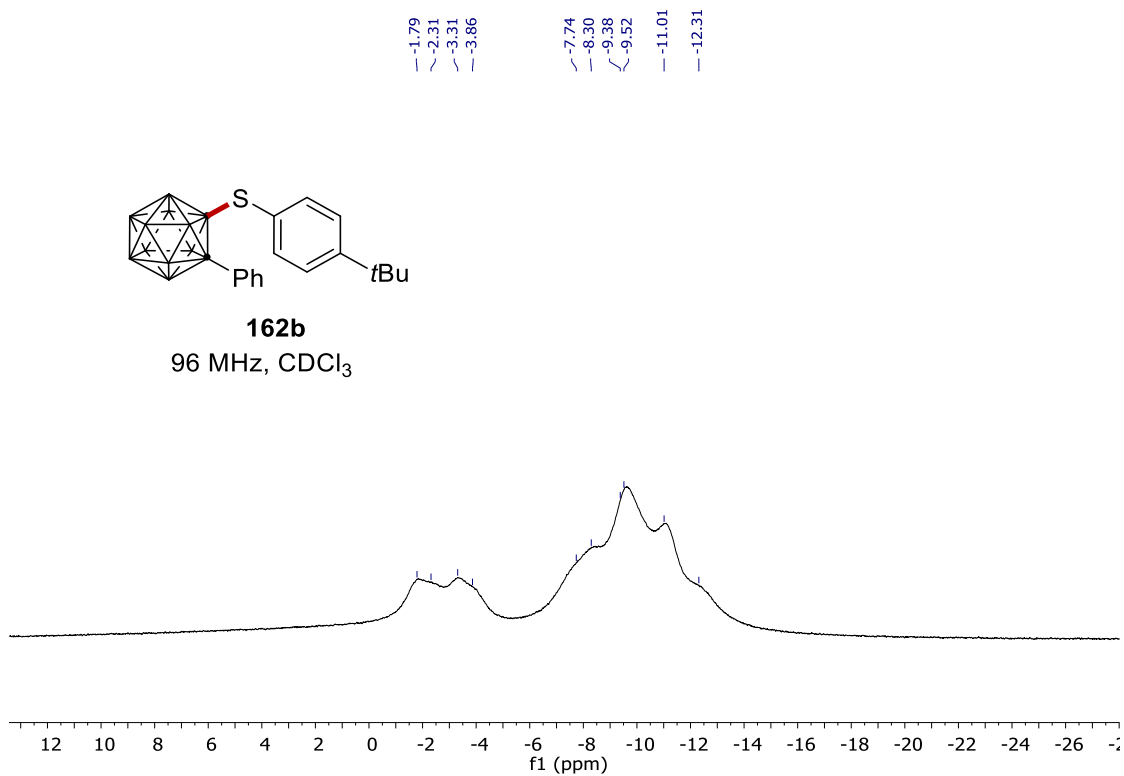
NMR Spectra



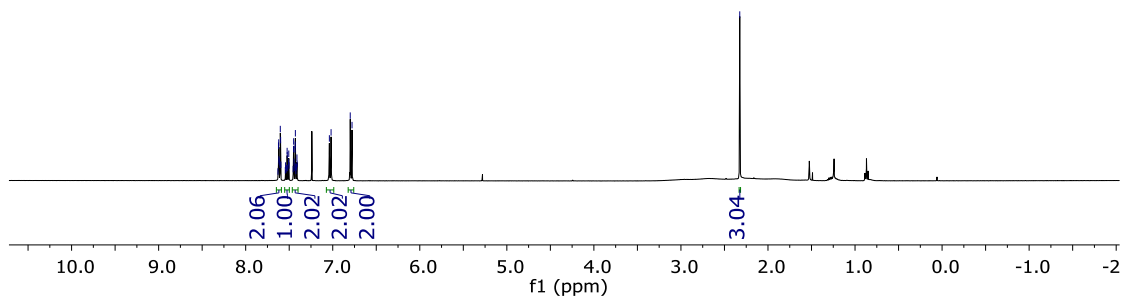
NMR Spectra



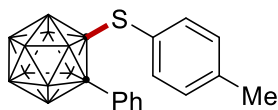
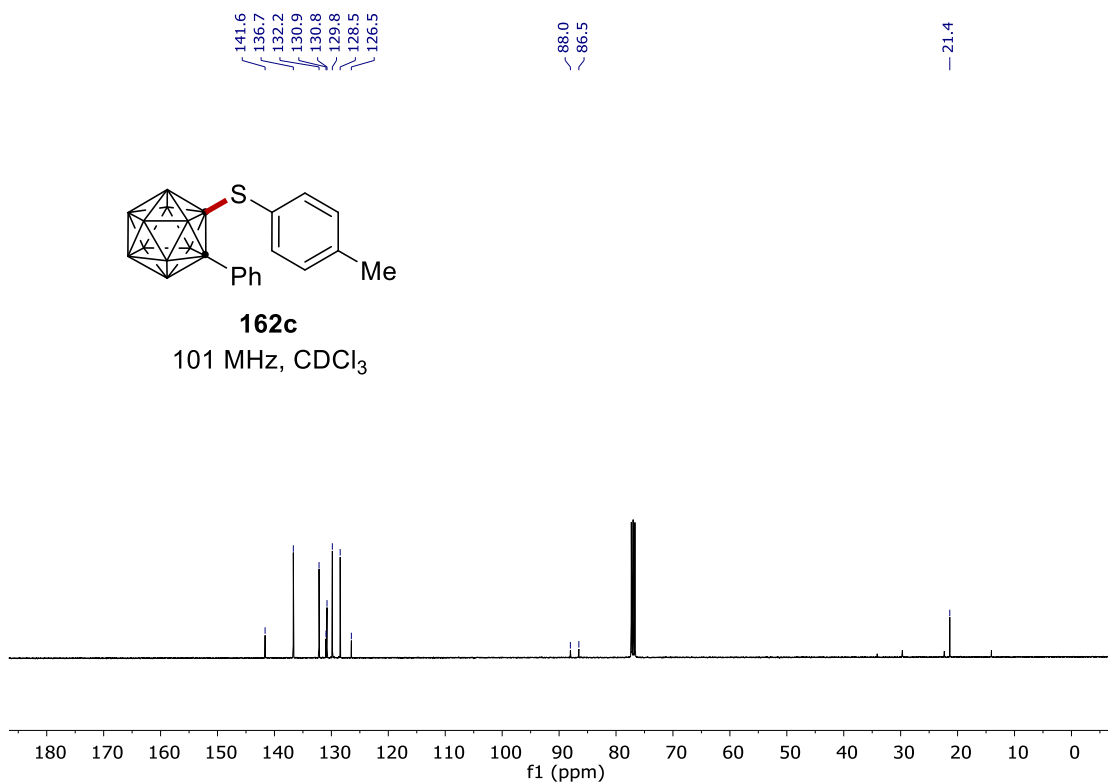
162b
96 MHz, CDCl₃



162c
400 MHz, CDCl₃

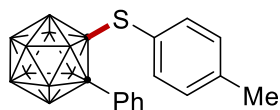
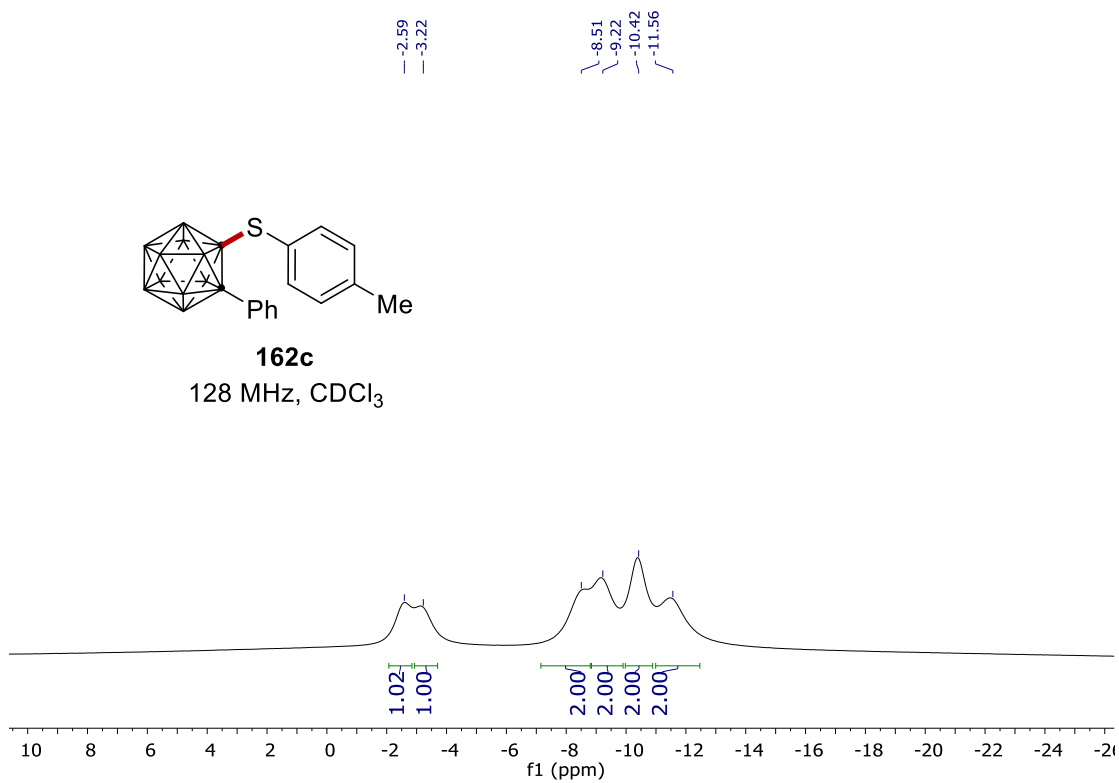


NMR Spectra



162c

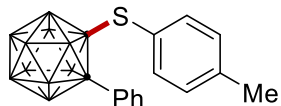
101 MHz, CDCl₃



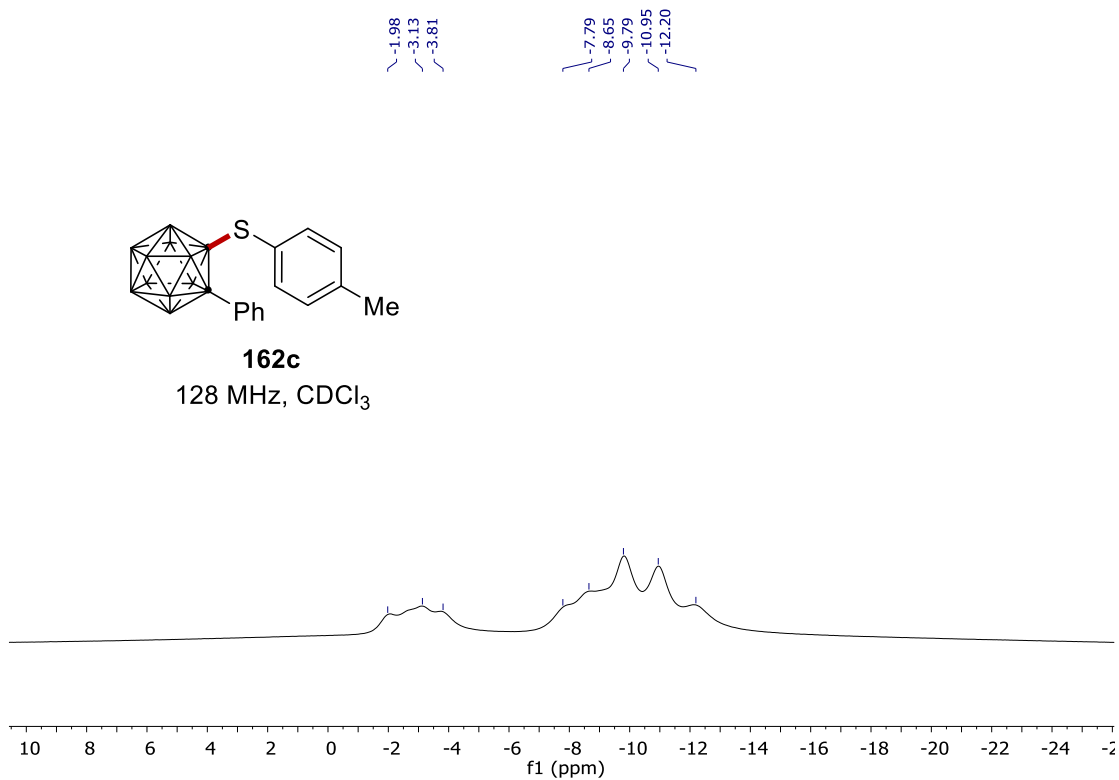
162c

128 MHz, CDCl₃

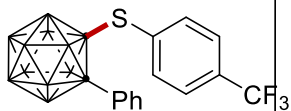
NMR Spectra



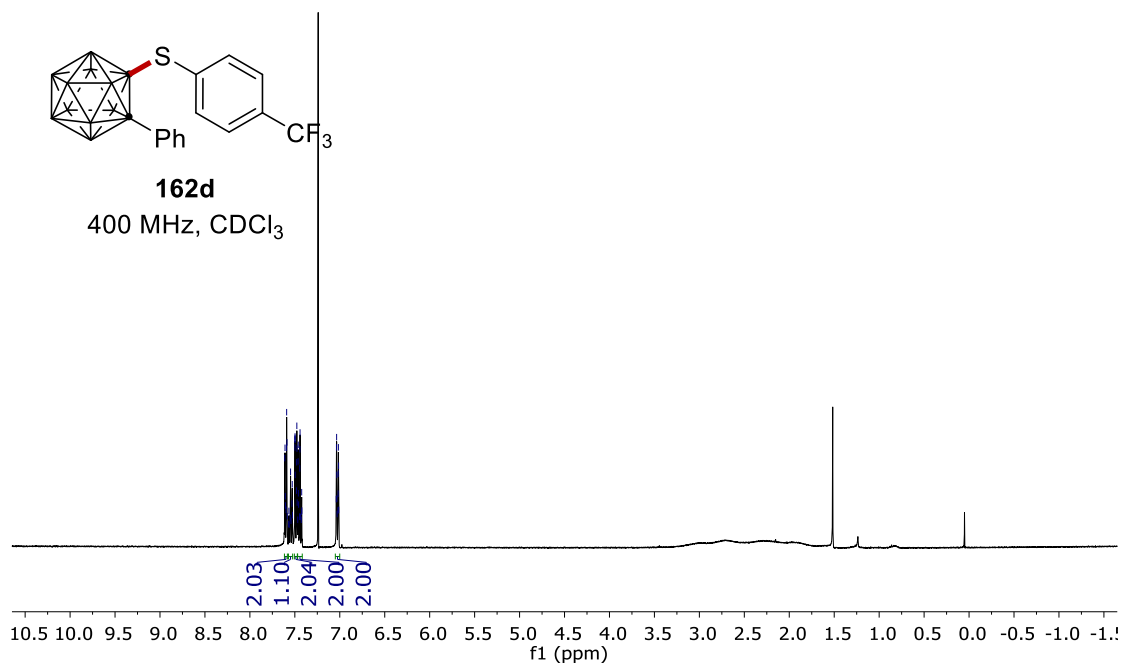
162c
128 MHz, CDCl₃



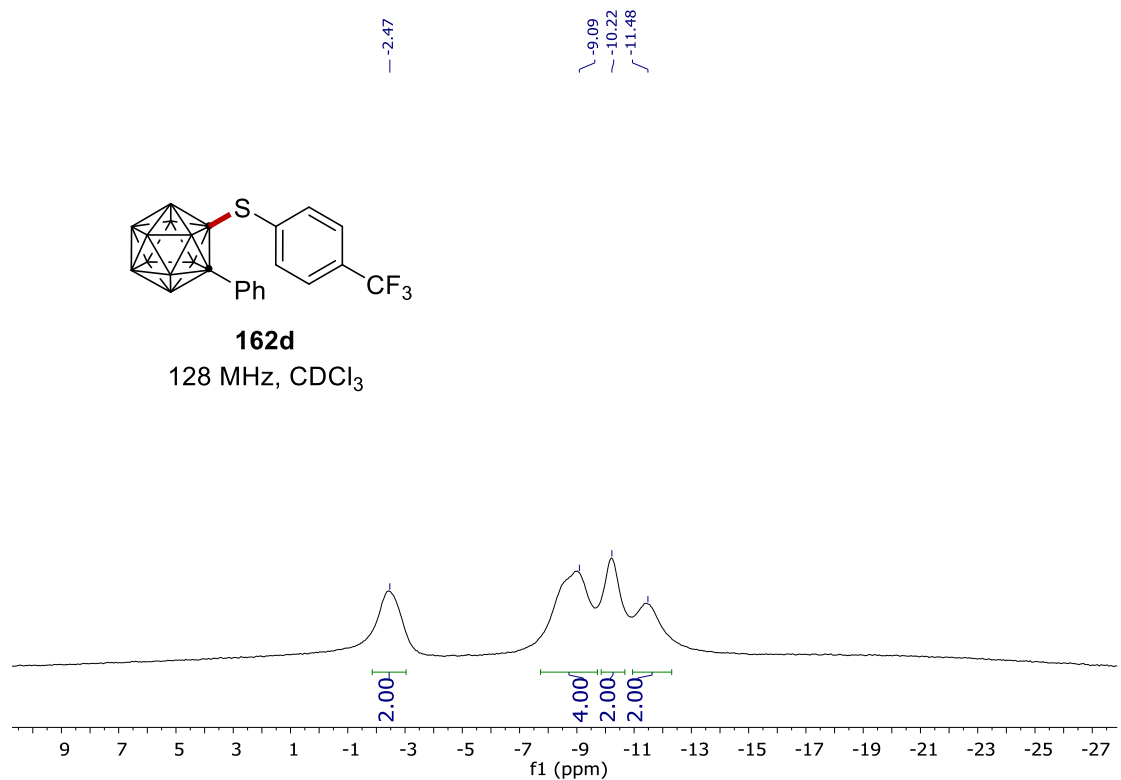
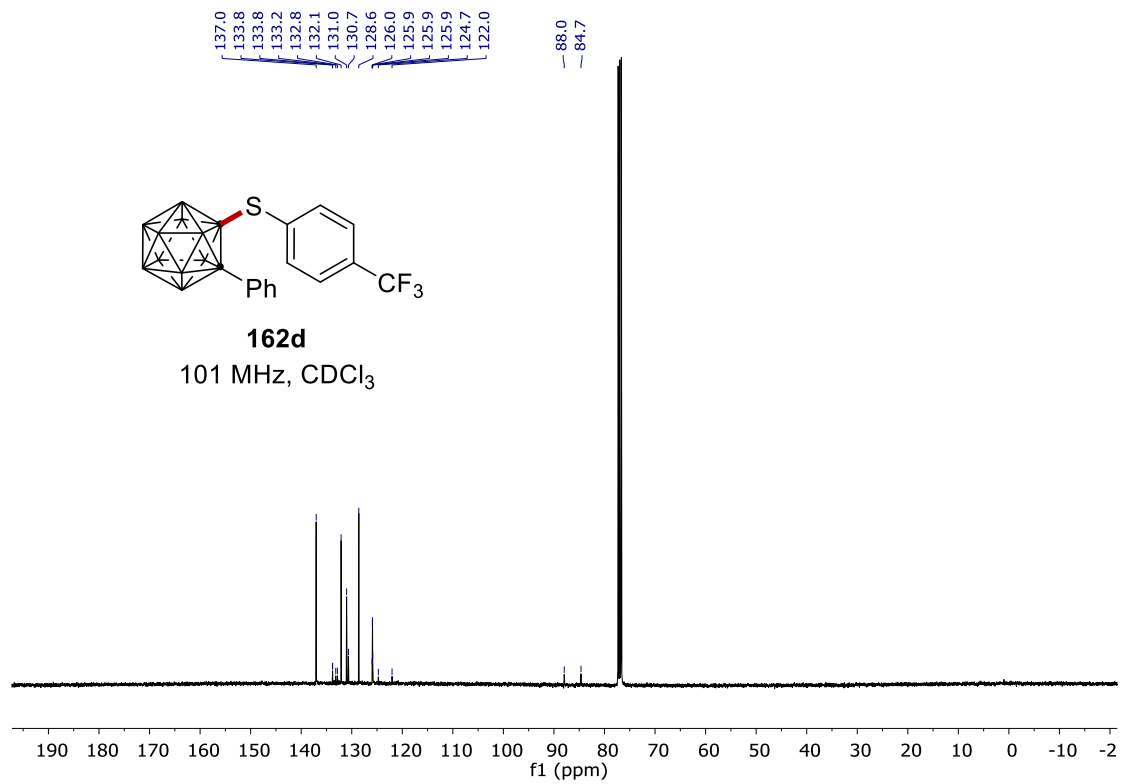
7.61
7.61
7.61
7.60
7.60
7.59
7.59
7.58
7.57
7.56
7.55
7.55
7.54
7.53
7.53
7.50
7.50
7.50
7.50
7.50
7.48
7.48
7.48
7.47
7.47
7.46
7.46
7.46
7.45
7.45
7.44
7.44
7.43
7.43
7.42
7.42
7.04
7.04
7.03
7.03
7.02
7.02
7.02
7.02
7.01
7.01



162d
400 MHz, CDCl₃

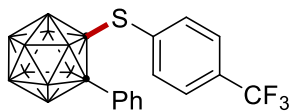


NMR Spectra

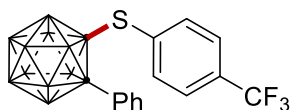
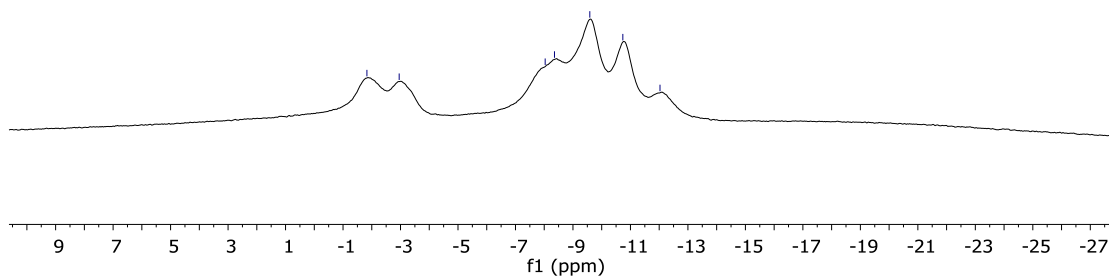


NMR Spectra

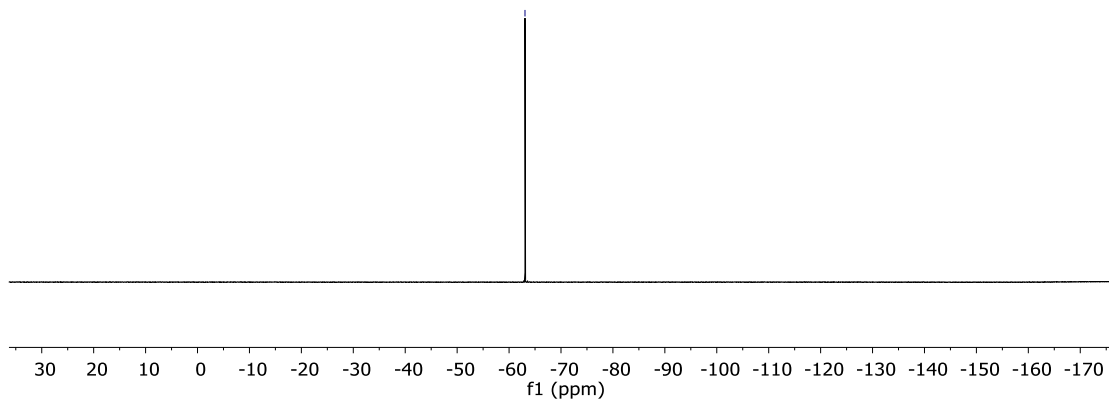
-1.83
-2.95
-8.03
-8.36
-9.59
-10.74
-12.03



162d
128 MHz, CDCl₃

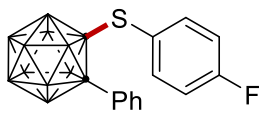


162d
376 MHz, CDCl₃



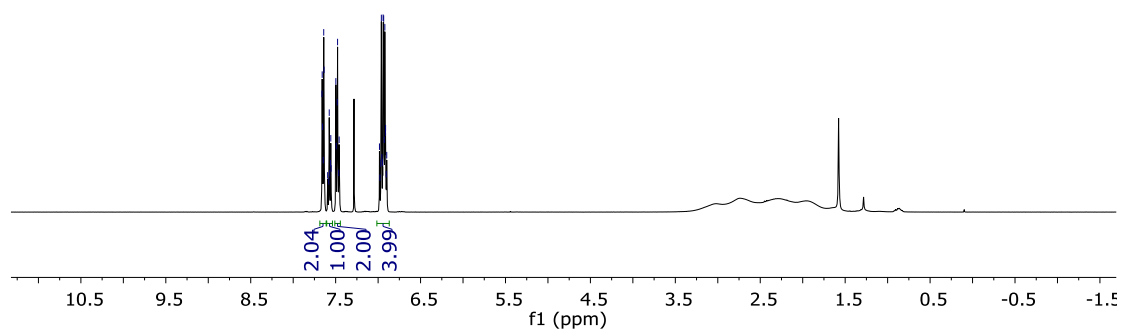
NMR Spectra

7.66
7.66
7.65
7.65
7.64
7.64
7.59
7.58
7.57
7.56
7.55
7.50
7.49
7.48
7.48
7.46
7.46
6.98
6.97
6.96
6.95
6.95
6.94
6.93
6.93
6.92
6.91
6.91
6.90
6.90

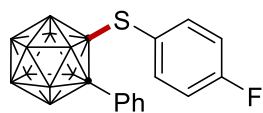


162e

400 MHz, CDCl₃

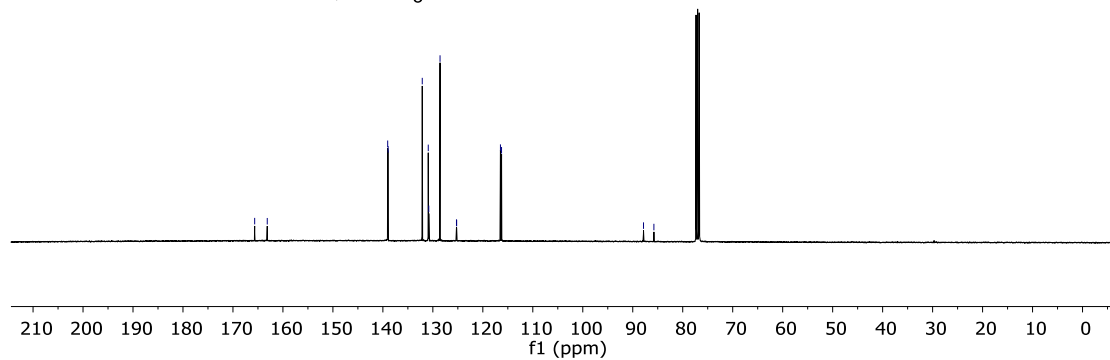


165.7
163.1
139.0
138.9
132.1
130.9
130.8
128.6
125.3
125.2
116.5
116.3
87.8
85.8

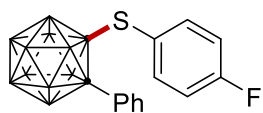


162e

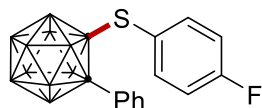
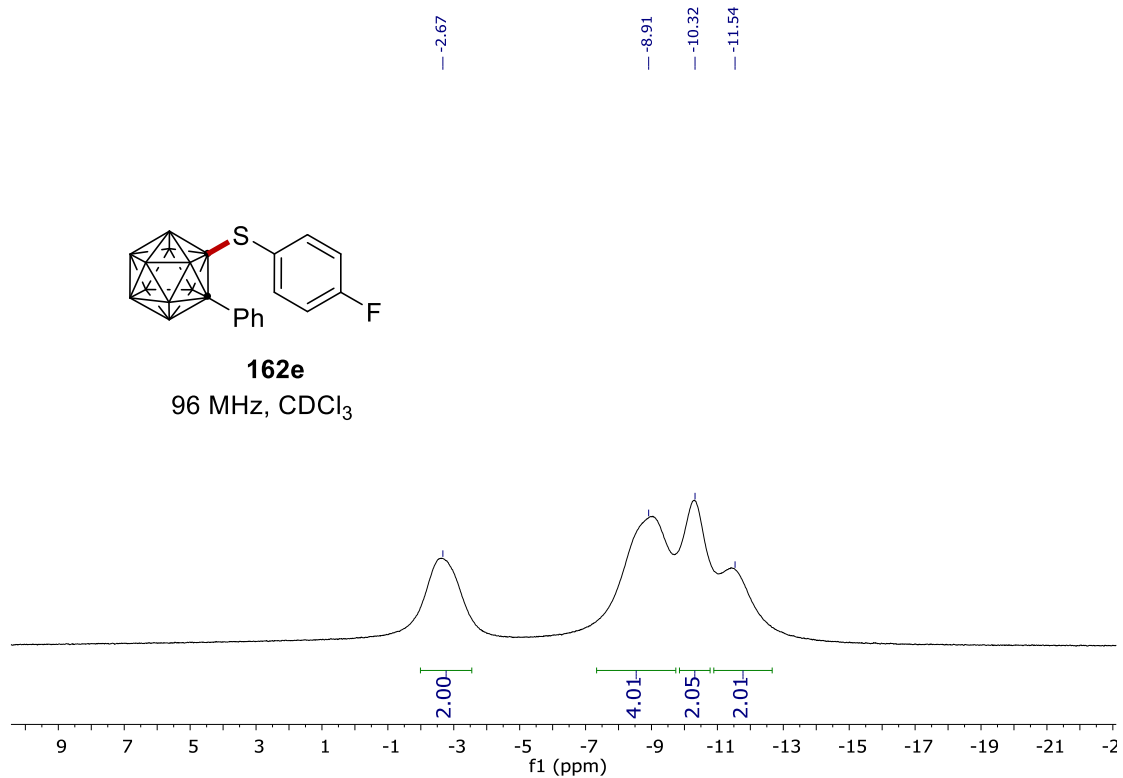
101 MHz, CDCl₃



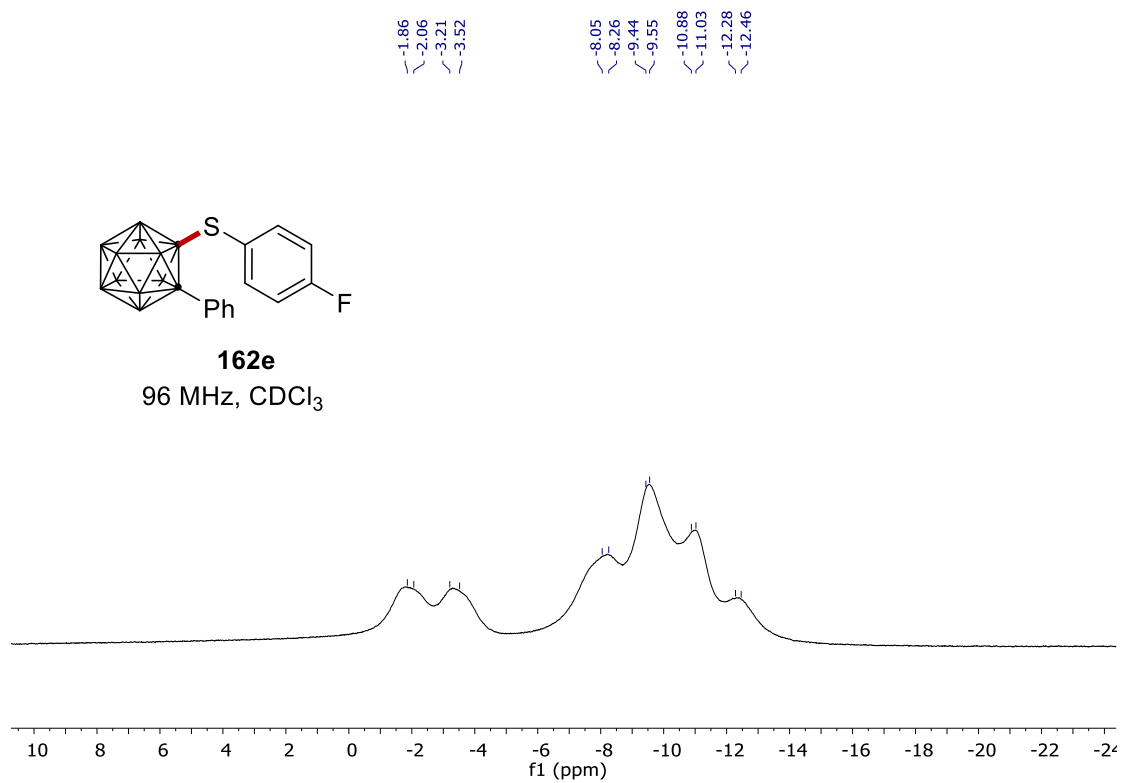
NMR Spectra



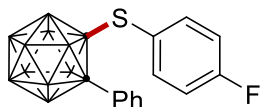
162e
96 MHz, CDCl₃



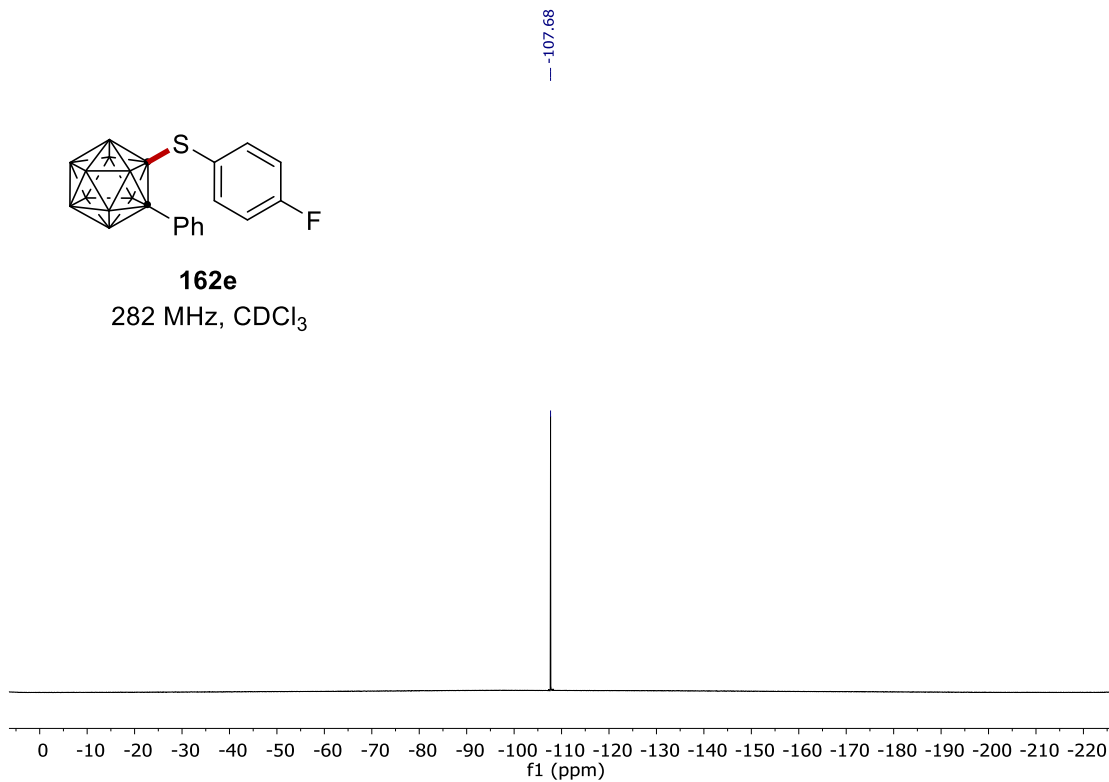
162e
96 MHz, CDCl₃



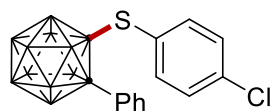
NMR Spectra



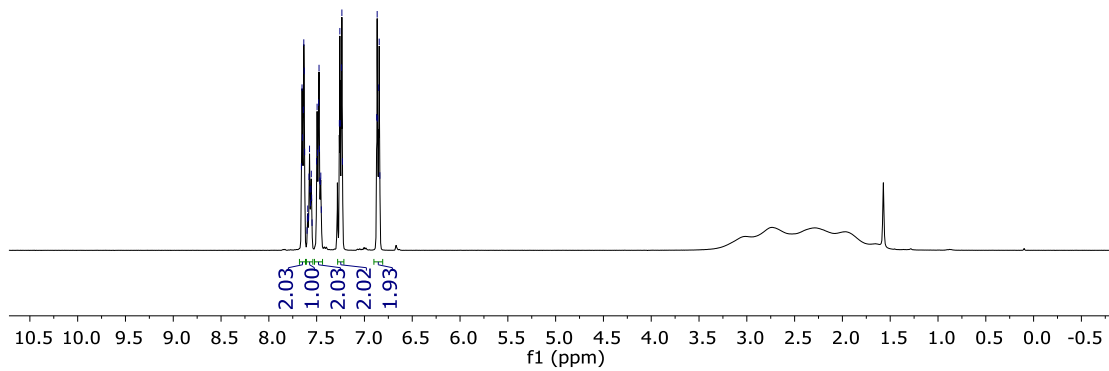
162e
282 MHz, CDCl₃



7.66
7.65
7.64
7.63
7.63
7.63
7.60
7.60
7.59
7.59
7.58
7.58
7.57
7.57
7.56
7.56
7.55
7.55
7.50
7.50
7.49
7.48
7.48
7.47
7.47
7.46
7.46
7.45
7.26
7.26
7.25
7.24
7.24
7.23
6.87
6.86
6.85
6.85
6.84



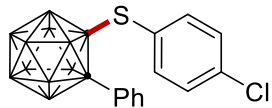
162f
400 MHz, CDCl₃



NMR Spectra

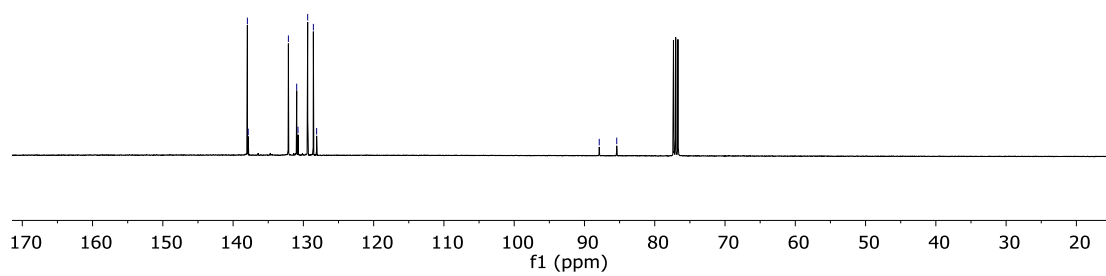
138.0
137.9
132.1
131.0
130.8
129.4
128.6
128.1

-87.9
-85.4



162f

101 MHz, CDCl₃

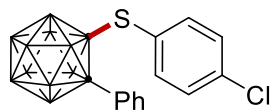


-2.60

-8.90

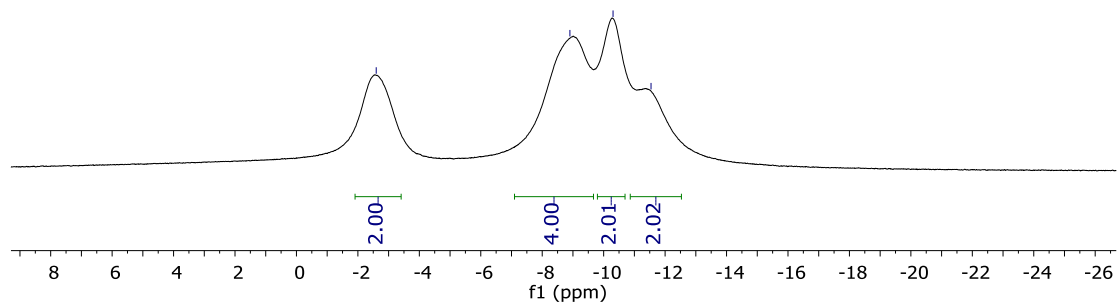
-10.31

-11.54

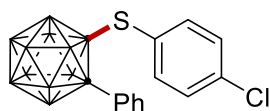


162f

96 MHz, CDCl₃

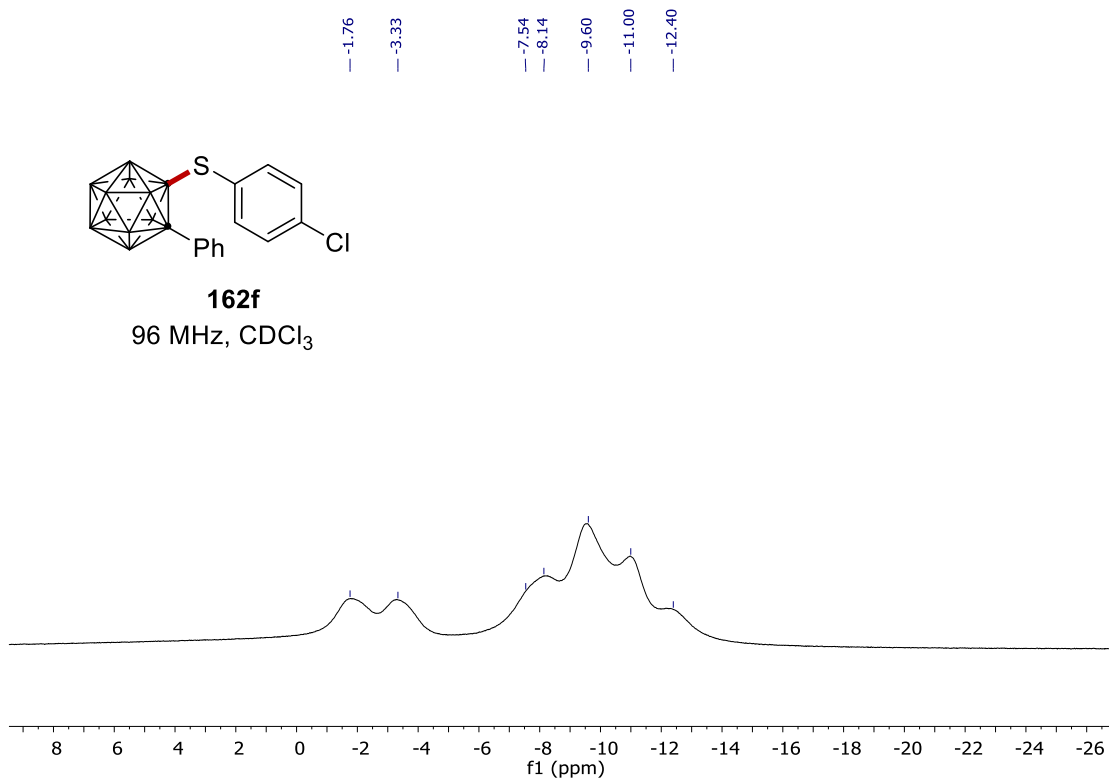


NMR Spectra

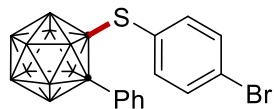


162f

96 MHz, CDCl₃

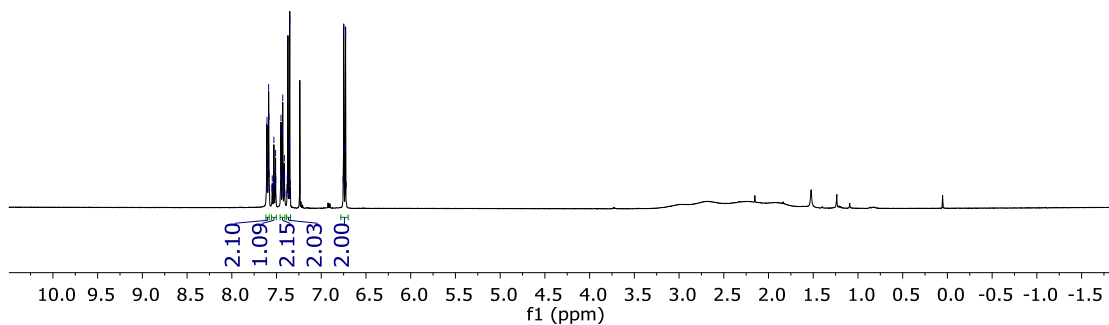


7.61
7.61
7.60
7.60
7.59
7.59
7.58
7.58
7.55
7.55
7.54
7.53
7.53
7.52
7.51
7.51
7.46
7.46
7.45
7.45
7.44
7.44
7.44
7.43
7.43
7.42
7.42
7.41
7.41
7.41
7.38
7.38
7.37
7.37
7.36
7.36
7.36
7.35
7.35
7.35
6.76
6.75
6.74
6.73
6.73
6.72



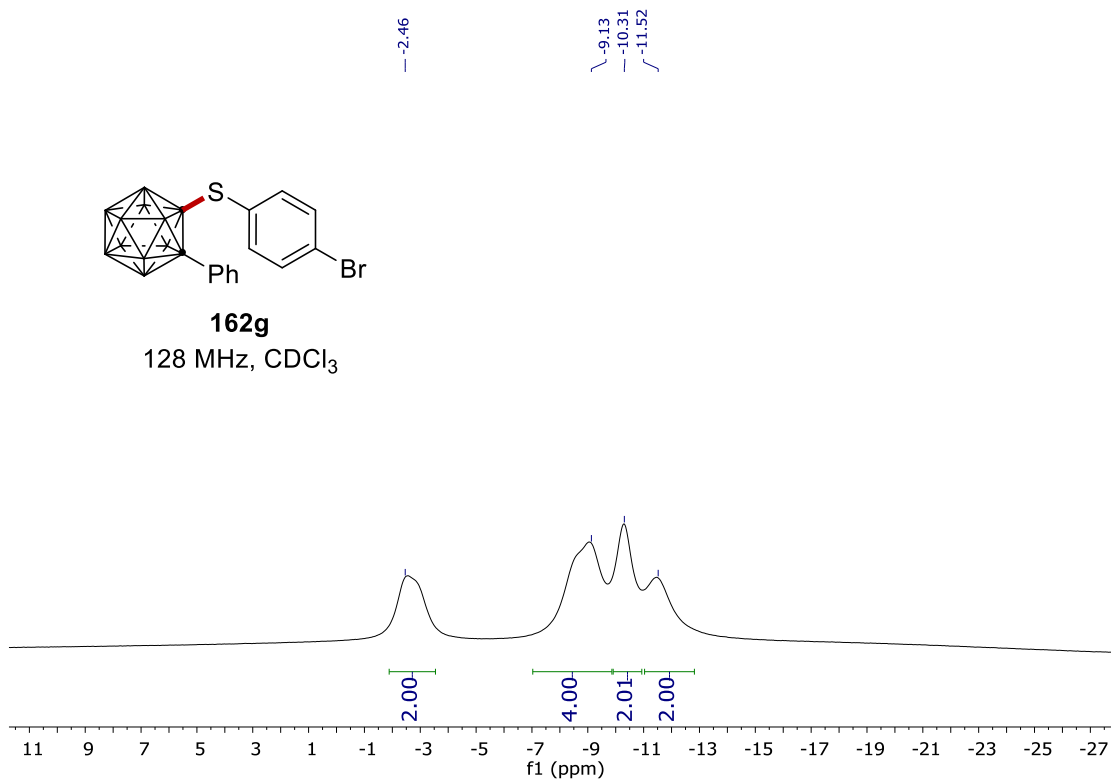
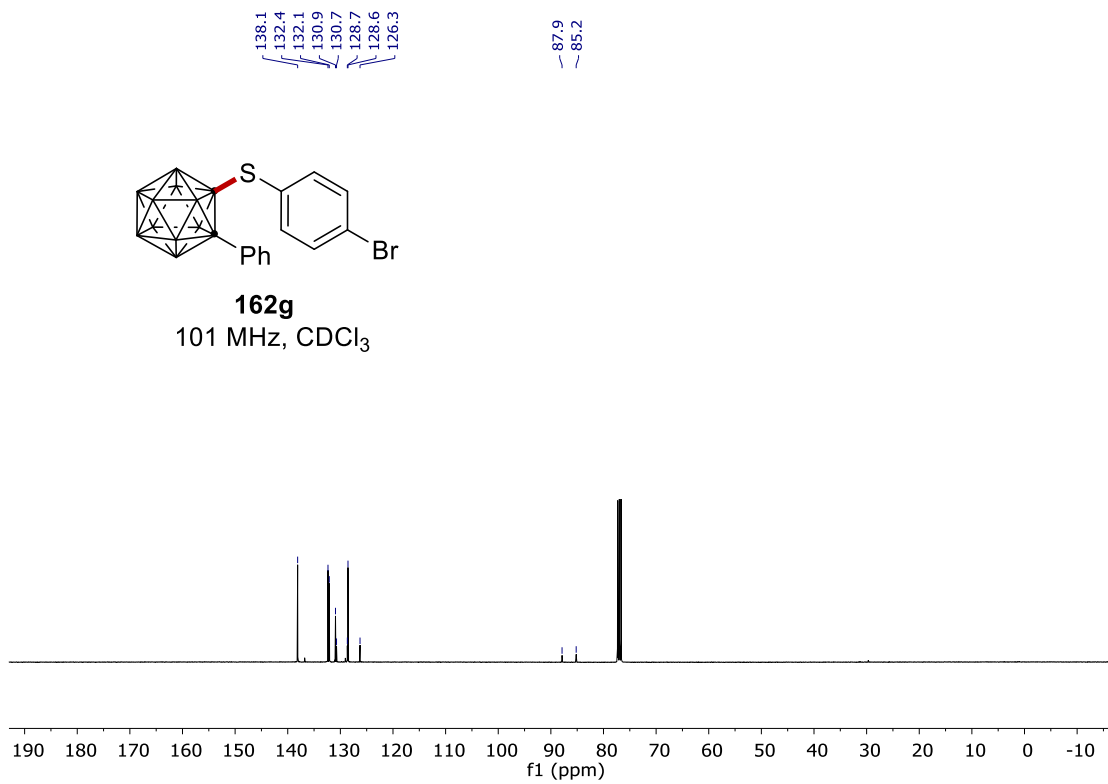
162g

400 MHz, CDCl₃

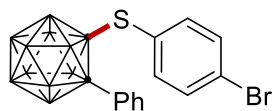


2.10
1.09
2.15
2.03
2.00

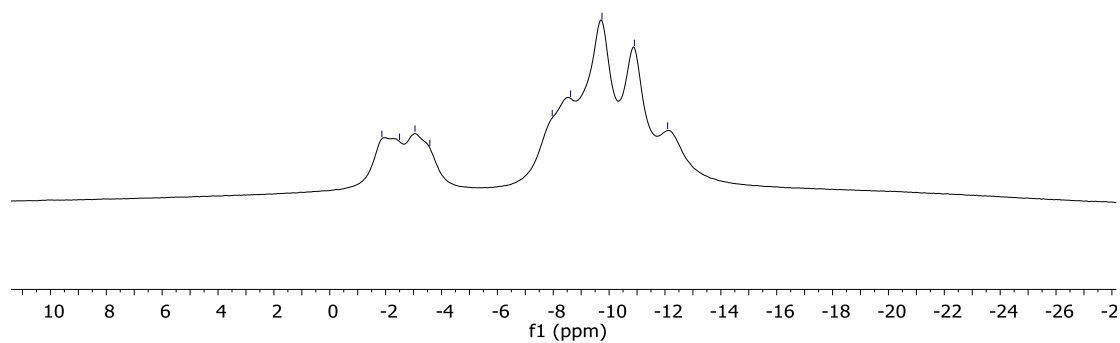
NMR Spectra



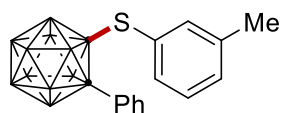
NMR Spectra



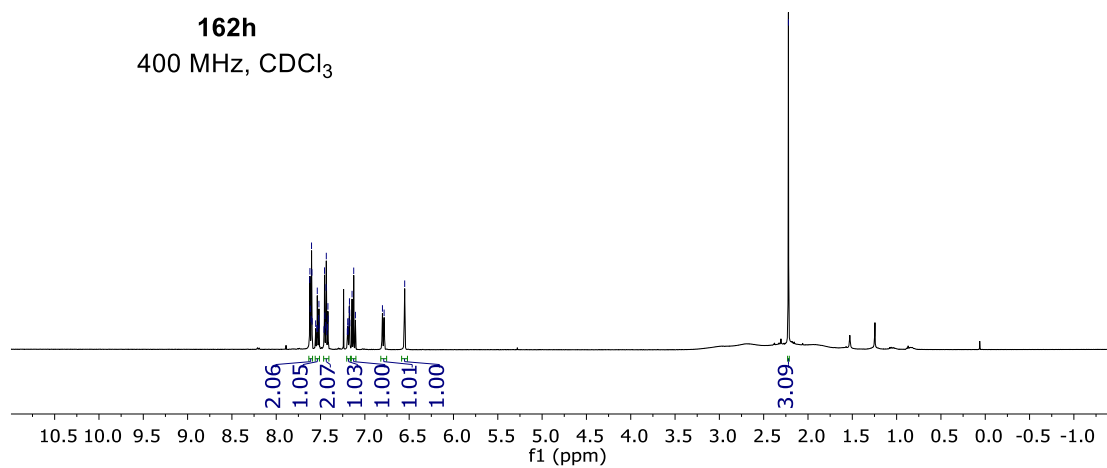
162g
128 MHz, CDCl₃



7.62
7.62
7.61
7.60
7.60
7.56
7.54
7.54
7.53
7.52
7.52
7.52
7.46
7.46
7.45
7.44
7.44
7.43
7.43
7.42
7.42
7.41
7.41
7.20
7.19
7.19
7.19
7.18
7.18
7.17
7.17
7.17
7.14
7.13
7.11
6.80
6.55
-2.22



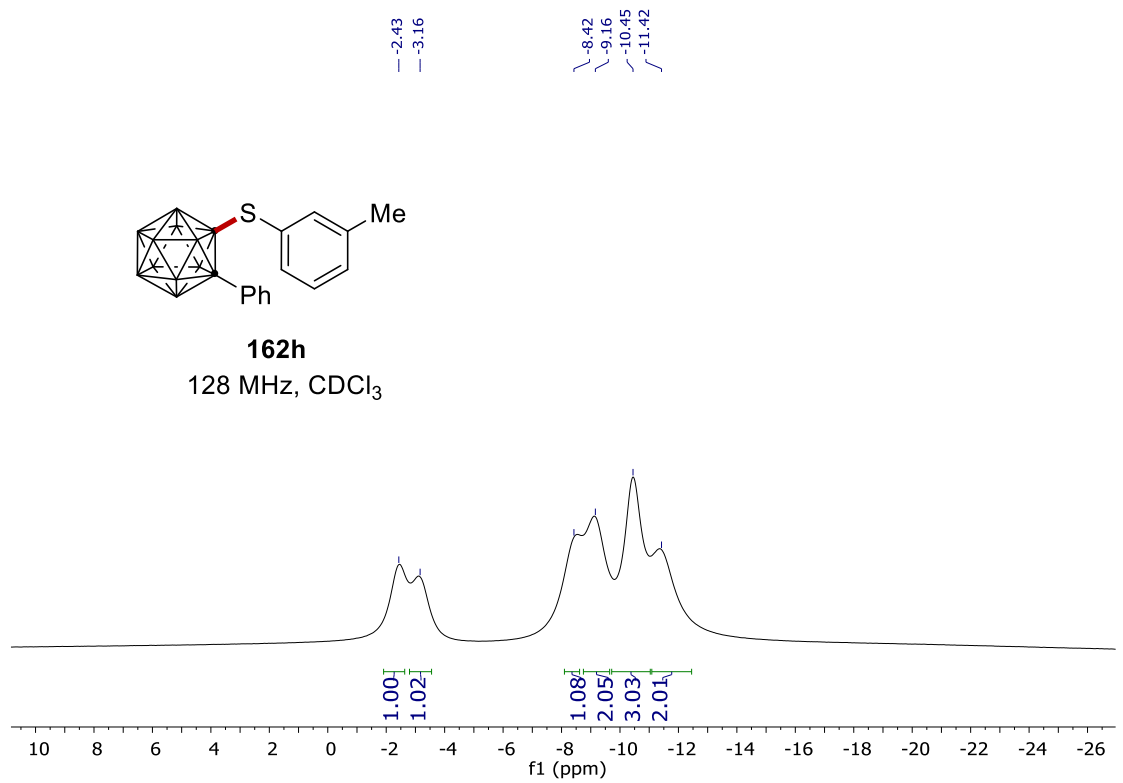
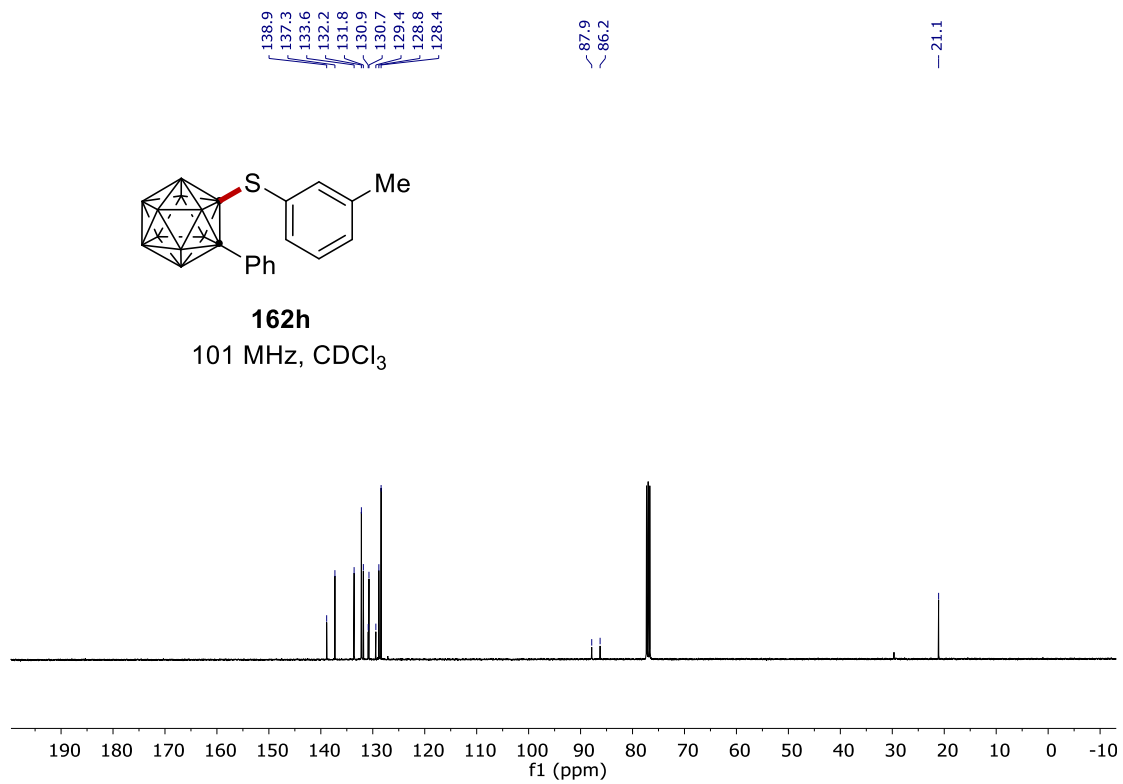
162h
400 MHz, CDCl₃



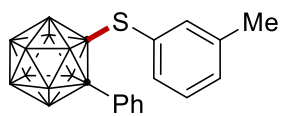
2.06
1.05
2.07
1.03
1.00
1.01
1.00

3.09

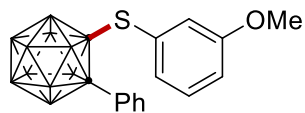
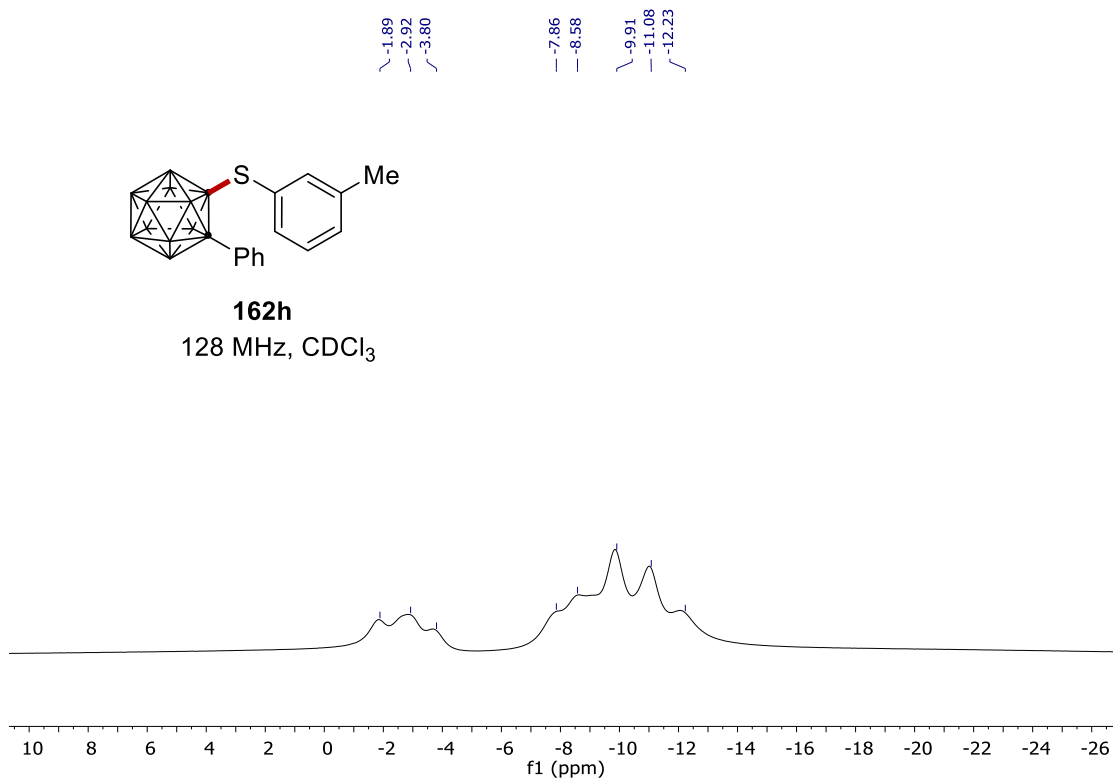
NMR Spectra



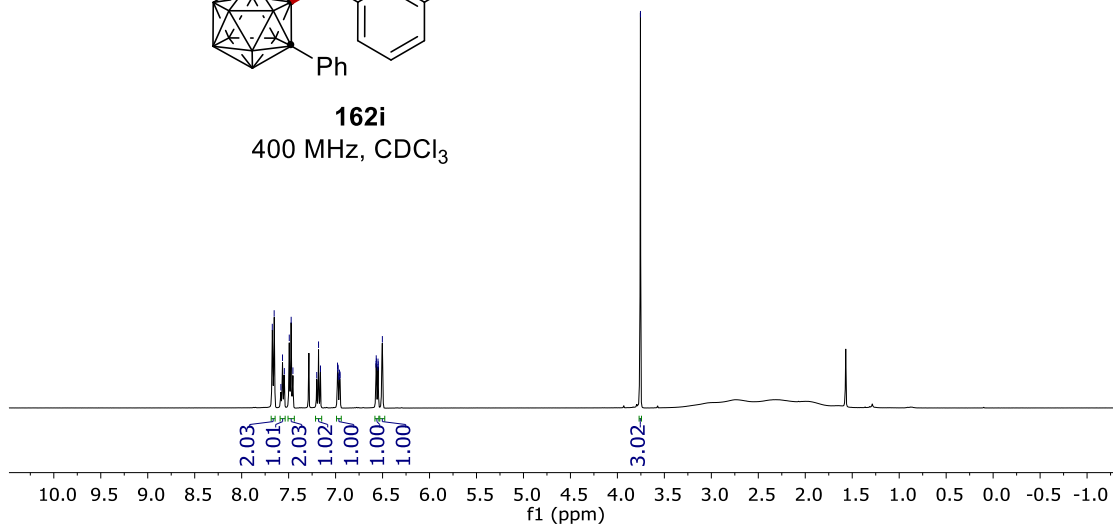
NMR Spectra



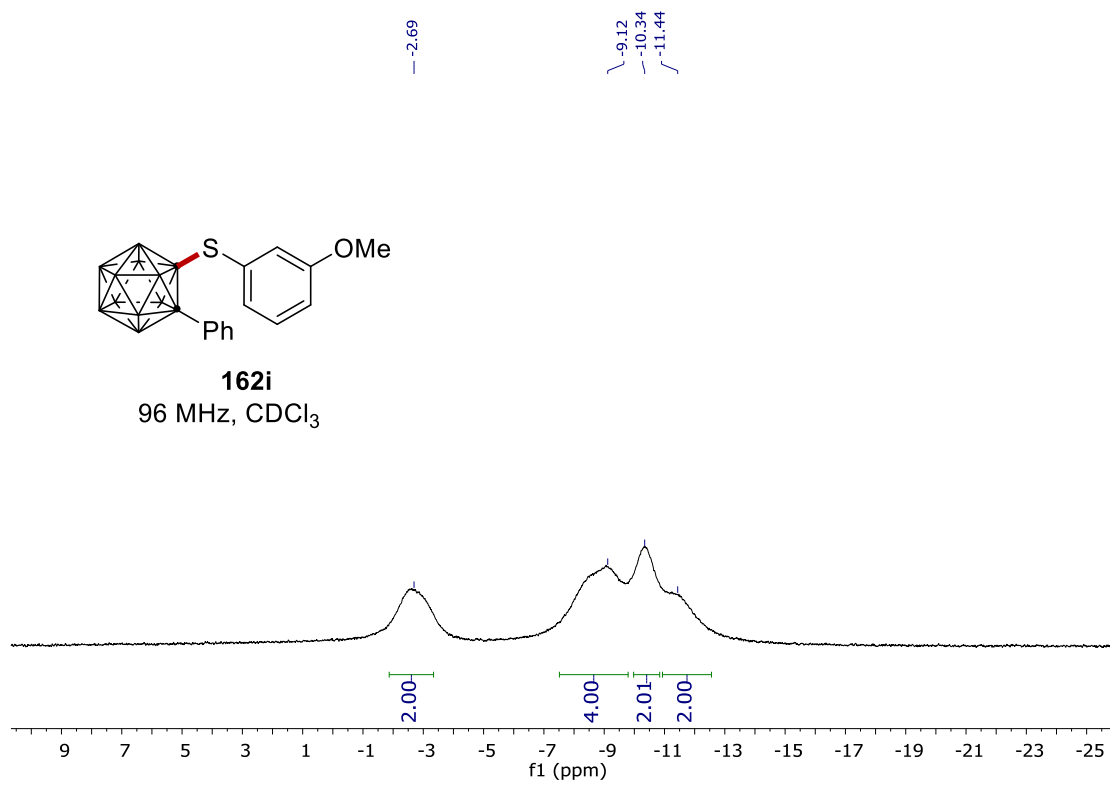
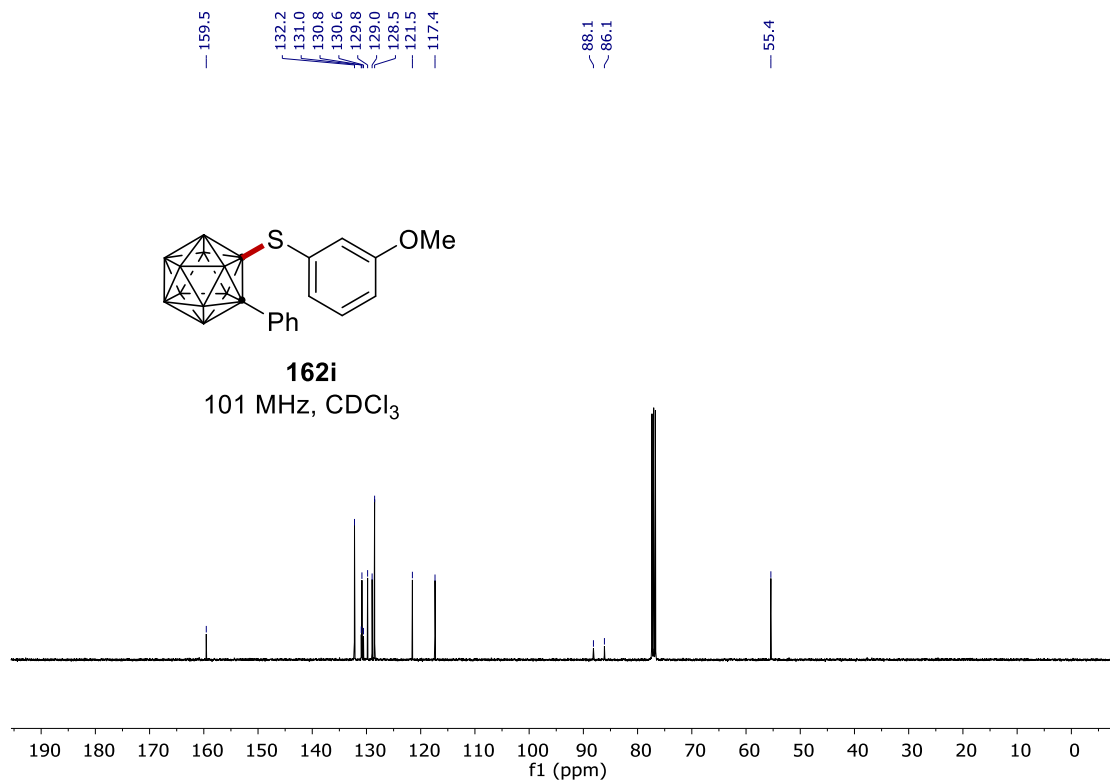
162h
128 MHz, CDCl₃



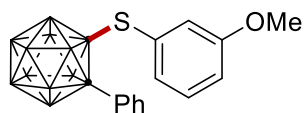
162i
400 MHz, CDCl₃



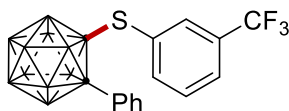
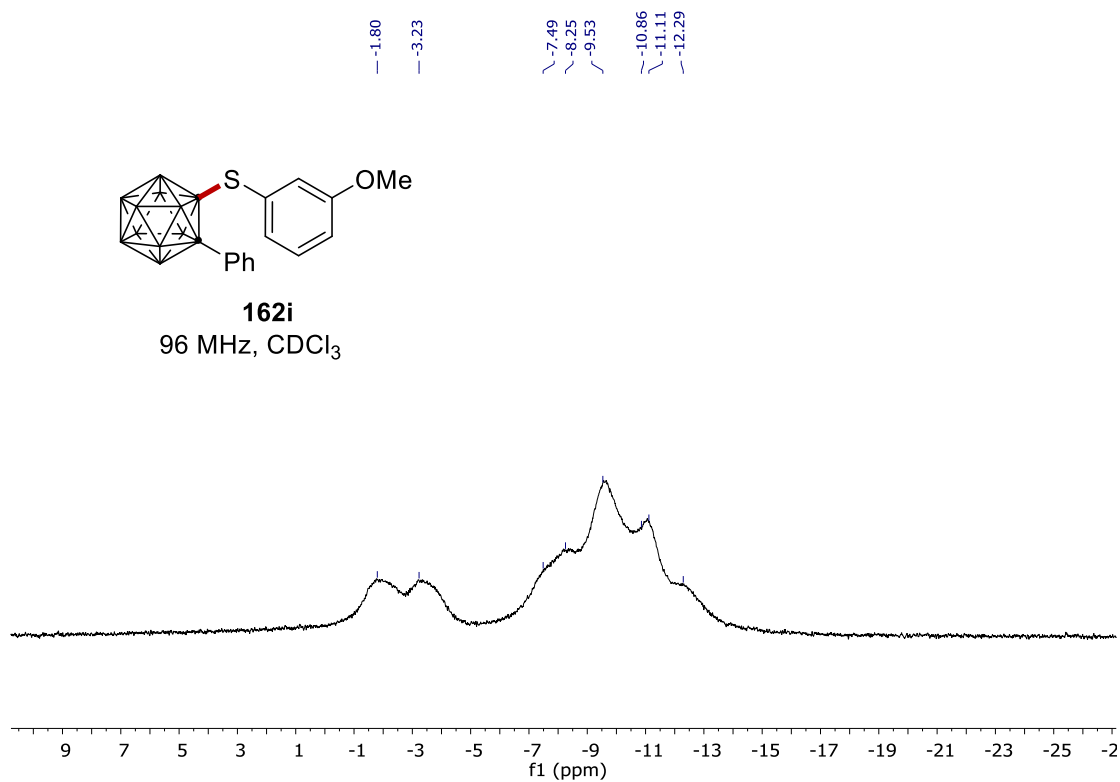
NMR Spectra



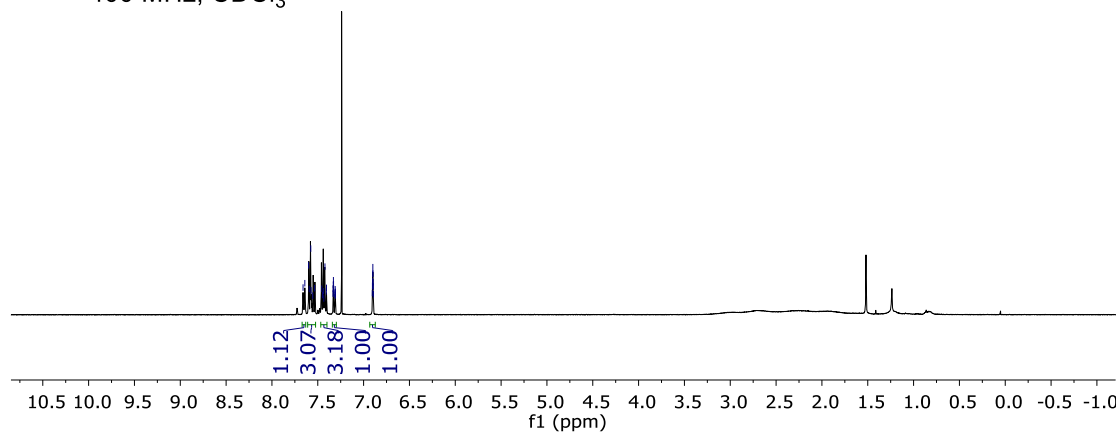
NMR Spectra



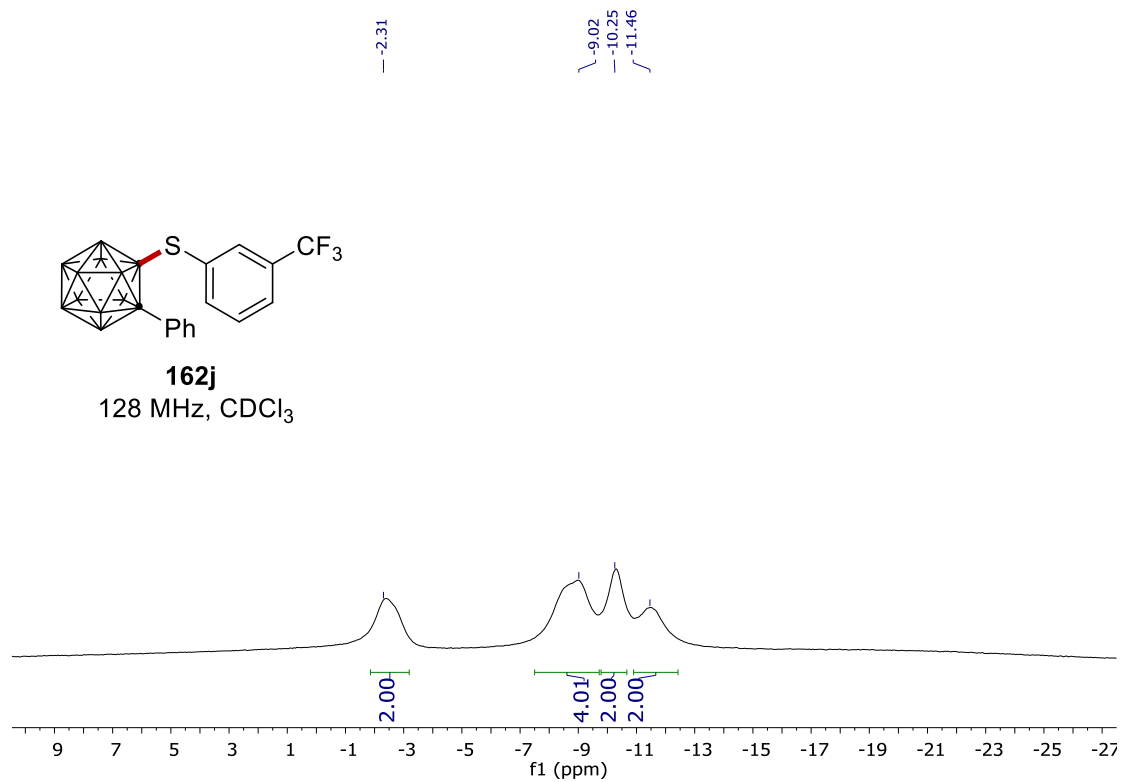
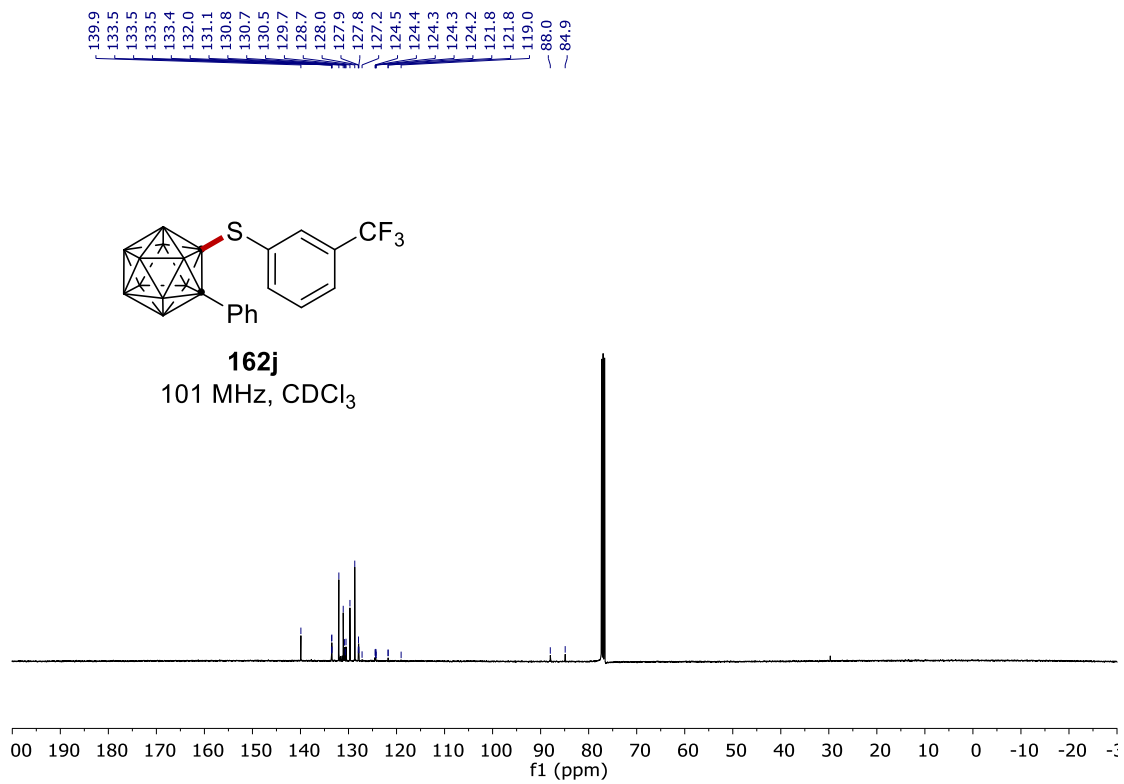
162i
96 MHz, CDCl₃



162j
400 MHz, CDCl₃



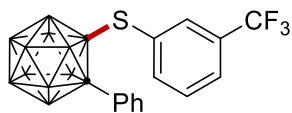
NMR Spectra



NMR Spectra

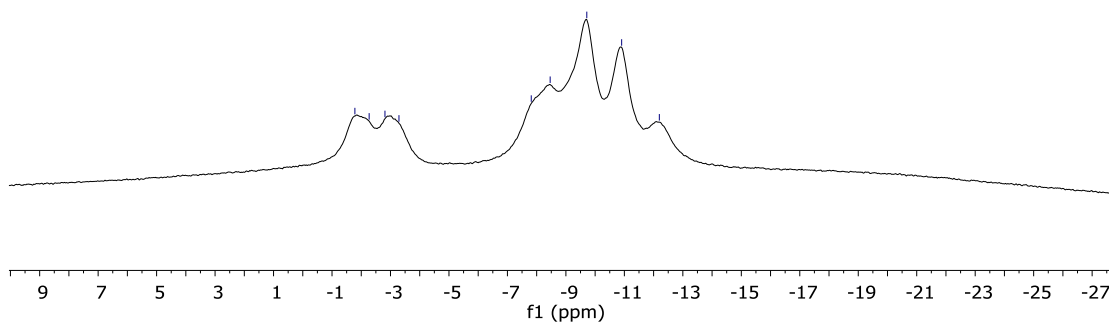
-1.78
-2.27
-2.81
-3.29

-7.81
-8.46
-9.72
-10.91
-12.20

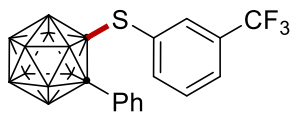


162j

128 MHz, CDCl₃

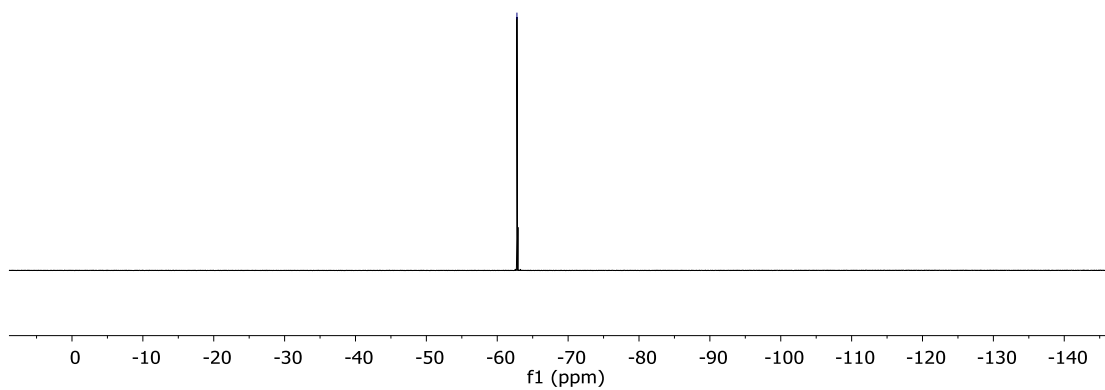


-62.78



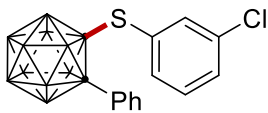
162j

376 MHz, CDCl₃

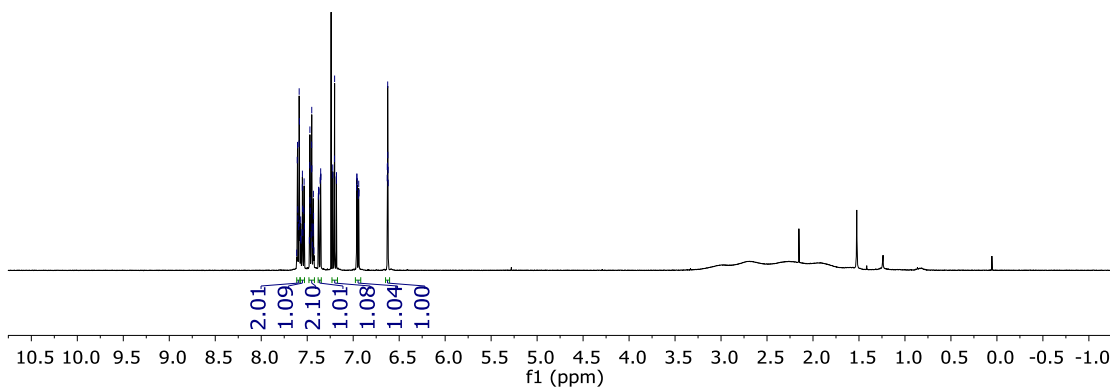


NMR Spectra

7.61
7.61
7.60
7.59
7.59
7.58
7.58
7.57
7.56
7.55
7.55
7.54
7.54
7.53
7.53
7.47
7.47
7.47
7.45
7.45
7.45
7.45
7.45
7.43
7.43
7.43
7.38
7.38
7.37
7.37
7.36
7.36
7.35
7.35
7.22
7.22
7.20
7.20
7.18
7.18
6.96
6.96
6.96
6.94
6.94
6.94
6.94
6.63
6.63
6.62
6.62
6.62
6.62

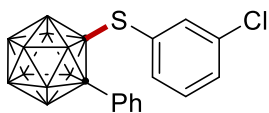


162k
400 MHz, CDCl₃

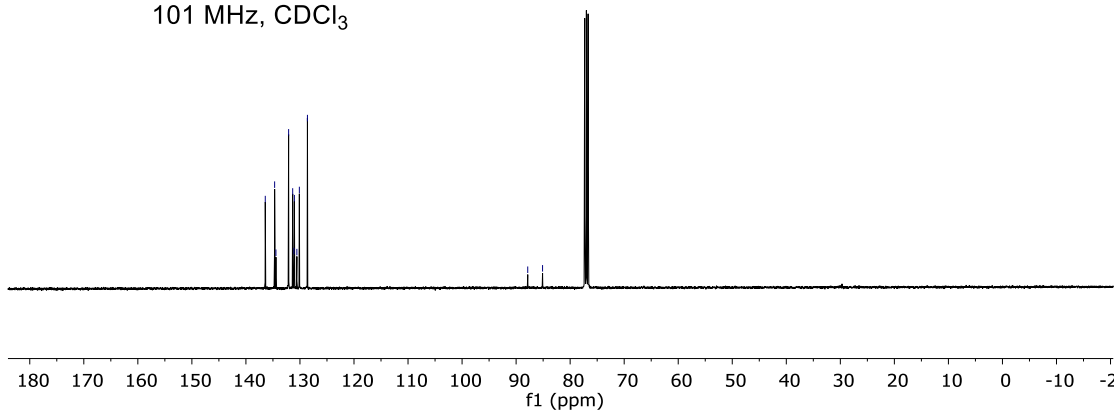


136.4
134.7
134.4
132.1
131.3
131.0
130.6
130.1
128.6

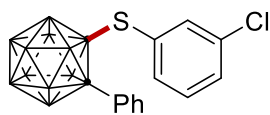
87.8
85.1



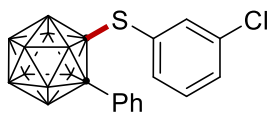
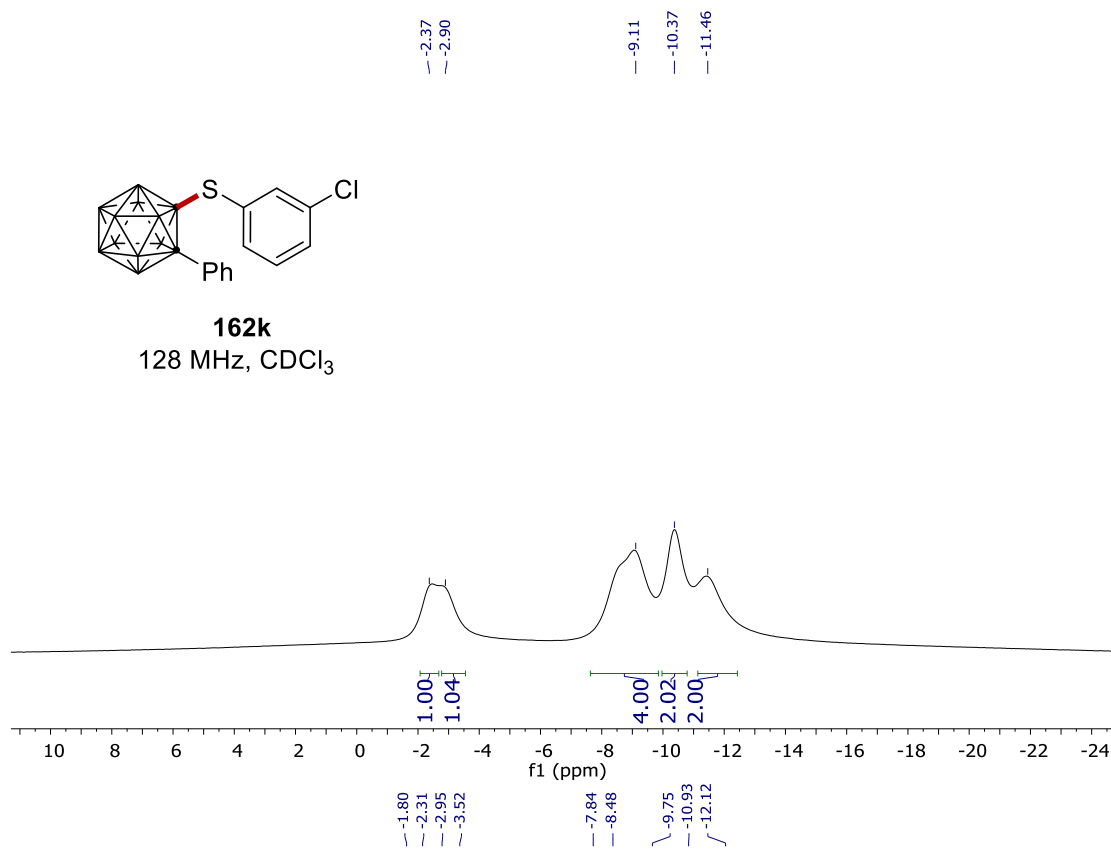
162k
101 MHz, CDCl₃



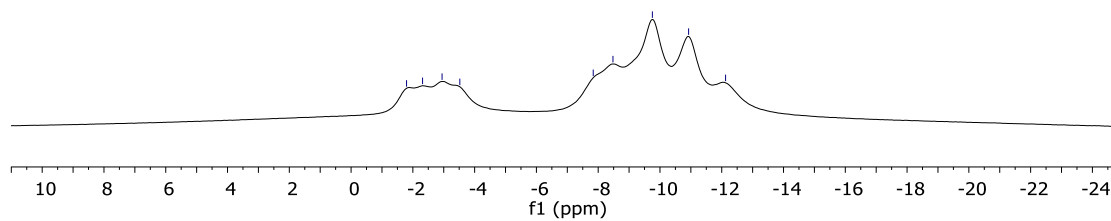
NMR Spectra



162k
128 MHz, CDCl₃

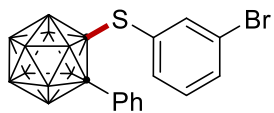


162k
128 MHz, CDCl₃



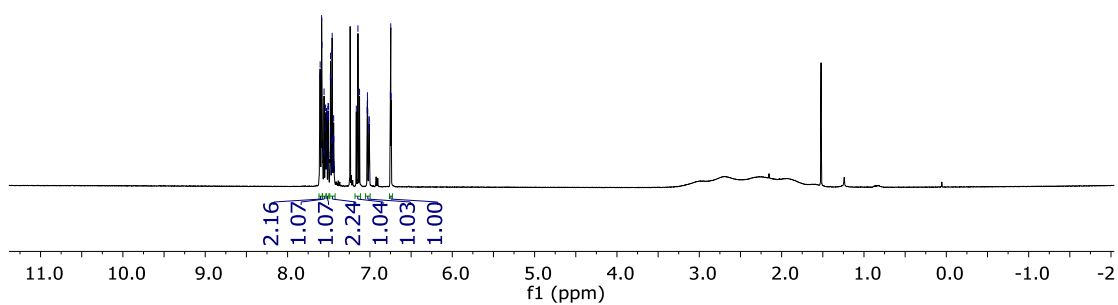
NMR Spectra

7.61
7.60
7.59
7.58
7.56
7.55
7.54
7.54
7.54
7.53
7.53
7.52
7.51
7.51
7.51
7.51
7.50
7.48
7.48
7.47
7.47
7.46
7.46
7.46
7.45
7.45
7.45
7.44
7.44
7.44
7.44
7.43
7.43
7.17
7.15
7.13
7.03
7.03
7.03
7.02
7.01
7.01
7.01
6.75
6.75
6.74



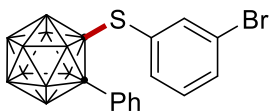
162I

400 MHz, CDCl₃



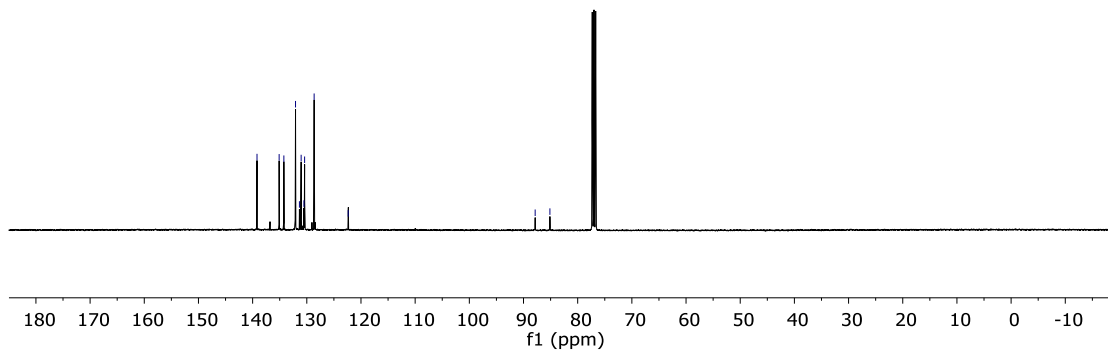
139.2
135.1
134.2
132.1
131.4
131.0
130.5
130.4
128.6
122.4

87.8
85.1

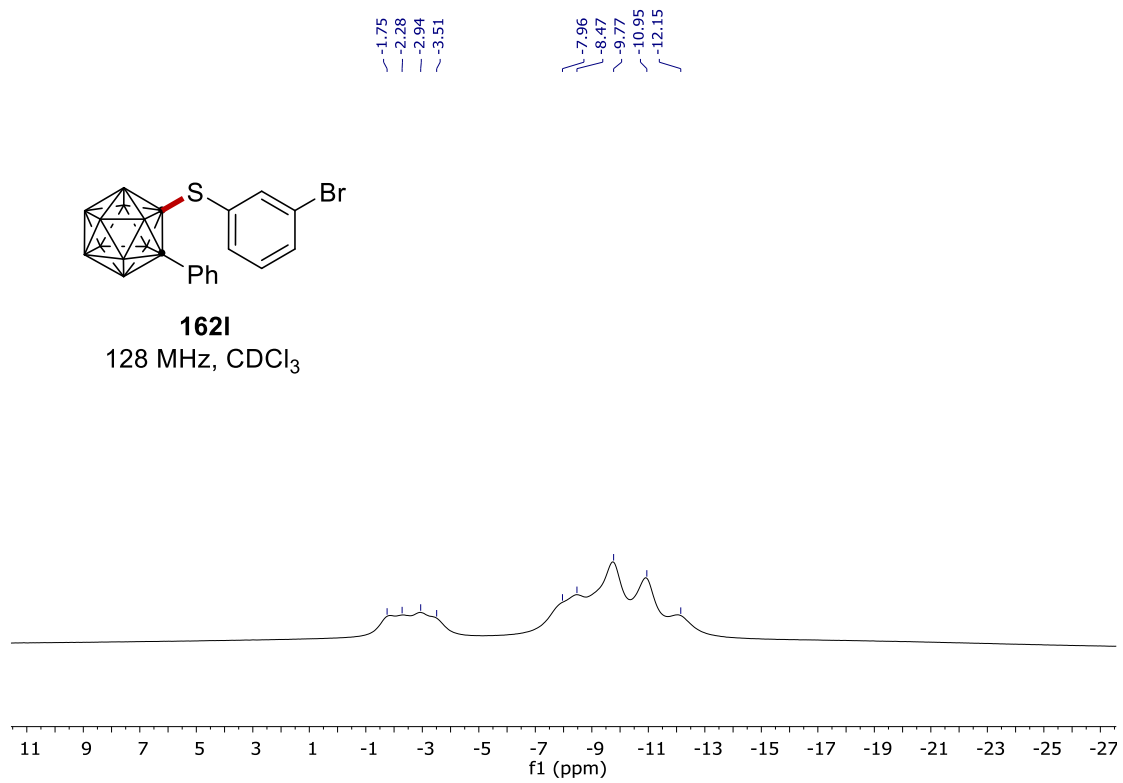
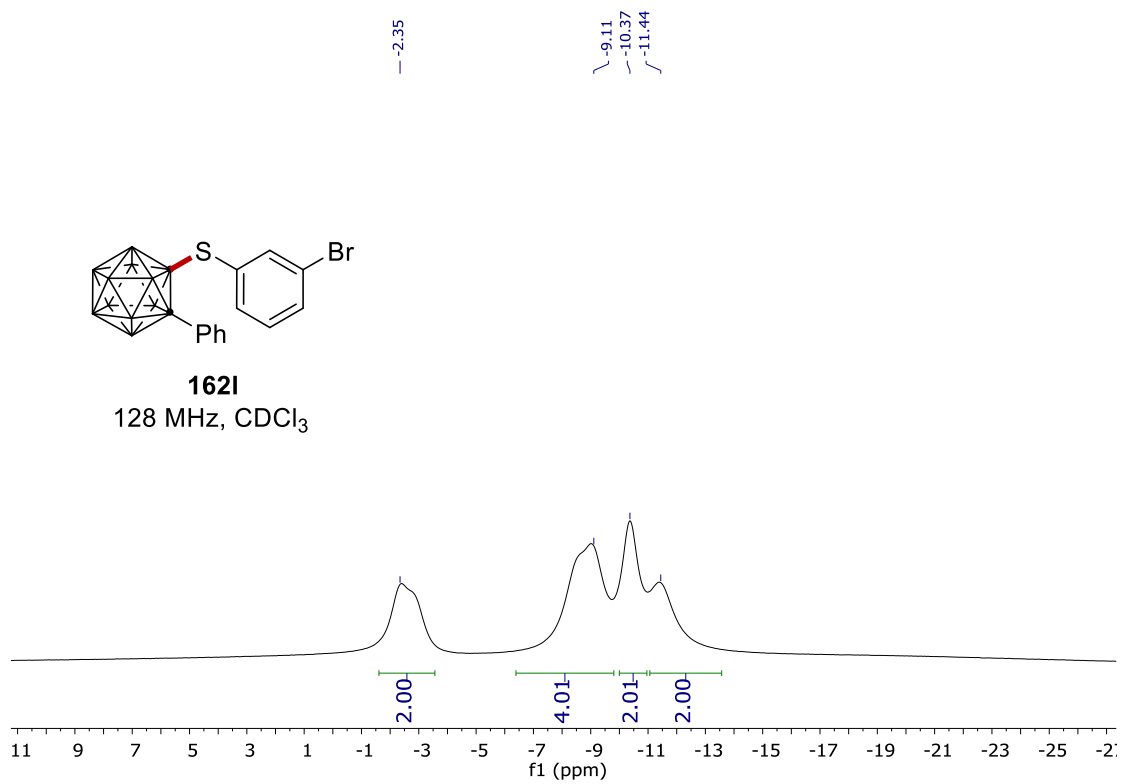


162I

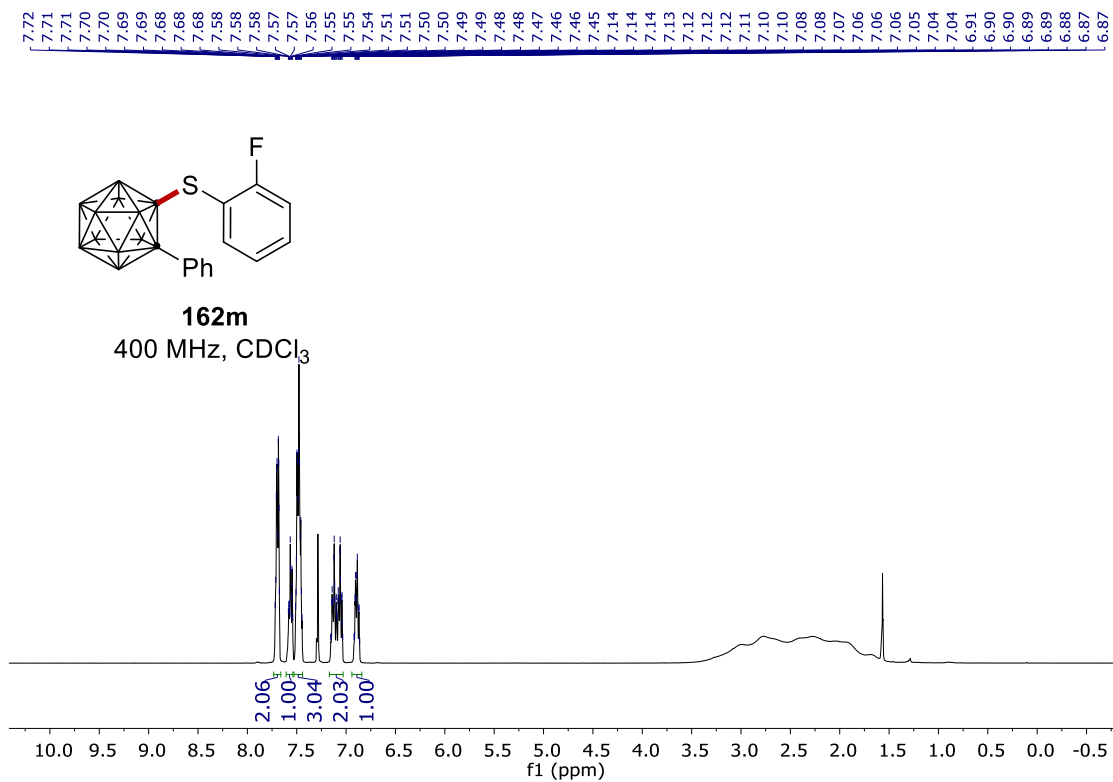
101 MHz, CDCl₃



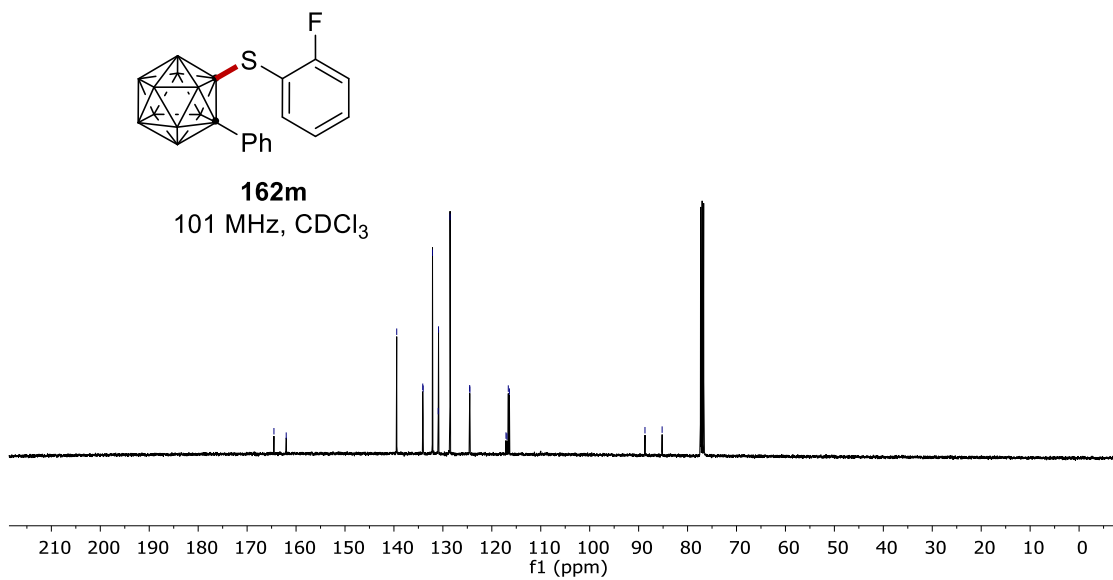
NMR Spectra



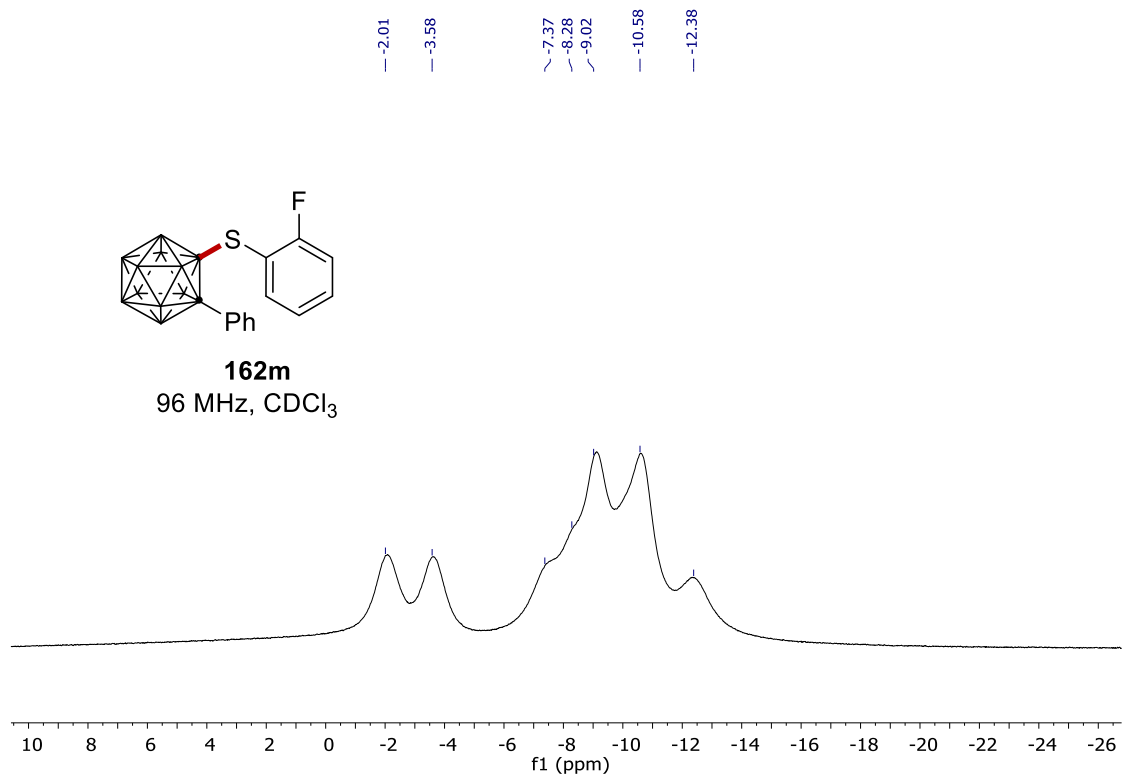
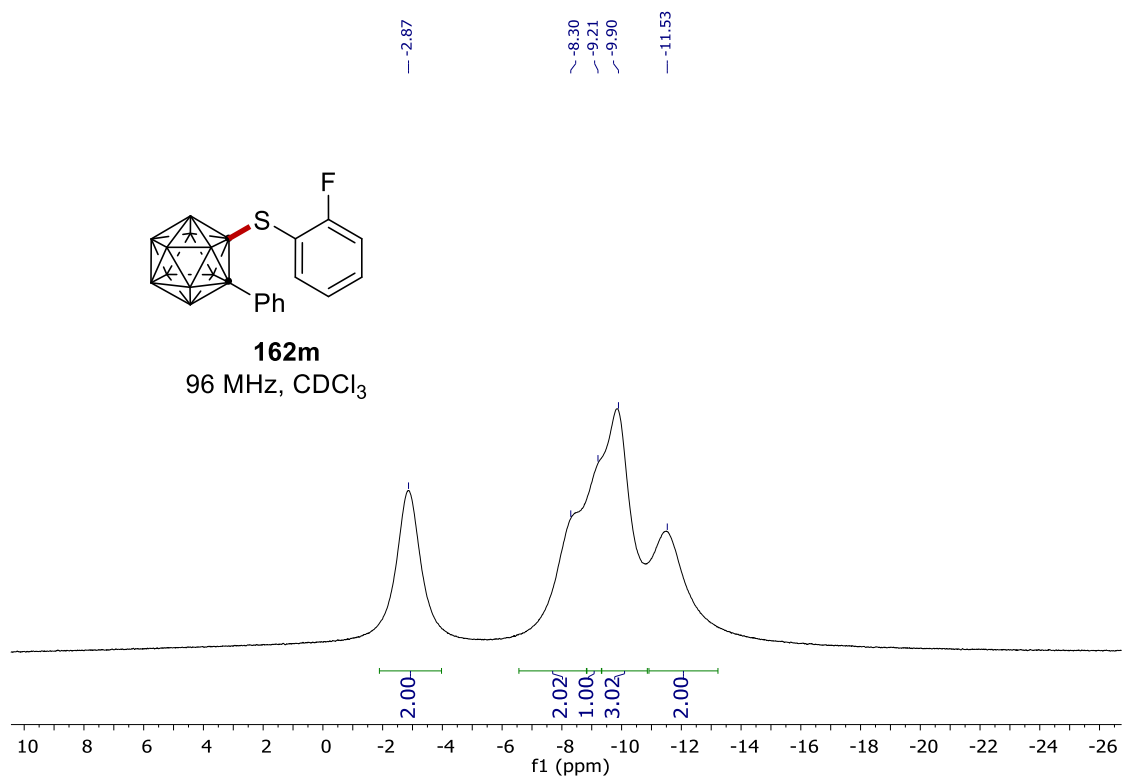
NMR Spectra



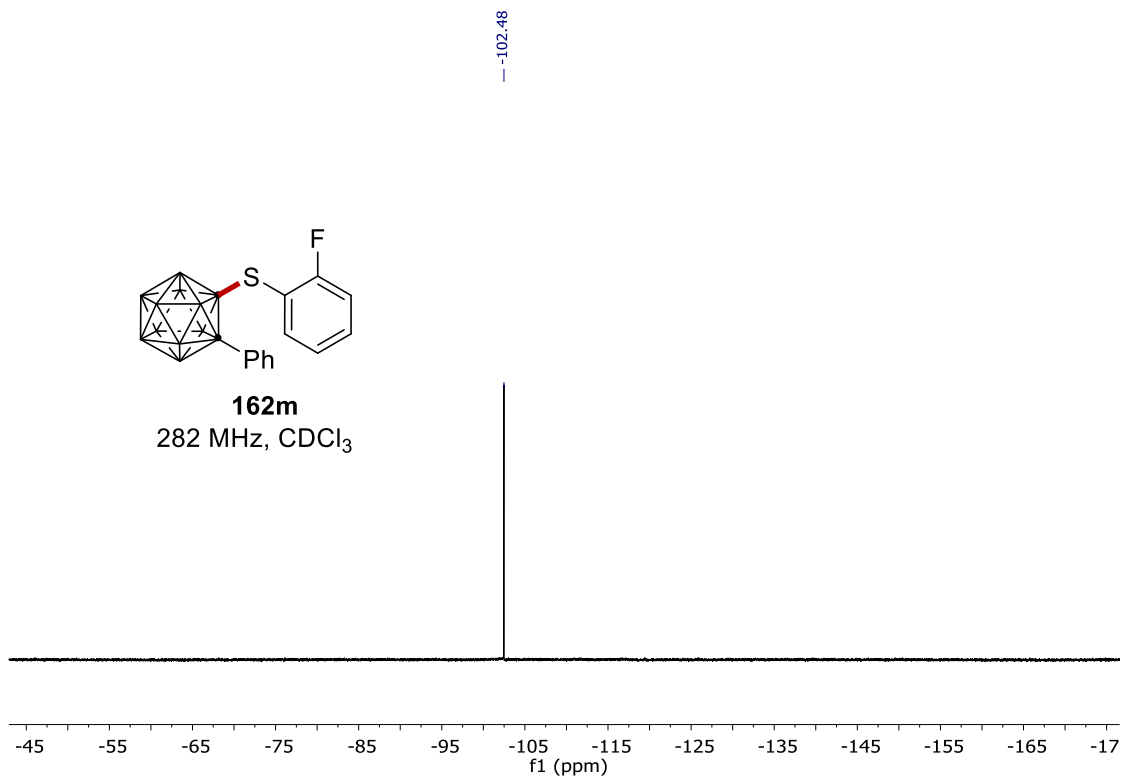
164.5
162.0
139.4
134.1
134.0
132.1
130.9
130.9
128.5
124.5
124.5
117.1
116.9
116.6
116.4
88.7
85.2



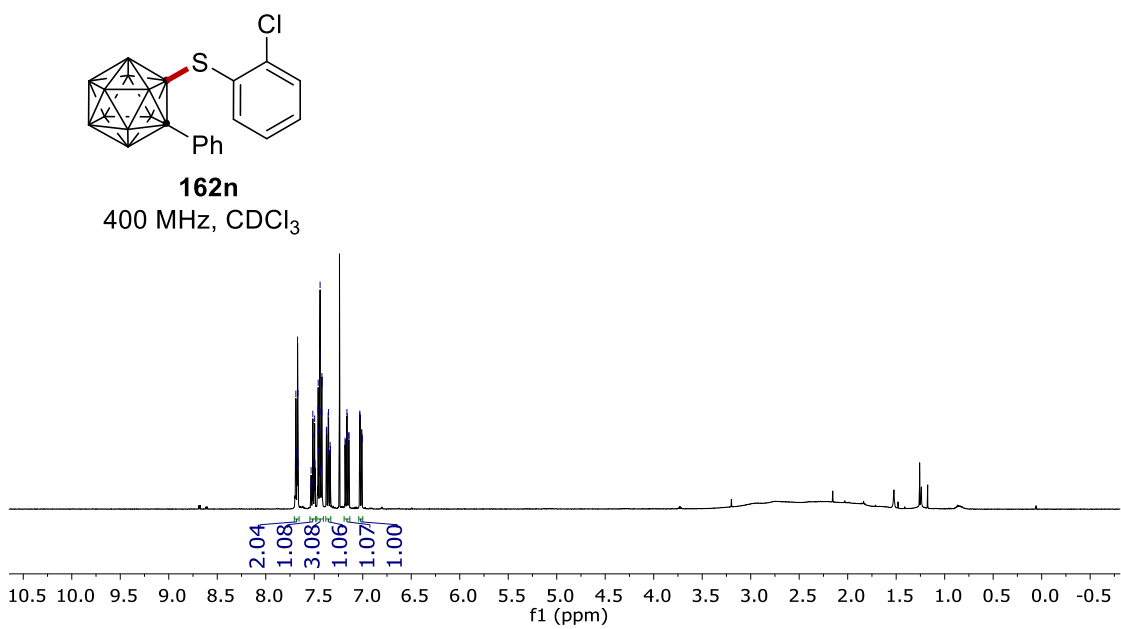
NMR Spectra



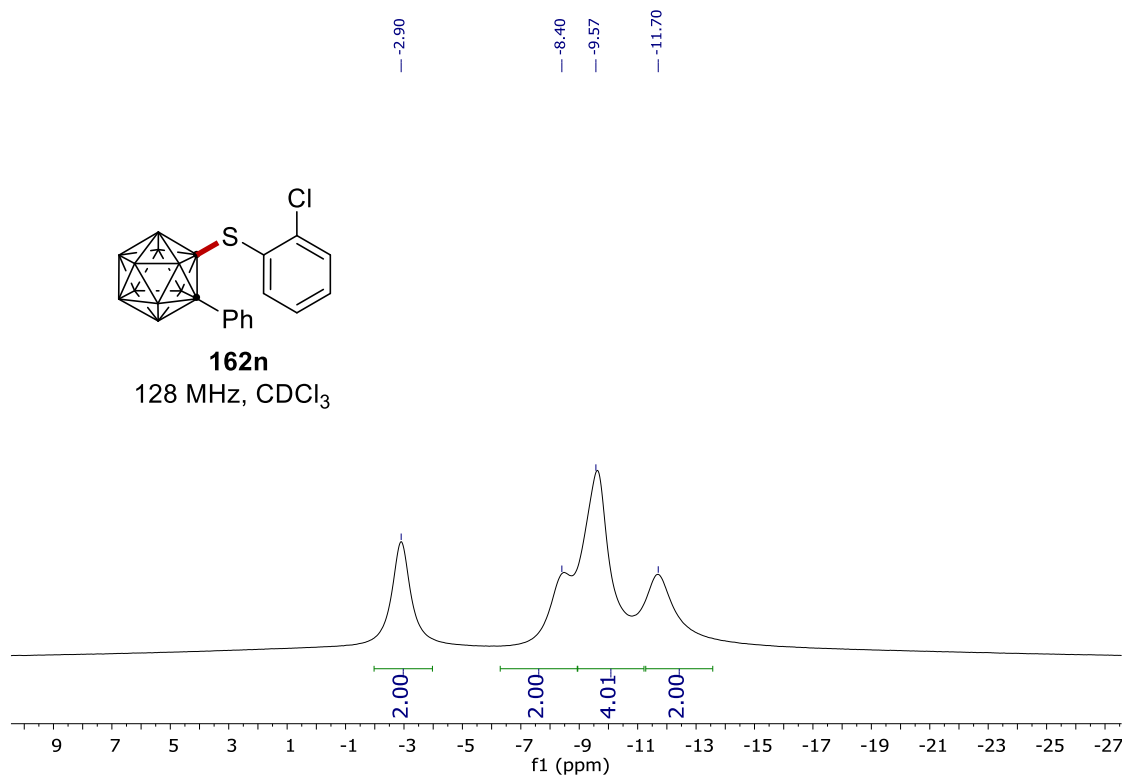
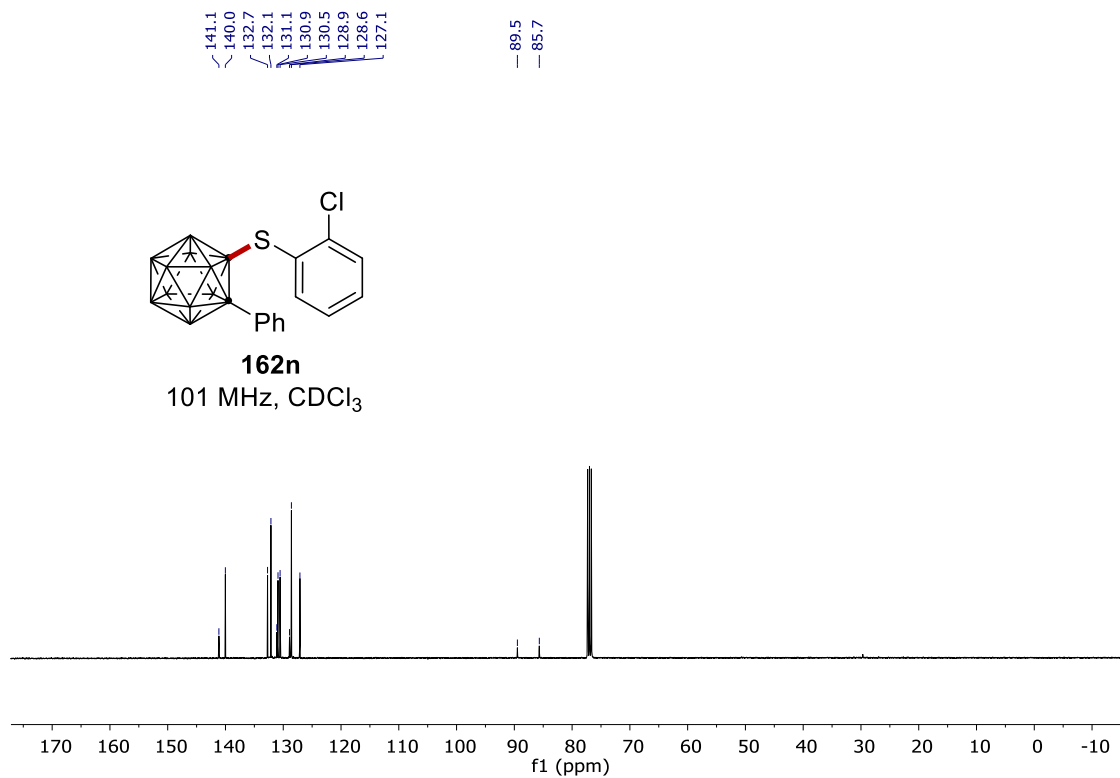
NMR Spectra



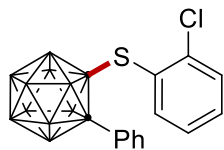
7.69
7.69
7.69
7.68
7.67
7.67
7.67
7.54
7.53
7.53
7.52
7.51
7.51
7.51
7.50
7.49
7.46
7.46
7.46
7.46
7.45
7.44
7.44
7.44
7.44
7.44
7.43
7.42
7.42
7.42
7.42
7.37
7.37
7.36
7.35
7.35
7.35
7.34
7.33
7.33
7.18
7.18
7.16
7.16
7.16
7.16
7.16
7.14
7.14
7.03
7.03
7.03
7.03
7.01
7.01
7.01



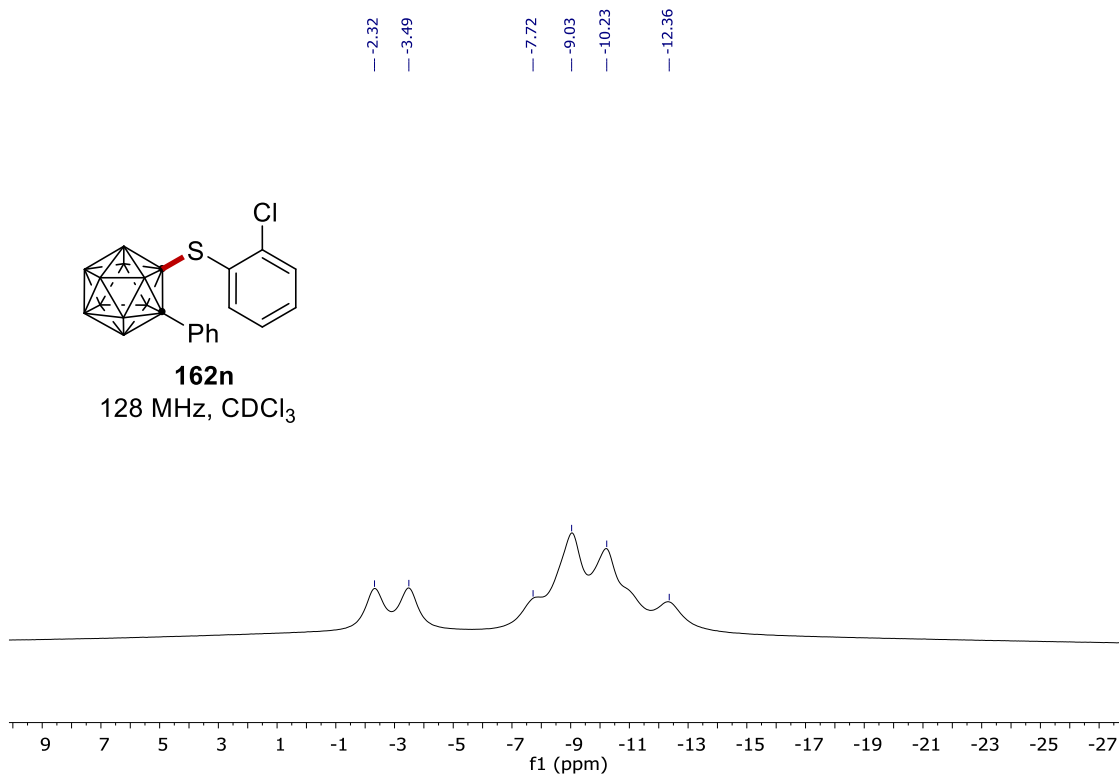
NMR Spectra



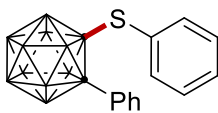
NMR Spectra



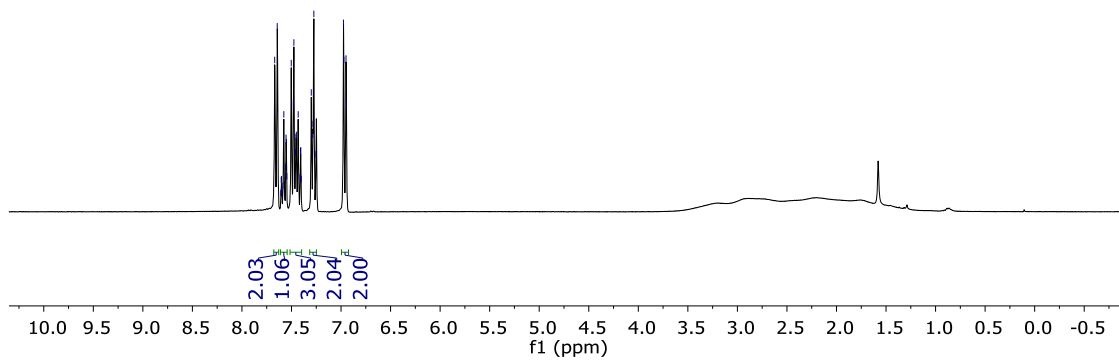
162n
128 MHz, CDCl₃



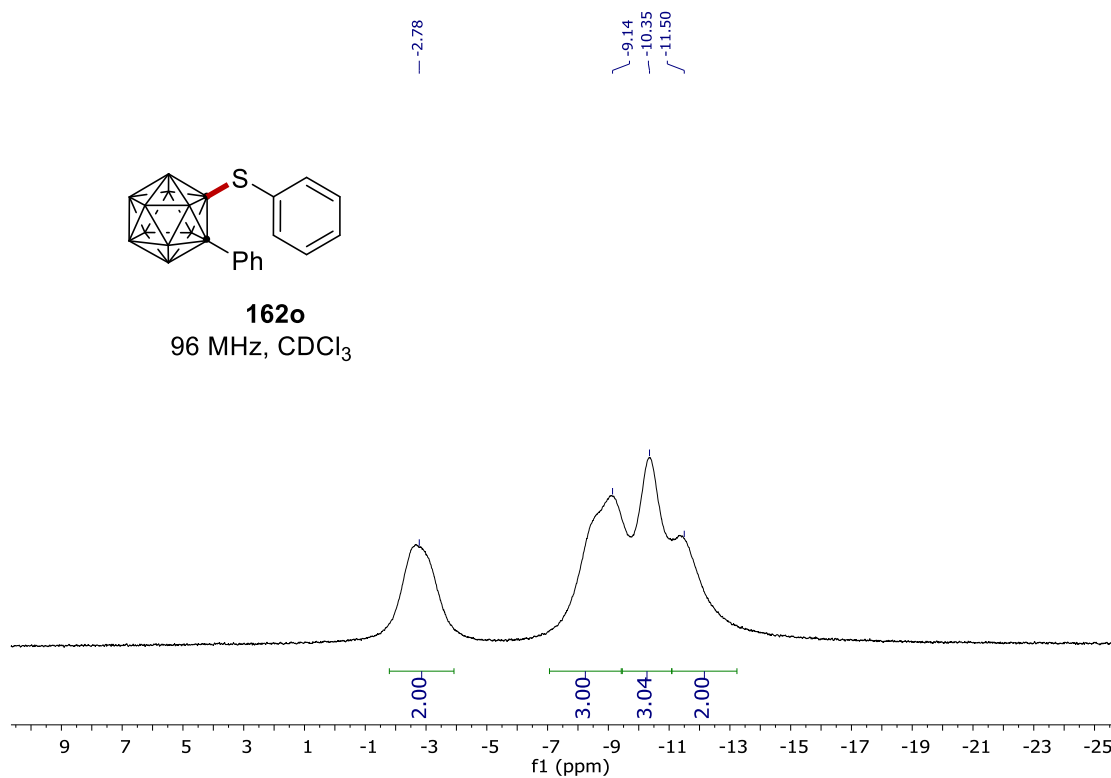
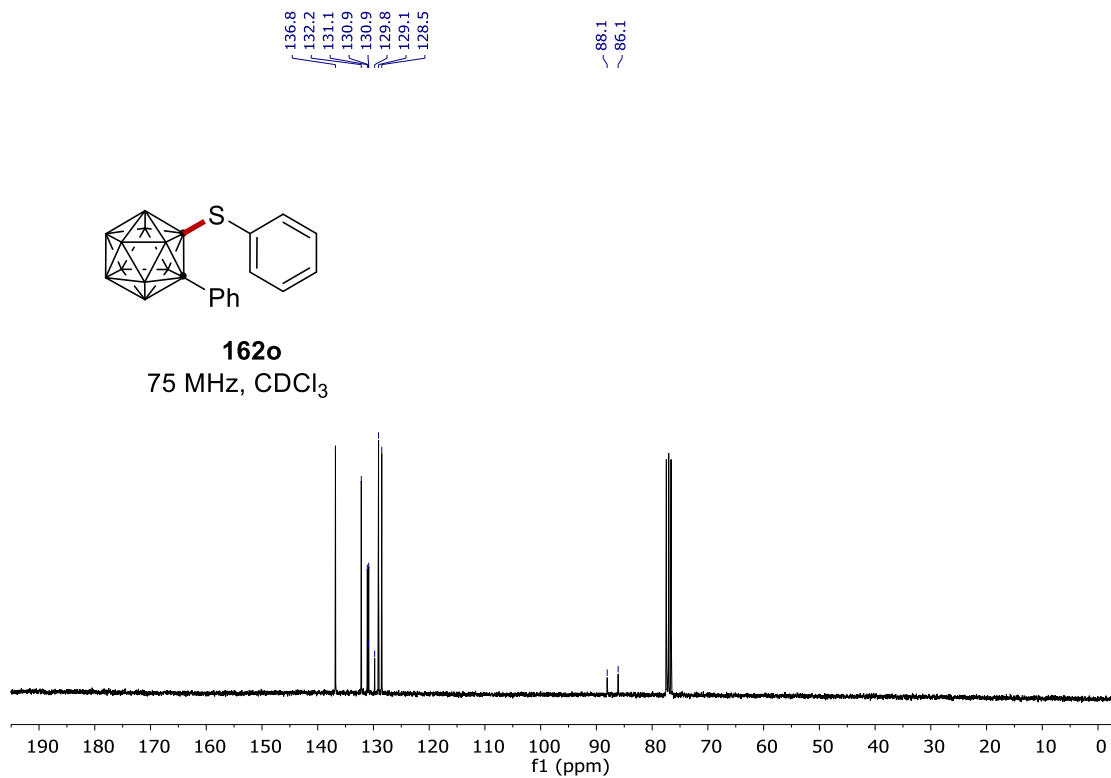
7.67
7.64
7.61
7.60
7.60
7.60
7.59
7.58
7.56
7.56
7.55
7.55
7.50
7.48
7.48
7.46
7.46
7.45
7.43
7.41
7.41
7.41
7.40
7.30
7.29
7.28
7.27
7.25
6.98
6.97
6.95
6.94



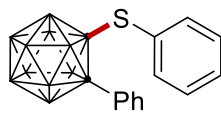
162o
300 MHz, CDCl₃



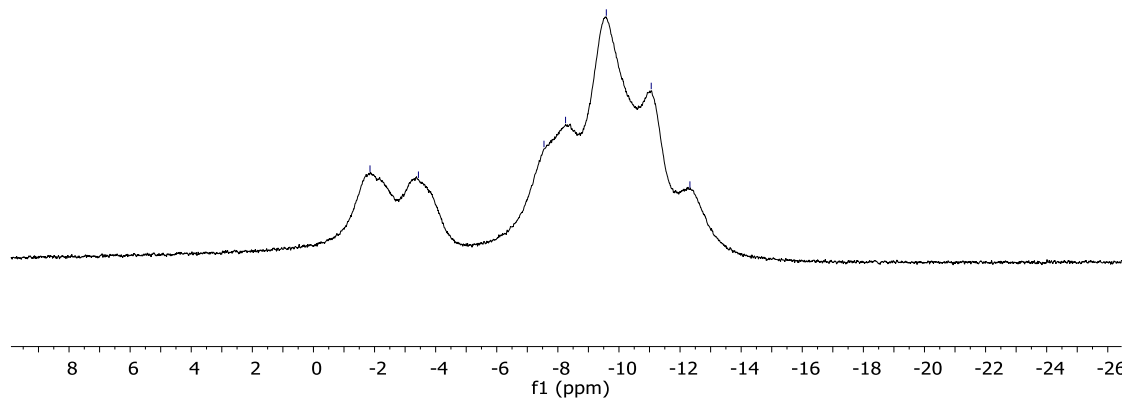
NMR Spectra



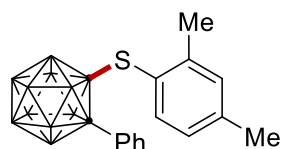
NMR Spectra



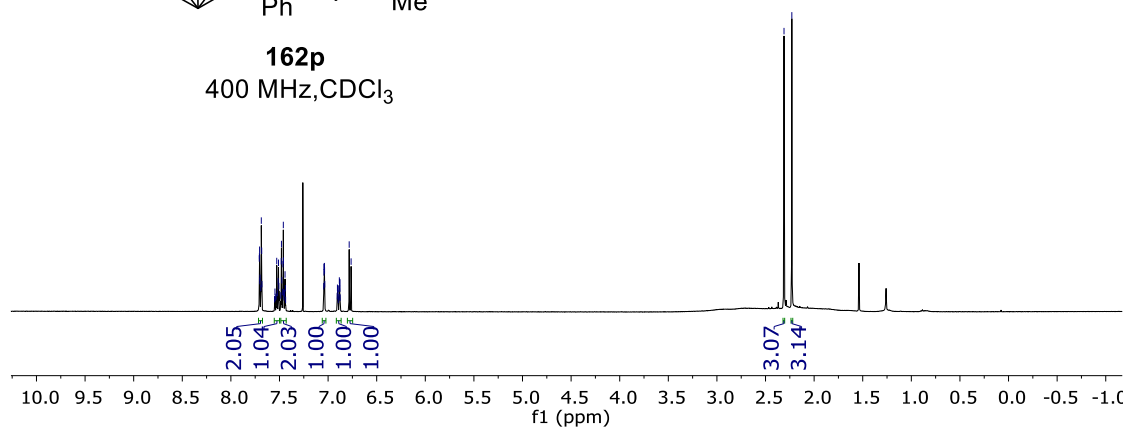
162o
96 MHz, CDCl₃



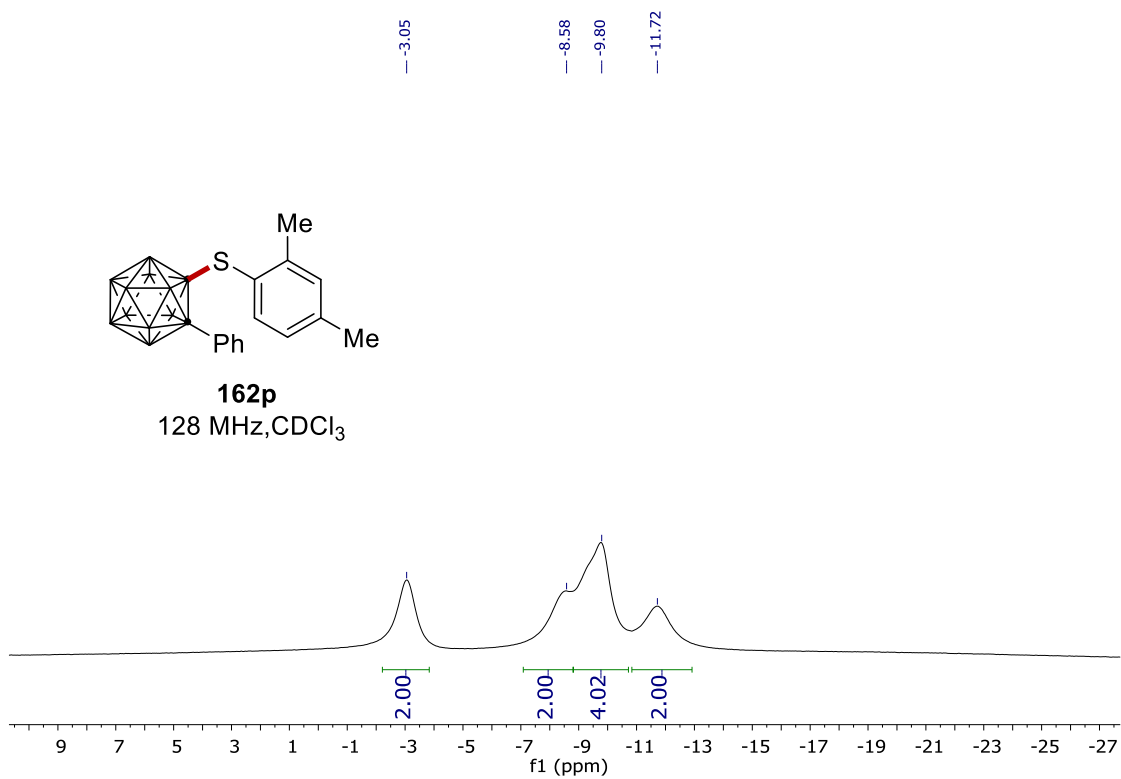
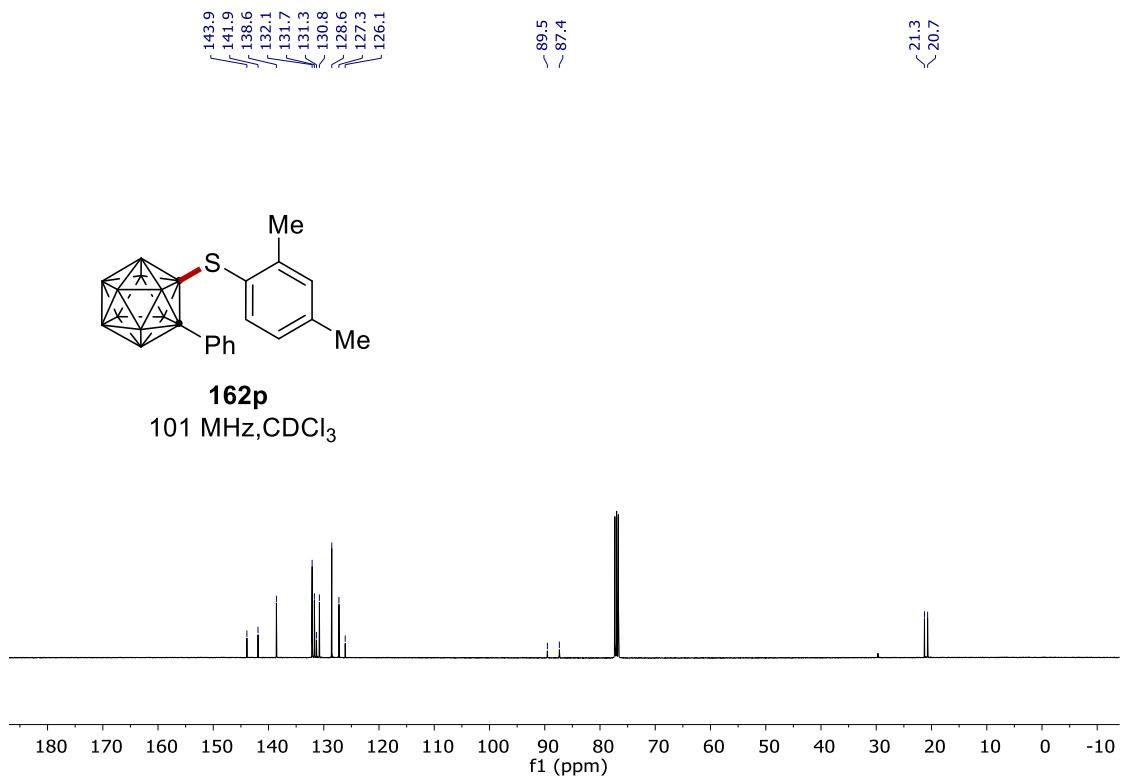
7.71, 7.71, 7.70, 7.70, 7.70, 7.69, 7.69, 7.68, 7.68, 7.55, 7.55, 7.54, 7.54, 7.53, 7.53, 7.52, 7.51, 7.51, 7.49, 7.49, 7.48, 7.48, 7.48, 7.47, 7.47, 7.46, 7.46, 7.46, 7.46, 7.45, 7.45, 7.44, 7.44, 7.44, 7.44, 7.04, 7.04, 7.04, 7.04, 7.04, 7.04, 7.03, 7.03, 6.91, 6.91, 6.90, 6.90, 6.90, 6.90, 6.89, 6.89, 6.88, 6.88, 6.88, 6.88, 6.88, 6.88, 6.78, 6.78, 2.31, 2.23



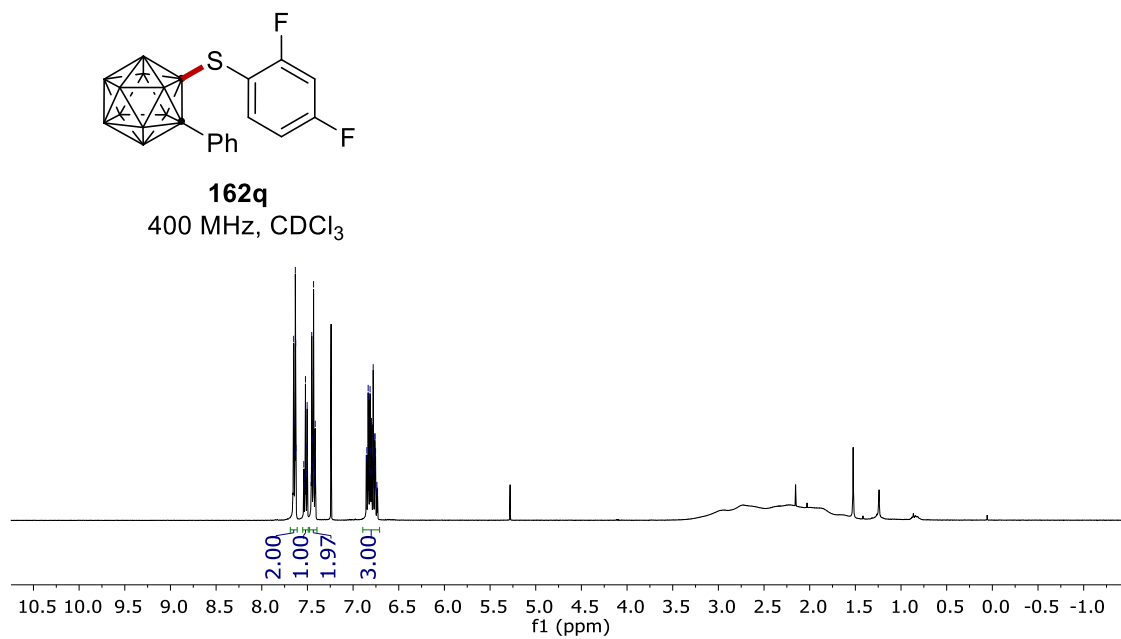
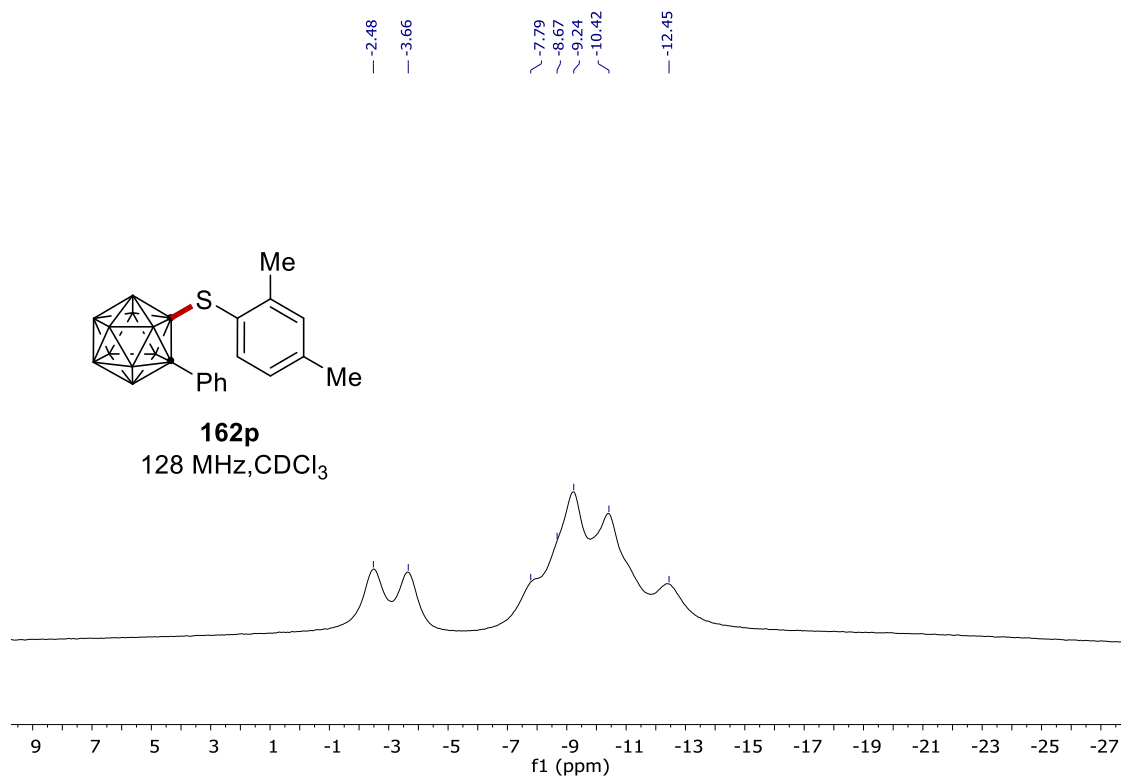
162p
400 MHz, CDCl₃



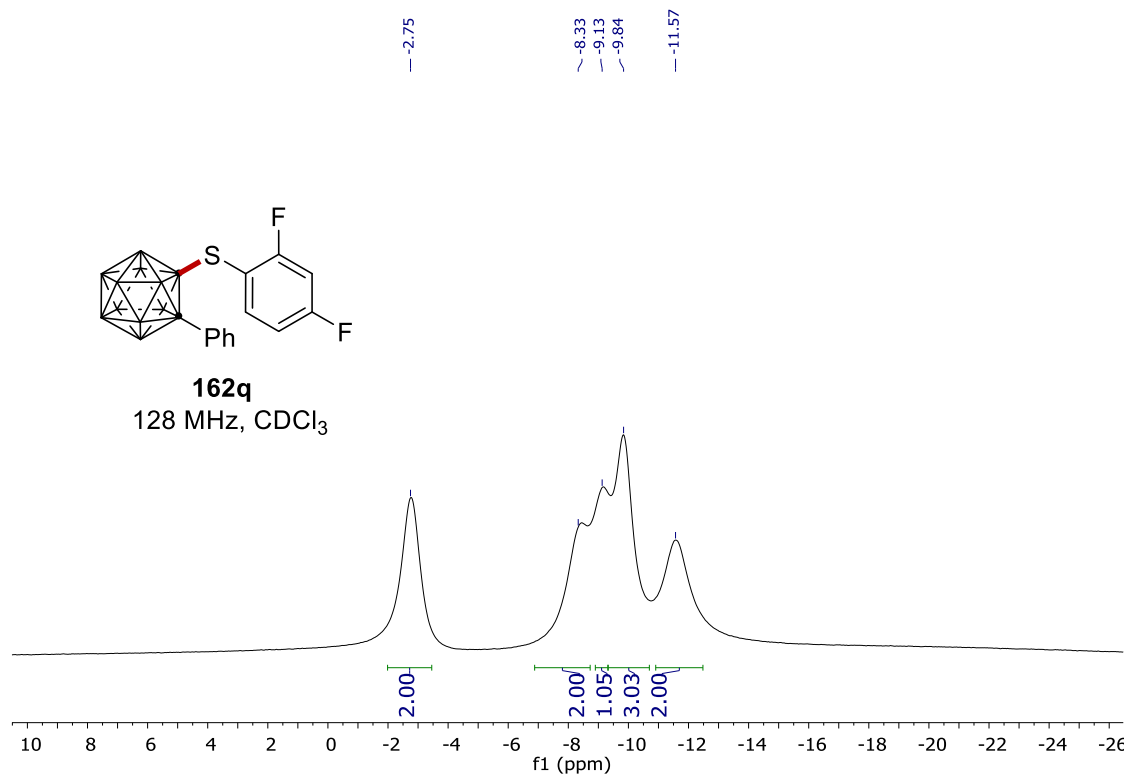
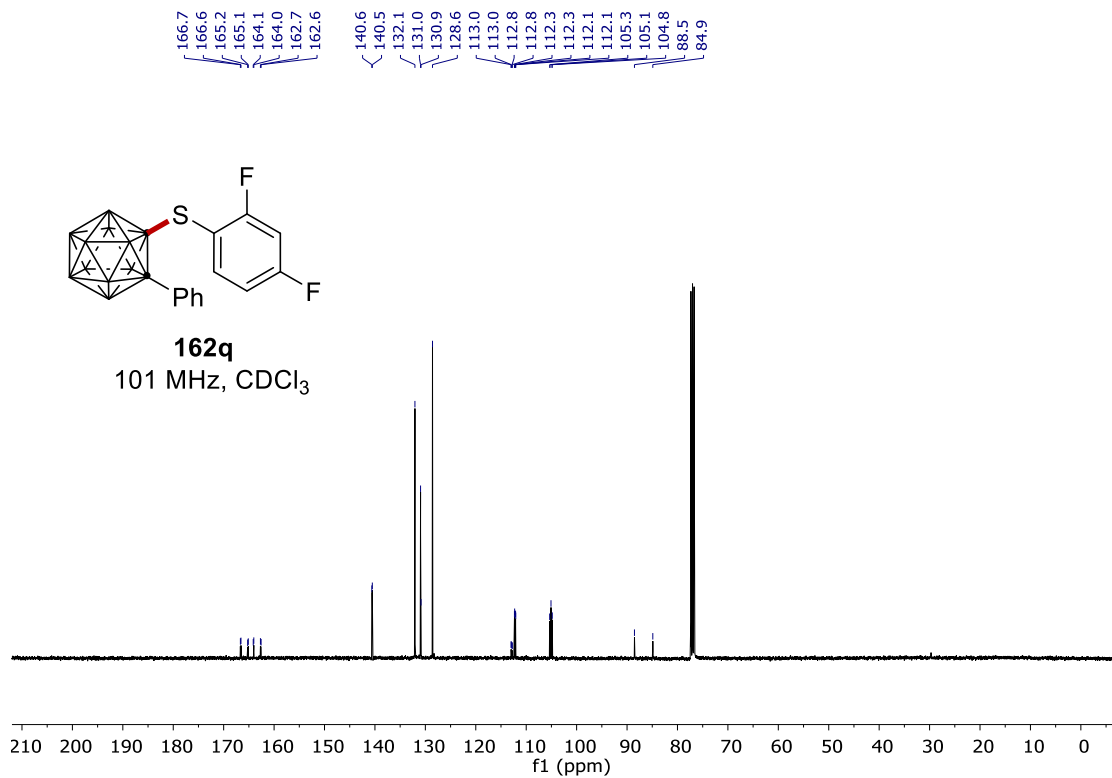
NMR Spectra



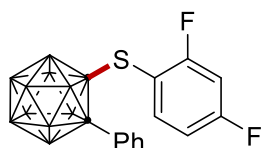
NMR Spectra



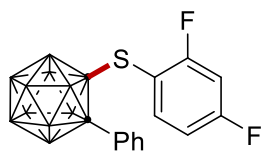
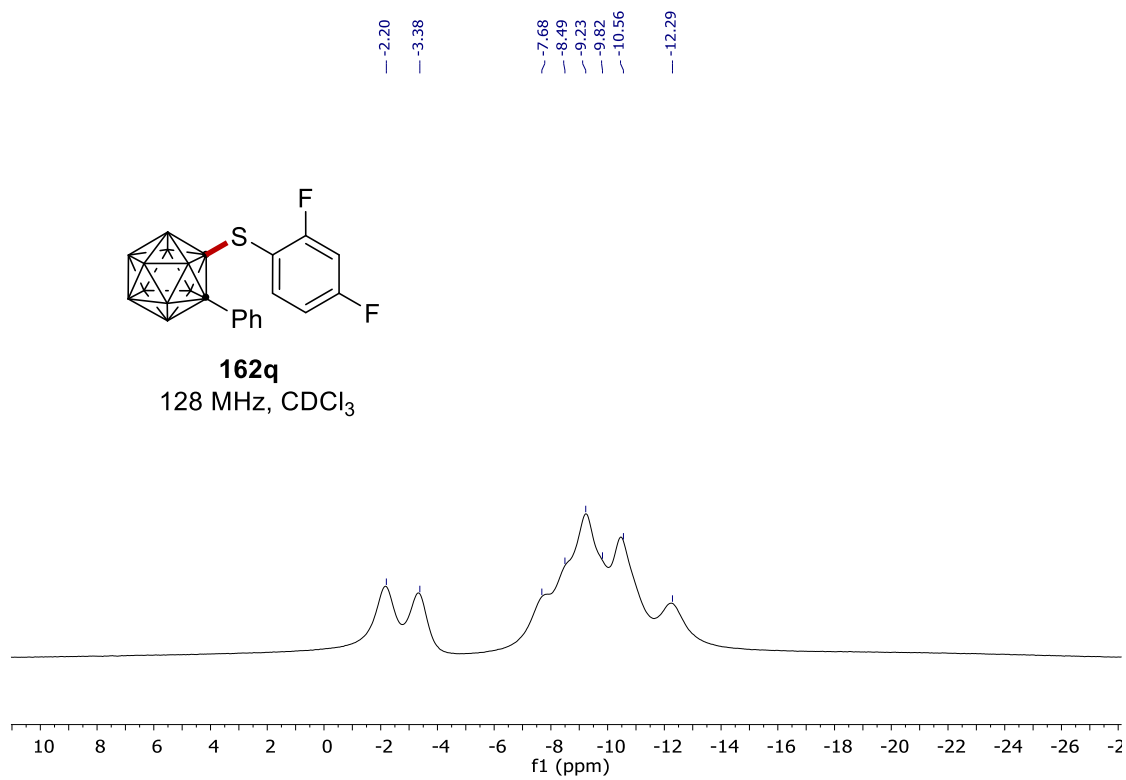
NMR Spectra



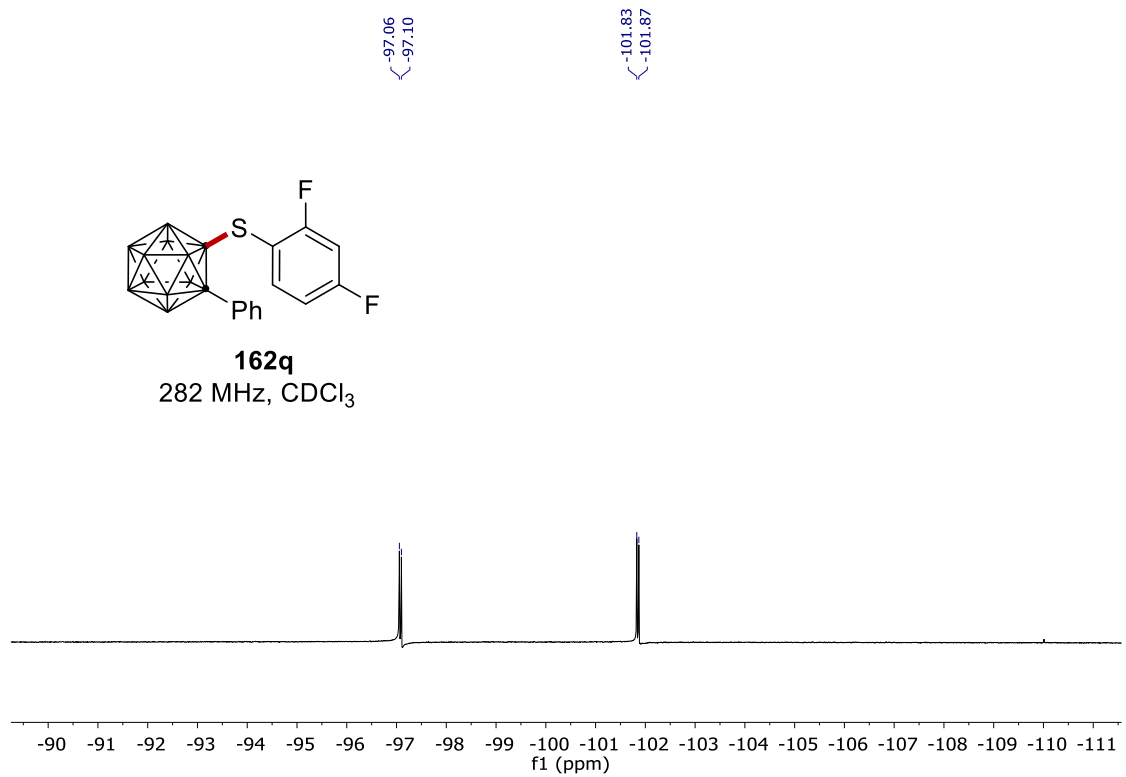
NMR Spectra



162q
128 MHz, CDCl₃

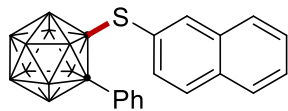


162q
282 MHz, CDCl₃



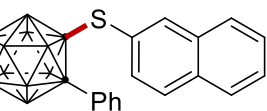
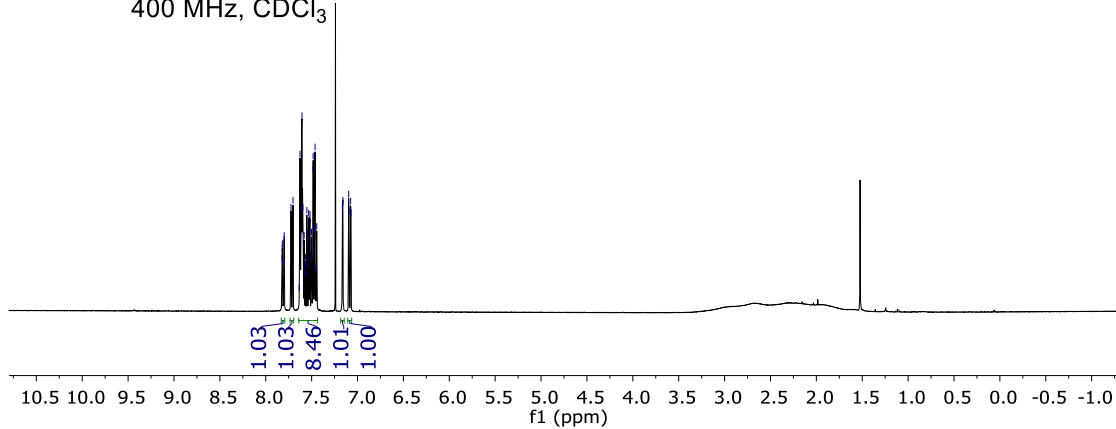
NMR Spectra

7.82
7.82
7.82
7.80
7.80
7.72
7.63
7.63
7.62
7.61
7.61
7.59
7.58
7.58
7.57
7.57
7.55
7.55
7.55
7.53
7.53
7.52
7.52
7.50
7.50
7.48
7.48
7.48
7.47
7.46
7.46
7.45
7.45
7.44
7.44
7.16
7.16
7.10
7.09
7.08
7.07



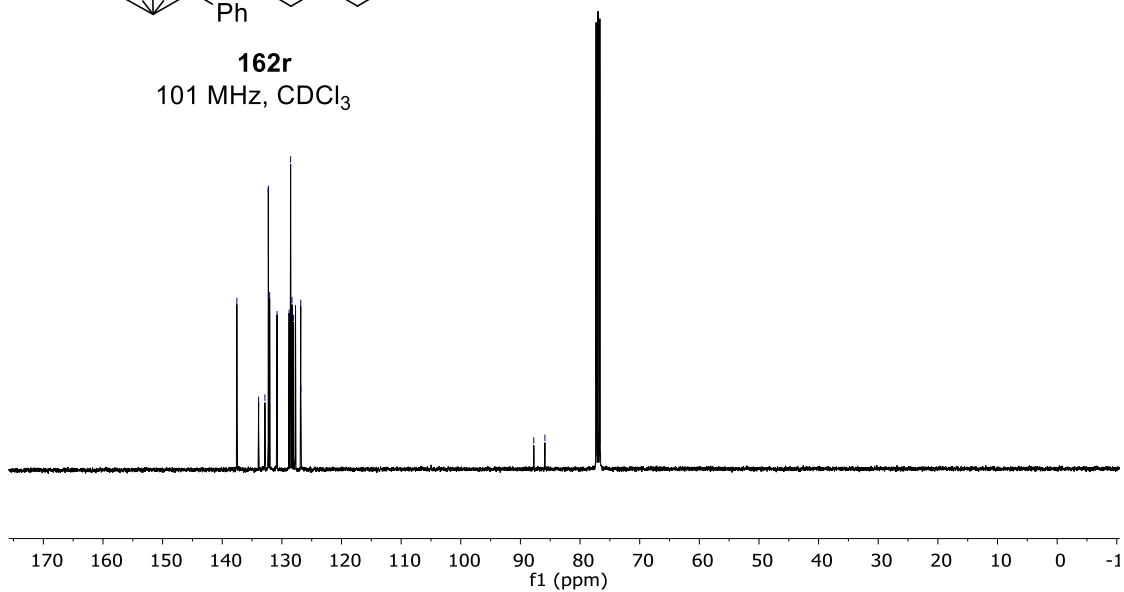
162r

400 MHz, CDCl₃

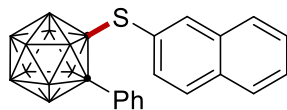


162r

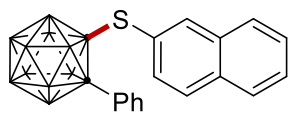
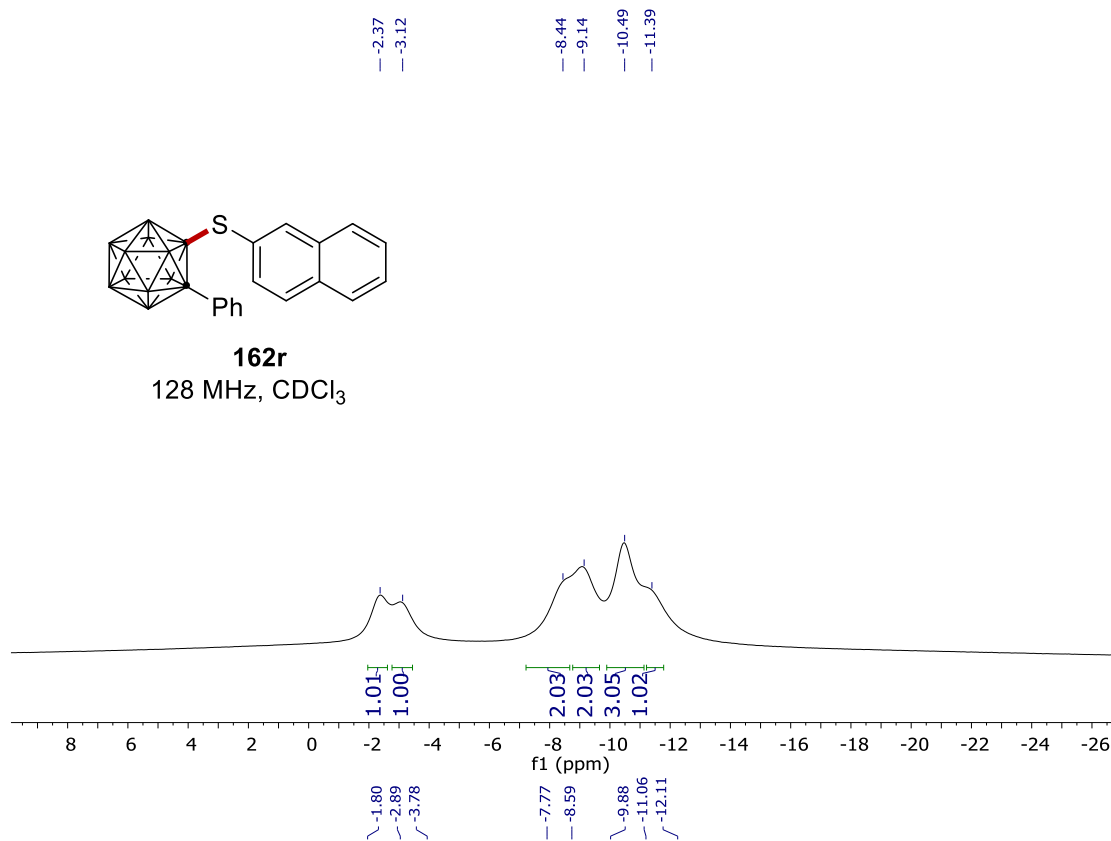
101 MHz, CDCl₃



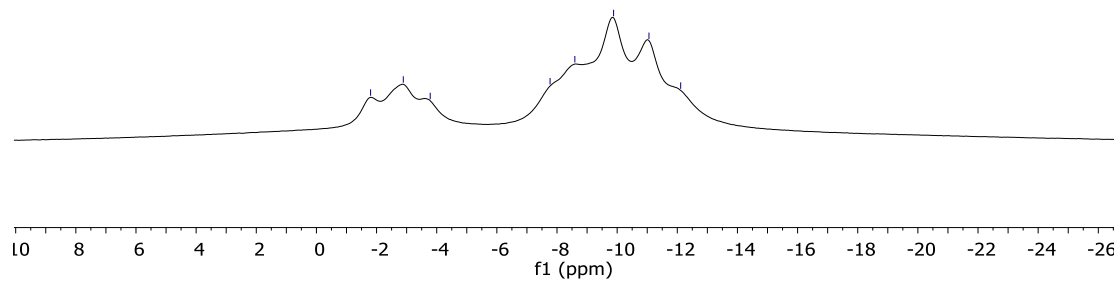
NMR Spectra



162r
128 MHz, CDCl₃

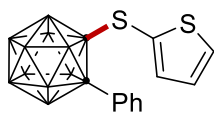


162r
128 MHz, CDCl₃

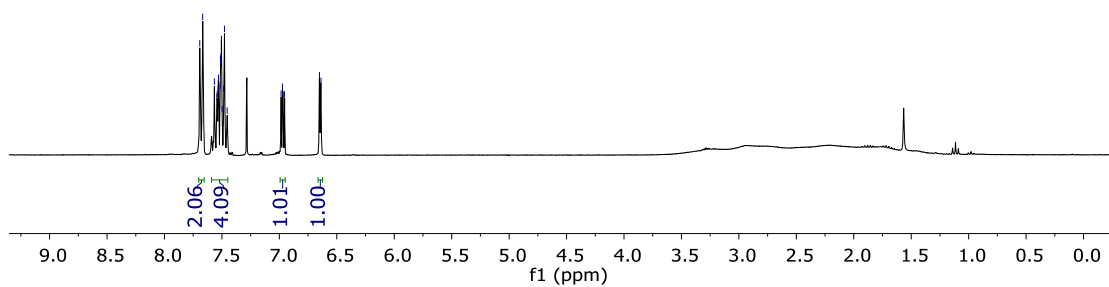


NMR Spectra

7.69
7.67
7.57
7.53
7.53
7.53
7.52
7.51
7.50
7.48
6.98
6.97
6.96
6.65
6.64

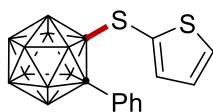


162s
300 MHz, CDCl₃

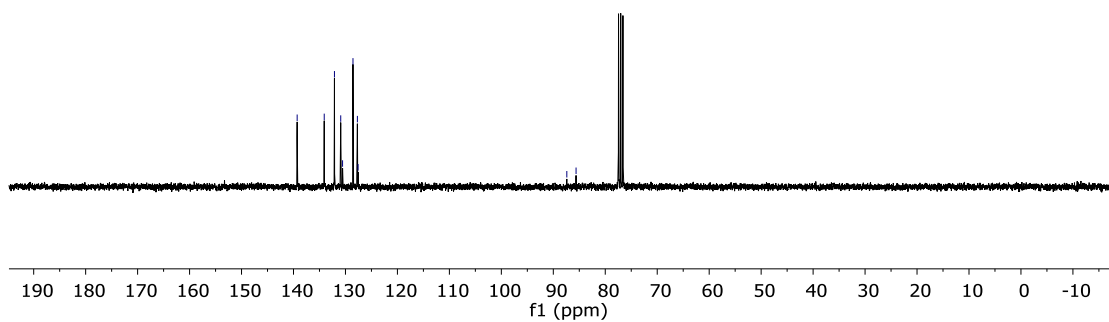


139.3
134.1
132.1
130.9
130.6
128.6
127.7
127.6

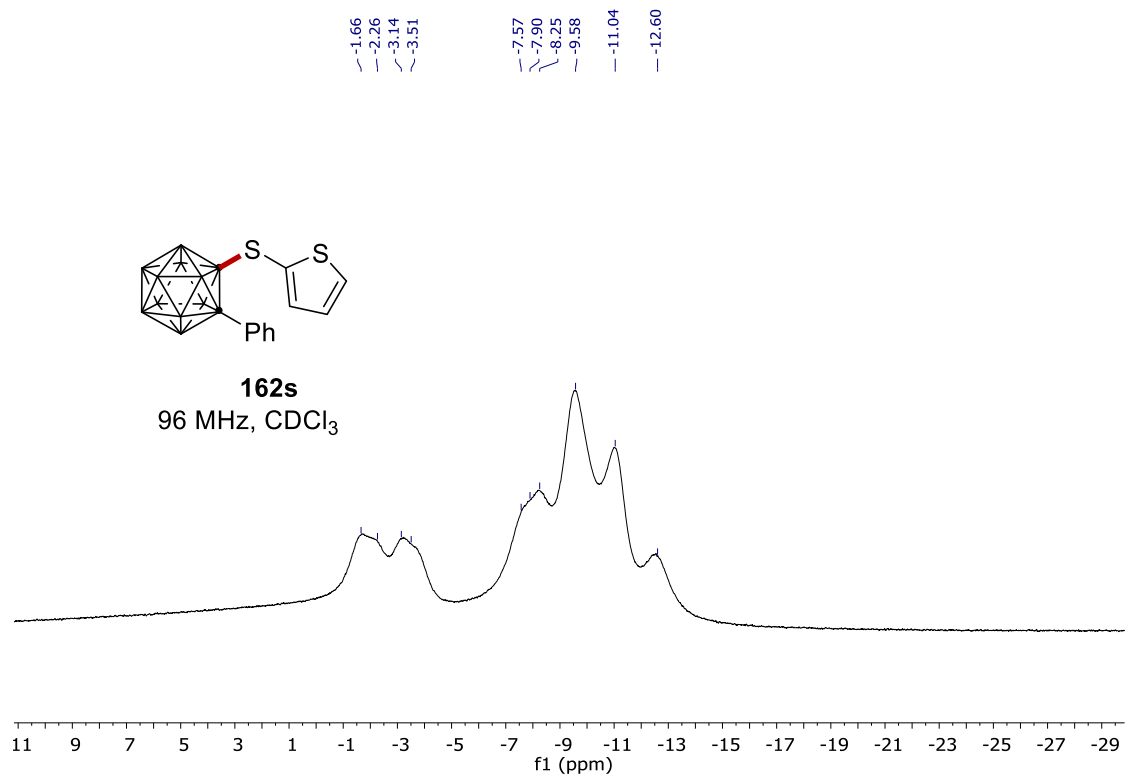
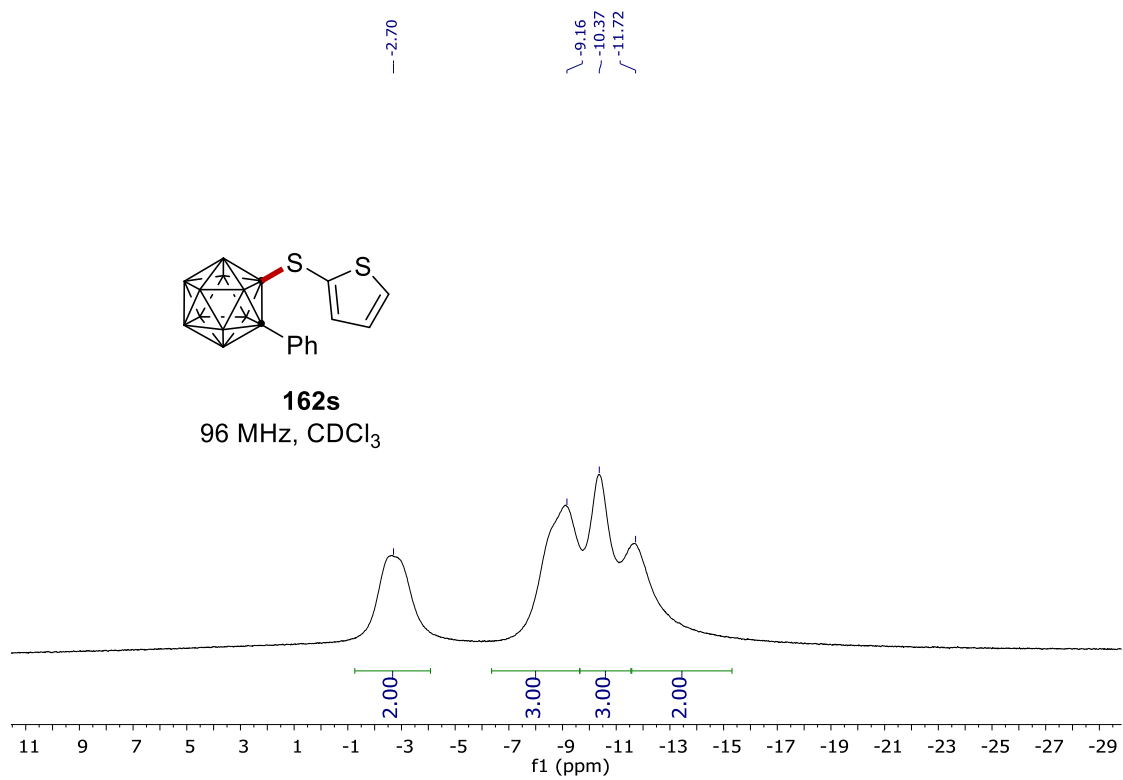
87.4
85.6



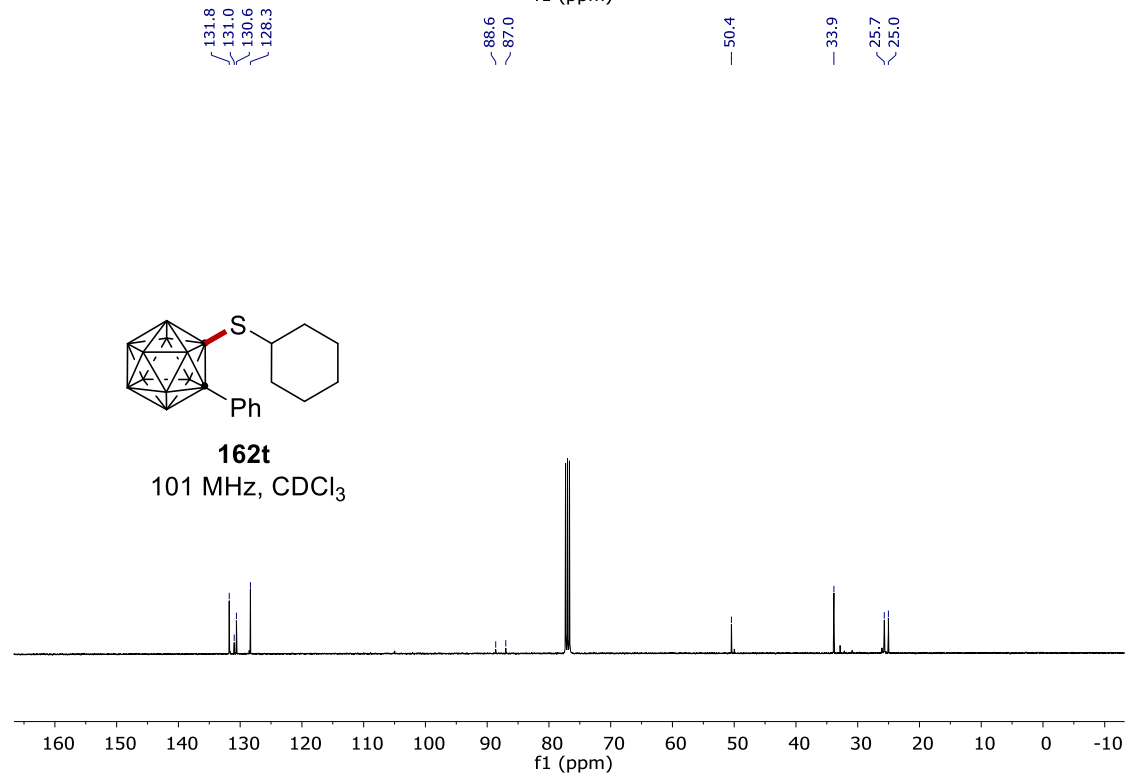
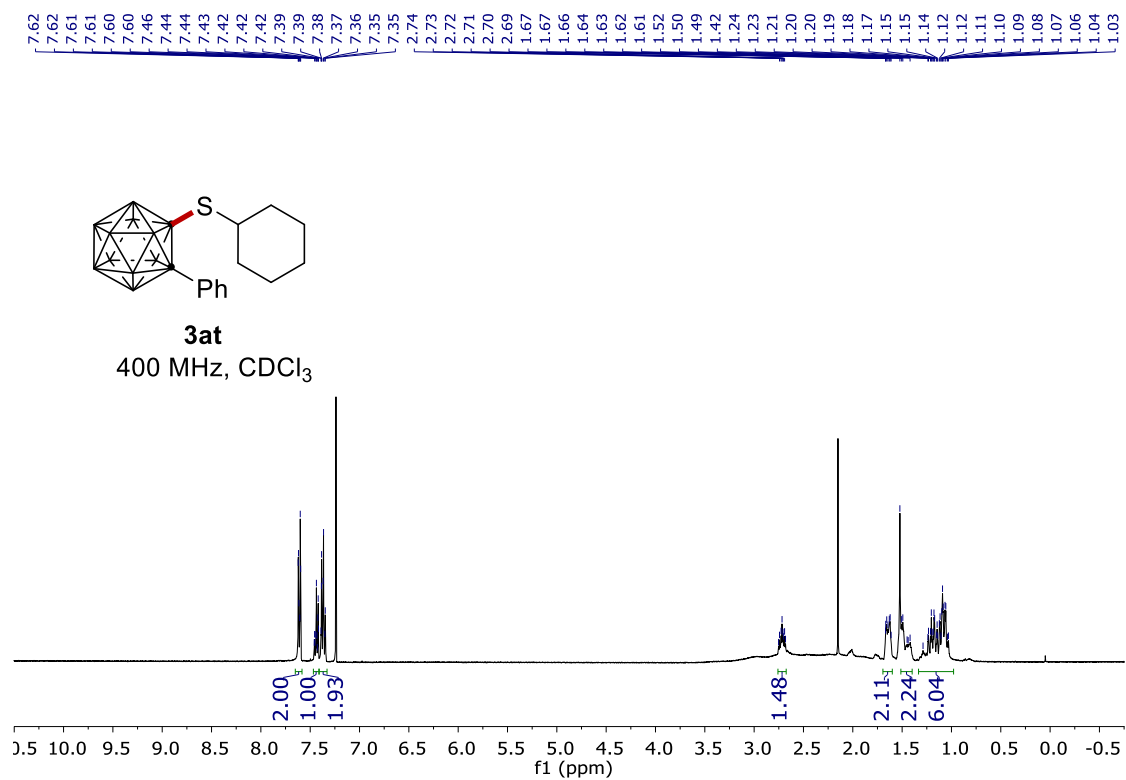
162s
75 MHz, CDCl₃



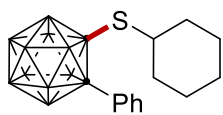
NMR Spectra



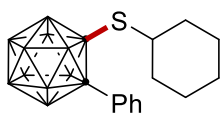
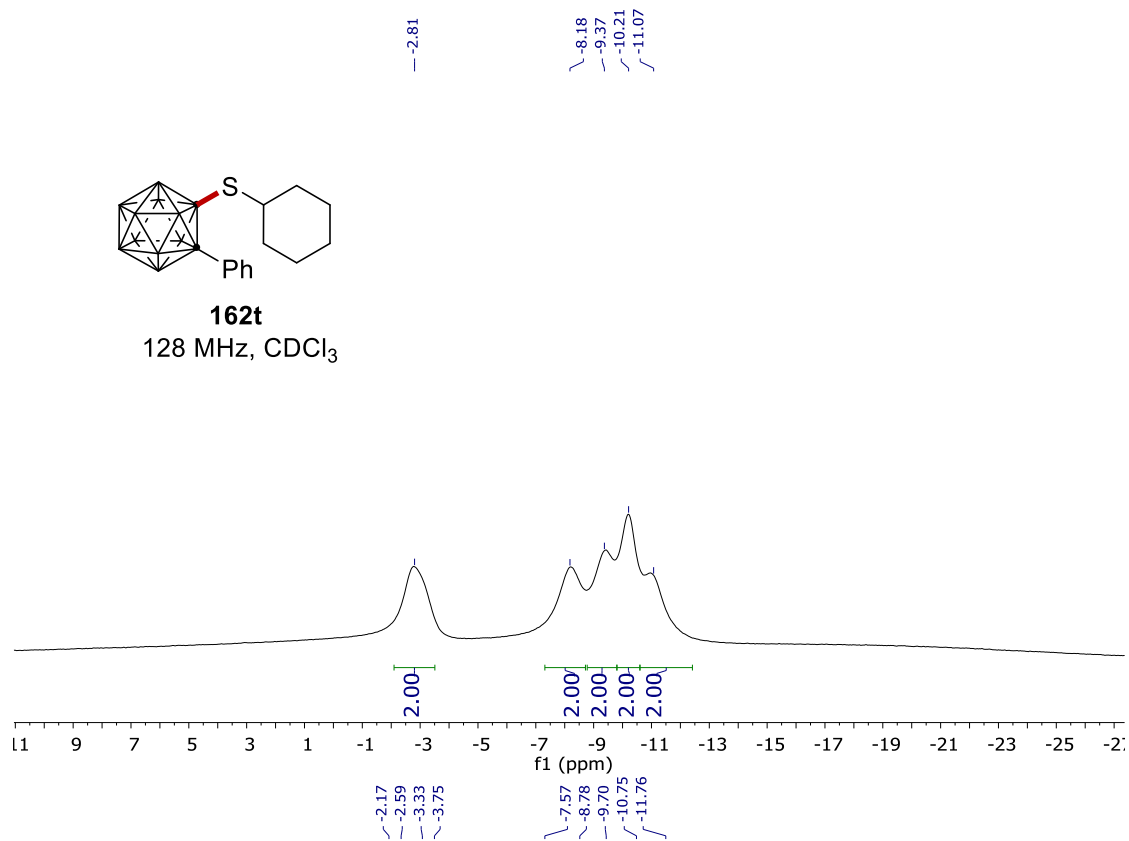
NMR Spectra



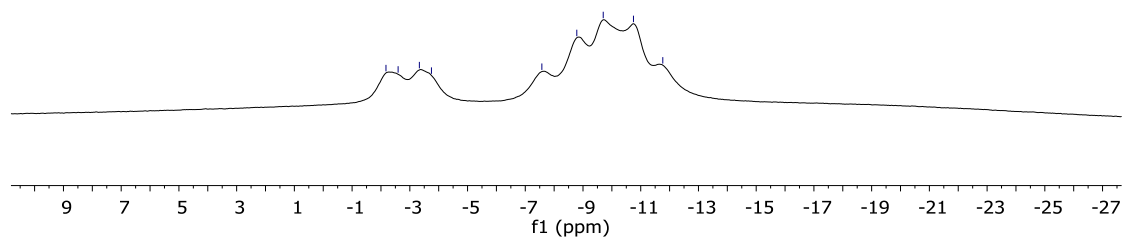
NMR Spectra



162t
128 MHz, CDCl₃



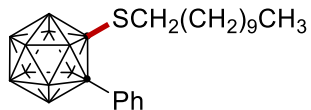
162t
128 MHz, CDCl₃



NMR Spectra

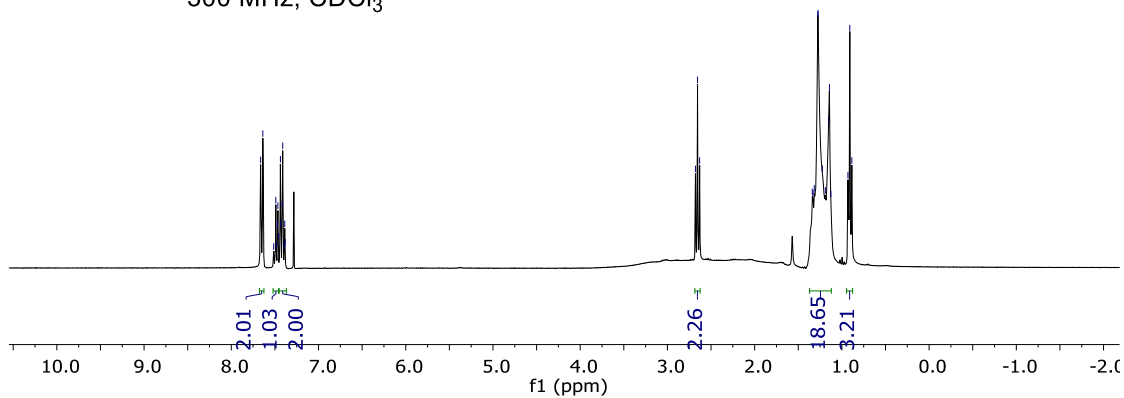
7.66
7.64
7.51
7.49
7.48
7.47
7.46
7.44
7.43
7.42
7.41
7.39
7.38

2.68
2.65
2.63
1.34
1.33
1.32
1.28
1.27
1.22
1.19
1.15
1.14
1.13
0.93
0.91
0.89



162u

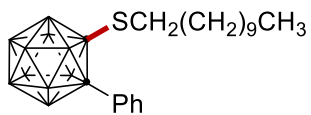
300 MHz, CDCl₃



131.6
131.1
130.7
128.5

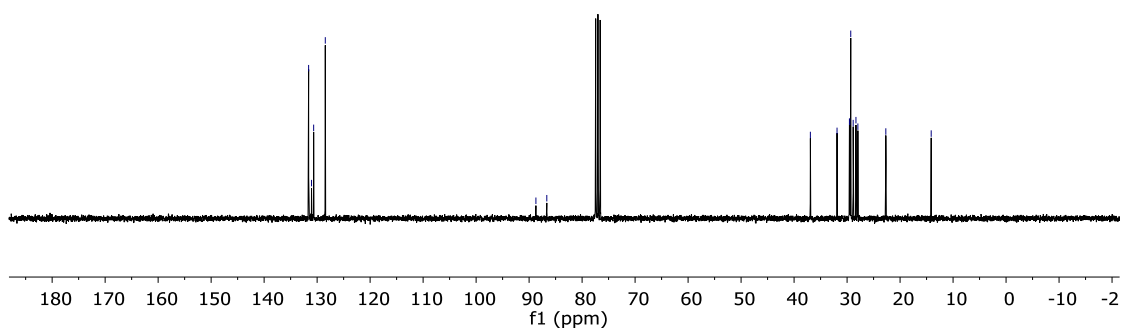
88.7
86.7

36.9
31.9
29.6
29.5
29.3
28.8
28.3
28.0
22.7
14.1

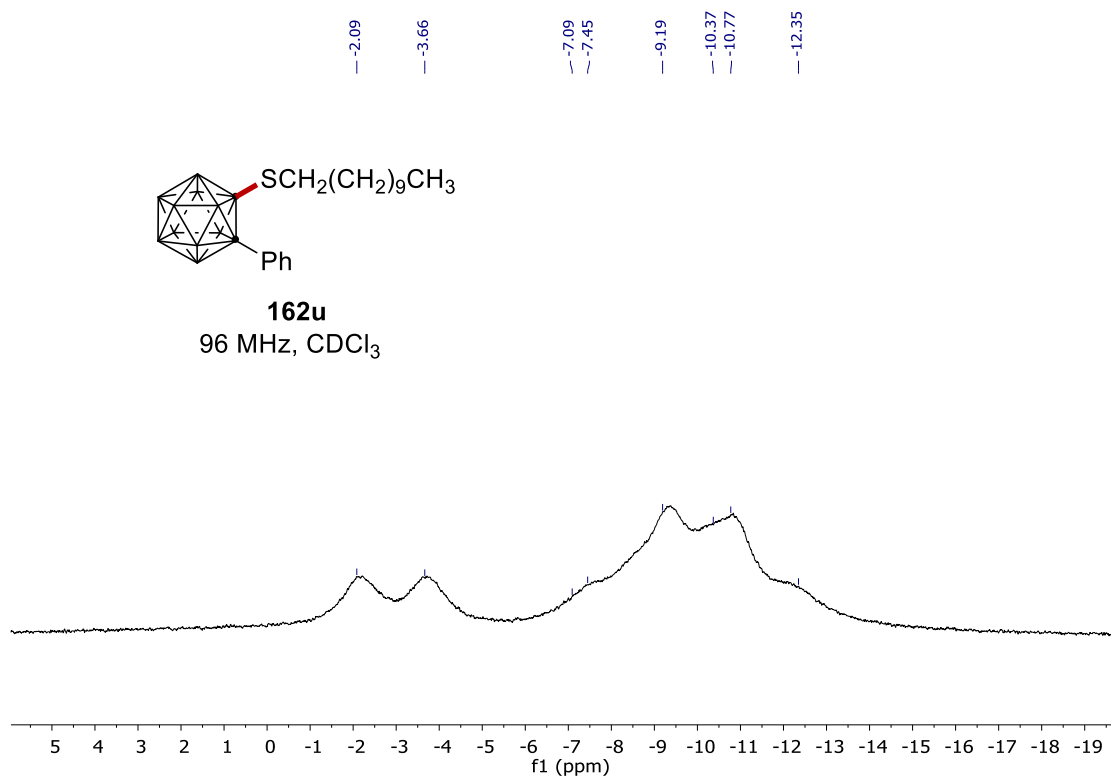
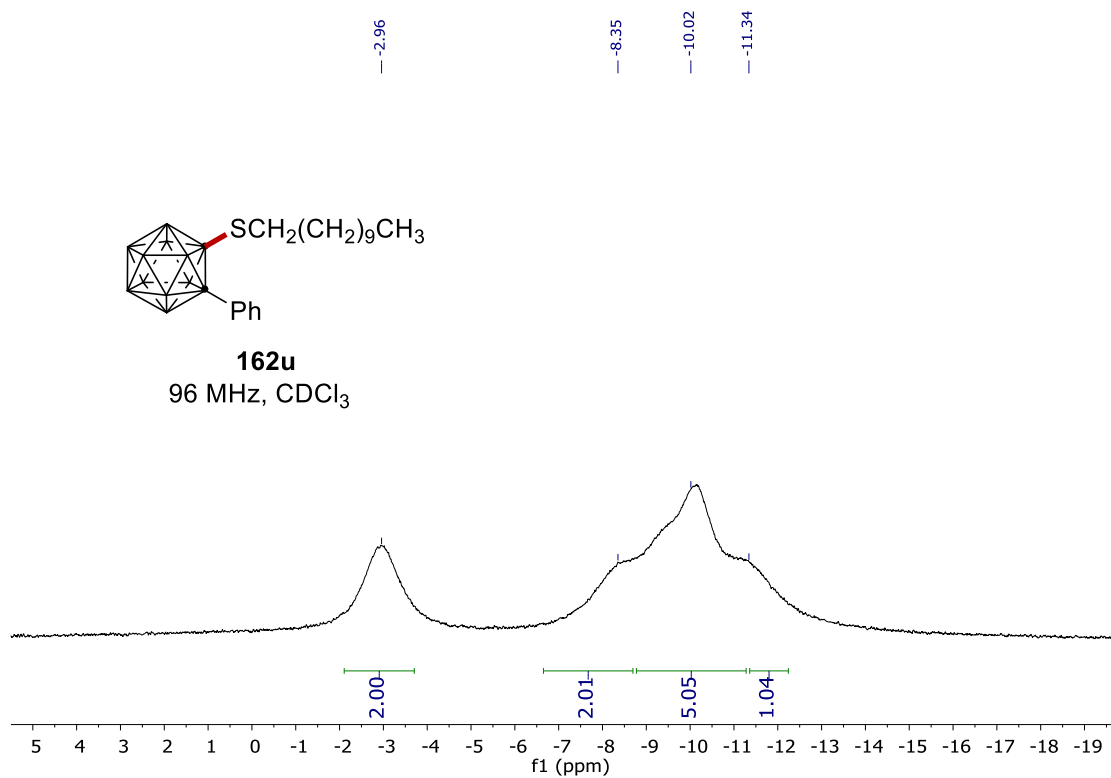


162u

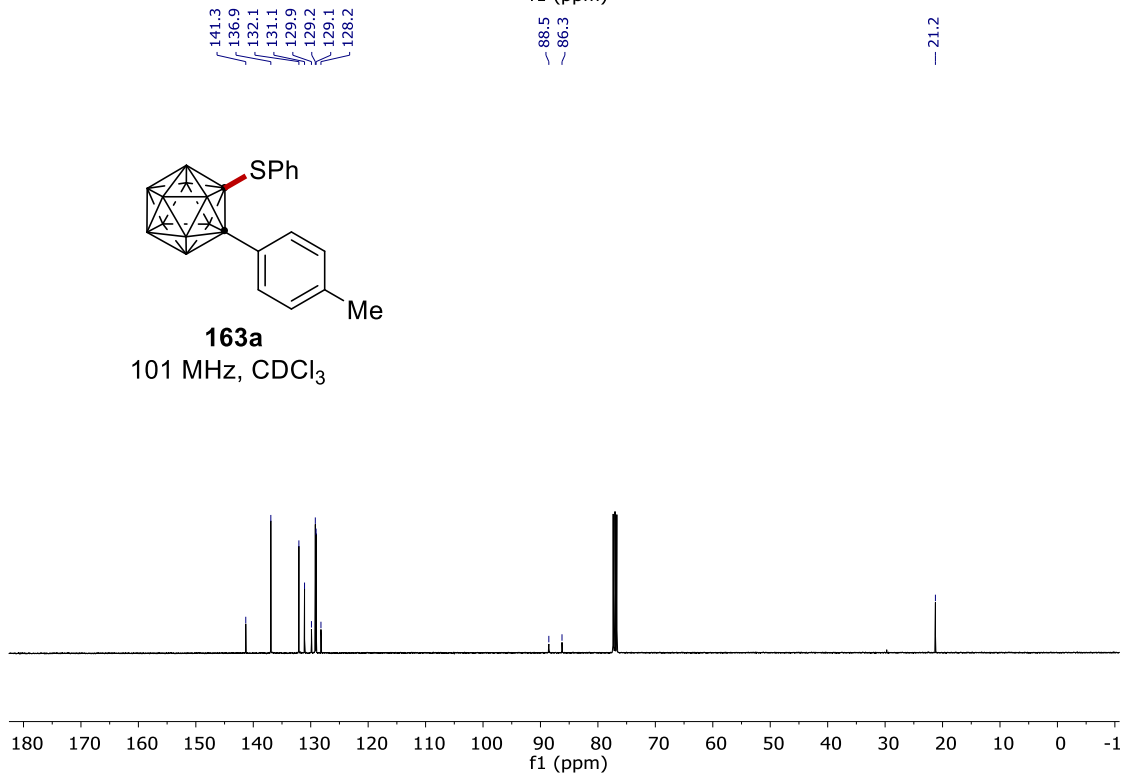
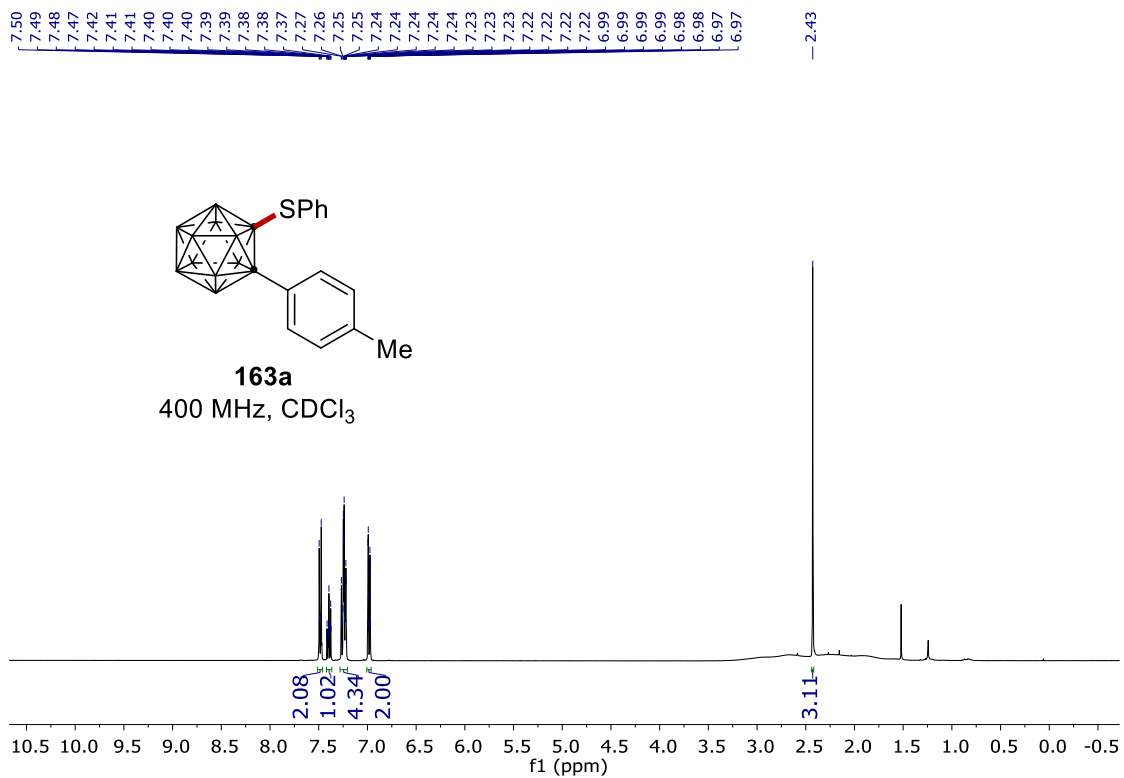
75 MHz, CDCl₃



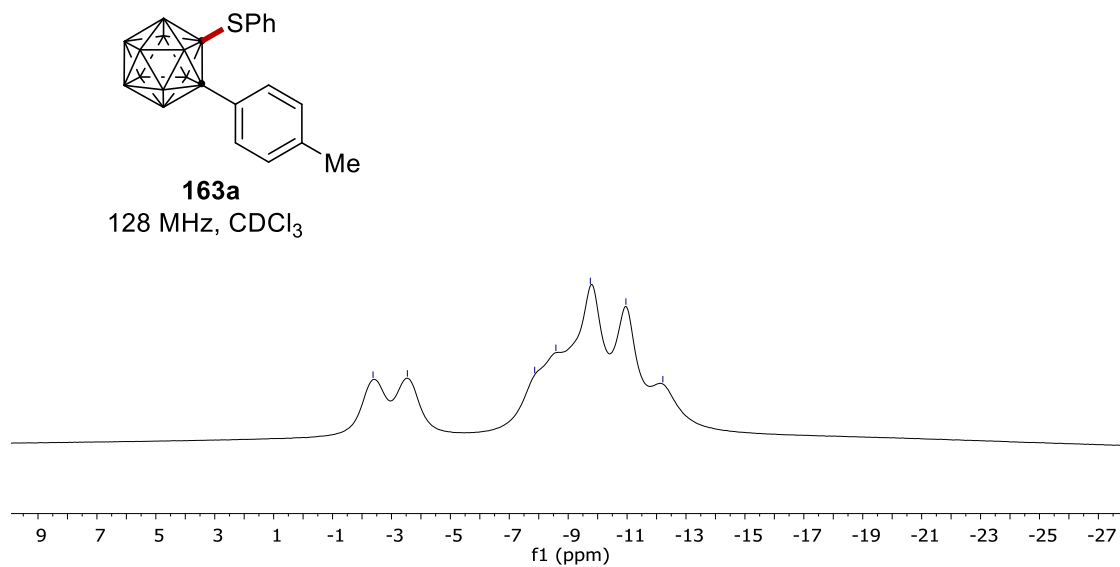
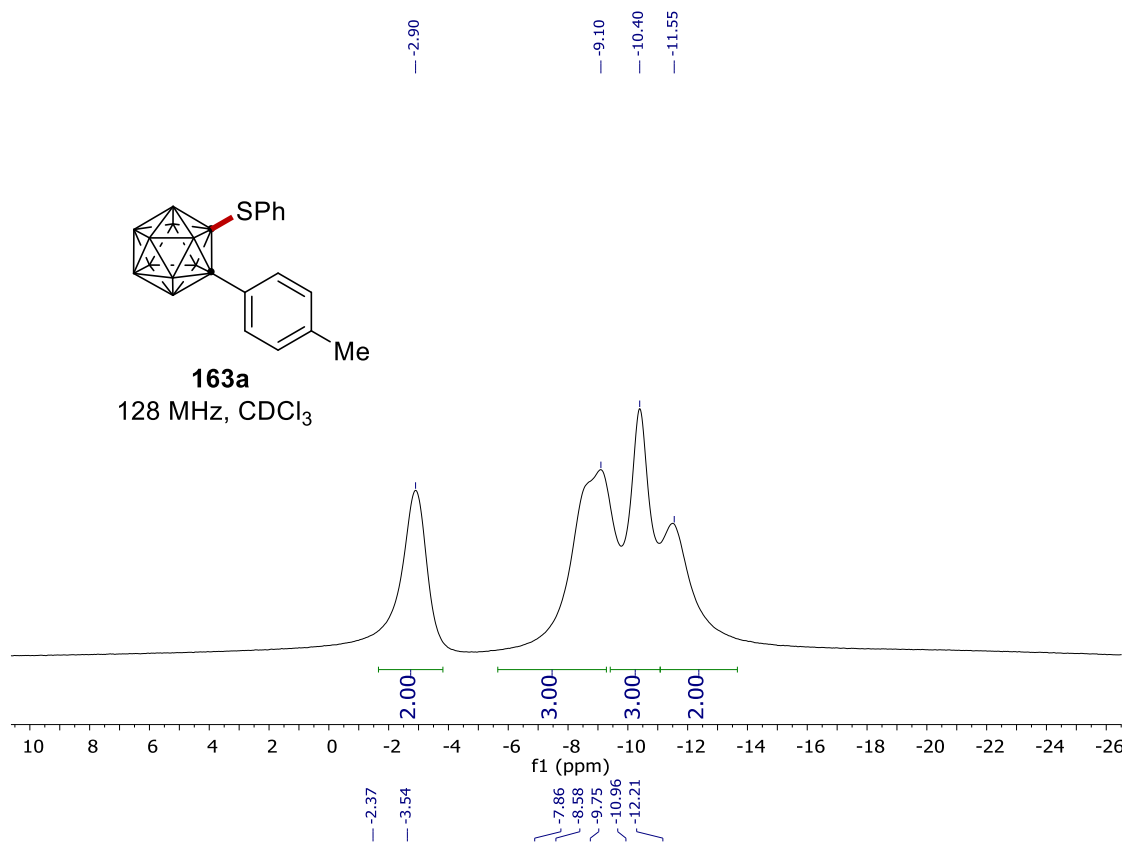
NMR Spectra



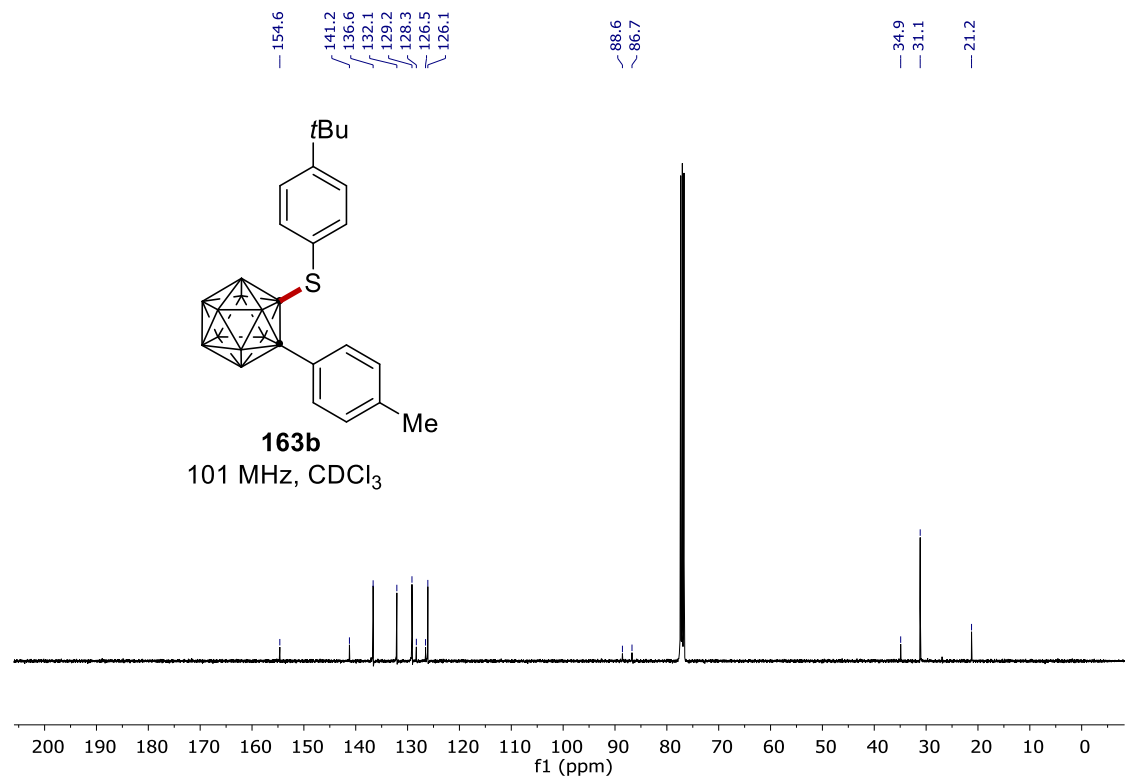
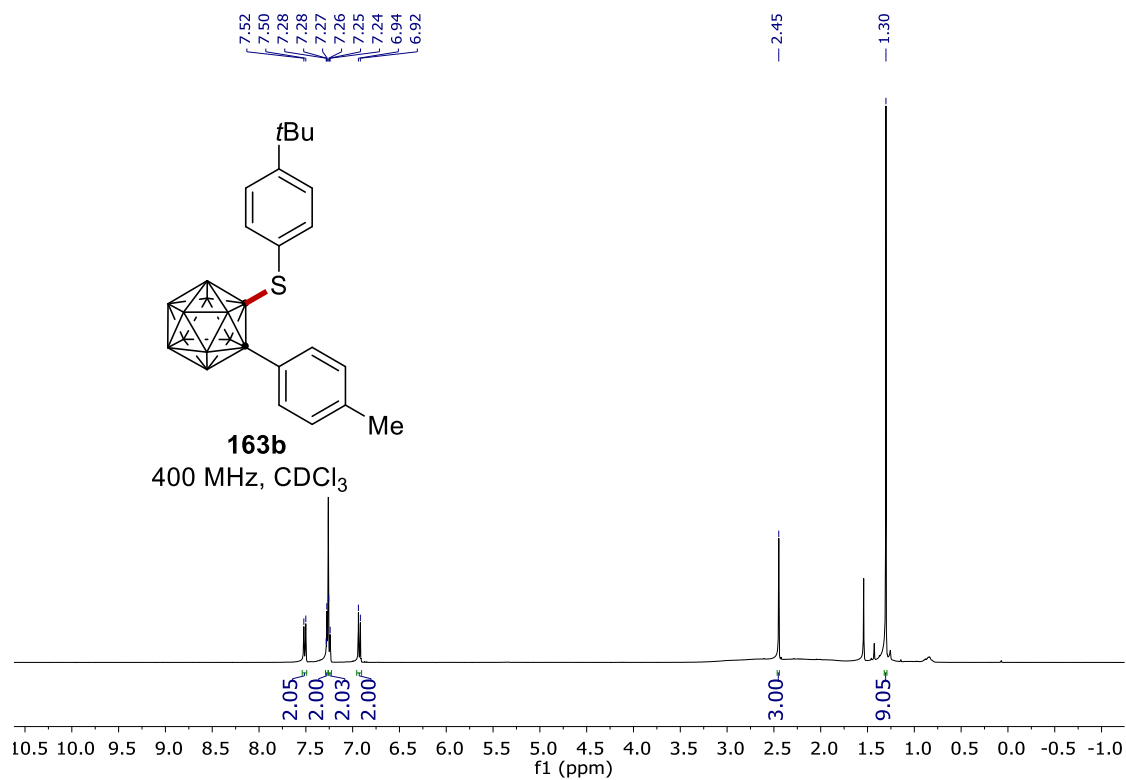
NMR Spectra



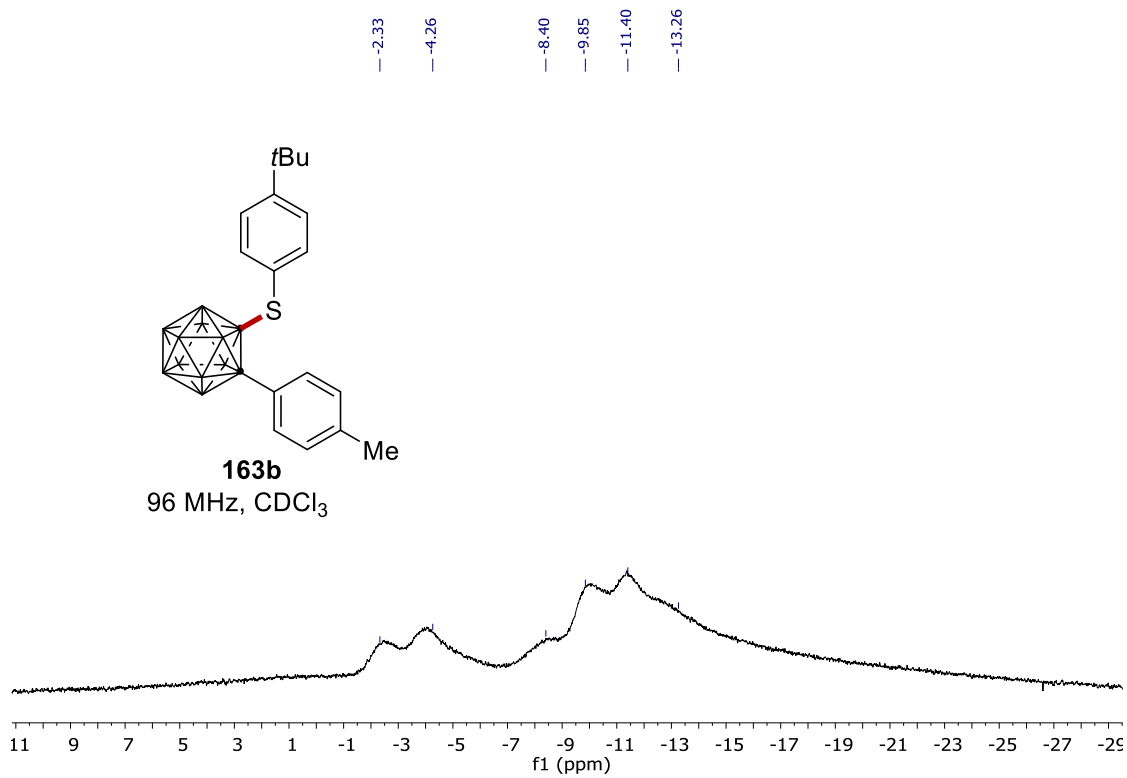
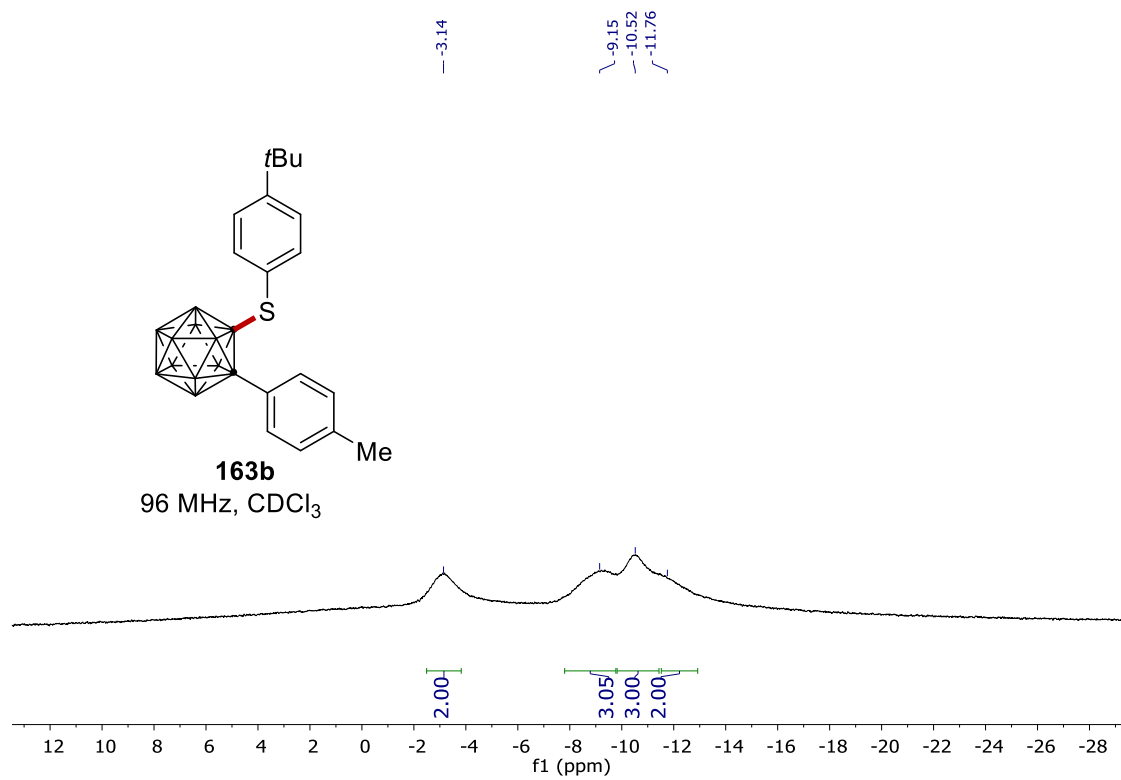
NMR Spectra



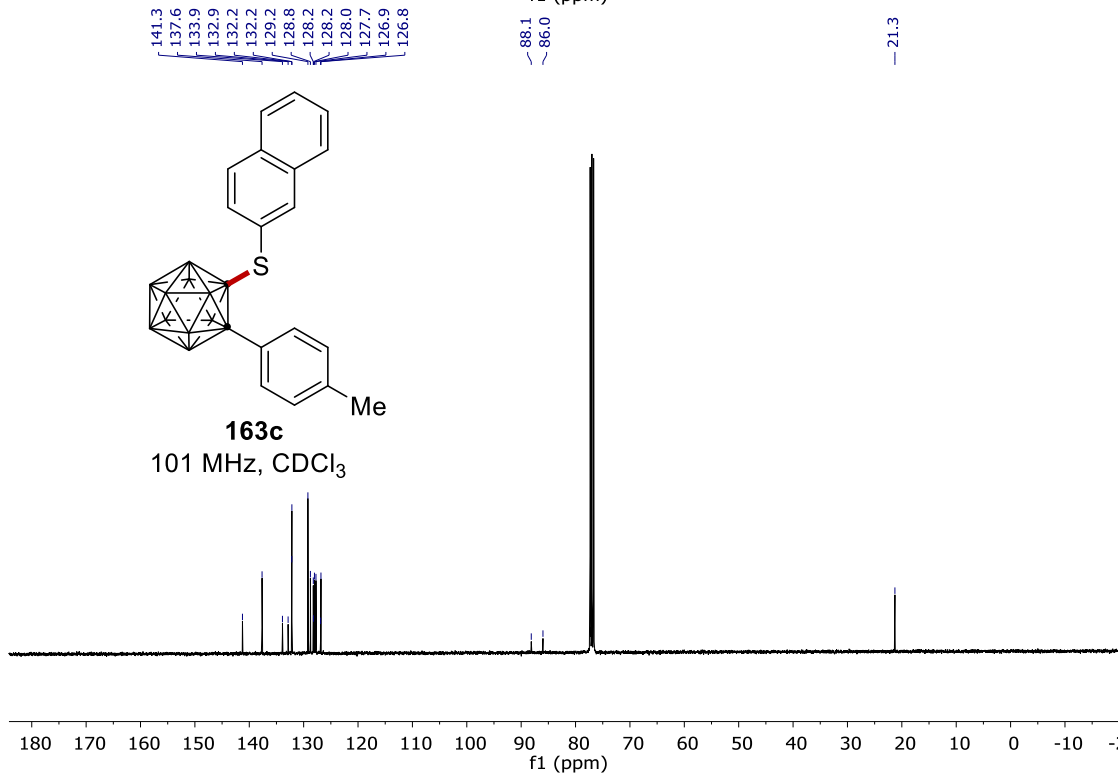
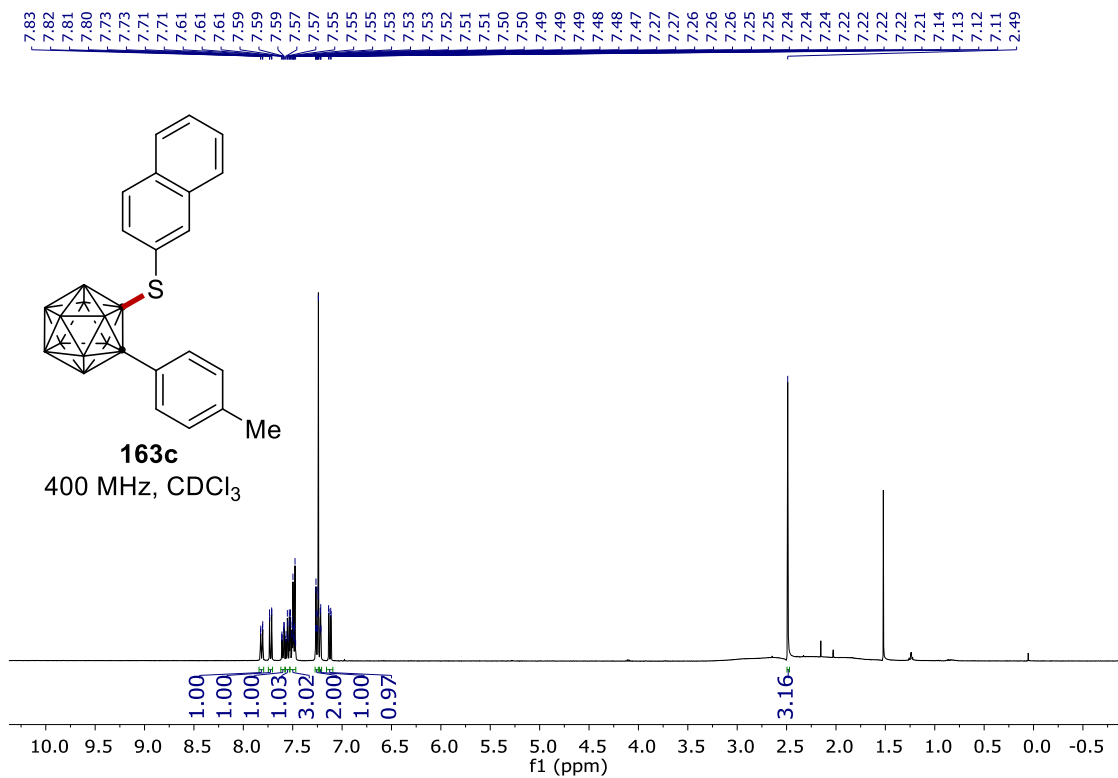
NMR Spectra



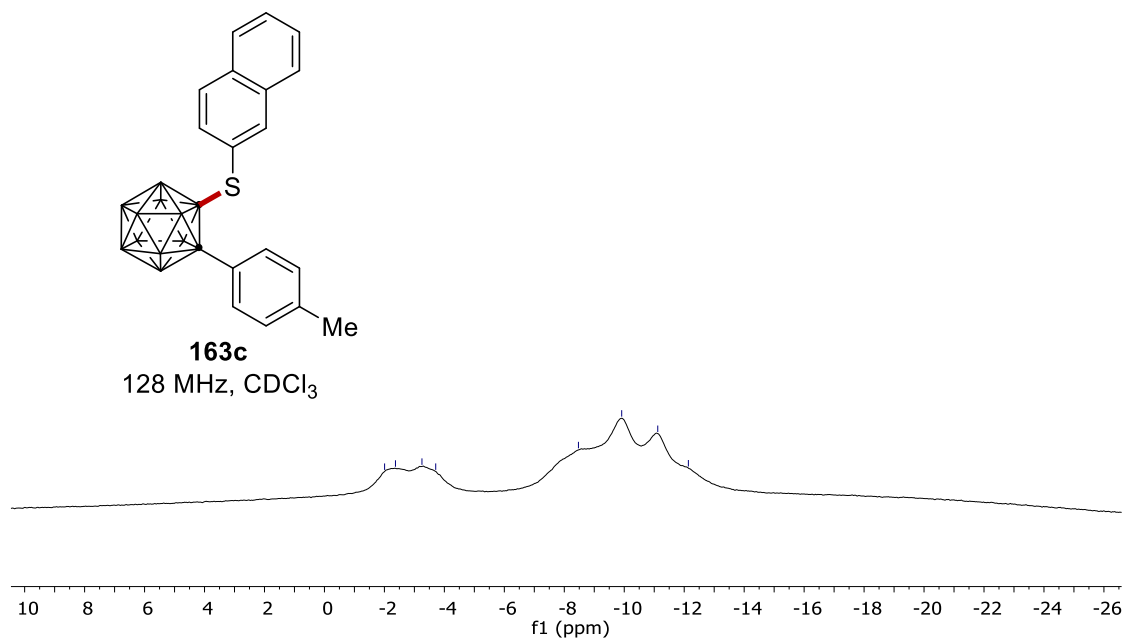
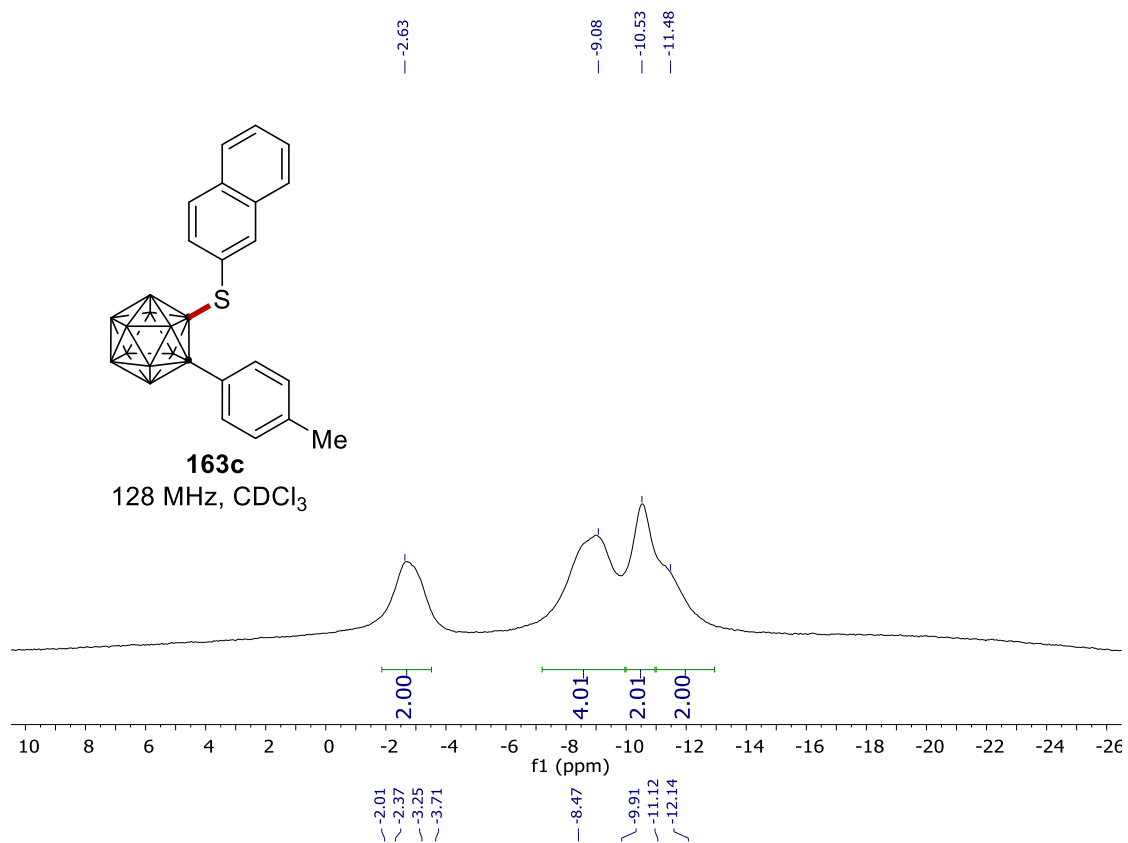
NMR Spectra



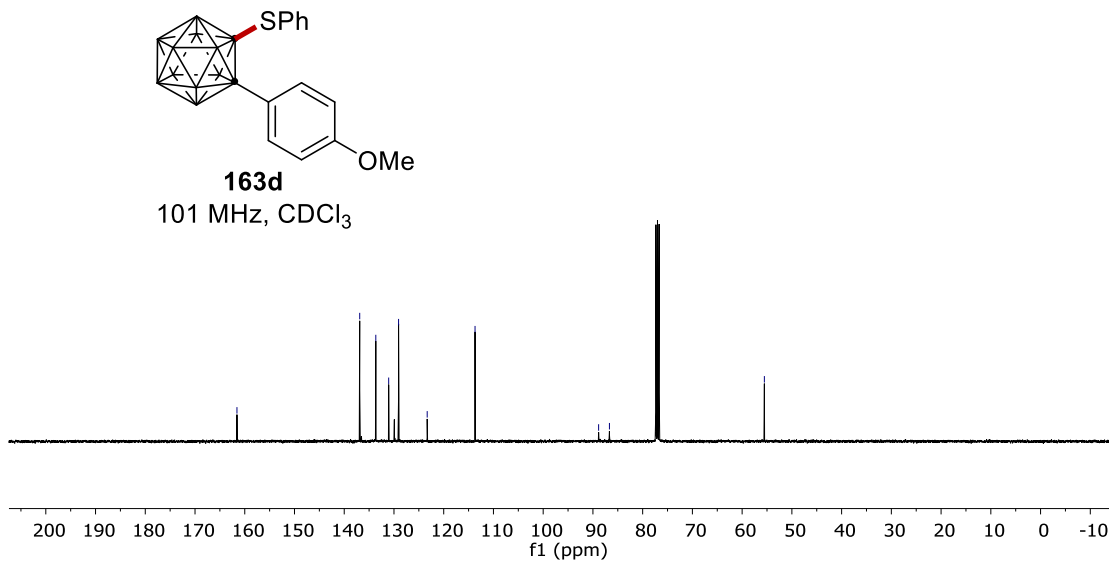
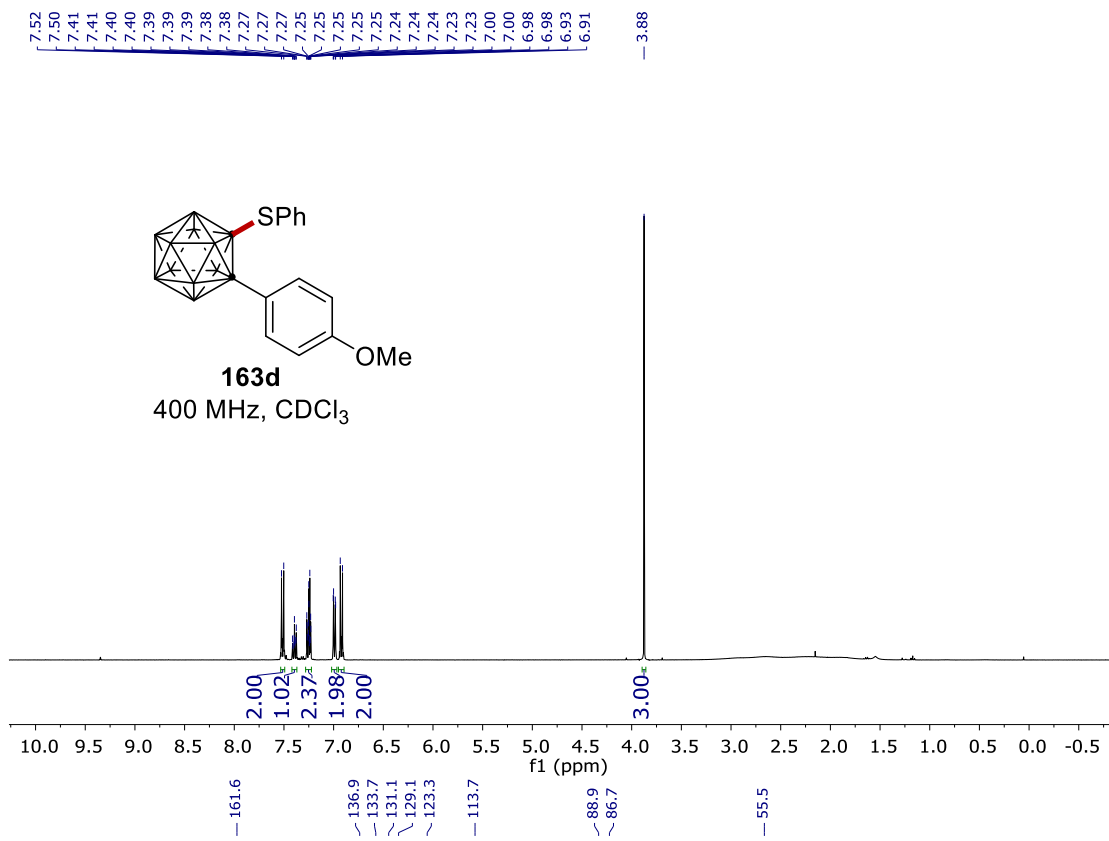
NMR Spectra



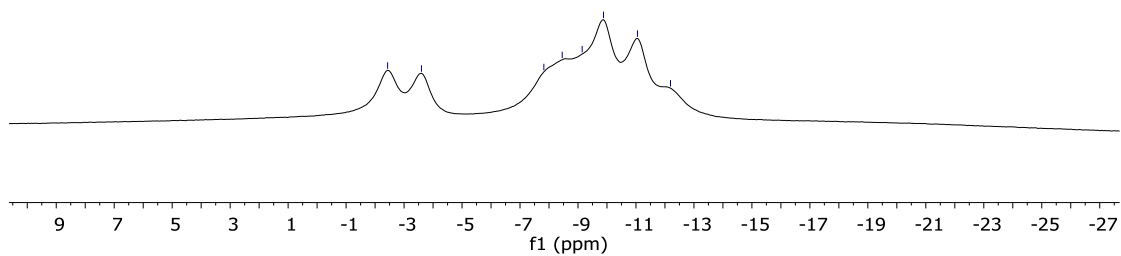
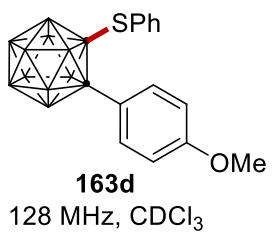
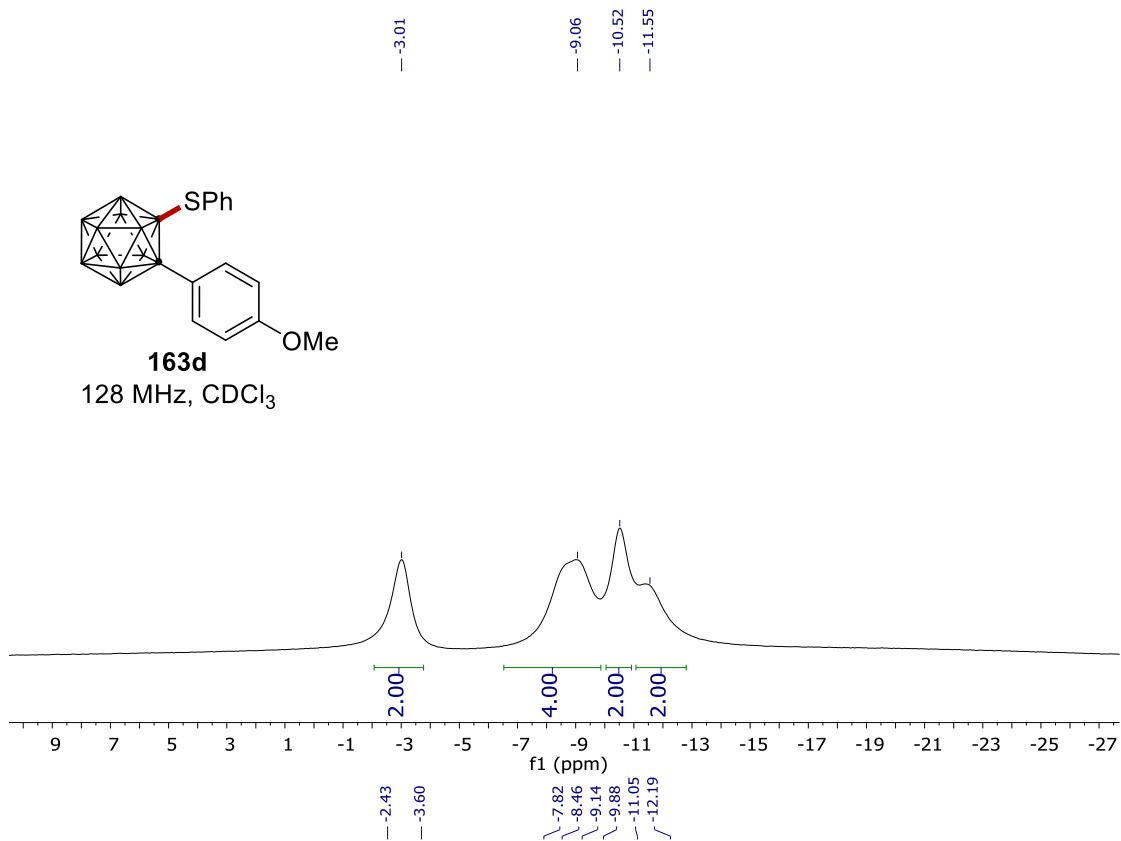
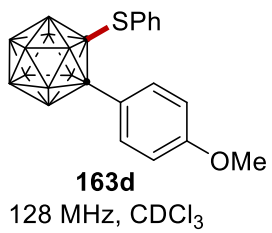
NMR Spectra



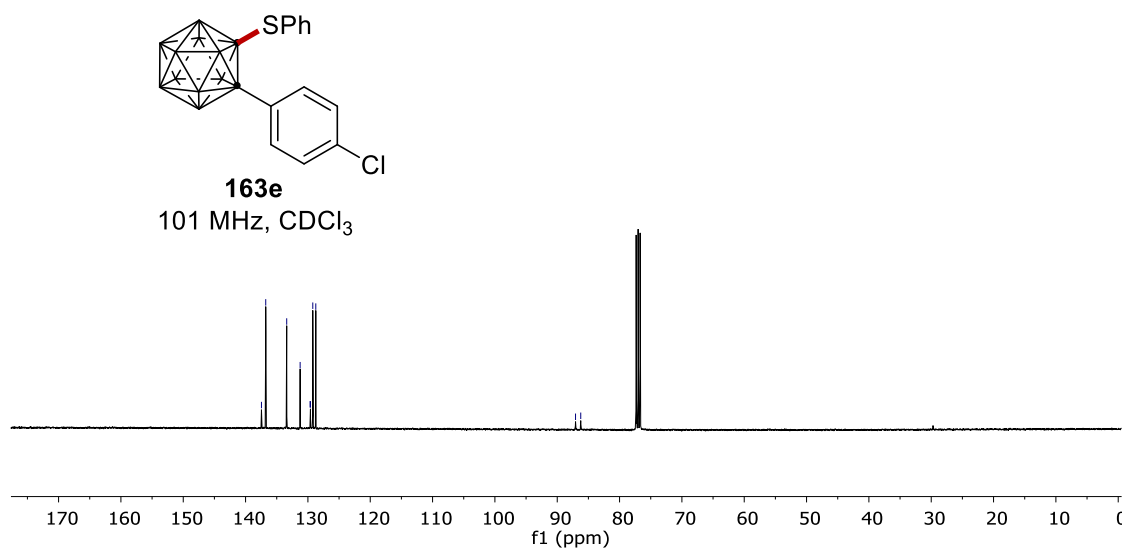
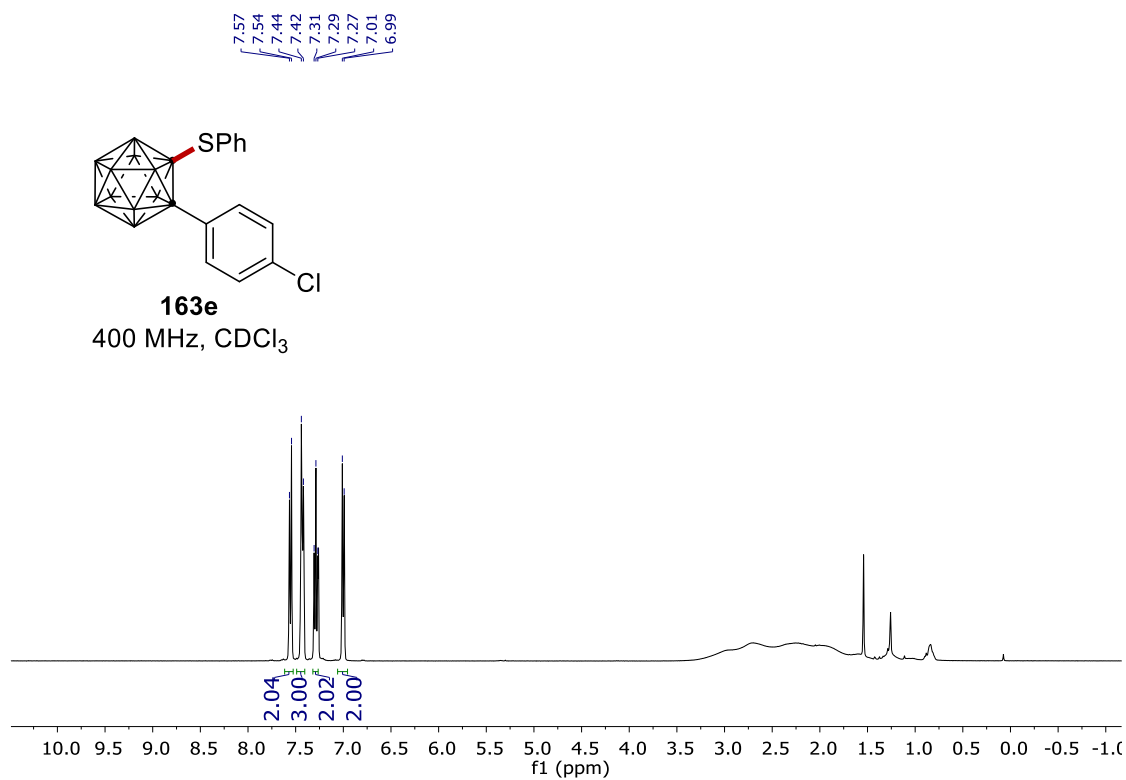
NMR Spectra



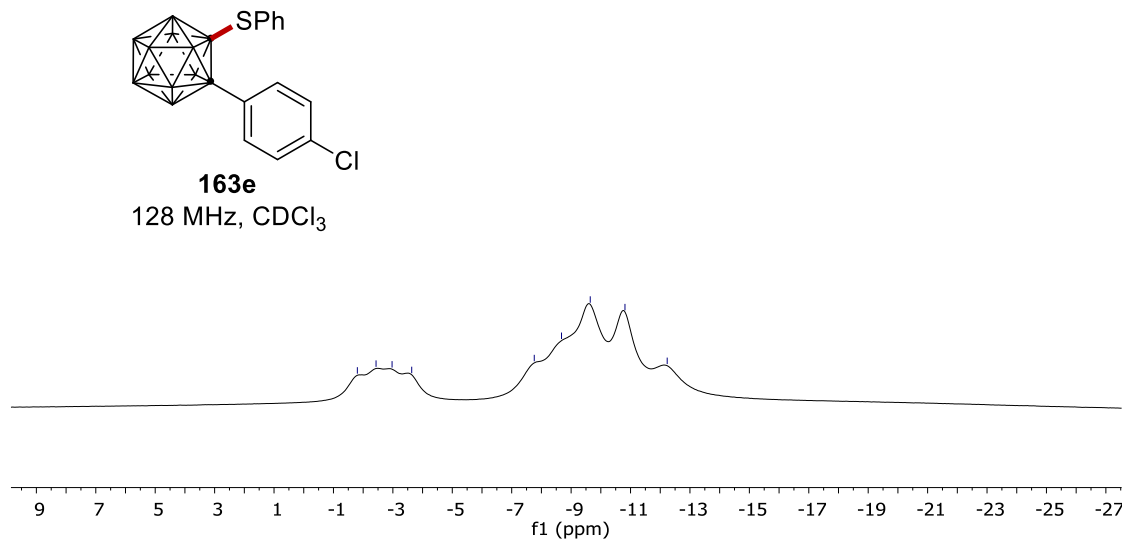
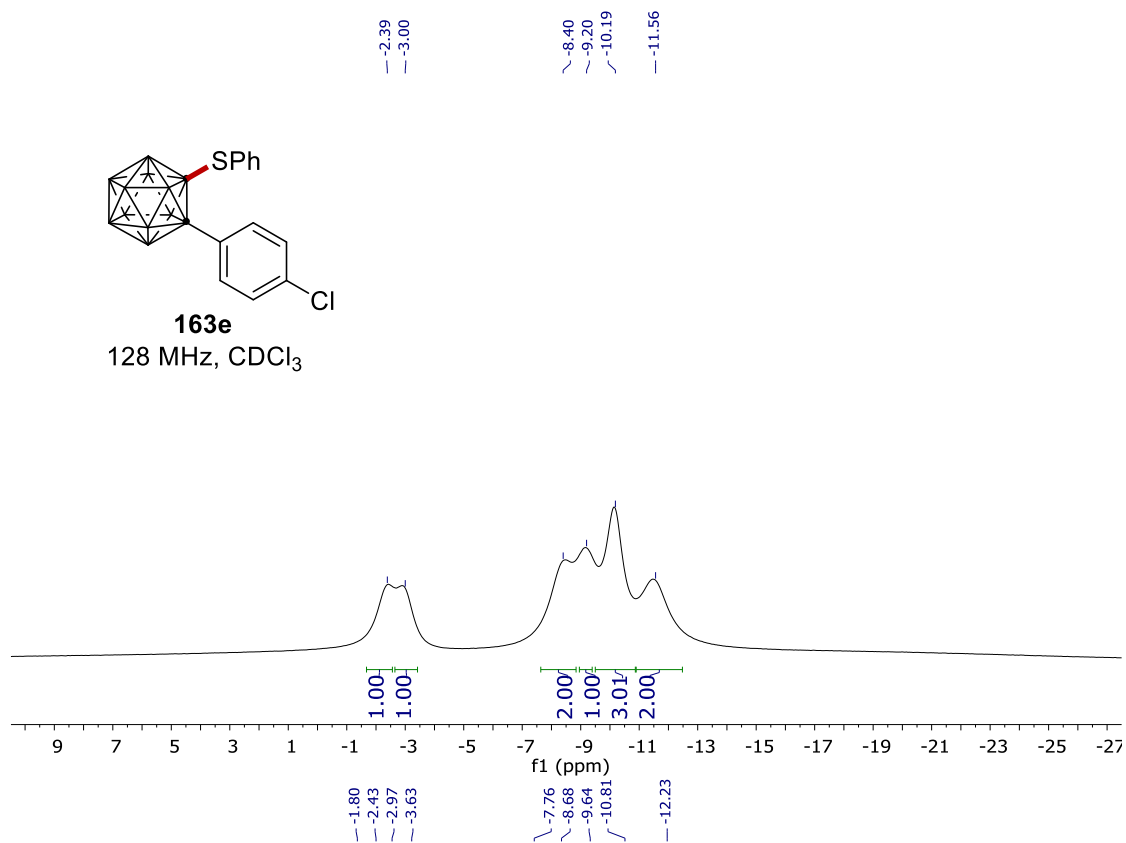
NMR Spectra



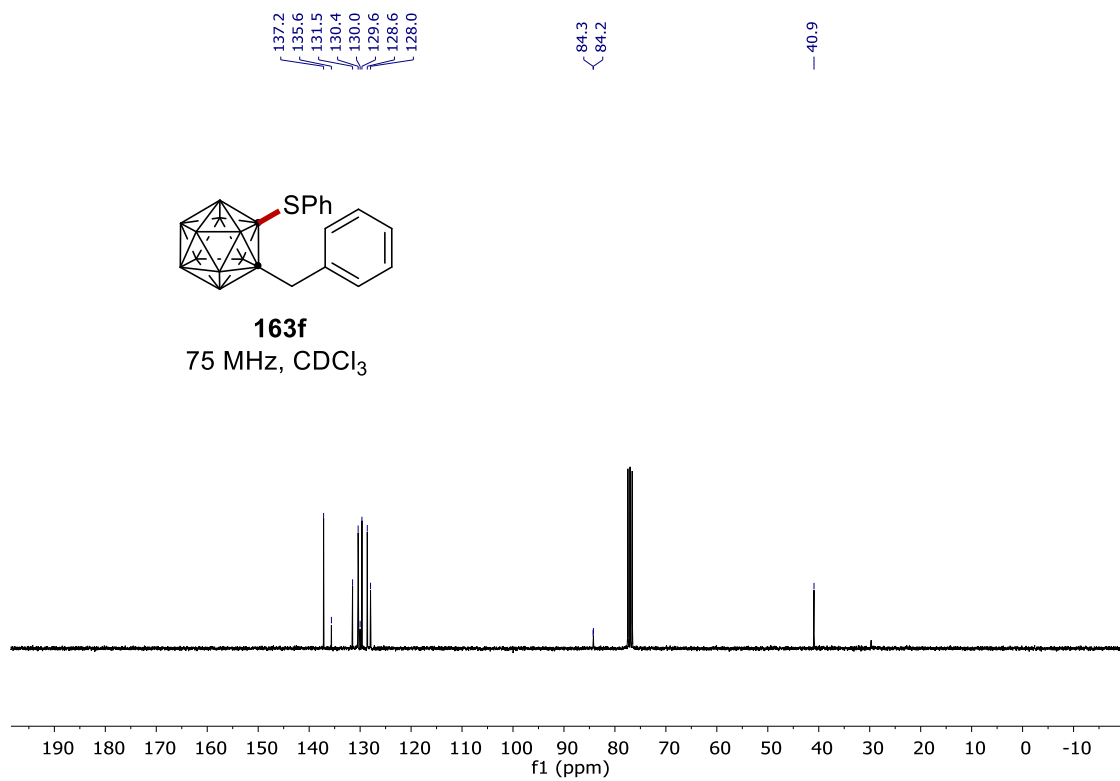
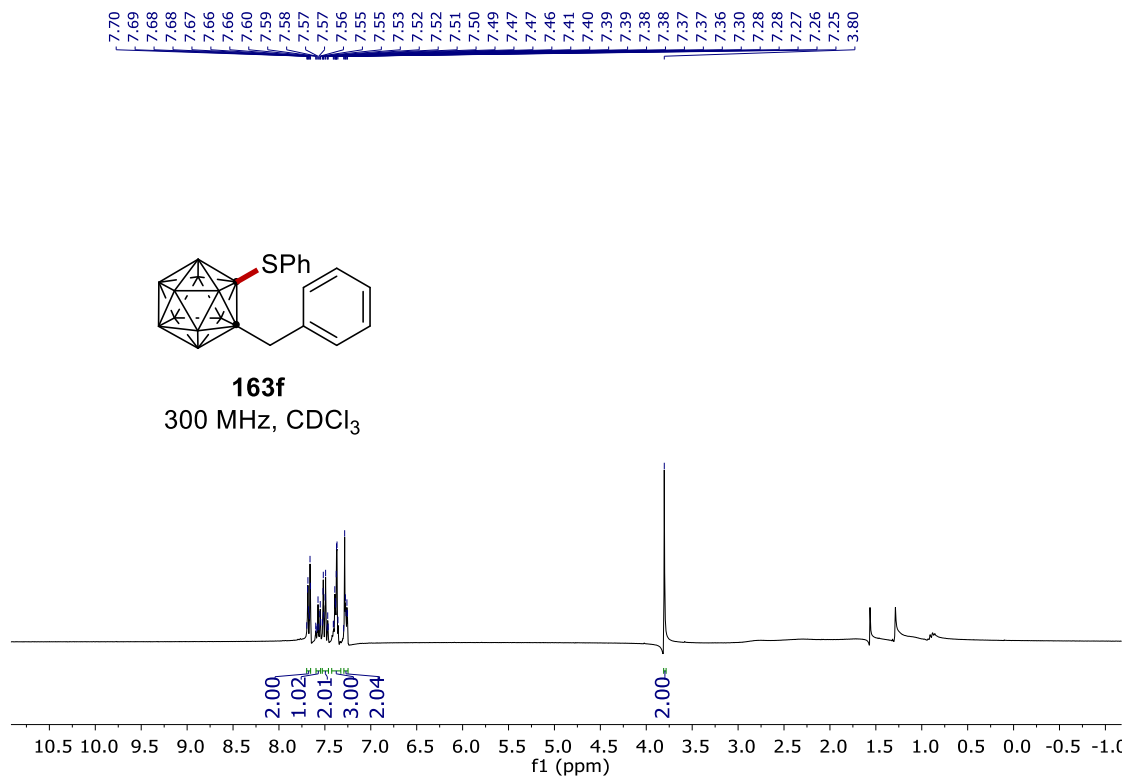
NMR Spectra



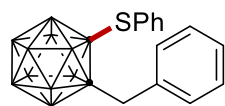
NMR Spectra



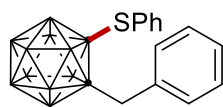
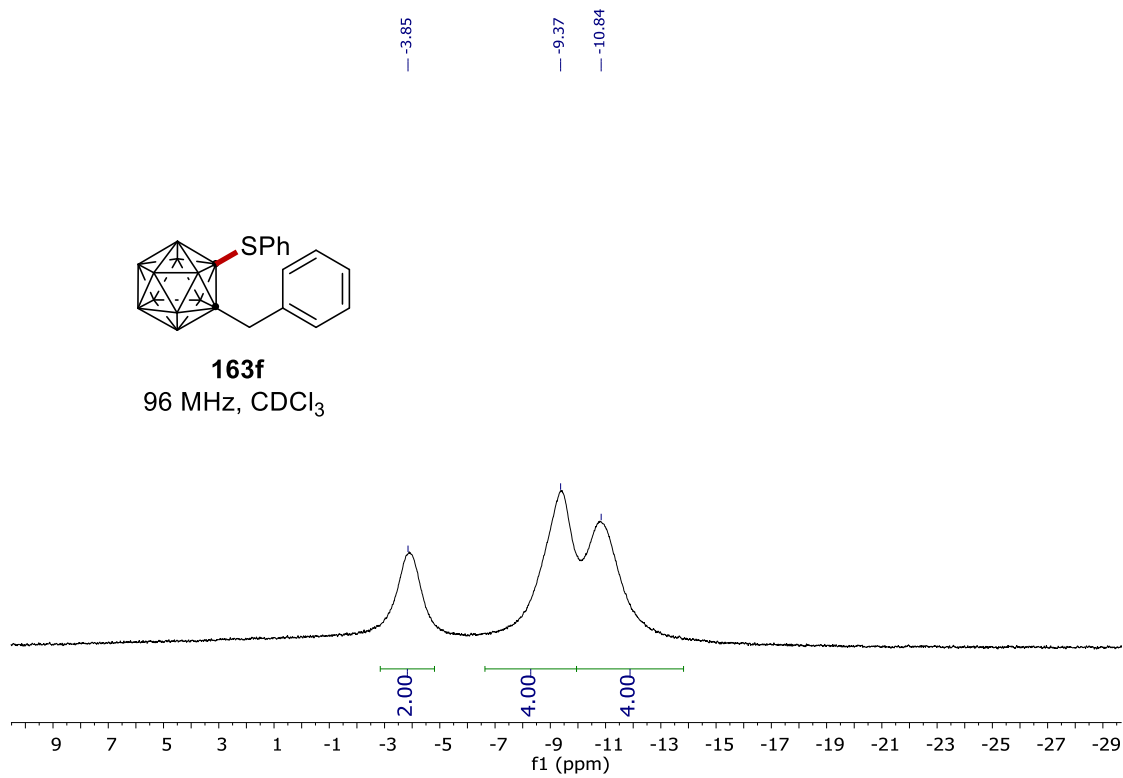
NMR Spectra



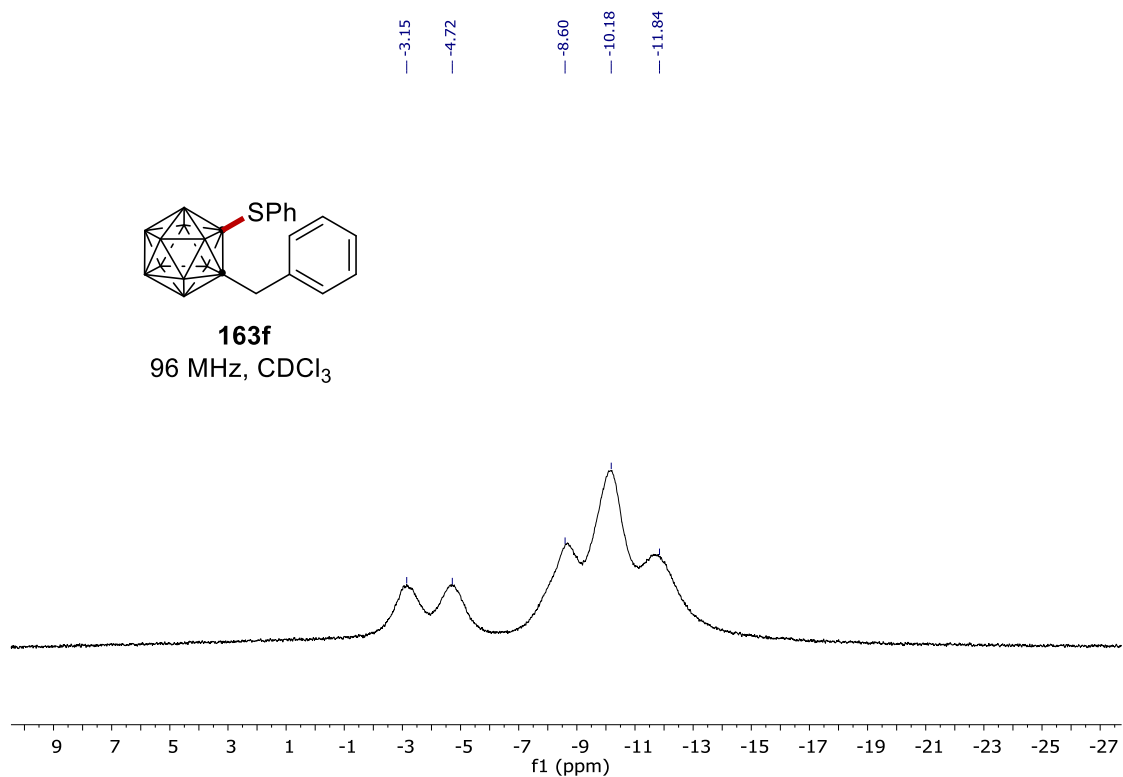
NMR Spectra



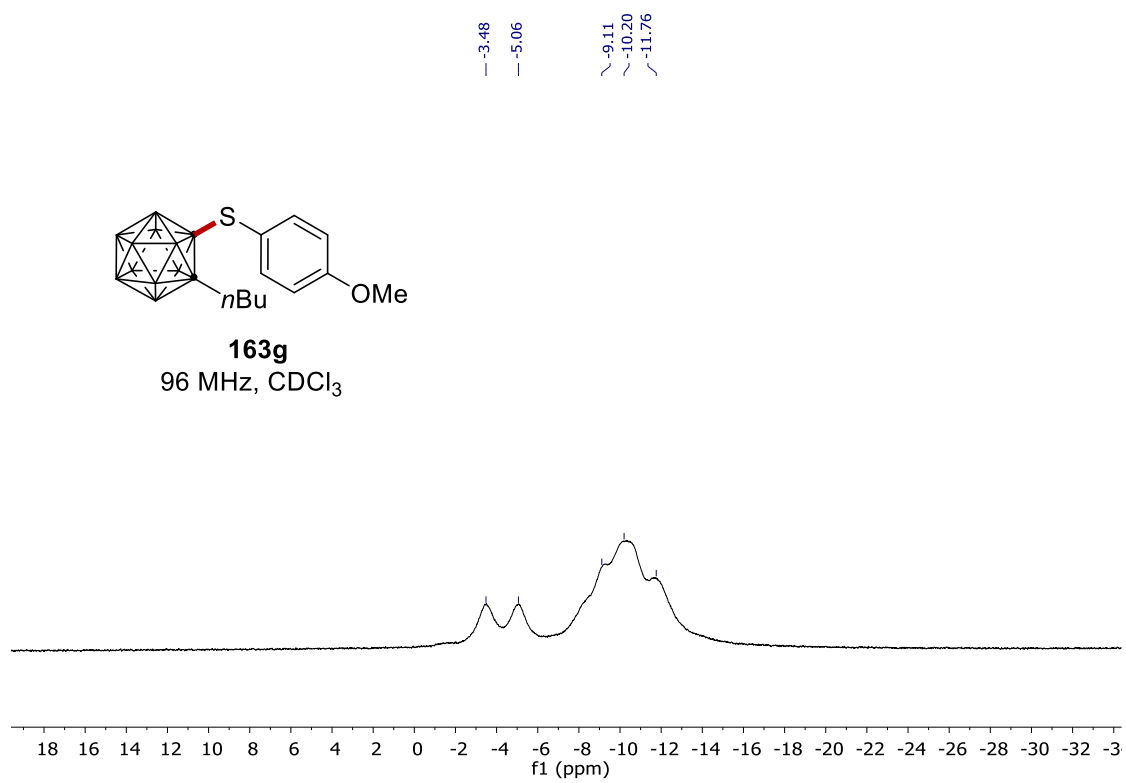
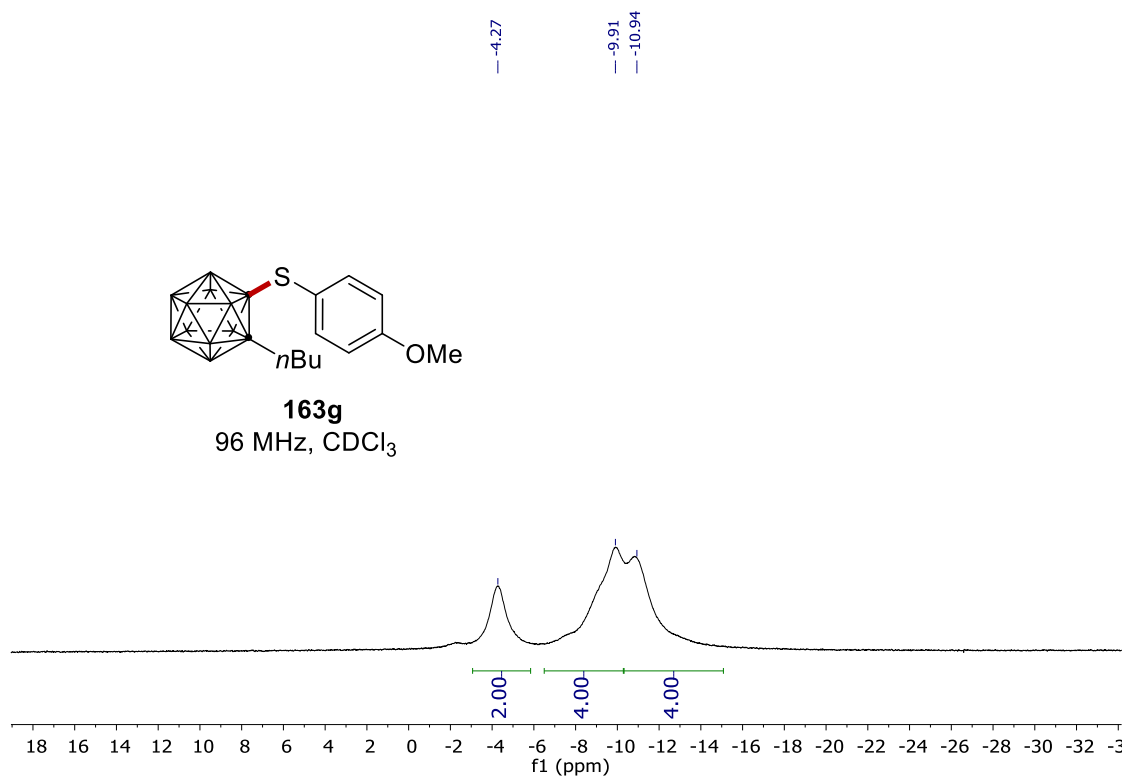
163f
96 MHz, CDCl₃



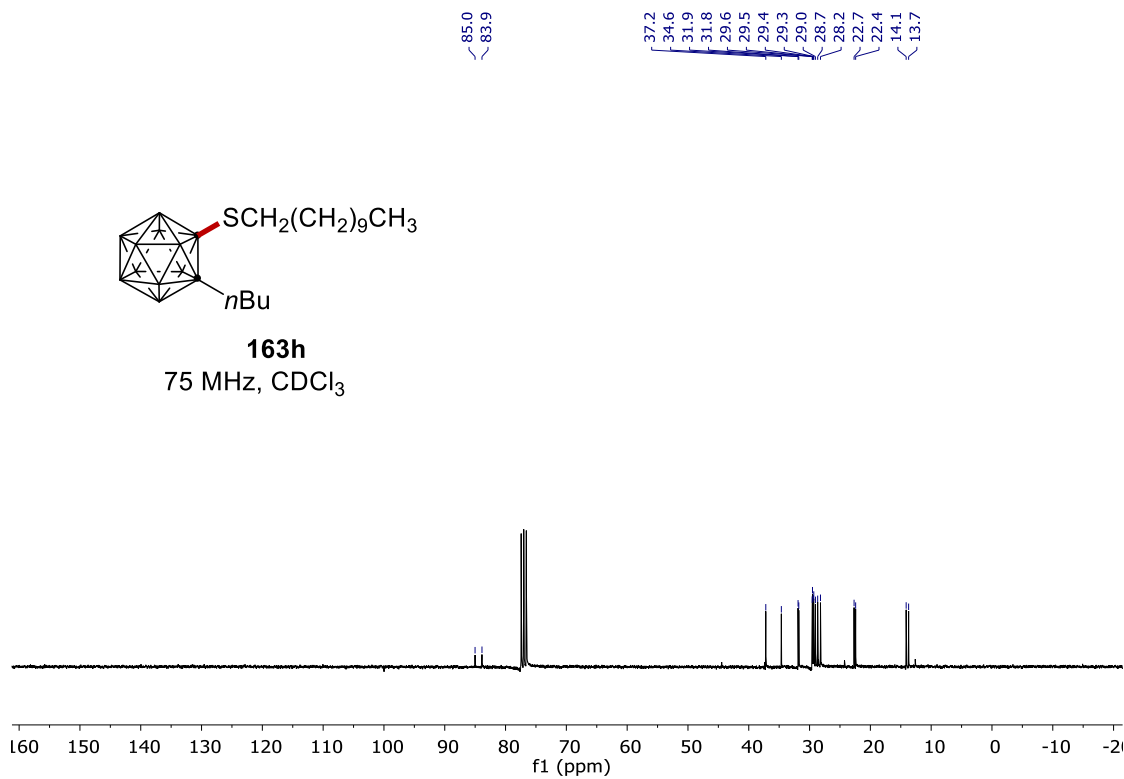
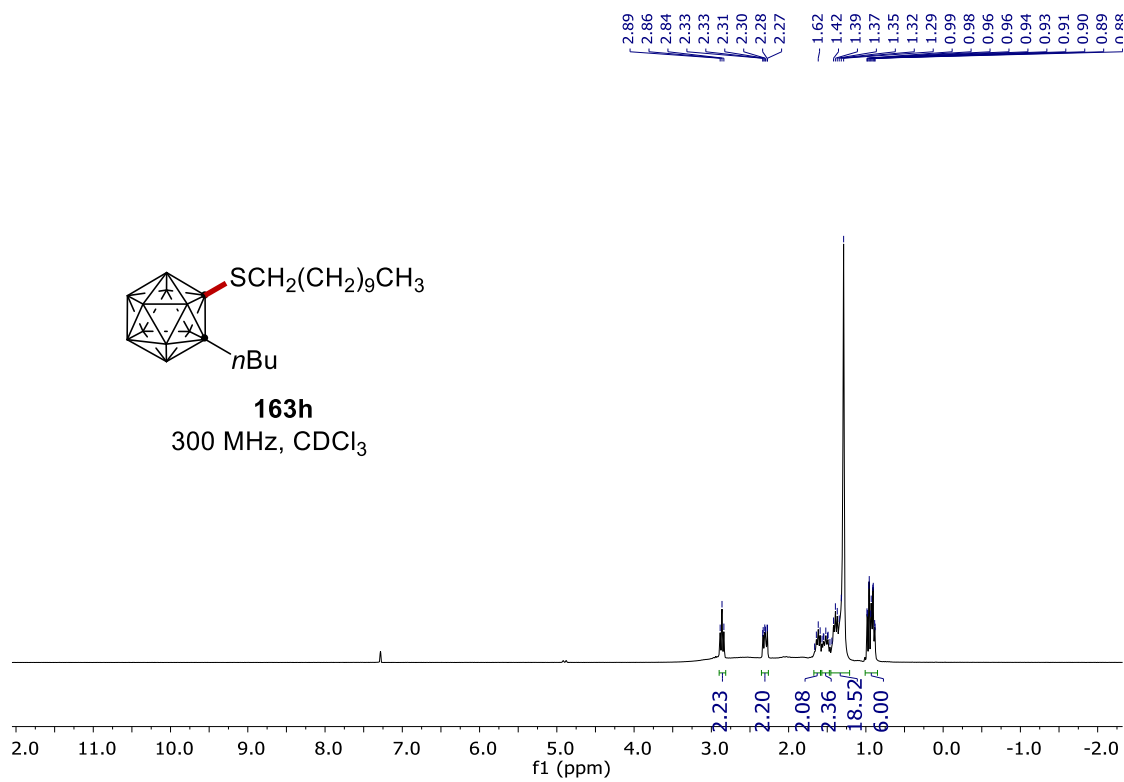
163f
96 MHz, CDCl₃



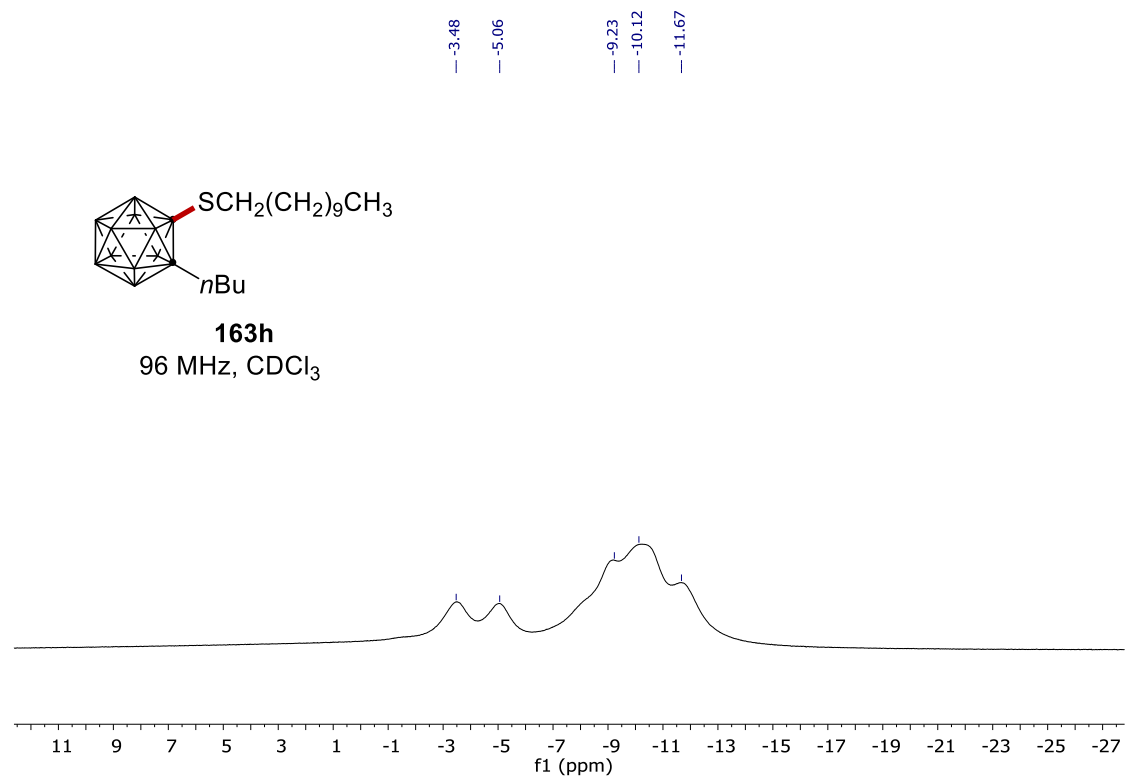
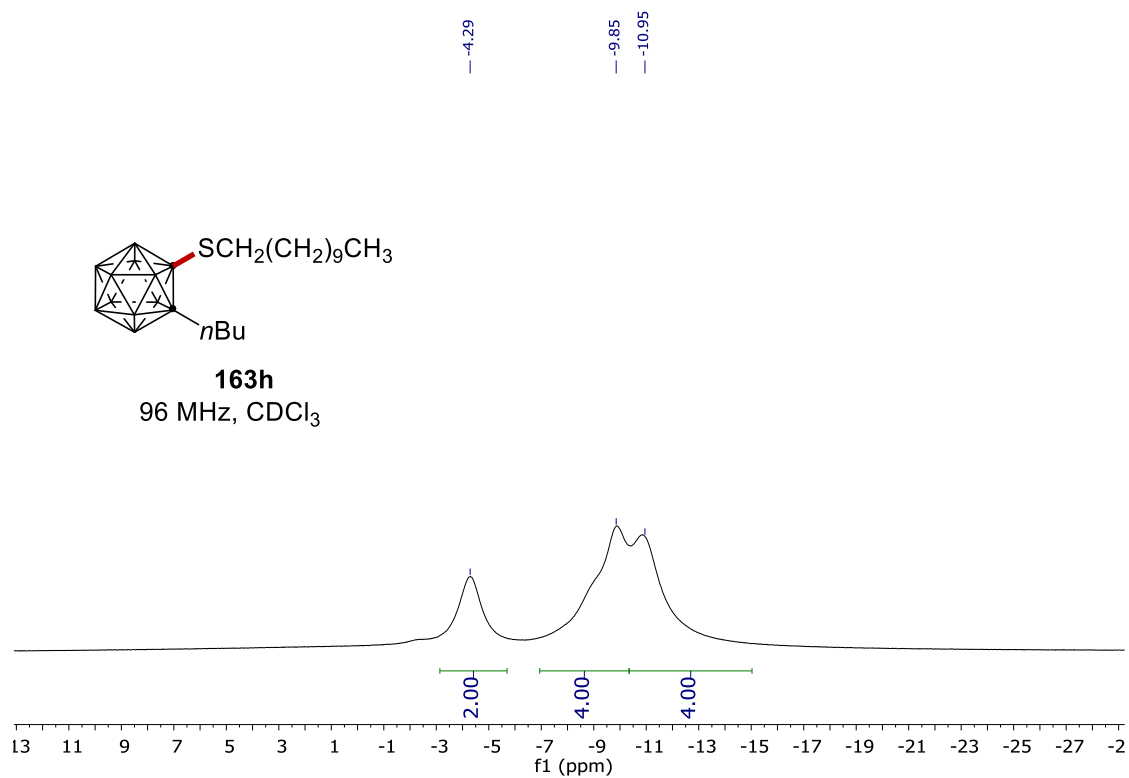
NMR Spectra



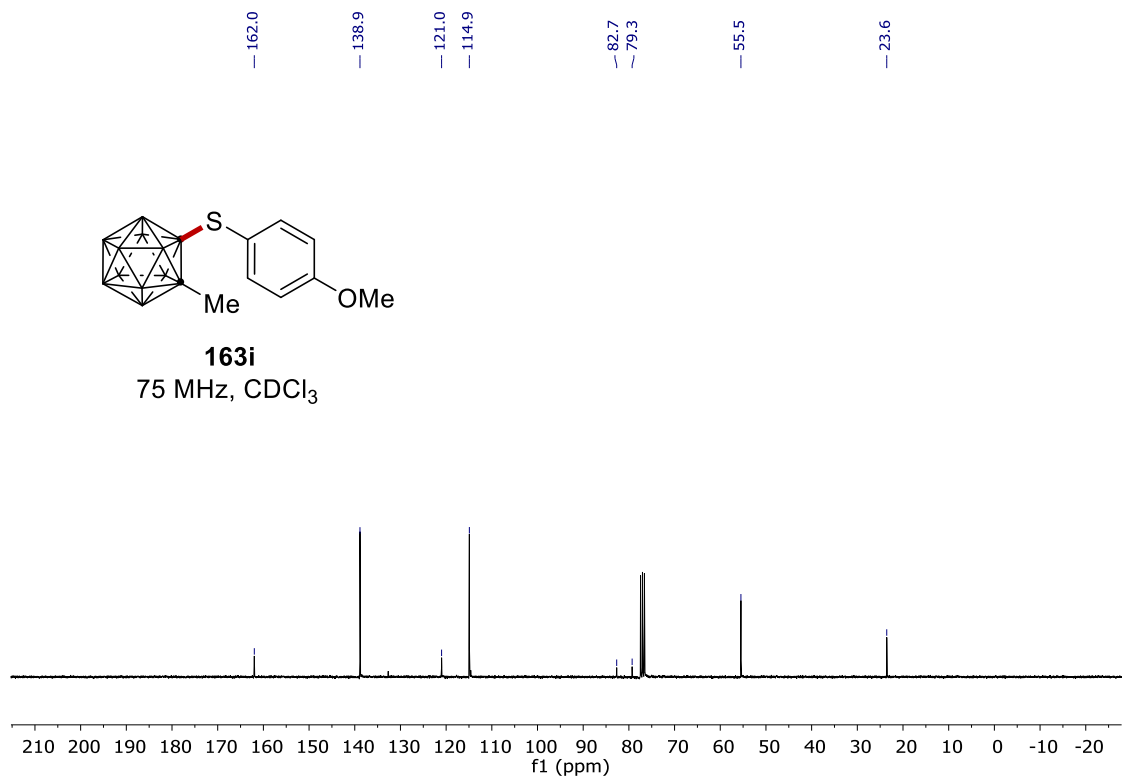
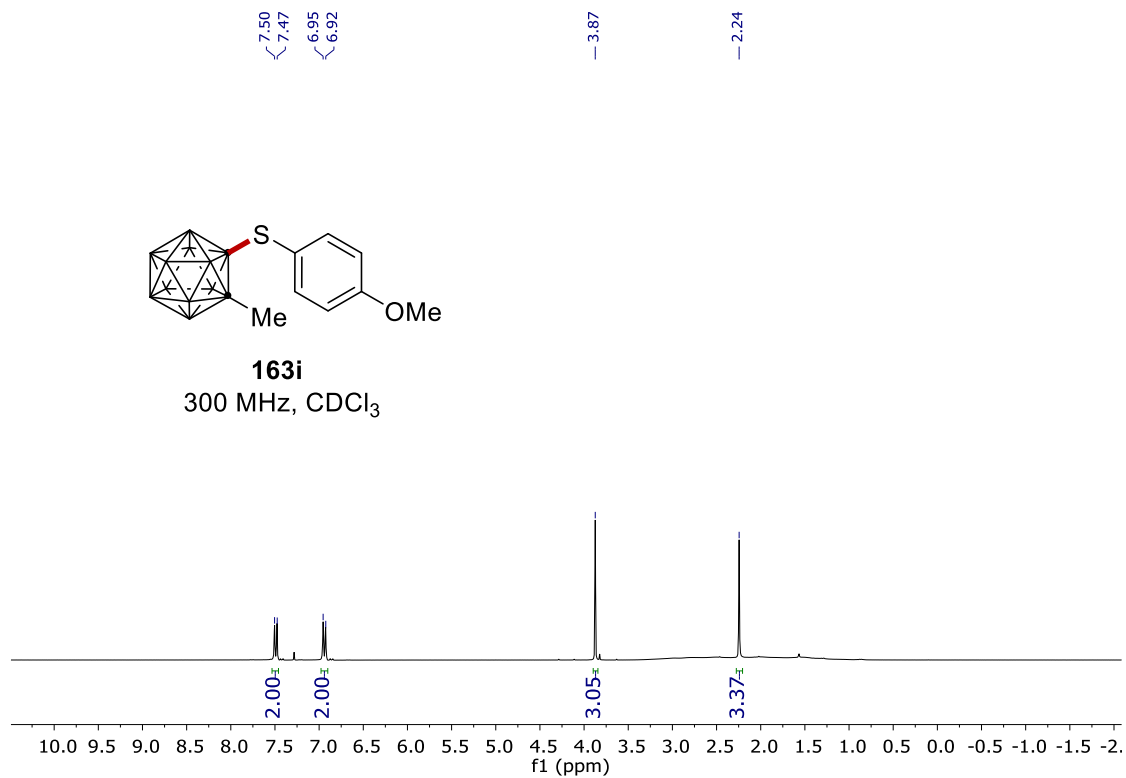
NMR Spectra



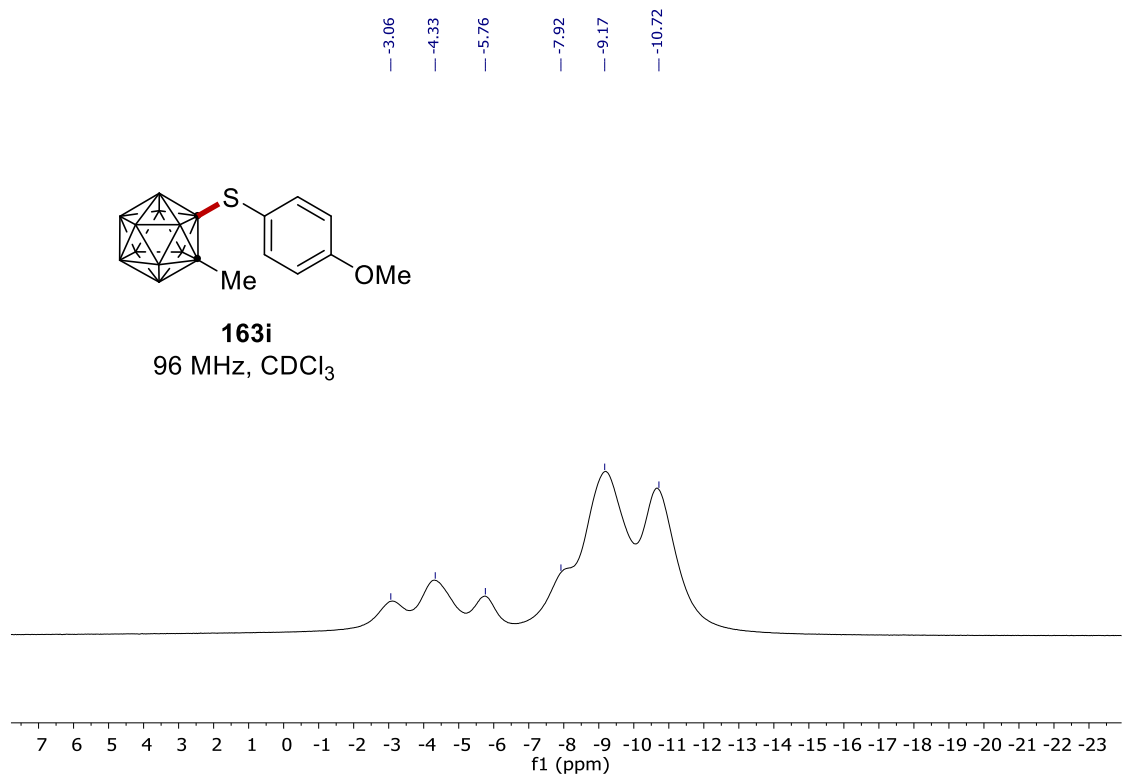
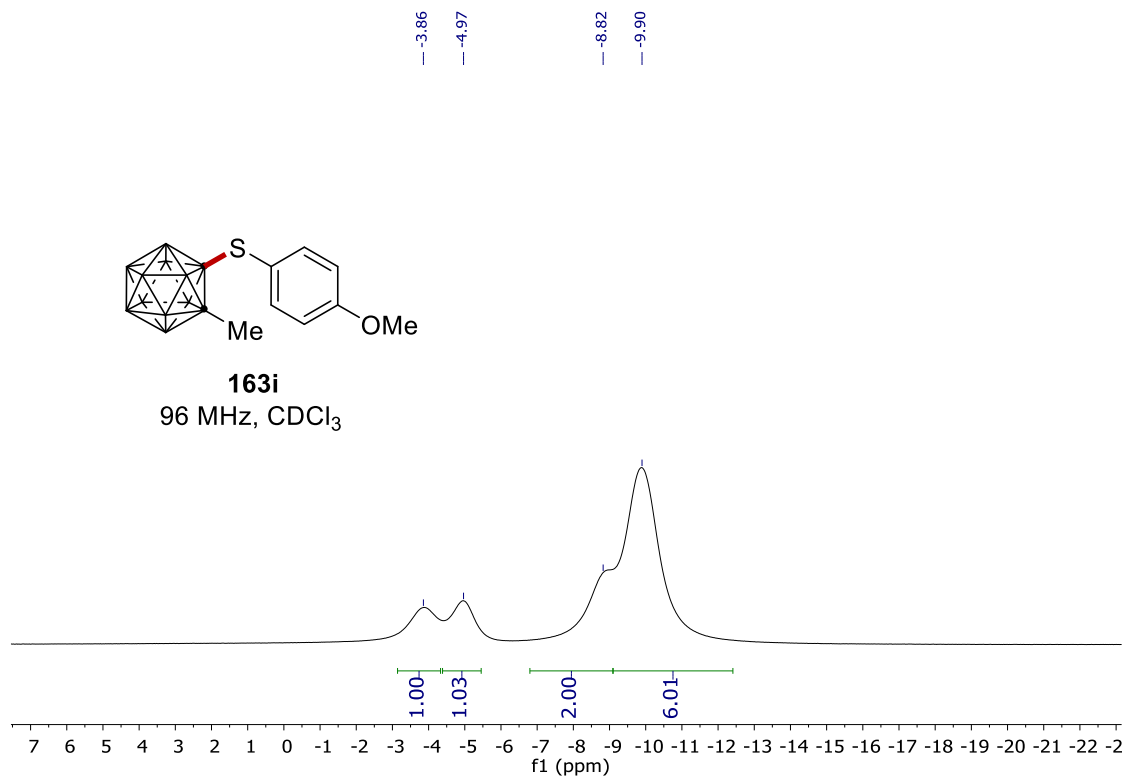
NMR Spectra



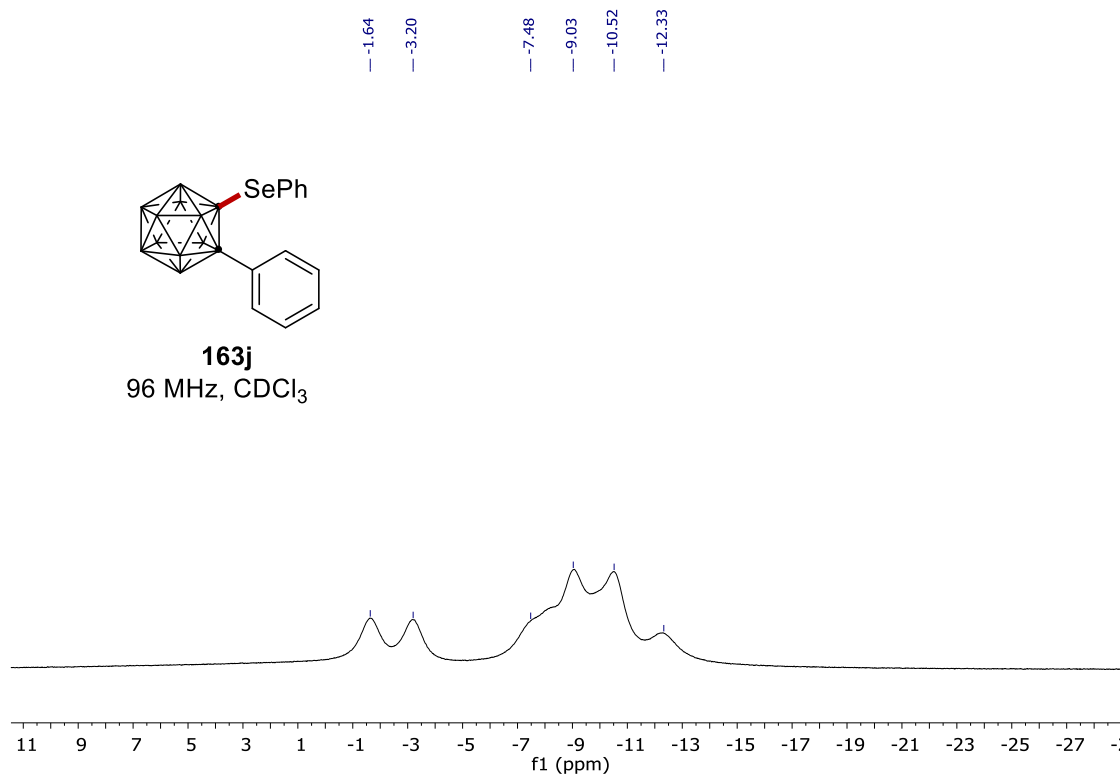
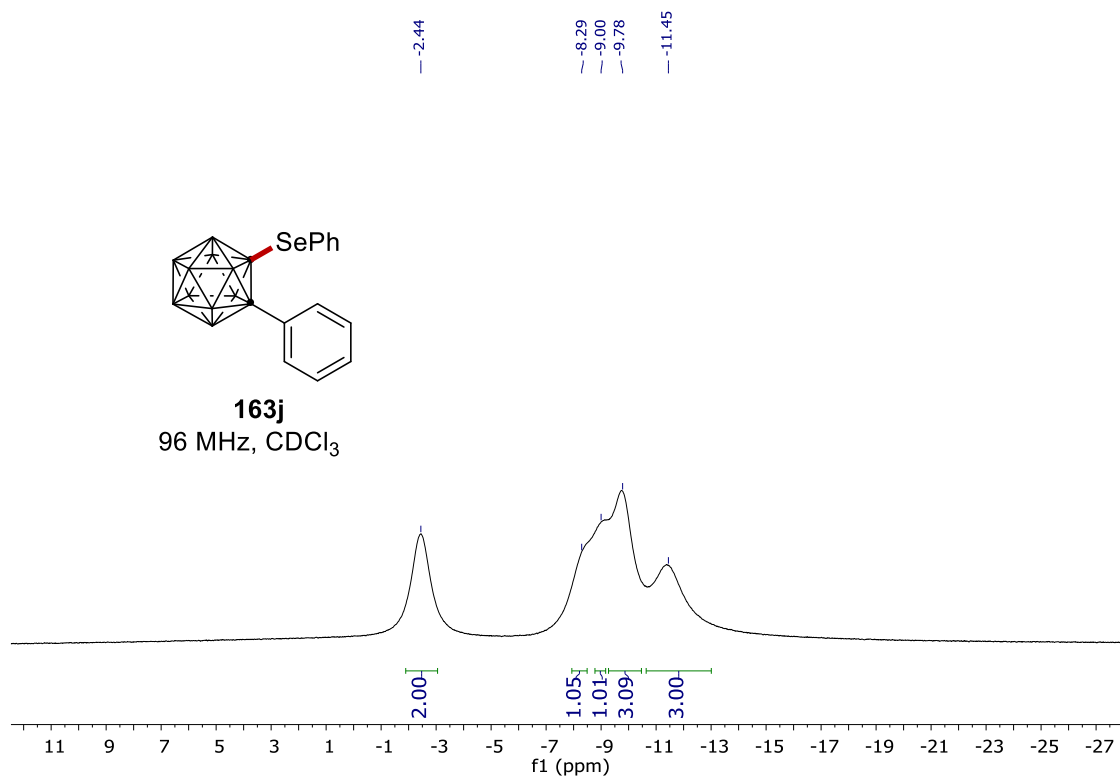
NMR Spectra



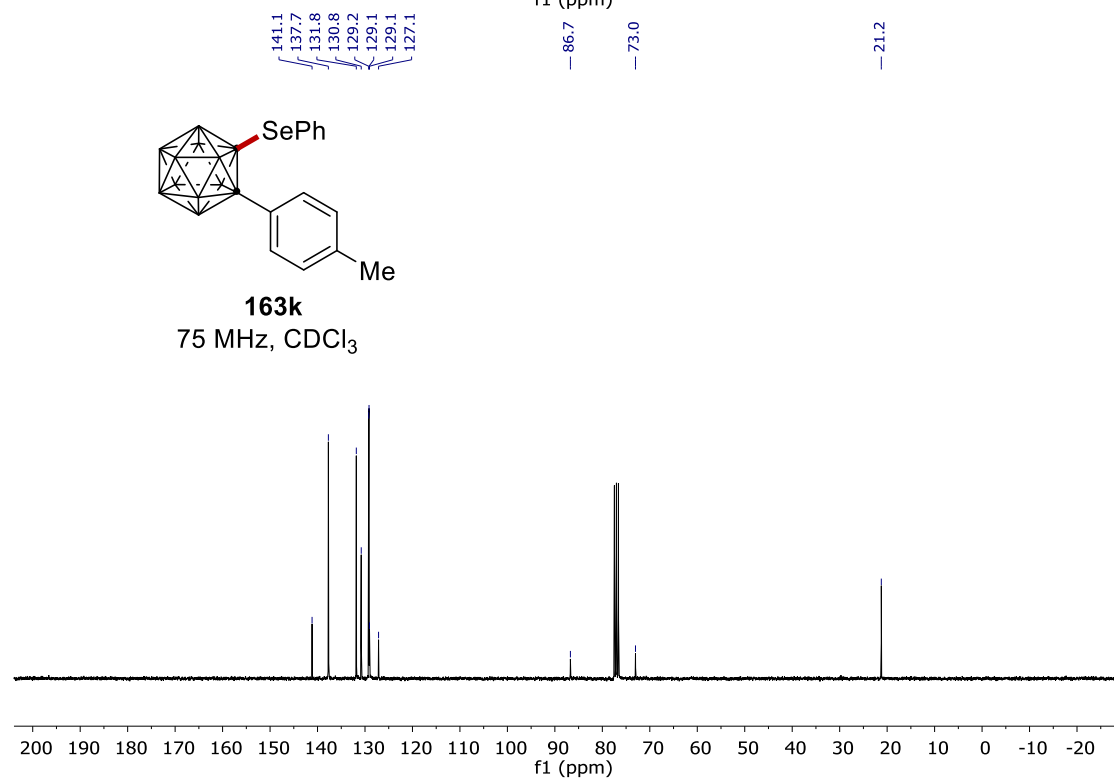
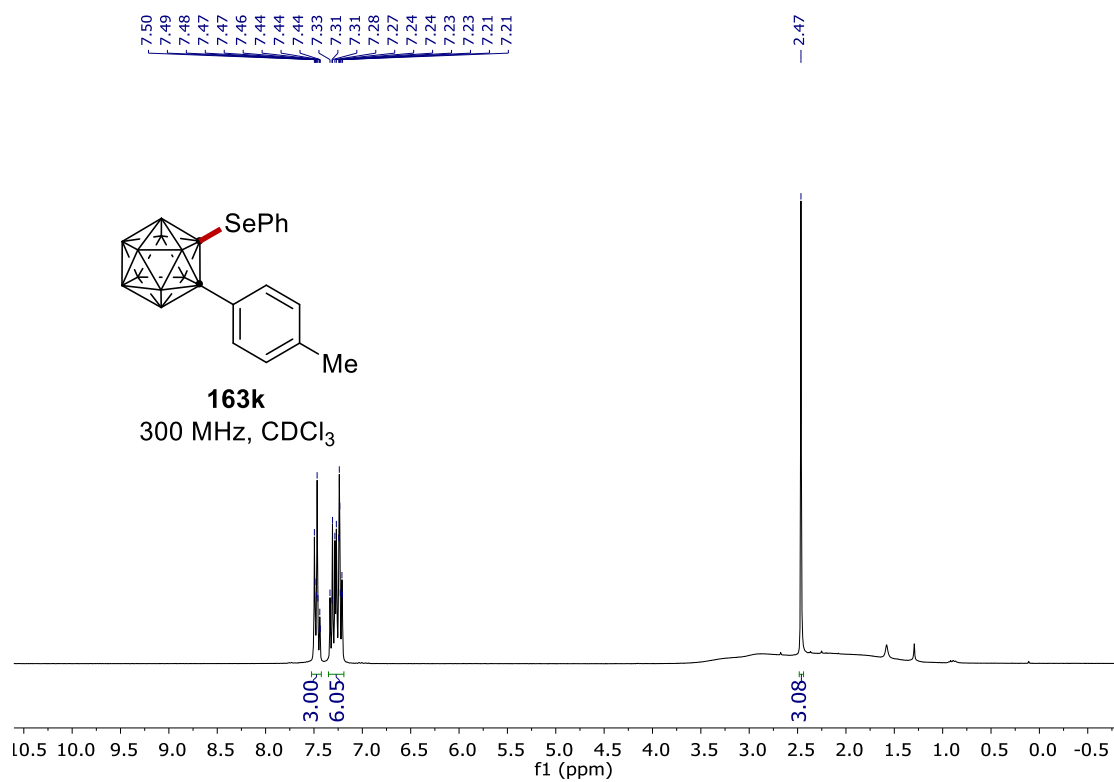
NMR Spectra



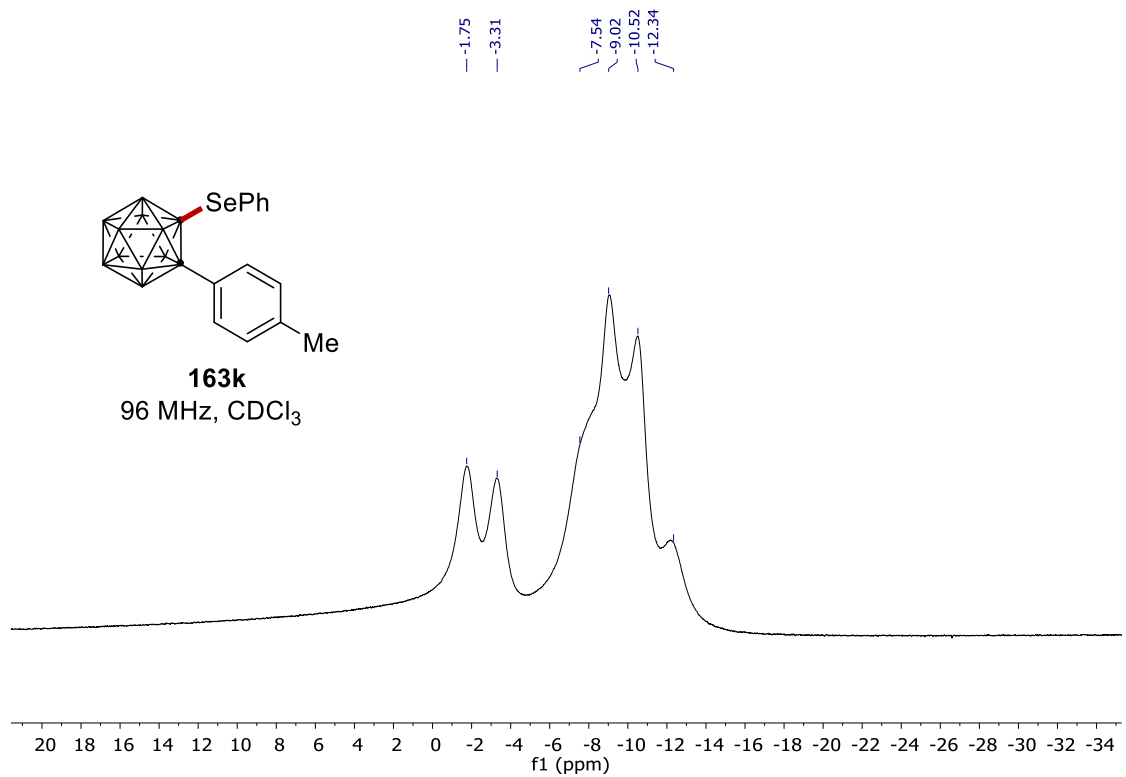
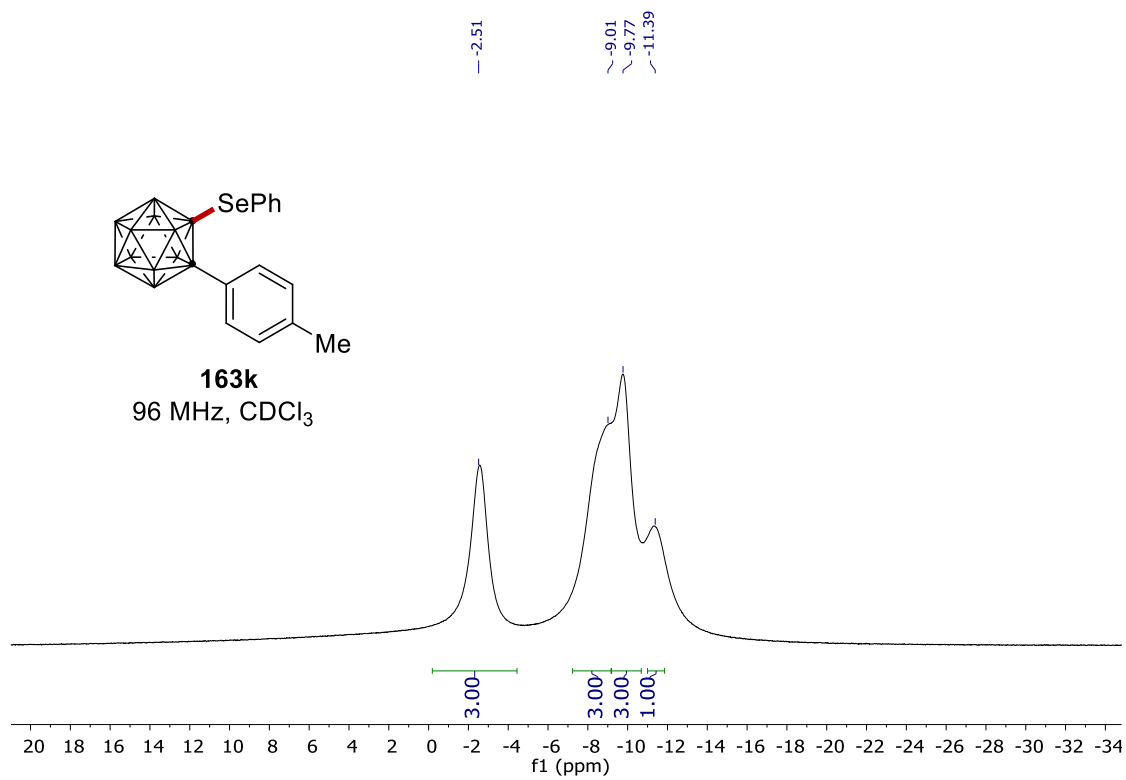
NMR Spectra



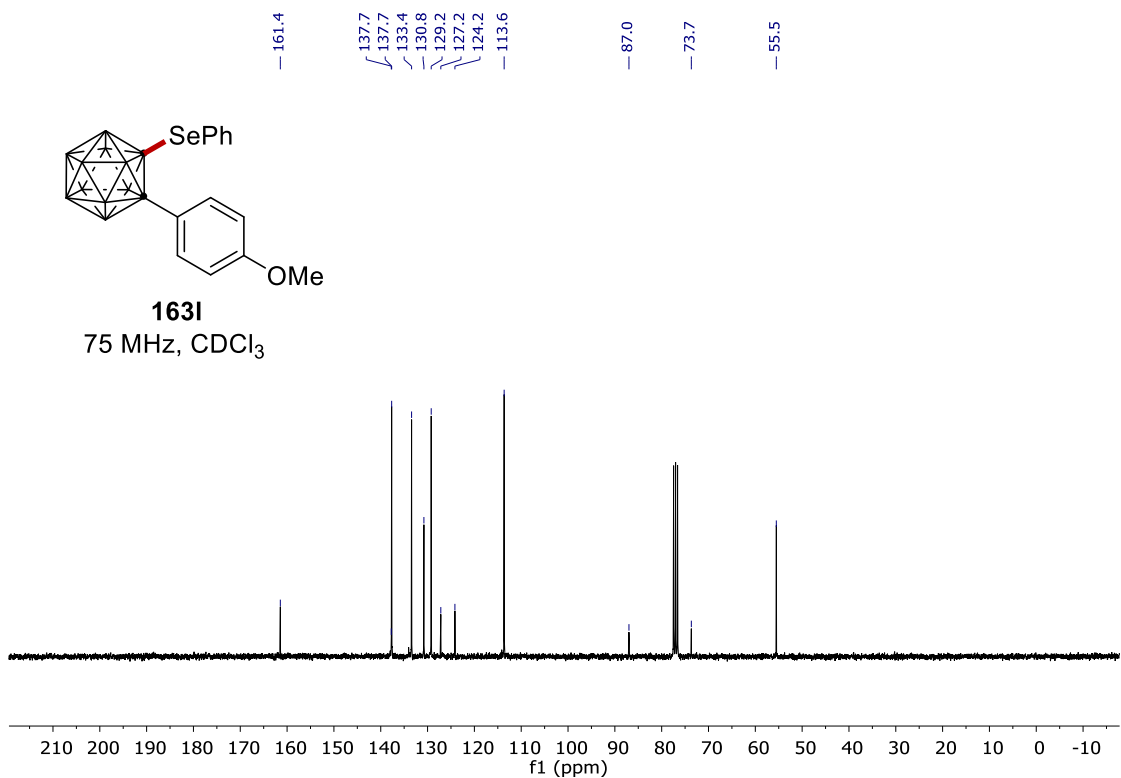
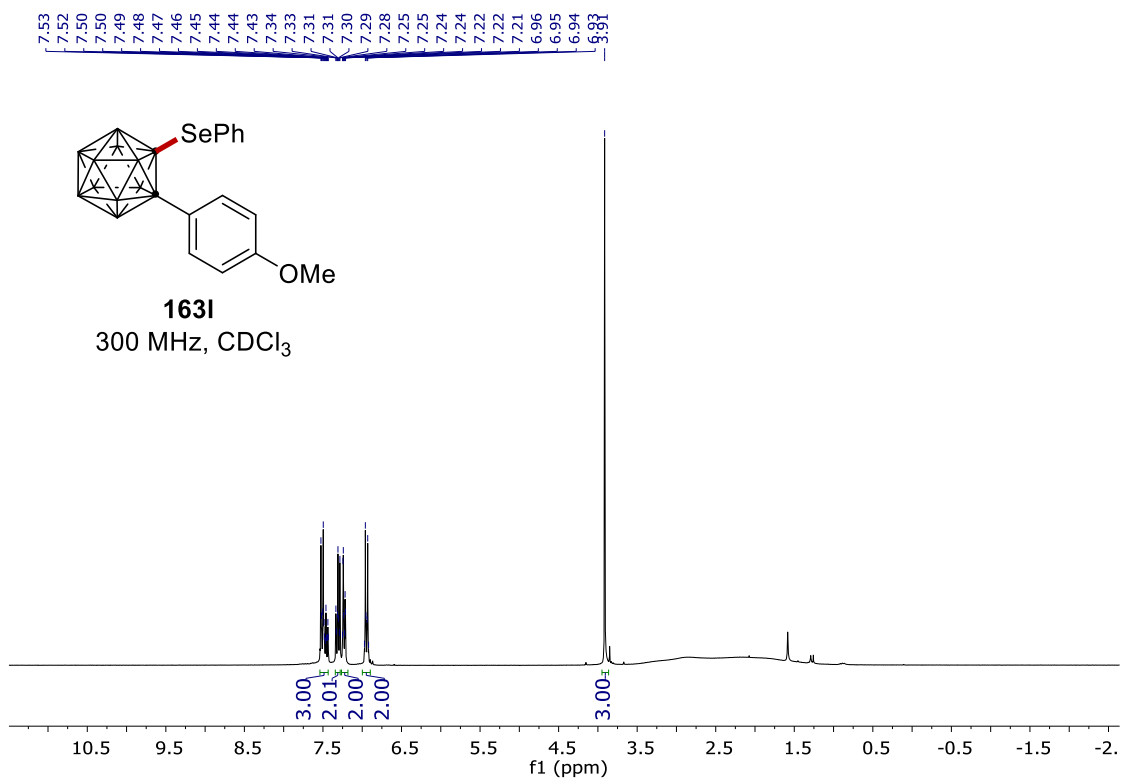
NMR Spectra



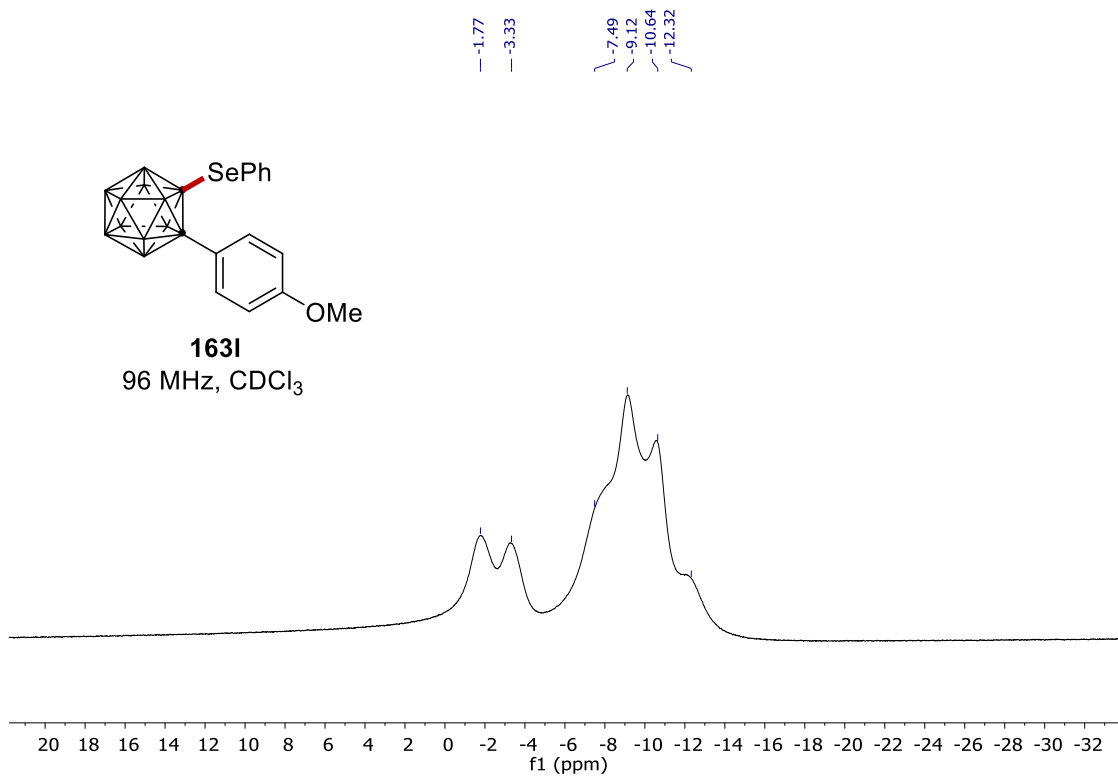
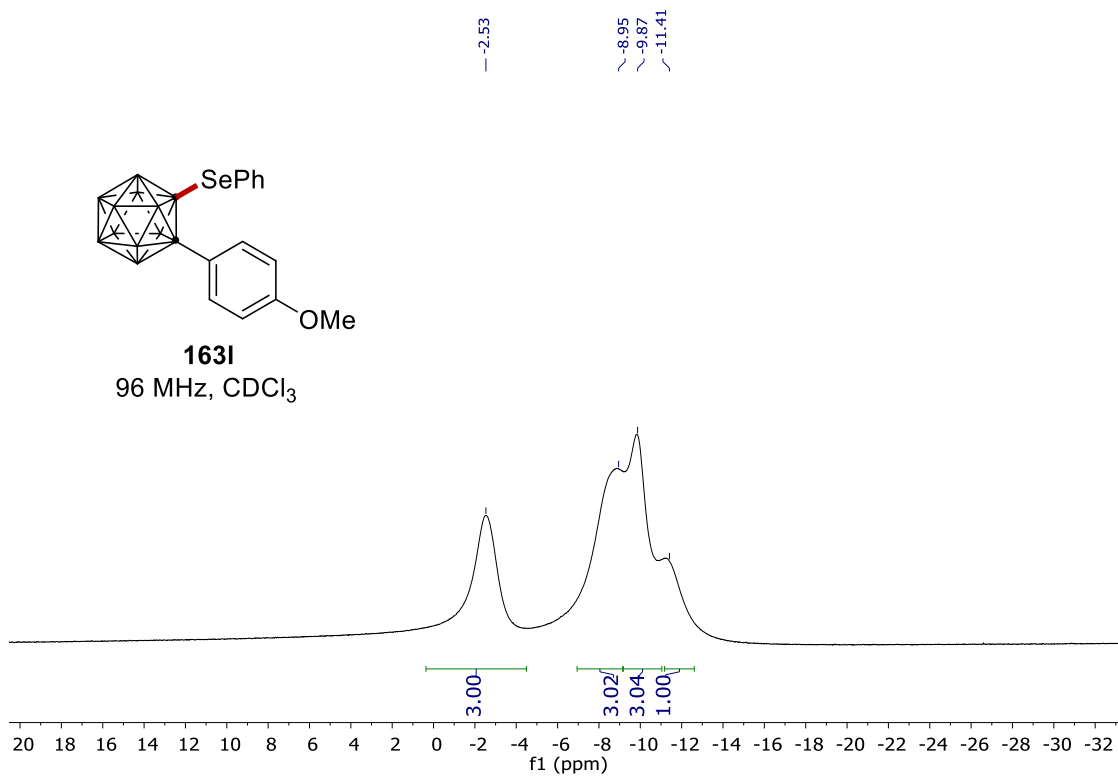
NMR Spectra



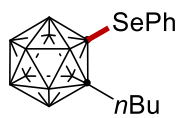
NMR Spectra



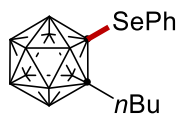
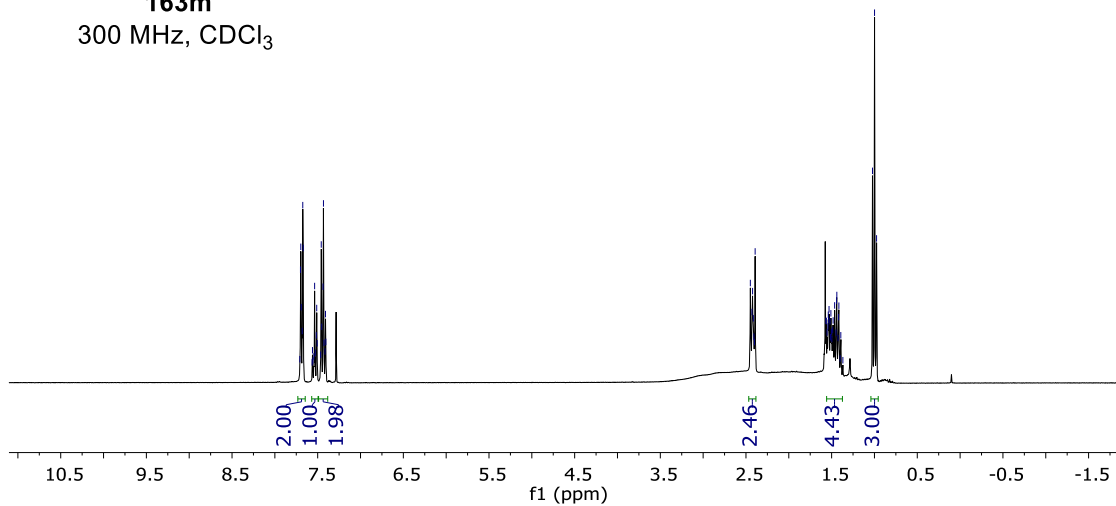
NMR Spectra



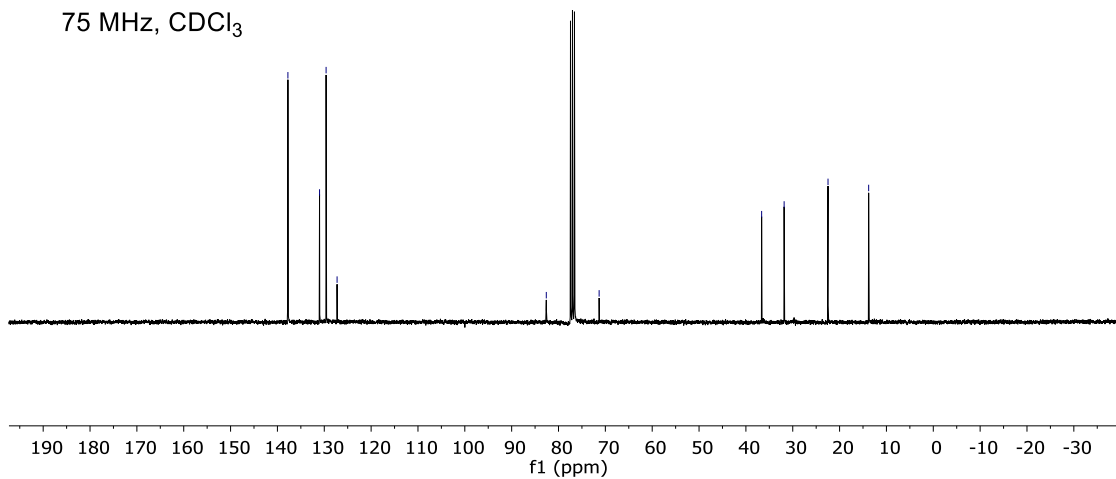
NMR Spectra



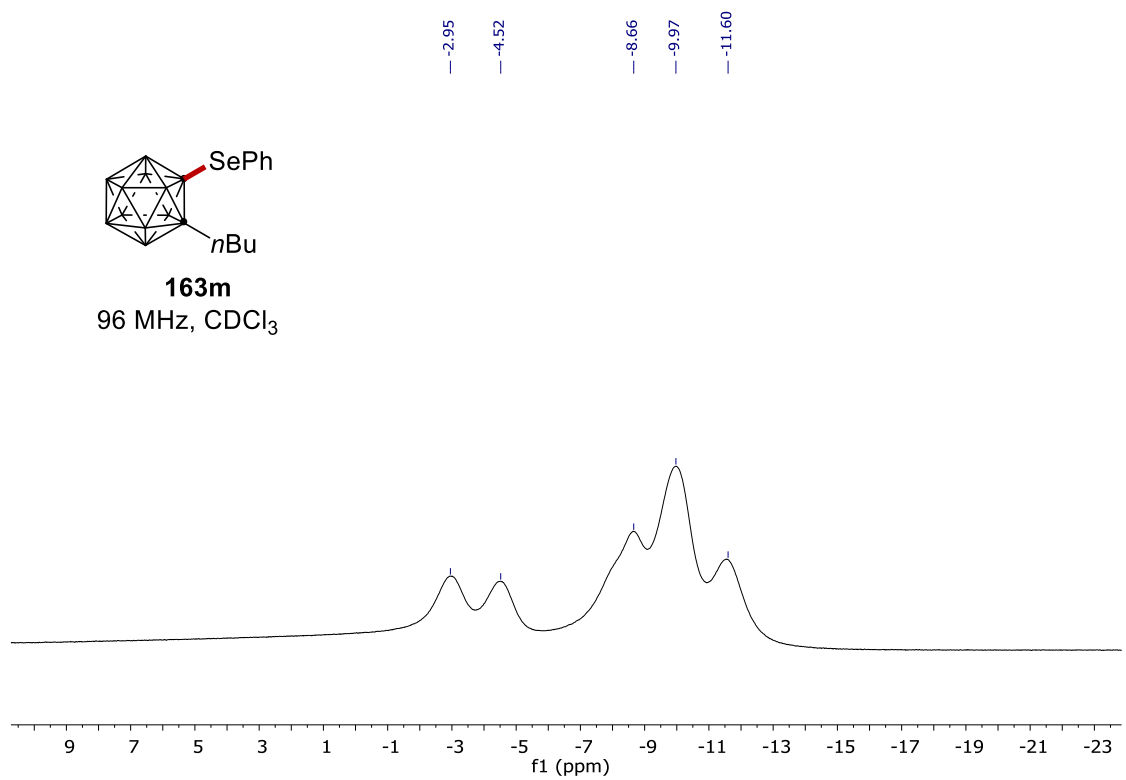
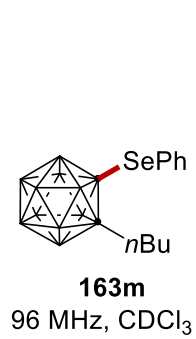
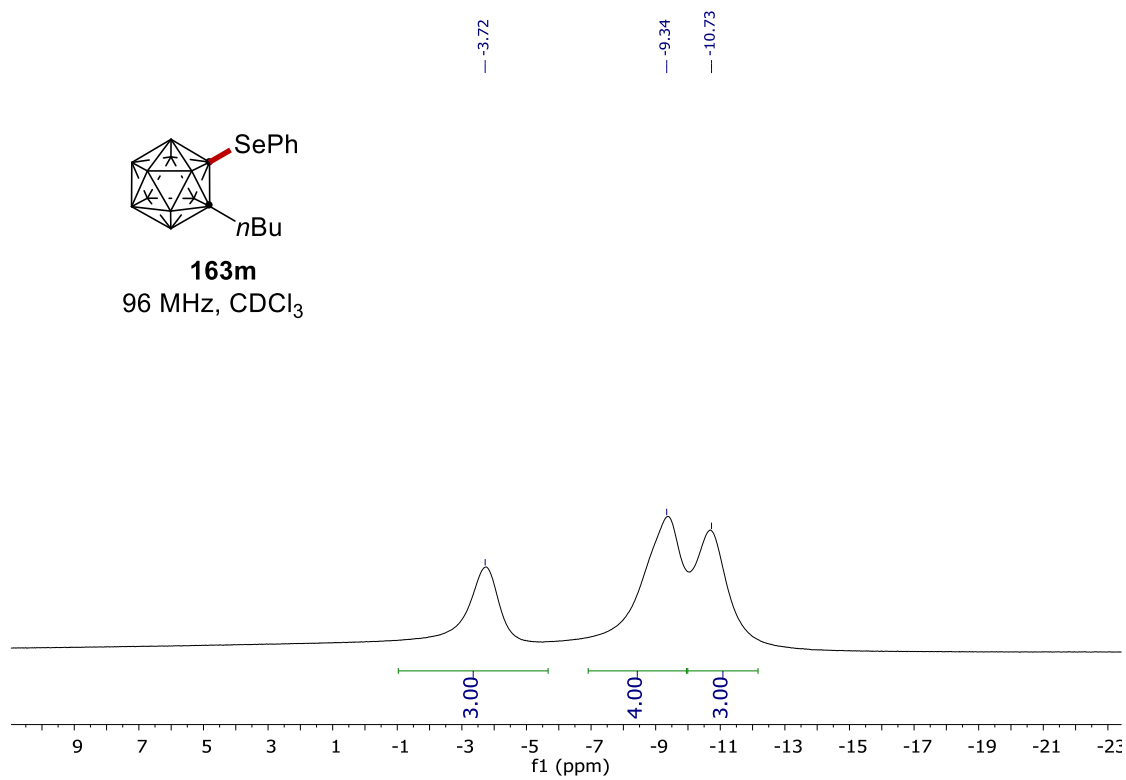
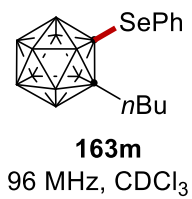
163m
300 MHz, CDCl₃



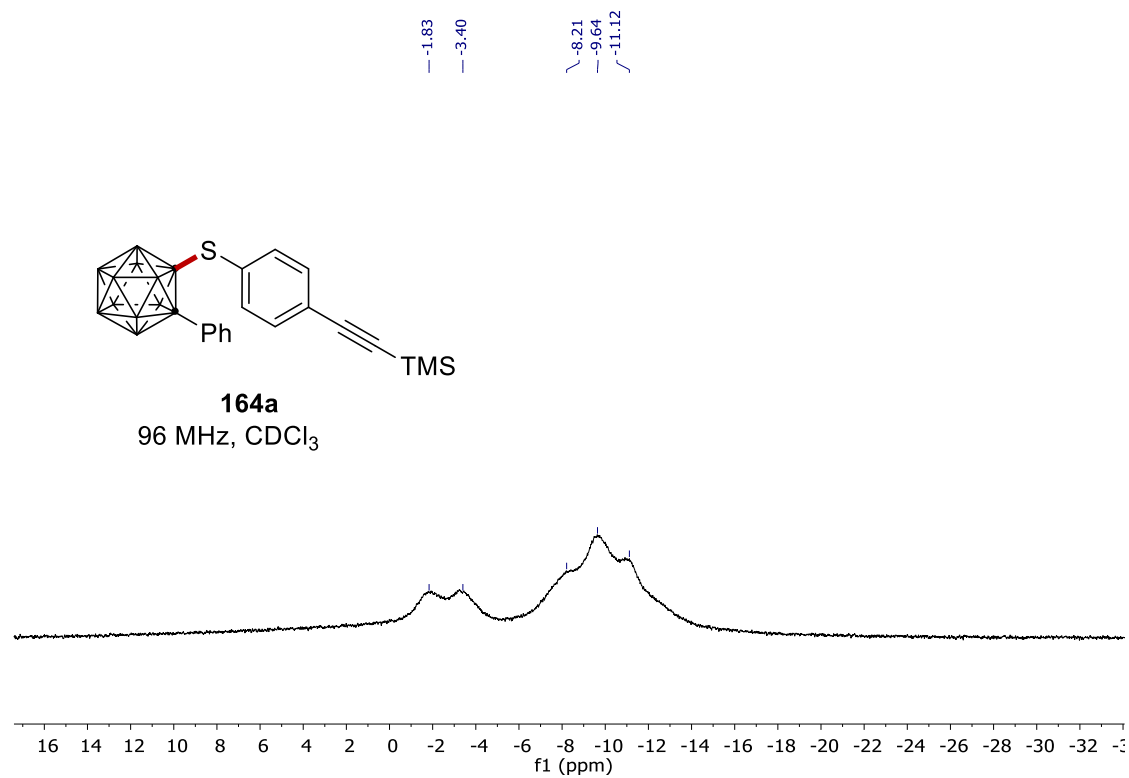
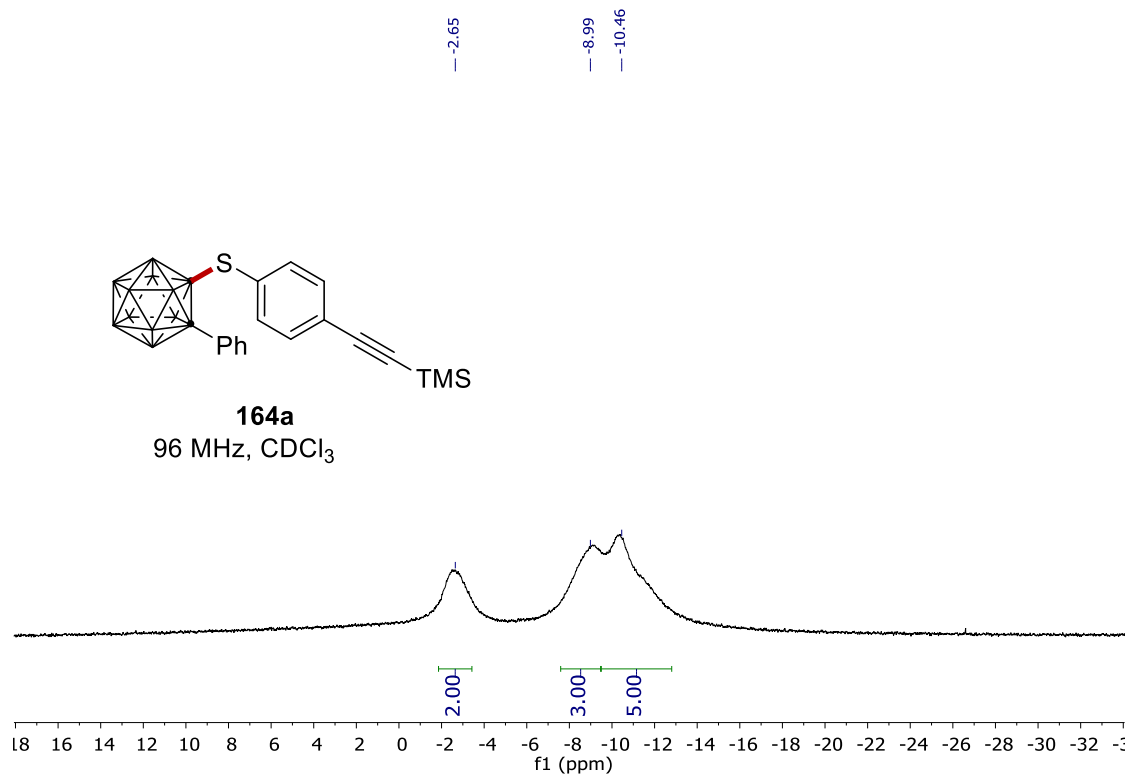
163m
75 MHz, CDCl₃



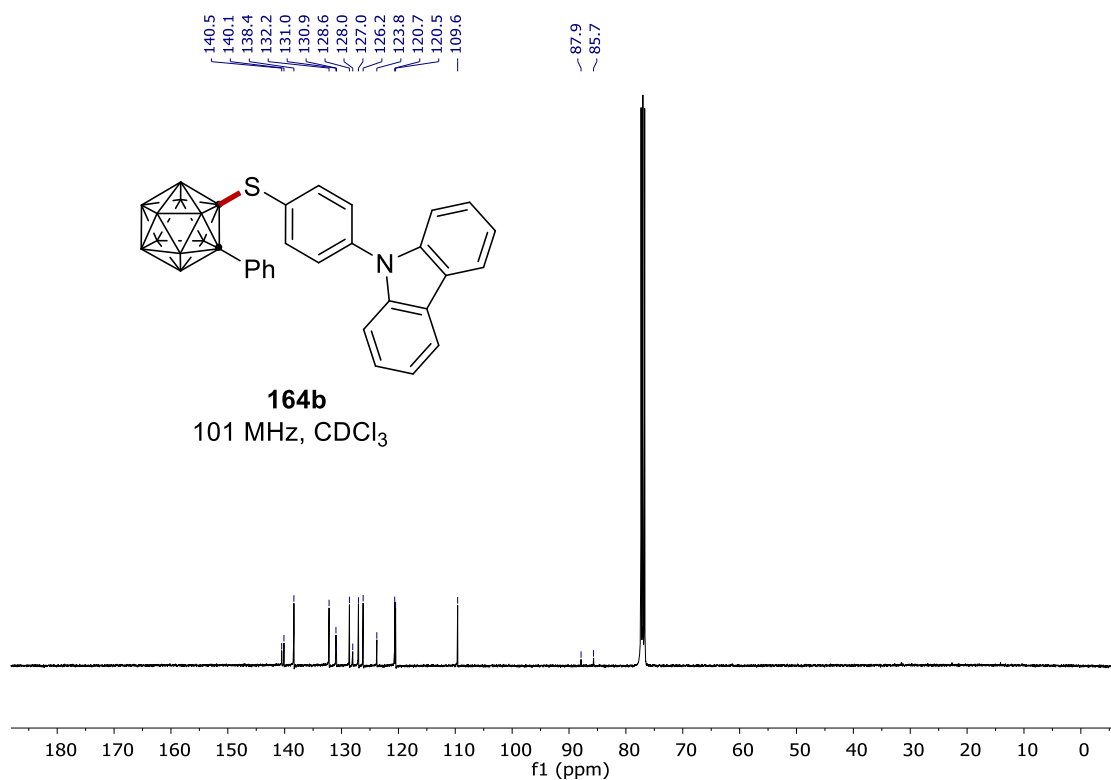
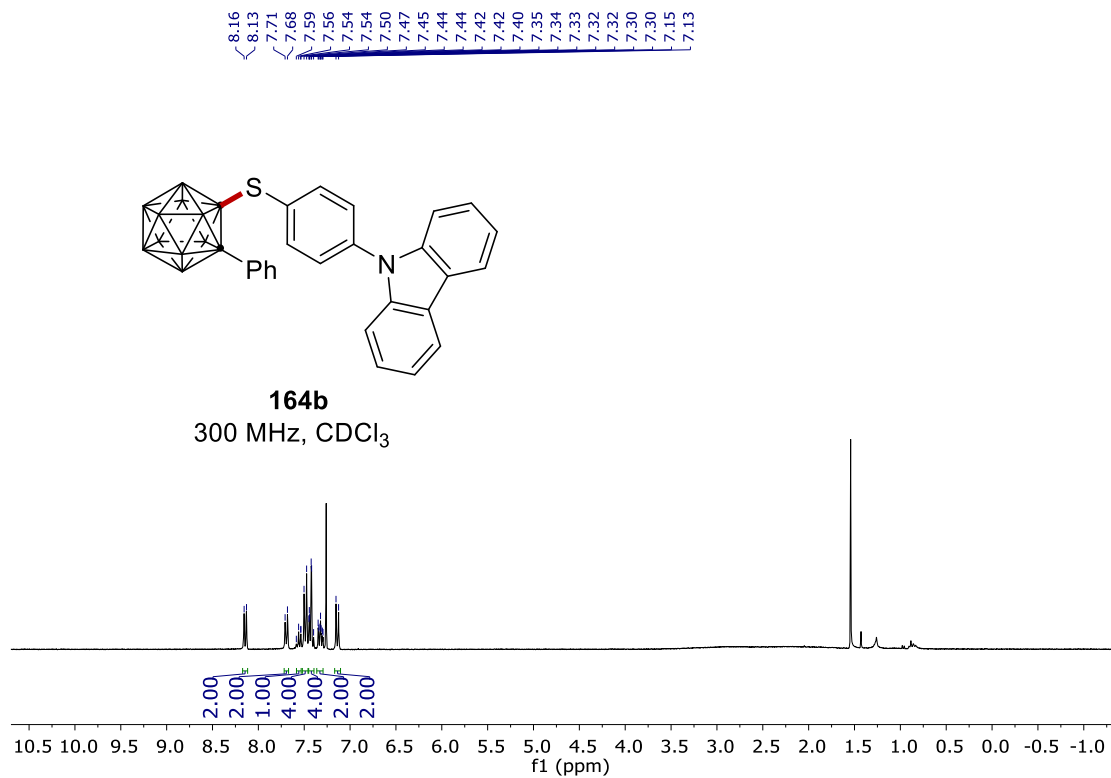
NMR Spectra



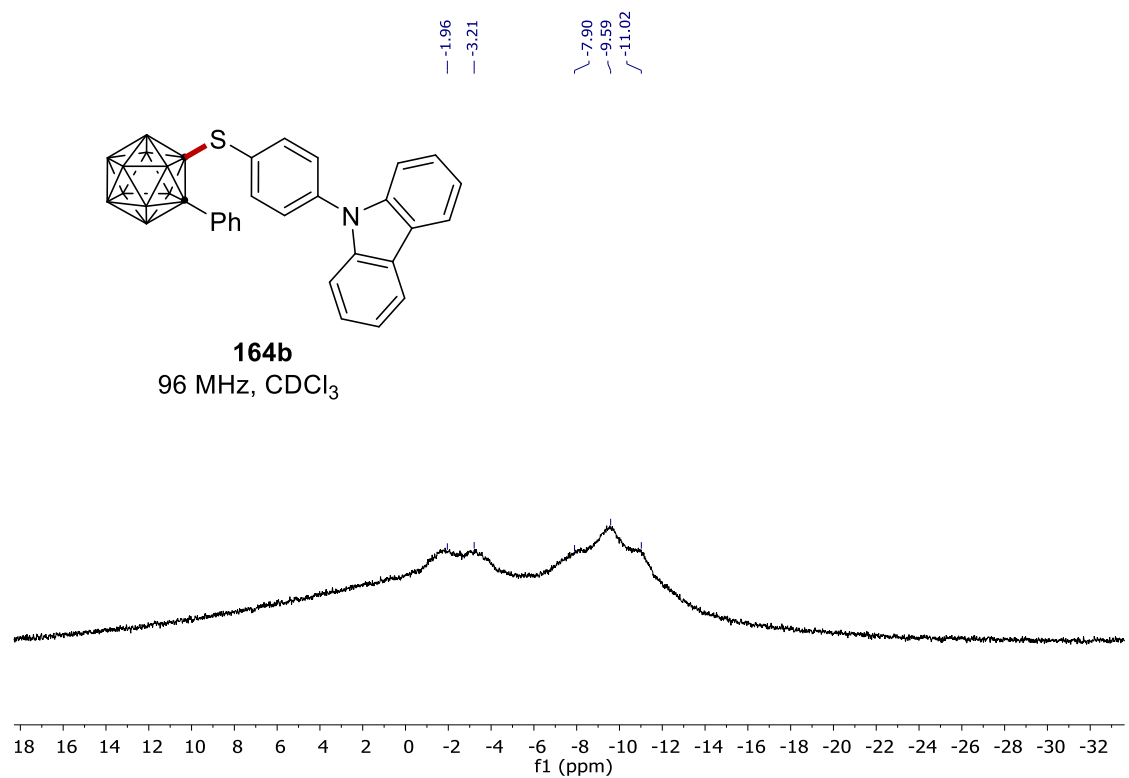
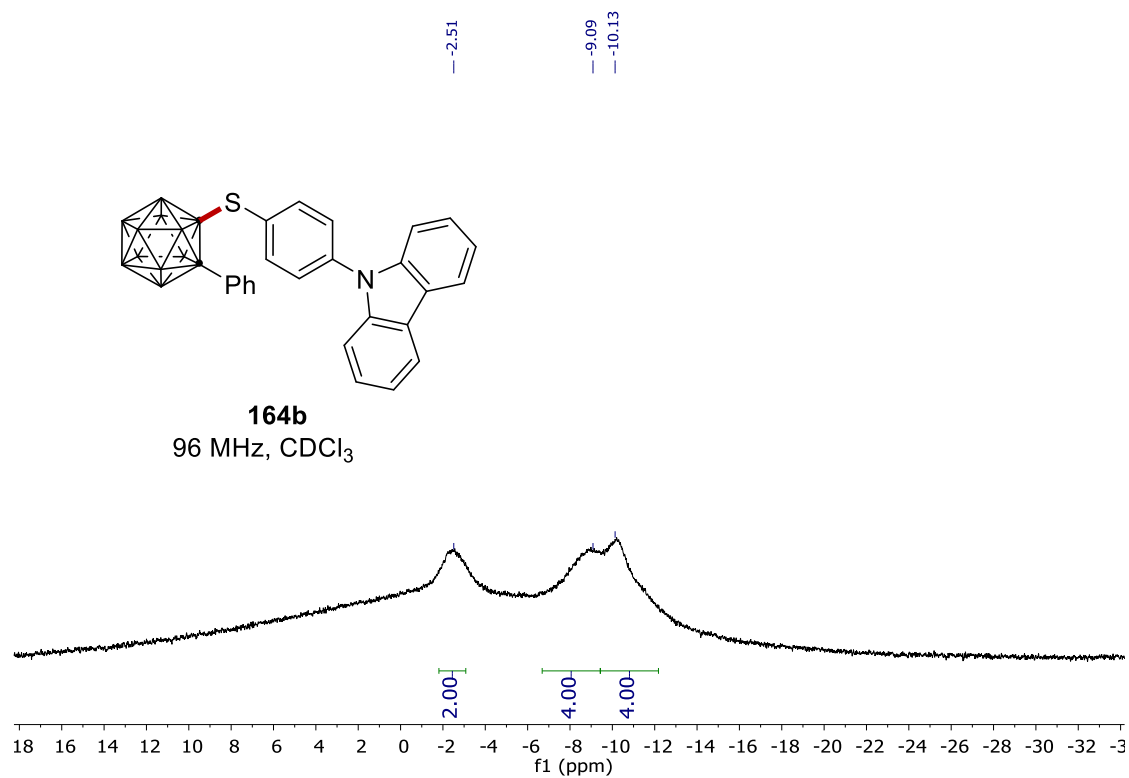
NMR Spectra



NMR Spectra



NMR Spectra



Acknowledgement

Herein, I would like to extend my sincere gratitude to my doctoral supervisor Prof. Dr. Lutz Ackermann for giving me this fascinating opportunity to carry out my PhD study here at University of Göttingen and sharing all those creative ideas, enlightening suggestions and helpful discussions with me throughout my research.

I am very grateful to Prof. Dr. Shoubhik Das for his kindly accepting to be the second supervisor. I also thank the other members of the examination committee, Prof. Dr. Dietmar Stalke, Jun.-Prof. Dr. Johannes C. L. Walker, Dr. Michael John, and Dr. Daniel Janßen-Müller.

I gratefully acknowledge China Scholarship Council (CSC) for the financial support during my research stay in Germany.

I thank Dr. Yu-Feng, Liang, Dr. Elżbieta Gońka, Dr. Fabio Pescioli, Dr. Rositha Kuniyil, Dr. Torben Rogge, Dr. Lars H. Finger, Dr. Antonis M. Messinis, Dr. Johanna Frey, Dr. A. Claudia Stückl, Becky Bongsuiru Jei, Ralf Steinbock, Alexej Scheremetjew, Dr. Yiyi Weng and Binbin Yuan, very much for their great contributions to my PhD projects. And many thanks to the people who helped me correct the doctoral thesis: Dr. Ramesh C. Samanta, Dr. Robert Connon, Dr. Bartłomiej Sadowski, Dr. Shou-Kun Zhang, Dr. Yulei Wang, Dr. Yanjun Li, Isaac Choi, Julia Struwe, Jun Wu and Becky Bongsuiru Jei.

I deeply appreciate Ms. Gabriele Keil-Knepel and Bianca Spitalieri for their kind assistance in the laboratory as well as in my daily life. I thank Mr. Stefan Beußhausen for the technical assistance with the instruments, and Mr. Karsten Rauch for his suggestions on the lab work and safety. I also want to thank all the members of the analytical departments of IOBC for their kind support in chemistry. I appreciate the help from Dr. Christopher Golz for the X-ray analysis.

I sincerely would also like to thank all the people who helped me to correct manuscripts and supporting information: Dr. Torben Rogge, Dr. Rositha Kuniyil, Dr. João C. A. de Oliveira, Dr. Lars H. Finger, Dr. Robert Connon, Dr. Tomasz Wdowik, Dr. Johanna Frey, Ralf Steinbock, Alexej Scheremetjew, Maximilian Stangier, Dr. Nikolaos Kaplaneris and Dr. Uttam Dhawa. I thank all the group members in Ackermann Group, particularly the past and current members in Lab 309, Dr. Fabio Pescioli, Dr. Yu-Feng Liang, Dr. Debasish Ghorai, Dr. Tomasz Wdowik, Dr. Robert Connon, Dr. Cong Tian, Dr. Elżbieta Gońka, Dr. Uttam Dhawa, Dr. Valentin Müller, Ralf

Acknowledgement

Steinbock, Becky Bongsuiru Jei, Weizhao Li, Rongxin Yin.

I really enjoyed the football and basketball games with Alexj Scheremetjew, Dr. Tjark Meyer, Maximilian Stangier, Dr. Ramesh C. Samanta, Dr. Youai Qiu, Leonardo Massignan, Dr. Wei-Jun Kong, Dr. Shou-Kun Zhang, Jun Wu, Dr. Thomas Müller, Dr. Antonis M. Messinis, Dr. Yan Zhang, Dr. João C. A. de Oliveira, Dr. Wei Wang, Dr. Zhigao Shen, Ralf Steinbock, Zhipeng Lin, Shan Chen, Dr. Yulei Wang, Dr. Yanjun Li, Hendrik Simon, Isaac Maksso, Takuya Michiyuki, Tsuyoshi Ohyama.

Last but not the least, I would like to express my deepest gratitude to my wife, my son and my parents. Their endless love, unconditional support and encouragement made it possible to come this far.

Curriculum Vitae

Personal Information

Name: Long Yang

Date of birth: February 14, 1991

Place of birth: Ganzhou, Jiangxi, P. R. China

Nationality: Chinese

Address: Tammannstrasse 2, 37077, Göttingen, Germany

Email: ylong@gwdg.de

Academic Education

10.2017–present Ph.D. Candidate in Organic Chemistry

Georg-August-Universität Göttingen

Supervisor: Prof. Dr. Lutz Ackermann

Thesis: Selective C–H Activation: Ruthenaelectro-Catalysis
and Carborane Cage Activation

09.2014–06.2017 M.Sc. in Organic Chemistry

Fuzhou University

Supervisor: Prof. Dr. Gang Li

Thesis: Palladium-Catalyzed *ortho*-C–H Bond Activation of Benzoic Acids
and *meta*-C–H Bond Activation of Anilines

09.2010–06.2014 B.Sc. in Chemical Engineering and Technology

Jinggangshan University

Attended Symposiums

1st Summer School on Organic Catalysis for Energy Conversion, Göttingen, Germany, September 24-29, 2017.

5th International Symposium on C–H Activation. Georg-August-Universität Göttingen, Germany, July 27-30, 2020.

ONLINE SYMPOSIUM: Earth-Abundant 3d Metal Catalysis BEILSTEIN ORGANIC CHEMISTRY SYMPOSIUM 2020, Germany, September 22-23, 2020

Visual Summer School organized within C–H•AIR project, Göttingen, Germany, June 22-24, 2021.

Publications

1. **L. Yang**,⁺ B. B. Jei,⁺ A. Scheremetjew, B. Yuan, A. C. Stückl and L. Ackermann,* "Electrooxidative *o*-Carborane Chalcogenations Without Directing Groups: Cage Activation by Copper Catalysis at Room Temperature" *Chem.Sci.* **2021**, *Accepted*.
2. **L. Yang**,⁺ B. B. Jei,⁺ A. Scheremetjew, R. Kuniyil, L. Ackermann,* "Electrochemical B–H Nitrogenation: Access to Amino Acid and BODIPY-Labeled *nido*-Carboranes" *Angew. Chem. Int. Ed.* **2021**, *60*, 1482-1487.
3. **L. Yang**, R. Steinbock, A. Scheremetjew, R. Kuniyil, L. H. Finger, A. M. Messinis, L. Ackermann,* "Azaruthena(II)-Bicyclo-[3.2.0]-Heptadiene: Key Intermediate for Ruthenaelectro(II/III/I)-Catalyzed Alkyne Annulations" *Angew. Chem. Int. Ed.* **2020**, *59*, 11130-11135.
4. **L. Yang**, J. Frey, L. Ackermann,* "Nickel-electrocatalyzed sulfide and phosphine oxygenations with water" *Sci. China Chem.* **2021**, *64*, 873-874.
5. Y.-F. Liang,⁺ **L. Yang**,⁺ B. B. Jei, R. Kuniyil, L. Ackermann,* "Regioselective B(3,4)–H Arylation of *o*-Carboranes by Weak Amide Coordination at Room Temperature" *Chem. Sci.* **2020**, *11*, 10764-10769.
6. E. Gońka,⁺ **L. Yang**,⁺ R. Steinbock, F. Pescioli, R. Kuniyil, L. Ackermann,* "π-Extended Polyaromatic Hydrocarbons by Sustainable Alkyne Annulations through Double C–H/N–H Activation" *Chem. Eur. J.* **2019**, *25*, 16246-16250.
7. Y.-F. Liang,⁺ **L. Yang**,⁺ T. Rogge,⁺ L. Ackermann,* "Ruthenium(IV) Intermediates in C–H Activation/Annulation by Weak O-Coordination" *Chem. Eur. J.* **2018**, *24*, 16548-16552.
8. **L. Yang**, S. Li, L. Cai, Y. Ding, L. Fu, Z. Cai, H. Ji, G. Li,* "Palladium-Catalyzed C–H Trifluoroethoxylation of *N*-Sulfonylbenzamides" *Org. Lett.* **2017**, *19*, 2746-2749.
9. **L. Yang**,⁺ L. Fu,⁺ G. Li,* "Incorporation of Carbon Dioxide into Carbamate Directing Groups: Palladium-Catalyzed *meta*-C–H Olefination and Acetoxylation of Aniline Derivatives" *Adv. Synth. Catal.* **2017**, *359*, 2235-2240.
10. Y.-F. Liang, R. Steinbock, **L. Yang**, L. Ackermann,* "Continuous Visible Light-Photo-Flow Approach for Manganese-Catalyzed (Het)Arene C–H Arylation" *Angew. Chem. Int. Ed.* **2018**, *57*, 10625-10629.
11. S. Li, L. Cai, H. Ji, **L. Yang**, G. Li,* "Pd(II)-catalysed *meta*-C–H functionalizations of benzoic acid derivatives" *Nat. Commun.* **2016**, *7*, 10443.
12. Y. Weng, H. Chen, N. Li, **L. Yang**, L. Ackermann,* "Electrooxidative Metal-Free Cyclization of 4-Arylamino coumarins Employing DMF as C1-Source" *Adv. Synth. Catal.* **2021**, *363*, 2773-2777. (*Equal contribution)